

# MODERN ELECTROCHEMISTRY 2A ELECTROCHEMISTRY 2A ELECTROCHEMISTRY 2A

Fundamentals of Electroics

SECOND EDITION

JOHN O'M. BOCKRIS, AMULYA K. N. REDDY,  
AND MARIA GAMBOA-ALDECO

*VOLUME 2A*

***MODERN  
ELECTROCHEMISTRY***

*SECOND EDITION*

*Fundamentals of  
Electrodics*

**This page intentionally left blank**

To J. A. V. Butler and Max Volmer



**This page intentionally left blank**

**VOLUME 2A**

**MODERN  
ELECTROCHEMISTRY**

**SECOND EDITION**

*Fundamentals of  
Electrodics*

**John O'M Bockris**

*Molecular Green Technology  
College Station, Texas*

**Amulya K. N. Reddy**

*President  
International Energy Initiative  
Bangalore, India*

*and*

**Maria Gamboa-Aldeco**

*Texas A&M University  
College Station, Texas*

**KLUWER ACADEMIC PUBLISHERS**

**NEW YORK, BOSTON, DORDRECHT, LONDON, MOSCOW**

eBook ISBN: 0-306-47605-3  
Print ISBN: 0-306-46166-8

©2002 Kluwer Academic Publishers  
New York, Boston, Dordrecht, London, Moscow

Print ©2000 Kluwer Academic/Plenum Publishers  
New York

All rights reserved

No part of this eBook may be reproduced or transmitted in any form or by any means, electronic, mechanical, recording, or otherwise, without written consent from the Publisher

Created in the United States of America

Visit Kluwer Online at: <http://kluweronline.com>  
and Kluwer's eBookstore at: <http://ebooks.kluweronline.com>

# ***PREFACE TO THE FIRST EDITION***

This book had its nucleus in some lectures given by one of us (J.O'M.B.) in a course on electrochemistry to students of energy conversion at the University of Pennsylvania. It was there that he met a number of people trained in chemistry, physics, biology, metallurgy, and materials science, all of whom wanted to know something about electrochemistry. The concept of writing a book about electrochemistry which could be understood by people with very varied backgrounds was thereby engendered. The lectures were recorded and written up by Dr. Klaus Muller as a 293-page manuscript. At a later stage, A.K.N.R. joined the effort; it was decided to make a fresh start and to write a much more comprehensive text.

Of methods for direct energy conversion, the electrochemical one is the most advanced and seems the most likely to become of considerable practical importance. Thus, conversion to electrochemically powered transportation systems appears to be an important step by means of which the difficulties of air pollution and the effects of an increasing concentration in the atmosphere of carbon dioxide may be met. Corrosion is recognized as having an electrochemical basis. The synthesis of nylon now contains an important electrochemical stage. Some central biological mechanisms have been shown to take place by means of electrochemical reactions. A number of American organizations have recently recommended greatly increased activity in training and research in electrochemistry at universities in the United States. Three new international journals of fundamental electrochemical research were established between 1955 and 1965.

In contrast to this, physical chemists in U.S. universities seem—perhaps partly because of the absence of a modern textbook in English—out of touch with the revolution in fundamental interfacial electrochemistry which has occurred since 1950. The fragments of electrochemistry which are taught in many U.S. universities belong not to the space age of electrochemically powered vehicles, but to the age of

thermodynamics and the horseless carriage; they often consist of Nernst's theory of galvanic cells (1891) together with the theory of Debye and Hückel (1923).

Electrochemistry at present needs several kinds of books. For example, it needs a textbook in which the whole field is discussed at a strong theoretical level. The most pressing need, however, is for a book which outlines the field at a level which can be understood by people entering it from different disciplines who have no previous background in the field but who wish to use modern electrochemical concepts and ideas as a basis for their own work. It is this need which the authors have tried to meet.

The book's aims determine its priorities. In order, these are:

1. **Lucidity.** The authors have found students who understand advanced courses in quantum mechanics but find difficulty in comprehending a field at whose center lies the quantum mechanics of electron transitions across interfaces. The difficulty is associated, perhaps, with the interdisciplinary character of the material: a background knowledge of physical chemistry is not enough. Material has therefore sometimes been presented in several ways and occasionally the same explanations are repeated in different parts of the book. The language has been made informal and highly explanatory. It retains, sometimes, the lecture style. In this respect, the authors have been influenced by *The Feynman Lectures on Physics*.

2. **Honesty.** The authors have suffered much themselves from books in which proofs and presentations are not complete. An attempt has been made to include most of the necessary material. Appendices have been often used for the presentation of mathematical derivations which would obtrude too much in the text.

3. **Modernity.** There developed during the 1950's a great change in emphasis in electrochemistry away from a subject which dealt largely with solutions to one in which the treatment at a molecular level of charge transfer across interfaces dominates. This is the "new electrochemistry," the essentials of which, at an elementary level, the authors have tried to present.

4. **Sharp variation is standard.** The objective of the authors has been to begin each chapter at a very simple level and to increase the level to one which allows a connecting up to the standard of the specialized monograph. The standard at which subjects are presented has been intentionally variable, depending particularly on the degree to which knowledge of the material appears to be widespread.

5. **One theory per phenomenon.** The authors intend a *teaching book*, which acts as an introduction to graduate studies. They have tried to present, with due admission of the existing imperfections, a simple version of that model which seemed to them at the time of writing to reproduce the facts most consistently. They have for the most part refrained from presenting the detailed pros and cons of competing models in areas in which the theory is still quite mobile.

In respect to references and further reading: no detailed references to the literature have been presented, in view of the elementary character of the book's contents, and the corresponding fact that it is an introductory book, largely for beginners. In the

“further reading” lists, the policy is to cite papers which are classics in the development of the subject, together with papers of particular interest concerning recent developments, and in particular, reviews of the last few years.

It is hoped that this book will not only be useful to those who wish to work with modern electrochemical ideas in chemistry, physics, biology, materials science, etc., but also to those who wish to begin research on electron transfer at interfaces and associated topics.

The book was written mainly at the Electrochemistry Laboratory in the University of Pennsylvania, and partly at the Indian Institute of Science in Bangalore. Students in the Electrochemistry Laboratory at the University of Pennsylvania were kind enough to give guidance frequently on how they reacted to the clarity of sections written in various experimental styles and approaches. For the last four years, the evolving versions of sections of the book have been used as a partial basis for undergraduate, and some graduate, lectures in electrochemistry in the Chemistry Department of the University.

The authors' acknowledgment and thanks must go first to Mr. Ernst Cohn of the National Aeronautics and Space Administration. Without his frequent stimulation, including very frank expressions of criticism, the book might well never have emerged from the Electrochemistry Laboratory.

Thereafter, thanks must go to Professor B. E. Conway, University of Ottawa, who gave several weeks of his time to making a detailed review of the material. Plentiful help in editing chapters and effecting revisions designed by the authors was given by the following: Chapters IV and V, Dr. H. Wroblowa (Pennsylvania); Chapter VI, Dr. C. Solomons (Pennsylvania) and Dr. T. Emi (Hokkaido); Chapter VII, Dr. E. Gileadi (Tel-Aviv); Chapters VIII and IX, Prof. A. Despic (Belgrade), Dr. H. Wroblowa, and Mr. J. Diggle (Pennsylvania); Chapter X, Mr. J. Diggle; Chapter XI, Dr. D. Cipris (Pennsylvania). Dr. H. Wroblowa has to be particularly thanked for essential contributions to the composition of the Appendix on the measurement of Volta potential differences.

Constructive reactions to the text were given by Messrs. G. Razumney, B. Rubin, and G. Stoner of the Electrochemistry Laboratory. Advice was often sought and accepted from Dr. B. Chandrasekaran (Pennsylvania), Dr. S. Srinivasan (New York), and Mr. R. Rangarajan (Bangalore).

Comments on late drafts of chapters were made by a number of the authors' colleagues, particularly Dr. W. McCoy (Office of Saline Water), Chapter II; Prof. R. M. Fuoss (Yale), Chapter III; Prof. R. Stokes (Armidale), Chapter IV; Dr. R. Parsons (Bristol), Chapter VII; Prof. A. N. Frumkin (Moscow), Chapter VIII; Dr. H. Wroblowa, Chapter X; Prof. R. Staehle (Ohio State), Chapter XI. One of the authors (A.K.N.R.) wishes to acknowledge his gratitude to the authorities of the Council of Scientific and Industrial Research, India, and the Indian Institute of Science, Bangalore, India, for various facilities, not the least of which were extended leaves of absence. He wishes also to thank his wife and children for sacrificing many precious hours which rightfully belonged to them.

**This page intentionally left blank**

## **PREFACE TO VOLUME 2A**

Bockris and Reddy is a well-known text in the electrochemical field. Originally published in 1970, it has had a very long life as an introduction to a vast interdisciplinary area. The updating of the book should have been carried out long ago, but this task had to compete with other needs, for example, preparation of an advanced graduate text (Bockris and Khan, *Surface Electrochemistry*, Plenum, 1993), and while the sales of the first edition continued to be significant, the inevitable second edition remained a future project. Its time has come.

It may first be restated for whom this book is intended. Its obvious home is in the chemistry and chemical engineering departments of universities. Electrochemistry is also often the basis of fields treated in departments of engineering, materials, science, and biology. However, the total sales of the first edition far exceeded the number of electrochemists in the Electrochemical Society—evidence that the book is used by scientists who may have backgrounds in quite other subjects, but find that their disciplines involve the properties of interfaces and thus, in practice, the interfacial part of electrochemistry (for the ionics part, see Vol. 1).

This broad audience, professionals all, affects the standard of the presentation, and it is important to stress that this book assumes an audience that has an undergraduate knowledge of chemistry. The text starts from the beginning and climbs quite high, from place to place reaching the frontier of a changing field in the late 1990s. However, it does not try, as graduate student texts must, to cover all the advancing fronts. Lucidity is the main characteristic where the book carries over from the first edition and lucidity needs increasingly more space as complexity increases. For those who want to see how the material developed here approaches a graduate standard, *Surface Electrochemistry* (1993) is available, as well as the monograph series, *Modern Aspects of Electrochemistry* (Kluwer-Plenum), which is published, roughly, at one volume per year.



*Modern Electrochemistry* was a two-volume work in 1970, but advances in the field since then have made it necessary to considerably enlarge the scope of this text. Whereas in Vol. 1 on ionics (Chapters 1 through 5), about a third of the first edition could be retained, the material in these two volumes, 2A and 2B, had to be nearly completely rewritten and six new chapters added.

The advances made since 1970 start with the fact that the solid/solution interface can now be studied at an atomic level. Single-crystal surfaces turn out to manifest radically different properties, depending on the orientation exposed to the solution. Potentiodynamic techniques that were raw and quasi-empirical in 1970 are now sophisticated experimental methods. The theory of interfacial electron transfer has attracted the attention of physicists, who have taken the beginnings of quantum electrochemistry due to Gurney in 1932 and brought that early initiative to a 1990 level. Much else has happened, but one thing must be said here. Since 1972, the use of semiconductors as electrodes has come into much closer focus, and this has enormously extended the realm of systems that can be treated in electrochemical terms.

Volume 2A consists of Chapters 6 through 9 and covers the fundamentals of electrodics. Chapters 10 through 15, which make up Vol. 2B, discuss electrodics in chemistry, engineering, biology, and environmental science. It would be a misapprehension to think of these chapters as being applied electrochemistry, for the considerations are not at all technological. The material presented serves to illustrate the breadth of fields that depend upon the properties of wet surfaces.

Each chapter has been reviewed by a scientist whose principal or even sole activity is in the area covered. The advice given has usually been accepted. The remaining inevitable flaws and choice of material are the responsibility of the authors alone.

A teaching book should have problems for students to solve and as explained in the preface to Vol. 1, acknowledgment must be made here to the classification of these problems according to a scheme used in Atkins, *Physical Chemistry* (Freeman).

## TEXT REFERENCES AND READING LISTS

Because electrochemistry, as in other disciplines, has been built on the foundations established by individual scientists and their collaborators, it is important that the student know who these contributors are. These researchers are mentioned in the text, with the date of their most important work (e.g., Gurney, 1932). This will allow the student to place these leaders in electrochemistry in the development of the field.

Then, at the end of sections is a suggested reading list. The first part of the list consists of some seminal papers, publications which, in the light of history, can be seen to have made important contributions to the buildup of modern electrochemical knowledge. The student will find these earlier papers instructive in comprehending the subject's development. However, there is another reason to encourage the reading

of papers written in earlier decades; they are generally easier to understand than the later, necessarily more sophisticated, papers.

Next in the reading list, are recent reviews. Such documents summarize the relevant field and the student will find them invaluable; only it must be remembered that these documents were written for the scientists of their time. Thus, they may prove to be less easy to understand than the text of this book, which is aimed at students in the field.

Finally, the reading lists offer a sampling of some papers of the past decade. These should be understandable by students who have worked through the book and particularly those who have done at least some of the exercises and problems.

There is no one-to-one relation between the names (with dates) that appear in the text and those in the reading list. There will, of course, be some overlap, but the seminal papers are limited to those in the English language, whereas physical electrochemistry has been developed not only in the United Kingdom and the United States, but also strongly in Germany and Russia. Names in the text, on the other hand, are given independently of the working language of the author.

ACKNOWLEDGEMENTS. Much help was obtained from colleagues in a general way. Their advice has been, by and large, respected. Dr. Ron Fawcett of the University of California, Davis, read and criticized part of Chapter 6. Chapters 8 and 9 were reported upon by Prof. Brian B.E. Conway, University of Ottawa. Chapter 9 was monitored by Dr. Rey Sidik at Texas A&M University. Chapter 10 was discussed with Prof. Nathan Lewis, Stanford University. Chapter 11 was commented upon by Dr. Norman Weinberg. Chapter 12 was studied and corrected by Dr. Robert Kelly, University of Virginia. Chapter 13 was read and criticized by Prof. A.J. Appleby, Texas A&M University and Dr. Supramaniam Srinivasan, Princeton University. Chapter 14 was commented upon by Dr. Martin Blank, State University of New York, and Chapter 15 by Dr. Robert Gale of Louisiana State University.

John O'M. Bockris, College Station, Texas  
Amalya K. Reddy, Bangalore, India  
Maria Gamboa-Aldeco, Superior, Colorado

**This page intentionally left blank**

# CONTENTS

## CHAPTER 6

### THE ELECTRIFIED INTERFACE

6.1.	Electrification of an Interface . . . . .	771
6.1.1.	The Electrode/Electrolyte Interface: The Basis of Electrodeics . . . . .	771
6.1.2.	New Forces at the Boundary of an Electrolyte . . . . .	771
6.1.3.	The Interphase Region Has New Properties and New Structures . . . . .	774
6.1.4.	An Electrode Is Like a Giant Central Ion . . . . .	774
6.1.5.	The Consequences of Compromise Arrangements: The Electrolyte Side of the Boundary Acquires a Charge . . . . .	775
6.1.6.	Both Sides of the Interface Become Electrified: The Electrical Double Layer . . . . .	775
6.1.7.	Double Layers Are Characteristic of All Phase Boundaries . . . . .	778
6.1.8.	What Knowledge Is Required before an Electrified Interface Can Be Regarded as Understood? . . . . .	778
6.1.9.	Predicting the Interphase Properties from the Bulk Properties of the Phases . . . . .	780
6.1.10.	Why Bother about Electrified Interfaces? . . . . .	780
6.2.	Experimental Techniques Used in Studying Interfaces . . . . .	782
6.2.1.	What Type of Information Is Necessary to Gain an Understanding of Interfaces? . . . . .	782
6.2.2.	The Importance of Working with Clean Surfaces (and Systems) . . . . .	782
6.2.3.	Why Use Single Crystals? . . . . .	784
6.2.4.	<i>In Situ</i> vs. <i>Ex Situ</i> Techniques . . . . .	785
6.2.5.	<i>Ex Situ</i> Techniques . . . . .	788
6.2.5.1.	Low-Energy Electron Diffraction (LEED). . . . .	788
6.2.5.2.	X-Ray Photoelectron Spectroscopy (XPS). . . . .	794

6.2.6.	<i>In Situ</i> Techniques . . . . .	797
6.2.6.1.	Infrared-Reflection Spectroscopy. . . . .	797
6.2.6.2.	Radiochemical Methods. . . . .	804
6.3.	The Potential Difference Across Electrified Interfaces . . . . .	806
6.3.1.	What Happens When One Tries to Measure the Potential Difference Across a Single Electrode/Electrolyte Interface? . . . . .	806
6.3.2.	Can One Measure Changes in the Metal–Solution Potential Difference? .	811
6.3.3.	The Extreme Cases of Ideally Nonpolarizable and Polarizable Interfaces .	813
6.3.4.	The Development of a Scale of Relative Potential Differences . . . . .	815
6.3.5.	Can One Meaningfully Analyze an Electrode–Electrolyte Potential Difference? . . . . .	817
6.3.6.	The Outer Potential $\psi$ of a Material Phase in a Vacuum . . . . .	821
6.3.7.	The Outer Potential Difference, ${}^M_S\psi$ , between the Metal and the Solution	822
6.3.8.	The Surface Potential, $\chi$ , of a Material Phase in a Vacuum . . . . .	823
6.3.9.	The Dipole Potential Difference ${}^M_S\chi$ across an Electrode–Electrolyte Interface . . . . .	824
6.3.10.	The Sum of the Potential Differences Due to Charges and Dipoles: The Inner Potential Difference, ${}^M_S\phi$ . . . . .	826
6.3.11.	The Outer, Surface, and Inner Potential Differences . . . . .	828
6.3.12.	Is the Inner Potential Difference an Absolute Potential Difference? . . . . .	829
6.3.13.	The Electrochemical Potential, the Total Work from Infinity to Bulk . . . . .	830
6.3.13.1.	Definition of Electrochemical Potential. . . . .	830
6.3.13.2.	Can the Chemical and Electrical Work Be Determined Separately? . . . . .	832
6.3.13.3.	A Criterion of Thermodynamic Equilibrium between Two Phases: Equality of Electrochemical Potentials . . . . .	833
6.3.13.4.	Nonpolarizable Interfaces and Thermodynamic Equilibrium.	834
6.3.14.	The Electron Work Function, Another Interfacial Potential . . . . .	834
6.3.15.	The Absolute Electrode Potential . . . . .	837
6.3.15.1.	Definition of Absolute Electrode Potential. . . . .	837
6.3.15.2.	Is It Possible to Measure the Absolute Potential? . . . . .	839
	Further Reading . . . . .	841
6.4.	The Accumulation and Depletion of Substances at an Interface . .	842
6.4.1.	What Would Represent Complete Structural Information on an Electrified Interface? . . . . .	842
6.4.2.	The Concept of Surface Excess . . . . .	843
6.4.3.	Is the Surface Excess Equivalent to the Amount Adsorbed? . . . . .	845
6.4.4.	Does Knowledge of the Surface Excess Contribute to Knowledge of the Distribution of Species in the Interphase Region? . . . . .	846
6.4.5.	Is the Surface Excess Measurable? . . . . .	847
6.5.	The Thermodynamics of Electrified Interfaces . . . . .	848

6.5.1.	The Measurement of Interfacial Tension as a Function of the Potential Difference across the Interface . . . . .	848
6.5.1.1.	Surface Tension between a Liquid Metal and Solution. . . . .	848
6.5.1.2.	Is It Possible to Measure Surface Tension of Solid Metal and Solution Interfaces? . . . . .	849
6.5.2.	Some Basic Facts about Electrocapillary Curves . . . . .	852
6.5.3.	Some Thermodynamic Thoughts on Electrified Interfaces . . . . .	854
6.5.4.	Interfacial Tension Varies with Applied Potential: Determination of the Charge Density on the Electrode . . . . .	858
6.5.5.	Electrode Charge Varies with Applied Potential: Determination of the Electrical Capacitance of the Interface . . . . .	859
6.5.6.	The Potential at which an Electrode Has a Zero Charge . . . . .	861
6.5.7.	Surface Tension Varies with Solution Composition: Determination of the Surface Excess . . . . .	862
6.5.8.	Summary of Electrocapillary Thermodynamics . . . . .	866
6.5.9.	Retrospect and Prospect for the Study of Electrified Interfaces . . . . .	869
	Further Reading . . . . .	870
6.6.	The Structure of Electrified Interfaces . . . . .	871
6.6.1	A Look into an Electrified Interface . . . . .	871
6.6.2.	The Parallel-Plate Condenser Model: The Helmholtz–Perrin Theory . . . . .	873
6.6.3.	The Double Layer in Trouble: Neither Perfect Parabolas nor Constant Capacities . . . . .	876
6.6.4.	The Ionic Cloud: The Gouy–Chapman Diffuse-Charge Model of the Double Layer . . . . .	876
6.6.5.	The Gouy–Chapman Model Provides a Potential Dependence of the Capacitance, but at What Cost? . . . . .	880
6.6.6.	Some Ions Stuck to the Electrode, Others Scattered in Thermal Disarray: The Stern Model . . . . .	882
6.6.7.	The Contribution of the Metal to the Double-Layer Structure . . . . .	887
6.6.8.	The Jellium Model of the Metal . . . . .	890
6.6.9.	How Important Is the Surface Potential for the Potential of the Double Layer? . . . . .	893
	Further Reading . . . . .	894
6.7.	Structure at the Interface of the Most Common Solvent: Water . . . . .	895
6.7.1.	An Electrode Is Largely Covered with Adsorbed Water Molecules . . . . .	895
6.7.2.	Metal–Water Interactions . . . . .	896
6.7.3.	One Effect of the Oriented Water Molecules in the Electrode Field: Variation of the Interfacial Dielectric Constant . . . . .	897
6.7.4.	Orientation of Water Molecules on Electrodes: The Three-State Water Model . . . . .	898
6.7.5.	How Does the Population of Water Species Vary with the Potential of the Electrode? . . . . .	900
6.7.6.	The Surface Potential, $\phi^s$ , Due to Water Dipoles . . . . .	904
6.7.7.	The Contribution of Adsorbed Water Dipoles to the Capacity of the Interface . . . . .	910

6.7.8.	Solvent Excess Entropy of the Interface: A Key to Obtaining Structural Information on Interfacial Water Molecules . . . . .	912
6.7.9.	If Not Solvent Molecules, What Factors Are Responsible for Variation in the Differential Capacity of the Electrified Interface with Potential? . . . . .	915
	Further Reading . . . . .	918
6.8.	Ionic Adsorption . . . . .	919
6.8.1.	How Close Can Hydrated Ions Come to a Hydrated Electrode? . . . . .	919
6.8.2.	What Parameters Determine if an Ion Is Able to Contact Adsorb on an Electrode? . . . . .	920
6.8.2.1.	Ion–Electrode Interactions. . . . .	920
6.8.2.2.	Solvent Interactions. . . . .	923
6.8.2.3.	Lateral Interactions. . . . .	924
6.8.3.	The Enthalpy and Entropy of Adsorption . . . . .	926
6.8.4.	Effect of the Electrical Field at the Interface on the Shape of the Adsorbed Ion . . . . .	929
6.8.5.	Equation of States in Two Dimensions . . . . .	931
6.8.6.	Isotherms of Adsorption in Electrochemical Systems . . . . .	933
6.8.7.	A Word about Standard States in Adsorption Isotherms . . . . .	936
6.8.8.	The Langmuir Isotherm: A Fundamental Isotherm . . . . .	937
6.8.9.	The Frumkin Isotherm: A Lateral Interaction Isotherm . . . . .	938
6.8.10.	The Temkin Isotherm: A Heterogeneous Surface Isotherm . . . . .	938
6.8.11.	The Flory–Huggins–Type Isotherm: A Substitutional Isotherm . . . . .	941
6.8.12.	Applicability of the Isotherms . . . . .	941
6.8.13.	An Ionic Isotherm for Heterogeneous Surfaces . . . . .	944
6.8.14.	Thermodynamic Analysis of the Adsorption Isotherm . . . . .	955
6.8.15.	Contact Adsorption: Its Influence on the Capacity of the Interface . . . . .	959
6.8.15.1.	The Constant-Capacity Region. . . . .	961
6.8.15.2.	The Capacitance Hump and the Capacity Minimum. . . . .	962
6.8.16.	Looking Back . . . . .	963
	Further Reading . . . . .	967
6.9.	The Adsorption Process of Organic Molecules . . . . .	968
6.9.1.	The Relevance of Organic Adsorption . . . . .	968
6.9.2.	Is Adsorption the Only Process that the Organic Molecules Can Undergo? . . . . .	969
6.9.3.	Identifying Organic Adsorption . . . . .	970
6.9.3.1.	Test 1: The Almost-Null Current. . . . .	970
6.9.3.2.	Test 2: The Parabolic Coverage-Potential Curve. . . . .	970
6.9.3.3.	Test 3: The Maximum of the Coverage-Potential Curve Lies Close to the pzc. . . . .	971
6.9.4.	Forces Involved in Organic Adsorption . . . . .	971
6.9.5.	The Parabolic Coverage-Potential Curve . . . . .	972
6.9.6.	Other Factors Influencing the Adsorption of Organic Molecules on Electrodes . . . . .	978
6.9.6.1.	Structure, Size, and Orientation of the Adsorbed Organic Molecules . . . . .	978

6.9.6.2.	Electrode Properties. . . . .	979
6.9.6.3.	Electrolyte Properties. . . . .	981
6.10.	The Structure of Other Interfaces . . . . .	984
6.10.1.	The Structure of the Semiconductor–Electrolyte Interface . . . . .	984
6.10.1.1.	How Is the Charge Distributed inside a Solid Electrode? . . .	984
6.10.1.2.	The Band Theory of Crystalline Solids. . . . .	985
6.10.1.3.	Conductors, Insulators, and Semiconductors. . . . .	988
6.10.1.4.	Some Analogies between Semiconductors and Electrolytic Solutions . . . . .	990
6.10.1.5.	The Diffuse-Charge Region Inside an Intrinsic Semiconductor: The Garrett–Brattain Space Charge . . . . .	992
6.10.1.6.	The Differential Capacity Due to the Space Charge. . . . .	995
6.10.1.7.	Impurity Semiconductors, <i>n-Type</i> and <i>p-Type</i> . . . . .	997
6.10.1.8.	Surface States: The Semiconductor Analogue of Contact Adsorption . . . . .	1000
6.10.2.	Colloid Chemistry . . . . .	1001
6.10.2.1.	Colloids: The Thickness of the Double Layer and the Bulk Dimensions Are of the Same Order . . . . .	1001
6.10.2.2.	The Interaction of Double Layers and the Stability of Colloids	1002
6.10.2.3.	Sols and Gels. . . . .	1005
6.11.	Double Layers Between Phases Moving Relative to Each Other . .	1006
6.11.1.	The Phenomenology of Mobile Electrified Interfaces: Electrokinetic Properties . . . . .	1006
6.11.2.	The Relative Motion of One of the Phases Constituting an Electrified Interface Produces a Streaming Current . . . . .	1008
6.11.3.	A Potential Difference Applied Parallel to an Electrified Interface Produces an Electro-osmotic Motion of One of the Phases Relative to the Other . . . . .	1011
6.11.4.	Electrophoresis: Moving Solid Particles in a Stationary Electrolyte . . .	1012
	Further Reading . . . . .	1015
	Exercises . . . . .	1015
	Problems . . . . .	1020
	Micro Research Problems . . . . .	1029
	Appendix 6.1 . . . . .	1031

## CHAPTER 7

### ELECTRODICS

7.1.	Introduction . . . . .	1035
------	------------------------	------



7.1.1.	Some Things One Has to Know About Interfacial Electron Transfer: It's Both Electrical and Chemical . . . . .	1035
7.1.2.	Uni-electrodes, Pairs of Electrodes in Cells and Devices . . . . .	1036
7.1.3.	The Three Possible Electrochemical Devices . . . . .	1036
7.1.3.1.	The Driven Cell (or Substance Producer). . . . .	1036
7.1.3.2.	The Fuel Cell (or Electricity Producer). . . . .	1039
7.1.3.3.	The Electrochemical Undevice: An Electrode that Consumes Itself while Wasting Energy . . . . .	1040
7.1.4.	Some Special Characteristics of Electrochemical Reactions . . . . .	1041
7.2.	Electron Transfer Under an Interfacial Electric Field . . . . .	1042
7.2.1.	A Two-Way Traffic Across the Interface: Equilibrium and the Exchange Current Density . . . . .	1047
7.2.2.	The Interface Out of Equilibrium . . . . .	1049
7.2.3.	A Quantitative Version of the Dependence of the Electrochemical Reaction Rate on Overpotential: The Butler–Volmer Equation . . . . .	1052
7.2.3.1.	The Low Overpotential Case. . . . .	1054
7.2.3.2.	The High Overpotential Case. . . . .	1054
7.2.4.	Polarizable and Nonpolarizable Interfaces . . . . .	1055
7.2.5.	The Equilibrium State for Charge Transfer at the Metal/Solution Interface Treated Thermodynamically . . . . .	1057
7.2.6.	The Equilibrium Condition: Kinetic Treatment . . . . .	1058
7.2.7.	The Equilibrium Condition: Nernst's Thermodynamic Treatment . . . . .	1058
7.2.8.	The Final Nernst Equation and the Question of Signs . . . . .	1062
7.2.9.	Why Is Nernst's Equation of 1904 Still Useful? . . . . .	1064
7.2.10.	Looking Back to Look Forward . . . . .	1065
	Further Reading . . . . .	1067
7.3.	A More Detailed Look at Some Quantities in the Butler–Volmer Equation . . . . .	1067
7.3.1.	Does the Structure of the Interphasial Region Influence the Electrochemical Kinetics There? . . . . .	1068
7.3.2.	What About the Theory of the Symmetry Factor, $\beta$ ? . . . .	1071
7.3.3.	The Interfacial Concentrations May Depend on Ionic Transport in the Electrolyte . . . . .	1072
	Further Reading . . . . .	1073
7.4.	Electrode Kinetics Involving the Semiconductor/solution Interface	1074
7.4.1.	Introduction . . . . .	1074
7.4.1.1.	General. . . . .	1074
7.4.1.2.	The $n$ - $p$ Junction. . . . .	1075
7.4.2.	The Current-Potential Relation at a Semiconductor/Electrolyte Interface (Negligible Surface States) . . . . .	1082
7.4.3.	Effect of Surface States on Semiconductor Electrode Kinetics . . . . .	1086
7.4.4.	The Use of $n$ - and $p$ -Semiconductors for Thermal Reactions . . . . .	1086
7.4.5.	The Limiting Current in Semiconductor Electrodes . . . . .	1088
7.4.6.	Photoactivity of Semiconductor Electrodes . . . . .	1089

Further Reading . . . . .	1090
7.5. Techniques of Electrode Kinetics . . . . .	1091
7.5.1. Preparing the Solution . . . . .	1091
7.5.2. Preparing the Electrode Surface . . . . .	1094
7.5.3. Real Area . . . . .	1095
7.5.4. Microelectrodes . . . . .	1097
7.5.4.1. The Situation. . . . .	1097
7.5.4.2. Lessening Diffusion Control by the Use of a Microelectrode . .	1098
7.5.4.3. Reducing Ohmic Errors by the Use of Microelectrodes. . . .	1099
7.5.4.4. The Downside of Using Microelectrodes. . . . .	1100
7.5.4.5. Arrays. . . . .	1100
7.5.4.6. The Far-Ranging Applications of Microelectrodes. . . . .	1102
7.5.5. Thin-Layer Cells . . . . .	1103
7.5.6. Which Electrode System Is Best? . . . . .	1103
7.5.7. The Measurement Cell . . . . .	1104
7.5.7.1. General Arrangement. . . . .	1104
7.5.7.2. More on Luggin Capillaries and Tips. . . . .	1107
7.5.7.3. Reference Electrodes. . . . .	1108
7.5.8. Keeping the Current Uniform on an Electrode . . . . .	1111
7.5.9. Apparatus Design Arising from the Needs of the Electronic Instrumentation . . . . .	1112
Further Reading . . . . .	1113
7.5.10. Measuring the Electrochemical Reaction Rate as a Function of Potential (at Constant Concentration and Temperature) . . . . .	1115
7.5.10.1. Temperature Control in Electrochemical Kinetics. . . . .	1121
7.5.11. The Dependence of Electrochemical Reaction Rates on Temperature . . . . .	1122
7.5.12. Electrochemical Reaction Rates as a Function of the System Pressure . . . . .	1123
7.5.12.1. The Equations. . . . .	1123
7.5.12.2. What Is the Point of Measuring System Pressure Effects? . .	1125
7.5.13. Impedance Spectroscopy . . . . .	1127
7.5.13.1. What Is Impedance Spectroscopy? . . . . .	1127
7.5.13.2. Real and Imaginary Impedance. . . . .	1128
7.5.13.3. The Impedance of a Capacitor in Series with a Resistor. . . .	1129
7.5.13.4. Applying ac Impedance Methods to Obtain Information on Electrode Processes . . . . .	1131
7.5.13.5. The Warburg Impedance. . . . .	1133
7.5.13.6. The Simplest "Real" Electrochemical Interface. . . . .	1133
7.5.13.7. The Impedance (or Cole–Cole) Plot. . . . .	1135
7.5.13.8. Calculating Exchange Current Densities and Rate Constants from Impedance Plots . . . . .	1136
7.5.13.9. Impedance Spectroscopy for More Complex Interfacial Situations . . . . .	1136
7.5.13.10. Cases in which Impedance Spectroscopy Becomes Limited .	1138
7.5.14. Rotating Disk Electrode . . . . .	1139

7.5.14.1.	General. . . . .	1139
7.5.14.2.	Are Rotating Disk with Ring Electrodes Still Useful in the Twenty-first Century . . . . .	1143
7.5.14.3.	Other Unusual Electrode Shapes. . . . .	1144
7.5.15.	Spectroscopic Approaches to Electrode Kinetics . . . . .	1145
7.5.15.1.	General. . . . .	1145
7.5.15.2.	FTIR Spectroscopy and Mechanisms on Electrode. . . . .	1147
7.5.16.	Ellipsometry . . . . .	1147
7.5.16.1.	What Is Ellipsometry? . . . . .	1147
7.5.16.2.	Is Ellipsometry Any Use in Electrochemistry? . . . . .	1148
7.5.16.3.	Some Understanding as to How Ellipsometry Works. . . . .	1149
7.5.16.4.	Ellipsometric Spectroscopy. . . . .	1152
7.5.16.5.	How Can Ellipsometry Be So Sensitive? . . . . .	1153
7.5.16.6.	Does Ellipsometry Have a Downside? . . . . .	1154
7.5.17.	Isotopic Effects . . . . .	1154
7.5.17.1.	Use of Isotopic Effects in the Determination of Electro-Organic Reaction Mechanisms . . . . .	1156
7.5.18.	Atomic-Scale <i>In Situ</i> Microscopy . . . . .	1157
7.5.19.	Use of Computers in Electrochemistry . . . . .	1159
7.5.19.1.	Computational. . . . .	1159
7.5.19.2.	Computer Simulation. . . . .	1160
7.5.19.3.	Use of Computer Simulation to Solve Differential Equations Pertaining to Diffusion Problems . . . . .	1161
7.5.19.4.	Use of Computers to Control Experiments: Robotization of Suitable Experiments . . . . .	1162
7.5.19.5.	Pattern Recognition Analysis . . . . .	1162
	Further Reading . . . . .	1164
7.6.	Multistep Reactions . . . . .	1166
7.6.1.	The Difference between Single-Step and Multistep Electrode Reactions . . . . .	1166
7.6.2.	Terminology in Multistep Reactions . . . . .	1167
7.6.3.	The Catalytic Pathway . . . . .	1167
7.6.4.	The Electrochemical Desorption Pathway . . . . .	1168
7.6.5.	Rate-Determining Steps in the Cathodic Hydrogen Evolution Reaction . . . . .	1168
7.6.6.	Some Ideas on Queues, or Waiting Lines . . . . .	1169
7.6.7.	The Overpotential $\eta$ Is Related to the Electron Queue at an Interface . . . . .	1171
7.6.8.	A Near-Equilibrium Relation between the Current Density and Overpotential for a Multistep Reaction . . . . .	1172
7.6.9.	The Concept of a Rate-Determining Step . . . . .	1175
7.6.10.	Rate-Determining Steps and Energy Barriers for Multistep Reactions . . . . .	1180
7.6.11.	How Many Times Must the Rate-Determining Step Take Place for the Overall Reaction to Occur Once? The Stoichiometric Number $\nu$ . . . . .	1182
7.6.12.	The Order of an Electrode Reaction . . . . .	1187
7.6.13.	Blockage of the Electrode Surface during Charge Transfer: The Surface-Coverage Factor . . . . .	1190

Further Reading . . . . .	1192
7.7. The Intermediate Radical Concentration, $\theta$ and Its Effect on Electrode Kinetics . . . . .	1193
7.7.1. Heat of Adsorption Independent of Coverage . . . . .	1193
7.7.2. Heat of Adsorption Dependent on Coverage . . . . .	1194
7.7.3. Frumkin and Temkin . . . . .	1195
7.7.4. Consequences from the Frumkin–Temkin Isotherm . . . . .	1195
7.7.5. When Should One Use the Frumkin–Temkin Isotherms in Kinetics Rather than the Simple Langmuir Approach? . . . . .	1197
7.7.6. Are the Electrode Kinetics Affected in Circumstances under which $\Delta G_\theta$ Varies with $\theta$ ? . . . . .	1197
Further Reading . . . . .	1201
7.8. The Reactivity of Crystal Planes of Differing Orientation . . . . .	1201
7.8.1. Introduction . . . . .	1201
7.8.2. Single Crystals and Planes of Specific Orientation . . . . .	1201
7.8.3. Another Preliminary: The Voltammogram as the Arbiter of a Clean Surface . . . . .	1203
7.8.4. Examples of the Different Degrees of Reactivity Caused by Exposing Different Planes of Metal Single Crystals to the Solution . . . . .	1205
7.8.5. General Assessment of Single-Crystal Work in Electrochemistry . . . . .	1209
7.8.6. Roots of the Work on Kinetics at Single-Crystal Planes . . . . .	1210
Further Reading . . . . .	1210
7.9. Transport in the Electrolyte Effects Charge Transfer at the Interface	1211
7.9.1. Ionics Looks after the Material Needs of the Interface . . . . .	1211
7.9.2. How the Transport Flux Is Linked to the Charge-Transfer Flux: The Flux-Equality Condition . . . . .	1213
7.9.3. Appropriations from the Theory of Heat Transfer . . . . .	1215
7.9.4. A Qualitative Study of How Diffusion Affects the Response of an Interface to a Constant Current . . . . .	1216
7.9.5. A Quantitative Treatment of How Diffusion to an Electrode Affects the Response with Time of an Interface to a Constant Current . . . . .	1218
7.9.6. The Concept of Transition Time . . . . .	1221
7.9.7. Convection Can Maintain Steady Interfacial Concentrations . . . . .	1225
7.9.8. The Origin of Concentration Overpotential . . . . .	1230
7.9.9. The Diffusion Layer . . . . .	1232
7.9.10. The Limiting Current Density and Its Practical Importance . . . . .	1235
7.9.10.1. Polarography: The Dropping-Mercury Electrode. . . . .	1237
7.9.11. The Steady-State Current–Potential Relation under Conditions of Transport Control . . . . .	1246
7.9.12. The Diffusion-Activation Equation . . . . .	1247
7.9.13. The Concentration of Charge Carriers at the Electrode . . . . .	1247
7.9.14. Current as a Function of Overpotential: Interfacial and Diffusion Control . . . . .	1248
7.9.15. The Reciprocal Relation . . . . .	1250

7.9.16.	Reversible and Irreversible Reactions . . . . .	1251
7.9.17.	Transport-Controlled Deelectronation Reactions . . . . .	1252
7.9.18.	What Is the Effect of Electrical Migration on the Limiting Diffusion Current Density? . . . . .	1253
7.9.19.	Some Summarizing Remarks on the Transport Aspects of Electrode Further Reading . . . . .	1254 1256
7.10.	How to Determine the Stepwise Mechanisms of Electrode Reactions . . . . .	1257
7.10.1.	Why Bother about Determining a Mechanism? . . . . .	1257
7.10.2.	What Does It Mean: "To Determine the Mechanism of an Electrode Reaction"? . . . . .	1258
7.10.2.1.	The Overall Reaction. . . . .	1258
7.10.2.2.	The Pathway. . . . .	1259
7.10.2.3.	The Rate-Determining Step. . . . .	1260
7.10.3.	The Mechanism of Reduction of $O_2$ on Iron at Intermediate pH's . . . .	1263
7.10.4.	Mechanism of the Oxidation of Methanol . . . . .	1269
	Further Reading . . . . .	1273
7.10.5.	The Importance of the Steady State in Electrode Kinetics . . . . .	1274
7.11.	Electrocatalysis . . . . .	1275
7.11.1.	Introduction . . . . .	1275
7.11.2.	At What Potential Should the Relative Power of Electrocatalysts Be Compared? . . . . .	1277
7.11.3.	How Electrocatalysis Works . . . . .	1280
7.11.4.	Volcanoes . . . . .	1284
7.11.5.	Is Platinum the Best Catalyst? . . . . .	1286
7.11.6.	Bioelectrocatalysis . . . . .	1287
7.11.6.1.	Enzymes. . . . .	1287
7.11.6.2.	Immobilization. . . . .	1289
7.11.6.3.	Is the Heme Group in Most Enzymes Too Far Away from the Metal for Enzymes to Be Active in Electrodes? . . .	1289
7.11.6.4.	Practical Applications of Enzymes on Electrodes. . . . .	1291
	Further Reading . . . . .	1292
7.12.	The Electrodeposition of Metals on Electrodes . . . . .	1293
7.12.1.	The Two Aspects of Electrodeposition . . . . .	1293
7.12.2.	The Reaction Pathway for Electrodeposition . . . . .	1294
7.12.3.	Stepwise Dehydration of an Ion; the Surface Diffusion of Adions . . . . .	1296
7.12.4.	The Half-Crystal Position . . . . .	1301
7.12.5.	Deposition on an Ideal Surface: The Resulting Nucleation . . . . .	1302
7.12.6.	Values of the Minimum Nucleus Size Necessary for Continued Growth . . . . .	1305
7.12.7.	Rate of an Electrochemical Reaction Dependent on 2D Nucleation . . . . .	1306
7.12.8.	Surface Diffusion to Growth Sites . . . . .	1307

7.12.9.	Residence Time . . . . .	1310
7.12.10.	The Random Thermal Displacement . . . . .	1312
7.12.11.	Underpotential Deposition . . . . .	1313
7.12.11.1.	Introduction. . . . .	1313
7.12.11.2.	Some Examples. . . . .	1313
7.12.11.3.	What Are the Causes of Underpotential Deposition? . . . . .	1315
7.12.12.	Some Devices for Building Lattices from Adions: Screw Dislocations and Spiral Growths . . . . .	1316
7.12.13.	Microsteps and Macrosteps . . . . .	1324
7.12.14.	How Steps from a Pair of Screw Dislocations Interact . . . . .	1327
7.12.15.	Crystal Facets Form . . . . .	1328
7.12.16.	Pyramids . . . . .	1334
7.12.17.	Deposition on Single-Crystal and Polycrystalline Substrates . . . . .	1334
7.12.18.	How the Diffusion of Ions in Solution May Affect Electrogrowth . . . . .	1335
7.12.19.	About the Variety of Shapes Formed in Electrodeposition . . . . .	1336
7.12.20.	Dendrites . . . . .	1338
7.12.21.	Organic Additives and Electrodeposits . . . . .	1339
7.12.22.	Material Failures Due to H Co-deposition . . . . .	1340
7.12.23.	Would Deposition from Nonaqueous Solutions Solve the Problems Associated with H Co-deposition? . . . . .	1341
7.12.24.	Breakdown Potentials for Certain Organic Solvents . . . . .	1341
7.12.25.	Molten Salt Systems Avoid Hydrogen Codeposition . . . . .	1344
7.12.25.1.	“Nonaqueous.” . . . .	1344
7.12.25.2.	Advantages of Molten Salts as Solvents for Electrodeposition . . . . .	1344
7.12.26.	Photostimulated Electrodeposition of Metals on Semiconductors . . . . .	1345
7.12.27.	Surface Preparation: The Established Superiority of Electrochemical Techniques . . . . .	1345
7.12.28.	Electrochemical Nanotechnology . . . . .	1345
7.13.	Current–Potential Laws For Electrochemical Systems . . . . .	1348
7.13.1.	The Potential Difference across an Electrochemical System . . . . .	1348
7.13.2.	The Equilibrium Potential Difference across an Electrochemical Cell . . . . .	1350
7.13.3.	The Problem with Tables of Standard Electrode Potentials . . . . .	1351
7.13.4.	Are Equilibrium Cell Potential Differences Useful? . . . . .	1356
7.13.5.	Electrochemical Cells: A Qualitative Discussion of the Variation of Cell Potential with Current . . . . .	1361
7.13.6.	Electrochemical Cells in Action: Some Quantitative Relations between Cell Current and Cell Potential . . . . .	1364
7.14.	The Electrochemical Activation of Chemical Reactions . . . . .	1371
	Further Reading . . . . .	1374
7.15.	Electrochemical Reactions That Occur without Input of Electrical Energy . . . . .	1374
7.15.1.	Introduction . . . . .	1374

7.15.2.	Electroless Metal Deposition . . . . .	1374
7.15.3.	Heterogeneous “Chemical” Reactions in Solutions . . . . .	1376
7.15.4.	Electrogenerative Synthesis . . . . .	1377
7.15.5.	Magnetic Induction . . . . .	1378
	Further Reading . . . . .	1379
7.16.	The Electrochemical Heart . . . . .	1380
	Further Reading . . . . .	1382

## CHAPTER 8

### TRANSIENTS

8.1.	Introduction . . . . .	1401
8.1.1.	The Evolution of Short Time Measurements . . . . .	1401
8.1.2.	Another Reason for Making Transient Measurements . . . . .	1403
8.1.3.	Is there a Downside for Transients? . . . . .	1407
8.1.4.	General Comment on Factors in Achieving Successful Transient Measurements . . . . .	1407
8.2.	Galvanostatic Transients . . . . .	1409
8.2.1.	How They Work . . . . .	1409
8.2.2.	Chronopotentiometry . . . . .	1411
8.3.	Open-Circuit Decay Method . . . . .	1412
8.3.1.	The Mathematics . . . . .	1412
8.4.	Potentiostatic Transients . . . . .	1414
8.4.1.	The Method . . . . .	1414
8.5.	Other Matters Concerning Transients . . . . .	1416
8.5.1.	Reversal Techniques . . . . .	1416
8.5.2.	Summary of Transient Methods . . . . .	1417
8.5.3.	“Totally Irreversible,” etc.: Some Aspects of Terminology . . . . .	1418
8.5.4.	The Importance of Transient Techniques . . . . .	1420
8.6.	Cyclic Voltammetry . . . . .	1422
8.6.1.	Introduction . . . . .	1422
8.6.2.	Beginning of Cyclic Voltammetry . . . . .	1424
8.6.3.	The Range of the Cyclic Voltammetric Technique . . . . .	1425
8.6.4.	Cyclic Voltammetry: Its Limitations . . . . .	1426
8.6.5.	The Acceptable Sweep Rate Range . . . . .	1427
	8.6.5.1. What Would Make a Sweep Rate Too Fast? . . . . .	1427
	8.6.5.2. What Would Make a Sweep Rate Too Slow? . . . . .	1427
8.6.6.	The Shape of the Peaks in Potential-Sweep Curves . . . . .	1428
8.6.7.	Quantitative Calculation of Kinetic Parameters from Potential-Sweep Curves . . . . .	1431

8.6.8.	Some Examples . . . . .	1432
8.6.9.	The Role of Nonaqueous Solutions in Cyclic Voltammetry . . . . .	1434
8.6.10.	Two Difficulties in Cyclic Voltammetric Measurements . . . . .	1434
8.6.11.	How Should Cyclic Voltammetry Be Regarded? . . . . .	1438
8.7.	Linear Sweep Voltammetry for Reactions that Include Simple Adsorbed Intermediates . . . . .	1438
8.7.1.	Potentiodynamic Relations that Account for the Role of Adsorbed Intermediates . . . . .	1438
	Further Reading . . . . .	1442

## CHAPTER 9

### SOME QUANTUM-ORIENTED ELECTROCHEMISTRY

9.1.	Setting the Scene . . . . .	1455
9.1.1.	A Preliminary Discussion: Absolute or Vacuum-Scale Potentials . . . . .	1457
9.2.	Chemical Potentials and Energy States of “Electrons in Solution” . . . . .	1458
9.2.1.	The “Fermi Energy” of Electrons in Solution . . . . .	1458
9.2.2.	The Electrochemical Potential of Electrons in Solution and Their Quantal Energy States . . . . .	1461
9.2.3.	The Importance of Distribution Laws . . . . .	1462
9.2.4.	Distribution of Energy States in Solution: Introduction . . . . .	1463
	9.2.4.1. The Gaussian Distribution Law. . . . .	1464
	9.2.4.2. The Boltzmannian Distribution. . . . .	1467
9.2.5.	The Distribution Function for Electrons in Metals . . . . .	1469
9.2.6.	The Density of States in Metals . . . . .	1471
	Further Reading . . . . .	1472
9.3	Potential Energy Surfaces and Electrode Kinetics . . . . .	1473
9.3.1.	Introduction . . . . .	1473
9.3.2.	The Basic Potential Energy Diagram . . . . .	1475
9.3.3.	Electrode Potential and the Potential Energy Curves . . . . .	1479
	9.3.3.1. A Simple Picture of the Symmetry Factor. . . . .	1479
	9.3.3.2. Is the $\beta$ in the Butler–Volmer Equation Independent of Over-potential? . . . . .	1484
9.3.4.	How Bonding of Surface Radicals to the Electrode Produces Electrocatalysis . . . . .	1484
9.3.5.	Harmonic and Anharmonic Curves . . . . .	1487
9.3.6.	How Many Dimensions? . . . . .	1488
9.4.	Tunneling . . . . .	1489
9.4.1.	The Idea . . . . .	1489
9.4.2.	Equations of Tunneling . . . . .	1490
9.4.3.	The WKB Approximation . . . . .	1492



9.4.4.	The Need for Receiver States . . . . .	1494
9.4.5.	Other Approaches to Quantum Transitions and Some Problems . . . . .	1494
9.4.6.	Tunneling through Adsorbed Layers at Electrodes and in Biological Systems . . . . .	1495
9.5.	Some Alternative Concepts and Their Terminology . . . . .	1496
9.5.1.	Introduction . . . . .	1496
9.5.2.	Outer Shell and Inner Shell Reactions . . . . .	1496
9.5.3.	Electron-Transfer and Ion-Transfer Reactions . . . . .	1497
9.5.4.	Adiabatic and Nonadiabatic Electrode Reactions . . . . .	1497
9.6.	A Quantum Mechanical Description of Electron Transfer . . . . .	1499
9.6.1.	Electron Transfer . . . . .	1499
9.6.2.	The Frank–Condon Principle in Electron Transfer . . . . .	1504
9.6.3.	What Happens if the Movements of the Solvent–Ion Bonds Are Taken as a Simple Harmonic? An Aberrant Expression for Free Energy Activation in Electron Transfer . . . . .	1504
9.6.4.	The Primacy of Tafel’s Law in Experimental Electrode Kinetics . . . . .	1507
9.7.	Four Models of Activation. . . . .	1511
9.7.1.	Origin of the Energy of Activation . . . . .	1511
9.7.2.	Weiss–Marcus: Electrostatic . . . . .	1512
9.7.3.	George and Griffith’s Thermal Model . . . . .	1514
9.7.4.	Fluctuations of the Ground State Model . . . . .	1515
9.7.5.	The Librator Fluctuation Model . . . . .	1516
9.7.6.	The Vibron Model . . . . .	1517
9.8.	Bond-Breaking Reactions . . . . .	1518
9.8.1.	Introduction . . . . .	1518
9.9.	A Quantum Mechanical Formulation of the Electrochemical Current Density . . . . .	1521
9.9.1.	Equations . . . . .	1521
9.10.	A Retrospect and Prospect For Quantum Electrochemistry . . . . .	1522
9.10.1.	Discussion . . . . .	1522
	Further Readings . . . . .	1523
Appendix.	The Symmetry Factor: Do We Understand It? . . . . .	1526
	A.1. Introduction: Gurney–Butler . . . . .	1526
	A.2. Activationless and Barrierless . . . . .	1528
	A.3. The Dark Side of $\beta$ . . . . .	1528
Index	. . . . .	xxix

## CHAPTER 6

# THE ELECTRIFIED INTERFACE

### 6.1. ELECTRIFICATION OF AN INTERFACE

#### 6.1.1. The Electrode/Electrolyte Interface: The Basis of Electrodeics

The situation inside an electrolyte—the *ionic* aspect of electrochemistry—has been considered in the first volume of this text. The basic phenomena involve—ion–solvent interactions (Chapter 2), ion–ion interactions (Chapter 3), and the random walk of ions, which becomes a drift in a preferred direction under the influence of a concentration or a potential gradient (Chapter 4). In what way is the situation at the electrode/electrolyte interface any different from that in the bulk of the electrolyte? To answer this question, one must treat quiescent (equilibrium) and active (nonequilibrium) interfaces, the structural and electrical characteristics of the interface, the rates and mechanism of changeover from ionic to electronic conduction, etc. In short, one is led into *electrodeics*, the newest and most exciting part of electrochemistry.

#### 6.1.2. New Forces at the Boundary of an Electrolyte

It has been stressed that as long as no irreversible transport processes occur, every particle (ion or solvent molecule) in the bulk of an electrolyte looks out upon a spherically symmetrical world. On a time average, the ions and water molecules (in aqueous solutions) experience forces that are independent of direction and position in the electrolyte.

Thus, if each water dipole is represented by a vector, the vectors are completely randomized in direction<sup>1</sup> (Fig. 6.1). There is no *net* resultant vector, i.e., there is no alignment of the solvent dipoles in any preferred direction. Further, the positive and

---

<sup>1</sup>In fact, the structure of the solvent water is a little more complicated (see Chapter 2).

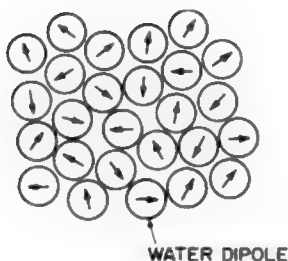


**Fig. 6.1.** A schematic representation of the random orientation of water dipoles in the interior of the electrolyte (the network structure of water is ignored in the diagram).

negative ions are equally distributed<sup>2</sup> in any given volume of electrolyte. Electroneutrality must prevail. Consider any lamina of electrolyte parallel to a planar electrode (Fig. 6.2). As long as the lamina is in the bulk of the electrolyte, the net charge on the lamina will be zero. Since the charges on any two parallel laminae are equal to zero, there will be no potential gradient inside the electrolyte under equilibrium conditions.

To summarize: Under equilibrium conditions, the time-average forces are the same in all directions and at all points in the bulk of the electrolyte (perfect isotropy and homogeneity), and there are no net preferentially directed electrical fields.

Every electrolyte, however, is bounded. It must ultimately contact some other material, e.g., the gas phase above the electrolyte or the metallic electrode or, for that matter, the walls of the container. The frontier is reached. What happens at such a phase boundary?

It will be shown further on that the phases on either side of the boundary become charged to an equal and opposite extent and this gives rise to a potential difference across the boundary. There are several ways in which this potential difference can arise. If one of the phases is an electronic conductor and the other is an ionic conductor, electron-transfer reactions can occur at the boundary and lead to the development of a potential difference. A discussion of this type of mechanism will be reserved for Section 7.5. Or, the electronic conductor can be deliberately charged by a flow of electrons from an external source of electricity. The electrolyte side of the boundary then responds with an equal and opposite charge, and a potential difference develops across the boundary. However, even without an external connection or the occurrence

<sup>2</sup>One is talking here of volumes that are large compared with the dimension  $\kappa^{-1}$  of the ionic cloud of Chapter 3.

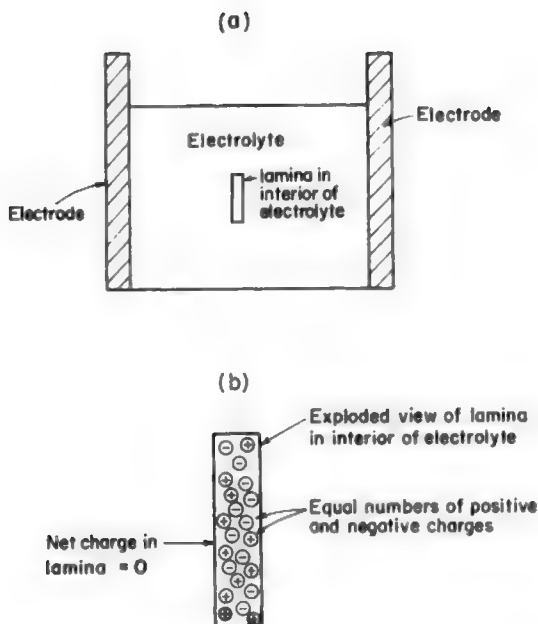


**Fig. 6.2.** A schematic representation of electroneutrality in the interior of an electrolyte. (a) A lamina in the bulk of the electrolyte. (b) An exploded view of the lamina showing that it contains an equal amount of positive and negative charge and therefore has a zero net charge.

of electron-transfer reactions, it is possible for a potential difference to develop across a phase boundary. How this comes about will now be described.

The electrolyte is terminated at the phase boundary by the presence of an alien material. One would expect, therefore, that the characteristics of the electrolyte (i.e., its properties) are also physically interrupted at the frontier. Now, the essential characteristics of the bulk of the electrolyte are homogeneity and isotropy. Are these uniform properties perturbed by the presence of the phase boundary?

Consider an ion near enough<sup>3</sup> the electrode to feel its influence. (Particles sense each other through the forces they exert on each other.) This ion sees its world as quite different from that of an ion in the bulk of the electrolyte. Things are not the same in all directions. When it looks toward the bulk of the electrolyte, it feels electrolyte forces, but when it looks across the frontier (the phase boundary), it feels new forces that it never experienced as long as it was content to stay deep inside the homogeneous electrolyte.

<sup>3</sup>The phrase "near enough" will be quantified later.

The forces operating on particles near the phase boundary are therefore *anisotropic*. They are different in a direction toward the boundary compared with the direction toward the electrolyte bulk. Further, the forces due to the phase (e.g., the electrode) on the other side of the phase boundary (e.g., the electrode-electrolyte boundary) should vary with distance from the boundary; the deeper the ion recedes into the bulk, the less the frontier influence is felt and the more things become normal again.

### 6.1.3. The Interphase Region Has New Properties and New Structures

The properties of any material are dependent on the particles present and the forces operating on the particles. Since these forces are different at the frontier than the forces in the bulk, the properties of the frontier region, the *interphase* region, will differ from the bulk properties. Thus, the uniform properties of the electrolyte are perturbed in the interphase region by the presence of another phase.

The arrangement of particles, however, depends on the forces operating on them. Since new forces exist near the phase boundary, new structures would tend to exist. The arrangement of particles in the interphase region is a compromise between the structures demanded by both phases. Thus, the electrode, e.g., would like the ions and water molecules of an electrolytic solution to assume a certain time-average arrangement. The solution, on the other hand, demands another arrangement. The ions and other particles, caught between contradictory demands, adopt compromise positions that are characteristic of the interphase region.

### 6.1.4. An Electrode Is Like a Giant Central Ion

An analogy between the situation just described and those involved in ion-solvent and ion-ion interactions can be drawn. The solvent water, for example, normally has a particular structure, the water network. Near an ion, however, the water dipoles are under the conflicting influences of the water network and the charged central ion. They adopt compromise positions that correspond to primary and secondary solvation (Chapter 2). Similarly, in an electrolytic solution, the presence of the central ion makes the surrounding ions redistribute themselves—an ionic cloud is formed (see Chapter 3).

Just as the central ion can perturb and cause a rearrangement of the surrounding solvent molecules and ions, the electrode itself can cause the surrounding particles to assume abnormal, compromise positions (relative to the bulk of the electrolyte). It will be seen later that an electrode also can get enveloped by a solvent sheath and an ionic cloud. There are, however, many other interesting phenomena arising from the fact that one can connect an external potential source (e.g., a battery) to the electrode by a metallic wire and thus control the electrode charge. New possibilities emerge that do not exist in the case of the central ion.

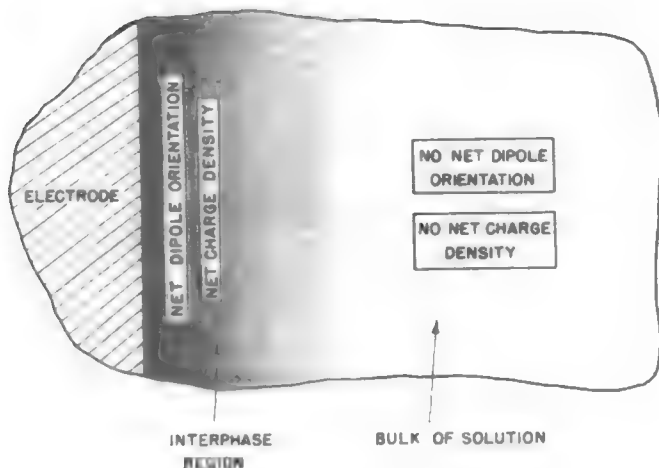


**Fig. 6.3.** A schematic diagram to illustrate that in the interphase region (indicated by shading) there generally is net dipole orientation and net, or excess, charge density.

### 6.1.5. The Consequences of Compromise Arrangements: The Electrolyte Side of the Boundary Acquires a Charge

The new forces operating at the electrode/electrolyte interface give rise to new arrangements of solvent dipoles and charged species. At the same time, they incite the particles of the electrolyte to be governed no longer by the characteristics of the situation inside the electrolyte, i.e., random orientation of dipoles and equal distribution of positive and negative charges in any macroscopic lamina of the electrolyte. These two laws are not applicable in the interphase region (Fig. 6.3). Thus, there can be (and generally is) a net orientation of the solvent dipoles and a net or excess charge on a lamina parallel to the planar electrode surface (because of unequal numbers of positive and negative charges present there).

All this means that electroneutrality has broken down on the electrolyte side of the phase boundary. The electrolyte side of the frontier has become charged or electrified (Fig. 6.4). How does this electrification affect the phase (e.g., the electrode) on the other side of the phase boundary?<sup>4</sup>

### 6.1.6. Both Sides of the Interface Become Electrified: The Electrical Double Layer

Once the electrolyte side of the phase boundary acquires a net, or excess charge, an electric force, or field, operates across the boundary. All charged particles feel this

<sup>4</sup>One is discussing here a situation in which the electrode is *not* deliberately charged by connecting it to an external source of electricity and in which electron-transfer reactions do *not* occur at the interface.

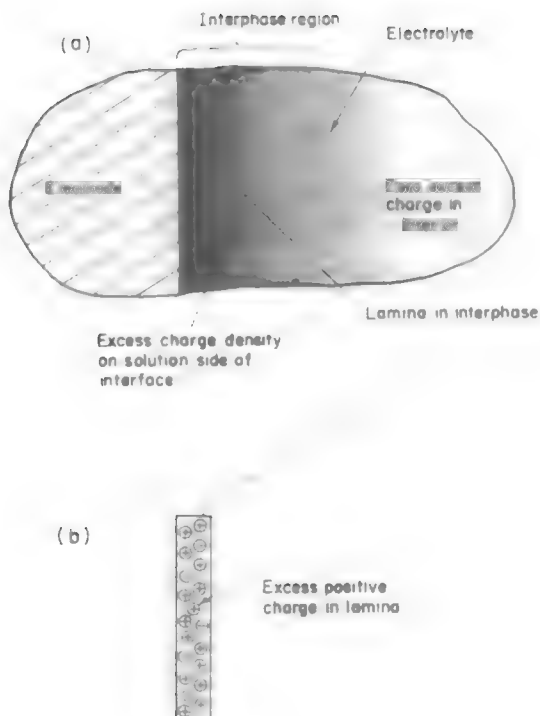


**Fig. 6.4.** A schematic representation of the charging of the solution side of an interface. (a) Shading indicates excess-charge density in the interphase region. (b) An exploded view shows that the positive charge in a lamina in the interphase exceeds the negative charge and there is a net, or excess, positive-charge density in the lamina.

field. But the other phase (e.g., the electrode) consists of charged particles. Hence, the charges of the second phase respond to the stimulus of the field arising from the charging of the electrolyte side of the boundary. The nature of their response depends on whether the nonelectrolyte phase is a conductor, a semiconductor, or an insulator. In any case, there *is* a response.

Consider that the other phase is a metallic conductor, i.e., an electrode. It consists of a three-dimensional, periodic network of positive ions and a communal pool of mobile electrons. The positive ions of the metallic lattice feel the field that is due to the excess charge at the boundary of the electrolyte, but they can move only with great difficulty.<sup>5</sup>

<sup>5</sup>Recall the treatment (Chapter 5) of hole formation and jumping in liquid electrolytes; the energies involved in solids are at least an order of magnitude greater than those in liquids.

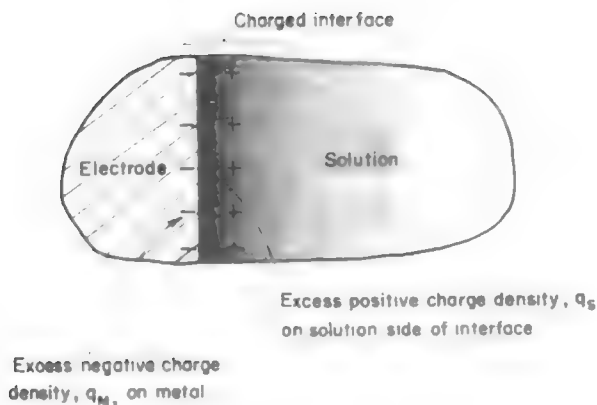


**Fig. 6.5.** The electrified interface. The excess-charge density  $q_s$  on the solution side of the interface is equal and opposite to that on the metal  $q_M$ .

In contrast to these clumsy, cumbersome ionic movements in a metal, the free electrons move with agility in response to the field produced by the charging of the electrolyte side of the frontier. The electrons move either toward or away from the boundary, depending on the direction of the field. Thus, a charge is induced on the metal. This induced charge is equal and opposite to that on the electrolyte side of the phase boundary (Fig. 6.5).

What has happened as a result of this induced charge? Separation of charge has occurred across the electrode/electrolyte interface, a net charge of one sign on the electrode side of the interface and a net charge of another sign on the electrolyte side. Note, however, that the interphase region as a whole (not any one side, but the two sides taken together) is electrically neutral.

When charges are separated, a potential difference develops across the interface. The electrical forces that operate between the metal and the solution constitute the electrical field across the electrode/electrolyte phase boundary. It will be seen that although the potential differences across the interface are not large ( $\sim 1$  V), the dimensions of the interphase region are very small ( $\sim 0.1$ ) and thus the field strength (gradient of potential) is enormous—it is on the order of  $10^7 \text{ V cm}^{-1}$ . *The effect of this enormous field at the electrode/electrolyte interface is, in a sense, the essence of electrochemistry.*

The term “electrical double layer,” or just “double layer,” is used to describe the arrangement of charges and oriented dipoles constituting the interphase region at the boundary of an electrolyte. The terms are a legacy from an early stage in understanding, when the interphase was pictured as always consisting of only two layers, or sheets, of charge,<sup>6</sup> one positive and the other negative. It is now known that the situation is

<sup>6</sup>It will be shown later that under some circumstances the electrified interface is indeed a double layer, and the term “double layer” is justified.



more complex. Nevertheless, the term “double layer” is still used, not in a literal sense, but loosely, as a near-synonym for electrified interface.

### 6.1.7. Double Layers Are Characteristic of All Phase Boundaries

The argument for the formation of the double layer has proceeded simply. The existence of a boundary for the electrolyte necessarily implies a basic anisotropy in the forces operating on the particles in the interphase region. Owing to this anisotropy, there occurs a redistribution of the mobile charges and orientable dipoles (compared with their distribution in the bulk of the phases). This redistribution is the structural basis of the potential difference across the interface.

The argument is so general that its particularization for the metal/electrolyte interface was only for convenience. One could have carried out the discussion with equal validity for the gas/electrolyte or the glass (container)/electrolyte boundary of the electrolyte. Of course, one would have had to note the difference between the particles that constitute gases and glass and those that compose a metal. In all these systems, the conclusion would be reached that forces are direction dependent at the phase boundary and therefore new and compromise arrangements are assumed by the particles (of the two phases) in the phase boundary. If the particles are charged or are dipoles, not only is there a redistribution of particles but also an electrification of the interface and the development of a potential difference across it.

Double layers, therefore, are *not a* special feature of the electrode/electrolyte interfaces; they are a general consequence of the meeting of two phases at a boundary. Across almost any junction between two phases (i.e., between two materials) a potential difference will develop. If the materials contain mobile free charges (electrons or ions), the potential difference arises from the electrification of the two sides of the boundary by the mechanism described above (see Section 6.1.6.) by the occurrence of charge-transfer reactions, or by connecting up the electronically conducting phase to an external source of electricity and charging it. Even if the materials consist, not of free charges, but of permanent dipoles or of molecules in which dipoles can be induced, a potential difference across the boundary can arise from a net orientation of the dipoles constituting it. Some examples of double layers are shown in Fig. 6.6.

### 6.1.8. What Knowledge Is Required before an Electrified Interface Can Be Regarded as Understood?

The double layer formed at a boundary between two phases containing charged entities has two fundamental aspects, the electrical aspect and the structural aspect. The electrical aspect concerns the magnitude of the excess-charge densities on each phase. (Recall that the total excess charge on one phase is always equal in magnitude to the total excess charge on the other phase.) It also concerns the variation of potential with distance from the interface. The structural aspect is a matter of knowing how the

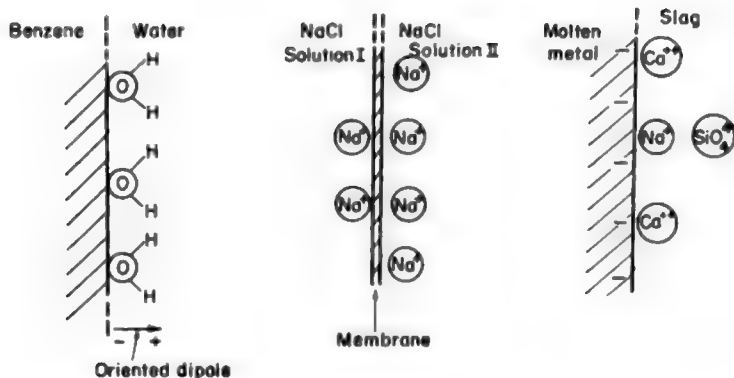


**Fig. 6.6.** Some examples of electrified interfaces.

particles of the two phases (ions, electrons, dipoles, neutral molecules) are arranged in the interphase region so as to electrify the interface. The electrical and structural aspects of the double layer are intimately related. The charge or potential difference is characteristic of the particular structure, and vice versa.

The formation of an electrified interface has been described in the following steps:

Redistribution of electrolyte particles → Charging of electrolyte side of interface → Induction of charge on metal side of interface → Charge separation → Development of interfacial potential difference

In systems in which one of the phases (e.g., a metal electrode) can be connected to an external source of charge, the formation of an electrified interface can be conceived in the following way:

Charge flows from outside source into one phase (e.g., metal) → Charging of one phase → Redistribution of electrolyte particles in the interface → Development of net charge on electrolyte side of interface → Charge separation across interface → Development of potential difference across interface

In fact, these processes occur almost simultaneously.

There is a functional relationship between the charge on each phase (or the potential difference across the interface) and the structure of the interphase region. The fundamental problem of double-layer studies is to unravel this functional relationship. One has understood a particular electrified interface if, on the basis of a model (i.e., an assumed type of arrangement of the particles in the interphase), one can predict the distribution of charge (or variation of potential) across the interphase.

### 6.1.9. Predicting the Interphase Properties from the Bulk Properties of the Phases

A deeper level of understanding is gained if the double-layer structure can be predicted on the basis of the properties of the bulk phases. Double layers are formed because in the interphase region particles are not distributed in the same way as in the bulk. For example, perhaps more positive ions than negative ions exist in a lamina in the interphase region. If, however, a lamina in the bulk were considered, the numbers of positive and negative ions would be equal. Evidently there is a depletion of negative ions or an accumulation of positive ions, or both, relative to the bulk. This phenomenon of substances collecting in or departing from a phase boundary is known as *adsorption*.

Why do particles tend to accumulate at or leave an interface? A phenomenological answer is in terms of the free-energy change associated with the adsorption process. If one knew these free energies of adsorption, one could state: Given these bulk compositions, this will be the composition of the interface and these will be the properties of the interface.

But why determine the free energies of adsorption from experiment? Instead, one can attempt to calculate the values from a knowledge of the particles, the forces between them, and the effect on the particles of the electric field operating on the electrified interface.

These, then, are some of the ultimate goals of double-layer research. They may be summarized thus: From a knowledge of the bulk phases, to determine the structure of the electrified interface and finally the potential variation across the interphase region.

### 6.1.10. Why Bother about Electrified Interfaces?

Why is the spatial distribution of charges in the interphase region between two phases of interest and importance? There is, of course, the philosophical reason stemming from the search for understanding and for a coherent picture of natural phenomena. Surfaces are found almost everywhere in nature, and many of them carry a charge. A substantial part of the understanding of nature is dependent upon a satisfactory model of charged interfaces.

However, there are also the reasons that arise from utilitarian needs that often inspire scientific quests. Thus, electrified interfaces are of vital importance in many aspects of everyday life. This fact can be demonstrated in many ways.

Consider, for example, colloidal particles, i.e., particles that are too small to display the properties of macroscopic objects, say,  $<0.01$  mm, and too large to behave like atoms and small molecules, approximately  $>10,000$  pm. These colloidal particles move under electric fields, and if they are pigments, electric fields can be used to “guide” the colloidal particles to deposit upon metals and color them. The hues formed in this way may be more permanent than paint. But why do the particles move? The

answer lies in the electrified interface between a colloid and the medium. In other words, the charge separation and the resulting potential difference at the particle's interface provide a handle with which the externally applied electrical field can guide the particle along. Thus, an understanding of double layers at the surface of colloidal particles is a basis for technological improvements in the coatings of metals.

A rather unusual example of the ubiquitous role of electrified interfaces is based on the friction between two solids which, in the presence of liquid films, may depend on the double layers at their interfaces. Thus, the efficiency of a wetted rock drill depends on the double-layer structure at the metal/drill/aqueous solution interface.

Electrode reactions that underlie the processes of metal deposition, etc., cannot be understood without knowing the potential difference at the electrode/solution interface and how it varies with distance from the electrode. The ions from the solution must be electrically energized to cross the interphase region and deposit on the metal. This electrical energy must be picked up from the field at the interface, which itself depends upon the double-layer structure. Thus, control over metal deposition processes can be improved by an increased understanding of double layers at metal/solution interfaces.

An electrodic process of vast practical significance is that resulting in the dissolution of a metal into solution or into a film of conducting moisture adhering to the metal surface. This process is corrosion. Processes connected with corrosion may lead to the breaking off of an aircraft's wing. Many things corrode slightly; it is the corrosion *rate* that determines the significance of the corrosion. This depends partly on the structure of the double layer (i.e., on the electric field across the interface), which in turn governs the rate of metal dissolution. Thus, double layers influence the stability of metal surfaces and hence the strength of metals. Nor must it be thought that these remarks apply only to metals in contact with a visible solution. They apply to all substances that corrode—for this always occurs by electrodic reactions across surfaces, even if the solution phase is a moist film only a few microns thick.

Molecular mechanisms in biology, too, depend to a great extent on electrified interfaces. Thus, the mechanism by which nerves carry messages from brain to muscles is based on the potential difference across the membrane that separates a nerve cell from the environment. What are the laws that apply to this electrified interface? If this question is answered, then the mechanism by which nerves transmit messages may be determined at the molecular level and the process concerned may become controllable.

These are only a few examples cited to stress the wide range of phenomena in which electrified interfaces play an important part. The number of such examples could be multiplied many times. They all emphasize the crucial role of double-layer studies as a basis for understanding at a molecular level many very practical happenings. Understanding the electrified interface is one of the most exciting aspects of electrochemistry.

## 6.2. EXPERIMENTAL TECHNIQUES USED IN STUDYING INTERFACES

### 6.2.1. What Type of Information Is Necessary to Gain an Understanding of Interfaces?

The previous section discussed the structure at the junction of two phases, the one a solid electron conductor, the other an ionic solution. Why is this important? Knowledge of the structure of the interface, the distribution of particles in this region, and the variation of the electric potential in the double layer, permits one to control reactions occurring in this region. Control of these reactions is important because they are the foundation stones of important mechanisms linked to the understanding of industrial processes and problems, such as deposition and dissolution of metals, corrosion, electrocatalysis, film formation, and electro-organic synthesis.

In the past decade, many new techniques have been developed and applied to the study of interfaces. While earlier measurements involved only macroscopic characteristics of the interface (e.g., surface charge, surface tension, and overall potential drop), new spectroscopic techniques have opened a window to the microstructure of the interface, and insight at the atomic level in this important region is now possible. Parallel to these discoveries and supported by them, more realistic theoretical models of the interface have been developed that combine quantum mechanical theories of metal surfaces and the statistical mechanics of solutions.

### 6.2.2. The Importance of Working with Clean Surfaces (and Systems)

It seems obvious to stress that the experimental setup of any experiment should start with a clean system. However, how clean is clean enough to study the interfacial region? What has to be cleaned? How does one clean the system and keep it clean?<sup>7</sup> To answer these questions, the experimenter starts by asking a defining question: What are the components of the system being studied? These are mainly the electrode and the electrolyte, since these compose the region of interest to the electrochemist.<sup>8</sup> However, one should not forget the electrochemical cell—the container in which the system studied is enclosed, and of course, the chemicals added to the systems (including any solids, liquids or gases). All these components should be cleaned and/or purified to ensure a successful experiment.

How clean a system should be depends greatly on the type of electrode the researcher is working with, as well as the type of experiment. The introduction of single crystals in electrochemistry, as well as the use of techniques involving a high

---

<sup>7</sup>The first researcher to discuss the importance of having a clean system was Frumkin, back in the 1930s. After that, Bockris and Conway stressed it in the 1950s and Schuldiner in the 1960s. Today research papers on surface electrochemistry routinely record the preparation methods for surfaces and solutions. The degree to which trace impurities are removed from solutions depends up whether electrocatalysis is an important aspect of the process and how long the electrode is in contact with the solution.

<sup>8</sup> With the exception of liquid/liquid interfaces, where obviously the studied region is between the two liquids.

vacuum, has stressed the importance of ultrapure clean electrode surfaces for obtaining meaningful and reproducible results.

Figure 6.7 shows some methods used to prepare and clean different components of an electrochemical system. For example, ideally and when available, the experimenter should start with high-purity materials (99.999%) as electrodes. Then, in spite of their initial purity, the materials have to be cleaned because handling and exposure to air may deposit impurities on their surfaces and/or form a surface layer of oxides that would obstruct the reaction one wants to study. Usually this procedure starts simply with degreasing the surface with acetone. Then other treatments follow, depending on the type of material one is using. For example, there are several electrochemical procedures to “activate” or remove oxides from the surface of electrodes. When not only the surface but also the bulk of the electrode material will take part in the electrochemical reaction, any stress in the metal has to be removed. This is done by annealing the electrode. In this procedure, the electrode is placed under vacuum at an appropriate high temperature (e.g., 1200 K for Pt or Fe, 770 K for Au) for about 1 hr, followed by slow cooling to room temperature.

CELL COMPONENTS	CLEANING PROCEDURE
Electrode Surfaces	<ul style="list-style-type: none"> <li>• Start with the highest purity material available(99.999%)</li> <li>• Degrease surface with acetone</li> <li>• Polish or electropolish surface</li> <li>• Electrochemical activation procedures</li> <li>• Ultrasonic cleaning</li> <li>• Flaming or annealing</li> <li>• Chemical treatments (e.g. dilute nitric acid followed by distillation for liquid metals like Hg)</li> </ul>
Solvents (water)	<ul style="list-style-type: none"> <li>• Catalytic pyrodistillation</li> <li>• Millipore purification system</li> <li>• Pre-electrolysis of inert electrolyte on a sacrificial anode or cathode</li> </ul>
Cell components	<ul style="list-style-type: none"> <li>• Teflon: overnight treatment in hot acid and then in hot alkali</li> <li>• Glass: steaming, standing overnight in chromic sulfuric acid or <math>\text{HNO}_3/\text{H}_2\text{SO}_4</math> bath and rinsing with purified water</li> </ul>
Solute Materials	<ul style="list-style-type: none"> <li>• Use of high-quality chemicals</li> <li>• Recrystallization of salts</li> <li>• Calcination to remove organic impurities from inorganic substances</li> <li>• Acids can be cleaned by normal or vacuum distillation</li> </ul>
Gases	<ul style="list-style-type: none"> <li>• For nitrogen and argon: passage through purification traps such as <math>\text{Mg}(\text{ClO}_4)_2</math> and molecular sieve to remove water, <math>\text{CO}</math>, and hydrocarbons; then deoxygenate in a furnace at 623 K with copper turnings</li> <li>• Organic impurities are removed from oxygen by catalytic burning at 1000 K</li> </ul>

**Fig. 6.7.** Procedures used to clean the different components in an electrochemical system.

One of the most common sources of contamination is the electrolyte since impurities in it would diffuse to the electrode and adhere to it during the course of the experiment. Impurities in the electrolyte can be reduced substantially by careful purification of solvent and solute. Distillation or ultrafiltration purifies water, the most common solvent. Usually solute materials can be bought in a very high purity, and whenever this is not the case, they can be cleaned by standard procedures such as recrystallization or calcination. Electrolysis of the electrolyte is also a common practice. Here, two sacrificial electrodes are immersed in the electrolyte and a potential is applied between them for about 36 hr in such a way that impurities are oxidized or reduced on their surfaces—the electrodes act as a garbage disposal; thus the name of “sacrificial” electrodes.

Finally the purification of gases, if they are used in the experiment, should not be forgotten. Gases such as nitrogen or helium can be cleaned by passing them through purification traps such as  $\text{Mg}(\text{C}10_4)_2$  and a molecular sieve to remove water. Passing a gas through a hot trap (620 K) with copper turnings oxidizes CO and hydrocarbons.

### 6.2.3. Why Use Single Crystals?

Single crystals are solids characterized by a certain constant arrangement of the atoms. This regularity is extended to all the atoms without interruption. In contrast, in a polycrystalline solid, there are several of these regular regions, which are large compared with the interatomic distances, but which have boundaries where the regular orientation suddenly changes. In other words, the polycrystalline solids are made of many small crystals with three-dimensional order, which intergrow, one against the other (Fig. 6.8).

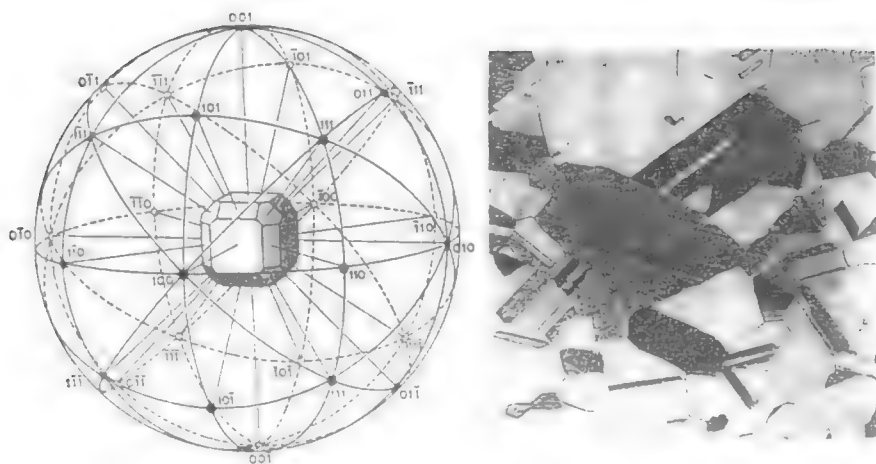


**Fig. 6.8.** (a) The spherical projection of the faces of a crystal. The numbers indicate the Miller indices of the corresponding planes. (b) Photomicrograph of a polycrystalline brass. (Reprinted with permission from Elizabeth A. Wood in *Crystals and Light. An introduction to Optical Crystallography*, 2nd ed., Dover, 1977, Plate III(2) and Fig. 4.5.)

Ideally, the experimenter would like to perform the experiment on single-crystal surfaces whose composition and atomic structure are uniform. That is why the use of single crystals in electrochemistry has become more and more required. However, one can point out that industrial electrochemical processes (e.g., control of corrosion, and manufacture of batteries and fuel cells) usually involve polycrystals. Thus, why study single crystals? On one hand, interpretation of results involving well-ordered surfaces is simpler than those involving complex polycrystals. Then, once the knowledge of the electrochemical process on these “simpler” structures has been acquired, it can be used to obtain an understanding of similar processes on the most complex polycrystalline surfaces. Furthermore, many electrochemical reactions are found to depend strongly on surface structure, and it is through the use of single crystals having different preferred orientations that these reactions can be studied (see Fig. 6.9).

### 6.2.4. *In Situ* vs. *Ex Situ* Techniques

The techniques used in studying interfaces can be classified in two categories: *in situ* techniques and *ex situ* techniques. *In situ* methods are those where a surface is probed by one or several techniques while immersed in solution and under potential control. In contrast, in *ex situ* methods, an electrochemical experiment is first carried out. Then the electrode is removed from solution and examined by one or several spectroscopic techniques, which generally require ultrahigh vacuum (UHV) conditions. Figures 6.10 and 6.11 show some of the most common *ex situ* and *in situ* techniques applicable to the study of the metal/solution interface.

Although *in situ* methods provide more direct information on the interfacial structure, the advantage of *ex situ* techniques is that once the electrode is removed from solution, the experimenter may use several of the UHV techniques developed to study the metal/gas interface. These techniques sometimes give more details on the structure of the surface at a molecular level than *in situ* methods do. The disadvantage is that in the UHV techniques, the electrode has to be removed from solution so that potential control is lost. Losing control of the potential across the interface is equivalent to losing the main factor that keeps the double layer intact. In addition, placing the electrode in UHV could also change the structure of the double layer because water molecules, which are important players in the game, get removed in the process.<sup>9</sup> Does this mean, then, that electrochemists are not able to obtain the great degree of detail and definition

---

<sup>9</sup>An option to keeping the solvent molecules on the electrodes after placing them in the ultrahigh vacuum (UHV) chamber is to hold the samples at temperatures below 200 K. Although one may argue that investigation at these temperatures has little relevance to room temperature experiments, there are several cases where it has been found that a certain degree of similarity exists. The name of the technique utilized to obtain double-layer properties in frozen electrolytes is *frozen electrolyte electrochemistry* (FREECE).

Another consequence of placing the electrode in a vacuum to study it is the removal of the solvent molecules. Thus, one may pose the following question: Are the results of spectroscopic examinations of the electrode surface *in vacuo* (no solvent present) relevant to the study of the electrochemical interfacial region in which the solvent plays a strong role?



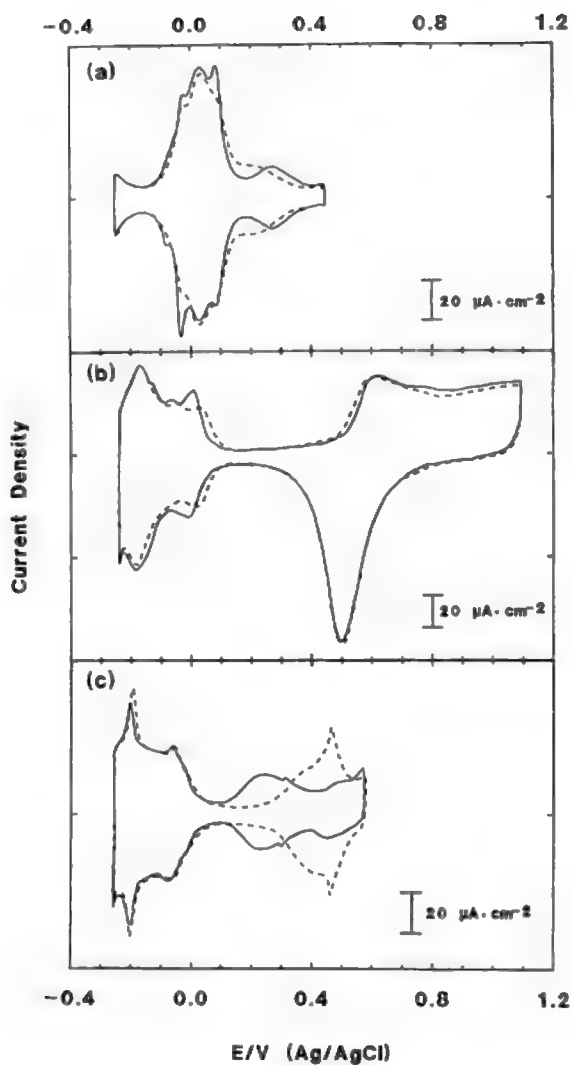


**Fig. 6.9.** Cyclic voltammetry of three platinum electrodes in clean  $0.1\text{ M HClO}_4$  solution (broken curves) and in the same solution containing  $1.0\text{ mM of H}_2\text{SO}_4$  (solid curves). (a) Pt(100), (b) Pt(poly), and (c) Pt(110). Scan rate  $50\text{ mV s}^{-1}$ . (Reprinted from Y-E. Sung, A. Thomas, M. Gamboa-Aldeco, K. Franaszczuk and A. Wieckowski, *J. Electroanal. Chem.* **378**:131 copyright, 1994, Fig. 13, with permission of Elsevier Science.)

UHV SPECTROSCOPIC METHOD	SOURCE OF EXCITATION	ANALYZED PARTICLE	INFORMATION OBTAINED FROM INTERFACIAL REGION
Low-energy electron diffraction (LEED)	Electrons (50-500 eV)	Backscattered electrons	• Structure and surface crystallography
Auger electron Spectroscopy (AES)	Electrons (1-10keV)	Auger electrons	• Elemental composition (except H and He) • electronic structure
X-Ray-photoelectron spectroscopy (XPS)	Monochromatic X-rays	Core level electrons	• Qualitative and quantitative analysis of elements • Depth profiling
Ultra-violet-photoelectron spectroscopy (UPS)	UV-light	Valence electrons	• Qualitative and quantitative analysis of elements • Depth profiling
High-resolution-electron-energy-loss spectroscopy (HREELS)	Low energy electrons (2-10 eV)	Backscattered electrons	• Adsorbate-metal vibrational energies
Thermal-Desorption-Spectroscopy (TDS)		Desorbed atoms and molecules	• Nature of adsorbed species • Thermodynamics of adsorption / desorption

**Fig. 6.10.** Some *ex situ* methods applied in the analysis of electrodes.

of spectral information available only by *ex situ* techniques? Not really. Electrochemists have tried to determine the structure of an electrode before and after its removal from solution. They are interested in determining whether *ex situ* techniques provide information about the structure of the surface as if the solution were still there, or whether the vacuum and the removal of water have spoiled the structure. It turns out that the success of the application of UHV to electrochemistry depends greatly on the strength of adsorption of the molecule studied, that is, on the adsorbed properties that

IN SITU METHOD	SOURCE OF EXCITATION	INFORMATION OBTAINED FROM INTERFACIAL REGION
Potentiostatic techniques	Applied potential	• Current related to surface processes
Infrared spectroscopy	IR light	• Nature of adsorbed species
Ellipsometry (optical method)	Monochromatic X-rays	• Thickness of adsorbed layer
Radiochemical techniques	UV light	• Number of adsorbed species
Scanning-tunneling microscopy (STM)	Low-energy electrons (2-10 eV)	• Structure of adsorbed species

**Fig. 6.11.** Some *in situ* methods applied to electrochemistry.

are the object of the experiment. If the strength is large (e.g., CO on platinum), *ex situ* methods provide information relevant to the electrochemical situation in which they were prepared. But if it is weaker (chloride ions on platinum, for example), the *ex situ* information may not be relevant to the original electrochemical process the researcher started studying.

### 6.2.5. *Ex Situ* Techniques

In UHV surface spectroscopies, the electrode under investigation is bombarded by electrons, photons, or ions, and an analysis of the electrons, ions, molecules, or atoms scattered or released from the surface provides information related to the electronic and structural parameters of the atoms and ions in the interfacial region. As mentioned before, the transfer of the electrode from the electrochemical cell to the UHV chamber is a crucial step in the use of these techniques. This has motivated a few groups to build specially designed transfer systems. Pioneering work in this area was done by Hubbard's group, followed by Yeager.

Two of the most common UHV-spectroscopic methods used in electrochemistry are briefly described next, and Fig. 6.10 lists other *ex situ* techniques, which can be reviewed in the literature by the inquisitive student.

**6.2.5.1. Low-Energy Electron Diffraction (LEED).** This is an example of a technique used to probe the surface structure of the electrode—in contrast to other techniques, which give its analytical composition. Surface structure involves mainly the arrangement of the atoms on the electrode surface.

Two main ideas are related to the development of this technique. The first one is the wave nature of the matter. As postulated by Louis de Broglie in 1924, a free electron with mass  $m$ , moving with speed  $v$ , has a wavelength  $\lambda$  related to its momentum ( $p = mv$ ) in exactly the same way as for a photon, that is,

$$\lambda = \frac{h}{mv} \quad (6.1)$$

with  $h$  being Planck's constant. Inserting values in this equation shows that electrons with an energy of 100 eV or velocity  $v = \sqrt{2E/m} \approx 6 \times 10^6 \text{ m s}^{-1}$ , are related to a wavelength of about 0.12 nm. This is the order of magnitude of spacing of adjacent atoms in a crystal (e.g., 0.28 nm in NaCl). This indicates that interference of these waves with periodically arranged atoms in a crystal is possible.<sup>10</sup>

<sup>10</sup>The discovery of the interaction of electrons with matter was, as many other times in science, the result of an accident. Davisson and Germer (1927, Bell Telephone Laboratories) were directing a beam of electrons to a nickel sample contained in a glass vessel at low pressures and high temperatures. In one instance the glass vessel broke and the sample oxidized. To remove the oxide, they heated the sample in a hydrogen atmosphere, and this caused the partial ordering of the atoms in the sample. As a result, they were the first witnesses of the wave character of electrons and their interaction with matter.

The second idea related to the LEED technique is, as its name indicates, the diffraction phenomenon. With the wave nature of the electrons established, information on the interaction of a beam of light with matter can be extrapolated to understand the interaction of a beam of electrons with a crystal. In this sense, the corresponding relationship is that of a monochromatic beam of light—that with a single frequency and single wavelength—with that of a beam of electrons of fixed energy.

When monochromatic light passes through a slit, the beam observed on the other side of the slit is not what would be expected from everyday experience. Instead of observing a sharp edge delimiting the illuminated zone from the shadowed one—that is, a beam with the same cross section as the slit—one observes that the beam is spread out vertically after passing through the slit (see Fig. 6.12).<sup>11</sup> This scattering of light is called *diffraction* and the pattern formed is called a *diffraction pattern*.

Why is this diffraction pattern formed? The light wave passing through the slit may be considered to consist of several wavelets or secondary waves that spread out in all directions with a speed equal to the speed of propagation of the original wave (Huygens' principle, 1678). Thus, light passing through the slit can be divided into several secondary waves propagating in all directions with the same speed as the original monochromatic light [Fig. 6.13(a)]. If a screen is placed to the right of the slit, it is possible to determine the resultant intensity at a point  $P$  by adding the contributions from the individual wavelets [Fig. 6.13(b)]. If the screen is far away, it can be assumed that the wavelets are parallel to each other. Consider for the moment, only two wavelets, one in the top and one in the center of the slit. The difference in the path length between these two wavelets is given by the distance  $a$  in Fig. 6.13(c). If this distance happens to be the same or equal to any multiple of  $\lambda$ , then the intensities of the two waves add to each other [Fig. 6.14(a)]—the waves *interfere constructively*—and a bright fringe is observed on the screen [ $P'$  in Fig. 6.13(c)]. The waves are said to be *in phase*. If now the distance equals  $\lambda/2$  or any multiple of this value, then the waves are *out of phase* and they *interfere destructively* [Fig. 6.14(b)] and a dark fringe appears on the screen [ $P''$  in Fig. 6.13(c)]. The wavelets propagating perpendicular to the slit ( $\theta = 0$ ) would give a wide bright band at  $P'''$  in Fig. 6.13(c) because in this case, light from the entire slit arrives in phase. Figure 6.13(c) also shows that the intensity of the light reaching the screen at the different fringes varies, with 85% of the total intensity lying in the central bright fringe.

What happens if instead of one slit there are a large number of equally spaced parallel slits with the same width? Figure 6.15 shows the cross section of four of these slits, which are perpendicular to the plane of the page. Suppose that the angle  $\theta$  in Fig. 6.15 is such that the difference in path lengths of the light passing through the slits is  $a = \lambda$ ,  $b = 2\lambda$ ,  $c = 3\lambda$ , etc., with  $\lambda$  being the wavelength of the incident light. Under these conditions, the waves from all the slits are in phase, and all their wavelengths

<sup>11</sup>Why do we not observe diffraction patterns from frosted light bulbs? The light from every point of the bulb *does* form its own diffraction pattern, but these patterns overlap to such an extent that no individual pattern can be observed.

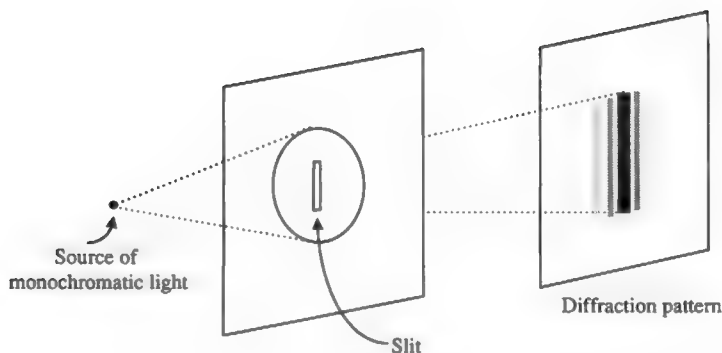


**Fig. 6.12.** Monochromatic light passing through a slit produces a diffraction pattern.

interfere constructively [Fig. 6.14(a)]. The result is a bright fringe detected on the screen placed far away on the right-hand of the slit plane (Fig. 6.15 point  $Q$ ). If the angle  $\theta$  is now slightly increased, the waves of the various slits are out of phase and the result is destructive interference among them [Fig. 6.14(b)]. A dark fringe appears on the screen. If the angle  $\theta$  increases even more until it reaches a value such that  $a = 2\lambda$ ,  $b = 4\lambda \dots$  (or in fact any value that satisfies the condition  $a = n\lambda$ ,  $b = 2n\lambda$ ,  $\dots$ , with  $n$  equal to an integer number) then again the waves are all in phase and another bright fringe appears on the screen. The general condition for an intensity maximum to appear can be written as

$$d' \sin \theta = n\lambda \quad (n = 0, \pm 1, \pm 2, \dots) \quad (6.2)$$

As described before, light passing through one slit would result in a broad maximum, but several slits produce several fringes. In fact, with the contribution of so many waves, the constructive interference occurs only when the path difference of the wavelets is *exactly* an integer number of wavelengths, and small deviations from these values drop the intensity of the fringe close to a zero value. The results are bright and sharp maxima. The phenomenon described here is called *interference*, and the pattern produced, an *interference pattern*. In fact, the pattern obtained in this type of experiment is called indiscriminately an *interference pattern* or a *diffraction pattern*.

What do the phenomena described here have to do with the LEED technique? Imagine now that instead of the incident light, a beam of low-energy electrons is directed to an array of atoms, as in a crystal [Fig. 6.16(a)]. Returning to de Broglie's postulate, the electrons can be viewed as electromagnetic waves moving with a speed  $v$  and a wavelength  $\lambda$ . The interaction of these waves with the atoms will induce oscillating electric dipole momenta in each atom. These dipoles act like antennas, emitting scattered waves. The interference of these waves as they move away from the atoms is of the same nature as the interference pattern observed when light passes

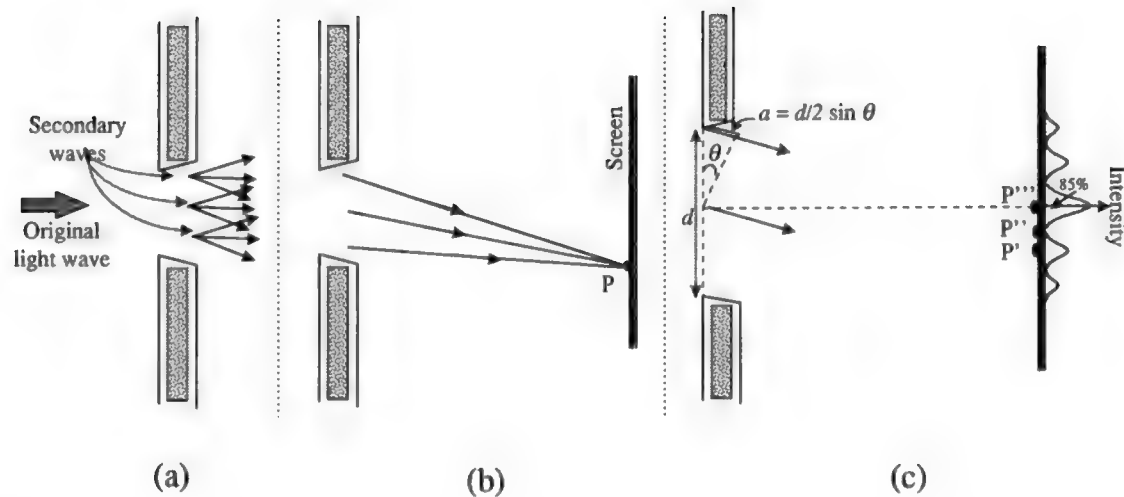


**Fig. 6.13.** Diffraction of light by a slit. (a) The original light wave can be split into secondary waves. (b) The resultant intensity at a point  $P$  can be determined by adding the individual wavelets (accounting for their phases and amplitudes), and if the screen is far away, the rays can be considered to be parallel to each other. (c) Differences in pathway of two wavelets (when  $a = \lambda/2$ , a minimum in intensity occurs ( $P''$ ), and 85% of the total intensity occurs at  $\theta = 0$ ). The appearance of fringes of different intensities on the screen is called *diffraction of light*.

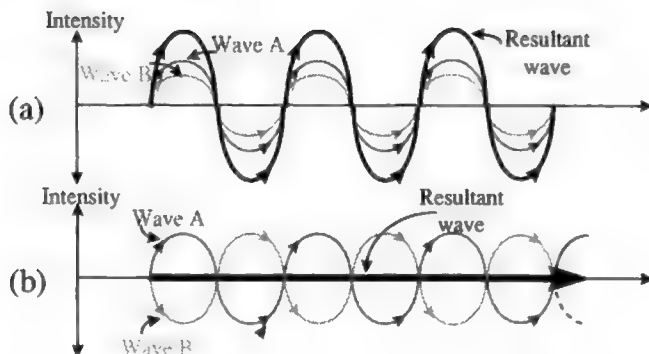


**Fig. 6.14.** (a) If the path difference of two waves is  $0, \lambda, 2\lambda, \dots$  the resultant wave is the addition of both waves. (b) However, two waves with the same amplitude but with a path difference equal to  $\lambda/2$  cancel each other.

through a large number of slits, as described previously. The only difference is that the waves emitted from the atoms are not all in phase as in the many-slits case.

Consider for example, that the atoms—or scatterers—are placed in an ordered manner in rows in a single plane, as shown in Fig. 6.16(a). The path length from the source of electrons to the observer (screen) is the same for all atoms in a single row, say row A in Fig. 6.16(b), and the scattered radiation from these atoms is in phase. What happens with the radiation emitted from atoms in parallel rows? The total

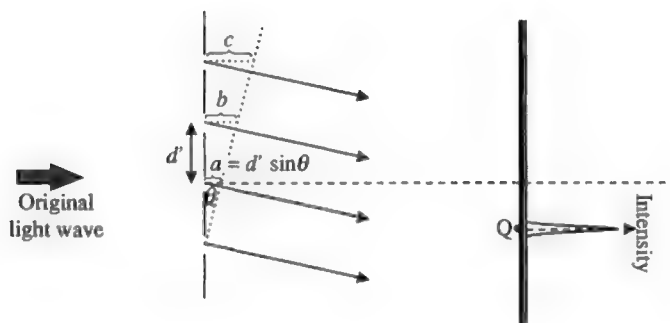


**Fig. 6.15.** Difference in pathways of several waves in several parallel slits. When  $a$  equals  $\lambda$  or any integer multiple of  $\lambda$ , the waves are in phase and they interfere constructively, producing a maximum in the intensity at Q. When  $a$  equals any other value of  $\lambda$ , the waves are out of phase and they interfere destructively. The fringes appearing on the screen are called an *interference pattern*.

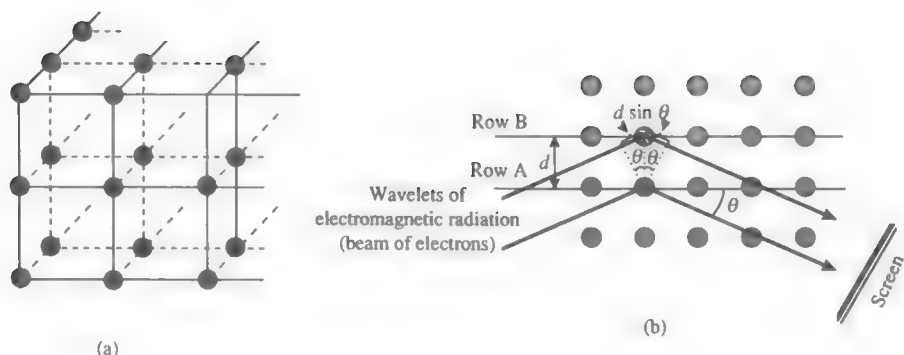


**Fig. 6.16.** (a) An array of atoms in a crystal. (b) Scattering of radiation from a plane of array of atoms.

difference in path of the electromagnetic wavelets between two adjacent rows, say rows A and B in Fig. 6.16(b), is  $2d \sin \theta$ . LEED experiments are usually performed with normal incidence of the electron beam; therefore the path difference simplifies to  $d \sin \theta$ . The condition needed for the wavelets to be in phase, and therefore to produce constructive interference, is that the path difference should be equal to an integer number of wavelengths, that is,

$$d \sin \theta = n\lambda \quad (n = 1, 2, 3, \dots) \quad (6.3)$$

What happens now, if as in a crystal, there are several planes of atoms? The condition described above should hold, but one more condition should be added. Now not only the difference in path length of adjacent rows in the same plane should equal an integer number of wavelengths, but also the difference in path of adjacent *planes* should equal  $n\lambda$ . It is only under these conditions that bright diffraction patterns can be observed.

In fact, the phenomenon and conditions described here can be applied not only to a beam of electrons, but also to a beam of X-rays.<sup>12</sup> What is the difference in the diffraction pattern when these different sources of radiation are applied to an ordered array of atoms? X-rays penetrate deeply into the crystal, and information between spacing of planes inside the crystal is obtained from the diffraction pattern. In contrast, the use of low-energy electrons as a source of incident radiation with energies in the range of 10 to 500 eV ensures that only atoms close to the surface (one or two planes) produce the diffraction pattern. Since this is the region in contact with a solution, the region where electrochemical processes occur, LEED is the technique used in electro-

<sup>12</sup>If this is the case, the technique is then called *X-ray diffraction*. The wavelength of the X-rays is on the order of 0.1 nm and the diffraction pattern produced is also called a *Laue pattern* (see Section 5.2.3).



chemistry to study the arrangement of atoms on the surface, that is, the surface structure.

Figure 6.17 shows a schematic of the LEED system. The sample is bombarded through the left by a beam of electrons. Only radiation or electrons (remember the wave nature of matter!) with the same energy as the incident beam are detected. These electrons are called *elastic backscattered electrons*. The detection system is a fluorescent screen placed in front of the sample. Holding the screen at a large positive potential accelerates the electrons. Once they reach it, they excite the phosphorus in the screen, marking it with bright spots characteristic of the diffraction pattern. Finally, a camera in front of the screen records the diffraction pattern.

As discussed above, only a well-ordered surface produces bright and well-defined spots. These spots broaden and lose intensity when they represent a less-ordered surface. From the intensity of the spots and its variation with the energy of the electron beam, it is also possible to elucidate the vertical distance of the atoms, using equations related to Eq. (6.3). Examples of LEED patterns are shown in Fig. 6.18.

**6.2.5.2. X-Ray Photoelectron Spectroscopy (XPS).** This technique is also known as *electron spectroscopy for chemical analysis (ESCA)*, and as this name implies, it is a surface analytical technique. At present it is probably the most versatile and generally applicable surface spectroscopic technique. It is called XPS because of the type of beam used to study the interfacial region, that is, X-rays. These X-rays consist of monochromatic radiation—radiation of a given energy—emitted by a metal target bombarded by an electron beam of several kiloelectron volts of kinetic energy

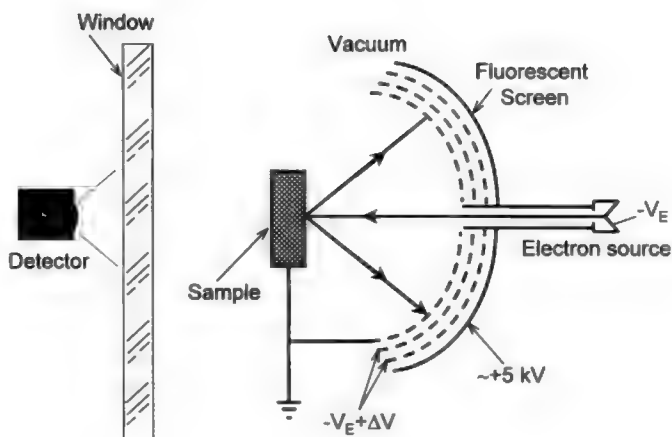


**Fig. 6.17.** Scheme of an LEED system. The potential  $V_E$  defines the electron energy as  $eV_E$ . (Reprinted with permission from D. P. Woodruff and T. A. Delchar, *Modern Techniques of Surface Science*, Cambridge University Press, 1990, Fig. 28.)

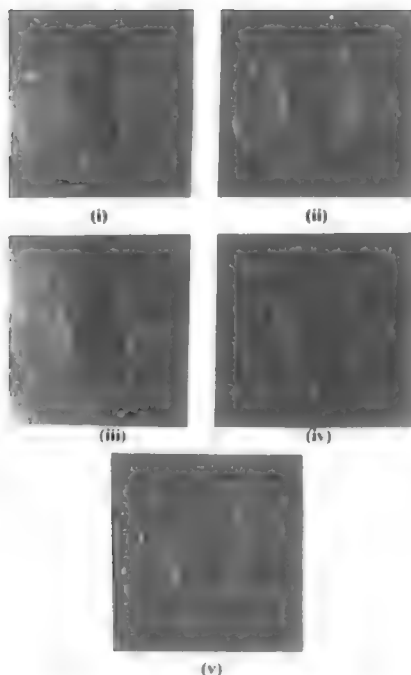


**Fig. 6.18.** Actual LEED patterns seen at various coverages of iodine on Ni(100): (i)  $c(2 \times 2)$ ,  $\theta = 1/2$ ; (ii) incommensurate,  $\theta = 0.313$ ; (iii) about  $2 \times 3$ ,  $\theta = 1/3$ ; (iv) incommensurate,  $\theta = 0.359$ ; (v) about  $2 \times 8$ ,  $\theta = 0.375$ . (Reprinted from R. G. Jones and D. P. Woodruff, *Vacuum*, 31:411, copyright 1981, Figs. 1 and 3, with permission from Elsevier Science.)

[Fig. 6.19(a)]. Typical targets are made of magnesium and aluminum, which emit radiation of 1.486 keV and 1.253 keV, respectively.

What do the X-rays do? They penetrate down into the solid, through the surface and surface region in which one is interested. On the way, these X-rays cause electrons to be emitted from the atoms or molecules that they meet (the excitation process). Analysis shows that the electrons emitted come not from the outer shells, but from the inner ones. What happens to these electrons? It depends on how deep they are in the material. Typically, electrons do not reach the surface if they are emitted from deep inside the electrode. But if the electrons belong to atoms closer to the surface, say a few nanometers, they escape into the vacuum

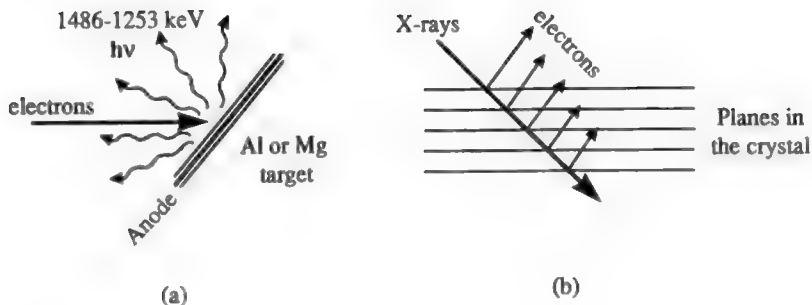


**Fig. 6.19.**(a) Emission of X-rays from an aluminum or magnesium target, and (b) the scattering behavior of diffracted X-rays. (Reprinted with permission from G. A. Somorjai, *Chemistry in Two Dimensions. Surfaces*, Cornell University Press, 1981, Fig. 2.8.)

[Fig. 6.19(b)]. Outside the surface one is examining there is a detector that finds out the energies of the electrons being emitted. If the binding energy of the ejected electrons is  $E_B$ , and the incident X-ray beam has an energy  $E = h\nu$ , then, the kinetic energy of the emitted electrons,  $E_{kin}$ , is

$$E_{kin} = h\nu - E_B \quad (6.4)$$

Data obtained from a typical experiment are plotted as the intensity of the electron emission as a function of the binding energy of the ejected electrons, as shown in Fig. 6.20. This graph or spectrum contains several maxima (peaks) positioned at the binding energies of the emitted electrons. Since these energies are characteristic of the atoms from which they were emitted, it is possible to identify the elements of the surface region of the material examined.

However, does this mean that the only information obtained from the spectrum is an elementary analysis of the surface region? Not really, but to understand this, one has to look closer to the position of the peaks. If a given atom in the interface region is in a different state than the base state (e.g.,  $\text{Na}^0$ ), for example, in an oxidation state ( $\text{Na}^+$ ), the binding energies of the core-level electrons that are ejected during the experiment are also different. What this means is that the position of the corresponding peak in the spectrum would somehow be shifted from its original one, and from this shift the experimenter is able to predict the state of the analyzed atoms (see Fig. 6.20). In addition, analysis of the peak shift can indicate the position of the atoms, that is, if the atoms are on the topmost surface layer (adsorbed) or if they belong to a deeper layer of the electrode studied. Another piece of information that can be extracted by XPS studies is a quantitative analysis of the surface, since the peak intensity—that is, the integrated area below a certain peak—is proportional to the number of atoms in the detected volume.

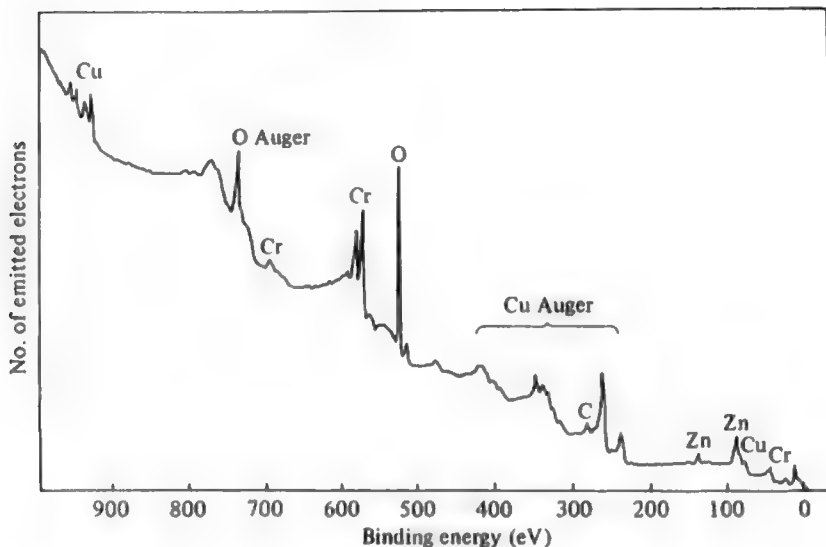


**Fig. 6.20.** Typical XPS spectrum taken using 1253-eV photons ( $\text{MgK}\alpha$ ). (Reprinted with permission from D. P. Woodruff and T. A. Delchar, *Modern Techniques of Surface Science*, Cambridge University Press, 1990, Fig. 3.8.)

## 6.2.6. *In Situ* Techniques

In this section, two *in situ* electrochemical techniques are presented, namely, infrared-reflection spectroscopy (IRS) and electrochemical methods. Examples are given in Fig. 6.21.

**6.2.6.1. Infrared-Reflection Spectroscopy.** As in other spectroscopic techniques, infrared reflection spectroscopy uses light as a source to explore the energy levels of molecules. The information obtained depends on the wavelength of the light source. For example, the range of the wavelengths of *microwave radiation* is on the order of millimeters and centimeters, and is used to explore rotational energy levels of molecules and therefore their bond lengths and bond angles. Then comes *infrared radiation*, with wavelengths from  $10^3$  to  $5 \times 10^5$  nm, which gives information on the vibration energy of the molecules studied. *Visible* and *ultraviolet* spectroscopies use radiation from 50 to  $10^3$  nm and are able to explore electronic energy levels of the molecules.

In a typical IRS experiment, the infrared light is separated into its frequencies so that the variation of the absorbed light,<sup>13</sup>  $A$ , with the light frequency,  $\nu$ , can be monitored. The separation of light into its frequencies is carried out in a spectrometer.

<sup>13</sup>Do not confuse *absorbance* with *adsorbance*!

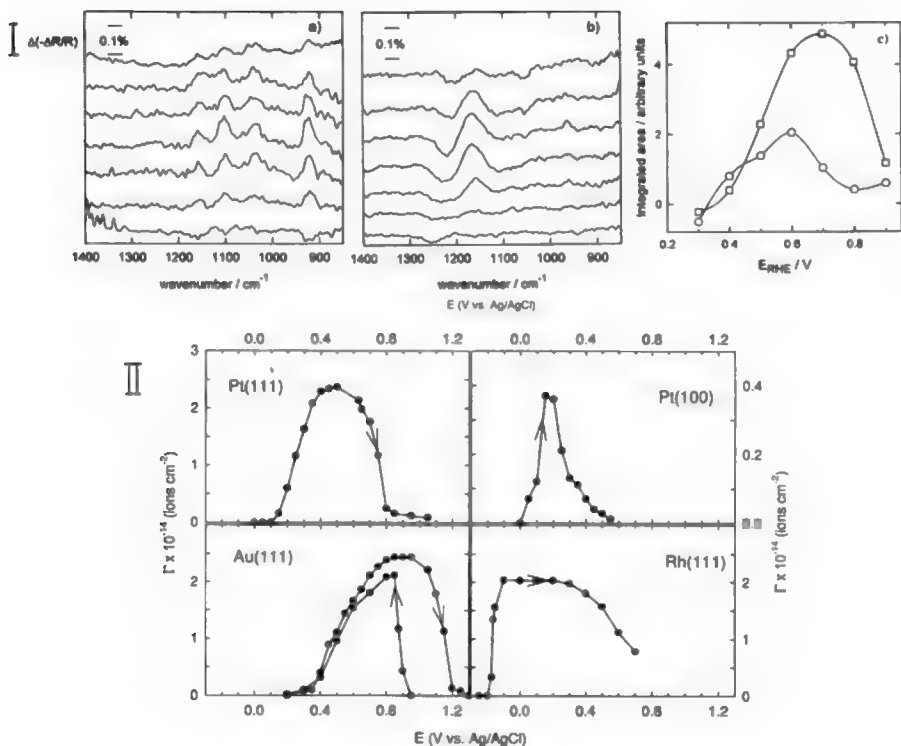
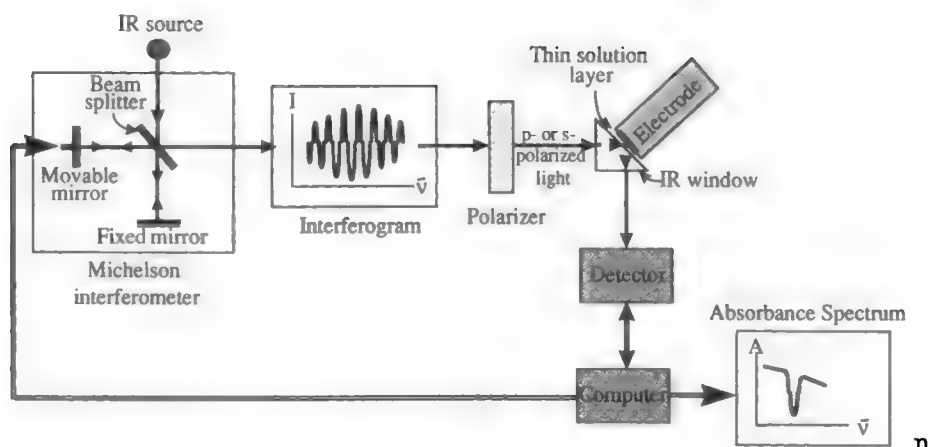


**Fig. 6.21.** FTIR spectra of Pt(111) in  $0.1 \text{ M HClO}_4 + 1 \text{ mM Ti}^+$  in (a) the absence and (b) in the presence of  $1 \text{ mM H}_2\text{SO}_4$ . (c) Dependence of integrated area on electrode potential for the bands shown in (a) and (b). (O) perchlorate bands, and ( $\square$ ) bisulfate bands. (Reprinted with permission from N. S. Marinković, W. R. Fawcett, J. X. Wang, and R. R. Adžić, *J. Phys. Chem.* **99**:17490, Figs. 3 and 4, copyright 1995, American Chemical Society.) (II) Bisulfate coverages in  $0.1 \text{ M HClO}_4$  supporting electrolyte, as measured by a radiotracer technique on: Pt(111),  $c_{\text{H}_2\text{SO}_4} = 1 \text{ mM}$ ; Pt(100),  $c_{\text{H}_2\text{SO}_4} = 0.1 \text{ mM}$ ; Au(111),  $c_{\text{H}_2\text{SO}_4} = 0.5 \text{ mM}$ ; and Rh(111),  $c_{\text{H}_2\text{SO}_4} = 1 \text{ mM}$ . (Reprinted from P. A. Rikvold, M. Gamboa-Aldeco, J. Zhang, M. Han, Q. Wang, H. L. Richards, and A. Wieckowski, *Surf. Sci.* **335**:389, copyright 1995, Fig. 6; M. Gamboa-Aldeco et al., *J. Electroanal. Chem.* **348**:451, copyright 1993, Figs. 2 and 3; and Z. Shi et al., *J. Electroanal. Chem.* **366**:317, copyright 1994, Fig. 5, with permission from Elsevier Science.)

One of these devices that is typically used in infrared spectroscopy is the Michelson interferometer (Fig. 6.22). This device works by splitting the beam into two components perpendicular to each other. Then each beam gets reflected by mirrors in such a way that the reflected beams recombine again at the beam splitter. In one of these beams a path difference is introduced by moving the mirror on which it reflects. This



splitter divides the incident beam into two components. The movable mirror produces a path difference in one of the beams. The recombination of the beams produces constructive or destructive interference (interferogram). In the polarizer, the light becomes p- or s- polarized before reaching the electrochemical vessel.

difference in path ( $m$ ) produces differences in the phases of the two beams in such a way that when they meet again, the recombination produces a constructive or a destructive interference (see Fig. 6.14). Since the mirror moves smoothly, the recombined signal oscillates as the two beams come into and out of phase. Thus, the intensity of the recombined signal,  $I^*$ , is determined by the changes in the path of the mirror. This intensity is related to the wavenumbers,  $\bar{\nu}$ , of the radiation by

$$I^* = \int_0^{\infty} I_{\bar{\nu}} (1 + \cos 2\pi \bar{\nu} m) d\bar{\nu} \quad (6.5)$$

What this equation indicates is that the intensity of the signal coming out of the beam splitter,  $I^*$ , can be written as the intensity in terms of wavenumbers,  $I_{\bar{\nu}}$ . This variable,  $I_{\bar{\nu}}$ , is the one the spectroscopist is interested in obtaining. However, this intensity is inside an integral; therefore, in order to obtain it, it is necessary to use a standard technique in mathematics called the *Fourier transformation*,

$$I_{\bar{\nu}} = 4 \int_0^{\infty} \left[ I_0 - \frac{1}{2} I(0) \right] \cos(2\pi \bar{\nu} m) dm \quad (6.6)$$

Because of this mathematical step, the technique is usually called *Fourier transform infrared spectroscopy* or *FTIR spectroscopy*. The Fourier transformation is a mathematical procedure that enables one to convert from the results of an interferogram back to intensities of a given wavelength. It is performed in a computer connected to the spectrometer. The result is the absorption spectrum of the sample, that is, the intensity of the absorbance as a function of the wavenumbers.

After being passed through the interferometer, the light is polarized (see below). Then it enters the electrochemical vessel, passes through a solution layer, reaches the mirror-polish electrode, where it is reflected, and then goes out of the electrochemical vessel after again crossing a solution layer. During this trajectory the light interacts with the molecules in its path, that is, those in solution and those in the interfacial region. These molecules absorb part of the incident light at certain frequencies that depend on the vibrational characteristics of the molecules.<sup>14</sup> According to the Beer–Lambert law, the intensity of the absorbed light is related to the concentration of the molecules in the sample by the equation

$$\log \frac{I}{I_0} = -\epsilon cd \quad (6.7)$$

where  $I_0$  is the incident intensity of the IR light at a particular wavelength,  $I$  is the intensity after passage through a sample of length  $d$ ,  $c$  is the concentration of the absorbing molecules, and  $\epsilon$  is the absorption coefficient. The left part of this equation is called the *absorbance* of the sample,  $A = \epsilon cd$ . Therefore, the absorbance can be determined by measuring the intensity of the incident and emerging light, and it is directly proportional to the amount of molecules in the sample. As a result, the experimenter obtains an absorption spectrum that carries information on the frequencies of the vibrational modes of the molecules (Fig. 6.22) and the concentration of the molecules on the sample.

One of the most difficult tasks of the IR spectro-electrochemist is to differentiate between the information that comes from the adsorbed molecules and that which comes from molecules in solution. If one compares the amount of molecules that are in the bulk of a solution (e.g.,  $\sim 10^{19}$  in  $10 \text{ cm}^3$  of a  $10^{-2} \text{ mol dm}^{-3}$  solution) with those adsorbed on the surface of the electrode ( $\sim 10^{15}$ ), it is easy to understand why: The IR absorbance from the electrolyte solution would be so much stronger (in our example 10,000 times stronger) than that from adsorbed molecules, that it would not be possible to detect the latter. To increase the sensitivity of the absorbance of the adsorbed molecules, the design of the electrochemical vessel is very important. Generally, the electrode is placed very close to the window through which the IR beam enters and then is reflected (Fig. 6.22). In this configuration, the amount of electrolyte solution

<sup>14</sup>Ideally, absorption should occur at a single wavelength, producing lines in the absorbance spectrum. However, absorption bands generally spread over a range of wavelengths, indicated by peaks in the spectrum. The total absorption is then given by the sum of the absorbance over the entire band.

is minimized and therefore its absorbance. Unfortunately this does not enhance the absorbance from the adsorbed molecules enough to obtain a detectable signal. To increase the selectivity of the technique in such a way that the absorbance of the molecules at the interface increases relative to the absorbance from the solution molecules, several techniques have been developed. They have to do with selection rules of polarized light, as explain in the following paragraphs.

One of the theorems involved in IR spectroscopy is a theorem due to Greenler. This theorem gives rise to a unique surface selection rule arising from the physics of the reflection of radiation from highly conducting surfaces. Consider for a moment the electrical component of an incident electromagnetic wave traveling in the  $z$ -direction, with components in the  $x$  and  $y$  directions. It is possible to differentiate these two components and divide them in such a way that only one of them remains and the other is completely suppressed. When only the component in the  $y$ -direction remains, it is said that the light is linearly polarized in the  $y$ -direction. In the same way, light with only  $x$ -displacements is called  $x$ -polarized light (Fig. 6.23). The names given to these

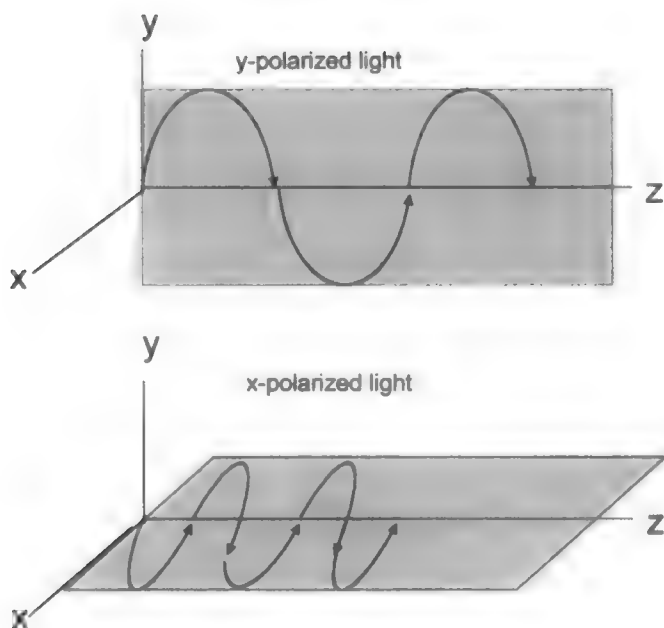


**Fig. 6.23.** The direction of the electric-field vector of the electromagnetic wave defines the direction of polarization. In the upper diagram, the electric-field vector travels in the  $y$ -direction ( $y$ -polarized light), and in the lower diagram, in the  $x$ -direction ( $x$ -polarized light).



components in IR spectroscopy are *parallel* (*p*-) and *perpendicular* (*s*-) polarized light, depending on position of the light with respect to the surface of the electrode; *p*-polarized light has its electric field oriented perpendicular to the surface, while *s*-polarized light has its electric field oriented parallel to the surface. What happens now when *p*- or *s*-polarized light strikes the surface of a mirror-polished electrode? The component of the light parallel to the surface would induce an image dipole in the metal that opposes the incident field, whereas the perpendicular component would induce an image dipole that is aligned with the incident component. As a result, the phase of the reflected light will differ from that of the incident light, and this will depend on the orientational difference between the incident electric field and the induced dipole. Figure 6.24 shows this change of phase of the light upon reflection for perpendicular and parallel-polarized light.

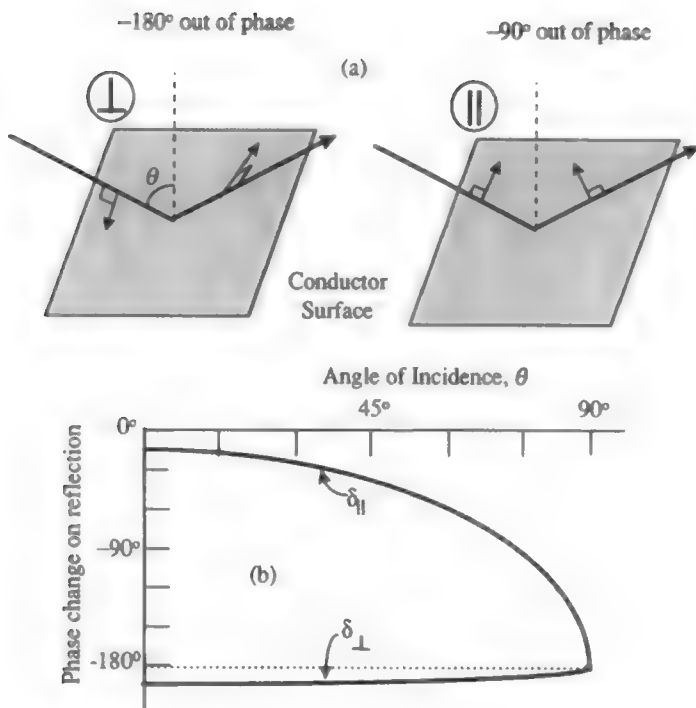


**Fig. 6.24.** (a) A representation of the phase change upon reflection at a large angle of incidence for perpendicular-polarized light, and parallel-polarized light. (b) The phase change upon reflection as a function of angle of incidence for both polarizations of light. (Reprinted with permission of the American Institute of Physics from R. G. Greenler, *J. Chem. Phys.* **44**:310, Figs. 1 and 2.)

It has been found also that this phase change depends on the incident angle ( $\theta$ ) of the light. At practically all angles of incidence, s-polarized light will suffer a phase shift of  $\sim 180^\circ$ , as shown in Fig. 6.24(a), and the net component at the surface resulting from the superposition of the incident and reflected vectors is zero. On the other hand, the effect on p-polarized light depends strongly on its incidence angle [Fig. 6.24(b)]. At small angles of incidence, the reflected light is phase shifted by only few degrees, but as the angle of incidence increases, the phase shift slowly increases. At large angles of incidence, the phase shift reaches  $90^\circ$  [Fig. 6.24(a)]. As a consequence, the net component of the light at the surface would also vary, having a minimum at a normal angle and increasing until reaching a maximum.

How would these differences in the net component of polarized light at the surface affect its interaction with adsorbed molecules? As discussed above, the net component at the surface when irradiated with perpendicular-polarized light would be zero at any angle of incidence, and therefore no interaction of s-polarized light with material on the surface would result. On the other hand, the net component of the parallel-polarized light will depend strongly on the angle of incidence and therefore its possible interaction with adsorbed molecules. At normal incidence ( $\theta \approx 0^\circ$ ) the net component is close to zero and there is negligible interaction of the light with material on the surface. As the angle increases, this interaction increases, and therefore the absorbance of the adsorbed molecules. It has been found that at high reflective surfaces, the detectability of the surface film has a maximum at an incident angle of  $79^\circ$ .

Therefore, as noted above, the resulting wave at the phase boundary will depend strongly on the optical properties of the substrate, the incidence angle of the light, and the polarization of the incident light. The conditions for high detectability at metals would be large angles of incidence with the use of p-polarized light.

How can these properties of light and the way it interacts with the surface be used to obtain information on adsorbed molecules in electrochemistry? The idea would be to use and combine the information obtained from experiments performed with either s- or p-polarized light. Since s-polarized light does not interact with molecules on the surface, it would carry information on the other molecules that it encountered in its path, i.e., only on molecules in solution. On the other hand, the reflected p-polarized light carries information on solution molecules, and may also contain information on the adsorbed film, depending on its incidence angle. Therefore, if the reflected beam is arranged so that the perpendicular mode of polarization (containing information from the solution) is subtracted from the parallel mode (containing information from the solution and from the surface), the result should be information from the molecules in the interfacial region, i.e., the region interesting to the electrochemist.

Another very important consequence due to the reflection rule described here is that only those fundamental vibrations of adsorbed species which have a finite value of the dipole derivative perpendicular to the surface can undergo interaction with the radiation. Consider a simple case of a diatomic molecule adsorbed on the surface (Fig. 6.25). When this molecule lies on the surface, its dipole moment is parallel to the

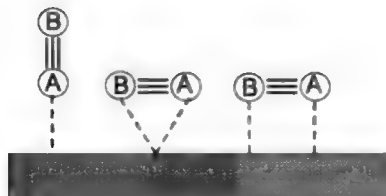


**Fig. 6.25.** Three possible orientations of  $A \equiv B$  molecule adsorbed on an electrode.

surface—no interaction between the incident light and the molecule occurs. On the other hand, if this molecule is standing, its dipole moment would be perpendicular to the surface and a full interaction would occur. Many times, there are changes in the orientation molecule when the electrode potential is changed. Studies of the IR-absorption spectra would allow these changes in species to be followed as a function of the electrode surface (see Section 7.3.1).

**6.2.6.2. Radiochemical Methods.** Radioactive isotopes are unstable atoms that decay to form other nuclides by emitting particles and electromagnetic radiation. These decay processes may occur in a period of microseconds to billions of years. These emitting particles, as found by the early researchers in the area (i.e., Marie and Pierre Curie and Rutherford), were found to be positively and negatively charged particles, as well as neutral particles. The names given to them were alpha, beta, and gamma particles.

The modern setup to study electrochemical adsorption processes by radiochemistry is based on the following idea. Radioactive molecules, preferentially  $\beta$ -emitters, and nonradioactive molecules exist in solution in a ratio specified by the experimenter. Usually this ratio is very small, on the order of 1 radioactive molecule for  $10^{11}$  nonradioactive molecules. The general idea is that when adsorption occurs on the electrode, a certain amount of the adsorbed molecules will be radioactive,<sup>15</sup> and they can be detected by a detector close to the electrode. The ratio of radioactive-adsorbed molecules to nonradioactive-adsorbed molecules is expected to be the same as in solution. Figure 6.26 shows a schematic representation of the measurement of adsorbed molecules using a radiochemical technique. Initially the electrode is in a position far from the detector, where the electrochemical reaction occurs, say, adsorption of ions on the electrode. Then, after the process is finished, the electrode is pushed against a glass scintillator. This is a piece of glass with specific compounds embedded in it, which get excited proportionally to the radioactivity in the nearby region; i.e.,

<sup>15</sup>The surface of the electrode is covered by about  $10^{15}$  molecules. If there is one radioactive molecule per  $10^{11}$  nonradioactive molecules, then there are approximately  $10^4$  radioactive molecules on the surface of the electrode.

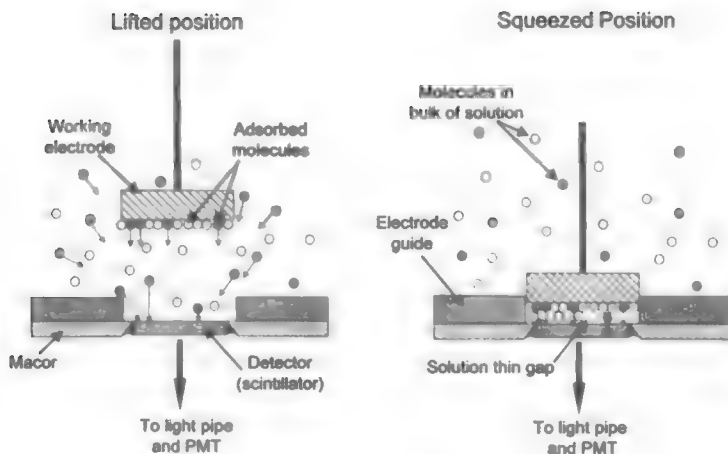


**Fig. 6.26.** Two electrode positions in a radiochemical technique. On the left, the electrode is lifted up for adsorbate equilibration and bulk counting rate measurement. On the right, the electrode is pressed down (squeezed) against the scintillator for surface counting rate measurement. (Reprinted with permission from M. E. Gamboa-Aldeco, K. Franaszczuk, and A. Wieckowski, "Radiotracer Study of Electrode Surfaces," in *Surface Imaging and Visualization*, A. T. Hubbard, ed., Ch. 46, CRC Press, Boca Raton, FL, p. 635, 1995, Fig. 46.4.)

the radioactive adsorbed molecules and the radioactive molecules in the solution trapped in the thin gap (Fig. 6.26). After becoming excited, the particles in the scintillator decay, producing flashes of light that are changed into electrons in the photomultiplier tube (PMT) beneath it. These electrons are proportional to the detected radiation and to a certain degree to the amount of material adsorbed on the electrode. The success of the experiment requires a mirror-polished electrode, so that the solution layer between the electrode and the glass scintillator is minimum, and the contribution of the radiation from solution molecules in the thin gap is reduced. The determination of the total surface concentration of adsorbed molecules (radioactive and nonradioactive),  $\Gamma$ , of an adsorbate can be obtained according to the following equation.<sup>16</sup>

$$\Gamma = \frac{N_{\text{ads}}}{N_{\text{bulk}}} \frac{N_A c 10^{-3}}{\mu f_b R e^{-\mu x}} \quad (6.8)$$

<sup>16</sup>In Section 6.4.2 we will find that  $\Gamma$  represents the Gibbs-surface excess, i.e.,  $\Gamma = N/A - N^0/A$ , where  $N^0$  is the number of molecules that would have been there if there had been no double layer, and  $N$  is the actual number of molecules in the interfacial region. However, when the bulk concentration of the species is small, i.e.,  $N^0 \rightarrow 0$ , then the number of adsorbed molecules tends to  $\Gamma$ , i.e.,  $\Gamma \rightarrow N/A$ .

where  $N_{\text{ads}}$  is the signal of radioactive molecules in the adsorbed state (counts  $\text{s}^{-1}$ ),  $N_{\text{bulk}}$  is the signal radioactive molecules in solution measured when the electrode is in the lifted position (counts  $\text{s}^{-1}$ ),  $N_{\text{A}}$  is Avogadro's number,  $c$  is the total concentration of the adsorbate in solution ( $\text{mol dm}^{-3}$ ),  $\mu$  is the linear absorption coefficient ( $\text{cm}^{-1}$ ),  $f_{\text{b}}$  is the backscattering factor that accounts for radiation reflected from the electrode toward the scintillator,  $R$  is the roughness factor of the electrode (real area / geometrical area), and  $x$  is the distance between the  **$\beta$ -emitter** and the scintillator, i.e., the gap distance between the electrode and the scintillator (cm).

What are the advantages of the radiochemical method compared with other *in situ* techniques? It offers a direct relationship between surface radiation ( $N_{\text{ads}}$ ) and surface concentration, which allows a direct measurement of the amount of adsorbed molecules on the electrode, a condition difficult to determine with other *in situ* techniques. The main limitation of the technique is the availability of radioactive forms of the compound the experimenter wants to study. In this respect, the type of radiation preferred is of the  **$\beta$ -type**, mainly because of the ease of detection and minimal safety hazards. Typical  **$\beta$ -emitters** used are  $^3\text{H}$ ,  $^{14}\text{C}$ ,  $^{35}\text{S}$ ,  $^{36}\text{Cl}$ , and  $^{32}\text{P}$ , which as constituents of molecules, open a great variability of compounds for study. Figure 6.21 shows some experimental results obtained for the measurement of adsorption on single crystals using this radiochemical method.

### 6.3. THE POTENTIAL DIFFERENCE ACROSS ELECTRIFIED INTERFACES

#### 6.3.1. What Happens When One Tries to Measure the Potential Difference Across a Single Electrode/Electrolyte Interface?

Consider the operations necessary to measure the potential difference across a metal/solution interface. Various potential-measuring instruments can be used: potentiometers, electrometers, etc. All these instruments have two metallic terminals that must be connected to the two points between which the potential difference is to be measured.

One terminal is connected directly to the electrode. But what does one do with the other terminal? It must be connected to the other phase, the potential of which is to be measured. This is the electrolyte. The second connecting wire has to be immersed in the solution (Fig. 6.27).

The connecting wires of potential-measuring devices are intended, however, to act as pure probes. They must be spectators of the potential scene. They must sense

<sup>17</sup> *Beta particles* consist of *electrons* traveling at very high speeds. These electrons do not come from the electron shield of the atoms, but from the nucleus itself. In the  **$\beta$ -decay** process, a neutron in the nucleus is transformed into a proton, an electron, and an antineutrino,  $\bar{\nu}$ . For example, the nucleus of  $^{14}\text{C}$  suffers the decay:  $^{14}_6\text{C} \rightarrow ^{14}_7\text{N} + ^0_{-1}\text{e} + \bar{\nu}$ . In this equation, the electron  $^0_{-1}\text{e}$  is called a  **$\beta^-$  particle**.

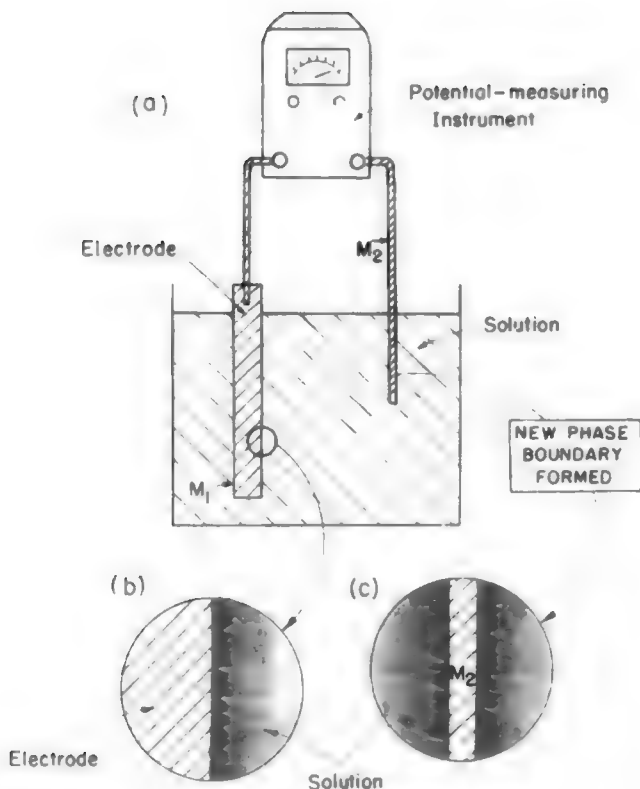


**Fig. 6.27.** (a) If the second terminal  $M_2$  of a potential-measuring instrument is dipped into the solution, an extra  $M_2$ /solution electrified interface is formed [see exploded view (c)] apart from the electrified electrode/solution interface under study [see exploded view (b)].

the potential without actively introducing any potential differences. But this is not possible because the immersion of the second connecting wire  $M_2$  in the electrolyte inevitably produces a new phase boundary, i.e., the  $M_2$ /solution interface (Fig. 6.27). At this interface, there must be a second double layer and a second metal/solution potential difference, i.e.,  $PD_{M_2/S}$ , which cannot be avoided.

Thus, the very operation of measurement cannot but involve a second double layer and a second potential difference. This is the difficulty. One sets out to measure one potential difference  $PD_{M_1/S}$  and in the attempt, one creates at least one additional potential difference. One ends up with the measurement of the sum of at least two potential differences (Fig. 6.28).

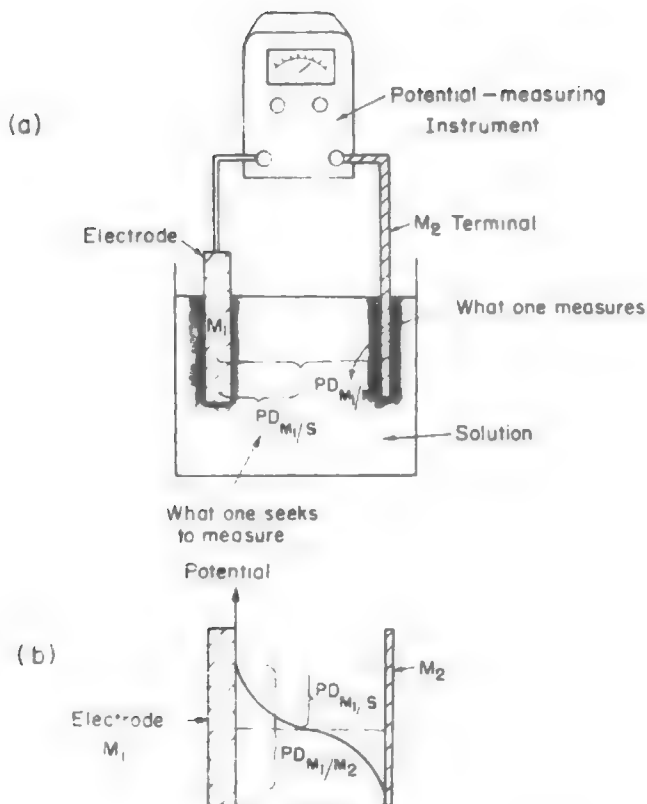


**Fig. 6.28.** (a) Though one seeks to measure the potential difference  $PD_{M_1/S}$  across the interface under study, one actually measures the potential difference  $PD_{M_1/M_2}$  across at least two interfaces  $M_1/S$  and  $M_2/S$ . (b) A schematic representation of the potential variation from electrode  $M_1$  to terminal  $M_2$ .

The system created by the measuring procedure is in fact an electrochemical system, or cell, consisting of two electronic conductors (electrodes) immersed in an ionic conductor (electrolyte). *All one can measure, in practice, is the potential difference across a system of interfaces, or a cell, not the potential difference across one electrode/electrolyte interface.*

In the particular cell (Fig. 6.28) generated by the measuring process, it will be only as a special case that the metal  $M_1$  (of the electrode/electrolyte interface under study) is identical with the metal  $M_2$  (the connecting wires of the measuring instrument). In general,  $M_1$  and  $M_2$  will be different metals, say, platinum and copper. The meeting of the platinum and copper phases produces another double layer and an

additional potential difference across the platinum/copper interface. This additional potential difference is known as the *contact potential difference*. Thus, the procedure of using a potential-measuring device has introduced, if  $M_1$  and  $M_2$  are dissimilar metals, two additional and unwanted potential differences (Fig. 6.29).

One can have more complicated cells (Fig. 6.30), and in all of them it can be seen that the attempted measurement of a metal-solution potential difference will conclude with the measurement of the sum of at least two interfacial potential differences, i.e., the desired  $PD_{M_1/S}$  and as many extra potential differences as there are new phase boundaries created in the measurement. In symbolic form, therefore, the potential difference  $V$  indicated by the measuring instrument can be expressed as

$$V = PD_{M_1/S} + \sum_{i=1}^n PD_i \quad (6.9)$$

where  $PD_i$  is the potential difference at the  $i$ th phase boundary created in the process of measurement, there being  $n \geq 1$  such phase boundaries. In the case of the particular system shown in Fig. 6.31, one has

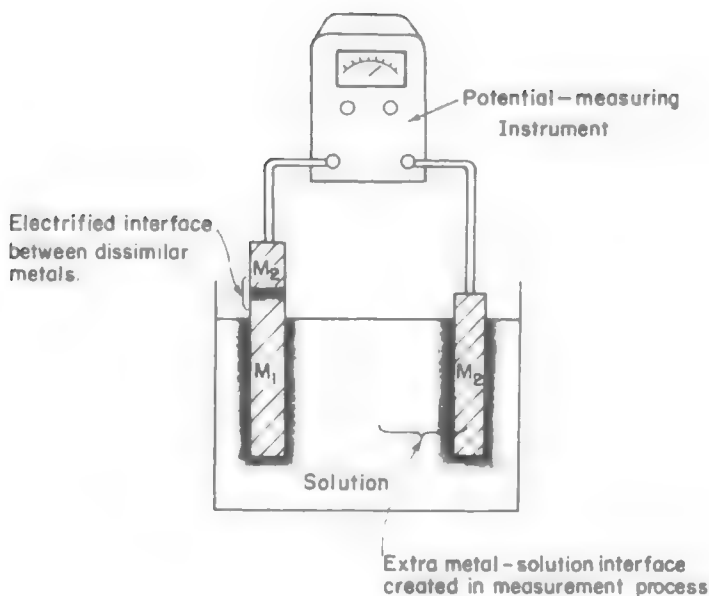


**Fig. 6.29.** If electrode  $M_1$  and the connecting wires  $M_2$  are dissimilar metals, a contact potential difference  $PD_{M_2/M_1}$  at the metal  $M_1$ /metal  $M_2$  interface is generated in the measurement process in addition to the extra metal-solution potential difference  $PD_{M_2/S}$ .



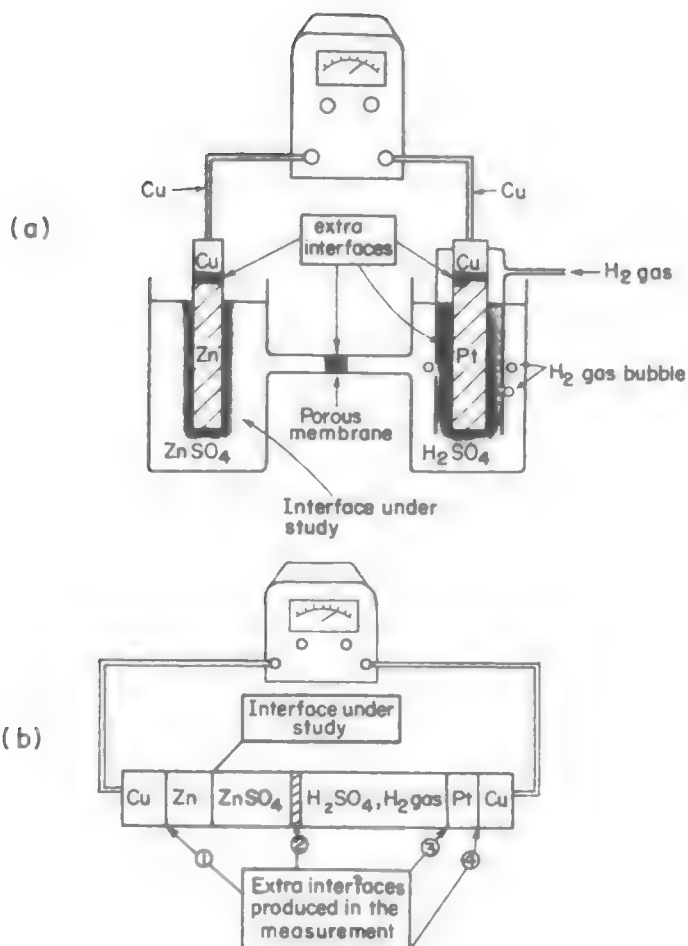


**Fig. 6.30.** (a) A more complex cell in which the two electrodes differ in nature from the copper connecting wires of the potential-measuring instrument. In addition, the solutions in contact with the two electrodes are different from each other and are separated by a porous membrane. (b) Another representation of the cell.

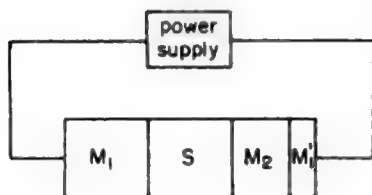


**Fig. 6.31.** A cell consisting of two metals  $M_1$  and  $M_2$  in contact with a solution  $S$ . The  $M_1'$  is a metal of the same composition as  $M_1$ .

$$V = PD_{M_1/S} + \sum_{i=1}^2 PD$$

$$= PD_{M_1/S} + PD_{S/M_2} + PD_{M_2/M_1} \quad (6.10)$$

The analysis of the process of measuring potential differences across phase boundaries demonstrates the impossibility of using standard potential measuring devices to determine the value of a single metal–solution potential difference. The electrochemist proceeds, therefore, somewhat humbled but not defeated. He or she must ask how much information about the potential difference across an electrode/electrolyte interface can be obtained.

### 6.3.2. Can One Measure Changes in the Metal–Solution Potential Difference?

In the preceding discussion, the electrochemical system was itself the origin of the potentials discussed, these potentials being measured by a device.

Consider now a situation where, instead of a measuring instrument, one inserts (Fig. 6.31) into the “circuit” a source of potential (e.g., an electronically regulated power supply). Here, the total potential difference across the cell must equal (in magnitude) that put out by the source.<sup>18</sup> This is, in fact, the law of conservation of energy applied to an electrical circuit, or Kirchhoff’s second law: The algebraic sum of all potential differences around a closed circuit must be equal to zero. For the simple hypothetical system shown in Fig. 6.32, one has

$$PD_{M_1/S} + PD_{S/M_2} + PD_{M_2/M_1'} + PD_{M_1'/M_1} = 0$$

<sup>18</sup> If a current passes through the electrolyte, the sum of potential differences will include an ohmic drop in addition to those at the interfaces. This potential difference due to the ohmic drop depends on the current  $I$  and the resistance  $R$  of the electrolyte and is equal to  $IR$ .

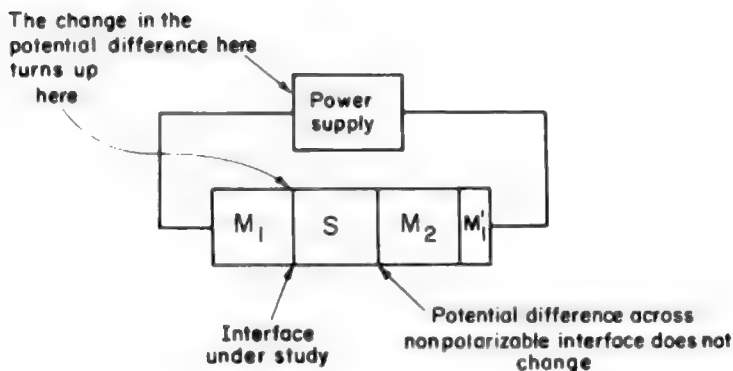


**Fig. 6.32.** By combining the  $M_1/S$  interface under study with a nonpolarizable  $M_2/S$  interface, changes in the potential difference across the source turn up at the interface under study.

or

$$PD_{M_1/S} + PD_{S/M_2} + PD_{M_2/M_1'} = -PD_{M_1'/M_1} = V \quad (6.11)$$

where, according to Kirchhoff's laws, the input potential  $V$  equals the potential difference  $PD_{M_1/M_1'}$  between the two metal leads.

Now, let the input potential<sup>19</sup> be changed by an amount  $\delta V$ . Since the changes in the potential of the source must be equal to the changes in potential in the system, one can write

$$\delta V = \delta PD_{M_1/S} - \delta PD_{M_2/S} + \delta PD_{M_2/M_1'} \quad (6.12)$$

It appears that the change  $\delta V$  at the source is distributed over all the interfaces and produces changes in the potential differences across them.

Imagine, however, at  $M_2/S$ , a nonpolarizable<sup>20</sup> interface (to be described further later) which is characterized by the fact that the potential across it does *not* change except under extreme "duress" (i.e., a large change in input potential). Then, for small changes  $\delta V$  at the external source, the potential difference across the nonpolarizable interface will not depart significantly from its "fixed" value, i.e.,

$$\delta PD_{M_2/S} = 0 \quad (6.13)$$

<sup>19</sup>For convenience of exposition, it is customary to use *potential* for the term "potential difference."

<sup>20</sup>To *polarize an interface* means to alter the potential difference across it; to be *polarizable* means to be susceptible to changes in potential difference. The quantitative definition of polarizability will be given in Section 7.7.1.

It is important to understand the way in which nonpolarizable interfaces resist changes in potential across them. A simple picture is as follows (a detailed description is given in Section 7.7.1) The potential variation across a double layer depends on the charge separation, or distribution, at the interface. The only way that the potential can change is by changing the magnitude of the charge on each side of the interface. Suppose, however, that any charge flowing into an interface from an external source promptly leaks across the interface; then the charge separation, and thus  $PD_{M_2/S}$ , stays constant. The interface has resisted changes in its potential. The more easily charges leak across the interface, the more resistant is the interface to changes in potential difference.

Further, the contact potential difference between two metals depends on the composition of the two metals and is unaffected by potential difference across the cell, and hence,

$$\delta PD_{M_2/M_1} = 0 \quad (6.14)$$

One can now resort to a simple artifice. Combine the interface under study,  $M_1/S$ , with an interface that resists changes in potential, i.e., a nonpolarizable interface  $M_2/S$  (Fig. 6.32). By using this electrochemical system, or cell, all changes in the potential of the source find their way to only one interface, i.e., that under study. An excellent method of producing changes in potential at one interface only has thus been devised. Then

$$\delta V \approx \delta PD_{M_1/S} \quad (6.15)$$

Of course, this argument implies that the  $M_1/S$  interface is completely polarizable. This is important. The point is that the power supply requires that the whole cell change its potential difference by an amount  $\delta V$ . Only if one interface is completely nonpolarizable and the other one completely polarizable can the latter wholly accept the changes of potential put out by the source. If both interfaces are partially nonpolarizable, then the potential differences across both of them will change and the experimenter will be at a loss to know the magnitude of the individual changes at each interface.

### 6.3.3. The Extreme Cases of Ideally Nonpolarizable and Polarizable Interfaces

Are nonpolarizable and polarizable interfaces fictions, or can one find them in the laboratory? The fact is that such interfaces can indeed be fabricated and have been used in double-layer studies. Of course, no interface is ideally nonpolarizable or ideally polarizable, i.e., nonpolarizable interfaces do change their potential to some extent and polarizable interfaces do resist such changes to some extent. The distinction is one of degree rather than kind.

What makes an interface polarizable? In other words, what makes an interface resist or accept potential changes? This question can be answered, but the answer has to be in terms of the rates at which charges transfer across the interface, i.e., in electrodic terms (see Section 7.2).

At this stage, therefore, an electrical analogy will be given. The electrical behavior of a metal/solution interface can be compared to that of a capacitor and resistor connected in parallel (Fig. 6.33). A circuit consisting of electrical components that simulates the electrical behavior of an electrified interface is referred to as an *equivalent circuit*. To understand the difference between nonpolarizable and polarizable interfaces in terms of a model consisting of a capacitor and resistor connected in parallel, consider what happens when the capacitor–resistor combination is connected to a source of potential difference. If the resistance is very high, then the capacitor charges up to the value of the potential difference put out by the source; this is the behavior of a polarizable interface. If, on the other hand, the resistance in parallel with the capacitor is low, then any attempt to change the potential difference across the capacitor is compensated by the charge's leaking through the low-resistance path; this is the behavior of a nonpolarizable interface.

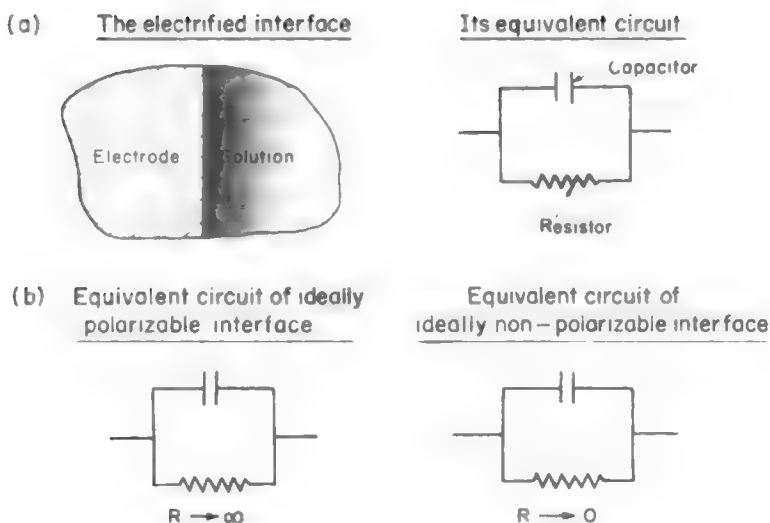


**Fig. 6.33.** (a) The equivalent circuit for an electrified interface is a capacitor and resistor connected in parallel. (b) In the equivalent circuit for an ideally polarizable interface, the resistance tends to infinity, and for a nonpolarizable interface, the resistance tends to zero.

### 6.3.4. The Development of a Scale of Relative Potential Differences

The essential feature of a nonpolarizable interface is that the potential difference across it remains effectively a constant as the potential applied to a cell that contains the nonpolarizable electrode changes. This property of nonpolarizable interfaces can be taken advantage of to develop a scale of relative potential differences across interfaces.

Thus, suppose that when one wishes to measure an interfacial potential difference  $PD_{M_1/S}$ , one connects the electrode with another electrode and measures the potential of this cell. Suppose one always keeps this second electrode constant in nature (i.e., the algebraic sum of the potentials associated with it is kept constant). Then, measurements of the potential of a cell in which the one (same) electrode and its associated solution were always present and the other [i.e., the first electrode mentioned here ( $M_1$ )] and its solution were changed would clearly reflect the changing interfacial potential difference  $PD_{M_1/S}$ . This is in fact what is done to measure the relative values of  $PD_{M_1/S}$  as  $M_1$  or  $S$  (or both) are varied.

It has long been a convention in this field to utilize an electrode at which the potentials are controlled by the reaction of the exchange of  $H^+$  between the solution and  $H_2$  gas, through the medium of a highly nonpolarizable interface, which exchanges electrons between  $H^+$  and  $H_2$  according to  $2H^+ + 2e_0 \rightleftharpoons H_2$  [gas]. This is called the *reversible hydrogen electrode (RHE)*. It will give rise to the same potential contribution to the cell as long as the hydrogen-ion activity in the solution and the pressure of  $H_2$  with which this is in equilibrium are kept always the same. The values chosen are unit activity for the hydrogen ion and unit pressure for the hydrogen gas. (Fig. 6.34).

Electrode potentials are measured by coupling electrodes in a cell, the second electrode of which is a certain constant one. The one that is chosen is usually a hydrogen electrode, as described previously.<sup>21</sup> It is then the potentials of such cells that are called *relative electrode potentials* or *potentials of electrodes on the standard hydrogen scale*. What is meant is that by an arbitrary convention, these particular cell potentials are no longer called *cell potentials* but relative electrode potentials, and, indeed, the word "relative" is often dropped because those in the know realize what is meant.

The above discussion has been given as may perhaps have been gathered, a little bit with tongue in cheek; it is not quite complete. The reason is that it started talking about absolute potential differences (i.e., the  $PD_{M_1/S}$ ) and then with a slight change in phraseology slid into an electrode potential.

<sup>21</sup>However, at least two other reference electrodes, calomel (Fig. 7.42) and silver-silver chloride electrodes, are in common use as secondary reference electrodes (they are easier to set up than the hydrogen reference electrode). Potentials of electrodes measured using one of the secondary reference electrodes can be directly converted to values on the hydrogen scale, if the potential of the secondary reference electrode with respect to the hydrogen electrode is known (see also Section 7.5.7.3).

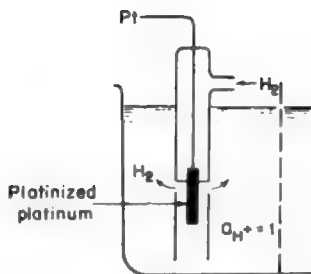


**Fig. 6.34.** The nonpolarizable standard hydrogen electrode.

Is electrode potential the same as  $PD_{M_1/S}$ , the potential difference of the metal/solution interface? The fact that it is not has already been implied in Eq. (6.11). An electrochemical cell consists of at least four potential differences.

Equation (6.11) may be repeated here in a slightly different form:

$$PD_{M_1/S} + PD_{S/M_{ref}} + PD_{M_{ref}/M_1'} = -PD_{M_1'/M_1} = V \quad (6.16)$$

The  $V$  is the voltmeter reading. The question to ask, therefore, is: What potentials are maintained constant when one measures a number of electrode potential in cells that always contain a standard hydrogen electrode (SHE)?

The answer to this question is relatively simple if one breaks down  $PD_{M_{ref}/M_1'}$  into two potentials,  $\phi_{M_{ref}}$  and  $\phi_{M_1'}$ . Then (6.16) becomes

$$(PD_{M_1/S} - \phi_{M_1'}) + \phi_{ref} + PD_{S/M_{ref}} = V \quad (6.17)$$

The part that is constant in the relative scale of potentials is therefore

$$\phi_{ref} + PD_{S/M_{ref}}$$

When one refers to the relative electrode potentials of a number of systems on the hydrogen scale and then equates these with the potentials of the cells made up of the systems (the electrode-solution systems concerned) in combination with a hydrogen electrode, the situation is that one is arbitrarily taking the constant

$$PD_{S/M_{ref}} + \phi_{ref} = 0 \quad (6.18)$$

Of course, if this constant is taken as zero for all the metals with which the potentials of the other systems are compared, there will be no effect of this constant, but one may never forget that the relative electrode potential, to which reference is so often made, is in fact *not* a metal-solution potential difference.

Before we leave this rather complicated subject, it is a good idea to point out what an electrode potential *is* rather than what it is not. Unfortunately, it is not a simple

thing at all. An electrode potential is not a metal–solution potential difference, not even on some arbitrary or relative scale; it is a combination of two potential differences, one at the metal/solution interface and the other part of (one may think of half the span of a bridge) the metal–metal potential difference in a cell (Fig. 6.35).

### 6.3.5. Can One Meaningfully Analyze an Electrode–Electrolyte Potential Difference?

The discussion so far can be summarized as follows: The value of the potential difference across a single electrode/electrolyte interface cannot be measured with potential measuring instruments. The sum of the potential differences across at least

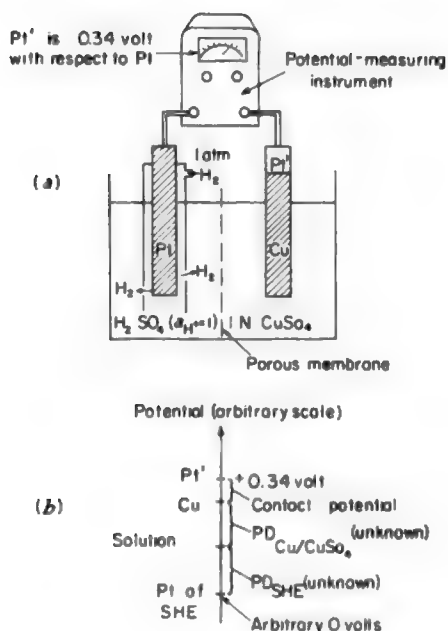


**Fig. 6.35.** The meaning of the relative potential difference across the  $\text{Cu}/\text{CuSO}_4$  interface, i.e., the relative electrode potential. (a) The electrochemical cell corresponding to the relative potential difference. (b) The relative potential difference includes a platinum–copper contact potential and the unknown potential difference across the SHE, apart from the absolute potential difference across the  $\text{Cu}/\text{CuSO}_4$  interface.



two interfaces (i.e., across an electrochemical cell) can be measured. Further, changes in the potential difference across any one interface can be measured provided the interface under study can be built into a system or cell, the other interface being a nonpolarizable one across which there is a constant potential difference.

Does the impossibility of measurement of a quantity preclude further thought about it? Discussion of a concept, even if it cannot be measured, often leads to better understanding of it. With this view, attempts will be made to probe further into the question of the absolute potential difference across an individual metal/solution interface.

Can the potential difference across an interface be “structured,” or separated into contributions? This potential difference depends on the arrangement of charges, oriented dipoles, etc. Can one speak of separate contributions to the total potential difference from the excess charges on the metal and solution phases, on the one hand, and from the oriented dipoles, on the other? Perhaps these individual contributions can be measured or calculated. Thereafter, one may be able to add them together to calculate the elusive metal–solution potential difference.

Consider a thought experiment in which the interface is conceptually disassembled in the following manner: The two phases are separated and each is placed in vacuum. Let the metal and solution phases now be charged to the extent they were charged in the presence of a double layer, i.e., before the interface was disassembled. What one has at this point is two isolated charged phases in vacuum. The process of carrying a unit test charge from infinity in vacuum toward each charged phase will now be analyzed.

The electric forces operating on the test charge consist basically of two types. First there are those forces that originate in Coulomb’s law. At large distances from the electrode, the potential will arise entirely from this long-range interactions of the charge in the electrode and the charge on the unit charge.<sup>22</sup> This potential is plotted in

---

<sup>22</sup> A point charge  $q$  in a vacuum exerts an electric force  $\vec{F}$  on charges ( $q'$ ) in the surrounding space. It produces an electric field  $\vec{X}$ , given by

$$\vec{X} = \frac{\vec{F}}{q} \quad \text{or} \quad \vec{X} = \frac{1}{4\pi\epsilon_0} \frac{q'}{r^2} \quad \left[ \frac{\text{newton}}{\text{coulomb}} \right] \quad (6.19)$$

where  $r$  is the distance between the charges  $q'$  and  $q$ . The potential energy,  $U$ , of the unit charge,  $q$ , in a point  $P$  in the electric field  $\vec{X}$  is defined as the work done to bring the unit charge in such a field from infinity to the point  $P$ ,

$$U = - \int_{\infty}^P q \vec{X} \cos \theta dx \quad [\text{joule}] \quad (6.20)$$

where  $\theta$  is the angle between the tangent of the trajectory of the test charge,  $dx$ , and the electric field  $\vec{X}$ . The potential at any point  $P$  on the electric field  $\vec{X}$  for the unit charge  $q$  is

$$\psi = \frac{U}{q} = - \int_{\infty}^P \vec{X} \cos \theta dx \quad [\text{volt}] \quad (6.21)$$

Fig. 6.36 as a function of the logarithm of the distance from the metal surface.<sup>23</sup> In this example it was assumed that the electrode is a flat one of  $1 \text{ cm}^2$  area and a charge of  $+3.11 \times 10^{-13} \text{ C}$ , so that the maximum contribution of this potential is 1 V.

At short distances from the surface of the electrode, the potential of the test particle will not be that given only by the Coulomb potential, but will be the sum of this potential and various potentials arising from short-range interactions, e.g., between the particle and its electrical image, between the particle and the dipole layer in the surface (see Section 6.3.8), and the dispersion interactions. That of longest range is the one due to image forces<sup>24</sup>.

What are the nature of these image interactions? When a charge approaches a material phase, it induces an equal and opposite charge on the surface of the material (Fig. 6.37). The spatial distribution of the induced charge is a complicated affair, and therefore the calculation of the interaction between the test charge and the metal is not simple. However, one can resort to a simple device: The metal is replaced by an "electrostatic mirror" located in the same position as the metal surface, in which case the test charge will have an image charge of equal magnitude and opposite sign as far behind the mirror as the test charge is in front of it (Fig. 6.37). The image interaction between the test charge and the metal is given by the Coulombic interaction between the test charge and the fictitious image charge.<sup>25</sup>

Thus, the image force acting on an unit charge  $q$  is

$$\vec{F}_{\text{image}} = -\frac{1}{4\pi\epsilon_0} \frac{|q q_{\text{image}}|}{4r^2} \quad (6.22)$$

The corresponding electrical field due to the fictitious charge is

$$\vec{X}_{\text{image}} = -\frac{1}{4\pi\epsilon_0} \frac{|q_{\text{image}}|}{4r^2} \quad (6.23)$$

and the potential of the unit charge  $q$  at a distance  $r$  from the metal surface (Fig. 6.37) due to this  $\vec{X}_{\text{image}}$  is

$$\Psi_{\text{image}} = -\int_{\infty}^r \vec{X} \, dr = \int_{\infty}^r \frac{1}{4\pi\epsilon_0} \frac{|q|}{4r^2} \, dr = -\frac{1}{4\pi\epsilon_0} \frac{|q|}{4r} \quad (6.24)$$

<sup>23</sup>To make the comparison with the image forces clearer, the charge of the electrode is taken as positive in such a way that the Coulombic forces are of repulsive character. Image forces are always of attractive character.

<sup>24</sup>Dispersion forces between a particle and the surface vary with  $x^{-6}$ .

<sup>25</sup>The image charge does not have physical reality in the sense of a well-defined unit charge moving inside the metal in accordance with the movement of the test charge toward the metal. It is a mathematical device, proved rigorously to be valid, by which simple equations can be derived that correctly describe the complex effect of an approaching test charge on the actual charge distribution in the metal.

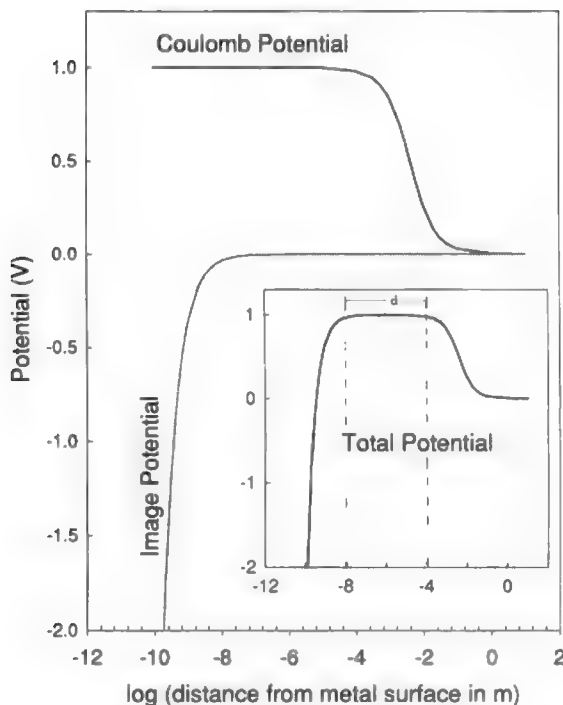


**Fig. 6.36.** Coulomb, image, and total potential in the interfacial region.

The negative sign in Eq. (6.24) indicates that this potential is of an attractive character.

Figure 6.36 shows the corresponding image potential, and the insert in the same figure shows the total potential, which is given by the sum of the Coulombic and image potentials. Thus, at very short distances from the surface, the potential due to the image force is dominant. At long distances, the Coulombic force determines the potential. There is an intermediate distance,  $d$ , where the contribution due to the image force is negligible, and the potential is that due to Coulombic forces alone. It is in this region,  $10^{-8} \text{ m} < x < 10^{-4} \text{ m}$ , that a test charge would experience the constant potential that is characteristic of the surface at a given charge density and negligibly affected by image interactions.

Now, it is very important that in the thought experiment, the unit charge being transported only test (or “probe”) the charge on the metal. The unit test charge must not itself interact with the metal; it should only sense the charge on the metal. It must be a spectator, not an actor. From this point of view, it is clear that when the test charge is involved in image interactions, it is not taking a detached view of the charge on the electrode. Thus, as long as the test charge is sufficiently far away from the phase, the

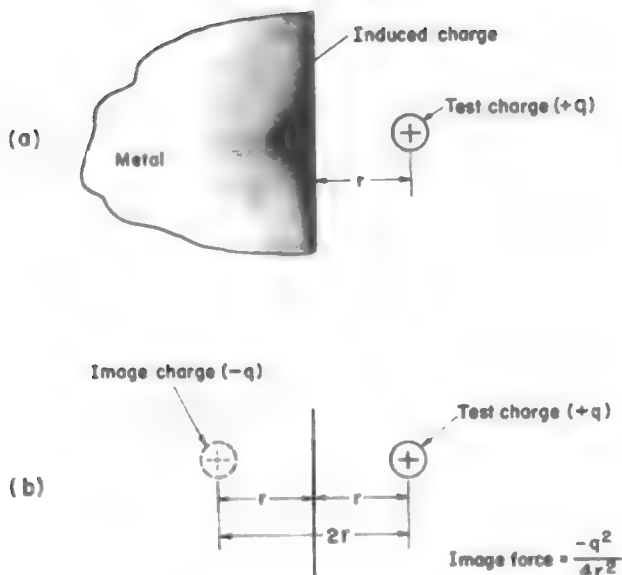


**Fig. 6.37.** When a charge comes near a material (e.g., a metal) it induces a charge that is distributed in a complicated way. (b) The interaction between the test and induced charges can be calculated by considering that the metal is replaced by an image charge (equal in magnitude and opposite in sign to the test charge) situated as far behind the plane corresponding to the metal surface as the test charge is in front of it.

Coulombic force characteristic of the electrode dominates. The closer the test charge comes to the phase, the greater becomes the magnitude of the short-range image interaction. The distance at which the short-range image forces start to become significant is on the order of  $10^{-8}$  m.

### 6.3.6. The Outer Potential $\psi$ of a Material Phase in a Vacuum

It may be recalled that the work done in bringing a unit test charge along the  $x$ -axis from infinity up to a point  $P$  defines the potential at the point. [cf. Eq. (6.21)]. Thus,

$$\text{Potential} = \psi = - \int_{\infty}^P \vec{F}_x dx \quad (6.25)$$

Consider that the point  $P$  is a point in vacuum and just outside the reach of the image-force interactions arising from the presence of the electrode. Then the work

done in bringing a unit test charge from infinity up to the point  $P$  and hence the potential at this point, is determined purely by the charge on the electrode and is not influenced by any image interactions between the test charge and the electrode. At the same time [Fig. 6.36], it is independent of distance. This potential just outside the charged electrode is termed, for obvious reasons, the *outer potential*. It is also referred to as the *psi ( $\psi$ ) potential* (Fig. 6.38).

### 6.3.7. The Outer Potential Difference, ${}^M\Delta^S\psi$ , between the Metal and the Solution

In Section 6.3.5, a real electrified interface was thought of as dismantled into two parts, a solution part and a metal part. Further, in a pure thought experiment, these two parts were imagined as placed separately in vacuum. Then (in Section 6.3.6) a unit test charge was brought to a point just outside the charged metal, and the outer potential, or  $\psi$  potential, was defined. But there is also the charged solution phase to be considered. Here, too, a unit test charge can be used to define the outer potential (Fig. 6.39).

Thus, by carrying out two thought experiments, one involving the electrode in a vacuum and the other the electrolyte in a vacuum, one obtains two outer potentials. The outer potential due to the charge on the metal electrode is termed  $\psi_M$  and that due to the charge on the electrolytic solution,  $\psi_S$ .

At this stage, let the two conceptually separated parts of the double layer be brought together again. The interface has been reassembled. One can now refer to the outer potential difference, sometimes called the *Volta potential difference*, between the metal and solution. This outer potential difference is written

$${}^M\Delta^S\psi = \psi_M - \psi_S \quad (6.26)$$

What is the physical significance of  ${}^M\Delta^S\psi$ ? The conditions of the thought experiment may be recalled. After separating the metal and solution phases, the phases were charged to the same extent that they would be if the double layer existed.

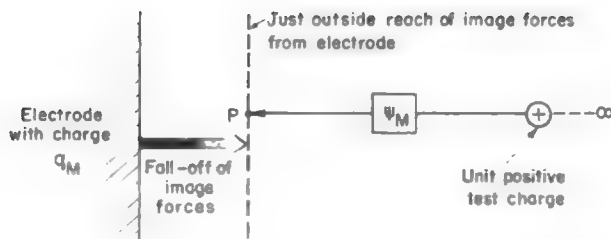


**Fig. 6.38.** The outer,  $\psi_M$  potential of the electrode is the work done to bring a unit of positive charge from infinity to a point  $P$  just outside the reach of the image forces from the electrode.

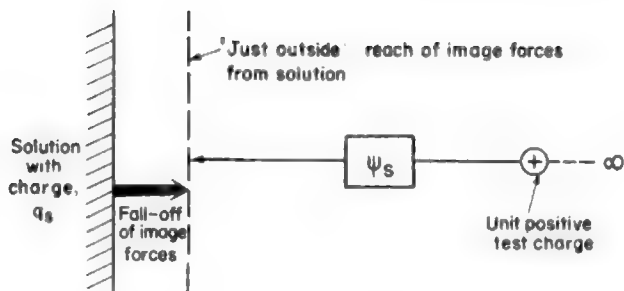


**Fig. 6.39.** The outer, or  $\psi_s$ , potential of the solution is the work done to bring a unit of positive charge from infinity to a point  $P$  just outside the reach of the image forces from the solution.

Hence, the  $\psi$  potentials of the metal and solution phases correspond to the charges that these phases actually have in the presence of the double layer at a metal/solution interface. The outer potential difference  ${}^M\Delta^S\psi$  is, therefore, the contribution to the potential difference across an electrified interface arising from the charges on the two phases.

The Volta potential difference is a quantity that can be measured experimentally (see Appendix 6.1). Further, if one chooses a plausible model of the arrangement of charges at the interface, the Volta potential difference can be calculated by simple electrostatic reasoning [see Eq. (6.118)]. It is for these reasons that the outer potential is an important aspect of the study of the electrified interface.

### 6.3.8. The Surface Potential, $\chi$ , of a Material Phase in a Vacuum

The basic picture of an electrified interface at an electrolyte boundary (Section 6.1.7) is now recalled. In general, not only is there charge separation, but there is also the possibility of a net preferential orientation of dipoles in the interphase region (Lange and Miscenko). When dipoles are tacked together so that more of them point one way than another (i.e., there is a net orientation), the arrangement is equivalent to a charge separation and therefore a potential difference occurs across the dipole layer. This dipole potential is an integral part of the potential difference across an electrified interface. Hence, the outer potential difference  ${}^M\Delta^S\psi$  is not the only contribution to the electrode-electrolyte potential difference; the dipole contribution must also be analyzed and added to the Volta potential to give the total electrode-electrolyte potential difference.

How can this dipole potential be visualized? Once again a thought experiment can be performed. The electrode and electrolyte phases are conceptually detached from each other and the double layer “turned off.” In this process, the excess charges and oriented-dipole layers that characterized the double layer are considered eliminated.

For the definition of the outer potential, the appropriate amounts of charge were then conferred on the two separated phases. Here, a layer of solvent dipoles will be fixed on the electrolyte so that the net orientation and the number per unit area of dipoles corresponds to that obtaining on the solution side of the double layer.

From this point on, the thought experiment proceeds as in Section 6.3.6 (Fig. 6.40). A test charge is brought in from infinity toward the dipole layer and then made to just cross it.<sup>26</sup> The work done in this process defines a potential. This potential has nothing to do with the excess charge on the solution phase because during the thought experiment, the excess charge on the solution phase is maintained at a value of zero. Since the work has to do with traversing a surface layer on the electrolyte, the corresponding potential is a *surface potential*. Equally, because the potential is that associated with a dipole layer, it may be termed a *dipole potential*. It is also referred to as a *chi* ( $\chi$ ) *potential*.

In the case of the electrolytic solution, what has been defined here is its surface potential  $\chi_s$ . Is there a  $\chi$  potential for a metal electrode? This question arises from the fact that in conceptually dismantling the interface and then transferring the oriented dipoles, one has placed all the oriented solvent dipoles on the electrolyte and left none on the metal. Does this mean that the metal has no surface potential, i.e.,  $\chi_M = 0$ , because it has no dipole layer? At first sight, this seems to be the case.

Further consideration, however, reveals that even in the case of a metal, there is what might be termed a dipole layer. The situation is roughly as follows (Fig. 6.41): The physical surface of the metal tries to confine the free electrons inside the metal. It is as if the electrons are in “potential wells.” But electrons have the characteristic of being able to penetrate potential barriers. If they succeed, a positive charge is left behind for every electron jumping out of the metal. This is tantamount to a charge separation and a dipole layer. Thus, there is a surface potential for metals, too, and therefore a  $\chi_M$  (see Section 6.6.8).

### 6.3.9. The Dipole Potential Difference ${}^M\Delta^S\chi$ across an Electrode–Electrolyte Interface

The two surface potentials  $\chi_s$  and  $\chi_M$  represent the work done to carry a unit test charge from infinity in a vacuum through and just across the dipole layers at the surfaces of an uncharged electrolyte and an uncharged metal. If, now, the electrode and solution phases are brought together, there will be dipole layers in the two phases. The work done to take a test charge across both these dipole layers is given by the difference of the two  $\chi$  potentials. Hence, this difference

$${}^M\Delta^S\chi = \chi_M - \chi_s \quad (6.27)$$

<sup>26</sup>Once the test charge enters the phase, it will begin to interact with the atoms and molecules of the phase. Such interactions and the corresponding work terms are excluded from the dipole potential since they are considered separately in the definition of the chemical potential (Section 6.3.13.1).

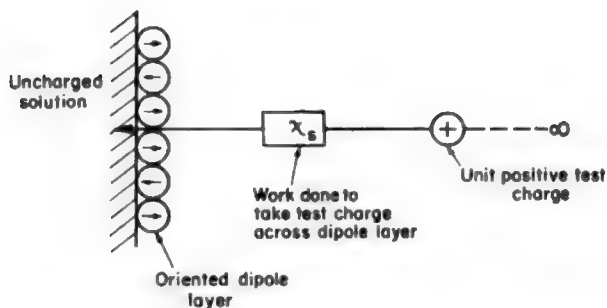


**Fig. 6.40.** The surface, or dipole, or  $\chi_s$ , potential of the solution is the work done to bring a unit of positive charge from infinity and take it across the oriented-dipole layer of the solution.

is the dipole contribution to the potential difference across the interface.

By conceiving a model for the dipole layers, it is possible to make some rough calculations for the individual surface potentials (see Section 7.4.30). In this presentation of surface potentials,  $\chi_M$  and  $\chi_s$  were conceived when both phases, the metal and the solution, were taken apart and placed separately in a vacuum. However, when there is a metal in contact with a solution (neither of the phases is in contact with a

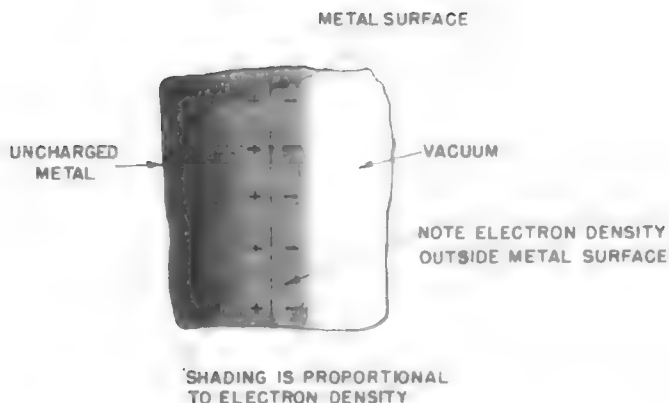


**Fig. 6.41.** A schematic representation of the origin of the surface, or  $\chi$ , potential of a metal. Because of the finite probability of an electron's being found outside the metal surface, the electron density decays to zero outside the metal. This phenomenon is equivalent to the formation of a dipole layer across the metal surface.



vacuum), the corresponding surface potentials,  $\chi^M$  and  $\chi^S$ , are in reality  $g^M$  and  $g^S$ , and the surface potential difference becomes,

$${}^M\Delta^S g = g^M - g^S \quad (6.28)$$

instead of  ${}^M\Delta^S \chi$ . The correlations between the surface potential in a vacuum and that in a solution are  $g^M = \chi^M + \delta\chi^M$  and  $g^S = \chi^S + \delta\chi^S$ , where  $\delta\chi^M$  and  $\delta\chi^S$  are the changes in the surface potential of the metal and solution arising upon contact between the phases (see Section 6.7.6). The surface potential difference is then

$${}^M\Delta^S g = \chi^M - \chi^S + \delta\chi^M - \delta\chi^S \equiv \chi^M - \chi^S + \delta\chi \quad (6.29)$$

where  $\delta\chi = \delta\chi^M - \delta\chi^S$  is the term that takes into account the changes in the orientation of the solvent dipoles and the electron overlap at the metal surface when the two phases are brought in contact with each other.

### 6.3.10. The Sum of the Potential Differences Due to Charges and Dipoles: The Inner Potential Difference, ${}^M\Delta^S \phi$

The result of the two thought experiments can be summarized thus: One experiment yielded the potential difference at an electrified interface arising only from the charges; the other experiment yielded the potential difference arising only from the dipole layers. The former was the  $\Delta\psi$  potential and the latter, the  $\Delta\chi$  potential. Thus, a conceptual separation of the charge and dipole contributions to the total potential has been achieved.

From the point of view of the outer and surface potentials, the charge separation and dipole orientation are the only two sources of a potential difference across an electrified interface and therefore the two contributions can be summed to give the total potential across the electrode/electrolyte interface

$$\begin{array}{l} \text{Total metal-solution potential difference} \\ \text{with respect to an uncharged infinite} \end{array} \equiv \Delta\phi = \Delta\psi + \Delta\chi \quad (6.30)$$

The term used for this total potential difference across an electrified interface is the *Galvani potential* or *inner potential difference*, and the symbol used is  $\Delta\phi$ .

The outer,  $\psi$ , and surface,  $\chi$ , potentials were conceived in two thought experiments, one involving a charged, dipole-free phase in vacuum and the other, an uncharged, dipole-covered phase in vacuum. What does the synthesis of these two imaginary situations represent? Obviously, it can be represented in terms of another thought experiment in which the phases constituting the interface are separated, the double layer is turned off, and the phases are charged and wrapped with a dipole layer (Fig. 6.42). The work done to transport a test charge from infinity to a point outside the charged phase defines the outer potential  $\psi$ ; the subsequent work done in taking the charge through the surface dipole layer defines the surface potential  $\chi$ .

Where is the test charge at this stage of the thought experiment? It is inside the material phase (Fig. 6.43). Thus, the work done to bring a unit test charge from infinity

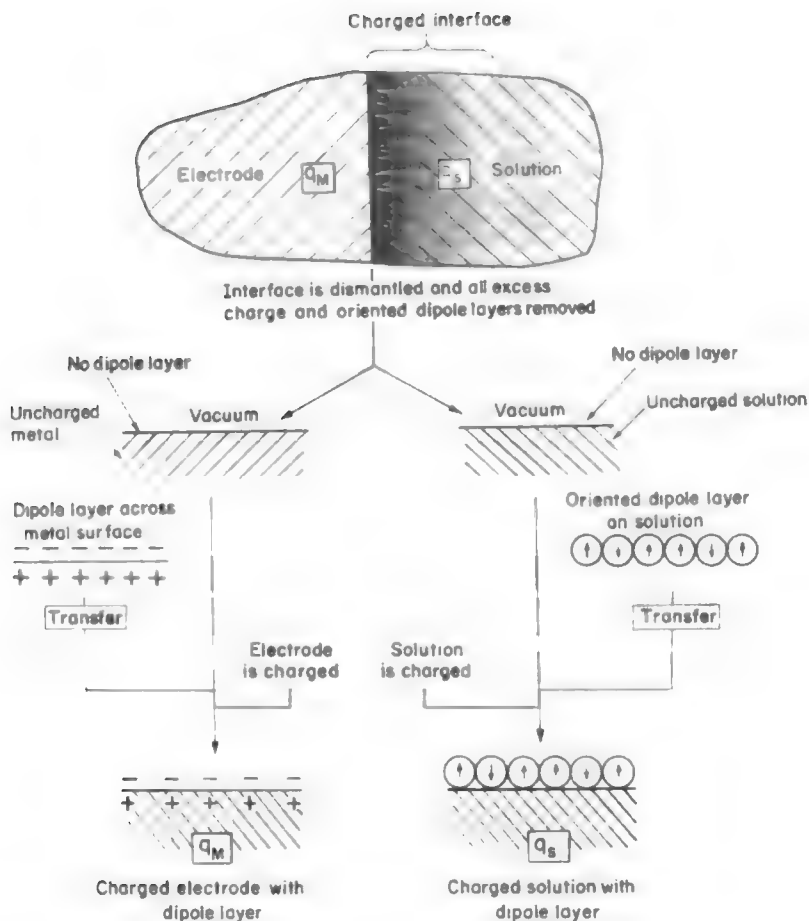


**Fig 6.42.** A thought experiment to define the total potential involves the following steps performed upon an electrified interface: (1) The interface is dismantled, and all excess charges and dipole layers are removed from the two phases. (2) Each phase is charged and covered with a dipole layer to reestablish its condition before the interface was dismantled.

across the charged surface covered with a dipole layer to a point inside<sup>27</sup> the phase is the inner potential  $\phi$ , the sum of the outer  $\psi$  and surface  $\chi$  potentials, i.e.,

$$\phi = \psi + \chi \quad (6.31)$$

<sup>27</sup>Even though the test charge is inside the phase, its interactions with the material of the phase are not included in the definition of the  $\phi$  potential, but are reserved for the computation of the chemical potential (see Section 6.3.13.1).

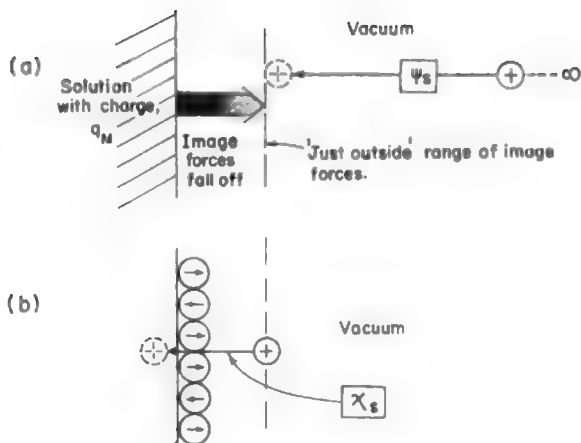


**Fig. 6.43.** The two stages of getting the inner, or  $\phi$ , potential: (a) The work done to bring a unit of positive test charge from infinity to a point just outside the range of the image forces defines the outer, or  $\psi$ , potential. (b) The charge on the solution is then removed, and the solution is wrapped in an oriented-dipole layer. The work done to transport the test charge across the oriented-dipole layer defines the surface, or,  $\chi$ , potential. Thus, the total work to bring the test charge from infinity to a point just inside the solution is given by  $\phi_s = \psi_s + \chi_s$ .

or

$$\text{Inner potential} = \text{outer potential} + \text{surface potential} \quad (6.32)$$

### 6.3.11. The Outer, Surface, and Inner Potential Differences

As long as test charges stand aloof from the potential scene and only measure it, the potential is measurable. This aloofness is guaranteed as long as the test charges are outside the material phases, i.e., where they do not interact with the particles of the material phases. Only the measurement of the outer potential satisfies this criterion. Hence, it is only the  $\psi$  potential and, correspondingly,  $\Delta\psi$ , which can be experimentally measured.

As for the surface potential  $\chi$ , it is the result of a thought experiment involving the transport of a unit test charge across a dipole layer. The final step in its journey is to a point on the inside “fence” of the double layer. If, now, the test charge looks in a direction away from the surface and toward the interior of the phase, there lies the

material medium (e.g., the electrolyte) with its particles, each one of which may interact with the test charge.

These interactions with the bulk of the phase (e.g., the electrolyte) have been tacitly ignored in the definition of the  $\chi$  potential. If test charge is an ion [e.g., all the ion-solvent (Chapter 2) and ion-ion (Chapter 3) interactions with the electrolyte bulk are switched off], this operation is possible only in a thought experiment. Hence, no direct physical operation can be prescribed for testing or probing or measuring the  $\chi$  potential inside a material phase, e.g., the electrolyte. One can probe potentials inside matter only with material probes which themselves interact with matter and thus invalidate the whole probing process.

Since surface potentials are not measurable, any quantity that includes them is also not measurable. The inner potential  $\phi$  is one such quantity since

$$\phi = \psi + \chi \quad (6.33)$$

Hence, the inner potential cannot be measured.

The argument just presented can be extended to the differences of the various potentials. The outer potential difference  $\Delta\psi$  can be measured (Klein and Lange; Appendix 6.1); the surface potential difference  $\Delta\chi$  cannot; and therefore the inner potential differences  $\Delta\phi = \Delta\psi + \Delta\chi$  also cannot be experimentally obtained.

### 6.3.12. Is the Inner Potential Difference an Absolute Potential Difference?

Knowledge of absolute electrode potentials would be of great usefulness in electrochemistry. It would allow us to predict the direction of electron flow when two electrodes are brought into electrical contact, as those in the cell in Fig. 6.29.

As explained in Section 6.3.11, the inner potential difference— $\Delta\phi$ —seems to encompass all the sources of potential differences across an electrified interface— $\Delta\chi$  and  $\Delta\psi$ —and therefore it can be considered as a total (or “absolute”) potential across the electrode/electrolyte interface. However, is the inner potential a practical potential? First, the inner potential cannot be experimentally measured (Section 6.3.11). Second, its zero point or reference state is an electron at rest at infinite separation from all charges (Sections 6.3.6 and 6.3.8), a reference state impossible to reach experimentally. Third, it involves the electrostatic potential within the interior of the phase relative to the uncharged infinity, but it does not include any term describing the interactions of the electron when it is inside the conducting electrode. Thus, going back to the question posed before, the inner potential can be considered as a kind of “absolute” potential, but it is not useful in practical experiments. Separation of its components,  $\Delta\chi$  and  $\Delta\psi$ , helped in understanding the nature of the potential drop across the metal/solution interface, but it failed when we tried to measure it and use it to predict, for example, the direction of reactions. Does this mean then that the electrochemist is defeated and unable to obtain absolute potentials of electrodes?

Fortunately not, but to measure the absolute potential at an interface, another reference state would have to be used, as well as the nature of the metal-electron interactions. Later, in Chapter 8, it will be shown that relevant calculations can be made of this difference of inner potentials (sometimes called the *Galvani potential difference*), but their accuracy is on the order of  $\pm 0.1$  V, which is not yet enough to compensate for our lack of ability to measure the quantity. In the next sections, some useful concepts will be described and in Section 6.7.2 we will return to the concept of absolute electrode potential and the possibility of creating a scale of practical absolute-electrode potentials.

### 6.3.13. The Electrochemical Potential, the Total Work from Infinity to Bulk

**6.3.13.1. Definition of Electrochemical Potential.** To understand the potential difference across an electrified interface, thought experiments were used to consider the work done in moving unit test charges. The following potentials emerged from the analysis: (1) the outer, or  $\psi$ , potential arising from the work done to transport a unit test charge to a point just outside a charged but dipole layer-free phase; (2) the surface, or  $\chi$ , potential arising from the work done to carry the unit charge across the dipole layer at the surface of an uncharged phase; (3) the inner, or  $\phi$ , potential arising from the work done to carry the test charge from infinity up to and across the dipole layer at a charged phase. In defining the  $\chi$  and  $\phi$  potentials, the test charges were prohibited from interacting with the bulk of the phases.

Now, what will happen if the material phase (e.g., the electrolytic solution) is imagined to be bereft of either surface charge or a surface dipole layer? Consider a thought experiment (Fig. 6.44) involving the transport of a test charge from infinity to a point deep inside the solution phase. The outer, or  $\psi$ , potential will be zero because the solution is uncharged. Similarly, the surface, or  $\chi$ , potential will be zero because there are no surface dipole layers. Hence, the inner, or  $\phi$ , potential will also be zero, which means that zero *electrical* work is done with the test charge.

But once the test charge begins to be affected by all the interactions due to the particles in the solution, work will have to be done to take it inside the solution. What interactions are these? The test charge will feel, for instance, ion-solvent interactions, ion-ion interactions, and the repercussions of solvent-solvent interactions. All these interactions can be lumped together and called *chemical*. In the thought experiment, therefore, one can use the chemical work (i.e., the work done against all these interactions with the particles of the material phase) to define the chemical, or  $\mu$ , potential (see Chapter 3). The chemical potential  $\mu_i$  of a particular species  $i$  is the work done to bring a mole of  $i$  particles from infinity into the bulk of an uncharged, dipole layer-free material phase.

Thus, a test charge not only interacts with the charges and dipole layers on the surface of the phases forming the interface, but it also interacts with the bulk of the phases. What, therefore, is the total work in taking a mole of charges from infinity in

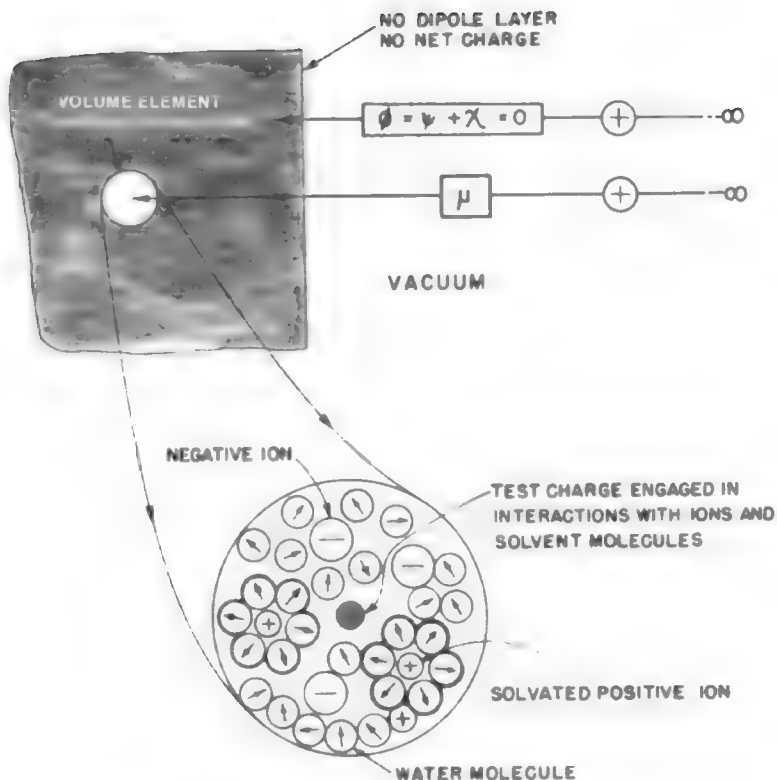


**Fig. 6.44.** A thought experiment for the definition of the chemical potential  $\mu$ . An uncharged solution without an oriented-dipole layer on its surface is taken. The work done to transport a unit of positive test charge from infinity into the interior of the phase is the chemical potential  $\mu$  of the phase. The electrical work  $\phi = \psi + \chi$  is zero because there is no charge and no oriented-dipole layer on the surface of the solution.

vacuum into the bulk of the material phase? It is the synthesis of the result of two thought experiments, one involving a material phase without either charges or dipole layer on the surface and the other involving only the charges and the dipole layer. The total work is the sum of the chemical work and the electrical work, i.e.

Total work = chemical work + electrical work per mole of charges

The symbol used for this catchall total work is the electrochemical potential  $\bar{\mu}$ . Hence,

$$\bar{\mu} = \mu + zF\phi = \mu + zF(\psi + \chi) \quad (6.34)$$

The factor  $zF\phi$  arises because  $\phi$  is the electrical work to bring a unit charge,  $z_i e_0 \phi$  is the electrical work to transport *one* particle bearing a charge  $z_i e_0$ , and  $N_A z_i e_0 \phi = z_i F \phi$

is the electrical work to bring an Avogadro number  $N_A$  of particles inside the material phases.

The electrochemical potential  $\bar{\mu}_i$  includes all types of work involved in bringing particles<sup>28</sup> (of charges  $z_i e_0$ ) into material phases. Nothing is left out. The  $\bar{\mu}$  includes the chemical work  $\mu$ , the charge contribution  $\psi$ , and the dipole contribution  $\chi$ .

The concept of electrochemical potential arose frequently in earlier chapters (e.g. Chapter 4). Just as the gradient of the chemical potential ( $\partial\mu/\partial x$  for the  $x$  component of this gradient) acts as the driving force in pure diffusion and the gradient of the electric potential ( $d\phi/dx$ ) acts as the driving force in pure conduction, the gradient of the electrochemical potential ( $\partial\bar{\mu}/\partial x$  for the  $x$  component) can be considered the total driving force for the transport of a charged species, the total transport process consisting of both diffusion and conduction. In the present context, instead of approaching the concept of electrochemical potential through the facts of transport, it has been arrived at in a discussion of the work done in transporting a charge into a phase.

**6.3.13.2. Can the Chemical and Electrical Work Be Determined Separately?** In the case of transport processes, the total driving force for the flow of a particular species  $j$ , i.e., the gradient of electrochemical potential,  $\partial\bar{\mu}_j/\partial x$ , was considered split up into a chemical (diffusive) driving force  $\partial\mu_j/\partial x$  and an electrical driving force for conduction,  $z_j F d\phi/dx$ ,

$$\frac{\partial\bar{\mu}_j}{\partial x} = \frac{\partial\mu_j}{\partial x} + z_j F \frac{d\phi}{dx} \quad (6.35)$$

It was also possible to set up experimental conditions in which either  $\partial\mu_j/\partial x$  or  $z_j F d\phi/dx$  could be reduced to zero. For example, by switching off the externally applied field,  $d\phi/dx$  inside the electrolyte could be reduced to zero. Similarly, by avoiding a concentration gradient inside the electrolyte,  $\partial\mu_j/\partial x$  can be directed to zero. Thus, the gradients of the chemical potential and the electric potential, i.e., the chemical and electrical driving forces, could be determined separately.

Separation into chemical and electrical terms is possible with gradients but not with quantities, i.e.,  $\mu_j$  and  $\phi$ , themselves. The reason is simple. The electrochemical potential  $\bar{\mu}_j$  was only conceptually separated into a chemical term  $\mu_j$  and an electrical term  $z_j F \phi$ . The conceptual separation was based on thought experiments; in practice, no experimental arrangement can be devised to correspond to the thought experiment described in Section 6.3.13.1. Thus, e.g., one cannot switch off the charges and dipole layer at the surface of a solution as one can switch off the externally applied field in a transport experiment. Only the combined effect of  $\mu_j$  and  $z_j F \phi$  can be determined.

<sup>28</sup>If the particles are uncharged, then  $z_i = 0$  and  $\bar{\mu}_i = \mu_i$ .

**6.3.13.3. A Criterion of Thermodynamic Equilibrium between Two Phases: Equality of Electrochemical Potentials.** It has been stated that the total driving force responsible for the flow or transport of a species  $j$  is the gradient  $d\bar{\mu}_j/dx$  of its electrochemical potential. However, when there is net flow or flux of any species, this means that the system is not at equilibrium. Conversely, for the system to be at equilibrium, it is essential that there be no drift of any species—hence, that there should be zero gradients for the electrochemical potentials of all the species. It follows, therefore, that, for an interface to be at equilibrium, the gradients of electrochemical potential of the various species must be zero across the phase boundary, i.e.,

$$\frac{d\bar{\mu}_j}{dx} = 0 \quad (6.36)$$

By integration, it follows that the value of the electrochemical potential of a species  $j$  must be the same on both sides of the interface, i.e.,

$$(\bar{\mu}_j)_M = (\bar{\mu}_j)_S \quad (6.37)$$

In other words, the change in electrochemical potential in transporting the species from one phase to the other must be zero, i.e.,

$$\Delta\bar{\mu}_j = 0 \quad (6.38)$$

Now, the electrochemical potential  $\bar{\mu}_j$  of the species  $j$  in a particular phase is the change in free energy of the system<sup>29</sup> resulting from the introduction of a mole of  $j$  particles into the phase while keeping the other conditions constant, i.e.,

$$\bar{\mu}_j = \left( \frac{\partial \bar{G}}{\partial n_j} \right)_{T, p, n_{i \neq j}} \quad (6.39)$$

Hence, the equality of electrochemical potentials on either side of the phase boundary implies that the change in free energy of the system resulting from the transfer of particles from one phase to the other should be the same as that due to the transfer in the other direction. This is only another way of stating that when a thermodynamic system is at equilibrium, its free energy is a minimum, i.e.,

$$d\bar{G} = 0 \quad (6.40)$$

This is a well-known thermodynamic truth.

<sup>29</sup>More rigorously, the electrochemical free energy  $\bar{G}$  should be used here. This is related to the free energy in the same way as the electrochemical potential  $\bar{\mu}$  is related to the chemical potential  $\mu$ .



**6.3.13.4. Nonpolarizable Interfaces and Thermodynamic Equilibrium.** It has just been shown that for an interface to be in thermodynamic equilibrium, the electrochemical potentials of all the species must be the same in both the phases constituting the interface. Since the difference in electrochemical potential of a species  $i$  between two phases is the work done to carry a mole of this species from one phase (e.g., the electrode) to the other (e.g., the solution), it must be the same as the work in the opposite direction. This implies a free flow of species across the interface. However, an interface that maintains an “open border” is none other than a nonpolarizable interface (see Section 6.3.3).

A simple conclusion follows: *Thermodynamic equilibrium exists at a nonpolarizable interface.* Hence, one can immediately apply the criterion of thermodynamic equilibrium to a nonpolarizable interface. That is, from Eq. (6.38),

$$\begin{aligned} {}^S\Delta^M\bar{\mu}_j &= {}^S\Delta^M(\mu_j + z_jF\phi) \\ &= {}^S\Delta^M\mu_j + z_jF{}^S\Delta^M\phi \\ &= 0 \end{aligned} \quad (6.41)$$

where  $j$  is the species that is exchanged across the nonpolarizable interface.<sup>30</sup> Hence,

$${}^S\Delta^M\phi = -\frac{1}{z_jF} {}^S\Delta^M\mu_j \quad (6.42)$$

or

$$d({}^S\Delta^M\phi) = -\frac{1}{z_jF} d\mu_j \quad (6.43)$$

This equation may be utilized whenever a nonpolarizable interface is treated.

### 6.3.14. The Electron Work Function, Another Interfacial Potential

Consider an uncharged metal and an electron “just outside” the metal.<sup>31</sup> The change of energy at a given temperature and pressure when the electron moves from the point “just outside” to the point inside the metal defines the binding energy of the electron to the material.<sup>32</sup> Consider now the reverse process, that is, when the electron

<sup>30</sup>When  $j$  is the species that is exchanged across the nonpolarizable interface (i.e., the species involved in the charge-transfer reaction leading to the leakage of charge across the interface), it is customary to say that the interface, or the electrode, is *reversible* with respect to the species  $j$ .

<sup>31</sup>The term “just outside” was discussed in Section 6.3.5 and refers to a point outside the electrode, out of the reach of its image forces.

<sup>32</sup>This process also defines the partial molar free energy of the electron.

moves from inside the metal to a point just outside it (Fig. 6.45). The energy involved is the same as in the first process, but with a reversed sign. This latest process, from the metal to just outside it, is what it is called the *work function* of the metal, represented by the symbol  $\Phi$ . This is a measurable quantity and it is a characteristic property of the phase.

At first sight it would look as if the definition of surface potential ( $\chi$ ) described in Section 6.4.8 would overlap with the definition of the work function. Does this mean that both quantities are the same but with opposite signs? To answer this question, let us look closer to the trajectory of the electron as defined in the work function (Fig. 6.45). The electron starts in a point deep inside the metal, where all different types of chemical bondings and interactions exist. After breaking all these forces, the electron moves itself free from inside the metal to a point close to the surface. Then, from here it has to cross the barrier of dipoles (see Section 6.3.8) to reach a point just outside the metal.

The first part of its trajectory involves short-range interactions of a chemical nature, and therefore these are usually called *chemical effects*. However, these chemical effects are nothing else than the chemical potential ( $\mu$ ),<sup>33</sup> of the electron with opposite sign (see Section 6.3.13).

On the other hand, the second part of the trajectory of the electron, the crossing of the dipole layer, defines an electrical part. This contribution is exactly what was defined as the surface contribution due to dipoles, i.e., the surface potential,  $\chi$ , but with opposite sign. Thus, the work function as described here has two contributions,

$$\Phi^M = -\mu_e^M - zF\chi^M \quad (6.44)$$

or, since the particle considered here is the electron,

$$\Phi^M = -\mu_e^M + F\chi^M \quad (6.45)$$

Is there any relevance of this new potential, work function, to electrochemistry? The main idea is that because of its nature, the work function can be considered “fingerprints” of individual metals. If the electrode studied is a metal, then the work function is expected to be a relevant physical property in electrochemistry. It is involved in all electrochemical processes and accounts for effects observed on metals with different surface orientations. An example of these effects is given in Fig. 6.46. Obviously, different metals would have different chemical potentials, and that would account for the different values of  $\Phi$  in Fig. 6.46. But what about the differences observed, for example, for two of the crystalline faces of silver (Ag)? For both crystals  $\mu_e$  is clearly the same; thus the work function difference arises from different dipole layers at surfaces with different surface geometry. Another important involvement of  $\Phi$  in electrochemistry is in the determination of the “absolute electrode potential,” as will be explained in the next section.

<sup>33</sup>Remember that it was established at the beginning of this section that the electrode is uncharged. Therefore  $\tilde{\mu}^M = \mu^M$  [see Eq. (6.34)].

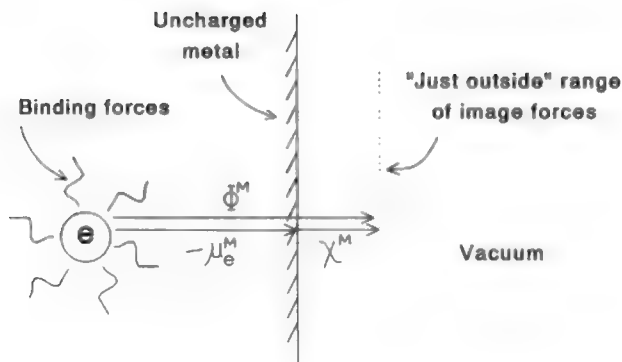


**Fig. 6.45.** The work function of a conductive material,  $\Phi_M$ , is the energy involved in moving an electron from inside the material to a point just outside it.

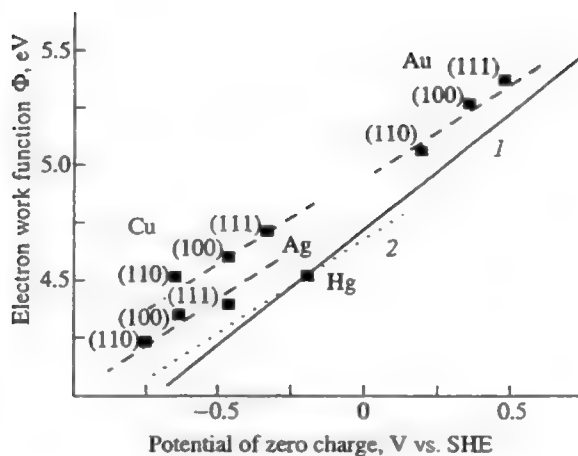


**Fig. 6.46.** Plot of the potential of zero charge vs. the electron work function for different crystal faces of silver (Ag), gold (Au), and copper (Cu) electrodes. (Reprinted from S. Trasatti, *Russ. J. Electrochem.* 31(8): 713, 1995, Fig. 3.)

### 6.3.15. The Absolute Electrode Potential

6.3.15.1. *Definition of Absolute Electrode Potential.* Consider the electrochemical system (see Fig. 6.29)

$$\text{M}|\text{S}|\text{R}|\text{M}' \quad (6.46)$$

where R is a reference electrode,  $\text{M}'$  and M are probes of the same metal, and S represents the solution phase. For this cell the measured cell potential difference is customarily written as [see Eq. (6.11)],<sup>34</sup>

$$V = PD_{\text{M}/\text{S}} - PD_{\text{R}/\text{S}} = E^{\text{M}} - E^{\text{R}} \quad (6.47)$$

where  $V$  is the electrochemical potential of M relative to R.  $V$  measures the work to bring a test charge from one electrode to another. Since electrons are the entities that move around in the external circuit, electrons will be taken as test charges. If each separate potential,  $E^{\text{M}}$  and  $E^{\text{R}}$ , could be measured with respect to a universal reference system, completely independent of any additional metal/solution interface, then, it would be possible to define an absolute electrode potential scale. Thus, Eq. (6.47) could be written as

$$V = E^{\text{M}}(\text{abs}) - E^{\text{R}}(\text{abs}) \quad (6.48)$$

with each one of these potentials,  $E^{\text{M}}(\text{abs})$  and  $E^{\text{R}}(\text{abs})$ , referred to this universal reference system. Thus, the problem of defining an absolute electrode potential consists in finding an appropriate reference level for electrons, independent of other electrodes.

Consider again the electrode potential difference,  $V$ , of the cell diagram of Eq. (6.46). It can be written as the energy difference of the electrons between the two electrodes through the external circuit:

$$V = - \frac{\tilde{\mu}_{\text{e}}^{\text{M}} - \tilde{\mu}_{\text{e}}^{\text{M}'}}{F} \quad (6.49)$$

where  $\tilde{\mu}_{\text{e}}$  is the electrochemical potential of the electron. According to Eq. (6.34),  $\tilde{\mu}_{\text{e}}$  can be written as

$$\tilde{\mu}_{\text{e}} = \mu_{\text{e}} - F\phi \quad (6.50)$$

where  $\mu_{\text{e}}$  is the chemical potential of the electron, and  $\phi$  is the inner electric potential. The sign in the second part of the equation is negative to account for the fact that the test charge considered here is the electron. The constant  $F$  has been included here to

<sup>34</sup>In Eq. (6.47) it is assumed that  $PD_{\text{R}/\text{M}'} \cong 0$ .

account for an Avogadro number  $N_A$  of electrons in the system. Therefore, Eq. (6.49) transforms into

$$V = - \left[ \left( \frac{\mu_e^M}{F} - \phi^M \right) - \left( \frac{\mu_e^{M'}}{F} - \phi^{M'} \right) \right] \quad (6.51)$$

However, the system is in equilibrium, and both materials, M and  $M'$ , are the same. Thus, their chemical potentials are the same, i.e.,

$$\mu_e^M = \mu_e^{M'} \quad (6.52)$$

Thus,

$$V = \phi^M - \phi^{M'} \quad (6.53)$$

This is an important relationship, and it defines the cell potential,  $V$ , as the difference in the inner potentials of phases M and  $M'$ .

In order to make the various components explicit, consider now the path of the electrons in the inside circuit, which goes from M to  $M'$ , not through the outside wire, but through the solution. In its traveling, the electron has to cross at least three interfaces, M/S, S/R, and  $R/M'$  [see Eq.(6.46)]. The potential is the same, independent of the path followed, thus, Eq. (6.53) can be written as

$$V = {}^M\Delta^{M'}\phi = {}^M\Delta^S\phi + {}^S\Delta^R\phi + {}^R\Delta^{M'}\phi \quad (6.54)$$

At the  $R/M'$  interface there is electronic equilibrium, and their electrochemical potentials are the same. Therefore,  $\tilde{\mu}_e^{M'} = \tilde{\mu}_e^R$ , and from the definition of  $\tilde{\mu}$  [see Eq. (6.34)],

$$\mu_e^{M'} - F\phi^{M'} = \mu_e^R - F\phi^R \quad (6.55)$$

or

$${}^R\Delta^{M'}\phi = \frac{\mu_e^R - \mu_e^{M'}}{F} = \frac{\mu_e^R - \mu_e^M}{F} \quad (6.56)$$

since  $\mu_e^{M'} = \mu_e^M$  [see Eq. (6.52)]. Substituting Eq. (6.56) into Eq. (6.54) and rearranging terms,

$$V = \left( {}^M\Delta^S\phi - \frac{\mu_e^M}{F} \right) - \left( {}^R\Delta^S\phi - \frac{\mu_e^R}{F} \right) \quad (6.57)$$

Comparing Eq. (6.57) with Eq. (6.48) leads to

$$E^M(\text{abs}) = {}^M\Delta^S\phi - \frac{\mu_e^M}{F} \quad (6.58)$$

This equation defines the absolute electrode potential (Bockris and Argade, 1968). Table 6.1 shows a summary of the different definitions of potential that have been discussed and that are found in electrochemical systems.

**6.3.15.2. Is It Possible to Measure the Absolute Potential?** Up to now a very important step has been given. We have defined the absolute potential. However, is it possible to experimentally determine values of  $E^M(\text{abs})$  for electrode systems?

It is understood that it would not be necessary to determine values of  $E^M(\text{abs})$  for all the existing electrode reactions. According to Eq. (6.48), if we could manage to determine at least one electrode system, say,  $E^R(\text{abs})$ , then, by measuring  $V$ , it would be possible to obtain the values of other systems, i.e., other  $E^M(\text{abs})$ . Since the hydrogen reaction has been already used to obtain the relative scale of electrode potentials (Section 6.3.4), it would be very convenient if the absolute value for this reaction could be determined. In this way we could simply add or subtract to the absolute potential of this reaction,  $E_{\text{H}_2/\text{H}^+}^0(\text{abs})$ , the appropriate values of a given

**TABLE 6.1**  
**Potentials at the Metal–Solution Interphase<sup>a</sup>**

Metal–Solution Potential Difference	$PD_{ij}$ ( $i, j$ phases in contact)	$PD_{M/S} = \Sigma$ potential contributions
Potential difference indicated by the instrument	$V$	$V = \Sigma PD_{i,j}$
Outer potential or Volta potential	$\psi$	The potential “just outside” (out of the reach of image forces) the charged phase. Depends purely on the phase charge
Surface potential or dipole potential	$\chi, g$	The potential due to the net preferential orientation of dipoles in the interphase region
Inner potential or Galvani potential	$\phi$	$\phi = \psi + \chi$
Electrochemical potential	$\tilde{\mu}$	$\tilde{\mu} = \mu + zF\phi = \mu + zF(\psi + \chi)$
Electron work function	$\Phi$	$\Phi^M = -\mu_e^M - zF\chi^M$
Absolute electrode potential	$E(\text{abs})$	$E^R(\text{abs}) = {}^R\Delta^S\phi - \frac{\mu_e^R}{F} = \frac{\Phi^M}{F} - \chi^S - V_{\text{pzc}}$

<sup>a</sup>The unit for potential is the volt (V).

reaction according to the table of relative potentials (see Section 6.3.4) to obtain the corresponding absolute potential.

Thus, a more appropriate question to ask is: Is it possible to measure the absolute potential of the hydrogen reaction,  $E_{\text{H}_2/\text{H}^+}^{\circ}(\text{abs})$ ? Actually it is possible. Remembering the definition of a standard hydrogen electrode potential (see Section 6.3.4), this was defined as the potential obtained when a metal comes in contact with a solution containing  $\text{H}^+$  under thermodynamically reversible conditions at unit activity, and  $\text{H}_2$  at 1 atm, at 298 K. As to the identity of the metal base, it can in principle be any metal at which it is possible to observe the reaction  $\frac{1}{2}\text{H}_2 \rightleftharpoons \text{H}^+ + \text{e}$  taking place at equilibrium. In practice, the metals used as substrates can only be noble metals because most other metals enter into equilibria with their own species in solution. Usually platinum is the metal chosen.

Now, to evaluate the absolute value of the electrode reaction, consider the cell in Eq. (6.46), with the  $\text{H}_2/\text{H}^+$  reaction taking place on, say, a platinum electrode as the reference electrode, and under conditions of  $q_{\text{M}} = 0$ . At these conditions the potential is known as the potential of zero charge, or  $pzc$  (see Section 6.5.6). Then, Eq. (6.54) can be written as

$$V_{pzc} = ({}^{\text{M}}\Delta^{\text{M}'}\phi)_{pzc} = ({}^{\text{M}}\Delta^{\text{S}}\phi)_{pzc} + {}^{\text{S}}\Delta^{\text{R}}\phi + {}^{\text{R}}\Delta^{\text{M}'}\phi \quad (6.59)$$

At  $q = 0$  the surface outer potential is zero, i.e.,  $({}^{\text{M}}\Delta^{\text{S}}\psi)_{pzc} = 0$  (see Section 6.3.7) and thus  $({}^{\text{M}}\Delta^{\text{S}}\phi)_{pzc} = {}^{\text{M}}\Delta^{\text{S}}\chi$  (see Section 6.3.11). From this consideration, and from Eq. (6.56), Eq. (6.59) becomes

$$V_{pzc} = (\chi^{\text{M}} - \chi^{\text{S}}) + \left( \frac{\mu_{\text{e}}^{\text{R}} - \mu_{\text{e}}^{\text{M}'}}{F} \right) + {}^{\text{S}}\Delta^{\text{R}}\phi \quad (6.60)$$

However, from the definition of work function,  $\Phi^{\text{M}} = F\chi^{\text{M}} - \mu_{\text{e}}^{\text{M}}$  (remember that  $\mu^{\text{M}} = \mu^{\text{M}'}$  because they are the same material) [see Eq. (6.45)], and then

$$V_{pzc} = \frac{\Phi^{\text{M}}}{F} - \chi^{\text{S}} + \frac{\mu_{\text{e}}^{\text{R}}}{F} + {}^{\text{S}}\Delta^{\text{R}}\phi \quad (6.61)$$

Therefore, from Eqs. (6.58) and (6.61),

$$E(\text{abs}) \equiv {}^{\text{R}}\Delta^{\text{S}}\phi - \frac{\mu_{\text{e}}^{\text{R}}}{F} = \frac{\Phi^{\text{M}}}{F} - \chi^{\text{S}} - V_{pzc} \quad (6.62)$$

Equation (6.62) indicates that  $E(\text{abs})$  can be obtained from measurements of work function and an estimation of the value of  $\chi^{\text{S}}$ <sup>35</sup> (Bockris and Argade, 1968) and from the value of the cell potential at the  $pzc$  ( $V_{pzc}$ ).

Several determinations of  $E_{\text{H}_2/\text{H}^+}^{\circ}(\text{abs})$  have been carried out in different laboratories, and different values have emerged. Scientists in the area are still elucidating

<sup>35</sup>It was established before that  $\chi$  cannot be determined experimentally. However, indirect estimation of this value is possible. It is on the order of 0.06 V. Therefore the error involved in the determination of  $E(\text{abs})$  if the term  $\chi^{\text{S}}$  could not be taken into account would be on the order of  $\pm 0.06$  V.

which value would be the correct one. The discussion has dropped so far to a range of values for the standard hydrogen reaction between 4.44 V and 4.78 V. The difference does not seem to be very large, but electrochemists interested in this area are not ready to leave this subject yet (see Chapter 8).

## Further Reading

### Seminal

1. W. Gibbs, *Collected Works: The Scientific Papers of J. Willard Gibbs* Vol 1: *Thermodynamics*, Dover, New York (1961).
2. A. Frumkin and A. Gorodetskaya, "Electrocapillary Phenomena with Amalgams," *Z. Phys. Chem.* **136**: 451 (1928).
3. E. Lange and K. P. Miščenko, "On the Thermodynamics of Ionic Solvation," *Z. Phys. Chem.* **A149**: 1 (1930).
4. R. Parsons, "Equilibrium Properties of Electrified Interphases," in *Modern Aspects of Electrochemistry*, J. O'M. Bockris and B. E. Conway, eds. Vol. 1, p. 103, Butterworths, London (1954).
5. J. E. B. Randies, "Real Hydration Energies from Ions," *Trans. Faraday Soc.* **52**: 1573 (1956).
6. J. O'M. Bockris and S. D. Argade, "Work Function of Metals and the Potential at which They Have Zero Charge in Contact with Solutions," *J. Chem. Phys.* **49**: 5133 (1968).
7. S. U. M. Khan, R. C. Kainthla, and J. O'M. Bockris, "The Redox Potential and the Fermi Level in Solution," *J. Phys. Chem.* **91**: 5974 (1987).

### Reviews

1. R. Parsons, "The Single Electrode Potential: Its Significance and Calculation" and "Standard Electrode Potentials: Units, Conventions and Methods of Determination," in *Standard Potentials in Aqueous Solution*, A. J. Bard, R. Parsons, and J. Jordan, eds. Chs. 1 and 2, Marcel Dekker, New York (1985).
2. S. Trasatti, "The Absolute Electrode Potential: An Explanatory Note," *Pure & Appl. Chem.* **58**(7): 955 (1986).
3. Howard Reiss, "The Absolute Electrode Potential—Tying the Loose Ends," *J. Electrochem. Soc.: Reviews and News* **135**: 247C (1988).

### Papers

1. S. Trasatti, *Electrochimica Acta* **35**(1): 269 (1990).
2. S. Trasatti, *Electrochimica Acta* **36**(11/12): 1659 (1991).
3. F. T. Wagner, in *Structure of Electrified Interfaces*, J. Lipkowski and P. N. Ross, eds., p. 309, VCH Publishers, New York (1993).
4. S. Trasatti, *Russian J. Electrochem.* **31**(8): 713 (1995).
5. I. Villegas, R. Gomez, and M. J. Weaver, *J. Phys. Chem.* **99**: 14832 (1995).
6. N. Sato, *Russian J. Electrochem.* **31**(8): 837 (1995).
7. S. Trasatti and L. M. Doubova, *J. Chem. Soc. Faraday Trans.* **91**(19): 3311 (1995).



## 6.4. THE ACCUMULATION AND DEPLETION OF SUBSTANCES AT AN INTERFACE

### 6.4.1. What Would Represent Complete Structural Information on an Electrified Interface?

In discussing the second law of thermodynamics, Maxwell, the great founder of the electromagnetic theory, conceived of a hypothetical being who could, in Lilliput fashion, enter a piece of matter, determine the velocities of the particles, and segregate the fast-moving (hot) particles and slow-moving (cold) particles into different regions. In this way, the being could create a temperature difference from a material that was originally at one temperature and thus reverse the equilibrating process by which heat flows from a hot region to a cold region. *Maxwell's demon* was the name given to this mythical being.

What would one expect of such a hypothetical being (a “Gibbs angel”)<sup>36</sup> in electrified interfaces? The being should be able to dive into the interphase region and quickly return with snapshots of the arrangements of ions and dipoles and neutral molecules that dwell in that area. The superposition of a sufficiently large number of snapshots would reveal the time-averaged structure of the interface: How the interface region is constituted, which ions and dipoles are in intimate contact with the electrode and in what numbers, and which ions swarm around the electrode and to what extent. This is the ideal type of information that one would like to have: the time-averaged positions of all the particles populating the electrified interface.

A Gibbs angel, like Maxwell's demon, unfortunately does not exist. Neither is there at present an experimental technique to achieve what could be accomplished by a Gibbs angel. Hence, one has to try to build up a picture of the structure of the interface by letting the mind play with the other types of cruder information that are available.

In the case of a metal/solution interface, the charge on the metal is one of the signals that can be picked up. This electrode charge is mirrored on the solution side by an equal and opposite net charge constituted of separate contributions of the positive and negative charges, i.e., the relative concentrations of cations and anions in the interphase. However, are these ions *on* the metal or *near* the metal?

The situation is not as trivial as in gas-phase adsorption where gas particles stick to the solid surface in partial or complete monolayer fashion. The adsorption at a metal/solution interface concerns a more extended and tenuous matter. It is simply a change of concentration near the interface, which may or may not include ions in contact with the metal.

Further, in gas-phase adsorption, the “solvent” for the gas particles, is a vacuum—an inert, indifferent, and noninterfering solvent. In solution, however,

---

<sup>36</sup>The angel is probably named after the great American physical chemist J. Willard Gibbs, who developed most of the theorems that permit the application of thermodynamics to interfaces.

the ions, etc., are dissolved in a solvent, usually water. This water, too, can change its concentration near the interface compared with its concentration in the bulk of the solution. Hence, the meaning of concentration in terms of gram ions per cubic centimeter is subtly different from that which it has in the bulk of the solution because the reference phase, water, may itself undergo a concentration change as the interphase is approached.

It is clear that the adsorption of species in the metal–solution interphase region needs a subtle analysis. The unraveling of the complex situation and the building up of a basic picture of the accumulation and depletion of species at an electrified interface is one of the principal achievements of the new electrochemistry and is largely due to the American electrochemist, Grahame.

#### 6.4.2. The Concept of Surface Excess

Suppose that a Gibbs angel, after taking snapshots of the arrangement of particles in the interphase region, plotted graphs showing the time-averaged concentrations of the various species against a distance  $x$  from some reference plane parallel to a planar electrode.

At the instant of immersion of the electrode in the electrolyte (i.e., at time  $t = 0$ ), the graph for some species  $i$ , say, the positive ions  $M^+$ , would show that the concentration was independent of  $x$  and equal to the bulk concentration  $c_i^0$  (Fig. 6.47). This is because at  $t = 0$ , the double layer has not yet been formed, i.e., the interface has not yet become electrified. For  $t > 0$ , the anisotropic forces at the boundary begin to operate, and the separation and sorting out of the various charges in the interphase take place.

Now, what would be the nature of the concentration profile at  $t \rightarrow \infty$ , i.e., after the steady-state double layer is formed? It is to be expected (Fig. 6.48) that the

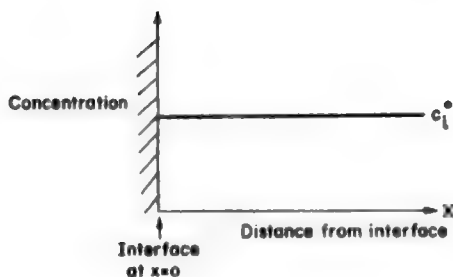


**Fig. 6.47.** The concentration  $c_i$  of the species  $i$  as a function of the distance  $x$  from the interface, at the instant of immersion ( $t = 0$ ) of the electrode in the solution.

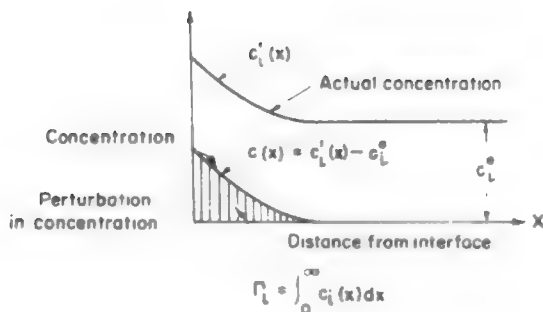


**Fig. 6.48.** A schematic representation of the distance variation of the concentration at  $t \rightarrow \infty$ , i.e., after the steady-state double layer is formed. The actual concentration,  $c_i'(x)$  and the concentration perturbation  $c_i(x) = c_i'(x) - c_i^0$  are both shown. The surface excess  $\Gamma_i$  of the species  $i$  is the definite integral  $\Gamma_i = \int_0^{\infty} c_i(x) dx$  indicated by the hatched area.

concentration  $c_i'(x)$  at  $t \rightarrow \infty$  would have altered from the initial value  $c_i^0$ , i.e., from the value before the double layer was formed.

As in the diffusion problems discussed in Chapter 3, it is more convenient not to discuss the actual concentrations  $c_i'(x)$  but the perturbations, or departures from the bulk concentrations. This is done by defining the perturbations thus

$$c_i(x) = c_i'(x) - c_i^0 \quad (6.63)$$

i.e.,

$$\begin{array}{l} \text{Perturbation} \\ \text{or excess concentration} \end{array} = \begin{array}{l} \text{actual} \\ \text{concentration} \end{array} - \text{bulk concentration} \quad (6.64)$$

A schematic representation of these perturbations or concentration changes is shown in Fig. 6.48.

What do these perturbations in concentration represent? They are quantitative measures of the accumulation or depletion of species in the interphase region. Unfortunately, only a Gibbs angel could directly provide the concentration-distance profile for the various cationic and anionic species in the double layer. At present, there are no techniques sensitive enough to experimentally determine the distance variation of the concentration changes in the various species in solution. One must settle for knowledge obtained by indirect argument and therefore of lesser certainty.

Gibbs conceived the idea of measuring adsorption in the interphase by using the integral of the perturbation in concentration with distance.<sup>37</sup> This is shown by the shaded area in Fig. 6.49. This integral represents the excess concentrations [Eq. (6.63)] in all the lamellae. The integration or summation is carried out from a reference plane  $x = 0$  up into the bulk of the electrolyte,  $x \rightarrow \infty$ . In the electrolyte bulk, the anisotropic forces of the interface are negligibly small and hence the perturbations tend to zero and do not contribute to the integral. The result of this summation is known as the *Gibbs surface excess*  $\Gamma$ , or simply the surface excess,

$$\Gamma_i = \int_0^{\infty} c_i(x) dx \quad (6.65)$$

It is easy to see that the surface excess is either a positive or a negative quantity, depending on whether the departure from the bulk concentration is positive or negative, i.e., on whether there is an accumulation or depletion of the particular species  $i$  in the interface.

#### 6.4.3. Is the Surface Excess Equivalent to the Amount Adsorbed?

Often the surface excess of a particular species has been simply assumed to be the quantity of that species adsorbed on the surface of an electrode. To examine this point of view, consider the profile of the actual concentration. The interphase region can be said to begin from the point where the actual concentration departs from the bulk value. The amount of the species that can be said to have adsorbed per unit area of the interface is equal to the *total* amount of the species existing inside the interphase region divided by the area of the interface. In Fig. 6.49 the adsorbed material is indicated by the hatched area.

The surface excess, however, is the amount of material *over and above that which would have existed had there been no double layer*. This surface excess is indicated by the shaded area in Fig. 6.49. It could also be represented by the expression

$$\Gamma_i = \int_0^{\infty} c_i(x) dx = \frac{1}{A} \int_0^{\infty} c_i(x) dV = \frac{1}{A} \int_0^{\infty} [c'_i(x) - c_i^0] dV$$

<sup>37</sup>Note the greater complexity of defining adsorption here in studies of electric double layers than, e.g., for metal-gas systems. With electric double layers, one is concerned with the whole interphasial region. The total adsorption is the sum of the increases of concentration over a distance, which in dilute solutions may extend for tens of nanometers. Within this total adsorption, there are, as will be seen, various types of adsorptive situations, including one, *contact adsorption*, which counts only those ions in contact with the electronically conducting phase (and is then, like the adsorption referred to in metal-gas systems, the particles on the surface). Metal-gas systems deal with *interfaces*, one might say, whereas metal-electrolyte systems deal primarily with *interphases* and only secondarily with interfaces.

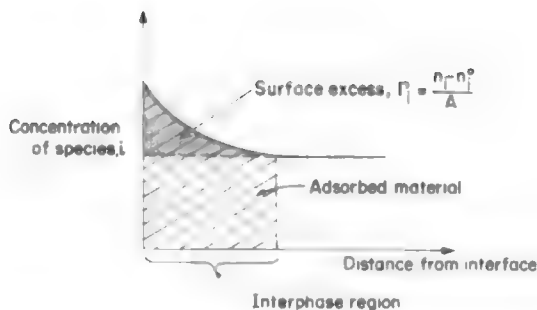


**Fig. 6.49.** The distinction between the amount of adsorbed material (hatched area) in the interphase region and the surface excess (shaded area).

$$\begin{aligned}
 &= \frac{1}{A} \int_0^{\infty} d(\Delta n_i) \\
 &= \frac{n_i}{A} - \frac{n_i^0}{A}
 \end{aligned} \tag{6.66}$$

where  $dV$  is the volume of an infinitesimally thin lamina having a cross section  $A$ ,  $n_i$  is the actual number of moles of species  $i$  in the interphase region, and  $n_i^0$  is the number of moles that would have been there if there had been no double layer.

It is now obvious that the amount of material adsorbed per unit area  $n_i/A$ , is not equal to the surface excess. Insofar as the bulk concentration, or  $n_i^0$ , tends to zero, the adsorption can be taken as approximately equal to the surface excess.

#### 6.4.4. Does Knowledge of the Surface Excess Contribute to Knowledge of the Distribution of Species in the Interphase Region?

Complete knowledge regarding the structure of the interface would consist of information regarding the arrangement of all the particles or what is the analytical equivalent, the variation of the actual or perturbed concentrations of the species with distance from the reference plane. Such knowledge would be on the microscopic level.

The definition of surface excess, on the other hand, starts with the concentration profile, but involves an integration between limits [Eq. (6.65)]. Once the integration is done and limits are inserted, one obtains a number (so many moles per square centimeter) and loses all knowledge of the function  $c_i(x)$ . In other words, after the integration is carried out and the surface excess evaluated, the concentration profile

cannot be discerned and the microscopic detail from the surface excess is lost. Surface excess is a macroscopic concept.

What then is the point of measuring surface excess? It will be shown that the surface excess affects many quantities, for example, the interfacial tension at the interface and the way in which it depends upon concentration. In fact it will be shown (see Section 6.5.1) that surface excess can be experimentally determined from thermodynamic measurements without recourse to modeling arguments.

Therefore, the purpose of measuring surface excess is to provide material for testing models of the electrified interface. From these models, one can calculate the variation in the concentration of the surface excess of any species. The extent of agreement between the variation calculated thus and that determined from thermodynamic reasoning (see Section 6.5.7) determines the extent of validity of the model. This is why the concept of surface excess is so useful, despite its macroscopic nature.

#### 6.4.5. Is the Surface Excess Measurable?

The surface excess is measurable. There are essentially two approaches to its measurement. One approach is to make use of the fact that the surface excess of a species is approximately equal to its adsorption on the electrode when the bulk concentration of that species is extremely low. Under these conditions, the surface excess can be approximately known by directly measuring adsorption. How can this be done?

One method of directly determining adsorption involves the use of radioactive isotopes, as explained in Section 6.6.2.2. Another way of getting the surface excess is based on the measurement of some property which depends on this surface excess. One such property is the surface tension, or, rigorously speaking, the interfacial tension.<sup>38</sup> The latter is to a surface what pressure is to a bulk volume. Work has to be done against the surface tension to increase the area of the interface, just as it has to be done against pressure to increase the volume of a bulk phase. The phenomenon of surface tension arises from the anisotropy of forces existing in an interphase. But these forces are affected by the particles in the interphase, and therefore the surface tension must be related to the degree to which these particles are present, i.e., to the surface excess.

The precise thermodynamic relationship between the surface tension and the surface excess can be worked out and the resulting relationship is rigorous and accurate (see Section 6.5.3). The catch is, however, that the method is only suited for the interface between a liquid metal (e.g., mercury) and a solution. This is because the surface tension of liquids can be easily determined (see Section 6.5.1.1) but not the

<sup>38</sup>The two terms "surface tension" and "interfacial tension" will be used interchangeably in this text, although the tension is strictly an interphasial tension (both phases determine it) rather than that of a surface.

surface tension of solids. However, indirect methods allow the determination of the surface tension of solids, as we will see in Section 6.5.1.2).

## 6.5. THE THERMODYNAMICS OF ELECTRIFIED INTERFACES

### 6.5.1. The Measurement of Interfacial Tension as a Function of the Potential Difference across the Interface

**6.5.1.1. Surface Tension between a Liquid Metal and Solution.** It has been emphasized that for liquid metals, the interfacial tension is a property that is measurable and is also directly relatable to the potential difference across the interface and the surface excess of various species in solution. How is this measurement done?

Consider mercury as the liquid metal under study. One of the advantages of this metal is that the mercury/solution interface approaches closest to the ideal polarizable interface (see Section 6.3.3) over a range of 2 V. What this means is that this interface responds exactly to all the changes in the potential difference of an external source when it is coupled to a nonpolarizable interface, and there are no complications of charges leaking through the double layer (charge-transfer reactions).

One electrochemical system that can be used to measure the surface tension of the mercury/solution interface is shown in Fig. 6.50. The essential parts are (1) a mercury/solution polarizable interface, (2) a nonpolarizable interface, (3) an external source of variable potential difference  $V$ , and (4) an arrangement to measure the surface tension of the mercury in contact with the solution.<sup>39</sup>

What are the capabilities of this system? Since the system consists of a polarizable interface coupled to a nonpolarizable interface, changes in the potential of the external source are almost equal to the changes of potential only at the polarizable interface, i.e., the changes in  $\Delta\phi$  across the mercury/solution interface are almost equal to changes in potential difference  $V$  across the terminals of the source. Hence, the system can be used to produce predetermined  $\Delta\phi$  changes at the mercury/solution interface (Section 6.3.11). Further, measurement of the surface tension of the mercury/solution interface is possible, and since this has been stated (Section 6.4.5) to be related to the surface excess, it becomes possible to measure this quantity for a given species in the interphase. In short, the system permits what are called *electrocapillary* measurements, i.e., the measurement of the surface tension of the

<sup>39</sup> Other advantages of using mercury (or any other liquid metal) as an electrode are prevention of surface contaminants and surface reproducibility. If a mercury-drop electrode is used, every time a drop falls and a new drop forms, the electrode presents a virgin surface to the solution. With a simple capillary connected to a reservoir, contamination problems are circumvented. Also, the use of liquid metals removes complications from the characteristic structure and topography present in solid surfaces. Liquid surfaces are nonstructured and highly reproducible.

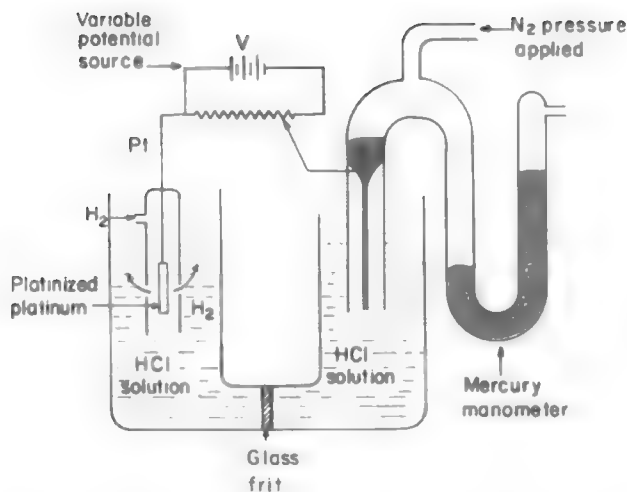


**Fig. 6.50.** Schematic apparatus for the measurement of the surface tension  $\gamma$  of mercury as a function of cell potential  $V$ .

metal (in contact with the solution) as a function of the electrical potential difference across the interface.

Surface tension is measured by using a fine capillary and adjusting the height of a mercury column so that the mercury in the capillary is stationary. Under these conditions of mechanical equilibrium, the surface tension  $\gamma$  is obtained approximately from a simple expression (Fig. 6.51)

$$\gamma = \frac{h\rho g r}{2} \quad (6.67)$$

What has been described is the simplest version of the capillary electrometer. The system can be made sophisticated by using controlled gas pressure to force the mercury in the capillary to desired distances from the tip, by using advanced optical systems in recording the height of the mercury column, and by connecting a sensing device of this height to the gas pressure and the applied potential. Even with the simple version of this system, it is amazing what an amount of useful information can be gained from the form of electrocapillary curves, i.e., plots of interfacial tension  $\gamma$  versus changes in interfacial potential difference  $\delta V$ .

**6.5.1.2. Is It Possible to Measure Surface Tension of Solid Metal and Solution Interfaces?** In contrast to measurement of surface tension for liquids, the direct measurement of surface tension for solids can be considered an impossible task. However, it is possible to apply indirect measurements to obtain electrocapillary curves of solid electrodes and therefore the information from these curves.



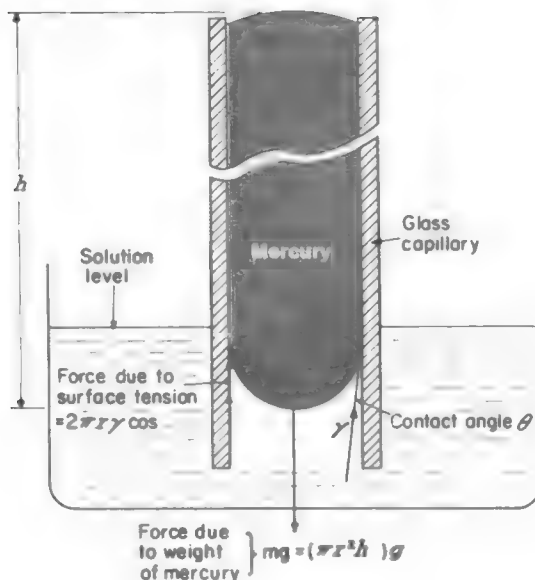


**Fig. 6.51.** When the mercury column in the capillary is stationary and therefore in mechanical equilibrium, its weight is exactly balanced by the total force of its surface tension. The weight of the mercury column acts downward and is equal to the density  $\rho$  times the volume of the column,  $\pi r^2 h$ , times the gravitational constant  $g$ ; this weight compensates for the surface-tension force, which is equal to the perimeter of the contact,  $2\pi r$  times the upward component  $\gamma \cos \theta$  of the surface tension. Since  $2\pi r\gamma \cos \theta = \pi r^2 h g$ , it follows that  $\gamma = rhg/2 \cos \theta$ . For the mercury glass interface,  $\theta \approx 0$ ; hence,  $\gamma = rhg/2$ .

For example, one can start by measuring the current,  $I$ , passing through the circuit as a function of time when the potential is changed from a value where adsorption does not occur to a value where adsorption occurs at a given concentration of species in solution (Lipkowski, 1986). Curves of this type (i.e., as a function of time) are called *transients*. Figure 6.52(a) shows an example of current transients. The charge of the electrode can be obtained by integrating these curves according to the equation,

$$\int_{(q_M)_0}^{(q_M)_\theta} dq_M = \int_0^t I \times dt \quad (6.68)$$

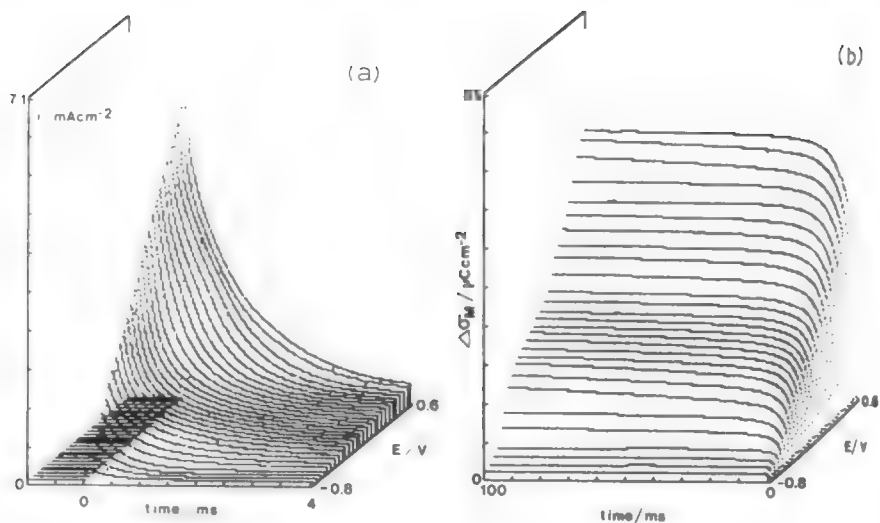


**Fig. 6.52.** (a) Three-dimensional representation of current transients recorded for a polycrystalline gold electrode in a solution that contains  $5 \times 10^{-4} M$  pyridine over the potential region  $-0.75 V$  to  $+0.6 V$  (vs. saturated calomel electrode). (b) Three-dimensional representation of charge transients obtained by integration of the current transients shown in (a). In this drawing  $\Delta\sigma_M = \Delta q_M$ . (Reprinted from J. Stolberg, J. Richer, and J. Lipkowski and D. E. Irish, *J. Electroanal. Chem.* 207:213, copyright 1986, Fig. 4, with permission of Elsevier Science.)

or

$$\Delta q_M = \int_0^t I \times dt \quad (6.69)$$

where  $\Delta q_M$  is defined by the equation:

$$\Delta q_M = (q_M)_\theta - (q_M)_0 \quad (6.70)$$

In this equation  $(q_M)_\theta$  is the charge density of the metal at a potential where the electrode is covered by adsorbate, and  $(q_M)_0$  in the absence of adsorbate. The value of  $(q_M)_0$  is obtained by an independent measurement and then  $(q_M)_\theta$  is obtained by applying Eq. (6.70). A set of  $\Delta q_M$  values as a function of time and potential is shown in Fig. 6.52(b).

Once the values of the charge of the electrode in the presence of adsorbates are obtained, i.e.,  $(q_M)_\theta$ , one may apply one of the electrocapillary equations that will be derived in Section 6.5.3. Specifically, Eq. (6.95) can be integrated to obtain values of

surface tension as a function of electrical potential difference, that is, the electrocapillary curve.

$$\gamma_{\theta} = - \int_{V_0}^{V_{\theta}} q_M dV + \gamma_0 \quad (6.71)$$

where the subscript 0 represents the variable with the electrode in the absence of adsorbate ( $\theta = 0$ ), and the subscript  $\theta$ , the variable when the electrode is covered by a fraction  $\theta$  of adsorbate.

### 6.5.2. Some Basic Facts about Electrocapillary Curves

The interfacial tension depends on the forces arising from the particles present in the interphase region. If the arrangement of these particles (i.e., the composition of the interface) is altered by varying, for example, the potential difference across the interface, then the forces at the interface should change and thus cause a change in the interfacial tension. One would expect therefore that the surface tension  $\gamma$  of the metal/solution interface will vary with the potential difference  $V$  supplied by the external source.

The experimental  $\gamma$  versus  $V$  curves obtained by electrocapillary measurements demonstrate this variation of surface tension  $\gamma$  with the potential difference  $V$  across the cell. What is informative, however, is the nature of the variation (Table 6.2). A typical electrocapillary curve is almost a parabola (Fig. 6.53). The potential at which

**TABLE 6.2**  
**Variation in Interfacial Tension of a Mercury–1.0 N CsCl Interface**  
**with Potential Difference**

Potential Difference (mV) vs Normal Calomel Electrode	Interfacial tension, (dynes cm <sup>-1</sup> )
-0	345.0
-100	376.4
-200	397.1
-300	410.2
-400	418.8
-500	422.6
-600	422.9
-700	419.9
-800	414.0
-900	405.6
-1000	395.1
-1100	382.9
-1200	369.2
-1300	356.6

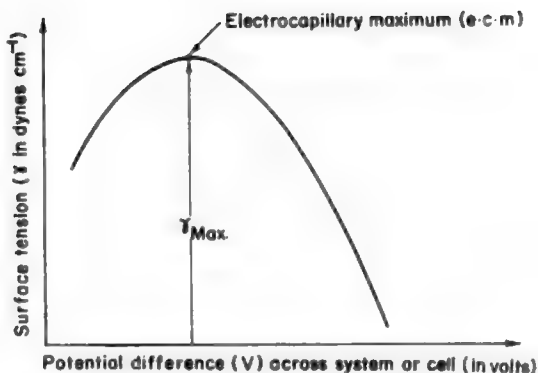


**Fig. 6.53.** A typical  $\gamma$  vs.  $V$  electrocapillary curve.

the surface tension is a maximum is known as that of the *electrocapillary maximum* (ecm).

The measurements also show that surface tension varies with the composition of the electrolyte (Table 6.3). This is easily seen by comparing electrocapillary curves obtained in solutions of different electrolyte concentrations. As the solution is diluted, the maximum of surface tension rises (Fig. 6.54).

The surface tension was stated (Section 6.4.5), on general grounds, to be related to the surface excess of species in the interphase. The surface excess in turn represents in some way the structure of the interface. It follows therefore that electrocapillary curves must contain many interesting messages about the double layer at the electrode/electrolyte interface. To understand such messages, one must learn to decode the electrocapillary data. It is necessary to derive quantitative relations among surface tension, excess charge on the metal, cell potential, surface excess, and solution composition.

**TABLE 6.3**  
**Variation in Interfacial Tension of an Hg/CsCl Interface with CsCl Concentration<sup>a</sup>**

CsCl Normality	Interfacial Tension, (dynes cm <sup>-1</sup> )
3.0	390.0
1.0	395.1
0.3	398.9
0.1	402.9
0.03	406.4
0.01	410.8

<sup>a</sup>The surface tension values are at a potential of  $-1000$  mV vs a calomel electrode in the same solution.

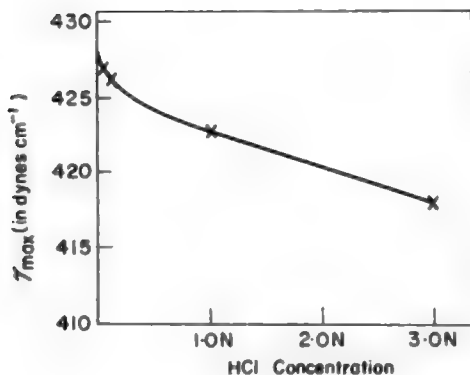


**Fig. 6.54.** The variation of  $\gamma_{\max}$  with electrolyte concentration.

### 6.5.3. Some Thermodynamic Thoughts on Electrified Interfaces

All thermodynamic thinking begins with a definition of the portion of the universe under study, i.e., the system. Here the system is an electrode/electrolyte interface; restrictions regarding the polarizability of the interface will be introduced as and when required.

The next step is to write down the first and second laws of thermodynamics for the system. If the system is a closed one (no matter enters or leaves it), the statement of the combined first and second laws is

$$dU = T dS - W \quad (6.72)$$

where  $TdS = Q$  is the heat reversibly supplied to the system in an infinitesimal change, and  $W$  is the work reversibly carried out by the system. For an open system, not only heat but also matter may be exchanged between the system and its surroundings. To introduce a mole of the species  $i$ , the chemical work done on the system is  $\mu_i$ . Hence, to alter the number of moles of  $i$  in the system by  $dn_i$ , the work done by the system is  $-\mu_i dn_i$ . For an open system, this chemical work must be included and the combined first and second laws must be written

$$dU = T dS - W - \sum \mu_i dn_i \quad (6.73)$$

where  $\sum \mu_i dn_i$  is the work done by the system in expelling  $dn_i$  moles of species  $i$ ,  $\mu_i$  being the work of transfer per mole.

In the case of an electrode/electrolyte interface  $M_1/S$ , what are the various possible types of work? There is first the work of volume expansion,  $p dV$ ; second, one might in some way increase the area of the interface by an amount  $dA$ , in which case the work

of increasing the area of the interface is  $\gamma dA$ , where  $\gamma$  is the interfacial tension; and finally, one might, for example, connect the metallic phase to an external source of electricity and alter the charge on the metal by an amount  $dq'_M$ , in which case the electrical work of transferring the charge  $dq'_M$  is  $^M\Delta^S\phi dq'_M$ .

Introducing these work terms in place of  $W$  in Eq. (6.73), the statement of the combined first and second laws of thermodynamics applied to the above system reads

$$dU = T dS - p dV - \gamma dA - ^M\Delta^S\phi dq'_M - \sum_i \mu_i dn_i \quad (6.74)$$

Each term on the right-hand side is a product of an intensive factor (one that does not depend on the amount of matter in this system) and an extensive factor (one that does depend on the amount of matter in the system). Thus,

$$dU = \sum \text{intensive factor} \times \text{extensive factor} \quad (6.75)$$

Keeping the intensive factors ( $T, p, \gamma, \Delta\phi, \mu$ ) constant, let the extensive factors be increased from their differential values to their absolute values for the system concerned,  $S, V, A, q'_M, n_i$ . One now has for the energy of the system

$$U = TS - PV - \gamma A - ^M\Delta^S\phi q'_M - \sum_i \mu_i n_i \quad (6.76)$$

On differentiating this equation, the result is

$$\begin{aligned} dU = & (T dS - p dV - \gamma dA - ^M\Delta^S\phi dq'_M - \sum_i \mu_i dn_i) \\ & + [S dT - V dp - A d\gamma - q'_M d(^M\Delta^S\phi) - \sum_i n_i d\mu_i] \end{aligned} \quad (6.77)$$

The two expressions (6.77) and (6.74) must be equal to each other. Hence, by equating them, one gets

$$0 = S dT - V dp - A d\gamma - q'_M d(^M\Delta^S\phi) - \sum_i n_i d\mu_i \quad (6.78)$$

which, at constant temperature and pressure, reduces to

$$0 = -A d\gamma - q'_M d(^M\Delta^S\phi) - \sum_i n_i d\mu_i$$

or

$$d\gamma = -\frac{q'_M}{A} d(M_1 \Delta^S \phi) - \sum_i \frac{n_i}{A} d\mu_i \quad (6.79)$$

Thus, surface tension changes have been related to changes in the absolute potential differences across an electrode/electrolyte interface and to changes in the chemical potential of all the species, i.e., to changes in solution composition. Only one other quantity is missing, the surface excess. This can be easily introduced by recalling the definition of surface excess [Eq. (6.66)], i.e.,

$$\frac{n_i}{A} = \Gamma_i + \frac{n_i^0}{A} \quad (6.80)$$

Hence, one can write

$$\frac{n_i}{A} d\mu_i = \Gamma_i d\mu_i + \frac{n_i^0}{A} d\mu_i \quad (6.81)$$

or

$$\sum_i \frac{n_i}{A} d\mu_i = \sum_i \Gamma_i d\mu_i + \sum_i \frac{n_i^0}{A} d\mu_i \quad (6.82)$$

It is known, however, from the Gibbs–Duhem relation that

$$\sum_i n_i^0 d\mu_i = 0 \quad (6.83)$$

Introducing this relation into Eq. (6.82), one gets

$$\sum_i \frac{n_i}{A} d\mu_i = \sum_i \Gamma_i d\mu_i \quad (6.84)$$

and, by substituting this expression for  $\sum_i (n_i/A) d\mu_i$  in Eq. (6.79), the result is<sup>40</sup>

$$d\gamma = -q_M d(M_1 \Delta^S \phi) - \sum_i \Gamma_i d\mu_i \quad (6.85)$$

<sup>40</sup>Note that  $q_M$ , the excess-charge *density* on the electrode, has been written instead of  $q'_M/A$ , the total excess charge on the electrode divided by its surface area.

Equation (6.85) contains the quantity  $d(M_1 \Delta^S \phi)$ , which is the change in the inner (or Galvanic) potential difference across the interface under study. It will be recalled, however (Section 6.3.11), that, though the absolute value of  $M_1 \Delta^S \phi$  cannot be determined, a change in  $M_1 \Delta^S \phi$ , i.e.,  $d(M_1 \Delta^S \phi)$ , can be measured provided (1) the  $M_1/S$  interface is a polarizable one and (2) the  $M_1/S$  interface is linked to a nonpolarizable interface  $M_2/S$  to form an electrochemical system, or cell. If such a cell is connected to an external source of electricity, one has

$$V = M_1 \Delta^S \phi + {}^S \Delta M_2 \phi + M_2 \Delta M_1' \phi \quad (6.86)$$

since the sum of the potential drops around a circuit must be zero. The inner potential difference  $M_2 \Delta M_1' \phi$  does not depend upon the potential  $V$  supplied from the external source or upon the solution composition; hence, on differentiating Eq. (6.86),

$$-d(M_1 \Delta^S \phi) = -dV + d({}^S \Delta M_2 \phi) \quad (6.87)$$

Substituting this expression for  $-d(M_1 \Delta^S \phi)$  in Eq. (6.85), it follows that

$$d\gamma = -q_M dV + q_M d({}^S \Delta M_2 \phi) - \sum \Gamma_i d\mu_i \quad (6.88)$$

The nonpolarizable characteristics of the second interface  $M_2/S$ , which is a necessary part of the cell and measuring setup, are now introduced. It is recalled that there is thermodynamic equilibrium at this interface, and thus

$$d({}^S \Delta M_2 \phi) = -\frac{1}{z_j F} d\mu_j \quad (6.89)$$

where  $j$  is the particular species involved in the leakage of charge across the nonpolarizable interface.<sup>41</sup> For example, if one uses a hydrogen electrode (see Fig. 6.34), one would write (with  $z_+ = 1$ )

$$d({}^S \Delta M_2 \phi) = -\frac{d\mu_{H^+}}{F} \quad (6.90)$$

Or, if one uses a calomel electrode in which  $Cl^-$  ions can be thought to do the leaking across the interface, then (with  $z_- = -1$ ),

<sup>41</sup>The nonpolarizable interface has been defined above (Section 6.3.3) as one which, at constant solution composition, resists any change in potential due to a change in cell potential. This implies that  $(\partial {}^S \Delta M_2 \phi / \partial V)_\mu = 0$ . However, the inner potential difference at such an interface can change with solution composition; hence, Eq. (6.89) can be rewritten in the form of  $d({}^S \Delta M_2 \phi) = (RT/z_j F) d \ln a$ , which is the Nernst equation [see Eq. (7.51)] in differential form for a single interface.



$$d(^S\Delta^M\phi) = + \frac{d\mu_{Cl^-}}{F} \quad (6.91)$$

By substituting Eq. (6.89) in Eq. (6.88), one obtains<sup>42</sup>

$$d\gamma = -q_M dV - \frac{q_M}{z_j F} d\mu_j - \sum \Gamma_i d\mu_i \quad (6.92)$$

This is the fundamental equation for the thermodynamic treatment of polarizable interfaces. It is a relation among interfacial tension  $\gamma$ , surface excess  $\Gamma_i$ , applied potential  $V$ , charge density  $q_M$ , and solution composition. It shows that interfacial tension varies with the applied potential and with the solution composition. This is in fact the relation that was desired. Its implications will now be analyzed.

#### 6.5.4. Interfacial Tension Varies with Applied Potential: Determination of the Charge Density on the Electrode

When an electrocapillary curve is obtained in the laboratory, a solution of a fixed composition is taken, i.e.,  $d\mu_i$  for all the species is zero. The conditions of electrocapillary-curve determinations correspond therefore to

$$\sum_i \Gamma_i d\mu_i = 0 \quad \text{and} \quad d\mu_j = 0 \quad (6.94)$$

from which it follows from Eq. (6.92) that

$$\left( \frac{\partial \gamma}{\partial V} \right)_{\text{const.comp.}} = -q_M \quad (6.95)$$

This equation, known as the *Lippmann equation*, is perhaps a surprising result: The slope of the electrocapillary curve at any cell potential  $V$  is equal to the charge density on the electrode (Fig. 6.55).

Actually, in the electrocapillary equation for a solid electrode, the first and last terms are strictly given by

$$d\gamma = - \left[ q_M + (\gamma - Y) \left( \frac{\partial \epsilon_e}{\partial V} \right)_{T,P,\mu_i} \right] dV - \frac{q_M}{z_j F} d\mu_j - \sum_i \left[ \Gamma_i + (\gamma - Y) \left( \frac{\partial \epsilon_e}{\partial \mu_i} \right)_{T,P,E} \right] d\mu_i \quad (6.93)$$

where  $Y$  is the elastic surface stress defined as the reversible work required to form a unit area of surface by stretching (in contrast to  $\gamma$ , defined as the reversible work required to form a unit area of surface by cleavage), and  $\epsilon_e$  is the elastic surface strain. The changes of  $\epsilon_e$  with  $V$  and  $\mu_i$  are minimal, and therefore the terms involving changes in this variable can be neglected. The result is that for solid electrodes, Eq. (6.92) can also be applied.

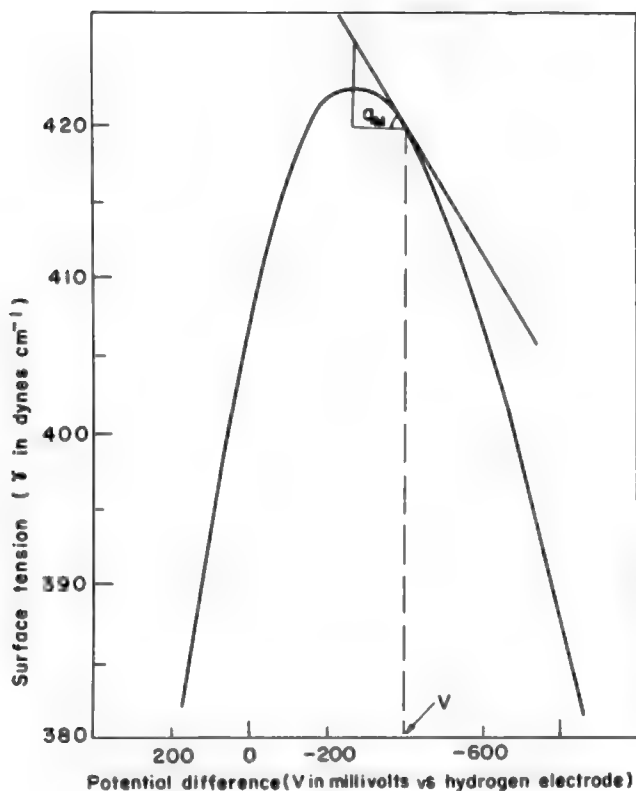


**Fig. 6.55.** The charge density on the electrode at a particular value of the potential difference  $V$  is given by the slope of the electrocapillary curve at that potential. The curve shown is for mercury in contact with 1.0  $N$   $HCl$ .

### 6.5.5. Electrode Charge Varies with Applied Potential: Determination of the Electrical Capacitance of the Interface

The next step is obvious. Differentiate the  $\gamma$  versus  $V$  electrocapillary curve at various values of cell potential, and plot these values of the slope (electrode charge) as a function of potential (Fig. 6.56). If the electrocapillary curve were a perfect parabola, then the charge (strictly, excess charge density) on the electrode would vary linearly with the cell potential (Fig. 6.56).

An electrified interface can be considered a system capable of storing charge, considering that it is a region where charges are accumulated or depleted relative to the bulk of the electrolyte. However, the ability to store charge is the characteristic

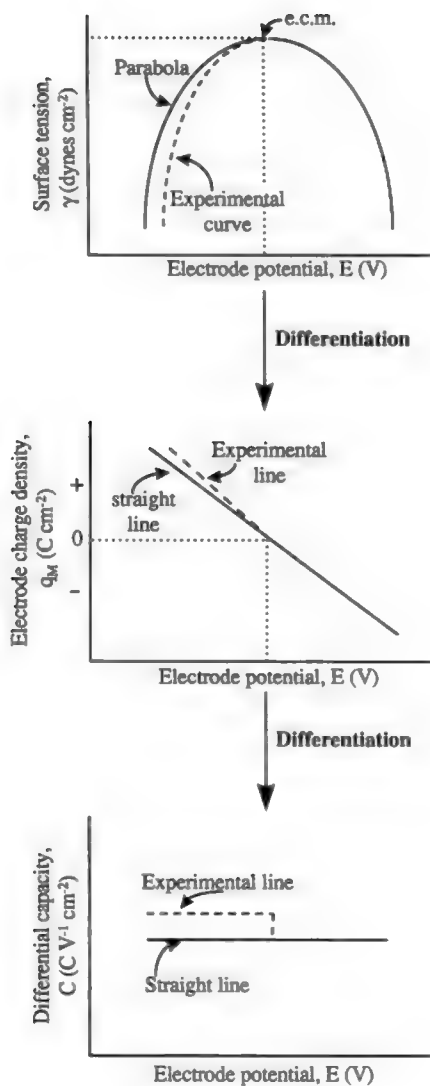


**Fig. 6.56.** When the electrocapillary  $\gamma$  vs.  $E$  curve is a perfect parabola, the electrode-charge density varies linearly with potential difference. A further differentiation gives a capacity that is potential independent. However, experimental electrocapillary curves are not perfect parabolas.

property of an electric capacitor. Hence, one can discuss the capacitance of an electrified interface in way similar to that with a condenser.

What is the capacitance of a condenser? It is given by the total charge required to raise the potential difference across the condenser by 1 V

$$K = \frac{q}{V} \quad (6.96)$$

This is the *integral* capacitance, and it is generally used for electrical capacitors where the capacity is constant and independent of the potential. This constancy of capacity may not be the case with electrified interfaces and in order to be prepared for this eventuality, it is best to define a *differential* capacity  $C$  thus

$$C = \left( \frac{\partial q_M}{\partial V} \right)_{\text{const.comp.}} = - \left( \frac{\partial^2 \gamma}{\partial V^2} \right)_{\text{const.comp.}} \quad (6.97)$$

What is the significance of this equation? It shows that the slope of the curve of the electrode charge versus cell potential yields the value of the differential capacity of the double layer. In the case of an ideal parabolic  $\gamma$  versus  $V$  curve, which yields a linear  $q$  versus  $V$  curve, one obtains a constant capacitance (Fig. 6.56).

### 6.5.6. The Potential at which an Electrode Has a Zero Charge

It can be seen from the  $q_M$  versus  $V$  curve (Fig. 6.56) that the charge on an electrode starts off with one sign and then changes its sign after passing through a zero-charge value. The potential difference across the system (or cell) at which the charge on the electrode is zero is the potential of zero charge and is given the symbol  $E_{q=0}$  or  $E_{\text{pzc}}$  if this potential is measured on the hydrogen scale.

Where is the pzc on the electrocapillary  $\gamma$  versus  $V$  curve? Since  $q_M$  is given by the slope of the curve, the pzc is defined by

$$q_M = - \left( \frac{\partial \gamma}{\partial V} \right)_{\text{const.comp.}} = 0 \quad (6.98)$$

Hence, the pzc is the potential at which the electrocapillary maximum (ecm) occurs (Fig. 6.56).

With liquid metals, the most convenient method of determining the pzc is by making electrocapillary measurements. From the  $\gamma$  versus  $V$  curve, the  $q_M$  versus  $V$  curve can be found and thus the value of  $E_{q=0}$  or  $E_{\text{pzc}}$ . The pzc, however, is such a fundamental characteristic of the interface that there is a considerable need to know its value for interfaces involving solid electrodes. Here, surface tensions cannot be determined with capillary electrodes, and one must resort to other methods of pzc determination. Some values of the pzc for solid metals are given in Table 6.4.

**TABLE 6.4**  
**The Potential of Zero Charge on Solids**

Metal	Solution	$E_{pzc}$ , V vs SHE
Aluminum	0.01 N KCl	-0.52
Antimony	0.10 HCl	-0.19
Bismuth	0.01 N KCl	-0.36
Cadmium	0.01 N KCl	-0.92
Cobalt	0.02 N Na <sub>2</sub> SO <sub>4</sub>	-0.32
Copper	0.02 N Na <sub>2</sub> SO <sub>4</sub>	+0.03
Gold	0.02 N Na <sub>2</sub> SO <sub>4</sub>	+0.23
Iron	0.001 N H <sub>2</sub> SO <sub>4</sub>	-0.37
Lead	0.01 N KCl	-0.69
Platinum	0.003 N HClO <sub>4</sub>	+0.41
Silver	0.02 N Na <sub>2</sub> SO <sub>4</sub>	-0.70

### 6.5.7. Surface Tension Varies with Solution Composition: Determination of the Surface Excess

Equation (6.92) describes changes in surface tension with both potential and composition. In order to find out how to determine the surface excess  $\Gamma_\gamma$ , one has first to eliminate one variable in this equation, the potential. This seems to be easy; electrocapillary curves obtained for various salt concentrations can be plotted in one diagram and a perpendicular erected to the cell-potential axis. This will then contain points relating  $\gamma$  to concentration when, in Eq. (6.88),  $dV = 0$ . Here, however, a very important and often not realized feature of this equation must be remembered. It contains the term  $d(S\Delta^M\phi)$ , i.e., changes in the potential difference across the reference electrode/solution interface produced by changes in solution composition via Eq. (6.89). Thus, the  $V$  read on the potentiometer refers, for every concentration in which the  $\gamma$  versus  $V$  relation is determined, to a reference electrode consisting of metal immersed in a solution of *the same* concentration as that surrounding the test electrode. It is this value of  $V$  (obtained *not* with a standard reference electrode, i.e., one always immersed in the solution of the same activity, but with reference electrodes differing according to the concentration of the ions that leak charge across the interface) that has to be kept constant.

In order to remember this often-forgotten fact, it is customary to denote these potential values, referred *not* to the standard electrode but to one reversible to ions of given (varying) concentration, as  $V_+$  or  $V_-$ , indicating at the same time whether the electrode is one at which cations or anions leak, respectively.

Now, a perpendicular erected on the axis of the cell potential  $V_+$  or  $V_-$  (Fig. 6.57) intersects the electrocapillary curves at points for which the condition  $dV = 0$  in Eq. (6.92) is satisfied, whereupon

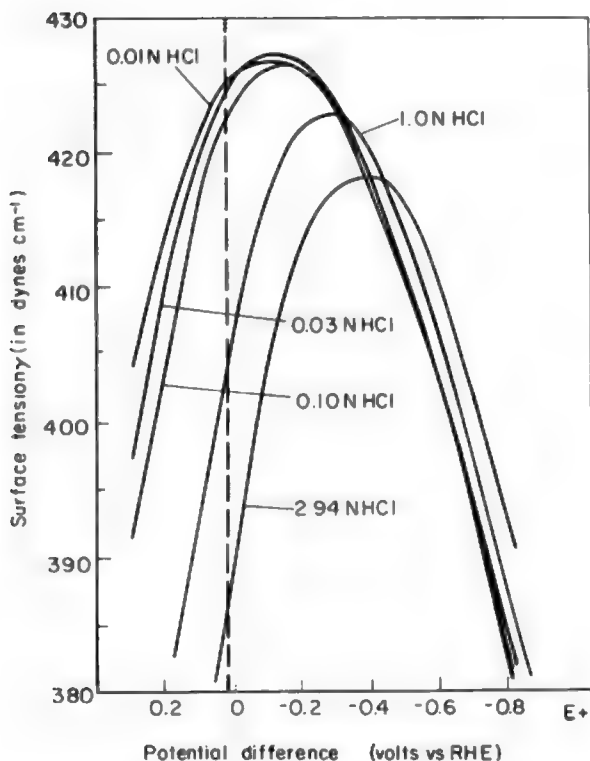


**Fig. 6.57.** Electrocapillary curves from solutions of different electrolyte (HCl) concentrations. The symbol RHE stands for a reversible hydrogen electrode immersed, not in a standard solution, but in the same electrolyte as the electrode under study.

$$d\gamma = -\frac{q_M}{z_j F} d\mu_j - \sum_i \Gamma_i d\mu_i \quad (6.99)$$

This equation describes the changes in surface tension with composition at any particular cell potential,  $V_+$  or  $V_-$  (Table 6.2).

Now consider a polarizable interface that consists of a metal electrode in contact with a solution of a 1:1-valent electrolyte (i.e.,  $z_+ = 1$  and  $z_- = -1$ ). It will be remembered that in order to apply electrocapillary thermodynamics to a polarizable interface  $M_1/S$ , the interface has to be assembled in a cell along with a nonpolarizable interface. Suppose that the nonpolarizable interface is one at which negative ions interchange charge with the metal surface, i.e.,  $z_j = -1$ . Hence, Eq. (6.99) for the polarizable interface becomes

$$d\gamma = +\frac{q_M}{F} d\mu_- - \Gamma_+ d\mu_+ - \Gamma_- d\mu_- \quad (6.100)$$

where the  $\Sigma$  of Eq. (6.99) has been expanded.

It would be convenient to transform this expression so that it would contain the concentration of the electrolyte used in the cell. The first step in effecting this transformation follows by noting that the chemical potential  $\mu$  of the electrolyte is the sum of the chemical potentials of the ions, i.e.,

$$\mu = \mu_+ + \mu_- \quad (6.101)$$

or

$$d\mu = d\mu_+ + d\mu_- \quad (6.102)$$

Using Eq. (6.102), one can substitute for  $d\mu_+$  in Eq. (6.100) to give

$$\begin{aligned} d\gamma &= \frac{q_M}{F} d\mu_- - \Gamma_+ d\mu + \Gamma_+ d\mu_- - \Gamma_- d\mu_- \\ &= -\Gamma_+ d\mu + \left( \frac{q_M + F\Gamma_+ - F\Gamma_-}{F} \right) d\mu_- \end{aligned} \quad (6.103)$$

The second step consists in affirming that there is electroneutrality across the interface, i.e., the charge on the metal is always equal and opposite to the total charge on the solution side of the interface. Before the double layer is formed, the metal is uncharged and in the solution, the charge per unit area of a lamina due to positive and negative ions is zero, i.e.,

$$F \left( \frac{n_+^0}{A} \right) - F \left( \frac{n_-^0}{A} \right) = 0 \quad (6.104)$$

After the double layer is formed, electroneutrality requires that

$$F \frac{n_+}{A} - F \frac{n_-}{A} + q_M = 0 \quad (6.105)$$

Subtracting Eq. (6.104) from Eq. (6.105), one gets

$$q_M + F \left( \frac{n_+ - n_+^0}{A} \right) - F \left( \frac{n_- - n_-^0}{A} \right) = 0 \quad (6.106)$$

But, according to the definition of surface excess [see Eq. (6.80)],

$$\Gamma_+ = \frac{n_+ - n_+^0}{A} \quad \text{and} \quad \Gamma_- = \frac{n_- - n_-^0}{A} \quad (6.107)$$

Hence, according to the electroneutrality condition,

$$q_M + F\Gamma_+ - F\Gamma_- = 0 \quad (6.108)$$

and, inserting this condition into Eq. (6.103) one finds that, for a polarizable interface built into a cell with a nonpolarizable interface that leaks negative ions, the second term is zero, so that

$$d\gamma = -\Gamma_+ d\mu \quad (6.109)$$

or

$$\left( \frac{\partial \gamma}{\partial \mu} \right)_{\text{const. } V_-} = -\Gamma_+ \quad (6.110)$$

Now,

$$\begin{aligned} \mu &= (\mu_+ + \mu_-) \\ &= (\mu_+^0 + \mu_-^0) + (RT \ln a_+ + RT \ln a_-) \\ &= (\mu_+^0 + \mu_-^0) + (RT \ln a_+ a_-) \end{aligned} \quad (6.111)$$

Instead of  $a_+ a_-$ , one can introduce the mean ionic activity  $a_{\pm}$ , obtained by multiplying Eqs. (3.71) and (3.72). Thus,

$$a_{\pm} = (x_{\pm} f_{\pm}) = (x_+ f_+)^{\frac{1}{2}} (x_- f_-)^{\frac{1}{2}} = (a_+ a_-)^{\frac{1}{2}} \quad (6.112)$$

or

$$a_+ a_- = a_{\pm}^2 \quad (6.113)$$

Hence, from (6.111) and (6.113),

$$\mu = (\mu_+^0 + \mu_-^0) + 2RT \ln a_{\pm} \quad (6.114)$$

or

$$d\mu = 2RT d \ln a_{\pm} \quad (6.115)$$



Hence, substituting Eq. (6.115) into Eq. (6.110),

$$\left( \frac{\partial \gamma}{2RT \partial \ln a_{\pm}} \right)_{\text{const. } V_-} = -\Gamma_+ \quad (6.116)$$

which shows that the slope of the surface tension versus  $\ln a_{\pm}$  curve at constant potential yields the surface excess. Of course, the activity of the electrolyte,  $a_{\pm}$ , is obtained by taking the bulk concentration and multiplying it by the mean activity coefficient at that concentration. Figure 6.58 shows three-dimensional plots of the surface excess,  $\Gamma$ , of ter-amyl alcohol on Au(100) as a function of the electrode potential,  $V$ , the logarithm of alcohol concentration,  $\ln c$ , and the metal charge,  $q_M$ .

An interesting point to note is that the surface excess of the positive ion is determined by choosing a nonpolarizable interface that leaks negative ions. Following an argument similar to that given above, one could have shown that a nonpolarizable interface that leaks positive ions enables the determination of the surface excess of negative ions. Thus, in a study of the Hg–HCl polarizable interface, the surface excess  $\Gamma_-$  of the  $\text{Cl}^-$  ions may be obtained by coupling the Hg/HCl interface with a hydrogen reference electrode that leaks hydrogen ions.

If the determination of surface excess is carried out at various cell potentials, then one can plot the surface excesses  $\Gamma_+$  and  $\Gamma_-$  of the positive and negative ions as a function of the cell potential  $V$ . It is more useful, however, to plot  $q^+ = z_+ F \Gamma_+$  and  $q^- = z_- F \Gamma_-$ , i.e., the excess-charge densities in the solution side of the interface due to the surface excesses of positive and negative ions (Fig. 6.59 and Table 6.5). Since the charge density  $q_S = -q_M$  in the solution is made up of the algebraic sum of the excess positive and excess negative charge densities,  $q^+$  and  $q_-$  are the components of the (excess) charge in the solution

$$\begin{aligned} -q_M = q_S &= q^+ + q^- \\ &= z_+ F \Gamma_+ + z_- F \Gamma_- \end{aligned} \quad (6.117)$$

The components-of-charge curve (Fig. 6.59) must be read as follows: When, e.g.,  $q^-$  is negative, it means that  $\Gamma_- = q^-/z_- F$  is positive, i.e., there is an accumulation of negative ions in the interphase relative to the bulk; and when  $q^-$  is positive,  $\Gamma_-$  is negative, which indicates a depletion of negative ions in the interphase. At the ecm,  $q_M = -q_S = 0$ ; hence,  $q^- = q^+$ .

## 6.5.8. Summary of Electrocapillary Thermodynamics

The thermodynamic equations applicable to a polarizable interface, which can be studied by means of a capillary electrometer, can now be summarized. The general equation is

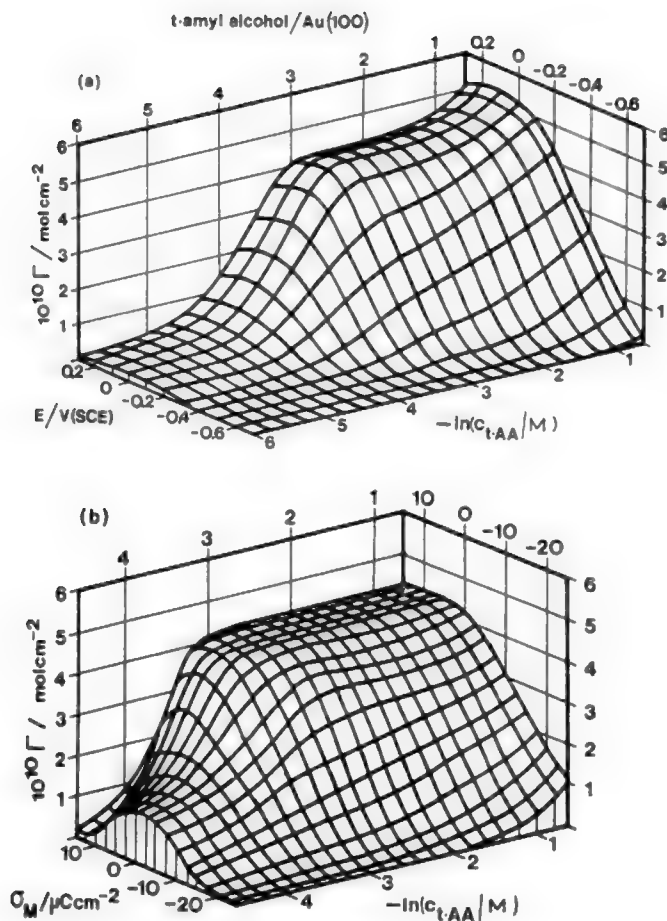


**Fig. 6.58.** Three-dimensional graphs representing the surface excess (approximately equivalent to the number of adsorbed molecules) of *ter*-amyl alcohol calculated with respect to (a) the electrode potential and (b) the charge density. The electrical variable varies along the axis "normal" to the plane of the figure. The maximum surface excess corresponding to the plateau on both graphs is equal to  $4.4 \times 10^{-10} \text{ mol cm}^{-2}$ . In this figure  $\sigma_M = q_M$ . (Reprinted from J. Richer and J. Lipkowski, *J. Electroanal. Chem.* **251**:217, copyright 1988, Fig. 12, with permission of Elsevier Science.)

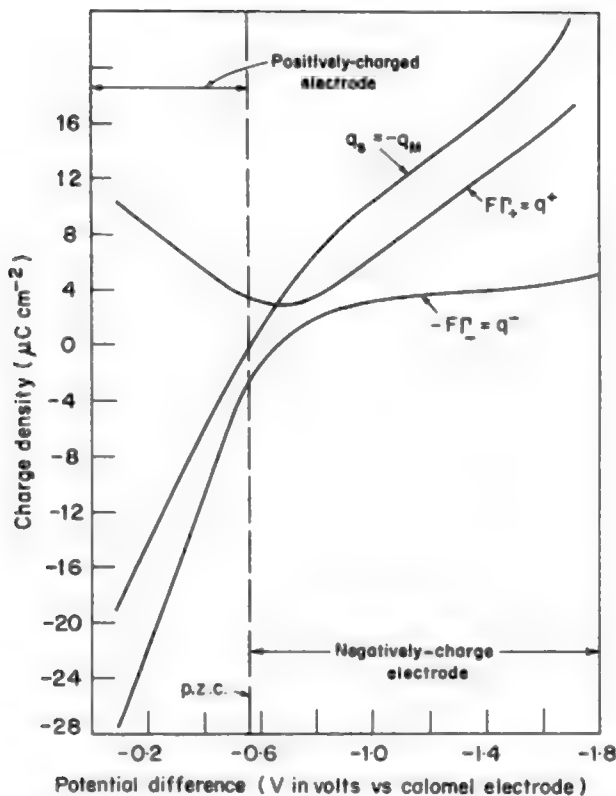


**Fig. 6.59.** Components of charge density as a function of the applied potential  $V$  in a 1  $N$  NaCl solution.

$$d\gamma = -q_M dV - \frac{q_M}{z_j F} d\mu_j - \sum_i \Gamma_i d\mu_i \quad (6.92)$$

By keeping the solution composition constant, i.e.,  $d\mu_i = 0 = d\mu_j$ , the charge density  $q_M$  on the metal is given by the slope of the interfacial tension  $\gamma$  versus the applied potential  $V$  curve

$$q_M = - \left( \frac{\partial \gamma}{\partial V} \right)_{\text{const. comp.}} \quad (6.95)$$

From the variation of this charge density with applied potential, the differential capacity of the interface is obtained

**TABLE 6.5**  
**Surface Excess of Cs<sup>+</sup> and Cl<sup>-</sup> Ions in a Mercury-1.0 N CsCl Interphase as a**  
**Function of Applied Potential**

Potential (mV) vs calomel electrode	$q^+ = F\Gamma_+$ ( $\mu\text{C cm}^{-2}$ )	$q^- = F\Gamma_-$ ( $\mu\text{C cm}$ )
-200	10.2	-26.8
-300	8.7	-19.2
-400	7.5	-13.4
-500	6.5	-8.5
-600	5.8	-4.4
-700	5.5	-0.9
-800	5.8	1.4
-900	6.9	2.6
-1000	8.5	2.8

$$C = \left( \frac{\partial q_M}{\partial V} \right)_{\text{const.comp.}} = - \left( \frac{\partial^2 \gamma}{\partial V^2} \right)_{\text{const.comp.}} \quad (6.97)$$

The surface excess of a species  $i$  is obtained from the plot of interfacial tension versus mean activity of the electrolyte taken under conditions of constant applied cell potential  $V$ . By considering various applied potentials, one can get the surface excess  $\Gamma_+$  and  $\Gamma_-$  and thus the excess-charge densities  $q^+ = z_+ F \Gamma_+$  and  $q_- = z_- F \Gamma_-$ , due to the positive and negative ions, as a function of the applied potential

$$\Gamma_{\pm} = - \left( \frac{\partial \gamma}{2RT \partial \ln a_{\pm}} \right)_{\text{const. } V_{\mp}} \quad (6.116)$$

### 6.5.9. Retrospect and Prospect for the Study of Electrified Interfaces

What has been learned so far about electrified interfaces? First, one has learned what a double layer is. It is an interphasial region (between two homogeneous phases) in which the charged constituents have been separated so that each side of the interface is electrified. The charges on the two sides are equal in magnitude but opposite in sign, making the interphase region electrically neutral as a whole.

Second, the inner potential difference across a double layer,  $\Delta\phi$ , was defined. It was determined that this inner potential can be resolved into two contributions. One of them, the outer potential difference or  $\Delta\psi$ , emerged from the charges in the electrode and/or in the solution, and was found to be a measurable quantity. The other potential, the surface potential difference or  $\Delta\chi$ , was due to the oriented dipoles existing on one

or both of the phases, and its immeasurability was determined. It was learned that the absolute value of the inner potential is also a quantity impossible to measure, although changes in this potential across a polarizable interface can be measured provided the other interface is nonpolarizable. With this in mind, it was determined that although it is conceptually important, the inner potential difference was not useful enough because of its immeasurable characteristic.

Then, an absolute electrode potential was defined,  $E^M(\text{abs})$ . It was established that the absolute electrode potential for the reference hydrogen electrode has a value between  $-4.44$  V and  $-4.78$  V, and a scale of absolute potentials for different reactions was obtained. This was an important step because knowledge of this scale allows one to predict the direction of electron flow when two electrodes are brought into electrical contact.

Third, a curious and subtle concept was explained, the concept of surface excess,  $\Gamma$ . This is not to be confused with adsorption, although the surface excess may become nearly identical to the total amount adsorbed under certain limiting conditions. The surface excess of a particular species is the excess of that species present in the surface phase relative to the amount that would have been present had there been no double layer. The surface excess, therefore, represents the accumulation or depletion of the species in the entire interphase region. Further, electrocapillary measurements and radiochemical experiments permit a direct experimental description of the surface excess of a species.

The surface excess of the various species in an interphase does not, however, reveal the time-average locations of the ions, dipoles, etc., i.e., the structure of the interphase. The various species (e.g., the ions) are distributed in the interphase region so that their concentrations vary with distance from the electrode. Knowledge of structure hinges upon knowing these concentration variations. It is by the integration of these concentrations that the surface excesses are obtained, but, being definite integrals, the surface excesses retain no information on that concentration variation.

What next? One must seek knowledge of the distribution of particles in the interphase region—the structure. One must also seek the variation of potential with distance and the interatomic forces that make up the interphasial structure. One seeks to develop the atomic theory of the interface. To achieve these tasks, one must learn to intuit models, for these are the crutches that can aid one in acquiring an atomic view of an electrified interface. A preview of these models will be presented in the next sections.

## Further Reading

### Seminal

1. G. Lippmann, *Ann. Chim. Phys.* (Paris) **5**: 494 (1875). Shows that electrocapillary curves yield surface charge.
2. W. Gibbs, *The Scientific Papers of J. Willard Gibbs*, Vol. 1: *Thermodynamics*, Dover, New York (1961).

3. E. A. Guggenheim and N. K. Adam, "Thermodynamics of Adsorption at the Surface of Solutions," *Proc. Roy. Soc. (London)* **A139**: 218 (1933).
4. D. C. Grahame, "The Electrical Double Layer and the Theory of Electrocapillary," *Chem. Revs.* **41**: 441 (1947).
5. R. Parsons, "Equilibrium Properties of Electrified Interphases," in *Modern Aspects of Electrochemistry*, J. O'M. Bockris and B. Conway, eds., Vol. 1, Butterworths London (1954).

## Reviews

1. A. Hamelin, "The Surface State and the Potential of Zero Charge of Gold (100)- A further Assessment," *J. Electroanal. Chem.* **386**(1-2): 1 (1995).

## Papers

1. J. Lipkowski and L. Stolberg, "Molecular Adsorption at Gold and Silver Electrodes," in *Adsorption of Molecules at Metal Electrodes*, J. Lipkowski and P. N. Ross, eds., p. 171, VCH Publishers, New York (1992).
2. I. R. Peterson, *Colloids and Surfaces: Physicochemical and Engineering Aspects*, **102**: 21 (1995).
3. M. J. Honeychurch and M. J. Ridd, *J. Electroanal. Chem.* **418**(1-2): 185 (1996).
4. J. Dabkowski, I. Zagorska, M. Dabkowska, Z. Koczorowski, and S. Trasatti, *J. Chem. Soc. Faraday Trans.* **92**(20): 3873 (1996).
5. I. O. Efimov and K. E. Heusler, *J. Electroanal. Chem.* **414**(1): 75 (1996).
6. M. L. Foresti, M. Innocenti, and G. Pezzatini, *Langmuir* **12**(4): 1061 (1996).
7. M. Turowska, D. Kazmierczak, and T. Blaszczyk, *Polish J. Chem.* **71**(2): 221 (1997).
8. J. H. Chen, S. H. Si, L. H. Nie, and S. Z. Yao, *Electrochimica Acta* **42**(4): 689 (1997).

## 6.6. THE STRUCTURE OF ELECTRIFIED INTERFACES

### 6.6.1. A Look into an Electrified Interface

Consider the picture of the metal/solution interface shown in Fig. 6.60. It looks complicated, but actually the picture will be seen to consist of simple elements. The metal is made up of a lattice of positive ions and free electrons. When the metal is charged with an excess-charge density  $q_M$ , it means that there is either an excess ( $q_M$  is negative), or a deficit ( $q_M$  is positive) of free electrons at the surface of the metal.

The metal surface can be compared to a stage occupied by this excess-charge density  $q_M$ . The particles of the solution constitute the audience that responds to the scene on the stage. The first row is largely occupied by water dipoles (Fig. 6.61). The excess charge on the metal produces a preferential orientation of the water dipoles. This is the *hydration sheath* of the electrode (see Chapter 2). The net orientation of the dipoles varies with the charge on the metal, and the dipoles can even turn around and look away from the electrode.

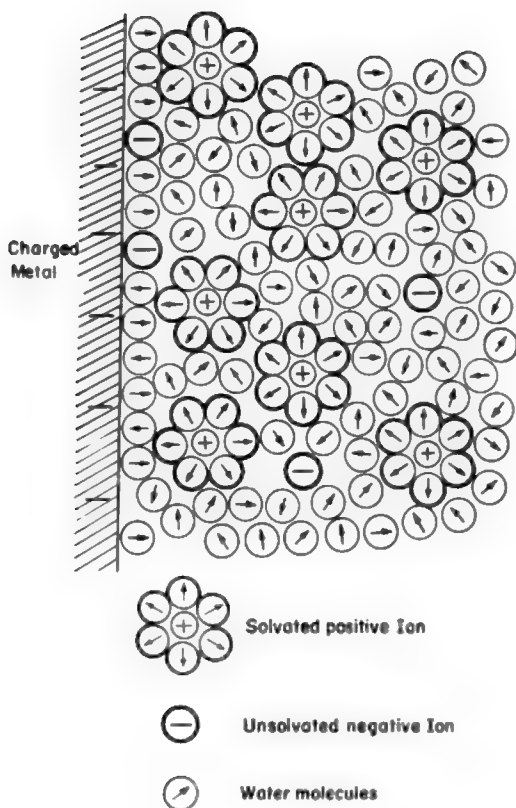


**Fig. 6.60.** A schematic representation of the structure of an electrified interface. The small, positive ions tend to be solvated, while the larger, negative ions are usually unsolvated (see Section 2.3.7).

The second row is largely reserved for solvated ions. The locus of centers of these solvated ions is called, for historical reasons, the *outer Helmholtz plane*, hereafter referred to as OHP (Fig. 6.61). On top of the first-row water (the primary water layer) and in between the solvated ions are other water molecules, a sort of secondary hydration sheath, feebly bound to the electrode.

The above paragraphs give a brief description of the metal/solution interface. However this is only a qualitative description without any detail on how ions or molecules in solution are arranged. At this point one may ask: Are the ions touching the electrode? Or do the solvent molecules interact with the ions in the interfacial region? Or does the material of the electrode matter? Or what happens if the electrode is positively charged?

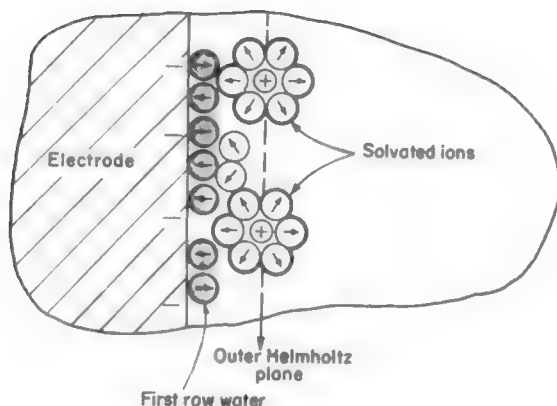


**Fig. 6.61.** A layer of solvated ions on the layer of first-row water. The locus of the centers of these solvated ions defines the OHP.

How can these questions be answered? One way to learn more about any system, in this case the interfacial region, is to propose a model of the system. Once this model is conceptually and mathematically defined, it can be tested by comparing it with data obtained from experiments. If the model fails, then a new model or a modification of the original model is tested again, until one obtains a reasonable match of the model's results with the experimental data. This is the procedure followed in the development of any theory. This is the way understanding of any system increases. Thus, to understand the structure of electrified interfaces, we should start looking at proposed models, design mathematical models of interfaces, and see how well their results fit with the experimental data. In this way we will gain a better understanding of the metal/solution interface.

### 6.6.2. The Parallel-Plate Condenser Model: The Helmholtz–Perrin Theory

The simplest model of the electrified interface arose from the work of Helmholtz and Perrin. They thought that the charge on the metal would draw out from the randomly dispersed ions in solution a counter-layer of a charge of an opposite sign. In this way the electrified interface will consist of two sheets of charge, one on the electrode and the other in the solution, as shown in Fig. 6.62(a). Hence, the term “double layer.” The charge densities on the two sheets are equal in magnitude but opposite in sign, exactly as in a parallel-plate capacitor [Fig. 6.62(b)]. The drop in potential between these two layers of charge is, then, a linear one [Fig. 6.62(c)].



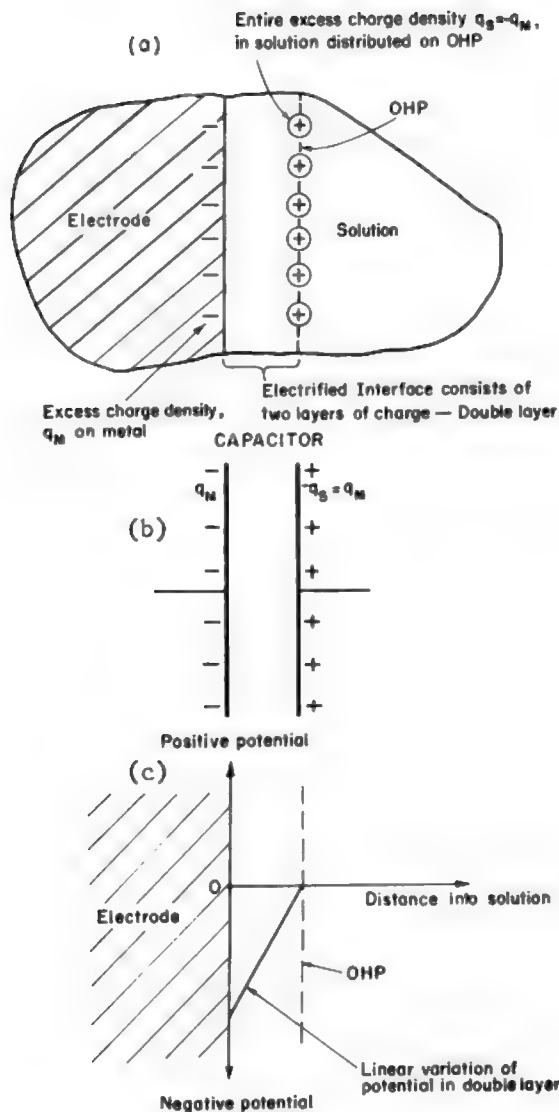


**Fig. 6.62.** The Helmholtz-Perrin parallel-plate model. (a) A layer of ions on the OHP constitutes the entire excess charge in the solution,  $q_s$ . (b) The electrical equivalent of such a double layer is a parallel-plate condenser. (c) The corresponding variation of potential is a linear one. (Note: The solvation sheaths of the ions and electrode are not shown in this diagram nor in subsequent ones.)

Once the electrical equivalence between an electrified interface and a capacitor is postulated, the electrostatic theory of capacitors can be used for double layers. It is known, for example, that the potential difference  $V$  across a condenser of unit area is

$$V = \frac{d}{\epsilon \epsilon_0} q_M \quad (6.118)$$

or

$$dV = \frac{d}{\epsilon \epsilon_0} dq_M \quad (6.119)$$

where  $d$  is the distance between the plates,  $\epsilon$  is the dielectric constant of the material between the plates, and  $\epsilon_0$  is a constant called the *permittivity of free space* ( $\epsilon_0 = 8.854 \times 10^{-12} \text{ C}^2 \text{ J}^{-1} \text{ m}^{-1}$ ).

What can it be done with this expression? For once it is possible to consider the Lippmann equation [Eq. (6.95)] and replace  $dV$  in Eq. (6.119). Thus one has

$$\int d\gamma = \frac{d}{\epsilon \epsilon_0} \int q_M dq_M \quad (6.120)$$

or, after integrating Eq. (6.120),

$$\gamma + \text{const} = \frac{d}{\epsilon \epsilon_0} \frac{q_M^2}{2} \quad (6.121)$$

To evaluate the constant, it is possible to apply the known condition that at  $q_M = 0$ ,  $\gamma = \gamma_{\max}$  (see Fig. 6.53), and therefore  $\text{const} = -\gamma_{\max}$ . Hence,

$$\gamma = \gamma_{\max} - \frac{d}{\epsilon \epsilon_0} \frac{q_M^2}{2} \quad (6.122)$$

or

$$\gamma = \gamma_{\max} - \frac{\epsilon \epsilon_0}{d} \frac{V^2}{2} \quad (6.123)$$

This is the equation for a parabola symmetrical about  $\gamma_{\max}$ , i.e., about the electrocapillary maximum.

Going a step further, what does the parallel-plate model of the double layer have to say regarding the capacity of the interface? Rearranging Eq. (6.119) in the form of the definition of differential capacity [Eq. (6.97)],

$$C = \frac{dq}{dV} = \frac{\epsilon\epsilon_0}{d} \quad (6.124)$$

Thus, if  $\epsilon$  and  $d$  are taken as constants, the parallel-plate model predicts a constant capacity, i.e., one that does not change with potential. So it appears that the Helmholtz–Perrin model would be quite satisfactory for electrocapillary curves that are perfect parabolas (Fig. 6.56).

### 6.6.3. The Double Layer in Trouble: Neither Perfect Parabolas nor Constant Capacities

However, is the electrocapillary curve a perfect parabola? Almost, but not quite. There is always a slight asymmetry (see Fig. 6.56), and that asymmetry precludes it from having constant capacities, as the Helmholtz–Perrin model predicts.

Also, the deviations from a parabolic shape are greater with some solutions than with others. Electrocapillary curves show, for instance, a marked sensitivity to the nature of the anions present in the electrolyte (Fig. 6.63). In contrast, the curves do not seem to be affected significantly by the cations present unless they are large organic cations, e.g., tetraalkylammonium ions.

It appears that an electrified interface does not behave like a simple double layer. The parallel-plate condenser model is too naïve an approach. Evidently some crucial secrets about electrified interfaces are contained in those asymmetric electrocapillary curves and the differential capacities that vary with potential. One has to think again.

### 6.6.4. The Ionic Cloud: The Gouy–Chapman Diffuse-Charge Model of the Double Layer

In the previous section it was seen that the Helmholtz–Perrin model fixes the solution charges onto a sheet parallel to the metal. However, this model was too rigid

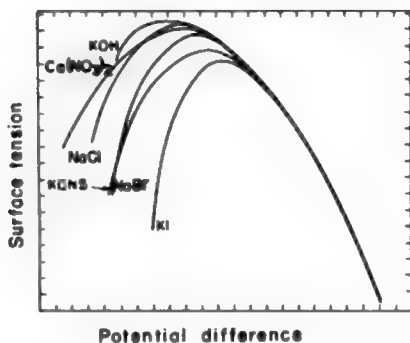


**Fig. 6.63.** The dependence of electrocapillary curves on the nature of the anions present in the electrolyte.

to explain the asymmetry of electrocapillary curves and the dependence of capacity upon potential. Perhaps it was the lack of freedom of the charges in the solution that precipitated the inconsistency. Why not free them from their restriction to a sheet? It was Gouy and Chapman who thought of liberating the ions from a sheet parallel to the electrode. However, once the ions are free, they become exposed to the thermal buffeting from the particles of the solution. The behavior of ions in the vicinity of the electrode is affected by the electric force arising from the charge on the electrode and by thermal jostling.

Thus, in the Gouy–Chapman model the excess-charge density on the OHP is not equivalent to that on the metal, but is less (Fig. 6.64). Some of the solvated ions leave their second-row seats and random walk in the solution. The excess-charge density in the solution decreases with distance from the electrode. The electrode has a sort of ionic atmosphere. Near the metal, its charge attracts the solvated ions to the second row. Further out, thermal motions have an influence comparable to the forces from the electrode. Sufficiently far into the solution, the net charge density is zero because positive and negative ions are equally likely in any region—thermal motion reigns supreme.

With the ionic cloud on the electrode, the resemblance of the Gouy–Chapman model to that of the theory of ion-ion interactions in solution reviewed in Chapter 3 is evident. There, it was necessary to arbitrarily choose one ion and spotlight it as the “central ion,” or source, of the field. Here, the discussion resolves on ion–electrode interactions with the electrode as the source of the field. The response of an ion, however, does not depend on how the electric field is produced (i.e., whether the source is a central ion or a charged electrode). It depends only on the value of the field at the location of the ion. Hence, the electrostatic arguments in the problems of ion–ion interactions and ion–electrode interactions must be similar.

There are, however, differences in the geometry of the two problems. These differences affect the mathematical development. Thus, the central ion puts out a spherically symmetrical field. In contrast, the electrode is like an infinite plane (infinite vis-à-vis the distances at which ion–electrode interactions are considered), and its field displays a planar symmetry. Otherwise, the technique of analysis of the diffuse double layer proceeds along the same lines as in the theory of long-range ion–ion interactions (Section 3.3).<sup>43</sup>

Thus, the corresponding field or gradient of potential at a distance  $x$  from the electrode according to the diffuse-charge model of Gouy and Chapman is given by the expression:

---

<sup>43</sup>However, it is interesting to note that the theory of the diffuse double layer was presented independently by Gouy and Chapman (1910) 13 years *before* the Debye–Hückel theory of ion–ion interactions (1923). The Debye–Hückel theory was immediately discussed and applied to the diffuse charge around an ion, doubtless owing to the preoccupation of the majority of scientists in the 1920s with bulk properties rather than those at surfaces.

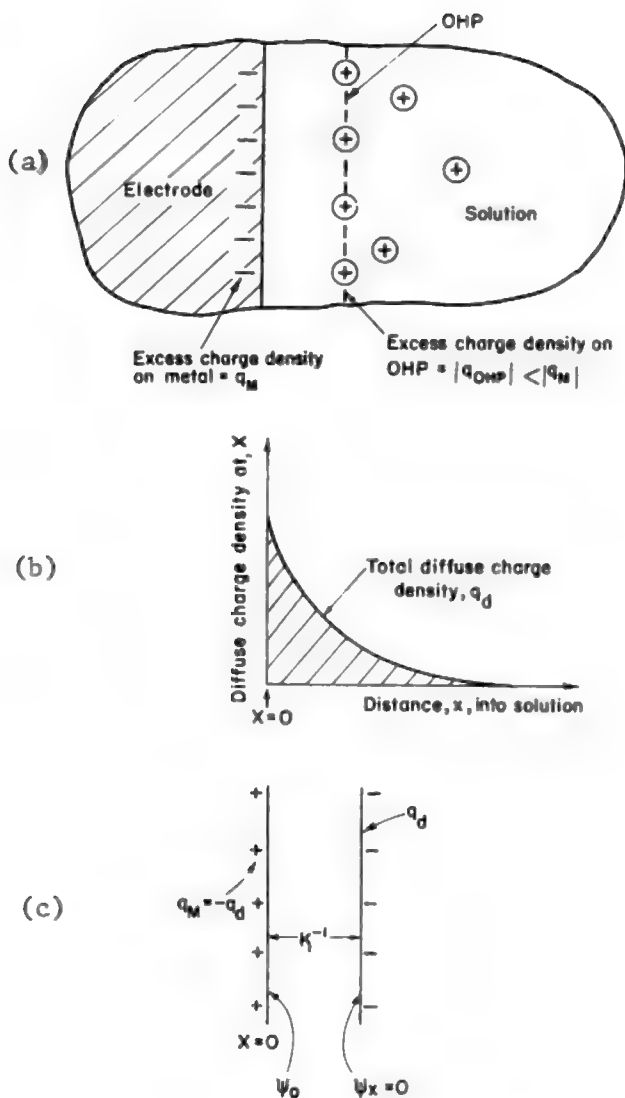


**Fig. 6.64.** The Gouy-Chapman model. (a) The excess charge density on the OHP is smaller in magnitude than the charge on the metal. The remaining charge is distributed in the solution. The diffuse charge region, (b), can be simulated by a sheath of charge  $q_d$  placed at a distance  $\kappa^{-1}$  from the  $x = 0$  plane, as depicted in (c).

$$\frac{d\psi}{dx} = - \left( \frac{8 k T c_0}{\epsilon \epsilon_0} \right)^{1/2} \sinh \frac{ze_0 \psi_x}{2 k T} \quad (6.125)$$

where  $c_0$  is the concentration of the  $i$ th species in the bulk of the solution,  $\epsilon$  is the dielectric constant of solution,  $\epsilon_0$  is the permittivity of free space, and  $\psi_x$  is the outer potential difference between a point  $x$  from the electrode and the bulk of the solution. Hence, Eq. (6.125) spells out the relation between the electric field and the potential at any distance  $x$  from the electrode.

Two important quantities that it would be interesting to know are the total diffuse charge in the solution,  $q_d$ , and how the potential varies with distance. According to Gauss's law from electrostatics, the charge contained within a closed volume (Gaussian box) is equal to  $\epsilon \epsilon_0$  times the area of the closed surface (taken here as unity) times the component of the field normal to the surface of the enclosed volume

$$q = \epsilon \epsilon_0 \frac{d\psi}{dx} \quad (6.126)$$

However, to determine the total diffuse-charge density,  $q_d$ , the Gaussian box should extend from a place very close to the electrode, e.g.  $x = 0$ ,<sup>44</sup> to a place deep inside the solution,  $x \rightarrow \infty$ , where  $\psi_x = 0$  and  $d\psi_x/dx = 0$ . Hence, with these conditions the total diffuse-charge density scattered in the solution under the interplay of thermal and electrical forces,  $q_d$ , is given from Eqs. (6.125) and (6.126),

$$q_d = -2(\epsilon \epsilon_0 c_0 k T)^{1/2} \sinh \frac{ze_0 \psi_0}{2 k T} \quad (6.127)$$

where  $\psi_0$  is the potential at  $x = 0$  relative to the bulk of the solution where the potential is taken as zero.

The second relationship, the variation of the potential with distance, can be obtained from the integration of Eq. (6.125). Thus, assuming that  $\sinh(ze_0 \psi_x)/(2kT) \approx (ze_0 \psi_x)/(2kT)$ ,

$$\ln \psi_x = - \left( \frac{2c_0 z^2 e_0^2}{\epsilon \epsilon_0 k T} \right)^{1/2} x + \text{const} \quad (6.128)$$

However, the quantity inside the brackets, i.e.,  $2c_0 z^2 e_0^2 / \epsilon \epsilon_0 k T$ , is nothing else than the familiar  $\kappa^2$  of the Debye-Hückel theory. The integration constant in Eq. (6.128) can be evaluated from the boundary condition that at  $x \rightarrow 0$ ,  $\psi_x \rightarrow \psi_0$ . Therefore,

<sup>44</sup>In the Gouy-Chapman model, the ions are considered as *point-charge ions*, so  $x = 0$  ensures that the Gaussian box contains all the diffuse charges.

$$\psi_x = \psi_0 e^{-\kappa x} \quad (6.129)$$

This is the expression we were looking for. What does it tell us? For one thing, that the potential decays exponentially as the distance from the electrode increases [Fig. 6.64(b)]. Further, as the solution concentration  $c_0$  increases,  $\kappa$  increases and  $\psi_x$  falls more and more sharply. This potential-distance relation [Fig. 6.64(b)] is an important and simple result from the Gouy–Chapman model. It forms a valuable basis for thinking about the interaction of the diffuse charges around what are called *colloidal* particles (see Section 6.10.2).

Let's now have a closer look at Eq. (6.129). Here the same  $\kappa$  used in the Debye–Hückel theory is used. However, what would be the meaning of this variable when instead of a central ion there is an electrode? In the ionic-cloud model, the cloud on the central ion was simulated by placing the entire charge of the cloud,  $-ze_0$ , at the distance  $\kappa^{-1}$  from the central ion (Chapter 3). Given the similarity between the two systems, it would be possible to follow a similar reasoning for the electrode and its diffuse charge. Thus, the diffuse charge of the electrode can be simulated by placing the total diffuse charge,  $q_d$ , at a distance  $\kappa^{-1}$  from the electrode. One has in effect a parallel-plate condenser situation, i.e., a charge of  $-q_d = q_M$  at the  $x = 0$  plate and the diffuse charge  $q_d$  at the  $x = \kappa^{-1}$  plate [Fig. 6.64(c)].

A third quantity that must be calculated is the differential capacity. This can be obtained by differentiating Eq. (6.127) with respect to the potential,  $V$  [see Eq. (6.97)]. However in Eq. (6.127) the variable is  $\psi_0$ , i.e., the potential at  $x = 0$ . Thus, what is the relationship between  $V$  and  $\psi_0$ ? At  $x=0$ ,  $V = \psi_0 - \psi_{\text{bulk}}$ , and therefore  $dV = d\psi_0$  because  $\psi_{\text{bulk}} = 0$ . Even more,  $\psi_0$  could be replaced by  $\psi_M$  since the ions are considered as point-charge ions. Thus, with  $dq_M = -dq_s = -dq_d$ , the differential is

$$C = \left( \frac{\partial q_M}{\partial V} \right)_{\text{const.comp.}} = - \left( \frac{\partial q_d}{\partial \psi_M} \right)_{\text{const.comp.}} = \left( \frac{2\epsilon\epsilon_0 z^2 e_0^2 c_0}{kT} \right)^{1/2} \cosh \frac{ze_0 \psi_M}{2kT} \quad (6.130)$$

Now, the cosh function gives inverted parabolas [Fig. 6.65(b)]. Hence, according to the simple diffuse-charge theory, the differential capacity of an electrified interface should not be a constant. Rather, it should show an inverted-parabola dependence on the potential across the interface. This, of course, is a welcome result because the major weakness of the Helmholtz–Perrin model is that it does not predict any variation in capacity with potential, although such a variation is found experimentally [Fig. 6.65(b)].

### 6.6.5. The Gouy–Chapman Model Provides a Potential Dependence of the Capacitance, but at What Cost?

After the initial jubilation that the diffuse-layer model has overcome the weakness of constant capacity with change of potential of the parallel-plate model, one has to

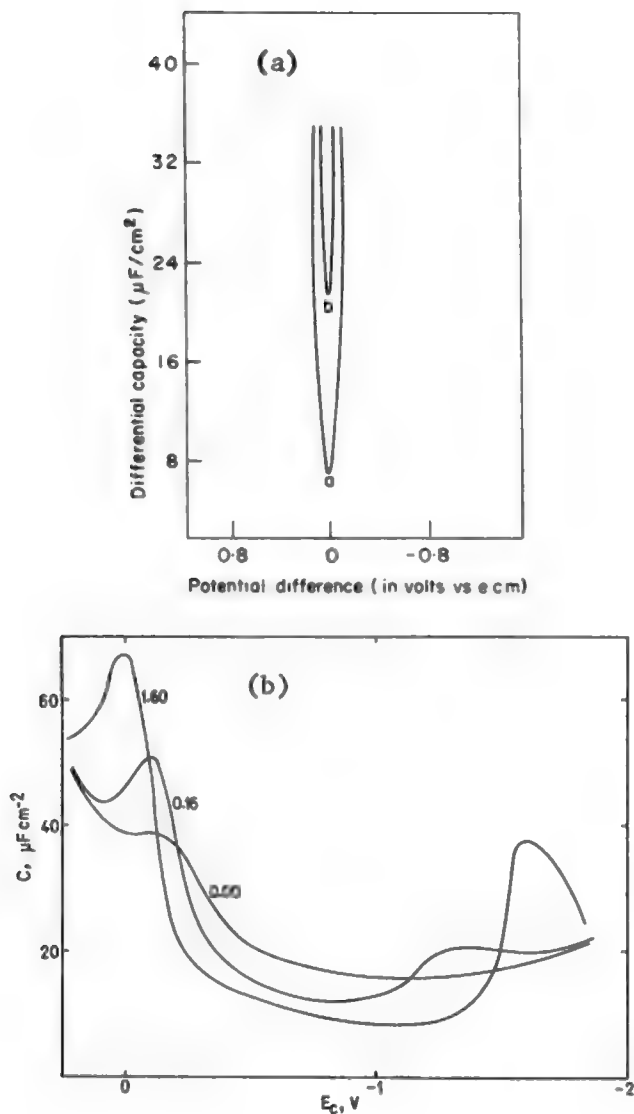


**Fig. 6.65.** (a) Representation of the Gouy–Chapman theory according to Eq. (6.130). (b) Plots of the differential capacity of the mercury/solution interface vs. electrode potential for various concentrations of  $N,N$  dimethylacetamide in 0.15  $M$   $\text{Na}_2\text{SO}_4$ -water. (Reprinted with permission from W. R. Fawcett, G. Y. Champagne, S. Komo, and A. J. Motheo, *J. Phys. Chem.* **92**: 6368, Fig. 6, copyright 1988, American Chemical Society.)



face a few more somber facts about the details of the model. The main fact is that the experimental capacity–potential curves are not the inverted parabolas that the Gouy–Chapman diffuse model predicts [Fig. 6.65(b)]. Only in very dilute solutions ( $<0.001 \text{ mol dm}^{-3}$  for 1:1 electrolytes) and at potentials near the pzc are there *portions* of the experimental curves that suggest that the interface is behaving in a Gouy–Chapman way.

We could point to several reasons why the model fails to predict reality. For one, it neglects ion–ion interactions, which definitely become important at high concentrations. A second error, and perhaps the most important, is the assumption of point-charge ions. Finally comes the value of the dielectric constant, which was taken as a constant in the region between the electrode and the bulk of the solution.

However, even taking all these facts into account, this theory is not able to reproduce the capacitance–potential curves in the regions beyond the pzc proximity. The model seems, in fact, to be in sharp disagreement with the experimental behavior. The Gouy–Chapman theory might best be described as a brilliant failure. However, as will be seen, it represents an important contribution to a truer description of the double layer; it also finds use in the understanding of the stability of colloids and, hence, of the stability of living systems (see Section 6.10.2.2).

### 6.6.6. Some Ions Stuck to the Electrode, Others Scattered in Thermal Disarray: The Stern Model

The next step is fairly obvious: the synthesis of the Helmholtz–Perrin thesis of a layer of ions in contact with the electrode and the Gouy–Chapman antithesis of the ions being scattered out in solution in thermal disarray. This synthesis was made by Stern.

The simplest version of the Stern theory consists in eliminating the point-charge approximation of the diffuse-layer theory. This is done in exactly the same way [Fig. 6.66(a)] as in the theory of ion–ion interactions (see Chapter 3); the ion centers are taken as not coming closer than a certain distance  $a$  from the electrode.

The second modification of the Stern theory consists in dividing the solution charge into two contributions. Thus, according to the Stern picture, part of the charge  $q_S$  on the solution is immobilized close to the electrode in the OHP (the Helmholtz–Perrin charge or  $q_H$ ), and the remainder is diffusely spread out in the solution (the Gouy–Chapman charge or  $q_G$ ), i.e.,

$$q_S = q_H + q_G \quad (6.131)$$

When, however, charges are separated, potential drops result. The Stern model implies, therefore, two potential drops, i.e.,

$$\phi_M - \phi_{\text{bulk}} = (\phi_M - \phi_H) + (\phi_H - \phi_{\text{bulk}}) \quad (6.132)$$

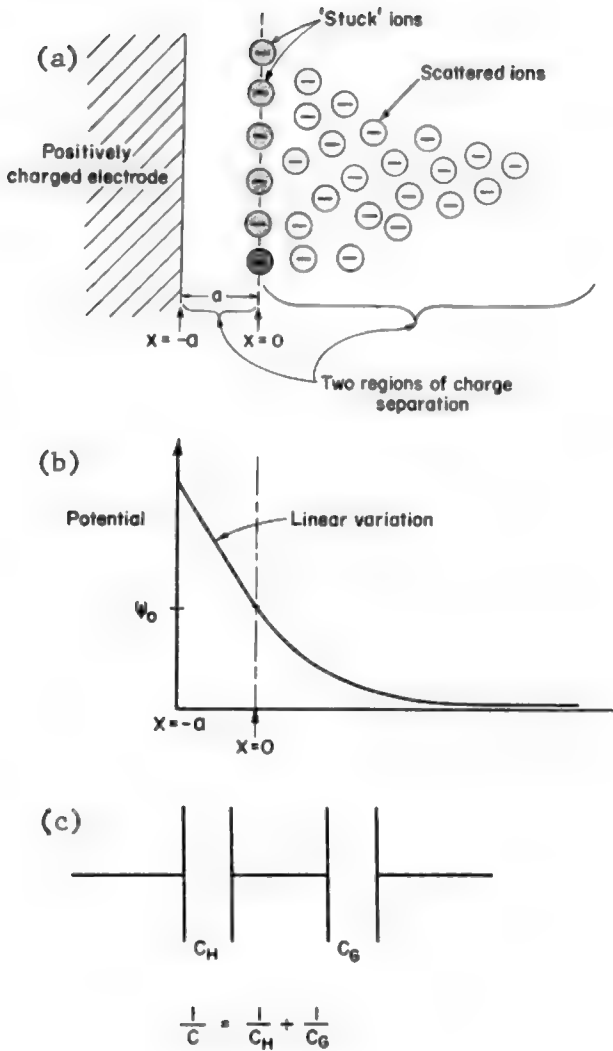


**Fig. 6.66.** The Stern model. (a) A layer of ions stuck to the electrode and the remainder scattered in cloud fashion. (b) The potential variation according to this model. (c) The corresponding total differential capacity  $C$  is given by the Helmholtz and Gouy capacities in series.

where  $\phi_M$  and  $\phi_H$  are the inner potentials at the metal and the Helmholtz planes, and  $\phi_{\text{bulk}}$  is the potential in the bulk of the solution.

What are the implications of Eq. (6.132)? The Stern synthesis of the two models implies a synthesis of the potential–distance relations characteristic of these two models [Fig. 6.66(b)]: a *linear* variation in the region from  $x = 0$  to the position of the OHP according to the Helmholtz–Perrin model (see Section 6.6.2), and an *exponential* potential drop in the region from OHP to the bulk of solution according to the Gouy–Chapman model (see Section 6.6.4), as shown in Fig. 6.67.

A second implication and one that would allow one to evaluate the new model, is that the separation of charges and potential regions also produces a separation of differential capacities. One may start by differentiating the potential difference across the interface [Eq. (6.132)] with respect to the charge on the metal,  $q_M$ ,

$$\frac{\partial(\phi_M - \phi_{\text{bulk}})}{\partial q_M} = \frac{\partial(\phi_M - \phi_H)}{\partial q_M} + \frac{\partial(\phi_H - \phi_{\text{bulk}})}{\partial q_M} \quad (6.133)$$

In the denominator of the last term, one can replace  $\partial q_M$  with  $\partial q_d$  because the total charge on the electrode is equal to the total diffuse charge, i.e.,

$$\frac{\partial(\phi_M - \phi_{\text{bulk}})}{\partial q_M} = \frac{\partial(\phi_M - \phi_H)}{\partial q_M} + \frac{\partial(\phi_H - \phi_{\text{bulk}})}{\partial q_d} \quad (6.134)$$

Now, examine each term in the equation. Each term represents the reciprocal of a differential capacity [see Eq. (6.97)]. Hence, Eq. (6.134) can be rewritten as

$$\frac{1}{C} = \frac{1}{C_H} + \frac{1}{C_G} \quad (6.135)$$

where  $C$  is the total capacity of the interface,  $C_H$  is the Helmholtz–Perrin capacity, and  $C_G$  is the Gouy–Chapman or diffuse-charge capacity.

This result is formally identical to the expression for the total capacity displayed by two capacitors in series [Fig. 6.66(c)]. The conclusion therefore is that an electrified interface has a total differential capacity that is given by the Helmholtz and Gouy capacities in series. Let's examine two extreme cases.

What happens when the concentration  $c_0$  of ions in solution is very large? Equations (6.124) and (6.130) indicate that while  $C_G$  increases with increasing  $c_0$ ,  $C_H$  remains constant. Thus, as  $c_0$  increases,  $(1/C_G) \ll (1/C_H)$ , and for all practical purposes,  $C \approx C_H$ . That is, in sufficiently concentrated solutions, the capacity of the interface is effectively equal to the capacity of the Helmholtz region, i.e., of the parallel-plate model. What this means is that most of the solution charge is squeezed onto the Helmholtz plane, or confined in a region very near this plane. In other words, little charge is scattered diffusely into the solution in the Gouy–Chapman disarray.

MODEL	RELEVANT EQUATIONS	SQUEMATIC	FACTS ABOUT THE MODELS
Helmholtz–Perrin Parallel-Plate Model	$q_M = -q_S = -q_{OHP}$ $C = \frac{\epsilon}{4\pi d}$ $E = \frac{4\pi d}{\epsilon} q_M$		It predicts constant differential capacities. Ions are arranged in a layer (OHP) close to the electrode
Gouy–Chapman Diffuse-Charge Model	$q_M = -q_d = -2 \left( \frac{\epsilon \epsilon_0 kT}{2\pi} \right)^{1/2} \sinh \frac{ze_0 \psi_0}{2kT}$ $C = \left( \frac{\epsilon z^2 e_0^2 C_0}{2\pi kT} \right)^{1/2} \cosh \frac{ze_0 \psi_M}{kT}$ $\psi_x = \psi_0 e^{-\kappa x}$		It predicts that differential capacities have the shape of inverted parabolas. Ions are considered as pointcharges. Ion-ion interactions are not considered. The dielectric constant is taken as a constant.
Stern Combination of Parallel-Plate and Diffuse-Charge Models	$q_M = -q_S = -[q_H + q_G]$ $\frac{1}{C} = \frac{1}{C_H} + \frac{1}{C_G}$ $M_{\Delta^b} \phi = M_{\Delta^b H} \phi + M_{\Delta^b G} \phi$		Ions are under the combined influence of the ordering electrical and the disordering thermal forces. Agrees with the experiment only for ions nonspecifically adsorbed on the electrode (e.g. NaF).

Fig. 6.67. Helmholtz–Perrin, Gouy–Chapman, and Stern models of the double layer.

What happens now at the other extreme case, i.e., at solutions with low concentrations? Under this condition  $(1/C_G) \gg (1/C_H)$  and therefore,  $C \approx C_G$ . This indicates that the electrified interface has become in effect Gouy–Chapman-like in structure, with the solution charge scattered under the simultaneous influence of electrical and thermal forces.

After all this analysis, can we say that the Stern model is consistent with experimental results? In other words, is the Stern model able to reproduce the differential capacity curves? Under certain conditions, it is. So, to some extent, the Stern model was successful. However, what are the restrictions the model imposes? Recall that in the Helmholtz–Perrin model the ions lay close to the electrode on the OHP. The condition for the Stern model to succeed is that ions not be in close proximity to the electrode; they are not to be adsorbed. Thus the model proved to be valid only for electrolytes such as NaF (Grahame, 1947).<sup>45</sup> Both of these ions,  $\text{Na}^+$  and  $\text{F}^-$ , are known to have a hydration layer strongly attached to them in such a way that even in the proximity of the electrode they are almost not interacting with the electrode surface. The Stern model works well representing noninteracting ions.

Nevertheless, when other ions such as  $\text{Cl}^-$ ,  $\text{Br}^-$ ,  $\text{I}^-$ , or  $\text{PO}_4^{3-}$  are in solution, they may come in close contact with the electrode and strongly interact chemically with it. They may *specifically adsorb*<sup>46</sup> on the electrode. The Stern model is not applicable in

---

<sup>45</sup>There seems no doubt that the person who made the most significant contribution to experimental work on the double layer in this century was David C. Grahame of Amherst College in Massachusetts. His comprehensive review of the field in a 1947 issue of *Chemical Review* set the tone for the next generation of workers in this field. The essence of his contribution was an extensive series of measurements of the double-layer capacitance at the mercury/solution interface that he published between 1947 and 1957. Not only did Grahame provide data of a breadth and accuracy not reached earlier, but he was also able to devise, on their basis, a regimen for distinguishing between ions in the interfacial region that were simply held there electrostatically and those that were chemisorbed.

Grahame was certainly a person to whom the description “workaholic” applies. His work was his life and his life was work; not just any work but measurements of the capacitance of the double layer, and what they meant. Amherst being a college and not a university had no graduate students and if (as was usual) faculty wished to do experimental research, they were forced to do it themselves or hire outsiders. Grahame hired women students from two nearby colleges. His rationale was that they were more “obedient” than male technicians. At the same time, Grahame demanded strict time keeping, for he paid by the hour, and to avoid any late arrival or early sloping off, he set unconventional times for the work day. For example, the assistants had to arrive at 7:58, but then they could leave at 4:58. Among the less usual characteristics possessed by this outstanding scientist was an abhorrence of scientific meetings. He thought them to be of no advantage for him because, as he said, “you just get the other fellows’ ideas.” However unusual this viewpoint, it paid off. In 1956 the United States was deep in the Cold War, but when the august Soviet Academy of Sciences held its first post-WWII international meeting in electrochemistry, David Grahame was one of only two U.S. scientists invited.

<sup>46</sup>The word “specific” is used because the extent of the phenomenon seems to depend on the chemical nature of the ion rather than on its charge (e.g., a chloride or fluoride ion, both having the same charge). The contact-adsorbing ion is partly oblivious to the charge on the metal, and it is possible that negative ions may even contact adsorb on a negatively charged electrode and positive ions on positively charged electrodes.

these cases. Thus, how can it be pictured as an interface with ions stuck on the metal? What are the forces that influence the sticking of ions to electrodes, i.e., the removal of the ionic hydration shell? What is the role of the solvent in this type of interface?

These are the types of questions fundamental to an understanding of the electrified double-layer region. These are the questions we will address in the following sections of this chapter. However, before doing that, we should have a closer look at the other part of the double-layer region (i.e., the electrode), which we put aside while focusing on the ions in solution in the interphasial region.

### 6.6.7. The Contribution of the Metal to the Double-Layer Structure

In Section 6.3.8 we discussed the possibility that electrons “jump” out of the metal, leaving behind a positive charge and therefore creating a surface potential,  $\chi_M$ . However, how are the electrons distributed on the metal of the surface, i.e., what model of the metal surface can be used to properly describe the metal–solution properties? How important is the contribution of the metal to these properties?<sup>47</sup>

Consider for a moment the relation of the potential of zero charge and the work function,  $\Phi^M$ , presented in Section 6.3.14, Eq. (6.61),

$$E_{\text{pzc}} = \frac{\Phi^M}{F} + \text{const} \quad (6.136)$$

as well as the corresponding graph, i.e., Fig. 6.46. What does this equation imply? One of the characteristics of  $\Phi^M$  is that it depends entirely on the metal properties. Thus the correlation between these two quantities indicates that the metal properties are somehow involved in the interfacial properties of the double layer.

This is not the only proof that the metal properties are important in the interfacial properties. We have already studied the capacitance curves and found that it is difficult to find a model that would describe the curves properly (Section 6.6.5). Would it be possible then, to think that the metal also contributes to the capacity of the interface and that it could, at least to some extent, explain the shape and asymmetry of the capacitance curves?

It was seen in Section 6.6.6 that the separation of charges and potentials in the double-layer region was done so that the total differential capacity could be divided into two capacities in series,

<sup>47</sup>This question was only considered important after about 1980 for most electrochemists (however, see *Modern Electrochemistry*, 1st ed, Section 725j, 1970). The failure of Rice’s early work (1928) to explain surface properties of metals using the Thomas–Fermi model encouraged scientists to focus on the solution side of the interface and forget any specific contribution of the metal, which was taken as a perfect conductor.

$$\frac{1}{C} = \frac{1}{C_H} + \frac{1}{C_G} \quad (6.137)$$

However, if the contribution of the potential difference of the metal (basically  $g_M$ ) should be included into the total capacity, it would be also in series with the other solution capacities (Fig 6.68), that is,

$$\frac{1}{C} = \frac{1}{C_M} + \frac{1}{C_{\text{soln}}} \quad (6.138)$$

where the term  $C_{\text{soln}}$  includes  $C_H$  and  $C_G$ , and  $C_M$  is the capacity of the metal.

How would  $C_M$  contribute to the total capacity of the double layer? We pointed out earlier that electrons are able to “jump” or come out of the electrode surface, and that they are the main contributors to the surface potential ( $\chi_M$  or  $g_M$ ), and therefore,

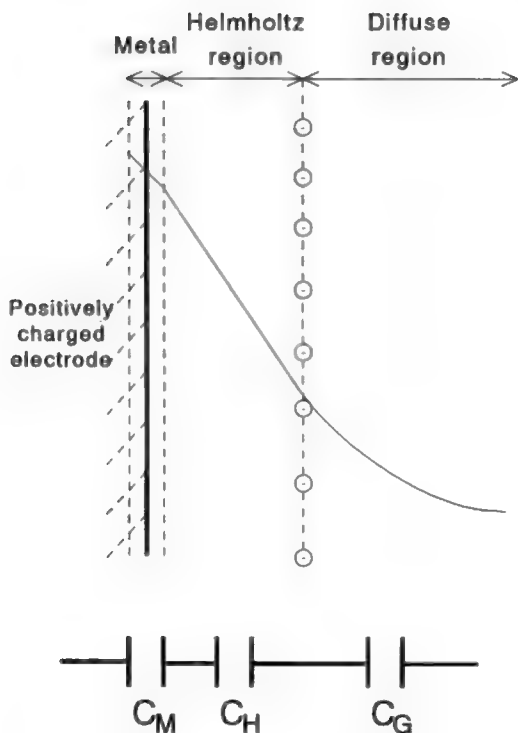


**Fig. 6.68.** Potential drops and capacitances found in the interfacial region.

to  $C_M (= q_M/\chi_M \text{ or } q_M/g_M)$ . Thus, how would this “tail” of electrons react to the positive or negative charging of the electrode? Consider an uncharged electrode that suddenly gets positively charged because electrons are being pumped out of it by an external circuit. The tail of electrons out of the electrode would be attracted by the positive charges and therefore they would tend to recoil toward the electrode [Fig. 6.69(a)]. Under such conditions, the surface potential would decrease, the value of  $C_M$  would increase, and as a consequence the total capacity would decrease. What if the electrode gets negatively charged because of electrons being pumped into it? The opposite situation would occur. A negatively charged electrode will repel the tail electrons, pushing them toward the solution [Fig. 6.69(b)];  $\chi_M$  would increase;  $C_M$  would decrease; and finally the total capacity,  $C$ , would increase.

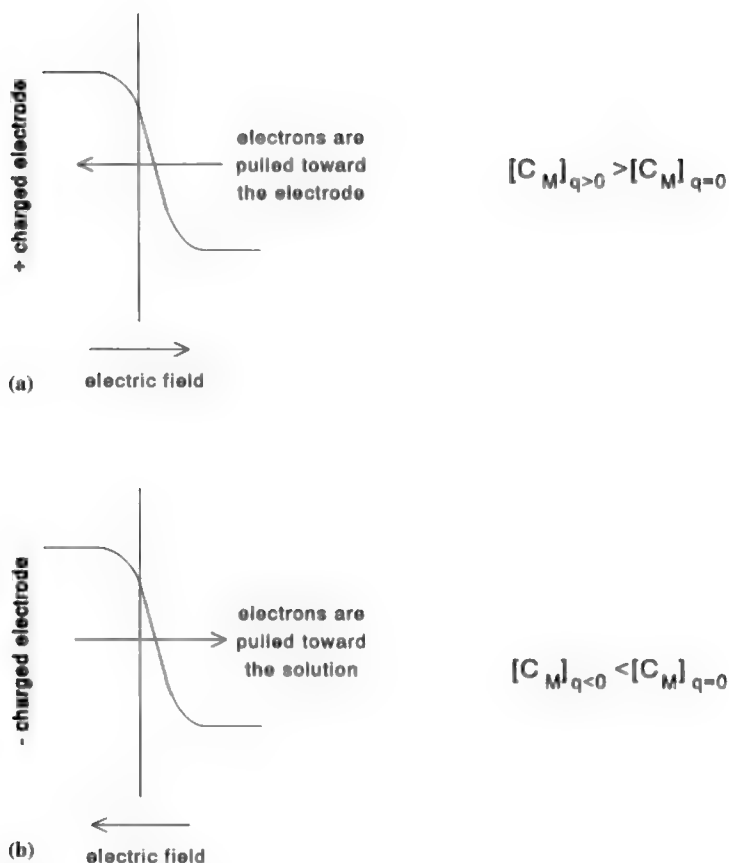


**Fig 6.69.** Effect of the charge of the metal on the spillover electrons and on the metal capacity of the double layer.



On this basis it seems that metal properties do affect the total capacity,  $C$ , through the changes in  $C_M$ . Thus, the next question seems quite obvious: Would it be possible to measure  $C_M$  and then corroborate its contribution to the total capacity of the double layer? Unfortunately a direct measurement of  $C_M$  is not possible because the metal will always form part of the total double layer and therefore only the total capacity can be measured. However, we may still have some weapons left. It is possible to obtain an indirect measurement of  $C_M$  in the absence of specific adsorption. The way to proceed is as follows. From Eq. (6.124) we see that  $C_H$  is independent of the concentration in solution, in contrast to the term  $C_G$ , which involves the term  $c_0$  [see Eq. (6.130)]. However,  $C_M$  should be independent of the concentration of the solution since it involves only the electrode properties. Thus, it is reasonable to combine the concentration-independent terms and say, for example, that the term  $C_M$  is included in the  $C_H$  term.<sup>48</sup> Thus, a plot of  $C_H$  vs. the charge of the electrode,  $q_M$ , would give an indication of the effect of  $C_M$  on the interfacial properties. Figure 6.70 shows one of those graphs. Thus, the shape of this graph, the asymmetric parabola, is most probably due to the influence of the properties of the metal in the interfacial properties.

### 6.6.8. The Jellium Model of the Metal

So far we have established in a qualitative way the importance of the metal properties on the characteristics of the interfacial region through two properties, the relation of  $\Phi_M$  vs.  $E_{pzc}$  and the capacitance of the double layer. What is next? At this point it would be good to obtain a detailed model of the metal region and then determine—now in a quantitative way—the influence of the metal on the interfacial properties, similarly to the procedure followed when studying the solution region (Section 6.6.1).

We saw in Section 6.6.7 that the metal electrons seem to carry the main responsibility for the metal properties. One of the models that seems to be more successful in explaining the distribution of electrons on the metal surface and thus their interactions with solution, is the so-called *jellium model*.

In this model, the metal is divided into two contributions, the positively charged ions and the negatively charged electrons. The ions form a continuous positive background that abruptly disappears at the edge of the metal (*jellium edge*) (Fig. 6.71). The electrons, on the other hand, are considered as a negative gas interacting with the positive background and therefore dispersed in an inhomogeneous fashion. Contrary to the positive background, the electron density does not drop at the metal edge. Rather, it slowly decays, in such a way that some electrons are localized outside the metal, on the other side of the metal edge, creating the tail of electrons that was mentioned in Section 6.6.7 (see also Fig.

<sup>48</sup> The  $C_H$  term can be determined from a plot of the inverse of the total measured capacity ( $1/C$ ) versus the inverse of the calculated Gouy–Chapman capacity ( $1/C_G$ ). This type of graph is called a *Parsons–Zobel* plot.

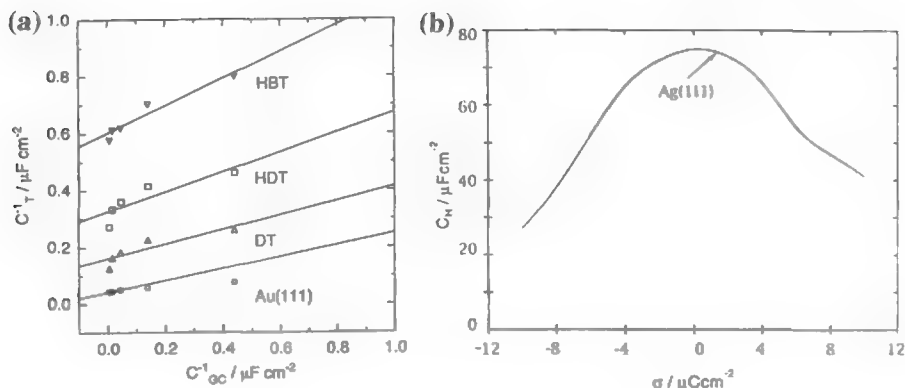


**Fig. 6.70.** (a) Parsons–Zobel plots of bare Au(111), covered with decanethiol (DT),  $\omega$ -hydroxydecanethiol (HDT), and 4'-hydroxy-4-mercaptobiphenyl (HBT). (Reprinted with permission from R. P. Janek, W. R. Fawcett, and A. Ulman, *J. Phys. Chem. B* **101**:8550, Fig. 12, copyright 1997, American Chemical Society.) (b) Helmholtz capacity ( $C_H$ ), as a function of the electrode charge for Ag(111) in contact with an aqueous solution of ions that are not specifically adsorbed. (Reprinted with permission from W. Schmickler, *Chem. Rev.* **96**:3177, Fig. 3, copyright 1996, American Chemical Society.)

6.71). This effect is formally called electron spillover, and can be as far as 0.1 to 0.2 nm from the metal edge (Fig. 6.71).<sup>49</sup> Since the electronic gas is the active part in the metal (the “moving” part), electrons are considered the main factor responsible for the properties of the metal.

However, electrons are the same independently of the type of material. Thus, how can we understand that different metals behave in different ways? How can we understand, for example, that the work function of different metals—say platinum and silver—are different (see Fig. 6.46)? Or how to explain the different behavior of different crystallographic surfaces of a given single crystal, say, Ag(111) and Ag(100)?

At this point one needs to remember that electrons are not completely independent particles, moving randomly in a positively charged background. They are a charged species and as such, they also interact with the positive ions (nucleus)

<sup>49</sup>How are electrons able to spill over the metal edge? At least at room temperature, electrons cannot jump over the barrier between the metal in which they exist and the surrounding environment. However, their quantum behavior allows them to leak or tunnel into the apparently impossible barrier at the metal edge. If receptors—or ions with electronic states of the same energy as that of the metal's electrons—are available in solution, the metal electrons tunnel through the potential barrier at the interface, giving rise to cathodic currents. However, even when receptors are not available in solution, there is always a probability of electron overlap or “incipient tunneling electrons.” A better account of the quantum behavior of the electron and how it tunnels through barriers will be given in Section 9.4.

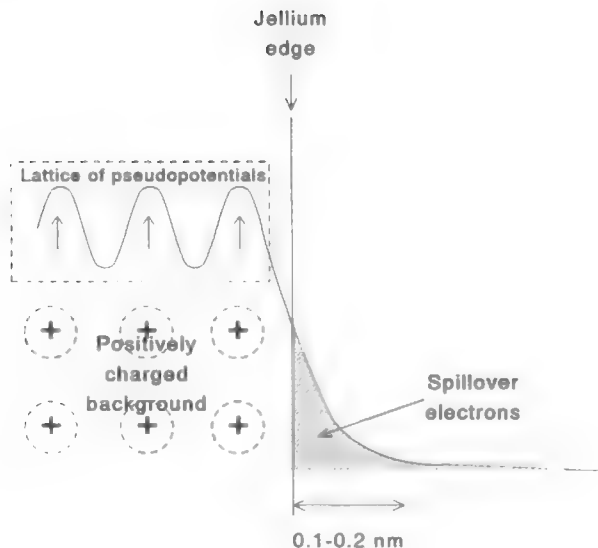


**Fig. 6.71.** The jellium model of the metal electrode. The positive background charge abruptly disappears at the jellium edge while spillover electrons can be found beyond the edge (shaded area). The continuous line represents the profile of electrons in the interfacial region. The positions of the ion cores are indicated by the arrows.

of the metal. Thus, the attractive and repulsive forces between the electrons and the positive background account for the different behavior of different metals. A higher attractiveness would recoil the electrons toward the metal, and a higher repulsiveness would repel the electrons more, increasing the tail of the spillover electrons.

However, what about when the metal is the same (i.e., same positive ions, such as  $\text{Ag}^+$ ), but only the crystal structure is different? The effect of the structure of the crystal is included in the following way: The positive ions are arranged in an orderly way inside the metal (Fig. 6.71). Close to the core of the ions, the electrons feel repulsive forces, and far from them, they get attracted due to Coulombic forces. The result is a lattice of local potentials or *pseudo-potentials* in the region around the ions, which are characteristic of the position of the ions (Fig. 6.71). If the positive ions are arranged in different ways even when they are of the same species (e.g.,  $\text{Ag}^+$  ions), their interactions with the electrons will be different because the pseudo-potentials will be closer or farther, depending on the structure of the crystal. Thus, silver ions arranged in a hexagonal fashion will interact differently than silver ions arranged in a cubic way. The electronic spillover distance would

then depend on the surface plane. Thus, the surface dipole and consequently the work function will also vary with the different single-crystal faces. The dependence of  $E_{\text{pzc}}$  on  $\Phi_{\text{M}}$  for different crystallographic structures can now be understood (see Fig. 6.46).

### 6.6.9. How Important Is the Surface Potential for the Potential of the Double Layer?

Through the jellium model of the metal we have explained the effect of the metal electrons on the interfacial properties. We also know that the spillover of electrons creates a separation of charges at the metal edge, and consequently, a surface potential. However, what is the magnitude of this surface potential? How important is its contribution to the total potential drop in the interfacial region?

As mentioned in Section 6.3.10, the surface potential cannot be measured. However, its value can be calculated (Bockris and Habib, 1976). Thus, from Eq. (6.60),

$$E_{\text{pzc}} = g^{\text{M}} - g^{\text{S}} + \frac{\mu_{\text{e}}^{\text{R}}}{F} - \frac{\mu_{\text{e}}^{\text{M}}}{F} + {}^{\text{S}}\Delta^{\text{R}}\phi \quad (6.139\text{a})$$

or

$$g^{\text{M}} = E_{\text{pzc}} + g^{\text{S}} - \frac{\mu_{\text{e}}^{\text{R}}}{F} + \frac{\mu_{\text{e}}^{\text{M}}}{F} - {}^{\text{S}}\Delta^{\text{R}}\phi \quad (6.139\text{b})$$

where  $g^{\text{M}}$  and  $g^{\text{S}}$ —the surface potential of the metal and of the solution in contact with each other instead of a vacuum (see Section 6.3.9)—has been written instead of  $\chi^{\text{M}}$  and  $\chi^{\text{S}}$ . Table 6.6 shows the different variables used in Eq. (6.139) to calculate  $g^{\text{M}}$  for two metals, cadmium and zinc, measured on the hydrogen scale.

According to Table 6.6, the value of  $g^{\text{M}}$  at the pzc is on the order of 1 V for both metals. Thus, comparing this value with the total potential drop at the interface,  $E_{\text{pzc}} = 4.6$ , it is seen that the metal constitutes almost one-fourth of the total value, which represents a considerable contribution and stresses the importance of the metal in the properties of the double-layer region.

The metal—or the electrode material—is the part of the interfacial region that has been less studied. However, as was seen in the above paragraphs, it is an important contributor to the properties of the double layer. Electrochemists are aware of this situation. Thus, in the 1990s the study of the specific properties of the metal on the double layer has been that of a frontier area, more so than other aspects of the interphasial structure.

**TABLE 6.6**  
**Calculated Values of the Electron Overlap Potentials at Metal/Solution Interfaces**

Variables Needed to Calculate $g^M$ and $\chi^M$	Metal	
	Cd	Zn
$E_{H^+/H_2}^o(\text{abs.})(V)$		
$(= R\Delta^S\phi - \mu_e^R)$	4.6	
$\mu_e^M(V)$	-2.57	-1.97
$E_{pzc}(V)$	-0.72	-0.63
$g_{pzc}^S(V)$	0.06	0.07
$g_{pzc}^M(V)$	1.08	1.78
$\Phi(eV)$	4.1	4.12
$\chi^M(V)$	1.53	2.15
$\chi^S(V)$	-0.45	-0.37

Source: J. O'M. Bockris and M. A. Habib, *J. Electroanal. Chem.* **68**: 367, copyright 1976, Table 1, with permission from Elsevier Science.

## Further Reading

### Seminal

1. H. L. von Helmholtz, "The Double Layer," *Wied. Ann.* **7**: 337 (1879).
2. G. Gouy, "Constitution of the Electric Charge at the Surface of an Electrolyte," *J. Physique* **9**: 457 (1910).
3. D. L. Chapman, "Diffuse Distribution of Adsorbed Ions," *Phil. Mag.* **25**: 475 (1913).
4. O. K. Rice, "Application of the Fermi Statistics to the Distribution of Electrons under Fields in Metals and the Theory of Electrocapillarity," *Phys. Rev.* **31**: 1051 (1928).
5. J. O'M. Bockris and M. A. Habib, "The Electron Overlap Potential at Metal-Solution Interfaces," *J. Electroanal. Chem.* **68**: 367 (1976).
6. W. Schmickler, "A Jellium-Dipole Model for the Double Layer," *Electroanal. Chem.* **150**: 19 (1983).

### Reviews

1. M. Philpott, "Electrochemical Contact Adsorption Site Changes Driven by Field and Charge: Fact and Theory," in *Cluster Models for Surface and Bulk Phenomena*, G. Pacchioni ed., Plenum, New York (1992).

2. W. Schmickler, "Electronic Effects in the Electric Double Layer," *Chem. Rev.* **96**: 3177 (1996).
3. J. W. Halley, "Studies of the Interdependence of Electronic and Atomic Dynamics and Structure at the Electrode–Electrolyte Interface," *Electrochim. Acta.* **41**: 2229 (1996).
4. R. Parsons, "The Metal–Liquid Electrolyte Interface," *Solid State Ionics* **94**: 91 (1997).

### Papers

1. P. A. Rikvol, *Electrochim. Acta* **36**: 1689 (1991).
2. V. Fieldman and M. Partenskii, *Electrochim. Acta* **36**: 1703 (1991).
3. W. Schmickler and E. Leiva, *Molecular Physics* **86**: 737 (1995).
4. X. P. Gao and H. S. White, *J. Electroanal. Chem.* **389**: 13 (1995).
5. S. Amokrane, *Electrochim. Acta* **41**: 2097 (1996).
6. J. W. Halley, *Electrochim. Acta* **41**: 2229 (1996).
7. J. N. Glosli and J. N. Philpott, *Electrochim. Acta* **41**: 2145 (1996).
8. B. B. Damaskin and V. A. Safonov, *Electrochim. Acta* **42**: 737 (1997).
9. Y. Shingaya and M. Ito, *Surface Science* **386**: 3 (1997).
10. D. R. Berard, M. Kinoshita, N. M. Cann, and G. N. Patey, *J. Chem. Phys.* **107**: 4719 (1997).
11. J. C. Shelley, G. N. Patey, D. R. Berard, and G. M. Torrie, *J. Chem. Phys.* **107**: 2122 (1997).
12. R. Kjellander and D. J. Mitchell, *Molec. Phys.* **91**: 173 (1997).
13. R. D. Armstrong and B. R. Horrocks, *Solid State Ionics* **94**: 181 (1997).
14. B. B. Damaskin and V. A. Safonov, *Electrochim. Acta.* **42**: 737 (1997).

## 6.7. STRUCTURE AT THE INTERFACE OF THE MOST COMMON SOLVENT: WATER

### 6.7.1. An Electrode Is Largely Covered with Adsorbed Water Molecules

A discussion of the structures of an electrified interface must begin with the statement that the majority of sites on an electrode surface are occupied by water molecules. It is possible to show by a very rough calculation that in the absence of directing forces, about 70% of the metal surface is covered with water molecules. This can be done by dividing the population density of *water molecules on a plane* in bulk water ( $n_w$  in molecules per square centimeter) by the *number of sites* on the metal surface ( $n_s$  in sites per square centimeter). The quantity  $n_w$  is roughly estimated in the following way: Imagine a unit volume ( $V_m$  in  $\text{cm}^3/\text{mole}$ ), say, a cube, of water molecules (Fig. 6.72). The total number of water molecules in this cube is then  $N_A/V_m$  or  $\rho N_A/M$ , where  $N_A$  is Avogadro's number,  $\rho$  is the water density, and  $M$  is its molecular weight. Thus, to determine the number of water molecules on one side of this cube ( $N_w$ ), one can take the total number of water molecules in the cube and elevate it to the  $2/3$  power, in a way similar to that of obtaining the area of one side of a cube if only its volume is known (Fig. 6.72). Thus,

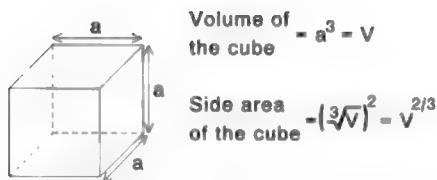


**Fig. 6.72.** The side area of a cube of volume  $V$  can be calculated as  $V^{2/3}$ .

$$N_w = \left( \frac{N_A}{V_m} \right)^{2/3} = \left( \frac{\rho N_A}{M} \right)^{2/3} \quad (6.140)$$

The number of sites on the metal surface per square centimeter can be taken as equal to the number of metal atoms per square centimeter (about  $1.5 \times 10^{15}$ ). Thus, the fraction of surface covered by water molecules,  $\theta_w$ , turns out (by inserting the appropriate numerical values into this zeroth-approximation approach) to be about 0.7.

### 6.7.2. Metal–Water Interactions

The value of 0.7 for water molecules covering the electrode was calculated in the previous section in a simple way, considering that the water molecules were close to the electrode, but not interacting with it. There are, however, forces operating between water molecules and the metal electrode. Consequently, the actual coverage with water molecules may be different from the calculated coverage of 70%. How can we determine a more accurate value of  $\theta_w$ ? A good place to start is to determine the type of interactions between the metal and the water molecules.

First, there are the *image forces* that were described earlier (Section 6.4.5). A water molecule is a dipole, i.e., it has two charges separated by a certain distance (see Section 2.4.2), and each one induces a charge on the metal. Thus, one can think that when this dipole comes close to the electrode, it generates an *image dipole* (Fig. 6.73). Therefore, the problem of calculating image interactions between the metal and the water molecule is reduced to computing dipole-dipole interactions.

A second type of force between water molecules and the metal consists of the *dispersion forces*. Dispersion forces (or London forces) can be seen classically as follows: A time-averaged picture of any atom shows spherical symmetry because the charge due to the electrons orbiting around the nucleus is smoothed out in time. An instantaneous picture of, say, a hydrogen atom, would, however, show a proton here and an electron there—two charges separated by a distance. Hence, every atom has an instantaneous dipole moment; of course, the time average of all these dipole moments is zero. This instantaneous dipole will induce an instantaneous dipole in a contiguous atom, and an instantaneous dipole–dipole force will arise. When these

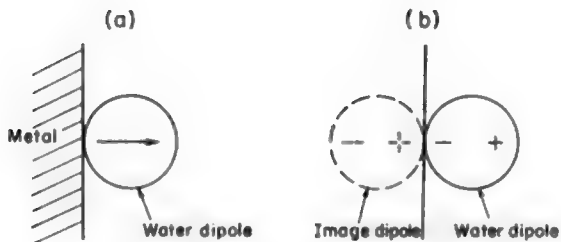


**Fig. 6.73.** (a) The interaction between a water molecule and a metal can be computed by (b) replacing the metal with an image dipole.

forces are averaged over all instantaneous electron configurations of the atoms, an attractive, nondirectional force arises, the dispersion force. Dispersion forces are important at electrified interfaces. They attract water molecules to the metal and contribute to their adsorption at electrodes.

A third kind of force is of a chemical nature. These are the forces that induce chemical bonding between the metal and the water molecule.

These three forces are operative at any time, even when the electrode is uncharged. Thus, although the electrode has no charge, it exerts attraction for water molecules. These attractive forces may overcome the forces that bind water molecules into networks in the liquid phase, and if this is the case, water adsorbs on the surface metal.

What happens when the metal is charged? Would other types of forces be involved? The forces of attraction between the metal and the water molecules still operate, but in addition, the charge on the metal will stimulate the water molecules to orient themselves. The process is similar to the orientation of dipoles in the solvent sheath around an ion (see Chapter 2).

However, it must not be imagined that the water molecules act by themselves and that they are unaffected by the presence of their neighbors. After all, dipoles interact with dipoles. Hence, the oriented water molecules also experience lateral interaction—a phenomenon that affects the net number of water molecules oriented in one direction and therefore the value of the dipole potential,  $g_{\text{dipole}}^S$  (Section 6.7.6). Once the dipole potential is affected, the total potential difference across the interface gets affected, and consequently, the properties of the interface.

### 6.7.3. One Effect of the Oriented Water Molecules in the Electrode Field: Variation of the Interfacial Dielectric Constant

We have seen that water molecules in the interfacial region are more oriented than those in the bulk water. This orientation, however, is not for free, and a price (consequence) should be attached to it. One of these prices is seen in the value of its



dielectric constant,  $\epsilon$ .<sup>50</sup> In the bulk region, where thermal disarray prevails, the value of  $\epsilon$  is about 78. However, close to the electrode, the value of  $\epsilon$  drops one order of magnitude (Fig. 6.74). How does the orientation of the molecules produce this dramatic effect?

The dielectric constant depends on the electric field strength of the environment (this fact was discussed in the treatment of hydration in Chapter 2). If the molecules in the environment contain charges (e.g., dipoles), the degree of ordering of these molecules would affect the strength of the electric field. Water molecules are dipoles, and as such have the capability to affect the strength of the electric field, and consequently, the dielectric constant.

Except near the potential of zero charge, the first layer of water molecules near the electrode (first hydration layer) is completely oriented; the molecules form a *saturated dielectric*. These water molecules do not affect the dielectric constant of the medium because they are not able to orient more in the presence of an electric field. The value of such an oriented water layer is approximately 6 (Fig. 6.74).

Consider now the water molecules cited in the next layer. These are molecules only partly oriented by the field arising from the charged electrode, but also partly disoriented by thermal and hydrogen-bonding influences of the particles of the solution. These dipoles are able to orient themselves more, and therefore they may contribute to  $\epsilon$ , at least to that part of the dielectric constant that arises from orientation polarization. The value of  $\epsilon$  in this second hydration layer is larger than the value of 6 found in the first one.

What about the dielectric constant of completely disoriented water, i.e., like the water in the bulk? The contribution of these dipoles to the dielectric constant is even larger than that of the second hydration layer. A value of 78 has been found for the dielectric constant of water molecules under these conditions.

#### 6.7.4. Orientation of Water Molecules on Electrodes: The Three-State Water Model

We have seen that water molecules—solvent dipoles—are affected by the presence of a charged electrode. Distant from it, they exist in thermal disarray, but close to it they order and orient. Now, the electrode can be positively or negatively charged. Would the water molecules always orient in the same way? Definitely not, because they are dipoles with a positive and a negative charge, and thus their orientation should depend on the charge on the electrode.

We can think of two limiting conditions on the relation between the charge on the electrode and the orientation of the dipoles relative to the surface of the metal (Bockris, Devanathan, and Muller, 1963). One limiting condition arises on an electrode that has

<sup>50</sup>A reminder: The electric force between two charges depends on the medium between them. The electric force in the presence of a material medium is less than that which operates when only a vacuum is present. The ratio of the force in a vacuum to the force in the medium is a characteristic of the medium and is known as its *dielectric constant*,  $\epsilon$ .

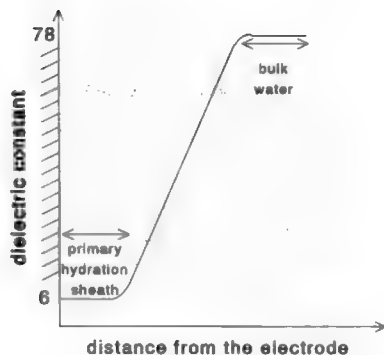


**Fig. 6.74.** The dielectric constant as a function of the distance from the electrode and the ordering of the dipole water molecules.

a highly positive charge. In such a field, dipoles reduce their potential energy by aligning themselves so that the dipole vector (which runs from the negative to the positive end of the dipole) becomes parallel to the field (Fig. 6.75). In other words, the water dipoles flip up so that the oxygen atoms are in contact with the electrode, and the hydrogen end of the water points into the solution. This is the *flip-up state* of oriented water molecules [Fig. 6.76(a)].

The other limiting condition occurs when electrons are pumped into the electrode to make it very negatively charged. What will the dipoles do? On the basis of a simple electrostatic argument, the flipped-up dipoles will turn around and flop down. In this new state, the hydrogens are facing the electrode and the oxygen atom is toward the solution [Fig. 6.76(b)].

These two orientations of water molecules, the flip-up and flip-down states, are extreme cases. However, there are several other possible states for the water molecules on the electrode. Evidence exists suggesting that water molecules in the interfacial region may be associated into groups (see Fig. 6.77). This gave rise to several models proposed to describe the water structure at the interface: Damaskin and Frumkin (1974), Parsons (1975), Fawcett (1978), and Guidelli (1986) (Fig. 6.78).

One possibility is that water molecules at the interface associate into groups of two molecules. Such entities are called *dimers*. What are the characteristics of these dimers? They consist of two water molecules associated in such a way that their dipole moments oppose each other (Fig. 6.79). As a consequence, the dimers do not have any net permanent dipole moment. They are neutral species.

To summarize, three possible species may populate the electrode surface: two types of monomers—the flip-up and flop-down water molecules—and one associated species—the dimers. This model is called, for obvious reasons, the *three-state water model* (Habib and Bockris, 1977).

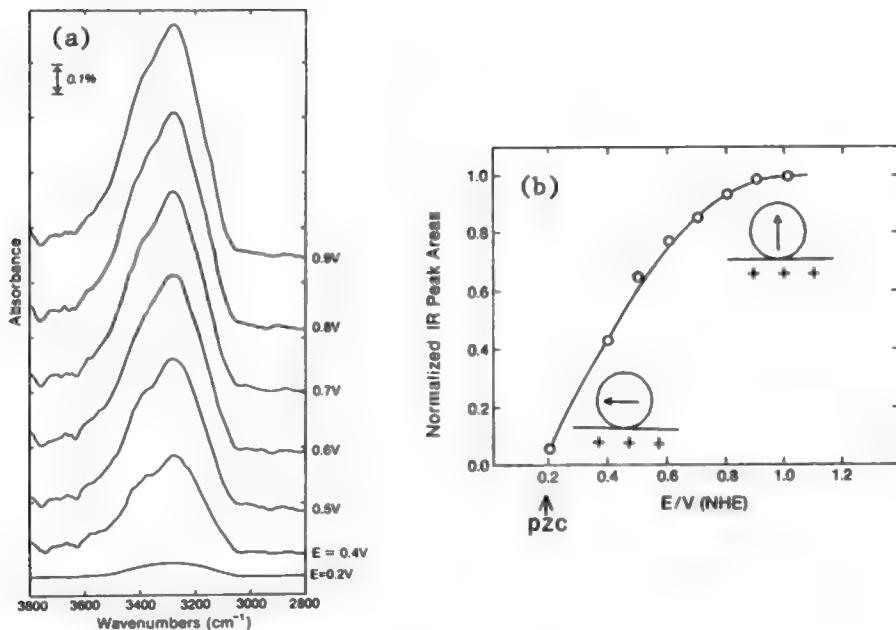


**Fig. 6.75.** (a) IR spectra in percent absorbance of O-H vibration in adsorbed water molecules on platinum at various potentials. These spectra are the differences between the spectra at the given potential and that at the reference potential (0.1 V). (b) Areas under the IR peaks of (a) as a function of the potential (normalized to 1 at the maximum). In the region close to the pzc, monomer water molecules are lying on the surface of the electrode with their dipole moment parallel to the surface. As the potential becomes more positive, they stand up, aligning themselves with the electric field and with their oxygens toward the electrode and their hydrogens toward the solution (flip-up configuration) in such a way that their dipole moments stand perpendicular to the surface. (Reprinted with permission from M. A. Habib and J. O'M. Bockris, *Langmuir* 2: 388, Figs. 1 and 2, copyright 1986, American Chemical Society.)

However, it is not enough to know only that three different water species populate the surface of the electrode. The electrochemist would like to know more about them, for example, to what extent does each of these three water states populate the surface? Or how do these water species affect the properties of the interfacial region? These are the questions that will be discussed in the following sections.

### 6.7.5. How Does the Population of Water Species Vary with the Potential of the Electrode?

One of the questions in the previous section referred to the relative amount of each of the three water species—two monomers and one dimmer—on the surface of the

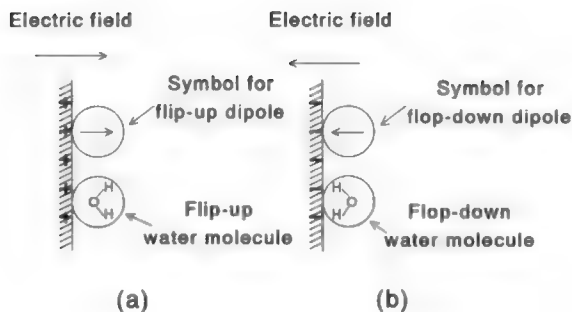


**Fig. 6.76.** (a) The flip-up orientation and (b) the flop-down orientation of a water molecule on an electrode.

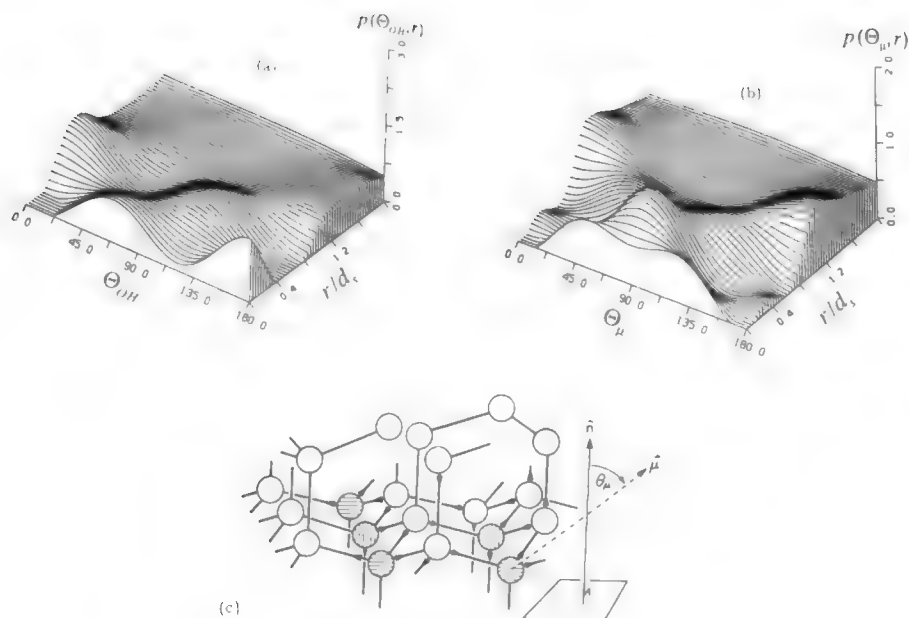


**Fig. 6.77.** Calculations done using the statistical mechanical theory of electrolyte solutions. Probability density  $p(\theta, r)$  for molecular orientations of water molecules (tetrahedral symmetry) as a function of distance  $r$  from a neutral surface (distances are given in units of solvent diameter  $d = 0.28$  nm): (a)  $\theta_{OH}$  OH bond orientation and (b) dipolar orientation. (c) Ice-like arrangement found to dominate the liquid structure of water models at uncharged surfaces. The arrows point from oxygen to hydrogen of the same molecule. The peaks at  $180$  and  $70^\circ$  in  $p(\theta_{OH}, r)$  for the contact layer correspond to the one hydrogen bond directed into the surface and the three directed to the adjacent solvent layer, respectively, in (c). (Reprinted from G. M. Torrie and G. N. Patey, *Electrochim. Acta* **36**: 1677, copyright 1991, Figs. 1 and 2, with permission from Elsevier Science.

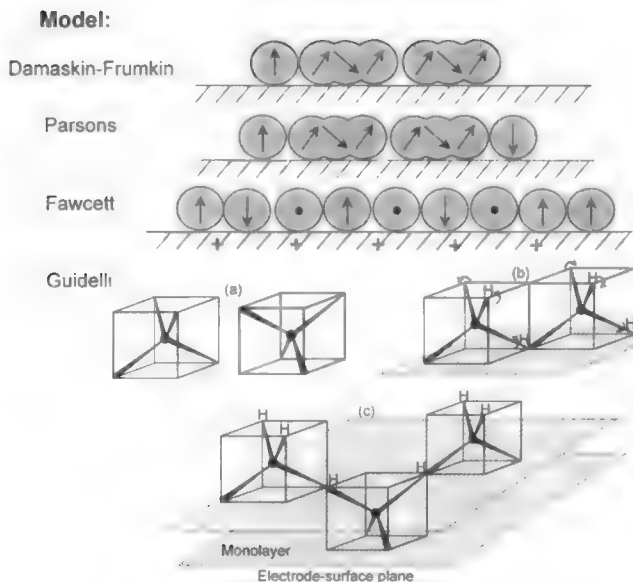


**Fig. 6.78.** Schematic representation of water molecules at the interface according to Damaskin–Frumkin’s monolayer model, Parson’s monolayer model, Fawcett’s three-state model, and Guidelli’s model. (a) Allowed orientations of water molecules with H bonds directed toward the vertices of the unit cell. (b) Rotations required to form H bonding between two water molecules of the monolayer. (c) H bonding of a chemisorbed water molecule in the monolayer with two bulk water molecules. (Reprinted from R. Guidelli and G. Aloisi, in *Electrified Interfaces in Physics, Chemistry and Biology*, R. Guidelli, ed., NATO ASI series, Vol. 355, 1992, p. 309, Figs. 6, 7, and 8; with kind permission of Kluwer Academic Publishers; R. Guidelli, in *Trends in Interfacial Electrochemistry*, F. Silva, ed., NATO ASI series, Vol. 179, p. 387, 1984, Figs. 8, 9, and 11, with kind permission of Kluwer Academic Publishers.)

electrode at a given potential. We established that at the two extreme potentials (i.e., at very positive or at very negative values) most of the water molecules are either in the flip-up or in the flop-down positions. However, what happens when the potential is in the region between these two limits, i.e., in the region close to the  $pzc$ ?

Here, not only the monomers (flip up and flop down) would be expected, but also the dimer species. The fraction of the electrode covered by these three configurations is obtained by the consideration of the following equilibrium cycle:

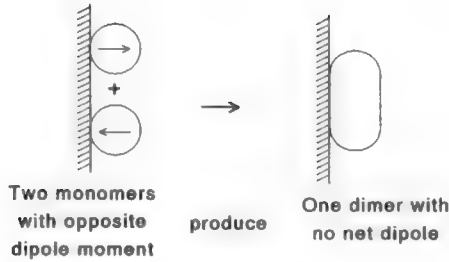
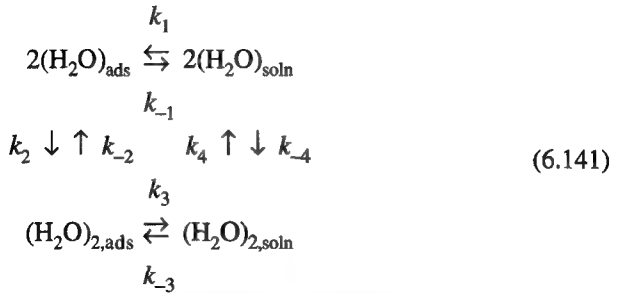


**Fig. 6.79.** Dimer molecule. It is made up of two water molecules oriented in opposite directions. The net dipole moment of the dimer molecule is zero.



where  $(\text{H}_2\text{O})_{\text{ads}}$  represents monomers and  $(\text{H}_2\text{O})_{2,\text{ads}}$  represents dimers on the uncharged surface. From the above cycle, simple kinetic considerations (see Chapter 7) indicate that the relative amounts of monomers and dimers on the surface follow from

$$\frac{d[(\text{H}_2\text{O})]_{\text{ads}}}{dt} = k_1 c_m (1 - \theta_m - \theta_d) - k_{-1} \theta_m^2 + k_{-2} \theta_d - k_2 \theta_m^2 \quad (6.142)$$

and

$$\frac{d[(\text{H}_2\text{O})_2]_{\text{ads}}}{dt} = k_{-3} c_d (1 - \theta_m - \theta_d) - k_3 \theta_d + k_2 \theta_m^2 - k_{-2} \theta_d \quad (6.143)$$

where  $c_m$ ,  $c_d$  are the concentrations of monomers and dimers in solution, and  $\theta_m$  and  $\theta_d$  are the fractions of the surface covered by monomers and dimers. The corresponding  $k$ 's represent the rate constants for each reaction. If we consider that

$$\theta_m + \theta_d = 1 \quad (6.144)$$

and that at equilibrium the rate of both reactions, i.e., Eqs. (6.142) and (6.143), is zero, then,

$$\theta_d(k_{-2}) - \theta_m^2(k_{-1} + k_2) = 0 \quad (6.145a)$$

$$\theta_d(k_3 + k_{-2}) - \theta_m^2(k_2) = 0 \quad (6.145b)$$

Equating these two equations, and substituting  $\theta_m^2$  for  $(1 - \theta_d)^2$ ,

$$\frac{\theta_d}{(1 - \theta_d)^2} = \frac{2k_2 + k_{-1}}{2k_{-2} + k_3} \quad (6.146)$$

Equation (6.146) gives the coverage of dimers as a function of the rate constants. One more simplification can be done to this equation, and that is to assume that  $k_2 \gg k_{-1}$  and that  $k_{-2} \gg k_3$ . Then Eq. (6.146) becomes

$$\frac{\theta_d}{(1 - \theta_d)^2} = \frac{k_2}{k_{-2}} \quad (6.147)$$

but  $k_2/k_{-2}$  is nothing other than the equilibrium constant for reaction 2 in Eq. (6.141),  $K_2 = k_2/k_{-2}$ , and it can be expressed in terms of the standard free-energy change,  $\Delta G_2^\circ$ , for the formation of dimers on the surface from the adsorbed monomers, that is,

$$\frac{\theta_d}{(1 - \theta_d)^2} = K_2 = e^{-\Delta G_2^\circ/RT} \quad (6.148)$$

The value of  $\Delta G_2^\circ$  is  $-4.7 \text{ kJ mol}^{-1}$  at 298 K. Thus, substituting this value in Eq. (6.148), and solving this equation for  $\theta_d$ , one finds that  $\theta_d = 0.68$  and  $\theta_m = 0.32$  for the coverage values of dimers and monomers in the region close to the pzc.

What does this result mean? It indicates that at the pzc most of the water molecules (i.e., 68%) are associated as dimers. The rest of the molecules, 32%, remain as monomers, most probably oriented parallel to the surface of the electrode (see Fig. 6.75). As the potential of the electrode changes to positive values, the dimers break into single water molecules and, together with the monomers, they stand with their oxygens close to the electrode, in the flip-up position (see Fig. 6.75).

### 6.7.6. The Surface Potential, $g_{\text{dipole}}^S$ , Due to Water Dipoles

So far we have found that water molecules in the interfacial region exist in three different states—two monomers and one dimer—and that the population of these species varies as the electrode potential changes. We went a step further and determined the relative amount of monomers and dimers at different electrode potentials.

What is next? The above results give only a particular view of one part of the interface, i.e., the solvent structure. It would be good to find how this solvent and its changes in configuration affect—if at all—the total interfacial properties, for example, properties that we are already familiar with, such as the surface potential or the capacity. Thus, what would be the expression for the surface potential due to a layer of oriented water dipoles, i.e.,  $g_{\text{dipole}}^S$ ? A dipole layer is electrically analogous to a parallel-plate condenser (Fig. 6.80), the thickness of the condenser being the thickness of the dipole,  $d$ , and the charge density on the condenser plates being the charge  $e$  at each end of the dipole times the number  $N$  of *net oriented dipoles* per unit area, i.e.,  $Ne$ . Thus, in this dipole condenser [see Eq. (6.118)],

$$g_{\text{dipole}}^S = \frac{Ne_0 d}{\epsilon \epsilon_0} = \frac{N\vec{\mu}}{\epsilon \epsilon_0} \quad (6.149)$$

where the dipole moment,  $\vec{\mu} = e_0 d$ , has been introduced in the second part of the equation.

Equation (6.149) gives the surface potential when all the dipoles are pointing in the same direction. Under such conditions,  $N$  is simply equal to the number of monomers on the surface. However, we know that this happens only during extreme conditions, i.e., when the electrode is either highly positively or highly negatively charged.

What then, is the expression for  $g_{\text{dipole}}^S$  in the charge region between these extreme cases? We know that in this in-between region it is more likely that there will be a mixture of flip-up and flop-down water molecules. Not all of the monomers are aligned in the same direction, and their individual contribution to the surface potential equations should be considered. And what about the dimers? Are they not also present

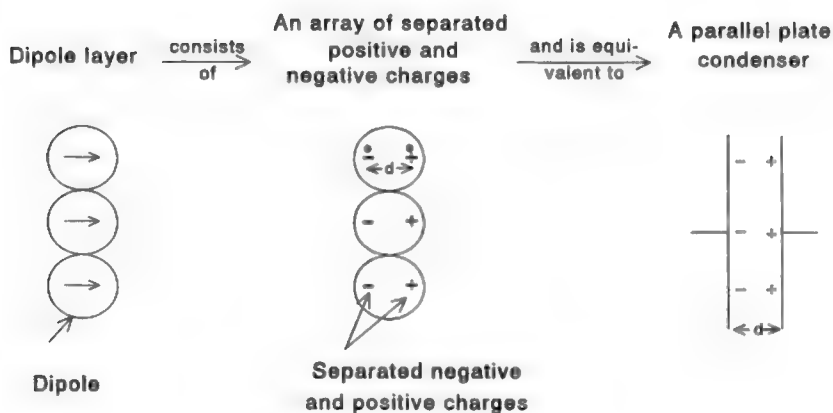


**Fig. 6.80.** A dipole layer is electrically equivalent to a parallel-plate condenser.



at the interface in this in-between charge region, and should they not be also considered in the corresponding  $g_{\text{dipole}}^S$  expression? At this point it is good to remember that dimers are neutral species (Section 6.7.4), without a net dipole moment, and as such do not contribute to the surface potential of the solvent. Thus, the main contributors to the surface potential are both monomer species.

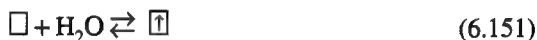
The two types of monomers have dipole moments that differ by  $180^\circ$ . Thus their contribution to the total  $g_{\text{dipole}}^S$  should be quite different. How can  $g_{\text{dipole}}^S$  be calculated in this situation? Looking closer at Eq. (6.149), we see that it involves the parameter  $N$ , that is, the *net* oriented dipoles per unit area. Thus, in order to obtain  $g_{\text{dipole}}^S$  in the presence of both monomers, the problem reduces to one of finding the value of  $N$ .

Let the symbol  $N_\uparrow$  represent the number per unit area of the flipped dipoles with the hydrogen end toward the solution, and  $N_\downarrow$  be the number per unit area of the flop-down position. The subtraction of these numbers should give the net number of dipoles oriented in the up ( $\uparrow$ ) direction, i.e.,  $N = N_\uparrow - N_\downarrow$ . Thus, Eq. (6.149) can be written as

$$g_{\text{dipole}}^S = \frac{\mu}{\epsilon \epsilon_0} (N_\uparrow - N_\downarrow) = \frac{\vec{\mu} N_m Z}{\epsilon \epsilon_0} \quad (6.150)$$

where  $N_m$  is the total number of monomers, and the parameter  $Z \equiv (N_\uparrow - N_\downarrow)/N_m = \theta_\uparrow - \theta_\downarrow$  has been introduced.

Now, to derive an expression for  $N_\uparrow$  and  $N_\downarrow$  (and therefore for  $Z$ ), a simple approach is to consider the adsorption of water in any one position as a chemical reaction. For example, for the flip-up water molecules,



where  $\square$  are free sites on the metal and  $\uparrow$  are sites occupied by flip-up water molecules. Thus, under equilibrium conditions,

$$\frac{N_\uparrow}{a_{\text{H}_2\text{O}} M} \approx \frac{N_\uparrow}{M} = e^{-\Delta G_\uparrow^\circ/RT} \quad (6.152)$$

where  $\Delta G_\uparrow^\circ$  is the standard free-energy change associated with the adsorption of water in the flip-up state,  $a_{\text{H}_2\text{O}}$  is the activity of water, which in dilute solutions can be taken as equal to unity, and  $M$  is the number of free sites on the metal.

Similarly, an equivalent equation for flop-down molecules would permit us to calculate  $N_\downarrow/M$ . Thus, from these two quantities,  $N_\uparrow$  and  $N_\downarrow$ , the variable  $Z$  becomes [see Eq.(6.150)],

$$Z = \frac{N_\uparrow - N_\downarrow}{N_m} = \frac{N_\uparrow - N_\downarrow}{N_\uparrow + N_\downarrow} = \frac{\exp(-\Delta G_\uparrow^\circ/RT) - \exp(-\Delta G_\downarrow^\circ/RT)}{\exp(-\Delta G_\uparrow^\circ/RT) + \exp(-\Delta G_\downarrow^\circ/RT)} \quad (6.153)$$

Equation (6.153) allows us to evaluate  $Z$ , but only if the values of  $\Delta G_{\uparrow}^{\circ}$  and  $\Delta G_{\downarrow}^{\circ}$  are known. What are these energy terms? They can be considered to be built by three contributions: (1) a *chemical* term related to the work of adsorption, represented by  $\Delta G_c^{\circ}$ , (2) an *electrical* or field term, and (3) a *lateral interaction* term.

The electrical work involves the free energy of a dipole in the electric field  $\vec{X}$  arising from the charge  $q_M$  on the metal. This free energy is given by  $-\vec{\mu}\vec{X} \cos \alpha$  where  $\alpha$  is the angle between the field vector and the unit vector drawn from the negative to the positive end of the dipole. Thus, the energy of the flip-up dipoles is  $+\vec{\mu}\vec{X}$  because  $\alpha = \pi$  [Fig. 6.81(a)], and that of the flop-down dipoles is  $-\vec{\mu}\vec{X}$  because  $\alpha = 0$  [Fig. 6.81(b)].

The lateral-interaction term can be determined by considering a flip-up dipole in its vicinity. Certainly the field of the reference flip-up dipole dies down quite rapidly (as  $r^{-3}$ ), allowing the reference dipole to interact only with a certain number  $x$  of surrounding dipoles. Even more, from this number of neighbor dipoles, a fraction is oriented in the flip-up position ( $\theta_{\uparrow} = N_{\uparrow}/N_T$ ) and another fraction in the flip-down position ( $\theta_{\downarrow} = N_{\downarrow}/N_T$ ). Thus, only  $x\theta_{\uparrow}$  and  $x\theta_{\downarrow}$  are the numbers of flipped and flopped dipoles with which the reference flip-up dipole interacts. The dipole-dipole interaction energy is minimum ( $-U$ ) when the neighboring dipole being considered is in the flop-down state, and maximum ( $+U$ ), when both dipoles have like orientations. Thus, the total interaction work for a flipped-up dipole is  $[(+U)x\theta_{\uparrow} + (-U)x\theta_{\downarrow}]$  or  $Ux(\theta_{\uparrow} - \theta_{\downarrow})$ .

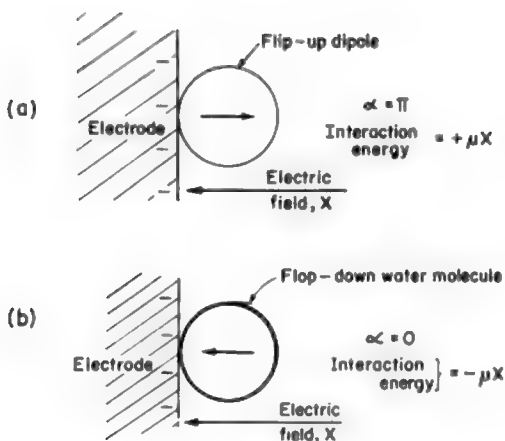


**Fig. 6.81.** (a) When a flip-up water molecule is on an electrode charged negative to the solution, the interaction energy is  $+\vec{\mu}\vec{X}$ , and (b) when a flop-down water molecule is on an electrode charged negative to the solution, the interaction energy is  $-\vec{\mu}\vec{X}$ .

Similarly, if the reference dipole is a flopped-down dipole, its total interaction energy is  $-Ux(\theta_{\uparrow} - \theta_{\downarrow})$ . The negative symbol arises because this dipole has a  $-U$  interaction energy with a flipped-up dipole and a  $+U$  with a flopped-down dipole.

Thus, the free-energy change of the flipped water molecules is expressed as  $\Delta G_{\uparrow}^{\circ} = (\Delta G_c^{\circ})_{\uparrow} - \vec{\mu} \vec{X} + Ux(\theta_{\uparrow} - \theta_{\downarrow})$ , and that of the flopped water molecules, as  $\Delta G_{\downarrow}^{\circ} = (\Delta G_c^{\circ})_{\downarrow} + \vec{\mu} \vec{X} - Ux(\theta_{\uparrow} - \theta_{\downarrow})$ . Thus, substituting these equations in Eq. (6.153), the variable  $Z$  can be written as

$$Z = \frac{\exp \left[ -\frac{(\Delta G_c^{\circ})_{\uparrow}}{RT} + \frac{y}{RT} \right] - \exp \left[ -\frac{(\Delta G_c^{\circ})_{\downarrow}}{RT} - \frac{y}{RT} \right]}{\exp \left[ -\frac{(\Delta G_c^{\circ})_{\uparrow}}{RT} + \frac{y}{RT} \right] + \exp \left[ -\frac{(\Delta G_c^{\circ})_{\downarrow}}{RT} - \frac{y}{RT} \right]} \quad (6.154)$$

where

$$y = \vec{\mu} \vec{X} - UxZ = \frac{\vec{\mu} q_M}{\epsilon \epsilon_0} - UxZ \quad (6.155)$$

In the second part of Eq. (6.155), the electric field has been written as  $\vec{X} = q_M / \epsilon \epsilon_0$ .

Let's have a closer look at Eq. (6.154). It involves the terms  $(\Delta G_c^{\circ})_{\uparrow}$  and  $(\Delta G_c^{\circ})_{\downarrow}$ . Is there any difference in the chemical energy of the flipped and the flopped molecules? In other words, if the molecules are the same (i.e., water), should their chemical interaction with the substrate not be the same? Would they not cancel out? Certainly not. Evidence exists proving that water molecules are preferentially adsorbed with their oxygen end toward the metal at the pzc (see Section 6.7.8). This means that the chemical interactions between the two states of water—flip-up and flop-down molecules—and the metal are different. The flipped dipoles, with their oxygens toward the metal, are more stable, and should have a more negative chemical energy. Thus,  $|(\Delta G_c^{\circ})_{\uparrow}| > |(\Delta G_c^{\circ})_{\downarrow}|$  and the difference between these two terms is

$$b = -[(\Delta G_c^{\circ})_{\uparrow} - (\Delta G_c^{\circ})_{\downarrow}] = -\Delta(\Delta G_c^{\circ}) \neq 0 \quad (6.156)$$

Now, if Eq. (6.154) is multiplied in its numerator and denominator by  $\exp [(\Delta G_c^{\circ})_{\downarrow}/RT + y/RT]$ , it can be simplified to give

$$Z = \frac{\exp \left[ \frac{b}{RT} + \frac{2y}{RT} \right] - 1}{\exp \left[ \frac{b}{RT} + \frac{2y}{RT} \right] + 1} \quad (6.157)$$

With all this mathematical procedure we have managed to finally find an expression for the variable  $Z$ . However, this was not the main concern of this treatment. This

was just one step in order to obtain the dipole potential in Eq. (6.150). The next step is to substitute Eq. (6.157) into Eq. (6.150). Hence,

$$g_{\text{dipole}}^s = -\frac{\vec{\mu} N_M \exp\left[\frac{b}{RT} + \frac{2y}{RT}\right] - 1}{\epsilon \epsilon_0 \exp\left[\frac{b}{RT} + \frac{2y}{RT}\right] + 1} \quad (6.158)$$

This is the expression we were looking for, and its graphical representation is given in Fig. 6.82. It tells us about the way the surface dipole varies with the charge of the electrode,  $q_M$ , which is found in the term  $y$  in Eq. (6.158) [see Eq. (6.155)]. The

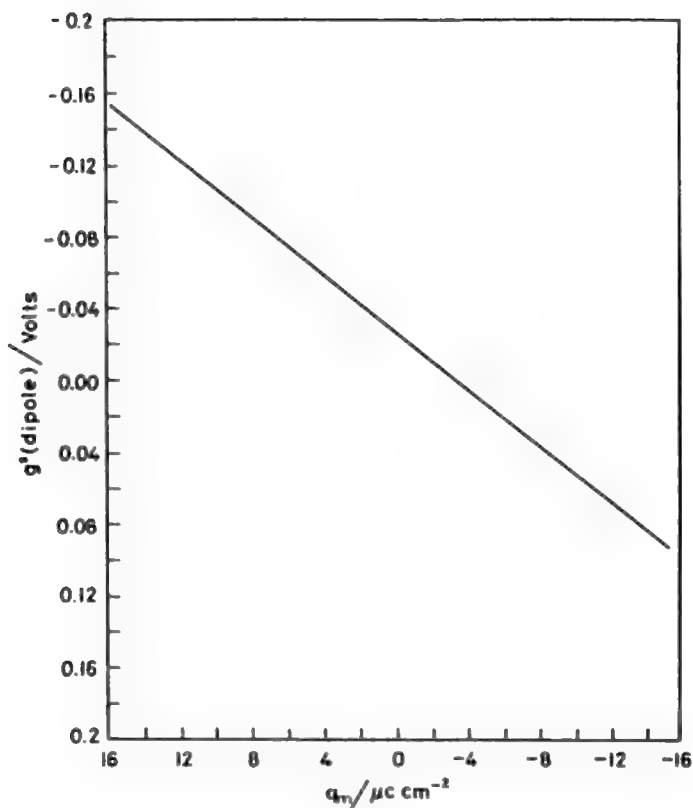


**Fig. 6.82.** Surface potential of water at the mercury/solution interface as a function of charge density on the metal. (Reprinted from J. O'M. Bockris and M. A. Habib, *Electrochim. Acta* **22**: 41, copyright 1977, Fig. 2, with permission from Elsevier Science.)

result is not strange to us. As the metal becomes more electropositive ( $q_M > 0$ ), the preferential adsorption of the flip-up water dipole increases and the bond strength between the metal and the oxygen increases. What this means is that  $[-\Delta\Delta G_c^0]$  increases with  $q_M$  [ $\Delta\Delta G_c^0$  becomes more negative, see Eq. (6.156)], and therefore  $Z$  increases [Eq. (6.157)]. Hence  $g_{\text{dipole}}^S$  also increases [see Eq. (6.158)].

However, the story is not finished yet. The contribution of the solvent dipole layer to the properties of the whole double layer has not been determined. One way to do it would be by comparing the calculated results of  $g_{\text{dipole}}^S$  with the total potential drop of the double layer. In this way we could determine how much the characteristics of the double layer are affected by the water layer in the interface, that is, if the water molecules behave more like "spectators" or more like "actors." Nonetheless, this is not the only way to proceed. A better course to follow would be to compare, instead of potentials, the capacity of the dipole layer,  $C_{\text{dipole}}$ , with the total capacity. The advantage of this comparison is that we are already familiar with the experimental data of the total capacity (see Fig. 6.65). The only thing we would have to do is to transform the dipole potential into a dipole capacity, a procedure we know how to do (see Section 6.5.5).

### 6.7.7. The Contribution of Adsorbed Water Dipoles to the Capacity of the Interface

From Eq. (6.124), in order to determine the capacitance due to a layer of water dipoles, one has only to differentiate the  $g_{\text{dipole}}^S$  potential [Eq. (6.158)] with respect to the electrode charge and take its inverse. Equation (6.158) contains the variable  $q_M$  in the numerator and in the denominator the variable  $y$ . Hence, from Eq. (6.158), and following the rules of differentiation,

$$\frac{dg_{\text{dipole}}^S}{dq_M} = -\frac{\vec{\mu}N_M}{\epsilon\epsilon_0} \frac{4\exp[(b+2y)/RT]}{RT\{\exp[(b+2y)/RT] + 1\}^2} \frac{dy}{dq_M} \quad (6.159)$$

The  $dy/dq_M$  term can be obtained from the differential of Eq. (6.155) with respect to  $q_M$ ,

$$\frac{dy}{dq_M} = \frac{\vec{\mu}}{\epsilon\epsilon_0} - \frac{4Ux}{RT} \frac{\exp[(b+2y)/RT]}{\{\exp[(b+2y)/RT] + 1\}^2} \frac{dy}{dq_M} \quad (6.160)$$

or,

$$\frac{dy}{dq_M} = \frac{\vec{\mu}}{\epsilon\epsilon_0} \frac{\{\exp[(b+2y)/RT] + 1\}^2}{\{\exp[(b+2y)/RT] + 1\}^2 + \frac{4Ux}{RT} \exp[(b+2y)/RT]} \quad (6.161)$$

Substituting Eq. (6.161) into Eq. (6.159), and taking the inverse of this value gives the capacitance of the dipole layer, i.e.,

$$C_{\text{dipole}} = \left( \frac{dg_{\text{dipole}}^S}{dq_M} \right)^{-1} = \frac{\epsilon^2 \epsilon_0^2 kT}{4N_M \mu^2} \frac{[\exp A + 1]^2 + \frac{4Ux}{kT} \exp A}{\exp A} \quad (6.162)$$

where  $A = \exp [(b + 2y)/RT]$ .

When the values of  $C_{\text{dipole}}$  calculated from Eq. (6.162) are plotted as a function of  $q_M$  (Fig. 6.83), it turns out that the values of the dipole capacity are extremely large compared with the experimental values of the capacity. What does this imply? Consider the complete expression for the total differential capacity of the interface:

$$\frac{1}{C} = \frac{d\Delta\phi}{dq_M} = \frac{d\Delta\psi}{dq_M} + \frac{d\Delta g_{\text{dipole}}^S}{dq_M} = \frac{1}{C_{\text{charge}}} + \frac{1}{C_{\text{dipole}}} \quad (6.163)$$

Here the term  $1/C_{\text{charge}}$  refers to the capacity due to contact with adsorbed ions (see Section 6.6.2), and  $C_{\text{dipole}}$  is the capacity due to the adsorbed water dipoles. From Eq. (6.163) it can be seen that when one of the capacitances, say,  $C_{\text{dipole}}$ , is large with

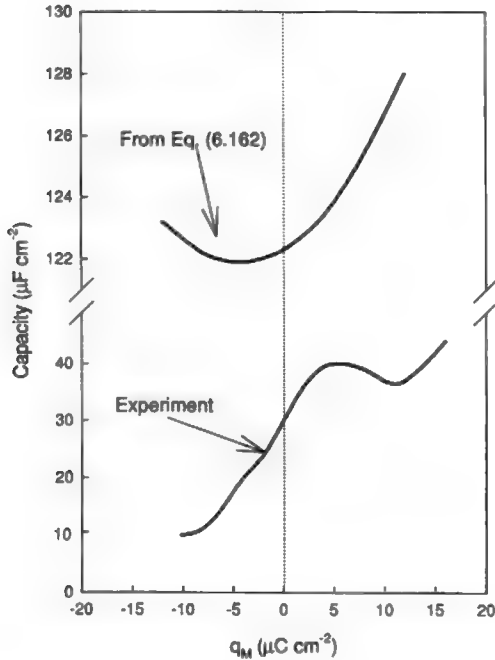


**Fig 6.83.** Comparison between the calculated values of the dipole capacity [from Eq. (6.162)] and the experimental capacity.

respect to the other, its effect on  $1/C$  is small. This is the case depicted in Fig. 6.83. The situation is analogous to that in the Stern theory, where the Gouy capacity made a negligible contribution to the total capacity whenever the magnitude of the Gouy capacity became large. Thus,

$$\frac{1}{C} \approx \frac{1}{C_{\text{charge}}} \quad (6.164)$$

and it is justifiable to ignore the contribution of the water dipoles constituting the hydration sheath of the electrode to the differential capacity of an electrified interface. Equation (6.164) indicates that the contribution of the capacity due to the water layer is very small, and it can be reasonably assumed that the capacity of the double layer—an important property of the double layer—is given by the capacity due to the adsorbed ions.

### 6.7.8. Solvent Excess Entropy of the Interface: A Key to Obtaining Structural Information on Interfacial Water Molecules

One point that remains unclear from the above discussion is the statement in Section 6.7.6 that the water molecules in the flip-up and in the flop-down positions have different energies of adsorption [i.e.,  $(\Delta G_c^\circ)_\uparrow \neq (\Delta G_c^\circ)_\downarrow$ ], and that therefore at the pzc, water preferentially adsorbs with its oxygen end toward the metal. This statement was thrown in without indicating its origins, and now it is time to do so. We can start by looking closer at the structure of water and analyzing any natural or spontaneous change it may have when lying on the surface of the electrode. How can we analyze these possible spontaneous changes? The thermodynamic property that deals with this type of phenomenon is the entropy of the system. Thus, to obtain information on why the water molecules prefer to orient with their oxygens toward the metal, it is necessary to analyze the entropy of these molecules when they are in the adsorbed state.

Figure 6.84(d) shows the experimental results of the entropy of adsorbed water molecules as a function of the electrode charge. This curve has a near-parabolic shape, with a maximum at a potential negative to the pzc, at about  $-3 \mu\text{C cm}^{-2}$ . From thermodynamic considerations we know that the entropy can be considered as a measure of the disarrangement of the system, i.e., the larger the entropy, the larger the disorder in the system studied. Thus, this peak represents a point of maximum disorder, that is, a point where water molecules are less oriented, i.e., they do not have any preferred orientation and can be in either the flip-up or in the flop-down positions. However, if both species would be likely to adsorb in the same way, then this peak would be expected to occur when the charge of the electrode is zero and there is no external field that would align the molecules with it, i.e., at the pzc. However, Fig. 6.84(d) indicates that is not the case. Why does this maximum not occur at the pzc?

To find an answer to this question, one should analyze different contributions of this solvent entropy when the solvent molecules are under the different stresses or

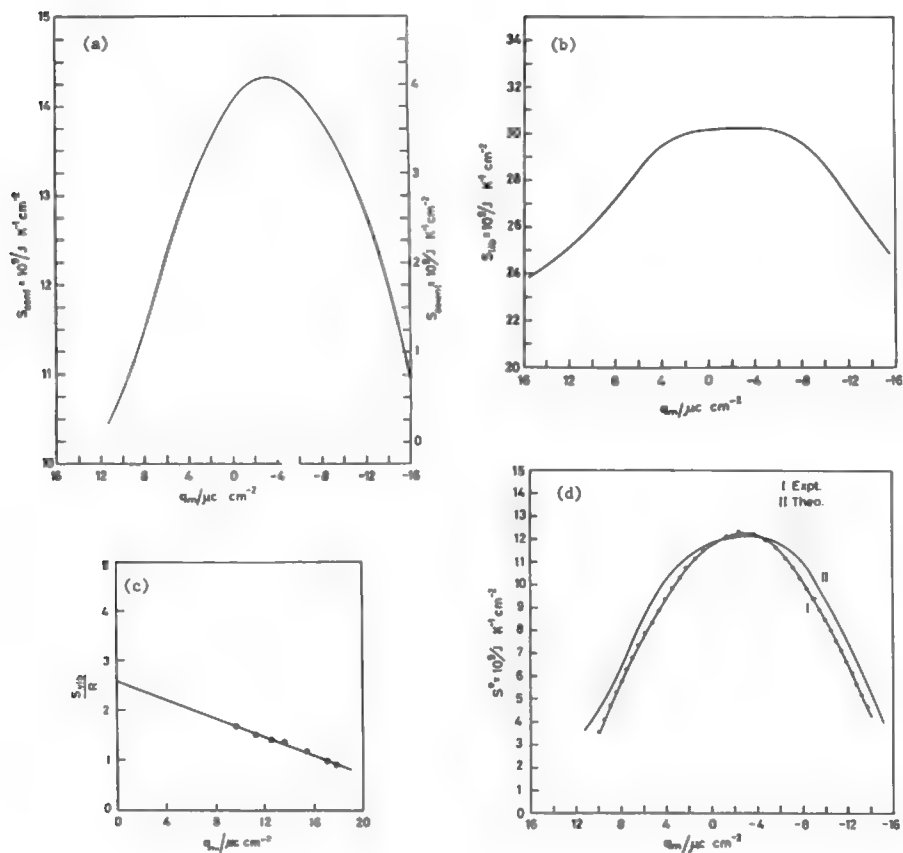


**Fig. 6.84.** (a) Configurational, (b) libratory, and (c) vibrational entropy of surface water as a function of charge density on metal. The addition of these three entropies according to Eq. (6.166) gives (d), the solvent excess entropy as a function of the electrode charge. The experimental curve also shown in this graph was obtained in 0.1 M NaCl solution. (Reprinted from J. O'M. Bockris and M. A. Habib, *J. Electroanal. Chem.* 65: 473, copyright 1975, Figs. 2, 3, 4, and 9, with permission from Elsevier Science.)

forces of the interface. We could start by splitting the solvent entropy,  $S^*$ , into two parts, one that depends on the charge,  $S_{q_M}$ , and one that does not depend on it,  $S_0$  (Table 6.7):

$$S^* = S_0 + S_{q_M} \quad (6.165)$$

The different constituents of  $S_0$  are shown in Table 6.7. However, since we want to know why the peak appears at a point different than the pzc, it would be more useful



**TABLE 6.7**  
**Different Components of  $S_0 \times 10^9 \text{ J K}^{-1} \text{ cm}^{-2}$**

$S_{\text{rot},d}$	$S_{\text{vib},d}$	$S_{\text{SB}}$	$S_{w-w}$	$S_0$
33.2	11.21	10.3	99.48	-44.77

Source: Reprinted from M. A. Habib, "Solvent Dipoles at the Electrode-Solution Interface," in *Modern Aspects of Electrochemistry*, J. O'M. Bockris and B. E. Conway, eds., Vol. 12, Ch. 13, 1977, Table 1.

to analyze that part of the entropy that varies with the electrode charge, i.e.,  $S_{q_M}$ . This entropy is made up of the following components:

$$S_{q_M} = S_{\text{conf}} + S_{\text{lib},m} + S_{\text{vib},m} \quad (6.166)$$

where  $S_{\text{conf}}$  is the *configurational* entropy,  $S_{\text{lib},m}$  the *libration* entropy of the monomers, and  $S_{\text{vib},m}$  the *vibrational* entropy of the monomers.

The  $S_{\text{conf}}$  is given by the distinct position (configurations) the monomers and dimers may acquire on the surface of the electrode [Fig. 6.85(a)]. To calculate it, one needs to consider all the possible combinations of positions the monomers and dimers may have on the electrode. However, when doing so, one has to consider that the bonding energy between the particles and the electrode differs according to the position considered. This bonding energy term is nothing other than the term  $\Delta G_c^\circ$  (see

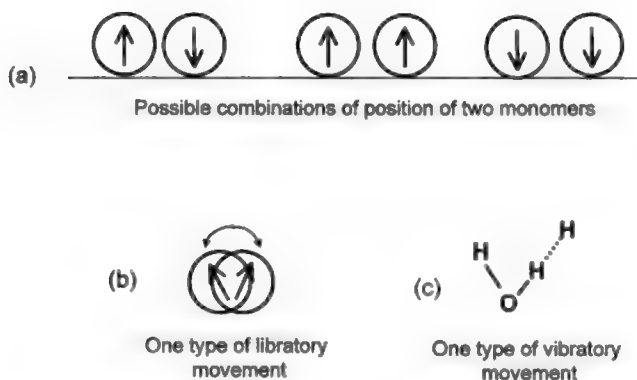


**Fig. 6.85.**  $S_{\text{conf}}$  is given by the different configurations the monomers and dimers may acquire on the electrode, such as those shown in (a) for two monomers.  $S_{\text{lib},m}$  is given by the libration of the monomers, such as that shown in (b).  $S_{\text{vib}}$  is given by vibration movements of the water molecule, such as that in (c).

Section 6.7.6). This means that to determine  $S_{\text{conf}}$ , one has to consider in the corresponding calculations the values of  $[\Delta G_c^\circ]_{\uparrow}$  and  $[\Delta G_c^\circ]_{\downarrow}$ . Figure 6.84(a) shows how  $S_{\text{conf}}$  varies as a function of the charge of the electrode.

The second term in Eq. (6.166),  $S_{\text{lib,m}}$ , represents the part of the entropy contributed by oscillations or balancing movements of the monomer around its axis. These oscillations constitute libratory motions (see Vol. 1) about the three mutually perpendicular axes with their origin at the center of mass [Fig. 6.85(b)]. Because of the charges in the dipole, the libratory movements are influenced by the changes in the electrode field; i.e., with a larger charge on the electrode, the molecules are more aligned to the generated field, with less possibility of oscillating, and therefore a smaller  $S_{\text{lib,m}}$ . Figure 6.84(b) shows the corresponding  $S_{\text{lib,m}}$  as a function of the charge of the electrode.

Finally,  $S_{\text{vib}}$  represents the internal vibrational entropy of the water molecules. These vibrations are represented mainly by H-bonding bendings and vibrations normal to the surface [Fig. 6.85(c)]. Their variation with  $q_M$  is shown in Fig. 6.84(c).

What conclusions can be obtained from these curves [Fig. 6.84(a–c)]? Both the configurational and the libratory entropy of surface water show a strong dependence on the charge of the electrode, showing a maximum at a potential negative to the pzc, just as the experimental results indicate [see Fig. 6.84(d)]. On the other hand, the vibrational entropy of surface water shows a small linear variation with the charge of the electrode. Furthermore, when these three contributions are added according to Eq. (6.166), the result is a curve very similar to that observed experimentally [see Fig. 6.84(d)].

Thus there are two factors responsible for the maximum in the solvent entropy and its deviation from the pzc. Those parameters are the different configurations the monomers and dimers are able to assume on the surface of the electrode, and that, as we discussed above, depend on the free energy associated with each configuration [Fig. 6.85(a)]. The second parameter is related to the entropy of libration, i.e., how the water molecules oscillate and how these oscillations are affected by the electrode charge [Fig. 6.85(b)]. The vibrational movements of the molecule do not greatly affect the position of the maximum in the entropy–charge curve.

### 6.7.9. If Not Solvent Molecules, What Factors Are Responsible for Variation in the Differential Capacity of the Electrified Interface with Potential?

Section 6.7.7 ended with an encouraging statement: The contribution of the water dipoles constituting the hydration sheath of the electrode can be ignored in the understanding of the differential capacity of the electrified interface. Thus, if water molecules, in spite of their large number in the interfacial region, are not responsible for this property of the double layer, what is? We also said that the total differential capacity of the interface could be divided into two contributions

$$\frac{1}{C} = \frac{1}{C_{\text{charge}}} + \frac{1}{C_{\text{dipole}}} \approx \frac{1}{C_{\text{charge}}} \quad (6.167)$$

but since  $C_{\text{dipole}}$  was a large number in comparison with  $C_{\text{charge}}$ , then the total capacity could be approximated as  $C_{\text{charge}}$ . What are the contributors to this  $C_{\text{charge}}$ , which are in control of the properties of the interface? The answer is, all the elements in our system that contain charges—the ions in the solution and the electrons in the metal.

The contribution of the metal to the double layer was discussed in Sections 6.6.7 to 6.6.9. However, we have said little about the ions in solution adsorbed on the electrode and how they affect the properties of the double layer. For example, when presenting the Stern model of the double layer (Section 6.6.6), we talked about ions sticking to the electrode. How does an interface look with ions stuck on the metal? What is the distance of closest approach? Are hydrated ions held on a hydrated electrode; i.e., is an electrode covered with a sheet of water molecules? Or are ions stripped of their solvent sheaths and in intimate contact with a bare electrode? What are the forces that influence the sticking of ions to electrodes?

Before going into this matter of ions, we should not take with us the impression that the solvent molecules are unimportant to the structure of the double layer. On the

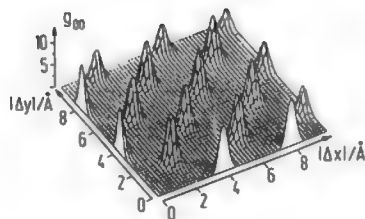
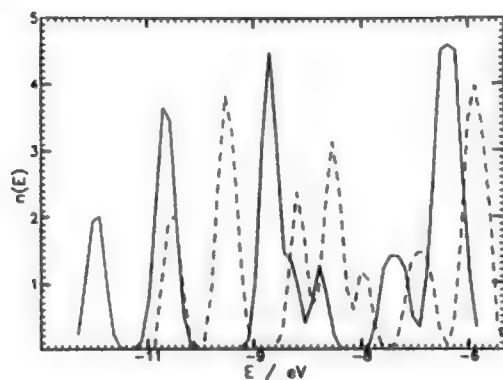
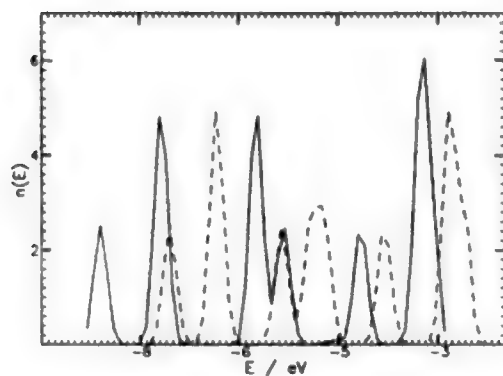


**Fig. 6.86.** Oxygen–oxygen pair correlation function obtained from molecular dynamic simulations on the adsorbed layer of a Pt(100) surface.  $\Delta x$  and  $\Delta y$  are the projections of the interatomic distances in the  $x$ - and  $y$ -directions, respectively. They reflect the positions of the oxygen atoms on the top site of the platinum lattice, and the pronounced form of the peaks refers to their relatively small displacement. (Reprinted from E. Spohr, G. Toth, and K. Heinzinger, *Electrochim. Acta* **41**: 2131, copyright 1996, Fig. 10a, with permission from Elsevier Science.)



(a)



(b)

**Fig. 6.87.** Density of electronic states of copper (111) surface calculated from quantum chemical modeling for the copper surface alone and with the water molecules adsorbed on top. The solid line represents the cluster (a)  $\text{Cu}_{19}$  and (b)  $\text{Cu}_{19}^-$ , and the dashed lines (a)  $\text{Cu}_{19}(\text{H}_2\text{O})_5$  and (b)  $\text{Cu}_{19}(\text{H}_2\text{O})_5^-$ . (Reprinted from R. R. Nazmutdinov and M. S. Shapnik, *Electrochem. Acta* **41**: 2253, copyright 1996, Fig. 4, with permission from Elsevier Science.)

contrary. In Section 6.7.1 it was established that water molecules often cover most of the surface of the electrode. We are also aware that ions possess hydration sheets. Thus, if the electrode and the ions have to strip themselves from water molecules so that the ions can adsorb on the metal, then the energy of adsorption of water molecules on the electrode as well as the hydration energy of the ions should play an important role in this adsorption process and therefore in the properties of the interface.

The structure and interactions of water are so important that they have been extensively studied throughout the history of electrochemistry. However, many of water's special properties remain unexplained at the molecular level, and with every new generation of experimental and theoretical tools, the subject of water is, and will continue, being revised (Figs. 6.86 and 6.87).

## Further Reading

### Seminal

1. A. Frumkin and A. Gorodetskaya, "Electrocapillary Phenomena and Layer Formation on the Surface of Liquid Gallium," *Z. Phys. Chem. (Leipzig)* **136**: 215 (1928).
2. L. Lange and K. P. Miščenko, "On the Thermodynamics of Ionic Solvation," *Z. Phys. Chem. (Leipzig)* **149**: 1 (1930).
3. N. F. Mott and R. J. Watts-Tobin, "The Interface Between a Metal and an Electrolyte," *Electrochim. Acta* **4**: 79 (1961).
4. J. O'M. Bockris, M. A. V. Devanathan, and K. Muller, "Water Molecule Model of the Double Layer," *Proc. Roy. Soc. (London)* **A274**: 55 (1963).
5. J. O' M. Bockris and M. A. Habib, "The Contribution of the Water Dipoles to Double-Layer Properties," *Electrochim. Acta* **22**: 41 (1977).
6. M. A. Habib and J. O'M. Bockris, "Potential-Dependent Water Orientation: An In Situ Spectroscopic Study," *Langmuir* **2**: 388 (1986).
7. M. A. Habib, "Solvent Dipoles at the Electrode-Solution Interface," in *Modern Aspects of Electrochemistry*, B.E. Conway and J. O'M. Bockris, eds., Vol. 12, Plenum, New York (1977).

### Reviews

1. K. Heinzinger, "Molecular Dynamics of Water at Interfaces," in *Structure of Electrified Interfaces*, J. Lipkowski and P. N. Ross, eds., p. 239, VCH Publishers, New York (1993).
2. F. Bensebaa and T. H. Ellis, "Water at Surfaces: What Can We Learn from Vibrational Spectroscopy?" *Prog. Surf. Sci.* **50**(1-4): 173 (1995).
3. J. W. Halley, "Studies of the Interdependence of Electronic and Atomic Dynamics and Structure at the Electrode-Electrolyte Interface," *Electrochim. Acta* **41**: 2229 (1996).
4. R. R. Nazmutdinov and M. S. Shapnik, "Contemporary Quantum Chemical Modelling of Electrified Interfaces," *Electrochim. Acta* **41**: 2253 (1996).
5. I. Benjamin, "Molecular Dynamic Simulations in Interfacial Electrochemistry," in *Modern Aspects of Electrochemistry*, J. O'M Bockris, B. E. Conway, and R. E. White, eds., Vol. 31, p. 115, Plenum, New York (1997).

## Papers

1. B. B. Damaskin and A. N. Frumkin, *Electrochim. Acta* **19**: 173 (1974).
2. R. Parsons, *J. Electroanal. Chem.* **59**: 229 (1975).
3. W. R. Fawcett, *J. Phys. Chem.* **82**: 1385 (1978).
4. R. Guidelli, *J. Electroanal. Chem.* **197**: 77 (1986).
5. G. M. Torrie and G. N. Patey, *Electrochim. Acta* **36**: 1677 (1991).
6. M. Xu, P. Yang, W. Yang, and S. Pang, *Vacuum* **43**: 1125 (1992).
7. F. Bensebaa and T. H. Ellis, *Prog. Surf. Sci.* **50**(1–4): 173 (1995).
8. E. Spohr, G. Tóth, and K. Heinzinger, *Electrochim. Acta* **41**: 2131 (1996).
9. K. Ataka, T. Yotsuyanagi, and M. Osawa, *J. Phys. Chem.* **100**: 10664 (1996).
10. J. C. Shelley, G. N. Patey, D.R. Berard, and G. M. Torrie, *J. Chem. Phys.* **107**: 2122 (1997).

## 6.8. IONIC ADSORPTION

### 6.8.1. How Close Can Hydrated Ions Come to a Hydrated Electrode?

In Chapter 2 we learned how ions in solution are solvated. Some of the water molecules that form the solvation sheet are left behind when ions random walk and drift around, while others—the primary hydration molecules—show a stronger attraction to the ion and follow it in its thermal, random movements.

The ion, wrapped in a primary hydration sheath, migrates up to the electrode. How close to the electrode can such a hydrated ion approach? On its way to the electrode, the ion proceeds until its water molecules collide with the water molecules of the hydrated electrode. At this point, the electron shells of the water molecules of both sides start overlapping and repelling. The ions cannot pass over the guarding water molecules of the electrode and they have to remain in the second layer. The ions are not able to contact the electrode [Fig. 6.88(a)]. The plane drawn through the locus of centers of these hydrated ions is called the *outer Helmholtz plane*.

A very important question now arises. Does this arrangement of hydrated ions in contact with a hydrated electrode always correspond to the configuration of lowest free energy? Are some ions capable of divesting themselves (at least partly) of their primary waters, making their way through the hydration sheet of the electrode, and coming into contact with it?

If we assume a priori that the ions can touch the electrode, we can define another plane through the locus of centers of these contact-adsorbed ions [Fig. 6.88(b)]. The name of this plane is the *inner Helmholtz plane* or *IHP*. Therefore, are ions capable of quitting the OHP and populating the IHP, and if so, under what circumstances can they do it?

No a priori answer can be given to these questions. The parameter that would tell us if the ions stay in the OHP or jump to the IHP is the free-energy change associated with this process (Fig. 6.89). One must calculate the free-energy change for (i.e., the work done by) an ion to move from the OHP to the IHP while at the same time the

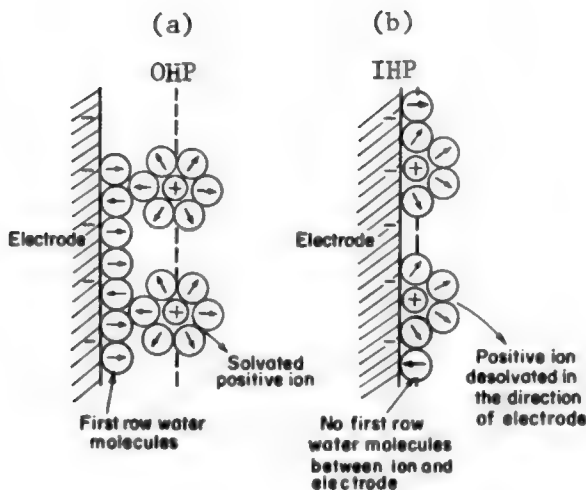


**Fig. 6.88.** The two positions the ions may acquire close to the electrode: (a) at the OHP, or (b) at the IHP in contact with the electrode.

appropriate number of adsorbed water molecules get displaced. If the free-energy change is negative, ions will make the move.

## 6.8.2. What Parameters Determine if an Ion Is Able to Contact Adsorb on an Electrode?

The process of contact adsorption can be viewed in the following way (Fig. 6.90): First, a hole of area of at least  $\pi r_i^2$ —where  $r_i$  is the radius of the bare ion—is swept free of water molecules in order to make room for the ion. At the same time, the ion strips itself of part of its solvent sheath and then jumps into the hole. During this process, the involved particles—electrode, ion, water molecules—break old attachments and make new ones (change of enthalpy,  $\Delta H$ ) and also exchange freedoms and restrictions for new freedoms (change of entropy,  $\Delta S$ ).

These changes in enthalpy and entropy can be classified into three groups: (1) changes in ion–electrode interactions, (2) changes in solvent interactions, including ion–solvent and electrode–solvent, and (3) changes in lateral interactions. The enthalpy and entropy and therefore, the free-energy changes corresponding to these groups will dictate whether the ions can come into contact adsorption with the electrode or stay solvated in the OHP.

**6.8.2.1. Ion–Electrode Interactions.** Similarly to water molecules in contact with the electrode (see Section 6.7.2), ions in contact with a charged metal experience different types of forces operating between the ion and the metal electrode. These include electric field forces, image forces, dispersion forces, and electronic forces.

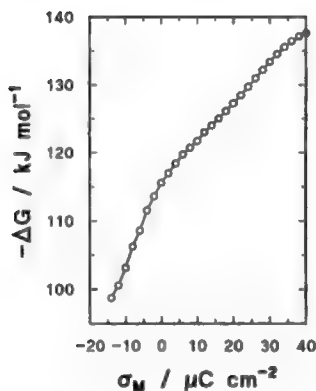


**Fig. 6.89.** Plot of the Gibbs energy of adsorption vs. electrode charge density for the adsorption of chloride ions at an Au(111) electrode by the chronocoulometry technique. Adapted from Z. Shi and J. Lipkowski, *J. Electroanal. Chem.* **403**: 225, copyright 1996, Fig. 7b, with permission of Elsevier Science.)

The *electric field forces* arise because the ions, with their negative or positive charges, are attracted or repelled by the charge on the metal (Section 6.3.5).

The *image forces* are those induced by the appearance of the fictitious charge on the metal (image charge) created by the ion's charge. Similarly to the adsorbed water molecules (Section 6.7.2), ions also experience *dispersion forces* due to the induction of instantaneous fluctuations in the electron density clouds of continuous atoms—the adsorbed ion and the metal atom. Both these forces are of attractive character and were discussed in Section 6.7.2.

Now, when the two atoms—the ion and the metal atom—are close enough, another type of force, having an *electronic nature*, appears. During the approach of the ion to a surface metal atom, the electron orbitals of the ion overlap the electron orbitals of the metal atom. If these orbitals are not compatible, they repel; the metal does not welcome the incoming ion.

Thus, when there is no charge on the electrode and the electric forces are off, there are three forces operating on the ion—two of attractive character and one of repulsive



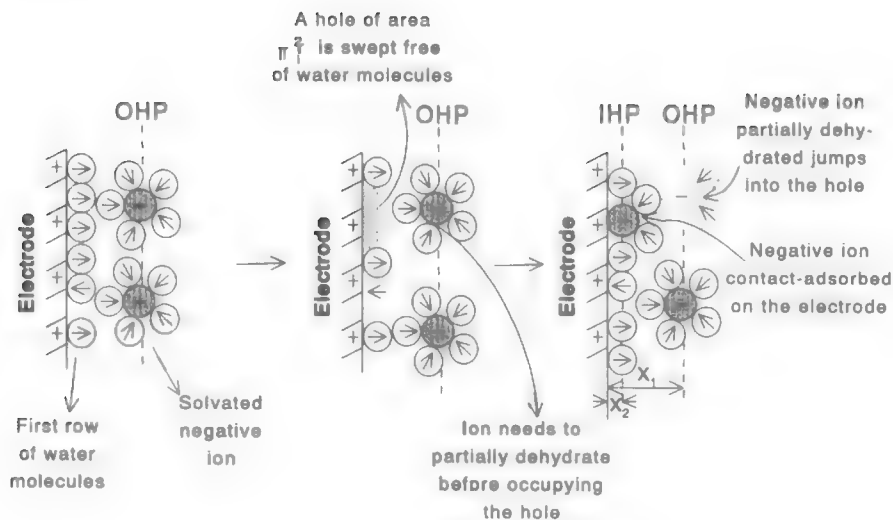


Fig. 6.90. The contact-adsorption process.

character if the electron orbitals of the metal and the ion are not compatible. If the repulsion force (electronic force) is larger than the image and dispersion forces, then repulsion between the ion and the metal occurs. The ion stays in the OHP and adsorption does not occur. In the opposite case (i.e., when image and dispersion forces are larger), ions may jump from the OHP to the IHP—of course, depending on the magnitude of the other interactions, i.e., solvent and lateral interactions. Then adsorption may take place. The process of *physisorption* occurs.

However, there are other possibilities. What if instead of an unsuccessful overlap of orbitals the overlap occurs in a suitable way, and instead of repulsion, attraction between the ion and the electrode atoms results? In this case strong bonds may be formed between the ion and the electrode. These bonds are the result of donation or acceptance of electrons by the ion, and are responsible for the *chemisorption* of molecules.

However, not everything is black or white; that is, complete bonding or no bonding at all between the ion and the metal atom. States in between may occur, and instead of a complete bonding—complete donation or acceptance of, say, one electron—only a partial transfer of electrons may occur (Lorenz and Salie, 1961). A parameter  $\lambda$  can be defined, which will indicate how much of the charge has been transferred from the ion to the electrode: a value of  $\lambda = 0$  will indicate that the ion retains all its charge and a value of  $\lambda = 1$  that it has donated all its charge to the electrode. If the adsorbed species is an anion,  $A^-$ , then  $\lambda = 0$  means that it gets adsorbed as  $A^-$ , but if  $\lambda = 1$ , then it gets adsorbed as an atom,  $A^0$ . A  $0 < \lambda < 1$  (e.g.,  $\lambda = 0.8$ ) is equivalent to saying that only a fraction of the electron charge (e.g.,

**TABLE 6.8**  
**Electrosorption Valencies ( $\gamma$ ) for Various Systems in Aqueous Solutions**

M	$S^z$	$\gamma$
<b>Anions</b>		
Au(111)	$\text{Cl}^-$	-0.8
Au(111)	$\text{Br}^-$	-0.78
Au	$\text{Br}^-$	-0.39
Au	$\text{I}^-$	-1.01
Au	$\text{S}^{2-}$	-2.0
Au	$\text{SO}_4^{2-}$	-1.0
Ag(110)	$\text{Cl}^-$	-0.53
Ag(100)	$\text{Br}^-$	-0.68
Ag(111)	$\text{S}^{2-}$	-1.4
Pt	$\text{Br}^-$	-0.9
<b>Cations</b>		
Au	$\text{Cu}^{2+}$	1.84
		1.40
Au	$\text{Cd}^{2+}$	1.6-2.0
Au	$\text{Bi}^{3+}$	2.2
		2.4
		2.7
Au	$\text{Tl}^+$	0.61
Au	$\text{Hg}_2^{2+}$	0.94
Au	$\text{Pb}^{2+}$	2.0
Pt(111)	$\text{Zn}^{2+}$	2.0
<b>Cosorption</b>		
Au(111)	$\text{Cu}^{2+}, \text{Br}^-$	1.6-1.8
Pt	$\text{Cu}^{2+}, \text{ClO}_4^-$	2.0
Pt	$\text{Cu}^{2+}, \text{SO}_4^{2-}$	1.75
		1.4-2.0

Source: Reprinted with permission from J. W. Schultze and D. Rolle, *Can. J. Chem.* **75**; 1750, (1997), Table 1.

0.8) has been donated to the electrode to make the bond (the electron is partially delocalized). Only partial transfer of electrons has occurred and the ion is adsorbed as  $\text{A}^{-0.2}$  (Table 6.8).<sup>51</sup>

**6.8.2.2. Solvent Interactions.** Consider an electrode surface originally free of contact-adsorbed ions. The metal is partially covered with solvent molecules, and the ions, beyond the IHP, may or may not be solvated (Fig. 6.90).

<sup>51</sup>Another parameter, the "electrosorption valence,  $\gamma$ " introduced by Vetter and Schulze (1973), is also widely used in electrochemistry. It is a macroscopic measure defined as  $\gamma = -(1/F)(\partial q_M / \partial \Gamma)_{\Delta\phi}$ . For most conditions,  $\lambda = -\gamma$ .

In order for the ions to come closer to the electrode, work has to be done to get rid of all or part of their solvation shield. This work is nothing other than the interaction energy of mainly primary solvent molecules with the ion. What are the parameters that determine the number of water molecules attached to the ion and how strong the attachment is?

In Chapter 2 it was said that the number of hydration molecules as well as the hydration energy depends mainly on the charge and size of the ion. Thus, small cations have a large number of hydration molecules attached strongly to the ion. They cannot easily get rid of their hydration sheet. They will not contact adsorb on the electrode. On the contrary, large anions and large cations have only a few primary water molecules or none loosely attached to the ion. For them, the ion-solvent interactions are less important than other interactions. They will tend to contact adsorb on the electrode (Fig 6.91).

What about the hydration sheet of the electrode? Some of the solvent molecules adsorbed on the metal have to be removed in order to make room for the ion to adsorb (Fig 6.90). Thus the work needed to remove water molecules from the electrode depends basically on the bonding energy of water molecules to the electrode. Also, we should not forget that water in the interphasial region changes its orientation in response to the variation of the electrode potential (see Section 6.7.5). Thus, the water-metal bond would be dependent also on the potential of the electrode.

Table 6.9 shows water-electrode and ion-water interaction energies as well as the ion-electrode interaction energy for several anions and cations. The free energies are positive for the water-electrode and ion-water processes, and for all the ions considered. What this means is that these two processes—water depletion of the electrode and water depletion of the ions—do not cooperate in the adsorbance of ions on the electrode. However, adding the three energies—water-electrode, ion-water, and ion-electrode—gives as a result different signs of total free-energy change and thus their differing attitudes to contact adsorption:  $\text{Cs}^+$ ,  $\text{Cl}^-$ ,  $\text{Br}^-$ , and  $\text{I}^-$ , with negative free energies, will tend to remove their hydration sheet and will make the transition to the IHP; on the other hand  $\text{Na}^+$ ,  $\text{K}^+$ , and  $\text{F}^-$ , with positive free energies, will tend to remain hydrated in the OHP.

**6.8.2.3. Lateral Interactions.** Besides the forces between the metal and the adsorbate, forces between the adsorbed molecules may exist and they may welcome or reject the adsorbing ion. To understand them, consider the adsorption of ions on a surface electrode. Now choose one of those ions and consider it as a reference ion. Since the ions adsorbed around the reference ion carry the same charge as the reference ion, electrostatic repulsion forces emerge between the reference ion and its neighbors (Fig. 6.92). These interactions are of long range, and they decay as  $1/r$ .

Another point that should not be forgotten is that adsorbed ions induce image charges on the electrode of equal magnitude but opposite charge (Section 6.3.5) (Fig. 6.92). Now, *all* the adsorbed ions induce image charges, including the ions surrounding the central ion. Thus we can expect that the reference ion interacts with its neighbor's

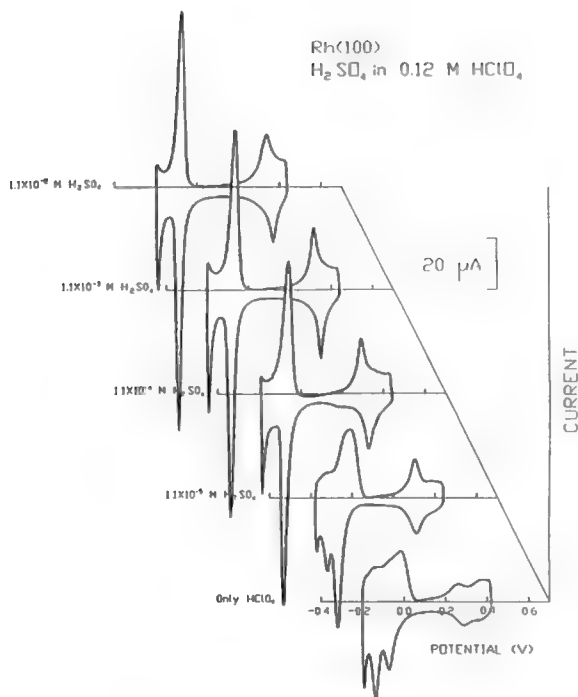


**Fig. 6.91.** Current vs. potential curves of Rh(111) in 0.12  $M$   $\text{HClO}_4$  with increasing amount of  $\text{H}_2\text{SO}_4$  ( $50 \text{ mV s}^{-1}$ ). (Reprinted from M. Gamboa-Aldeco, Ch. K. Rhee, A. Nahlé, Q. Wang, J. Zhang, H. L. Richards, P. A. Rikvold, and A. Wieckowski, Electrochemical Society meeting proceedings, copyright 1994, Fig. 13, with permission from Elsevier Science.)

image charges, and these interactions should be attractive. Also, because of its closeness, short-range forces—dispersion forces (Section 6.7.2)—will appear between the reference ion and its neighbors.

Finally, the central ion may be surrounded, not only by similar ions, but also by solvent molecules adsorbed on the surface. Interactions with solvent molecules could also be important to the adsorption process of the ion (Fig. 6.93).

From this discussion we can see that it is not so simple to determine the value of the lateral interactions of the reference ion. To do so it is necessary to know what type of molecules are surrounding the ion. The type of molecules and their number depend greatly on the state of adsorption, i.e., how many ions are already adsorbed on the electrode. And this value will depend largely on the charge of the electrode. Thus the lateral interactions are a function of the charge of the electrode.

**TABLE 6.9**  
**The Thermodynamics of Contact Adsorption<sup>a</sup>**

Ion	Ion–Electrode Interactions			Water–Electrode Interactions			Ion–Water Interactions			Sum
	$\Delta H$	$\Delta S$	$\Delta G$	$\Delta H$	$\Delta S$	$\Delta G$	$\Delta H$	$\Delta S$	$\Delta G$	$\Sigma_i \Delta G_i$
Na <sup>+</sup>	−49.1	1.5	−49.6	28.1	3.6	27.0	39.5	11.2	36.1	+13.5
K <sup>+</sup>	−48.2	2.0	−48.8	21.1	6.7	19.1	33.9	5.2	32.3	+2.6
Cs <sup>+</sup>	−43.5	3.3	−44.5	20.9	10.7	17.7	17.7	−12.2	21.4	−5.4
F <sup>−</sup>	−47.1	1.4	−47.5	38.1	6.7	36.1	35.0	6.4	33.1	+21.7
Cl <sup>−</sup>	−49.3	2.1	−49.9	22.0	12.4	18.3	17.7	−16.6	22.7	−8.9
Br <sup>−</sup>	−49.2	2.8	−50.0	21.6	14.5	17.2	14.7	−22.4	21.4	−11.4
I <sup>−</sup>	−49.2	3.6	−50.3	21.9	18.0	16.5	10.9	−32.6	20.7	−13.1

<sup>a</sup> $\Delta H$  and  $\Delta G$  given in kcal mol<sup>−1</sup> and  $\Delta S$  in kcal mol<sup>−1</sup> K<sup>−1</sup>.

### 6.8.3. The Enthalpy and Entropy of Adsorption

In the previous section we found that some molecules tend to adsorb while others prefer to stay in solution, and that the main factor that determines which molecules do what is the free energy of adsorption. Consider the general adsorption reaction of, say, an anion, on an electrode:

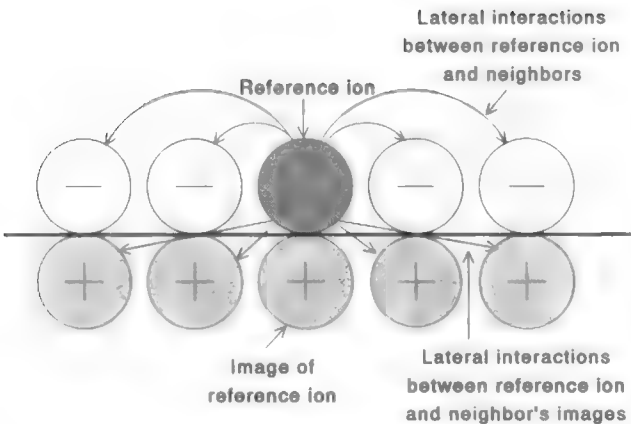
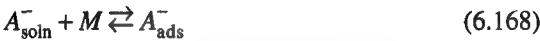


**Fig. 6.92.** Electrostatic forces between the reference ion and its neighbors and the neighbor's image charges.



**Fig. 6.93.** A typical equilibrium configuration for a model of bisulfate adsorption on Rh(111), generated by Monte Carlo methods in the ordered  $(\sqrt{3} \times \sqrt{7})$  phase region at  $-150$  mV. Bisulfate ions are represented by O, hydrogen as +, and empty lattice sites as •. (Reprinted from P. A. Rikvold, M. Gamboa-Aldeco, J. Zhang, M. Han, Q. Wang, H. L. Richards, and A. Wieckowski, *Surf. Sci.*, copyright 1995, Fig. 7, with permission from Elsevier Science.)

The free energy of adsorption of this reaction can be split into an enthalpy and an entropy term,

$$\Delta G_{\text{ads}} = \Delta H_{\text{ads}} - T\Delta S_{\text{ads}} \quad (6.169)$$

Thus, we could find the variation of  $\Delta G_{\text{ads}}$  by finding out the corresponding variation in the enthalpy and entropy of adsorption. However, the knowledge of  $\Delta H_{\text{ads}}$  and  $\Delta S_{\text{ads}}$  leads to some interesting questions related to the adsorption process. The bond strength between the adsorbed ion and the metal is determined by the value of the enthalpy. Is this enthalpy value constant through the whole adsorption process (i.e., from the first adsorbed ions to the last ones), or does  $\Delta H_{\text{ads}}$  vary as the population of the adsorbed ions increases?

Evidence exists indicating that  $\Delta H_{\text{ads}}$  decreases linearly with the coverage, i.e., the  $\Delta H_{\text{ads}}$  is not constant.<sup>52</sup> The fact that  $\Delta H_{\text{ads}}$  is not constant during the adsorption process should not surprise us because we know about the presence of lateral interactions between the adsorbed molecules (Section 6.8.2.2), and thus, ions adsorbing when the surface is clean (no other adsorbates) should have different energies than ions adsorbing when the surface is already highly populated. The change in enthalpy of the adsorption process of Eq. (6.168) is  $\Delta H_{\text{ads}} = H_{\text{A}_{\text{ads}}}^- - H_{\text{A}_{\text{soln}}}^-$ . From these two terms, only  $H_{\text{A}_{\text{ads}}}^-$  is affected by the other adsorbed ions. When the surface is clean of adsorbates,

<sup>52</sup>Whenever the adsorption process can be represented by a Temkin isotherm (see Section 6.8.10), a linear decrease of  $\Delta H_{\text{ads}}$  with  $\theta$  exists because this is the basis of the Temkin isotherm.

$H_{A_{\text{ads}}}^-$  is given only by the attractive forces between the ion and the electrode. As the population of ions on the surface increases, the repulsive interactions between the adsorbed ions increase, and as a consequence of this,  $H_{A_{\text{ads}}}^-$  and therefore  $\Delta H_{\text{ads}}$ , decreases (becomes less negative).

There is another factor that may contribute to the decrease of  $\Delta H_{\text{ads}}$ . Solid surfaces are rarely homogeneous and have irregularities or different sites on the surface characterized by different energies (Fig. 6.94).<sup>53</sup> These types of surfaces are said to be *heterogeneous* surfaces. At the beginning of the adsorption process, when there are not many adsorbed ions, the adsorbing ion may "choose" an appropriate "site," generally one of low energy (one with a more negative  $H_{A_{\text{ads}}}^-$ , such as one of the "irregularities" on the surface) to form strong bonds with the substrate. As the population on the surface increases, the most active sites are already occupied, and the incoming ions have to choose the least active sites (less negative  $H_{A_{\text{ads}}}^-$ ). The result is the decrease of  $\Delta H_{\text{ads}}$  as the surface coverage increases.

While the change in enthalpy tells us how strong the bonds are that have to be broken and formed during the adsorption process, the entropy of adsorption gives us other types of information, for example, how "mobile" the ion is in its adsorbed site. Consider a nonlinear molecule composed of  $N$  atoms. It will have a total of  $3N-6$  vibrational degrees of freedom.<sup>54</sup> Consider now the case in which this molecule adsorbs on the surface without any possible movement—the molecule is *immobilized* [Fig. 6.95(a)]. Under this circumstance the molecule loses all the translational and rotational degrees of freedom that it had in solution. These degrees of freedom are transferred into vibrations in the adsorbed molecule. Each molecule adsorbed in this manner will have a total of  $3N$  vibrational degrees of freedom.

At the other extreme, we have a molecule that upon adsorption loses only one of the translational degrees of freedom that it had in solution [Fig. 6.95(b)]. This translational degree of freedom is transformed into a vibration perpendicular to the surface. What about the other degrees of freedom? In this case the molecule retains the rest of them, and thus it can move freely on the surface of the electrode and rotate as it pleases. The molecule is adsorbed in a nonlocalized fashion.

In general, the internal vibrational degrees of freedom of a molecule are relatively unaffected on adsorption, since surface forces are usually weak compared with the restoring forces of the internal vibrations of a molecule. However, rotational and translational motion may be seriously affected by adsorption. It may be completely

<sup>53</sup>The heterogeneities referred to here are the different type of surfaces, e.g., (111), (100) that have different bonding energies. Also, dislocations, point defects, steps, etc. (see Fig. 7.110), are sites with stronger bonding energies than flat surfaces.

<sup>54</sup> $3N$  coordinates—degrees of freedom—are needed to describe a system (molecule). From these, three coordinates describe the position of its center of mass (translation of the molecule); three coordinates describe its orientation in space if the molecule is nonlinear (rotation of the molecule); the  $3N-6$  degrees of freedom left are used to describe the bond distances and angles in the molecule (vibration of the molecule).

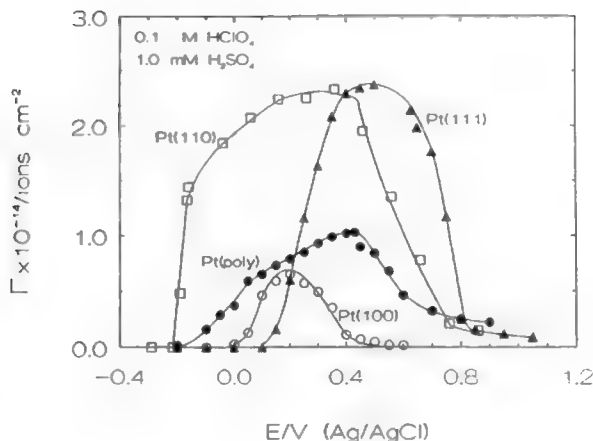


**Fig. 6.94.** Comparison of adsorption properties of different electrode surfaces. Bisulfate adsorption as a function of electrode potential on different platinum planes: (110), (111), (100); and on polycrystalline platinum. Data obtained by the radiotracer technique. (Reprinted from Y.-E. Sung, A. Thomas, M. Gamboa-Aldeco, K. Franaszczuk and A. Wieckowski, *J. Electroanal. Chem.* **378**: 131, copyright 1994, Figs. 14 and 15, with permission from Elsevier Science.)

transformed into vibrational motion or may change into some intermediate state of hindered rotation or translation (libration).

#### 6.8.4. Effect of the Electrical Field at the Interface on the Shape of the Adsorbed Ion

One effect important to mention here is the effect of the electric field,  $\vec{X}$ , which can be as strong as  $10^7 \text{ V cm}^{-1}$ , on the shape of the adsorbing species. The effect of this electrical field on the ion can be understood in the following way: The electrical field is directed perpendicularly to the electrode, toward the solution, as shown in Fig. 6.96. It can be considered equivalent to having an electrical force acting on the adsorbed ion. If we consider a negative ion (anion) adsorbed on the surface, this force is given by

$$F_{\vec{X}} = q_{\text{ads.ion}} \vec{X} = -ze_0 \vec{X} \quad (6.170)$$

The negative sign in this equation indicates that the electrical force acts in a direction opposite to that of the electric field from where it originates, i.e., it is directed



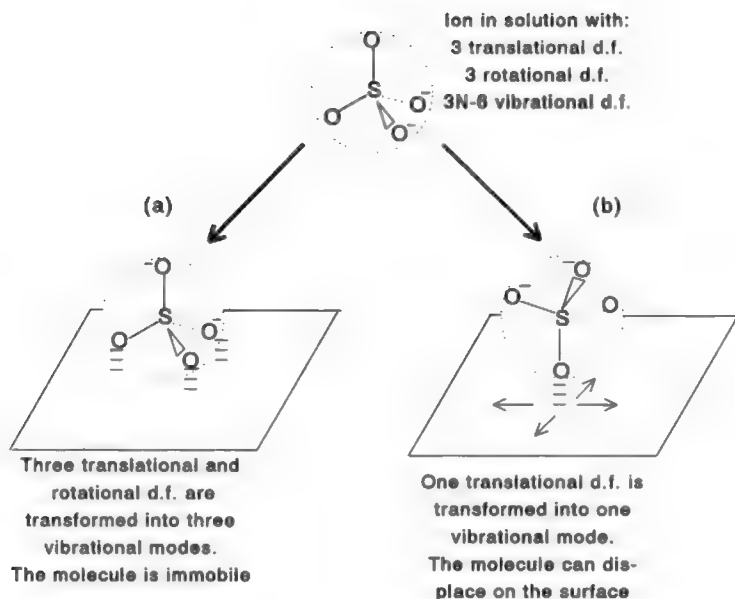


**Fig. 6.95.** Two of the possible ways a sulfate ion may adsorb on the surface: (a) The ion is immobilized and loses its translational and rotational degrees of freedom (d.f.), and (b) the ion is nonlocally adsorbed by losing only one of its translational degrees of freedom.

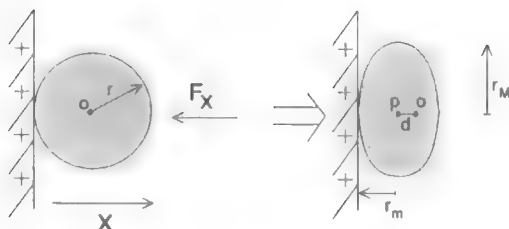


**Fig. 6.96.** Deformation of the adsorbed ion due to the electric field at the metal-solution interphase. (Reprinted from J. O'M. Bockris, M. Gamboa-Aldeco, and M. Szklarczyk, *J. Electroanal. Chem.* **339**: 355, copyright 1992, Fig. 16, with permission from Elsevier Science.)

toward the electrode (Fig. 6.96). How would this force affect the ion? As any other force would do, it would push the ion toward the electrode, crushing it, as depicted in Fig. 6.96. As a consequence of this crushing, the radius of the ion changes. For example, if the ion has a spherical shape in solution, in the adsorbed state it will have an elongated shape. Its radius perpendicular to the electrode will differ from that parallel to it.

### 6.8.5. Equation of States in Two Dimensions

So far we have had an overview of the forces involved in the adsorption process for ions in solution. However, we have not yet said anything about how to determine these forces or how to describe the adsorbed state of the ion. Physical quantities such as pressure, volume, temperature, and amount of substance describe the conditions in which a particular material exists; that is, they describe the *state* of a material. These quantities are interrelated and one cannot be changed without causing a change in one or more of the others. The mathematical relationship among these physical quantities is called the *equation of state* of the system. Well-known examples of equations of states for gases are the ideal gas ( $PV = nRT$ ) and the virial [ $P = RT(n/V) + RTB_{2,T}(n/V)^2 + \dots$ ] equations of state.

Pressure and volume are quantities that are applicable only in a three-dimensional system, such as a gas contained in a cylinder. However, molecules adsorbed on surfaces constitute a two-dimensional system. In these systems, the variable  $P$  does not make sense. Thus, there is a need to define a surface pressure,  $\Pi$ . While  $P$  is defined as force/area, the surface pressure  $\Pi$  is given as force/length. In the same way, instead of volume,  $V$ , in the two-dimensional system, the appropriate variable is the area,  $A$ .

How does the equation of state look in a two-dimensional system? Let's consider, for example, the virial equation of state. If  $\Pi$  is written instead of  $P$ , and  $A$  instead of  $V$ , then the corresponding equation of state in two dimensions is (Parsons, 1961),

$$\begin{aligned}\Pi &= RT \left( \frac{n}{A} \right) + RTB_{2,T} \left( \frac{n}{A} \right)^2 + RTB_{3,T} \left( \frac{n}{A} \right)^3 + \dots \\ &= RT\Gamma + RTB_{2,T}\Gamma^2 + RTB_{3,T}\Gamma^3 + \dots\end{aligned}\quad (6.171)$$

where  $B_{2,T}, B_{3,T}, \dots$ , are the second and third virial coefficients and are functions of temperature; in the second part of Eq. (6.171),  $n/A$  has been replaced by the surface excess,  $\Gamma$  (see Section 6.4.3).<sup>55</sup>

In Eq. (6.171) a new variable was introduced,  $\Pi$ . How can this variable be determined? One way is to relate it to another variable that we already know, i.e., the surface tension,  $\gamma$  (see Section 6.4.5). Thus,  $\Pi \equiv \gamma^* - \gamma$ , where  $\gamma^*$  is the surface tension

<sup>55</sup>The surface excess is defined as  $\Gamma = n_i/A - n_i^0/A$  [see Eq. (6.66)]. However, since the bulk concentration tends to zero,  $\Gamma \approx n_i/A$ .

of pure water and  $\gamma$  is the surface tension in the presence of the adsorbate ions. Substituting  $\gamma^* - \gamma$  by  $\Pi$  in Eq. (6.171) and differentiating it with respect to  $\Gamma$  ( $\gamma^*$  is constant),

$$\frac{d\Pi}{d\Gamma} = -\frac{d\gamma}{d\Gamma} = RT + 2RTB_{2,T}\Gamma + 3RTB_{3,T}\Gamma^2 + \dots \quad (6.172)$$

We know from Section 6.5.7 (Eq. 6.116) that at constant potential of the electrode,

$$d\gamma = -2RT\Gamma d(\ln a_{\pm}) \quad (6.173)$$

Substituting Eq. (6.173) into Eq. (6.172),

$$2RT\Gamma \frac{d(\ln a_{\pm})}{d\Gamma} = RT + 2RTB_{2,T}\Gamma + 3RTB_{3,T}\Gamma^2 + \dots \quad (6.174)$$

and integrating this equation,

$$\int d(\ln a_{\pm}^2) = \int \left( \frac{1}{\Gamma} + 2B_{2,T} + 3B_{3,T}\Gamma + \dots \right) d\Gamma \quad (6.175)$$

or

$$\ln a_{\pm}^2 = \ln \Gamma + 2B_{2,T}\Gamma + \frac{3}{2}B_{3,T}\Gamma^2 + \dots + \text{const} \quad (6.176)$$

where “const” is the constant of integration. Here several simplifications can be done. First, we can neglect the terms higher than  $B_{2,T}\Gamma$ . Then from Eq. (6.113),  $\ln a_{\pm}^2 = \ln a_+ + \ln a_-$ . If the anion is the only adsorbing species, then the term  $\ln a_+$  can be introduced in the constant in Eq. (6.176). Calling this constant  $\ln \beta$ , and dropping the subscript in  $a_-$ , Eq. (6.176) becomes

$$\ln a + \ln \beta = \ln \Gamma + 2B_{2,T}\Gamma \quad (6.177)$$

or,

$$\alpha\beta = \Gamma e^{2B_{2,T}\Gamma} \quad (6.178)$$

Equation (6.178) forms part of a very important set of equations, called *isotherms*. These isotherms are equivalent to the equations of state and therefore they are used to describe the adsorption process in electrochemical systems.

### 6.8.6. Isotherms of Adsorption in Electrochemical Systems

In the previous section we saw how the equation of state of the adsorbed ions can be expressed as isotherms. What are the characteristics of these isotherms? Isotherms, as equations of state, relate the physical quantities that define the adsorbed molecules in the electrochemical system. These physical quantities are the number of adsorbed molecules ( $\Gamma$  or  $\theta$ ), the activity of ions in solution ( $a$ ), the charge ( $q_M$ ) or potential of the electrode ( $E$ ), and the temperature of the system ( $T$ ). When the last two variables,  $q_M$  and  $T$ , are kept constant, the mathematical expression that relates all the variables is called an *isotherm*. Now, if the variables that are kept constant are the activity and temperature, the name given to the equation is *isoconc*.<sup>56</sup>

At this point it can be said that there are many techniques used to determine the surface coverage,  $\Gamma$  or  $\theta$ , as a function of the different parameters. Figure 6.97 shows some techniques used for this purpose.

Consider the following adsorption reaction. The molecule  $A_{\text{soln}}$  in solution gets adsorbed on the substrate M, and the adsorbed molecule  $A_{\text{ads}}$  remains in equilibrium with the species in solution,



The corresponding electrochemical potentials of  $A_{\text{soln}}$  and  $A_{\text{ads}}$  are [see Eq. (6.114)]

$$\bar{\mu}_{A,\text{soln}} = \bar{\mu}_{A,\text{soln}}^0 + RT \ln a \quad (6.180)$$

and

$$\bar{\mu}_{A,\text{ads}} = \bar{\mu}_{A,\text{ads}}^0 + RT \ln f(\theta) \quad (6.181)$$

where  $\bar{\mu}_{A,\text{soln}}^0$  and  $\bar{\mu}_{A,\text{ads}}^0$  are the standard electrochemical potentials of the molecule in solution and in adsorbed states, respectively. The parameter  $f(\theta)$  is a function of the surface concentration expressed in terms of surface coverage of the adsorbed ion,  $\theta$ . Since equilibrium exists between the adsorbed molecules and those in solution, Eqs. (6.180) and (6.181) are equal,

$$\bar{\mu}_{A,\text{soln}}^0 + RT \ln a = \bar{\mu}_{A,\text{ads}}^0 + RT \ln f(\theta) \quad (6.182)$$

or

$$f(\theta) = ae^{-\Delta G^\circ/RT} \quad (6.183)$$

<sup>56</sup>An isoconc is also an isotherm. The names are given to differentiate the other variables that are constant besides the temperature.

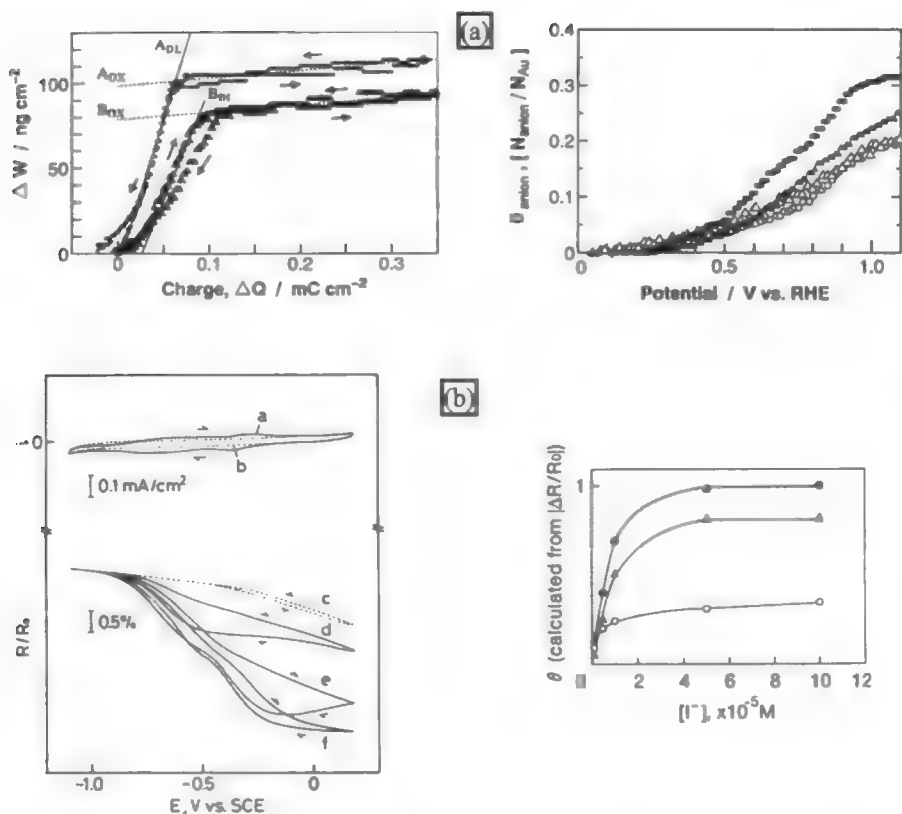
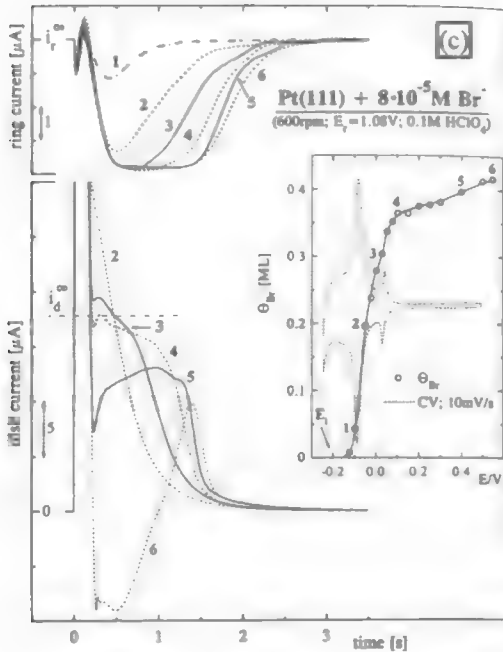
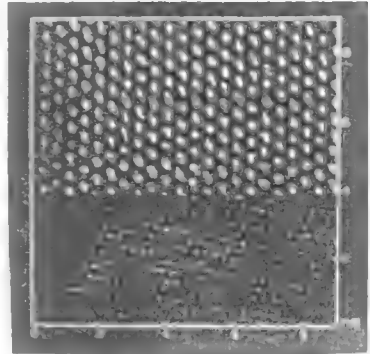


**Fig. 6.97.** Some techniques used in the study of isotherms: (a) Electrochemical quartz crystal microbalance: mass change ( $\Delta W$ ) vs. quantity of electricity ( $\Delta Q$ ) [Au,  $0.1 \text{ M HClO}_4$  ( $\blacktriangle$ ), and  $0.05 \text{ M H}_2\text{SO}_4$  ( $\bullet$ )]; and anion coverage vs. electrode potential [poly-Au (open symbols), and Au(111) (dark symbols);  $\text{HSO}_4^-$  (circles); and  $\text{ClO}_4^-$  (triangles)]. Reprinted from H. Uchida, N. Iwada, and M. Watanabe, *J. Electroanal. Chem.* **42**, copyright 1997, Figs. 3 and 5, with permission of Elsevier Science.) (b) Specular reflection method: reflectivity change vs. potential [Au,  $\text{HClO}_4$  with NaI: (b) and (c)  $0 \text{ M}$ , (d)  $5 \times 10^{-6}$ , (e)  $5 \times 10^{-5} \text{ M}$ , (a) and (f)  $1 \times 10^{-4} \text{ M}$ ]; and coverage vs. iodide concentration [ $-0.2 \text{ V}$  ( $\bullet$ );  $0.2 \text{ V}$  ( $\blacktriangle$ );  $-0.6 \text{ V}$  ( $\circ$ )]. (Reprinted from K. Arai, F. Kusu, K. Ohe, and K. Takamura, *Electrochim. Acta* **42**: 2493, copyright 1997, Figs. 2 and 6, with permission from Elsevier Science.) (c) Rotating-ring-disk electrode: disk current vs. time at different electrode potentials [Pt(111),  $0.1 \text{ M HClO}_4$  and  $8 \times 10^{-5} \text{ M Br}^-$  (600 rpm)]; and  $\theta_{Br}$  at different potentials. (Reprinted with permission from H. A. Gasteiger, N. M. Markovic, and P. N. Ross, Jr., *Langmuir* **12**: 1414, copyright 1996, American Chemical Society, Fig. 3.) (d) STM composite image of Au(111) in a KI solution. The iodide adlayer is observed on the top half of the image. (Reprinted with permission from X. Gao and M. J. Weaver, *J. Am. Chem. Soc.* **114**: 8544, Fig. 2c, copyright 1992, American Chemical Society.)



(d)



where  $\Delta G^\circ (= \bar{\mu}_{A,ads}^0 - \bar{\mu}_{A,soln}^0)$  is the standard electrochemical free energy of adsorption. Equation (6.183) can be written in a general form as

$$f(\theta) = \alpha\beta \quad (6.184)$$

where  $\beta = \exp(-\Delta G^\circ/RT)$ .

Equation (6.183) or Eq. (6.184) can be identified as the relation between the coverage, the activity in solution of the adsorbed species, and the temperature of the system. Thus, in order to define the system well, only one variable is missing, the charge of the electrode. However this variable is intrinsically expressed in the term  $\Delta G^\circ$ . Thus, Eq. (6.183) or Eq. (6.184) represents the isotherm of the system given by the reaction in Eq. (6.179).

In Section 6.8.5 we were able to derive one specific isotherm, the virial isotherm. However, can all the adsorption systems be described by this isotherm? There is a difficulty. The isotherms, similarly to the equations of state in the gas phase, have restrictions that make them suitable for use only under certain conditions.<sup>57</sup> For

<sup>57</sup>A typical example in the gas phase is the ideal gas equation of state,  $PV = nRT$ , which can represent the system *only* when the gaseous molecules do not interact with each other, i.e., at low pressures or high temperatures.

example, in the virial isotherm, the second virial coefficient is related to interactions between two contiguous molecules (short-range interactions). However, when ions are the considered species, long-range forces (Coulombic forces, see Section 6.8.2.3) are the predominant ones and the virial coefficient is not applicable anymore. The virial isotherm cannot be used to describe the adsorption of ions from solution.

Some of the most useful adsorption isotherms will be presented in the following sections, together with a complete isotherm for ionic adsorption. However, before that, it would be useful to stress some points about standard states in isotherms.

### 6.8.7. A Word about Standard States in Adsorption Isotherms

Standard states of species adsorbed on the surface and in solution have been given a lot of thought by scientists in the area (Conway, 1974; Nikitas, 1984; Bockris, 1986; Trasatti, 1987). The importance of finding convenient standard states is that in doing so we are able to compare the adsorption energies of different adsorption processes calculated by different isotherms.

Standard states are well defined for pure substances. We know that for a pure solid or liquid, the standard state is defined as the state with pressure  $P = 1 \text{ atm}$  ( $10^5 \text{ Pa}$ ) and temperature  $T$ , where  $T$  is some temperature of interest determined in such a way that for each value of  $T$  there is a single standard state.<sup>58</sup>

In the case of adsorbed species, a unique standard state—one that makes the bottom part of the logarithm equal to zero—is not defined because it will depend on the type of isotherm chosen to describe the process, i.e., it will depend on the function  $f(\theta)$  in Eq. (6.184) characteristic of each isotherm. Thus, it would be impossible to compare the adsorption energies (i.e.,  $\Delta G^\circ$ 's) of different adsorbates if they were represented by different adsorption isotherms. However, instead of a unique standard state, it is possible to define convenient standard states common to any isotherm. The way to choose this convenient standard state is explained in the following analysis of the Langmuir isotherm.

The Langmuir isotherm is obtained by considering the reaction given in Eq. (6.179) (see also Section 6.8.8),

---

<sup>58</sup>Consider, for example, a pure gas, under conditions in which it behaves as an ideal gas. The chemical potential is given by  $d\mu = dG_m = -S_m dT + V_m dP$ , where the subscript  $m$  indicates molar quantities. Thus, at constant temperature,  $d\mu = V_m dP = (RT/P)dP$ . Integration of this equation from  $P^0$  to  $P$  gives

$$\mu_{T,P} = \mu_{T,P^0} + RT \ln \frac{P}{P^0} \quad (6.185)$$

Here  $P^0$  represents a "convenient" pressure (reference pressure) and defines a "convenient-standard state." If this pressure is  $1 \text{ atm}$  ( $10^5 \text{ Pa}$ ), then the convenient-standard state corresponds to the conventional standard state, and

$$\mu_{T,P} = \mu^0 + RT \ln P \quad (6.186)$$

where  $\mu^0$  is given by  $\mu_{T,P=1 \text{ atm}}$ . The utility of using this standard state is that the bottom part of the logarithm in the equation becomes zero.



and the chemical potential is found from statistical-mechanical considerations

$$\mu_{A_{\text{ads}}} = -kT \ln f_A - kT \ln \frac{1 - \theta}{\theta} \quad (6.188)$$

where  $f_A$  is the partition function of the adsorbed species and  $(1 - \theta)$  the number of free sites on the metal. Keeping the temperature constant and differentiating with respect to  $\theta$  ( $f_A$  does not depend on  $\theta$ ):

$$\frac{d\mu_{A_{\text{ads}}}}{d\theta} = -kT \frac{\partial}{\partial \theta} \left( \ln \frac{1 - \theta}{\theta} \right) \quad (6.189)$$

Integrating this equation gives

$$\int_{\mu_{A_{\text{ads}}}^0}^{\mu_{A_{\text{ads}}}} d\mu_{A_{\text{ads}}} = -kT \int_{\theta_0}^{\theta} \frac{\partial}{\partial \theta} \left( \ln \frac{1 - \theta}{\theta} \right) d\theta \quad (6.190)$$

or

$$\mu_{A_{\text{ads}}} = \mu_{A_{\text{ads}}}^0 - kT \left( \ln \frac{1 - \theta}{\theta} - \ln \frac{1 - \theta_0}{\theta_0} \right) \quad (6.191)$$

where  $\mu_{A_{\text{ads}}}^0$  depends on the temperature and  $\theta_0$ . Subtracting Eq. (6.191) from Eq. (6.188),

$$\mu_{A_{\text{ads}}}^0 = -kT \ln f_A - kT \ln \frac{1 - \theta_0}{\theta_0} \quad (6.192)$$

The value of  $\theta_0$  can be chosen arbitrarily. In this case, the most convenient value is  $\theta_0 = 0.5$  because it makes the logarithmic term disappear and under such conditions,  $\mu_{A_{\text{ads}}}^0 = -kT \ln f_A$ .

### 6.8.8. The Langmuir Isotherm: A Fundamental Isotherm

Consider again the reaction given in Eq. (6.179). The rates of reaction of the forward and backward reactions are given by

$$\vec{r} = k_1(1 - \theta)a_A^- \quad (6.193)$$



$$\bar{r} = k_2 \theta \quad (6.194)$$

where  $(1 - \theta)$  represents the number of free sites on the metal and  $\theta$  is the coverage of the metal by the adsorbent. At equilibrium both these equations are equal, thus,

$$k_1(1 - \theta)a_A = k_2 \theta \quad (6.195)$$

or

$$\frac{\theta}{1 - \theta} = \beta a \quad (6.196)$$

where  $\beta = k_1/k_2$ . This is the Langmuir isotherm (Fig. 6.98). This is one of the first isotherms, derived back in 1918.

### 6.8.9. The Frumkin Isotherm: A Lateral Interaction Isotherm

The Frumkin isotherm is one of the earliest isotherms (1925) that deals with lateral interactions among adsorbed species (Fig 6.98). The isotherm can be written as<sup>59</sup>

$$\frac{\theta}{1 - \theta} e^{-2A\theta} = \beta c \quad (6.197)$$

The interactions among adsorbed molecules are considered in the term  $A$ ,

$$A = - \frac{N_a \phi}{2kT} \quad (6.198)$$

where  $\phi$  is the interaction energy of one molecular pair and,  $N_a \phi$  is the interaction energy of one molecule with its  $N_a$  nearest neighbors on the completely covered surface. A positive value of  $A$  means attraction between the adsorbed particles, and a negative value, repulsion between the molecules. When the parameter  $A$  is equal to zero (no interactions), the Frumkin isotherm reduces to the Langmuir isotherm.

### 6.8.10. The Temkin Isotherm: A Heterogeneous Surface Isotherm

Temkin (1941) approached the development of an adsorption isotherm by considering a heterogeneous surface (Section 6.8.3) where no molecular interactions exist. He divided the surface into different patches, and since there are no interactions between molecules, in each patch the Langmuir isotherm can be applied [see Eq. (6.196)] (Fig. 6.98). Thus, for the  $i$ th patch,

<sup>59</sup>The activity,  $a$ , and the concentration,  $c$ , of the ion in solution will be used here indistinguishably. This assumption is valid at low concentrations, where  $a \approx c$  (see Section 3.5).

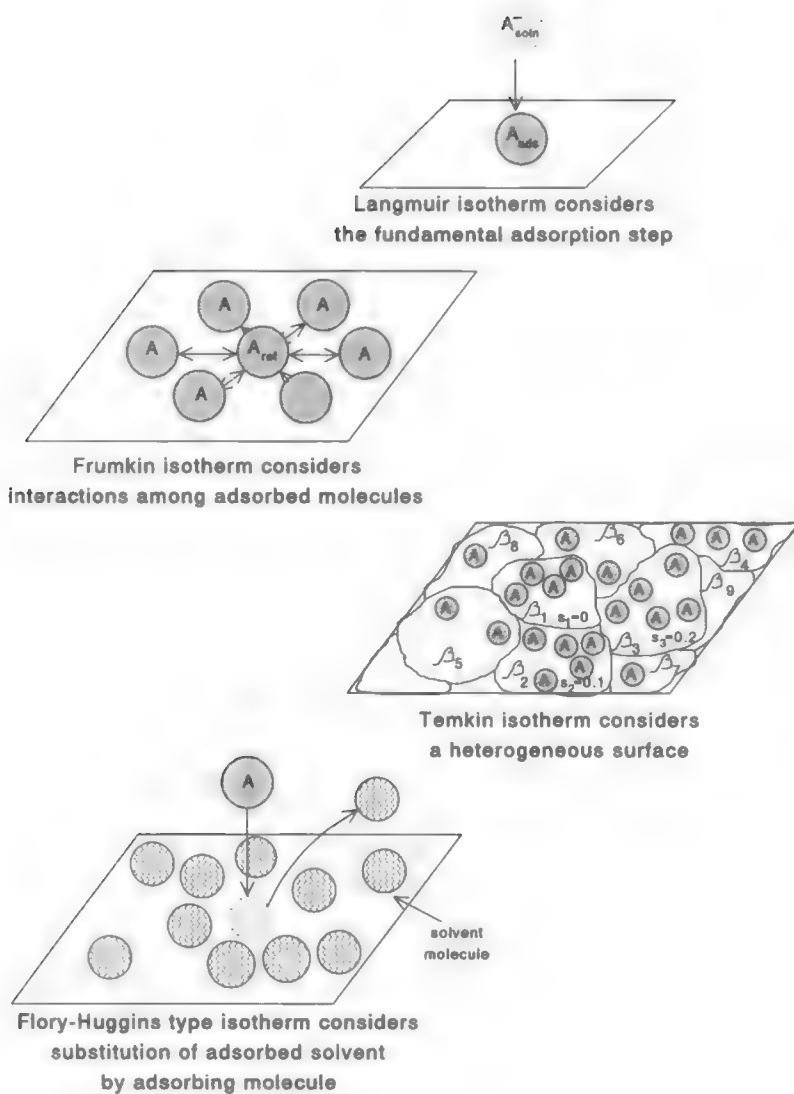


**Fig. 6.98.** Fundamental ideas of some adsorption isotherms.

$$\theta_i = \frac{\beta_i c}{1 + \beta_i c} \quad (6.199)$$

Each patch is characterized by a different energy of adsorption, i.e., different heat (enthalpy) of adsorption  $Q_i$ . Thus,  $\beta_i$  will be also different for each patch because

$$\beta_i = W \exp(Q_i/kT) \quad (6.200)$$

Here  $W$  is a parameter related to the distribution of the molecules in solution and the adsorbed ones.

One more characteristic of these patches is that they are arranged in a random way on the surface of the electrode. We can number the patches according to their value of  $Q_i$ , and label them with a parameter  $s$  that will vary from 0 to 1, i.e.,  $0 < s < 1$ . Thus, the heat of adsorption for each patch can be written as

$$Q_i = Q_0 - Ks_i \quad (6.201)$$

where  $K$  is a constant and  $Q_0$  is the heat of adsorption when  $s = 0$ . Dividing Eq. (6.201) by  $kT$ ,

$$\frac{Q_i}{kT} = \frac{Q_0}{kT} - \frac{K}{kT}s_i = \frac{Q_0}{kT} - fs_i \quad (6.202)$$

where  $f = K/kT$ . Substituting Eq. (6.202) into Eq. (6.200),

$$\beta_i = W e^{(Q_0/kT - fs_i)} = \beta_0 e^{-fs_i} \quad (6.203)$$

where  $\beta_0 = W e^{Q_0/kT}$ . Substituting Eq. (6.203) into Eq. (6.199),

$$\theta_i = \frac{\beta_0 c e^{-fs_i}}{1 + \beta_0 c e^{-fs_i}} \quad (6.204)$$

However, this equation gives the coverage of only one patch, the one characterized by the parameter  $s_i$ . To obtain the coverage of the whole surface,  $\theta$ , we need to integrate over the whole range of the parameter  $s_i$ , i.e., from  $s = 0$  to  $s = 1$ :

$$\int_0^1 \theta_i = \int_0^1 \frac{\beta_0 c e^{-fs_i}}{1 + \beta_0 c e^{-fs_i}} ds_i \quad (6.205)$$

or

$$\theta = -\frac{1}{f} \ln \frac{1 + \beta_0 c e^{-f}}{1 + \beta_0 c} = -\frac{1}{f} \ln \frac{1 + \beta_1 c}{1 + \beta_0 c} \quad (6.206)$$

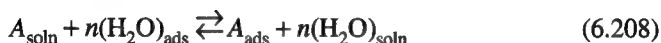
This is the complete Temkin isotherm. In the second part of this equation, the term  $\beta_1$  represents the value of  $\beta$  when  $s = 1$ , and  $\beta_0$ , the value of  $\beta$  when  $s = 0$ . If the appropriate conditions exist such that  $\beta_1 c \ll 1 \ll \beta_0 c$ , i.e., all the patches with large  $\beta$  are full and the others are empty independently of the concentration, then,

$$\theta = \frac{1}{f} \ln \beta_0 c \quad (6.207)$$

which is the best-known form of the Temkin isotherm. It is usual to call this isotherm the *logarithmic* isotherm.

### 6.8.11. The Flory–Huggins-Type Isotherm: A Substitutional Isotherm

In the Flory–Huggins<sup>60</sup> isotherm, the process of adsorption is considered a substitutional process (Fig 6.98). The molecule in solution that is going to be adsorbed makes room on the surface of the electrode by displacing some of the water molecules that cover it. This isotherm also takes into account the size of the molecules. The process can be represented by



which gives the isotherm

$$\frac{\theta}{(1 - \theta)^n} e^{(1-n)} = \beta c \quad (6.209)$$

The main characteristic of this isotherm is the appearance of the term  $\theta/(1 - \theta)^n$ .

### 6.8.12. Applicability of the Isotherms

Now that we have presented all these different types of isotherms, does it mean that any of them can be used to describe the ionic process of adsorption? Before answering this question, we should talk a little bit about the conditions involved in the development of these isotherms.

For example, although it is easy to deduce, the Langmuir isotherm (Section 6.8.8) has several drawbacks: Originally it was derived for the adsorption of molecules from

<sup>60</sup>The original treatment of this type of displacement isotherm was developed by Flory and Huggins separately, back in 1942. They developed the isotherm for adsorption of large molecules (polymers). However, applicability to small molecules (e.g., ions) displacing only few water molecules has been proved.

the gas phase and consequently it does not explicitly consider the different types of interactions involved in the adsorption process in solution (Section 6.8.2). This results in a heat of adsorption independent of coverage (Section 6.8.3) and therefore of the electrode charge. This is a severe limitation since in order to apply it to electrochemical systems not only should lateral interaction vanish, but the surface should also be completely homogeneous (no dislocations, steps, etc.) and all the sites should have the same energy (Section 6.8.3). However, because it addresses the fundamental adsorption step [Eq. (6.179)], the Langmuir isotherm is used as starting point in the derivation of many other complex isotherms.

Although the Frumkin isotherm (Section 6.8.9) considers lateral interactions, it has two main restrictions when it is applied to ionic systems: It considers lateral interactions only from the first circle of neighbors, and the strength of these lateral interactions should be weak (like dispersion forces). In ionic systems, the main type of forces involved are of long-range character (Coulombic forces, see Section 6.3.5). Also, when corresponding calculations are done by taking into account interactions with the ions beyond the first-layer neighbors, the result is an infinite energy of repulsion, leading to the absurd idea that adsorption of the same type of ions (anions or cations) could not occur. This dilemma of infinite repulsion makes the Frumkin isotherm unacceptable for describing adsorption of ionic species.

In Section 6.8.10 we saw that the Temkin isotherm is based on the Langmuir isotherm. One advantage of the Temkin isotherm is that it considers the heterogeneity of the surface. However, like the Langmuir isotherm, it does not take into account lateral interactions between the adsorbates.

Finally, the Flory–Huggins isotherm has the advantage of considering the size of the molecules as well as the replacement of adsorbed solvent molecules by the adsorbing molecule. However, its applicability to ionic systems depends on the parameters included in the term  $\beta$ —lateral interactions, surface heterogeneity, etc.

Table 6.10 gives a list of several isotherms, including the ones already discussed, and some of their main characteristics. The isotherms we have presented here are focused on particular aspects of the adsorption phenomenon. For example, the Langmuir isotherm focuses on the basic process of transferring a molecule from the bulk to the electrode; the Temkin isotherm focuses on interpreting the adsorption process in terms of the heterogeneity of the adsorbing surface; etc.

However, when adsorption of ionic species takes place on solid electrodes, it is difficult to decide what particular characteristic—surface heterogeneity, transfer of charge, lateral interactions, displacement of adsorbed solvent, size of the ions, etc.—is dominant in the process or which one can be neglected. Nonetheless, would it not be possible to include all these effects in a single isotherm? It is possible, although not easy. In the following sections we will introduce the development of one isotherm for ionic adsorption where many of these distinctive characteristics of ionic adsorption are considered.

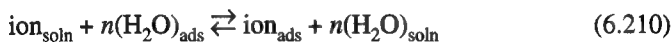
**TABLE 6.10**  
**Some Isotherms Used in Describing the Adsorption of Ions**

Langmuir	$\beta a = \frac{\theta}{1 - \theta}$	Considers the fundamental step of the adsorption reaction: $A_{\text{soln}} + M \rightleftharpoons M - A_{\text{ads}}$
Frumkin	$\beta a = \frac{\theta}{1 - \theta} e^{-2a\theta}$	Isotherms characterized to consider lateral interactions
Virial	$\beta a = \Gamma e^{2B_{2,T}\Gamma}$	
Temkin	$\beta a = e^{f\theta}$	Considers the heterogeneity (sites with different energies) of the surface
Conway and Angerstein-Kozłowska	$\beta a = \frac{\theta}{1 - \theta} \exp(K\theta^{3/2} - \gamma PV/RT)$	Considers the partial transfer of charge between the adsorbed molecule and the substrate
Parsons	$\beta a = f(\Gamma) \exp\left\{e_0 \Delta \phi \frac{K}{K_q} [g_z - \lambda(1-g)]\right\}$ $\times \exp\left\{e_o \frac{q'}{K'_q} [zh - \lambda(1-h)]\right\}$	
Habib and Bockris	$\beta a = \frac{\theta}{e^{p-1}(1-\theta)^p}$ $\times \exp\left\{a_3 \theta^{1/2} \sum_{n=1}^{\infty} \left[1 - \left(1 + \frac{h'\theta}{n^2}\right)^{-1/2}\right]\right\}$ $\times \exp\left\{a_4 \theta^3 \sum_{n=1}^{\infty} \frac{1}{n^5} \left[1 + \left(1 + \frac{h'\theta}{n^2}\right)^3\right]\right\}$	This isotherm is of the Flory-Huggins type (considers displacement of solvent molecules). It also considers lateral interactions between the adsorbed species.

Source: Reprinted from M. Gamboa-Aldeco, dissertation, Texas A&M University, 1992.

### 6.8.13. An Ionic Isotherm for Heterogeneous Surfaces

We can start developing the isotherm by considering a heterogeneous surface with regions of different energies of adsorption (Temkin formalism, Section 6.8.10). Then it can be considered that in order for the ion to adsorb, it has to displace  $n$  solvent molecules (water molecules) (Flory–Huggins formalism, Section 6.8.11). If in each of these regions (patches), equilibrium exists between the adsorbed ions and those in solution, the adsorption process in one of these regions can be represented by the following equation:



According to the Flory–Huggins formalism (Section 6.8.11), the isotherm corresponding to this equilibrium is given by

$$\frac{\theta_j}{(1 - \theta_j)^n} = e^{n-1} \beta \frac{c}{c_w} \quad (6.211)$$

where  $\theta_j$  represents the partial surface coverage on sites with adsorption energy  $U_j$ , and  $c$  and  $c_w$  represent the bulk concentrations of ion and water in solution.

What parameters should be included in the  $\beta$  term? It should include not only the energy of adsorption of the metal,  $U_j$ , but also all the interactions we discussed in Section 6.8.2, i.e., ion electrode, solvent, and lateral interactions.

Let us divide the parameters into three terms: (1) one representing chemical interactions of the ion and the water molecules that is independent of the charge or potential of the electrode,  $\Delta G_{\text{ch}}^\circ$ ; (2) a charge or electrode potential-dependent term for the ion and the solvent molecules,  $\Delta G_E$ ; and (3) a lateral interaction term,  $\Delta G_L$ .

Then  $\beta$  in Eq. (6.211) can be written as

$$\beta = \exp[-(\Delta G_{\text{ch}}^\circ + \Delta G_E + \Delta G_L)/kT] \quad (6.212)$$

and substituting  $\beta$  in Eq. (6.211),

$$\frac{\theta_j}{(1 - \theta_j)^n} = e^{n-1} \frac{c}{c_w} e^{-(\Delta G_{\text{ch}}^\circ + \Delta G_E + \Delta G_L)/kT} \quad (6.213)$$

Each of these energy terms is discussed below.

1. The  $\Delta G_{\text{ch}}^\circ$  represents a coverage and potential-independent term for the different interactions of the water molecule and the ion during the adsorption process and it can be split into  $\Delta G_{\text{ch}}^\circ = \Delta G_{\text{ch},i}^\circ + \Delta G_{\text{ch},w}^\circ$ . These interactions include dispersion and electronic forces (Section 6.8.2.1) of the ion and water molecules, as well as partial dehydration of the ion and the metal (Section 6.8.2.2).

In order to introduce the heterogeneity of the surface, these ion and water interaction energies can be divided into two groups. One of them corresponds to the energy involved when the ion gets rid of its hydration sheet, the breaking of the bond between the  $n$  water molecules and the metal that the ion needs to displace to get adsorbed, and finally, the part of the ion-metal interaction (bond) that arises from the ion's orbitals, i.e.,  $\Delta G_{\text{ch},i}^{\circ,1}$  and  $\Delta G_{\text{ch},w}^{\circ,1}$  (see Fig. 6.90).

The second part includes the metal side of the ion-metal and water-metal bonds at the  $j$ th site. This term depends on the heterogeneity of the surface and is given by  $U_{j,i}$  and  $U_{j,w}$ . Therefore the chemical term  $\Delta G_{\text{ch}}^{\circ}$  is written as

$$\Delta G_{\text{ch}}^{\circ} = (\Delta G_{\text{ch},i}^{\circ,1} + U_{j,i}) + (\Delta G_{\text{ch},w}^{\circ,1} + U_{j,w}) \quad (6.214)$$

If  $U_{j,i}$  can be considered to be much greater than  $U_{j,w}$ , then the previous equation can be written as<sup>61</sup>

$$\Delta G_{\text{ch}}^{\circ} = (\Delta G_{\text{ch},i}^{\circ,1} + U_{j,i}) + \Delta G_{\text{ch},w}^{\circ,1} \quad (6.215)$$

2. The term  $\Delta G_E$  represents the electrical work done in moving an ion of charge  $ze_0$  and water molecules with dipole moments  $\vec{\mu}$  between the outer Helmholtz layer and the inner Helmholtz layer in the electric field,  $\vec{X}$ , arising from the charge of the metal (Section 6.8.2.1). Thus, it can split into  $\Delta G_E = \Delta G_{E,i} + \Delta G_{E,w}$ . If some transfer of charge (Section 6.8.2.1) occurs during the adsorption process, Eq. (6.210) can be written as

$$A_{\text{soln}}^z + n(\text{H}_2\text{O})_{\text{ads}} + (z - z')e^- \rightleftharpoons A_{\text{ads}}^{z'} + n(\text{H}_2\text{O})_{\text{soln}} \quad (6.216)$$

where  $ze_0$  is the charge of the ion in solution and  $z'e_0$  is the charge of the adsorbed ion.<sup>62</sup>

The electrical interaction with the field is a matter of the work of taking a charged ion through a distance  $x_2 - x_1$ , i.e., from the OHP to the IHP. The electrical field,  $\vec{X}$ , in a parallel-plate condenser is  $q_M/\epsilon\epsilon_0$ . From Eq. (6.20), the difference in energy in bringing a test charge  $z'e_0$  from  $x_2$  to  $x_1$  in this electrical field is

$$\Delta G_{E,i} = - \int_{x_2}^{x_1} z'e_0 \vec{X} dx = \frac{z'e_0 q_M (x_2 - x_1)}{\epsilon\epsilon_0} \quad (6.217)$$

where  $q_M$  is the charge on the metal per unit area,  $\epsilon$  is the dielectric constant of the interface (Section 6.7.3),  $\epsilon_0$  is the permittivity of free space, and  $x_2$  and  $x_1$  are the

<sup>61</sup>For example, consider the adsorption of  $\text{HSO}_4^-$ . If it adsorbs through three of its oxygens (see Fig. 6.95), it has three oxygens bonded to the surface. On the other hand, water molecules would be bonded through one oxygen when  $E > pzc$ . Thus, in a zeroth approximation we can assume that the bonding energy per oxygen in the bisulfate ion is the same as in the water molecule. Thus,  $U_{j,i} \approx 3U_{j,w}$ .

<sup>62</sup>A better approximation would be to consider in Eq. (6.217), not the charge of the adsorbed ion,  $e_0 z'$ , but an average of the charge the ion has between the OHP and the IHP, e.g.  $(z'e_0 + ze_0)/2$ .



distances from the outer and inner Helmholtz planes to the electrode, respectively (Fig. 6.90).

The term  $\Delta G_{E,w}$  has two possibilities, depending on the sign of the electrode potential.<sup>63</sup> At  $E > E_{pzc}$ , the net dipole moment of the water molecule,  $\vec{\mu}$ , is directed toward the solution ( $\uparrow$ ), and at  $E < E_{pzc}$  toward the electrode ( $\downarrow$ ) (Section 6.7.3). Then,

$$\Delta G_{E,w} = \Delta G_{E,\uparrow} = \frac{\vec{\mu} \cdot \vec{X}}{\epsilon \epsilon_0} = \frac{\vec{\mu} q_M}{\epsilon \epsilon_0} \quad \text{when } E > E_{pzc} \quad (6.218)$$

$$\Delta G_{E,w} = \Delta G_{E,\downarrow} = -\frac{\vec{\mu} \cdot \vec{X}}{\epsilon \epsilon_0} = -\frac{\vec{\mu} q_M}{\epsilon \epsilon_0} \quad \text{when } E < E_{pzc} \quad (6.219)$$

Therefore the total  $\Delta G_E$  is

$$\Delta G_E = -\frac{z'e_0(x_2 - x_1)}{\epsilon \epsilon_0} q_M + \frac{\vec{\mu}}{\epsilon \epsilon_0} q_M \quad \text{when } E > E_{pzc} \quad (6.220)$$

$$\Delta G_E = -\frac{z'e_0(x_2 - x_1)}{\epsilon \epsilon_0} q_M - \frac{\vec{\mu}}{\epsilon \epsilon_0} q_M \quad \text{when } E < E_{pzc} \quad (6.221)$$

3. The term  $\Delta G_L$  represents the different interactions among the adsorbed species (Section 6.8.2.3). These interactions can be Coulombic interactions ( $\Delta G_{Coul}$ ), which are of the long-range type, or dispersive interactions ( $\Delta G_{disp}$ ) that act only at short distances. As discussed in Section 6.8.2.3, these interactions include not only forces between neighboring ions, but also between the reference ion and the neighbor's image charges.<sup>64</sup> The total lateral interaction term,  $\Delta G_L$ , can be written as

$$\Delta G_L = \Delta G_{Coul} + \Delta G_{disp} \quad (6.222)$$

Let us find now an expression for the long-range interaction energy,  $\Delta G_{Coul}$ .

Consider a reference ion surrounded by similar ions arranged in a hexagonal fashion around the reference ion (Fig. 6.99), with each ion of radius  $r$  occupying an area of hexagonal shape (unit cell). The area of one of these unit cells is  $\sqrt{3}R^2/2 \text{ cm}^2 \text{ cell}^{-1}$ , which means that there are  $2/\sqrt{3}R^2$  cells per unit area. Since there is one ion per cell, the number of contact-adsorbed ions per unit area is  $n_{CA} = 2/\sqrt{3}R^2$ . Hence,

<sup>63</sup>In the region close to the pzc, these equations would not hold because in this region a mixture of up and down dipoles exists (Section 6.7.5). In such region,  $\Delta G_{E,w}$  would more likely involve  $(\theta_{\uparrow}\mu_{\uparrow} + \theta_{\downarrow}\mu_{\downarrow})$  instead of  $\vec{\mu}$  shown in these equations.

<sup>64</sup>The lateral interactions between the adsorbed ion and the water molecules are considered inside the  $\Delta G_{ch}^o$  term.

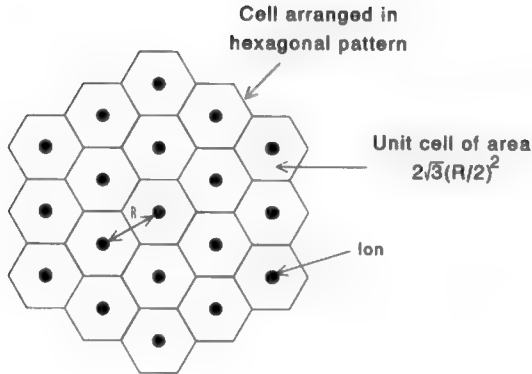


**Fig. 6.99.** The contact-adsorbed ions in a hexagonal array at the IHP. Ions are considered spatially distributed in cells, with the centers of the cells corresponding to the time-average positions of the ions. (Reprinted from J. O'M. Bockris, M. Gamboa-Aldeco, and M. Szklarczyk, *J. Electroanal. Chem.* **339**: 355, copyright 1992, Fig. 51, with permission from Elsevier Science.)

$$R = \left( \frac{2}{\sqrt{3}n_{CA}} \right)^{1/2} \times \left( \frac{\sqrt{3}}{\sqrt{3}} \right)^{1/2} = \left( \frac{2\sqrt{3}}{3n_{CA}} \right)^{1/2} \quad (6.223)$$

The surrounding ions of the hexagonal array are effectively in circular rings about the reference ion (Fig. 6.100). The ring radii increase as  $1R, 2R, 3R, \dots, mR$ . Thus, if the charge of one adsorbed ion is  $z'e_0$ , then the charge in the first ring is  $6z'e_0$ ; in the second ring,  $12z'e_0$ , ...; and in the  $m$ th ring,

$$\sigma_{\text{ring}} = 6mz'e_0 \quad (6.224)$$

With this information, the long-range interaction energy between the reference ion and the ions in the  $m$ th ring can be calculated. This is given as [(charge on the  $m$ th ring  $\times$  charge of the reference ion)/(dielectric constant  $\times$  distance of the  $m$ th ring to the reference ion)], or

$$\frac{\sigma_{\text{ring}} z' e_0}{4\pi\epsilon_0 \epsilon m R} \quad (6.225)$$

The next step is to calculate the long-range interaction energy between the reference ion and the image charges due to the  $m$ th ring. Every charged ring on the

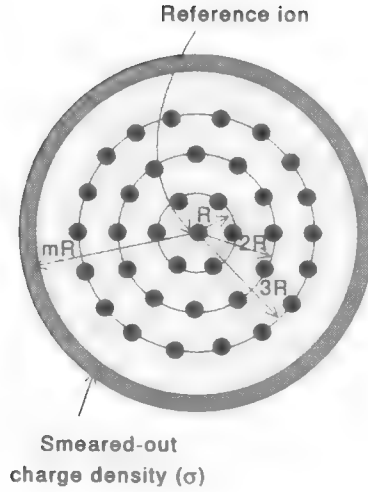


**Fig. 6.100.** The contact-adsorbed ions are effectively in circular rings, with  $6m$  ions in the  $m$ th ring of radius  $mR$ .

IHP has associated with it a ring of image charge located at a distance  $[(nR)^2 + (2r)^2]^{1/2}$  (Fig. 6.101) from the reference ion. Following a reasoning similar to that for Eq. (6.225), the attractive interaction between the reference ion and the  $m$ th ring of the image charge is

$$-\frac{\sigma_{\text{ring}}' e_0}{4\pi\epsilon_0\epsilon} \frac{1}{[(mR)^2 + (2r)^2]^{1/2}} \quad (6.226)$$

and the interaction energy between the reference ion and the  $m$ th ring plus the interaction energy of the ion with the image charge due to the  $m$ th ring is

$$\frac{\sigma_{\text{ring}}' e_0}{4\pi\epsilon_0\epsilon mR} \left[ 1 - \frac{1}{[1 + (2r/mR)^2]^{1/2}} \right] \quad (6.227)$$

Now the total lateral-interaction energy,  $\Delta G_L$ , needs to be determined. This is obtained by summing over all the rings as follows:

$$\Delta G_{\text{Coul}} = \sum_{m=1}^{\infty} \frac{\sigma_{\text{ring}}' e_0}{4\pi\epsilon_0\epsilon mR} \left[ 1 - \frac{1}{[1 + (2r/mR)^2]^{1/2}} \right] \quad (6.228)$$

In this equation, the number of contact-adsorbed ions is given by

$$n_{\text{CA}} = \Gamma = \theta \Gamma_{\text{max}} \quad (6.229)$$

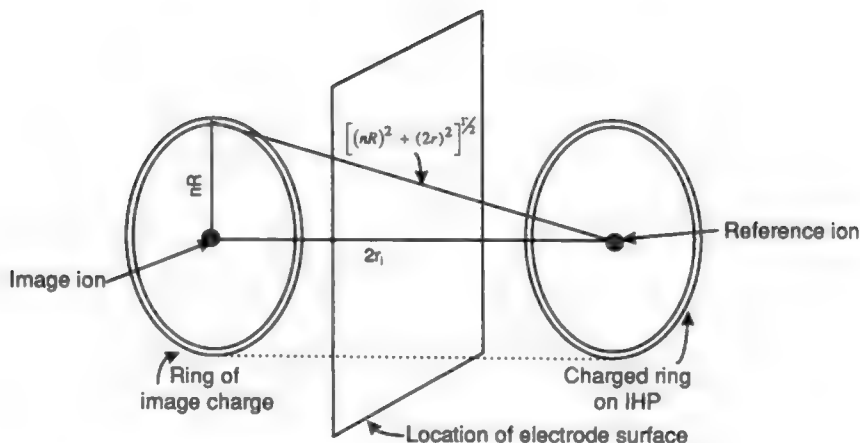


**Fig. 6.101.** Every charged ring on the IHP produces a ring of image charge as far behind the metal surface as the IHP is in front of it.

where  $\Gamma$  is the surface concentration of adsorbed ions, and  $\Gamma_{\max}$  is the maximum surface concentration that can be achieved (see Section 6.4.3).

Substituting Eqs. (6.223), (6.224), and (6.229) into Eq. (6.228) and dividing both sides by  $kT$ ,

$$\frac{\Delta G_{\text{Coul}}}{kT} = A \frac{z'^2 \Gamma_{\max}^{1/2} \theta^{1/2}}{\epsilon T} \sum_{m=1}^{\infty} \left[ 1 - \frac{1}{[1 + Br^2 \Gamma_{\max} \theta_m / m^2]^{1/2}} \right] \quad (6.230)$$

where  $A = 6(3/4)^{1/4} e_0^2 / (k4\pi\epsilon_0)$  and  $B = 2\sqrt{3}$ .

The short-range interaction energy term,  $\Delta G_{\text{disp}}$ , can be calculated similarly to the long-range term, but taking into consideration only those forces like the dispersive one (Habib-Bockris, 1976). Thus, the energy of dispersion between a reference ion and its neighboring ions as well as their images (a hexagonal array is also considered) is

$$\Delta G_{\text{disp}} = \sum_{m=1}^{\infty} \frac{3}{4} \frac{h\nu\alpha^2\sqrt{s}(6m)}{\epsilon_{\text{op}}} \left\{ \frac{1}{[mr]^6} + \frac{1}{[(mr)^2 + (2r)^2]^{3/2}} \right\} \quad (6.231)$$

where  $\nu = e_0 / 2\pi\sqrt{\alpha M_e}$  is the frequency occurring in dispersive coupling between two like ions, with  $M_e$  being the reduced mass;  $\alpha$  is the polarizability of the ion;  $s$  is the number of electrons in the outer shell; and  $\epsilon_{\text{op}}$  is optical dielectric constant.

Substituting these terms in the previous equation, and dividing by  $kT$ ,

$$\frac{\Delta G_{\text{disp}}}{kT} = A' \frac{r^{9/2} \sqrt{s} \Gamma_{\text{max}}^3 \theta^3}{\epsilon_{\text{op}} T} \sum_{m=1}^{\infty} \frac{1}{m^5} \left\{ 1 + \frac{1}{[1 + B' r^2 \Gamma_{\text{max}} \theta / m^2]^3} \right\} \quad (6.232)$$

where  $A' = (27\sqrt{3}/16)(h\nu/k)$  and  $B' = 2\sqrt{3}$ . Figure 6.102 shows the variation of  $\Delta G_{\text{Coul}}$  and  $\Delta G_{\text{disp}}$  as a function of  $q$  for the adsorption of some anions.

So far, we have determined the different terms of the free energy of adsorption, that is,  $\Delta G_{\text{ch}}^{\circ}$  [Eq. (6.215)],  $\Delta G_E$  [Eqs. (6.220) and (6.221)], and  $\Delta G_L$  [Eqs. (6.222), (6.230) and (6.232)], in Eq. (6.213). Table 6.11 shows some of the main structural parameters obtained in the calculation of the above free energies.

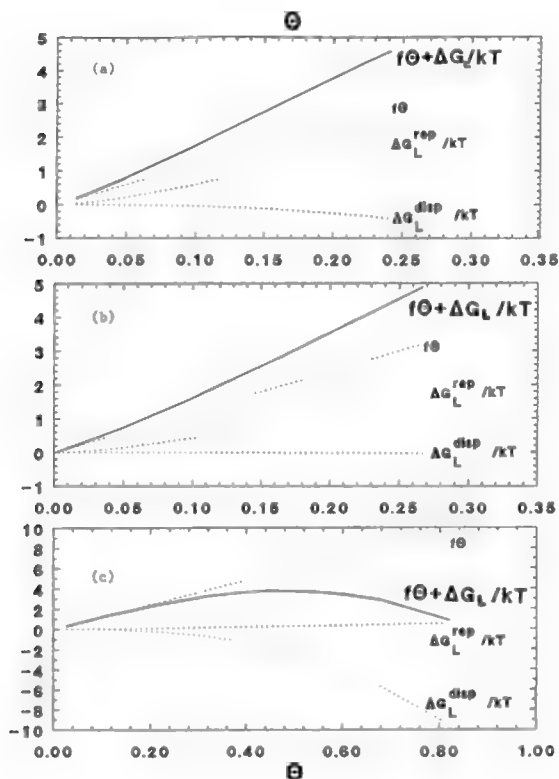


**Fig. 6.102.** Variation of the free energy of dispersion interactions ( $\Delta G_{\text{disp}}$ ) (represented as  $\Delta G_L^{\text{disp}}$  in the figure) and the free energy of Coulombic interactions ( $\Delta G_{\text{Coul}}$ ) (represented as  $\Delta G_L^{\text{rep}}$  in the figure) for the adsorption of bi-sulfate ions (a), chloride ions (b), and iodide ions (c), on platinum. (Reprinted from M. Gamboa-Aldeco, Ph.D. dissertation, 1992, Texas A&M University.)

**TABLE 6.11**  
**Some Parameters Needed to Calculate  $\Delta G_{\text{ch}}^\circ$  [Eq. (6.215)],  $\Delta G_E$  [Eqs. (6.220) and (6.221)], and  $\Delta G_L$  [Eqs. (6.222), (6.230), and (6.232)] for the Adsorption Isotherm in Eq. (6.246) of Bisulfate, Chloride, and Iodide Anions on Platinum Electrodes**

Parameter	Bisulfate	Chloride	Iodide
$T(\text{K})$	298	298	298
$z'$	0.8	0.4	0.1
$r_M (\text{\AA})$	2.04	1.33	1.48
$r_m (\text{\AA})$	1.82	1.29	1.30
$x_2 - x_1 (\text{\AA})$	2.80	3.28	3.69
$\ln c_w = \ln 55.5$	4.02	4.02	4.02
$F$	12	12	12
$\epsilon$	16	20	22
$S$	17	8	8
$\alpha (\text{\AA}^3)$	1.09	1.42	1.80
$\epsilon_{\text{op}}$	2	2	2
$\Gamma_{\text{max}} (\text{mol cm}^{-2})$	$1.15 \times 10^{-9}$	$2.71 \times 10^{-9}$	$2.19 \times 10^{-9}$
$N$	1	1	1

Source: Reprinted from J. O'M. Bockris, M. Gamboa-Aldeco, and M. Szklarczyk, *J. Electroanal. Chem.* **339**: 355, copyright 1992, Table 3, with permission from Elsevier Science.

If only one water molecule is displaced during the adsorption process represented in Eq. (6.216) i.e.,  $n = 1$ , then after substituting Eq. (6.215), the partial isotherm in Eq. (6.213) becomes

$$\frac{\theta_j}{1 - \theta_j} = \frac{c}{c_w} \exp \left[ - \left( \frac{\Delta G_{\text{ch},i}^{\circ,1} + U_j}{kT} + \frac{\Delta G_{\text{ch},w}^{\circ,1}}{kT} + \frac{\Delta G_E}{kT} + \frac{\Delta G_L}{kT} \right) \right] \quad (6.233)$$

This partial isotherm was constructed by considering a heterogeneous surface built by patches of different energy  $U_j$ , and the equation is then applicable only in the  $j$ th patch. This partial isotherm can be rearranged by grouping on the left the terms that are related to the heterogeneity of the surface, i.e.,  $\theta_j$  and  $U_j$ ,

$$\frac{\theta_j}{1 - \theta_j} e^{U_j/kT} = \beta' c \quad (6.234)$$

where

$$\beta' = (1/c_w) \exp \left[ - (\Delta G_{\text{ch},i}^{\circ,1} + \Delta G_{\text{ch},w}^{\circ,1} + \Delta G_E + \Delta G_L)/kT \right] \quad (6.235)$$

Now, as said before,  $\theta_j$  represents the coverage of one of these patches. What would be the total coverage of the whole surface? To find it out, it is necessary to sum over all the different patches represented by the energy term  $U_j$ . Even more, if  $\theta_j$  is considered to be a continuous function of  $U_j$ , then the sum can be replaced by an integral covering the whole range of energies, i.e.,  $-\infty < U_j < 0$ ,

$$\theta = \int_{-\infty}^0 \theta_j \Psi_{U_j} dU_j \quad (6.236)$$

where  $\Psi_{U_j}$  represents the *site energy distribution function*.

From Eq. (6.234),

$$\theta = \frac{\beta' c e^{-U_j/kT}}{1 + \beta' c e^{-U_j/kT}} \quad (6.237)$$

and the total coverage calculated by substituting (6.237) into (6.236) is

$$\theta_j = \int_{-\infty}^0 \frac{\beta' c e^{-U_j/kT}}{1 + \beta' c e^{-U_j/kT}} \Psi_{U_j} dU_j \quad (6.238)$$

In order to solve this equation, it is necessary to have the distribution function,  $\Psi_{U_j}$ . What is this distribution function? It is a way to describe how the sites are distributed according to their energies, i.e., how many surface sites have energy  $U_1$ , how many  $U_2$ , etc. One of these functions is (Nikitas, 1988)

$$\Psi_{U_j} = \begin{cases} 0 & U < U_m - U_0 \text{ and } U > U_m + U_0 \\ \frac{1}{2U_0} & U_m - U_0 \leq U \leq U_m + U_0 \end{cases} \quad (6.239)$$

where  $U_m$  and  $U_0$  are energy parameters characteristic of the lattice. A plot of this function is shown in Fig. 6.103. Thus, substituting Eq. (6.239) into Eq. (6.238),

$$\theta = \int_{U_m - U_0}^{U_m + U_0} \frac{\beta' c e^{-U_j/kT}}{1 + \beta' c e^{-U_j/kT}} \frac{1}{2U_0} dU_j \quad (6.240)$$

and the corresponding equation after integrating Eq. (6.240) is

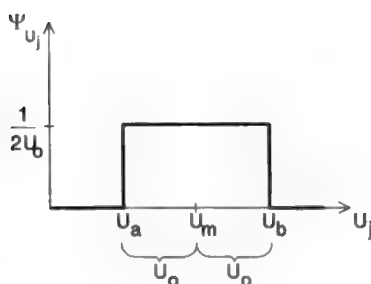


**Fig. 6.103.** Distribution of sites according to the "uniform distribution" model of Nikitas: Sites of very low or very high energies are not present or are not available for adsorption; sites with energies between  $U_a$  and  $U_b$  are distributed equally on the surface. (Reprinted from J. O'M. Bockris, M. Gamboa-Aldeco and M. Szklarczyk, *J. Electroanal. Chem.* **339**: 355, copyright 1992, Fig. 15, with permission from Elsevier Science.)

$$\theta = -\frac{kT}{2U_0} \ln \frac{1 + \beta' c e^{-(U_m + U_0)/kT}}{1 + \beta' c e^{-(U_m - U_0)/kT}} \quad (6.241)$$

This is the equation, the isotherm, we were seeking. It is a generalized isotherm for the adsorption of ionic species on a heterogeneous surface. It considers the adsorption reaction as a substitution process, with the possibility of transfer of charge between the ion and the electrode and also lateral interactions among adsorbed species.

If the following conditions apply,

$$\beta' c e^{-(U_m - U_0)/kT} \ll 1 \ll \beta' c e^{-(U_m + U_0)/kT} \quad (6.242)$$

then the isotherm, Eq. (6.241) reduces to

$$\theta = -\frac{kT}{2U_0} \left( \ln \beta' c - \frac{U_m + U_0}{kT} \right) \quad (6.243)$$

or after substituting  $\beta'$  from Eq. (6.235)



$$\theta = -\frac{kT}{2U_0} \left( -\frac{\Delta G_{\text{ch},i}^{\circ,1} + U_m}{kT} - \frac{\Delta G_{\text{ch},w}^{\circ,1}}{kT} - \frac{\Delta G_E}{kT} - \frac{\Delta G_L}{kT} - \frac{U_0}{kT} + \ln \frac{c}{c_w} \right) \quad (6.244)$$

The term  $U_m$  can be considered as the average energy of the surface. Then the term  $(\Delta G_{\text{ch},i}^{\circ,1} + U_m)$  involves the average bonding of the ion on the surface and  $\Delta G_{\text{ch},i}^{\circ} = \Delta G_{\text{ch},i}^{\circ,1} + U_m$ . If

$$f = -2U_0/kT \quad (6.245)$$

then,

$$\theta = \frac{1}{f} \left( -\frac{\Delta G_{\text{ch},i}^{\circ}}{kT} - \frac{\Delta G_{\text{ch},w}^{\circ}}{kT} - \frac{\Delta G_E}{kT} - \frac{\Delta G_L}{kT} + \frac{f}{2} + \ln \frac{c}{c_w} \right) \quad (6.246)$$

Table 6.12 shows the corresponding terms of the free energies of adsorption represented in Eq. (6.246) for different adsorbing ions.

What does Eq. (6.246) mean? This equation represents the adsorption process of ions on metallic surfaces. It includes several conditions that are characteristic of the adsorption process of ionic species, namely, surface heterogeneity, solvent displacement, charge transfer, lateral interactions, and ion size. However, is this equation capable of describing the adsorption process of ions? In other words, what is the success of the isotherm described in Eq. (6.246)? Figure 6.104 shows a comparison of data obtained experimentally for the adsorption of two ions—chloride and bisulfate—on polycrystalline platinum, with that obtained applying Eq. (6.246). The plots indicate that the theory is able to reproduce the experimental results quite satisfactorily. The isotherm may be considered a success in the theory of ionic adsorption.

**TABLE 6.12**  
**The Chemical Part of the Free Energy  $\Delta G_{\text{ch}}^{\circ}$ , the Potential-Dependent Part of the Free Energy,  $\Delta G_E$ , and the Lateral Interaction Part of the Free Energy,  $\Delta G_L$ , for the Adsorption Isotherm in Eq. (6.246)**

	Bisulfate	Chloride	Iodide
$(\Delta G_{\text{ch},i}^{\circ} + \Delta G_{\text{ch},w}^{\circ})/kT$	-5.21	-6.50	-13.40
$\Delta G_E/kT \ E > E_{\text{pzc}}$	(1.01-4.24E)	(0.73-3.11E)	(-0.42 + 1.60E)
$\Delta G_E/kT \ E < E_{\text{pzc}}$	(3.69-15.49E)	(5.98-25.48E)	(4.83 -18.44E)
$f\theta + \Delta G_L/kT \ E > E_{\text{pzc}}$	(0.66 + 4.24E)	(0.84 + 3.11E)	(4.29 - 1.60E)
$f\theta + \Delta G_L/kT \ E < E_{\text{pzc}}$	(-2.03 + 15.49E)	(-4.40 + 23.48E)	(-0.96 + 18.44E)

Source: Reprinted from J. O'M. Bockris, M. Gamboa-Aldeco, and M. Szklarczyk, *J. Electroanal. Chem.* 339: 355, copyright 1992, Table 7, with permission from Elsevier Science.

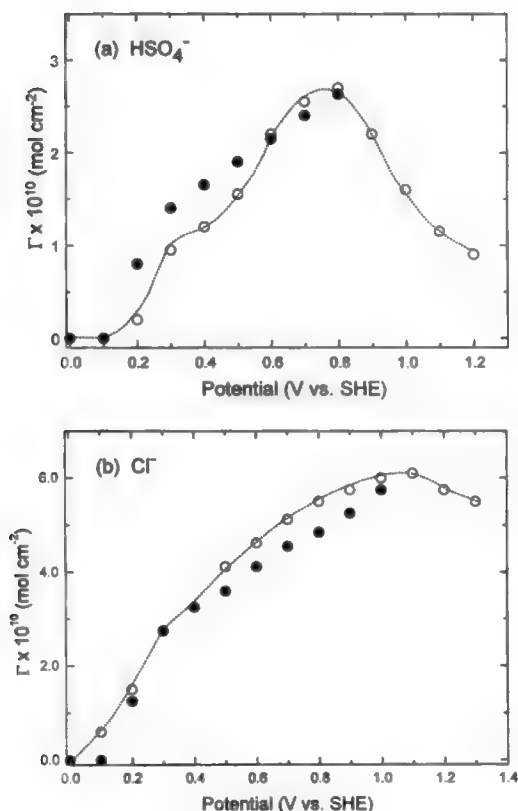


**Fig. 6.104.** Surface concentration vs. electrode potential for the adsorption of (a)  $\text{HSO}_4^-$ ,  $4 \times 10^{-3} M$ , and (b)  $\text{Cl}^-$ ,  $10^{-3} M$  ions on platinum electrodes. The calculated values are represented by the filled circles, while the open circles represent the experimental points. (Reprinted from J. O'M. Bockris, M. Gamboa-Aldeco, and M. Szklarczyk, *J. Electroanal. Chem.* **339**: 355, copyright 1992, Fig. 21, with permission from Elsevier Science.)

#### 6.8.14. Thermodynamic Analysis of the Adsorption Isotherm

In the previous section we developed an isotherm, Eq. (6.246), which was intended to represent the adsorption process of ions on metallic surfaces. It included conditions such as the heterogeneity of the surface, displacement of solvent molecules, transfer of charge, lateral interactions, and size of the ions; some of the main parameters involved in this isotherm were shown in Tables 6.11 and 6.12 for three adsorbing ions.

Also, in Section 6.8.3 we talked about the importance of thermodynamic parameters involved in the adsorption process. Thus, the next step is to connect these two sections and find the corresponding  $\Delta G^\circ$ ,  $\Delta H^\circ$  and  $\Delta S^\circ$  of the adsorption process using the developed isotherm. How can this be done?

Equation (6.246) can be written as

$$\theta = -\frac{1}{f} \left( \frac{\Delta G_{\text{ads}}^\circ}{kT} + \ln c_w \right) + \frac{1}{f} \ln c \quad (6.247)$$

where

$$\frac{\Delta G_{\text{ads}}^\circ}{kT} = -\frac{\Delta G_{\text{ch,i}}^\circ}{kT} - \frac{\Delta G_{\text{ch,w}}^\circ}{kT} - \frac{\Delta G_E}{kT} - \frac{\Delta G_L}{kT} + \frac{f}{2}$$

and represents the free energy of the total adsorption process given by Eq. (6.216). When  $\theta$  vs.  $\ln c$  is plotted, according to Eq. (6.247) the intercept of the corresponding curve is equal to

$$-\frac{1}{f} \left( \frac{\Delta G_{\text{ads}}^\circ}{kT} + \ln c_w \right)$$

from which  $\Delta G_{\text{ads}}^\circ$  could be obtained. Also, basic thermodynamic relationships indicate that

$$\left[ \frac{\partial(\Delta G_{\text{ads}}^\circ/T)}{\partial(1/T)} \right]_P = \Delta H_{\text{ads}}^\circ \quad (6.248)$$

$$\left[ \frac{\partial \Delta G_{\text{ads}}^\circ}{\partial T} \right]_P = -\Delta S_{\text{ads}}^\circ \quad (6.249)$$

Therefore, the slope of a plot of  $(\Delta G_{\text{ads}}^\circ)/T$  vs.  $1/T$  gives the  $\Delta H_{\text{ads}}^\circ$ , and the slope of a plot of  $\Delta G_{\text{ads}}^\circ$  vs.  $T$  gives the  $\Delta S_{\text{ads}}^\circ$  of the adsorption reaction. Figure 6.105 shows the corresponding graphs to determine  $\Delta H_{\text{ads}}^\circ$  and  $\Delta S_{\text{ads}}^\circ$  for the adsorption of bisulfate on polycrystalline electrodes.

What information can be obtained from  $\Delta H_{\text{ads}}^\circ$ ? One important parameter involved in the enthalpy of the reaction is the ion-metal bond. However,  $\Delta H_{\text{ads}}^\circ$  includes all the different interactions involved in the adsorption process, e.g., the breaking of the hydration sheet of the electrode and the ion, lateral interactions, and heterogeneity of the surface. One can subtract all these energy terms from  $\Delta H_{\text{ads}}^\circ$  and obtain in this way the energy (or strength) of the ion-metal bond. For the example of the adsorption of bisulfate ions on polycrystalline platinum (Fig. 6.105), the ion-metal bond was found to be  $-214 \pm 60 \text{ kJ mol}^{-1}$ .

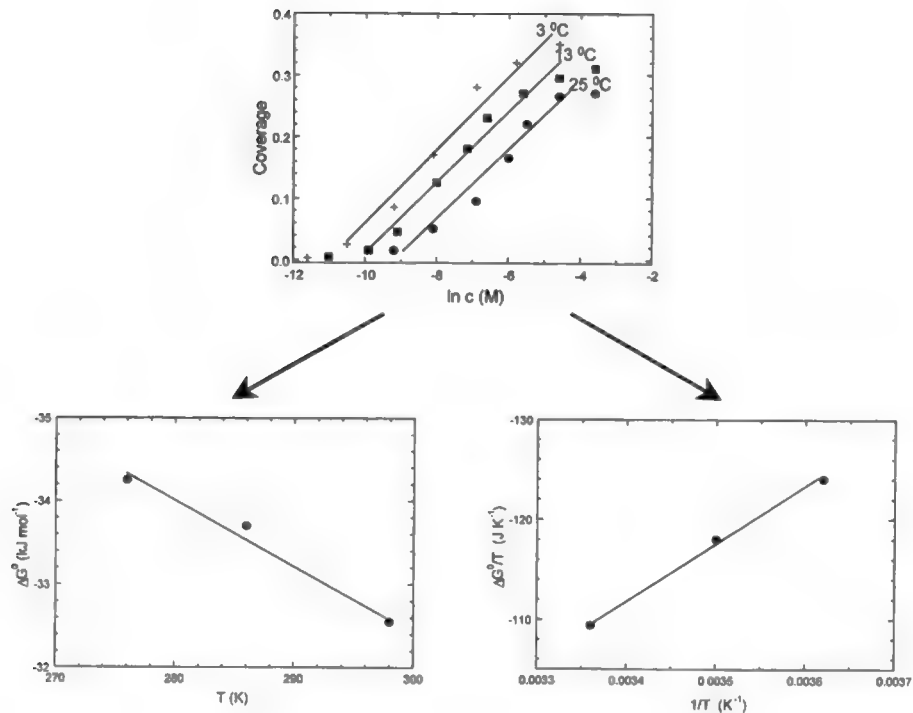
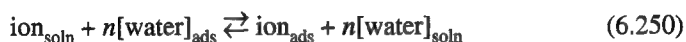


**Fig. 6.105.** From the intercepts of the curves in the graph  $\theta$  vs.  $\ln c$ , the values of  $\Delta G^\circ_{\text{ads}}$  at different temperatures are obtained. The slope of  $\Delta G^\circ_{\text{ads}}$  vs.  $T$  gives  $-\Delta S^\circ_{\text{ads}}$ . The slope of  $\Delta G^\circ_{\text{ads}}/T$  vs.  $1/T$  gives  $\Delta H^\circ_{\text{ads}}$ . (Reprinted from J. O'M. Bockris, M. Gamboa-Aldeco, and M. Szklarczyk, *J. Electroanal. Chem.* **339**:355, copyright 1992, Fig. 23, with permission of Elsevier Science.)

What information can be obtained from the  $\Delta S_{\text{ads}}^\circ$ ? Consider the adsorption reaction:



The entropy change associated with this reaction is

$$\Delta S_{\text{ads}}^\circ = (S_{\text{i,ads}}^\circ + nS_{\text{w,soln}}^\circ) - (S_{\text{i,soln}}^\circ + nS_{\text{w,ads}}^\circ) \quad (6.251)$$

From statistical thermodynamic treatments it is possible to calculate the terms on the right-hand side of Eq. (6.251). This is done by assuming a given model of the species considered, e.g., whether the adsorbed ion is immobilized or nonlocalized on the surface of the electrode (Section 6.8.3), and how many cells it occupies. Then one adds the corresponding entropies according to Eq. (6.251) and finally compares the calculated values of  $(\Delta S_{\text{ads}}^\circ)_{\text{model}}$  with the value obtained experimentally,  $(\Delta S_{\text{ads}}^\circ)_{\text{exp}}$ . The model that gives the value more similar to that obtained experimentally corresponds to the model closer to reality.

Table 6.13 shows the calculated values of entropy of adsorption for different models of the adsorption reaction of bisulfate on polycrystalline platinum electrodes, as well as its comparison with the experimental value. The conditions that best describe the experiments are those shown on line 4. This means that in solution the bisulfate

**TABLE 6.13**  
**Calculated Entropy Values (in  $\text{J K}^{-1} \text{mol}^{-1}$ ) of the Individual Species of the**  
**Adsorption Reaction:  $(\text{HSO}_4^-)_{\text{soln}} + (\text{water dimer})_{\text{ads}} \rightleftharpoons (\text{HSO}_4^-)_{\text{ads}} + 2(\text{H}_2\text{O})_{\text{soln}}$ <sup>a</sup>**

$S_{\text{i,ads}}^\circ$	$+2S_{\text{w,soln}}^\circ$	$-S_{\text{i,soln}}^\circ$	$-S_{\text{dimer,ads}}^\circ$	$-\Delta S_{\text{ads}}^\circ$
(1) 63.33 2 d.f. one cell	$2 \times 70$	-178.10 3 d.f. communal	-58.75 2 d.f. one cell	-33.52
(2) 63.33 2 d.f. one cell	$2 \times 70$	-169.80 3 d.f. one cell	-58.75 2 d.f. one cell	-25.22
(3) 6.67 no translation	$2 \times 70$	-178.10 3 d.f. communal	-58.75 2 d.f. one cell	-90.18
(4) 6.67 no translation	$2 \times 70$	-169.80 3 d.f. one cell	-58.75 2 d.f. one cell	-81.88
(5) 6.67 no translation	$2 \times 70$	-169.80 3 d.f. one cell	-16.12 no translation	-39.25
			Experimental	-77.89

Source: Reprinted from M. Gamboa-Aldeco, dissertation, Texas A&M University, 1992.

<sup>a</sup>Comparison with the experimental value indicates that the conditions that best describe the experiments are those in line 4: in solution the  $\text{HSO}_4^-$  translates in a restricted way and upon adsorption the ion loses its translational mobility and retains only a restricted rotation around its axis perpendicular to the surface. The degrees of freedom (d.f.) allowed for the movement of each species as well as the area covered in their movement (one cell, communal) are indicated in each case.

ion translates in a restricted way within one cell; upon adsorption, the ion loses its translational mobility and retains only a restricted rotation around its axis perpendicular to the surface. Also, the adsorbed water dimer maintains a restricted translation within one cell, as well as a restricted rotational movement around its axis perpendicular to the surface.

### 6.8.15. Contact Adsorption: Its Influence on the Capacity of the Interface

When we revised the different models of the interface, namely, the Helmholtz–Perrin, Gouy–Chapman, and Stern models, we left the corresponding section (Section 6.6.6) with the idea that these models were not able to reproduce the differential capacity curves [Fig. 6.65(b)]. We said that when ions specifically adsorb on the electrode, the models fail to explain the experimental facts.

We have studied the forces and parameters related to the adsorption of ions. We have gained knowledge of the different interactions involved in the contact adsorption process. Now it is time to return and look again at the experimental capacitance curves and try to explain them via the new knowledge we have gained about the interphasial structure.

Consider the interphasial region with some ions contact adsorbed at the IHP [Fig. 6.88(b)]. If now it is assumed that the solution is concentrated, all the diffuse charges will be perched on the OHP, and the potential drop beyond the OHP into the solution could be neglected. The total potential difference across this interphase could be resolved into two components, one from the metal to the IHP and another from the IHP to the OHP:

$$\phi_M - \phi_S = (\phi_M - \phi_{\text{IHP}}) + (\phi_{\text{IHP}} - \phi_{\text{OHP}}) \quad (6.252)$$

Each of these potential drops can be expressed in terms of the corresponding integral capacities, i.e. [see Eq. (6.96)]

$$\phi_M - \phi_{\text{IHP}} = \frac{q_M}{K_{M \rightarrow \text{IHP}}} \quad (6.253)$$

and

$$\phi_{\text{IHP}} - \phi_{\text{OHP}} = \frac{q_d}{K_{\text{IHP} \rightarrow \text{OHP}}} \quad (6.254)$$

Substituting these two equations into the total potential drop, e.g., Eq. (6.252), gives

$$\phi_M - \phi_S = \frac{q_M}{K_{M \rightarrow \text{IHP}}} + \frac{q_d}{K_{\text{IHP} \rightarrow \text{OHP}}} \quad (6.255)$$

The total capacity is defined as  $C = dq_M/d(\phi_M - \phi_S)$ . Thus, the inverse of the total capacity can be obtained by differentiating Eq. (6.255) with respect to  $q_M$ ,

$$\frac{1}{C} = \frac{d(\phi_M - \phi_S)}{dq_M} = \frac{1}{K_{M \rightarrow IHP}} + \frac{1}{K_{IHP \rightarrow OHP}} \frac{dq_d}{dq_M} \quad (6.256)$$

The condition of electroneutrality of the interface as a whole says that

$$q_M = q_{CA} + q_d \quad (6.257)$$

and differentiating this equation with respect to  $q_M$  gives,

$$1 = \frac{dq_{CA}}{dq_M} + \frac{dq_d}{dq_M} \quad (6.258)$$

Substituting  $dq_d/dq_M$  from Eq. (6.258) into Eq. (6.256) gives

$$\frac{1}{C} = \frac{1}{K_{M \rightarrow IHP}} + \frac{1}{K_{IHP \rightarrow OHP}} \left( 1 - \frac{dq_{CA}}{dq_M} \right) \quad (6.259)$$

or

$$\frac{1}{C} = \left( \frac{1}{K_{M \rightarrow IHP}} + \frac{1}{K_{IHP \rightarrow OHP}} \right) - \frac{1}{K_{IHP \rightarrow OHP}} \frac{dq_{CA}}{dq_M} \quad (6.260)$$

The first part of this equation is nothing other than the integral capacity of the region between the metal and the OHP in the absence of contact-adsorbing ions, i.e.,  $(1/K_{M \rightarrow OHP}) = (1/K_{M \rightarrow IHP}) + (1/K_{IHP \rightarrow OHP})$ , and thus Eq. (6.260) can be rearranged to give

$$\frac{1}{C} = \frac{1}{K_{M \rightarrow OHP}} - \left( \frac{1}{K_{M \rightarrow OHP}} - \frac{1}{K_{M \rightarrow IHP}} \right) \frac{dq_{CA}}{dq_M} \quad (6.261)$$

This is the expression for the capacity of an interface in the presence of contact adsorption. Note how the differential capacity is affected by contact-adsorbed ions populating the IHP through the quantity  $dq_{CA}/dq_M$ .

Would Eq. (6.261) for the total differential capacity be able to reproduce the experimental capacity curves? Let us have a look again at one of the complete capacity-potential curves shown in Fig. 6.65(b) and illustrated in Fig. 6.106 in this section. This is not a simple curve. It breaks out into "breaks and flats," and it has a complicated fine structure that depends upon the ions that populate the interphasial region. Whereas there is a region of "constant" capacity at potentials more negative than the electrocapillary maximum, there is also a "hump" in the capacity-potential

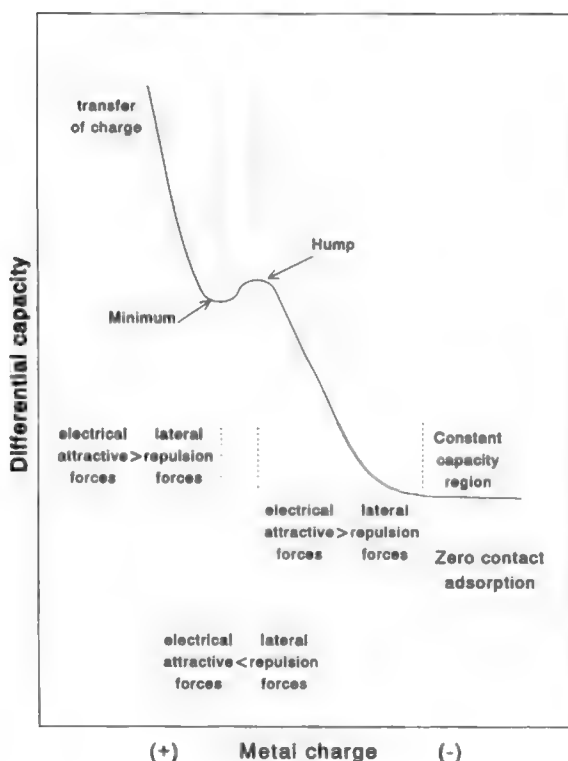


**Fig. 6.106.** The lateral-repulsion model for the explanation of the capacity-potential curve.

curve in a region positive to the ecm. At potentials positive to the hump region, the capacity goes through a minimum and then starts increasing rapidly. Perhaps this is because the interface is on the verge of leaking and becoming nonpolarizable, in which case the  $q$  in  $C = dq/dE$  is contributed to by the transfer of charge across the double layer. Thus, in general terms, the capacity-potential curve presents two basic challenges: the challenge of interpreting the constant-capacity region, and that of interpreting the hump and the minimum.

**6.8.15.1. The Constant-Capacity Region.** When one sees a relatively constant capacity region (e.g., on the negative side of the capacitance curve in Fig. 6.106), one's thoughts turn naturally to a simple parallel-plate condenser model (the Helmholtz-Perrin model), because such a model yields a potential-independent capacity. One plate is located at the metal surface, but where is the second plate? On the IHP or on the OHP?

Experimental data may give us another clue to answering these questions. It is known that the capacity in this region is not only constant with potential over a region



of a few hundred millivolts, but is also virtually independent of the nature of the ions that occupy the double layer. The capacity stays constant at a value of 16 to 17  $\mu\text{F cm}^{-2}$  irrespective of the radii of the ions. What is the implication of this constancy of double-layer capacity?

In the Helmholtz–Perrin model, we found that (Section 6.6.2)

$$C = \frac{q}{\Delta\phi} = \frac{\epsilon\epsilon_0}{d} \quad (6.262)$$

where  $d$  is the distance between the condenser plates. If ions were contact adsorbed and populating the IHP, then the two plates constituting the condenser would be the metal and the IHP. Thus,  $d$  for this condenser would simply be the radius of the ions contact adsorbed in the IHP, i.e.,  $r_i$ . Hence the capacity should be very sensitive to differences in radii of the ions. However, experiment does not show this radius dependence of the capacity. It seems, therefore, that there are no ions in the IHP. In other words, a constant capacity implies the absence of contact adsorption of ions. The ions then should be populating only the OHP.

Would ions populating only the OHP explain the constancy of capacity? It will tend to do so because when it is considered that the ions are in the OHP, the  $d$  term in Eq. (6.262) will become  $r_i$  plus other terms connected with the radii of water molecules separating the ions from the electrode [see Fig. 6.88(a)]. The total separation distance would be much less dependent on the radius of the ion because it consists also of the water molecules around the ion and those hydrating the electrode. The variation in  $r_i$  would affect  $d$  to a lesser degree. Constant capacity means, then, that ions do not contact adsorb on the electrode, but populate the OHP.

**6.8.15.2. The Capacitance Hump and the Capacity Minimum.** A discussion of the hump should really begin with a consideration of the question: Why does the differential capacity of the interface increase when the electrode charge becomes positive with respect to the constant-capacity region? Why doesn't the capacity maintain the constant value of 16 or 17  $\mu\text{F cm}^{-2}$  as the potential difference across the interface changes?

Let us have a look at the general expression for the capacity of the electrode/electrolyte interface, i.e., Eq. (6.261),

$$\frac{1}{C} = \frac{1}{K_{M \rightarrow \text{OHP}}} - \left( \frac{1}{K_{M \rightarrow \text{OHP}}} - \frac{1}{K_{M \rightarrow \text{IHP}}} \right) \frac{dq_{\text{CA}}}{dq_{\text{M}}} \quad (6.261)$$

This equation says that  $C$  is constant when the second term is zero, i.e., when there is no change in the amount of the contact-adsorbed ion with a change in the electrode charge ( $dq_{\text{CA}}/dq_{\text{M}} \rightarrow 0$ ). But this condition is given only when there is zero contact adsorption, as we discussed in the previous paragraphs.

Equation (6.261) also indicates that  $1/C$  decreases, or in other words, that  $C$  increases, when the term  $dq_{CA}/dq_M$  becomes nonzero, i.e., the capacity increases when  $q_{CA}$  increases with  $q_M$ . However, according to this argument, the capacity should keep on increasing as the potential difference across the double layer becomes more positive. In practice,  $C$  does not go on increasing indefinitely. It increases up to a point and then decreases, giving place to the hump that we are trying to explain (Fig. 6.106). The hump means, therefore, that as the electrode charge becomes positive, the population of contact-adsorbed ions increases more and more, and then at the apex of the hump, the rate of growth begins to decline. What makes this rate of adsorption decrease?

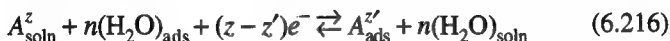
In Section 6.8.2 we studied the main forces involved in the contact-adsorption process, i.e., in the migration of an ion from the OHP to the IHP. We found that this process involves chemical and electrical forces, as well as lateral interactions. If the charges of the adsorbing ions and the electrode are of opposite sign, then the electrode charge encourages the growth of the population of contact-adsorbed ions and thus the accumulation of charges,  $q_{CA}$ , in the IHP. However, this process sets out another type of force that inhibits further growth—the ion–ion lateral interaction forces (Fig. 6.92).

It is this negative feedback—electrical attracting forces giving rise to lateral repulsion forces—that generates the hump. At charges in the region of constant capacities,  $q_{CA} \approx 0$ , as the electrode charge increases,  $q_{CA}$  starts growing in an exponential fashion. However, with the increasing departure of  $q_{CA}$  from zero, the lateral repulsion forces also increase in significance. They slow down the rate of growth of the population of contact-adsorbed ions. They make the capacity go through the hump.

After this decrease in capacity, the attracting forces between the metal charge and the ion charge overcome the lateral repulsion forces. The rate of adsorption increases and the capacity also increases after passing through a minimum after the hump. This lateral-repulsion model is able, then, to explain and reproduce the maximum (the hump) and the minimum in the  $C$ - $q_M$  curve (Table 6.14).

### 6.8.16. Looking Back

In these sections we learned about the processes and forces involved in the adsorption of ions from solution on electrodes, which can be represented by



where  $A_{\text{soln}}^z$  is the ion in solution with charge  $ze$ ,  $A_{\text{ads}}^{z'}$  is the adsorbed ion with a net charge  $z'e$ ,  $(z - z')e^-$  is the charge being transferred from the ion to the electrode, and  $n$  is the number of water molecules displaced from the electrode surface during the adsorption process.

First we went through a qualitative presentation of the main factors affecting the adsorption process. In order for ions to migrate from the OHP and contact adsorb on

**TABLE 6.14**  
**Surface Coverage at Which the Capacitance Hump and Inflection on Contact**  
**Adsorption Charge-Metal Charge Curve Occurs**

Ions	Concentration ( <i>N</i> )	$\theta_{\text{hump}}$		$q_M$ at $C_{\text{min}}$ ( $\mu\text{C cm}^{-2}$ )		$\theta_{\text{minimum}}$
		Exptl.	Theor.	Exptl.	Exptl.	Theor.
$\text{Cl}^-$	0.3	0.01	0.070	10.0	0.10	0.31
$\text{Br}^-$	0.1	0.10	0.075	7.0	0.13	0.32
$\text{I}^-$	0.1	0.12	0.082	3.0	0.19	0.33
$\text{ClO}_3^-$	0.1	0.07	0.100	13.0	0.11	0.27
$\text{BrO}_3^-$	0.1	0.12	0.100	11.6	0.13	0.27
$\text{NO}_3^-$	0.1	0.10	0.100	11.1	0.25	0.30
$\text{ClO}_4^-$	0.3	0.10	0.095	11.5	0.24	0.27
$\text{SCN}^-$	1	0.07	0.065	20.0	0.19	0.28

Source: Reprinted from M. A. Habib and J. O'M. Bockris, "Specific Adsorption of Ions," in *Comprehensive Treatise of Electrochemistry*, Vol. 1, Ch. 4, J. O'M. Bockris, B. E. Conway, and E. Yeager, eds., Plenum, 1980, Tables 7 and 8.

the electrode at the IHP, a series of steps should occur: The metal has to get rid of part of its hydration sheath; the ion has to remove at least part of its solvation layer; and it is only then that the ion can move to a position closer to the electrode and interact with it (Fig. 6.90). It is the free energy of adsorption of the whole process ( $\Delta G_{\text{ads}}$ ) that dictates if the ion is ready to make the translation to the IHP region, and the strength of the bonds keeping the ions there. To understand how this happens, we split the total  $\Delta G_{\text{ads}}$  into changes in ion-electrode interactions (electric field forces, image forces, and dispersion forces), changes in solvent interactions (ion-solvent, metal-solvent) and changes in lateral interactions (interactions between a reference ion and its neighbor ions and their image charges, as well as with other species that may be adsorbed on the electrode) (Section 6.8.2).

The free energy of adsorption is formed by the enthalpy and the entropy of the adsorption process (Section 6.8.3). The enthalpy indicates the strength of the bonds that have to be broken and formed during the adsorption process [including those related to the different electrode sites (Fig. 6.94)]. Meanwhile, the entropy indicates how mobile the ions are in their adsorbed site (Fig. 6.95).

Another effect due to the strong electric field at the interface is the deformation of the contact-adsorbed ions, as shown in Fig. 6.96.

The next step was to quantitatively determine some of the parameters involved in the adsorption of ions. We started by comparing equations of states in three dimensions (gas in a cylinder) with those in two dimensions (adsorbed molecules) (Section 6.8.5). This led us to define adsorption isotherms in electrochemical systems: They are relationships relating the physical quantities [number of adsorbed molecules ( $\Gamma$  or  $\theta$ ), activity of ions in solution ( $a$ ), charge or potential of the electrode ( $q_M$  or  $E$ ) and

temperature of the system ( $T$ )] that define the adsorbed state at the interface in an electrochemical system (Section 6.8.6).

With this in mind, some important adsorption isotherms were introduced, and we found that each of them describes important characteristics of the adsorption process (Table 6.10). Thus, the Langmuir isotherm considers the basic step in the adsorption process; the Frumkin isotherm was one of the first isotherms involving lateral interactions; the Temkin is a surface heterogeneity isotherm; and the Flory–Huggins-type isotherms include the substitution step of replacing adsorbed water molecules by the adsorbed entities (Fig. 6.98).

However, adsorption is a complex process that cannot be described by only one parameter. Thus we developed an isotherm for adsorption of ions that included most of the parameters already described (Section 6.8.13). It included heterogeneity of the surface, displacement of solvent molecules from the electrode, transfer of charge, deformation of the adsorbing ions, ion size, lateral interactions, etc.

Finally, we returned to an old problem that we had left unresolved in previous sections: the understanding of the capacity-potential curve [Fig. 6.65(b)]. With the knowledge we acquired on ionic adsorption, we were able to explain the features characteristic of the capacitance curves (Fig. 6.106). A constant-capacity region indicates that ions do not contact adsorb, but populate the OHP. The increase in capacitance as the potential departs from this constant-capacity region was understood to be due to the increase of the population of adsorbed ions on the surface of the electrode. However, as the adsorbed population increases, lateral repulsion forces tend to increase also. This continues until a point—the hump position—at which these repulsion forces overcome the electrical attracting forces and the rate of adsorption decreases, giving rise to the hump. After this, the attracting forces take over again and the capacity increases.

What is next? Several examples were given of modern experimental electrochemical techniques used to characterize electrode–electrolyte interactions. However, we did not mention theoretical methods used for the same purpose. Computer simulations of the dynamic processes occurring in the double layer are found abundantly in the literature of electrochemistry. Examples of topics explored in this area are investigation of lateral adsorbate–adsorbate interactions by the formulation of lattice-gas models and their solution by analytical and numerical techniques (Monte Carlo simulations) [Fig. 6.107(a)]; determination of potential-energy curves for metal–ion and lateral–lateral interaction by quantum-chemical studies [Fig. 6.107(b)]; and calculation of the electrostatic field and potential drop across an electric double layer by molecular dynamic simulations [Fig. 6.107(c)].

The specific methodology involved in these simulations is beyond the scope of this chapter. So, instead of extending our knowledge of adsorption of ions on electrodes, in the next section we will study the characteristics of the adsorption process of other types of species, the adsorption of organic molecules.

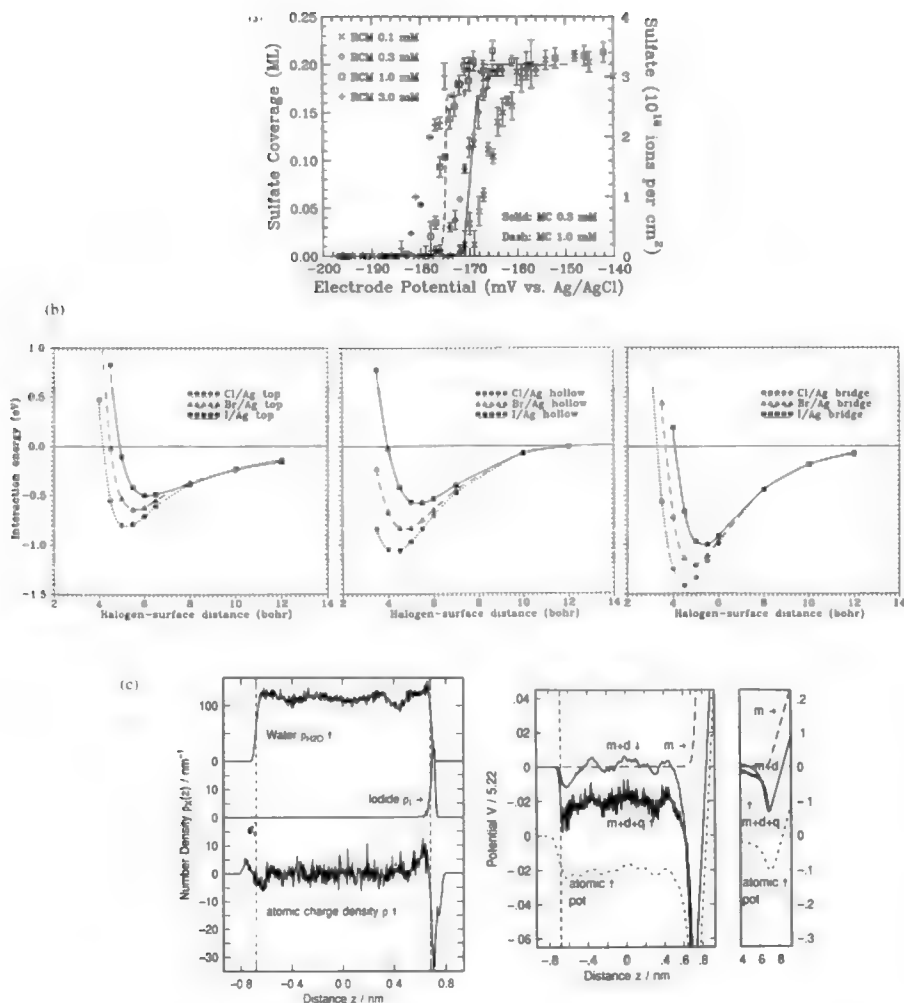


**Fig. 6.107.** Computer simulations of the processes occurring in the double layer. (a) Monte Carlo (MC) simulation results for the adsorption of bisulfate on Rh(111) electrodes, and its comparison with the experimental radiotracer technique (RCM). (Reprinted from P. A. Rikvold, M. Gamboa-Aldeco, J. Zhang, M. Han, Q. Wang, H. L. Richards, and A. Wieckowski. *Surf. Sci.*, **335**: 389, copyright 1995, Fig. 6, with permission of Elsevier Science.) (b) Potential–energy curves for the interaction of chloride, bromide, and iodide ions on top, fourfold hollow, and bridge sites of Ag clusters. (Reprinted from G. Pacchioni, *Electrochim. Acta* **41**: 2285, copyright 1996, Figs. 4, 5, and 6, with permission from Elsevier Science.) (c) Density profiles for iodide and water molecules (metal electrode on right-hand side), and potential drop across the system (m, monopole; d, dipole; q, quadrupole; image charge on metal +1, metal on right-hand side). (Reprinted from J. N. Glosli and M. R. Philpott, *Electrochim. Acta* **41**: 2145, copyright 1996, Figs. 5 and 6, with permission from Elsevier Science.)

## Further Reading

### Seminal

1. I. Langmuir, "The Adsorption of Gases on Plane Surfaces of Glass in Mica and Platinum," *J. Am Chem. Soc.* **40**: 1361 (1918).
2. A. N. Frumkin, "Surface Tension Curves of the Higher Fatty Acids and the Equations of Conditions of the Surface Layer," *Z Physik. Chem.* **116**: 466 (1925).
3. M. Temkin, "Adsorption Equilibrium and the Kinetics of Processes on Non-Homogeneous Surfaces and in the Interaction Between Adsorbed Molecules," *Zhurnal Fizicheskoi i Khimii* **15**: 296 (1941).
4. P. J. Flory, "Thermodynamics of High-Polymer Solutions," *J. Chem. Phys.* **10**: 51 (1942).
5. M. L. Huggins, "Thermodynamic Properties of Solutions of Long Chain Compounds," *Ann. N. Y. Acad. Sci.* **43**: 6 (1942).
6. W. Lorenz and G. Salie, "Mechanism of the Electrochemical Phase Boundary Reaction," *Z Phys. Chem. (Leipzig)* **218**: 259 (1961).
7. J. O'M. Bockris, M. A. V. Devanathan, and K. Muller, "Water Molecule Model of the Double Layer," *Proc. Roy. Soc. (London)* **A274**: 55 (1963).
8. K. J. Vetter and J. W. Schultze, "Experimental Determination and Interpretation of the Electrosorption Valency,  $\gamma$ ," *J. Electroanal. Chem.* **44**: 63 (1973).
9. B. E. Conway and H. Angerstein-Kozłowska, "Interaction Effects in Electrodeposited Monolayers and the Role of the 'Electrosorption Valency' Factor," *J. Electroanal. Chem.* **113**: 63 (1980).
10. R. Parsons, "The Contribution to the Capacity of an Electrode from a Species Adsorbed with Partial Charge Transfer," *Can. J. Chem.* **59**: 1898 (1981).
11. M. A. Habib and J. O'M. Bockris, "Adsorption at the Solid/Solution Interface," *J. Electrochem. Soc.* **132**: 108 (1985).
12. J. O'M. Bockris, M. Gamboa-Aldeco, and M. Szklarczyk, "Ionic Adsorption at the Solid-Solution Interphase using Three In Situ Methods," *J. Electroanal. Chem.* **339**: 355 (1992).

### Review

1. A. J. Bard, H. D. Abruña, C. E. Chidsey, L. R. Faulkner, S. W. Feldberg, K. Itaya, M. Majda, O. Melroy, R. W. Murray, M. D. Porter, M. P. Soriaga, and H. S. White, "The Electrode/Electrolyte Interface—A Status Report," *J. Phys. Chem.* **97**: 7147 (1993).
2. J. O'M. Bockris, S. Fletcher, J. J. Gale, S. U. M. Khan, D. M. Kol, D. J. Mazur, K. Uozaki, and N. L. Weinber, "Electrochemistry (1992–1995)," in *Annual Reports of the Royal Society of Chemistry*, Section C, Vol. 92, p. 23 (1996).
3. R. Parsons, "The Metal–Liquid Electrolyte Interface," *Solid State Ionics* **94**: 91 (1997).
4. J. Schultze and D. Rolle, "The Partial Discharge of Electrosorbates and Its Influence in Electrocatalysis," *Can. J. Chem.* **75**: 1750 (1997).

### Papers

1. R. Parsons, *Proc. Royal Soc. (London)* **A261**: 79 (1961).

2. B. E. Conway, H. Angestein-Kozłowska, and H. P. Dhar, *Electrochim. Acta* **19**: 455 (1974).
3. P. Nikitas, *J. Electroanal. Chem.* **170**: 353 (1984).
4. P. Zelenay, M. A. Habib, and J. O'M. Bockris, *Langmuir* **2**: 393 (1986).
5. J. Jastrzebska, M. Jurkiewicz-Herbich, and S. Trasatti, *J. Electroanal. Chem.* **216**: 21 (1987).
6. P. Nikitas, *Electrochim. Acta* **33**: 647 (1988).
7. I. Betova, G. Neykov, R. Raicheff, and E. Lazarova, *Langmuir* **9**: 3452 (1993).
8. W. Schmickler, in *Structure of Electrified Interfaces*, J. Lipkowski and P. Ross, eds., p. 201, VCH Publishers, New York (1993).
9. Z. Shi, J. Lipkowski, M. Gamboa, P. Zelenay, and A. Wieckowski, *J. Electroanal. Chem.* **366**: 317 (1994).
10. P. A. Rikvold, M. Gamboa-Aldeco, J. Zhang, M. Han, Q. Wang, H. L. Richards, and A. Wieckowski, *Surface Science* **335**: 389 (1995).
11. M. Gamboa-Aldeco, K. Franaszczuk, and A. Wieckowski, in *Handbook of Surface Imaging and Visualization*, p. 635, CRC Press, Boca Raton, FL (1995).
12. P. Mrozek, Y.-E. Sung, M. Han, M. Gamboa-Aldeco, A. Wieckowski, Ch.-H. Chen, and A. Gewirth, *Electrochim. Acta* **40**: 17 (1995).
13. G. Pacchioni, *Electrochimica Acta* **41**: 2285 (1996).
14. J. N. Glosli and M. R. Philpott, *Electrochim. Acta* **41**: 2145 (1996).
15. H. A. Gasteiger, N. M. Markovic, and P. N. Ross, Jr., *Langmuir* **12**: 1414 (1996).
16. J. J. Calvente, Z. Kováčová, R. Andreu, and W. R. Fawcett, *J. Electroanal. Chem.* **401**: 231 (1996).
17. Z. Shi and J. Lipkowski, *J. Electroanal. Chem.* **403**: 225 (1996).
18. A. Hamelin, in *Nanoscale, Probes of the Solid/Liquid Interface*, A. A. Gewirth and H. Siegenthaler, eds., Vol. 288, p. 285, NATO ASI Series, Series E: Applied Sciences, Reidel, Dordrecht.
19. B. K. Niece and A. A. Gewirth, *Langmuir* **13**: 6302 (1997).
20. H. Uchida, N. Dceda, and M. Watanabe, *J. Electroanal. Chem.* **424**: 5 (1997).
21. K. Arai, F. Kusu, K. Ohe, and K. Takamura, *Electrochim. Acta* **42**: 2493 (1997).

## 6.9. THE ADSORPTION PROCESS OF ORGANIC MOLECULES

### 6.9.1. The Relevance of Organic Adsorption

The adsorption of organic substances is one of the big topics in electrochemistry. Its importance lays not only in the structural information of the double layer that can be obtained from its study or the basic information that it provides to organic chemistry, bioelectrodics, or bioelectrochemistry. Organic electrosorption is also involved in fundamental industrial processes. For example, organic substances are added as brightening, leveling, and antipitting agents that help produce bright, smooth, and pit-free electrodeposits. Some organic molecules play an essential role as inhibi-

tors in attempts to reduce corrosion, and others act as electrocatalysts. In other cases, the consequences of organic adsorption have deleterious effects, e.g., organic impurities may block the electrode surface, impede charge transfer and thus slow down the desired reactions.

### 6.9.2. Is Adsorption the Only Process that the Organic Molecules Can Undergo?

Does the reacting species reside in the double layer—in the OHP or in the IHP? Does it remain solvated or does it remove its water sheet? Does the molecule undergo electron transfer and reaction? What is its orientation? Does the nature of the electrode influence the adsorption process? These are some of the questions the electrochemists find when studying organic adsorption.

In general, the adsorption of organic compounds on electrodes can be classified into two categories. In the first, the molecules adsorb but retain their chemical individuality. The adsorption bond between the molecule and the adsorbate is relatively weak, and adsorbed organic molecules may exchange readily with their peer molecules from solution:



This type of adsorption is said to be *reversible* and the thermodynamic laws of the surface phenomena (e.g., isotherms, determination of  $\Delta G^\circ$ ,  $\Delta H^\circ$ , and  $\Delta S^\circ$  as explained in Section 6.8.3) are valid.

In contrast, the interaction between the molecule and the electrode may be very strong. This may result in a charge-transfer reaction between the adsorbate (organic molecule) and the adsorbent (electrode). As a consequence, new species may form, which may adsorb as such or further react to become other species. Under such conditions, the equilibrium between the original organic molecules in solution and the chemisorbed particles on the electrode no longer exists. Such a reaction can be written as



and the organic molecules are said to be adsorbed in an *irreversible* fashion. Under such conditions the thermodynamic laws are no longer applicable.

However, one process does not exclude the other. While adsorption of an organic molecule may take place under certain experimental conditions (potential, temperature, etc.), under other conditions the same molecule may undergo other electrode reactions, such as oxidation, reduction, or polymerization of the adsorbed organic molecules.<sup>65</sup> These types of processes are so important that they are studied separately,

<sup>65</sup>Destructive adsorption can be found especially in the case of low molecular weight organic compounds such as methanol and formic acid, and it is mainly the products of such transformations that are the ones adsorbed on the electrodes.



under the title of organoelectrochemistry. Chapter 11 in this book deals with these types of reactions.

### 6.9.3. Identifying Organic Adsorption

It is not always easy to identify the path the organic molecule has undertaken. As explained in the previous section, the molecule may be adsorbed on the surface in a way similar to how ions adsorb on the electrode, or they may undergo further reactions. Thus, the electrochemist may perform three experimental tests in aqueous solutions to figure out whether the process under study is related to adsorption or to an electrode transfer reaction.

**6.9.3.1. Test 1: The Almost-Null Current.** Consider an organic molecule undergoing adsorption on the surface of an electrode. The adsorbed organic molecule is in equilibrium with its peer molecules in solution, as shown in Eq. (6.263). Under such conditions, there is no complete transfer of electrons between the adsorbed molecule and the adsorbate.<sup>66</sup> The current,  $I$ , is defined as the charge transferred per unit time ( $I = q/t$ ). However, since during the adsorption process the transfer of electrons does not occur, the process is characterized by an almost null current, as shown in Fig. 6.108. The close to zero current is dependent on the potential of the electrode because at sufficiently positive potentials, all organic molecules undergo oxidation and decompose to form  $\text{CO}_2$  as a final product. These reactions might involve a large number of electrons, and large currents can be detected, as shown on the right side of Fig. 6.108. On the other hand, at sufficiently negative potentials, the adsorbed organic molecule may undergo other reactions, such as hydrogenation or reduction. These processes may involve as well a large number of electrons and large currents (left side of Fig. 6.108).<sup>67</sup> Thus, adsorption processes are characterized by close to zero currents, in contrast to other charge-transfer processes where large currents may be detected.

**6.9.3.2. Test 2: The Parabolic Coverage-Potential Curve.** It has been found that in aqueous solutions, an adsorbed (nonreactive) organic molecule always undergoes a parabolic dependence on coverage,  $\theta$ , with the potential of the electrode. In contrast, if the organic molecule follows other reaction paths, and a modified original molecule or its fragments is the one adsorbed, then the  $\theta$  vs. potential curve may differ considerably from that of the parabolic behavior found for the adsorption process, as shown in Fig. 6.109.

<sup>66</sup>However, as explained in Section 6.8.2.1 for the case of ionic adsorption, partial transfer of electrons may occur during the adsorption process of organic molecules.

<sup>67</sup>The solvent in which the organic molecule is dissolved may undergo oxidation or reduction as the organic molecule. However, to make this discussion clearer, it is assumed that such processes take place at much more positive (oxidation) or negative (reduction) potentials than those for the organic molecule.

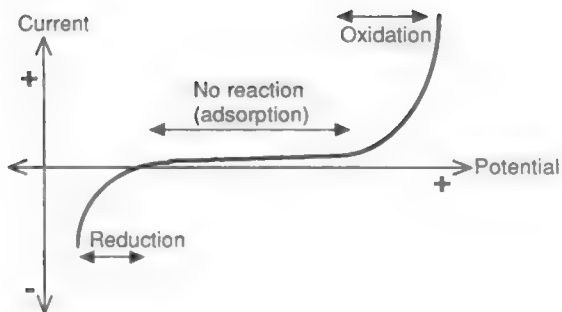


**Fig. 6.108.** Current vs. potential curve for the adsorption of organic molecules on electrodes. The current due to adsorption of organic molecules is a currentless process. When oxidation, reduction, or other electron-transfer reactions take place, high currents may be detected.

**6.9.3.3. Test 3: The Maximum of the Coverage–Potential Curve Lies Close to the pzc.** The coverage of the adsorbed molecule is not alone in following a parabolic curve as the potential increases. It has been found that the coverage of all adsorbing organic molecules passes through a maximum when the charge of the electrode is close to that of zero charge, i.e., at the potential of zero charge (see Fig. 6.109).

If the organic molecule under study follows the behavior described in these three tests, it can be said that the molecule is undergoing an adsorption reaction. Although it was explained why the current should be almost zero when adsorption occurs, we did not explain why the adsorption should follow a parabolic shape with a maximum close to the pzc. This behavior will be explained shortly, but before that, some fundamentals of the adsorption process of organic molecules should be pointed out.

## 6.9.4. Forces Involved in Organic Adsorption

Will an organic molecule adsorb onto the electrode? In principle, this question is no different from asking: Will an ion contact adsorb? The parameter responsible for the adsorption of ions, as pointed out in Section 6.8.1, is the free energy of adsorption,  $\Delta G_{\text{ads}}^\circ$  and the same variable is also responsible for the adsorption of organic molecules. A minimum value of  $\Delta G_{\text{ads}}^\circ$  corresponds to a maximum value of the adsorptivity of the organic molecule, and this maximum frequently lies at a value of the metal charge,  $q_M$ , that is close to the pzc (i.e.,  $q_M = 0$ ).<sup>68</sup> Figure 6.110 shows an example of this behavior for the adsorption of various *n*-alcohols on mercury.

<sup>68</sup>For example, in mercury, the  $(\Delta G_{\text{ads}}^\circ)_{\text{max}}$  lies in between  $-1$  and  $-3 \mu\text{C cm}^{-2}$ . Positive values of  $(\Delta G_{\text{ads}}^\circ)_{\text{max}}$  are found only with some polyfunctional organic compounds (Guidelli, 1992).

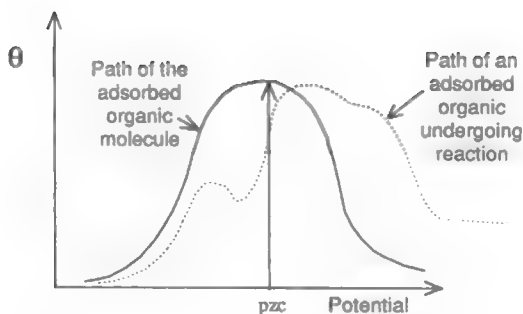


**Fig. 6.109.** Coverage vs. potential curve for the adsorption of organic molecules on electrodes. The coverage due to the adsorption process of an organic molecule from solution follows a parabolic path, with a maximum close to the pzc.

Correspondingly, the forces involved in the adsorption of organic molecules can be classified into three categories: organic molecule–electrode forces, water–electrode forces, and lateral interactions. These forces are the same as those we studied in the adsorption of ions on electrodes, and their nature was described in Section 6.8.2.

Thus, adsorption of organic molecules and ions are very similar processes. However, certain differences are evident. These are mainly related to the structure of the organic molecules with respect to the ions we studied in Section 6.8. For example, ions are usually smaller than organic molecules, which may be as large as a protein or a carbohydrate; organic molecules may be neutral, with different types of active groups that give different characteristics to the molecule; organic molecules may have aromatic rings, with delocalized electrons that interact differently with the electrons of the electrode, etc.

Thus, in the following sections we will discuss the characteristic behavior that organic molecules follow (i.e., the coverage vs. potential curve) and that we already pointed out. Then we will indicate how some of the structural features of the organic molecules as well as of the electrode and the electrolyte may affect their adsorption behavior.

### 6.9.5. The Parabolic Coverage–Potential Curve

In Section 6.9.3 it was pointed out that it has been found experimentally that the coverage of organic molecules adsorbing on an electrode follows a parabolic path with potential, and that this curve passes through a maximum that lies close to the pzc of the electrode. How can this behavior be explained?

We can start by qualitatively understanding this adsorption process. As in the case of ionic adsorption, the adsorption of organic molecules is highly influenced by the

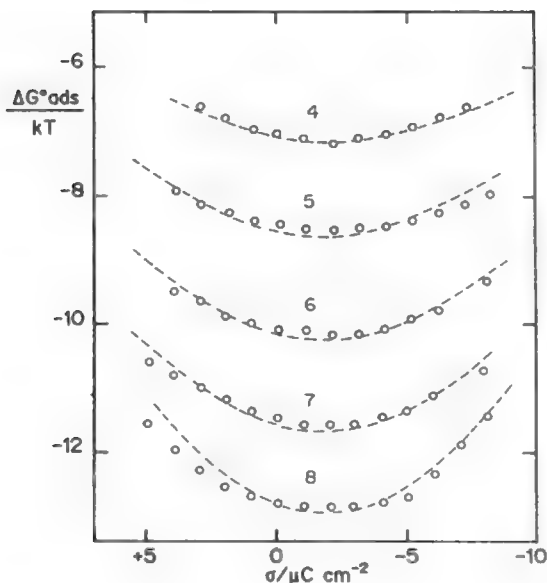


**Fig. 6.110.**  $\Delta G_{\text{ads}}^{\circ}/kT$  vs. electrode charge ( $\sigma$ ) for the adsorption of  $n$ -aliphatic alcohols on mercury from aqueous  $0.5\text{ M Na}_2\text{SO}_4$ . The number on each plot is that of the carbon atoms of the given alcohol ( $n$ ). The dashed curves were calculated by the authors of the graph. (Reprinted from R. Guidelli, in *Adsorption of Molecules at Metal Electrodes*, J. Lipkowski, and P. N. Ross, p. 1, Fig. 1.24, copyright 1992, Wiley. Reprinted by permission of John Wiley & Sons, Inc.)

adsorbed water molecules. Thus, the adsorption of organic molecules can be seen—as in the case of ionic adsorption—as a substitution process. The adsorption reaction of an organic molecule may be written as:



where  $n$  water molecules on the electrode have to be displaced to accommodate one organic molecule. In fact, this reaction could be seen as water molecules surrendering their position of contact adsorption on the electrode in favor of the organic molecules. Thus, the dependence of organic adsorption upon electrode charge will relate to the way the electrode charge decides the “desorbability” of the water molecules on the surface. If these are not attracted strongly, the organic molecules tend to replace them on the surface, and vice versa.

Consider the situation when the electrode is highly charged with excess electrons, i.e.,  $q_M \ll 0$  [Fig. 6.111(a)]. The water dipoles are nearly all in the flopped-down position, i.e., nearly all of them are aligned and tightly held with their hydrogens on the surface of the electrode. Not much organic can adsorb under such circumstances, and  $\theta_{\text{Org}}$  is small.

What happens as the electrode charge is made less negative? An increasing fraction of the water molecules change their position from that in which the hydrogen is in contact with the electrode (flop-down) to that in which the oxygen is in contact with the electrode (flip-down), and more and more dimers are formed (see Section 6.7.3). Hence, as the electrode charge decreases from a highly negative value to a value of zero, the net water-electrode interaction energy decreases, the water desorbs more and more easily, and organic adsorption becomes more and more facilitated. To a first

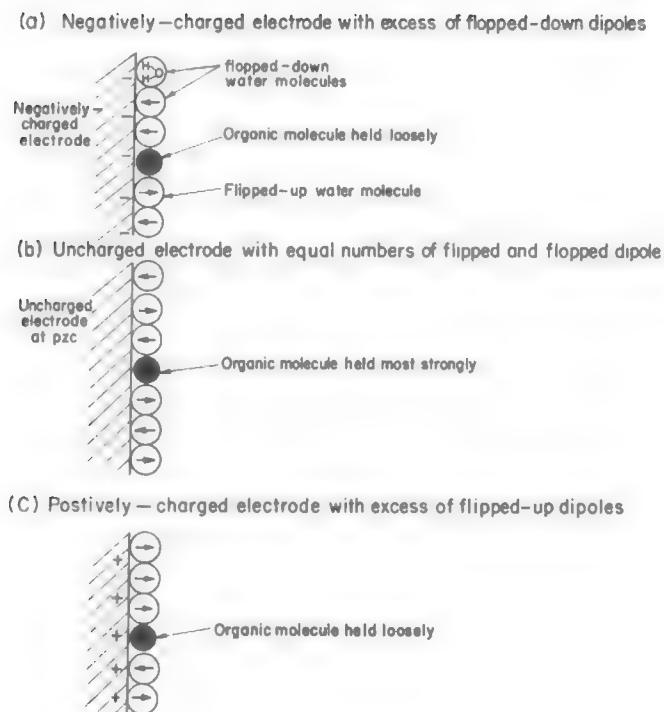
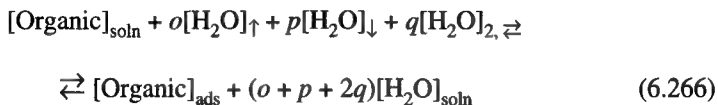


**Fig. 6.111.** The relation between the electrode charge and organic adsorption: (a) A negatively charged electrode with an excess of flopped-down dipoles has weak organic adsorption. (b) An uncharged electrode with equal numbers of flipped and flopped dipoles and dimers shows strong organic adsorption. (c) A positively charged electrode with an excess of flipped-up dipoles has weak organic adsorption.

approximation, the water molecules are held most lightly at the pzc, and consequently the organic molecules will be held relatively tightly—and thus more numerous—to the electrode at this potential [Fig. 6.111(b)]. The maximum of organic adsorption should then occur at the pzc.

What happens at the positive side of the pzc? The tendency is for water dipoles to flip up with hydrogens away from the electrode. The amount of flip-up dipoles increases with increasingly positive charge on the electrode, and at the same time the net attraction of water to the surface becomes increasingly strong. Organic adsorption reduces to a point where all the organic molecules are displaced by the tightly adsorbed flipped-up dipoles [Fig 6.111 (c)]. The amount of adsorbed organic material will have a maximum at the pzc and will die down asymptotically to zero at extremes of positive and negative charges.

This brief introduction has helped us to understand the adsorption process of the organic molecules. The next step is to consider a more detailed process and develop an equation that would describe the parabolic curve observed in the coverage vs. potential plots. As stated before, we can start by considering the organic adsorption process as a solvent substitution process, where the water-solvent molecules are assumed to adopt three configurations at the interface: monomers pointing toward the solution (flip-up monomers,  $\uparrow$ ), monomers pointing toward the electrode (flip-down monomers,  $\downarrow$ ), and dimers with no net dipole ( $\rightleftharpoons$ ) (see Fig. 6.79). Thus the adsorption reaction may be written as (Jeng et al., 1992):



The adsorption process should also be greatly influenced by the heterogeneity of the surface, as discussed in Section 6.8.3, and by the lateral interactions among the adsorbed species (Section 6.8.2.3). Thus, from Eq. (6.266) it follows that

$$\mu_{\text{Org,soln}} + o\mu_{\text{w},\uparrow} + p\mu_{\text{w},\downarrow} + q\mu_{\text{w},\rightleftharpoons} = \mu_{\text{Org,ads}} + (o + p + q)\mu_{\text{w,soln}} \quad (6.267)$$

where the  $\mu$ 's are the chemical potentials of the corresponding species. In Table 6.15 an account of the corresponding variables is given. Thus, substituting the corresponding  $\mu$ 's into Eq. (6.267) gives

$$\frac{x_{\text{Org}}}{(x_{\text{w},\uparrow})^o (x_{\text{w},\downarrow})^p (x_{\text{w},\rightleftharpoons})^q} \exp \left( \frac{U_{\text{Org}} - oU_{\text{w},\uparrow} - pU_{\text{w},\downarrow} - qU_{\text{w},\rightleftharpoons}}{kT} \right) \exp \left( \frac{\sum_j \omega_{\text{Org},j}}{kT} \right) = \frac{c_{\text{Org}}}{55.5} K' \quad (6.268)$$

where  $U_i$  and  $x_i$  are the corresponding adsorption energy and molar fractions of adsorbed species, and  $\omega$  indicates the lateral interaction energies between adsorbed molecules.

**TABLE 6.15**  
**Variables Used in the Deduction of Eq. (6.270)**

Chemical Potentials:

$$\mu_{i,ads}: \quad \mu_{i,ads} = kT(\ln x_i - \ln f_i) + U_i + \sum_j \omega_{i,j}$$

$$\mu_{i,sol}: \quad \mu_{i,sol} = \mu_{i,sol}^0 + kT \ln x_{i,sol}$$

Lateral interactions:

$$\sum_j \omega_j \approx r_2 \theta^{3/2} + r_3 \theta^3$$

Surface heterogeneity:

$$rU_{Org} - oU_{w,\uparrow} - pU_{w,\downarrow} - qU_{w,\rightleftharpoons} = \Delta H_{\theta=0} + \Delta \Delta H_{\theta} = \Delta H_{\theta=0} + r\theta$$

Equilibrium constants:

$$K' = \left( \frac{f_{Org}}{f_{w,\uparrow}^o f_{w,\downarrow}^o f_{w,\rightleftharpoons}^o} \right) \exp \left( \frac{\sum_i \sum_j d_i \omega_{wi,j}}{kT} \right) \exp \left( \frac{\mu_{Org,sol}^0}{kT} \right) \exp \left( \frac{-n \mu_{w,sol}^0}{kT} \right)$$

$$K = K' \exp(-\Delta H_{\theta=0}/kT) = \frac{K_{Org}}{K_w}$$

Mole fractions:

$$x_{Org} = \frac{\theta}{\theta + 0.66n(1 - \theta)} \quad x_{w,\rightleftharpoons} = \frac{0.32n(1 - \theta)}{\theta + 0.66n(1 - \theta)}$$

$$x_{w,\uparrow} = \frac{0.32n(1 - \theta)}{\theta + 0.66n(1 - \theta)} \frac{e^y}{e^y + e^{-y}} \quad x_{w,\downarrow} = \frac{0.32n(1 - \theta)}{\theta + 0.66n(1 - \theta)} \frac{e^{-y}}{e^y + e^{-y}}$$

Coefficients of adsorption:

$$o = \frac{0.32ne^y}{0.66(e^y + e^{-y})} \quad p = \frac{0.32ne^{-y}}{0.66(e^y + e^{-y})} \quad q = \frac{0.17n}{0.66}$$

**TABLE 6.15**  
**Continued**

Where:

$x_i$  = molar fraction of the adsorbed species  $i$   
 $f_i$  = molecular partition function

$U_i$  = adsorption energy

$\omega$  = lateral interaction energies between adsorbed molecules

$\mu_{i,\text{sol}}^0$  = chemical potential of the pure substance

$x_{i,\text{sol}}$  = molar fraction of the species in solution  $x_{w,\text{sol}} \approx 1$

$x_{\text{Org},\text{sol}} \approx c_{\text{Org}}/55.5$

$r_1$  = change in  $\Delta H$  due to the effect of heterogeneity of the electrode surface

$r_2$  = dipole-dipole interactions

$r_3$  = dispersion interactions

$d_i$  = one of the coefficients  $o$ ,  $p$ , or  $q$

$\theta$  = surface coverage of adsorbed organic species

$$y = \frac{\vec{\mu}_w \vec{X}}{kT} - \frac{0.32 U_w c_w B_w}{kT}$$

$\vec{X}$  = electric field

$U_w$  = nearest-neighbor dipole interaction of water molecules

$c_w$  = coordination number = 6

0.32 is the fraction of coverage that has effective dipole-dipole interaction

$$B_w = x_{w\uparrow} - x_{w\downarrow} = \frac{0.32(e^y - e^{-y})}{0.66(e^y + e^{-y})}$$

$$= 0.485 \tanh y$$

$K_w = \exp(-\Delta G_w^\circ/kT)$  = equilibrium constant for water

$K_{\text{Org}} = \exp(-\Delta G_{\text{Org}}^\circ/kT)$  = equilibrium constant for the organic molecules

$\vec{\mu}$  = dipole moment

The effect of surface heterogeneity may be included in the  $U$  terms in Eq. (6.268), and the lateral interactions, which are mainly composed of dipole-dipole and dispersion interactions (see Eq. 6.232), are included as a sum of  $\omega$ 's. Introducing these effects into Eq. (6.268) (see Table 6.15) gives

$$\frac{x_{\text{Org}}}{(x_{w,\uparrow})^o (x_{w,\downarrow})^p (x_{w,\rightleftharpoons})^q} \exp[(r_1 \theta + r_2 \theta^{3/2} + r_3 \theta^3)/kT] = \frac{c_{\text{Org}}}{55.5} K \quad (6.269)$$

where  $r_1$  is the change in enthalpy due to the effect of heterogeneity of the electrode surface,  $r_2$  represents dipole-dipole interactions, and  $r_3$  dispersion interactions. The corresponding variables are described in full in Table 6.15. Equation (6.269) can be written as

$$\begin{aligned} & \frac{x_{\text{Org}}}{(x_{w,\uparrow})^o (x_{w,\downarrow})^p (x_{w,\rightleftharpoons})^q} \exp[(r_1 \theta + r_2 \theta^{3/2} + r_3 \theta^3)/kT] \\ &= \frac{c_{\text{Org}}}{55.5} \exp\left(\frac{-\Delta G_{\text{Org}}^\circ + n\Delta G_w^\circ}{kT}\right) \exp\left(\frac{\vec{\mu}_{\text{Org}} \vec{X}}{kT} - \frac{n\vec{\mu}_w \vec{X} B_w}{kT} + \frac{0.32 n U_w c B_w^2}{kT}\right) \quad (6.270) \end{aligned}$$



Equation (6.270) can be used to compare the experimental results of the coverage vs. potential curve. The result is shown in Fig. (6.112) for the adsorption of *n*-valeric acid and phenol on platinum electrodes.

Thus, Eq. (6.270) is an isoconic (see Section 6.8.6), which describes the adsorption of organic molecules on electrodes as a substitution process of solvent molecules and takes into account the surface heterogeneity and lateral interactions among the adsorbed species. This isoconic is able to successfully describe and reproduce the parabolic shape—with its maximum in the vicinity of the pzc—of the adsorption process of organic molecules.

### 6.9.6. Other Factors Influencing the Adsorption of Organic Molecules on Electrodes

**6.9.6.1. Structure, Size, and Orientation of the Adsorbed Organic Molecule.** In general, hydrocarbon chains, whether linear or branched, are expected to interact relatively weakly, both with water molecules and with the electrode material. Aliphatic molecules with functional groups (e.g., diols, sugars, or thiourea) may interact strongly with water molecules via H bonds and this interaction affects

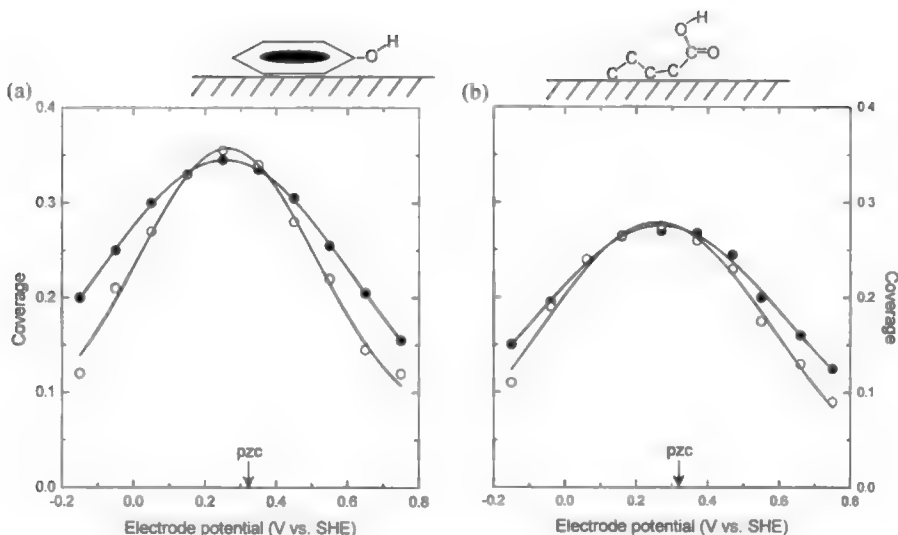


**Fig. 6.112.** Comparison of coverage vs. potential curves for (○) experimental and (●) theoretical [Eq. (6.270)] results predicted by the adsorption model for the adsorption of (a)  $10^{-5}$  M phenol and (b)  $10^{-4}$  M *n*-valeric acid on platinum electrodes. Under these experimental conditions, the pzc was found to be at about 0.35 V. (Reprinted from J. O'M. Bockris and K. T. Jeng, *J. Electroanal. Chem.* **330**: 541, Copyright 1992, Figs. 18, 19, and 20, with permission of Elsevier Science.)

the adsorptivity of the molecule. Aromatic compounds, with their  $\pi$ -electrons, tend to interact strongly with neighboring molecules and with electrodes.

The orientation of the adsorbed organic molecule may also vary with the type of molecule. Thus, linear aliphatic compounds adopt a vertical position that gives them a more negative free energy of adsorption [Fig. 6.113(a)]. Compounds with benzene rings tend to adopt a flat orientation due to strong interaction between  $\pi$ -electrons of the rings and the electrode. Unsaturated linear compounds generally adopt an orientation with their multiple bonds parallel to the surface.

Functional groups play an important role in the orientation of molecules as well, as in the case of thiophenol, which attaches to the surface vertically through its sulfur atom (instead of through its benzene ring) (Krznaniec et al., 1978), or urea, which bonds to Pt(100) through its  $\text{NH}_2$  groups (Fig. 6.114). Figure 6.113 shows how 16-mercaptohexadecanol molecules adsorb preferentially with their alkyl chains all tilted by the same angle of  $30^\circ$ , while 22-mercaptodocosanoic acid adsorbs with a large amount of disorder (Dannenberger et al., 1997). Naphthyl compounds adsorb more than phenyl compounds, and these latter more than butyl compounds in polycrystalline platinum electrodes.<sup>69</sup>

It is not uncommon to find that the adsorbed species change their orientation (reorientation process) under certain circumstances, such as an increase in the adsorbed population or a change in electrode potential. For example, adsorption of nicotinic acid on Pt(111) at negative potentials leads to attachment exclusively through its nitrogen, while at the most positive potential, both the aromatic nitrogen and carboxylate moiety are bonded to the surface (Hubbard, 1990). These reorientation processes may occur even when the changes produce a less favorable position, i.e., a position that produces a less negative free energy of adsorption. Also, this process is most commonly seen in compounds of the aromatic type, which tend to change from a flat to an edgewise orientation.

**6.9.6.2. Electrode Properties.** Another parameter that seems to play a significant role in the adsorption of organic molecules is the roughness of the electrode.<sup>70</sup> Roughness is sometimes a determining factor in how the organic molecules adsorb on an electrode. For example, the concentration of the adsorbed species tends to be smaller and the adsorption process slower on a rough surface than on a smooth one. Also, surface roughness inhibits flat-to-vertical reorientation of simple aromatics (White et al., 1984).

<sup>69</sup>Actually, the differences in adsorbability are impressive: naphthyl compounds adsorb  $10^4$  times more than butyl compounds and phenyl compounds adsorb  $10^2$  times more than the same butyl compounds (Jeng, 1992).

<sup>70</sup>The roughness is defined as the real area divided by the geometric area. Thus, consider a circular electrode of a 0.56-cm diameter and a geometric area of  $1 \text{ cm}^2$ . If this electrode is perfectly polished, its real area equals the geometric one and has a roughness nearly equal to 1. On the other hand, a highly rough surface (e.g., of real area  $100 \text{ cm}^2$ ) has a roughness equal to  $100/1 = 100$ .

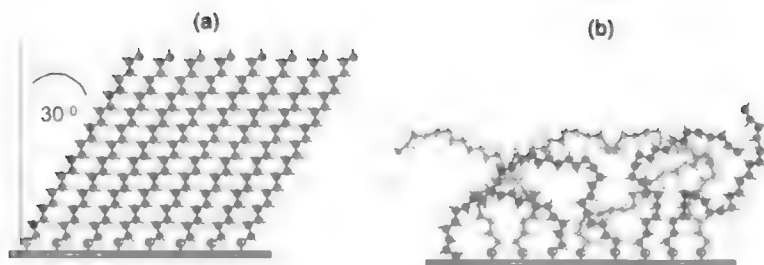


**Fig. 6.113.** Models for (a) 6-mercaptohexadecanol and (b) 22-mercaptopododecanoic acid, adsorbed on gold substrates investigated by near-edge X-ray absorption fine structure (NEXAFS) spectroscopy and X-ray photoelectron spectroscopy. (Reprinted from O. Dannenberger, K. Weiss, H. J. Himmel, B. Jäger, M. Buck, and Ch. Wöll, *Thin Solid Films* **307**: 183, copyright 1997, Fig. 6, with permission from Elsevier Science.)

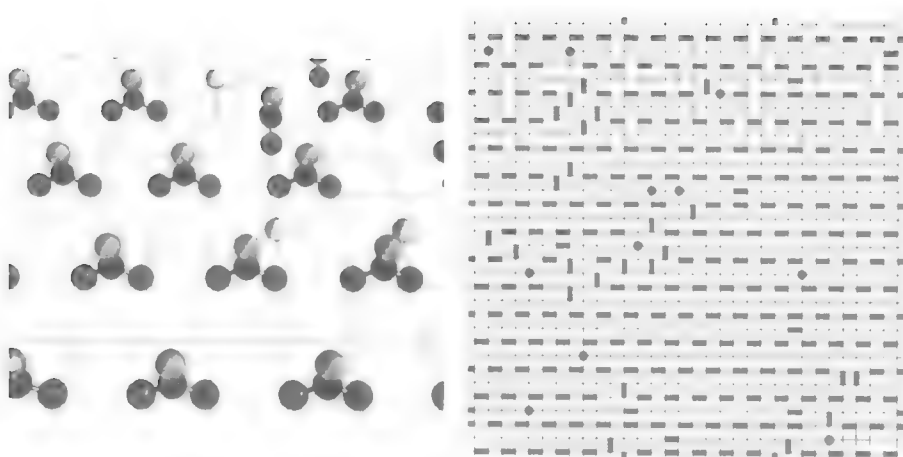


**Fig. 6.114.** (a) Illustration of a microscopic model of urea molecules, with their  $\text{NH}_2$  groups (dark gray) on the square Pt(100) lattice sites and their  $\text{C}=\text{O}$  groups (C, black and O, lighter gray) pointing away from the surface. The hydrogen atoms are shown as single light-gray spheres. (b) A typical equilibrium configuration is generated by Monte Carlo methods in the ordered  $c(2 \times 4)$  phase region at  $-60$  mV (urea, black rectangles and hydrogen, black circles). (Reprinted from P. A. Rikvold, M. Gamboa-Aldeco, J. Zhang, M. Han, Q. Wang, H. L. Richards, and A. Wieckowski, *Surf. Sci.* **335**: 389, copyright 1995, Fig. 3, with permission of Elsevier Science.)

Similarly, the crystal structure of the electrode influences the adsorption process of organic molecules. Adsorption on the most compact surfaces is generally stronger than in the most open surfaces. Thus, organic molecules tend to adsorb in the following order: (111) > (100) > (110), as shown in Figure 6.115 for the adsorption of various organic substances on different crystal faces of various metals (Trasatti, 1995).

Also, as would be expected, the type of metal (i.e., the electronic structure of the electrode) influences the adsorbability of the organic molecules. For example, Fig. 6.116 shows the free energy of adsorption of amyl alcohol and acetonitrile on different metals. This figure indicates how the adsorption energy of the organic molecule decreases as the strength of metal-water interaction increases (the  $\Delta X$  parameter in Fig. 6.116) (Trasatti, 1995).

**6.9.6.3. Electrolyte Properties.** As in the case of ionic adsorption, during the adsorption of organic species, solvent bonds have to be broken and formed, contributing to the total free energy of adsorption and influencing the adsorption of the organic species. Organic molecules are generally larger than the ions we studied in Section 6.8. Thus, during the adsorption process, several water molecules have to break their bonds with the metal to make room to adsorb the organic molecule. Similarly, the organic molecules may need to get rid of some of their hydration waters

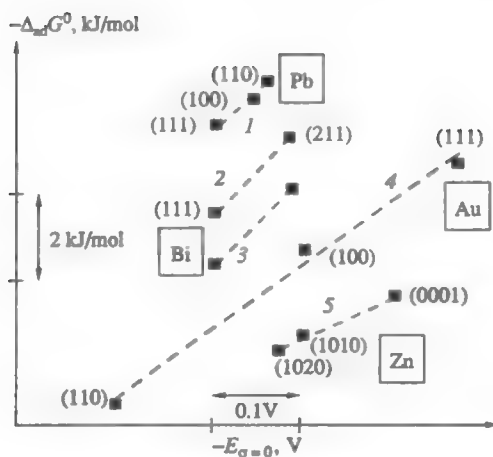


**Fig 6.115.** Gibbs energy change for adsorption of organic substances on different crystal faces of various metals, as a function of the corresponding potential of zero charge: cyclohexanol (1), camphor (2), cyclohexanol (3), diethylether (4), and cyclohexanol (5). (Reprinted from S. Trasatti, *Russ. J. Electrochem.* **31**: 713, 1995, Fig. 7.)

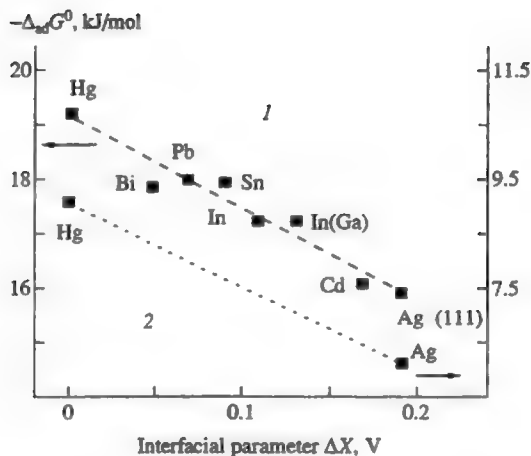


**Fig. 6.116.** Gibbs energy change for adsorption of amyl alcohol (1) and acetonitrile (2) on a number of sp-metals and Ag, as a function of the relative interfacial parameter. (Reprinted from S. Trasatti, *Russ. J. Electrochem.* **31**: 713, 1995, Fig. 8.)

before reaching the IHP. In this case, the hydrophilic (affinity of the organic for water) properties of the organic compound enable the water molecules to influence the orientation of the adsorbed species.

Another important aspect to consider is the solubility of the organic compound in the electrolyte. Compounds that are not very soluble will tend to adsorb easily on electrodes, where they may acquire a more stable (lower energy) position. For example, the less soluble naphthyl compounds show stronger adsorbidities on mercury than the more soluble butyl and phenyl compounds (Blomgren et al., 1961). Also, high concentration in solution (allowed by the solubility of the compound) accounts for faster adsorption and larger surface coverages.

Figures 6.117 and 6.58 show examples of the amount of surface covered by different organic molecules as a function of the concentration of the organic molecule in the electrolyte. We can identify these curves as isotherms (see Table 6.10). In organic adsorption, the most-used isotherm is the Frumkin one, namely,

$$\frac{\theta}{1 - \theta} = \beta c e^{-2a\theta} \quad (6.271)$$

where  $a$  is the *Frumkin interaction factor*, involving interaction of the adsorbed molecules. However, as in the case of adsorption of inorganic ions and as stated in the derivation of the isocon in Section 6.8.12, the adsorption of organic molecules is a far more complex process, where other factors besides the lateral interactions should

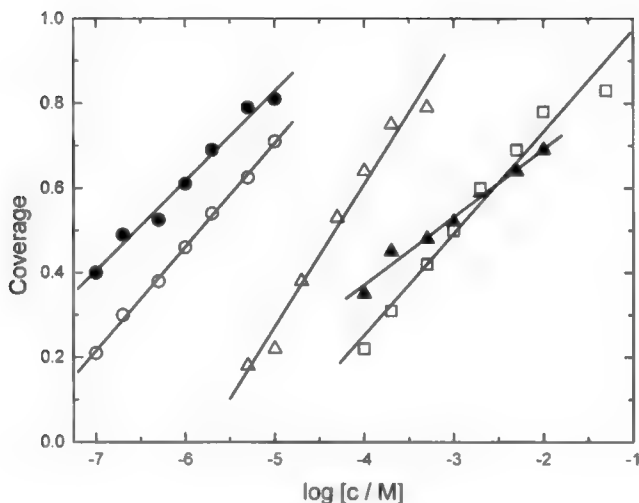


**Fig. 6.117.** Adsorption isotherms for various organic species on platinum in 0.01 *N* HCl solution, obtained with the radiotracer technique: valeric acid (▲), butanol (□), benzoic acid (△), naphthoic acid (●), naphthol (○). All the data are taken at the maximum adsorption potential. (Reprinted from J. Jeng, dissertation, Texas A&M University, 1991.)

be considered. Thus, in order to represent the isotherm appropriately through equations, the researcher should be sure to include all parameters that may influence the adsorption process of the organic molecule. There are several of these parameters. For example, in Section 6.9.5 it was seen how the adsorption of organic molecules should be considered as a substitution process of solvent molecules. Because of the sometimes large size of the adsorbing organic molecules, more than one solvent molecule may be displaced, as in the case of pyridine, which displaces *four* water molecules during its adsorption on platinum electrodes. The orientation of water dipoles and in many cases the organic molecule itself, are potential dependent and should be included as a parameter in the adsorption isotherms. It should not be forgotten that lateral interactions are important to consider during the adsorption process of molecules (see Section 6.9.4), and that these interactions are active, not only between the adsorbed organic molecules, but also between them and the solvent molecules. Properties of the adsorbent surface, such as its heterogeneity, may also play an important role, especially in the case of polycrystalline electrodes.<sup>71</sup>

<sup>71</sup>As explained in Section 6.8.10, the Temkin isotherm—the “logarithmic” isotherm—is derived by considering a heterogeneous surface. It can be written as [cf. Eq. (6.207)]  $\theta = 1/f \ln \beta_0 + 1/f \ln c$ . Thus, a plot of  $\theta$  vs.  $\ln c$  giving a straight line—as in the case of Fig. 6.117—suggests that the adsorption process giving rise to that curve is likely to be Temkin-like, i.e., governed by the heterogeneity of the surface.

## Further Reading

### Seminal

1. A. N. Frumkin, "The Influence of an Electric-Field on the Adsorption of Neutral Molecules," *Z. Phys.* **35**: 792 (1926).
2. E. Blomgren, J. O'M Bockris, and C. Jesch, "Adsorption of Aromatic Amines at the Interface of Mercury–Aqueous Solutions," *J. Phys. Chem.* **65**: 2000 (1961).
3. J. O'M. Bockris and K. T. Jeng, "In situ Studies of Adsorption of Organic Compounds on Platinum Electrodes," *J. Electroanal. Chem.* **330**: 541 (1992).

### Reviews

1. R. Guidelli, "Molecular Models of Organic Adsorption at Metal–Water Interfaces," in *Adsorption of Molecules at Metal Electrodes*, J. Lipkowski and P. N. Ross, eds., p. 1, VCH Publishers, New York (1992).

### Papers

1. D. Krznanric, P. Valenta, H. W. Nurnberg, and M. Branica, *J. Electroanal. Chem.* **93**:41 (1978).
2. J. H. White, M. P. Soriaga, and A. T. Hubbard, *J. Electroanal. Chem.* **117**: 89 (1984).
3. A. T. Hubbard, *Langmuir* **6**: 97 (1990).
4. E. J. Lust, K. K. Lust, and A. A. J. Jänes, *Russian J. Electrochem.* **31**(8): 807 (1995).
5. E. Umbach, C. Seidel, J. Taborski, R. Li, and A. Soukopp, *Phys. Stat. Sol (b)* **192**: 389 (1995).
6. V. Lazarescu, *Surface Sci.* **335**: 227 (1995).
7. M. H. Holzle, D. M. Kolb, D. Drznaric, and B. Cosovic, *Berichte der Bunsen Gesellschaft für Physikalische Chemie—An International J. of Phys. Chem.* **100**(11): 1779 (1996).
8. P. Nikitas, *Electrochim. Acta* **41**(14): 2159 (1996).
9. J. L. E. Campbell and F. C. Anson, *Langmuir* **12**: 4008 (1996).
10. B. N. Afanas'ev, Yu. P. Akulova, G. S. Aleksandrova, and I. A. Cherepkova, *Russ. J. Electrochem.* **33**(7): 700 (1997).
11. R. J. Hamers, J. S. Hovis, S. Lee, H. Liu, and J. Shan, *J. Phys. Chem. B* **101**(9): 1489 (1997).
12. J. F. E. Gootzen, A. H. Wonders, A. P. Cox, W. Visscchr, and J. A. R. van Veen, *J. Molec. Catalysis A: Chemical* **127**: 113 (1997).
13. Th. Dretschkow, A. S. Dakkouri, and Th. Wandlowski, *Langmuir* **13**(10): 2844 (1997).
14. R. H. Terrill, T. A. Tanzer, and P. W. Bohn, *Langmuir* **14**: 845 (1998).
15. E. Lust, A. Jänes, K. Lust, and A. Piidla, *J. Electroanal. Chem.* **442**: 189 (1998).

## 6.10. THE STRUCTURE OF OTHER INTERFACES

### 6.10.1. The Structure of the Semiconductor-Electrolyte Interface

6.10.1.1. *How Is the Charge Distributed inside a Solid Electrode?* Phenomena that depend on electric double layers comprise a general and very widespread part of the science of surfaces. They occur wherever phases (containing charged

particles or permanent or induced dipoles) meet to form an interface. Thus, double layers appear at air/solution, metal/solution, and solution/solution interfaces. Nevertheless, an impression might have been gained that only *metal*/solution interfaces are of consequence. If so, the impression will now be corrected by dealing in a very elementary way with another type of interface that is intellectually stimulating and technologically important, the *semiconductor*/electrolyte interface. This aspect of electrochemistry extends the scope of the subject beyond considerations of the *metal*/solution interface to all<sup>72</sup> interfaces at which electrons are exchanged. It thus opens up the prospect of understanding the electrochemistry of nonmetals, e.g., interfaces in biological systems and interfaces involving solid oxides.

In dealing with the metal/electrolyte interface, consideration of the metal was restricted to the statement that the charge density  $q_M$  was confined close to the surface of the metal and to a narrow region—a few angstroms—extending into the solution, (see Section 6.6.7). Thereafter, attention was turned to the solution side of the interface, i.e., toward the ionic double layer, and it was asked how the excess charges are arranged there as a function of distance from the metal, how the potential decays, how the concentration in the electrolyte affects the picture, etc. Now the viewpoint will be reversed. The situation in the solution will be considered to be understood, and the distribution of excess charge inside the electrode, i.e., the electronic double layer, will be scrutinized.

Consider a concentrated electrolytic solution. For all intents and purposes, the entire Gouy–Chapman diffuse charge will be located on the OHP (Section 6.6.4). Further, let there be no contact adsorption, so that the IHP is unpopulated. What is being considered, therefore, is a single layer of charge on the solution side of the interface.

What is the situation inside the electrode? That depends upon whether the electrode is a metal or a semiconductor. What is the most important difference between a metal and a semiconductor? Operationally speaking, it is the order of magnitude of the conductivity. Metals have conductivities on the order of about  $10^6 \text{ ohm}^{-1} \text{ cm}^{-1}$ ; and semiconductors, about  $10^2\text{--}10^{-9} \text{ ohm}^{-1} \text{ cm}^{-1}$ . These tremendous differences in conductivity reflect predominantly the concentration of free charge carriers. In crystalline solids, the atomic nuclei are relatively fixed, and the charge carriers that drift in response to electric fields are the electrons. So the question is: What determines the concentration of mobile electrons? One has to take an inside look at electrons in crystalline solids.

**6.10.1.2. The Band Theory of Crystalline Solids.** Consider a crystalline solid. The atoms are arranged according to a three-dimensional pattern (or lattice) in which they have equilibrium interatomic distances. A thought experiment is now performed. The lattice is expanded, i.e., the interatomic distances are increased.

<sup>72</sup>The theory of the electrochemistry of insulators derives from the theory of the semiconductor/solution interface.



Eventually the atoms are so far apart that they can be considered isolated and independent atoms, as in a gas.

The electrons in a gaseous atom are arranged in shells. The shell structure is a result of the energy levels of the electrons' having to follow quantum rules. Thus, only a set of discrete energy states is allowed, and all other energies are forbidden. The energy states are occupied by electrons in accordance with the Pauli exclusion principle: The maximum number of electrons per energy state is two, and these two electrons must have opposite spins. The energy states fall into groups or shells.

As one shell fills up with electrons, the Pauli principle rules that any further electrons have to move to shells more removed from the nucleus. (The electrons in an incomplete outermost shell are known as *valence* electrons, and those in filled inner shells are known as *core* electrons.) The location of the various electrons can be described by talking of an *electron cloud*; the density of this cloud at any point is a measure of the probability of finding the electron at that point.

Suppose now that two gaseous atoms are made to approach each other. As long as the electron clouds of the two atoms do not overlap, the electron-energy states continue to follow the quantum rules for gaseous atoms. When, however, the electron clouds begin to overlap and the electrons interact with both atoms, the rules for electron-energy states are upset and they start changing.

They change in an interesting way; each energy state from a gaseous atom splits into two states, one with a higher energy and the other with a lower energy (Fig. 6.118). If three atoms are brought together, then each energy state of the gaseous atoms splits into three energy states; if six atoms are brought together, the splitting is into six states; and, in general, if there are  $N$  atoms, each energy state of a gaseous atom splits into  $N$  states. Some of these levels may be degenerate, i.e., they may have exactly the same energy, but none can be lost or created, i.e., the number of energy levels, or states, in a crystal made up of  $N$  particles must equal  $N$  times the number of electronic states in each particle to satisfy Pauli's exclusion principle. The upper and lower levels shown in Fig. 6.118 arise because of the symmetrical and antisymmetrical linear combination of atomic orbitals.

The spacing between these  $N$  energy states depends on the value of  $N$ ; the larger the value of  $N$ , the closer together are the energy levels. In a bulky, solid electrode where there may be some  $10^{22}$  atoms  $\text{cm}^{-3}$ , the energy levels are spaced so close together that it is more convenient to ignore the discreteness of the levels and think of a continuous band of allowed energies.<sup>73</sup>

This means that as the expanded lattice is contracted in the thought experiment, the discrete energy states of the atoms are replaced by energy bands. Thus, when the lattice-contraction thought experiment is finally halted with atoms at their equilibrium interatomic distances, the electron-energy states show a band structure.

<sup>73</sup>For example, if the total energy range is 10 eV and the  $10^{22}$  levels are spaced equally apart, the distance between any two will be  $10^{-21}$  eV, or  $2.3 \times 10^{-17}$  cal mol<sup>-1</sup>, compared with the average thermal energy of about  $6 \times 10^2$  at room temperature.

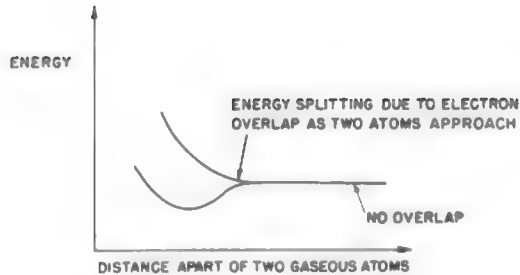


**Fig. 6.118.** The splitting of the energy into two energy states when two atoms approach each other.

The energy states of gaseous atoms split because of the overlap between electron clouds. Obviously, therefore, atoms must come much closer before the clouds of the core electrons begin to overlap compared with the distance at which the clouds of outer (or valence) electrons overlap (Fig. 6.119). Hence, at the equilibrium interatomic distances, the energy levels of the core electrons (in contrast to the valence electrons) do not show any band structure and therefore will be neglected in the following discussion. This simplified picture of the band theory of solids will now be used to explain the differences in conductivity of metals, semiconductors, and insulators.

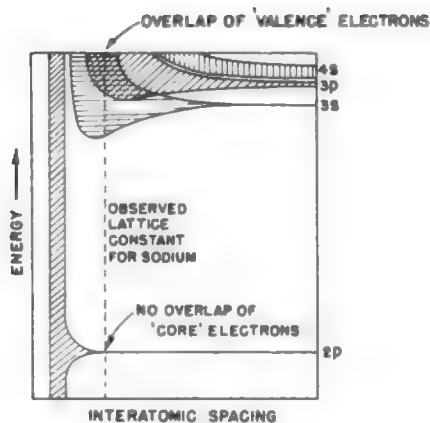


**Fig. 6.119.** The energy levels of the core electrons do not show any band structure. The band picture is for sodium (1s electrons not shown).

**6.10.1.3. Conductors, Insulators, and Semiconductors.** The essence of electrical conductivity is that charges must be able to move under an applied electric field. In solids, conduction requires the movement of electrons.<sup>74</sup> But, for an electron to move, there must be a partially vacant energy band. If all energy states in a band are completely filled, then an electron cannot move, for where can it move to when the Pauli principle says it cannot go into a filled state? So differences in conductivity between different substances must be a matter of vacant, or partially filled, bands.

Consider the electron-energy versus interatomic-spacing diagram (Fig. 6.120) picturing the result of the thought experiment in which an expanded lattice is contracted. Let this contraction be stopped when the equilibrium interatomic spacing is  $d_M$  (see Fig. 6.120). Then inside the crystal, the electron-energy states would be grouped into bands (see Fig. 6.120). One can talk of the lower, or valence band, which results from the overlap of filled valence orbitals of the individual atoms and the upper, or conduction band, which results from overlap of partially filled or empty higher orbitals of the atoms involved. In such a material, mobile electrons can arise in two ways. Either the valence band containing electrons is only partially filled and thus gives rise to electron states to which electrons can migrate, or, even if this band (valence band) is completely filled, it can overlap an unfilled band (conduction band) where unoccupied energy states permit electron drift (Fig. 6.120). Since there are plenty of valence electrons (at least one valence electron per atom) and also plenty of vacant states, the concentration of mobile charge carriers is high and so will be the conductivity that depends upon this concentration. *The crystal (e.g., copper) will show metallic conduction.*

If, however, the equilibrium interatomic spacing in a certain solid is  $d_1$  (Fig. 6.121), it is noticed that there exists a large range of forbidden energies between the first and second bands. Now, what happens if there are just enough available valence electrons to fill the first band, the valence band (Fig. 6.121)? Then, these electrons will not be able to find any easily accessible vacant energy states in the valence band for them to move into. Further, if the energy gap  $E_g$  is large compared with the thermal energy  $kT$  of the electrons, the electrons cannot be significantly thermally excited into the conduction band. In effect, therefore, there will be no mobile electrons in either band. *The material (e.g., diamond) will behave like an insulator.*

A third and most interesting possibility is when the equilibrium interatomic spacing in the solid is  $d_{SC}$  (Fig. 6.122). It will be noticed that here, too, the essence of this situation is that there is an energy gap separating the valence band from the upper band. But this energy gap, in contrast to that in the case of insulators, is not much more than the thermal energy of the electrons and therefore is small enough for electrons in the valence band (i.e., the electrons used for bonding atoms together) to be excited into the upper band (Table 6.16). The energy required for the excitation of electrons into the upper band may come from the thermal motions of electrons or from light shining

<sup>74</sup>Conduction involving the drift of ions is not under consideration here.

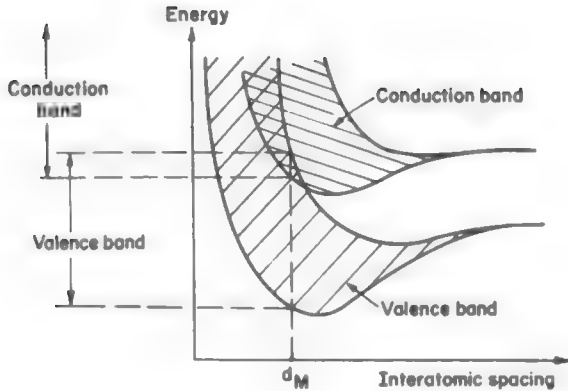


**Fig. 6.120.** The band picture of a metal with an interatomic spacing of  $d_M$ , showing an overlap of the valence and conduction bands.

on the material. Once they are in the upper band, these electrons find plenty of unoccupied energy states into which they can move. Hence, the conduction-band electrons can conduct electricity. *This is how an intrinsic semiconductor (e.g., silicon) conducts electricity.*

When an electron is excited across the energy gap  $E_g$  to the conduction band in an intrinsic semiconductor, an unoccupied energy state, or hole, is left behind in the normally full valence band. This vacant state can be jumped into by another electron

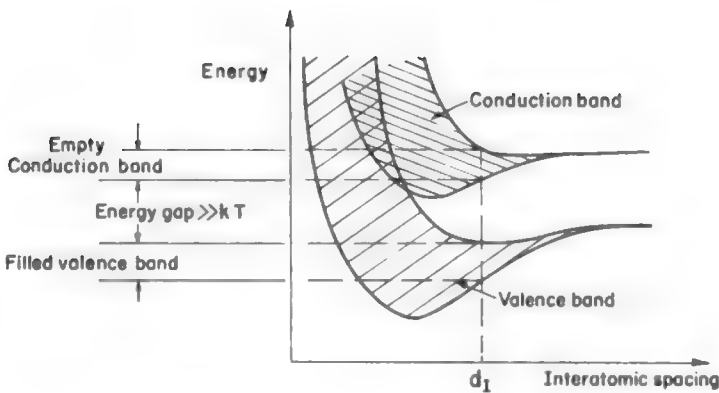


**Fig. 6.121.** The band picture of an insulator with an interatomic spacing of  $d_I$ , showing the filled valence band separated from the empty conduction band by a large energy gap.

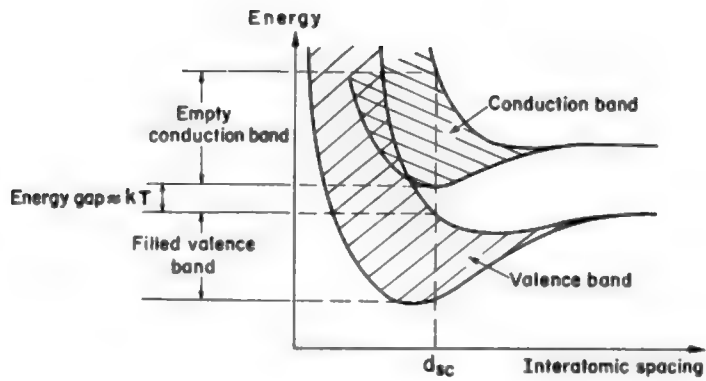


**Fig. 6.122.** The band picture of a semiconductor with an interatomic spacing of  $d_{sc}$ , showing the small energy gap between the valence and conduction band.

in the valence band (Fig. 6.123), but this leads to a vacant state in the place where the jumping electron was. The motion of electrons into unoccupied energy states, or holes, in the valence band is therefore equivalent to the movement of the vacant states, or holes, in the opposite direction. Since an electric field moves holes in an opposite direction to electrons, the holes may be treated as if they were positively charged (Fig. 6.124).

*6.10.1.4. Some Analogies between Semiconductors and Electrolytic Solutions.* Since the electrons of the valence band are used for bonding together atoms, the removal of a valence electron by excitation into the conduction band implies the rupture of a bond in the lattice. The creation of an electron-hole pair may therefore be treated as an ionization reaction

**TABLE 6.16**  
**Room-Temperature Energy Gap for Some Materials**

Substance	Energy gap (eV)
<i>Insulator</i>	
C, diamond	5.6
<i>Semiconductors</i>	
Germanium	0.656
Silicon	1.089
Tellurium	0.34
GaAs	1.35
InSb	0.17
PbS	0.37

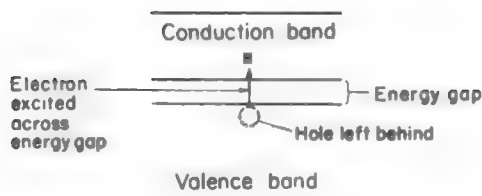
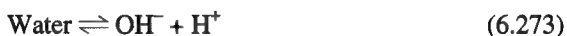


**Fig. 6.123.** The formation of a hole when an electron from the valence band is excited into the conduction band.



Viewed thus, it turns out that there are remarkable parallels between the ionization of the lattice of an intrinsic semiconductor and the ionization of water



Both equilibrium “reactions” can be treated by the law of mass action. Just as the product of the concentrations of hydroxyl ions and hydrogen ions remains a constant at a fixed temperature,

$$c_{\text{H}^+} \times c_{\text{OH}^-} = K_{\text{H}_2\text{O}} \quad (6.274)$$

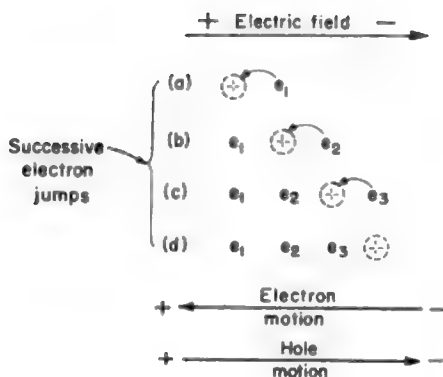


**Fig. 6.124.** Since hole motion is in a direction opposite to electron motion, a hole behaves as if it were positively charged.

the product of the electron  $n$  and hole  $p$  concentrations also remains a constant at a fixed temperature. The constant depends on the energy gap  $E_g$  across which the valence electrons must be excited into the conduction band

$$np = K_{sc} \quad (6.275)$$

where  $K_{sc}$  is a constant characteristic of the intrinsic semiconductor. Further, just as in pure water the concentrations of hydroxyl and hydrogen ions are equal, the electron and hole concentrations in an intrinsic semiconductor are equal

$$n = p = K_{sc}^{1/2} \quad (6.276)$$

When one examines the value of  $n = p$ , it turns out that the density of charge carriers in an intrinsic semiconductor (Table 6.16) at room temperature is in the range of  $10^{13}$  to  $10^{16} \text{ cm}^{-3}$ , compared with about  $10^{22} \text{ cm}^{-3}$  in a metal. It is this relatively low concentration of charge carriers in intrinsic semiconductors that is responsible for the most important differences between semiconductor electrodes and metal electrodes.

**6.10.1.5. The Diffuse-Charge Region inside an Intrinsic Semiconductor: The Garrett-Brattain Space Charge.** After this elementary account of the constitution of an intrinsic semiconductor, one can consider the basic question posed in Section 6.10.1.1. Given a layer of charge on the OHP of the electrolyte, how do the electrons and holes inside an intrinsic semiconductor distribute themselves as a function of distance from the interface?

Garrett and Brattain were the first to attack this problem by elaborating on its formal similarity to the problem of a diffuse charge in solution. Inside the electrolyte, the positive and negative ions are the charge carriers; inside the semiconductor, there are the holes and electrons. In the electrolyte bulk, the excess-charge density in any volume element is zero because the numbers per unit volume of positive and negative charges are exactly equal; similarly, deep inside the intrinsic semiconductor, the excess-charge density is zero because of the equality of the density of electrons  $n^0$  and holes  $p^0$ . Thus, for the semiconductor bulk,

$$n^0 = p^0 \quad (6.277)$$

and

$$e_{\text{bulk}} = e_0 p^0 - e_0 n^0 = 0 \quad (6.278)$$

The charged electrode exerts an electric field on the positive and negative ions in the electrolyte; similarly, the sheet of charge on the OHP exerts an electric field on the holes and electrons in the intrinsic semiconductor so that relatively near the surface, electrons and holes are not present in equal numbers.

The charge density  $\rho_x$  on any electrolyte lamina parallel to the electrode and a distance  $x$  from it can be obtained by the application of electrostatics (Poisson's equation) and the Boltzmann distribution. Similarly, one can write for the *intrinsic semiconductor*, Poisson's equation

$$\rho_x = -\epsilon\epsilon_0 \frac{d^2\psi_x}{dx^2} \quad (6.279)$$

and the Boltzmann distribution

$$\begin{aligned} \rho_x &= e_0(p_x - n_x) \\ &= e_0(p^0 e^{-e_0\psi_x/kT} - n^0 e^{e_0\psi_x/kT}) \end{aligned} \quad (6.280)$$

where  $\psi_x$  is the Volta potential of the semiconductor at a distance  $x$  from the electrode surface ( $\psi_{x \rightarrow \infty}$  is taken as zero). Using the relation (6.277), one has

$$\begin{aligned} \rho_x &= -e_0 n^0 (e^{e_0\psi_x/kT} - e^{-e_0\psi_x/kT}) \\ &= -2e_0 n^0 \sinh e_0\psi_x/kT \end{aligned} \quad (6.281)$$

The two expressions for the charge density can be equated to give the Poisson-Boltzmann equation

$$\frac{d^2\psi_x}{dx^2} = \frac{2e_0 n^0}{\epsilon\epsilon_0} \sinh \frac{e_0\psi_x}{kT} \quad (6.282)$$

This differential equation for the space variation of the potential inside the semiconductor can be easily identified with that for the space variation of the potential inside the electrolyte in the Gouy-Chapman theory of the diffuse layer (Section 6.6.1). The solution can therefore be borrowed from the diffuse-layer theory. One has, from Eq. (6.125),

$$\frac{d\psi_x}{dx} = - \left( \frac{8kTn^0}{\epsilon\epsilon_0} \right)^{1/2} \sinh \frac{e_0\psi_x}{2kT} \quad (6.283)$$

and, from Eq. (6.127)

$$q_{sc} = 2(\epsilon\epsilon_0 n^0 kT)^{1/2} \sinh \frac{e_0\psi_s}{2kT} \quad (6.284)$$



where  $q_{sc}$  is total space charge, and  $\psi_s$  is the potential at the surface of the semiconductor.

These results have important consequences. By linearizing the hyperbolic sine function<sup>75</sup>

$$\sinh \frac{e_0 \psi_x}{2kT} \approx \frac{e_0 \psi_x}{2kT} \quad (6.285)$$

and solving the differential equation (see Section 6.6.4)

$$\frac{d\psi_x}{dx} = - \left( \frac{2n^0 e_0^2}{\epsilon \epsilon_0 kT} \right)^{1/2} \psi_x = -\kappa \psi_x \quad (6.286)$$

one gets

$$\psi_x = \psi_s e^{-\kappa x} \quad (6.287)$$

There is (Fig. 6.125) thus an exponential decay of potential due to the space charge inside the semiconductor.

This potential decay implies that there is a field inside the semiconductor and that the excess-charge density slowly decays to zero as if there were an electronic cloud analogous to the ionic cloud adjacent to an electrode in solution. It can be seen that the potential due to the atmosphere of holes and electrons is characterized by the same parameter

$$\kappa = \left( \frac{2n^0 e_0^2}{\epsilon \epsilon_0 kT} \right)^{1/2} \quad (6.288)$$

as that which occurs in the Debye-Hückel ionic cloud and the Gouy-Chapman diffuse-charge treatments. The term  $\kappa^{-1}$  is the measure of the thickness of the Garrett-Brattain space charge inside a semiconductor. The value of  $\kappa^{-1}$  diminishes as the bulk concentration of charge carriers increases. What this means is that as the carrier concentration increases, the thickness of the space-charge region decreases. This is one way of looking at a metal; because of its high concentration of charge carriers, the space charge is all squeezed onto the surface. The situation here is analogous to the diffuse charge in solution, which gets compressed on the OHP when the electrolyte concentration is sufficiently high.

It has just been pointed out that owing to the existence of a layer of charge in the solution, there is a space charge and a potential drop inside the semiconductor. Any electron in this space-charge region will interact with the field, and its energy will

<sup>75</sup>The system still gives an equation of the form of (6.287) even when the linearization condition is dropped.

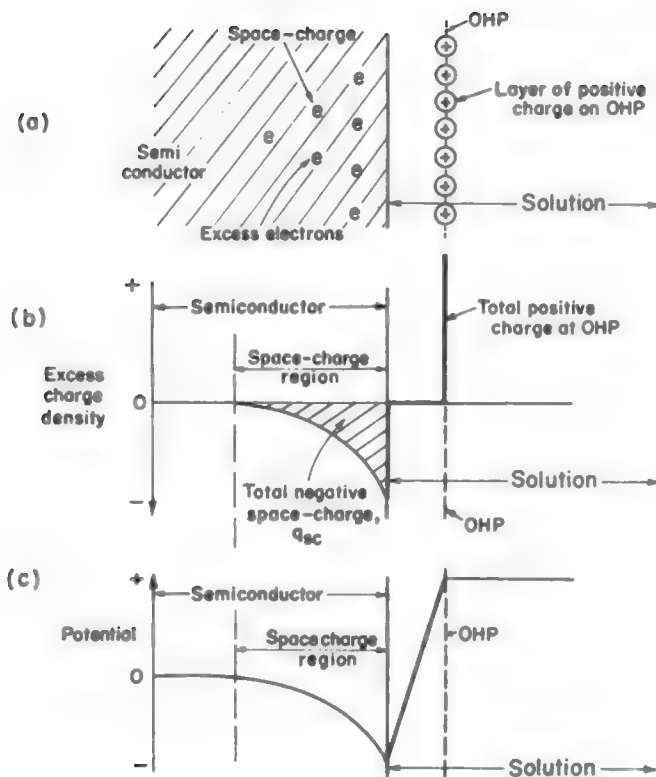


**Fig. 6.125.** (a) The space charge inside a semiconductor, (b) the corresponding charge-density variation, and (c) the potential variation.

either increase or decrease compared with the value in the absence of the field. The value of the electron energy in the absence of the field has been shown to be given by the band structure of the solid.

What this implies is that the energy bands near the surface of an intrinsic semiconductor are disturbed by the existence of a field. The electron energies are given by the sum of the energies due to the intrinsic-band structure and that due to the deviation of the inner potential from its zero value in the bulk. Thus, near the surface, there is a bending of the bands up or down, depending upon the sign of the ionic charge populating the OHP (Fig. 6.126).

**6.10.1.6. The Differential Capacity Due to the Space Charge.** When capacity measurements are carried out on a semiconductor/electrolyte interface, one must not forget that the space-charge region inside the semiconductor has the ability to store charge. The contribution of this region to the differential capacity of the interface can

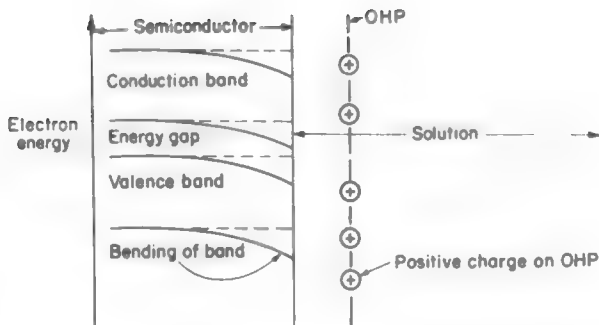


**Fig. 6.126.** The bending of bands near the surface of a semiconductor.

be easily calculated. One simply differentiates the expression (6.284) for  $q_{sc}$  by the potential drop  $\Psi_s$  inside the intrinsic semiconductor. Thus,

$$C_{sc} = \frac{dq_{sc}}{d\Psi_s} = 2 (\epsilon\epsilon_0 n_0 kT) \cosh \frac{e_0 \Psi_s}{kT} \quad (6.289)$$

One expects that the differential capacity of a semiconductor/electrolyte interface due to the space charge inside an intrinsic semiconductor will vary in a hyperbolic cosine manner with the potential. Such a variation is shown in Fig. 6.127.

It will be seen that the values of the space-charge capacities are low ( $\sim 0.01\text{--}1 \mu\text{F cm}^{-2}$ ) compared with the capacities ( $\sim 17 \mu\text{F cm}^{-2}$ ) of the region between the semiconductor surface and the OHP plane, the Helmholtz–Perrin parallel-plate region. That is why the space-charge capacities (the inverted parabolas) are noticed, for the observed capacity is given by two capacitors in series, the space charge,  $C_{sc}$ , and Helmholtz–Perrin  $C_{HP}$  capacitors. Thus,

$$\frac{1}{C_{obs}} = \frac{1}{C_{sc}} + \frac{1}{C_{HP}} \quad (6.290)$$

but  $C_{HP} \gg C_{sc}$  and hence,

$$\frac{1}{C_{obs}} \approx \frac{1}{C_{sc}} \quad (6.291)$$

When the electrolyte is dilute, then a diffuse-charge region will appear in the solution, too. There will be three potential drops: one inside the semiconductor, the Garrett–Brattain drop  $\Delta\phi_{sc}$ ; a linear Helmholtz–Perrin drop  $\Delta\phi_{HP}$ ; and, finally, the Gouy–Chapman drop  $\Delta\phi_{GC}$  in the solution. The total  $\Delta\phi$  across the interface is given by

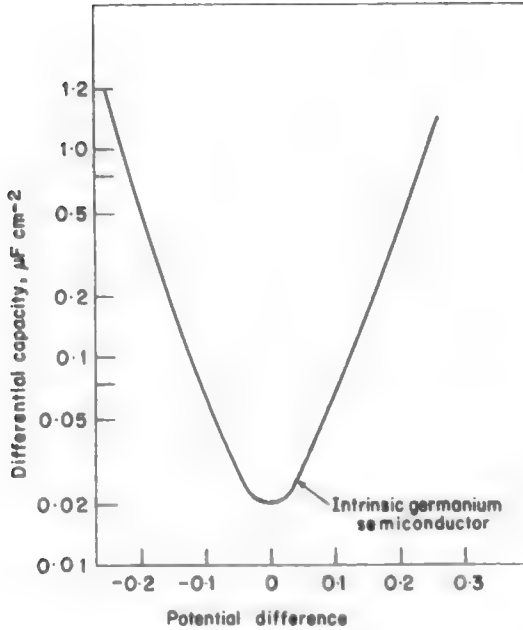


**Fig. 6.127.** The differential capacity of a semiconductor/electrolyte interface has a cosh dependence on the potential.

$$\Delta\phi = \Delta\phi_{\text{sc}} + \Delta\phi_{\text{HP}} + \Delta\phi_{\text{GC}} \quad (6.292)$$

and the total differential capacity by

$$\frac{1}{C} = \frac{1}{C_{\text{sc}}} + \frac{1}{C_{\text{HP}}} + \frac{1}{C_{\text{GC}}} \quad (6.293)$$

Thus, there are three capacitors in series at a semiconductor/electrolyte interface rather than two capacitors as at a metal/solution interface. What is observed largely depends upon the electron concentration in the semiconductor (how low it is) and the ionic concentration in solution.

**6.10.1.7. Impurity Semiconductors, n-Type and p-Type.** The discussion has been restricted so far to pure intrinsic semiconductors exemplified by germanium and silicon. In these substances, there is a low concentration of charge carriers (compared with metals). Further, the hole and electron concentrations are equal, and their product is a constant given by the law of mass action

$$np = K_{\text{sc}} \quad (6.294)$$

Intrinsic semiconductors have been compared to pure water in which the  $\text{OH}^-$  and  $\text{H}^+$  concentrations are equal and the product of these concentrations is a constant  $K_w$

$$C_{\text{OH}^-} C_{\text{H}^+} = K_w \quad (6.295)$$

In the case of water, however, the concentration of either the  $\text{OH}^-$  or  $\text{H}^+$  ions can be decreased by adding proton donors (acids) or proton acceptors (bases). Thus, a proton donor releases hydrogen ions into the solution (i.e.,  $C_{\text{H}^+}$  increases), and the only way the product  $K_w$  (i.e.,  $C_{\text{OH}^-} C_{\text{H}^+}$ ) remains a constant is by a decrease in  $C_{\text{OH}^-}$ .

Is there an analogous situation in semiconductors? If one adds an electron donor (say, arsenic) to an intrinsic semiconductor (say, germanium), then the ionization of arsenic



releases electrons into the system, and the hole concentration goes down to preserve the constancy of the product  $np$  [see Eq. (6.294)]. In this way, the electron concentration can be made so large compared with the hole concentration that the conduction is predominantly by electrons; the substance is known as an  $n$ -type of semiconductor.

There is also a parallel in semiconductors to the effect of adding a base, or proton acceptor, to water. This involves the addition of an electron acceptor (say, gallium) to an intrinsic semiconductor. The electron acceptors ionize thus



and by accepting electrons force up the hole concentration in the valence band. Such a “doped” semiconductor will conduct mainly by holes; it is known as a  $p$ -type of semiconductor.

What the addition of electron acceptors and donors means in the band picture can be easily understood from Figs. 6.128 and 6.129. The electron acceptors and donors enter the lattice of the semiconductor and introduce electron-energy levels between the valence and conduction bands. Thus, with an  $n$ -type of semiconductor (Fig. 6.128), only a small part of the electrons in the conduction band arise by thermal excitation from the valence band; the rest come from the ionization of electron donors. The hole concentration, however, depends only upon the number of valence electrons that are excited into the conduction band. The hole concentration can therefore be made small.

The band-picture explanation of the  $p$ -type of semiconductor (Fig. 6.129) is in terms of the electron-acceptor levels appearing in the energy gap near the top of the valence band. The electron-acceptor atoms can then easily receive electrons from the valence band. Thus, holes are created in the valence band without the corresponding electrons in the conduction band. The conduction, therefore, is essentially by holes—a  $p$ -type of semiconductor.

The conclusion from this description of  $n$ - and  $p$ -types of semiconductors is that the concentration of holes and electrons is not only low, but it can be varied by doping

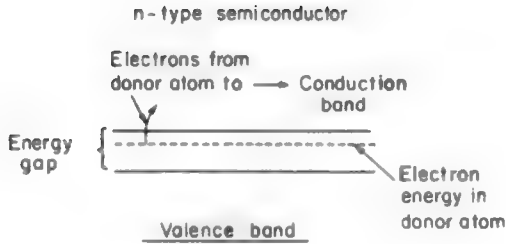


**Fig. 6.128.** The band picture of *n*-type semiconductors.

the material with varying amounts of electron acceptors or donors. Apart from this variability in the choice of electron and hole concentrations, the treatment of the space charge in *n*- and *p*-types of semiconductors is basically the same as that of intrinsic semiconductors. One important difference, however, is that even though the excess-charge density is zero in the bulk of the impurity semiconductor, this is not simply because the electron and hole concentrations are equal. Rather, the electroneutrality condition must be written as

$$n^0 + n_A = p^0 + n_D \quad (6.298)$$

where  $n^0$  and  $p^0$  are the bulk concentrations of electrons and holes, and  $n_A$  and  $n_D$  are the numbers per unit volume of electron acceptors and electron donors which are added to the intrinsic semiconductor. In other words, in the bulk of the impurity semiconductor, the total negative-charge density is equal to the total positive-charge density, taking into account the added donor or acceptor ions.

Another point to remember in the treatment of the diffuse charge inside a doped, or impurity semiconductor is that although the electron acceptors and donors affect the electroneutrality, they should be considered immobile and fixed in the lattice. Thus,

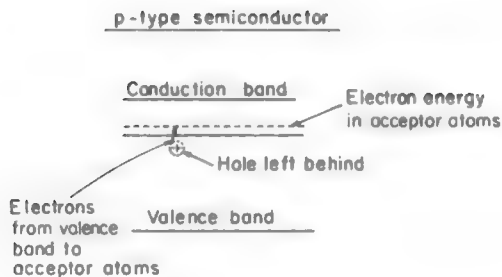


**Fig. 6.129.** The band picture of *p*-type semiconductors.

their concentration remains uniform inside the doped semiconductor, in contrast to that of the electron and hole concentrations, which are decided by the interplay of electrical and thermal forces.

These differences between intrinsic and doped, or impurity, semiconductors complicate the mathematics of the solution of the Poisson–Boltzmann equation, but the picture that emerges remains basically the same: A charged cloud, or space charge, and therefore a potential drop, develops inside the semiconductor; the space charge contributes to the capacity of the interphase, etc.

**6.10.1.8. Surface States: The Semiconductor Analogue of Contact Adsorption.** In the simple theory of the space charge inside a semiconductor, it was assumed that all the electrons and holes are free to move up to the surface. Being susceptible to thermal motion, their concentrations from  $x = 0$  to  $x \rightarrow \infty$  were said to be given by the interplay of electrical and thermal forces only, as expressed by the Boltzmann distribution law and Poisson's equation.

What happens, however, if electrons become bound in such a way that they cannot move in a direction normal to the interface? Then the simple theory of the space charge will have to be modified. There is a charge trapped in the surface energy states (i.e., those energy levels for electrons or holes which are different from those present in the bulk and which are localized at the surface of the semiconductor). The trapped charge will have to be excluded from a space-charge analysis in which the only charges considered were those that could distribute themselves freely under thermal and electric fields.

Surface states force a change in the picture of the double layer inside the semiconductor in the same way that contact-adsorbed ions alter the simple Gouy–Chapman picture of the diffuse charge in solution (Fig. 6.130). The presence of contact-adsorbed ions at a metal/solution interface means that the total Gouy–Chapman diffuse charge in solution and the potential drop across the diffuse-charge region is reduced. Similarly, the existence of surface states means that charge and the potential drop across the Garrett–Brattain space-charge region is reduced. At a high enough density of surface states, it can be assumed that there is hardly any space charge and hardly any potential drop inside the semiconductor. The semiconductor is in fact behaving like a metal—most of its charge is on the surface. This is analogous to the situation in metal/solution interfaces where the magnitude of the charge due to contact-adsorbed ions is almost equal to that on the metal. Under these circumstances, there is hardly any Gouy–Chapman diffuse charge.

What is the atomistic nature of surface states? A complete answer to this question is not yet available, but there is strong evidence that one source of surface states is the adsorption of atoms on the semiconductor surface. Thus, hydrogen atoms adsorbed on a germanium surface apparently behave as surface states. The space charge is then reduced so drastically that the germanium/solution interface behaves like a metal/solution interface, e.g., the capacities come into the approximate  $10 \mu\text{F cm}^{-2}$  range.

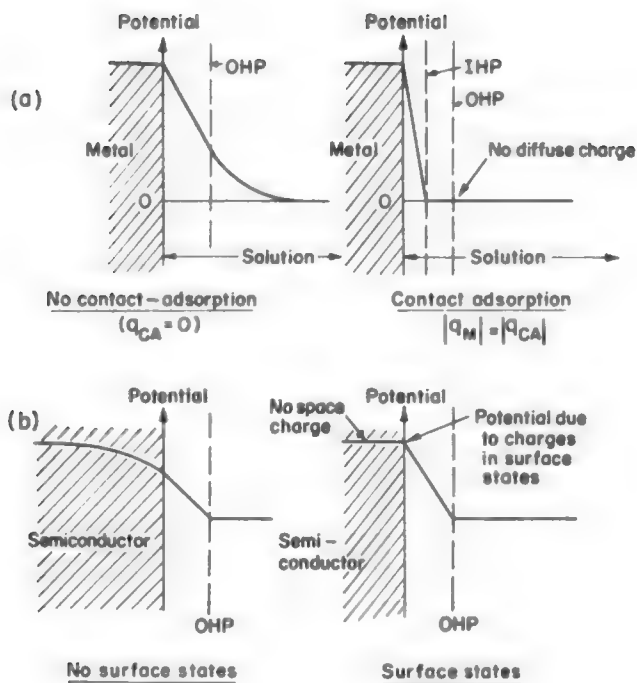


**Fig. 6.130.** The analogy between the role of surface states in the semiconductor and contact-adsorbed ions in the solution.

The study of surface states, therefore, is vital to an understanding of the semiconductor/electrolyte interface.

## 6.10.2. Colloid Chemistry

**6.10.2.1. Colloids: The Thickness of the Double Layer and the Bulk Dimensions Are of the Same Order.** The sizes of the phases forming the electrified interface have not quantitatively entered the picture so far. There has been a certain extravagance with dimensions. If, for instance, the metal in contact with the electrolyte was a sphere (e.g., a mercury drop), its radius was assumed to be infinitely large compared with any dimensions characteristic of the double layer, e.g., the thickness  $\kappa^{-1}$  of the Gouy region. Such large metal spheres, dropped into a solution, sink to the bottom of the vessel and lie there stable and immobile.

What would happen if the radii of the spheres were made smaller and smaller? In general, changes in the magnitude of a parameter (size, temperature, time, velocity, field, etc.) ultimately lead to new phenomena. Thus, the engineer knows well that “scaling up” or “scaling down” generally results in new modes of behavior.



In the case of the “shrinking” metal spheres, too, important new aspects of behavior arise when such spheres attain submicroscopic dimensions (10 to 10,000 Å), i.e., dimensions of the same order of magnitude as, and smaller than, the wavelength of the light used by microscopes. The little metal spheres begin to show the behavior of what is called the *colloidal* state of matter—an in-between world where the particles are too gross to display the fine behavior of atoms and too minute to reveal the bulk properties of macroscopic matter. The key to understanding the colloidal state lies in knowledge of the structure of electrified interfaces: Colloid chemistry is electrochemistry. How double layers assume such significant roles will now be briefly sketched.

Referring again to the metal spheres of submicroscopic dimensions, one point becomes clear. The smaller they are (~ microns), the more they react to the thermal “kicks” from the ions and water molecules of the electrolyte; they take off on a random walk through the solution. Large (~ centimeters) spheres also exchange momentum with the particles of the solution, but their masses are huge compared with those of ions or molecules, so that the velocities resulting (to the spheres) from such collisions are essentially zero.

Once the microspheres begin to jump about in Brownian movement in the solution, some of them collide with each other. What should happen when two approximately  $10^{-5}$ -cm metal spheres collide? Many aspects of colloidal chemistry—and hence of molecular biology, including the electrochemical basis of the stability of blood and the forming of clots—are illuminated by a consideration of this subject.

#### 6.10.2.2. *The Interaction of Double Layers and the Stability of Colloids.*

The first thing to remember is that each metal sphere sees its environment through its charged interface; each sphere is enveloped in a double layer. All the concepts and pictures of the electrified interface that have been developed in this chapter are of immediate relevance<sup>76</sup> to the microspheres rushing toward a collision.

Considering dilute solutions and no contact-adsorbing ions, one can picture each metal sphere surrounded by a (Gouy–Chapman) region of diffuse charge. Note, however, that the Gouy–Chapman layers of both colliding spheres contain charges of the *same sign*. Thus, there is *Coulombic repulsion as the two spheres come close*. This repulsion energy depends on the distance apart  $r$  of the spheres and varies with distance in the same way as the Gouy–Chapman potential. This dependence on distance is approximately given by  $\Psi_0 e^{-\kappa r}$  (see Section 6.6.4). One is talking here about the interaction of two double layers.

Not only do double layers interact with double layers, the metal of one sphere also interacts with the metal of the second sphere. There is what is called the *van der Waals attraction*, which is essentially a dispersion interaction that depends on  $r^{-6}$ , and the electron overlap repulsion, which varies as  $r^{-12}$ . These interactions between the bulk

<sup>76</sup>The surfaces being considered are not planar, and therefore instead of Helmholtz–Perrin parallel-plate condensers, one has concentric-sphere capacitors; Gouy–Chapman regions show radial instead of planar symmetry. All such points complicate the mathematics, but lead to few new truths. Hence, such details will be ignored in this very simple account of the dominating role of double layers in colloid chemistry.

of the two colloidal metal spheres will be represented by a term  $-Ar^{-6} + Br^{-12}$ , where  $A$  and  $B$  depend on the chemical composition of the phase dispersed in the solution.

The total interaction between the two metal spheres can therefore be classified into two parts: (1) the surface, or double-layer, interaction determined by the Gouy–Chapman potential  $\psi_0 e^{-\kappa r}$  and (2) the volume, or bulk, interaction  $-Ar^{-6} + Br^{-12}$ . The interaction between double layers ranges from indifference at large distances to increasing repulsion as the particles approach. The bulk interaction leads to an attraction unless the spheres get too close, when there is a sharp repulsion (Fig. 6.131). The total interaction energy depends on the interplay of the surface (double layer) and volume (bulk) effects and may be represented thus

$$U_{\text{total}} = \psi_0 e^{-\kappa r} + (-Ar^{-6} + Br^{-12}) \quad (6.299)$$

This approximate formula contains information concerning what happens when two colloidal particles (the two metal spheres) collide. One has to plot this total interaction energy  $U_{\text{total}}$  against the distance apart of the particles.

Consider one type of energy-distance diagram (Fig. 6.131). It is seen that for the first type of behavior where electrostatic repulsion dominates, the net energy  $U_{\text{total}}$  is always positive; this means that two metal spheres under this condition cannot stick together stably. Note that (Fig. 6.131), if the spheres did not wrap themselves in double layers, the interaction between the particles themselves, neglecting the double-layer repulsion, would dominate and have a minimum in a negative potential energy region corresponding, therefore, to a favoring of the aggregation of colloidal particles. Thus,

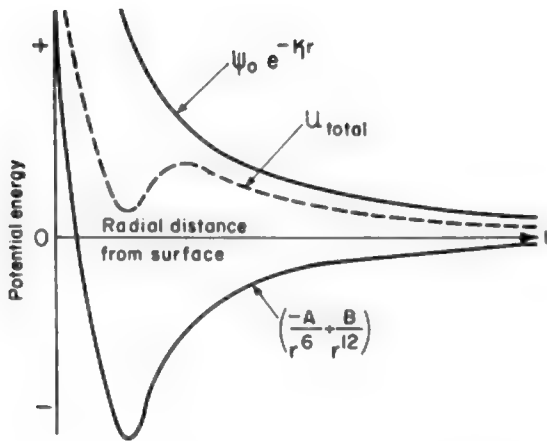


**Fig. 6.131.** The energy of interaction between two colloidal particles as a function of their distance apart, when the conditions factor stability of the colloid.

particles of colloidal dimensions survive aggregation into macroscopic phases *only* because their boundaries are guarded by electrified interfaces. The repulsion between double layers is the key to the stability of colloids.

It has been shown, however, in some detail (Section 6.6.4), that the structure of an electrified interface and therefore the potential drop across it markedly depend on the composition of the electrolyte. Make the solution concentrated by adding some electrolyte, and the Gouy–Chapman region starts being reduced in thickness and the potential falls sharply. Put in contact-adsorbing ions, and they start populating the IHP, which gives a region of linear potential drop. All this means that by varying the solution composition one can exert indirect control over the double-layer contribution and therefore the total interaction energy for two colloidal particles. One can control the stability of colloids.

How can colloidal particles be made to aggregate? The bulk-interaction curve is given by nature for a given material; it cannot be altered. Hence, what one has to do is to get lower Gouy–Chapman potentials at the  $r_{\min}$  distance. This is easy; one adds more electrolyte to the solution. The  $n^0$  of Eq. (3.43) increases,  $\kappa$  increases, and, since  $\psi = \psi_0 e^{-\kappa r}$ ,  $\psi$  falls more sharply with distance. In other words, the Gouy–Chapman region is compressed, and the total interaction curve becomes negative and shows a minimum at  $r_{\min}$  (Fig. 6.132). Two metal spheres approaching each other get irreversibly stuck together at this distance. The colloid has lost its stability. This is known as *coagulation*, or *flocculation*.

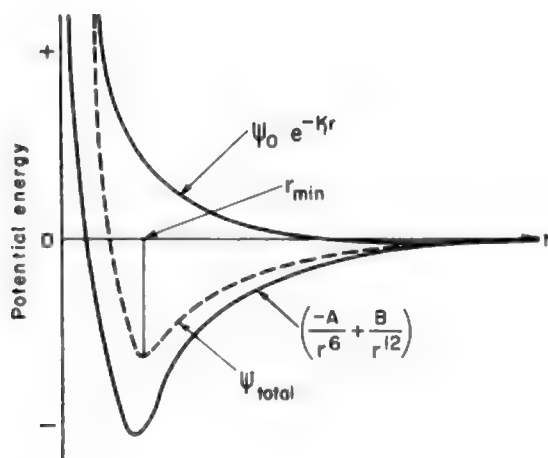


**Fig. 6.132.** The energy of interaction between two colloidal particles as a function of their distance apart, when the conditions factor coagulation of the colloid.

There is another way of bringing about this irreversible flocculation. Recall that by contact adsorption of ions, the bulk of the potential drop across the interface can be made to occur between the metal and the IHP. Thus, by the addition of contact-adsorbing ions, the value of  $\psi_0$  can be reduced without significantly changing the concentration of the bulk electrolyte. The effect of this will be qualitatively similar to that shown in Fig. 6.132 and is shown in Fig. 6.133. The value of  $U_{\text{total}}$  again comes into the negative potential-energy region, i.e., a stable configuration of particles in contact may exist, and a flocculation thus again occurs.

**6.10.2.3. Sols and Gels.** The essence of the behavior characteristic of the colloidal state is that double-layer interactions are as significant as bulk interactions. In other words, surface interactions are on a par with volume interactions. This condition can therefore be realized in all systems where the surface-to-volume ratios are high, i.e., at submicroscopic dimensions.

One type of colloidal system has been chosen for discussion, a system in which the solid metal phase has been shrunk in three dimensions to give small solid particles in Brownian motion in a solution. Such a colloidal suspension consisting of discrete, separate particles immersed in a continuous phase is known as a *sol*. One can also have a case where only two dimensions (e.g., the height  $z$  and breadth  $y$  of a cube) are shrunk to colloidal dimensions. The result is long spaghetti-like particles dispersed in solution—macromolecular solutions.

Instead of having one phase discontinuous and in the form of separate particles, it is possible to have the phase as a continuous matrix with pores of very fine dimensions running through it. This is a porous mass, or membrane, also known as a

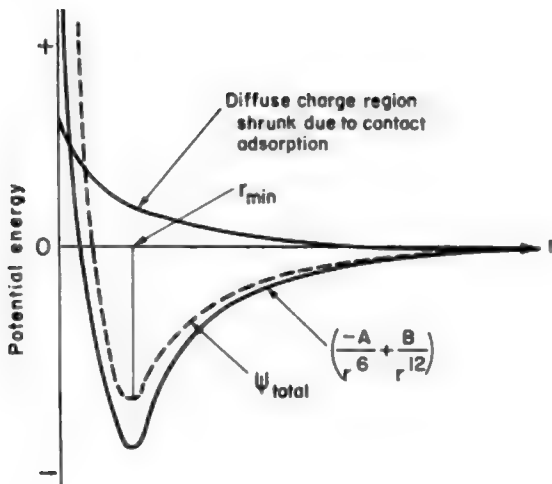


**Fig. 6.133.** The effect of the contact adsorption of ions on the condition of the stability of a colloid.

*gel*. In such membranes, interactions inside the pores become highly dependent on double-layer interactions.

Sols and gels are frequently partakers in biological processes. A living cell is separated from the outside by a membrane (a gel), and inside is a collection of colloidal particles held in suspension by interacting Gouy layers. A vivid example of this is given by the electrochemical mechanism of the clotting of blood. Blood clots at a metal/solution interface when the potential difference across it exceeds a critical value. This provides a basis for the control of thrombosis. Electrified interfaces are indeed essential to life, but there is something else that is essential, too. Charge transfer must occur for life to go on. In other words, charges must leak across electrified interfaces, as for example in the consumption of oxygen at the interfaces of biological cells. This transfer of charge across electrical double layers, which constitutes the very extensive field of *electrodics*, will be examined in other chapters of this book.

## 6.11. DOUBLE LAYERS BETWEEN PHASES MOVING RELATIVE TO EACH OTHER

### 6.11.1 The Phenomenology of Mobile Electrified Interfaces: Electrokinetic Properties

The double layer has hitherto been considered still, or static, in the sense that the bulk phases that meet at the interface are at rest relative to each other. When, however, one of the phases moves relative to the other, interesting electrical phenomena arise—*electrokinetic phenomena*.

Consider that a potential difference is applied across a glass capillary tube filled with an electrolytic solution (Fig. 6.134). What would one expect? Of course, one would expect a current to flow through the capillary according to Ohm's law. In practice, however, a remarkable and unexpected phenomenon is observed. In addition to the current, the solution itself begins to flow—the phenomenon of *electro-osmosis*. Liquid flow is generally associated with the application of a pressure gradient, but in this case it appears that a potential difference is doing the job normally achieved by a pressure difference.

This phenomenon of electro-osmosis can be treated in mathematical form. The fact is that the velocity of flow of electrolyte,  $v$ , depends not only on its usual driving

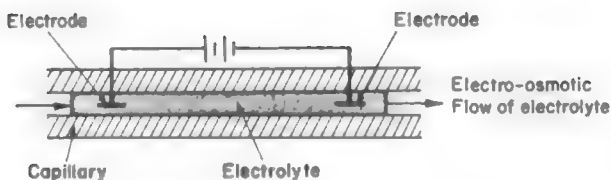


**Fig. 6.134.** The phenomenon of electro-osmosis.

force (i.e., a pressure gradient  $\Delta P$ ) but also on the electric field  $\vec{X}$ . When the driving forces are small, it can always be assumed that there are linear relations between driving forces and the resulting flows. Hence,

$$v = a_1 \Delta P + a_2 \vec{X} \quad (6.300)$$

Even when the usual driving force  $\Delta P$  is absent ( $\Delta P = 0$ ), one still has

$$v = a_2 \vec{X} \quad \text{or} \quad \frac{v}{\vec{X}} = a_2$$

Thus the coefficient  $a_2$  describes the electro-osmotic flow velocity per unit of potential gradient, i.e., the electro-osmotic mobility.

An obvious idea arises now. If an electric field  $\vec{X}$  can achieve what a pressure difference  $\Delta P$  normally does, namely, produce a liquid flow, then perhaps a pressure difference will produce an electric current, which is normally the result of an electric field. Experiment (Fig. 6.135) once again yields an interesting answer; an electric current known as a *streaming current* is in fact produced by a pressure difference.

One can transcribe the phenomenon in the form of an equation following the same thinking as for electro-osmosis. One says: A current density  $j$  results not only from an electric field but also from a pressure difference  $\Delta P$ , and, for small  $\vec{X}$  and  $\Delta P$ ,

$$j = a_3 \Delta P + a_4 \vec{X} \quad (6.301)$$

Even when the usual driving force  $\vec{X}$  is absent ( $\vec{X} = 0$ ), one still has

$$j = a_3 \Delta P \quad \text{or} \quad \frac{j}{\Delta P} = a_3 \quad (6.302)$$

The streaming-current constant  $a_3$  is the streaming-current density produced by a unit pressure difference.

If both sides of Eq. (6.302) are divided by the specific conductivity  $\sigma$  of the electrolyte, it is clear that

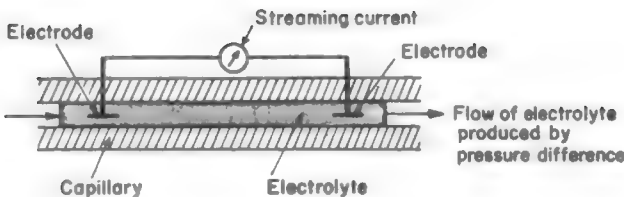


Fig. 6.135. The phenomenon of streaming current.

$$\vec{X} = \frac{i}{\sigma} = \frac{a_3}{\sigma} \Delta P \quad (6.303)$$

In words, the application of a pressure difference in an electrolyte should produce a potential difference and a corresponding electric field. This is the phenomenon of *streaming potential*.

What has been done so far is to take experimental laws and express them in the form of phenomenological equations, i.e., Eqs. (6.300) and (6.301). Just as the phenomenological equations describing the equilibrium properties of material systems constitute the subject matter of equilibrium thermodynamics, the above phenomenological equations describing the flow properties fall within the purview of nonequilibrium thermodynamics. In this latter subject, the Onsager reciprocity relation occupies a fundamental place (see Section 4.5.7).

The Onsager reciprocity relation, when applied to the present context, predicts that the cross coefficients  $a_2$  and  $a_3$ , which determine the rate of flow of liquid due to the applied electric field and the current passing due to a hydrostatic pressure difference, respectively, are equal, i.e.,

$$\left( \frac{i}{\Delta P} \right)_{X=0} = a_3 = a_2 = \left( \frac{v}{X} \right)_{P=0} \quad (6.304)$$

In words, the prediction is that the current per unit of pressure gradient should be equal to the fluid flow velocity per unit of electric field. Experiments prove that this is indeed the case.

As long as one remains within the framework of thermodynamics (whether the equilibrium or nonequilibrium variety), one always has to appeal to experiment for the values of coefficients. To calculate them, one must leave phenomenology and turn to models so that the atomistic mechanisms underlying the phenomenological laws are revealed. This will be done now, and, interestingly enough, it will be seen that the electrokinetic phenomena—electro-osmosis, streaming current, and streaming potential—depend on the electrification of the interface between the two phases.

### 6.11.2. The Relative Motion of One of the Phases Constituting an Electrified Interface Produces a Streaming Current

To give an atomistic interpretation of electrokinetic phenomena, one must consider questions such as: What happens when one of the phases moves relative to the other? For example, what happens when the electrolyte is made to flow past an electrode at rest?

Consider a plane electrode in an electrolytic solution dilute enough for there to be a “thick” diffuse layer, i.e., one that is hundreds or thousands of angstroms thick. Suppose now that a pressure difference is applied on the electrolytic solution in a direction parallel to the electrode. The electrolyte will begin to flow. When the liquid

attains a steady velocity (zero acceleration), the pressure difference is equal to the viscous force, i.e., to the viscosity,  $\eta$ , times the velocity gradient,  $dv/dx$ ,

$$\Delta P = \eta \frac{dv}{dx} \quad (6.305)$$

How does the velocity  $v$  vary with the distance  $x$  from the electrode? The velocity of the viscous fluid depends on  $x$ , as shown in Fig. 6.136. At  $x = 0$ , i.e., at the solid surface, the velocity is zero because the solid exerts forces on the fluid particles and does not allow them to slip past. This is equivalent to considering that the charges on the IHP and OHP are fixed and immobile. As one goes away from the electrode and from the OHP, the fluid velocity increases (assumed linear increase) and reaches a constant value.

The thickness of the diffuse-charge region is given by  $\kappa^{-1}$ , i.e., the Debye-Hückel parameter (Section 6.6.4). Thus, if the fluid velocity is  $v$  at the distance  $\kappa^{-1}$ , then the velocity gradient is given by

$$\frac{dv}{dx} = \frac{v}{\kappa^{-1}} \quad (6.306)$$

The charge in the diffuse layer can be considered equivalent to the Gouy charge density  $q_d$  placed at a distance  $\kappa^{-1}$  from the OHP. This gives rise to a parallel-plate condenser model. The potential at one plate—deep in the solution side—is taken at zero, while the potential at the other plate—which coincides with the OHP—is  $\psi_0$ . This latter potential is often referred to in the study of electrokinetic phenomena as the *zeta* ( $\zeta$ ) *potential*. Thus,

$$\psi_0 = \frac{4\pi q_d \kappa^{-1}}{\epsilon} \quad (6.307)$$

or

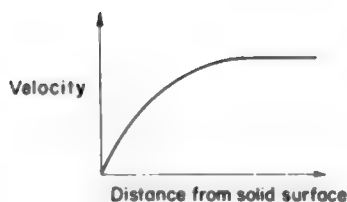


**Fig. 6.136.** The variation of fluid velocity with distance from the solid surface.



$$\frac{1}{\kappa^{-1}} = \frac{4\pi q_d}{\Psi_0 \epsilon} \quad (6.308)$$

This expression (6.308) for  $1/\kappa^{-1}$  can be inserted into Eq. (6.306), and the result into Eq. (6.305) to obtain

$$\Delta P = \left( \frac{4\pi\eta}{\Psi_0 \epsilon} \right) q_d v \quad (6.309)$$

According to the model (Fig. 6.137), a charge of  $q_d$  coulombs is in a unit area ( $1 \text{ cm}^2$ ) of a plane parallel to the immobile, solid phase. When this charge moves through a transit plane of unit area ( $1 \text{ cm}^2$ ) normal to the solid phase, it means that a charge of  $q_d$  coulombs  $\text{cm}^{-3}$  moves with a velocity of  $v \text{ cm s}^{-1}$  and gives rise to a current density  $j = q_d v$ . Hence, substituting this equation into Eq. (6.309), and transforming,

$$\frac{j}{\Delta P} = \frac{\Psi_0 \epsilon}{4\pi\eta} = a_3 \quad (6.310)$$

Thus, one has obtained an atomistic picture for the streaming-current density, i.e., the current density produced per unit of pressure gradient.

If one divides both sides by the specific conductivity of the electrolyte, one gets an atomistic expression for the streaming potential [see Eq. (6.302)],

$$\frac{\vec{X}}{\Delta P} = \frac{\Psi_0 \epsilon}{4\pi\eta\sigma} = \frac{a_3}{\sigma} \quad (6.311)$$

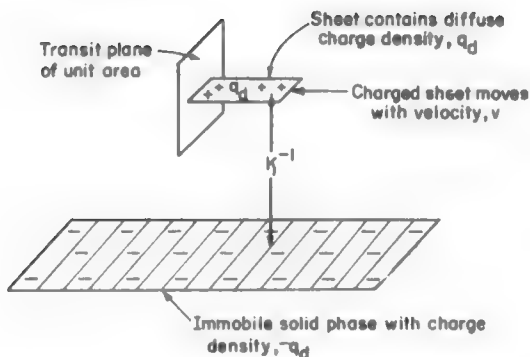


**Fig. 6.137.** A schematic diagram for the computation of the streaming-current density.

where  $\vec{X}$  is the electric field, or the gradient of the streaming potential in the direction of movement of the liquid, caused by the pressure difference  $\Delta P$ .

The phenomenon turns out to depend on the fact that there is a diffuse-charge region near the electrode. If there is no diffuse charge [i.e., if all the diffuse charge is “fixed” on the OHP (as in concentrated solutions)], there are no excess charges in any volume element in the solution and the phenomenon of a streaming current and streaming potential disappears. Any factor (e.g., contact adsorption of ions or concentration of electrolyte) that affects  $\psi_0$  also affects the streaming current.

### 6.11.3. A Potential Difference Applied Parallel to an Electrified Interface Produces an Electro-osmotic Motion of One of the Phases Relative to the Other

Instead of applying a pressure difference, one can apply a potential difference to the electrolyte in a direction parallel to the interface (Fig. 6.138). Once again a layer of charge  $q_d$  at a distance  $\kappa^{-1}$  from the solid, immobile phase will be assumed to represent the diffuse-charge region of the interface.

This layer of diffuse charge  $q_d$  will experience an electric force  $q_d \vec{X}$ . The charged layer on the solution side will begin to move. But the motion of the charged fluid is opposed by a viscous force that is once again given [see Eq. 6.309] by  $\eta(v/\kappa^{-1})$  or  $(4\pi\eta/\psi_0\epsilon)q_d v$ . When the electrolyte attains a steady velocity, the electric and viscous forces are exactly equal. Hence,

$$\vec{X} q_d = \frac{4\pi\eta}{\psi_0\epsilon} q_d v \quad (6.312)$$

or [from (6.304)],

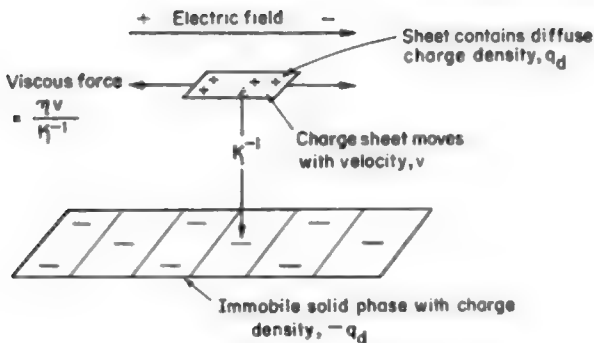


**Fig. 6.138.** A schematic diagram for the computation of the electro-osmotic mobility.

$$\frac{v}{\vec{X}} = \frac{\Psi_0 \epsilon}{4\pi\eta} = a_2 \quad (6.313)$$

But  $v/\vec{X}$  is the electro-osmotic velocity of the fluid per unit of electric field, i.e., the electro-osmotic mobility. It is interesting to note that both the electro-osmotic mobility  $v/\vec{X} = a_2$  and the streaming-current coefficient  $j/\Delta P = a_3$  have been proved to be equal to each other and to  $\Psi_0 \epsilon / 4\pi\eta$ . This only means that the Onsager reciprocity relation has been shown to be consistent with a simple model of some electrokinetic phenomena.

#### 6.11.4. Electrophoresis: Moving Solid Particles in a Stationary Electrolyte

Electrokinetic phenomena depend on the relative motion of the phases constituting the double layer. In the treatment of electro-osmotic mobility, the electrolyte was considered to move within a stationary capillary—a moving cylinder of liquids within a static cylinder of solid. But the arguments only need relative motion; the arguments would be equally valid if one considered a moving cylindrical solid within a stationary liquid.

The solid phase must be large enough to have at its interface a double layer. Then, equating the viscous force created by the movement of the particle to the electrical force due to the interaction of the field with the charge on the particle, one obtains

$$\frac{v}{\vec{X}} = \frac{\Psi_0 \epsilon}{4\pi\eta} \quad (6.314)$$

This equation was derived above for the movement of a liquid through a stationary solid phase. Its application here to the movement of colloidal particles under experimental conditions that render the liquid medium immobile implies that the solid particle is large compared with the dimensions of the diffuse double layer  $\kappa^{-1}$ . It is customary to term this movement of the solid phase electrophoresis. The phenomenon is observed with particles suspended in a liquid (Fig. 6.139).

The charge  $q_d$  in the diffuse double layer around a colloidal particle moving in the electric field has the same problem as the ionic atmosphere around a moving ion (see Section 4.6.4). On the one hand, it tries to move with the particle to which it is attached. On the other hand, it is influenced by the electric field, which pulls it in the opposite direction. The particle apparently wins. It moves through the liquid with a diffuse double layer surrounding it, although it is not actually carrying the oppositely charged ionic atmosphere with it but leaving part of it behind and rebuilding it in front as it moves along. The tendency of the ions in the diffuse double layer to move in the direction opposite to the movement of the particles has its effect on the particle. It produces a “drag” that slows down the movement of the particle much as the ionic cloud slows down the movement of ions and affects their mobility (see Section 4.6.4).

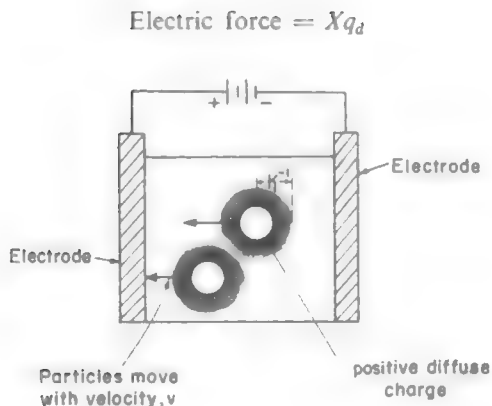


**Fig. 6.139.** The phenomenon of electrophoresis.

Equation (6.313) indicates that electrophoretic mobility is independent of the shape of the particles. Suppose, however, that the particle is spherical. Then one could arrive at the electrophoretic mobility in a completely different way and in a manner used to calculate the electrophoretic effect in conduction (see Section 4.6.4). One starts with Stokes' law (see Section 4.4.8)

$$\text{Viscous force} = 6\pi\kappa^{-1}\eta v \quad (6.315)$$

and say that (Fig. 6.139) the moving entity has a radius  $\kappa^{-1}$  (i.e., a particle of radius  $a$  contained in its thick ionic cloud of radius  $\kappa^{-1}$ ). The electric force on the particle plus cloud is given by the field times the charge on the cloud, which is  $q_d$ . Now,  $q_d$  can be related to the potential  $\Psi_0$  (at the surface of the particle) in a manner characteristic of the decay of potential from a charged sphere, i.e.,

$$\Psi_0 = \frac{q_d}{\epsilon\kappa^{-1}} \quad (6.316)$$

(This assumes that the radius  $a$  of the sphere  $\ll \kappa^{-1}$ .) Hence, the electric force is  $\vec{X}\Psi_0\epsilon\kappa^{-1}$ .

When the particle attains a steady-state velocity, the electric and viscous forces are exactly equal and by utilizing Stokes' law with  $\kappa^{-1}$  as the radius,

$$\frac{v}{X} = \frac{\Psi_0\epsilon}{6\pi\eta} \quad (6.317)$$

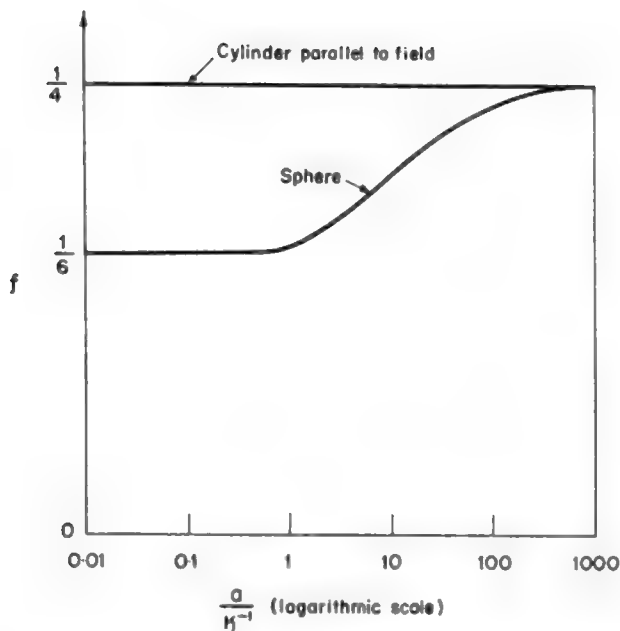


**Fig. 6.140.** The variation of the numerical factor  $f$  with the ratio of the radius  $a$  of the particle to the effective thickness  $\kappa^{-1}$  of the diffuse-charge region.

If one compares Eqs. (6.317) and (6.314) everything is fine, except that this Stokes' law approach gives a numerical factor  $f = \frac{1}{6}$ , whereas the electro-osmotic approach gives  $f = \frac{1}{4}$ . It turns out that each is right for a particular set of conditions. This conclusion comes out of an accurate mathematical treatment that results in the following expression for the electrophoretic velocity:

$$\frac{v}{X} = f \frac{\epsilon \Psi_0}{\pi \eta} \quad (6.318)$$

The quantity  $f$  is a numerical factor that depends on the ratio  $a/\kappa^{-1}$ , where  $a$  is the radius of the spherical or cylindrical particle. In other words,  $f$  depends on the ratio of the radius of the particle to the effective thickness  $\kappa^{-1}$  of the diffuse layer. When  $a/\kappa^{-1}$  is large, (the particle large in comparison with the diffuse-charge thickness), the numerical factor is always equal to  $\frac{1}{4}$  irrespective of the shape of the particle. When the particle is small compared with the thickness of the double layer,  $f$  is  $\frac{1}{4}$  for cylindrical particles parallel to the field and  $\frac{1}{6}$  for spherical particles (Fig. 6.140).

## Further Reading

### Seminal

1. B. V. Deryaguin and L. V. Landau, "The Basic Theory of Interactions Between Colloid Particles," *Acta Physicochim.* **44**: 633 (1941).
2. E. J. W. Verwey and J. Th. G. Overbeck, *Theory of the Stability of Lyophobic Colloids*, Elsevier, Amsterdam (1948).

### Reviews

1. S. S. Dukhin, "Electrochemical Characterization of the Surface of a Small Particle and Nonequilibrium Electric Surface Phenomena," *Adv. Coll. Interf. Sci.* **61**: 17 (1995).
2. K. Sarmini and E. Kenndler, "Influence of Organic Solvents on the Separation Selectivity in Capillary Electrophoresis," *J. Chromatog.* **792**(1-2): 3 (1997).
3. A. M. Grancaric, T. Pusic, I. Soljagic, and V. Ribitsch, "Influence of Electrokinetic Potential on Adsorption of Cationic Surfactants," *Textile Chemist Colorist* **29**(12): 33 (1997).

### Modern

1. E. Rodier and J. Dodds, *Particle Systems Characterization* **12**(4): 198 (1995).
2. J. E. Sandoval and S. M. Chen, *Anal. Chem.* **68**(17): 2771 (1996).
3. H. G. Herz and S. K. Ratkje, *Electrochim. Acta* **41**(1): 159 (1996).
4. J. C. Liu and M. C. Wu, *Water Science & Technology* **36**(4): 127 (1997).
5. A. Williams and G. Vigh, *Anal. Chem.* **69**(21): 4445 (1997).
6. K. J. Kim, A. G. Fane, M. Nystrom, and A. Pihlajamaki, *J. Membrane Sci.* **134**(2): 199 (1997).
7. A. Szymczyk, A. Pierre, J. C. Reggiani, and J. Pagetti, *J. Membrane Sci.* **134**(1): 59 (1997).
8. M. Pontie, X. Chasseray, D. Lemordant, and J. M. Laine, *J. Membrane Sci.* **129**(1): 125 (1997).
9. T. Jimbo, T. M. Higa, N. Minoura, and A. Tanioka, *Macromolecules* **31**(4): 1277 (1998).

## EXERCISES

Note to the reader: You will find that a number of the exercises and problems have a name in parentheses at the end. The problems have been taken from a wide range of sources, and have been supplied by scientists from all over the world. It is their names that appear in the parentheses.

1. Define the following terms used in Section 6.1: (a) adsorption, (b) absorption, (c) interphase, and (d) electrical double layer. (Gamboa-Aldeco)
2. (a) Draw a schematic representation of the charges at a metal solution interphase region. Consider the metal negatively charged (say, eight negative charges).

Refer to Figs. 6.4 and 6.5 in the text. (b) Draw a schematic representation of the charges in the bulk of solution. Refer to Fig. 6.2. (c) Draw a schematic representation of the charges at a metal solution interphase. Consider the metal positively charged, (d) Bring the three schematics into one drawing to form an electrochemical cell. How many charges should be drawn to maintain electroneutrality in the cell? (Gamboa-Aldeco)

3. (a) When the terminals of a 100-V battery are connected to two parallel plates 1 cm apart, what is the electrical field in the region between the plates? (b) How does it compare with the field in the interphase region? (Gamboa-Aldeco)
4. Describe the formation of an electrified interface with and without one of the phases connected to an external source of charge. (Gamboa-Aldeco)
5. Write down in an explicit form [cf Eq. (6.9)] the potential difference of the system in Fig. 6.31. (Gamboa-Aldeco)
6. A point charge in a vacuum has a charge of  $1 \times 10^{-9}$  C. Compute the electric field,  $\vec{X}$ , caused by this charge at 0.1, 0.5, 0.8, 1.0, and 1.5 cm. Plot  $\vec{X}$  as a function of the distance from the point charge. (Gamboa-Aldeco)
7. Define the following terms used in Section 6.2: (a) single crystal, (b) polycrystalline solid, (c) *in situ* technique, (d) *ex situ* technique, (e) diffraction pattern, (f) infrared radiation, (g) s-polarized and p-polarized light, and (h) radioactive isotope. (Gamboa-Aldeco)
8. Figure 6.47 shows that different crystalline faces of a given metal have different electron work functions,  $\Phi$ . Explain this tendency. Determine the difference in surface potential of the gold faces (100) and (111) with respect to the (110) in volts. (Gamboa-Aldeco)
9. Define the following terms used in Section 6.3: (a) electrochemical cell, (b) ideally nonpolarizable and polarizable interfaces, (c) relative electrode potential, (d) outer potential, (e) inner potential, (f) surface potential, (g) image forces, (h) Coulombic forces, (i) electrochemical potential, (j) chemical potential, (k) electron work function, (l) "just outside the metal," and (m) absolute potential. (Gamboa-Aldeco)
10. (a) Name and describe three recognized potentials in terms of which the interfacial region can be discussed. (b) What are the corresponding potential differences that they make up? (c) Can any of these potentials or potential differences be measured and if so, which ones? (Bockris)
11. Table E.1 is a list of reduction potentials of several reactions given in the *relative*-electrode potential scale. Write the potentials of the same reactions in

the *absolute*-electrode potential scale. Consider the absolute potential of the  $\text{H}^+/\text{H}_2$  pair as 4.61 V. (Gamboa-Aldeco)

TABLE E.1

Reaction	Potential, V
$2\text{H}^+ + 2\text{e}^- \rightleftharpoons \text{H}_2$	0.000
$\text{Cu}^{2+} + \text{e}^- \rightleftharpoons \text{Cu}^+$	+0.158
$\text{Fe}^{2+} + 2\text{e}^- \rightleftharpoons \text{Fe}$	-0.409
$\text{Hg}^{2+} + 2\text{e}^- \rightleftharpoons \text{Hg}$	+0.851
$\text{Ni}^{2+} + 2\text{e}^- \rightleftharpoons \text{Ni}$	-0.230
$\text{Ag}^+ + \text{e}^- \rightleftharpoons \text{Ag}$	+0.800
$\text{Au}^+ + \text{e}^- \rightleftharpoons \text{Au}$	+1.68
$\text{Pt}^{2+} + 2\text{e}^- \rightleftharpoons \text{Pt}$	~+1.2

12. Calculate the inner potential difference across (a) an  $\text{Na}^-/\text{Na}^+$  standard reversible electrode and (b) a standard reversible hydrogen-nickel electrode.  $^R\Delta^S\phi$  can be calculated provided one has knowledge of the chemical potential of electrons in the reference electrode, i.e.,  $\mu_e^R$ , and the surface potential,  $g^S$  [note that  $g^S$  is used instead of  $\chi^S$  in (Eq. 6.61)]. Data pertinent to the calculation are:  $V_{\text{pzc}}^{\text{Hg}} = -0.20$  V,  $\Phi^{\text{Hg}} = 4.52$  eV,  $g^S = -\chi^S + \delta_\chi = +0.06$  V,  $\mu_e^{\text{Na}}/F = -3.2$  V, and  $\mu_e^{\text{Ni}}/F = -5.5$  V. (Gamboa-Aldeco)
13. Define the following terms used in Section 6.4: (a) surface excess, (b) contact adsorption, (c) interface and interphase, and (d) interfacial tension. (Gamboa-Aldeco)
14. Define the following terms used in Section 6.5: (a) electrocapillary measurements, (b) ecm, (c) Lippmann equation, (d) integral capacitance, (e) differential capacitance, and (f) potential of zero charge. (Gamboa-Aldeco)
15. A purely thermodynamic approach to adsorption in the double layer allows one to obtain the Gibbs surface excess for both cations and anions. Describe an approach for breaking up the  $\Gamma$  into diffuse layer and contact-adsorbed contributions. Be careful in making the assumptions. (Bockris)
16. In an electrocapillary measurement, mercury is in contact with a solution. If the height of the column is 2 cm, the inner diameter of the capillary tube is 0.5 mm, and the density of mercury at 25 °C is  $13.5457 \text{ g cm}^{-3}$  and at 0 °C is  $13.5951 \text{ g cm}^{-3}$ , what are the surface tension values of mercury at these two temperatures? (Gamboa-Aldeco)
17. The Lippmann equation gives the charge density of the electrode based on electrocapillary measurements. This equation can be approximate as  $(\Delta\gamma/\Delta V)_{\text{const.comp}} = -q_M$ . Measurements of surface tension of Hg in contact with 1.0 N HCl gave the following data:



TABLE E.2

$\gamma$ (dynes $\text{cm}^{-1}$ )	414	406	391
cell potential (V)	-0.10	0.00	+0.10

Based on the above approximation, calculate (a) the charge of the electrode,  $q_{M1}$ , for the change in potential from -0.10 to 0.00 V; (b) the charge of the electrode,  $q_{M2}$ , for the change in potential from 0.00 to +0.10 V.

(c) If  $q_{M1}$  is assigned a potential of -0.05 V, and  $q_{M2}$  of +0.05 V, calculate the differential capacitance of the interface assuming that  $C = \Delta q_M / \Delta V$ . (Gamboa-Aldeco)

18. Starting from the Lippmann equation, derive an expression for the variation of the radius of a mercury drop as a function of potential in a solution where there is no specific adsorption. Assume that the double layer at the mercury solution interface can be treated as a parallel-plate capacitor. (Contractor)
19. The potential across a parallel-plate condenser is 100 V. If the distance between plates is 1 cm, calculate the charge of the plates of the condenser if (a) there is vacuum between the plates and (b) the dielectric constant between the plates is 80. (Gamboa-Aldeco)
20. Verify that the right side of Eq. (6.130) has units of capacitance. (Gamboa-Aldeco)
21. Define the following terms used in Section 6.7: (a) image forces, (b) image dipole, (c) dispersion forces, (e) chemical forces, (f) saturated dielectric, (g) water monomers and water dimers, (h) configurational entropy, (i) libration entropy, and (j) vibrational entropy. (Gamboa-Aldeco)
22. In describing adsorption on an electrode, it is common to write  $\theta$  for the fraction of the surface covered. However, in purely thermodynamic analyses, the symbol  $\Gamma$  is used for the Gibbs surface excess. Describe the difference in meaning between these two quantities and the conditions under which they may tend to become nearly equal. (Bockris)
23. Show that the fraction of electrode covered by water is on the order of 70%. Take the density of water as  $1 \text{ g cm}^{-3}$  and its molecular weight as  $18 \text{ g mol}^{-1}$ . (Gamboa-Aldeco)
24. Calculate the capacity of the Helmholtz layer per unit area for an interface of mercury in contact with a 0.01M NaF electrolyte. Model the value of "the double layer thickness" assuming a two-state water model, a positive charge on the electrode, and a local dielectric constant of six. (Bockris)

25. Prove that Eq. (6.157) originates from Eq. (6.154) when  $|\Delta G_c^\circ|_T > |\Delta G_c^\circ|_L$ . (Gamboa-Aldeco)
26. What isotherm does the Frumkin isotherm become when: (a)  $A = 0$  and (b)  $\theta = 1/2$ ? (Gamboa-Aldeco)
27. How does the Temkin isotherm (Eq. 6.206) reduce at (a) very low concentrations and (b) very high concentrations? (Gamboa-Aldeco)
28. Calculate the diffuse-layer charge according to the classical Gouy theory for a mercury electrode in contact with an aqueous electrolyte of 0.001 M NaF, the zeta potential being +8 mV and the temperature 28 K. The dielectric constant can be taken as that of water at this temperature. (Bockris)
29. Consider a simple interfacial region at a mercury/solution interface. The electrolyte is 0.01 M NaF and the charge on the electrode is 10  $\mu\text{C}$  negative to the pzc. The zeta potential is -10 mV on the same scale. What is the capacitance of the Helmholtz layer and that of the diffuse layer? Calculate the capacitance of the interfaces. Take the thickness of the double layer as the distance between the center of the mercury atoms and that of hydrated  $\text{K}^+$  in contact with the electrode through its water layer. (Bockris)
30. Silver crystallizes in the face-centered cubic (fcc) form. (a) Make a sketch of the three basal faces of silver with the Miller indices [i.e., (100), (110), and (111)] and calculate the atom densities on these faces in atoms per  $\text{cm}^2$ . The interatomic distance of Ag-Ag is equal to 0.2889 nm. (b) If only geometric factors are responsible for differences in the adsorption, what is the sequence of the surface concentration of adsorbed species on the individual planes? (Bockris)
31. At a semiconductor/solution interface, an  $n$ -type semiconductor (carrier density of  $10^{17}$  electrons  $\text{cm}^{-3}$ ) is in contact with a nonaqueous system using a redox system, i.e., no surface states. The capacity of this interface is 4  $\mu\text{F cm}^{-2}$ . Evaluate the potential differences within the semiconductor. (Bockris)
32. Under what conditions are colloids stable? Explain qualitatively (with schematic diagrams) the forces between colloidal particles. How does the force of repulsion between them vary with concentration? As the concentration of the colloid increases, there is the tendency to coagulate and in fact the critical concentration for coagulation gets *less* as the valence of the ions present increases (Schulze-Hardy rule). Give a detailed, although qualitative, rationalization of this law. (Bockris)
33. A measurement of electrophoretic mobility  $v/x$ , gives  $x = 0.02 \text{ cm s}^{-1}$ , where  $v$  is the velocity observed under a field, and  $x$  the mobility. Calculate the zeta potential of the colloid concerned. (Bockris)

# PROBLEMS

- Two slits 0.5 mm apart are placed 1 m from a screen. If the slits are illuminated with a light of a wavelength of 500 nm, what is the distance between the first and second, and the first and third lines of the interference pattern? (Gamboa-Aldeco)
- Experimental parameters were obtained from the adsorbance of bisulfate ions on polycrystalline electrodes using a radiotracer technique slightly different from that described in the text, where the working electrode is placed on top of the scintillator. These values are listed in Table P.1.

**TABLE P.1**

Concentration (mol dm <sup>-3</sup> )	Activity (mCi cm <sup>-3</sup> )	$N_b$ (counts per s)	$N_a$ at max. ads. (counts per s)	R
10 <sup>-9</sup>	0.0018	15	746	60
10 <sup>-7</sup>	0.0011	74	572	60
10 <sup>-5</sup>	0.0005	38	253	60
10 <sup>-2</sup>	0.0030	205	96	66

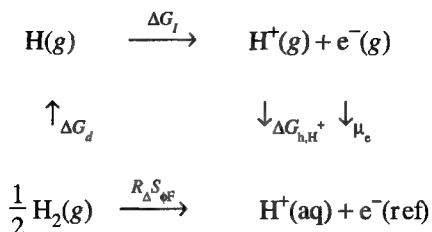
The surface concentration in this technique is determined by an equation similar to Eq. (6.8), i.e.,

$$\Gamma = \frac{N_a}{N_b} \frac{c}{\mu R}$$

- (a) What is the ratio of radioactive to nonradioactive molecules in solution for the 10<sup>-5</sup> M solution? In measuring the activity of the solution, 1 Ci = 3.7 × 10<sup>10</sup> counts s<sup>-1</sup>. (b) Calculate the surface concentration of bisulfate ions on the electrode at each concentration. The value of the linear absorption coefficient for <sup>35</sup>S, i.e., μ<sub>35S</sub>, is 266 cm<sup>-1</sup>. (Gamboa-Aldeco)
- (a) Draw an electrochemical cell similar to that in Fig. 6.30, where one of the electrodes is Fe and the other is the hydrogen electrode. The connecting wires are made of Pt. (b) Draw the direction of the flux of electrons in this cell as well as the corresponding reactions and the balance of potential drops in the system. (Gamboa-Aldeco)
  - (a) Draw an electrochemical cell similar to that in Fig. 6.30, with one of the electrodes made of nickel and the other of silver. Each electrode is connected to the measuring device by silver wire and is immersed in a solution with nickel and silver ions, respectively, separated by a porous membrane. (b) Based on the table in Exercise 11, indicate the direction of the flux of electrons and the

corresponding reactions at each electrode, as well as the balance of potential drops in the system, (c) What potential is expected at the measuring device when the circuit is closed? (Gamboa-Aldeco)

5. Estimate the value of the surface potential of water,  $\chi_{\text{H}_2\text{O}}$ , using the following thermodynamic cycle (Bockris and Argade, 1968):



where  $\Delta G_{\text{d}} = 48.48 \text{ kcal mol}^{-1}$  is the free energy of dissociation,  $\Delta G_{\text{I}} = 313.22 \text{ kcal mol}^{-1}$  is the free energy of ionization,  $\Delta H_{\text{h,H}^+} = -260.7 \text{ kcal mol}^{-1}$  is the enthalpy of hydration,  $\Delta S_{\text{h,H}^+} = -31.0 \text{ cal K}^{-1} \text{ mol}^{-1}$  is the entropy of hydration,  $\mu_{\text{e}}$  is the chemical potential of the electron and  $R\Delta^{\text{S}}\phi$  is the inner potential difference between the reference electrode and solution. Other data can be obtained from Fig. 6.47. (Gamboa-Aldeco)

6. If in Problem 5 the change in surface potential arising upon contact between the two phases is taken into consideration, i.e.,  $\delta\chi^{\text{S}}$ , what is the value of  $\chi^{\text{S}}$ ? The value of  $\delta\chi^{\text{S}}$  is +0.27 V. (Gamboa-Aldeco)
7. (a) From the data in Table 6.2, plot  $\gamma$  vs. the potential difference across the electrochemical cell, (b) Does this graph correspond to a perfect parabola? (c) Differentiate the curve to obtain the electrode charge density and plot it against the potential difference, (d) Does this curve correspond to a single eight line? (e) Differentiate this curve to obtain the capacitance and plot the values vs. the potential difference, (f) Does this graph give one or more straight lines? What is the pzc of this system? (Gamboa-Aldeco)
8. Obtain the surface concentration from the slope of  $\gamma$  vs.  $\ln c$  (consider  $c \cong a$ ) at -1.0 V for the data in Table 6.3. (Gamboa-Aldeco)
9. (a) Calculate the differential capacities for a mercury electrode at the pzc in NaF solutions of concentrations 0.001, 0.01, 0.1, and 1.0 N. Consider  $\epsilon = 78$  and  $\psi \sim 0$  at room temperature. The experimental values of the differential capacities found for each one of these concentrations are 6.0, 13.1, 20.7, and  $25.7 \mu\text{F cm}^{-2}$ . (b) Discuss the similarity and discrepancy of your calculated results with those found experimentally. (Gamboa-Aldeco)
10. Figure 6.84(d) shows some experimental results indicating that the entropy of adsorption of water molecules varies in a parabolic way with the electrode

charge. It was established in the text that if the amount of water molecules at the surface is considered as constant, the variation of entropy with the electric field of the electrode should be attributed to changes in the molecular entropy of the adsorbed water molecules due to changes in its orientation (flip-up, flop-down, and lying down). However, another hypothesis indicates that these entropy changes should be attributed to changes in the amount of water at the interface, with a constant value for the molecular entropy of the water at the interface. (a) Considering this second hypothesis as valid, if the amount of adsorbed water molecules at the pzc is  $10^{15}$  molecules  $\text{cm}^{-2}$ , determine the amount of molecules at  $-16 \mu\text{C cm}^{-2}$ . (b) What is the increase in the number of water molecules when going from one electrode charge to the other? Comment on your results. (Gamboa-Aldeco)

11. Equation (6.148) involves the term  $\Delta G_2^\circ$ , which represents the standard free energy change for the formation of dimers on the surface from adsorbed monomers. The energy in the formation of one dimer from one up and one down water molecule involves the following terms. For the dimers: The hydrogen-bond energy,  $U_{\text{HB}} = -18.81 \text{ kJ mol}^{-1}$ . The dimer-metal attraction energy,  $U_{\text{dim-att}} = -C r^{-3}$ , where  $C$  is a constant characteristic of the adsorbent atoms and adsorbate molecules, and  $r = r_{\text{adsorbent}} + r_{\text{adsorbate}}$ . For a dimer adsorbed on mercury:  $C = 6.0 \times 10^{-22} \text{ kJ mol}^{-1} \text{ cm}^3$ ,  $r_w = 1.38 \times 10^{-8} \text{ cm}$ , and  $r_{\text{Hg}} = 1.5 \times 10^{-8} \text{ cm}$ . The dimer-metal repulsion energy,  $U_{\text{dim-rep}} = A r^{-9}$ , where  $A$  is given by

$$\frac{dU_{\text{dim-rep}}}{dr} = \frac{d}{dr} \left( -\frac{C}{r^3} + \frac{A}{r^9} \right) = 0.$$

For the monomers; (d) the image interaction of one water molecule is given by

$$U_{\text{image}} = -\frac{1}{4\pi\epsilon_0} \frac{\mu_w^2}{(2r_w)^3}$$

where  $\bar{\mu} = \mu_w/\sqrt{3}$ , and  $\mu_w$  is the dipole moment of water (1.84 D). The monomer-metal attraction interaction is  $U_{\text{mon-att}} = U_{\text{dim-att}}/\text{two molecule of monomer water}$ . The monomer-monomer lateral interaction term is  $U_L = -(1/4\pi\epsilon_0)(\bar{\mu}^2/(2r_w)^3)$ . The monomer-metal repulsive energy is given by  $U_{\text{mon-rep}} = 13.71 \text{ kJ/two molecules water}$ .

- (a) Write the equation of dimer formation. Determine: (b)  $U_{\text{dim-att}}$ , (c)  $U_{\text{dim-rep}}$ , (d) the interaction energy of an adsorbed dimer on mercury, (e)  $U_{\text{image}}$  for one molecule of up and one mol of down monomer, (f)  $U_L$  (Is this term of attractive or repulsive character? Explain), and (g) the energy of one molecule of up and one molecule of down monomers,  $U_{\text{mon}}$ . (h) Calculate the value of the enthalpy

of formation of a dimer from one up and one down water molecule, i.e.,  $\Delta H_2^\circ$ . (Gamboa-Aldeco)

12. In Problem 11, the enthalpy of formation of a dimer from two monomers was addressed. The entropy change,  $\Delta S_2^\circ$ , can be determined by considering the formation of one molecule dimer from one molecule up monomer and one down monomer molecules. When these two molecules of up and down monomers are present on the surface, the configurational entropy can be calculated as  $S_{\text{mon}} = 2k \ln(N_o! / N_\uparrow! N_\downarrow!)$ . (a) Using Stirling's approximation for large  $N$ , i.e.,  $\ln N! = N \ln N - N$ , prove that  $S_{\text{mon}} = 2k N_o \ln 2$ . (b) If  $N_o$  equals Avogadro's number, what is the value of  $S_{\text{mon}}$ ? (c) What is the configurational entropy for one molecule of dimers? (d) What is the value of  $\Delta S_2^\circ$ ? (e) Considering the value of  $\Delta H_2^\circ$  obtained in problem 11, what is the value of  $\Delta G_2^\circ$  at 25 °C? (Gamboa-Aldeco)

Equation (6.156) indicates that the difference in free energies of the up and down monomers is different from zero, i.e.,  $\Delta(\Delta G_c^\circ) \neq 0$ . This quantity is made up of the following terms (for definition of terms, please refer to Problems 11 and 12): difference in the image interaction in the two orientations, favoring the case in which the oxygen atom is oriented toward the metal because the dipole is then 0.05–0.1 Å closer to the metal,  $\Delta U_{\text{image}} \approx - (1/4\pi\epsilon_0)(3\mu^{-2}d/2r_w^4)$ , where  $d$  is the difference in the distances between the centers of two molecules oriented oppositely ( $d = 0.05$  Å); and a difference in dispersion interaction of the two different water positions with the metal due to the difference in the distances of their centers from the metal surface,  $\Delta U_{\text{disp}} = C[(1/(r-d)^3) - (1/(r+d)^3)]$ . Determine the value of  $\Delta(\Delta G_c^\circ)$  for the mercury/water interface. (Gamboa-Aldeco)

14. It is assumed that the molecules adsorbed on the electrode surface behave as a two-dimensional gas that can be described by an equation of state. For ideal noninteracting molecules, Henry's law,  $\beta a = RT\theta$ , is fulfilled. When the mutual interaction between adsorbed molecules is taken into account, the equation with the virial coefficient  $B'$  can be presented in the form:

$$\Phi = RT\Gamma + B'\Gamma^2$$

where  $\Phi$  is a surface energy. The change of the surface energy is described by the Gibbs equation:

$$d\Phi = -d\gamma = \frac{RT\Gamma}{a} da$$

where  $a$  is the activity. Derive the virial isotherm from the above equation of state. (Sobkowski)

15. Develop the standard state equations, i.e.,  $\mu_{A,ads}^0 = \mu_{A,ads}^0(T, f_A^0, n, \theta_0)$  and  $\mu_{w,ads}^0 = \mu_{w,ads}^0(T, f_w^0, n, \theta_0)$  for the Flory-Huggins isotherm [Eq. (6.208)]. The chemical potentials from statistical mechanical considerations of the adsorbate A and water molecules in their adsorbed states are:  $\mu_{A,ads} = -kT \ln f_A + kT[(1 - \theta)(1 - n) + \ln \theta]$  and  $\mu_{w,ads} = -kT \ln f_w + kT[\theta(1 - 1/n) + \ln(1 - \theta)]$ . Choose a convenient value for  $\theta_{zero}$  when  $n = 1$ . (Gamboa-Aldeco)
16. Benzoic acid was adsorbed on polycrystalline gold electrode at different potentials. It was found that the process is reversible in respect to the bulk concentration of benzoic acid and electrode potential. The maximum of adsorption was found at 1.3 V vs. potential of hydrogen electrode in 0.1 M  $\text{HClO}_4$ . The dependence of the surface concentration of benzoic acid adsorbed from 0.1 M  $\text{HClO}_4$  on the bulk concentration is given in Table P.2:

TABLE P.2

$c \times 10^{-4} \text{ (mol dm}^{-3}\text{)}$	0.3	0.5	1.0	1.5	2.5	5.0	10.0
$\Gamma \times 10^{-14} \text{ (molecules cm}^{-2}\text{)}$	1.12	1.48	2.14	2.55	3.06	3.67	4.18

The maximum surface concentration of benzoic acid obtained by extrapolation of the experimental data is  $\Gamma_{\max} = 5.1 \times 10^{14} \text{ molecules cm}^{-2}$ . Determine the parameters  $\beta$  and  $A$  in the Frumkin equation of adsorption. Calculate the Gibbs energy of adsorption. Compare the results with the Langmuir isotherm. (Sobkowski)

17. (a) Consider the surface of an electrode in solution and a central ion in the middle of it. Consider further concentric rings around the central ion that contains adsorbed ions of the same sign as that of the central one. Work out the Coulombic repulsion between a ring of ions and the central ion, and integrate so that you have the total repulsion energy per unit area for anion adsorption. Show that electrostatic repulsion between adsorbed ions makes ionic adsorption, calculated thus, impossible. (b) However, anion adsorption is a fact. Obviously, *chemical* interactions of nonhydrated adsorbed ions and the metal overcome the repulsion calculated. However, there is another force, the image force, which will reduce the net free energy of interaction and may draw it into the negative region. Add, therefore, to your earlier analysis the effect of image forces of the adsorbing ion with the metal (neglect imaging in solution) and determine if this interaction alone explains adsorption. (Bockris)
18. The Langmuir isotherm can be derived from a statistical mechanical point of view. Thus, for the reaction  $M + A_{\text{gas}} \rightleftharpoons A_{\text{ads}}$ , equilibrium is established when the chemical potential on both phases is the same, i.e.,  $\mu_{\text{gas}} = \mu_{\text{ads}}$ . The partition function for the adsorbed molecules as a system is given by

$$F_{\text{ads}} = \frac{N_{\text{M}}!}{N_{\text{ads}}!(N_{\text{M}} - N_{\text{ads}})!} (f_{\text{ads}})^{N_{\text{ads}}}$$

and that for the molecules in the gas phase (considered as an ideal gas). (Gamboa-Aldeco)

19. All chemists have heard of Langmuir's isotherm. It should apply only to smooth surfaces where the adsorbing particles do not interact. Known mainly to surface and electrochemists, Temkin's logarithmic isotherm results from recognizing that surfaces have areas that adsorb much more strongly than others. Two other isotherms, that of Frumkin and that of Flory-Huggins, come into the work of physical electrochemists and, for the latter equation, polymer chemists. All these are described in the text. Figure P6.1 shows the adsorption of  $\text{CF}_3\text{SO}_3^-$  and  $\text{H}_3\text{PO}_4$  as a function of concentration and temperature, and Fig. P6.2 shows the temperature dependence of the standard free energy of adsorption of these ions. Considering the Temkin and Flory-Huggins isotherms, is it possible to show a superior fit with either of these isotherms? Interpret your results. (Bockris)

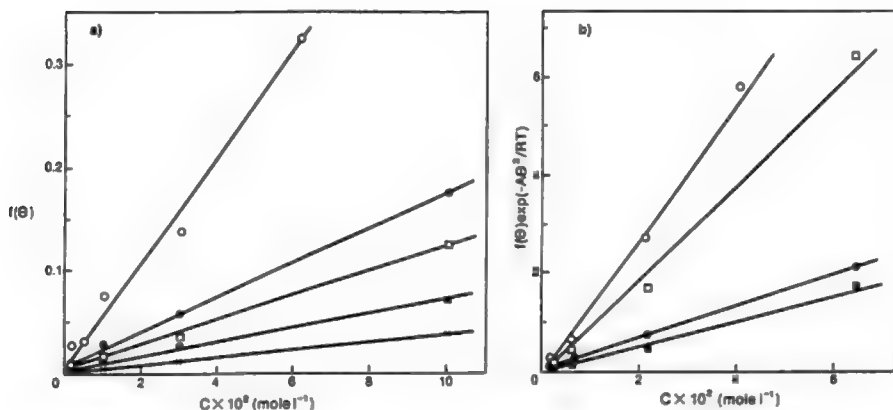


**Fig. P6.1** Adsorption of  $\text{CF}_3\text{SO}_3^-$  and  $\text{H}_3\text{PO}_4$  at 0.80 V as a function of concentration and temperature: (a) Adsorption of  $\text{CF}_3\text{SO}_3^-$  at 298 K ( $\circ$ ), 323 K ( $\bullet$ ), 333 K ( $\square$ ), 343 K ( $\blacksquare$ ) and 353 K ( $\times$ ); (b) adsorption of  $\text{H}_3\text{PO}_4$  at 298 K ( $\circ$ ), 308 K ( $\square$ ), 318 K ( $\bullet$ ), and 328 K ( $\blacksquare$ ).  $f(\theta) = \theta / (1 - \theta) [\theta + n(1 - \theta)]^{n-1} / n^n$  is the configurational term in the Bockris-Swinkels isotherm, where the number of water molecules displaced upon adsorption,  $n$ , is 3 for both  $\text{CF}_3\text{SO}_3^-$  and  $\text{H}_3\text{PO}_4$ . (Reprinted from P. Zelenay, B. R. Scharifker, J. O'M. Bockris, and D. Gervasio, *J. Electrochem. Soc.* **133**: 2262, copyright 1986, Fig. 3, with permission of Elsevier Science.)



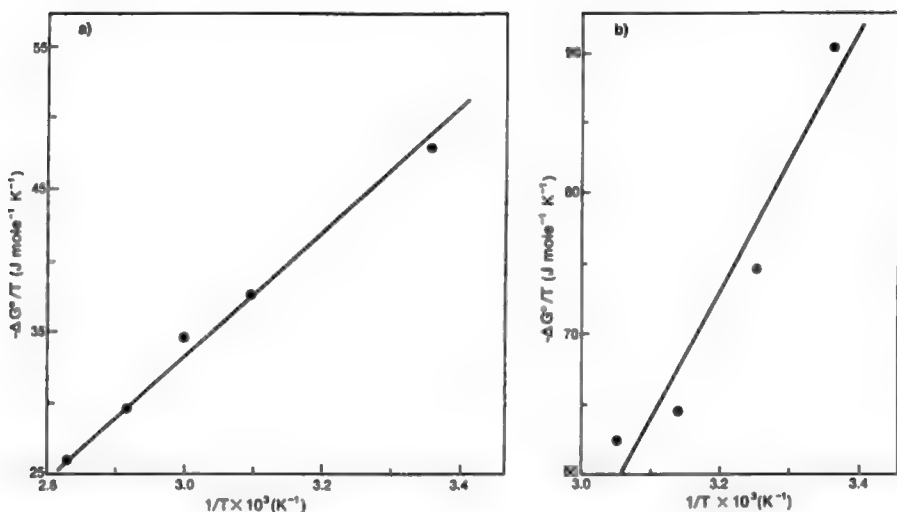


**Fig. P6.2.** Temperature dependence of the standard free energy of adsorption for (a)  $\text{CF}_3\text{SO}_3^-$  and (b)  $\text{H}_3\text{PO}_4$  ( $E = 0.80 \text{ V}$ ). (Reprinted from P. Zelenay, B. R. Scharifker, J. O'M. Bockris, and D. Gervasio, *J. Electrochem. Soc.* **133**: 2262, copyright 1986, Fig. 4, with permission of Elsevier Science.)

20. When organic molecules adsorb on solid electrodes, they undergo oxidation at sufficiently positive potential or reduction at a significant rate at sufficiently negative potentials, and their subsequent behavior then becomes part of organo-electrochemical kinetics (Chapter 11). However, on some electrodes, there is a substantial potential region, even up to an 0.8-V range, where currents observed in voltammograms (current–potential curves) are largely due to charging currents, i.e.,  $C(dV/dt)$ , and not to reaction currents. In these regions, it is best to regard the organic molecules as adsorbed on the electrode surface and in equilibrium with molecules of the species dissolved in solution. The first step in understanding this adsorption of organic molecules—the two-state model—is to regard the electrical properties of the organic molecules as outside the Helmholtz plane formed by the supporting electrolyte. The electrode field would mainly affect the water molecules as far as they are intact and not strongly chemisorbed on the surface. Thus, the water molecules should turn over at or near the pzc, where their adsorption passes through a minimum so that the adsorption of organic molecules goes through a maximum. For many types of organic molecules, the maximum of the adsorption occurs near  $\pm 0.1 \text{ V}$  from the pzc, as shown in Table P.3.

**TABLE P.3**  
**Differences between the pzc and the Adsorption Maxima of Various Organic Compounds in 0.01 M HCl Solution on Platinum**

Compounds	$V_{\max}/V$ (SHE)	$V_{\text{pzc}}/V(\text{SHE})$ ( $\theta = 0.5$ )	$V_{\text{pzc}} - V_{\max}$ ( $\theta = 0.5$ )	Comments
<i>n</i> -Butyl alcohol	0.40	0.263	-0.137	Neglect effect of organic dipole
<i>n</i> -Valeric acid	0.30	0.263	-0.037	Neglect effect of organic dipole
<i>n</i> -Valeraldehyde	0.30	0.263	-0.037	Neglect effect of organic dipole
<i>n</i> -Butylamine	0.30	0.263	-0.037	Neglect effect of organic dipole
<i>n</i> -Valeronitrile	0.20	0.263	0.063	Neglect effect of organic dipole
<i>l</i> -Butylmercaptan	0.50	0.263	-0.237	Neglect effect of organic dipole
<i>n</i> -Valeroylchloride	0.50	0.263	-0.237	Neglect effect of organic dipole
Phenol	0.30	0.452	0.152	
Benzoic acid	0.30	0.446	0.146	
Benzaldehyde	0.55	0.421	-0.129	
Aniline	0.40	0.451	0.051	
Benzonitrile	0.20	0.395	0.195	
Thiophenol	0.30	0.450	0.150	
Benzoyl chloride	0.50	0.426	-0.074	
<i>l</i> -Naphthol	0.35	0.440	0.090	$V_{\max}$ not well determined
<i>l</i> -Naphthoic acid	0.50	0.436	-0.064	$V_{\max}$ not well determined
<i>l</i> -Naphthaldehyde	0.30	0.426	0.126	$V_{\max}$ not well determined
<i>l</i> -Naphthamine	0.55	0.439	-0.111	$V_{\max}$ not well determined
<i>l</i> -Naphthoyl chloride	0.30	0.424	0.124	$V_{\max}$ not well determined

Source: Reprinted from J. O'M. Bockris and K. T. Jeng, *J. Electroanal. Chem.* **330**: 541, Table 5, copyright 1992 with permission from Elsevier Science.

Consider the deviations of  $\theta_{\max}$  from the pzc quantitatively. Can you associate them with the probable orientation of the adsorbed organic molecules on the surface? Or perhaps on image potentials formed by dipoles of the organic with the metal? Perform simple calculations to determine whether breakdown of the first approximation assumption of zero interaction of the organic molecule with the field, or image forces, explains the deviation of  $V_{\max}$  of the organic molecule from the pzc. (Bockris)

21. (a) Figure P6.3 shows diagrams from an examination of organic adsorption of a number of organic substances on platinum. (a) From the diagrams of  $\theta$  against  $V$ , obtain the  $V_{\max}$  and pzc values. (b) Explain the deviation from the  $V_{\max}$  values and the pzc values as  $\pm \Delta V_{\max}$ . (c) What fact do these figures suggest? (d) What

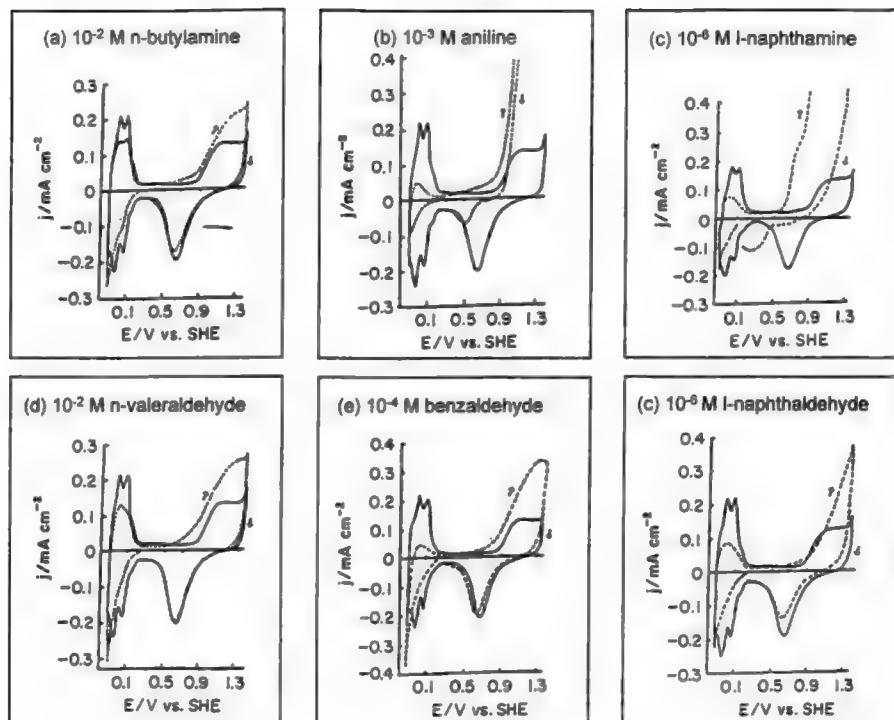


**Fig. P6.3.** I, Voltammograms (current density vs. potential) and isoconcs (coverage vs. potential) diagrams for several organic molecules adsorbed on platinum. I, Solid line, pure electrolyte (0.01 M HCl; broken line, addition of organic species. Sweep rate,  $50 \text{ mV s}^{-1}$  298 K. II. Measurements taken with radiotracer (RT) FTIR spectroscopy, and ellipsometric (ELIP) techniques. (Reprinted from J. O'M. Bockris and K. T. Jeng, *J. Electroanal. Chem.* **330**: 54, copyright 1992, Figs. 5 and 6, with permission of Elsevier Science.)

theoretical conclusion do they imply? Consider the current-potential diagrams in which the compounds are being reduced or oxidized (dotted lines). (e) What are the potential regions in which the minimal current suggests that the electrochemical reactivity in this region is negligible? (f) What does this suggest related to the state of the adsorbed organic molecules on the electrode surface? (g) Is this information consistent with the conclusion concerning the shape of the  $\theta$ -potential, curves and the result from the  $V_{\max}$  examination? The continuous lines represent the current density potential of the platinum electrodes in the absence of organic compounds. It has been suggested (Wieckowski, 1993) that

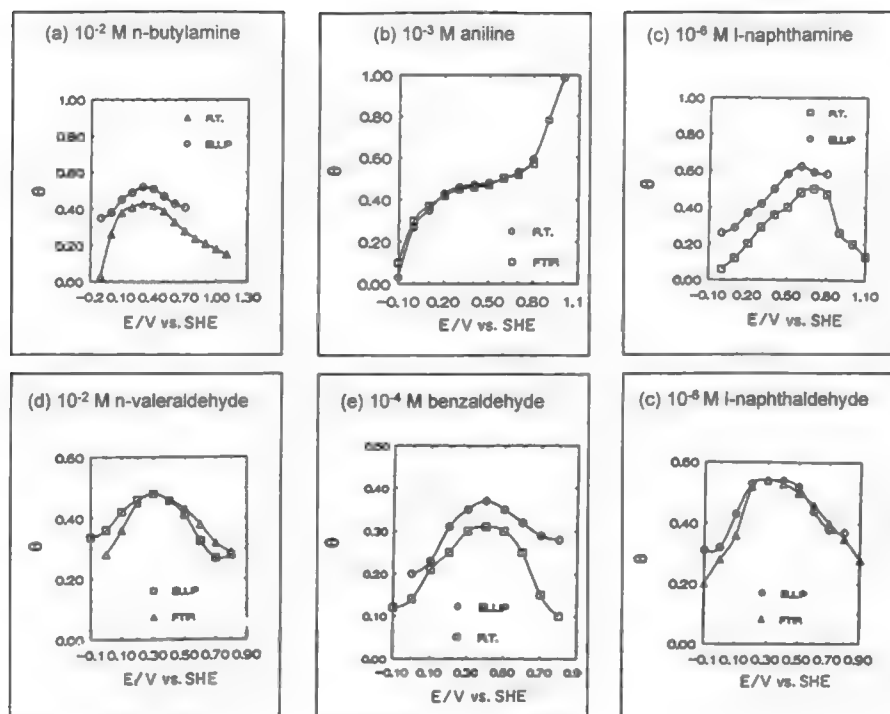


Fig. P6.3. Continued

the organic molecules do not remain undissociated upon adsorption in the potential region of the  $\theta$ -potential curves (i.e., reaction dominates equilibrium adsorption of the molecules). (h) Evaluate this view. (Bockris)

22. Figure P6.4 shows the logarithmic dependence of the adsorption of chloride ions,  $\log(\Gamma - \Gamma_i/\Gamma)$ , on time,  $t(\text{min})$ . The adsorbing metal is aluminum, the concentration of chloride ions in solution is  $10^{-3} \text{ mol dm}^{-3}$  at pH 12, and the potential in the hydrogen scale is  $-0.9 \text{ V}$ . On the assumption that the adsorption is diffusion controlled, determine the standard free energy of adsorption of chloride ions on the surface concerned.

## MICRO RESEARCH PROBLEMS

- (a) Calculate the potential originating from Coulombic forces at various distances from the electrode surface for a flat electrode of  $1 \text{ cm}^2$  of area and a

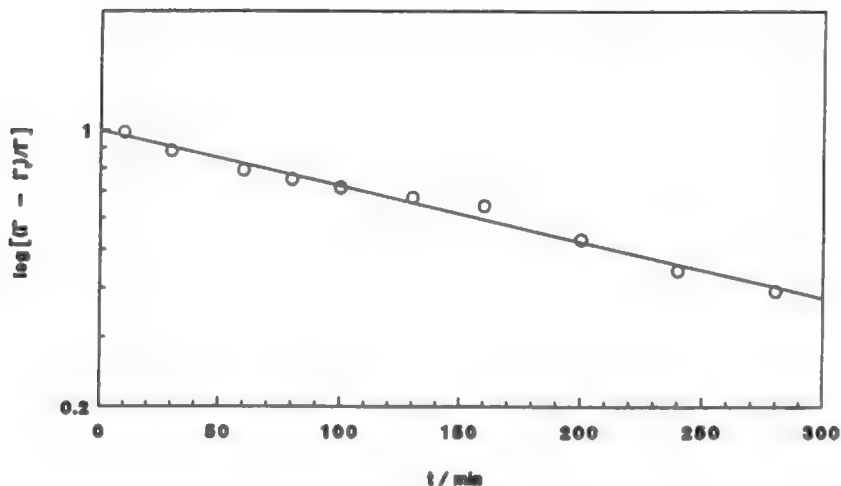


**Fig. P6.4.** Logarithmic dependence of adsorption on time for  $10^{-3}$  M chloride ions on aluminum at pH 12,  $V = -0.9$  V. (Reprinted from J. O'M. Bockris and L. Minevski, *J. Electroanal. Chem.* **349**: 375, copyright 1993, Fig. 4, with permission of Elsevier Science.)

- charge of  $3.11 \times 10^{-13}$  C. (b) Calculate the potential due to image forces at various distances from the electrode surface. (c) Plot the Coulombic potential and the image potential on one graph. Add these two values to approximately obtain the total potential due to the test charge near a charged electrode. (d) How far from the electrode are the image forces dominant over the Coulombic forces, i.e., image potential > Coulombic potential? (e) At what distance from the electrode do the Coulombic forces fade out? (f) What is the importance of this calculation?
- Several more advanced theories of organic adsorption have succeeded the simple two-state model of Bockris, Devanathan, and Muller (BDM) (1963). They allow, for example, for clustering among the water molecules and heterogeneity on the metal surface. (a) Make a quantitative appraisal of the degree to which the more sophisticated models have improved the simple two-state first approximation of the BDM theory. Consider the fitting of data without calibrating the theory beforehand (use data in the chapter or in the literature cited for this material). (b) Under what circumstances is it valid to make models of the adsorption of organic molecules on solid metals, assuming that the adsorbed—intact—molecule is in equilibrium with dissolved species of the same structure? (Bockris)

## APPENDIX 6.1. MEASUREMENT OF THE ELECTRODE-SOLUTION VOLTA POTENTIAL DIFFERENCE

The value of the Volta potential difference between a metal  $\alpha$  and a solution can be obtained by performing two measurements, in one of which the electrode  $\alpha$  is in contact with the solution (Fig. A6.1), whereas, in the second, it is separated from the latter by a space filled with ionized unreactive gas at a low pressure (Fig. A6.2). Electrode  $\alpha$  and another electrode of a metal  $\gamma$ , reversible to ions  $M^{Z+}$  in solution, are connected to a potentiometer  $P$  by wires  $\beta$  and  $\beta'$  made of the same metal.

Consider first the arrangement shown in Fig. A6.1. By adjusting the potentiometer to a reading  $V$  such that the galvanometer  $G$  indicates no current flowing, conditions of electronic equilibrium are created between  $\alpha$  and  $\beta$ , i.e.,

$$\bar{\mu}_{el}^{\alpha} = \bar{\mu}_{el}^{\beta} \quad (\text{A6.1})$$

and between  $\beta'$  and  $\gamma$ , i.e.,

$$\bar{\mu}_{el}^{\beta'} = \bar{\mu}_{el}^{\gamma} \quad (\text{A6.2})$$

The potentiometer reading  $V$  is equal to the Galvani potential difference between  $\beta$  and  $\beta'$ , i.e.,

$$V = \phi^{\beta} - \phi^{\beta'} \quad (\text{A6.3})$$

By multiplying Eq. (A6.3) by  $F$  and adding and subtracting  $\mu_{el}^{\beta}$  (chemical potential of electrons in phase  $\beta$ ),

$$FV = \bar{\mu}_{el}^{\beta} - \bar{\mu}_{el}^{\beta'} \quad (\text{A6.4})$$

Substituting Eq. (A6.1) and (A6.2) in Eq. (A6.4), one obtains

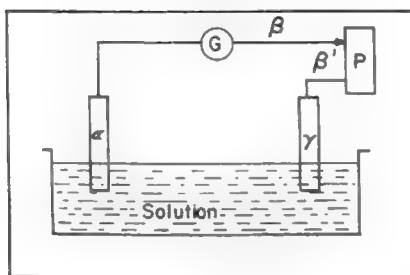


**Fig. A6.1.** The measurement of the Volta potential.

$$FV = \bar{\mu}_{el}^{\gamma} - \bar{\mu}_{el}^{\alpha} \quad (\text{A6.5})$$

At the  $\gamma$ -solution interface, an equilibrium exists



(for simplicity univalent ions are considered), and thus

$$\mu^{\gamma} = \bar{\mu}_{M^+}^{\text{sol}} + \bar{\mu}_{el}^{\gamma} \quad (\text{A6.6})$$

Eliminating  $\bar{\mu}_{el}^{\gamma}$  between Eqs. (A6.5) and (A6.6), one obtains

$$FV = \mu^{\gamma} - \bar{\mu}_{M^+}^{\text{sol}} - \bar{\mu}_{el}^{\alpha} \quad (\text{A6.7})$$

Using Eq. (6.31),

$$\bar{\mu}_{M^+}^{\text{sol}} = \mu_{M^+}^{\text{sol}} + F\psi^{\text{sol}} + F\chi^{\text{sol}} \quad (\text{6.31})$$

and

$$\bar{\mu}_{el}^{\alpha} = \mu_{el}^{\alpha} - F\psi^{\alpha} - F\chi^{\alpha} \quad (\text{6.31})$$

and denoting

$$\mu_{M^+}^{\text{sol}} + F\chi^{\text{sol}} = \alpha_{M^+}^{\text{sol}}$$

and

$$\mu_{el}^{\alpha} - F\chi^{\alpha} = \alpha_{el}^{\alpha}$$

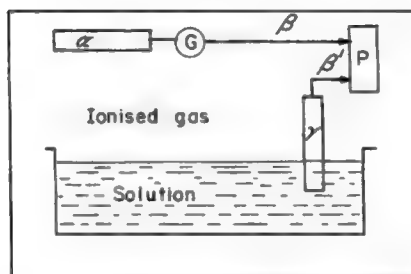


**Fig. A6.2.** Principle of measurement of the Volta potential difference.

Eq. (A6.7) may be transformed into

$$FV = \mu^\gamma - \alpha_{M^+}^{\text{sol}} - \alpha_{el}^\alpha - F(\psi^{\text{sol}} - \psi^\alpha) \quad (\text{A6.8})$$

We shall return to this equation after consideration of the arrangement shown in Fig. A6.2.

By adjusting the potentiometer to a reading  $V'$  such that the galvanometer indicates no current flowing when  $\alpha$  is moved relative to the solution, conditions are created such that there is no *field* between  $\alpha$  and the solution and thus

$$\psi^\alpha = \psi^{\text{sol}} \quad (\text{A6.9})$$

Equations describing equilibria between phases  $\alpha$  and  $\beta$ ,  $\beta'$  and  $\gamma$ ,  $\gamma$  and solution obtain as previously, and by the same reasoning one arrives at an equation analogous to (A6.8):

$$FV' = \mu^\gamma - \alpha_{M^+}^{\text{sol}} - \alpha_{el}^\alpha - F(\psi^{\text{sol}} - \psi^\alpha) \quad (\text{A6.8a})$$

Now, however,  $\psi^\alpha = \psi^{\text{sol}}$  [Eq. (A6.9) and thus (A6.8a)] reduces to

$$FV' = \mu^\alpha - \alpha^{\text{sol}} - \alpha^\alpha \quad (\text{A6.10})$$

Subtracting Eq. (A6.10) from equation (A6.8), one obtains

$$\psi^\alpha - \psi^{\text{sol}} = V' - V \quad (\text{A6.12})$$

in which the left-hand side is the single-electrode Volta potential between phase  $\alpha$  and the solution.

It is obvious from the above reasoning that introduction of phases  $\beta$  and  $\beta'$  is immaterial; the same argument could be carried out if potentiometer leads were made of metal  $\alpha$  or  $\gamma$  or if any amount of various metallic phases was introduced between  $\alpha$  and  $\gamma$ .



**This page intentionally left blank**

# CHAPTER 7

## ELECTRODICS

### 7.1. INTRODUCTION

Volume 1 of this text was devoted to the study of charged particles—ions, usually with an attached sheath of water molecules—darting about in solution. This second volume presents the other half of electrochemistry, the bigger half, the part that involves surfaces (Chapter 6). When an electronically conducting surface is in contact with a solution, and a stream of electrons is passed into the electronic conductor (most often a metal), randomly moving ions in the solution get caught up in the gradient of concentration thus created and this gradient acts on the ions in a way analogous to the drag felt by a boat approaching a waterfall, forcing them onward toward the electrode. Finally, the ion and its hydration sheath are up against the electrode, separated from it by only a single water layer. What happens after that, how *electron transfer* occurs between the electronic conductor and the ions next to its surface, is the subject of this chapter on electrode kinetics or electrodics.

There is a special property of the region between a metal electrode in contact with a solution, and the layer of ions that collide with it in their wandering and stay there awhile. This property is the electric field between the electrode and this layer. It is a colossally strong electric field ( $10^9 \text{ V m}^{-1}$ ) but extends only some 0.5 nm into the solution. A billion volts per meter is a bigger field strength than one can engineer in a macrodevice in a laboratory. It is electrochemistry's special strength.

#### 7.1.1. Some Things One Has to Know About Interfacial<sup>1</sup> Electron Transfer: It's Both Electrical and Chemical

First, it is important to absorb the meaning of one of the several definitions of electrochemistry. This (which covers only the electrochemistry of this volume) runs

---

<sup>1</sup>Is interfacial the same as “interphasial”? In practice, it is nearly always so. When an electron leaves the surface of mercury and enters the electronic shell of an ion in solution, although adherent to the surface,

as follows: *Electrochemistry is the subject that describes the making of substances by means of electricity and the making of electricity by consuming substances.*

This sounds like a grand definition. It is, and one can see what it means by looking at Figs. 7.1 and 7.2. In Fig. 7.1, one sees the first part of the definition (substances from electricity). Copper ions, invisible and dissolved in solution, are converted into visible metallic copper by means of the electrons flowing across the interfaces to the copper ions in solution. A new substance is produced by means of the flow of electricity. In Fig. 7.2, the reverse occurs: One puts in a substance at one electrode and another substance at the other, and gets electricity! So, electrochemistry has (as its name suggests), a chemical and an electrical side.

## 7.1.2. Uni-electrodes, Pairs of Electrodes in Cells and Devices

Much of the following text—and the results of the research to which it corresponds—deals with a single electrode (“a uni-electrode system”). One can only *imagine* uni-electrode systems. It is true that anyone who has a beaker of solution can place in it a single electrode, a platinum wire, say, and connect it to a source of electrical power outside the beaker (Fig. 7.3). But one cannot *operate* with it, pass electrons in and out of it, say, unless there is a second electrode (Fig. 7.1). Thus, to make up an electrochemical cell, one has to have two electrodes, and these can then act in three ways as devices (see next section).

## 7.1.3. The Three Possible Electrochemical Devices

**7.1.3.1. The Driven Cell (or Substance Producer).** The first of the electrochemical devices is the one most familiar; it is encountered in high school labs under the title of “electrolyzer” (see Fig. 7.4). Here the two electron-transfer reactions that can be seen occurring in the cell have to be driven by an outside source of electric power. Thus, all chemical reactions, under set conditions, have a spontaneous tendency to go to the right or to the left. However, they can be driven backward (acting endergonically), against their spontaneous chemical tendencies to act exergonically, by an outside electrical power source.

What happens inside a water electrolyzer is a case in point. It is well known that the reaction



tends to go from left to right, and if a catalyst is present, the reaction occurs explosively.

---

it is undergoing *interfacial* (between surfaces) electron transfer. However, the electronic conductor, mercury, is also a *phase* (liquid mercury), and the solution adherent to it is another phase (e.g., 0.1 *M* aq. sulfuric acid). So the electron transfer is also *interphasial*. The electrical double layer (0.5 nm in thickness) provides the interphase.

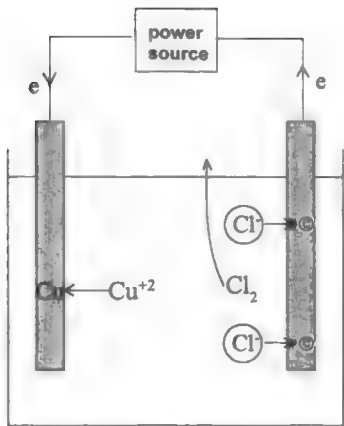


**Fig. 7.1.** An electrochemical system that acts as a substance producer upon passage of current.

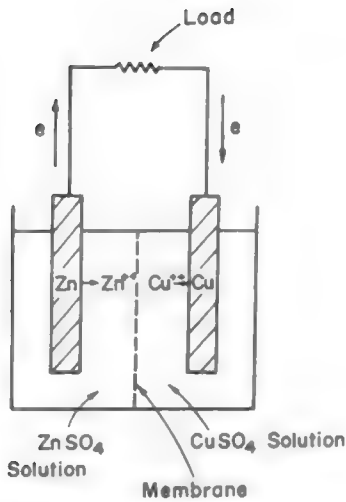


**Fig. 7.2.** An electrochemical system that acts as a producer of electrical energy.

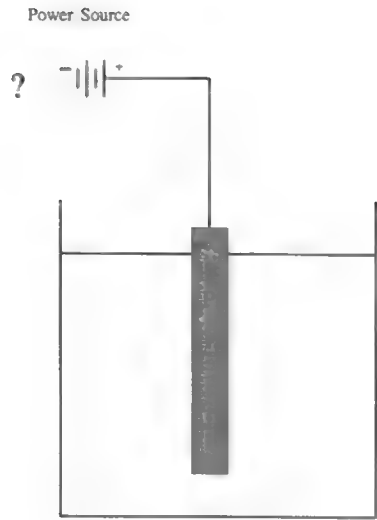


**Fig. 7.3. A uni-electrode system.**

In a vessel containing these three substances, there is no tendency to go the other way, from water to form hydrogen and oxygen. This can be made to occur, however, if an electrolyte such as NaOH is put into the water to produce ionic conduction and the conditions of a driven cell (Fig. 7.4) are set up (the two electrodes and the outside power source).

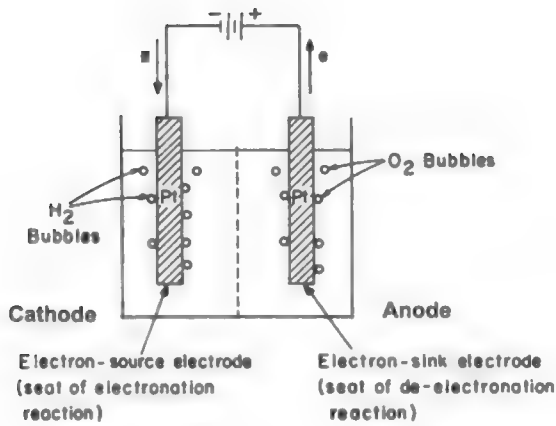
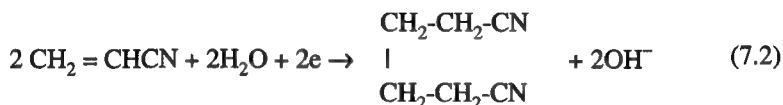


**Fig. 7.4. A driven cell or substance producer.**

Many such driven systems are known in electrochemistry and some of them will be explained in the chapters of this volume. One of them, indeed, is a step in the synthesis of nylon. This is the polymerization of acrylonitrile by means of the following electrochemical reaction:



This step is carried out on a large scale in the United States and the United Kingdom by Monsanto, and in Japan by Asahi.

**7.1.3.2. The Fuel Cell (or Electricity Producer).** A fuel cell is shown schematically in Fig. 7.5. Instead of pushing the reactions at the electrodes to go against their spontaneous tendency, the fuel cell consumes chemicals (their fuels), and the overall result of the reactions at its two electrodes is the consequence of allowing the reaction in the cell to occur spontaneously. As can be seen from the figure, the electrons produced from the oxidation of the lithium fuel at the one electrode pass out of the cell and travel on through a "load" (which could be an electric motor) and then pass on to reduce chlorine to chloride at the second electrode (Fig. 7.5).

The pollution-free production of electricity within electrochemical generators is a major step forward in technology. In the twenty-first century, transportation—cars, trains, and ships—will all be driven by electric motors powered by electricity derived from fuel cells (Chapter 13).

Thus, the electric cars that the Big Three auto makers are now planning in the United States will be moved by means of electric motors receiving electric power from

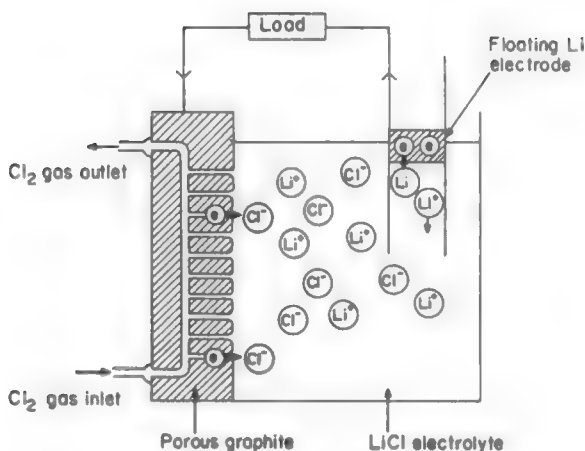


**Fig. 7.5.** A driving (fuel) cell or electricity producer.

fuel cells rather than from batteries. This is because batteries (storers of electricity produced elsewhere) give electric cars a range of not much over 100 miles, after which there has to be a pause for recharging that takes several hours. However, the fuel cell-electric motor combination (the electrochemical engine) will not be limited in range, which will depend, as with gasoline-powered internal combustion engines, only on the size of the fuel tank. The use of electric cars powered by fuel cells will eliminate the main cause of air pollution (emissions from gasoline-fueled cars) that all cities have to bear right now, together with the smog that develops over some. The way in which fuel cells work will be explained in Chapter 13.

**7.1.3.3. The Electrochemical Undevice: An Electrode that Consumes Itself while Wasting Energy.** It has been stated that in order to produce chemicals electrically (Fig. 7.4) and to obtain electricity directly from chemicals (Fig. 7.5), it is necessary always to have two electrodes in the cell. In this third device, which has the greatest economic significance of any part of electrochemistry, there are still two electrodes, but they both are contained in one piece of metal. It makes two electrodes

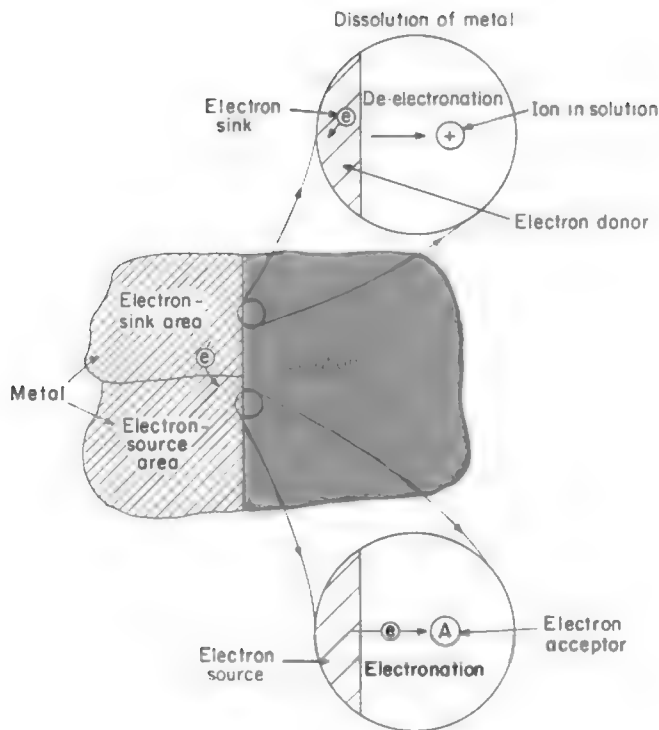


**Fig. 7.6.** Processes occurring in an electrochemical undevice, the electrochemical corrosion of metals.

because two different electron-transfer reactions take place upon different parts of it. The basic scheme is shown in Fig. 7.6.

On some surface sites the atoms of the metal give up their electrons to the bulk of the metal itself and leave the surface as ions, dissolving into the surrounding solution (or adherent moisture layer). Since the device shown in Fig. 7.6 is electrically isolated—does not have any wires attaching it to an outside power source—the piling up of electrons from the dissolving atoms in the metal has to be compensated by some electron-removing process that takes up the excess electrons and thus allows the dissolution of the metal to continue. In this way, the electrode (which is typically a piece of steel or aluminum) goes on consuming itself indefinitely.

What has been described here is corrosion (Chapter 12), the universally observed gradual decay of metals. A metal structure unprotected by an oxide film or a suitable paint layer will go on corroding, gradually breaking down. Although there are plenty of ways of thwarting corrosion, it is the metallurgical analogue of aging in biology, and limits the life of machines, planes, ships, etc., to a few decades.

#### 7.1.4. Some Special Characteristics of Electrochemical Reactions

All students of physical chemistry are taught something about the mechanism of chemical reactions and that knowledge can be summarized thus: The essential prerequisite for a chemical reaction is a collision between the molecules of the reactants. However, only if the colliding particles are sufficiently energized does a reaction occur.

It is therefore surprising to state that in the corresponding electrochemical reactions, the reactants never meet. They do collide, but with electronically conducting electrodes and not with each other. Thus, when Li and  $\text{Cl}_2$  are fed separately into an electrochemical cell, each in contact with a specific electrode (Fig. 7.5), there is electron transfer from the Li atoms to the electrode with which they are in contact. These electrons (messengers from the Li atoms, one might say) get around to the  $\text{Cl}_2$  molecules in contact with the second electrode and react with it to form  $\text{Cl}^-$  ions (making the pure electrolyte, lithium chloride). Thus, the overall reaction ( $\text{Li} + 1/2 \text{Cl}_2 \rightarrow \text{LiCl}$ ) takes place with the reactants separated: it is marriage by correspondence. The partners never actually meet, although their connection effectively leads to an offspring: electricity.

There is a second difference between electrochemical and chemical reactions. When chemical reactants meet in collision (and if they are to stick together), there is usually energy left over in the form of heat (an *exothermic* reaction). However, when the same reaction occurs electrochemically, the corresponding free energy change is converted directly to electricity without any heat of reaction reaching the surroundings.<sup>2</sup> Some have described the electrochemical process as being *cold combustion*.

<sup>2</sup>This statement is thermodynamically true. However, when fuel cells work, there may be a heating effect due to the passage of the current through the solution.



This conversion of the free energy of the chemical reaction occurring in the cell to electricity is what occurs in a fuel cell (Chapter 13). There, the energy of a chemical reaction goes directly into electricity, potentially to drive an electric motor, instead of some of the available energy being lost in the form of heat wasted on the surroundings, as occurs in heat engines, which work by means of chemical combustion. The fuel cell–electric motor combination is hence intrinsically a more efficient means of converting chemical energy to mechanical power than is the internal combustion engine. In fact, for many applications, fuel cell efficiencies are twice those of internal combustion engines.

So, there are two characteristics of electrochemical reactions that distinguish them from chemical reactions. While students are introduced to chemical reactions first, this is the reverse of the order in which we encounter reactions in real life. For example, digestive processes in the body are associated with electrochemical reactions on the surfaces of energy-converting mitochondrial cells. In fact, the electrochemical oxidation of, for example, glucose, coupled to the electrochemical reduction of oxygen taking place in these cells is part of the process by which our bodies get the electrical charges to work our musculature or the energy to power the compressions of the heart pump.

The great natural process of photosynthesis works by means of an electrochemical step as well. In it, water is split photoelectrochemically to produce atomic H and  $O_2$ , and the H produced later reacts chemically with  $CO_2$  present in the air to provide food for green plants, which then enter the food chain and give back to us solar energy to power the moving parts of our bodies.

Finally there is the mechanism by which metallic materials gradually break down in moist air. This process—corrosion—was described in Section 7.1.3.3.

These three great natural processes (conversion of biological energy into muscle power; collection and storage of solar energy in green plants, including grass and trees; and the breakdown of materials) all involve electrochemistry and embrace a significant part of normal life. *Purely chemical* reactions are less prominent in the natural world.

## 7.2. ELECTRON TRANSFER UNDER AN INTERFACIAL ELECTRIC FIELD

Electrode reactions are interfacial electron-transfer reactions, with the special circumstance that the electron transfer occurs between the solution and an electronic conductor, or vice versa. In Section 4.2.17 it was pointed out that the jump frequency of an ion is given by

$$\nu = \frac{kT}{h} c_i e^{-\Delta G^{\ddagger}/RT} \quad (7.3)$$

where  $\Delta G^{\ddagger}$  is the free energy of activation of the reaction.

Let a thought experiment be performed. In it, the metal electrode (a silver foil, say) is introduced into an aqueous solution (containing, say, ions of silver) so quickly (and without causing any disturbance in the solution) that suddenly the metal atoms of the silver foil, the molecules of water, and the  $\text{Ag}^+$  ions are confronting each other, none of them having had time to adjust to the newly created situation.

There will not yet be built up any of the excess surface charges that were examined in Chapter 6. Hence, there will be, for a tiny instant of time, maybe up to  $10^{-10}$  s, no intense electric field across the interface. Thus, as far as the  $\text{Ag}^+$  ions are concerned, they may experience a chemical force to move to the electrode, but there can be nothing as yet electrical in the influences on the ion from the electrode surface.

Wait, however, a short time, much less than a microsecond, and there will come about an orientation of water molecules and adsorption of  $\text{Ag}^+$  ions in the layer next to the electrode, which leads to the setting up of a specific interfacial region (called a *double layer*). Very soon there are positively charged ions lined up on the solution side of the layer at the electrode and negatively charged electrons on the electrode side, and the result is a strong electric field across this interfacial region (Fig. 7.7). The product of the electric field strength in volts times the thickness of the potential region is the potential difference across the interface, which is usually a few volts.

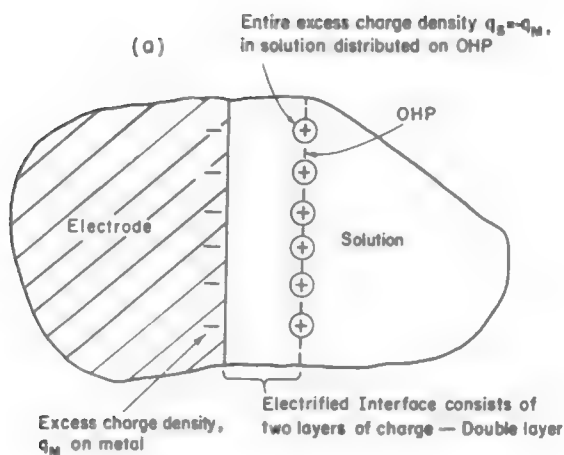


**Fig. 7.7.** (a) A double layer, a simple hypothetical type of electrified interface in which a layer of ions on the outer Helmholtz plane constitutes the entire excess charge  $q_{\text{soln}}$  in the solution. The solvation sheaths of these ions and the first row of water molecules on the electrode are not shown in the diagram. (b) The electrical equivalent of such a double layer is a parallel-plate condenser.

How can this electric field affect the rate of transfer of electric charge across the interface? To see how this can be done, assume the charge is carried all the way on the  $\text{Ag}^+$  ions that are to deposit on the electrode as atoms. For the moment, consider only the metal ion as an electric charge carrier and neglect the electrons, which presently will be seen transferring to neutralize the  $\text{Ag}^+$  and form a metal atom. Thus (see Fig. 7.8), the ion can be imagined as moving from right to left in the picture. On the right, there is imagined a layer of ions near the electrode, called the outer Helmholtz plane. One can assume that the electrode bears an excess negative electrical charge and the  $\text{Ag}^+$  ion, of course, is positively charged.

Suppose the interfacial potential  $^M\Delta^S\phi$  is divided (still in this thought experiment) into two parts. Each part will be less than the full  $^M\Delta^S\phi$ , which plays out across the whole double layer (or interphasial region between metal and solution). Suppose one takes a fraction of the potential difference,  $\Delta\phi$ , i.e.,  $\beta\Delta\phi$ , where ( $0 < \beta < 1$ ) and regards this fraction of the interfacial potential difference as that which (when multiplied by the electric charge,  $e_0$ , on the ion) lowers the chemical energy barrier for the ion's movement right to left by  $\beta e_0 \Delta\phi$ , as shown in Fig. 7.9. Thus, because this electrostatic energy is *helpful* (i.e., serves to attract the ion to move from right to left), one thinks of it as *lowering the energy barrier* for the transfer of the  $\text{Ag}^+$  from the layer in the solution nearest to the electrode and onto the electrode.<sup>3</sup> Thus, one could define  $\beta$  at this stage as

$$\beta = \frac{\text{Distance across around half the interfacial region}}{\text{Distance across the whole of the interfacial region}}$$

Correspondingly,  $(1 - \beta)\Delta\phi e_0$  is the amount (in energy terms) by which the energy barrier is raised for the converse metal  $\rightarrow$  solution reaction.

Thus,

$$\Delta\vec{G}^{\circ*} = \Delta\vec{G}_{\text{chem}}^{\circ*} + \beta e_0 \Delta\phi \quad (7.4)$$

It follows that

$$\vec{v}_e = \frac{kT}{h} e^{-\Delta\vec{G}_{\text{chem}}^{\circ*}/RT} e^{-\beta\Delta\phi e_0/RT} = \vec{v}_{\text{chem}} e^{-\beta\Delta\phi e_0/RT} \quad (7.5)$$

<sup>3</sup>The picture given here is merely illustrative. In a cathodic reaction (the electron leaves the metal to the solution), it is easy to see that a charged ion moving from the solution and surmounting an energy barrier will be helped if the electrode is negative to the ion's positive one. But what happens when an atom leaves the electrode and heads off for the solution? Atoms are not charged! So the picture only works for the reverse reaction if one assumes that the metal "atoms" in the surface of the electrode are already charged. Then it is easy to see that for an ion that wishes to leave the metal and go to the solution side, an increasingly positive charge will repel it and increase the velocity of reaction. A much more complete model of charge transfer is given in Chapter 9.

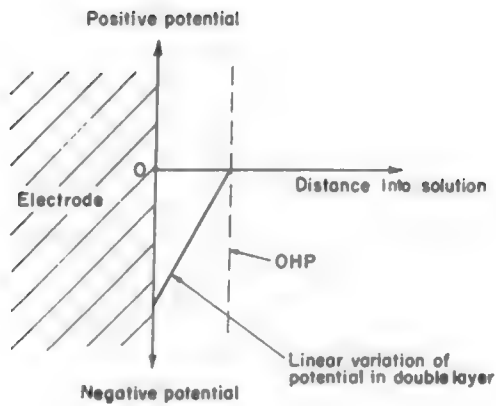


**Fig. 7.8.** The linear variation of potential corresponding to the double layer of Fig. 7.7(b).

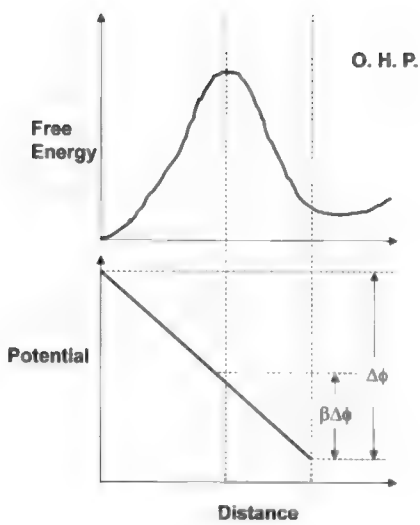


**Fig. 7.9.** The electrical work of activating the ion is determined by the potential difference across which the ion has to be moved to reach the top of the free energy-distance relation.

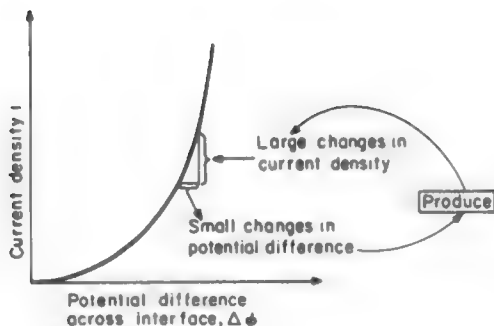


**Fig. 7.10.** The exponential nature of the current–potential dependence results in large changes in current for small changes in potential.

Here  $v_e$  is the number of ions per unit time and area transferring from the solution layer next to the electrode, to the electrode. It will at once be noticed that as long as the interfacial potential difference  $\Delta\phi$  is *negative*, the electrostatic work term  $\beta\Delta\phi e_0$  increases the velocity of the ion transfer reaction in an exponential way (Fig. 7.10).

One can write Eq. (7.5) in another form. Thus,  $e_0$  is the electrical charge of a *single ion* and  $k$  is the gas constant *per molecule*. Converting now to gram-ions, or moles,  $k$  becomes  $R$  and  $e_0$  becomes  $F$ , the faraday, the charge on an Avogadro's number of ions. Then:

$$\vec{v}_e = \frac{kT}{h} c_{Ag^+} e^{-\Delta G^*/RT} e^{-\beta F \Delta\phi / RT} \quad (7.6)$$

and this also represents the rate of the ion crossing the interface. When this is multiplied by the charge per mole of positive charges, it becomes the current density,  $i$ , in  $A\,cm^{-2}$ .

$$i = F \frac{kT}{h} c_{Ag^+} e^{-\Delta G^*/RT} e^{-\beta F \Delta\phi / RT} \quad (7.7)$$

This last relation, that for the electric current *density* (so called because it is per unit area and time), represents the bridge relation between chemistry (where the rate of a surface reaction is expressed in moles  $cm^{-2}\,s^{-1}$ ) and electrochemistry, where it is expressed in amperes (A)  $cm^{-2}$ .

One can put it in a simpler way that demonstrates this important link between the two kinds of velocities, the velocity,  $v$ , and the current density,  $i$ :

$$v = \frac{i}{F} \quad (7.8)$$

where  $v$  represents the chemical way of expressing an interfacial reaction rate and  $i$  represents the electrochemical way for a one-electron transfer reaction.

Now, if the ions in the layer next to the electrode keep on coming across and delivering their charge to the electrode (and if the latter is not connected to any compensating source of potential), then all the excess charge on either side of the double layer will be reduced to zero. The electrical help to the transfer of ions across the double layer (which is proportional to the excess charge on the interface), will slow down and stop, a miserable end to a promising beginning of a thought experiment.

### 7.2.1. A Two-Way Traffic Across the Interface: Equilibrium and the Exchange Current Density

The slowdown toward zero of the thought experiment current described at the end of the last section clearly won't do, and something has been left out of the thoughts that led to it. One of the principles of physical chemistry is called the principle of microscopic reversibility. Put in a simple but correct way, it states that something that happens in one direction will also happen in the other direction *along the same path*. What we have been looking at in the last section could be written as



where  $M^+$  is a metal ion and  $A$  a metal atom.

Presumably, therefore



The first of these two reactions could well be called *electronation* and the second, *deelectronation*. One can easily write the equation for it by using the expression  $(1 - \beta)F\Delta\phi$  for the effect of the interfacial potential upon the energy barrier for the deelectronation reaction. By reference to Eq. (7.7), one would get for the current density in the reverse direction to that expressed in Eq. (7.9):

$$\vec{i} = Fk_{\text{chem}}c_A e^{(1-\beta)F\Delta\phi/RT} \quad (7.11)$$

where  $c_A$  is the surface concentration of atoms on the electrode.

Now, this possibility of ionization happening to atoms in metal surfaces (by which they become ions), as well as ions in solution forming atoms on the electrode, does help the dilemma of the diminishing current referred to at the end of the last section,  $M^+ + e \rightarrow A$ , slowing down to zero. If the atoms also ionize ( $A \rightarrow M^+ + e_M$ ), the electronic charge on the interface will be increased and therefore (with ions and electrons going *both* ways across the interfacial region) one will clearly end up (as far as a charge on the electrode is concerned) in a compromise. This is because an electrode reaction going in one direction uses up charge and a reaction going in the other direction produces it.

However, there might be another possibility. Suppose that one has the electrode (the Pt plate, for example) not just sitting in the solution and exchanging ions and electrons with the solution, but with an electronic connection (a wire in fact) leading from the electrode in the solution to an outside source of electric power—an electron supply house.

The addition of an outside potential source—and one that can vary the electrical potential level of the electrons in the Pt plates—widens the possibilities of what happens to the excess (or scarcity) of electronic charge on the electrode surface.<sup>4</sup> Because the interfacial potential difference,  $\Delta\phi$ , is proportional to the excess electric charge on the surface of the electrode, the currents in the two directions, the electro-nation and deelectronation currents as they have been called, will change with change of charge and  $\Delta\phi$  [cf. Eqs. (7.7) and (7.11)]. Before we explore the opening this connection gives us, it is interesting to consider what conditions make the backward and forward movement of ions equal in rate.

The importance of this equality is that it will represent equilibrium and thus it provides an important bridge, that between electrochemical kinetics (to which an introduction is being given here) and thermodynamics. Before we deduce the condition for an equal rate of exchange of ions to electrode (as atoms) and atoms to solution (as ions), it is important to mention the name of a seminal figure in the history of electrochemistry. J. A. V. Butler,<sup>5</sup> the British physical chemist, was the first to write down a treatment of the kind discussed here, i.e., he was the first to connect the kinetic electrochemistry built up in the second half of the twentieth century with the thermodynamic electrochemistry that dominated the first half.

However, Butler did not get it all quite right and therefore it is necessary to give credit also to Max Volmer, a great German surface chemist of the 1930s<sup>6</sup> and his student (at that time), Erdey-Gruz.<sup>7</sup> Butler's very early contribution in 1924 and the

---

<sup>4</sup>To be able to have an electronic device to control the potential of the electrode under consideration so that a continuous current passes, there has to be another electrode as well to complete the circuit. (See the examples in the figures showing the three basic electrochemical devices.)

<sup>5</sup>J. A. V. Butler had to his credit, not only the first exponential relation between current and potential (1924), but also (along with R. W. Gurney, Chapter 9) the introduction of energy-level thinking into electrochemistry (1951). Later he contributed to biochemistry relevant to cancer research. Butler was the quintessential absent-minded research scientist of legend, often lost to the world in thought. During such periods of contemplation he sometimes whistled softly to himself, though he was known on occasion to petulantly instruct nearby colleagues to be *quiet*.

<sup>6</sup>Volmer held the prestigious chair of physical chemistry at the University of Berlin. That chair had previously been held by the great Walther Nernst, whose work led to the third law of thermodynamics. In his years in Berlin, Volmer was best known for his early contributions to models for crystal growth, both under chemical and electrochemical conditions.

After World War II (WWII), the Communist government of East Germany forcibly removed Volmer to a position in Russia. However, scientists of his stature were given privileges far above those of their Russian colleagues, so that their position was described as being in a "golden cage."

<sup>7</sup>Much later, this student became the minister for education in Hungary.

Erdey-Gruz and Volmer contribution in 1930 form the basis of phenomenological kinetic electrochemistry.

With the possibility of an outside connection to an electric power source allowing the entry and exit of an excess electronic charge on the electrode surface, the potential difference,  $\Delta\phi$ , across the metal/solution interface can be varied at will. If it is made more positive, there will be a faster ionization (or deelectronation) current [cf. Eq. (7.11)]. If it is made more negative, the electronation current will increase. Hence there must occur a value of  $\Delta\phi$  (it is reasonable to call it  $\Delta\phi_{\text{equilibrium}}$ , or  $\Delta\phi_e$ ) at which the two rates will be equal.

Then [from Eqs. (7.7) and (7.11)]:

$$\vec{i} = \vec{k} c_M^* e^{-\beta \Delta\phi_e F/RT} = \overleftarrow{i}_0 = \overleftarrow{k} c_A e^{(1-\beta) \Delta\phi_e F/RT} \quad (7.12)$$

The significance of these equal and opposite current densities is easy to comprehend. They represent the kinetic side of equilibrium. Equilibrium is not a static business, as it often seems to be from thermodynamics. It is better to regard it as a two-way traffic of ions and electrons across the interface. The word “exchange” is used quite aptly here—there is an exchange of ions between electrode and solution, and at the equilibrium potential the rate of exchange in each direction is equal in magnitude though opposite in direction.

Thus, the exchange current density,  $i_0$ , is a useful arbiter of the dynamic nature of the electrode reaction. The larger the  $i_0$ , the faster the exchange of ions and charge takes place, although because it is equilibrium, there is no net electronation or deelectronation current. We will see shortly that  $i_0$  determines the rate of electrode reactions at any potential  $\Delta\phi$ —and indeed leads to the study of electrodes acting as catalysts.

## 7.2.2. The Interface Out of Equilibrium

So far it has been shown that

1. The “current density” (or electrochemical reaction rate) that signifies the rate of electric charge flow (e.g., electrons leaving the metal to go to ions in an adjacent layer in solution) is given by, for example, Eq. (7.7) by putting the constant terms  $kT/h$  and  $\exp(-\Delta G^\circ)$  together as  $\vec{k}$ :

$$\vec{i} = \vec{k} c_M^* e^{-\beta \Delta\phi F/RT} \quad (7.7a)$$

2. The reverse of this, the electrons being donated back to this metal, would be given by

$$\overleftarrow{i} = \overleftarrow{k} c_M^* e^{(1-\beta) F \Delta\phi / RT} \quad (7.11)$$



Up until now, the special case of equilibrium:

$$\vec{i} = \vec{i} \quad (7.13)$$

has been considered. In this section, a further step will be taken. By adjusting the settings on the outside power source away from that set for equilibrium, it is possible to provoke more charge flow in one direction than another, hence to have a net flow of electric current across the interface (for, at equilibrium, the net flow is zero).

Now, it is necessary to define a new and central term. It is called the *overpotential*,  $\eta$ . It refers to the departure of the potential of the electrode from its equilibrium value,  $\Delta\phi_e$ . By making  $\eta$  negative, one can push excess electrons into the electrode and provoke a net exiting of electrons from metal to solution; one can provoke the entry of electrons. Suppose we impose (using the outside power source) a shift ( $\eta$ ) in the electrode potential from the equilibrium value in a negative direction. The new interfacial potential is to be  $\Delta\phi$ . Then, the definition of overpotential is

$$\eta = \Delta\phi - \Delta\phi_e \quad (7.14)$$

In words, the overpotential is a deviation of the Galvani potential of the electrode from the value it has when the rate of charge flow across its interface with the solution is equal in each direction for the reaction concerned (i.e.,  $\text{M}^{z+} + ze \rightleftharpoons \text{M}$ ). The definition given in Eq. (7.14) is general, although it is necessary to define the electrode reaction concerned, the solution composition, etc., because the value of the thermodynamic  $\Delta\phi_e$  is different for each electrode reaction, concentration of reactant, and temperature.

There is a technical name given to electric currents in which electrons leave the electrode bound for ions in the solution. They are called *cathodic*, and an electrode in the state of such emission is called a cathode.

Correspondingly, the outside power source can be adjusted so that it reduces the density of excess surface electrons below that of equilibrium. Then,  $\Delta\phi$  is more positive than the value for equilibrium and hence  $\eta = \Delta\phi - \Delta\phi_e$  is positive. The technical name given to electric currents in which the electrons leave particles in the solution and enter the electrode is “anodic” and the electrode in this positively charged state is termed an *anode*.<sup>8</sup>

<sup>8</sup>These terms “anode” (electron sink) and “cathode” (electron source) are both due to a suggestion made to the great Michael Faraday by his friend, the Reverend Whewell. “If we admit the magnetism of the Globe as due to Electric Currents running... from East to West, and if a portion of water under decomposition by an electric current be placed so that the current through it shall be parallel to that considered as circulating round the earth, then the oxygen will be rendered towards the east... and hydrogen towards the west .... Eastode and Westode, however, are names which a scholar could not suffer,” and thus Reverend Whewell, a well-known (among other things) philologist, suggested “anode” and “cathode” as words that also might signify an eastern and western “way.”

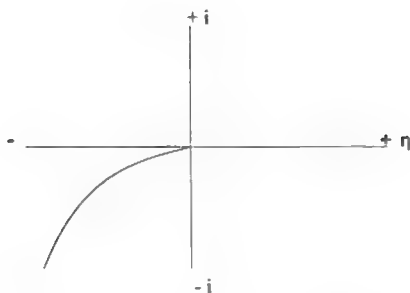


**Fig. 7.11.** Dependence of current density (or reaction rate) on negative overpotential.

What has been said so far about overpotential and cathodic and anodic current densities can be shown in two figures (Figs. 7.11 and 7.12). The results of a negative overpotential are shown in Fig. 7.11 and the use of a positive overpotential is shown in Fig. 7.12. The way these figures have been drawn, the cathodic and anodic rates of electron flow, or current densities, seem the same except for the sign of the overpotential, which is positive for the anodic current (electrons entering the electrode from the solution) and negative for electrons ejected from the metal electrode to the solution. The corresponding currents also have signs, positive for the anodic current and negative for the cathodic one.

In practice, one often has cases where the course of the cathodic and anodic current densities across the electrode with change of overpotential is symmetrical (except for the signs for the same numerical value of  $\eta$ ). It will be seen in the next section that this is so if the symmetry factor,  $\beta$ , is exactly 0.50. More often, the anodic and cathodic curves are nearly symmetrical. However, sometimes they are importantly and even dramatically different. For example, the anodic current is oxidizing and could provoke

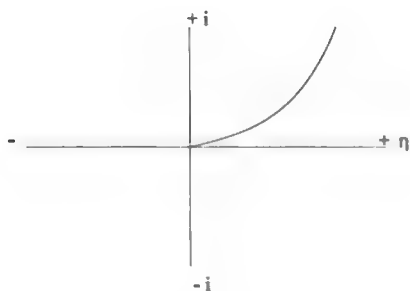


**Fig. 7.12.** Dependence of current density on positive overpotential.

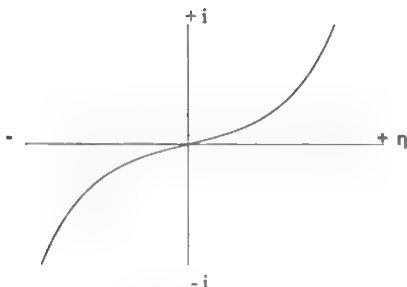


**Fig. 7.13.** Dependence of current density on overpotential.

the formation of a resistive film on the electrode, and this may cause the current to decrease with increasingly positive overpotential, in contradiction to what is shown in Fig. 7.12.

One more thing should be discussed before becoming acquainted with a famous equation. This is to put Figs. 7.11 and 7.12 together. One gets Fig. 7.13.

### 7.2.3. A Quantitative Version of the Dependence of the Electrochemical Reaction Rate on Overpotential: The Butler–Volmer Equation

From what has been described so far, there can be a flow of cathodic current, or of anodic current at an electrode/solution interface, according to the value (and particularly the sign) of the overpotential, i.e., of the displacement from equilibrium of the electric potential of the electrode. The equilibrium referred to is that of some specific interfacial electron transfer reaction (e.g., the cathodic reduction of  $O_2$  ( $O_2 + 4H^+ + e \rightarrow 2H_2O$ )) or the anodic oxidation of ethylene,  $C_2H_4 + 4H_2O \rightarrow 2CO_2 + 12H^+ + 12e$ .

At equilibrium and only at equilibrium, the two partial current densities at the electrode are equal in magnitude and opposite in direction. When  $\eta$  is negative, there will be a net *cathodic* electron flow to the first layer of ions in contact with the electrode, and the corresponding current density:

$$i_{\text{cath}} = \vec{i} - \overleftarrow{i} \quad (\Delta\phi < \Delta\phi_e) \quad (7.15)$$

If  $\eta$  is positive, there will be a net *anodic* current (electron from the solution layer to the electrode), and the corresponding anodic current density is

$$i_{\text{an}} = -\overleftarrow{i} - \vec{i} \quad (\Delta\phi > \Delta\phi_e) \quad (7.16)$$

At equilibrium,  $\Delta\phi = \Delta\phi_e$ :

$$\vec{i} = \vec{i} \quad (7.17)$$

$$i_{\text{cath}} = i_{\text{an}} = 0 \quad (7.18)$$

For a net cathodic current density:

$$i_{\text{cath}} = F\vec{k}c_i e^{-\beta\Delta\phi F/RT} - F\vec{k}c_A e^{(1-\beta)\Delta\phi F/RT} \quad (7.19)$$

where  $c_i$  is the concentration of an ionic species  $i$  and  $A$  is atoms.

If  $\Delta\phi = \Delta\phi_e$ ,

$$i_{\text{cath}} = 0 \quad (7.20)$$

Hence,

$$F\vec{k}c_i e^{-\beta\Delta\phi_e F/RT} = i_0 = F\vec{k}c_A e^{(1-\beta)\Delta\phi_e F/RT} \quad (7.21)$$

where  $i_0$  is called the *exchange current density*.

From (7.14):

$$\Delta\phi = \eta + \Delta\phi_e \quad (7.22)$$

Then, from Eq. (7.19):

$$i_{\text{cath}} = i_0 (e^{-\beta\eta F/RT} - e^{(1-\beta)\eta F/RT}) \quad (7.23)$$

This is the famous Butler–Volmer (B–V) equation, the central equation of phenomenological electrode kinetics, valid under conditions where there is a plentiful supply of reactant (e.g., the  $\text{Ag}^+$  ions) by easy diffusion to and from electrodes in the solution, so that the rate of the reaction is indeed controlled by the electric charge transfer at the interface, and not by transport of ions to the electrode or away from it.

The B–V equation has been derived here for the case of a negative  $\eta$  whereupon the current passing will be cathodic, i.e., electrons will flow from the electrode to the solution. There can be an exactly similar anodic deduction and the result will be

$$i_{\text{an}} = i_0 (e^{(1-\beta)\eta F/RT} - e^{-\beta\eta F/RT}) \quad (7.24)$$

Here the first (anodic) term dominates,  $\eta$  is positive, and the current will be by means of transfer of electrons from the solution to the electrode.

There are two limiting cases of the Butler–Volmer equation. They are given in the following two sections.

**7.2.3.1. The Low Overpotential Case.** If  $\eta$ , the overpotential, is numerically less than  $RT/\beta F$  (around 50 mV at room temperature in most cases), expansion of the B–V equation under this condition (using the usual Taylor–MacClaurin expansion) gives:

$$i = i_0 \frac{\eta F}{RT} \quad (7.25)$$

i.e., the current density (the rate of electron transfer across the electrode/solution interface) is linear with the overpotential,  $\eta$ . The sign of the current density will be determined by that of  $\eta$ , negative for a cathodic (electronation) current and positive for an anodic (or deelectronation) one.

**7.2.3.2. The High Overpotential Case.** If  $\eta$  is numerically greater than  $RT/\beta F$ , then for cathodic current densities ( $\eta$  negative),

$$e^{-\beta\eta F/RT} > e^{(1-\beta)\eta F/RT} \quad (7.26)$$

therefore (and if  $\eta$  is sufficiently negative):

$$i_{\text{cath}} = i_0 e^{-\beta\eta F/RT} \quad (7.27)$$

Thus, as  $\eta$  becomes increasingly negative, the current rises exponentially.

It is trivial to show that from Eq. (7.27),

$$\eta = \frac{RT}{\beta F} \ln i_0 - \frac{RT}{\beta F} \ln i \quad (7.28)$$

For a given reaction and temperature,  $i_0$ , the exchange current density (Section 7.2.1) is constant so that for a given reaction and constant temperature:

$$\eta = a - b \log i \quad (7.29)$$

where  $a$  and  $b$  are constants, and  $b = 2.303 RT/\beta F$  (Tafel's equation, 1905). At 298 K,

$$2.303 RT/F = 2.303 (8.315)(298)/9.65 \cdot 10^4 = 0.058. \quad (7.30)$$

Of course, for an anodic reaction, a corresponding argument with  $\eta$  sufficiently<sup>9</sup> positive gives

<sup>9</sup>“Sufficiently”?  $\eta > 0.05 \text{ V}$  makes the current in one direction more than 10 times the current in the other.

$$i = i_0 e^{(1-\beta)\eta F/RT} \quad (7.31)$$

and

$$\eta = a + b \log i \quad (7.32)$$

Hence, if  $\beta \approx 1/2$ ,  $b \approx (2.303)2 RT/F = 0.116$ . In fact, experiments show that for simple electron- and ion-transfer reactions, one often finds that  $\partial\eta/\partial \log i \approx 0.12$  V, i.e., they agree with the simplest supposition,  $\beta = 1/2$ , which corresponds to the picture one gets if the energy barrier at the surface is symmetrical.

There are two kinds of charge-transfer reactions at electrodes. An *electron-transfer* reaction is the first kind and is exemplified by the reduction of  $\text{Fe}^{3+}$  to  $\text{Fe}^{2+}$  at the interface. The ions in the layer hardly move while the electron comes from the electrode or leaves the ions in the layer of solution adjacent to the electrode and goes to the electrode. The charge transfer is dominated by means of electrons transferring from electrode to ions and vice versa.

An *ion-transfer* reaction, on the other hand, is one in which, for example, in the cathodic deposition of  $\text{Ag}^+$  ions, the  $\text{Ag}^+$  ion begins in the solution layer nearest the electrode but toward the electrode. At some point on the way, electron transfer occurs. The point is, the ion has also transferred. Correspondingly, for anodic ion-transfer reactions, a surface atom leaves the electrode, becoming in this act an ion and leaving an electron behind in the metal.

## 7.2.4. Polarizable and Nonpolarizable Interfaces

In Section 6.3.3 the polarizability of an interface was discussed. To revise what was said earlier, the ideal polarizable interface is one in which, when the potential on the metal side is forced to move in the positive or negative direction, there is a change of potential across the interphasial region, but no consequent passage of charge across the interface.

Indeed, a small current does flow, though not across the interphase. It is called a *charging current*, i.e., a current observed because there is an electron flow either out of the electrode or into it. But this latter current does not result in any electrons crossing the interphase; it's like charging the plates of a condenser. A perfectly polarizable electrode is the analogue of an absolutely leakproof condenser.

At the other end of the scale is the idealization of a nonpolarizable electrode—and that means an electrode that is “completely leaky,” i.e., when one flows electrons in from the outside circuit to give excess electrons to the electrode, they do not stay there, but go straight across and neutralize particles on the other side. In contrast to the behavior of a polarizable electrode, the potential of the electrode does not change because, of the electrons that flow in, none stay, i.e., no extra charge builds up on the electrode surface, but instead flows away to the solution. In the same way, when a nonpolarizable electrode is stimulated to flow electrons from the solution to the

electrode, electrons promptly flow across the double layer from the ions in the electrode surface, rather than the ions accumulating on the electrode surface making the potential more positive.

As implied, no real electrode is exactly like a polarizable or a nonpolarizable electrode. But the idealizations of completely polarizable (potential changes, but no current flows across the interphase), or completely nonpolarizable (current passes, but there is no potential change) electrodes are useful. Real electrodes tend to be more like the one or the other of the two ideals.

The real case, a partly polarizable (and hence partly nonpolarizable) electrode, can be described in terms of the exchange current density  $i_0$ . From the linearized Butler–Volmer equation [Eq. (7.25)], then:

$$\frac{\partial i}{\partial \eta} = \frac{F}{RT} i_0 \quad (7.33)$$

Or,

$$\frac{\partial \eta}{\partial i} = \frac{RT}{F} \left( \frac{1}{i_0} \right) \quad (7.34)$$

According, however, to Ohm's law,

$$E = I R_{CT} \quad (7.35)$$

Or

$$\frac{\partial E}{\partial I} = \frac{RT}{i_0 F} = R_{CT} \quad (7.36)$$

where  $R_{CT}$  is the differential charge-transfer resistance.

The resistance to current flow at

$$\eta < \frac{RT}{\beta F} \quad (7.37)$$

is therefore proportional to  $1/i_0$ . A relatively large  $i_0$  (e.g.,  $10^{-3} \text{ A cm}^{-2}$ ) will mean a relatively small resistance to electron transfer so that such an electrode would tend to be nonpolarizable. But if  $i_0$  were very small ( $10^{-10} \text{ A cm}^{-2}$ , say), the resistance of the interface would be very large, i.e., it would tend to be polarizable.

Thus, the resistance to electron flow across the double layer is (at 298 K),

$$R_{CT} = \frac{0.025}{i_0} \text{ ohms cm}^{-2} \quad (7.38)$$

For  $i_0 = 10^{-3} \text{ A cm}^{-2}$ , this resistance is  $0.025 \times 10^3 = 25 \text{ ohms cm}^{-2}$ . But if  $i_0 = 10^{-10} \text{ A cm}^{-2}$ , the resistance is  $25 \times 10^7 \text{ ohms cm}^{-2}$ . This, then, puts a more quantitative face on the terms “polarizable” and “nonpolarizable.” The first electrode of the two examples is fairly nonpolarizable and the second distinctly polarizable.

## 7.2.5. The Equilibrium State for Charge Transfer at the Metal/Solution Interface Treated Thermodynamically

Thermodynamic treatments in physical chemistry were effectively identical with the theory of the subject in the nineteenth century. No one understood electron transfer at interfaces at that time (J. J. Thompson did not discover the electron until 1897). But whereas the molecular kinetic approach gradually seeped into many parts of chemistry by the 1930s, the chemistry of electrode processes remained reluctantly bound up with the older thermodynamic viewpoint. The Faraday Society meeting in Manchester, U.K. in 1947 was a turning point in the application of a molecular-level concepts and even of quantum mechanics. By the mid-1950s, research papers in electrode process chemistry (except for those dealing with electroanalytical themes)<sup>10</sup> were fully kinetic.

Nevertheless, the earlier thermodynamic treatment left one significant equation still very much present and effective when a change toward the kinetic approach occurred. This equation (Nernst’s law) is used today and probably will be used even when all electrochemical calculations are wrapped up inside various companies’ software offerings. Nernst’s equation,<sup>11</sup> which treats the electrode/solution interface at equilibrium in a thermodynamic way, is the subject of the following section.

<sup>10</sup>Electroanalytical chemistry—the application of an understanding of electrode processes to analyze materials in solution—requires attention to just that aspect of the story one tries to diminish in the study of happenings at the interface. One needs to think of diffusion and migration to the electrode and how they affect its potential. By measuring the rate of this migration, it is possible to find the concentration of entities in the solution. Thus, an ideal electrode, from the electroanalytical viewpoint, is a nonpolarizable one. Changes in potential that occur because the electron passage across the interface is balky are simply a complication thwarting the electroanalytical purpose.

If this is the case, the interest in the phenomenology of  $i$ – $\eta$  in terms of the Butler–Volmer equation (no diffusion control, all electron transfer at the interface) is lessened. It will be acceptable to use equilibrium concepts at the interface for many purposes, and concentrate on the rate-determining transport process outside the interfacial region.

Electroanalytical chemists *do* deal with what they call “irreversible reactions” because they exist at and interfere with a transport-oriented approach. But the focus of interest in electroanalytical chemistry (rather reasonably), is on the usefulness of electrode processes to analysis and in this case one should aim for an electrode showing the highest  $i_0$ , and hence the least  $\eta$  for a given current density.

<sup>11</sup>Walther Nernst (see also Vol. 1, Section 3.4.8) was the epitome of the “God professor,” a man regarded by all who knew him as not only more knowledgeable but also much more intelligent and self-disciplined than other men. He suggested a theorem according to which  $\Delta S$  for chemical reactions tends to zero as  $T$  tends to zero, and this theorem led directly to the third law of thermodynamics. Like many great scientists, Nernst was not limited to one field. Late in life he switched his attention to cosmology and made a suggestion that is now at the forefront of theories that may soon replace the Big Bang.



## 7.2.6. The Equilibrium Condition: Kinetic Treatment

According to Eq. (7.21) in which the concept of the exchange-current density was introduced, at equilibrium,

$$F\vec{k}c_{A^+}e^{-\beta\Delta\phi_e F/RT} = i_0 = F\vec{k}c_D e^{(1-\beta)\Delta\phi_e F/RT} \quad (7.21)$$

where  $c_{A^+}$  is the concentration of an electron-acceptor ion,  $c_D$  is that of an electron donor. Hence,

$$\Delta\phi_e = \frac{RT}{F} \ln k + \frac{RT}{F} \ln \frac{c_{A^+}}{c_D} \quad (7.39)$$

Since the first term is not a function of concentration, one can write it as a constant. Hence,

$$\Delta\phi_e = \Delta\phi_{e,o} + \frac{RT}{F} \ln \frac{c_{A^+}}{c_D} \quad (7.40)$$

This kinetically deduced equation relates  $\Delta\phi_e$ , the metal-solution potential difference [a Galvani potential difference (Section 6.3.10)], to the concentration (and in a more complete treatment, the activity) of those ions in the solution that undergo electron transfer at the interface. It will be seen later that (7.40) is quite near the famous equation that bears Nernst's name.

## 7.2.7. The Equilibrium Condition: Nernst's Thermodynamic Treatment

Consider a  $z$  electron exchange reaction occurring at an interface of an electrode in solution. It can be written:



Then the general thermodynamic condition for equilibrium in a reaction involving charged particles and electrons is

$$\mu_M = \bar{\mu}_{M^{z+}} + z\bar{\mu}_e \quad (7.42)$$

since the electrochemical potential of the neutral metal atoms is equal to the chemical potential  $\mu_M$ . Now [Eq. 6.34],

$$\bar{\mu}_{M^{z+}} = \mu_{M^{z+}} + zF\phi_s \quad (7.43)$$

and

$$\bar{\mu}_e = \mu_e - F\phi_M \quad (7.44)$$

the  $M^{z+}$  and  $e$  species being on the solution side and on the metal side of the interface, respectively. The  $\phi_M$  and  $\phi_S$  are the inner potentials of two phases, respectively, and the negative signs on  $F\phi_M$  reflect the fact that the charge on an electron is  $-1$ .

Introducing these into Eq. (7.42) one obtains

$$\mu_M = \mu_{M^{z+}} + \mu_e + zF(\phi_S - \phi_M) \quad (7.45)$$

Thus, according to the convention that the potential difference across the interface is the inner potential of the metal minus the inner potential of the solution, one has

$$\Delta\phi_e = \phi_M - \phi_S = \frac{1}{zF} (\mu_{M^{z+}} + \mu_e - \mu_M) = -\frac{\Delta G}{zF} \quad (7.46)$$

However, it will be recalled that chemical potentials are related to activities by the familiar expression  $\mu_i = \mu_i^\circ + RT \ln a_i$ . Since the atoms in the metal are of a metal in the pure form, they are in its standard state, so that their activity is considered to be 1; it follows that  $a_M = 1$ . The electrons are also in their standard state,  $a_e = 1$ , and the equation becomes

$$\Delta\phi_e = \frac{(\mu_{M^{z+}}^\circ + \mu_e^\circ - \mu_M^\circ)}{zF} + \frac{RT}{zF} \ln a_{M^{z+}}$$

and where  $a_M = 1$ ,

$$\Delta\phi_e^\circ = \frac{(\mu_{M^{z+}}^\circ + \mu_e^\circ - \mu_M^\circ)}{zF} = -\frac{\Delta G^\circ}{zF}$$

which results in

$$\Delta\phi_e = \Delta\phi_e^\circ + \frac{RT}{zF} \ln a_{M^{z+}} \quad (7.47)$$

This equation is virtually identical to the kinetically deduced version of Eq. (7.40). However, it is not yet formally identical with that of Nernst, which was deduced long before the concept of a Galvani potential difference ( $^M\Delta^S\phi$ ) across the metal/solution interface was introduced (Lange and Misenko, 1930). Nernst's original treatment was in terms of the electrode potential and symbolized by  $V$ . It is possible to show (see Section 3.5.15) that for a given electrode,  $^M\Delta^S\phi - V + \text{const.}$  (i.e., the factors that connect the measured electrode potential to the potential across the actual interface) do not depend on the activity of ions in the solution. Hence, using now the relative electrode potentials,  $V_i$  in place of the absolute potentials  $\Delta\phi$ ,

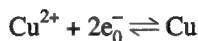
$$V_e = V_e^0 + \frac{RT}{zF} \ln a_{M^{z+}} \quad (7.47a)$$

which is the classical law of Nernst, and the same equation as that deduced kinetically, i.e., Eq. (7.40).

Correspondingly, it can be shown that for a more general case of an acceptor  $A^{z+}$  that accepts  $z$  electrons in its equilibrium with an electron donor  $D$ ,

$$\Delta\phi_e = \Delta\phi_e^0 + \frac{RT}{zF} \ln \frac{a_{A^{z+}}}{a_D} \quad (7.47b)$$

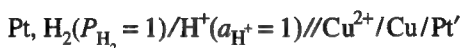
In discussing this modification, it is helpful to consider a concrete example. Suppose that the electron-transfer reaction at the interface under study is



i.e., the electron acceptor  $A$  is  $\text{Cu}^{2+}$  and the electron donor  $D$  is  $\text{Cu}$ . The Nernst equation for the interface reads (on setting,  $a_{\text{Cu}} = 1$ ):

$${}^{\text{Cu}}\Delta^{\text{S}}\phi_e = {}^{\text{Cu}}\Delta^{\text{S}}\phi_e^0 + \frac{RT}{2F} \ln a_{\text{Cu}^{2+}} \quad (7.48)$$

At this stage, two facts may be recalled. First, the potential difference across an electrochemical cell, or system, is measurable. Thus, if the  $\text{Cu}^{2+}/\text{Cu}$  interface is incorporated into an electrochemical along with a second metal/solution interface, the potential difference across the whole cell is measurable (Fig. 7.14). Second, if the second interface is nonpolarizable (i.e., its potential does not depart significantly from the equilibrium value on the passage across it of a small current), it contributes a constant value to the potential difference across the cell. Thus, by choosing a standard hydrogen electrode as the nonpolarizable interface, the following system can be built (Fig. 7.14):



In this representation,  $\text{Pt}'$  (and not  $\text{Pt}$ ) has been written in at the right to show that a contact potential difference will arise where the platinum wire from the high-input impedance voltmeter (Fig. 7.14) contacts the copper electrode. The symbol  $//$  is used to indicate that the potential due to the junction between the solutions containing the  $\text{H}^+$  and  $\text{Cu}^{2+}$  has been minimized.

This is, in fact, the way electrode potentials are measured in practice. A cell is made up of the electrode of interest (the working electrode, e.g.,  $\text{Cu}$  in Fig. 7.14) and a reference electrode made of  $\text{Pt}$  over which is bubbled  $\text{H}_2$ . No current passes through the reference electrode, which is therefore at its thermodynamically reversible potential. A counter-electrode (not shown in Fig. 7.14) is coupled through a power source

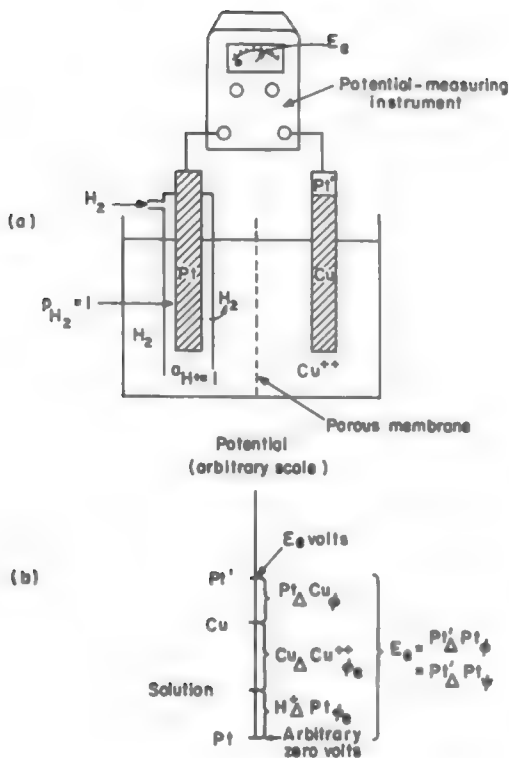


**Fig. 7.14.** A galvanic cell composed of a copper electrode in cupric ion solution and a standard hydrogen electrode (a) gives a measurable potential difference  $E_g$  (b).

to the working electrode. Thus, the working electrode potential is measured by coupling it with a thermodynamically reversible reference electrode, and when that is the standard reversible hydrogen electrode, the latter is arbitrarily taken as zero (cf. the zero in the centigrade side for temperature).

The potential difference  $V$ , across this cell (i.e., the reading on the voltmeter) consists of the following potential differences [cf. Eq. (6.12)]:

$$E_e = {}^{\text{Pt}}\Delta^{\text{Pt}'}\phi = {}^{\text{Cu}}\Delta^{\text{S}}\phi_e + {}^{\text{S}}\Delta^{\text{Pt}}\phi_e^0 + {}^{\text{Pt}'}\Delta^{\text{Cu}}\phi \quad (7.49)$$

Similarly, if the copper ions are at unit activity,  $a_{\text{Cu}^{2+}} = 1$ , one has

$$E_e^0 = {}^{\text{Pt}}\Delta^{\text{Pt}'}\phi^0 = {}^{\text{Cu}}\Delta^{\text{S}}\phi_e^0 + {}^{\text{S}}\Delta^{\text{Pt}}\phi_e^0 + {}^{\text{Pt}'}\Delta^{\text{Cu}}\phi \quad (7.50)$$

Note that  ${}^S\Delta\phi_e^{\text{Pt}^0}$  and  ${}^{\text{Pt}}\Delta\phi^{\text{Cu}}$  are constant quantities, the former because the hydrogen electrode is nonpolarizable and the latter because the inner potential difference of two metals *in contact*,  ${}^{\text{Pt}}\Delta\phi^{\text{Cu}}$ , depends purely on the two metals and not on what is happening inside the solution (i.e., it does not depend on the activity of the solution ions).

Now, adding Eqs. (7.48)–(7.50) together gives us a very convenient expression, the Nernst equation for the cell potential (i.e., that of the copper electrode in equilibrium with cupric ions in the solution, together with the standard  $\text{H}_2$  electrode, Fig. 7.14)<sup>12</sup>:

$$E_e = E_e^\circ + \frac{RT}{2F} \ln a_{\text{Cu}^{2+}} \quad (7.51)$$

One could determine  $E_e^\circ$ , the cell potential, when the solution has  $a_{\text{Cu}^{2+}} = 1$ , and once  $E_e^\circ$  is known, one could predict the cell potential for any other activity of copper ions from (7.51).

## 7.2.8. The Final Nernst Equation and the Question of Signs

The question is: How can one get an equation of the form (7.51) from Eq. (7.48)? One is at liberty to add constants to both sides of an equation. So, one can add  ${}^S\Delta\phi_e^{\text{Pt}^0}$  and  ${}^{\text{Pt}}\Delta\phi^{\text{Cu}}$  to both sides of Eq. (7.48) and obtain

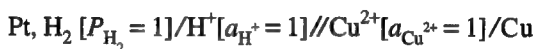
$$\left[ {}^{\text{Cu}}\Delta\phi_e^S + {}^S\Delta\phi_e^{\text{Pt}^0} + {}^{\text{Pt}}\Delta\phi^{\text{Cu}} \right] = \left[ {}^{\text{Cu}}\Delta\phi_e^S + {}^S\Delta\phi_e^{\text{Pt}^0} + {}^{\text{Pt}}\Delta\phi^{\text{Cu}} \right] + \frac{RT}{2F} \ln a_{\text{Cu}^{2+}}$$

substituting Eqs. (7.49) and (7.50) into the above expression gives

$$E_e = E_e^\circ + \frac{RT}{2F} \ln a_{\text{Cu}^{2+}} \quad (7.51)$$

What is  $E_e^\circ$ ? It is the potential difference  ${}^{\text{Pt}}\Delta\phi^{\text{Pt}}$  across the cell (shown in Fig. 7.14) containing the standard hydrogen electrode when the copper ion in solution has a unit activity.

The reading measured on the voltmeter can be used then to define the *equilibrium potential* for the reaction  $\text{Cu}^{2+} + 2e_0^- \rightleftharpoons \text{Cu}$ . For example, it is said that the *standard electrode potential*  $E^\circ$  of this reaction is +0.337 V at 25 °C. This means (Fig. 7.15) that when a cell is constructed thus:



the voltmeter shows that the cell potential is 0.34 V at 25 °C with the copper electrode positive. From Eq. (7.49) it is obvious that measuring the standard electrode potential

<sup>12</sup>Thus, one uses  $V$  for the single electrode potential and  $E$  for a cell potential.

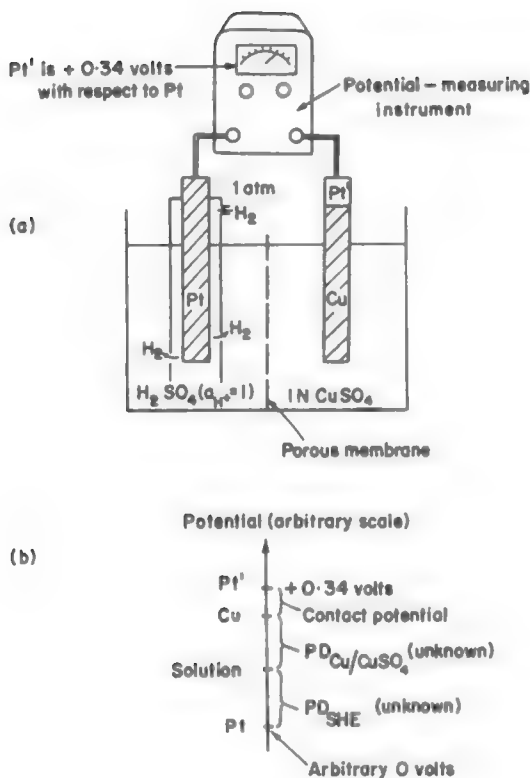


**Fig. 7.15.** When the cell is so constructed that the activity of cupric ions is unity, the voltmeter should show 0.34 V at 25 °C, which is then the standard potential of copper on the standard hydrogen scale.

on the standard hydrogen scale (i.e., the special kind of cell potential that arises when one has the electrode concerned made up in a cell with a standard  $\text{H}_2$  electrode) is not at all the same as measuring the absolute potential difference  $\Delta\phi$  across the  $\text{Cu/Cu}^{2+}$  interface; the value  $E^\circ$  contains also the  $\Delta\phi$  across the Pt/Cu interface, the  $\Delta\phi$  across the  $\text{Pt/H}^+$  interface, and, if not reduced to a negligible quantity, a small liquid junction potential at the junction between the  $\text{H}^+/\text{Cu}^{2+}$  solutions.<sup>13</sup>

<sup>13</sup>Measuring electrode potentials with respect to a reference electrode (Figs. 7.14–7.16) (there are other reference electrodes than the basic hydrogen one; Section 6.3.4) is similar to the conventional measurement of temperature on the centigrade scale. Just as there is a more fundamental way of stating the temperature (i.e., in terms of “degrees absolute”), so there is a more fundamental way of measuring and stating electrode potentials (Section 6.3.4). However, in contrast to the temperature situation, the absolute potential of the hydrogen electrode is not yet sufficiently well defined numerically to allow its use as a *practical* measure of the absolute potential of an electrode.

Once this “standard electrode potential” is known by means of experimental measurements, the Nernst equation permits a calculation of what the electrode potential will be when the solution has any other  $a_{\text{Cu}^{2+}}$  than the value of unity used in the standard potential. For example, the electrode potential of a copper electrode on the standard hydrogen scale immersed in a  $\text{Cu}^{2+}$  solution of  $a_{\text{Cu}^{2+}} = 2 \times 10^{-2}$  would be (Fig. 7.16)

$$E = 0.337 + (0.059/2) \log (2 \times 10^{-2}) = 0.287 \text{ V}$$

### 7.2.9. Why Is Nernst’s Equation of 1904 Still Useful?

This question is easy to answer: There is always an equilibrium condition at the base of the discussion of any kinetic process. Nernst’s equation is the electrochemical version of the well-known thermodynamic equation,  $\Delta G = \Delta G^\circ + RT \ln a_{\text{products}}/a_{\text{reactants}}$ , which forms a basic part of the treatment of equilibrium in chemical reactions and which is deduced and discussed in every thermodynamics text. Indeed, one can deduce Nernst’s equation from it. For at equilibrium:

$$\sum_i \bar{\mu}_i = 0 \quad (7.52)$$

where  $\bar{\mu}_i$  is the electrochemical potential of a typical species taking part in the reaction. Hence,

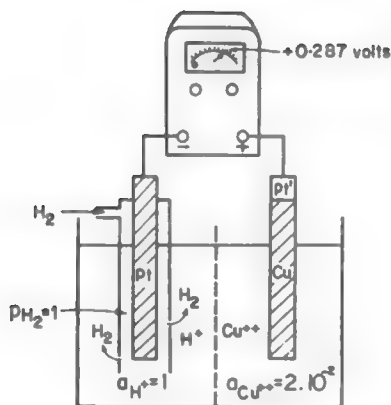


**Fig. 7.16.** If the activity of cupric ions is changed, e.g., to  $2 \times 10^{-2}$  mol/liter, the voltage of the cell should decrease to 0.287 V, as can be calculated from the Nernst equation.

$$\bar{\mu}_i = \mu_i + zF\phi \quad (7.53)$$

where  $\mu_i$  is the chemical potential of  $i$  and  $\phi$  is the inner potential inside the phase concerned. Hence, at equilibrium

$$\sum_i \mu_i = -zF \sum_i \phi_i \quad (7.54)$$

The algebraic sum of the  $\phi$ 's will be equal to the potential of the entire electrolytic cell (see Fig. 7.14). Correspondingly,  $\sum_i \mu_i = \Delta G$ , the free energy of the chemical reaction in the cell.

Hence,

$$\begin{aligned} -nFE &= \Delta G^\circ + RT \ln \frac{\Pi a_{\text{product}}}{\Pi a_{\text{reactant}}} \\ E &= -\frac{\Delta G^\circ}{nF} - \frac{RT}{nF} \ln \frac{\Pi a_{\text{reactant}}}{\Pi a_{\text{product}}} \\ &= E^\circ - \frac{RT}{nF} \ln \frac{\Pi a_{\text{reactant}}}{\Pi a_{\text{product}}} \end{aligned} \quad (7.55)$$

for



Nernst's equation is timeless. Theories of the mechanism of electrode reaction may change as a consequence of the availability of new experimental results and new ideas for interpreting them. However, thermodynamic treatments involve no molecular assumptions. They depend only on the validity of the two great generalizations of experience that constitute the first two laws of thermodynamics. Therefore, conclusions reached by applying them are not expected to change.

## 7.2.10. Looking Back to Look Forward

Once some of the possible applications of electrochemical systems are glimpsed, electron transfer across the electrode/electrolyte interface demands understanding. It is to consider this problem that one begins to look at what happens at the interface.

Things are simple at the instant of immersion of a metal in an electrolytic solution. There is no field and no potential difference across the interface. Reactions (e.g.,  $\text{M}^+ + e \rightarrow \text{M}$ ) run for a very short while chemically. However, the very occurrence of a charge-transfer reaction across the interface in one direction creates an electric field, a fraction of which puts a brake on the reaction  $\text{M}^+ + e \rightarrow \text{M}$ . The same field, however, has an accelerating effect on the charge-transfer reaction in the opposite direction,  $\text{M} \rightarrow \text{M}^+ + e$ .



Thus, the electronation and deelectronation reactions modify the electric field across the interface, and the field, in feedback style, alters the rates until the rates of  $\mathbf{M}^+ + \mathbf{e} \rightarrow \mathbf{M}$  and  $\mathbf{M} \rightarrow \mathbf{M}^+ + \mathbf{e}$  become equal. This is equilibrium. Underlying the condition of zero net current, an equilibrium exchange-current density  $i_0$ , flows across the interface in both directions. The potential difference across the interface at equilibrium depends upon the activity ratio of electron acceptor to electron donor in the solution. Alter the ratio, and the equilibrium potential changes.<sup>14</sup>

If all interfaces remained at equilibrium, electrochemical devices would be limited in their possibilities. Substances could not be produced electrochemically; neither would power production in fuel cells be possible. Net currents must flow across interfaces for devices to work. There must be net electronation or net deelectronation. Interfaces need to move away from equilibrium and the corresponding Galvani potential difference,  $\Delta\phi_e$ .

It turned out in our considerations that the current density  $i$  across an interface is linked to the *overpotential*, or excess potential,  $\eta = \Delta\phi - \Delta\phi_e$ . In a driven electrochemical system, it is the excess-potential difference  $\eta$  [or, rather, the corresponding excess electric field ( $\delta X$ ) that drives the current density. Make  $\eta = \Delta\phi - \Delta\phi_e$  more positive, and the net deelectronation current density  $i = \vec{i} - \vec{i}$  increases. Increase the net deelectronation current density, and the excess potential at the electron-sink electrode (anode) becomes more positive. In a self-driving cell, the action is spontaneous, the reaction in the cell works itself, and the resulting current density  $i$  sets up an excess field  $\delta X$  and an overpotential  $\eta$ . The quantitative description of these features of an interface during charge transfer is crystallized in the well-known equation of phenomenological electrodics, the Butler–Volmer equation, which is an  $i$  vs.  $\eta$  relation.

This general equation covers charge transfer at electrified interfaces under conditions both of zero excess field, low excess fields, and high excess fields, and of the corresponding overpotentials. Thus the Butler–Volmer equation spans a large range of potentials. At equilibrium, it settles down into the Nernst equation. Near equilibrium it reduces to a linear  $i$  vs.  $\eta$  (Ohm's law for interfaces), whereas, if  $\eta > (RT/\beta F)$  (i.e., one is ~50 mV or more from equilibrium at room temperature), it becomes an exponential  $i$  vs.  $\eta$  relation, the logarithmic version of which is called *Tafel's equation*.

The Butler–Volmer equation has yielded much that is essential to the first appreciation of electrode kinetics. It has not, however, been mined out. One has to dig deeper, and after electron transfer at one interface has been understood in a more general way, electrochemical systems or cells with two electrode/electrolyte interfaces must be tackled. It is the theoretical descriptions of these systems that provide the basis

<sup>14</sup>The language used here is more easily understood in terms of inert electrodes such as Pt in solutions containing redox couples, e.g.,  $\text{Fe}^{3+}/\text{Fe}^{2+}$ . For a metal (e.g., Ag) in equilibrium with its ions in solution, there is still a ratio, but one part of it—that of the metal (e.g., Ag)—has the unit activity because it is in the metal's standard state (e.g., at 25 °C).

for efficient electrochemical-energy production, electrochemical synthesis, the stability of metals, and the functioning of some, perhaps many, biological systems.

The Nernst thermodynamic equation was also introduced in this section. Although first deduced a quarter of a century before the Butler–Volmer equation, this famous thermodynamic relation is still alive and well today. Nernst's law acts as a kind of fatherly underlayer to the younger (and much more sprightly) Butler–Volmer equation. Not only does it tell us the variation of the equilibrium potential with activity of the ions in equilibrium via electron exchange reactions with the metal of the electrode, but it also relates electrochemistry to thermodynamics, for it is the standard potential of the Nernst equation that connects up to the standard free energy of the corresponding chemical reaction through the basic equation  $\Delta G^\circ = -nFE^\circ$ . In this way, Nernst's law also is relevant to the energetics of fuel cells and the future of the power source for transportation.

## Further Reading

### Seminal

1. W. Nernst, *Z. Physikal. Chem.* **47**:52 (1904).
2. J. Tafel, *Z. Physikal. Chem. (Leipzig)* **50**:641 (1905).
3. J. A. V. Butler, *Trans. Faraday Soc.* **19**:729 (1924).
4. T. Erdey Gruz and M. Volmer, *Z. Physikal Chemie* **203**:250 (1930).

### Reviews

1. J. O'M. Bockris, *Chem. Rev.* **3**:525 (1948) (hydrogen oriented); *Modern Aspects of Electrochemistry*, Vol. 1, Ch. 4, Butterworths, London (1954). First comprehensive article on electrode kinetics as such.
2. K. J. Vetter, *Electrode Kinetics*, Springer-Verlag, Berlin (1961). First textbook on electrode kinetics.
3. B. E. Conway, *Theory of Principles of Electrode Processes*, Ronald Press, New York (1964).

## 7.3. A MORE DETAILED LOOK AT SOME QUANTITIES IN THE BUTLER–VOLMER EQUATION

The interphasial region constitutes the essential parts of an electrochemical system, and its structure has been dealt with in Chapter 6. The active behavior of the system depends on the charge-transfer reactions that occur at the interfaces. The basic law of charge-transfer reactions has been expressed through the Butler–Volmer electrodic equation (7.23). Written for a net cathodic current (electrons leaving the metal in the solution):

$$i = i_0 \left( e^{-\beta n F / RT} - e^{(1-\beta) n F / RT} \right) \quad (7.23)$$

with

$$i_0 = F\vec{k}c_e e^{-\beta\Delta\phi_e F/RT} = F\overleftarrow{k}c_A e^{(1-\beta)\Delta\phi_e F/RT} \quad (7.21)$$

There are, however, several questions that can be raised. For example, is the simple interpretation (Section 7.2) of  $\beta$  as dividing the potential at the interface which acts on the forward and backward movement of charge sufficient? Should one not get a better comprehension of  $\beta$ ? Can one relate it to molecular quantities?

The basic electrodic equation also conceals a geographic problem. The whole analysis has proceeded from the statement that the electron acceptors and donors are positioned near the electrode before being involved in the charge-transfer reaction. Where? Does it matter? It would surely be expected to, and very much. Both the potential and concentrations of various species can vary near the interface. As the location of the initial state of the reaction is altered, the potential differences and concentrations appearing in the basic equation also vary (see Fig. 7.9).

What, therefore, is the potential difference to be used? Is it  $^M\Delta^{\text{IHP}}\phi$ , the potential difference from the metal to the contact adsorption plane, or IHP (inner Helmholtz plane, see Fig. 6.88), or is it  $^M\Delta^{\text{OHP}}\phi$ , the potential difference from the metal to the OHP (outer Helmholtz plane, see Fig. 6.88), or  $^M\Delta^{\text{S}}\phi$ , the entire potential difference from the bulk of the metal to the bulk of the electrolytic solution? In respect to  $\beta$ , does one consider it to multiply the whole potential difference across the interface or only a fraction of this potential difference? Similarly, what concentrations of electron acceptors and donors must be fed into the basic equation? Bulk values or the values at the OHP or the values at the contact-adsorbed species (Fig. 6.88)?

It is clear that these questions cluster around some basic quantities that appear in the Butler–Volmer electrodic equation, such as  $\beta$ , the interfacial concentrations of electron acceptors and donors, and the potential difference that affects the reaction rate. Some attempts must be made to answer these questions.

### 7.3.1. Does the Structure of the Interphasial Region Influence the Electrochemical Kinetics There?

The equations for the rate of charge transfer across the interphasial region given so far are basically primitive. To make things easy to comprehend in a first reading, the model used two assumptions that are not strictly true. The first tacit assumption was that the potential difference across the interphasial region simply consists of a linear change with distance, starting at the electrode surface and ending a couple of molecular diameters out into the solution (see Fig. 7.9). But the structure of the interphasial region is not that simple—as will have been learned in Chapter 6. It is best not to bring into account as yet the full complexity of the model of the interface,

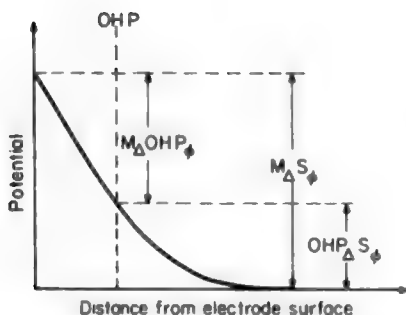


**Fig. 7.17.** The potential difference across the interface can be divided into the linear portion of the layer extending to the OHP, at which the ions ready to discharge are located, and a portion in the diffuse part of the double layer, which is called the *electrokinetic* or *ζ potential*.

but to give at least a somewhat more realistic version than that used so far. This is shown in Fig. 7.17.

Charge transfer is assumed to occur *only* between the electrode and the *first* layer of ions out from the metal. The plane of these ions is that illustrated in Fig. 7.17 by the OHP.<sup>15</sup> Hence, it is not the full Galvani potential difference,  $^M\Delta\phi^S$  that acts on electron transfer, but only  $^M\Delta\phi^S - ^{OHP}\Delta\phi^S$  where  $^{OHP}\Delta\phi^S$  is the potential difference between the OHP and the solution bulk.

However, this realization (i.e., that the ions that react at interfaces are at a potential and hence energy different from that in the bulk of the solution) means that they are also at a different concentration from that of the bulk. Thus:

$$c_M^{z+,OHP} = c_M^{z+,bulk} e^{-zF^{OHP}\Delta\phi^S/RT} \quad (7.56)$$

where  $zF^{OHP}\Delta\phi^S$  is (charge  $\times$  potential) the amount of electrostatic energy by which ions in this OHP differ from the average electrostatic energy of ions in the bulk of the solution.

It follows that the exchange current density,  $i_0$ , previously written in a rudimentary form, needs modifying to account for the structure at the interface (implied in Fig. 7.17). Thus [cf. Eq. (7.21)], the corrected  $i_0$  becomes

<sup>15</sup>It is probable that ions—the physisorbed ones—do react from this outer plane. However, there is a closer plane—the inner Helmholtz plane (see Fig. 6.88)—and this is occupied principally by ions that chemisorb on the electrode (and are not separated from the electrode by a water layer).

$$(i_0)_{\text{correct}} = F \vec{k} c_M^{z^+} e^{-z^+ F \Delta \phi^{\text{OHP}} / RT} e^{-\beta F (\Delta \phi_e^{\text{OHP}} - \Delta \phi^{\text{S}}) / RT} \quad (7.57)$$

Does this more correct version of the basic exchange current density make any significant difference to the value of the current density (or electrochemical reaction rate)? Under certain circumstances, it can (see Fig. 7.18):

1. Because  $\Delta \phi^{\text{OHP}}$  varies with concentration, there can be an effect upon the concentration dependence of the current density at constant potential. This effect is more significant at low ionic concentrations (e.g.,  $10^{-4} - 10^{-2} M$ ) and fades away at higher concentrations, becoming negligible at concentrations above  $0.1 M$  because the value of  $\Delta \phi^{\text{OHP}}$  attains a value of only a few millivolts.

2. There can be an effect on the rate of the variation of the current density with potential which, under the approximation that neglects the interphasial structure, is simply  $\partial \ln i / \partial \Delta \phi = RT / \beta F$ . However, the value of  $(\partial^{\text{OHP}} \Delta \phi^{\text{S}} / \partial \Delta \phi)_{c,T}$  is significant only in a potential region, about  $0.2 V$  either side of the potential of zero charge (Section 6.5.6). At other potentials, such effects become insignificant (Fig. 7.19).

A calculation of these effects was on the frontier of research in the 1930s, not so much because it helped obtain evidence for mechanisms of electrochemical reactions, but because it was an indirect way of probing the structure of the interface. However, in modern times, many direct methods of probing the interface are available, and the effects of the variation of the potential of the outer Helmholtz plane with the electrode potential can be left to exercises in the problems section of this chapter.

One other effect that deals with the structure of the interface and how it affects electrochemical reaction rates can be mentioned. As explained in Chapter 6, some ions (usually anions) chemisorb on the electrode, bending back their solvation sheaths so that the ion itself comes into contact with the electrode surface and forms valence bonds with it. Such effects are potential dependent, and since the adsorption will tend to block the electrode surface, it will change the dependence of  $\log i$  on  $\Delta \phi$  assumed earlier [Eq. (7.7)]. Such effects are particularly important in organoelectrochemistry (see Chapter 11) where the reactants themselves may adsorb in contact with the electrode as a function of potential and complicate the theory of the dependence of the rate of reaction (or current density,  $i$ ) on potential.

A discussion of the effects of the structure of the interface on electrode kinetic rates is the right moment to introduce a seminal figure in electrochemistry, a person who played a part later than—but hardly less than—that of Butler and of Volmer and Erdey-Gruz, in establishing the basis of the modern subject. It was A. N. Frumkin who first introduced interfacial structure considerations into electrode kinetics, in 1932. However, to leave a mention of Frumkin at that would sadly underdescribe a great leader whose influence in creating physical electrochemistry was outstanding.<sup>16</sup>

<sup>16</sup> It was Frumkin who, from 1936 to 1976, led a group of several hundred Russian scientists at an institute of the Academy of Sciences in Moscow. Here, full-blown treatments of electrochemical reaction rates in kinetic terms were being published in the 1930s (long before the Faraday meeting of 1947, mentioned earlier as the beginning of a new stage in the chemistry of electrode processes). For some 20 years,

### 7.3.2. What About the Theory of the Symmetry Factor, $\beta$ ?

A deeper consideration of the origin of the symmetry factor,  $\beta$  (in addition to that given in Section 7.2) has not yet been presented. This important coefficient will be considered from a more molecular point of view in Chapter 9. A preliminary word is said here.

In the picture already given (Section 7.2), the symmetry factor was described as a factor reflecting the *shape* of the potential-energy diagram in an ion-transfer reaction. When an ion moves toward the electrode from its position in the outer Helmholtz plane, electrostatic work is done on the ion by *part* (and that is the point—*what* part?) of the potential difference between the electrode surface and the bulk of the solution (Fig. 7.9). Is there no more to it than that? This electrostatic work covers the energy of activation for the reaction and hence increases the ion-transfer rate. For example, if one considers the metal/solution interface, each side is different (one is a metal surface with its electrons, the other a solution with its ions) so it does not follow as obvious that the barrier is symmetrical. However, when we bring in experimental results for comparison, it is found that a value of nearly 1/2 (which would correspond to exact symmetry of the potential energy barrier in the interfacial region) is what experiment demands. Thus, there may be something more to say about the molecular version of the value of  $\beta$ . However, it is best to put off further discussion until the chapter concerned with quantum mechanical matters (Chapter 9) is reached because we must not only think of ions traveling across the interfacial region but also of electrons, and they are quantum particles. The coefficient  $\beta$  has been a bit mysterious for the three-quarters of a century of its life and it will be seen later that there are still matters about it that are not going to be solved until we have much more information on electrode kinetics at very high current densities and very low temperatures.

---

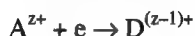
particularly in the 1950s and 1960s, this huge group was at the cutting edge of physical electrochemistry and stimulated much of the post-WWII work in this field in Europe and eventually also in the United States, where its influence was felt on work leading to the fuel cells used in NASA's early space flights. The dominance of the Russian group was relinquished only when spectroscopic and computer-based techniques, which were easily available in the West, became essential to research in physical electrochemistry but were not available (because of the supply problems in Communist countries) to scientists in the Soviet Union.

Frumkin himself has been called in an obituary, "The Great Academician," not only because of his wide knowledge, including contact with the current humanistic literature in Russia, England, Germany, and France (he spoke fluently the language of all four), but because he was a leading member of the Academy of Sciences of the Soviet Republics, the most prestigious organ of Russian science. He was in the best sense an active intellectual, and it seems appropriate to regard Frumkin as the successor to the great Nernst. He was eager to discuss virtually any subject. He did not agree with the Darwinian theory of evolution, asking how it would be possible for the mechanism of the human eye to develop via a series of *accidental* changes in gene structure. He showed an encyclopedic knowledge of flowers and trees. In spite of these virtues, Alexander Naumovitch (his name to close colleagues) did not believe in the objective evaluation of a scientist's work. Asked his view of a specific scientist, his reaction was a frown or a smile. The frown was succeeded by a terse expression of disgust and the phrase "Terrible work," the smile was succeeded by a lively "Him I like. *Excellent work.*"

Because we are putting off the discussion of a molecular theory of  $\beta$  until Chapter 9, this does not mean that  $\beta$  is an academic matter having purely theoretical importance. When we change the overpotential,  $\eta$  [see Eq. (7.23)], we change the current density (or rate of the electrochemical reaction). But the *fraction* of the change of  $\eta$  that affects the current density is determined by the numerical value of  $\beta$ ! It follows that in the practical example of an electric car powered by a fuel cell or battery, the value of  $\beta$  determines the power increase that a change of potential (i.e., a pressing of the accelerator) gives. In fact, it is not too much to say that  $\beta$  is at the heart of electrode kinetics and that is why an attempt must be made to relate it to the molecular activities at the interface during a reaction.

### 7.3.3. The Interfacial Concentrations May Depend on Ionic Transport in the Electrolyte

Observe (Fig. 7.18) what happens at the OHP (referred to as the  $x = 0$  plane) when a constant current is driven across the interface. The electron acceptors at the  $x = 0$  plane are *consumed* at a constant rate by the reaction



To keep the reaction going and the electronation current constant, a steady supply of electron-acceptor ions must be maintained by transport from the electrolyte bulk. This transport may be by diffusion (random walk) or migration under an electric field (drift) [cf. Eq. (4.226)].

In considering the effect of the double-layer structure on electrode kinetics (Section 7.3.1), it was pointed out that the existence of a diffuse charge region causes the concentration at the outer Helmholtz plane to differ from the bulk concentration (Fig. 7.19). The consumption of electron acceptors by the electronation reaction and

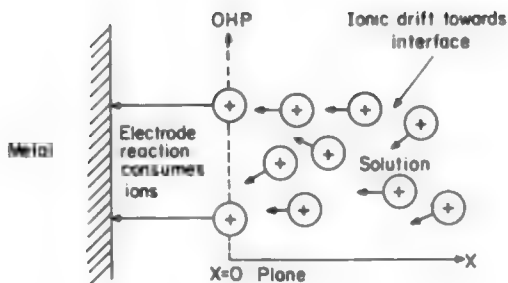


**Fig. 7.18.** As the electrode reaction consumes ions from the OHP, their concentration is bound to decrease because the ionic drift diffusion from the bulk of the solution can start only after a certain concentration gradient is established.

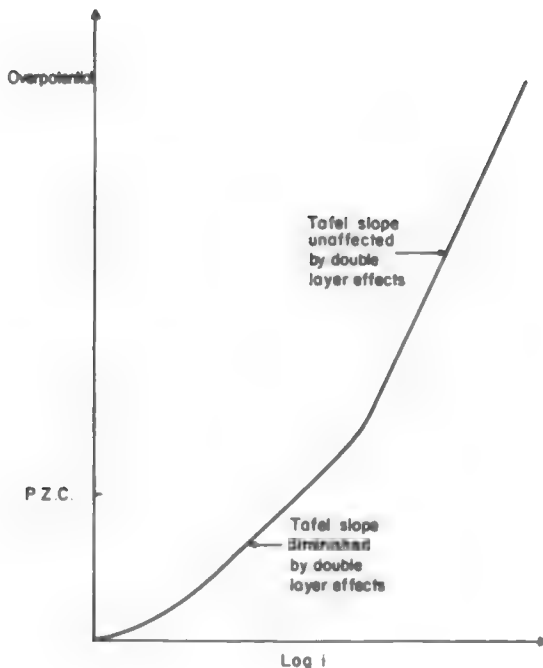


**Fig. 7.19.** The existence of the region of diffuse charge in the electrified interface has an effect on the Tafel relation, making it change the slope and deviate from linearity.

the need for transport processes to maintain the supply may be yet another reason for the interfacial concentration of electron acceptors to deviate from the bulk concentrations. Thus arises an effect of transport processes upon the rates of electrode reactions. The possibility of this effect is only mentioned here; this influence of ionics upon electrodics is elaborated upon in Section 7.9.1.

## Further Reading

1. A. N. Frumkin, *Z. Physikal Chem.* **164A**:121 (1933). Effect of the double-layer structure on the concentration dependence of a reaction rate.
2. J. O'M. Bockris, I. A. Ammar, and A. K. M. S. Huq, *J. Phys. Chem.* **61**:879 (1957). Effect of the double-layer structure on the potential dependence of the electrochemical reaction rate.

## Historical

1. J. O'M. Bockris, "The Life of A. N. Frumkin," *Proc. Roy. Austr. Chem. Inst.* 19–21 (1971).



## Modern

1. C. M. A. Brett and A. M. O. Brett, *Electrochemistry*, Oxford University Press, Oxford (1993).
2. C. H. Hamman, A. Hamnett, and W. Vielstich, *Electrochemistry*, Wiley-VCH, Weinheim (1995).

## Elementary Phenomenological Electrode Kinetics

1. J. O'M. Bockris, *J. Chem. Ed.* 48:352 (1971).
2. E. Gileadi, *Electrode Kinetics for Chemists, Engineers and Material Scientists*, VCH Publisher, Weinheim (1993).
3. W. Schmickler, *Interfacial Electrochemistry*, Ch. V, Oxford University Press, Oxford (1995).

## 7.4. ELECTRODE KINETICS INVOLVING THE SEMICONDUCTOR/SOLUTION INTERFACE

### 7.4.1. Introduction

**7.4.1.1. General.** So far, the account given of charge-transfer reactions has concerned the *metal*/solution interface. The electronic structure inside the metal has not been dealt with at all. Suffice it to say (see Section 7.2.2) that a change in an outside power source, pouring more electrons into the metal, or an alternative type of change in the power source, withdrawing electrons to the outer power source, causes the interfacial charge-transfer reaction to change its velocity, the dependence of the velocity of the transfer reaction on the electrode potential being exponential [see, e.g., Eq. (7.31)].

Now, electrochemical reactions also take place at *semiconductor*/solution interfaces as well as those involving metals. Until the 1960s, the number of non-metals that were thought to be sufficiently conducting to sustain electron current flow was regarded as being restricted to a very small group of oxides and sulfides, exemplified by conducting  $\text{Fe}_3\text{O}_4$ . However, with the invention of the transistor and the accompanying shift to semiconductor electronics and the *n-p* junction, it became clear that the process of adding tiny amounts of electron donating or accepting foreign materials ("doping") brought the conductivity of hundreds of non-metals into a range in which they could be thought of as electrodes, thereby greatly extending the breadth of the electrochemical field. In this section, an introduction will be given to semiconductor electrochemistry.<sup>17</sup> (See the discussion on the semiconductor/solution interface in

<sup>17</sup> It will be seen that although normal (or "thermal") electrochemical reactions can be sustained at low current densities using semiconductors (i.e., they act as electron-poor metals), they really do not come onto center stage until their photoelectrochemistry is studied (see Chapter 10). Thus, semiconductor electrodes are responsive to light when metals are almost unreactive to it.

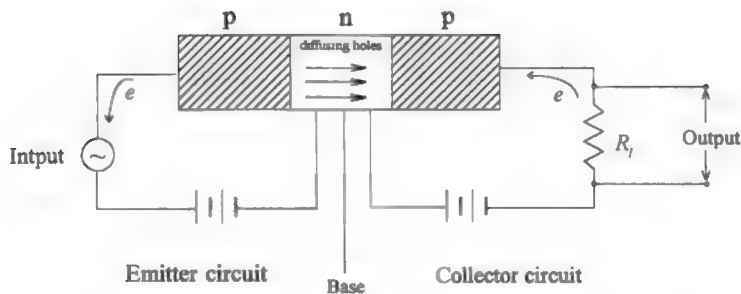


**Fig. 7.20.** Basic construction and operation of the junction transistor.

Section 6.9, which gives the meanings of “*n*” and “*p*” as they relate to doped semiconductors.)

**7.4.1.2. The *n-p* Junction.** Before beginning a discussion of electron transfer at interfaces between *n*-type semiconductor/solution interfaces, it is helpful to describe something of the theory of the famous *n-p* junction. This is not a part of electrode-process chemistry (which deals with electron-transfer reactions between electronically and ionically conducting phases), but it is the basis of so much modern technology (e.g., the transistor in computers) that an elementary version of events at the junction should be understood. Further, knowing about the *n-p* junction makes it easier to understand electrochemical interfaces involving semiconductors.

A junction transistor consists of two *p-n* junctions joined together, back to back, with a common *n* region (Fig. 7.20). It acts as an amplifier, the strength of which can be easily increased by controlling the potential across the junction. The revolutionary impact on TV, computers, etc., consists in the fact that it provides amplification of currents without the large, clumsy, fragile vacuum tubes earlier used. Solid-state transistors can now be made in very small sizes and cheaply. In an integrated circuit, transistors are developed cheaply by depositing layers of material and etching patterns to delineate current paths, thus constructing large numbers of transistors as well as capacitors and resistors on the same piece of semiconductor. The purpose here is to have a look at the current-potential relations for *n-p* junctions or interfaces while keeping in mind charge transfer at an electrode/electrolyte interface and its basic law, the Butler–Volmer equation:

$$i = i_0 \left( e^{-\beta \eta F/RT} - e^{(1-\beta) \eta F/RT} \right) \quad (7.23)$$

Consider an interface formed by joining together an *n*-type semiconductor (e.g., germanium “doped” with arsenic atoms, which donate electrons to the conduction

band of the semiconductor; Table 7.1) and a *p*-type semiconductor (e.g., germanium doped with gallium atoms, which accept electrons from the valence band of this substance, leaving behind “holes” in the valence band). The charge carriers in the *n*-type material will be mostly electrons, and the *p*-type material will carry a current by means of its majority of holes.

Before the junction is formed, there is overall electroneutrality in both types of materials. Thus, the positive charge on the immobile arsenic donors in the *n*-type of material exactly balances the negative charge of the free electrons; and the negative charge on the fixed gallium acceptors in the *p*-type of material balances out the positive charge on the mobile holes. Once the two types of material are brought face to face to form a junction, electrical contact is established and a path is provided for electrons and holes to move from one side of the junction to the other [Fig. 7.21 (a)].

Consider the hole movement first. In the *n*-type of material, holes are generated when electrons from the valence band jump to acceptor atoms. These holes can random walk across the junction into the *p*-type of material [Fig. 7.21(b)]. Conversely, holes from the *p* side can random walk into the *n*-type of material, where they are consumed in a hole-electron recombination process (the reverse of a hole-generation process). Both electrons and holes have considerable mobility (Table 7.2).

Since one starts off with a larger hole concentration in the *p*-type of material than exists in the *n*-type of material, there will initially be more holes taking the  $p \rightarrow n$  random walk than the  $n \rightarrow p$  random walk. One has stated in microscopic language that there will be diffusion of holes in the  $p \rightarrow n$  direction [Fig. 7.21(b)]. What is the result of this  $p \rightarrow n$  hole diffusion? The net *p* transport of holes leaves a negative charge on the *p* material and confers a positive charge on the *n* material [Fig. 7.21(c)]. A potential difference develops [Fig. 7.21(d)]. Further, this charging of the two sides of the interface and the resultant potential difference acts precisely in such a manner as to oppose further  $p \rightarrow n$  hole diffusion (Fig. 7.22).

**TABLE 7.1**  
**Summary of Features of Impurity Conduction in Silicon and Germanium**

Conductivity Type	<i>n</i> -Type or Excess	<i>p</i> -Type or Defect
Conduction by	(Excess) electrons	Holes
Energy band in which carrier moves	Conduction band	Valence band
Sign of carrier	Negative	Positive
Name for impurity atom	Donor	Acceptor
Typical impurities	Elements of Group V: Phosphorus, P Arsenic, As Antimony, Sb	Elements of Group III: Boron, B Aluminum, Al, Gallium, Ga Indium, In

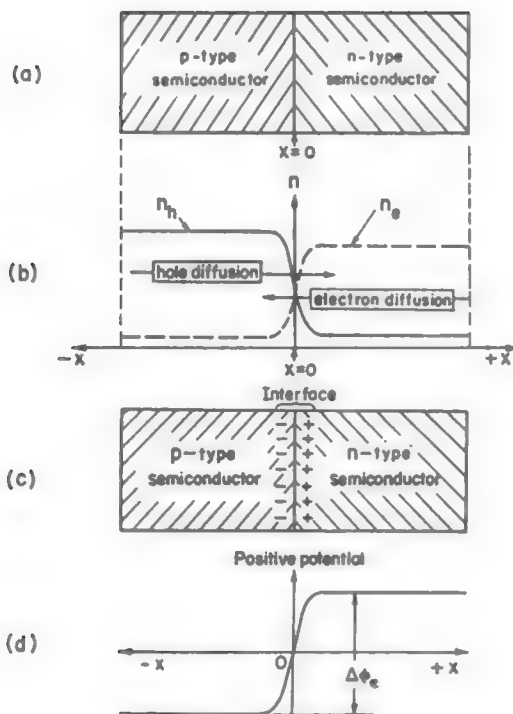


**Fig. 7.21.** When a junction between a *p*-type and an *n*-type of semiconductor is established (a), a diffusion of holes and electrons in the opposite direction takes place (b). This results in a separation of charge (c) and the formation of an electrical potential difference across the interface (d).

Equilibrium is reached when the driving force for the diffusion (the concentration gradient) is compensated for by the electric field (the potential gradient). Under these equilibrium conditions, there is an equilibrium net charge on each side of the junction and an equilibrium potential difference  $\Delta\phi_e$ . This process is analogous to the way charge transfer across a nonpolarizable electrode/solution interface results in the establishment of an equilibrium potential difference  $\Delta\phi_e$  across the interface.

Since there is no net diffusion under equilibrium conditions, the  $n \rightarrow p$  hole current is equal to the  $p \rightarrow n$  hole current. These equilibrium currents are analogous to the equilibrium exchange currents at an electrode/solution interface. They represent the exchange of holes across the junction between the *n*- and *p*-types of material and will be designated by the symbol  $i_{0,h}$ . This  $i_0$  will now be examined more carefully.

**TABLE 7.2**  
**Room-Temperature Energy Gap and Electron and Hole Mobilities for Some Semiconductors**

Semiconductor	Energy Gap (eV)	Electron Mobility, $v_e$ ( $\text{cm}^2\text{V}^{-1}\text{s}^{-1}$ )	Hole Mobility, $v_p$ ( $\text{cm}^2\text{V}^{-1}\text{s}^{-1}$ )
Carbon (diamond)	5.6	1800	1200
Germanium	0.66	3900	1700
Silicon	1.0	91,420	250
Tellurium	0.34	300	200
PbS	0.37	500	150
ZnO	3.1–3.2	85	—
AlSb	1.52	50	150
GaAs	1.35	4000	400
GaSb	0.7	5000	1000
InP	1.3	3500	700
InSb	0.17	80,000	4000
Mg <sub>2</sub> Si	0.7–0.8	400	70
Mg <sub>2</sub> Ge	0.6–0.7	500	100
Mg <sub>2</sub> Sn	0.2	300	250

Consider the holes that are making the  $p \rightarrow n$  crossing. The number of holes approaching a unit of area of the junction per second is proportional to the number per unit volume of holes on the  $p$  side, i.e.,  $n_{h,p}$ . Will they cross the junction? Each hole approaching the interface finds that it has to surmount the potential difference  $\Delta\phi_e$ , and the probability that it will climb the barrier is given by the Boltzmann term<sup>18</sup>  $e^{-F\Delta\phi_e/RT}$ . Hence, the  $p \rightarrow n$  hole current density at equilibrium is

$$\begin{aligned}\vec{i}_{h,\Delta\phi_e} &\propto n_{h,p} e^{-e_0\Delta\phi_e/kT} \\ &= \vec{k} n_{h,p} e^{-e_0\Delta\phi_e/kT}\end{aligned}\tag{7.58}$$

where the arrow over the  $i$  represents  $p \rightarrow n$  crossings and  $\vec{k}$  is the proportionality constant.

Now think of the  $n \rightarrow p$  hole current. When the holes from the  $n$ -type of medium reach the junction [see Fig. 7.21(c)], they do not see any barrier due to an electrical potential difference, so they simply tumble over the potential drop. Hence, the  $n \rightarrow p$  hole current density at equilibrium is controlled only by diffusion and is simply proportional<sup>19</sup> to the number of holes,  $n_{h,n}$ , in the  $n$ -type of material:

<sup>18</sup>The absence of  $\beta$  in this expression will be commented on later.

<sup>19</sup>The proportionality constant depends on the fraction moving normal to, and colliding with, the interface per second. Hence, if the velocities of holes in both types of material are the same, the  $\vec{k}$ 's in Eqs. (7.58) and (7.59) can be assumed to be equal.

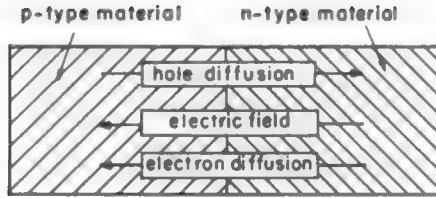


**Fig. 7.22.** The established electric field opposes further diffusion of holes across the interface.

$$\overleftarrow{i}_{h, \Delta\phi_e} = \overleftarrow{k} n_{h,p} \quad (7.59)$$

where the arrow  $\leftarrow$  over the  $i$  indicates  $p \leftarrow n$  crossings. Hence, at equilibrium (Fig. 7.22):

$$i_{0,h} = \overrightarrow{i}_{h, \Delta\phi_e} = \overleftarrow{i}_{h, \Delta\phi_e} \quad (7.60)$$

Now, what happens if the potential difference across the junction is lowered by an amount  $\eta$  (Fig. 7.23)? The holes making the  $p \rightarrow n$  crossing find a smaller barrier to climb, and hence the  $p \rightarrow n$  hole current density becomes

$$\begin{aligned} \overrightarrow{i}_{h, (\Delta\phi_e - \eta)} &= \overrightarrow{k} n_{h,p} e^{-e_0(\Delta\phi_e - \eta)/kT} \\ &= i_{0,h} e^{-e_0\eta/kT} \end{aligned} \quad (7.61)$$

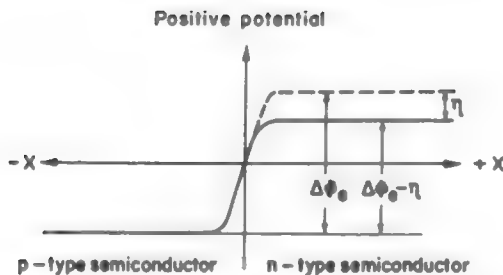


**Fig. 7.23.** As the potential difference across the interface is lowered by superimposing an external field, the current starts flowing.

But the holes crossing from the  $n$ - to  $p$ -type of material still have no barrier to climb. Hence, the  $n \rightarrow p$  hole current density still depends only on the number of holes in the  $n$ -type of material and

$$\vec{i}_{h,(\Delta\phi_e-\eta)} = i_{0,h} \quad (7.62)$$

not on the potential difference across the junction, i.e.,  $i_h [n \rightarrow p]$  is unaffected by the field. The net hole current density is given by the difference in the hole current densities for the two directions:

$$\begin{aligned} i_h &= \vec{i}_{h,(\Delta\phi_e-\eta)} - \overleftarrow{i}_{h,(\Delta\phi_e-\eta)} \\ &= i_{0,h} e^{e_0\eta/kT} - i_{0,h} \\ &= i_{0,h} (e^{e_0\eta/kT} - 1) \end{aligned} \quad (7.63)$$

All these arguments can be applied to the electrons making  $n \rightarrow p$  and  $p \rightarrow n$  crossings and giving rise to electron current densities. The net electron current density is given by an expression similar to (7.63), i.e.,

$$i_e = i_{0,e} (e^{e_0\eta/kT} - 1) \quad (7.64)$$

The total current density across the junction is therefore equal to the sum of the electron and hole current densities, just as the total ionic-migration current density in an

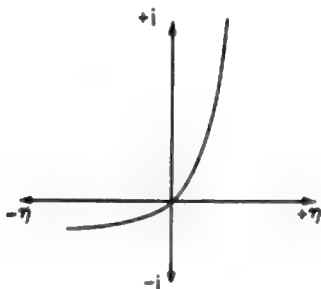


**Fig. 7.24.** The current-potential relation at a  $p$ - $n$  semiconductor junction differs from that of an electrode/solution interface by being totally asymmetrical.

electrolyte is equal to the sum of the current densities due to positive and negative ions [cf. Eq. (6.158)].

Hence, the current-potential law for an  $n$ - $p$  junction is (Fig. 7.24)

$$i_e = i_0(e^{e_0\eta/kT} - 1) \quad (7.65)$$

where

$$i_0 = i_{a,h} + i_{0,e} \quad (7.66)$$

Notice that as  $\eta$  (the departure from the equilibrium potential) increases,  $e^{e_0\eta/kT}$  increases in comparison to unity until, when  $e^{e_0\eta/kT} \gg 1$ ,

$$i_e = i_0 e^{e_0\eta/kT} \quad (7.67)$$

the exponential law for  $n$ - $p$  junctions.

One is now in a position to compare the current-potential law for an electrode/electrolyte interface<sup>20</sup> (which has been referred to as an  $e$ - $i$  junction) with that for any  $n$ - $p$  junction:

$$i = i'_0[e^{e_0\eta/kT} - 1] \quad [n\text{-}p \text{ junction}] \quad (7.65)$$

$$i = i_0[e^{(1-\beta)e_0\eta/kT} - e^{-\beta e_0\eta/kT}] \quad [e\text{-}i \text{ junction}] \quad (7.68)$$

For large departures from equilibrium, i.e., large  $\eta$ , both types of interfaces tend to give an exponential  $i$  vs.  $\eta$  law. Thus,

$$i = i_0 e^{(1-\beta)e_0\eta/kT} \quad [e\text{-}i \text{ junction}] \quad (7.69)$$

For small departures from equilibrium, i.e., small  $\eta$ , a linear  $i$  versus  $\eta$  law is obtained for both  $e$ - $i$  and  $n$ - $p$  junctions:

$$i = i_0 e_0 \eta / kT \quad [e\text{-}i \text{ junction}] \quad (7.70)$$

$$i = i'_0 e_0 \eta / kT \quad [n\text{-}p \text{ junction}] \quad (7.71)$$

It is seen, therefore, that there are basic similarities in the  $i$  vs.  $\eta$  laws for both types of interfaces, but there is an important difference. There is no symmetry factor  $\beta$  in the exponential  $i$  vs.  $\eta$  law for semiconductor  $n$ - $p$  junctions. Why?

<sup>20</sup>To facilitate the comparison,  $e_0/k$  is written instead of  $Ne_0/Ink = F/R$ .



Think back to the origin of the symmetry factor in *electroodic expressions*. The main point to be noted is that there is a hill-shaped potential energy barrier *even in the absence of an electrified field*. This barrier has to do with the atomic movements in bond stretching, which are a prerequisite of processes such as chemical reactions and diffusion of atoms and ions. What the electric field does in the case of charged particles is to modify the already existing potential barriers. The modification is such that only a fraction  $(1 - \beta)$  of the input electric energy  $e_0\eta$  turns up in the change of activation energy and hence in the rate expression. This is because the atom movements necessary for the system to reach the barrier peak are only a fraction of the total distance over which the potential difference extends.

The situation in the case of the transfer of holes (or electrons) across *n-p* junctions is different. First, the only difficulty the electron has to overcome is that due to the electric field. When there is no field, there is no barrier. This is because the barrier is not an expression of the energies involved in atomic movements; there are no atomic movements as prerequisites to the movements of holes or electrons. Second, whereas potential-energy barriers for atom movements and reactions are like hills, the barrier for hole and electron movements is like a cliff with its attendant implication that “falling over the cliff” does not involve an activation energy [Fig. 7.21(d)]. Finally, since the holes and electrons reach the barrier top only after traversing the whole distance over which the field extends, the entire  $e_0\eta$ —not a fraction  $(1 - \beta)e_0\eta$ —affects the hole and electron movements.

There is therefore one essential conclusion from the comparison of electroodic *e-i* junctions and semiconductor *n-p* junctions: The symmetry factor  $\beta$  originates in the atomic movements that are a necessary condition for the charge-transfer reactions at electrode/electrolyte interfaces. Interfacial charge-transfer processes that do not involve such movements do not involve this factor. By understanding this, ideas on  $\beta$  become a tad less underinformed. Chapter 9 contains more on this subject.

## 7.4.2. The Current-Potential Relation at a Semiconductor/Electrolyte Interface (Negligible Surface States)<sup>21</sup>

From the point of view of kinetics, the main difference between the metal and semiconductor cases is the location of the potential difference (p.d.), which affects the rate of electron transfer. In the metal–solution case, any potential difference inside the metal is neglected. This is because there is a huge excess of electrons in the metal and

<sup>21</sup>In metals, the density of electronic states is given by the Fermi distribution law, and little attention is paid to special (or Tamm) states which exist at a metal/vacuum (cf. metal/solution) interface. For semiconductors, as shown in Section 6.10.1, two cases occur. In the first (semiconductors without surface states), the distribution of electrons (concentration vs. distance back to the semiconductor bulk) is known, being deduced originally by Kingston and Nenstätter in 1936. The electrons spread themselves out, back into the interior of the semiconductor. But in another type of semiconductor (the more numerous in practice), the electrons tend to settle in “surface states,” and their concentration back toward the bulk is smoothed out, thus changing the potential profile within the semiconductor (see Section 6.10.1.8).

the kind of current densities used in electrochemistry are far too low to disturb the large electron concentration. As the overpotential changes from that at equilibrium ( $\eta = 0$ ) to that at a certain finite net reaction rate,  $\eta = \eta$ , the quantity that varies is the potential difference in the Helmholtz layer.

On the other hand, in a semiconductor, the electron concentration may be some  $10^6$  to  $10^8$  times less than in a metal. Thus, at a semiconductor/solution interface, the excess charge on the semiconductor is spread out inside the semiconductor because the interfacial activity is enough to significantly use up or add to the sparsely available electrons. In the absence of the special traps called *surface states*, there is a negligible excess charge at the semiconductor surface (conversely, in the metal, the excess charge is exactly on the surface of the metal). Thus, for a *p*-type semiconductor/solution interface, the two situations for the potential-distance plot inside the semiconductor corresponding to  $\eta = 0$  and  $\eta = \eta$  are as shown in Fig. 7.25.

To deduce a current-potential relation at a semiconductor/solution interface, one can make an approximate argument. But how approximate will it be? The basic approximation is that there are no "surface states," which in practice means a surface state concentration of  $< 10^{10} \text{ cm}^{-2}$ . If no surface states for electrons exist, the charge is spread back into the semiconductor and the charge actually *at* the surface will be small compared with the surface concentration of electrons at metal/solution interfaces. It follows that the electrical double layer on the solution side will have no adherent Helmholtz layer and the charge on the solution will be spread out (but be equal in magnitude though opposite in sign to the charge on the semiconductor).

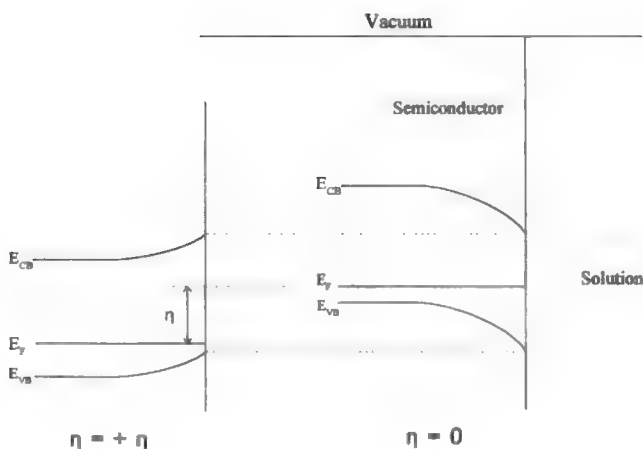


**Fig. 7.25.** Changes in the potential energy of the electrons in a *p*-type semiconductor at the semiconductor/solution interface when there are no surface states at the semiconductor electrode surface.

It is easy to see how the concentration of electrons at the surface will depend on the overpotential. As shown above, in dealing with the rate of electron transfer at an  $n$ - $p$  junction, the form of the expression [outside the reversible region, i.e., for  $\eta > (RT/F)$ ] is given by

$$i = i_0 e^{-\eta F/RT} \quad (7.72)$$

for an electron-transfer reaction from an  $n$ -type semiconductor to an acceptor. There is no  $\beta$ . Thus, the concentration of electrons at the surface can be expressed in a Nernst-type way:

$$\eta = \frac{RT}{F} \ln \frac{c_{e,\text{equil}}}{c_{e,\eta}} \quad (7.73)$$

i.e.,

$$c_{e,\eta} = c_{e,\text{equil}} e^{-\eta F/RT} \quad (7.74)$$

The reaction rate between these interfacial electrons from the  $n$ -type semiconductor and receptor in solution (say, on an  $\text{Fe}^{3+}$  ion) will be given by an expression for the electrochemical rate of reaction by

$$i = Fkc_{e,\eta} c_{\text{Fe}^{3+}} \quad (7.75)$$

Or from Eq. (7.74)

$$i = Fkc_{e,\text{equil}} c_{\text{Fe}^{3+}} e^{-\eta F/RT} \quad (7.76)$$

Thus,

$$\eta = \frac{RT}{F} \ln \frac{i_0}{i} \quad (7.77)$$

An important distinction between metals and semiconductor electrodes is apparent. Thus, if one puts (7.77) in the form of a Tafel equation:

$$\eta = a - \frac{RT}{F} \ln i \quad (7.78)$$

The corresponding form of the equation for metals is (from 7.28):

$$\eta = a - \frac{RT}{\beta F} \ln i \quad (7.29a)$$

(with  $\beta \approx 1/2$ ).

Thus, in a region in which the current density at a driven semiconductor/solution interface is low enough that the electrons in the semiconductor are in equilibrium between surface and bulk (i.e., *not* rate-determined by charge carrier transport—

diffusion—inside the semiconductor), the gradient of the overpotential with respect to  $\log i$  will be half that for a metal.

However, all this (i.e., the dependence of  $i$  on  $\eta$  before exhaustion of charge carriers occurs) is less stressed in the practical use of semiconductors in electrochemistry because diffusion-limited currents caused by electron or hole exhaustion inside the semiconductor (rather than exhaustion of transporting ions in solution as with metals) are usually orders of magnitude less than the limiting current densities due to difficulties with ion transport in solution. For this reason, published diagrams of current potential dependence at the semiconductor/solution interface show limiting currents more often than Tafel behavior. Thus, in Fig. 7.26, the  $p$ -type electrode shows exponential behavior on the anodic side (plenty of holes to receive electrons from redox ions undergoing oxidation), but only a low limiting current when electrons are required. The converse is true for the electron-rich  $n$ -type.

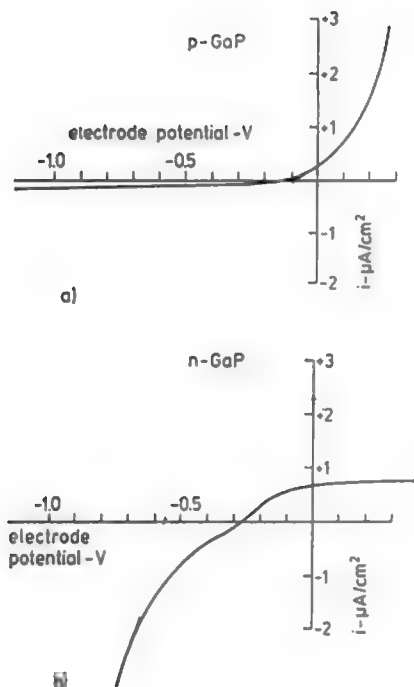


**Fig. 7.26.** Current-potential dependence at  $n$ - and  $p$ -type GaP in  $0.1\text{ N H}_2\text{SO}_4$ . (Reprinted from K. Memming and G. Schwandt, *Electrochim. Acta* 13: 1299, copyright 1983 with permission from Elsevier Science.)

### 7.4.3. Effect of Surface States on Semiconductor Electrode Kinetics<sup>22</sup>

The situation described so far with semiconductor electrode kinetics is the simplest case: The semiconductor has no states for electrons or holes at the surface. More frequently met—particularly for semiconductors that evolve  $\text{H}_2$  or  $\text{O}_2$ , are semiconductors *with* surface states. In such a case, the potential–distance relation inside the semiconductor becomes flatter, and the behavior of the semiconductor becomes more like that of a metal. Thus (see Fig. 7.27), for the high surface-state case for a *p*-type semiconductor anode, there reappears a substantial p.d. in the solution; the p.d. inside the semiconductor is reduced toward a small value.

A first approximation view of the semiconductor/solution interface is analogous to the view of the metal/solution interface with no specific adsorption (see Section 6.10.1.8). Of course, it is easier to theorize about metal/solution interfaces that have no interfering anions chemisorbed on these surfaces. In reality, however, there is plenty of evidence to show that most anodic situations (and some cathodic ones) do have to suffer the complexity of adsorbed layers, discussed in Section 6. In an analogous manner, most semiconductor/solution interfaces *do* have the surface states described above, and a good number of them, particularly those with adsorbed H and O, have the high concentration of surface states that makes the semiconductor/solution interface more like that involving a metal. In such a case, and insofar as the p.d. at the electrode is now predominantly (see Fig. 7.27) in the Helmholtz layer and not inside the semiconductor, the current-potential relation at currents lower than the limiting current inside the semiconductor can be that of the Butler–Volmer equation (7.23). However, easy electron or hole exhaustion means that *i*- $\eta$  behavior will be more often near that of the limiting current (see Fig. 7.26) than that of a Tafel region.

### 7.4.4. The Use of *n*- and *p*-Semiconductors for Thermal Reactions

Semiconductor electrodes are always used in the doped state (i.e., the state in which small quantities of materials have been added to the pure semiconductor, which ionize upon dissolution and make it conducting). They can be doped *n*-type, or *p*-type.

---

<sup>22</sup>What are surface states? In an ideal semiconductor, the electron distribution in the conduction band follows Fermi's distribution law and the assumptions behind the deduction is that the conduction electrons are mobile ("free"). In this model, electrons may come to the surface and overlap or underlap a bit, but there are no traps to spoil the sample distribution.

In a more realistic model, traps (the "surface states") can occur at the semiconductor/solution interface. What effect this has on the electron distribution depends on the number of traps per unit area. If they cover only 0.1 % of the total surface, the surface states can be neglected because they will not affect the electron distribution. At surface state concentrations of 1% of the surface and higher, there is a strong effect and the electrons that would have been distributed deeply in the bulk of the semiconductor tend to concentrate increasingly at the surface, just as excess electrons put into a metal electrode (taken from it) tend to change its surface concentration of electrons.

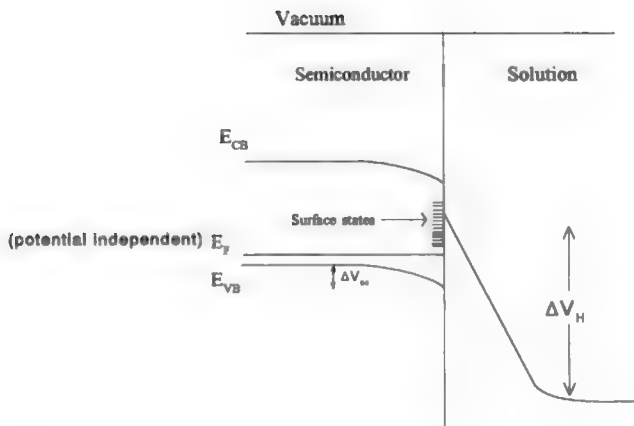


**Fig. 7.27.** Changes in the potential energy of the electron in the *p* semiconductor and the potential drop at the semiconductor/solution interface when there are surface states at the semiconductor electrode surface.

The *n*-type electrodes acting thermally (i.e., without the stimulation of light) have an excess of electrons in their conduction bands (the actual concentration depends on the concentration of dopant) and this enables them to serve in thermal (i.e., normal) cathodic reactions in which electrons leave the electrode and are donated to ions in the solution. The reverse is true for *p*-type semiconductors (see Section 6.10.1.7), acting without light stimulation. Here the doping agent is typically Ga and now it is the doping agent that sucks up electrons from the valence band (thus becoming an anion by a process such as  $\text{Ga} + e \rightarrow \text{Ga}^-$ ) and hence produces “holes” (cavities in the valence band occupied by electrons before the dopant removed them in the ionization process). The result of the doping, here, is to make plenty of “holes” in the valence band, but very few electrons in the conduction band.

The question of *n*- and *p*-type (excess charge carriers in conductivity and valence band, respectively) mechanisms of semiconductors is shown in Figs. 7.28 and 7.29. For this reason, *p*-type electrodes will be suitable as anodes,<sup>23</sup> i.e., a deelectronation reaction, in which electrons are accepted from ions in the solution layer next to the electrode into the waiting holes in the valence band. Semiconductor doped “*n*” will be cathodes.

In this discussion, electrochemical reactions with semiconductors are referred to as “thermal.” The reason is that semiconductors are particularly sensitive to incident light, which stimulates electron emission and causes photocurrents to flow. They are

<sup>23</sup>Perhaps not so very well suitable! Thus, semiconductor electrodes exhibit limiting currents that arise from the transport of the charge carrier inside the semiconductor. In practice, this means that it is difficult to get current densities above  $\sim 1 \text{ mA cm}^{-2}$  at moderately doped semiconductors. No such limitation occurs with metals that have roughly 1 electron per atom free to move under an electron field gradient. The limiting currents that arise with metals are due to the limitation in supply of materials in the solution.

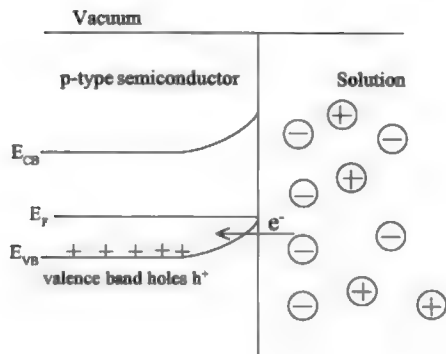


**Fig. 7.28.** A *p*-type semiconductor acts as an anode in thermal reaction under dark conditions.

more often used as “photoelectrodes,” and produce phenomena that are similar to a kind of “wet photovoltaics.” Hence, the nonilluminated electrochemical reactions involving semiconductors are called *thermal*. Photoelectrochemistry is a whole field to itself and is described in Chapter 10.

#### 7.4.5. The Limiting Current in Semiconductor Electrodes

As already stated, when metal electrodes are used in electrochemical reactions and one speaks of a limiting diffusion current, one is referring to ionic charge carriers

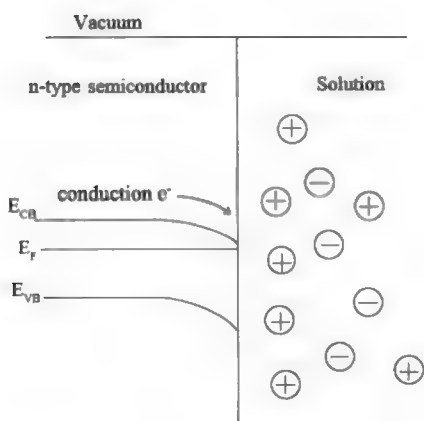


**Fig. 7.29.** An *n*-type semiconductor acts as a cathode in thermal reaction under dark conditions.

in solution, which cannot diffuse up to the electrode at a sufficient rate to donate or pick up the number of charges demanded by the electrode potential. Although the same phenomenon is possible with semiconductor electrodes, a limiting current usually arises because of a limiting transport rate of charge carriers in the electrode. Thus, in an  $n$ -type semiconductor with no surface states, electrons must be transported to the semiconductor/solution interface. They do this partly under a diffusion gradient that impels them to the surface, but their direction is also affected by the electric field near the electrode surface (Fig. 7.29).

Similar statements can be made about holes. They, too, have to be transported to the interface to be available for the receipt of electrons there. These matters all come under the influence of the Nernst–Planck equation, which is dealt with in (Section 4.4.15). There it is shown that a charged particle can move under two influences. The one is the concentration gradient, so here one is back with Fick’s law (Section 4.2.2). On the other hand, as the particles are charged, they will be influenced by the electric field, the gradient of the potential–distance relation inside the semiconductor. Electrons that feel a concentration gradient near the interface, encouraging them to move from the interior of the semiconductor to the surface, get “seized” by the electric field inside the semiconductor and accelerated further to the interface.

Holes, too, are subject to analogous events. They carry a positive charge<sup>24</sup> and diffuse and act under potential gradients just as electrons do, except that they react in an opposite way to electric fields because they have an opposite charge.

#### 7.4.6. Photoactivity of Semiconductor Electrodes

In the discussions of semiconductors and electrochemistry in this section, it has been assumed that the sole source of electrons and holes that are transported to the interface to take part in electrode reactions is the electrons injected into the conduction band from doping ( $n$ -type) and holes made in the valence band by doping for  $p$ -type. In the latter, holes migrate to the electrode surface to receive electrons from ions in the solution.

When light is incident on semiconductors, it may (as long as the photons are sufficiently energetic) *promote* electrons from the valence band to the conduction band, thus creating new electrons and holes. A whole new series of electrochemical

---

<sup>24</sup>There is a need to be cautious about raised eyebrows when one talks about the positive charge on holes (they have equivalent mass, too, see Appendix 5.1). Holes are the result of electron motion. In a  $p$ -type semiconductor, the act of doping has withdrawn electrons from the valence band and hence, in the position formerly occupied by these electrons, there now exist vacancies. However, the vacancies are surrounded by electrons. If an electron moves from right to left to jump *into* a hole, it clearly creates a hole where it had just been before it moved into the available hole created by doping. A number of electrons moving to the left is equivalent to a number of holes moving to the right. Hence, the equivalent charge and even an equivalent mass, for the acceleration of the holes depends upon the dynamics of electron movement and electrons certainly have mass.



reactions can now occur, for the electron and hole availability is no longer dependent only on doping, but depends also on the incident radiation. This gives rise to the new field of photoelectrochemistry, which is treated in Chapter 10. The field is important because it allows direct light to be used for conversion processes (e.g., incident light leads to electron ejection and the production of  $\text{H}_2$  from water). It is also the basis of one of the most basic processes known—photosynthesis, the production of food in green plants and biomass.

## Further Reading

### Seminal

1. H. Brattain and G. Garrett, *Ann. N.Y. Acad. Sci.* **58**:951 (1954). First treatment (thermodynamic) of semiconductors as electrodes.
2. M. Green, "Electrochemistry of the Semiconductor Solution Interface," in *Modern Aspects of Electrochemistry*, J. O'M. Bockris, ed., Vol. II, Butterworths, London (1959). First kinetic treatment of electron transfer at semiconductor/solution interfaces.
3. H. Gerischer, "Semiconductor Electrode Reactions," in *Recent Advances in Electrochemistry*, P. Delahay, ed., Interscience, New York (1961). Electrode kinetics involving conductivity and valence bands.
4. J. F. Dewald, "Semiconductor Electrodes," in *Semiconductors*, H. B. Hannay, ed., Reinhold, New York (1964). First diagrammatic presentation of electron exchange between redox species in solution and semiconductor bands.

### Modern

1. F. Gutmann, H. Keyzer, and L. E. Lyons, *Organic Semiconductors*, Part B, Malabar, FL (1983).
2. G. DiGirolamo, *Electrochemical Migration*, J. McHardy and F. Ludwig, eds., Noyes, Park Ridge, NJ (1992).
3. K. Uosaki and M. Koinuma, "STM and Semiconductor-Solution Interfaces," *Faraday Disc.* **94**:361 (1992).
4. R. DeMattel and R. S. Feigelson, "Electrochemical Deposition of Semiconductors," in *Electrochemistry of Semiconductors*, J. McHardy and F. Ludwig, eds., Noyes, Park Ridge, NJ (1992).
5. P. Allongue, in *Advances in Electrochemical Science and Engineering*, H. Gerischer and C. Tobias, eds., VCH Publishers, Weinheim (1995). STM on semiconductor electrodes.
6. W. Schmickler, *Interfacial Electrochemistry*, pp. 81–94, Oxford University Press, Oxford (1996).
7. W. Jaegerman, "Semiconductor Electrolyte Interface: A Surface Science Approach," in *Modern Aspects of Electrochemistry*, R. E. White, B. E. Conway, and J. O'M. Bockris, eds., Vol. 30, Plenum, New York (1996).
8. C. Hamann, A. Hamnett, and W. Vielstich, *Electrochemistry*, pp. 207–208, VCH-Wiley, New York (1998).

## 7.5. TECHNIQUES OF ELECTRODE KINETICS

### 7.5.1. Preparing the Solution

In the early days of electrode kinetics studies (1928–1950), the results of the measurements of rates of electrode reactions on solid electrodes obtained in one laboratory were usually irreproducible and disagreed by large percentages with those obtained in another laboratory. It was found (Bockris and Conway, 1949) that for electrode reactions involving intermediate radicals adsorbed on the electrode, as little as  $10^{-10}$  mol liter $^{-1}$  of impurity in the solution affected the measured rate of the electrode reaction (Fig. 7.30). There are two mechanisms by which impurities (usually traces of organics from the environment) can interfere with a satisfactory measurement.

1. A dissolved impurity can diffuse to the electrode surface and react there, in competition with the electrode reaction being examined. Usually the side reaction with the impurities contributes significantly to the current density only when this is low (e.g., in the microampere cm $^{-2}$  range). This was first shown quantitatively by Huq (1956), who measured the evolution of oxygen at extremely low rates (tenths of nanoamperes cm $^{-2}$ ) in experiments, the aim of which was to reach the value of the potential of the reversible oxygen reduction reaction  $O_2 + 4H^+ + 4e \rightleftharpoons 2H_2O$ . The effect of successive degrees of purification of the solution on the current-potential relation is shown in Fig. 7.31.

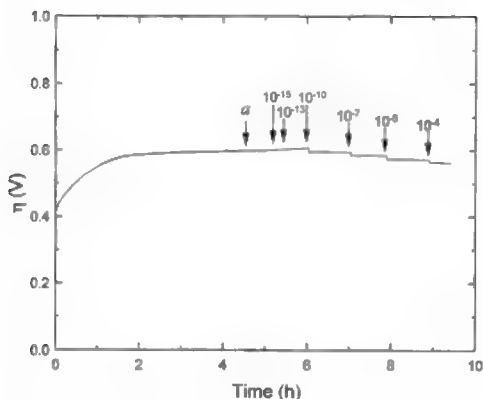


**Fig. 7.30.** Poisoning of Ni by  $As_2O_3$  in 0.1 N aq. HCl at  $10^{-2}$  M. *a* in the diagram represents 50 drops of 0.1 N HCl added as blank. Arrows show concentration of  $As_2O_3$  in mols/liter. (Reprinted with permission from J. O'M. Bockris and B. E. Conway, *Trans. Faraday Soc.* 45: 989, 1949.)

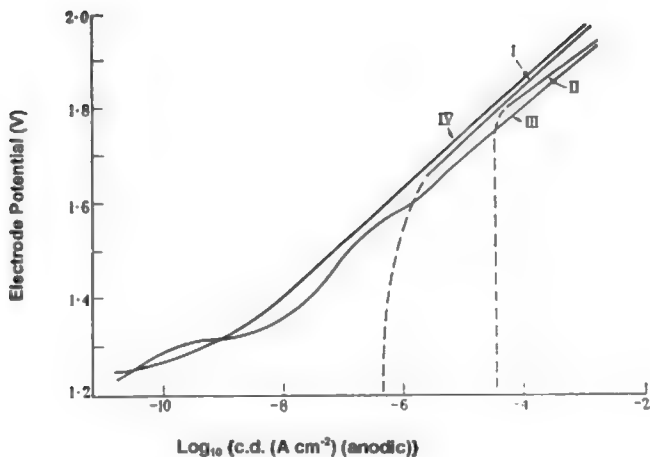


**Fig. 7.31.** Typical Tafel lines for oxygen evolution as a function of preelectrolysis conditions. I, no preelectrolysis; II, cathodic preelectrolysis at  $10^{-2} \text{ A cm}^{-2}$  for 24 hr; III, only anodic preelectrolysis at  $10^{-2} \text{ A cm}^{-2}$  for 48 h; IV, cathodic preelectrolysis for 24 h, anodic for 48 hr at  $10^{-2} \text{ A cm}^{-2}$ . (Reprinted with permission from J. O'M. Bockris and A. K. M. S. Huq, *Proc. Roy. Soc. London A237*: 277, 1956.)

A second mechanism by which impurities present in the solution interfere with measurements in electrode kinetics is associated less with their providing alternative paths to reactions and more with their adsorption on the electrode surface. The presence of adsorbed impurity material on the electrode surface may affect the rate of an intended reaction, particularly where there is an intermediate in the mechanism of the intended reaction.<sup>25</sup> Thus, the adsorbed impurity may block reactive sites on the electrode. Since the intended reaction (say, the reduction of oxygen) cannot now use the blocked active sites on the electrode surface, its kinetics are slowed down, particularly when the impurity adsorbs on the most active catalytic sites on the electrode. Again,

<sup>25</sup>Some electrochemists in the 1960s and 1970s stressed working with *redox* reactions. The prototypical redox reaction is the reduction of ferric ions to ferrous. In such reactions, the reacting ions do not actually adsorb chemically in actual contact with the electrode surface. Some workers chose these systems to avoid what they saw as the “complexities of adsorption.” However, in doing this, they missed the catalytic aspects of electrode kinetics. Further, nearly all electrode reactions (the central reactions of hydrogen evolution and oxygen reduction, but also most organoelectrochemical reactions, together with reactions in fuel cells and reactors, corrosion and bioelectrochemistry) involve reaction intermediates, so it is of little use trying to learn electrochemistry by examining electrode reactions that have no intermediates.

because different impurities turned up in the solutions used in different laboratories, the measurements disagreed.<sup>26</sup>

What are ways out of this extreme sensitivity to impurities in electrode kinetics for most electrochemical reactions? One way to reduce the effects of trace impurities from the solution in electrode kinetics is to use a liquid electrode because such electrodes can be made to form drops, the lifetime of which is small, so that the impurities from the solution don't have time to adsorb on the drops before they break off from the electrode. The electrode material then has to be mercury (the only metal that is liquid at room temperatures), so this approach is limited because mercury is a poor catalyst and one wishes particularly to work with electrode materials that catalyze electrode reactions well.<sup>27</sup>

One general method may always be used to reduce the effect of impurity adsorption on electrodes, and that is to work only for short times. Impurities take substantial times to adsorb. If the time in which the measurement is made is short enough, the adsorption aspect of impurity interference with electrode kinetic measurements can be reduced. Many of the techniques for doing this are described in Chapter 8 (transients). However, this approach does not eliminate the difficulty that at low current densities impurities in the solution may compete with electrons from the electrode. Further, although transient measurements may greatly reduce the adsorption of impurities during the measurement, it is difficult to arrange techniques so that the electrode is in contact with the solution for seconds only.

For these reasons, purification of the solution in electrode kinetics is often necessary. There are several steps.

1. The water used should not only be distilled but also passed through a reverse osmosis filter, or an ion-exchange membrane. Exposure to UV radiation may be used to eliminate bacteria.
2. The solute (electrolyte, dissolved reactant) must be analytical grade.
3. Care must be taken to guard the electrochemical cell from dirty (i.e., normal) air.<sup>28</sup>

<sup>26</sup>It's surprising how tiny are the concentrations in solution that can be significant in interrupting the normal behavior of an electrode reaction by covering up a substantial fraction of surface sites. Half of a platinum electrode can be covered with moderately complex organic molecules (e.g., anthracene) with a molar concentration of about  $10^{-6}$ . At an impurity concentration of  $10^{-10} M$  (see Fig. 7.29), the coverage would be  $< 0.01\%$ , and hence blockage by the impurity of critical catalytic sites of great activity would affect the intended reaction.

<sup>27</sup>There is a good economic reason for this. Look back at the Butler-Volmer equation (Eq. 7.24); the larger the  $i_0$  (i.e., the better the catalysis), the smaller the overpotential needed to get a given rate of reaction. However, the smaller the overpotential, the less the total cell potential, and hence the kilowatt hours, to produce a given amount of a substance in an electrochemical reactor.

<sup>28</sup>Tobacco smoke is a supercontaminant. If a cell used to carry out an experiment involving adsorbed intermediates gets contaminated, it may need lengthy treatment in oxidizing acid mixtures and steaming out, etc., to remove the contaminants adsorbed on the cell surface (but later transferred to the solution and thus coming into contact with the electrode).

4. *Scavenging* of residual impurities in the solution may be necessary if the rate-potential relation betrays the effects of impurities in the solution by some kind of aberrant behavior. One introduces a large auxiliary electrode of high area platinum black and changes the potential on it slowly and cyclically over the range of potentials of the intended experiment (Bockris and Conway, 1949). A day or so of this cycling may be necessary and the platinum black sheet (which now contains deposited or adsorbed impurities) must be removed carefully with the potential still on (so that the impurities do not desorb back into the solution).

The only test of a satisfactorily purified solution is constancy of the electrochemical reaction rate upon an increase in the degree of purification. Solution purification in electrode kinetics is expensive and time consuming. Each system should be considered in respect to the degree of purification necessary. For example, a solution containing redox reactions examined in the milliamperes  $\text{cm}^{-2}$  range may need far less purification than catalytically affected reactions examined in the microampere range. Kinetics (e.g., in bioelectrochemistry) where only transient changes are to be noted yield information where “purification” would be meaningless.

### 7.5.2. Preparing the Electrode Surface

Basically, three types of solid electrode surfaces are used in research laboratories.

1. Polycrystalline electrodes (e.g., flags of metal about  $1 \text{ cm}^2$  in area) or wires (e.g., 1–2 mm in diameter).
2. Single crystals with a surface prepared so it exposes a certain crystal plane.<sup>29</sup>
3. Films of the electrode material, about  $1 \text{ }\mu\text{m}$  in thickness, evaporated onto some unreactive substrate, e.g., graphite.

There are pros and cons for each method of electrode preparation. The polycrystalline electrodes are cheap and also are nearest in character to those used in practical reactors in industry. However, a polycrystal consists of innumerable grains (bits) of the electrode material, each having a different crystal orientation and hence a different catalytic property. One way of manufacturing an original metal may differ from another in the distribution of crystal faces of different kinds. Thus, irreproducibility of results in electrode kinetics is not only due to inadequate purification of solution,

<sup>29</sup>Planes that are cut through crystals in differing directions project a different arrangement of atoms. Not surprisingly, such different arrangements of the surface atoms give different rates of electrode reactions because the forces acting from the surface on adsorbed atoms differ with each crystal arrangement. Hence, measurements on well-defined single-crystal electrode surfaces are more informative than those on polycrystals.

it may also be caused by nonconstant crystal composition of a polycrystal surface or differing degrees of imperfection in the surface structure.

Single crystals, cut so that a certain crystal face is exposed to the solution, offer better definition and therefore reproducibility of results. By using electron diffraction measurements (which require a vacuum), one can determine the crystal face exposed to the solution before and after electrochemical measurements and hence ascertain if any change in crystal orientation has occurred as a result of contact with the solution. Such techniques, introduced by Hubbard in the 1970s, began a seminal change in electrode kinetics, the full fruits of which are still to be obtained.

Thin evaporated films are polycrystalline, but allow a more reproducible and defined surface than the use of bulk metal in wire or flag form.

What needs to be done to the electrode before immersion in the solution and the start of the experimental program depends on which of the above types of electrode one is using. Polycrystalline wires or flags are repeatedly washed in distilled water and treated with a polishing machine. After these steps, there are some alternatives. One is to introduce the electrode (which may still be covered by an invisibly thin oxide film) into the solution and subject it to a series of cyclical potential changes that repeatedly oxidize and reduce the surface ("activation"). Another is to subject it briefly to a hydrogen-oxygen flame, thus accomplishing removal of organics, reduction of oxides, etc. (Clavillier, 1974). A method has to be devised by which the electrode is then introduced into the solution without contaminating it or exposing it to dirty air. For example, it can be sealed in a thin glass bulb in an  $\text{H}_2$  atmosphere, and the bulb removed after its introduction into the solution. Measurement can begin immediately after removal of the protective glass bulb brings the solution into contact with the electrode.

### 7.5.3. Real Area

The apparent surfaces of polycrystals, measured geometrically, are often 2–3 times smaller than the real area because the latter is relatively rough—it has hills and valleys that are invisible to unaided sight (see Fig. 7.32). Because various metals—and different samples of the same metal—may have different "roughness factors"

$$\left( = \frac{\text{atomic scale real area}}{\text{geometrically measured apparent area}} \right)$$

and because the velocity of an electrode reaction has to be standardized to the real area, the roughness factor has to be determined.

It is easy to do this if the electrode is a noble metal, i.e., does not itself easily oxidize on anodic polarization. One evolves  $\text{H}_2$  cathodically until the entire surface is covered with H atoms ( $\theta_{\text{H}} = 1$ ) and then reverses the direction of the current, making it anodic and dissolving the adsorbed H atoms ( $\text{MH} \rightarrow \text{M} + \text{H}^+ + e$ ). It is easy, by use of a cathode ray oscillograph, to record the  $i_t$ - $t$  relation during dissolution at a constant potential. Apart from an initial charging potential, one obtains the coulombs used in

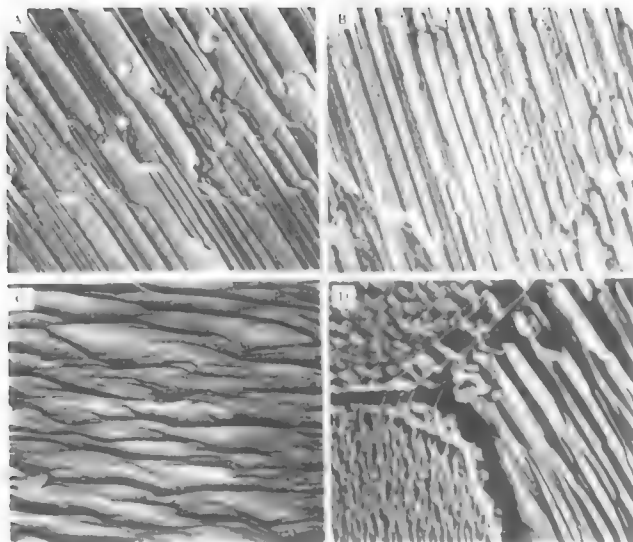


**Fig. 7.32.** The real area of polycrystals is often 2–3 times larger than the apparent area because of hills and valleys. SEM pictures of deposition at 50 mV. The mark represents  $20\mu$ . A, Electrode No. 1,  $16.5 \text{ C/cm}^2$ ; B, electrode No. 3,  $11.5 \text{ C/cm}^2$ ; C, electrode No. 4,  $14 \text{ C/cm}^2$ ; D, electrode No. 1,  $20 \text{ C/cm}^2$ . (Reprinted from J. O'M. Bockris, Z. Nagy, and D. Drazic, *J. Electrochem. Soc.* **120**(1): 40, 1973, Fig. 19. Reproduced by permission of The Electrochemical Society, Inc.)

dissolving the H from the linear section in a time,  $\tau$ . Dividing the coulomb determined by  $F$ —the electrical charge on a mole of  $\text{H}^{++}$ s—gives the moles of H atoms per *real* unit area. Knowing the area occupied by one adsorbed H atom gives the real area.

When the metal substrate is not noble, it dissolves along with the H, and it is difficult to separate the H dissolution current out of the total. There are alternatives. Thus:

- 1.a One determines the steady-state current for, e.g., anodic dissolution of the metal substrate per unit *apparent* area. Then one prepares a thin evaporated film on a substrate made nearly atomically flat (a cleaved crystal; a well-defined surface of a single crystal) and measures the steady-state current on a unit area. Then  $i_{\text{apparent}}/i_{\text{flat}} = \text{real area}$  per unit of apparent geometric area.
- 2.b One uses a small organic compound ( $^{14}\text{C}$  marked) to measure the radioactivity and thus the number of molecules when one is sure that  $\theta_{\text{org}} = 1$ . Knowing how the organic is lying on the surface (flat? standing up?), one can know the area per molecule and thus the number of molecules per geometric unit area.

The various methods of determining the real surface area usually agree only to about  $\pm 25\%$ . One of the advantages of single crystals with a well-defined face exposed is that the real area is a known property of the exposed crystal face (see Section 7.8.2 on Miller indices).

## 7.5.4. Microelectrodes

**7.5.4.1. The Situation.** There are two difficulties in making measurements on electrodes of normal size and shape, e.g., a square plate with sides of 1 cm. The first is that when the current density becomes sufficiently high, the rate of the reaction at the electrode is no longer controlled by interfacial processes such as electron transfer or a surface chemical reaction, but by the rate of transport of materials to the electrode surface. There are circumstances where that is just what is wanted (e.g., in electro-analytical situations where one needs a proportionality between the current and the concentration of reactant). However, if the mechanism of the reaction at the metal/solution interface is the objective of the examination, it is desirable to have some interfacial process (in contrast to transport in the solution) be rate determining. There is a quantity,  $i_L$  (see Section 7.9.10) called the *limiting current density* (the maximum current density at which diffusion to a unit area of an electrode can occur) and it is desirable that this be as high as possible for a given concentration of reactant because if the current density of measurement approaches (gets within 1/10 of) the highest possible current density for transport, the measurements no longer reflect only the interfacially controlled situation, but are increasingly determined by the characteristics of transport of the charge carriers in the solution to the electrode.

It is shown elsewhere (Section 7.9.2) that an approximate numerical formula for this limiting diffusion current  $i_L$  is  $i_L = 0.02 nc$ , where  $n$  is the number of electrons used in one step of the overall reaction in the electrode and  $c$  is the concentration of the reactant in moles liter<sup>-1</sup>. Hence, at 0.01 M, and  $n = 2$ , say,  $i_L = 0.4 \text{ mA cm}^{-2}$ —a current density less than may be desirable for many purposes. The problem is how to increase this diffusion-controlled limiting current density and obtain data on the interfacial reaction free of interference by transport at increasingly high current densities.

Now, there is another problem. As the current density of the measurement increases, there is an increase in the ohmic potential difference between the end of the (so-called) Luggin capillary (see Section 7.5.7.2) and the electrode. As shown in Section 7.5.7.2, the value of this ohmic error is given by the equation  $\eta_{\text{ohmic}} = i_L/\kappa$  where  $L$  is the distance between the Luggin tip and the electrode, and  $\kappa$  is the specific conductivity of the electrode. Thus, to make measurements of overpotential that contain less than, say, 0.01 V of this unwanted ohmic error,  $i_L/\kappa < 0.01 \text{ V}$ . With  $L \sim 0.01 \text{ cm}$  and  $\kappa \sim 10^{-3} \text{ S}$  (the kind of value observed for an 0.01 M solution),  $i_{\text{max}}$  is  $1 \text{ mA cm}^{-2}$ .

It is desirable to have much higher current density values available for investigation without the disturbing influences of a limiting rate of diffusion or inclusion in the



mechanism of the unwanted IR drop. One of the ways of solving this problem is to use a "microelectrode." If an electrode is made hemispherically with a radius of curvature of  $<0.01$  cm, the maximum (free of transport effects) current density can be increased, compared with that for a planar electrode, and furthermore, the interfering ohmic drop between the Luggin and the electrode can be greatly reduced.

**7.5.4.2. Lessening Diffusion Control by the Use of a Microelectrode.** For steady-state diffusion to a flat-plate electrode, it is known (Section 7.9.3) that  $i_L = DcF/\delta$ , where  $i_L$  is the maximum current density allowed by diffusion,  $D$  is the diffusion coefficient,  $c$  is the reactant concentration in moles  $\text{cc}^{-1}$ ,  $F$  is the faraday in coulombs  $\text{mol}^{-1}$ , and  $\delta$  is the steady-state diffusion layer thickness in centimeters. This quantity becomes constant after about 1 s of electrolysis owing to the intervention of convection<sup>30</sup> superimposed on diffusion and has a value in a solution that is not artificially stirred of about 0.05 cm.

In work connected with the theory of the growth of dendrites on electrodes, it was found (Barton and Bockris, 1961) that for a spherical electrode of a radius less than this diffusion layer thickness (i.e., less than 0.05 cm), the maximum diffusion-controlled current is no longer given by  $DcF/r$ , but rather by  $Dc_f F/r$ .

This finding opens the possibility of obtaining increased limiting diffusion currents (i.e., for hemispherical electrodes with  $r < \delta$ ) and increasing the range of current densities at which reaction rates can be measured without disturbance by interfering diffusion reactants to or from the electrode. To find out what the advantage could be, let it be supposed that one has a microelectrode with a tip radius as low as  $0.1 \mu\text{m}$ ,  $10^{-5}$  cm. Thus,  $\delta/r = 0.05/10^{-5} = 5000$ . Depending on need, therefore, by using a microelectrode, one can increase the maximum current density that remains free from transport control by several thousand times, a considerable improvement for anyone who, say, wants to investigate the range over which the Butler–Volmer equation (which is applicable only to reactions free from diffusion control) is valid.

However, advantageous applications of micro- and ultramicroelectrodes are not limited to fundamental investigations. Such electrodes open up possibilities for work in very low concentrations of solute. Whatever can be done at a planar electrode can be done at a concentration about a thousand times lower by using an ultramicroelectrode without reaching the limiting diffusion current. This means that one could even obtain responses from solutes of 1 ppb (assuming a measured current density of  $1 \mu\text{A cm}^{-2}$ ).

Another advantage in the use of microelectrodes is that the limiting diffusion current is independent of disturbances in the solution. Thus, for a planar electrode, the

<sup>30</sup>"Natural" convection sets itself up very near an electrode because the electrode process either adds ions to the solution and makes it heavier, or deposits ions from it and makes it lighter. Either of these practices leads to a difference in density between the region very near the electrode and the rest of the solution, and this in turn causes the solution layers near the electrode to rise or sink, thus causing a stirring motion.

limiting current density depends on the diffusion layer thickness,  $\delta$ , but this in turn is only  $\sim 0.05$  cm in an undisturbed solution. Any kind of flow in the solution (e.g., stirring) decreases  $\delta$ , and hence  $i_L$  at a planar electrode becomes an unreliable quantity, particularly in practical (i.e., industrial) circumstances, where the solution is often disturbed. With microelectrodes, however, the limiting current density is controlled by the radius of curvature of the electrode and is independent of the flow conditions of the solution. This is clearly of great practical value if measurements are to be made (e.g., in a pipe) where the flow rate may be uncertain.

**7.5.4.3. Reducing Ohmic Errors by the Use of Microelectrodes.** In Section 7.5.7.2, it is shown that the IR drop between the end of a Luggin capillary and a planar electrode is given by  $i_L/\kappa$ , where these quantities have been defined. Consider now the arrangement shown in Fig. 7.33, which shows a microelectrode of radius  $r$  surrounded by a radial counter-electrode, e.g., a basket of platinum mesh of radius  $R$ . Then since the current  $I$  equals  $iA$ , where  $i$  is the current density and  $A$  is the area of the microelectrode:

$$IR = \frac{I}{\kappa} \int_r^R \frac{dR}{4\pi R^2} = \frac{4\pi r^2 i}{\kappa} \left| \frac{1}{r} - \frac{1}{R} \right| \quad (7.79)$$

For  $r \ll R$ , the IR drop is given by  $ir/\kappa$ . Thus, the lessening in the unwanted IR component in an overpotential measurement ( $iL/\kappa = \text{planar electrode}$ ) is  $L/r$  times. Taking  $L \sim 0.1$  and  $r \sim 10^{-5}$ , the improvement could be as much as  $10^4$  times.

Consider deionized water. This has a  $\kappa$  value of about  $3 \times 10^{-8}$ . Hence, if  $r \sim 10^{-5}$  cm,  $ir/\kappa = i \cdot 10^{-5} / 3 \times 10^{-8} \approx 333i$ . Thus, for  $ir/\kappa < 0.01$ , a current density of as much as  $30 \mu\text{A cm}^{-2}$  could be measured at an ultramicroelectrode in deionized water current. Correspondingly, ultramicroelectrodes have made possible valid potential electrochemical measurements in the electrolysis of steam (Bond and Fleischmann, 1984).

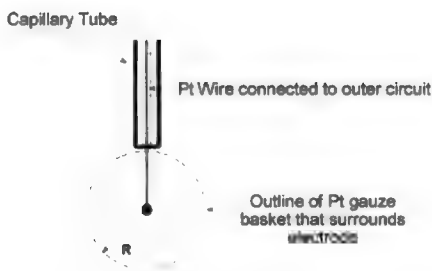


**Fig. 7.33.** Microelectrode of radius,  $r$ , surrounded by a basket of platinum gauze of radius  $R$ .

**7.5.4.4. The Downside of Using Microelectrodes.** Since microelectrodes extend the current density that can be measured by several orders of magnitude and allow a great reduction in the concentration range amenable to measurement, one might think they would be the electrode of choice for most measurements. However, there are some downside problems to ponder in using microelectrodes.

1. A reduction in the IR drop by using a microelectrode is obtained by using a very small electrode area. Suppose one takes  $1 \text{ mA cm}^{-2}$  as a typical current density for measurement in electrode kinetics. Then, if the microelectrode is an *ultramicroelectrode* and has a radius of only  $0.1 \text{ }\mu\text{m}$ , or  $10^{-5} \text{ cm}$ , its area is that of a sphere, i.e., it is  $4\pi 10^{-10} \approx 1.25 \cdot 10^{-9} \text{ cm}^2$ . The current ( $I$ ) at an electrode is  $iA$ . On the assumption chosen then, the  $I$  is  $\sim 10^{-12} \text{ A}$ . Now, modern instrumentation in the laboratory can easily measure  $1 \text{ pA}$ . Outside a research laboratory, however, measurement of such a low current may pose problems.<sup>31</sup>

Again, if microelectrodes are so sensitive that they can allow measurements in distilled water ( $c_0 = 10^{-7} \text{ mol liter}^{-1}$ ), they will also react to impurities present at the same order of magnitude, i.e., around  $0.001 \text{ ppm}$ . This means that impurities have to be removed from the solution to, say,  $0.0001 \text{ ppm}$ . This can be done by using scavenger electrolysis on a large auxiliary electrode, but one may have to use a quartz cell to guard against impurities dissolving out of the glass, and be cautious about the possibility of trace impurities from possible dissolved ions from the counter-electrode.

A corresponding impurity-related problem is adsorption of (nonreacting) impurities from the solution. In a microelectrode, there is a far greater volume/area ratio than with a planar electrode, i.e., a greater reservoir of impurities is available for adsorption onto the tiny electrode area. It is impractical to remove impurities to a level at which there are not enough impurities to be adsorbed on the fraction of the electrode that contains the active sites, so that one has to depend on the *rate* of adsorption and keep the time of the experiment down so that adsorption is negligible. Experiments show that the rate of adsorption of organics is quite slow so that if the impurity level in the solution is, say,  $< 0.01 \text{ }\mu\text{mol}^{-1}$  (about  $0.001 \text{ ppm}$ ), one has about  $1 \text{ hr}$  before adsorption on Pt is significant.

**7.5.4.5. Arrays.** One can compensate for the tiny currents produced by microelectrodes by working with many of them placed together within a board of an insulating material (connected at the back so that all the currents add) (see Fig. 7.34). Then, if  $r$  is the radius of each electrode (assumed to be disklike in shape) and  $n$  the number per unit area,  $n\pi r^2$  is the total active area. If  $L$  is the distance between the “spots,”  $(\sqrt{n}L)^2$  is the total area. Hence,

<sup>31</sup>For example, one needs shielded and grounded cables, for such tiny currents may be exceeded by stray currents from nearby electrical machinery.

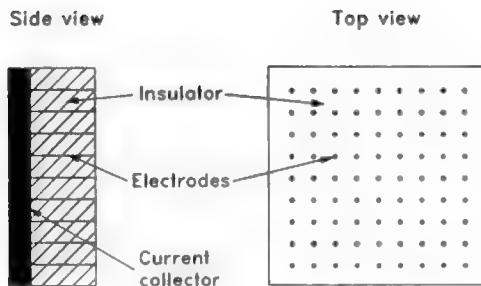


**Fig. 7.34.** An ensemble of ultramicroelectrodes. (Reprinted from E. Gileadi, *Electrode Kinetics for Chemists, Chemical Engineers, and Materials Scientists*, VCH Publishers, 1993, p. 450. Copyright © 1993 John Wiley. Reprinted by permission of John Wiley & Sons, Inc.)

$$\frac{n\pi r^2}{(\sqrt{n}L)^2} = \pi \left( \frac{r}{L} \right)^2 \quad (7.80)$$

is the ratio of active to total area. The current per ensemble is increased by  $n$  (e.g., 10) times over that for a single microelectrode.

Microelectrode arrays also have their Achilles heel. At sufficiently short times, they do indeed provide a current total  $n$  times greater than that at an individual microelectrode. However, as time increases, the diffusion situation around each electrode begins to blur (i.e., there is a spread of the areas—indeed volumes—around each microelectrode until, instead of each electrode “spot” acting as if it were an individual microelectrode, the overlap of the individual diffusion gradients begins to spoil the intended functioning of the ensemble by which the very high limiting current densities for each microelectrode could be added. Eventually, at sufficiently high times, as far as the limiting diffusion current density is concerned, the array behaves as though it were simply a single planar electrode, the limiting current being that of a planar electrode of an area that is the sum of the areas of the microelectrodes. This is illustrated in Fig. 7.35.

The question, then, is, how long is the time during which one can avoid this pesky overlap of the diffusive regions so that the ensemble functions ideally and gives the total of the limiting current for, e.g., 100 microelectrodes? A precise answer needs a very lengthy calculation. It can be stated that this “safe” time covers a range as low as  $10^{-2}$  s and as high as 1 s. In view of the relatively short times used in transient (or sweep) measurements, this range may be acceptable. However, arrays of microelec-

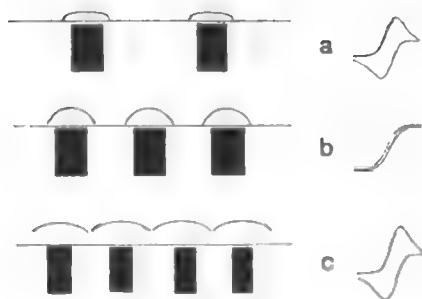


**Fig. 7.35.** Development of diffusion concentration profiles in ensembles of microelectrodes. Concentration distortions at very short times during chronoamperometry or fast sweep rates during (a) cyclic voltammetry, (b) intermediate times or sweep rates, and (c) long times or slow sweep rates. Voltammetric responses are shown schematically. (Reprinted from B. R. Scharifker, "Microelectrode Techniques in Electrochemistry," in *Modern Aspects of Electrochemistry*, Vol. 22, J. O'M. Bockris, B. E. Conway, and R. E. White, eds., Plenum, 1992, p. 505.)

trodes are not useful for examining the kinetics of electrode reactions that reach the steady state at times longer than 1 s. This limits the use of the technique to electrode reactions involving catalysis of solid electrodes where adsorption of ions or radicals on the electrode surface may take  $> 1$  s to reach its final value at a given potential for the steady-state reaction mechanism concerned.

#### 7.5.4.6. The Far-Ranging Applications of Microelectrodes.

Although spherical diffusion to electrodes has been understood since the 1960s, microelectrodes only came into general use in electrochemistry in the 1980s. The range of their applicability will still be explored in the twenty-first century. They facilitate electrochemical measurements at low concentrations and high current densities. They may be used to investigate the electrochemical changes in tiny but interesting spaces, such as inside the pits formed in corroding metals (Section 7.1.4 and Volume 2B). Within bioelectrochemistry, they allow investigation of *in vivo* systems on a realistic scale (i.e., on the scale of biological cells,  $\sim$  microns), and particularly processes relevant to the electrochemistry of the brain. Their use is liable to increase in many areas of electrochemistry.

### 7.5.5. Thin-Layer Cells

Cells can be made in which the cathode–anode distance is only  $10^{-3}$  cm. Such cells have the advantage that the total impurity present is very small and may not be enough to cover more than 0.1% of the electrode surface if they were all adsorbed. Thus, suppose the impurity concentration were  $10^{-6}$  mol liter $^{-1}$  or  $10^{-9}$  mol cc $^{-1}$  or  $10^{-12}$  mol in the cell. Because an electrode surface can carry (at most) about  $10^{-9}$  mol cm $^{-2}$ , the maximum fraction of the surface covered with impurity molecules is 0.1%. Does work with thin-layer cells eliminate the impurity problem in electrode kinetics? It improves it. However, active sites on catalysts may occupy less than 0.1% of an electrode and preferentially attract newly arriving impurities, so that even thin-layer cells may not entirely avoid the impurity difficulty,<sup>32</sup> particularly if the electrode reaction concerned (as with most) involves adsorbed intermediates and electrocatalysis.

### 7.5.6. Which Electrode System Is Best?

The answer to this question depends on the mission. Single crystals with a preferred orientation exposed to the solution give the most well-defined and repeatable surface, and here rightly been called by Hubbard and Soriaga “well-defined” electrodes. Intense and continuous purification of solution allows the attainment of steady-state conditions on polycrystalline electrodes, even when the current density or rate of the reaction is very low. Measurements at abnormally high current densities or at abnormally low concentrations are best achieved using microelectrodes. Another factor is the time range. Some systems “last” only for seconds before impurities adsorb or concentrations at the interface begin to change: On the other hand, attainment of the steady state in catalyzed reactions may require as much as  $10^2$  s.

Table 7.3 summarizes some of the insights as to the properties of electrode systems gained in the preceding section. The numbers in it have been calculated with assumptions as to what is “reasonable” for the parameters used. In real situations, the quantities tabulated should be more exactly defined using the actual parameters pertaining to the situation.

In the present discussion, attention has been given to the physical size and shape of the various types of electrodes. In Chapter 8, the time variable will be introduced and it will be seen to what degree using transient techniques for making measurements can contribute to the best compromise between short times that help to lessen the

---

<sup>32</sup>Such cells have been used as a means towards “examining adsorption” by subjecting them to a high vacuum (i.e., removing the liquid from the solution) and examining what remains “adsorbed.” However, the interfacial region at an electrode involves the solvent and stretches out into the solution for  $\sim 1$  nm. The removal of the solvent leaves unaffected only an indeterminate number of tightly bound chemisorbed ions. An examination of the structure of the interfacial region this way has the advantage of being able to apply ultrahigh voltage methods, e.g., Auger, XPS, LEED, to the remains left by removing the solvent. The procedure is analogous to researching the structure of a building by examining what remains with a microscope after the building has been knocked down by a tornado.

**TABLE 7.3**  
**Some Electrode Types and Their Realms of Usefulness**

Type	Time during Which One Can Work without Impurity Interference	Definition of Catalytic Surface	Highest $i$ in 1 $M$ solution	Lowest conc. for 1 mA cm <sup>-2</sup>	Sensitivity to 10 <sup>-6</sup> $M$ impurity
Flag polycrystal	Several hours if scavenger electrolysis of solution is used	Poor	0.1 A cm <sup>-2</sup>	0.1 $M$	Sensitive
Single crystal		Excellent	0.1 A cm <sup>-2</sup>	0.1 $M$	Sensitive
Specific orientation exposed	0.1 hr if scavenger electrolysis of solution is used	Better	0.1 A cm <sup>-2</sup>	0.1 $M$	Sensitive
Evap. film		Usually uncontrolled, but could be electrochemically faceted	500 A cm <sup>-2</sup>	10 <sup>-7</sup> $M$	Not sensitive if time < 0.1 hr
Microelectrode	1 s	The same as for microelectrode	500 A cm <sup>-2</sup> at times of < 1 s	10 <sup>-6</sup> $M$	Same as microelectrode
Microelectrode array					
Rotating disk, 10,000 rpm	< 0.1 hr	Poor	1 A cm <sup>-2</sup>	5 10 <sup>-3</sup> $M$	Not sensitive in time < 0.1 hr
Thin-layer cell	> 1 hr	Normally poor; single crystal use?	1 A cm <sup>-2</sup>	10 <sup>-3</sup> $M$	Insensitive

disturbing effects of diffusion control and contamination, and the longer times sometimes necessary to attain steady state at a given potential.

### 7.5.7. The Measurement Cell

**7.5.7.1. General Arrangement.** It has been stressed (Section 6.3.1) that the absolute value of the potential difference, the Galvani potential difference,  $\Delta\phi$ , across an interface cannot be measured. How then is it possible to determine the overpotential,  $\eta = \Delta\phi - \Delta\phi_e$ , which is the difference between two absolute potentials, one ( $\Delta\phi$ ) corresponding to a current density  $i$  and the other ( $\Delta\phi_e$ ) to equilibrium?

In principle, the approach is similar to that of Section 6.3.2. There it was shown (see, e.g., Fig. 7.14) that by setting up a two-electrode system (i.e., by coupling the

interface under study, the test or working electrode, with a nonpolarizable interface, the reference electrode), two quantities can be measured: (1) the changes in the potential of the test electrode and (2) the potential of the test electrode relative to the reference electrode. Such a two-electrode system is quite adequate for the measurement of equilibrium relative electrode potentials.

To determine an overpotential, however, it is necessary to alter the above two-electrode system by introducing an extra auxiliary electrode, which is termed the *auxiliary* or *counter-electrode*. Thus a three-electrode arrangement is set up as shown in Fig. 7.36. In such a setup, the counter electrode is connected to the test electrode via a polarizing circuit (e.g., a power source) through which a controllable current is made to pass and produce alterations in the potential of the test electrode. Between the nonpolarizable reference electrode and test electrode is connected an instrument that is capable of measuring the potential difference between these electrodes.

When no current flows through the polarizing circuit and there is equilibrium at the test electrode/electrolyte interface, the potential difference,  $E_e$ , between the test and reference electrodes is given by

$$E_e = \Delta\phi_e + \Delta\phi_{\text{contact}} + \Delta\phi_{\text{ref}, e} \quad (7.81)$$

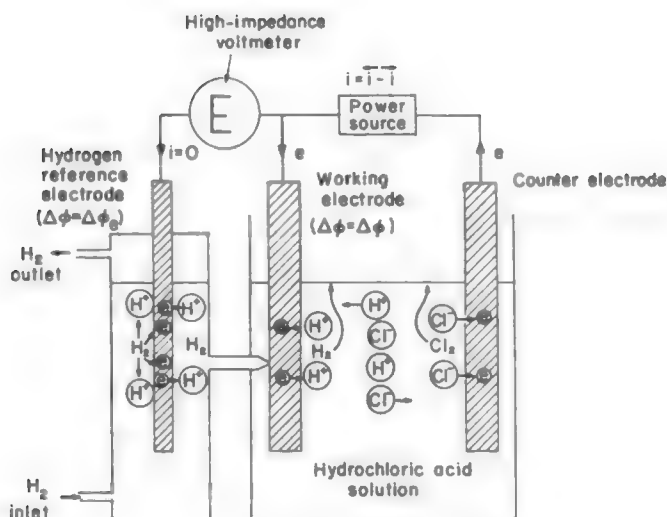


**Fig. 7.36.** The three-electrode system required to measure electrode overpotentials, i.e.,  $\Delta\phi - \Delta\phi_e$ . The potential between the working electrode and the reference electrode when both  $\Delta\phi$  and  $\Delta\phi_e$  correspond to the same reaction is equal to the overpotential,  $\eta$ . The tube joining the reference electrode and the working electrode is a Luggin capillary. It helps diminish the inclusion of illicit IR drop in the measurement.



where  $\Delta\phi_{\text{contact}}$  and  $\Delta\phi_{\text{ref}, e}$  are the potential differences across the metal–metal contact and reference interfaces.

When a current  $I$  is passed through the polarizing circuit (i.e., between the test and counter-electrodes), (1) the potential of the test electrode changes from  $\Delta\phi_e$  to  $\Delta\phi$ ; (2) the potential difference across the metal–metal contact can be considered to be unchanged; (3) the potential of the reference electrode remains at the equilibrium value,  $\Delta\phi_{\text{ref}, e}$ , because no current flows through the measuring circuit (i.e., between the reference and test electrodes); and (4) a potential drop occurs in the electrolyte through which the polarizing current flows. Thus, under these conditions, the measured potential difference between the test and reference electrodes is

$$E = \Delta\phi + \Delta\phi_{\text{contact}} - \Delta\phi_{\text{ref}, e} + IR \quad (7.82)$$

In this equation  $IR$  is the potential drop developed when the polarizing current  $I$  overcomes the resistance  $R = 1/\sigma A$  of the electrolyte between the test electrode and the *Luggin tip* or probe by means of which the reference electrode makes ionic or electrolytic contact with the test electrode.

From Eqs. (7.81) and (7.82), it follows that

$$\eta = \Delta\phi - \Delta\phi_e = (E - E_e) + IR \quad (7.83)$$

The  $IR$  error can be reduced by minimizing  $R$ , i.e., by choosing high-conductivity electrolytes and using small distances between the test electrode and Luggin tip (see Section 7.5.7.2).

When  $\eta$  values are obtained at various currents, it is possible to obtain  $\eta$  vs.  $\log i$  plots. Such  $\eta$  vs.  $\log i$  plots are known as *Tafel* lines, in recognition of Julius Tafel,<sup>33</sup> who first (1903) published measurements that showed the behavior of Eq. (7.83). An

<sup>33</sup>Julius Tafel started his academic life as an organic chemist, working with the great Emil Fischer, who became a Nobel laureate because of his work on carbohydrates. It was during Tafel's work on the structure of strychnine in Fischer's laboratory that he discovered it would be possible to reduce at electrodes substances for which he had not found other reduction methods. Tafel applied this organoelectrochemical discovery to many compounds and proposed from this work the catalytic mechanism for hydrogen evolution (rate-determining step: the chemical combination of hydrogen atoms) which bears his name. He may have been the first to use the technique of preelectrolysis for purifying solutions and, above all, he discovered the first law of electrochemistry, Tafel's law, which showed the exponential relation between the reaction rate and the overpotential.

Tafel was one of those scientists whose life is not well known, although the equation that bears his name is certainly as important to the overall understanding of kinetics in nature as is the corresponding equation due to Arrhenius. Tafel's life was rather short. He retired at the age of 48, due to poor health and spent his last years in spas attempting to regain his vigor, frequently attended by pupils at his bedside, even during fever spells. In his last years he wrote as many as 60 book reviews covering practically every field of chemistry. He died at the age of 56. A review of Tafel's life has been published by Klaus Müller, *J. Res. Inst. Catalysis*, Hokkaido University, **17**: 54 (1969).

example is shown in Fig. 7.37. It will be noticed that the intercept  $a$  in the Tafel plot permits a determination of the equilibrium exchange current density  $i$ .

**7.5.7.2. More on Luggin Capillaries and Tips.** A Luggin capillary (Fig. 7.38) is used in electrochemical cell measurements to reduce toward zero what is called "the IR error." Zero net current flows over the reference electrode itself for it to register the potential corresponding to the equilibrium value of a reaction. There will therefore be no potential drop in the tube leading from the reference electrode to the end of the Luggin. The Luggin tip is at the potential of the solution in contact with the electrode. Then the potential difference relevant to an "electrode potential" measurement is that between the interior of the electrode and that of the solution. One should not press the Luggin capillary against the electrode because that would shield a part of the electrode from receiving the normal current density.

Suppose the solution-filled space between the electrode and the tip of the Luggin capillary is of length  $L$  and the current on the electrode is  $I$ . The resistance of the electrolyte column is  $(1/\kappa)(L/A)$  where  $\kappa$  is the specific resistivity of the electrolyte between the tip of the capillary and the electrode,  $L$  is the length of the electrolyte column, and  $A$  is the cross-sectional area of the gap. The current  $I$  is  $iA$ . If one can consider the electrode-Luggin distance as a small cylinder of solution (Fig. 7.38), then:

$$IR \text{ error} = (iA) \frac{1}{\kappa} \frac{L}{A} = i \frac{L}{\kappa} \quad (7.84)$$

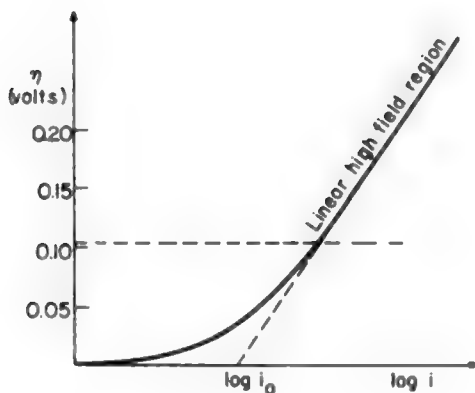


**Fig. 7.37.** A typical Tafel line for a one electron-transfer electrode reaction, showing the exponential relationship at high overpotentials, which makes the relation between  $\eta$  and  $\log i$  linear.

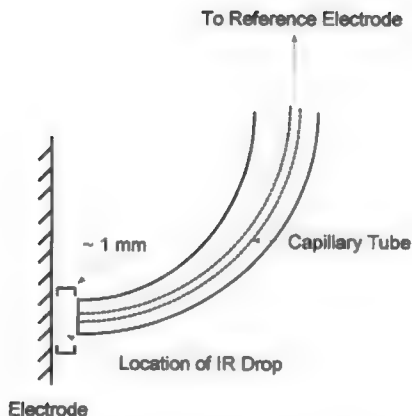


**Fig. 7.38.** An enlarged schematic of the relevant features of a Luggin capillary.

Consider a 1 M solution of a typical fully dissociated electrolyte. The  $\kappa$  value will be around  $0.1 \text{ S cm}^{-1}$ . For  $L = 0.1 \text{ cm}$ ,  $\eta_{\text{ohmic}} = i(0.1/0.1)$  and for  $i = 1 \text{ mA cm}^{-2}$ , the ohmic error is an acceptable 1 mV. A rather favorable case has been chosen as the example. For  $\kappa = 0.01$  and  $i = 10 \text{ mA cm}^{-2}$ , the ohmic error is 0.1 V, which is too great to be neglected.

To reduce this “ohmic error,” one could diminish  $L$  to 0.1 mm, but this would mean screening the length of solution still remaining between the electrode and the Luggin tip from current lines. Instead, it is best to use electronic devices that distinguish the superfast change in potential that occurs in this IR portion when the current density is switched on and off from the slower change of the electrode potential itself, where the charging of the interfacial capacitor takes time. The ohmic correction (eliminating the IR error) can be made automatically. However, it is in any case desirable to minimize the value of the IR error to be corrected to as small a fraction of the total measured potential as is practical. The failure to make such corrections is one of the most frequently made errors in electrochemical kinetics (particularly in potential sweep measurements—Chapter 8—near the current peaks).

**7.5.7.3. Reference Electrodes.** The potential offered by a standard hydrogen electrode is defined as the fundamental reference electrode. The arrangement is shown in Fig. 7.39. The platinum is usually of what is called the “black” variety, having a very rough surface and hence a very high real area per geometric area, electrodeposited from a solution of  $\text{H}_2\text{PtCl}_6$  under especially prescribed conditions. The solution is made up of a mineral acid ( $\text{HCl} \sim \text{H}_2\text{SO}_4$ ) with a mean activity on  $\text{H}^+$  at  $25^\circ \text{C}$ .  $\text{H}_2$  gas is bubbled across the electrode.

A well-behaved  $\text{H}_2$  reference electrode is splendid to perceive and use. However, the truth is that well-behaving  $\text{H}_2$  reference electrodes are difficult to set up; for

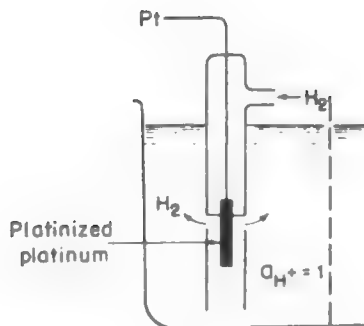


**Fig. 7.39.** The nonpolarizable standard hydrogen electrode.

example, they get poisoned and may then deviate significantly from their proper thermodynamic value. Setting them up so that they behave well is time consuming and can be stressful to the experimenter.

For this reason, secondary reference electrodes are often used in place of the standard hydrogen electrode. Their potentials are more stable; they are easier to set up; and one knows by measurement what potential they exhibit at a given temperature, with respect to the standard hydrogen electrode. Thus, one can measure an electrode process at a “working electrode,” and measure it against a secondary standard as a reference electrode. Then (knowing the potential of the secondary standard against hydrogen) one can convert the reading to express the working electrode’s potential on the primary standard, the standard hydrogen electrode.

The most-used secondary standard is the calomel electrode, shown in Fig. 7.40. It consists basically of a pool of mercury on top of which is spread a thin layer of  $\text{Hg}_2\text{Cl}_2$  (calomel), a substance only slightly soluble in water. A  $\text{KCl}$  solution (either at the unit activity with respect to  $\text{Cl}^-$  or saturated) is in contact with the calomel  $\text{Hg}$  system and a  $\text{Pt}$  wire connects the electrode to the rest of the circuit.

Hence, from Eq. (7.47):

$$V = V_0 + \frac{RT}{2F} \ln a_{\text{Hg}_2^{2+}}$$

However (since calomel is sparingly soluble and present as a solid):

$$\frac{a_{\text{Hg}}^2 a_{\text{Cl}^-}^2}{a_{\text{Hg}_2\text{Cl}_2}} = K_S$$

Thus the calomel electrode is reversible with respect to

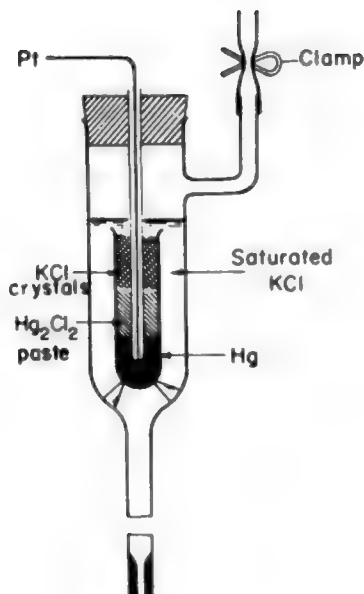


**Fig. 7.40.** The nonpolarizable calomel electrode. (One must be careful to avoid currents passing across the interface sufficient to form  $\text{HgO}$ , for this irreversibly spoils the electrode's reversible function.)

$$V_0^1 - \frac{RT}{F} \ln a_{\text{Cl}^-} \quad (7.85)$$

In the  $\text{Hg-Hg}_2\text{Cl}_2$  system, the calomel electrode becomes a secondary standard, having a value at  $T = 25^\circ \text{C}$  for 1 M KCl of 0.281 V at  $25^\circ \text{C}$  or for saturated KCl, 0.242 at  $25^\circ \text{C}$ .

There are other secondary standard electrodes, and one that is often used as a secondary standard is the Ag-AgCl electrode. It consists of an Ag wire that has been made an anode in a chloride-containing solution. The resulting evolution of  $\text{Cl}_2$  forms a thin porous film of AgCl on the silver wire. The wire and its layer are immersed in a standard KCl solution and the electrode is reversible with respect to  $\text{Cl}^-$  on the grounds of reasoning similar to that presented for calomel. The potential of this electrode is 0.222 V versus the standard  $\text{H}_2$  electrode.

A whole series of "ion selective" electrodes also exists. They are not reference electrodes in the same sense as the three electrodes discussed above, but serve to

indicate the presence (and concentration) of specific ions, and these specific ions only. Ion-selective electrodes exist for Cu, Pb, Fe, Zn, and Ca. The mechanism by which they work involves a membrane (see Fig. 7.41). A substance that preferentially forms a complex with the test ion to be measured is on the electrode side of the membrane, and when the test ion diffuses from the solution through the membrane and comes into contact with the complexer, it sets up a certain new characteristic concentration, different from, but a function of, the concentration of the ions concerned in the test solution. This potential of the Ag-AgCl electrode in the ion-selective apparatus, compared with that of some other reference electrode in the outer solution, then gives a measure of the concentration of the test ion in the solution.

### 7.5.8. Keeping the Current Uniform on an Electrode

If one envisages a very *simple* electrochemical cell, one in which the two electrodes face each other and only these two faces are active (e.g., the backs are covered with an insulating layer), then the current lines between them are essentially uniform, although they may deviate somewhat at the edges. This would not be so for the back of these two electrodes if they were not insulated, for the current lines would have to circle around the front and come around the back. Assuming for the moment a nonpolarizable electrode reaction (see Section 6.3.3), the distribution of the current will depend simply and solely on the resistance of the solution and the strength of the current passing through it. In the extreme of high solution concentration and low current, the value of the ohmic drop for current lines “coming around the back” will be negligible and the current uniform both back and front. Conversely, then, the current to the back sides of the two electrodes will be less than at the front insofar as the

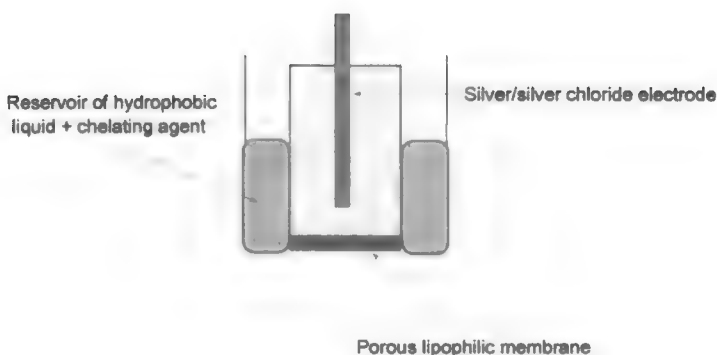


**Fig. 7.41.** The structure of an ion-selective electrode to be chelated through the lipophilic membrane. (Reprinted with permission from P. W. Atkins, *Physical Chemistry*, 5th ed., W. H. Freeman, 1994, Fig. 10.16.)

concentration of the electrolyte in the solution is low (hence, its resistance high) and the current high. In an extreme case, the current lines will barely reach the back (too much IR opposing them).

This *primary current distribution* becomes important in practical electrochemical devices, e.g., fuel cells. Here, one uses porous electrodes to try to increase the active electrode area for a unit apparent external area. This seems a good idea at first, but in reality the resistance of the solution down the pores prevents ions produced in the fuel cell reaction from “getting out” and often only a small length of the pore in a porous electrode is active.

However, there is another kind of influence on current distribution that may even the score. This is called *secondary current distribution* and describes the resistances set up at the interface of the working electrodes in a cell in which the interface tends to be polarizable. For example, it was shown [Eq. (7.36)] that when  $\eta < RT/F$ , the interfacial resistance per unit area is  $RT/i_0F$ . If  $i_0$  is very small (e.g.,  $10^{-10} \text{ A cm}^{-2}$ , hence, an interfacial resistance  $\text{cm}^{-2}$  of  $2.6 \times 10^8$  ohms), it is this interfacial resistance and not the ohmic resistance in the bulk solution that determines the current distribution. Thus, in an extreme case of high solution concentration (low solution resistance) and low  $i_0$ , a substantial fraction of the length of the pores in a porous electrode remains active.<sup>34</sup> Considerations such as these, together with resistance effects at edges, all count in cell design.

### 7.5.9. Apparatus Design Arising from the Needs of the Electronic Instrumentation

Two contradictory requirements arise from the point of view of the electronics of measuring the potential of the working electrode versus that of the reference electrode.

1. On the one hand, it is important that the current that bears the signal making the voltmeter register be very small. The reason is that it must not disturb the reference electrode from its position of thermodynamic reversibility by providing it with significant overpotential. Since, according to Eq. (7.25),

$$i = i_0 \frac{F}{RT} \eta \quad (7.25)$$

then at 25° C,  $RT/F$  is 0.026, so that  $i = 38.46 i_0 \eta$ . One can take the attitude that “no disturbance” means  $\eta < 10^{-3} \text{ V}$  (1 mV) and hence  $i < 38.46 i_0 10^{-3} \text{ V}$ . In practice, the experimental values are  $10^{-10} < i_0 < 10^{-3}$  so that for  $\eta < 10^{-3}$ , the  $i$  that may pass without disturbance of the reference electrode may have to be as little as a picoampere

<sup>34</sup>There are other cases in practical electrochemical devices in which current distribution is important. Because of the interplay of interfacial and electrolyte resistance effects (primary and secondary current distribution, respectively), the detailed calculation involve much mathematics. Electroplating deep into crevices of the object to be plated is an example of where current distribution considerations often dominate behavior. “Throwing power” is a term that describes the degree of penetration of the current—hence the plating—into fissures and irregularities in electrodeposition.

$\text{cm}^{-2}$ , but could be as much as  $0.01 \text{ mA cm}^{-2}$ . To be absolutely sure for all likely  $i_0$ 's that the shift of  $\eta$  in the reference electrode should be  $< 10^{-3}$ , the current in the measuring circuit should be not greater than a picoampere. In practice, electronic voltmeters have a resistance of  $10^{12} \text{ ohms}$ , so that the likely currents across them would be given by  $E/10^{12}$ . Thus, if  $E \approx 1 \text{ V}$ ,  $i \approx 10^{-12} \text{ A cm}^{-2}$ , so that even reference electrodes that function with  $i_0 \approx 10^{-12}$  will not be disturbed from reversibility. In practice, the value of the exchange current density at the reference electrode,  $i_0$ , is likely to be much higher than  $10^{-10} \text{ A cm}^{-2}$  so that the condition for negligible disturbance of a reference electrode from its reversibility by reason of a current passing across it during measurement is always easily reached.

2. However, there is a counter requirement. In order to function, some electronic instruments need a larger current to function than the low currents that the reversibility of the reference electrode requires. It may be necessary, therefore, to calculate in more detail what current densities particular reference electrodes may pass without developing significant departures from reversibility. Here, the standard hydrogen electrode itself is particularly good—its  $i_0$  may be  $> 10^{-3} \text{ A per geometric cm}^{-2}$  and the current density it can pass without the electrode departing from equilibrium by more than  $10^{-3} \text{ V}$ , is

$$i = i_0 \frac{F}{RT} \eta = \frac{10^{-3}}{0.026} \eta, \text{ i.e., for } \eta = 10^{-3} \text{ V, } i = 33 \cdot 10^{-6} \text{ A cm}^{-2} \quad (7.86)$$

which is quite enough for the functioning of potentiostats.<sup>35</sup>

## Further Reading

### Seminal

1. F. Haber, *Z. Elektrochemie* **7**: 13 (1900). Luggin capillary as a means to avoid IR errors.
2. W. Nernst, *Z. Elektrochemie* **7**: 253 (1900). Hydrogen reference electrode.
3. F. P. Bowden and E. K. Rideal, *Proc. Roy. Soc.* **120A**: 59, 80 (1928). First measurements of "real" areas.
4. S. Levina and W. Silberfarb, *Acta Physicochim. USSR* **4**: 282 (1936). First cells aimed at steady-state pure solution measurements.
5. S. Levina and W. Sarinsky, *Acta Physicochim. USSR* **6**: 491 (1937). Clean solutions, preelectrolysis.

<sup>35</sup>Note that some electrochemical cells use, instead of conventional reference electrodes, "indicator electrodes." These are electrodes that are not thermodynamically reversible but which may hold their potential constant  $\pm 1 \text{ mV}$  for some minutes—enough to make some nonsteady-state measurements (see Chapter 8). Such electrodes can simply be wires of inert materials, e.g., smooth platinum without the conditions necessary to make it a standard electrode exhibiting a thermodynamically reversible potential. However, many different electrode materials may serve in this relatively undemanding role.



6. A. Hickling, *Trans. Faraday Soc.* **33**: 1540 (1937). The first paper on electronic potentiostats.
7. F. P. Bowden and J. Grew, *Discuss. Faraday Soc.* **1**: 91(1947). Measurements at very low current densities,  $10 \text{ nA cm}^{-2}$ .
8. J. O'M. Bockris and B. E. Conway, *J. Sci. Instrum.* **19A**: 23 (1948). Preparation of electrodes in a hydrogen flame.
9. J. O'M. Bockris and B. E. Conway, *Trans. Faraday Soc.* **45**: 989 (1949). Effects of trace impurities in solution.
10. A. M. Azzam, J. O'M. Bockris, B. E. Conway, and H. Rosenberg, *Trans. Faraday Soc.* **46**:918 (1950). Technique of steady-state electrode kinetics on solid electrodes involving intermediates.
11. C. Wagner, *J. Electrochem. Soc.* **98**: 116 (1951). Resistance and current lines in solution.
12. S. Schuldiner, *J. Electrochem. Soc.* **99**: 488 (1952). Clean cells made of Teflon.
13. J. Barton and J. O'M. Bockris, *Proc. Roy. Soc. London A***268**: 485 (1962). Spherical diffusion control experimentally established.
14. E. Schmidt and H. R. Gygas, *Chimia* **16**:105 (1962). The first, but primitive, thin-layer cell.
15. C. C. Christensen and F. C. Anson, *Anal. Chem.* **35**: 205 (1963). The first real thin-layer cell.
16. H. Angerstein-Kozłowska, in *Comprehensive Treatise of Electrochemistry*, E. Yeager, J. O'M. Bockris, B.E. Conway, and S. Sarangapani, eds., Vol. 9, p. 15, Plenum, New York (1985).

## Reviews

1. R. Varma and J. R. Selman, *Techniques for Electrodes*, Wiley, New York (1991).
2. D. Genders and N. Weinberg, *Electrochemistry for a Cleaner Environment*, Electrosynthesis Co., Buffalo, NY (1992).
3. B. R. Scharifker, in *Modern Aspects of Electrochemistry*, J. O'M. Bockris, B. E. Conway, and R. E. White, eds., Vol. 5, p. 467, Plenum, New York (1992). Microelectrodes.
4. R. J. Gale, in *Electrochemistry, 1992-95*. Royal Society of Chemistry, London (1996). Instrumentation.
5. J. Bemhofer, *Pract. Spectroscopy* **15**: 233 (1993). Cells for optical measurements.
6. P. A. Christensen and A. Hamnett, *Techniques and Mechanisms of Electrochemistry*, Blackie Academic and Professional, London (1994).
7. R. C. Salvarazza and A. J. Arvia, in *Modern Aspects of Electrochemistry*, B. E. Conway, J. O'M. Bockris and R. E. White, eds., Vol. 28, Ch. 5, Plenum, New York (1996). Roughness measurement.
8. M. E. Clark, J. L. Ingram, E. E. Blakely, and W. T. Bowes, *J. Electroanal. Chem.* **385**: 105 (1995). Miniature cells for Tafel measurements.
9. Z. Li and X. Lin, *J. Electroanal. Chem.* **386**: 83 (1995). Cells for infrared measurements.
10. R. T. Baker, I. S. Metalfe, and P. H. Middleton, *J. Catal.* **155**: 21 (1995). Cells coupled to mass spectrographs.

11. Y. Iwasaki and M. Moritz, *Curr. Sep.* **14**: 2 (1995). Arrays of microelectrodes.

### 7.5.10. Measuring the Electrochemical Reaction Rate as a Function of Potential (at Constant Concentration and Temperature)

In chemical reaction kinetics, the basic measurement is that of rate ( $v$ ) per unit area as a function of temperature, with application of the classical Arrhenius equation,  $v = Ae^{-E/RT}$ . Electrochemical reactions also vary with temperature (see Section 7.5.14). However, the basic measurement for electrochemical kinetics is the rate as a function of potential<sup>36</sup> at constant temperature, with application of the corresponding Tafel equation,  $v = A'e^{\pm nF/RT}$ .

The obvious way to measure  $i$  as a function of the overpotential  $\eta$  is to fix  $\eta$  at a number of values,  $\eta_1, \eta_2, \eta_3$ , and record the corresponding electrochemical rates, or current densities,  $i_1, i_2, i_3$ , corresponding to the fixed value of  $\eta$ . This "potentiostatic approach" at a series of  $\eta$ 's sounds straightforward and indeed is analogous to the procedure in chemical kinetics where one measures various  $v$ 's corresponding to a number of fixed  $T$ 's. However, there is another procedure possible in electrochemical kinetics, and that is to fix the overpotentials and measure the corresponding current densities ("galvanostatic" approach). There is no corresponding procedure in chemical kinetics.

On the whole, it is better to use the potentiostatic procedure, i.e., use a series of fixed overpotentials while measuring the corresponding rate. This way of measuring rate as a function of potential will be the principal one described here, but it will be seen later that use of the galvanostatic (i.e., constant current density) approach also has advantages so that it won't be altogether abandoned.<sup>37</sup>

First, it is desirable to show the quintessential potentiostatic and galvanostatic phenomena in a schematic way. Figure 7.42 is a schematic presentation of the potentiostatic transient at one chosen overpotential. The potential is applied at time  $t =$

<sup>36</sup>In these presentations, potential and overpotential are used somewhat interchangeably. Strictly speaking, it is the overpotential  $\eta$  (the deviation of the potential from the reversible value  $\eta = V - V_{\text{rev}}$ ) which is the variable to which the rate relates. It can be seen from the Butler-Volmer equation (7.24) that at  $\eta = 0$ , the electrochemical rate (i.e., the current density) is also zero. Here it is helpful to remind the reader of the basic relation between current density and rate per unit area, i.e.,  $i/nF = v$ , where  $i$  is the current in  $\text{A cm}^{-2}$ ,  $n$  is the number of electrons in one act of the overall reaction,  $F$  is the Faraday, and  $v$  is the interfacial reaction rate in  $\text{mol cm}^{-2} \text{s}^{-1}$ .

<sup>37</sup>The application of these two basic techniques in making electrode-kinetic measurements implicitly assumes that a reaction can be observed "in the steady state." When one switches on an electrode reaction, either under potentiostatic or galvanostatic conditions, a short pause occurs for charging the double layer and then the electrode reaction begins to settle down to a velocity called the *steady state*. In this second period, a number of adjustments occur (e.g., of radicals adsorbed on the electrode surface). In simple redox reactions, there are no adsorbed intermediates. In the majority of electrode reactions, there is one or more intermediate and the electrode reaction may take seconds to find its steady state (or more than that if variations in the character of the surface occur). Finally, the current at constant potential may feel the influence of diffusion control and gradually fall as the diffusion of reactants from the bulk affects the rate.

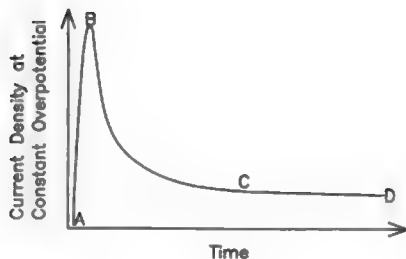


**Fig. 7.42.** A potentiostatic transient. The current (A-B) ascends almost vertically after being switched on, because all of it goes to charge the double layer. In B-C, the current is increasingly used in the form of electrons crossing the double layer. After C the current should decline slowly as diffusion control sets in. In reality, at solid polycrystalline electrodes, in reactions involving adsorbed intermediates, there is often some further variation of  $i$ , owing to, e.g., surface crystalline rearrangements and the effect of impurities from the solution.

0 and the current density rises rapidly to a maximum value. Part A-B in Fig. 7.42 represents the current (i.e., the rate of flow of electrons) used to charge up the metal of the electrode and establish between it and the solution a potential difference corresponding to the chosen overpotential.<sup>38</sup>

In section B-C, the fraction of the current used to charge the interfacial region to the designated overpotential is progressively reduced and more and more of the current flowing between electrode and solution is due to electrons that cross the interfacial region and take part in the electrochemical reaction. By C, all the electrons (for  $i$ , at  $\eta_1$ ) are being used in the electrode reaction which then, from a simplistic point of view, should continue to flow at a constant rate independent of time.

<sup>38</sup>The working electrode is connected to a reference electrode through an electronic voltmeter, and the overpotential is the difference between the potential of the working electrode and that of the reversible electrode for the reaction occurring at the working electrode. This is a clear, experimental quantity. However, it is *not* the same as the potential difference across the metal solution interface (the meaning of an “electrode potential”) (see Section 6.3).

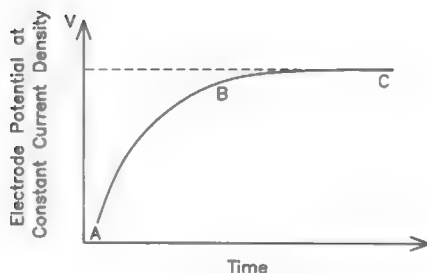


**Fig. 7.43.** Idealized galvanostatic result shown as a plot of potential against time at constant current density. A-B is largely double layer charging through the current and becomes used increasingly by electrons crossing the interfacial region. About one-fourth to one-half of this section in practice is linear and can be used to obtain the capacity of the interface from  $i_L = C \, dV/dt$ . B-C shows the current changeover to be entirely taken up (at C) with electrons crossing the interfacial region.

In contrast to the  $i$ - $t$  plot at a given  $\eta$ , the idealized *galvanostatic* result is a plot of potential against time at constant current density as shown in Fig. 7.43.<sup>39</sup> Here, the section A to B represents the change in potential as the double layer is being charged at constant current density.<sup>40</sup> Initially, this section is virtually all condenser charging and in this section, then,

$$i \approx C_v \left( \frac{\partial V}{\partial t} \right)_{i,t} \quad (7.87)$$

<sup>39</sup>The reader will note the use of "potential" and not overpotential as the variable here. This is indeed the definition of a galvanostatic transient. Since the overpotential is the difference of the electrode potential and the reversible potential for the reaction being studied, potential and overpotential are here equivalent because the reversible potential (at a constant solution concentration and temperature) is constant with time. Thus,  $\eta = V - V_{\text{rev}}$  and  $V = \eta + V_{\text{rev}} = \eta + \text{constant}$ . Variation with time of  $V$  will follow the variation with time of  $\eta$ , both at the fixed current density.

<sup>40</sup>The reader will sometimes find "current" and sometimes "current density" ( $\text{A cm}^{-2}$ ) used in the text (some texts use  $\text{mA cm}^{-2}$ ). The relation between the current (amperes),  $I$  passing through an electrode and the current density ( $i$ ) ( $\text{A cm}^{-2}$ ),  $i$ , is  $I/A = i$ . Strictly speaking,  $A$  should be the *real* area (Section 7.5.3), but in practice many electrochemists use the geometric (or, "visible") area. Thus, one should refer to the real or apparent current density, respectively.

where  $C$  is the capacitance per unit area of the interface at the potential  $V$ , corresponding to the varying time,  $t$ . By the time  $B$  is reached (Fig. 7.43), the current is being used (predominantly) for the passage of electrons across the region between the electrode and solution, and the electrochemical reaction concerned is then taking place. By  $C$ , the double layer is fully charged, corresponding to the charge that follows from the potential,  $V$ . In a simple analysis,  $V$  now remains constant and the electrode reaction proceeds at the chosen constant current density,  $i$ . There are several things to explain here, to make the ideal descriptions of these two methods more realistic.

1. In the potentiostatic technique, how is a constant potential maintained? This is done by means of a device called a *potentiostat*. The first potentiostat was described by Hickling in 1937; it turned out to be a seminal invention. Its working depends on a continuing measurement of the potential difference between the working electrode and the reference electrode. This is set at a chosen value, say, +0.333 V, with respect to the reference electrode. Various events tend to change the potential from the set value. The potentiostat senses the deviation from the designated +0.333 V. If the charging value is positive to this, the potentiostat reduces the anodic current (electrons flowing away from the electrode to the counter electrode) until the 0.333 is reattained. If the potential of the working electrode becomes negative to the desired 0.333, the potentiostat increases the anodic current between the working and the counter-electrode until 0.333 is reached. In this way, the electrode potential is maintained effectively constant.<sup>41</sup>

One of the advantages of the galvanostatic technique is that it is easier to set up a circuit that gives a constant current than one that holds the electrode at a constant potential. All that is necessary is to have a power source applied to a series circuit involving the electrochemical cell and a large available resistance. Variation of this controls the current passing through the circuit. Now, if the variable series resistance controlling the current is always much greater than the resistance of the experimental cell, the phenomena involved, including the change of the interfacial resistance that occurs when the cell functions at various currents and potentials, will have a negligible effect on the chosen current,<sup>42</sup> which therefore remains effectively constant (although it can be varied in steps by the experimenter), while the electrode potential varies with time when it is switched on at another step in the series of current density changes, as shown in Fig. 7.43.

2. What is the time at which to take the results of steady-state measurements?

<sup>41</sup>Electrochemists were slow to adopt Hickling's excellent invention. Potentiostats were first made commercially by a technician called Wenking in Germany in the 1950s. They soon became generally available. But there are some limitations on the availability of potentiostats for large industrial plants and for measurements at time less than  $\sim 10 \mu\text{s}$ .

<sup>42</sup>One refers here to "current" and not current density. Later, when the raw results of an experiment are being tabulated, to find the relation of rate to potential, the current is divided by the area of the electrode and then called the *current density*.

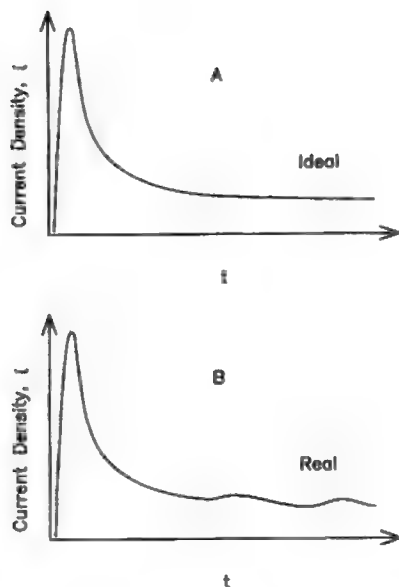


**Fig. 7.44.** (A) The identified “perfect” potentiostatic transient (cf. Fig. 7.42). (B) A schematic of a more realistic potentiostatic transient “as it occurs,” i.e., on polycrystalline electrodes in reactions involving intermediates.

a. The lower limit. Potentiostatic and galvanostatic measurements, such as those portrayed simplistically in Figs. 7.43 and 7.44, are called *transients*, and the theory of such measurements is discussed further in Chapter 8.<sup>43</sup> The time scale of such measurements stretches over microseconds to tens and even hundreds of seconds. The lower limits of such measurements are controlled by the time constant of the electronic instruments (about  $1\mu\text{s}$ ). The time required to charge the double layer (i.e., the condenserlike interfacial region between the electrode surface and the layer of ions adjacent to it) is another factor that limits the time span of electrochemical measurements at the lower end. Some rough idea of the duration of this charging time can be obtained by regarding the interface as a pure condenser, i.e., one assumes the ideal case of an electrode that is completely polarizable. Then,

<sup>43</sup>This is the general name for electrochemical rate measurements in which the rate varies with time on the way to achieving the final steady-state rate. Potentiostatic measurements are also called *potential step*, and galvanostatic measurements *current step*, measurements.

$$C = \frac{\partial q}{\partial V} = i \frac{dt}{dV} \approx i \frac{\tau}{\Delta V} \quad (7.88)$$

where  $q$  is charge,  $C$  is capacitance (per unit area), and  $\tau$  is the charging time. Use of a median value for these quantities suggests a middle range of tens of milliseconds. However, very small electrode areas and very high current densities (both are possible with microelectrodes) drive the condenser charging time to the microsecond range, where the lower limit in respect to time lies in the electronic potentiostat. Correspondingly, very large electrodes and small current densities can make the charging time last for seconds.

b. The higher limits. There is usually not much trouble in the lower time limit for measurements of transients. The limiting behavior at higher times is sharply different, depending upon whether the control is constant potential or constant current.

At constant potential, in a simple reaction with no surface intermediates, the  $i$ - $t$  line will tend to become constant after the double-layer charging is over. If at this time the current density is well below the limiting current density,  $i_L$  (Section 7.9.10), there should be nothing to interfere with the continuation of the steady-state constant current. If the current density after double-layer charging is above the limiting current, the current will decline with time. This is discussed quantitatively in Chapter 8.

For a more complex (more usual) reaction involving surface intermediates, it is possible that their adjustment to steady-state value may lengthen the time at which the potentiostated current density reaches constancy, even at current densities well below the limiting diffusion-current density.

At constant current, above the limiting-current density, a more dramatic event limits the time of the transient. As the current is being kept constant, it may be that the interfacial region runs out of a supply of the requisite ions to supply the reaction. Then a rapid and dramatic change in potential occurs at a time called the *transition time*. This can be calculated from a well-known equation (Sand's equation, Eq. 7.181). For example, if the concentration of the reacting ion is  $\sim 10^{-3}$  and the constant-current density is  $\sim 10^{-3} \text{ A cm}^{-2}$ , the transition time is  $\sim 0.1 \text{ s}$ .

With solid electrodes—particularly polycrystals—and less purified solutions, other changes can make the potentiostatic and galvanostatic measurement less clearly defined as to the final time at which the value of the current density at a given potential (or the final potential at a given current) should be taken. What sort of “other changes” are relevant here (apart from possible changes due to adsorption of impurities)?

3. On a polycrystal (on which most reaction rates are measured), the distribution of the various crystal planes on the surface may vary, partly due to time-dependent adsorption of impurities if the solution is not completely clean and partly due to differing dissolution rates of the varying crystal planes in the substrate for an anodic current. Until these unstable factors have been taken care of, the reaction rate will vary with time.

4. Diffusion into the electrode. If the surface radical is H, there may be diffusion into the electrode and this may cause a change in the character of the surface and the atoms immediately beneath it. Hence, for surface-catalyzed reactions on real surfaces, finding the steady state in the  $i_t$ - $t$  curve at constant potential may show complexities (Fig. 7.44). Where is the steady state in Fig. 7.44(b)? It becomes a matter of judgment. The best plan is to take the first time-invariant section and to reject the further variations, which simply indicate a nonconstant surface.<sup>44</sup>

**7.5.10.1. Temperature Control in Electrochemical Kinetics.** Electrochemical currents at constant current density vary by a few (1–3) millivolts per degree Celsius. It is consequently not worth maintaining a temperature of measurement more constant than  $\pm 0.5^\circ \text{C}$ , and this is easily and simply done in an air thermostat.<sup>45</sup>

Measurements between zero and  $100^\circ \text{C}$  can be done in this way; temperatures below that of the surroundings can be reached by blowing air over solid  $\text{CO}_2$  or a thermoelectrically cooled couple. At the higher temperatures, simple resistance heating and a fan to blow warmed air into the bath is satisfactory.

There is sometimes a need for very low temperatures, e.g., to examine electrode kinetics at superconductors in frozen electrolytes, say, at  $<100 \text{ K}$ . Here it may be necessary to use a more advanced degree of cooling, e.g., work within a cryostat using liquid  $\text{H}_2$ , by which experiments to a few degrees above absolute zero can be made (Bockris and Wass, 1989).

Temperatures much above  $100^\circ \text{C}$  can best be attained by heating the electrode alone by means of supplemental ac currents. Owing to the “skin effect,” such currents (at sufficiently high frequencies) travel along the metal surface and hence make the necessary power load for heating relatively small (Velev, 1990).

#### **7.5.10.2. Further Observations on the Technique of Steady-State Electrochemical Kinetic Measurements**

1. In potentiostatic measurements, the appropriate interval of potential between each measurement depends on the total range of potential variation. It may be between 10 and 50 mV and can be automated and computer controlled (Buck and Kang, 1994). It is helpful to observe a series of steady-state currents at, say, 20 potentials taken from least cathodic to most cathodic, and the same series taken from most cathodic to the least cathodic. The two sets of current densities should be equal at each of the chosen constant potentials. In practice, with reactions involving electrocatalysis, a degree of disagreement up to  $\pm 25\%$  in the current density at constant potential is to be tolerated.

<sup>44</sup>The ultimate case of a changing surface in electrode kinetics is that of the deposition of one metal on another where the surface changes intrinsically. The study of such systems involves processes described under the title of underpotential deposition (Section 7.12.11).

<sup>45</sup>Immersing an electrochemical cell in a water bath creates problems. The procedure makes electrical isolation of the connections in the cell more difficult. Electrical leaks are then encouraged and may cause errors of measurement. In any case, there are few measurements in which the added sensitivity to temperature control that a water thermostat implies is necessary.



2. If the overall desired pH is between 4 and 9, it may be necessary to include a buffer. Thus, if an electrode reaction involves the creation or annihilation of  $\text{H}^+$  or  $\text{OH}^-$ , the pH in the viscosity of the electrode will tend to differ from that of the bulk.

3. The surface of the electrode must remain constant as the potential is changed in a series of potentiostat, steady-state measurements. Apart from difficulties connected with impurity adsorption, which are reduced if the experiments are carried out sufficiently quickly (Chapter 8), it may be that thermodynamically the most stable state of the surface changes with potential most commonly by means of oxide formation. If this is suspected, it is helpful to keep observing the electrode surface during the potential measurements. The methods used must be *in situ* spectroscopic ones (see Section 7.5.15); FTIR or ellipsometry are the most readily applied (see Sections 7.5.15.2 and 7.5.16, respectively).

### 7.5.11. The Dependence of Electrochemical Reaction Rates on Temperature

In *chemical* kinetics, the most basic measurement is that of rate as a function of temperature. This is because such measurements lead to a determination of the *heat of activation*, a quantity that represents the energy colliding molecules must have before they react to a new product.

In *electrochemical* kinetics, there is a need to determine a similar quantity. However, there are complexities in the electrochemical case, because the reversible potential of the electrode reaction under examination varies with temperature.<sup>46</sup> Thus, for a simple one-step electrode reaction, and substituting in the equation of the absolute reaction rate theory for the rate constant,  $k$  (cf. Eq. 4.112):

$$i_0 = \kappa \frac{kT}{h} a_i e^{-\Delta G_{\text{rev}}^{\text{ox}}/RT} e^{-\beta V_{\text{rev}} F/RT} \quad (7.89)$$

There is a relation derived in textbooks of physical chemistry that runs:

$$nFV_{\text{rev}}^{\circ} = -\Delta G_{\text{rev}}^{\circ} = T\Delta S^{\circ} - \Delta H^{\circ} \quad (7.90)$$

where these are equations applicable to reactions in the thermodynamically reversible state.

Using (7.90) in (7.89) and taking  $\kappa(kT/h)a_i e^{\Delta S_{\text{ox}}^{\circ}/R}$  as relatively independent compared with the influence of the exponential terms,

$$\ln i_0 = \ln k_0 - \beta \frac{\Delta S_{\text{ox}}^{\circ}}{R} - \frac{\Delta H_{\text{ox}}^{\circ} - \beta \Delta H^{\circ}}{RT} \quad (7.91)$$

<sup>46</sup>This complication was pointed by Baxendale in 1947. However, there was a theoretical treatment of the same material by the Russian physical electrochemist, Temkin in 1941.

Thus:

$$-R \frac{\partial \ln i_0}{\partial \frac{1}{T}} = \Delta H_{\text{ox}} - \beta \Delta H^\circ \quad (7.92)$$

The value of the gradient of  $\ln i_0$  versus  $1/T$  is clearly measurable; one determines the exchange current density at a number of temperatures. But Eq. (7.92) shows that the result is not the heat of activation of the electrode reaction at the reversible potential (that's what one would like to have), but that quantity diminished by the heat of reaction of the reaction (e.g.,  $\text{O}_2 + 4\text{H}^+ + 4\text{e} \rightarrow 2\text{H}_2\text{O}$ ) being examined.

Traditionally, the quantity given by  $-R(\partial \ln i_0 / \partial 1/T)$  is termed the *apparent* heat of activation at the reversible potential. The word “apparent” is a code word for the fact that the quantity delivered by (7.92) has a mixed meaning (because it is partly concerned with the energy barrier to the reaction and partly with the thermodynamics of the reaction occurring reversibly).

One of the reasons physical electrochemists have been walking gently over the ice here instead of working to be in a position to place a solid ladder across it, is that virtually all measurements of temperature dependence in the literature in the past came from experiments which for a given electrode surface take a long time, several hours in fact. Such long times of exposure of an electrode surface to a solution bring about undesirable adsorption of impurities from the solution and/or re-formation of the (usually used) polycrystalline surface. Both these factors introduce unwanted effects on the rate of the reaction. While this was the case, a more penetrating discussion of how one might extract  $\Delta H_{\text{ox}}$  from  $\Delta H_{\text{rev}}^\circ$  seemed unjustified.

Since the early 1990s, however, the use of a powerful laser to fire pulses of increasing intensity at the back of an electrode in the form of a thin plate (Velez, 1991) has allowed reaction rates at a series of increasing temperatures to be measured in a few minutes. Such measurement times may be short enough (in systems where good control is practiced to reduce impurities) to make values of  $i_0$  independent of changes in the electrode surface that occur with time. The more meaningful data on temperature effects measured with this technique will stimulate attention to clear up the effects of the inclusion of  $\Delta H_{\text{rev}}^\circ$  in Eq. (7.89), which seeks to get only at  $\Delta H_{\text{ox}}$ .

### 7.5.12. Electrochemical Reaction Rates as a Function of the System Pressure

**7.5.12.1. The Equations.** It is possible to view the effects of pressure on electrochemical reaction rates in two ways. On the one hand, the partial pressure of a gaseous reactant, (e.g.,  $\text{O}_2$ ) takes its place in kinetic equations and has an effect on the reaction rate similar to that of the concentration of an ionic reactant.

However, there is another way of looking at “pressure,” and that is if the whole system (solution, electrodes) is subject to an increased or decreased pressure. One can assess the effect of a *system* change in pressure by use of the ideal gas approximation:

$$PV_M = RT \quad (7.93)$$

where  $V_M$  is the molar volume of the gas. But,  $3/2 RT$  is the kinetic energy of a mole of gas. It follows that  $RT$  and hence  $PV_M$  have the dimensions of energy. The rate of a chemical gas reaction is affected by system pressure in the following way:

$$k_p = k_1 e^{-P(V^x - V)/RT} \quad (7.94)$$

where  $k_p$  is the rate constant at a pressure  $P$  and  $k_1$  that at 1 atm,  $V^x$  is the volume of the activated state in the reaction and  $V$  is that of the initial state. No more detailed proof of Eq. (7.94) is needed, because in the theory of absolute reaction rates, rate constants are proportional to

$$e^{-(G_{ox} - G_{in})/RT} \quad (7.95)$$

where  $G_{ox}$  is the standard free energy of the activated complex and  $G_{in}$  that of the initial state of the reaction.

One could take Eq. (7.95) and rewrite it, for a reaction in solution, in terms of the partial molar volume because the  $V$ 's of the reactants and products in solution represent a *volume change in the system* caused by the addition of 1 mol of the entities concerned to a large volume of solution. Then,

$$k_p = k_1 e^{-P\Delta V^x/RT} \quad (7.96)$$

where  $\Delta V^x$  is the activation volume, i.e., the partial molar volume of the activated state diminished by that of the initial state.

In electrochemical reactions, however, there is a complication because the way one represents the reaction rate at the equilibrium potential<sup>47</sup> involves the reversible potential, and this quantity itself depends on pressure. Hence, an exchange current density written to take account of changes in pressure of the whole system would be [cf. Eq. (7.89)]

$$i_0 = \kappa \frac{kT}{h} a_i e^{-\frac{\alpha F V_{rev}}{RT}} e^{-\frac{\alpha \eta F}{RT}} e^{-\frac{P \Delta \bar{V}_{ox}}{RT}} \quad (7.97)$$

<sup>47</sup>A “reaction rate at equilibrium” is not an oxymoron. To be sure, there is no *net* reaction rate at equilibrium, but that is because the equilibrium consists of two reactions having velocities equal in magnitude but opposite in direction. The exchange current density (see Section ??) represents one of these and must therefore be finite.

Remembering that

$$-nFV_{\text{rev}}^0 = \Delta G^\circ$$

and that

$$\frac{(\partial \Delta G^\circ)_T}{\partial P} = \Delta V$$

where  $\Delta V$  is the change with pressure of the standard volume of the overall reaction being considered, then one obtains:

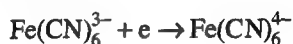
$$\left( \frac{\partial \ln i_0}{\partial P} \right)_{\eta, T} = -\frac{\Delta \bar{V}_0^x}{RT} + \frac{\alpha V^0}{RT} \quad (7.98)$$

It is relatively easy to figure out  $\Delta \bar{V}_0^0$  as long as the partial molar volumes of the reactants and products are known, as they are for most ordinary reactants. Thus, if one can measure  $(\partial \ln i_0 / \partial P)_{\eta, T}$ ,  $\Delta \bar{V}_{\text{ox}}$  can be obtained.

It is not an easy experiment to measure electrode reaction rates as a function of the system pressure. Using a fluid and a pump to apply the pressure will cause the gas to dissolve in the solution and bring about an unwanted concentration change in the reactant molar volume. Again, working the pump to bring about pressure changes in the kilobar range takes hours rather than minutes, and during this time the electrode surface is likely to change, thus causing an irrelevant alteration in the reaction rate, which may well be greater than that of the direct pressure effect one is trying to measure.

Jovancicevic brought progress to this area in 1987 by introducing an apparatus in which a change in pressure in the kilobar range could be communicated to the cell by bringing about pulsed pressure changes outside a membrane that formed one of the cell's walls using a pulsed high-current source to evolve an electrolytic gas into a small volume, one part of which is in contact with the membrane (Fig. 7.45). This technique allows the effect of, say, five pressure changes to be measured in as many minutes, thus reducing the problems (i.e., contamination, etc.) that prolonged exposure of the surface to the solution may bring about.

**7.5.12.2. What Is the Point of Measuring System Pressure Effects?** A good example of the use of pressure effects to give some information on mechanisms arises from an analysis of these changes for the overall redox reaction by Conway and Currie (1978):



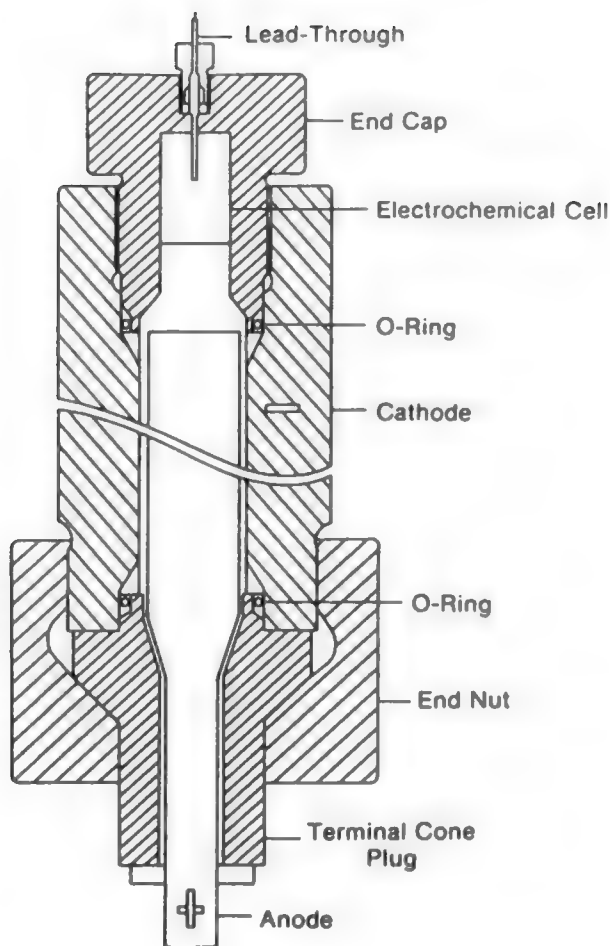


**Fig. 7.45.** Pressure-pulse apparatus. (Reprinted with permission of the American Institute of Physics from V. Jovančević and J. O'M. Bockris, *Rev. Sci. Instrum.* **58**: 1252, 1987, Fig. 3.)

One of the questions here is the degree to which a change in volume during the formation of the activated state [i.e., the  $\Delta V_{\text{ox}}$ , which can be obtained from Eq. (7.97)] occurs as a result of pressure changes in regions *outside* the ion's inner solvation shell (caused by the experimental change in pressure on the solution); or whether one has to seek an explanation for it from the change in local pressure in the first layer around the Fe ions. Thus, during this change from  $\text{Fe}^{\text{III}+}$  to  $\text{Fe}^{\text{II}+}$ , the pressure due to the electrostatic field of the ions on the hydration shell gets less. According to some

researchers, the origin of the activation energy in redox reactions is in the “outer sphere” (outside the hydration shell). According to others (see Chapter 9), the origin of the energy is in the first layer next to the ion.

For the reduction reaction  $\text{Fe}(\text{CN})_6^{3-} + e \rightarrow \text{Fe}(\text{CN})_6^{4-}$ , the  $\Delta V_{\text{ox}}$  was *negative* by 20.3 ml per mole. If the volume decrease is largely due to changes in the immediate vicinity of the ion (i.e., changes in pressure due to an increase in charge on the complex), this figure can be rationalized. If, on the other hand, it is assumed that the origin of the activating process in the charge transfer is in the outer sphere (see Chapter 9), there is no way such large values can be understood as being due to the applied pressure. Thus, the Conway and Currie work is an example of mechanism information collected from  $(\partial \ln i_0 / \partial P)_\eta$ .

### 7.5.13. Impedance Spectroscopy

**7.5.13.1. What Is Impedance Spectroscopy?** The words “impedance spectroscopy” imply the dependence of impedance on a wavelength and therefore on frequency. The frequency here is not that of an incident light beam, but of an alternative current applied to a cell, and then the question is: What is impedance?

It is best to regard impedance as a “generalized resistance.” The concept of “resistance” comes in with metallic wires where impedance and resistance are identical and equal (Ohm’s law) to the potential difference (caused by the flow of current) through the wire divided by the magnitude of the flowing current. Thus,  $V/I = R$ . *Impedance* is the term given to  $V/I$  for systems other than metallic resistors. As will be explained later, the quantity  $V/I$  for these other systems (including, indeed, electrode/solution interfaces of various kinds) contains two kinds of information. One is a magnitude—here one thinks of resistance again—but there is also something called a “phase difference,” and this refers to the angle by which the “current leads the voltage.” The angle involved refers to the magnitude of  $\omega t$  where  $\omega = 2\pi\nu$ , and  $\nu$  is the frequency of the ac applied in the system,  $t$  being the time within one of the cycles of the sinusoidal oscillations of the current applied to the system. This phase angle,  $\alpha$ , may stretch from zero (current and voltage *in phase*) to  $90^\circ$  (the current angle leads the voltage by  $\omega t = \pi/2$ , i.e., current and voltage are *out of phase* by this angle).

Now, this quantity impedance ( $Z$ ) turns out upon detailed analysis to contain within the characteristics of its variation with frequency,<sup>48</sup> properties of the reaction occurring at the electrode/solution interface. For example, if a reaction occurring there has as its rate-determining step the electron transfer, then the variation of the impedance with frequency will have certain characteristics different from those shown in the  $Z - \log \omega$  plot if the rate-determining step involves instead diffusion in the solution. So, by working out how  $Z$  varies with  $\log \omega$  according to a chosen mechanism

<sup>48</sup>As stated,  $\omega = 2\pi\nu$ . However, one often carelessly refers to  $\omega$  as the frequency. In any calculation, of course, the fact that  $\nu = \omega/2\pi$  must be taken into account.

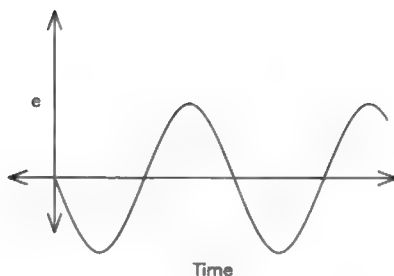


**Fig. 7.46.** The relation of  $V$  to  $t$  for a given constant  $\omega$ .

hypothesis, A; then working out how  $Z$  should vary with a function of  $\omega$  according to an alternative mechanism hypothesis, B; and comparing the real, observed behavior with the predictions of the behavior based, respectively, on A and B, one finds out which (if either) of the two hypotheses fits the facts and hence obtains evidence favorable to A or to B as the most important happening in the analysis of the mechanism of the electrode reaction being studied. That, in essence, is the role impedance analysis plays in electrode kinetics. It is usual, with modern apparatus, to work from 0.01 cps to about 100 kHz.

**7.5.13.2. Real<sup>49</sup> and Imaginary Impedance.** One of the characteristics of electrochemical research papers on the application of impedance spectroscopy to find mechanisms is that they usually involve  $i$  ( $i = \sqrt{-1}$ ), and the word “imaginary.” This needs some explanation.

It is a fact that alternating current voltages can be represented by the equation:

$$V = V_0 \sin \omega t \quad (7.99)$$

The variation of  $\omega$  from 0 to  $2\pi$  radius (0 to  $360^\circ$ ) corresponds to the rotation of a vector and when sketched out, the relation of  $V$  to  $t$  for a given constant  $\omega$  (or frequency) represents the well-known shape of a sine wave (Fig. 7.46).

It turns out that mathematically, equations such as (7.99) can also be written as

$$V = V_0 e^{i\omega t}$$

and from de Moirre’s theorem:

$$V = V_0 (\cos \omega t + i \sin \omega t) \quad (7.100)$$

<sup>49</sup>What is “real” in mathematics has varied over the centuries. The Greeks argued that there were three dimensions. Thus,  $x^3$  could be real, but  $x^4$  imaginary. The years have led to a change in their view. Similarly, a so-called imaginary impedance has perfectly real implications.

This shows that the potential response to the applied current has two parts, one part *not* containing  $i$  and another term containing it.

Because for historical reasons the quantity  $i$  is “imaginary,” everything it multiplies suffers the same terminological fate. However, it is not true to think that the part of a mathematical expression that contains  $i$  is unreal in a physical sense. It is just as real as the first part.

Impedance is a vector and is characterized by a phase angle,  $\alpha$ ; i.e., it can be resolved into two components, the impedance component *in phase* with the cell voltage and the impedance component at  $90^\circ$  to it, which is called the *imaginary* part of the impedance. Indeed, one method of studying the impedance of an electrochemical circuit is to determine  $Z$  as a function of frequency and then resolve it into  $Z_{\text{real}}$  and  $Z_{\text{imag}}$ . Then one can plot  $Z_{\text{real}}$  against  $\log \omega$ , or  $Z_{\text{imag}}$  against  $\log \omega$  (the Bode plot) and each of these plots will have a shape characteristic of events at the chosen electrode in the cell. Alternatively, one may plot  $Z_{\text{real}}$  against  $Z_{\text{imag}}$ , each point on the graph using values of  $Z_{\text{real}}$  and  $Z_{\text{imag}}$  [for the same frequency (the Cole-Cole plot); see Fig. 7.47].

**7.5.13.3. The Impedance of a Capacitor in Series with a Resistor.** This circuit is shown in Fig. (7.48). The impedance of a resistor is simply the resistance itself. What about the impedance of a capacitor? Now,

$$Z = \frac{V}{I} = \frac{V_0 e^{i\omega t}}{I} \quad (7.101)$$

But  $I = dQ/dt$

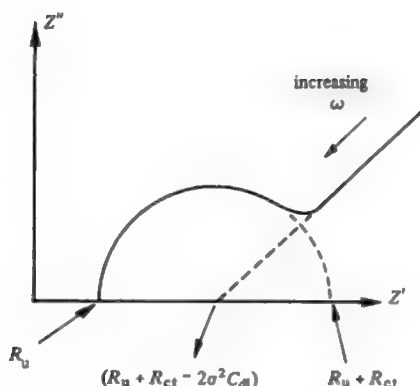


**Fig. 7.47.** Cole–Cole impedance plot. (Reprinted from Southampton Electrochemistry Group, *Instrumental Methods in Electrochemistry*, Ellis Harwood, 1985, p. 268.)





Fig. 7.48. Series circuit.

Also:

$$C = Q/V$$

$\therefore$

$$I = C dV/dt$$

with

$$V = V_0 e^{i\omega t}$$

$$I = Ci\omega V_0 e^{i\omega t}$$

$$Z = \frac{V_0 e^{i\omega t}}{Ci\omega V_0 e^{i\omega t}} = \frac{1}{i\omega C} \quad (7.102)$$

The impedance of resistor and capacitors are additive. Hence,

$$Z_{R+C \text{ in series}} = R + 1/i\omega C \quad (7.103)$$

This expression shows an interesting result. As the frequency ( $\omega = 2\pi\nu$ ) is increased, the resistor becomes dominant (i.e., the capacitive impedance tends toward zero). On the other hand, at low frequencies, the capacitive impedance dominates. Indeed, as  $\omega \rightarrow 0$ ,  $Z \rightarrow \infty$ ; this fulfills a commonsense expectation, i.e., that a direct current ( $\omega = 0$ ) cannot pass across a capacitor, which becomes then an infinite resistance.

The inverse of an impedance is called an *admittance* and represented by the symbol  $Y$ :

$$Z = V/I$$

So,

$$Y = I/V$$

or

$$I = VY$$

$$= \frac{V_0 e^{i\omega t}}{R + \frac{1}{i\omega C}} = \frac{V_0 e^{i\omega t} i\omega C}{1 + \frac{1}{i\omega C}} \quad (7.104)$$

Following through a number of algebraic steps, one finds:

$$I = \frac{V}{(|Z|)} e^{i\omega t + \alpha} \quad (7.105)$$

where

$$|Z| = \frac{(1 + \omega^2 C^2 R^2)^{1/2}}{\omega C} \quad (7.106)$$

and the phase angle is given by

$$\alpha = \tan^{-1} \frac{1}{\omega CR} \quad (7.107)$$

Thus, in a resistor-capacitance circuit, the phase angle  $\alpha$  depends on frequency. If  $\omega \rightarrow 0$ ,  $\alpha \rightarrow \pi/2$  radians ( $90^\circ$ ) and if  $\omega \rightarrow \infty$ ,  $\alpha \rightarrow 0$ . These equations have a practical use, for if one can measure  $Z$  and  $\alpha$ ,  $C$  and  $R$  can be readily obtained and their values can be used diagnostically to test various hypotheses of the mechanism of the electrode reaction concerned.

**7.5.13.4. Applying ac Impedance Methods to Obtain Information on Electrode Processes.** The discussion so far has been at a rather simple level, but it can be understood that impedance spectroscopy offers possibilities for modeling electrode processes. One determines the impedance,  $Z$ , as a function of  $\omega$ , and then tries out the different ways of representing the electrode process (but in terms of its electrical analogue of resistance, capacitance, and inductance in various arrangements corresponding to the possibilities of the physical model. Then, a match in the  $Z$ - $\omega$  or  $Z_{\text{real}} - Z_{\text{imag}}$  for a particular model of the interface encourages one to believe in that model arrangement. It indicates what is happening in the electrode process more than alternative models that give less good matches with the types of  $Z$ - $\omega$  (or  $Z_{\text{real}} - Z_{\text{imag}}$ ) relations observed experimentally.

There are a couple of matters that have to be cleared up now, before going on to equivalent circuits more practical than the simple resistor-capacitance arrangement so far discussed.

1. Electrochemistry is studied in cells, which consist of a working electrode (where the process to be studied occurs) and the counter-electrode necessary to complete the circuit in which one electrode emits electrons and the other receives them; i.e., a direct current passes through the whole cell. (There is a third electrode, the reference electrode, which is necessary to measure the overpotential of the working electrode; see Section 6.3.4.)

In the material given so far, the attitude has been that there is only the electrode/solution interface at which the impedance is to be studied. However, there is always also the counter-electrode in the circuit of the cell, and things must be arranged so that the impedance measured is almost entirely that of the working electrode and contains only a negligible contribution from the counter-electrode. Basically, this is done by arranging for the resistance of the counter-electrode to be negligible compared with that of the working electrode and for the capacitance of the counter-electrode to be very large compared with that of the working electrode. Since resistances in series add and capacitances in series add reciprocally, the influence of the counter-electrode can be eliminated simply by making its area large compared with that of the working electrode. The larger area of the counter-electrode, the smaller is its interfacial resistance and the larger (i.e., lesser in influence) is its capacitance. In practice, the counter-electrode size should be as much as 100 times the area of the working electrode; often this can be achieved by the use of electrodes of large real to apparent area, e.g., platinized platinum.

Another practical matter is the frequency range to be used. One wants this range to be as large as possible so that the chance of discovering information-giving types of behavior (which may show up in various frequency ranges in the impedance spectrum) is increased.

In practice, the limit at high frequencies is controlled by the inductance in the circuit,  $\omega L$ . The influence of this on the impedance (in contrast to that of the capacitance) increases with an increase in frequency. The difficulty is that the inductance that becomes significant when the frequency exceeds, say,  $10^4$  cps, is often more an irrelevant inductance, not one caused by the electrode process. Thus, it may arise because of some contribution from the wire connections to the cell and their interaction with the surroundings. Hence, very short leads to the cell should be used. It is possible to build circuits that compensate for the inductance effects, but usually the practice is to keep the frequency within the 10 kilocycle/s upper range, so as to make  $\omega L$  negligible.

In the low-frequency direction, the capacitive impedance ( $1/i\omega C$ ) dominates. It is remarkable how in recent years the capability of commercial ac bridges to measure very low frequencies ( $10^{-3}$  to  $10^{-4}$  cycles  $s^{-1}$ ) has increased. However, the limit here is not so much in the electronics, but more in the stability of the interface. A frequency of  $10^{-4}$  cycles  $s^{-1}$  means a cycle some 3 hr in duration, and it is difficult to maintain a clean and stable solid/solution interface for this length of time.

**7.5.13.5. The Warburg Impedance.** The study of the impedance of the actual electrode/solution interface was begun by Dolin and Erschler in 1940. The use of impedance spectroscopy for analyzing mechanisms became widespread only some 30 years later. However, much earlier than either of these events, in fact before the beginning of mechanistic electrode kinetics by Tafel in 1905, Warburg (1899) published an analysis in 1899 that described the impedance offered by the diffusive movement of ions under an ac field. As the potential passes into its positive phase, it causes movement of the negative ions toward the electrode and repels the positive ones, but this influence lasts only until the potential has changed to the negative phase, etc.

Warburg showed that this impedance would have a phase angle of  $45^\circ$  and be proportional in magnitude to  $\omega^{-1/2}$ . Its value was shown to be

$$\frac{1}{2} \frac{RT}{(zF)^2} \frac{1}{c_i} \left( \frac{1}{D_i} \right)^{1/2} \quad (7.108)$$

where  $D_i$  is the diffusion coefficient of the ion concerned,  $c_i$  is its concentration, and  $z_i$  is its charge. At sufficiently high frequencies and concentration, the Warburg impedance becomes small compared with the other impedances of the electrode/solution interface.<sup>50</sup>

**7.5.13.6. The Simplest "Real" Electrochemical Interface.** Although the Warburg impedance is a well-known term in the field of impedance spectroscopy because of the early date at which it was published, the formulation came before the rest of the properties of the interface were known. In fact, for nearly all real situations examined in electrochemistry, the Warburg impedance is relatively small. Thus, for a concentration of  $1 \text{ mol liter}^{-1}$  and a frequency of  $1 \text{ kilocycle s}^{-1}$ , and using the normal parameters for room temperature, the resistance is in the milliohm  $\text{cm}^{-2}$  range.

Three further quantities are far more important in making up the impedance measured in a cell (for a simple redox system in contact with an inert electrode):

1. *The Solution Resistance.* The size of this quantity will depend on the concentration of the electrolyte and the dimension of the cell. Consider a column of electrolyte, cylindrical in shape, with a cross-sectional area ( $A$ ) of  $2 \text{ cm}^2$  and a length ( $L$ ) of 1 cm, containing a  $0.1 \text{ M}$  salt solution. The specific resistance of such a solution will be about  $0.01 \text{ ohm cm}^{-1}$ . Since the solution resistance  $R = (1/\kappa)(L/A)$ ,  $R = (1/0.01)(1/2) = 50 \text{ ohms}$ .

2. *The Resistance of the Interface.* As long as the amplitude of the ac superimposed on the circuit is small (e.g., 5 mV), one can regard the resistance as that

<sup>50</sup>But what happens to the Warburg impedance at  $\omega = 0$ , i.e., for a direct current? The answer is that (7.107) was derived by Warburg assuming *diffusion* was still in control. In fact, at frequencies less than 1 Hz, convection begins to play a part in transport at the interface, and the equation is no longer valid (Hamnett, 1997).

corresponding to the linear region in the  $i$ - $\eta$  relation (see Eq. 7.38). Then the resistance  $\text{cm}^{-2}$  is  $RT/i_0F = 0.026/i_0$  at 25 °C. The range of  $i_0$  values observed in electrochemistry is large, about 10 powers of 10, so let an intermediate value be taken on a log scale, say,  $10^{-5} \text{ A cm}^{-2}$ . In this case, the resistance  $\text{cm}^{-2}$  is  $2.6 \times 10^3 \text{ ohms cm}^{-2}$ , an order of magnitude greater than the solution resistance.

3. *The Capacitance of the Double Layer.* It has been seen that the impedance of the double layer is frequency dependent. Taking a frequency of 1 kilocycle, and a capacitance value of  $50 \mu\text{F cm}^{-2}$ , one has

$$Z_{\text{capac}} = \frac{1}{6.3 \times 10^3 \cdot 50 \times 10^{-6}} = \frac{1}{3.15 \times 10^{-1}} = 3.2 \text{ ohms cm}^{-2}$$

As stated above, the value of the capacitance is great at low frequencies and small at high frequencies.

The question now is how to arrange these elements in an equivalent circuit whose net impedance and behavior with frequency can be calculated and compared in a  $Z$  vs.  $\omega$  plot for the cell being examined.

In drawing an appropriate equivalent circuit, it is clear that the resistance of the solution should be placed first in the intended diagram, but how should the capacitive impedance be coupled with that of the interfacial resistance? One simple test decides this issue. We know that electrochemical interfaces pass both dc and ac. It was seen in Eq. (7.103) that for a series arrangement of a capacitor and a resistor, the net resistance is infinite for  $\omega = 0$ , i.e., for dc. Our circuit must therefore have its capacitance and resistance in parallel for under these circumstances, for  $\omega = 0$ , a direct current can indeed pass; the impedance has become entirely resistive.<sup>51</sup>

How does the simplest electrochemical interface look, in terms of an equivalent circuit? The appropriate circuit element is shown in Fig. 7.49. It is worth noting that the famous Warburg impedance has been left out! The reason is that for most situations in which relatively fast electrode reactions occur, it is negligible.

The first equivalent circuits involving interfacial resistance were published by the Russian authors, Dolin and Erschler, in 1940. This publication came out early in World War II and was not easily available to Western electrochemists. The British electrochemist, Randies, published an analysis somewhat similar to that of Dolin and Erschler (but derived independently of them) in the Faraday Discussion of Electrode Processes of 1947. Because of the easy availability of his work, his name is associated in most Western literature with the beginning of equivalent circuit work in electrochemistry.

<sup>51</sup>How does this fit in with the idea (see Section 7.7.1) of a completely polarizable electrode "across which no electrons pass?" It is a matter of degree. A *completely* polarizable electrode is an idealization, i.e., some electrons always pass across the interface. In practice, highly polarizable electrodes are those with exchange current densities (or rate constants) that are very low, i.e., the resistance of the interface ( $= RT/i_0F$ ) is very high.

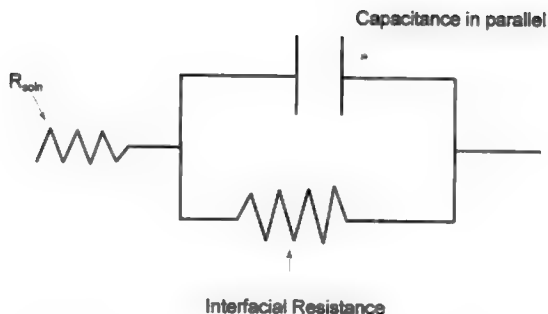


**Fig. 7.49.** Simplest electrochemical interface, in terms of an equivalent circuit.

**7.5.13.7. The Impedance (or Cole–Cole) Plot.** In the preceding discussion, the attitude was that one should calculate  $Z$ , the impedance of the circuit one thinks best represents events at the interface, as a function of  $\omega$  and find if the  $Z$ – $\omega$  plot<sup>52</sup> from the model of the interface fits the plot from experiment.

However, the Cole–Cole plot usually makes calculations (done automatically within the impedance bridge concerned) of the two components into which any measured impedance can be resolved. The components consist of the “real” part of the impedance, which is in phase with the applied voltage, and the “imaginary” part, which is  $90^\circ$  out of phase. One can plot either of these quantities against  $\log \omega$  to obtain mechanism-indicating plots.

In the Cole–Cole (or “complex impedance”) plot, one takes the  $Z_{\text{real}}$  as ordinate and the  $Z_{\text{imag}}$  part as abscissa. Each point on the resulting diagram is made up of a  $Z$  resolved into two components measured at a chosen frequency. There may be 20–30 points, each at different frequencies. Such plots tend to be semicircles (see Fig. 7.47), but even simple equivalent circuits have some structure (i.e., deviations from the semicircle), and these deviations provide information concerning events at the electrode/solution interface.

The deviation from a semicircle on the right provides information. One can obtain from its slope the value of  $R_{\text{interface}}$ . There are two values in the real axis at which the plot (or its extrapolation) intercepts with the axis. The one at the high-frequency side of Fig. 7.47 turns out to give the solution resistance; the low-frequency one gives the solution resistance together with the interfacial resistance (which can be determined later). The maximum of the semicircle must be associated with a certain value of  $\omega$  and this value is  $1/C_{\text{DL}} R_{\text{interface}}$ . One can see that Cole–Cole plots provide a lot of information.

<sup>52</sup>In fact, one does not plot  $Z$  itself, a quantity that mathematicians call “complex,” because expressions for it contain  $i$ . One resolves  $Z$  into its two components,  $Z_{\text{real}}$  and  $Z_{\text{imag}}$ , and plots either of these against  $\log \omega$ , or, alternatively, plots one against the other.

**7.5.13.8. Calculating Exchange Current Densities and Rate Constants from Impedance Plots.** If one takes the Butler–Volmer equation (7.24) under the “reversible condition,” i.e., that in which the overpotential,  $\eta$ , tends to zero, then,

$$\frac{\partial i}{\partial \eta} = \frac{1}{R_{\text{interfacial}}} = i_0 \frac{F}{RT} \quad (7.33)$$

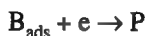
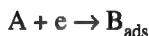
The relation of the exchange current density to the rate constant  $k_0$  at equilibrium is

$$i_0 = zF\chi k_0 c_i \quad (7.109)$$

where  $\chi$  is the thickness of the reaction ion layer.

**7.5.13.9. Impedance Spectroscopy for More Complex Interfacial Situations.** The electrochemical interfacial equivalent circuits shown in Figs. 7.48 and 7.49 are the simplest circuits that can be matched to actual electrochemical impedance measurements. The circuit in Fig. 7.49 would be expected to apply to an electrode reaction that involves only electron transfer (e.g., redox systems of the type  $\text{Fc}^{3+} + e \rightleftharpoons \text{Fc}^{2+}$ ), no adsorbed intermediate.

Most real electrochemical reactions are not so simple. The truth is that most of them involve one or several adsorbed intermediates. A rather simple situation would involve two parallel (charge-transfer) reactions, such as



It is possible to show that insofar as diffusion control can be neglected, such a reaction can be represented by Fig. 7.50.

$R_{\text{CT}}$  and  $R_{\text{R}}$  are the charge transfer and resistances in the two parallel reactions, respectively, and  $L$  is an inductance that arises from functions of the adsorbed species,  $B$ . (This inductance has nothing to do with the irrelevant inductance mentioned earlier, the one thought to occur at high frequencies as a consequence of stray inductances in wires of the circuit.)

A more complicated model situation is demanded if one thinks of the equivalent circuit for an electrode covered with an oxide film. One might think of Al and the protective oxide film that grows upon it during anodic polarization. One has to allow for the resistance of the solution, as before. Then there is an equivalent circuit element to model the metal oxide/solution interface, a capacitance and interfacial resistance in parallel. The electrons that enter the oxide by passing across the interfacial region can be shown to go to certain surface states (Section 6.10.1.8) on the oxide surface, and they must be represented. Finally, on the way to the underlying metal, the electron

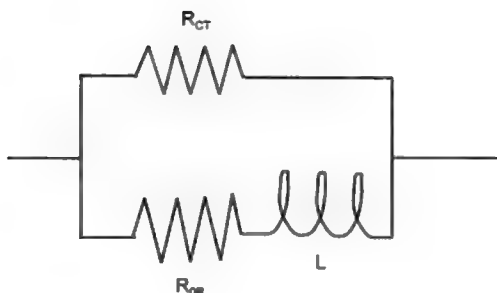


**Fig. 7.50.** Electrochemical reactions involving adsorbed intermediates.  $R_{CT}$  and  $R_{OR}$  are the charge transfer resistances in two parallel reactions, and  $L$  is an inductance that arises from functions of the adsorbed species,  $B$ .

experiences the special properties of semiconductors. The entire interface can be represented by Fig. 7.51.

Each of the three circuit elements in every circuit given above can be represented by an equation of the type:

$$\frac{R\omega^2 C}{1+\omega^2 C^2 R} \quad (7.110)$$

Of course, each  $C$  and  $R$  should bear an appropriate suffix that would indicate what particular element is to be understood (i.e., is it for electron transfer across the double layer, etc.?) (Fig. 7.51). It turns out that frequently the impedance plots due to the various elements maximize at characteristic frequencies, and if these maxima occur at

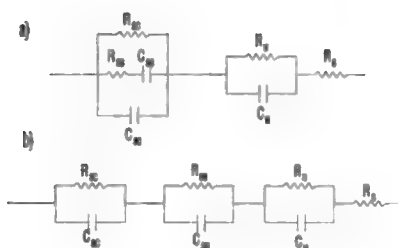


**Fig. 7.51.** Equivalent circuits for a semiconductor/solution interface. (a) Conventional equivalent circuit. (b) Equivalent circuit used in this work.



frequencies that are sufficiently far apart, each maximum may be taken to represent an element in the equivalent circuit. Thus, one maximum represents the interface (I), another the surface state (SS), and a third the semiconductor properties (SC) of the electrode's oxide.

At a maximum of an element sufficiently separated from the others:

$$\omega_{\max} C_e R_e = 1$$

or

$$C_e = 1/\omega_{\max} R_e \quad (7.111)$$

so that such an element may be determined. Deconvolution techniques can be used to enhance the plot and find individual maxima, which tend to get mixed up together and seem to form one peak.

It is usually possible from  $Z_{\max}$  to calculate  $C$  and  $R$  for the circuit element associated with the maximum. One of the many applications to which impedance plots can be put is that of determining the "surface states" of semiconductors.

#### 7.5.13.10. *Cases in which Impedance Spectroscopy Becomes Limited.*

One might say that if one understands an interface well, the results of  $Z-\omega$  measurements can be readily understood. Of course, the interest is in the other direction, in using  $Z-\omega$  plots when one does not understand the interface. Then the task is to find an interfacial structure and mechanism (and its resulting equivalent circuit) that provides a  $Z$  that is consistent in its dependence on  $\omega$  with the experimental results of the impedance measurement. This requires finding reasonable parameters to fit the value of the  $C$ 's and  $R$ 's as a function of  $\omega$  for the individual elements in the various equivalent circuits. If the shape of the calculated  $Z-\omega$  plot can only be made to match experiment by using  $C$ 's and  $R$ 's that are physically unreasonable, the proposed structure and the equivalent circuit to match it are not acceptable and another must be tried.

Several things can go wrong in this matching. Matches of calculated and experimental  $Z-\omega$  plots are seldom exact. Personal judgment becomes involved. One researcher may consider  $Z-\omega$  plots using a certain circuit satisfactory, but a more critical researcher may not accept that there is a fit and point to the use of parameters (perhaps values of the surface state  $C$ 's and  $R$ 's) that are too far away from those known by independent methods to be likely for the system concerned.

One of the techniques that can be used here is computer simulation. A computer can be programmed to find values of the parameters in the elements of the competing equivalent circuit that maximize the fit over a large frequency range. As already mentioned, the extension of the plots to very low frequencies is desirable to cover a range that may be very information-bearing. But what of the stability of the electrode surface after, say, 1 hr in the solution?

Finally, the microroughness of the electrode surface (due, e.g., to imperfections in the lattice structure) may make a significant contribution to the net impedance, which is, however, irrelevant (and thus disturbing) to the purpose of analyzing a reaction mechanism.

With all its complications and uncertainties, impedance spectroscopy, as seen at the end of the twentieth century, is a growing technique in fundamental electrodic analysis [cf. the seminal contributions of (independently) D. D. and J. R. MacDonald]. Among its advantages is that the necessary equipment is less expensive than that of competing spectroscopic equipment and that it can provide information on any electrochemical situation (e.g., it is not limited by, say, the need for specular reflectance, as in ellipsometry).

## 7.5.14. Rotating Disk Electrode

**7.5.14.1. General.** The central goal of fundamental electrochemical kinetics is to find out what electrons, ions, and molecules do during an electrode reaction. In this research, one is not only concerned with the initial state (i.e., the metal and the reactants in the solution next to the electrode surface before the reaction begins) and the final product of the reaction, one also has to know the intermediate species formed along the way. Thus, all practical electrode reactions (say, the electro-oxidation of methanol to  $\text{CO}_2$ ) consist of several consecutive and/or parallel steps, each involving an intermediate radical, e.g., the adsorbed  $\text{C-OH}$  radical. However, one finds that intermediates can be classed into two types.

1. The intermediate remains on the electrode until it is transformed into another particle during the consecutive steps that make up the overall reaction. The simplest example is (Section 7.6.2) the mechanism of hydrogen evolution, in which one possible step involves chemical recombination between adsorbed  $\text{H}$ 's, put onto the electrode surface by means of the discharge of  $\text{H}_2\text{O}^+$  from acid or  $\text{H}_2\text{O}$  from alkaline solutions. The adsorbed  $\text{H}$  is the intermediate radical.

2. In some electrode reactions, there are intermediates of a different kind, species more uncertain as to what they want to do. They do not always bond sufficiently to the substrate to remain there and undergo a consecutive surface reaction step, as does  $\text{H}$  that combines to  $\text{H}_2$ . This latter type of intermediate "comes loose" from the electrode surface. It may then contact the electrode again and react further, or quit the scene and diffuse off into the bulk of the solution, remaining lost to any continued reaction sequence that would be possible if the radical had stayed on the electrode surface for further consecutive reaction steps.

An example of this type of intermediate would be  $\text{H}_2\text{O}_2$ , which turns up in some mechanisms involving the reduction of  $\text{O}_2$ . Thus, at first,



Then,  $\text{H}_2\text{O}_2$  (the undecided intermediate) may react further with the electrode:



However, it may also be that at least part of the  $\text{H}_2\text{O}_2$  leaves the electrode after (A) and forgoes (B). Its fate is eventual decomposition to  $\text{O}_2 + \text{H}_2\text{O}$  in the bulk of the solution.

In order to study electrode reactions involving intermediates that could come loose from the electrode, partly diffuse away, and/or partly react further on the electrode, it is possible to use a device invented by Ivanov and Levich<sup>53</sup> in 1959. Ivanov and Levich considered the hydrodynamic problem presented when a disk is rotated in contact with a solution. Sticking for the moment to the electrochemical oxygen reduction for the example, a first reaction step in the two-part sequence described above produces  $\text{H}_2\text{O}_2$ . Radicals that do not remain adsorbed on the metal of the rotating disk will be thrown sideways across the disk. Ivanov and Levich's idea was to detect such radicals ( $\text{H}_2\text{O}_2$  in our example) by encircling the central disk electrode by a second "ring" electrode, electrically isolated from the disk and held at a potential at which  $\text{H}_2\text{O}_2$  would be expected to react. Thus, in a rotating disk electrode *with a ring* (see Fig. 7.52), the ring is electrically isolated from the disk and each is controlled at appropriate different potentials by separate potentiostats. The key hydrodynamic contribution made by Levich and Ivanov was an equation for the ring current, namely:

$$I_{\text{ring}} = \frac{J_0 N}{1 + k_3 \frac{\delta_\omega}{D}} \quad (7.112)$$

In Eq. (7.112),  $J_0$  is the current that forms the intermediate, i.e., the current in reaction (A).  $N$  is a geometric factor that can be written from theory if the relative sizes of ring and disk are known. The factor  $\delta_\omega$  is basically the same in meaning as the diffusion-layer thickness. As pointed out earlier,  $\delta$  is stirring dependent. A rotating disk electrode involves a kind of stirring (in fact, *super*-stirring since the revolutions per minute can be as much as 25,000). Hence,  $\delta$  is not a fixed value, but depends on the rate of stirring

---

<sup>53</sup>V. G. Levich spent a major part of his career in the world's largest institute of physical electrochemistry, The Frumkin Institute in Moscow. He was a man who had the good fortune to create a subfield in science and to dominate it during his lifetime. The field concerned is hydrodynamics applied to the relative movement of the solution near an electrode. His early work is encapsulated in a famous book *Physico-chemical Hydrodynamics*, which was finally published in English only in 1962. The most useful equation in this book is one used in this section [Eq. (7.112)]. Later, he was persuaded by Frumkin to apply his talents to the quantum theory of charge transfer, where he led a research group of some twenty-five members.

When Levich announced his plans to emigrate to Israel, it was still Soviet times and his announcement attracted intense scrutiny by the KGB, who wanted to prevent his leaving the USSR (they said he held military secrets). This generated angry protests from those western colleagues who appreciated his work. When he eventually arrived in the City College of New York, he returned to his old love, hydrodynamics.

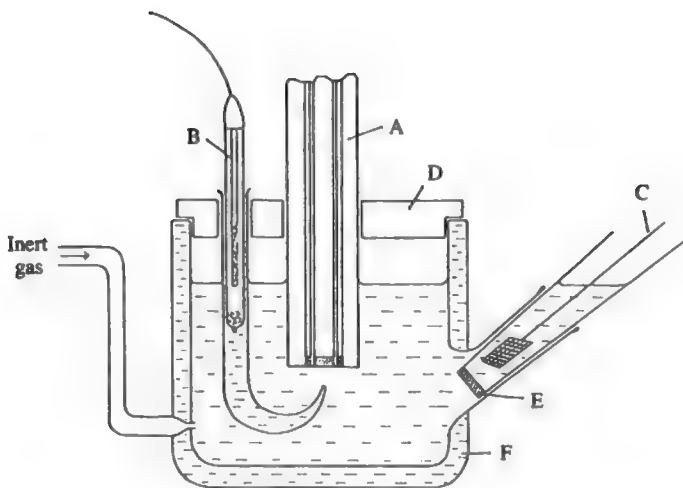


**Fig. 7.52.** Cell for the rotating disk electrode. A, ring-disk electrode; B, reference electrode with Luggin capillary; C, auxiliary electrode; D, Teflon lid; E, porous frit; F, thermostatted water jacket. (Reprinted with permission of Oxford University Press from C. M. A. Brett and A. M. O. Brett, *Electrochemistry: Principles, Methods, and Applications*, Oxford University Press, 1993, p. 156.)

(or rotation rate of the disk) and is written  $\delta_\omega$ , where  $\omega$  is the angular velocity of the ring. The equation that Levich derived for the coefficient  $\delta$  under hydrodynamic stirring conditions is

$$\delta_\omega = 1.61 D^{1/3} \nu^{1/6} \omega^{-1/2} \quad (7.113)$$

where  $D$  is the diffusion coefficient,  $\nu$  is the kinematic viscosity,<sup>54</sup> and  $\omega$  is the angular velocity (radians  $\text{s}^{-1}$ ).

Frumkin and Nekrassow then applied Levich's equation to an analysis of intermediate production when the intermediate could leave the electrode surface, with the possibility of reacting again at the ring or leaving for the bulk. Damjanovic et al. developed the Ivanov and Levich equation to include a term,  $x$ , the ratio of the velocity of the two parallel reactions (A) and (B), thus increasing the helpful information obtained by using the equation. Damjanovic et al.'s equation for the ratio of disk current to ring current is

$$\frac{I_{\text{disk}}}{I_{\text{ring}}} = \frac{x+1}{N} + \frac{(x+2)k'}{N\omega^{1/2}} \quad (7.114)$$

<sup>54</sup>The kinematic viscosity is the ratio of the electrolyte coefficient of viscosity and its density.

where  $k' = 1.61 D^{-2/3} \nu^{1/6} k_3$ , and  $k_3$  is the rate constant for the reduction of the intermediate. Of course, determination of  $k^1$  is equivalent to the determination of  $k_3$ , the rate constant for the decomposition of the intermediate on the electrode.

By determining  $I_{\text{disk}}/I_{\text{ring}}$  as a function of  $\omega^{-1/2}$ , one finds from the intercept  $x + 1/N$  (and therefore  $x$ ) and from the slope  $(x + 2) k'/N$  and hence  $k_3$ . Thus, if only the first reaction  $\text{ox} + n\text{e} \rightarrow \text{red}$  occurs, there will be no ring current.

Alternatively, if only the reaction for the reduction of the intermediate  $\text{ox} + (n-m)\text{e} \xrightarrow{k_3} \text{Int}$  occurs, and the intermediate does not react further,  $k_1 = 0 = k_3$ ,

$$\frac{I_{\text{disk}}}{I_{\text{ring}}} = \frac{1}{N} \quad (7.115)$$

In a plot of  $I_{\text{disk}}/I_{\text{ring}}$  against  $\omega^{-1/2}$ ,  $I_{\text{disk}}/I_{\text{ring}}$  will have the ratio  $1/N$ , and the plot will be a straight line parallel to the  $\omega^{-1/2}$  axis.

Another possibility is that only the second and third steps occur. There is no parallel reaction and hence  $x = 0$ . Equation (7.114) becomes

$$\frac{I_{\text{disk}}}{I_{\text{ring}}} = \frac{1}{N} + \frac{2k'}{N\omega^{1/2}} \quad (7.116)$$

The  $I_{\text{disk}}/I_{\text{ring}} - \omega^{-1/2}$  plot should be straight and dependent on potential; from the slope, one can determine  $k_3$ . (This is the case most often considered.)

A fourth possibility is that the first and second reactions occur but the third reaction does not, so that an intermediate is produced, but does not react further. Then,

$$\frac{I_{\text{disk}}}{I_{\text{ring}}} = \frac{x+1}{N} \quad (7.117)$$

Finally, all reactions may occur, and no simplification of Eq. (7.114) is possible. Both the slope of the plot and the intercept will be potential dependent and the latter will be greater than  $1/N$ . These possibilities are all portrayed in Fig. 7.53. From such results the conclusions drawn for oxygen reduction on a pure Fe surface were that on the bare iron, the rate-determining step involves the formation of  $\text{O}_2^-$ , while on the passive layer it is oxygen chemisorption under Temkin conditions.

The value of  $N$  in (7.117) is generally found by calibration for each ring disk electrode.  $N$  is defined as the fraction of species formed at the disk that arises at the ring and reacts there. It is determined prior to use of the electrode, using a simple redox electrode reaction, e.g.,  $\text{Fe}^{3+} + \text{e} \rightarrow \text{Fe}^{2+}$ . At the disk, the potential is set so that  $\text{Fe}^{2+} \rightarrow \text{Fe}^{3+} + \text{e}$  occurs; on the other hand, the ring potential is held at a value such that  $\text{Fe}^{3+}$  is reduced at a rate which is that of the limiting current. Then the ring current results from the  $\text{Fe}^{3+}$  produced by anodic reduction on the disk and transported to the ring by hydrodynamic convection (the swirling of the solution). Under these conditions, the

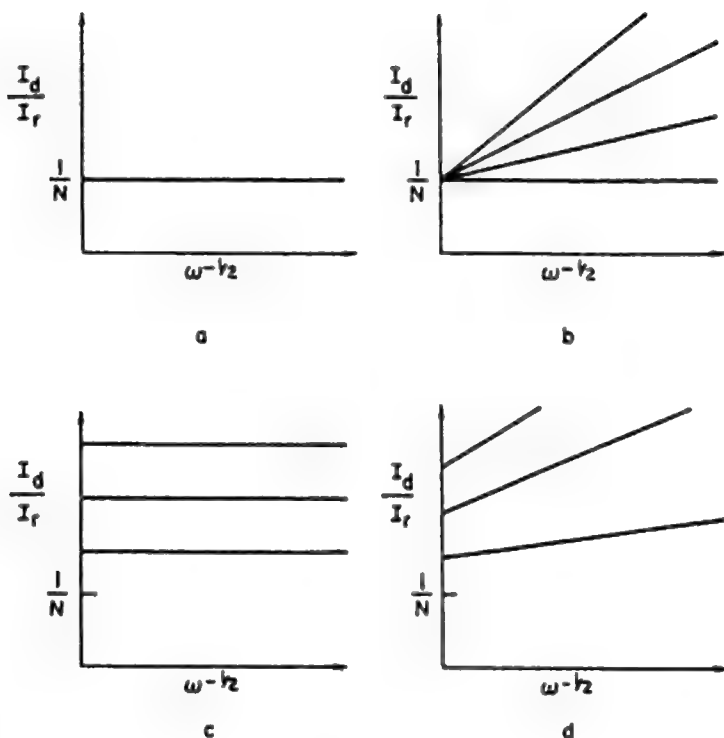


**Fig. 7.53.** Plots of  $I_{\text{disk}}/I_{\text{ring}}$  vs.  $\omega^{-1/2}$ : (a) Electrode reaction proceeds along a single path with the formation of intermediates that do not really react further. (b) Reaction proceeds along a single path with intermediates that readily react further. (c) Intermediates are produced in a parallel reaction and do not react further. (d) Intermediates are produced in a parallel reaction, but do not react further. (Reprinted with permission from A. Damjanovic, M. A. Genshaw, and J. O'M. Bockris, *J. Chem. Phys.* **45**: 4057, Fig. 1, copyright 1966, American Chemical Society.)

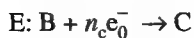
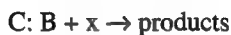
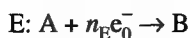
situation is very simple and  $(I_{\text{disk}}/I_{\text{ring}}) = (1/N)$ . There are theoretical equations for this ratio (derived of course by Ivanov and Levich), but in practice one finds  $N$  as above.

**7.5.14.2. Are Rotating Disk with Ring Electrodes Still Useful in the Twenty-first Century?** When the rotating disk electrode was first used, it was the 1960s; since that time, many new methods for measuring electrode reactions (above all, spectroscopic ones, e.g., those in Section 7.5.15), have been invented. Furthermore, microelectrodes have made it possible, in effect, to reduce  $\delta$  by as much as 1000 times compared with that in a still solution, so that one of the uses of the rotating disk

electrode (no ring, no two potentiostats), namely, making  $\delta$  smaller as rotation rate is increased, is taken care of in an easier way. Rotating disk electrodes are demanding mechanically. With rotation rates up to 25,000 rpm, they need a completely straight spindle to avoid vibration and a very stable bench.

Although new spectroscopic methods have reduced the need for some functions of the rotating disk electrode, there are a number of situations in which it remains the most effective technique. The detection of  $\text{H}_2\text{O}_2$  as an intermediate in the reduction of  $\text{O}_2$ , described above, is one example. Here are a few others.

1. There is a class of electrode reaction in which the first step involves an electron-transfer reaction (E), the second a chemical reaction (C), and the third another electrode in a transfer reaction different from the first (E):



The disk electrode potential is controlled to bring about the reaction indicated for A. The ring is held at a potential to cause B to react to C. Then the fraction of B obtained on the ring is  $N$ . Knowledge of this helps in understanding the formation of C, hence the mechanism of the overall reaction. There are many reactions of this type (called *E.C.E. reactions*). Some proteins undergo bromination in this sequence, the bromination step reaction being at B.

2. In the deposition of certain metals (e.g., Fe),  $\text{H}_2$  is produced in a parallel reaction. The amount of  $\text{H}_2$  formed can be determined by holding the disk at a potential for the co-deposition of Fe and  $\text{H}_2$  and the ring at a potential for the oxidation of  $\text{H}_2$ . The current produced on the ring can be combined with a knowledge of  $N$  to give the total current of  $\text{H}_2$  evolution on the disk, and thus deduce the rate of the cathodic deposition of Fe, free from interference by  $\text{H}_2$  deposition of  $\text{H}_2$ .

3. In some metal oxidation reactions (e.g., those involved in  $\text{Ni-NiO}_2$  electrodes), unwanted  $\text{O}_2$  is co-evolved. By setting the disk potential to oxidize the Ni and (unintentionally) evolve  $\text{O}_2$  and the ring current at a potential to reduce  $\text{O}_2$ , the amount of  $\text{O}_2$  production along with Ni oxidation can be obtained.

**7.5.14.3. Other Unusual Electrode Shapes.** Various modifications of the rotating disk electrode are described in the literature. For example, the rotating disk electrode with ring sometimes suffers from bubbles that collect in the center and make it difficult to determine the fraction of the disk available for electrode reactions. One remedy is to use a cone-shaped electrode; the ring is on the side of the cone and the disk at the tip. Bubbles don't like tips and skelter.

Cylindrical electrodes are mentioned sometimes, and there can be inner cylinders that can counter-rotate, also. Then there are jet electrodes (see Fig. 7.54). The jet

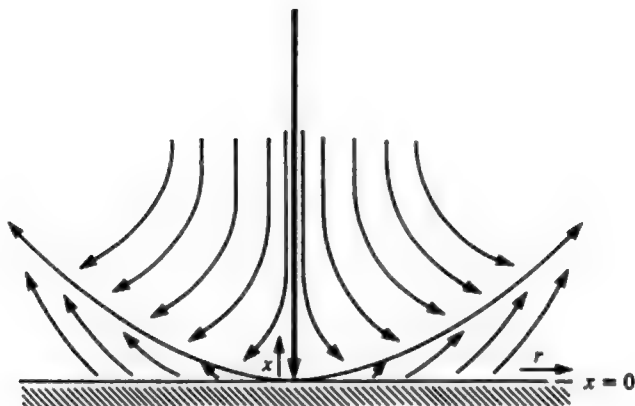


**Fig. 7.54.** The wall-jet electrode: schematic streamlines. (Reprinted with permission of Oxford University Press, from C. M. A. Brett and A. M. O. Brett, *Electrochemistry*, Oxford University Press, 1993. p. 155.)

electrode shoots the electrolyte at the electrode, and near the point of contact there will be a very low  $\delta$ , i.e., a very high limiting current density. The counter-electrode can be situated near the mouth of the jet. Thus, in mass production, it may be necessary to implant contacts on electronic devices (e.g., computer chips) passing by on a rapidly moving band. As each device comes beneath the jet, the latter is made to jut out momentarily at the device, which is arranged to be a cathode. The electronic contact is thus electrodeposited on the chip.

### 7.5.15. Spectroscopic Approaches to Electrode Kinetics

**7.5.15.1. General.** In the minds of many, spectroscopy involves the use of intensity–wavelength curves to determine the wavelength at which maxima occur in the absorption of the incident light. These maxima indicate the unique value of wavelength (or frequency) at which a specific chemical bond absorbs energy. Thus, absorption spectroscopy enables the researcher to identify bonds present in the system under examination. Observation of evidence for a characteristic combination of bonds enables the experimenter to determine the presence of a certain compound.

Electrode surfaces involve mostly submonolayers of ions, molecules, and radicals, surrounded by a layer of solution that is much thicker than the layer of atoms being observed. Can spectroscopic methods be found that are sufficiently sensitive to react to, say, one tenth of a monolayer on the surface, when the light has to pass through the adherent layer of solution, which contains a large excess of the bonds to be detected? Clearly, the answer to these questions must, somehow, be yes or there would be no section with the above title. But first let us deal with one of the controversial



questions of electrochemistry in 2000, the pros and cons of making spectroscopic measurements *in situ* and *ex situ*.

*In situ* measurements (i.e., those done on an electrode while it is in contact with the solution under a controlled potential) are described below (see also Section 6.2.4). However, there are plenty of reports in the electrochemical literature of the use of *ex situ* methods for looking at electrochemical situations. In these, the electrochemical reactions are duly carried out, sometimes using a thin-layer cell, and then the solution is rapidly removed from the thin-layer cell, e.g., by applying a vacuum. The electrode (one of the plates in the thin-layer cell) and whatever remains on it as a result of electrochemical activity while it was in contact with the solution, can then be examined at leisure, using a number of spectroscopic methods, including those that only function *in vacuo*.

The big advantage of making *ex situ* measurements is that they allow the application of methods used in surface chemistry when no solution is present. Some of these *ex situ* methods (LEED or XPS) are described in Chapter 6. In electrochemical situations in which the critical questions concern, for example, passivation of metals involving oxides or sulfide films, there is no accompanying disadvantage in the use of these well-developed and accurate methods.

However, in many electrochemical situations (e.g., methanol oxidation), the question is one of what entities and how many of them are present on the surface when a certain potential is applied to the electrode, *while the solvent layer is still adsorbed on the electrode*. One has to ponder the effect of removing the electric potential that orients the reactants on the electrode and the solvent (this happens when one applies a vacuum) and ask: Is the information that can now be extracted from the surface (i.e., in *ex situ* measurements) still relevant to what is wanted—information on entities present during the electrochemical reaction, which must necessarily involve a certain potential applied across the reactants, in the presence of the solvent?

Two extreme answers can be considered. Those who stress the use of *ex situ* methods (Hubbard, Soriaga, Wieckowski) might point to the idea of the photograph. What is a photograph but a “freezing in place” of action at a certain moment? Is the sudden removal of solvent and solute, as well as the interfacial structure across which there is the intense electric field that occurs in *ex situ* determinations, nothing but a “freezing in place” of events during an electrochemical reaction?

Those who stress the *in situ* methods (Neugebirt, Fleischmann, and Pons) and focus less on the *ex situ* ones, point to the destruction of the system before observations are made. The solvent in the reactant layer on the electrode, which is held in a certain orientation by the electric field, is similar to that of the bricks and mortar of a house. Removing the potential and destroying the solvent layer is like knocking down the walls of the building. Certainly, some of the contents of the house may be found in the ruins, but would it not be better to observe them in their proper setting?

The practice of physical electrochemistry at the turn of the twenty-first century is to use both *in situ* and *ex situ* methods. In this section our description will be restricted

to explaining how two *in situ* spectroscopic methods can provide information on certain electrochemical reactions.

**7.5.15.2. FTIR Spectroscopy and Mechanisms on Electrode.** The basis of Fourier transform infrared spectroscopy was described in Section 6.2.6. One of the more difficult aspects of detecting the mechanism of electrode reactions is that of knowing the nature of the intermediate radicals on the electrode surface. Infrared spectroscopy measures chemical bonds, so it is an ideal method for detecting which bonds are present and hence which intermediate radicals are taking part in a surface reaction at a given potential, etc.

The basic measurement in the FTIR technique (Fig. 7.55) is that of interference between two beams of white light that contain the full range of frequencies. The degree of interference is dependent on the wavelength, so when the beams interact there is light of different intensities, depending on the wavelength. This “interfered with” light (an interferogram) is impinged on the electrode containing the radical intermediates. Absorption will occur if there is a match between light of a given wavelength and a bond that vibrates at the corresponding frequency reflected off the electrode; from this it is possible to determine what is there. Fourier transform mathematics takes this light back to a spectrum (Fig. 7.56). In this way, the charge, growth, and decay of radicals gives an objective measure of steady state. During the 1990s, much progress was made in improving the speed at which all this occurs. A measurement that took 15 min in the 1960s has been reduced to about 1 ms.

## 7.5.16. Ellipsometry

**7.5.16.1. What Is Ellipsometry?** Ellipsometry uses the properties of polarized light. Light can be regarded as consisting of oscillations of electrostatic and magnetic fields at right angles to each other. Ordinary (nonpolarized) light consists of oscillations in all planes, no preference being given to any one. However, when light

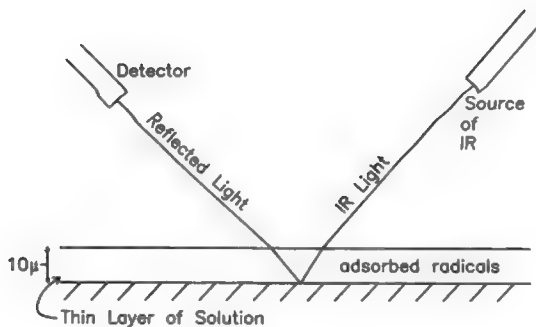


**Fig. 7.55.** Incident IR beam passing through a layer of solution.

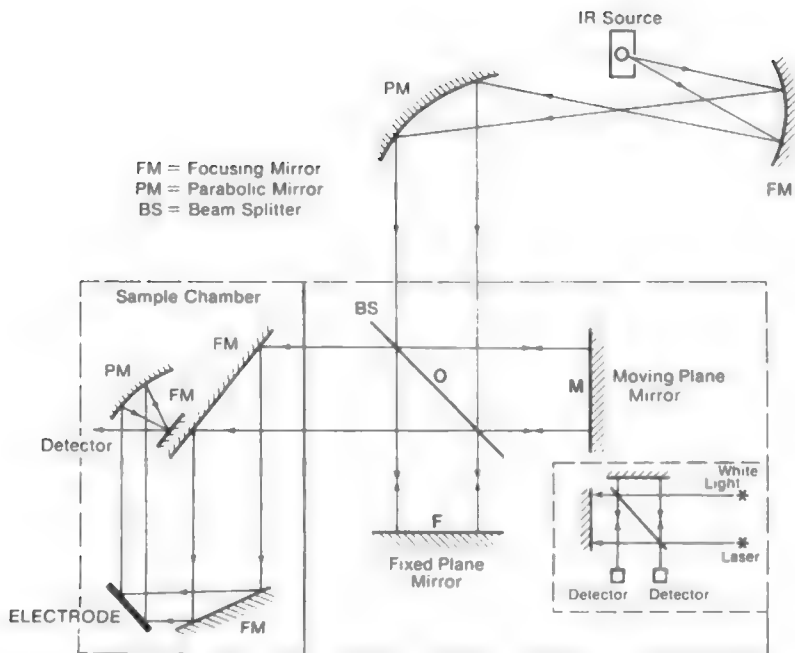


**Fig. 7.56.** The optical arrangements of an FTIR spectrometer. (Reprinted from M. A. Habib and J. O'M. Bockris, *J. Electroanal. Chem.* **180**: 290, copyright 1984, Fig. 2, with permission from Elsevier Science.)

passes through certain crystalline substances, it becomes “plane polarized”; the resulting light oscillates in only one plane.

When plane-polarized light contacts a new phase, the state of polarization of the light changes. Instead of being plane polarized (electrical and magnetic oscillations equal in amplitude and perpendicular to each other), there is a difference in phase in the amplitude of the electrical and magnetic components. Such a beam is shown in Fig. 7.57. If one follows the path of the *tip* of the electric vector resulting from the two components of the light, one finds it forms an ellipse.

Ellipsometry is the technique that uses changes in the polarization properties of light when it strikes the object of investigation to determine the properties thereof. As will be seen, it allows one to calculate the thickness of extremely thin layers on electrodes and gather some information as to the identity of what is present. This remarkable technique is sensitive to less than one-tenth of a monolayer.

**7.5.16.2. Is Ellipsometry Any Use in Electrochemistry?** Like the use of infrared spectra in FTIR to determine adsorbed entities, ellipsometry is an *in situ* technique. It uses (initially) ordinary light that after being converted to polarized light

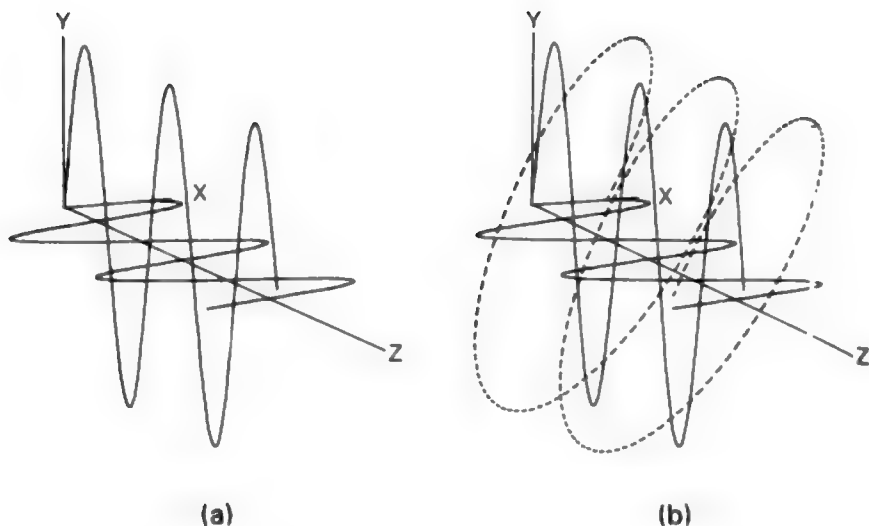


**Fig. 7.57.** Perspective view of the x and y components of an elliptically polarized wave. The ellipse results as a resolute of the two components. (Reprinted from R. A. Serway, C. J. Moses, and C. A. Moyer, *Modern Physics*, Saunders College Publishing, 1997, p. 208.)

passes through a solution to impinge upon materials adsorbed on the electrode. Measurement of the changes in the state of polarization of this beam of plane-polarized light after it is reflected from the surface under investigation can then be used in three main ways.

1. Ellipsometry is unrivaled for the measurement of the properties of thin films, particularly those on electrodes in solution. It has extraordinary sensitivity and can measure films from submonolayers up to films having a thickness near to that of the wavelength of the light incident upon the electrode surface. Moreover, ellipsometry gives not only the thickness of the film but also its refractive index and, in the case of conducting films, the absorption coefficient.

2. The great sensitivity of ellipsometry allows it to measure “films” down to a “thickness” of 0.1 monolayer, with possibilities of even greater sensitivity in sight. Such measurements can be applied not only to thickness but also to the examination of the adsorption of ions and organic molecules on the surface of metals (see Fig. 7.58).

3. Carrying out the measurements as a function of  $\lambda$  (i.e., wavelength) allows a new kind of spectroscopy (see following discussion).

**7.5.16.3. Some Understanding as to How Ellipsometry Works.** In consideration of what happens in ellipsometric measurements of a film on an electrode

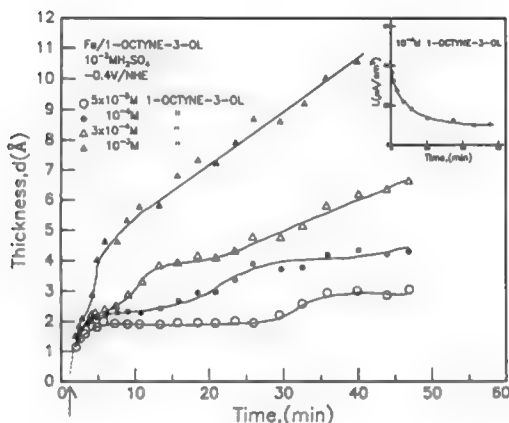


**Fig. 7.58.** Ellipsometrically measured thickness of an adsorbed layer of 1-octyne-3-ol on iron. (Reprinted from V. Jovancicevic, B. Yang, and J. O'M. Bockris, *J. Electrochem. Soc.* **135**: 94, 1998. Reproduced by permission of The Electrochemical Society, Inc.)

surface, it is helpful to look at a model of the interaction of light with the film and the electrode (see Fig. 7.59). The measuring device is shown in Fig. 7.60. One begins on the left with a light source. The light passes through a polarizer that produces plane-polarized light. Upon entering the cell, the light interacts with the film and is reflected after changes in the state of polarization, whereupon these changes are detected and recorded.

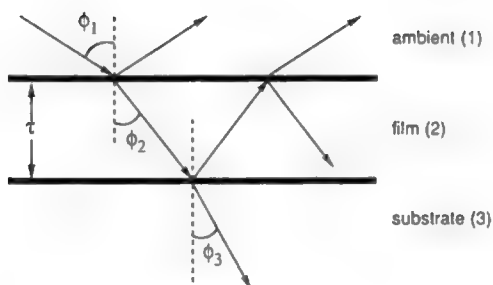


**Fig. 7.59.** Optics of a film-covered surface. (W. Paik, "Ellipsometry in Electrochemistry," in *Modern Aspects of Electrochemistry*, Vol. 25, J. O'M. Bockris, B. E. Conway, and R. E. White, eds., Plenum, 1993, p. 200.)

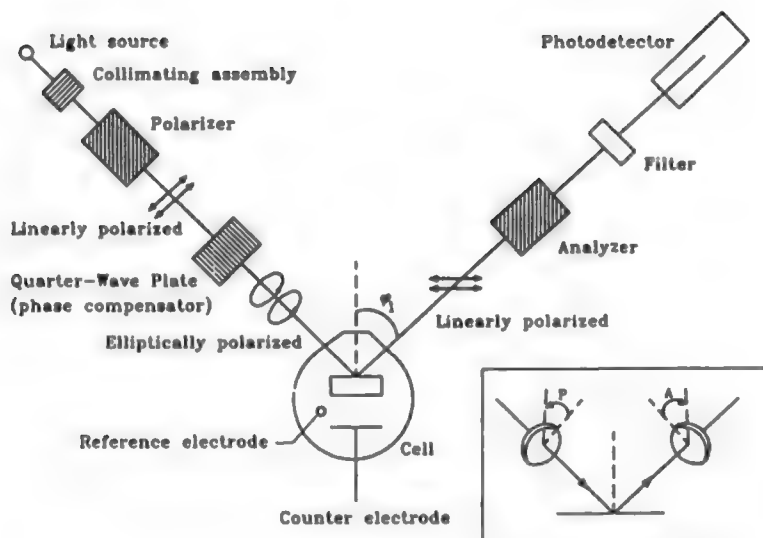


**Fig. 7.60.** A manual ellipsometer. (Reprinted from W. Paik, "Ellipsometry in Electrochemistry," in *Modern Aspects of Electrochemistry*, Vol. 25, J. O'M. Bockris, B. E. Conway, and R E. White, eds., Plenum, 1993, p. 200.)

One of the basic equations of ellipsometry is

$$\frac{r^p}{r^s} = \tan \psi e^{i\Delta} \quad (7.118)$$

Here, the  $r$ 's are reflection coefficients (outgoing to incoming intensities) and  $p$  and  $s$  refer to the parallel and perpendicular components of the light, respectively. The quantity  $\psi$  represents the change in amplitude of the light on contacting the film, and  $\Delta$  represents the change in phase difference similarly caused; these two variables are related to the thickness  $\tau$  and the refractive index  $n$  of the film.

It is possible to obtain  $\Delta$  and  $\psi$  from Eq. (7.118).<sup>55</sup> However, the *extraction of the refractive index of the film and its thickness* involves Fresnel's equation for the interaction of light with matter, and this mathematical manipulation was impractically laborious before the introduction of computers in the 1960s.

The situation may become more complex if the film being examined *absorbs* the light as well as reflects it. This is tantamount to introducing an absorption coefficient,  $\kappa$ , a third unknown (in addition to the refractive index,  $n$ , and the thickness of the film,  $\tau$ ). However, three unknowns cannot be obtained from two equations. It is necessary to obtain an extra datum.

<sup>55</sup>Equation (7.118) is really two equations because it contains real and imaginary parts.

One way to get this third quantity (Paik, 1972) is to measure not only the changes in the polarization states ( $\Delta$  and  $\Psi$ ) but also the intensity of the reflection,  $I$ , as a function of the angle of incidence. This change in intensity can also be expressed in terms of the variables  $n$ ,  $\tau$ , and  $\kappa$ . Then with  $I$ ,  $\Delta$ , and  $\Psi$ , the thickness  $\tau$ , refractive index  $n$ , and the absorption coefficient  $\kappa$ , can all be determined.

**7.5.16.4. Ellipsometric Spectroscopy.** Electrochemical applications of ellipsometry are usually made at a constant wavelength, measuring  $\Delta$  and  $\Psi$ , that is, the changes in the state of polarization of the light when the light strikes the electrode surface and interacts with material absorbed on it. However, it is also possible to make ellipsometric measurements as a function of wavelength,  $\lambda$ , from the near IR, visible, and even somewhat into the UV. Then one obtains  $n$  and  $\kappa$ , as indicated above (the film thickness is kept constant), but at a series of different wavelengths, using a monochromator to vary the wavelength of the incident light. In this way,  $n$  (Fig. 7.61) and  $\kappa$  (Fig. 7.62) may be plotted as a function of  $\lambda$ . These plots are in fact spectra and from them one can draw conclusions about the oxidation state of the species present in a film covering the electrode at a certain potential. Such information, obtained at

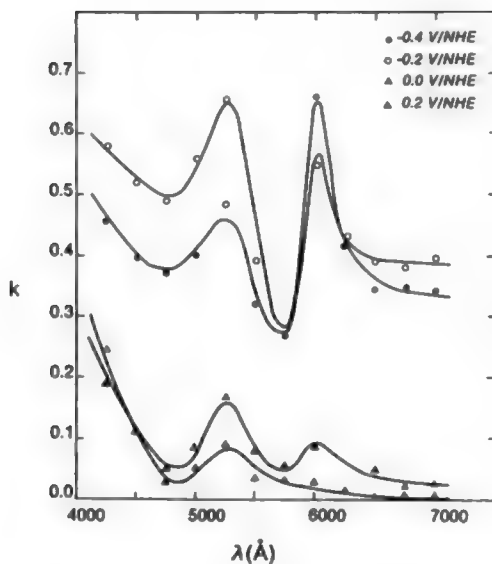


**Fig. 7.61.** Extinction coefficient spectra of iron for different potentials. (Reprinted with permission from V. Jovancicevic, R. C. Kainthla, Z. Tong, B. Yang, and J. O'M. Bockris, *Langmuir*, **3**: 392, Fig. 11, copyright 1987, American Chemical Society.)

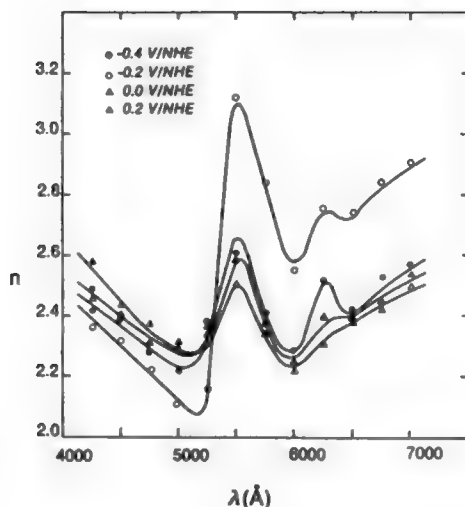


**Fig. 7.62.** Refractive index spectra of iron for different potentials. (Reprinted with permission from V. Jovancicevic, R. C. Kainthla, Z. Tong, B. Yang, and J. O'M. Bockris, *Langmuir*, **3**: 392, Fig. 12, copyright 1987, American Chemical Society.)

several potentials, provides a basis for understanding changes in the nature of the passive film with potential.

The availability of automatic ellipsometers<sup>56</sup> greatly helps all this. It is possible to program the ellipsometer to print a readout of, for example, refractive index and thickness as a function of potential. The technique could be applied more widely, a developmental possibility being that it could enable the operator to follow changes in spectra (and thus interpret what molecular changes cause them) in the millisecond range. One of the frontiers of development of techniques in electrochemistry could be the use of ellipsometric spectroscopy.

**7.5.16.5. How Can Ellipsometry Be So Sensitive?** Some students who approach ellipsometry for the first time find the extraordinary sensitivity of ellipsometry in measuring thickness difficult to believe. Thus, their first thought is that the minimum size of an object that disturbs a beam of electromagnetic radiation is that of the wavelength in the incident light. If the disturbing entity, a film, say, is less than  $\lambda$  in thickness (about 500 nm), it will not be “seen” except by some form of

<sup>56</sup>By “automatic” is meant ellipsometers that calculate  $n$  and  $\tau$  directly (and in a short time) from the measurement of  $\Delta$  and  $\Psi$ .



interferometry that can measure thicknesses of about 100 Å. Yet, ellipsometers are sensitive to fractions of monolayers.

However, such reasoning is irrelevant to ellipsometry. This technique works because the presence of a new phase on the electrode changes the polarization properties of the light. Detailed examination shows that detectable changes in  $\Delta$  and  $\Psi$  occur, even for a submonolayer of material on an electrode surface, and thus information on  $n$ ,  $\kappa$ , and  $\tau$  for such systems can be obtained for the entities comprising the submonolayer.

**7.5.16.6. Does Ellipsometry Have a Downside?** Any method of observing reactions on a surface in solution will be bound to have some limitation. That is why the examination of an electrode surface during a reaction has to be done by at least two different methods, each with its own strength and weakness.

Modern ellipsometers can measure changes in  $\Delta$  and  $\Psi$  quickly so that the technique can be used to observe adsorbed materials in transient situations (in contrast to FTIR, which can only be applied over longer times). However, ellipsometric detection and measurement of surface material can only take place<sup>57</sup> on specularly reflecting surfaces; roughness reduces the efficacy of ellipsometry and sufficient roughness can make it inapplicable. Thus, electrodes to which ellipsometry is to be applied must be highly polished and reflective. Such a situation can usually be achieved in the research laboratory, but it prevents the application of ellipsometry to surfaces that cannot be prepared in advance.

### 7.5.17. Isotopic Effects

It has been known for about 40 years that the reaction rates of the various isotopes of the same element are different, the lighter isotope reacting faster than the heavier one. The effect is most marked in reactions involving H and its isotopes, deuterium,  $^2\text{H}$  or D; and tritium,  $^3\text{H}$  or T, because here the ratio of the masses of the isotopes concerned is much greater than that of other electrochemically important isotopes, e.g.,  $^{16}\text{O}$  and  $^{18}\text{O}$ . In fact, the rate-constant ratios during the evolution of  $\text{H}_2$  and corresponding isotopic species (e.g., HT) on some electrode materials reach as much as 18 (i.e., reactions involving H are as much as 18 times faster than the same reactions involving T).

What is the use of this in electrode kinetics? First, it is easy to determine experimentally the relative rate constants between  $^1\text{H}$  and  $^3\text{H}$  because  $^3\text{H}$  is radioactive; then only very small amounts of  $^3\text{H}$  in solution are needed in an experiment.  $^3\text{H}$  can be detected simply by observing the number of scintillations caused by the emission

<sup>57</sup>It is easy to figure out why this is. The theory of ellipsometry assumes that the surface is atomically flat. It is possible to model roughness as a series of declivities in the surface. These are taken as being full of solution. Thus, the ellipsometer "sees" pools of solution where it assumes the electrode surface should be. Especially in the determination of submonolayers, the result can contain significant errors in  $n$  and  $\kappa$  that have been calculated on the assumption of a completely smooth surface (Brusic and Cahan, 1969).

of  $\beta$ -particles in the radioactive decay of tritium. This tritium-containing solution can be dissolved in a “cocktail” that emits flashes of light in the presence of this radiation. The number of flashes is recorded in a counter and converted to concentrations of the tritium that caused them.

The values of the separation factors thus determined relate to the mechanism for the hydrogen evolution reaction. Reactions involving hydrogen can take place in different paths and with different rate-determining steps within a given pathway. However, each mechanism predicts a specific and characteristic separation factor. Moreover, the differences in the separation factors of each step are large so that even if the experiments are uncertain by  $\pm 10\%$ , the mechanism of the hydrogen evolution reaction is indicated by matching the experimental value to the predicted value for a certain rate-determining step.

Why do isotopes of the same element react at different rates? The basic principles can be readily discerned from Fig. 7.63. The larger the zero-point energy, the smaller the heat of activation and the larger the rate. The isotope with the larger zero-point energy will (other factors being the same) react faster than that with the smaller zero-point energy. Tunneling, too, greatly favors H compared with the heavier D or T, as can be seen from the Gamow equation for the rate of barrier penetration. This runs:

$$P_E \propto e^{-\frac{4\pi l(\sqrt{2m(E-U)})}{h}} \quad (7.119)$$

Here  $m$  is the mass,  $l$  is thickness of the barrier the proton has to penetrate,  $E$  is the total energy, and  $U$  is the potential energy of  $\text{H}^+ - \text{O}$ , or correspondingly  $\text{D}-\text{O}$  or  $\text{T}-\text{O}$ . Clearly, unless  $l$ ,  $E$ , and  $U$  are strongly different for the various isotopes, the  $m$  factor

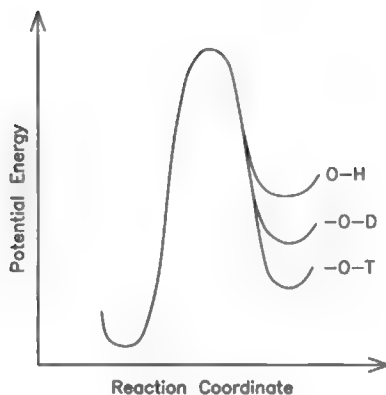


**Fig. 7.63.** Influence of zero-point energies on isotopic reaction rate.

will act to make the probability of penetrating the barrier vary according to the sequence for the velocities in which  $V_H > V_D > V_T$ . Table 7.4 indicates likely ratios.

**7.5.17.1. Use of Isotopic Effects in the Determination of Electro-Organic Reaction Mechanisms.** Much work has been carried out on the mechanism by which hydrocarbons can be electrochemically oxidized. Were that easy, it might be possible to use available oil in electrochemical devices (fuel cells) to convert chemical to electrical energy 2–3 times more efficiently than do heat engines (Chapter 13).

There are several possible rate-determining steps here. For example,

1. No breaking of O–H bonds.

Thus, the rate-determining step (rds) might be



There will be no isotopic effect connected with the differences in zero-point energy because the bonds broken are the same in each sequence. Hence, the predicted result is

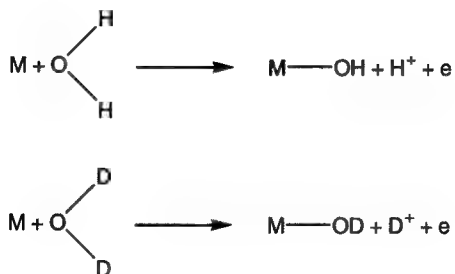
**TABLE 7.4**  
**Experimental H–T Separation Factors at a Current Density of  $10^{-2}$  A cm $^{-2}$  and at a Temperature of 25°C and Mechanisms Indicated**

Metal	Electrolyte	Separation Factor	Mechanism
Pt	0.5 N H <sub>2</sub> SO <sub>4</sub>	9.6±0.4	Fast discharge-slow recombination
Pt	0.5 N NaOH	15.3±0.8	Fast discharge-slow electrochemical desorption
Rh	0.5 N H <sub>2</sub> SO <sub>4</sub>	10.7±0.4	Fast discharge-slow recombination
W	0.5 N H <sub>2</sub> SO <sub>4</sub>	6.0±0.2	Linked discharge-electrochemical desorption
W	0.5 N NaOH	4.4±0.5	Slow discharge-fast recombination
Ni	0.5 N H <sub>2</sub> SO <sub>4</sub>	18.0±0.9	Fast discharge-slow electrochemical desorption
Ni	0.5 N NaOH	4.1±0.3	Slow discharge-fast recombination
Cu	0.5 N H <sub>2</sub> SO <sub>4</sub>	18.1±2.4	Fast discharge-slow electrochemical desorption
Hg	0.5 N H <sub>2</sub> SO <sub>4</sub>	5.8±0.3	Slow discharge-fast recombination
Pb	0.5 N H <sub>2</sub> SO <sub>4</sub>	6.7±0.7	Linked discharge-electrochemical desorption
Pb	0.5 N NaOH	7.2±0.8	Linked discharge-electrochemical desorption
Cd	0.5 N H <sub>2</sub> SO <sub>4</sub>	9.2±0.5	Linked discharge-electrochemical desorption

Source: Reprinted with the permission of the Royal Society of Chemistry from J. O'M. Bockris, S. Srinivasan, and D. B. Matthews, *Discuss. Faraday Soc.* **39**: 239, 1965, Table 5.

$$i_{\text{H}}/i_{\text{D}} \approx 1$$

2. Alternatively, the rds might involve the breaking of O–H or O–D bonds in the rate-determining water discharge:



where M is a site on the electrode. Here the major effect arises from the difference in zero-point energies of M–OH and M–OD. The difference is such that

$$i_{\text{H}}/i_{\text{D}} \approx 2.7$$

Several other possibilities exist for the mechanism of hydrocarbon oxidation, and in the application to ethylene oxidation, this isotopic determination of the reaction rate involving H and D was the main diagnostic of the mechanism determination for this reaction on Pt.

### 7.5.18. Atomic-Scale *In Situ* Microscopy

Atomic-scale observation of surfaces has long been available by means of electron microscopy. However, this technique must be carried out in a vacuum because the presence of a solution above the specimen absorbs and scatters the incoming electrons. What is needed is the ability to look at surfaces on an atomic scale *in situ*.

An entirely novel technique, the scanning tunneling microscope (STM), was invented by Binnig and Rohrer in 1983 (who were awarded the Nobel prize in physics in 1986). It allows the observation of surfaces on an atomic scale without a vacuum. The basic principle of the technique involves a probe with an exceedingly fine tip. The radius of curvature of the tips should be less than 1 nm. Now, if the tip of such a probe is brought very near (say, 1 nm) a surface in solution, and the potential difference between the surface and the probe tip is set appropriately, electron tunneling occurs between the electrode surface and the ultramicrotip. The intensity of the tunneling current in such a situation is proportional to  $e^{-\alpha x}$ , where  $\alpha$  is a constant characteristic of the apparatus and  $x$  is the distance between the tip and the surface. The electron current between the surface just under the tip and the tip is *very* sensitive to the probe–surface distance. Most surfaces are inherently rough on an atomic scale. Hence,

the current due to the tunneling of electrons between tip and surface would vary greatly as the probe is moved over the surface because the changes in local topography would give rise to significant changes in  $x$ . Alternatively, if a device can be arranged to maintain the current constant as the tip crosses the surface, there must be movement of the probe tip to follow the ups and downs of the surface as the probe moves across it, so that the distance (and hence the current) is always the same.

How can one make the tip move on an atomic scale and in the  $x$ -,  $y$ -, and  $z$ -directions? This is done by the use of piezoelectric crystals (e.g., barium titanate), which have the characteristic of undergoing minute changes in length when a potential is applied to them (see Fig. 7.64). One of the prerequisites of such microscopy is an equipment platform free from traffic vibrations. This usually means an elaborate arrangement; for example, the apparatus is supported on a heavy slab of stone placed on inflated inner tubes, tires, etc., and the whole assembly rests on a massive table.

The sensitivity of images of metal surfaces obtained through the solution is less than that in air. Crystal steps on a 1-nm scale can be discerned and in a few cases (e.g., Pb on C; Szklarczyk and Bockris, 1989) individual atoms can be distinguished and the interatomic distance measured. An STM picture is shown in Fig. 7.65.

The use of STM in electrochemistry has been growing rapidly since 1990, particularly for situations in electrodeposition and corrosion where knowledge of the changing surface on an atomic scale is informative in understanding the way corrosion

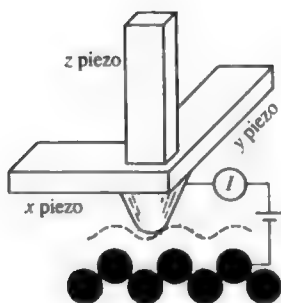


**Fig. 7.64.** Scheme of operation of piezoelectric drive in STM. (Reprinted with permission of Oxford University Press from C. M. A. Brett and A. M. O. Brett, *Electrochemistry: Principles, Methods, and Applications*, Oxford University Press, 1993, p. 269.)

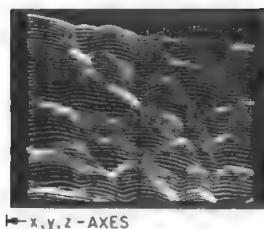


**Fig. 7.65.** STM image of a thin gold film (Reprinted from J. Schneir, R. Sonnenfeld, O. Marti, P. K. Hansma, J. E. Demuth and R. J. Hamers, *J. Appl. Phys.* **63**: 717 (1988).

occurs, e.g., how individual crystal planes of different indices dissolve at different rates on the various crystal forms that occur on a corroding surface.

STM has also been used to study the adsorption of large biomolecules on a surface in solution (Roscoe, 1996). However, caution must be exercised because of the tendency of the probe tip itself to push the biomolecule, i.e., interfere with its own measurement.

Another device that yields results of the same kind as STM is atomic force microscopy (AFM) (Binning, 1986). This avoids dependence on an electron stream (which cannot be obtained from insulators)<sup>58</sup> and relies on the actual interatomic forces between a microtip and nearby surface atoms. The forces experienced at a given point by the tip are sensed by a cantilever spring. The movements of this are slight, but they can be measured by means of interferometry and in this way the movement of the tip can be quantified. The sensitivity of the atomic force microscope is less than that of STM, but its action is independent of the electrical conductivity of the surface and it is therefore to be preferred over STM, particularly for studies in bioelectrochemistry.

## 7.5.19. Use of Computers in Electrochemistry

**7.5.19.1. Computational.** Computers used as advanced electronic calculating machines began to be available in U.S. universities in the early 1960s. A good example of the use of computers in this way in electrochemistry occurs in ellipsometry. The ideas of ellipsometry and the equations for dealing with changes in polarization when polarized light strikes matter were first devised by Raleigh in the nineteenth century. Their solution in situations such as the three-phase case was not practical

<sup>58</sup> This is a relative statement. STM works well for surfaces covered with thin oxide films that probably contain surface states.

before computers could be used to solve the equations in an acceptable time. Here is a case where the introduction of the computer made the subject viable and brought to life a major investigatory technique.

**7.5.19.2. Computer Simulation.** There are various ways in which a suitably programmed computer can predict (in a practical time) alternative hypothetical mechanisms based on simulated steps for an experimentally known reaction. The model that predicts behavior that most closely fits that of the real reaction indicates its mechanism.

An example can be given in the field of impedance spectroscopy (see Fig. 7.66). The figure shows the imaginary impedance of a GaP electrode in contact with a solution of 95% dimethyl formamide and 5% water, containing 0.1 *M* tetrabutylammonium phosphate under illumination. The experimental  $Z''_{\text{imag}} - \log \omega$  plot shows one clear maximum at the high-frequency end (about 1 kilocycle) and two further inflections that may indicate maxima.

Along with this experimental result are the results of four simulations, each of which corresponds to different assumptions about the arrangement of the components

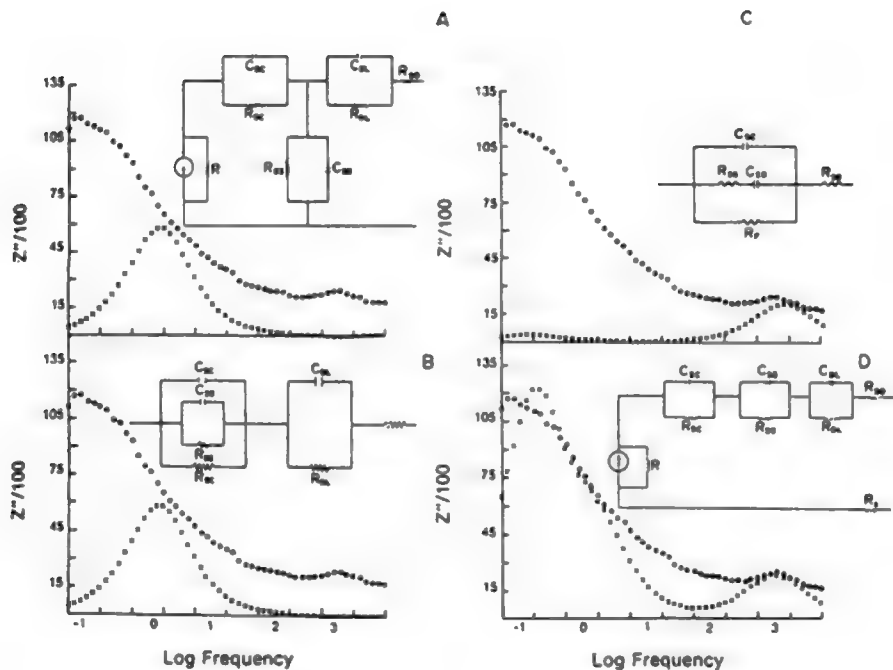


**Fig. 7.66.** Simulated imaginary-impedance-frequency plot. (Reprinted from K. Chandrasekaran and J. O'M. Bockris, *Electrochim. Acta* 32: 1398, copyright 1987, Fig. 10, with permission from Elsevier Science.)

that are likely to function in a semiconductor in contact with a solution. Thus, there will be a solution resistance,  $RS$ , the capacitance  $C$ , and resistance  $R$ , of the charge-transfer reaction across the interfacial region; the corresponding quantities to represent possible surface electronic states; and finally the capacitance and resistance ( $C_{sc}$ - $R_{sc}$ ) pair for the semiconductor space charge region.

The experimenter calculates the imaginary impedance of each of these circuit elements, using the equation

$$Z'' = \frac{R^2 \omega C}{1 + \omega^2 C^2 R^2} \quad (7.120)$$

The impedances of each circuit element are then added and the result, particularly that with respect to the concordance of the shape of the  $Z''$ - $\log \omega$  plots and the position of the maxima, are compared with experiment. This is done for each of the four circuits proposed (there may be others) and the ability of each and any circuit to replicate the experiment is then examined to choose the one giving the best fit (in the example in the figure, this is clearly D).

An important aspect of the use of the computer here comes about in the following way. Few of the components of the various surface elements are known accurately. On the other hand, a rough idea of these quantities is known from experiment on other systems and from theory. A computer can be programmed with a range of "reasonable" numbers for the  $R$ 's and the  $C$ 's of each of the circuit elements concerned and asked to find those values which, for the given model, fit the experimental impedance curves.

The key point here is the "reasonable limits" given to the computer for the quantities to be fitted into the appropriate circuit elements. There must be a limited range to each quantity found from independent data for the quantities concerned. Thus, for  $C_{DL}$ , the range taken was 10–100  $\mu F\ cm^{-2}$ . Choosing realistic ranges for the unknown parameters prevents a computer simulation from degenerating into a curve-fitting game, unconnected to reality. The operator must keep his integrity and not accept an "impossible" value of a parameter just because it yields an excellent fit between the  $Z''$ - $\omega$  plot calculated for a given equivalent circuit using it and that obtained experimentally.

**7.5.19.3. Use of Computer Simulation to Solve Differential Equations Pertaining to Diffusion Problems.** As shown earlier (Section 4.2.11), differential equations used in the solutions of Fick's second law can often be solved analytically by the use of Laplace transform techniques. However, there are some cases in which the equations can be solved more quickly by using an approximate technique known as the finite-difference method (Feldberg, 1968).

The basic principle in this technique is to replace derivatives by finite differences, i.e.,  $dy/dx$  is replaced by  $\Delta y/\Delta x$ . The differential equation is then rewritten using these difference quotients in place of the derivatives and the boundary conditions of the problem introduced. The equations can then be solved analytically. Space and time



are divided into arbitrarily small but finite quantities. Diffusion, electron transfer, and surface chemical reactions are each treated separately and consecutively. Detailed accounts of the procedures that have developed from Feldberg's 1968 initiative are to be found elsewhere.<sup>59</sup>

**7.5.19.4. Use of Computers to Control Experiments: Robotization of Suitable Experiments.** Many experimental methods can be carried out by robots. For example, in an experiment in a bioelectrochemical method for the production of hydrogen, it may be necessary to sample the amount of hydrogen produced in a series of, e.g., 50 flasks placed in a line. Each flask contains an aqueous mixture, the principal component of which is a specific enzyme difference for the mixture in each flask. A robot running on rails is programmed to move up and down the row of flasks, stopping at each, orienting its nose (a hollow needle) toward the given flask, then dipping it down through a rubber septum closing each flask and sniffing (sampling) for the hydrogen. The sample containing the hydrogen—mixed with air for each flask—is then transferred by the robot to a gas chromatograph, which measures and records the hydrogen produced in a given time in a certain flask. The robot continues to work the flasks, moving up and down on its rails, for as long as the experiment lasts—a week or more. In this way, the amount of hydrogen produced by 50 different enzymes can be measured as a function of time over weeks. The operator simply collects and stores the data once a day.

This is a simple example. It is possible for robots to carry out quite complex protocols that involve, e.g., mixing liquids to certain specified degrees, shifting and manipulating flasks, and recording current and potential.<sup>60</sup> Ultimately, robots will be able to perform complex experiments. The question will always be whether it is cheaper to buy such robots or hire technicians. The robot, of course, works around the clock and may be an economic and satisfactory way to do research if the experiment is sufficiently repetitive.

#### 7.5.19.5. Use of Computers in Pattern Recognition Analysis

**1. Water Electrolysis.** An example of the use of computers in pattern recognition can be given from work on the use of coal slurries to provide alternative anodic reactions in the electrolysis of water, with the aim of producing cheap hydrogen for fuel cells. In the presence of the coal slurries, the evolution of oxygen (the usual anodic reaction in the electrolysis of water) does not occur. Instead, a large number of

<sup>59</sup>A painstakingly clear account with all the mathematical details is given in *Instrumental Methods of Electrochemistry*, Southampton Electrochemistry Group, Harwood, Chichester, U.K., 1985.

<sup>60</sup>In a visit to a Japanese university laboratory in the mid-1990s, one of us was taken by the professor to visit what he called his team. In the poorly lit laboratory could be seen eleven shapes, each near a circular shelf on which some movement in beakers and apparatus, including the pouring of liquids, was to be seen. Trailing onto the floor from some of the shelves was a lot of paper, covered with columns of figures. However, off in a corner, one could see one white-coated human figure, also pouring liquids and taking readings. "Very sorry," said the professor, "Still have one man working with own hands."

anodic organic reactions take place. Because the average overpotential for these is less than that for the oxygen evolution that they replace, the cell potential for water electrolysis is significantly reduced. Since the cost of the electricity needed to produce a unit quantity of hydrogen is proportional to the cell potential (which itself is proportional to the anode overpotential), the use of coal slurries (which are cheap) leads to a reduction in the cost of hydrogen by means of water electrolysis.

In order to understand the processes occurring, it is necessary to know the principal organic compounds produced in the anodic reaction. This, however, presents a difficulty because of the great number (more than 50) of compounds involved. Moreover, coal is partly soluble in aqueous acid solution, so that even at the start of the electrolysis, a large number of organic compounds have already been introduced into the solution. It is therefore necessary to identify both qualitatively and quantitatively several dozen compounds present before electrolysis and the greater number of different compounds present afterward.

Because of the large numbers of compounds involved, the analytical problem seems to present a barrier to the investigation. However, it can be solved by making gas chromatographic (GC) and mass spectroscopic (MS) measurements on the solution before and after the electrolysis. The (GC-MS) readings from a given solution are then sent electronically to a suitably programmed computer in a distant university, and the computer scans the GC-MS patterns. Programmed in the memory of this computer are the GC-MS patterns of about 6000 compounds. The computer is able to judge the degree to which the GC-MS patterns provided by the researcher fit particular compounds in its memory. Clearly, fits of less than 90% raise doubts as to whether the compound chosen as a best fit by the computer is the one present in the coal slurry mixture. The method does not usually give "highly probable" fits for more than 20–30% of the compounds present, but it turns a hopeless task into a possible one.

**2. Automated Mechanism Analysis.** Reddy (1975) was the first to record the suggestion of using pattern recognition in analyzing electrochemical mechanisms. One might think of an electrode and solution setup as being prepared at a high degree of purity beforehand. Then a computer, together with easily available electrochemical equipment, would be programmed to carry out (for example) the following series of measurements:

1. Current-potential sweeps over a chosen potential range and repeated at several different sweep rates.
2. A series of current-time measurements, each at a certain fixed potential.
3. Measurement of interfacial impedance and phase angle over a frequency range of, say,  $10^{-3}$  to  $10^3$  s<sup>-1</sup>. Corresponding calculation of  $Z_{\text{real}}-\omega$ ;  $Z_{\text{imag}}-\omega$ , and  $Z_{\text{real}}-Z_{\text{imag}}$  plots.
4. Subjection of the cell to a series of pressures and measurement of current as a function of pressure over a range of one to a few thousand atmospheres.

From such an experimental program, several dozen derived plots can then be compared with those stored in the computer memory for the alternative reaction pathway and rate-determining steps that are possible for the type of reaction being studied.

Methods associated with the use of computers and robots often meet an initial resistance from research workers. This is partly because they fear losing their jobs. However, there are some disadvantages in using computers and robots in research (e.g., in an  $i$ - $t$  curve, one has to judge the steady state). The wisdom of attempting robotization has to be evaluated in each case for the likely gain in time and economics versus the loss of the “judgment” inherent in human comprehension.<sup>61</sup>

## Further Reading

### Seminal

1. J. Tafel, *Z. Physikal. Chem.* **50**:641 (1905). First experiment indicating that current density depends on the exponential value of the overpotential.
2. F. P. Bowden and E. K. Rideal, *Proc. Roy. Soc. London* **120A**: 59 (1928). First real area measurements, first transients.
3. P. Bakendale, *Discuss. Faraday Soc.* **1**: 46 (1947). Rational interpretation of meaning of temperature coefficients.
4. M. Temkin, *Zhur. Fiz. Khim.* **15**: 296 (1941). Analysis of heats of activation.
5. G. J. Hills and D. R. Kinniburgh, *J. Electrochem. Soc.* **113**:1111 (1960). Rate as a function of pressure.
6. Y. R. Ivanov and V. C. Levich, *Dokl. Akad. Nauk., SSSR* **126**: 1029 (1959). First theory, rotating disk with ring.
7. A. N. Frumkin and L. N. Nekrasov, *Dokl. Akad. Nauk., SSSR* **126**:115 (1959). First use, rotating disk with ring.
8. P. Dolin and B. Erschler, *Acta Phys. Chem.* **13**: 747 (1940). First use, equivalent circuit, in electrode kinetics.
9. J. C. B. Randies, *Discuss. Faraday Soc.* **1**:11 (1947). A simple derivation of the exchange current density from impedance measurements.
10. M. Neugebauer, G. Nauer, N. Brinda-Knopik, and G. Gidaly, *J. Electroanal. Chem.* **122**: 237 (1981). First Fourier transform infrared spectra on electrodes.
11. A. K. N. Reddy, M. A. U. Devanathan, and J. O'M. Bockris, *J. Electroanal. Chem.* **6**: 61 (1963). First use of ellipsometry to follow a dynamic electrode process.
12. W. K. Paik and J. O'M. Bockris, *Surf. Sci.* **18**:61 (1971). First exact ellipsometric solutions in one measurement.
13. S. G. Christov, *Electrochim. Acta* **4**: 306 (1961). Separation factors analysis in electrode kinetics.

<sup>61</sup>Reminded that George Washington spent most nights of his presidency in bed in the town bearing his name, and told that this involved the nightly act of resting his right leg on the bed, a computer might be asked where he rested his left leg. It would begin a search in its memory for Washington, president, George, left leg, in bed, and would be likely to continue searching for a very long time.

14. J. O'M. Bockris, D. G. M. Matthews, and S. Srinivasan, *Discuss. Faraday Soc.* **39**: 329 (1965). Use of quantum theory-derived values of separation factors in mechanism analysis for hydrogen evolution.
15. R. Sonnenfeld and P. K. Hansma, *Science* **232**: 211 (1986). First use of STM in electrochemistry.
16. M. Szklarczyk and J. O'M. Bockris, *J. Electrochem. Soc.* **137**: 452 (1990). First STM report of distinguishability of atoms on surface in contact with liquid.
17. S. W. Feldburg, in *Analytical Chemistry*, A. J. Bard, ed., Vol. 3, p. 199; (1969). First application of explicit finite-difference method to electrochemistry.
18. M. Szklarczyk, O. Velev, and J. O'M. Bockris, *J. Electrochem. Soc.* **136**: 2433 (1989). First atomic resolution in *in situ* electrochemistry.

## Papers

1. Z. Nagy, "D. C. Relaxation Techniques in Electrode Kinetics," in *Modern Aspects of Electrochemistry*, R. E. White, B. E. Conway, and J. O'M. Bockris, eds., Vol. 21, p. 137, Plenum, New York (1990).
2. R. Sonnenfeld, J. Schnei, and P. Hansma, "Scanning Tunneling Spectroscopy—A Natural for Electrochemistry," in *Modern Aspects of Electrochemistry*, R. White, B. E. Conway, and J. O'M. Bockris, eds., Vol. 21, p. 1, Plenum, New York (1990).
3. H. D. Abruna, "X-rays as Probes of the Electrochemical Interface," in *Modern Aspects of Electrochemistry*, J. O'M. Bockris, R. E. White, and B. E. Conway, eds., Vol. 20, p. 205, Plenum, New York (1989).
4. R. Adzic, "Reaction Kinetics on Single Crystals," in *Modern Aspects of Electrochemistry*, R. E. White, B. E. Conway, and J. O'M. Bockris, eds., Vol. 21, p. 163, Plenum, New York (1990).
5. T. Z. Fahidy and Z. H. Gu, "Dynamics of Electrode Processes," in *Modern Aspects of Electrochemistry*, R. E. White, J. O'M. Bockris, and B. E. Conway, eds., Vol. 27, p. 383, Plenum, New York (1995).
6. D. B. Sepa, "Energies of Activation," in *Modern Aspects of Electrochemistry*, J. O'M. Bockris, B. E. Conway, and R. E. White, eds., Vol. 29, p. 1, Plenum, New York (1997).
7. V. Jovancicevic and J. O'M. Bockris, "Pressure Dependence of Reaction Rate," *Rev. Sci. Inst.* **58**:1251(1987).
8. R. J. Nichols, "IR Spectroscopy at the Solid-Solution Interface," in *Adsorption of Molecules at Metal Electrodes*, J. Lipkowski and P. N. Ross, eds., VCH Publishers, Weinheim (1992).
9. W. K. Paik, "Ellipsometry in Electrochemistry," in *Modern Aspects of Electrochemistry*, J. O'M. Bockris, B. E. Conway, and R. E. White, eds., Vol. 25, p. 191, Plenum, New York (1993).
10. P. A. Christensen and A. Hamnett, *Techniques and Mechanisms in Electrochemistry, in Particular Impedance*, pp. 154–168, Blackie, London (1994).
11. C. M. A. Brett and A. M. D. Brett, *Electrochemistry*, pp. 156–189, Oxford University Press, Oxford (1993).

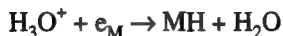
12. *Techniques for the Characterization of Electrodes and Electrode Processes*, R. Varma and J. R. Selman, eds., Wiley, New York (1994).
13. *Physical Electrochemistry*, I. Robinstein, ed., Marcel Dekker, New York (1995).
14. T. Iwasite and F. C. Nart, "FTIR," in *Advances in Electrochemical Science and Engineering*, C. W. Tobias and H. Gerischer, eds., Vol. 4, p. 123, Interscience, New York (1990).
15. W. Plith, W. Kozlowski, and T. Twomey, "Ellipsometry of Organic Layers," in *Adsorption of Molecules on Metals*, J. Lipkowski and P. N. Ross, eds., p. 1, VCH Publishers, Weinheim (1992).
16. A. Aramata, "On Single Crystal Techniques in Electrode Kinetics," in *Modern Aspects of Electrochemistry*, J. O'M. Bockris, R. E. White, and B. E. Conway, eds., Vol. 31, p. 181, Plenum, New York (1997).
17. M. Makri, G. C. Vayenas, S. Bebelis, K. H. Besocke, and C. Cavalca, "Atomic Resolution Solution by STM," *Surf. Sci.* **369**:351 (1996).
18. G. Wu and D. Baikey, "Atomic Force Microscopy Study of Cu Deposition in Motion," *J. Electrochem. Soc.* **144**:2261 (1997).
19. K. Chandrasekaran and J. O'M. Bockris, "In Situ Spectroscopic Study of Intermediates in an Electrochemical Reaction," *Surf. Sci.* **185**:495 (1987).
20. A. Szucs, D. Kitchens, and J. O'M. Bockris, "Ellipsometric Study of Di-pyridyl on Au," *Electrochim. Acta* **37**:403 (1992).
21. G. S. Popkirov and S. Ottow, 0147 *In Situ Impedance Spectroscopy of Electrochemical Si Formation*," *J. Electroanal. Chem.* **429**:47 (1997).
22. J. F. Aebersold and D. A. Stadelmann, "Rotating Disc Techniques," *Ultramicroscopy*, **62**:157 (1996).

## 7.6. MULTISTEP REACTIONS

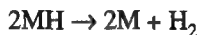
### 7.6.1. The Difference between Single-Step and Multistep Electrode Reactions



represents the deposition of silver portrayed as a single-step reaction,



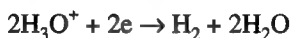
seems to be a single-step reaction but surprisingly continues to a second step:



In fact, single-step reactions are rare in electrochemistry and so it is necessary to learn about the more normal electrochemical reactions, those that occur in several steps and involve intermediate radicals.

## 7.6.2. Terminology in Multistep Reactions

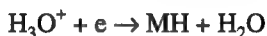
To begin with, there is, of course, always an “overall reaction.” This is the reaction seen from afar, without discrimination as to how it might be functioning. The simplest multistep reaction is that of hydrogen evolution and dissolution. Its overall reaction involves hydrated protons in solution discharging at the electrode and then with a follow-up evolution of hydrogen in gaseous form. Correspondingly,  $\text{H}_2$  can go back again to form hydrated protons via an interaction with the electrode that involves dissociation of  $\text{H}_2$ , adsorption of its atoms, and ionization of the atoms to  $\text{H}_3\text{O}^+$  ions in solution. Thus, two directions of the overall reaction would be written:



and



Then there is the question of the path. In acid solution, the proton is in the form of  $\text{H}_3\text{O}^+$  and this diffuses up to the electrode and discharges onto its surface, M:



However, to get the adsorbed H off the electrode and into the form of gaseous  $\text{H}_2$ , there are two possible paths.

1.  $\text{MH} + \text{MH} \rightarrow \text{H}_2$  (catalytic path)
- or 2.  $\text{MH} + \text{H}_3\text{O}^+ + e \rightarrow \text{H}_2\text{O}$  (electrochemical desorption path)

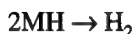
Thus, the hydrogen evolution reaction could have either of the two pathways, and it may function along either one, depending on the electrode.

## 7.6.3. The Catalytic Pathway

The catalytic pathway consists of a consecutive heterogeneous electrochemical reaction:



followed by

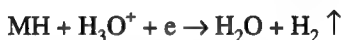


At first, when the current is switched on from the outside power source, the surface may be empty of adsorbed H. The protons discharge at first onto the entire empty surface. The coverage of the latter ( $\theta_{\text{H}}$ ) builds up with time, and consequently the

available free surface for discharge gets less. At the same time, the combination reaction for H atoms increases in rate (proportional to  $\theta^2$ ). Eventually, depending on the overpotential (but in the range of milliseconds), the rate of the discharge reaction slows down because it is discharging onto a decreasing fraction ( $1 - \theta_H$ ) of the surface and  $\theta_H$  is increasing with time at a constant overpotential. The increasing  $\theta_H$  makes the desorptive recombination reaction increase in rate according to  $k_2(\theta_H)^2$ . After an appropriate relaxation time, the rate of discharge onto the decreasingly available surface equals the rate of recombination of H and desorption as  $H_2$ , so that steady-state evolution of  $H_2$  is reached.

#### 7.6.4. The Electrochemical Desorption Pathway

The desorption pathway differs in kind from the catalytic one. It does not consist of two consecutive reactions (as does the catalytic path), but has two *simultaneous*, or *parallel*, paths. At first (and starting with the imaginary electrode surface empty of H),  $H^+$  discharge occurs onto empty sites on the metal, and the discharge reaction slows down as  $\theta_H$  builds up and  $(1 - \theta_H)$ , the fraction of free sites, decreases. However, for this second model, it is assumed that the chemical catalytic path has a negligible rate. To bring about desorption, a second parallel discharge reaction is envisaged. When  $\theta_H$  is large enough, the number of collisions of  $H_3O^+$  onto the surface-adsorbed MH becomes significant:



Hence, one has here “electrochemical desorption.”

Eventually, in steady state,  $\theta_H$  will be large (approaching 0.9, say). Most of the surface becomes occupied by the electrochemical desorption reaction. The discharge reaction into the remaining small area of the bare metal of the electrode will occur in parallel to that of the electrochemical desorption reaction (at steady state), which will have the same rate in the desorption reaction. Both reactions occur in parallel.

#### 7.6.5. Rate-Determining Steps in the Cathodic Hydrogen Evolution Reaction

In the catalytic mechanism, the two consecutive reactions are likely to have radically different rate constants. If the reaction for the proton discharge is relatively small compared with that for the catalytic desorption, the former reaction will determine the rate of the overall reaction in steady state. The catalytic reaction will react quickly when there are adsorbed H atoms to deal with. Since the recombination reaction is assumed here to have a relatively high rate constant ( $k_2$ ), then as soon as some H atoms arrive on the surface, they will form adsorbed H, which will recombine to  $H_2$ . After gathering a few  $H_2$ 's together, these will nucleate to form a tiny bubble, which will grow and detach itself from the electrode surface. Because the recombination rate constant is large, the adsorbed H is quickly removed, and  $\theta_H$  remains small.

Such a mechanism is called *rate-determining discharge with fast catalytic desorption*. The terms “fast” and “slow” refer to the rate constants. The actual rate of each of the two reactions must eventually be equal in the steady state for  $d\theta_{\text{H}}/dt$  to be zero.

Now, consider the other possibility, i.e., that the recombination reaction has a small rate constant compared with that of the rate constant for proton discharge. Of course,  $\theta_{\text{H}}$  will build up (since  $k_2\theta_{\text{H}}^2$  is relatively slow), and maybe not reach the rate of the discharge reaction until  $\theta_{\text{H}} > 0.01$  (though  $< 0.5$ ). Here, much depends on the value of  $k_2$  (the rate constant for the catalytic desorption). However, the reaction possesses a feature not seen in the first version (the rate-determining proton discharge). This feature is *pseudo-equilibrium*. Thus, if the rate constant for the discharge of protons onto the bare surface and the corresponding ionization of H back to  $\text{H}_3\text{O}^+$  is large, it is likely that while waiting for the lethargic recombination reaction to occur, ionization of H back to protons will take place. A thought experiment might envisage  $10,000,000 \text{ protons s}^{-1} \text{ cm}^{-2}$  discharging and  $9,900,000 \text{ cm}^{-2} \text{ s}^{-1}$  reionizing so that 100,000 would be left over and form  $50,000 \text{ H}_2 \text{ cm}^{-2} \text{ s}^{-1}$ . The imaginary quantities used in this illustration merely make a point: Pseudo-equilibrium is the state of a foregoing reaction, a fast reaction, *before* a rate-determining step. It is not quite an equilibrium, hence the word “pseudo” but in our mathematical development, it will be assumed as a viable approximation that the forward and backward reaction rates are equal. Thus, the catalytic path here occurs either with a rate-determining step in the proton discharge (then  $\theta_{\text{H}} < 1$ ) or with the rds in the recombination reaction ( $0.01 < \theta_{\text{H}} < 0.5$ ). In this latter case, the discharge reaction is taken as being in pseudo-equilibrium.

The rate-determining step in the electrochemical desorption path follows thinking similar to that for the catalytic path. If the rate constant for the discharge of  $\text{H}_3\text{O}^+$  onto a bare surface is relatively low (and the alternative of a catalytic recombination reaction is still lower), there will be an rds for discharge and a rapid electrochemical desorption. But such a pathway is less likely because its rate must be proportional to  $\theta_{\text{H}}$ , and this is low by definition (rapid removal of H by fast desorption). A more likely rds for the reaction mechanism is that with a fast discharge reaction onto the bare surface, the holdup being the removal of the adsorbed H. Then  $\theta_{\text{H}}$  will grow with time to be relatively large (so that electrochemical desorption becomes more likely). Here, there is no pseudo-equilibrium—the discharge reaction occurs *always* in forward mode (as long as one is sufficiently removed from the reversible region) and is equal, in steady state, to the rate of the desorption reaction,  $\text{H}_3\text{O}^+ + \text{MH} + \text{e}_0^- \rightarrow \text{H}_2$ . The two are said to be coupled (Fig. 7.67).

### 7.6.6. Some Ideas on Queues, or Waiting Lines

Before examining multistep reactions, it is worthwhile giving qualitative consideration to the general problem of the formation of queues, or waiting lines. This problem can be posed in the following familiar terms (Fig. 7.68).



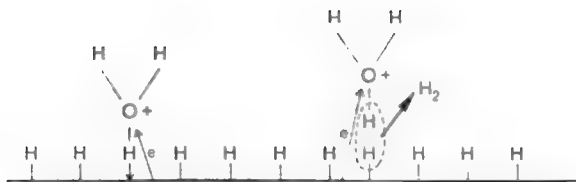


**Fig. 7.67.** Kobosew and Nekrassow model. Recombination is very slow, hence  $\theta_H \rightarrow 1$ . The desorption stage is the discharge of  $H^+$  on an absorbed H, and this reaction determines the availability of empty sites for fast proton discharge onto the metal. (Reprinted from J. O'M. Bockris and S. U. M. Khan, *Surface Electrochemistry*, Plenum, 1993, p. 316.)

Suppose that passengers (undertaking a train journey) arrive at the ticket counter. At the counter, they have to be serviced, i.e., issued tickets, information, etc. It is obvious that if the arrival rate of passengers at the ticket counter (to be referred to as a *servicing center*) is greater than the servicing rate, then a queue, or waiting line, of passengers builds up.

This is not an isolated example. One can speak of queues of customers at a supermarket counter, of automobiles at traffic lights, of airplanes at an airport, of patients at the receiving ward of a hospital, of telephone calls at a switchboard or exchange, of components on a factory assembly line, of fluids flowing through narrow constrictions, etc.

In all these cases, something arrives at a servicing center, and any servicing delay leads to the buildup of a queue. Since the basic pattern in all these examples is the same, a general theory, known as *queueing* or *waiting-time theory* has been developed. Its concern is to relate the magnitude of the queue to the arrival and servicing rates. Its utilitarian purpose is of course to understand how to minimize and possibly eliminate the queue.

Now, servicing centers are generally quite complex. They invariably consist of subcenters. An intermediate-stop airport, e.g., is a servicing center for airplanes, but there are several subcenters—landing, taxiing, unloading passengers and freight,



**Fig. 7.68.** If the rate of arrival is high enough, the throughput of passengers will depend entirely on the rate of servicing, and a waiting line will build up at the servicing center.

refueling, loading passengers, etc. Similarly, a town through which automobiles pass is a complex servicing center consisting of several traffic lights.

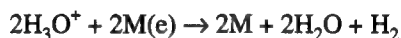
Whenever there is more than one subcenter in the servicing center, a central question emerges in queueing theory: Which subcenter of the complex servicing center is mainly responsible for the queue? Or, alternatively, which subcenter determines the overall servicing rate? For example, which particular traffic light is mainly responsible for the traffic jam? Or, in an automobile factory, what controls the overall rate of production, component manufacture, parts assembly, or final finishing?

### 7.6.7. The Overpotential $\eta$ Is Related to the Electron Queue at an Interface

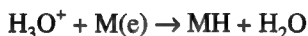
What have these thoughts on queues to do with electrodic reactions? Think of the electrified metal/solution interface as a servicing center for the electrons that flow into it from the metal to participate in the electronation reaction. The electrodic reaction represents the servicing of the electrons.

Any servicing difficulties and delays, such as preconditions that must be satisfied before electron tunneling occurs, lead to a queue of electrons on the electrode. In other words, the excess charge  $q_M$  on the electrode becomes more negative, and thus the potential difference across the interface departs from the equilibrium value. The overpotential, therefore, is determined by the electron queue.

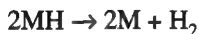
As in other complex servicing centers, the electrodic reaction may consist of a number of steps. For example, it has just been indicated that the overall electrodic reaction



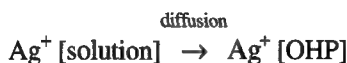
includes the following steps:



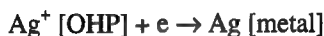
and



Or, as another example, the discharge of silver ions may consist of the transport of ions from the bulk of the solution:



and charge transfer:



Thus, the basic queueing problem arises in the case of electrodic reactions, also. Which particular subcenter (i.e., step) of the overall servicing center (i.e., electrode reaction) is the cause of the waiting line of electrons (and therefore of the overpotential  $\eta$ )? Correspondingly, which particular subcenter (or step) controls the overall servicing rate?

It can easily be seen that whichever of the unit steps in the above reactions causes the holdup in the servicing center, there will be a waiting line of electrons forming. If, e.g., the recombination reaction of hydrogen evolution (succeeding the charge transfer) is slow, the electrons will accumulate as they wait for the product of the transfer to pass through this bottleneck. If, on the other side, the transport of  $\text{Ag}^+$  ions (as a step preceding electron transfer) is slow, the electrons will accumulate as they wait for their partners like unfinished products on an assembly line waiting for parts to come to a particular place.

These problems are obviously of crucial importance. Once there is an understanding of electron waiting lines, i.e., of the origin of the current-produced potential,  $\eta$ , then one can consider how to control the factor that causes the electron waiting line and, therefore, how to control  $\eta$  and perhaps significantly reduce it.

### 7.6.8. A Near-Equilibrium Relation between the Current Density and Overpotential for a Multistep Reaction

It has been stated that though an overall electrodic reaction may consist of several steps, it is usually possible to single out one step and regard it as the essential cause of the overall electron queue and hence the overpotential  $\eta$ . What is the justification for this discriminatory attitude toward the one step?

Consider an overall electrodic reaction that takes place in  $n$  steps (Fig. 7.69). Let it be assumed, for convenience of exposition, that each step is a charge-transfer reaction with an electron acceptor receiving an electron. To simplify the treatment, let it also be assumed that the  $n$  individual electronation reactions are only slightly off equilibrium and that therefore, for each reaction, one can use the *linear* current-density-overpotential law [Eq. 7.25]. The rate of any one step in such a case is proportional to its overpotential  $\eta_j$ <sup>62</sup>:

$$i_j = \sigma_j \eta_j \quad (7.121)$$

where, in analogy to Ohm's law,  $\sigma_j$  is the reciprocal *resistance*, or the *conductivity*, of the reaction step  $j$ .

<sup>62</sup>One can ask at this point how it is possible to have different overpotentials for different steps of a reaction at one and the same metal/solution interface. Here it is necessary to remember that overpotential as a driving force is the difference between the reversible potential and the actual electrode potential. Hence, different overpotentials at one and the same actual potential attained by the electrode mean that in the process of establishing the steady state, each unit step has established a different reversible potential. This is achieved by changing the concentrations of various intermediate species or participants in the steps.

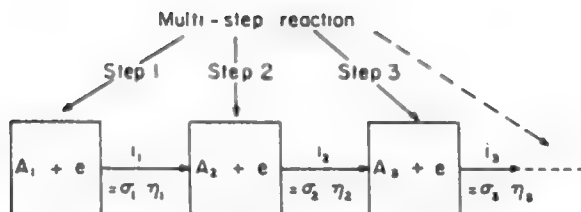


**Fig. 7.69.** In a multistep electron-exchange reaction, each step produces its individual current density. At a steady state, all these currents must be equal.

Each of the  $n$  electronation steps has associated with it an individual current density produced by a corresponding overpotential at the interface. Thus, one can write

$$\begin{aligned} i_1 &= \sigma_1 \eta_1 \\ i_2 &= \sigma_2 \eta_2 \\ &\vdots \end{aligned} \quad (7.122)$$

$$i_n = \sigma_n \eta_n$$

Now consider the situation where the overall reaction settles down and the intermediates do not change with time, i.e., when steady-state conditions are reached. Since consecutive currents are being considered, the current density from one reaction must be equal to the current density for the following reaction. Thus, the current densities of all the steps are equal to each other, i.e.,

$$\begin{aligned} i_1 &= i_2 = \cdots = i_n = i_j [j = 1, 2, 3, \dots, n] \\ &= \sigma_1 \eta_1 = \sigma_2 \eta_2 = \cdots = \sigma_n \eta_n \\ &= \frac{\eta_1}{1/\sigma_1} = \frac{\eta_2}{1/\sigma_2} = \cdots = \frac{\eta_n}{1/\sigma_n} \end{aligned} \quad (7.123)$$

The equalities (7.123) can also be written as

$$i_j \frac{1}{\sigma_1} = \eta_1$$

$$i_j \frac{1}{\sigma_2} = \eta_2$$

$$i_j \frac{1}{\sigma_n} = \eta_n \quad (7.124)$$

and summing all the equations, one obtains

$$i_j \left( \frac{1}{\sigma_1} + \frac{1}{\sigma_2} + \cdots + \frac{1}{\sigma_n} \right) = \eta_1 + \eta_2 + \cdots + \eta_n \quad (7.125)$$

or

$$i_j = \frac{\sum_{j=1}^n \eta_j}{\sum_{j=1}^n (1/\sigma_j)} \quad (7.126)$$

But the steps behave as parallel to each other as far as the electron flow through the interface is concerned. Hence, the total current must also be equal to the sum of those individual currents, i.e.,

$$i = i_1 + i_2 + \cdots + i_n = n i_j$$

The total current flowing through the interface is from (7.126):

$$i = \frac{\sum_{j=1}^n \eta_j}{\frac{1}{n} \sum_{j=1}^n (1/\sigma_j)} \quad (7.127)$$

The inverse of the conductivity of each reaction is its resistivity, and the sum of all the resistivities divided by their number gives the average resistivity,  $R_F$ , of the reaction,

$$\frac{1}{n} \sum_{j=1}^n \frac{1}{\sigma_j} = R_F \quad (7.128)$$

This total resistivity,  $R_F$ , will be called the faradaic resistance of the interface.

The argument can be generalized without restricting it to near the equilibrium. The only difference is that far from equilibrium, exponential current-density-potential relations are operative and the resistances of individual reactions as well as the faradaic

resistance are not constant any more, but dependent on overpotential. This is the basic operational difference between the faradaic and ohmic resistances.

### 7.6.9. The Concept of a Rate-Determining Step

Observe what happens in expressions (7.126) and (7.127) if the conductivity  $\sigma$  for one step  $r$  is much smaller than that for any other step,  $j \neq r$ , i.e.,

$$\sigma_r \ll \sigma_j [j \neq r] \quad (7.129)$$

In that case,

$$\sum_{j=1}^n \frac{1}{\sigma_j} = \frac{1}{\sigma_1} + \frac{1}{\sigma_2} + \dots + \frac{1}{\sigma_r} + \dots + \frac{1}{\sigma_n} \approx \frac{1}{\sigma_r} \quad (7.130)$$

because all the terms  $1/\sigma_j [j \neq r]$  become insignificant in comparison with  $1/\sigma_r$ .

Also, because of the equalities expressed in (7.123), the same must apply to the overpotentials  $\eta$ . They must all become insignificant compared with  $\eta_r$ :

$$\eta_r \gg \eta_j [j \neq r] \text{ or } \eta \approx \eta_r \quad (7.131)$$

Thus Eq. (7.127) can be rewritten as

$$i = \frac{\eta}{(1/n)(1/\sigma_r)} \quad (7.127a)$$

Hence, a single step will control the overall rate if its conductivity is much smaller (or its resistivity is much larger) than that of any other step.

The conductivity  $\sigma_j$  of any step is determined largely by its equilibrium exchange-current density  $i_{0,j}$ . The smaller the  $i_{0,j}$  is for the step, the lower is its conductivity. Thus one can say that the step with the smallest  $i_{0,j}$  generally determines the overall current.<sup>63</sup>

In fact, one can imagine (Fig. 7.70) that the electrodic reaction is like a resistor and the faradaic resistance of the overall reaction is a series combination of resistors in an electrical circuit. Then the overall conductance of the circuit is approximately given by the smallest conductance or largest resistance as long as one of the resistors is significantly—say, 10 times—larger than any of the other resistors.

One should note that  $i_{0,j}$  consists of two factors, the rate constant and the concentration of the substrate in the given step. Hence, either of those being small can be the cause of a slow rate-determining step.

<sup>63</sup>The relation of  $\sigma_r$  to the exchange current density will be discussed in more detail at the end of this section.

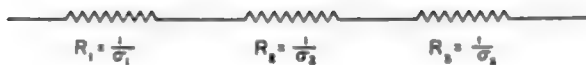


**Fig. 7.70.** The total electrical resistance of an electrode reaction consisting of a series of consecutive steps is obtained as a series combination of individual resistors.

There is another interesting result of the concept of an rds. If all the exchange-current densities except that for the rds are very large, it means that the overpotentials due to all other steps are negligibly small [cf. Eq. (7.131)]. Since the magnitude of the overpotential for a step is a measure of how far the step is from equilibrium, then if  $\eta_j \rightarrow 0$  [ $j \neq r$ ], one concludes that the  $j$ th step is almost in equilibrium, i.e., it is in *quasi-equilibrium*. Hence, the existence of a unique rds usually implies that other steps are virtually in equilibrium.

The electron waiting-line problem is hence clear. In a particular multistep electron-transfer reaction, the step with the lowest servicing rate or conductivity produces the largest queue and, indeed, the total queue is virtually a simple multiple of the queue at the rds. In other words, *in the steady state, all  $n$  steps proceed at the rate of the rate-determining step  $i_r$* , [cf. Eq. (9.4)], and the total net current is

$$i = ni_r \quad (7.132)$$

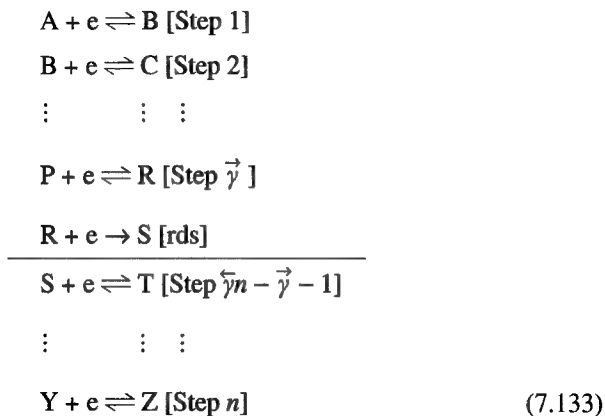
where  $n$  is the number of single-electron transfer steps in the overall reaction. Since

$$i_r = \vec{i}_r - \overleftarrow{i}_r$$

then

$$i = n(\vec{i}_r - \overleftarrow{i}_r) \quad (7.132a)$$

In order to develop the Butler–Volmer equation for a multistep reaction, expressions for  $\vec{i}_r$  and  $\overleftarrow{i}_r$  must be found for this case. Consider a multistep reaction



in which  $R + e \rightarrow S$  is the single-electron transfer rds preceded by  $\vec{\gamma}$  other single-electron transfer steps and followed by  $\overleftarrow{\gamma}$  such steps.<sup>64</sup>

The current  $\vec{i}_r$  of the forward (electronation) reaction in the rds is equal with

$$\frac{k \vec{i} e}{n} - \frac{\Delta G^{\circ\ddagger}}{RT} = k$$

to

$$\vec{i}_r = F \vec{k}_R c_R e^{-\beta F \Delta \phi / RT} \quad (7.7a)$$

Equation (7.7), in which  $c_R$  is the concentration of an intermediate, may give an erroneous impression that the current-potential relation is completely determined by the exponential term in  $\Delta \phi$ . However, species  $R$  was the result of a series of charge-transfer mechanisms, and thus its concentration, as shown below, is also potential dependent. To unravel this dependence, it will be recalled that all steps preceding and following the rds can often be assumed to be at equilibrium. Then, one can equate their forward and backward rates, e.g., for the first step  $A + e^- \rightleftharpoons B$ ,

$$\vec{i}_1 \approx \overleftarrow{i}_1$$

or, using Eqs. (7.7) and (7.11),

$$F \vec{k}_1 c_A e^{-\beta F \Delta \phi / RT} \approx F \overleftarrow{k}_1 c_B e^{(1-\beta) F \Delta \phi / RT}$$

From this,

$$c_B = K_1 c_A e^{-F \Delta \phi / RT} \quad (7.134)$$

where

$$K_1 = \frac{\vec{k}_1}{\overleftarrow{k}_1}$$

Similarly,

<sup>64</sup>The number of electrons transferred in the overall reaction is  $n$ ;  $\vec{\gamma}$  electrons are transferred in the steps preceding the rds; one electron is transferred in the rds. Thus,  $\overleftarrow{\gamma} \equiv (n - \vec{\gamma} - 1)$  electrons are transferred in the steps after the rds.



$$c_C = K_2 c_B e^{-F\Delta\phi/RT} = K_2 K_1 c_A e^{-2F\Delta\phi/RT}$$

$$c_D = K_3 c_C e^{-F\Delta\phi/RT} = K_3 K_2 K_1 c_A e^{-3F\Delta\phi/RT}$$

and, finally,

$$c_R = \left[ \prod_{i=1}^{\vec{\gamma}} K_i \right] c_A e^{-\vec{\gamma} F \Delta\phi / RT} \quad (7.134a)$$

By substituting Eq. (7.134a) in (7.7)

$$\vec{i}_R = F \vec{k}_R \left[ \prod_{i=1}^{\vec{\gamma}} K_i \right] c_A e^{-(\vec{\gamma} + \beta) F \Delta\phi / RT} = i'_{0,R} e^{-(\vec{\gamma} + \beta) F \eta / RT} \quad (7.135)$$

where

$$i'_{0,R} = F \vec{k}_R \left[ \prod_{i=1}^{\vec{\gamma}} K_i \right] c_A e^{-(\vec{\gamma} + \beta) F \Delta\phi_e / RT} \quad (7.135a)$$

The prime at  $i'_{0,R}$  indicates that the rate is now related to the concentration of the initial product  $A$  and not  $R$ . In complete analogy, the rate of the backward (deelectronation) reaction,



can be related to the concentration of the final product  $Z$  by the equations

$$\begin{aligned} \overleftarrow{i}_R &= F \overleftarrow{k}_R \left[ \prod_{i=n-\vec{\gamma}-1}^n K_i \right] c_Z e^{(\vec{\gamma}+1-\beta) F \Delta\phi / RT} \\ \overleftarrow{i}_R &= i'_{0,R} e^{(\vec{\gamma}+1-\beta) F \eta / RT} \end{aligned} \quad (7.135b)$$

where

$$i'_{0,R} = F \tilde{\kappa}_R \left[ \prod_{i=n-\vec{\gamma}-1}^n K_i \right] c_2 e^{(\vec{\gamma}+1-\beta)F\Delta\phi_s/RT} \quad (7.135c)$$

Thus, the Butler–Volmer equation for multistep reactions can be written as follows [cf. Eqs. (7.132a), (7.135), and (7.135b)]:

$$\begin{aligned} i &= n(\vec{\gamma}_R - \vec{i}_R) = n i'_{0,R} [e^{(\vec{\gamma}+1-\beta)F\eta/RT} - e^{-(\vec{\gamma}+\beta)F\eta/RT}] \\ &= i_0 [e^{(\vec{\gamma}+1-\beta)F\eta/RT} - e^{-(\vec{\gamma}+\beta)F\eta/RT}] = i_0 [e^{(n-\vec{\gamma}-\beta)F\eta/RT} - e^{-(\vec{\gamma}+\beta)F\eta/RT}] \end{aligned} \quad (7.136)$$

since  $\vec{\gamma} = n - \vec{\gamma} - 1$  and where

$$i_0 = n i'_{0,R} \quad (7.137)$$

and  $i'_{0,R}$  is given by Eqs. (7.135a) and (7.135c)

In the high-overpotential case (cf. Section 7.2.3b.2), the first exponential term can be neglected for  $n \ll 0$ , i.e., for net electronation, and the second exponential term for  $\eta \gg 0$ , i.e., for net deelectronation. In the *low-field* approximation, where both exponential terms in the Butler–Volmer equation can be linearized, Eq. (7.136) becomes

$$i = i_0 \left( \frac{nF}{RT} \eta \right) \quad (7.138)$$

This treatment remains valid for two other possible reaction sequences; these are sequences in which there are (a) chemical, i.e., noncharge-transfer, steps before and after a charge-transfer rds and (b) charge-transfer steps before and after a chemical rds. In the latter case, where no charge transfer occurs in the rds, the number of electrons transferred after the rds will be  $n - \vec{\gamma}$ . There will be no effect of potential on the rate of the rds except that arising from previous charge-transfer steps; thus, the Butler–Volmer equation for a chemical rds is given as

$$i = i_0 [e^{(n-\vec{\gamma})F\eta/RT} - e^{-\vec{\gamma}F\eta/RT}] \quad (7.139)$$

which, when the low-field approximation is applied, produces Eq. (7.138). Equations (7.136) and (7.138) may be written in a general form by including a factor  $r$ ,<sup>65</sup> e.g.,

$$i = i_0 [e^{(n-\vec{\gamma}-\beta r)F\eta/RT} - e^{-(\vec{\gamma}+\beta r)F\eta/RT}] \quad (7.136a)$$

Comparison of Eqs. (7.127a) and (7.138) allows the term  $\sigma_r$  to be identified as

<sup>65</sup>When the rds is a charge-transfer step,  $r = 1$  and, when the rds is a chemical step,  $r = 0$ .

$$\sigma_r = i'_{0,R} \frac{\eta F}{RT} \quad (7.140)$$

where  $i'_{0,R}$  is given by Eqs. (7.135). Thus, Eq. (7.127a) can be rewritten as

$$i = n i'_{0,R} \frac{nF}{RT} \eta = i_0 \frac{nF}{RT} \eta \quad (7.127b)$$

Note that Eqs. (7.136) and (7.139) pertain to a case where the rds occurs once per one occurrence of the reaction sequence. A more general expression will be given in Section 7.6.11.

### 7.6.10. Rate-Determining Steps and Energy Barriers for Multistep Reactions

Every reaction has an energy barrier associated with it. When, therefore, there are a series of consecutive reactions, one has a series of consecutive barriers (Fig. 7.71). The overall reaction corresponds to the passage in one direction of the point representing the system across all the barriers.

Suppose the standard free energy barrier is as shown in Fig. 7.72. It will be noticed that step 1 has a larger standard free energy of activation<sup>66</sup> than step 2, i.e.,

$$\Delta G_{A \rightarrow B}^{\circ \ddagger} > \Delta G_{B \rightarrow C}^{\circ \ddagger}$$

On the other hand, the activated state of step 2,  $B^*$  is higher with respect to the initial state  $A$  than step 1's activated state  $A^*$ . The question is: Which step will determine the overall rate of the reaction?

Assume that step 1 determines the overall rate  $\vec{v}$ . One has

$$\vec{v}_{\text{step 1}} = \frac{kT}{h} c_A \exp \left( -\frac{\vec{\Delta} G_{A \rightarrow B}^{\circ \ddagger}}{RT} \right) \quad (7.3)$$

If, however, step 2 is controlling the overall rate, then

$$\vec{v}_{\text{step 2}} = \frac{kT}{h} c_B \exp \left( -\frac{\vec{\Delta} G_{B \rightarrow C}^{\circ \ddagger}}{RT} \right)$$

One may take into account the fact that steps other than the rds can be considered in virtual equilibrium. Hence the substance  $B$  is in equilibrium with the reactants of  $A$ . Therefore, the law of mass action can be used, i.e.,

<sup>66</sup>The quantity  $\Delta G_{A \rightarrow B}^{\circ \ddagger}$ , and like quantities, is the standard free energy of activation, which governs the rate of passage of a representative point in the system from  $A$  to  $B$ . It is *not*  $G_B^\circ - G_A^\circ$ , but  $G_A^{\circ \ddagger} - G_A^\circ$  (see Fig. 7.72).

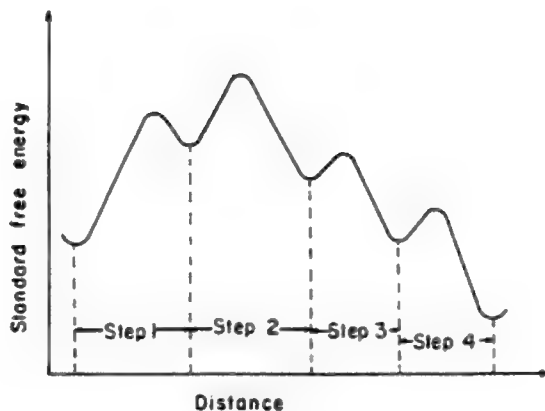


**Fig. 7.71.** Activation-energy barrier for a multistep reaction.

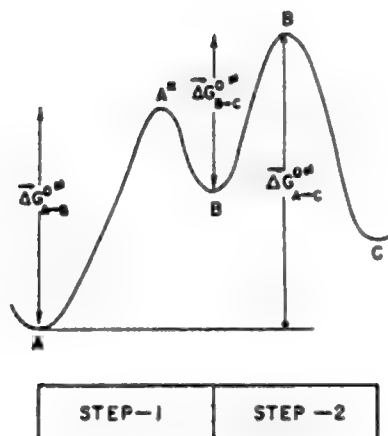


**Fig. 7.72.** The activation-energy barrier is the total change in energy between the initial state and the activated state with the highest standard free energy.

$$\frac{c_B}{c_A} = \exp \left( -\frac{\Delta G_{A \rightarrow B}^\circ}{RT} \right)$$

where  $\Delta G_{A \rightarrow B}^\circ$  is the standard free energy of formation of the substances at B. Hence, by substituting for  $c_B$  in Eq. (8.11a), one gets

$$\begin{aligned} \vec{v}_{\text{step 2}} &= \frac{kT}{h} c_A \exp \left( -\frac{\Delta G_{A \rightarrow B}^\circ}{RT} \right) \exp \left( -\frac{\Delta G_{B \rightarrow C}^{\circ\dagger}}{RT} \right) \\ &= \frac{kT}{h} c_A \exp \left( -\frac{\Delta G_{A \rightarrow C}^{\circ\dagger}}{RT} \right) \end{aligned}$$

On comparing expressions for  $\vec{v}_{\text{step 1}}$  and  $\vec{v}_{\text{step 2}}$ , it is clear that because

$$\Delta G_{A \rightarrow C}^{\circ\dagger} > \Delta G_{A \rightarrow B}^{\circ\dagger}$$

one has

$$\vec{v}_{\text{step 2}} < \vec{v}_{\text{step 1}}$$

That is, step 2 determines the overall rate  $\vec{v}$ , or

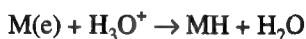
$$\vec{v} \approx \vec{v}_{\text{step 1}}$$

*One concludes that to qualify as the rds, it is not which step has the highest activation standard free energy with respect to the energy of the previous state that is important, but which step has the highest standard free energy of the activated state compared with that of the initial state.*

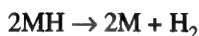
### 7.6.11. How Many Times Must the Rate-Determining Step Take Place for the Overall Reaction to Occur Once? The Stoichiometric Number $\nu$

The essential result of these last sections is that a single step, the rds, out of a sequence of steps, can determine the rate of the overall reaction. It was quickly assumed, however, that if the rds occurs once, the overall reaction also occurs once. In other words, it has been assumed that there is a one-to-one correspondence between the occurrence of the rds and the overall reaction. Is this always so?

Consider, e.g., that the electronation of hydrated protons, i.e.,



is the rds in the hydrogen-evolution reaction. If this rds occurs only once, then only one adsorbed hydrogen atom has been produced. But it takes two hydrogen atoms to produce a hydrogen molecule:



Hence, in this example, two occurrences of the rds are required to produce one occurrence of the overall reaction. One says that the *stoichiometric number*  $\nu$  of such a reaction scheme is 2. Thus, a stoichiometric number of  $\nu$ , as introduced by Horiuti in 1939, indicates that there is a  $\nu$ -to-one correspondence between the occurrences of the rds and the overall reaction.

In situations where the stoichiometric number is  $\nu$ , what is the theoretical relationship between the current density  $i$  and the overpotential  $\eta$ ? It has been shown [Eq. (7.127a)] that, when  $\nu = 1$ , the overall current density is given by

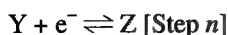
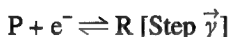
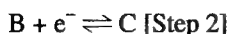
$$i = \frac{nF}{RT} i_0 \eta \quad (7.127b)$$

under conditions where the use of the linear law is justified. Thus, the conductivity for the overall reaction is determined by  $(nF/RT)i_0$ . Is this the case when the rds occurs more than once, i.e.,  $\nu$  times, for each occurrence of the overall reaction?

Up to now we have dealt with  $n$  electrons, out of which one was transferred in the once-occurring rds and  $n - 1$  were transferred in  $n - 1$  other, faster steps. The situation is changed now in that  $\nu$  electrons are now transferred in  $\nu$  times repeated rds and  $n - \nu$  electrons in the remaining, faster steps.

The rate-determining step,  $R + e^- \rightarrow S$  would have to be repeated  $\nu$  times if (1) more than one  $R$  particle is formed by the preceding  $\vec{\gamma}$  steps or (2) more than one particle  $S$  is required for the following sequence involving now  $\vec{\gamma} = n - \vec{\gamma} - \nu$  charge-transfer steps (since, not one, but  $\nu$  electrons are now transferred in the  $\nu$  times repeated rds).

Consider now a more general case of a multistep reaction  $A + ne^- \rightarrow Z$ :



(7.133a)

Applying the law of mass action for the steps in quasi-equilibrium, one has, in analogy to those equations related to (7.134)

$$c_B = K_1 c_A e^{-F\Delta\phi/RT}$$

$$c_C = K_2 c_B e^{-F\Delta\phi/RT} = K_1 K_2 c_A e^{-2F\Delta\phi/RT}$$

$$c_D = K_3 c_C e^{-F\Delta\phi/RT} = K_1 K_2 K_3 c_A e^{-3F\Delta\phi/RT}$$

Taking now the products of all terms to  $c_R$  and remembering that this rds occurs  $\nu$  times, one finds that  $c_{R^P}$  and  $c_R$  are equal to

$$c_{R^P} = \left[ \prod_{i=1}^{\vec{\gamma}} K_i \right] c_A^{1/\nu} e^{-\vec{\gamma} F \Delta\phi / RT} \quad (7.134b)$$

and

$$c_R = \left[ \prod_{i=1}^{\vec{\gamma}} (K_i) \right]^{1/\nu} c_A e^{-(\vec{\gamma}/\nu) F \Delta\phi / RT} \quad (7.134c)$$

The rate of the rds [cf. Eq. (7.7)] is expressed as

$$\vec{i}_R = F \vec{k}_R c_R e^{-r\beta F \Delta\phi / RT}$$

which, when Eq. (7.134c) is substituted for  $c_R$ , becomes

$$\vec{i}_R = F \vec{k}_R \prod_{i=1}^{\vec{\gamma}} (K_i c_A)^{1/\nu} e^{-(\vec{\gamma}/\nu) F \Delta\phi / RT} e^{-r\beta F \Delta\phi / RT} \quad (7.141)$$

$$\vec{i}_R = i'_{0,R} e^{-[(\vec{\gamma}/\nu) + r\beta] F \eta / RT}$$

and, hence, using Eq. (7.137), one can obtain for the total forward current  $\vec{i}$ ,

$$\vec{i} = i_0 \exp \left[ - \left( \frac{\vec{\gamma}}{\nu} + r\beta \right) \frac{F \eta}{RT} \right]$$

since  $i'_{0,R} = i_0/n$  and  $\vec{i} = n \vec{i}_R$ .

The same reasoning can be applied to the backward reaction:



the result being

$$c_{\text{S}} = \prod_{n=\vec{\gamma}-r\nu}^n (K_i c_i)^{1/\nu} e^{(\vec{\gamma}/\nu)F\Delta\phi/RT}$$

and, further,

$$\overset{\leftarrow}{i}_{\text{R}} = i'_{0,\text{R}} e^{[(\vec{\gamma}/\nu)r-r\beta]F\eta/RT} \quad (7.141\text{a})$$

and, finally,

$$\overset{\leftarrow}{i} = i_0 \exp \left[ \left( \frac{\vec{\gamma}}{\nu} + r - r\beta \right) F\eta/RT \right] \quad (7.141\text{b})$$

The total current  $i = \overset{\leftarrow}{i} - \overset{\rightarrow}{i}$  is then found to be

$$i = i_0 \left\{ \exp \left[ \left( \frac{n - \vec{\gamma}}{\nu} - r\beta \right) \frac{F\eta}{RT} \right] - \exp \left[ - \left( \frac{\vec{\gamma}}{\nu} + r\beta \right) \frac{F\eta}{RT} \right] \right\} \quad (7.142)$$

or, alternatively,

$$i = i_0 \left\{ \exp \left[ \left( \frac{\vec{\gamma}}{\nu} + r - r\beta \right) \frac{F\eta}{RT} \right] - \exp \left[ - \left( \frac{\vec{\gamma}}{\nu} + r\beta \right) \frac{F\eta}{RT} \right] \right\}$$

Both these equations are general forms of the Butler–Volmer equation; when  $\nu = 1$ , these equations reduce to (7.136).

In order to obtain the low-field approximation, both exponential terms in (7.142) are linearized, which yields

$$i = i_0 \left( \frac{nF\eta}{\nu RT} \right) \quad (7.127\text{c})$$

and the general expression for the conductivity of the reaction [cf. Eq. (7.140)],

$$\sigma_r = i'_{0,\text{R}} \frac{nF}{\nu RT}$$

where



$$i'_{0,R} = \frac{i_0}{n} \quad (7.137)$$

With reference again to Eq. (7.142), the terms  $[(n - \vec{\gamma})/\nu] - r\beta$  and  $(\vec{\gamma}/\nu) + r\beta$  are called *transfer coefficients* and are denoted by

$$\frac{n - \vec{\gamma}}{\nu} - r\beta = \tilde{\alpha}$$

and

$$\frac{\vec{\gamma}}{\nu} + r\beta = \vec{\alpha} \quad (7.143)$$

It can be easily seen that

$$\vec{\alpha} + \tilde{\alpha} = \frac{n}{\nu} \quad (7.143a)$$

These are the coefficients that determine the slope of the log  $i$  versus  $\eta$  curve (i.e., the Tafel slope of a multistep reaction) and are of primary importance in mechanism determinations.

In terms of the transfer coefficients,  $\tilde{\alpha}$  and  $\vec{\alpha}$ , Eq. (7.142) can be written from (7.24) thus:

$$i = i_0 [e^{\tilde{\alpha}F\eta/RT} - e^{-\vec{\alpha}F\eta/RT}] \quad (7.144)$$

Equation (7.144) is the most general form of the Butler–Volmer equation; it is valid for a multistep overall electrodic reaction in which there may be electron transfers in steps other than the rds and in which the rds may have to occur  $\nu$  times per occurrence of the overall reaction. This generalized equation is seen to be of the same form as the simple Butler–Volmer equation for a one-step, single-electron transfer reaction:

$$i = i_0 \left[ e^{(1-\beta)F\eta/RT} - e^{-\beta F\eta/RT} \right] \quad (7.24)$$

In comparing the general and the simple equations, it is seen that the transfer coefficients play the same role in a multistep,  $n$ -electron-transfer reaction as the symmetry factor does in one-step, one-electron transfer reaction, i.e., the  $\alpha$ 's determine how the input electrical energy ( $F\eta$ ) affects the reaction rate. Table 7.5 shows the tabulation of values for  $\vec{\gamma}$ ,  $r$ ,  $\nu$ ,  $\tilde{\gamma}$ , and  $n$ , from which  $\vec{\alpha}$  and  $\tilde{\alpha}$  have been evaluated.

**TABLE 7.5**  
**Tabulation of the Transfer Coefficients  $\vec{\alpha}$  and  $\vec{a}$  for Several Mechanisms (assuming  $\beta = 0.5$ ), where  $\vec{\gamma}$ ,  $r$ ,  $v$ ,  $\vec{\gamma}$ , and  $n$  Are Known<sup>a</sup>**

$\vec{\gamma}$	$r$	$v$	$\vec{\gamma}$	$n$	$\vec{\alpha}$	$\vec{a}$
0	0	1	1	1	0	1.0
1	0	1	2	3	1.0	2.0
1	0	2	1	2	0.5	0.5
2	0	2	2	4	1.0	1.0
0	1	1	1	2	0.5	1.5
1	1	1	2	4	1.5	2.5
1	1	2	1	4	1.0	1.0
2	1	2	2	6	1.5	1.5

<sup>a</sup>For example,  $\vec{\gamma} = 0$ ,  $r = 1$ ,  $v = 1$ ,  $\vec{\gamma} = 1$ , and  $n = 2$  is a two-step, two-electron transfer overall reaction, a reaction involving two electrochemical steps, the first of which is the rds, which occurs once per act of the overall reaction.

### 7.6.12. The Order of an Electrodic Reaction

In the kinetics of chemical reactions, the order of a reaction is a straightforward concept. One simply observes the exponents of the concentration terms in the expression for the reaction rate, e.g.,

$$-\frac{dc_A}{dt} = kc_A^a c_B^b \cdots c_N^n \quad (7.144)$$

Each exponent is termed the *order of reaction* for the species concerned, while the sum of the exponents of the concentration terms defines the *overall order* of a reaction.

Individual reaction orders are often expressed as derivatives of the log of the rate relative to the log of concentration of the particular species, at constant concentrations of all other species, for it follows from (7.144) that

$$\left( \frac{\partial \log \text{rate}}{\partial \log c_A} \right)_{c_B \cdots c_N} = a$$

or, in a general case,

$$\left( \frac{\partial \log \text{rate}}{\partial \log c_i} \right)_{c_{j \neq i}} = p_i \quad (7.145)$$

In electrodics, the reaction rate is expressed in terms of current density  $i$  (Section 7.2.1). Thus one would expect, by analogy, the electrochemical order of the reaction to be given by an expression similar to (7.145) which should result from the Butler–Volmer expression:

$$i = n(\vec{i}_r - \overleftarrow{i}_r) = nF(k_r c_A^a c_B^b \dots e^{\vec{a}F\Delta\phi/RT} - k_r c_A^{a'} c_B^{b'} \dots e^{-\vec{a}F\Delta\phi/RT}) \quad (7.146)$$

where  $A', B', \dots$  are the products of charge-transfer reactions involving  $A, B, \dots$ , respectively. The exponents  $a, b, \dots$  and  $a', b', \dots$  in (7.146) which relates the rate of reaction (current density) to the concentration of various species, are termed the *electrochemical-reaction orders*. It is stressed here that these electrochemical-reaction orders can only be related to equations such as (7.145) when  $\Delta\phi$  is constant (see below) and hence constant  $\Delta\phi$  becomes an essential part of the definition of electrochemical-reaction orders as given above.

It follows from Eq. (7.146) that each reactant  $A, B, \dots$  has a cathodic- and an anodic-reaction order, e.g.,  $a', b', \dots, a, b, \dots$ . At potentials sufficiently anodic to neglect the cathodic reaction, Eq. (7.146) can be expressed in the form of Eq. (7.145), e.g.,

$$\left( \frac{\partial \log i}{\partial \log c_A} \right)_{c_B, c_C, \dots, \Delta\phi} = a$$

$$\left( \frac{\partial \log i}{\partial \log c_B} \right)_{c_A, c_C, \dots, \Delta\phi} = b$$

At potentials sufficiently cathodic to neglect the anodic reaction, the electrochemical-reaction orders  $a'$  and  $b'$  are defined as

$$\left( \frac{\partial \log i}{\partial \log c_{A'}} \right)_{c_B, c_C, \dots, \Delta\phi} = a'$$

$$\left( \frac{\partial \log i}{\partial \log c_{B'}} \right)_{c_A, c_C, \dots, \Delta\phi} = b'$$

In a general form,

$$\left( \frac{\partial \log \overleftarrow{i}}{\partial \log c_i} \right)_{c_{j \neq i}, \Delta\phi} = p_{i,an}$$

and

$$\left( \frac{\partial \log \vec{i}}{\partial \log c_i} \right)_{c_{\neq i}, \Delta\phi} = p_{i, \text{cath}} \quad (7.147)$$

Note that in all these equations for electrochemical-reaction orders,  $\Delta\phi$  has been stipulated as a constant.

It is necessary to examine the terms in these equations more closely, particularly the concentration terms and the condition that  $\Delta\phi$  is a constant. The concentration terms in a rate equation for a multistep reaction usually have the following characteristics:

1. They refer to species other than the reactants in the rds.
2. Reaction orders do not necessarily reflect the molecularity of the rds, since reaction orders may be affected by preceding steps in quasi-equilibrium.
3. Reaction orders do not indicate the stoichiometry of the overall reaction.
4. The concentration of the given species may appear with different exponents in the rate equations for the cathodic and anodic reactions.
5. Reaction rates may be influenced by the concentration of a species that does not appear in the overall reaction.

The last point is well illustrated in the case of iron dissolution and deposition and can be generalized for all cases in which a species is formed in the reaction sequence *before* the rds and consumed *in* or *after* the rds. Very often such species are  $\text{OH}^-$  or  $\text{H}^+$ , which produces a pH dependence of the reaction rate and yet they are not involved in the overall reaction.

It has been stressed that the reaction order must be measured at a constant potential difference across the electrode/solution interface at which the reaction occurs. It will be recalled that the condition  $\Delta\phi = \text{constant}$  is tantamount to the condition that the potential of the electrode relative to a standard reference electrode is constant (Section 7.5.7.3). Thus, in order to obtain in practice the reaction order of, say, species A, one would measure current densities obtained at a certain potential  $E$  referred to a standard electrode potential, in solutions containing various concentrations of A and constant concentrations of all other reactants (Fig. 7.73). The potential  $E$  must be chosen sufficiently far from the reversible potential  $E$ , so that the exponential law (Section 7.2.3b.2) applies even at the highest concentrations of the given species in deelectronation reactions and at the lowest concentrations in electronation reactions.

One additional word of caution has to be added in this regard. In the above derivation, it was tacitly assumed that the change of concentration of the species whose reaction order was determined did not affect the potential distribution in the double layer, i.e., that  $\Delta\phi \equiv {}^M\Delta\text{OHP} = \text{constant}$  (Section 7.3.1). This is true only if the concentration of ions in the double layer remains high and unchanged with varying concentrations of the ionic species investigated. This condition can be closely approxi-

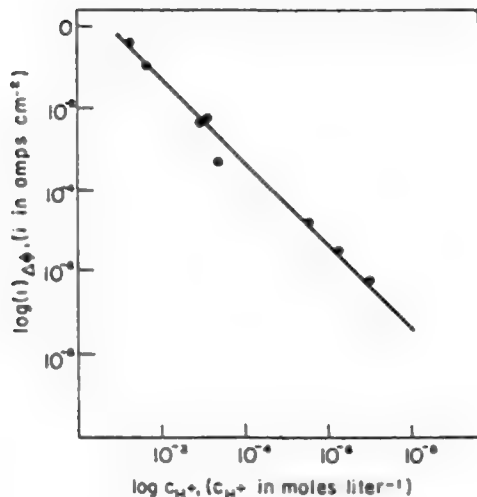


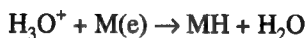
**Fig. 7.73** The reaction order of the hydrogen-evolution reaction (on mercury) in respect to a hydrogen ion is equal to 1, as seen from the slope of the straight line.

mated if the ionic strength of the solution is kept high and constant by the addition of foreign ions, i.e., of a supporting electrolyte that does not participate in the reaction.

### 7.6.13. Blockage of the Electrode Surface during Charge Transfer: The Surface-Coverage Factor

In writing out the Butler–Volmer equation, it has been assumed that, apart from factors concerning the potential-energy barrier, the current density depends only on the concentrations of reactants on the *solution* side of the interface. The metal surface was always considered empty, i.e., not blocked with any species, intermediate radical, or products.

The electrode, however, is fairly completely covered, at least by water molecules (see Section 6.7.1). Further, there may also be contact-adsorbed ions and organic molecules populating the region between the metal surface and the OHP. It depends on the radical and the reaction. For instance, the water molecules that cover most of the metal surface do not have direct effects on the reaction:



On the other hand, adsorbed hydrogen atoms do block the surface for the same reaction. If  $\theta$  is the *fraction* of the surface covered (i.e., the coverage) with adsorbed hydrogen atoms, the reaction can proceed only on the *free* surface, i.e., on  $1 - \theta$  of the electrode

surface. So, in writing out the exponential form of the Butler–Volmer equation, one has to introduce a correction. This is done as follows: In the expression for the exchange-current density, one reckons with the equilibrium coverage  $\theta_e$

$$i_0 = \frac{kT}{h} e^{-\vec{\Delta}G^{\circ \ddagger}/RT} e^{-\beta F \Delta \phi_e / RT} c_{\text{H}_3\text{O}^+} (1 - \theta_e)$$

When the overpotential goes into the exponential  $i$  vs.  $\eta$  region, the surface coverage may change from  $\theta_e$  to  $\theta$  where  $\theta$  is the (overpotential-dependent) coverage at  $\eta$ . So one has to write

$$\begin{aligned} &= \frac{kT}{h} e^{-\vec{\Delta}G^{\circ \ddagger}/RT} e^{-\beta F \Delta \phi_e / RT} c_{\text{H}_3\text{O}^+} (1 - \theta) e^{-\beta F \eta / RT} \\ &= [kT/h e^{-\vec{\Delta}G^{\circ \ddagger}/RT} e^{-\beta F \Delta \phi_e / RT} c_{\text{H}_3\text{O}^+} (1 - \theta_e)] \frac{(1 - \theta)}{(1 - \theta_e)} e^{-\beta F \eta / RT} \\ &= i_0 \frac{(1 - \theta)}{(1 - \theta_e)} e^{-\beta F \eta / RT} \end{aligned} \quad (7.148)$$

and, under the special circumstance where  $\theta_e \rightarrow 0$ , Eq. (7.148) reduces to

$$\vec{i} \approx i_0 (1 - \theta) e^{-\beta F \eta / RT} \quad (7.149)$$

The procedure for correcting for the departure from equilibrium to nonequilibrium surface coverage consists in (1) writing down the actual concentration in the Butler–Volmer equation or its relevant special case and (2) transforming this expression into one involving the equilibrium exchange-current density  $i_0$ , which contains the bulk concentration.

In the case of the deelectronation of adsorbed hydrogen, it is precisely the fraction of the surface covered that comes into the Butler–Volmer equation. One has

$$\vec{i} = i_0 \theta e^{(1-\beta)F\eta/RT}$$

It may be asked why the water can be neglected as a blocking agent, i.e., no  $1 - \theta_{\text{water}}$  term was taken into account, whereas one has to take into account a coverage term for the adsorbed hydrogen. The answer is simple if one considers the energies with which water and adsorbed hydrogen atoms are adsorbed on the electrode. Water is bound relatively lightly (10 to 20 kcal mol<sup>-1</sup>) for most electrode surfaces. In contrast, hydrogen atoms and many other substances adsorb on the electrode surface with much greater binding energies (~50 kcal mol<sup>-1</sup>) than that of water. Hence, if there is to be a competition for the surface, as there is when the products of charge transfer have to be adsorbed, water loses out. It gets desorbed during reaction because the charge-

transfer products (e.g., adsorbed hydrogen atoms) knock the water off the surface and are able to land even on the sites formerly occupied by water.

The introduction of  $\theta$  in the equations for current density need by no means refer only to the adsorbed *intermediates* in the electrode reaction. What of other entities that may be adsorbed on the surface? For example, suppose one adds to the solution an organic substance (e.g., aniline) and this becomes adsorbed on the electrode surface. Then, the  $\theta$  for the adsorbed organic substance must also be allowed for in the electrode kinetic equations. So, in Eq. (7.149), the value of  $\theta$  would really have to become a  $\Sigma\theta$ , where the summation is over all the entities that remain upon the surface and block off sites for the discharging entities. Many practical aspects of electrodictics arise from this aspect of the Butler–Volmer equation. For example, the action of organic corrosion inhibitors partly arises in this way (adsorption and blocking of the surface of the electrode and hence reduction of the rate of the corrosion reaction per apparent unit area).<sup>67</sup>

## Further Reading

### Seminal

1. R. Parsons, *Trans. Faraday Soc.* **147**: 1332 (1951). General scheme for current-potential relations and mechanism determination.
2. E. C. Potter, *J. Chem. Phys.* **20**: 614 (1952). Use of the stoichiometric number.
3. K. J. Vetter, *Electrochemical Kinetics*, Ch. 3, on electrochemical reaction orders, Academic Press, New York (1967).

### Papers

1. J. O'M. Bockris, *J. Chem. Ed.* **50**: 839 (1973).
2. I. Taniguchi, in *Modern Aspects of Electrochemistry*, J. O'M. Bockris, R. White, and B. E. Conway, eds., Vol. 20, p. 137, Plenum, New York (1989). Mechanism in the reduction of  $\text{CO}_2$ .
3. L. M. Vracar and D. M. Drazic, *J. Electroanal. Chem.* **265**: 171 (1989). More knowledge from current potential curves.
4. P. Nowak and W. Vielstich, *J. Electrochem. Soc.* **137**: 1036 (1990). Polymerization reactions.
5. A. Zagieli, P. Natashan, and E. Gileadi, *Electrochim. Acta* **35**: 1019 (1990). Complex mechanisms.
6. T. Z. Fahidy and Z. H. Gu, in *Modern Aspects of Electrochemistry*, R. E. White, B. E. Conway, and J. O'M. Bockris, eds., Vol. 27, p. 383, Plenum, New York (1995). Dynamics of electrode processes.
7. M. M. Scherer, J. C. Westall, M. Ziomek-Moroz, and P. G. Tratnyek, *Environ. Sci. Technol.* **31**: 2385 (1997). Kinetics of carbon tetrachloride reduction.

<sup>67</sup>One should note that the surface coverage can affect the standard free energy of intermediate states and thus also the activation-energy barrier and in this indirect way, the current density of the reaction.

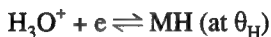
8. T. Frelink, W. Visscher, A. P. Cox, and J. A. R. van Veen, *Ber. Günsenges Phys. Chem.* **100**:599 (1996). The role of surface oxides.
9. R. Adzic, in *Modern Aspects of Electrochemistry*, R. E. White, B. E. Conway, and J. O'M. Bockris, eds., Vol. 21, p. 163, Plenum, New York (1990). Reaction kinetics on metal single-crystal electrode surfaces.

## 7.7. THE INTERMEDIATE RADICAL CONCENTRATION, $\theta$ AND ITS EFFECT ON ELECTRODE KINETICS

### 7.7.1. Heat of Adsorption Independent of Coverage

In previous material—when discussing the mechanisms of hydrogen evolution—the value  $\theta_H$  has been an important factor in the argument. For example, if  $\theta_H$  is large (approaching unity), it is likely that the mechanism of desorption of H from the surface to form  $H_2$  will be via the electrochemical desorption step rather than that of recombination.

However, in the discussion of  $\theta_H$ , our considerations have been arbitrary—taking  $\theta_H$  as “small” or “large.” Now, when the discharge reaction occurs in equilibrium, i.e.,



there is a relation between  $\theta_H$ , the concentration of  $H_3O^+$  in solution, and the electrode potential, or overpotential. To derive such a relation, one of the pieces of information one needs concerns the dependence of the heat of adsorption on  $\theta$ , and much experimental work has been done on this subject. However, to start with, and for the sake of simplicity, let it at first be assumed that  $\partial\Delta H/\partial\theta = 0$ . If a similar assumption goes for the entropy as well, one could write:

$$\tilde{k}(1 - \theta_H)c_{H^+} e^{-\beta\Delta\phi F/RT} = \tilde{k}\theta_H e^{(1-\beta)\Delta\phi F/RT} \quad (7.150)$$

rearranging gives

$$\frac{\theta_H}{1 - \theta_H} = Kc_{H^+} e^{-\Delta\phi F/RT} \quad (7.150a)$$

$$\theta = \frac{Kc_{H^+}e^{-\Delta\phi F/RT}}{1 + Kc_{H^+}e^{-\Delta\phi F/RT}} \quad (7.151)$$

Here,  $k/\tilde{k} = K = e^{-\Delta G^\circ/RT}$ , where  $\Delta G^\circ$  is the standard free energy of the above reaction. This is where the assumption about the independence of  $\Delta H$  on  $\theta_H$  comes into question.  $\Delta G_\theta = \Delta H_\theta - T\Delta S_\theta$  and, as a first approximation, it is assumed that the quantities of



this equation remain constant when the amount of adsorbed H in the steady state changes (e.g., with change of potential). Equations (7.150) and (7.151) are the electrochemical version of a famous equation developed by Langmuir.

The quantity  $\Delta\phi$  was discussed earlier (see Section 6.3.10). It is the Galvani potential difference and refers to the potential difference between the interior of the metal and the interior of the solution adjacent to the metal. The actual electrode potential as measured against a standard reference electrode is given by

$$V = \Delta\phi + \text{const} \quad (7.152)$$

where the constant involves other potential differences in the cell, such as that in which remain without change when  $\Delta\phi$  or the solution concentration vary and so we could absorb the constant in Eq. (7.152) into  $K$  and rewrite Eqs. (7.150) and (7.151) with  $V$  instead of  $\Delta\phi$ .

Thus,

$$\frac{\theta}{1 - \theta} = K c_{\text{H}^+} e^{-VF/RT} \quad (7.153)$$

This is the practical version of the electrochemical Langmuir equation. It indicates how the intermediate coverage changes with potential when the circumstances are such that the variation of the heat of adsorption with coverage is negligible in the range of  $\theta$  concerned.

### 7.7.2. Heat of Adsorption Dependent on Coverage

As mentioned earlier, much experimental work has been done on  $\Delta H_\theta$  as a function of  $\theta$  in gas-phase reactions. The heat of adsorption is usually a negative quantity and it is found experimentally that it gets less negative as  $\theta$  increases.

Assuming now that the standard entropy of adsorption remains constant with coverage, then the experimental phenomena are approximately expressed by

$$\Delta G_\theta = G_{\theta=0}^\circ + r\theta \quad (7.154)$$

Introducing (7.154) into (7.155), one obtains

$$\frac{\theta}{1 - \theta} = c_i e^{-\frac{(\Delta G^\circ + r\theta)}{RT}} e^{-VF/RT} = K_0 c_i e^{-r\theta/RT} e^{-VF/RT} \quad (7.155)$$

If one considers a region in which  $0.2 < \theta < 0.8$ , the variation of  $\ln(\theta/1 - \theta)$  is much less than that of the  $e^{r\theta/RT}$  term. As an approximation, for the limits of  $\theta$  stated, the variation of  $\ln \theta/1 - \theta$  is neglected [and  $\ln(\theta/1 - \theta)$  taken as zero], whereupon:

$$\frac{r\theta}{RT} = \ln K_0 c_i - \frac{VF}{RT} \quad (7.156)$$

### 7.7.3. Frumkin and Temkin

Frumkin (see Section 7.3.1) was the originator of equations such as (7.155). His view of the physical meaning of  $r$  was related to early studies he and his group had made on the dependence of organic molecule adsorption on the electrode potential. On the one hand there were situations in which the dipole moments of some organics (dipoles adsorbed head to head, say) caused repulsion between the adsorbed molecules, and hence lowered  $\Delta G_\theta^\circ$ , i.e., made it less negative. But Frumkin also discerned some situations in which (when the  $\theta_{\text{org}}$  was particularly high) there would be attraction between the molecules, due to dispersion force interactions. In this case,  $r$  would be negative, and  $\Delta G_\theta^\circ$  would become increasingly negative at high  $\theta_{\text{org}}$ .

Frumkin's work was largely with liquid mercury electrodes (which are easy to keep clean by frequent renewal of the liquid surface). Temkin, on the other hand, considered mostly solid electrode surfaces and here the question arises of heterogeneity—some sites on the metal surface (at ledges and corners of the structures on the surface) have metal atoms that are less bound to other metal atoms and so are more reactive to molecules that may try to adsorb there. Temkin stressed the idea that the surface of a metal would have all manner of  $\Delta H^\circ$ 's at the various types of sites. When adsorption begins ( $\theta_{\text{org}}$  is at first small), the adsorbed molecules would bind to the more attracting sites (i.e., those with the greatest bonding power), where  $\Delta G_\theta^\circ$  would be therefore highly negative. However, as the surface fills up, the more active sites (more negative  $\Delta G^\circ$ 's) become used up and therefore, for higher  $\theta$ 's,  $\Delta G_\theta^\circ$  would be less negative.

It has recently been shown (Nikitas, 1992) that (with certain approximations) the heterogeneity argument leads to the equation:

$$\Delta G_\theta = \Delta G_{\theta=0} + r\theta \quad (7.157)$$

which was earlier quoted on empirical grounds.

As to when to use Frumkin's approach or that of Temkin, as long as one is willing to accept the approximation leading to Eq. (7.156), it does not matter as far as the resulting kinetic equations (see below) are concerned. However, the thought process behind Frumkin's equation is to take account of the interaction between the adsorbed entities and that behind Temkin's is to allow for the difference in adsorption energies in different sites on the surface equation.

### 7.7.4. Consequences from the Frumkin–Temkin Isotherm

From (7.156), at constant  $V$ ,

$$\theta = \text{const} + \frac{RT}{r} \ln c_i \quad (7.158)$$

This equation is logically called *the logarithmic isotherm*. It shows that under the conditions chosen (constant  $V$  and  $0.2 < \theta < 0.8$ ),  $\theta$  is linear with  $\ln c_i$ .

Thus, in the Langmuir isotherm, there is a rather short range of  $c$ 's in which  $\theta$  varies with  $c_i$ . In a Temkin-type isotherm (Fig. 7.74),  $c$  can vary by an order of magnitude for  $\theta$  to vary by  $\sim 0.5$ . Conversely, however, an adsorbing entity obeying the Frumkin or Temkin isotherm takes three orders of magnitude of concentration change to bring about the same degree of change of  $\theta_i$  (see Fig. 7.74). It is reasonable to say that when conditions are such that  $\Delta H_{\text{ads}}$  varies with  $\theta$ , the Frumkin–Temkin isotherm is applicable and spreads out the region of linearity between  $\theta$  and  $\log c_i$ , i.e., it slows down the variation of  $\theta$  with  $c_i$ .

Consider, now the dependence of  $\theta$  upon potential under the condition that  $\Delta G_\theta$  varies with  $\theta$ . It will be less dramatic (i.e.,  $d\theta/dV$  will be much smaller) than in the situation represented by the original, simpler, corresponding, Langmuir equation [Eq. (7.153)]. If the latter isotherm is applicable to a variation of  $\theta$  with potential at constant concentration, the surface is effectively either empty of intermediate ( $\theta \ll 1$ ) or near to  $\theta \approx 1$ . With Frumkin–Temkin in control,  $\theta$  varies linearly and more slowly with  $V$  than it does with the Langmuir equation. Thus, from (7.156), at constant  $c_i$ ,

$$\theta = \text{const} - \frac{VF}{r} \quad (7.159)$$

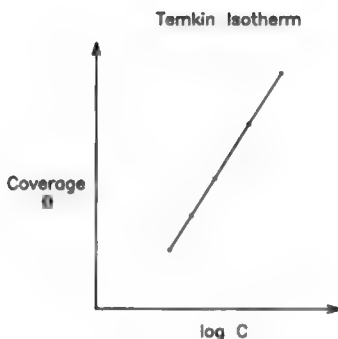


**Fig. 7.74.** In a Temkin-type isotherm, the coverage of a surface with an adsorbing entity varies with  $\log c$  (the change of  $\theta$  with  $c$  is much slower than with a Langmuir isotherm).

One thing should be noted, however, and that is that at the extreme of  $\theta$  (when  $\theta$  is less than 0.1 or very near to 1), it does not matter in practice what the applicable isotherm is. Thus, if  $\theta \ll 1$ , the term in  $e^{r\theta}$  is too small to be effective. If  $\theta \rightarrow 1$ , it can hardly vary more with either concentration or potential. In both these extremes, the Langmuir equation is applicable.

### 7.7.5. When Should One Use the Frumkin–Temkin Isotherms in Kinetics Rather than the Simple Langmuir Approach?

1. If the relative values of the rate constants among the consecutive or parallel steps in reactions such as that of hydrogen evolution have the most decisive influence here, Frumkin–Temkin should be used. If they lead to a situation in which the intermediate radical coverage tends toward zero or one, the matter is decided. As remarked above, for  $\theta \rightarrow 0$  or  $\theta \rightarrow 1$ , the Frumkin and Temkin isotherms coincide in effect with that of Langmuir.

2. If  $\theta$  is in the middle range,  $0.2 < \theta < 0.8$ , say, the appropriate isotherm could still be that of Langmuir. This would be likely to be the case for the academic systems of liquid electrodes (mercury and occasionally, liquid gallium). On solid surfaces, the effects of heterogeneity will apply and the appropriate isotherm will be that of Temkin.

Finally, a Frumkin isotherm *may* apply on Hg, also, when the adsorbed materials are substantially interactive. Usually this interaction is a Coulombic repulsion, but sometimes with concentrated situations in which  $\theta \rightarrow 1$ , ions adsorb strongly enough ( $\theta > 0.5$ ) so that attractive forces (arising from what is called “dispersive interaction”) come in and pull the particles together (cluster formation).

### 7.7.6. Are the Electrode Kinetics Affected in Circumstances under which $\Delta G_\theta$ Varies with $\theta$ ?

When one examines the rate of an electrochemical reaction and how it varies with overpotential, it is often found that equations such as (7.150) and (7.150a) (which depend on a Langmuir assumption as to the implied isotherm) are obeyed, and there is no need to modify the kinetic equations to allow for a special isotherm.

The matter is important in determining the mechanism of electrode reactions because one of the pieces of data that contributes to the evidence indicating pathway and rds is  $d \log i / d\eta$ , the gradient of the logarithmic of the rate of the reaction against the overpotential. The commonly quoted values of this coefficient (see Section 7.6.5) are derived with the assumption that  $\Delta H$  is independent of  $\theta$  ( $\theta$  tends to zero or unity). If, on the contrary,  $\theta$  is at some intermediate value, its variation with potential may affect the dependence of  $\log i$  on  $\eta$  in a mechanism-indicating way. It had better be known, therefore, which isotherm to use to express  $\theta$  as a function of  $\eta$  or  $V$ . For, if one goes on using a Langmuir assumption, the indicated value of  $d \log i / d\eta$  may not be appropriately derived and hence no longer be a valid indicator of mechanism.

In the following discussion, an example is given that serves to show that introducing a Frumkin–Temkin isotherm *does* affect the kinetic relation between the current density,  $i$ , and the corresponding overpotential. The example chosen will use the hydrogen evolution reaction once more because it is relatively simple but at the same time involves consecutive steps and alternative pathways; thus it has characteristics of many practical electrode reactions likely to be met in practice.<sup>68</sup>

Let it be assumed that there are some electrodes on which the hydrogen evolution reaction occurs by means of the catalytic desorption pathway; that the initial discharge of protons to form H atoms and the back-reaction of these to form protons is relatively fast compared with the following desorption reaction. Then the proton discharge reaction is in pseudo-equilibrium with that of H dissolution back to protons in solution. Let it be supposed that this pseudo-equilibrium will be followed by a rate-determining catalytic combination, the potential back-reaction of readsorption of  $\text{H}_2$  being assumed to be negligible in rate. Let there be two successive calculations of the overpotential ( $\eta$ )– $\log i$  relation. In the one, Langmuir conditions are observed and in the other Frumkin–Temkin.

In the Langmuir case, the rate of the rate-determining catalytic reaction is  $k_2\theta^2$ . The dependence of the rate upon potential is entirely fixed by the variation of  $\theta_{\text{H}}$  with potential. Thus,  $k_2$  is assumed not to vary with potential. Hence, as [cf. Eq. (7.153) at  $\beta < 1$

$$\theta_{\text{H}} = Kc_{\text{H}}e^{-VF/RT} \quad (7.160)$$

then,

$$i = 2Fk_2K^2\theta_{\text{H}}^2 = 2Fk_2c_{\text{H}}^2e^{-2VF/RT}$$

Or:

$$\ln i = \ln 2Fk_2K^2c_{\text{H}}^2 - \frac{2VF}{RT} \quad (7.161)$$

Therefore:

$$V = \frac{RT}{2F} \ln 2Fk_2K^2c_{\text{H}}^2 - \frac{RT}{2F} \ln i \quad (7.162)$$

Alternatively, as  $V = \eta + V_{\text{rev}}$ ,

<sup>68</sup>It differs, thereby, from simple redox reactions such as  $\text{Fe}^{3+} + e \rightleftharpoons \text{Fe}^{2+}$ . Such reactions do not involve an intermediate radical and lack consecutive steps and alternative pathways. Study of their kinetics, therefore, omits characteristics of most electrochemical reactions met, e.g., in electrochemical synthesis, energy conversion and storage, or corrosion.

$$\eta = \text{const} - \frac{RT}{2F} \ln i \quad (7.163)$$

On the other hand, in the Frumkin–Temkin case,  $k_2$  varies with potential. The reason for this can be seen in Fig. 7.75, where one sees potential energy (p.e.) curves for the surface recombination reaction of two adsorbed H atoms in close proximity reacting to form  $\text{H}_2$ , which is regarded as having a negligible heat of adsorption. The potential energy curve on the left is that for the oscillations of a single adsorbed H. It combines with another similar adsorbed H (p.e. curve not shown) to form the  $\text{H}_2$ .

On the left-hand side, the lower of the two curves represents the condition where  $\theta_{\text{H}}$  is low (and negligible). This condition pertains to an overpotential just above  $RT/F$  in value. The H is relatively tightly adsorbed and the two adsorbed H atoms react relatively slowly. As the electrode potential becomes more negative,  $\theta$  increases. Because of the Temkin equation  $\Delta G_{\theta} = \Delta G_{\theta}^{\circ} + r\theta$ , the increase of  $r\theta$  for the upper curve makes  $\Delta G_{\theta}^{\circ}$ , the free energy of adsorption of the H atoms, less negative. The binding of H atoms to the surface is less tight and the  $\text{H}_{\text{ads}} + \text{H}_{\text{ads}} \rightarrow \text{H}_2$  reaction increases in rate.

One still has (as with the Langmuir deduction),  $i = 2F k_2 \theta^2$ , but now  $k_2$ , the rate constant, varies with  $\theta$ . The amount of this variation can be seen from the diagrams; when the potential energy curve for M-H “rises” (the  $\Delta G_{\theta}^{\circ}$  becomes less negative), the

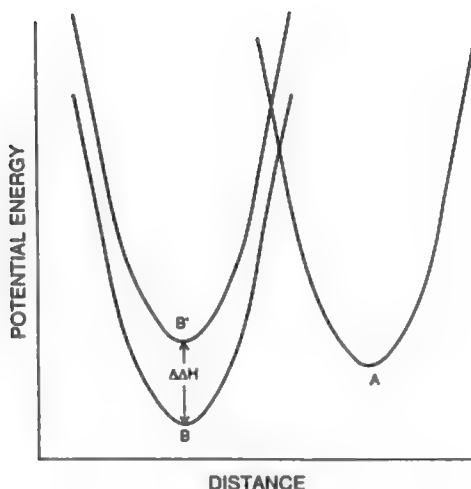


**Fig. 7.75.** The effect of the variation of the  $\Delta H$  ( $\Delta \Delta H$ ) on the potential energy distance diagram. (Reprinted from J. O'M. Bockris and S. U. M. Khan, *Surface Electrochemistry*, Plenum, 1993, p. 264.)

energy of activation is decreased. Thus, the minimum of the curve gets less negative by  $r\theta$ , but the effect of the change of  $\theta$  is less than  $r\theta$  because the intersection point of this MH curve with the p.e. curve for H-H (the curve on the right in Fig. 7.75) also moves “up,” but only by  $\gamma r \theta$ , where  $0 < \gamma < 1$ . Hence, the net change in energy of activation of the reaction due to a change in  $\theta$  from negligible to  $\theta$  for the 2 MH's is  $2r\theta - 2\gamma r\theta = 2(1 - \gamma)r\theta$ :

$$v_{2H \rightarrow H_2} = k_{2,0} \theta^2 e^{+2(1-\gamma)r\theta/RT} \quad (7.164)$$

However, from (7.159),

$$r\theta = \text{const} - VF \quad (7.159)$$

Thus,

$$i = 2Fk_{2,\theta=0} \theta_{(\eta)}^2 e^{-2(1-\gamma)VF/R} \quad (7.165)$$

One takes  $V = V_{\text{rev}} - \eta$ , and absorbs the constant exponential term in  $V_{\text{rev}}$  in the constant,  $k_{2,0}$ .

It is easy to show that if the potential energy functions in Fig. 7.75 are symmetrical,  $\gamma = 1/2$ . The effect of the linear variation with  $\theta$  is trivial compared with that of  $e^{r\theta/RT}$  (where  $r$  values range from 50 to 100 kJ mol<sup>-1</sup>) when  $\theta$  moves from, say, 0.01 to, say, around 0.5. Hence, one rewrites the equation as

$$i = 2Fk_{2,\theta=0} e^{-\eta F/RT} \quad (7.166)$$

Or,

$$\frac{\partial \ln i}{\partial \eta} = F/RT \quad (7.167)$$

This (Frumkin–Temkin) expression is to be compared with that using a Langmuir isotherm in Eq. (7.158). The value of

$$\partial \eta / \partial \ln i = -RT/2F \quad (\text{Langmuir})$$

$$= -RT/F \quad (\text{Frumkin–Temkin})$$

Thus, the applicable isotherm does indeed change the predicted kinetics (in the form of the variation of overpotential with respect to the log of the current density) in an important way. It is therefore critical, before one uses the coefficient  $\partial \eta / \partial \ln i$  in the evaluation of a mechanism, to know what kind of isotherm is effective in any adsorption equilibria that may exist in the mechanism.

## Further Reading

### Seminal

1. A. N. Frumkin, *Z. Physik*, **35**: 792 (1926).
2. M. Temkin, *Acta Physicachim. URSS*, **12**: 327 (1940).
3. E. Gileadi and B. E. Conway, in *Modern Aspects of Electrochemistry*, J. O'M. Bockris, and B. E. Conway, eds., Vol. 3, p. 347, Plenum, New York (1964).

### Modern

1. C. M. A. Brett and A. M. O. Brett, *Electrochemistry*, p. 55, Oxford Science Publications, Oxford University Press, Oxford (1993).
2. F. A. Christensen and A. Hamnett, *Techniques and Mechanism in Electrochemistry*, p. 10, Blackie, London (1993).
3. E. Gileadi, *Electrode Kinetics for Chemists, Engineers and Materials Scientists*, pp. 266–271, VCH Publishers, Weinheim (1993).
4. C. Hamann, A. Hamnett, and W. Vielstich, *Electrochemistry*, VCH Publishers, Weinheim (1998) (particularly Chapter 6).

## 7.8. THE REACTIVITY OF CRYSTAL PLANES OF DIFFERING ORIENTATION

### 7.8.1. Introduction

Most electrochemical kinetic measurements have been made on polycrystals, i.e., “normal” metals. However, metal surfaces, in reality, consist of many facets—patches—on each of which the crystals have what is called a “specific orientation.” In this section, some results of electrodic measurements are described in which the surfaces of the electrode catalysts are no longer the ill-defined mixture of many kinds of crystal orientations found in polycrystals. The results described here will be those obtained on crystals prepared in such a way that one crystal face only—having a specific, known orientation—is exposed to the solution.

Before getting to these more sharply defined results, it is necessary to define *single* crystals, the terminology by which the various crystal planes are described, and record a few words about how these individual crystal surfaces can be made in the laboratory.

### 7.8.2. Single Crystals and Planes of Specific Orientation

First, if one allows a liquid or solution to crystallize without involving it in special conditions, the solid that results will be a polycrystal—as is easily revealed by electron microscopy. An analogy can be considered: The polycrystal is rather like a collection of stones on the beach; each stone has a different shape, size, and position.



Now, there are methods available by which the crystal formed from the liquid (or vapor, or electrolyte solution) is no longer a series of little bits, but is made into just one crystal, a single crystal. Although single crystals in the shape of cubes and having a 12-inch side can be made, most single crystals used in laboratory investigations are 1–2 cm in diameter. However, they consist of one continuous crystal, not a great number of tiny crystals. In terms of the analogy of stones on a beach, the single crystal is a piece of solid rock.

By what techniques are those single crystals made? There are several methods. Here it will suffice to say that in one of these (growth from a vapor), the metal is evaporated from a polycrystal wire by heating the latter to a temperature near its melting point. In the path of the evaporating metal vapor is placed a freshly cleaved<sup>69</sup> mica surface maintained at a temperature below the melting point of the metal. The operation is carried out in an atmosphere of inert gas. Control of the rate of evaporation is the key to the successful formation of a single crystal on top of the mica.

A single crystal prepared in this way is already oriented; for example, it is oriented parallel to the face of the cleaved mica crystal base. Crystals starting on this seed are pulled out of a melt. Another method of forming a single crystal is to have it “cut” and polished. Cutting is done with a spark cutter on the crystal cradled in the arms of a goniometer, which allows the angle of the spark cutter to be precisely oriented in the direction of the desired plane.

Consider the three-dimensional arrangement of ions in a metal crystal. The ions are closely packed. If one imagines a plane cutting the assembly, then, depending on the direction of cut, characteristic arrangements of ions are exposed at the surface (Fig. 7.76). Each arrangement is generated by the repetition of a unit pattern. In silver, e.g., the unit patterns might consist (Fig. 7.77) of silver ions in the center of other silver ions arranged in hexagons or squares. The silver ions could also be arranged in rectangles as shown. The regular internal arrangement of ions in a silver crystal advertises itself at the surface through the characteristic unit pattern which represents different faces of the crystal. This is why they are known as crystal faces. Every face in a crystalline lattice can be identified precisely in terms of *Miller indexes*. For cubic lattices (e.g., silver), to describe exactly each face, plane, or direction in the lattice, three space vectors,  $x$ ,  $y$ , and  $z$  are required: one vector  $y$  in the vertical plane intersecting at right angles, two vectors  $x$  and  $z$  in the horizontal plane. Figure 7.76 shows three crystal faces of the cubic lattice (a)(111), (b)(100), and (c)(110), crystal planes. For a hexagonal lattice (e.g., zinc), to describe lattice faces and planes exactly, one requires four space vectors because this lattice structure is now compared with the four-sided cubic lattice: one vector  $y$  in the vertical plane intersecting at right angles

<sup>69</sup>Certain materials can be “cleaved,” i.e., shocked into splitting into two halves *along a specific crystal plane*. This method limits the choice of planes available, but a single crystal can be cut along other planes by using a spark to remove the unwanted parts of the crystal and a goniometer (an instrument for measuring interfacial angles of crystals) to guide the spark cutter.

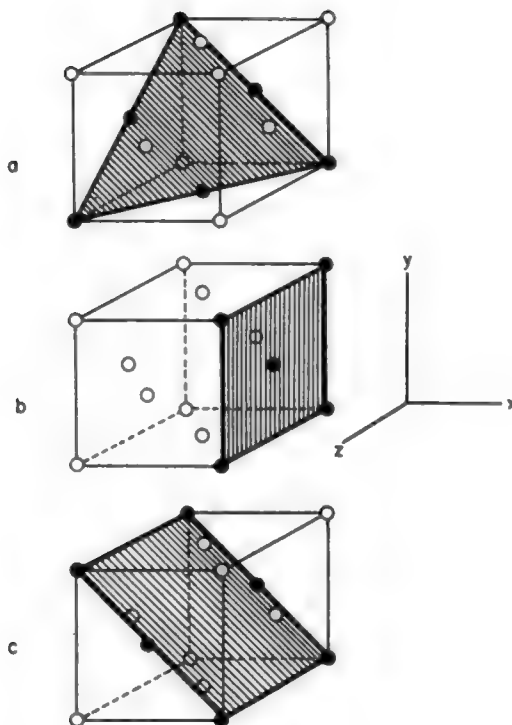


**Fig. 7.76.** Three faces of a cubic lattice showing how the atomic arrangement varies with the direction of the plane chosen.

three vectors  $u$ ,  $x$ , and  $z$ , each describing a  $60^\circ$  angle to the other in the horizontal plane. The Miller index is then the reciprocal of the length described along each vector and expressing the ratio of each vector length in integral numbers. For example, Fig. 7.76 describes a unit-cell length along the  $x$  vector and infinity along the  $y$  and  $z$  vectors. Taking the reciprocal of these lengths and expressing it as a ratio, one to another, produces for  $xyz$  the (100) plane. A small (e.g., 100-nm) square face is known as a *facet*. Figure 7.77 shows what the arrangement of three surface planes looks like for the closely packed cubic lattice of silver.

### 7.8.3. Another Preliminary: The Voltammogram as the Arbiter of a Clean Surface

It is important to make absolutely sure that no interference by adsorption of contaminants from solution gets in the way of understanding the effects of a change

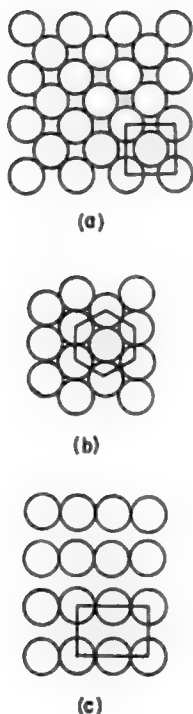


**Fig. 7.77.** Three crystallographic arrangements as seen for the close-packed cubic lattice of silver.

in crystal plane on electrode kinetics. It was first suggested by Conway and Angerstein-Kozłowska (1973) that the precise details of the shape of the current-potential sweep relation (or “voltammogram,” see Section 8.6.6), done on platinum can be used to indicate the degree of “cleanness” of a surface. On gold, it has been possible to confirm this. Surface spectroscopic observations show the adsorbed contaminant, and one can see the change it brings about in the voltammogram. One finds that if the potential of the electrode is “swept” up and down through its range a few times (thus oxidizing or “burning off” the contaminant), the shape of the voltammogram returns to that known from experience to represent (e.g., in  $0.1\text{ M H}_2\text{SO}_4$  etc.) behavior in the uncontaminated state. Such a shape is, as it were, the reference state—the evidence for integrity—when it comes to finding differences due to a change in crystal orientation (Fig. 7.78).

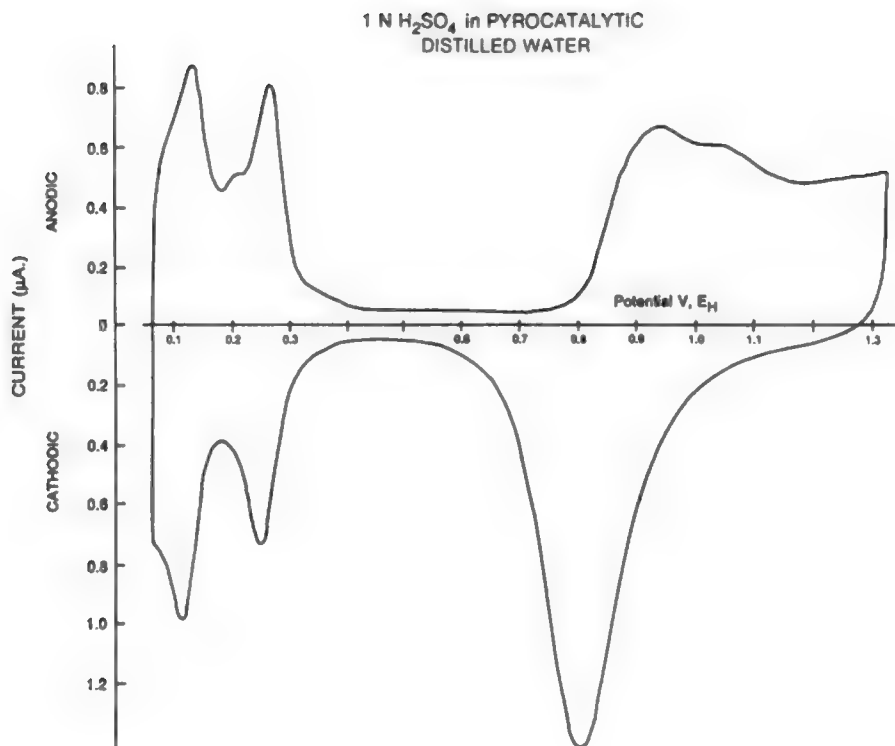


**Fig. 7.78.** Electrochemical spectrum of a clean Pt electrode in 0.5 M  $\text{H}_2\text{SO}_4$  solution. (Reprinted from H. Angerstein-Kozłowska, in *Comprehensive Treatise of Electrochemistry*, Vol. 9, E. Yeager, J. O'M. Bockris, B. E. Conway, and S. Sarangapani, eds., Plenum, 1984, pp. 15–61.)

#### 7.8.4. Examples of the Different Degrees of Reactivity Caused by Exposing Different Planes of Metal Single Crystals to the Solution

As expected, H ionizes from the surface of a platinum electrode previously used to evolve  $\text{H}_2$ , when the electrode is swept anodically. However, *two* peaks, each at a characteristic anodic potential, are always observed (even after the electrode has been subjected to an  $\text{H}_2\text{-O}_2$  flame to remove contamination) (Fig. 7.78).

The reason for these two peaks was first elucidated by Will (1965). He exposed the 111, 100, and 110 planes sequentially to 0.1 M  $\text{H}_2\text{SO}_4$ . On the 111 plane (Fig. 7.79), a large peak was observed as the potential grew more anodic, and of the two peaks observed on the polycrystal, only the one large peak was observed on this

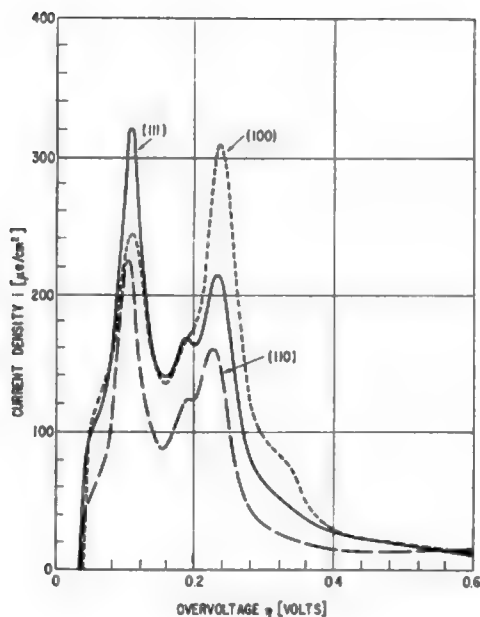


**Fig. 7.79.** Current-voltage sweep curves on platinum single-crystal faces (100), (111), and (110) at 25 °C. Sweep range 50–1550 mV, sweep rate 0.1 V/s. (Reprinted from F. G. Will, *J. Electrochem. Soc.* **112**(4): 451, 1965. Reproduced by permission of The Electrochemical Society, Inc.)

exclusively 111 electrode. On the corresponding 100 electrode, a peak was also observed, but it was shifted in potential from that on the 111 plane, and its maximum coincided with that of the more anodic peak on the polycrystal, indicating that here (in the 100 plane) H was more tightly bound than was the H on the 111 plane. No second peak was observed in the 100 plane, and the 110 plane exhibited no peaks at all.

These results are most informative as far as electrode structures and electrocatalysis are concerned. They show clearly that the two peaks on the polycrystal arise because the crystal consists of a mixture of 111, 110, and 100 planes. Evidently, our earlier crude perception that H is uniformly adsorbed in the electrode must be radically modified. It is adsorbed heterogeneously, and it ionizes from the 111 and 100 planes of the polycrystal sequentially, in relation to the potential when the latter is swept anodically.

Experiments on the 111 planes of platinum have shown a detailed structure in the anodic sweep (0.05 to 0.6 RHE),<sup>70</sup> but this structure is extinguished if contamination from the solution is present. Another interesting effect occurs if the  $\text{H}_2\text{SO}_4$  solution is replaced by  $\text{HClO}_4$ . In the potential range 0.05 to 0.5 (RHE) on the anodic side, the voltammogram splits into two parts in the presence of  $\text{ClO}_4^-$ .

The cause of this unexpected behavior turns out to be a change in structure of the platinum surface, evidently brought about by adsorbed  $\text{ClO}_4^-$ . The long-range order (flat planes) present in 111 has been changed to a more stepped surface. The importance is not so much in the detail here, but in the fact that work with the individual planes of single crystals can reveal much about electrode processes—even about the nature of the surface—and how it is changed by the nature of the solution, and what ions adsorb from it.

The study of the reduction of  $\text{O}_2$  on well-defined crystal planes (Adzic, 1984) confirms that the character of an electrode depends sharply on the crystal plane exposed to the solution. Measurements made on polycrystals reflect a mixture of properties characteristic of each plane. The results are much clearer if one sticks to observations from one plane. For example, a study of  $\text{O}_2$  reduction on the three planes of Au gives quite different Tafel lines (Fig. 7.80).

On the 100 plane there are diagnostic criteria, which are collected in Table 7.6. These data fit the following mechanism:



Further reduction of  $\text{HO}_2^-$  probably involves a direct pathway:



The rate constants for the various planes show differences of up to 5 times (see Table 7.7).

The last example here concerns the mechanism of the oxidation of methanol. This is an important mechanism because methanol is a likely fuel for fuel cells powering electric cars. The single crystal work on methanol oxidation is associated with the

<sup>70</sup>When an electrode potential is measured against the standard hydrogen electrode (Section 7.2.7), this is indicated by the abbreviation SHE. Alternatively, if the measurement is made against an  $\text{H}_2$  electrode at the same conditions of pH and temperature as in the solution of the test electrode, and at the same 1 atm hr pressure, the potential of the test electrode is designated RHE, for “reversible hydrogen electrode.”

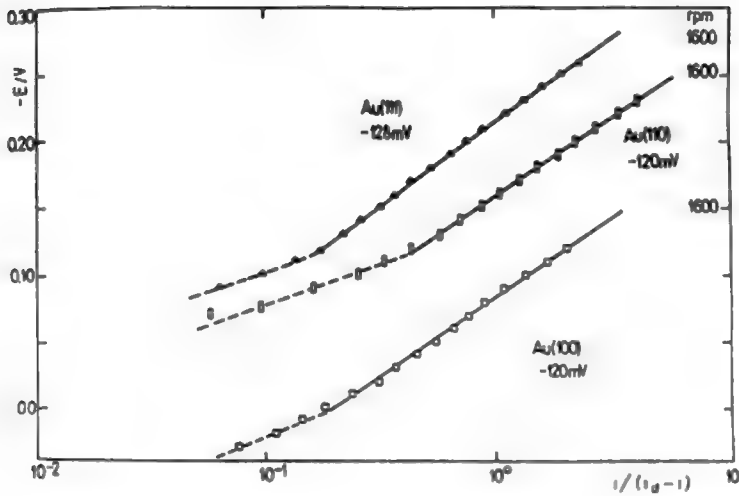


**Fig. 7.80.** Tafel plots for  $\text{O}_2$  reduction on Au single-crystal electrodes in 0.1 M NaOH. (Reprinted from R. Adzic and N. M. Markovic, *J. Electroanal. Chem.* **138**: 189, copyright 1982 with permission from Elsevier Science.)

**TABLE 7.6**  
**Experimental Values of Diagnostic Criteria for  $\text{O}_2$  Reduction on the Au(100) Surface**

Quantity	$\text{O}_2$ reduction	$\text{HO}_2^-$ reduction	$\text{HO}_2^-$ oxidation
$\frac{\partial E}{\partial \ln i}$	$-2RT/F$	$-2RT/F$	
$\left( \frac{\partial \ln i}{\partial \ln a_{\text{O}_2}} \right)_{a_{\text{OH}^-}, E}$	1	—	—
$\left( \frac{\partial \ln i}{\partial \ln a_{\text{HO}_2^-}} \right)_{a_{\text{OH}^-}, E}$	0	—	—
$\left( \frac{\partial \ln i}{\partial \ln a_{\text{HO}_2^-}} \right)_{a_{\text{OH}^-}, E}$	—	1	$\frac{1}{2}$

Source: R. R. Azic and N. M. Markovic, *J. Electroanal. Chem.* **165**: 105, Table 4, copyright 1984 with permission from Elsevier Science.

**TABLE 7.7**  
**Rate Constants for O<sub>2</sub> Reduction on Low-Index Single-Crystal Electrodes in 0.1 M NaOH**

$-E$ (V)	Au(100) $n = 4$	Au(110) $n = 2$	Au(111) $n = 2$
0.05	6.4		
0.07	8.5		
0.10	13.7		
0.15		9.9	
0.18		13.7	5.0
0.19			5.73
0.20	32.7	22.3	6.5
0.21		28.3	7.07
0.22			8.5
0.23			9.43

Source: R. R. Azic and N. M. Markovic, *J. Electroanal. Chem.* **165**: 121, Table 5, copyright 1984 with permission from Elsevier Science.

possibility of blocking by radicals such as  $\text{—C—OH}$ . On the 111 plane, sweeps from 0.2 to 0.8 V RHE give a broad peak, and the number of coulombs involved is the same when the sweep is run cathodic to anodic or anodic to cathodic. The maximum current density is  $1.5 \text{ mA cm}^{-2}$ , which is not as high as might be desired, but the important thing here is to compare this rate of reaction, or current density, with that observed for sweeps over the same potential range on 110 and 100 planes. The fact is that on these planes, for a sweep in the anodic direction, no current is registered at all. On the other hand, if the sweep is reversed in direction (reducing whatever is there), there is a significant current.

The conclusion here is therefore that activity in methanol oxidation on platinum is limited to the 111 plane. The other planes are blocked with a radical, probably adsorbed CO or  $\text{—C—OH}$ . It is not known at present what fraction of the electrode corresponds to each plane, but it is clear that greatly improved electrocatalysis of  $\text{CH}_3\text{OH}$  to  $\text{CO}_2$  would be observed if electrodes containing only the 111 plane were available.

### 7.8.5. General Assessment of Single-Crystal Work in Electrochemistry

Single crystals are expensive. Arrangements to expose only one plane to a solution increase their cost. However, there is no doubt that for academic and fundamental work, the initiatives taken (Hubbard, Hamelin) in using well-defined single-crystal electrodes give much more information than that which can be obtained by the use of polycrystals. The truth is that each crystal plane exhibits radically different reactivities.

As to the technological side (whether to use single-crystal planes or polycrystals), it is clearly a matter of the cost saved by using an exposed active plane versus the cost



of making it. Practical electrochemical cells, either reactors for producing new substances, or fuel cells for producing energy efficiently, need square meters, not square centimeters, of electrodes. For such situations, the cost of manufacturing large single-crystal surfaces, or putting a number of smaller ones together, has to be shown to be less than the gain in economics due to larger rates per unit area on specific “catalytic” planes.

### 7.8.6. Roots of the Work on Kinetics at Single-Crystal Planes

Much work was done in the 1950s and 1960s on electrode kinetics with single-crystal planes of specific orientation. A few examples are given in the reading list. By and large, the results indicated smaller effects (differences of 2–3 times) in respect to kinetic rate constants for the same reaction on different planes than were reported later. In these earlier experiments there was no before-and-after measurement of the crystal planes, exposed—as developed later (by Hubbard in the 1970s)—to verify that the face exposed was indeed that intended and not a mixture of faces due to recrystallization in solution. These latter effects, if they occurred, would mean that the surface exposed to the solution was in fact mixed in the orientations present. This smoothed out the differences in activity among the planes intentionally exposed and gave a far smaller effect than that observed later when care was taken that such recrystallizations in solution did not occur.

### Further Reading

#### Seminal

1. A. Damjanovic, T. H. V. Setty, and J. O'M. Bockris, *J. Electrochem. Soc.* **113**: 429 (1960).
2. H. Seither, H. Fischer, and L. Albert, *Electrochim. Acta* **2**: 97 (1960).
3. R. Piontelli, G. Poli, and G. Serrevalle, in *Transactions of the Symposium on Electrode Processes*, E. Yeager, ed., p. 245, Wiley, New York (1961).

#### Modern

1. J. Clavillier, R. Faure, G. Guinet, and R. Durand, *J. Electroanal. Chem.* **107**: 205 (1980).
2. A. Hamlin, in *Modern Aspects of Electrochemistry*, R. E. White, B. E. Conway, and J. O'M. Bockris, eds., Vol. 16, p. 1, Plenum, New York (1985).
3. K. Adzic, in *Modern Aspects of Electrochemistry*, R. E. White, B. E. Conway, and J. O'M. Bockris, eds., Vol. 21, p. 188, Plenum, New York (1990).
4. H. Gasteiger, N. Markovic, P. N. Ross, and C. J. Cairns, *J. Phys. Chem.* **97**: 12020 (1993).
5. H. A. Gasteiger, N. Markovic, P. N. Ross, and C. J. Cairns, *J. Electrochem. Soc.* **141**: 1795 (1994).
6. T. Fukuda and A. Aramato, *Electrochem. Soc. Proc.* **96-8**: 96 (1996).
7. H. You, Z. Nagy, D. J. Zurewsky, and R. P. Chierello, *Electrochem. Soc. Proc.* **96-8**: 136 (1996).

8. C. Stuhlmann, B. Wohlmann, M. Kruff, and K. Wandelt, *Electrochem. Soc. Proc.* **96-8**:203 (1996).

## 7.9. TRANSPORT IN THE ELECTROLYTE EFFECTS CHARGE TRANSFER AT THE INTERFACE

### 7.9.1. Ionics Looks after the Material Needs of the Interface

The electrodic events at an interface have been the center of attention so far. Quite justifiably, the view has been interface centered (electrodics), for charge transfer is the essence of electrochemistry. It should not be forgotten, however, that for an electrodic reaction to keep going, the electron acceptors and electron donors have to move to the interface. It is through this transport of matter from the electrolyte bulk to the interface that ionics (i.e., the behavior of ions in solution) figures in the scheme of things. Thus, ionics looks after the logistics of charge transfer and links up with electrodicts to make electrochemical systems run (Fig. 7.81).

The preoccupation with the interface that has characterized the discussion so far is based on an important assumption: The transport aspects of ionics are playing their supply role so well that one has not been aware of the logistic problems of charge transfer. Except for some preliminary indications (cf. Section 7.3.1), the interface has been assumed never to fall short of its needs (of electron acceptors and donors). But there are situations where the charge-transfer reaction is inadequately supplied with its material requirements (e.g., of electron acceptors). Here, a supply problem arises. The *transport* of electron acceptors and donors in the solution becomes the important event. Ionic transport begins to control the rate of charge transfer across the interface; then the viewpoint has to become electrolyte centered.

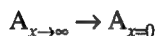
There is another way of looking at these situations where the lack of a sufficient supply of the needs of the interface compels one to look at the transport processes in solution. The broader view demands that one see the charge-transfer reaction as preceded by a drift of the reaction participants to the interface. In fact, one must think of transport in solution and charge transfer as consecutive steps of an overall reaction.

For example, consider an electron-transfer reaction

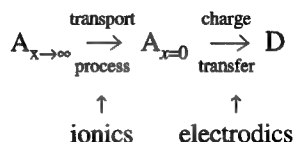


**Fig. 7.81.** The behavior of electrochemical systems is dependent on both the ionics and the electrodicts.

where the subscript  $x = 0$  emphasizes that in the initial state of the reaction, the electron acceptors are lined up at the OHP  $x = 0$  before being serviced by the electrons in a single or multistep reaction. The step preceding the charge transfer is the transport of the electron acceptors from the electrolyte bulk  $x \rightarrow \infty$  to the interface  $x = 0$ , i.e.,



Hence, the overall process is



Now, as in any consecutive reaction, one can pose the question: Which step controls the overall rate of the reaction? Or, which is the rds? Does the transport process or the charge-transfer reaction determine the overall rate? It has been argued (cf. Section 4.2.18) that the transport processes of diffusion and migration are rate processes. Hence, they are also connected with activation-energy barriers. These, however, are usually lower than the energy barriers of the electrodic reactions. If diffusion is to be rate controlling, does that mean that its activation-energy barriers have to be higher than those for charge transfer? It does not (Fig. 7.82). One should remember that rates of processes are determined also by concentration. Hence, if the

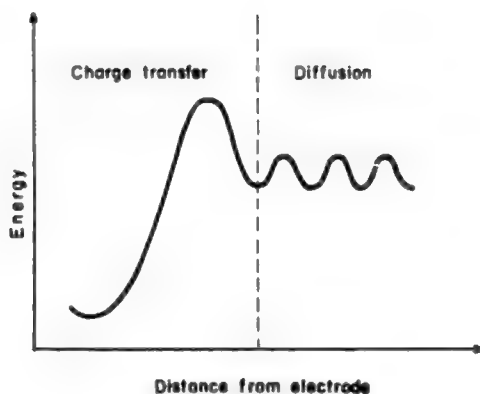


**Fig. 7.82.** Transport processes are interpretable in terms of the concept of energies of activation (which are, however, relatively very low) and concentration gradients.

concentration becomes small, the diffusion process can become the rds even though its energy barriers remain low.

### 7.9.2. How the Transport Flux Is Linked to the Charge-Transfer Flux: The Flux-Equality Condition

A simple idea is used to relate the current density across an interface to the rate at which electron acceptors (or electron donors) arrive at (or move away from) the interface. One starts off with the definition of steady state according to which the concentration of all the intermediates in the reaction must be constant with time. This condition can be achieved if the products of one step are used up in the succeeding step as fast as they are produced. If the first of two consecutive steps proceeded at a faster rate than the second, then the products of the first step would start accumulating (Fig. 7.83) and this would contradict the definition of steady state.

Hence, *in the steady state*, all steps in a consecutive reaction are proceeding at the same rate.<sup>71</sup> If the steps involve charge transfer or charge transport, one says that the net<sup>72</sup> current densities corresponding to all the steps are equal. This is an example of Kirchhoff's first law for electrical currents (Fig. 7.84), which says that the sum of the steady inflowing currents at a junction must be equal to the sum of outflowing currents. Thus, under steady-state conditions, the charge-transfer current density  $i_{\text{CTR}}$  must be set equal to the current density due to transport,

$$i = i_{\text{CTR}} = i_{\text{transport}} \quad (7.172)$$

(The junction at which this current equality holds is the  $x = 0$ , or OHP.) But the transport-current density is the charge transported per mole of ions (i.e.,  $nF$ ) times the transport flux  $J_{\text{transport}}$  (i.e., the number of moles of ions transported across  $1 \text{ cm}^2$  of a transit plane per second). If the electron acceptors are not charged species (ions), one can still state the equality of currents in terms of fluxes by expressing (7.172) in terms of moles per unit area and time arriving at, and being reacted in, the interphase

$$\frac{i}{nF} = \frac{i_{\text{CTR}}}{nF} = J_{\text{transport}} \quad (7.173)$$

If diffusion is the transport mechanism, the flux equality condition becomes

$$\frac{i}{nF} = \frac{i_{\text{CTR}}}{nF} = J_D \quad (7.174)$$

where  $J_D$  is the diffusion flux.

<sup>71</sup>This idea was used previously (cf. Section 7.6.5) to illustrate the concept of the rds.

<sup>72</sup>The word "net" is used to emphasize that one is not talking of the component forward and backward current densities  $\vec{i}$  and  $\vec{i}$ , but of the resultant current density  $i = \vec{i} - \vec{i}$ .

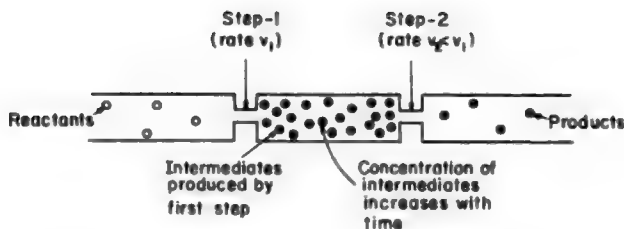


**Fig. 7.83.** The steady state cannot be established if some intermediates go on accumulating with time.

The flux continuity or flux equality condition can be applied even when the current density  $i$  and the transport flux  $J_{\text{transport}}$  are changing with time. One simply structures  $dt$  into small time intervals and says that the condition is valid within this infinitesimal time.

Once this flux equality condition (7.173) is formulated, one simply works out  $J_{\text{transport}}$  as a pure transport problem and equates it to  $1/nF$  times the current density across the interface since  $n$  faradays per mole are required for the transported material to be electronated. If the transport process consists of pure diffusion (i.e., there is no contribution from either migration or hydrodynamic flow), then the flux is given by Fick's first law (see Section 4.2.2), i.e.,

$$J_D = -D \frac{dc}{dx} \quad (7.175)$$

so one has to know the concentration gradient in the region where the flux is being considered, i.e., in the region about  $x = 0$  (Fig. 7.85). This requires a knowledge of the variation of concentration as a function of distance from the interface, and if the diffusion is in response to either a constant stimulus switched on at  $t = 0$  or a time-varying stimulus (see Section 7.7), then one must also know the *time* variation of the concentration at a particular distance from the interface. To obtain the space and



**Fig. 7.84.** Kirchhoff's law says that the sum of the inflowing currents at a junction must be equal to the sum of outflowing currents.

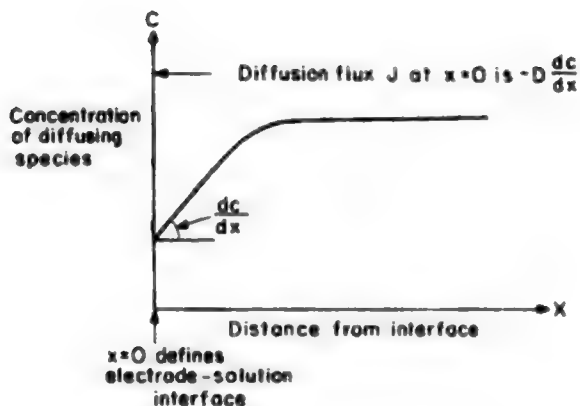


**Fig. 7.85.** The diffusion flux at  $x = 0$  depends on the concentration gradient at this point.

time variation of the concentration, it is necessary to solve Fick's second law under the appropriate initial and boundary conditions, as has been discussed in Section 4.2.9.

### 7.9.3. Appropriations from the Theory of Heat Transfer

The Laplace transformation method of solving nonsteady-state diffusion problems was briefly treated in Chapter 4. Thus, one can study all sorts of problems by using various types of current or potential stimuli (as in researches using transients; see Section 7.7) and analyzing how transport in solution influences the response of the system. For example, a sinusoidally varying current, density can be used with

$$i = I \sin \omega t \quad (7.176)$$

( $I$  and  $\omega$  are the amplitude and angular frequency of the current wave), and the corresponding variation of the potential difference across the interface with time can be measured. It will be recalled, however (see Section 4.2.10), that, once one has obtained the solution of the problem involving a constant stimulus (e.g., a current) switched on at  $t = 0$ , then one can get the solutions for other types of stimuli by using the simple property of Laplace transforms treated in Section 4.2.8.

Another approach can also be rewarding. A common practice in finding solutions to problems of the diffusion of ions in solution is, in fact, to look for analogous heat-flow problems. Since the basic laws of diffusion and heat flow are mathematically similar, the solution of a given heat-flow problem can be used as a solution for the analogous diffusion problem—of course, after changing temperature to concentration and thermal diffusivity to diffusion coefficient (Table 7.8). Solutions to a large number of heat-flow problems have been given in the classic treatise, *Heat Conduction in*

**TABLE 7.8**  
**Analogous Parameters in Heat Transfer and Mass Transfer**

Mass-Transfer-Controlled Electrode Reaction	Heat-Transfer systems, i.e., Heat Transfer Involved in Cooling Molten Metals
Current	Heat flow
Diffusion coefficient	Thermal diffusivity
Concentration gradient	Temperature gradient
Diffusion-layer thickness	Thermal-boundary layer

*Solids*, by Carslaw and Jaeger, a book that has become a bible for electro-chemists studying diffusion-controlled reaction rates.

#### 7.9.4. A Qualitative Study of How Diffusion Affects the Response of an Interface to a Constant Current

The best way to acquire a feel for what happens when the transport of ions determines the overall rate of a reaction at an interface is to consider a specific problem in detail. However, before tackling such a problem, it is essential to point out that transport processes in electrochemical systems have been analyzed with clarity and inadequate detail in many excellent treatises.<sup>73</sup> The present treatment, therefore, is elementary in approach and restricted in content. All that is intended is to sketch in a connected way some of the main concepts relevant to transport-controlled electrochemicals. Caution must be exercised before extending the ideas to more complex situations.

For example, *the treatment of diffusion that is to follow is solely restricted to semi-infinite linear diffusion*, i.e., diffusion that occurs in the region between  $x = 0$  and  $x \rightarrow +\infty$ , *to a plane of infinite area*. Thus, diffusion to a point sink—called *spherical diffusion*—is not treated, though it has been shown to be relevant to the particular problem of the electrolytic growth of dendritic crystals from ionic melts.

Consider the electronation of the species  $M^{n+}$



where M is deposited on the metal electrode. The electrolyte is assumed to be one with a small concentration of the electron acceptor  $M^{n+}$  compared with a large concentration of another positive ion  $N^+$ , which is “indifferent” to the charge-transfer reaction, i.e., it does not accept electrons at the given electrode at the potential concerned. Because

<sup>73</sup>It is of interest to note that transport to and from electrodes was understood at a sophisticated level many decades before charge-transfer theory began to enter the literature. Some of the frustrations of electrochemists before the 1950s stemmed, indeed, from attempting to deal with the theory of interfacial charge-transfer reactions with an overstress on diffusion and transport and a neglect of the energy barrier and charge-transfer theory.

of the large excess of the indifferent ions  $\text{N}^+$ , these assume the major part of the burden of carrying the conduction current. It will be recalled (Section 4.5.2) that the particular fraction of the conduction current carried by an ionic species depends on its transport number, which in turn depends upon its concentration. Hence, since the electron acceptor  $\text{M}^{n+}$  is present at relatively low concentrations, it has to reach the interface predominantly by diffusion<sup>74</sup> rather than by electrical migration. Suppose that at a time  $t = 0$ , a constant current density  $i_g$  is switched on, i.e., the stimulus is similar to that considered in the analysis of transients (Section 7.7). What will happen?

Initially, the current will largely go toward changing the structure of the interface; this is the double-layer charging discussed earlier. The basic principle in all situations where an external power supply forces a constant current through the interface is that the inflowing charge is consumed in the fastest available process. At the beginning, after switching on a current, this charging of an interface transfer without electrons is the easiest process; all that has to be done is to change the charge density on both sides of the interface. At the metal surface, this means moving in excess electrons, and on the solution side, it means making the excess charge density due to an unequal distribution of ions more positive by moving some positive ions toward the interface or negative ions away from it.

After the current has passed for a time, the reaction soon gets going at a considerable rate. In this section, for simplicity of treatment, we are considering transport-controlled reactions with the charge transfer in virtual equilibrium, i.e., the charge-transfer reaction is assumed to have a high exchange-current density. Hence, one can legitimately use the equilibrium case of the Butler–Volmer relation (Section 7.2.7), i.e., the Nernst equation

$$\Delta\phi = \Delta\phi^0 + \frac{RT}{nF} \ln c_{x=0} \quad (7.177)$$

where  $c_{x=0}$  is the concentration of  $\text{M}^{n+}$  at the interface.

It is in relating  $c_{x=0}$  to the  $c$  in the bulk that one applies the theory of diffusion. As the electron acceptor  $\text{M}^{n+}$  gets consumed by the charge-transfer reaction, its concentration at the interface  $x = 0$  departs from its initial value, which is the bulk concentration  $c^0$ . This is a question of logistics. The diffusion process does not replenish all the electron acceptors that are used up. Thus, the concentration  $\text{M}^{n+}$  at  $x = 0$ , namely,  $c_{x=0}$ , will start diminishing. But this means that the potential difference across the interface will start falling [cf. Eq. (7.177)]. Finally, after a certain time called the *transition time*, the concentration of  $\text{M}^{n+}$  is almost zero, which implies [Eq. (7.177)] that  $\ln c_{x=0}$  and therefore the potential difference  $\Delta\phi$  should sink toward  $-\infty$ .

<sup>74</sup>At this stage, the complicating factor of mass transport by a hydrodynamic flow of the electrolyte is not considered (see, however, Section 7.9.7).



Thus, when a constant current is imposed on an interface at which the rate of the electronation process is determined by diffusion (i.e., the other reaction steps, particularly electronation, in the overall reaction sequence are relatively fast), it is principally the interfacial concentration of  $M^{n+}$  that determines how the potential difference across the interface varies with time. The variation of  $c_{M^{n+}}$  with time must therefore be analyzed.

### 7.9.5. A Quantitative Treatment of How Diffusion to an Electrode Affects the Response with Time of an Interface to a Constant Current

In considering the time dependence of a concentration at a given point when this is determined by diffusion (Section 4.2.7), it has been shown that the variation in concentration with time and distance in a rectangular volume with one side parallel to the electrode depends on how the semi-infinite linear diffusion process is stimulated. Diffusion occurs only when a concentration gradient is set up. If the gradient arises from a constant rate of removal of the species across one face of the volume, then this constant flux,  $J_D$ , makes the concentration of the diffusing species vary with distance and time (Fig. 7.86) according to an expression derived in Section 4.2.12 by solving the partial differential equation for diffusion (Fick's second law) under the appropriate initial and boundary conditions. Concentration gradients also result when the interface, instead of removing a species, produces one (Fig. 7.87). From Eq. (4.75) and considering the case where  $c < c^0$

$$c_{x,t} = c^0 - \frac{2J_D t^{\frac{1}{2}}}{D^{\frac{1}{2}} \pi^{\frac{1}{2}}} e^{-x^2/4Dt} + \frac{J_D x}{D} \operatorname{erfc} \frac{x}{\sqrt{4Dt}} \quad (7.178)$$

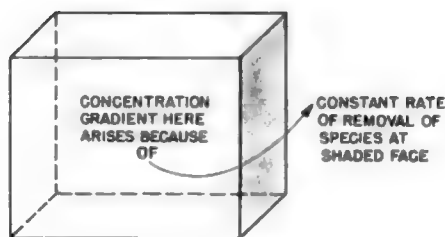


**Fig. 7.86.** A constant flux at one face of a volume element makes the concentration of the diffusing species vary with distance and time.

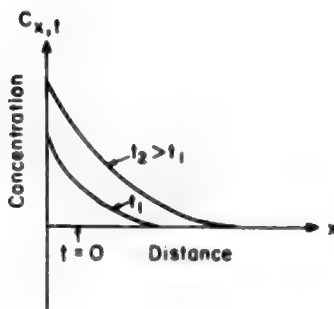


**Fig. 7.87.** As the substance is being generated, its concentration at the surface increases with time and a positive concentration gradient is established.

In this equation,  $c_{x,t}$  is the concentration of  $M^{n+}$  at a distance  $x$  from the  $x = 0$  plane at a time  $t$  after the switching on of the constant electronation current density,  $c^0$  is the bulk concentration of  $M^{n+}$ , and the other terms have their usual significance.

To link the constant-flux problem (of Section 4.2.12) to the constant-current problem discussed here, one can assume that the constant flux arises only from the imposed constant current  $i_g$ . Thus, one considers that the boundary of the diffusion problem is the electrified interface  $x = 0$  at which there is equality of the charge transfer (from electrode to ion) and diffusion fluxes (from solution to electrode), i.e.,

$$\frac{i_g}{nF} = J_D \quad (7.174)$$

This expression of  $J_D$  must be inserted back into the expression for the concentration  $c_{x=0}$  at the interface, i.e., into the expression obtained by setting  $x = 0$  in Eq. (7.178), whereupon one obtains

$$c_{x=0} = c^0 - \frac{2i_g}{nF} \sqrt{\frac{t}{\pi D}} \quad (7.179)$$

By writing

$$P = + \frac{2i_g}{nF} \sqrt{\frac{t}{\pi D}} \quad (7.180)$$

Eq. (7.179) becomes

$$c_{x=0} = c^0 - Pt^{\frac{1}{2}} \quad (7.181)$$

This expression, known as *Sand's equation*, gives the variation of the interfacial concentration of  $M^{n+}$  with time after application of a constant current density. But one seeks also to know the time variation of the potential difference across the interface at which the electronation reaction  $M^{n+} + ne \rightarrow M$  is occurring. To obtain this information, one recalls that the charge-transfer reaction across the interface is assumed in the present treatment to be virtually in equilibrium and therefore the Nernst equation (7.177) can be used to relate the potential difference to the concentration at the interface. That is, by substituting (7.181) in (7.177),

$$\Delta\phi = \Delta\phi^0 + \frac{RT}{nF} \ln(c^0 - Pt^{\frac{1}{2}}) \quad (7.182)$$

The shape of such potential-time transients as the one represented by (7.182) is interesting (Fig. 7.88). It appears that after the lapse of a certain time, the potential starts falling very rapidly. One must understand what is happening here. Before moving to examine this certain time more closely, consider instead of a metal-deposition reaction  $M^{n+} + ne \rightarrow M$ , an electronation reaction in which both the electron acceptor A and electron donor D are in solution ( $A + ne \rightarrow D$ ), i.e., a *redox* reaction (an example of such a reaction is the electronation of ferric ions to form ferrous ions,  $Fe^{3+} + e \rightarrow Fe^{2+}$ ), then one would also have had to consider the diffusion of the electron donor *away from* the electrode and the variation of its interfacial concentration with time. Since the electron donor D is being continuously generated by charge transfer from the electron acceptor A, the interfacial concentration of D will increase (Fig. 7.87) with time (not decrease, as in the case of the A that is being depleted). If 1 mol of D

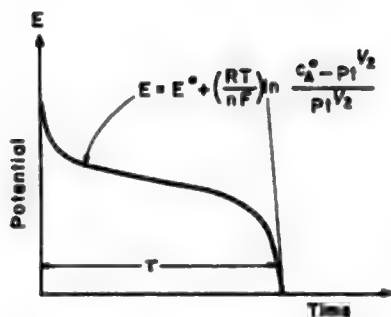


**Fig. 7.88.** The potential-time transient in a redox system with no reduced species at the beginning is an S-shaped curve.

is formed from 1 mol of A and their diffusion coefficients are the same, one will obtain, not the minus sign, but

$$c_{D,x=0} = c_D^0 + Pt^{\frac{1}{2}} \quad (7.183)$$

Further, the Nernst equation will take the form [see Eq. (8.61)]

$$\Delta\phi = \Delta\phi^0 + \frac{RT}{nF} \ln \frac{c_{A,x=0}}{c_{D,x=0}} \quad (7.184)$$

i.e.,

$$\Delta\phi = \Delta\phi^0 + \frac{RT}{nF} \ln \frac{c_A^0 - Pt^{\frac{1}{2}}}{c_D^0 + Pt^{\frac{1}{2}}} \quad (7.185)$$

Now suppose that one starts off the constant current with a zero or negligibly small concentration of electron donor D in the electrolyte. Then  $c_D^0 \approx 0$ , and Eq. (7.185) reduces to

$$\Delta\phi = \Delta\phi^0 + \frac{RT}{nF} \ln \frac{c_A^0 - Pt^{\frac{1}{2}}}{Pt^{\frac{1}{2}}} \quad (7.186)$$

By combining the interface under study with a nonpolarizable interface (i.e., a reference electrode) the potential difference across the system, or cell, will change with time (Fig. 7.88) according to the expression

$$E = E^0 + \frac{RT}{nF} \ln \frac{c_A^0 - Pt^{\frac{1}{2}}}{Pt^{\frac{1}{2}}} \quad (7.187)$$

### 7.9.6. The Concept of Transition Time

Consider the expression (7.186) for the time variation of the potential difference across an interface at which a diffusion-controlled electronation reaction is stimulated by a constant current switched on at  $t = 0$ :

$$\Delta\phi = \Delta\phi^0 + \frac{RT}{nF} \ln \frac{c_A^0 - Pt^{\frac{1}{2}}}{Pt^{\frac{1}{2}}} \quad (7.186)$$

The product  $Pt^{\frac{1}{2}}$  is zero at  $t = 0$ . Hence,  $c_A^0/Pt^{\frac{1}{2}}$  tends to infinity and so does the  $\log$  term in (7.186), i.e., the potential is supposed to start from plus infinity. Now,  $Pt^{\frac{1}{2}}$  grows with the passage of time, and at some value of time—let it be represented by  $\tau$  (Fig.

7.88)—it must become equal to  $c_A^0$ . As this time  $\tau$  is approached,  $c_A^0 - P\tau^{\frac{1}{2}}$  tends to zero,  $\ln(c_A^0 - P\tau^{\frac{1}{2}})$  tends to minus infinity, and the potential changes very much. In fact, it sinks till it has become sufficiently negative so that some other charge-transfer reaction (e.g., the electronation of the indifferent ions that were inert to electron acceptance at less negative potentials) can utilize the current.

What is the physical meaning that  $c_A^0 - P\tau^{\frac{1}{2}}$  is equal to zero? This is easy to see from

$$c_{A,x=0} = c_A^0 - P\tau^{\frac{1}{2}} \quad (7.181)$$

At  $t = \tau$ ,  $c_A = P\tau^{\frac{1}{2}}$ , and hence the interfacial concentration of the electron acceptors has fallen to zero (Fig. 7.89)

$$t = \tau \quad \text{when} \quad c_{A,x=0} = 0 \quad (7.188)$$

This time  $\tau$  at which the interfacial concentration attains a value of zero is known as the *transition time*.

The transition time has been operationally defined in terms of the rapid variation of potential with time, i.e., it is the time corresponding to the potential jump shown in Fig. 7.88. But one can easily get an explicit expression for it. By making use of the fact that at  $\tau$ ,  $c_{A,x=0} = 0$ , one has, using Eqs. (7.180) and (7.181)

$$c_{A,x=0} = 0 = c_A^0 - P\tau^{\frac{1}{2}} = c_A^0 - \frac{2i_g}{nF} \sqrt{\frac{\tau}{\pi D}} \quad (7.189)$$

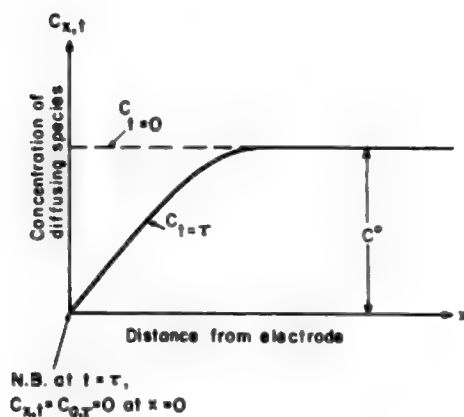


**Fig. 7.89.** As the transition time is reached, the concentration of the diffusing species at the OHP becomes virtually zero.

or

$$\tau^{\frac{1}{2}} = \frac{nF}{2i_g} c_A^0 \sqrt{\pi D} = \frac{c_A^0}{P} \quad (7.190)$$

This is a form of Sand's equation and dates from the remarkably early time of 1901. It reminds us that there was much progress made in the early days of electrochemistry with diffusion-related situations; one might call it the macrophase of the subject. (The Warburg impedance was derived even earlier; it deals with impedance due to diffusion. See Section 7.5.13.5.) Consideration on a microscale (the things that happen during charge transfer over 5 Å at the interface) had another 50 years before it became a funded research topic.

With this expression for  $\tau^{\frac{1}{2}}$  one has

$$c_A^0 = P\tau^{\frac{1}{2}} \quad (7.191)$$

which, in combination with (7.187), gives

$$E = E^0 + \frac{RT}{nF} \ln \frac{\tau^{\frac{1}{2}} - \bar{t}^{\frac{1}{2}}}{\bar{t}^{\frac{1}{2}}} \quad (7.192)$$

The equation for  $\tau^{\frac{1}{2}}$  [i.e., (7.187)] indicates two main conclusions. First, at a particular concentration  $c_A^0$ , the larger the constant current used, the shorter the transition time (Fig. 7.90 and Table 7.9). Second, for a fixed constant current  $i_g$ , the square root of the transition time is proportional to the bulk concentration; the higher the bulk concentration, the longer the transition time.

The considerations of the last two sections have concerned diffusion control of reactions at a constant applied *current*—galvanostatically, as it is called. The picture is very plain. When a constant current is switched on across an interface, and diffusion of charge carriers from the bulk to the interface is in rate control, it is the potential of the electrode that changes with time. The course of that change is given in Fig. 7.88, where one sees that the transition time,  $\tau$ , marks a point at which a dramatic change in the electrode potential occurs. Physically, the interface is running out of fuel; the demand of the constant current (a stream of electrons) is too much for the supply of ions to partner them and as the latter exhausts at  $\tau$ , the electrode potential changes to reach the switch-on potential of another process, one that will use up an alternative charge carrier until that reaches *its*  $\tau$ , and so on. The final particle to be used is water; in aqueous solutions one cannot run out of that.

Sand's equation, then, relates strictly to galvanostatic regimes. One is stimulated to ask what happens, then, in respect to time under diffusion control, if it is the *potential* of the electrode that is kept constant, i.e., the situation is potentiostatic. This case was treated a year after that given by Sands, although it was another 35 years before the

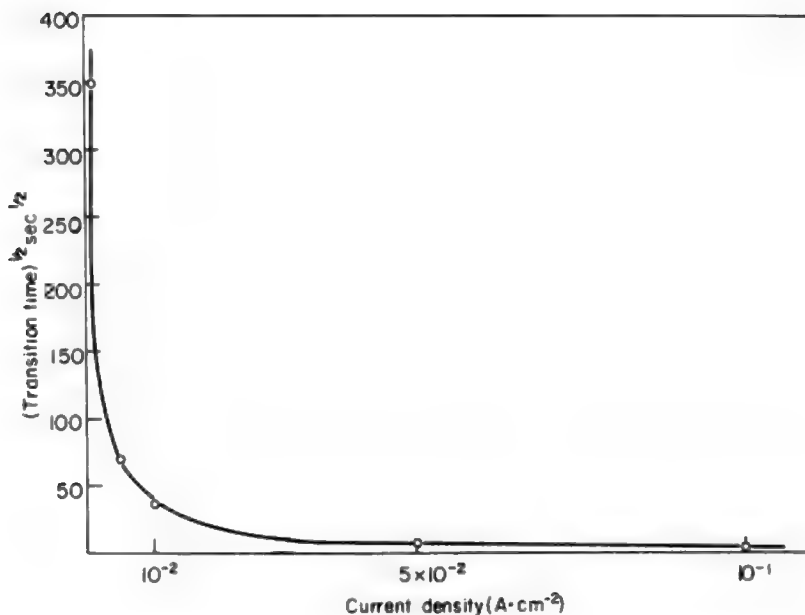


**Fig. 7.90.** Illustration of the hyperbolic relationship that exists between the square root of the transition time and the current density.

electronic equipment was available to make it practical to carry out potentiostatic experiments. It was Cottrell (1902) who deduced the time dependence of a current under diffusion control, the potential of the electrode being kept constant. Here there can, by definition, be no wandering of the potential to find an alternative supply of

**TABLE 7.9**  
**Transition Time for  $\text{Fe}^{2+}$  Discharge in 0.062 M  $\text{FeSO}_4$  + 0.1 M  $\text{Na}_2\text{SO}_4$  Solution at pH 3.4**

Current density ( $\text{A cm}^{-2}$ )	Experimental $\tau_{\text{Fe}^{2+}}$ ( $\text{s} \times 10^{-3}$ )	Calculated $\tau_{\text{Fe}^{2+}}$ ( $\text{s} \times 10^{-3}$ )
0.35	9	6
0.32	10	8
0.30	10	9
0.26	13	12
0.24	14	14
0.20	24	20
0.15	40	38
0.08	140	125
0.06	290	222

charge carriers and therefore as the supply is depleted, the current slowly falls. The Cottrell equation governs this fall and is expressed (for unit electrode area) by:

$$i_t = \frac{nF D^{1/2} c_i}{\pi^{1/2} t^{1/2}} \quad (7.193)$$

Rearrangement of the equation to make an expression for  $t^{1/2}$  will show the reader the similarity between Cottrell's equation for a diffusion-controlled current as a function of time at constant potential and Sand's equation for the time at which, under diffusion control at constant current, the potential takes off to seek a new supply of charge carriers for its electron stream.

### 7.9.7. Convection Can Maintain Steady Interfacial Concentrations

It follows from Eq. (7.190) that for relatively small concentrations of the reacting species and for not too small currents, transition times are relatively small, on the order of seconds or less. With both increasing concentration and decreasing current density, the calculated transition times increase, reaching, e.g., for a solution with 0.1 *M* concentration of the reactant and for a current density of  $10^{-4} \text{ A cm}^{-2}$ , a value on the order of several hours. Are there any practical limitations in observing the long transition times that Eq. (7.191) predicts?

A problem does indeed arise when the calculated transition time becomes more than a few seconds. The constant depletion of the electron acceptor makes the electrolyte density near the interface different from that in the bulk. These density differences in different regions of the electrolyte upset the initial condition of hydro-

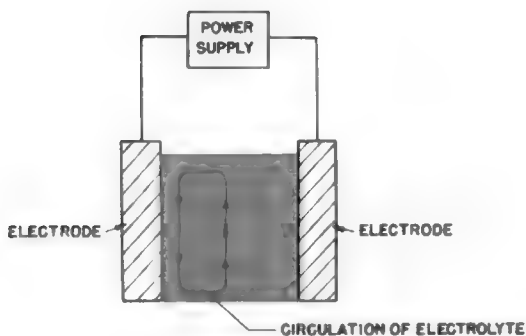


**Fig. 7.91.** The change in electrolyte concentration produces a change in the density of the electrolyte; a flow of electrolyte results from natural convection; and the hydrostatic equilibrium is thus upset.



static equilibrium, and the electrolyte begins to flow to compensate for the density changes (Fig. 7.91). This type of hydrodynamic flow is known as *natural convection*.

Though there is fluid flow in the bulk of the electrolyte, it is found that there is a layer adjacent to the electrode in which the electrolyte is stationary, or stagnant. Thus the electron acceptors travel by convection from the bulk up to the stagnant layer and then cross the remaining boundary layer by diffusion. This transport by a convection-with-diffusion mechanism has not been taken into account so far. The equations for the time and space variation of concentration [i.e., Eq. (7.178)], for the transition time [Eq. (7.190)], and for the time variation of potential [Eq. (7.192)] have been derived for convection-free conditions, and they break down when convection becomes significant. The first approximation theory given above, therefore, deviates from experiment if the constant current is applied sufficiently long (times on the order of seconds) for convection to be important.

Convection plays an important part in electrochemical systems and it is of interest here to state a few of its properties. The transport processes that have been dealt with so far are diffusion and migration. In diffusion, it is found that the movement of the dissolved entities follows  $(\partial c / \partial x)_{y,z}$ , i.e., they follow the concentration gradient in the one direction, usually that perpendicular to the electrode. In migration, it is the movement of ions only that is being discussed and they travel at the bidding of, and hence in the direction of, the electric field in the region of the solution being considered.

Convection arises through pressure gradients. In the example given, the solution moves because one part of it has been made heavier (more concentrated) than another. Pressure gradients in solution may turn up as a result of natural processes such as changes in concentration near electrodes, but also as a result of processes purposely imposed on the solution, such as making a propeller turn in it.

There are two kinds of convective flow. The kind dealt with here is called *laminar*, which means smooth or honeylike in flow. There is another kind that is much more difficult to deal with theoretically; this is turbulent flow, the kind of rough flow that occurs at waterfalls.

Laminar flow occurs when the movement of the liquid is slow. As the rate of flow increases, a condition arises in which *vortices* begin to form behind a cylinder placed in the path of the flow. Now if the rate is increased still further, these vortices pass out into the rest of the liquid after it has passed the cylinder. The flow has become turbulent.

There is an equation for the turnover point from honeylike to this rough, turbulent kind of flow. The relation is

$$(\rho/\eta)vd > N_{\text{Re}} \quad (7.194)$$

Here,  $\rho$  is the density,  $\eta$  the viscosity,  $v$  the velocity, and  $d$  the diameter of the pipe in which the flow takes place.  $N_{\text{Re}}$  is the Reynolds number. As soon as the expression on the left exceeds  $N_{\text{Re}}$  (having an order of magnitude of 1000), the flow becomes turbulent.

The complexities of turbulent flow are outside the province of this book. However, there are two further properties of laminar convective flow that are relevant to understanding the electrochemical situation. The first is easily understood by considering an excellent illustration of it—river flow. It is a matter of common observation that rivers (which flow convectively as a result of being pushed by gravity) move at maximum rate in the middle. At the river bank there is hardly any flow at all. This observation can be transferred to the flow of liquid through a pipe. The flow reaches a maximum velocity in the center. The liquid actually in contact with the walls of the pipe does not flow at all. The stationary layer is a few micrometers in thickness, about 1 % of the thickness of the diffusion layer set up by natural convection in an unstirred solution when an electrode reaction in steady state is occurring.

The resistance of the stationary layer is illustrated in an electrochemical situation by considering a solution being jetted against an electrode. The motion near the electrode is illustrated in Fig. 7.92. The jetted material never quite reaches the electrode as a consequence of the jet, which, however, serves to bring the material very near (maybe a micrometer from) the electrode, and the rest (through the remaining stationary layer) has to be done by diffusion and migration.

This brings us to the quantitative side of convection. In Section 4.2.2 it was seen that under stationary conditions in the solution (no natural or forced convection and no applied field), the flux involved per unit area and time is given by Pick's first law,

$$J = -D \frac{\partial c}{\partial x} \quad (4.16)$$

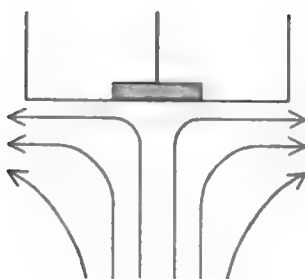


**Fig. 7.92.** Solution being jetted against an electrode. (Reprinted with permission from K. B. Oldham and J. C. Myland, *Fundamentals of Electrochemical Science*, Academic Press, 1994, p. 247.)

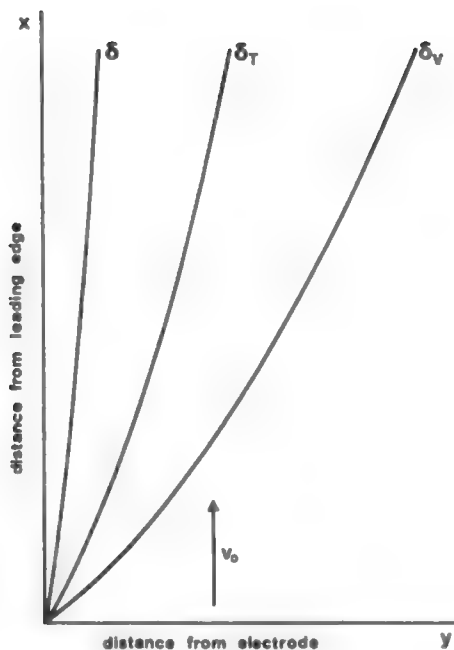


**Fig. 7.93.** Influence of location on boundary layer thickness in laminar flow along an electrode;  $\delta$ ,  $\delta_T$ , and  $\delta_v$  are the thicknesses of the diffusion, thermal, and hydrodynamic boundary layers, respectively.

When convection delivers ions or molecules to react at an electrode, there is (in addition to any diffusion) a *convective* flux, and this quantity is given by Fick's first law.

$$J_{\text{convec}} = v_x c_i$$

along the  $x$ -coordinate.<sup>75</sup> Hence,

$$J_{\text{total}} = -D_i \frac{\partial c}{\partial x} + v_x c_i$$

<sup>75</sup>As with other matters concerned with transport to electrodes, detailed treatments were set up very early. Various boundary layers at interfaces under flow were suggested by Prandtl as early as 1904. Three are shown in Fig. (7.93). The  $\delta_T$  is the well-known "diffusion layer" due to Nernst (Section 7.9.9). The  $\delta$  is the thermal boundary layer and the  $\delta_v$  signifies the thickness of the layer (Prandtl's layer) in a flowing liquid in which the velocity slows an approach perpendicular to the surface.

Correspondingly, the new version of Fick's second law becomes

$$\frac{\partial c_i}{\partial t} = D \frac{\partial^2 c_i}{\partial x^2} - v_i \frac{\partial c_i}{\partial x} \quad (7.195)$$

The most significant effect of a convective-diffusive transport mechanism is to counteract the tendency of the electronation-current density to reduce the interfacial concentration of electron acceptors to zero. Further, since the interfacial concentration of electron acceptors then remains at a value above that given by the diffusion-based equations, a transition time, indicated by a rapid potential variation, need not be attained.

Thus, the phenomenon of convection (which sets in significantly soon—seconds—after switching on a current) radically alters the picture of the potential-time transient resulting from the switching on of a constant current. When a constant current density is switched on to provoke semi-infinite linear diffusion, a rapid variation of potential is observed, provided the transition time is attained before the onset of natural convection. If, however, the current density is too low and the electron-acceptor concentration is too high, the initial transport process of pure diffusion is soon replaced by a process of convection with diffusion. This convective-diffusion process prevents the electron-acceptor concentration from sinking to zero, and a transition time, marked by a rapid fall of potential, is not attained. Instead, the potential difference across the interface remains at a steady value for an indefinite time, even though a constant current density is flowing.

The matter under discussion is of great practical importance. The potential jump associated with the transition time is both the basis of an electroanalytical technique for measuring concentration and also a cause for a lowering of efficiency in substance-producing or energy-converting electrochemical devices. Thus, the direct proportionality [Eq. (7.190)] between the square root of the transition time and the bulk concentration of electron acceptors suggests the use of transition-time measurements for analytical purposes (Section 7.9.6). Workers making such measurements must ensure that they do so under conditions of pure diffusion, i.e., that the transition time is unaffected by convection. They must choose the current density  $i_g$  so that the transition time in the concentration range concerned is reached before the onset of natural convection. The question of how long it takes for natural convection to begin can be answered only by a detailed hydrodynamic analysis of the system, e.g., the concentration of reacting species, current density, viscosity, diffusion coefficient, electrode reaction, and geometry and orientation of the reaction interface. The transition time must be less than a certain time (seconds) to avoid convection effects.

There are, however, many situations in which the potential variations (Fig. 7.88) associated with the approach to a transition time must be scrupulously avoided. Reference is made here to energy-conversion and substance-producing devices in which a departure of the potential from the equilibrium value represents a waste of

electrical energy. Thus, workers interested in such devices (in contrast to those interested in electroanalysis) try to avoid conditions that lead to a transition time. They use appropriately high values of concentration of the ion reacting at the interface to ensure that migration augments mass transport and, above all, they utilize natural convection aided by forced convection (stirring by mechanical means, bubbling of gases, or rotation of the electrode). In this way, the exhaustion of ions at the electrode interface and the rise in overpotential (and corresponding loss in energy) associated with it are avoided.

What is the quantitative relationship between the steady state, convection-with-diffusion current density and the potential difference across the interface? How is the steady-state potential difference at a steady current density related to the zero-current, or equilibrium, potential difference? These questions are the relevant ones for steady passage of current in convection-aided situations.

### 7.9.8. The Origin of Concentration Overpotential

What will be discussed, again for simplicity, is a situation where the charge-transfer reaction is in virtual equilibrium, but the interfacial concentration  $c_{x=0}$  of the electron acceptor  $M^{n+}$  is not the bulk value  $c^0$  but less than that, i.e.,  $c_{x=0} < c^0$ . If a current is passing through the interfaces, the question is: What is the value of the potential difference across the interface?

Experiment shows that when the transport of reactants cannot keep pace with the charge-transfer reaction, the potential  $\Delta\phi$  observed at the current density  $i$  is not equal to the zero-current, or equilibrium potential difference  $\Delta\phi_{i=0} = \Delta\phi_e$ . If an electronation reaction is considered,



the potential sinks to more negative values than that corresponding to equilibrium, although the exchange-current density  $i_0$  has been assumed to be very high (negligible departure from  $\Delta\phi_e$  caused by electron transfer). A simple explanation for this phenomenon can be given.

Since the charge transfer is assumed to be virtually at equilibrium, one can again use the Nernst equation to express the potential difference across the interface. Thus, when the current is zero,

$$\Delta\phi_e = \Delta\phi_{i=0} = \Delta\phi^0 + \frac{RT}{nF} \ln c^0 \quad (7.196)$$

But, what concentration should one use in the Nernst equation for the potential difference corresponding to a current density of  $i$ ? This cannot be the bulk concentration  $c^0$  because it is known that, owing to diffusional holdup, the interfacial concentration is less than the bulk value. One has to write

$$\Delta\phi = \Delta\phi^0 + \frac{RT}{nF} \ln c_{x=0} \quad (7.197)$$

This means that the passage of the current has made the potential depart from the zero current value  $\Delta\phi_e$ . The  $\Delta\phi$  has directly resulted from the departure of the interfacial concentration of electron acceptors from the initial bulk value  $c^0$  to a new value  $c_{x=0} \neq c^0$ . Thus,  $\Delta\phi - \Delta\phi_e$  is a potential difference produced by a concentration change at the interface. This concentration-produced<sup>76</sup> potential difference is often known as a *concentration overpotential*  $\eta_c$  to distinguish it from the usual overpotential<sup>77</sup>  $\eta_a$ , which results from the charge-transfer reaction and was treated at length in Section 7.2.3. Hence, one writes

$$\eta_c = \Delta\phi - \Delta\phi_e = \frac{RT}{nF} \ln \frac{c_{x=0}}{c^0} \quad (7.198)$$

Since  $c_{x=0}$  in cathodic reactions is always smaller than  $c^0$ , the concentration polarization has a negative sign, which adds to the activation overpotential in causing the electrode to depart from the equilibrium potential in the negative direction for an electronation reaction.

At this stage, it is worthwhile pointing out a feature of the simplified treatment adopted here. During the discussion of the Butler–Volmer equation (7.23) and the current-produced or activation overpotential  $\eta_a$ , it was assumed that there were no transport limitations on the charge-transfer reaction ( $c_{x=0} = c^0$ , bulk concentration). Correspondingly, in the present very simple version of transport-controlled electrochemistry, it has been assumed that charge-transfer limitations are completely absent, i.e., the charge-transfer reaction has such a high exchange current density that the activation overpotential  $\eta_a$  tends to zero for the current density used [as it would do with a sufficiently high  $i_0$ , cf. Eq. (7.24)].

It is now necessary to take a more unified view by considering situations in which the rate of the electrochemical process at the interface is subject both to activation and to transport limitations. One refers to a *combined activation-transport control* of the electrochemical reaction. Under such conditions, there will be, in addition to the overpotential  $\eta_c$  produced by the concentration change (from  $c^0$  to  $c_{x=0}$ ) at the interface, an activation overpotential  $\eta_a$  because the charge-transfer reaction is not at equilibrium. The total overpotential  $\eta$  is the difference between the interfacial-potential difference

<sup>76</sup>The change of concentration is the immediate cause of the change  $\Delta\phi - \Delta\phi_e$  of potential difference across the interface, but the concentration change itself is the result of a current. So, when one refers to concentration-produced overpotential,  $\eta_c$ , as opposed to the current-produced overpotential of Section 7.2.7, one is stressing immediate causes.

<sup>77</sup>To keep the distinction clear, a suffix “a” is hereafter attached to the overpotential arising from the fact that in the charge-transfer reaction an activation process is necessary. Hence,  $\eta_a$  is sometimes known as the *activation overpotential*.

$\Delta\phi$ , corresponding to a current density  $i$ , and the equilibrium-potential difference  $\Delta\phi_e$

$$\eta = \Delta\phi - \Delta\phi_e \quad (7.199)$$

but now it is possible to resolve (Fig. 7.94) this total overpotential into two portions: (1) a portion  $\eta_a$  arising from the fact that the charge-transfer reaction must be electrically driven or activated to make it go at a particular rate; and (2) another portion,  $\eta_c$ , arising from the shift in equilibrium potential produced by the transport-induced fall in interfacial concentration

$$\eta = \Delta\phi - \Delta\phi_e = \eta_a + \eta_c \quad (7.200)$$

It must be mentioned here that the activation overpotential  $\eta_a$ , as given by the Butler–Volmer equation (7.24), contains implicit concentration terms hidden in  $i_0$ ; these concentration terms refer to the concentrations at the OHP and not to bulk values. Only in certain circumstances can the concentration at the OHP be placed equal to the bulk concentration, e.g., when  $^{\text{OHP}}\Delta^S\phi = 0$  and  $\eta_c = 0$ .

### 7.9.9. The Diffusion Layer

When transport is not able to do its job adequately and there is a change in the interfacial concentrations of electron acceptors and donors from the bulk values, there is a variation of concentration with distance from the interface toward the bulk of the solution. What matters, however, as far as the charge-transfer reaction is concerned, is the gradient of concentration *at the interface* because it is this gradient that drives the diffusion flux  $J_D$ . Even when there is convection with a laminar flow of electrolyte, the transport in the (assumed) stagnant layer adjacent to the electrode is by diffusion

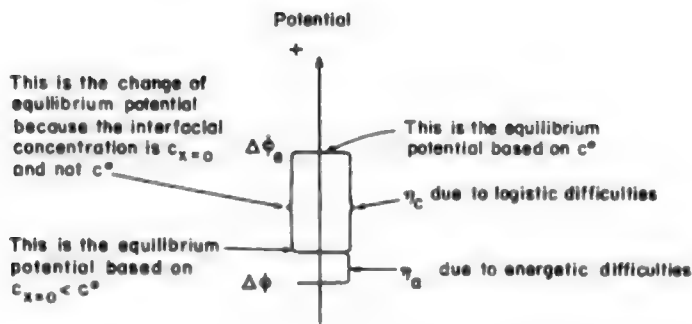


**Fig. 7.94.** The change in potential during the passage of a current in a cathodic process is negative and due to logistic and energetic difficulties.

and the flux  $J$  is governed by the concentration gradient in the layer. Thus, using Fick's law of diffusion (see Section 4.2.2), one has

$$\frac{i}{nF} = J_D = -D \left( \frac{dc}{dx} \right)_{x=0} \quad (7.201)$$

Now, in general, this concentration profile is such that there is a linear variation of concentration over small distances from the interface and then the concentration asymptotically approaches the bulk value. In this context, Nernst put forward a simplifying suggestion. One might extrapolate (Fig. 7.95) the linear part of the concentration vs. distance curve until it intersects the bulk value of the concentration at some distance  $\delta$  from the interface. Then the gradient of the concentration at  $x = 0$ , i.e.,  $(dc/dx)_{x=0}$ , can be replaced by  $(c^0 - c_{x=0})/\delta$  to give [from 7.201]

$$\frac{i}{nF} = J_D = -D \frac{c^0 - c_{x=0}}{\delta} \quad (7.202)$$

In this approximation, therefore, one can consider that the diffusion occurs across a region parallel to the interface, i.e., across a *Nernst diffusion layer* of effective thickness  $\delta$ .

The diffusion-layer concept is an artifice for handling the flux arising from what would be, if treated in a proper hydrodynamic way, a complicated space variation of concentration at the interface. There is always some gradient of concentration at the interface; there is an initial region in which the concentration changes linearly with distance, but there is, in the real case, no sharply defined layer of definite thickness, even when convection (natural or forced) produces a steady-state concentration

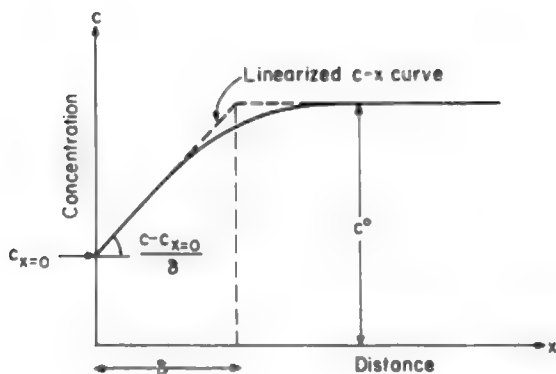


**Fig. 7.95.** The Nernst diffusion-layer thickness is obtained by extrapolating the linear portion of the concentration change to the bulk concentration value.



profile. If the concentration profile is not stabilized by forced convection, the effective diffusion-layer thickness varies with time in the case of semi-infinite linear diffusion [cf. Eq. (7.204)] until natural convection sets in and fixes the concentration profile (Fig. 7.96). In the case of forced convection, e.g., stirring, where the convective transport of species to and from the electrode is much faster than for natural convection, the concentration gradients extend over a much shorter distance  $\delta$ . The precise value of the Nernst diffusion-layer thickness  $\delta$  depends largely on the effectiveness of forced convection, being smaller the greater the effectiveness. Generally, the convection is laminar where the value of  $\delta$  and hence of the concentration gradient is governed by the electrode geometry, the kinematic viscosity.<sup>78</sup> The diffusion coefficient, and the velocity of the liquid caused by stirring; turbulent flow is also usually involved when the electrolyte is stirred. Both types of convection have been described mathematically by Levich.

Since  $\delta$  represents only an approximate and simplifying property, it is difficult to evaluate it numerically from fundamental theory. However, it turns out that in a very rough and order-of-magnitude sense, a numerical value for  $\delta$  of about 0.05 cm in solutions in which no forced convection has been artificially introduced is useful for calculations pertaining to transport-controlled electrochemicals.<sup>79</sup> As artificial convection (stirring, electrode rotation) is introduced, the value of  $\delta$  that must be introduced into (7.206) depends entirely on the degree of stirring. The value can be reduced to some  $10^{-3}$  cm and even smaller values with sufficiently high stirring. A hydrodynamic theory of  $\delta$  is available if the hydrodynamic conditions are sufficiently well defined, as, e.g., they are for the rotating-disk electrode (Section 7.5.14). Table 7.10 indicates the value of  $\delta$  under three conditions, calculated by assuming a rotating disk of a geometry shown in Fig. 7.97 and a value of  $\delta$  of 0.05 cm in stationary solutions.

The time variation of  $\delta$  before the onset of natural convection depends on how the diffusion process is provoked. If a constant current density is switched on at  $t = 0$ , then the time variation of the effective diffusion-layer thickness can be obtained from Eqs. (7.179) and (7.202)

$$c^0 - c_{x=0} = -\frac{i_g}{nF} \frac{\delta}{D} = -\frac{2i_g}{nF} \sqrt{\frac{t}{\pi D}}$$

$$\delta = \frac{2}{\sqrt{\pi}} \sqrt{Dt} \quad (7.203)$$

showing that the effective diffusion-layer thickness increases as the square root of time. It can be shown equally well that if one considers a diffusion-controlled electronation process occurring under a constant potential switched on at  $t = 0$ , the diffusion-layer thickness is given as

<sup>78</sup>The kinematic viscosity is the ratio of the electrolyte coefficient of viscosity and its density.

<sup>79</sup>For example,  $\delta \approx 0.05$  cm yields the correct order of magnitude for the maximum current—the limiting current,  $i_L$  [cf. Eq. (7.206)], that a particular charge-transfer reaction can support. This maximum is determined by the maximum transport flux of reactants under diffusion control, in the steady state.

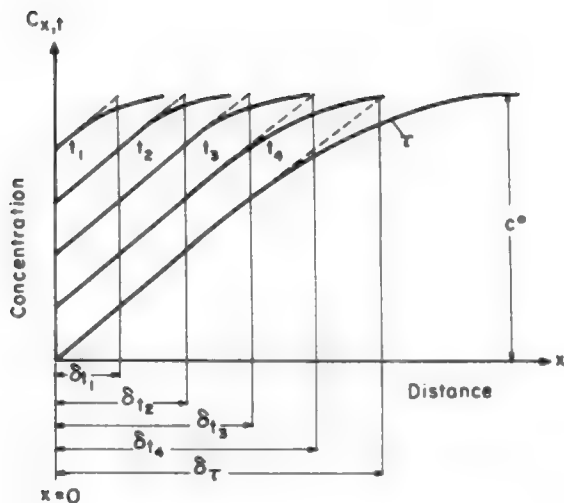


**Fig. 7.96.** When diffusion is not disturbed by convection, it can be shown that the diffusion-layer thickness  $\delta$  varies with the square root of time.

$$\delta = \sqrt{\pi D t} \quad (7.204)$$

which is also a square-root dependence of  $\delta$  on time.

Very much more is known about the theory of concentration gradients at electrodes than has been mentioned in this brief account. Experimental methods for observing them have also been devised, based on the dependence of refractive index on concentration (the Schlieren method) by means of interferometry (O'Brien, 1986). Nevertheless, the basic concept of an effective diffusion-layer thickness, treated here as varying in thickness with  $t^{1/2}$  until the onset of natural convection and as constant with time after convection sets in (though decreasing in value with the degree of disturbance, Table 7.10), is a useful aid to the simple and approximate analysis of many transport-controlled electrodic situations. A few of the uses of the concept of  $\delta$  will now be outlined.

### 7.9.10. The Limiting Current Density and Its Practical Importance

When an electronation reaction is occurring at an interface, the equality of the charge-transfer flux and the transport flux requires that

$$\frac{i}{nF} = -D \left( \frac{dc}{dx} \right)_{x=0} \quad (7.201)$$

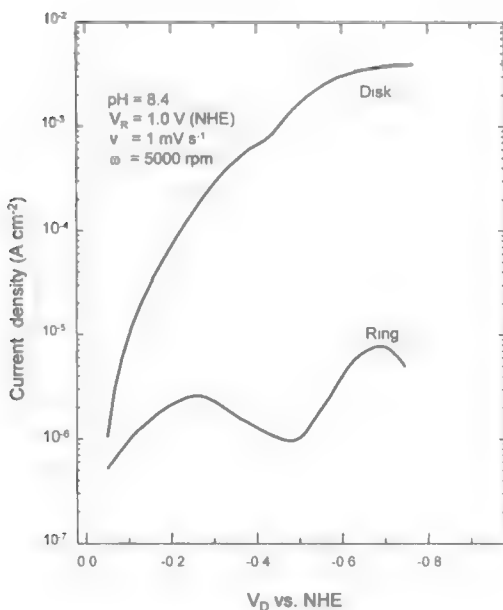


**Fig. 7.97.** Disk and ring currents as a function of the disk potential for O reduction and H<sub>2</sub>O<sub>2</sub> oxidation. Rotation rate is 5000 rpm. (Reprinted from V. Jovancicevic and J. O'M. Bockris, *J. Electrochem. Soc.* **133**(9) 1799, 1986. Reproduced by permission of The Electrochemical Society, Inc.)

**TABLE 7.10**  
Influence of Rotating Disk Electrode Condition (Stationary or Rotating) on the Diffusion-Layer Thickness and the Limiting Current Density for the Reaction  $I_3^- + 2e \rightarrow 3I^-$ <sup>a</sup>

Electrode Condition	Limiting Current Density $i_L$ ( $\mu\text{A cm}^{-2}$ )	Diffusion-Layer Thickness $\delta$ (cm)
Stationary	28.9	0.05
Rotated at 50 rpm	134.1	0.011
Rotated at 240 rpm	292.1	0.005

<sup>a</sup>Concentration of KI<sub>3</sub> is  $6.6 \times 10^{-4} M$  and the diffusion coefficient of I<sub>3</sub><sup>-</sup> is  $1.14 \times 10^{-5} \text{ cm}^2 \text{ s}^{-1}$ .

In terms of the diffusion-layer concept (Section 7.9.9), this condition becomes

$$\frac{i}{nF} = -D \left( \frac{dc}{dx} \right)_{x=0} = -D \frac{c^0 - c_{x=0}}{\delta} \quad (7.202)$$

It is obvious that the concentration gradient has a maximum value for  $c_{x=0} = 0$ . Placing this limit upon Eq. (7.202) produces

$$\lim_{c_{x=0} \rightarrow 0} \left( \frac{dc}{dx} \right)_{x=0} = \lim_{c_{x=0} \rightarrow 0} \frac{c^0 - c_{x=0}}{\delta} = \frac{c^0}{\delta} \quad (7.205)$$

This maximum-concentration gradient corresponds to a maximum or *limiting current density* denoted by  $i_L$  and given from (7.202) and (7.205) by

$$i_L = -\frac{DnFc^0}{\delta} \quad (7.206)$$

For a given electronation reaction, this is the maximum attainable current density. The reaction cannot go faster than  $i_L$  because the transport process in the electrolyte bulk is incapable of supplying the electron acceptor to the interface at a faster rate.

The concept of a limiting current density is of great practical importance. Table 7.11 shows some typical experimental limiting current densities for four energy producers employing oxygen (where the calculation of limiting current density is more complicated than that of (7.206).

**7.9.10.1. Polarography: The Dropping-Mercury Electrode.** The proportionality between  $i_L$  and  $c^0$  [cf. Eq. (7.206)] constitutes the basis of *polarography*, a powerful electroanalytical technique introduced by Heyrovsky. The essential part of the polarographic setup (Fig. 7.98) is a dropping-mercury electrode consisting of a glass capillary tube out of which mercury converges at the rate of a drop every few seconds. To the solution is added a large excess ( $\sim 1 M$ ) of a substance termed an *indifferent electrolyte* because its ions do not participate in, or are indifferent to, the

**TABLE 7.11**  
**Typical Experimental Limiting Current Density (per Geometric External Square Centimeter of a Porous Electrode) for Four Energy Producers**

Cell	Limiting Current Density ( $A\text{ cm}^{-2}$ )
Propane-oxygen	0.6
Hydrogen-oxygen	0.8
Hydrogen-air	0.13
Hydrazine-oxygen	0.64

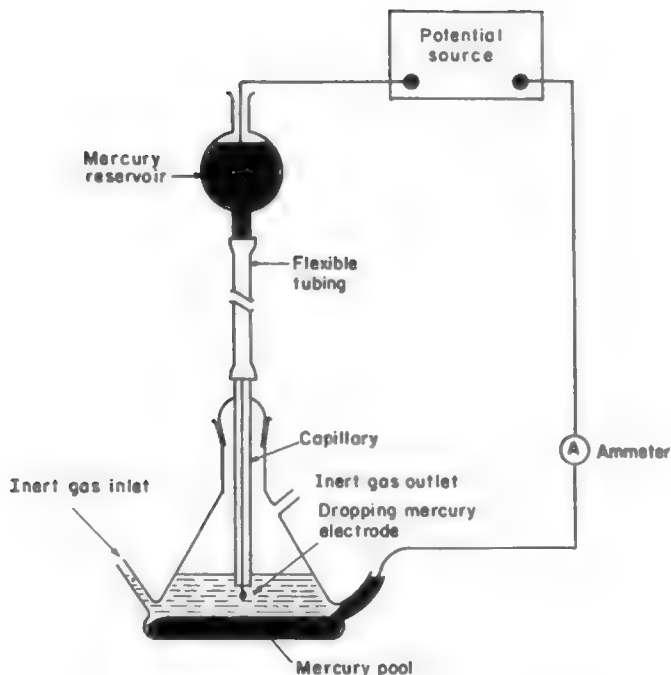


**Fig. 7.98.** The dropping mercury electrode arrangement.

charge-transfer reaction at the drop/solution interface. In contrast, the species A under polarographic analysis exists in the solution at a very small concentration ( $\sim 10^{-3} M$ ). This wide disparity in the concentrations of A and the indifferent electrolyte ensures that the ions of the indifferent electrolyte carry the migration current and that any transport of species A occurs by a process of pure diffusion.

In a polarographic experiment, a potential difference  $E$  is applied across the cell consisting of the dropping-mercury electrode and a nonpolarizable interface (e.g., a calomel electrode). In response to this potential difference, a current density  $i$  flows across the drop/solution interface. As each drop grows and falls, however, the surface area of the drop also grows, and then becomes effectively zero when the drop falls. Thus, the instantaneous current (current density times surface area) shows fluctuations, but the mean current is a unique function of the potential difference across the drop/solution interface, and therefore of that across the cell.

The relationship between the mean current and the potential (Fig. 7.99) will now be derived. Suppose that at the drop/solution interface, an electronation reaction:  $A + ne \rightarrow D$  is driven by the imposition of a constant potential,  $E$ . The reaction results in the depletion of A in the interfacial region, and therefore in the diffusion of A toward the drop/solution interface. Let it be assumed that the species D produced by the

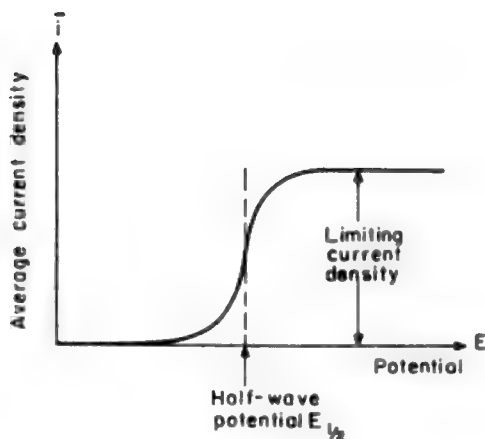


**Fig.7.99.** The polarographic wave is the current-potential dependence in which, at some sufficiently high potential values, the current becomes entirely diffusion controlled.

electrode reaction is soluble either in the electrolyte or in mercury (i.e., D is an amalgam-forming metal). Then, since there is generation of D in the interfacial region, there will be a diffusion of D away from the drop/solution interface either toward the electrolyte or into the mercury.

It is clear that since the mercury drop approximates a sphere, the theory of *spherical*, and *not* linear, diffusion might have to be used. However, detailed considerations accessible in monographs show that if the electrodic reaction is driven for a sufficiently short time ( $t < \text{a few seconds}$ ) and if the mercury-drop radius is not too small ( $r > 0.05 \text{ cm}$ ), then the equations of linear diffusion can be used with validity. Thus, the partial differential equations for the diffusion of A and D are [see Fick's second law; cf. Eq. (4.32)]

$$\frac{\partial c_A(x, t)}{\partial t} = D_A \frac{\partial^2 c_A(x, t)}{\partial x^2} \text{ and } \frac{\partial c_D(x, t)}{\partial t} = D_D \frac{\partial^2 c_D(x, t)}{\partial x^2} \quad (7.207a)$$

The initial conditions are

$$c_A(x, 0) = c^0 \text{ and } c_D(x, 0) = 0 \quad (7.207b)$$

i.e., before the imposition of the potential difference  $E$ , the concentrations of A and D for any  $x$  are  $c^0$  and zero, respectively.

The first boundary condition to be satisfied by solutions of the differential equations (7.207a) arises from the fact that the only source for the material D is the

electrode transformation of A by the reaction  $A + ne \rightarrow D$ . For each mole of A reacting at the interface (i.e., at  $x = 0$ ), one mole of D is produced; hence, the sum of the fluxes of A and D at  $x = 0$  must be equal to zero:

$$D_A \left( \frac{\partial c_A(x, t)}{\partial x} \right)_{x=0} + D_D \left( \frac{\partial c_D(x, t)}{\partial x} \right)_{x=0} = 0 \quad (7.207c)$$

The second boundary condition involves a relation between the concentrations of A and D and the potential  $E$ . The simplest relation is obtained by (initially) *assuming that there is charge-transfer equilibrium at the interface* ( $x = 0$ ), in which case the Nernst equation (7.47) can be applied:

$$E = E^0 + \frac{RT}{nF} \ln \frac{a_A(0, t)}{a_D(0, t)} = E^0 + \frac{RT}{nF} \ln \frac{c_A(0, t)f_A}{c_D(0, t)f_D} \quad (7.207d)$$

where  $a_A, f_A$  and  $a_D, f_D$  are the activities and activity coefficients of the species A and D, respectively.

Finally, the situation far away from the drop can be assumed to be unperturbed by the reaction  $A + ne \rightarrow D$ . Thus, one has

$$c_A(\infty, t) = c^0 \text{ and } c_D(\infty, t) = 0 \quad (7.207e)$$

Before attempting to solve the differential equations (7.207a) in the context of the initial and boundary conditions (7.207b)–(7.207e), two variables,  $\theta$  and  $c_1(x, t)$ , will be defined thus:

$$\theta = \frac{c_A(0, t)}{c_D(0, t)} = \frac{f_D}{f_A} \exp \left[ \frac{nF}{RT} (E - E^0) \right] \quad (7.208)$$

and

$$c_1(x, t) = c^0 - c_A(x, t) \quad (7.209)$$

In terms of these two variables, the differential equations (7.207a) and the initial and boundary conditions (7.207b)–(7.207e) become

$$\frac{\partial c_1(x, t)}{\partial t} = D_A \frac{\partial^2 c_1(x, t)}{\partial x^2} \text{ and } \frac{\partial c_D(x, t)}{\partial t} = \frac{\partial^2 c_D(x, t)}{\partial x^2} \quad (7.210a)$$

$$c_1(x, 0) = 0 \text{ and } c_D(x, 0) = 0 \quad (7.210b)$$

$$-D_A \left( \frac{\partial c_1(x, t)}{\partial x} \right)_{x=0} + D_D \left( \frac{\partial c_D(x, t)}{\partial x} \right)_{x=0} = 0 \quad (7.210c)$$

$$\frac{c^0 - c_1(0, t)}{c_D(0, t)} = \theta \quad (7.210d)$$

$$c_1(\infty, t) = 0 \text{ and } c_D(\infty, t) = 0 \quad (7.210e)$$

The corresponding Laplace transforms of equation (7.210a) are

$$p\bar{c}_1(x, p) - c_1(x, 0) = D_A \frac{d^2 \bar{c}_1(x, p)}{dx^2}$$

and

$$p\bar{c}_D(x, p) - c_D(x, 0) = D_D \frac{d^2 \bar{c}_D(x, p)}{dx^2}$$

These total differential equations can be combined with the initial condition (7.210b) and solved. The result is

$$\bar{c}_1(x, p) = A_1 \exp[-x \sqrt{p/D_A}] + A_2 \exp[+x \sqrt{p/D_A}] \quad (7.211a)$$

$$\bar{c}_D(x, p) = B_1 \exp[-x \sqrt{p/D_D}] + B_2 \exp[+x \sqrt{p/D_D}] \quad (7.211b)$$

The integration constants  $A_2$  and  $B_2$  must be zero in order to satisfy the boundary conditions (7.210e), in which case

$$\bar{c}_1(x, p) = A_1 \exp[-x \sqrt{p/D_A}] \quad (7.212a)$$

$$\bar{c}_D(x, p) = B_1 \exp[-x \sqrt{p/D_D}] \quad (7.212b)$$

To evaluate  $A_1$  and  $B_1$ , it is necessary to use boundary conditions (7.210c) and (7.210d), which after Laplace transformation are

$$\bar{c}_1(0, p) + \theta \bar{c}_D(0, p) = c^0/p \quad (7.213a)$$



$$D_A \left( \frac{d\bar{c}_1(x, p)}{dx} \right)_{x=0} - D_D \left( \frac{d\bar{c}_D(x, p)}{dx} \right)_{x=0} = 0 \quad (7.213b)$$

If equations (7.212a) and (7.212b) are used in (7.213a) and (7.213b), the integration constants  $A_1$  and  $B_1$  turn out to be

$$A_1 = \frac{c^0}{1 + \theta m} \frac{1}{p} \quad (7.214a)$$

$$B_1 = mA_1 \quad (7.214b)$$

where

$$m = \sqrt{D_A/D_D} \quad (7.214c)$$

Thus, the solutions of the total differential equations are

$$\bar{c}_1(x, p) = \frac{c^0}{1 + \theta m} \frac{\exp[-(x/\sqrt{D_A}) \sqrt{p}]}{p} \quad (7.215a)$$

and

$$\bar{c}_D(x, p) = \frac{c^0 m}{1 + \theta m} \frac{\exp[-(x/\sqrt{D_D}) \sqrt{p}]}{p} \quad (7.215b)$$

It is known, however, that the Laplace transform (see Table 7.12) of  $\text{erfc}(k/2 \sqrt{t})$  is  $e^{-k\sqrt{p}}/p$ , i.e.,

$$\mathcal{L}[\text{erfc}(k/2 \sqrt{t})] = \int_0^{\infty} e^{-pt} \text{erfc}(k/2 \sqrt{t}) dt = e^{-k\sqrt{p}}/p$$

hence

$$c_1(x, t) = \frac{c^0}{1 + \theta m} \text{erfc} \left( \frac{x}{2\sqrt{D_A t}} \right) \quad (7.216)$$

or

$$c_A(x, t) = c^0 \left[ \frac{\theta m + \text{erf}(x/2\sqrt{D_A t})}{1 + \theta m} \right] \quad (7.216a)$$

and

**TABLE 7.12**  
**Error Functions and Error Function Complements<sup>a</sup>**

$y$	$\text{erf}(y)$	$\text{erfc}(y)$
0	0	1
0.05	0.05637	0.94363
0.1	0.11246	0.88754
0.2	0.22270	0.77730
0.4	0.42839	0.57161
0.8	0.74210	0.25790
1.0	0.84270	0.15730
2.0	0.99532	0.00468
3.0	0.99998	0.00002

<sup>a</sup>Equation (7.216) includes the term  $\text{erfc}[x/2(D_A t)^{1/2}]$ , which can be rewritten as  $1 - \text{erf}[x/2(D_A t)^{1/2}]$ . The error function can be written generally as  $\text{erf}(y) = (2/\sqrt{\pi}) \int_0^y e^{-u^2} du$ , where  $u$  is simply a "dummy" variable;  $u$  does not appear in the final answer since integrating between 0 and  $y$  produces a final result dependent on  $y$ . Let  $y = x/2(D_A t)^{1/2}$ ; then  $\text{erf}[x/2(D_A t)^{1/2}] = (2/\sqrt{\pi}) \int_0^{x/2(D_A t)^{1/2}} e^{-u^2} du$ . Tabulations of the  $\text{erf}(y)$  as a function of the upper limit of integration  $y$  are available, examples of which are given.

$$c_D(x, t) = \frac{c^0 m \text{erf}(x/2\sqrt{D_D t})}{1 + \theta m} \quad (7.217)$$

At time  $t$ , the instantaneous current  $i_t$  is given by Fick's first law:

$$i_t = nFA_t D_A \left( \frac{\partial c_A(x, t)}{\partial x} \right)_{x=0} \quad (7.218)$$

where  $A_t$  is the surface area of the drop at time  $t$ . It is necessary, therefore, to get an explicit expression for the concentration gradient  $[\partial c_A(x, t)/\partial x]_{x=0}$  at the interface. This expression is obtained by differentiating Eq. (7.216a) with respect to  $x$  and then setting  $x = 0$  in the result. Thus, with

$$\frac{d \text{erf}[\lambda(x)]}{dx} = \frac{2}{\sqrt{\pi}} e^{-[\lambda(x)]^2} \frac{d[\lambda(x)]}{dx}$$

the result of the differentiation is

$$\left( \frac{dc_A(x, t)}{dx} \right)_{x=0} = \frac{c^0}{\sqrt{\pi D_A t}} \frac{1}{1 + \theta m} \quad (7.219)$$

Combining Eqs. (7.217) and (7.218), one obtains

$$i_t = \frac{nFA_t \sqrt{D_A} c^0}{\sqrt{\pi t}} \frac{1}{1 + \theta m} \quad (7.220a)$$

$$= i_L \frac{1}{1 + \theta_m} \quad (7.220b)$$

since the current, when  $\theta = c_A(0, t)/c_D(0, t) = 0$ , i.e., when  $c_A(0, t) = 0$ , is equal to the limiting current,  $i_L$ ,

$$i_L = \frac{nFA_i \sqrt{D_A} c^0}{\sqrt{\pi t}} \quad (7.220c)$$

By eliminating  $\theta$  between Eqs. (7.220b) and (7.207) one obtains the required current-potential relation:

$$E = E^0 - \left[ \frac{RT}{nF} \ln \left( \frac{f_D}{f_A} \right) \left( \frac{D_A}{D_D} \right)^{\frac{1}{2}} \right] + \frac{RT}{nF} \ln \frac{i_L - i_t}{i_t} \quad (7.221a)$$

$$= E_1 + \frac{RT}{nF} \ln \frac{i_L - i_t}{i_t} \quad (7.221b)$$

where  $E_1$  is termed the *half-wave potential* because the  $i_t$  versus  $E$  curve—the *polarographic wave*—is of the form shown in Fig. 7.98 and  $E = E_1$  when  $i_t = \frac{1}{2}i_L$ , i.e., when  $i_t$  has attained half the wave height  $i_L$ . The potential  $E_1$  also corresponds to an inflection point in the  $i_t$  versus  $E$  curve, for it may be shown that the second derivative of the  $i_t$  versus  $E$  curve is equal to zero—the criterion for an inflection point—when  $i_t = \frac{1}{2}i_L$ .

The half-wave potential  $E_1$  (Table 7.13) might be called a pseudo-fundamental quantity in polarographic analysis since, in the absence of disturbing factors, particularly the heat of amalgam formation, it should be equal to the standard electrode potential  $E_0$  [Eq. (7.221a)]. It was once thought that by determination of the half-wave potential and the assumption that this potential corresponded to the standard thermodynamic potential of the reaction at the mercury/solution interface, a qualitative identification of the species in solution could be made. However, the approximations involved in Eq. (7.221) reveal this as untrue; thus, the identification of the half-wave potential as the standard thermodynamic electrode potential depends not only upon the neglect of amalgam formation between the product  $D$  and the mercury but also upon the assumption made in Eq. (7.221) that the activation overpotential is negligible. It may well be true that for a number of reactions,  $\eta_A$  is negligible at the current densities obtained in polarographic analysis. However, it is too gross an assumption to allow polarography anything but a historical claim to applications in qualitative analysis.

**TABLE 7.13**  
**Polarographic Half-Wave Potentials  $E_{1/2}$  in Volts (vs. SCE), for Certain Metal Cations in the Presence of Either Ammonia–Ammonium Chloride Mixture or Tetraethylammonium Hydroxide as the Indifferent Electrolyte**

Indifferent Electrolyte Present in Excess	Metal Cation	$E_{1/2}$ (V, SCE)
Ammonia–ammonium chloride mixture	Mn <sup>2+</sup>	–1.66
	Ga <sup>3+</sup>	–1.60
	Fe <sup>2+</sup>	–1.49
	Zn <sup>2+</sup>	–1.35
	Co <sup>2+</sup>	–1.29
	Ni <sup>2+</sup>	–1.10
	Cd <sup>2+</sup>	–0.81
	Cu <sup>2+</sup>	–0.51
	Tl <sup>+</sup>	–0.48
	Li <sup>+</sup>	–2.31
Tetraethylammonium hydroxide	Mg <sup>2+</sup>	–2.30
	Ca <sup>2+</sup>	–2.22
	Sr <sup>2+</sup>	–2.11
	K <sup>+</sup>	–2.10
	Na <sup>+</sup>	–2.07
	Ba <sup>2+</sup>	–1.92
	Cr <sup>2+</sup>	–1.58

Quantitative analysis is, however, possible since, in Eq. (7.221), the existence of a limiting current density and its relationship to the concentration of species undergoing electronation are unaffected by the approximations involved. However, as Eq. (7.206a) shows,  $i_L$  is a function of time and as  $t$  rises, the diffusion-controlled current decreases toward zero. This is one disadvantage of working at a stationary electrode. Another disadvantage is the effect of impurities that accumulate at the surface. In order to avoid these difficulties, a dropping-mercury electrode is used where each drop extends only over a short time, which is determined by the flow rate  $v$ . The same law of nonstationary linear diffusion can be applied; however, a correction must be made for the variation of the surface area with time. The surface area  $A_t$  can be calculated, on assuming perfectly spherical drops, as follows. The weight of the drop at time  $t$  is given by

$$vt = \frac{4\pi r^3}{3} d$$

where  $r$  and  $d$  are the radius and density of the mercury drop, respectively. Then,

$$A_t = 4\pi r^2 = 4\pi \left( \frac{3}{4\pi d} vt \right)^{\frac{2}{3}}$$

and, at 25 °C,

$$A_t = 0.8515(vt)^{\frac{2}{3}} \quad (7.222)$$

The thickness of the diffusion layer, as first shown by Ilkovic, will be changed in that instead of Eq. (7.204), one has now for an expanding spherical drop

$$\delta = \left( \frac{3}{7} \pi D t \right)^{\frac{1}{2}} \quad (7.223)$$

From Eqs. (7.206), (7.222), and (7.223), the limiting current at time  $t$  is given by

$$i_L = i_{\text{lim}} = (7.082 \times 10^4) n v^{\frac{2}{3}} t^{\frac{1}{3}} D_A^{\frac{1}{2}} C^0 \quad (7.224)$$

This equation—in which  $i$  is in amperes,  $v$  in grams per second,  $t$ , in seconds,  $D_A$  in square centimeters per second, and  $c^0$  in moles per cubic centimeter—is known as the *Ilkovic equation*.

### 7.9.11. The Steady-State Current–Potential Relation under Conditions of Transport Control

The concept of limiting current density permits a simple derivation of a relation between the steady-state concentration overpotential  $\eta_c$  and the current density  $i$  if the reaction is such that other forms of overpotential are negligible. One starts from the expression for the concentration overpotential  $\eta_c$  [cf. Eq. (7.198)]

$$\eta_c = \frac{RT}{nF} \ln \frac{c_{x=0}}{c^0} \quad (7.198)$$

the electronation current density is given by

$$i = -DnF \frac{c^0 - c_{x=0}}{\delta} \quad (7.202)$$

and one can write

$$c^0 - c_{x=0} = \frac{-\delta}{DnF} i$$

or

$$\frac{c_{x=0}}{c^0} = 1 + \frac{\delta}{DnF c^0} i \quad (7.202)$$

But, from (7.206),

$$\frac{\delta}{DnFc^0} = -\frac{1}{i_L} \quad (7.206)$$

hence,

$$\frac{c_{x=0}}{c^0} = 1 - \frac{i}{i_L} \quad (7.225)$$

### 7.9.12. The Diffusion-Activation Equation

In the assumptions that were made in this chapter up to the beginning of this section, it was assumed that transport of charge carriers to and from the electrode played no part in rate control because it was always plentiful. Thus, in the evolution of hydrogen from acid solutions, the current density in most experimental situations is less than 10 times the limiting diffusion current and for this reason there is a negligible contribution to the overpotential due to an insufficiency of charge carriers. Like water from the tap in a normal city, the rate of supply of carriers is both tremendously important but seldom considered, for there is always plenty available.

Now, in this section on transport, the situation has been reversed. It has been assumed (at the other end of the spectrum, so to speak) that the events at the interface and on the electrode itself are very fast. Whatever they have to do to get things done, they do with lightning speed. One can see the result of this—the rate of supply of charge carriers to (or from) the interface may no longer be sufficient. It is as though the house with its plentiful water supply had become, say, a laundromat with a tremendous need for water. Suddenly the rate at which the water arrives may become a critical factor.

All this is clear enough, but nature of course does not always arrange itself in this clean-cut either-or manner. There may be reactions in which the parameters of the electron transfer at the interface are not fast enough compared with that of the transport reaction to be neglected, i.e., the overpotential developed by the interfacial happenings may be sufficiently large that it can no longer be neglected in considering the kinetics of a reaction in which diffusion control plays an important part. In these cases, the limiting equations that have so far been thought to represent “reality” have to be modified and equations deduced that express the influence of both transport and interfacial reactions.

### 7.9.13. The Concentration of Charge Carriers at the Electrode

In order to convert a current-potential relation from one based on the assumption that transport is plentiful to one that takes into account both transport and the interfacial reactions, it is first necessary to relate  $c_e$ , the concentration of the reactant ion (or

molecule) at the interface, to that in the bulk. Thus, the steady-state current at the electrode is given by

$$i = -DF \frac{\partial c_i}{\partial x} = -\frac{DF}{\delta} (c_{i,e} - c_{i,0}) \quad (7.226)$$

$$i = -FD \frac{\partial c}{\partial x} \quad (7.227)$$

where  $c_{i,0}$  is the concentration of the reacting particle in the bulk, and  $c_{i,e}$  is that of the reacting entity at the electrode.

The value of  $c_{i,0}$  is independent of the electrode process, but that of  $c_{i,e}$  decreases with an increase in cathodic current density (see Fig. 7.85). The maximum value of  $i$  is reached when  $c_e = 0$ . Then

$$i_L = + \frac{DzF}{\delta} c_{0,i} \quad (7.228)$$

From (7.227) and (7.228):

$$\frac{c_{e,i}}{c_{0,i}} = 1 - \frac{i}{i_L}, \quad c_{i,e} = c_{0,i} \left( 1 - \frac{i}{i_L} \right) \quad (7.229)$$

Thus, when  $i \ll i_L$ , so that  $i/i_L \rightarrow 0$ ,  $c_{e,i} \rightarrow c_{0,i}$ , i.e., the interfacial concentration is that of the bulk.<sup>80</sup> Correspondingly, at sufficiently high current densities, the concentration of reactant particles at the interface ( $c_{e,i}$ ) tends to zero. It is clear the current can increase no more; that is why the corresponding current density,

$$i_L = \frac{DzF}{\delta} c_{0,i} \quad (7.230)$$

is called the *limiting current density*. However, we are interested in the general case in which  $0 < c_{e,i} < c_{0,i}$  and Eq. (7.229) is then applicable.

### 7.9.14. Current as a Function of Overpotential: Interfacial and Diffusion Control

The Butler–Volmer equation (Eq. 7.23) is a relation for current density,  $i$ , as a function of the overpotential,  $\eta$ , applicable from  $\eta = 0$  to the value of the overpotential

<sup>80</sup>In Section (6.1.6) the effect of the double-layer structure on concentration at the interface compared with that in the bulk was considered. It causes a difference between the bulk concentration and that at the interface. Such differences fade away toward zero when the concentration increases. In the present treatment, they have been neglected.

at which the influences of a limiting diffusion control become significant. To obtain a mathematical relation that allows for this influence of diffusion, the Butler–Volmer equation will be simplified to the Tafel from Eq. (7.29), i.e., that which applies to  $\eta > RT/F$ . Taking the situation of electronation, i.e., the cathodic case in which  $\eta$  is a negative quantity:

$$i = i_0 e^{-\beta\eta F/RT} \quad (7.27)$$

In the equation for  $i_0$ , there is a term for the reactant concentration. This has been assumed to be that of the bulk. In a cathodic reaction, the reactant concentration at the electrode,  $c_{e,i}$  will always be somewhat less than that in the bulk because it is being used up at the electrode surface. In the treatment to follow, it will be assumed that this deviation is significant and that the value corrected for diffusion can be given with the help of Eq. (7.229).

Then, from (7.27) and (7.229):

$$i = i_0 \left( \frac{c_{e,i}}{c_{0,i}} \right) e^{-\beta\eta F/RT} \quad (7.231)$$

Or, from (7.229)

$$i = i_0 \left( 1 - \frac{i}{i_L} \right) e^{-\beta\eta F/RT} \quad (7.232)$$

If one extracts  $i$ , there follows:

$$i = \frac{i_0 e^{-\beta\eta F/RT}}{1 + \frac{i_0}{i_L} e^{-\beta\eta F/RT}} \quad (7.233)$$

One can see at once two extremes from this approximation.<sup>81</sup> If  $i_0 e^{-\eta F/RT} \ll i_L$ , one obtains again

$$i = i_0 e^{-\beta\eta F/RT}$$

which is a form of Tafel's equation (7.29).

If, on the other hand,

$$i_0 e^{-\beta\eta F/RT} \gg i_L$$

<sup>81</sup>This is an approximation because in (7.231),  $i_0$  contains a term in concentration of the reactant  $i$  (which is assumed to cancel with  $c_{0,i}$  on the bottom line), but in fact, the concentration term in  $i_0$  is raised to the power  $(1 - \beta)$ .



$$i = i_L$$

If one takes the entire Butler–Volmer equation, not only the first term, it is easy to show that the condition  $i_0 \gg i_L$  leads for a cathodic reaction to

$$i = i_L(1 - e^{\eta F/RT}),$$

a relation which gives the current–potential relation for a steady-state current under dominating diffusion control.

### 7.9.15. The Reciprocal Relation

Using a relation such as 7.229, one might write a general relation for an electrochemical reaction rate as

$$i = \vec{k}_v F c_0 \left( 1 - \frac{i}{i_L} \right) \quad (7.234)$$

Here,  $\vec{k}_v$  is an electrochemical rate constant, and  $F$  is the faraday, the charge on 1 mol of univalent ions. It contains the exponential term for the electrode potential (assuming a cathodic reaction in a region in which the rate of the back anodic reaction can be neglected). However, it does take into account the effect of diffusion on the observed current density,  $i$ .

Now one could write:

$$i_F = \vec{k}_v F c_0 \quad (7.235)$$

because  $i_F = \vec{k}_v F c_0$  would be the current density if there were no effects of transport control on the reaction (as indeed we have been assuming in all of this chapter except in this section).

So, if one writes:

$$i = i_F \left( 1 - \frac{i}{i_L} \right)$$

it is simple to find:

$$\frac{1}{i} = \frac{1}{i_F} + \frac{1}{i_L} \quad (7.236)$$

This is a simple and helpful relation in understanding the interplay of the Faradaic current density,  $i_F$ , and the diffusion-controlled limiting current density,  $i_L$ . Obviously [as with Eq. (7.233)], there are two limiting cases. If  $i_L \gg i_F$ , one has the situation that one has assumed in earlier sections of this book. If the limiting current is not approached (say, the current density being used is less than 1% of the limiting current density), one can neglect considerations of transport.

However, if  $i_F \gg i_L$ , then the observations of the current density,  $i$ , and its behavior will be very much dependent on  $i_L$ , i.e., on transport and diffusion. By observing such a current, one would gather much information about the concentration of entities in the solution. However, the physicochemical content of  $i_0$  (Chapter 9) would be obscured. Clearly, there will be cases in which  $i_F \approx i_L$  and both diffusion and transport as well as the properties of the interfacial reaction will influence  $i$ .

### 7.9.16. Reversible and Irreversible Reactions

In its most common use in chemistry, the term “reversible” means that a reaction can be made to go in the forward direction or the opposite one easily, e.g., by a change in pressure or temperature. In thermodynamics, the term has a more restricted and specialized meaning. A thermodynamically reversible reaction is one in which the direction can be changed by the application *of an infinitesimally small counter-force*. In practice, a thermodynamically reversible reaction is one that is well balanced at equilibrium, and that can be made to go in either direction by the influence of limitingly small changes in the factors influencing the reaction. For example, one might have an electrochemical reaction “at equilibrium” where by definition no net current can pass in either direction; however, if the potential of the electrode is made just 1 mV (say) more anodic, a significant current passes. One says that the reaction is “in the reversible region.” Were one to go back to equilibrium and apply a bias of 1 mV in the cathodic direction, a significant current (opposite, of course, in direction to that of the anodic) would also be observed.

In electrochemistry, it is envisaged that reactions can fall into two classes, depending on the physical nature of the forces that cause their departure from the equilibrium state (see Table 7.14). If the variations are simply due to concentration changes at the interface, the departure from equilibrium may be small (e.g.,  $\eta < RT/F$ ) and the reaction is said to be *reversible*; the small deviation from equilibrium can be represented by equations that are thermodynamic in origin. Such a situation arises in electrochemistry in transport control and the associated concentration overpotential.

However, electrochemical reactions generally occur at  $\eta \gg RT/F$ . Such reactions are called *irreversible* and the physical occurrences that govern the degree of overpotential that has to be developed to make a given  $i$  flow depend on the chemical physics of the interface—the work function of the electrode and the bond strength of its surface atoms, etc.<sup>82</sup> (Chapter 9).

<sup>82</sup>Thus, an irreversible interfacial reaction is one taking place far from equilibrium; one, for example, determinedly unidirectional, with the influence of the back-reaction (which was still being felt in the reversible region) quite expunged. But the fact that the cathodic evolution (say) of hydrogen occurs irreversibly in the cathodic direction does not mean that the reaction cannot be reversed in direction. Indeed, by adjusting the electrode potential to a value positive to the reversible potential for, say, hydrogen evolution, the anodic dissolution of molecular hydrogen to form protons can be made to occur. The irreversible cathodic reaction has been reversed.

**TABLE 7.14**  
**Comparison of the Rate Equation and the Characteristics of the Two Types of**  
**Catalysis, Chemical (or Thermal) Catalysis and Electrocatalysis**

	Chemical Catalysis	Electrocatalysis
Rate depends on	$e^{-\Delta G^\ddagger/RT}$	$e^{\Delta G^\ddagger/RT} e^{-\alpha F \Delta \phi / RT}$
Potential dependent	No	Yes
Temperature dependent	Yes	Yes
Operating temperature range	Usually above 150 °C	Usually below 150 °C
Activation energy, kcal mol <sup>-1</sup>	10–100	5–35

### 7.9.17. Transport-Controlled Deelectronation Reactions

The above treatment has been solely concerned with electronation reactions, but it is equally valid for deelectronation reactions in which the electron donor is in solution and has to be transported to the interface. It is necessary only to introduce some changes in signs in the equations.

However, for deelectronation reactions in which the electron donor is the solid electrode itself (as in the dissolution of a metal), some changes must be made in the analysis. The main point is that the electron donor (the metal) is in inexhaustible supply and can keep on building up (Fig. 7.100); the concentration gradient therefore keeps on increasing. Thus, the diffusion away gets faster and faster. Strictly speaking, therefore, there should be no limiting current for such a process. In practice, however, the product of the dissolution (i.e., the metal ion) often starts to precipitate out at some

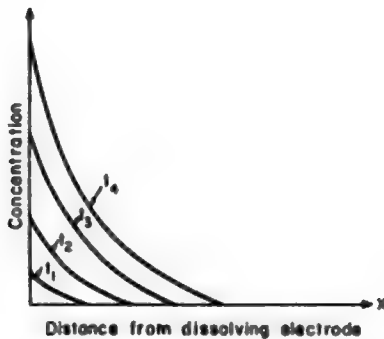


**Fig. 7.100.** In an anodic dissolution process, the concentration of the metal ions at the electrode surface increases with time from  $t_1$  to  $t_4$ .

limiting value of the anodic current density because the solubility product of one of the salts is exceeded. For example, the dissolution of nickel metal may lead to the precipitation of nickel hydroxide.

### 7.9.18. What Is the Effect of Electrical Migration on the Limiting Diffusion Current Density?

Unless there is a large excess of indifferent ions that assume the burden of carrying the current (as indeed was assumed above), the electron acceptors and donors do not move only by diffusion or convection; they also move under the influence of the electric field. In fact, this is generally the case unless one has diminished the fraction of the current in the solution which reactants need for carrying, by adding an excess of ions of another kind that do not undergo electrodic reaction, e.g., the indifferent electrolyte. How must the current-potential equations be modified?

In the steady state, the situation is simple. The basic condition is that at the  $x = 0$  plane, the number of moles per square centimeter per second being transformed by charge transfer is equal to the number of moles arriving per square centimeter per second by electrical migration and by diffusion. The material coming by migration is given by  $t_A(i/nF)$ , where  $t_A$  is the transport number or fraction of the current density carried by the electron-acceptor species A undergoing charge transfer. The diffusion flux is of course given by Fick's law (Section 4.2.2). Hence,

$$\frac{i}{nF} = \frac{t_A i}{nF} + D \frac{c^0 - c_{x=0}}{\delta}$$

or

$$i = + \frac{DnF}{1 - t_A} \frac{c^0 - c_{x=0}}{\delta} \quad (7.237)$$

It is seen from Eq. (7.237) that the current density  $i$  is always greater than in the case of pure diffusion [Eq. (7.202)], in which case  $t_A = 0$  and Eq. (7.237) reduces to (7.202). Similarly, the limiting current density must be greater for migration plus diffusion than for pure diffusion [Eq. (7.206)] and is given by

$$i_L = + \frac{DnF}{1 - t_A} \frac{c^0}{\delta}$$

This is good; when one wants to make substance-producing or energy-producing devices, one wants to maximize charge transfer and one does not like to be limited by transport in the bulk of the electrolyte. Hence, in such systems, the electron-acceptor species must carry as much of the current as possible; the larger its transport number  $t_A$ , the greater is its limiting current density. As  $i_L$  increases,  $\eta_c$  decreases and there is

a minimum waste of electrical energy utilized to combat transport limitations. This is of course only the case when migration helps the transport *toward* the electrode.

When migration enters the transport picture, it is important to realize that the direction of electrical migration of a charged species depends on the sign of the charge. Negatively charged species (anions) migrate to the positive, or electron-sink, electrode (the anode), and positively charged species (cations) migrate to the electron-source electrode (the cathode). It is known, however, that ions that accept electrons do not always have to be positively charged, as might at first be thought, e.g., the negatively charged  $[\text{Ag}(\text{CN})_2]^-$  is electronated at a negative electron-source electrode. The question is: If such ions migrate under the applied field gradient away from the electron-source electrode, how are they transported to it? This question was analyzed in Section 4.4.15. It will be referred to here by pointing out that it is the diffusion flux [i.e., the term  $DnF(c^0 - c_{x=0})/\delta$  of Eq. (7.202)] that has to sustain now not only the charge-transfer reaction but also the loss of ions from the reacting layer due to electrical migration away. Negatively charged particles can be electronated at the negative electrode as long as the diffusion flux *toward* the electrode is greater than the electrical migration *away* from the electrode.

### 7.9.19. Some Summarizing Remarks on the Transport Aspects of Electrodeics

In volume 1 (Chapters 4 and 5) a fairly detailed treatment of the movement and transport of ions was presented; qualitative pictures and quantitative accounts were given of the diffusion and electrical migration of ions in the bulk of the electrolyte. In the treatment of electrodic processes, no mention was made at first of a connection between the transport in solution and processes at electrodes. It was then realized that this neglect of ion transport in solution (ionics) was tantamount to assuming that at no stage in the course of a charge-transfer reaction did the interfacial concentrations of electron acceptors and donors depart from their bulk values.

This section began with the realization that the supply of the material requirements of the interface may sometimes not be sufficient to meet the demands of charge transfer and therefore one has to be able to analyze such supply problems. The transport of particles through the solution is one of the essential steps that join with the step (or steps) of the charge-transfer reaction to constitute the overall reaction. Hence, the rate of the transport may at relatively high current densities determine the overall rate. Thus, one began to think of current densities that may be transport controlled. It turned out that diffusion control, in particular one type of transport process, is easy to describe in a very simple physical way.

The treatment of nonsteady-state diffusion is a question of solving Fick's second law of diffusion. In many cases, however, the equations can be taken from the treatments of the analogous problems in heat flow in solids. The point is that heat flow and diffusion are described by mathematically similar methods.

The analysis of one problem, namely, how semi-infinite linear diffusion affects the response of an interface to the switching on of a constant current showed that after a certain time known as the *transition time*, the potential difference at the interface undergoes a rapid change. This rapid variation occurs because the interfacial concentrations of the particles diffusing to the interface tend to zero. Application of this fact to a simple equation relating the potential difference at the interface to concentration shows that when  $c_{x=0}$  tends to zero, the corresponding potential difference tends to highly negative values.

However, the onset of natural convection or a deliberate resort to stirring the solution may hold the interfacial concentrations at steady values. Under these steady-state conditions, one may use Fick's first law, and the equality of the flows of particles up to and across the interface for an electronation reaction can be written as

$$\frac{i}{nF} = -D \left( \frac{dc}{dx} \right)_{x=0} \quad (7.201)$$

In reality, the concentration gradient is constant for only a short distance from the interface and then becomes asymptotic to zero in the bulk. But one can resort to a linearization of the concentration profile, and then one can use the artifice of an imagined (i.e., simplified) diffusion layer in which the concentration is taken as if it changed in a linear fashion from the interfacial value  $c_{x=0}$  to the bulk value  $c_0$ . The effective thickness  $\delta$  of the diffusion layer, which can be taken as a constant independent of time only under steady-state conditions in which natural convection occurs, proved a useful quantity. With its aid, one can write out the flux-equality condition in the form

$$\frac{i}{nF} = \frac{D}{\delta} (c^0 - c_{x=0}) \quad (7.202)$$

The change of the interfacial concentrations from the bulk values at zero current to different values at finite currents produces an extra potential difference  $\eta_c = \Delta\phi_i - \Delta\phi_{i=0}$ . Because one is here in "the reversible region" this concentration overpotential can be obtained by inserting into the Nernst equation the interfacial concentrations  $c^0$  at  $i = 0$  and  $c_{x=0}$  at  $i$

$$\eta_c = \frac{RT}{nF} \ln \frac{c_{x=0}}{c^0} \quad (7.198)$$

The link between the current density and the concentration overpotential under steady-state conditions for systems in which the exchange-current density is relatively large compared with the limiting current density (hence, the activation overpotential is negligible) was established through the concept of a limiting current  $i_L$  arising from the fact that there is a maximum rate at which electron acceptors can move to an

interface. In terms of the limiting current density  $i_L$ , an exponential current–potential law was obtained for diffusion-controlled current densities involving electronation reactions:

$$i = i_L(1 - e^{nF\eta_c/RT}) \quad (7.210)$$

Electric migration of electron acceptors to the interface aids the transport process. The electron acceptors are driven by concentration gradients as well as by the electrical field in the bulk of the electrolyte between the electrodes. Here their transport number, the fraction of the concentration current carried by the electron acceptors compared with that carried by the other ions, plays a role.

All this material about the influence of the rate of transport in a solution, and how if it is too slow it influences the overall current density observed, has again used an extreme situation—the opposite of the diffusion-free picture given in earlier sections. In this section a relation is deduced that connects the diffusion control to the interfacial control. It is

$$\frac{1}{i} = \frac{1}{i_F} + \frac{1}{i_L} \quad (7.236)$$

Usually one tries to emphasize the one (interfacial) control or the other (diffusion).

## Further Reading

### Seminal

1. A. E. Fick, *Pogg. Ann.* **94**: 59 (1855). The first paper relating current density to diffusion.
2. H. J. S. Sand, *Phil. Mag.* **1**: 45 (1900). The transition time at constant current, diffusion control.
3. F. C. Cottrell, *Z. Physikal. Chem. (Leipzig)* **42**: 358 (1903). Time dependence of current under diffusion control at constant potential.
4. T. R. Rosebrugh and W. L. Miller, *J. Phys. Chem.* **14**: 816 (1910). Generalization of current as a function of time—particularly under periodic function of time.
5. D. Ilkovic, *Coll. Czech. Chem. Comm.* **6**: 495 (1934).
6. V. G. Levich, *Acta Physicochem. URSS* **17**: 252 (1942). Early paper in applying hydrodynamic theory to electrochemistry.
7. J. N. Agar, *Discuss. Faraday Soc.* **1**: 26 (1947). First paper on dimensional analysis applied to electrochemical equations.
8. C. Wagner, *J. Electrochem. Soc.* **95**: 161 (1949). Calculation of current at vertical electrodes with natural convection.
9. C. R. Wilke, M. Eisenberg, and C. W. Tobias, *J. Electrochem. Soc.* **100**: 513 (1953). Hydrodynamic factors and the limiting current.
10. W. Vielstich, *Z. Elektrochemie* **57**: 646 (1953). Diffusion layer related to hydrodynamic boundary layer.

11. V. G. Levich, *Physicochemical Hydrodynamics*, Prentice-Hall, Englewood Cliffs, NJ (1962). The classic text in the field.

## Modern

1. P. Delahay, *New Instrumental Methods in Electrochemistry*, Interscience, New York (1952). Contains much seminal work showing the evolution away from the pure diffusion control and the introduction of "activation" overpotential, i.e., interfacial control.
2. A. C. Riddiford, "Rotating Disc Systems," in *Advances in Electrochemistry and Electrochemical Engineering*, P. Delahay and C. W. Tobias, eds., Vol. IV, Ch. 2, Interscience, New York (1966).
3. N. Ibl, "Fundamentals of Transport," in *Comprehensive Treatise in Electrochemistry*, E. Yeager, J. O'M. Bockris, B. E. Conway, and S. Sarangapani, eds., Vol. 6, p. 133, Plenum, New York (1987).
4. C. M. Brett and A. M. A. Brett, *Electrochemistry*, Ch. 8 (hydrodynamics), Oxford University Press, Oxford (1993).
5. Keith R. Oldham and Jan C. Myland, *Fundamentals of Electrochemical Science*, Ch. 7, (transport), Academic Press, San Diego (1994).
6. A. Bard and B. Faulkner, *Electrochemical Methods*, 2nd ed., Interscience, New York (1998). A classic text oriented to transport and its role in electroanalytical chemistry.

N.B. The source of much modern work in transport control in electrochemical engineering is found in papers by Newmann and Tobias and others, particularly R. E. White, who has led much of the development of modeling on electrochemistry. These appear mostly in the *Journal of the Electrochemical Society*.

## 7.10. HOW TO DETERMINE THE STEPWISE MECHANISMS OF ELECTRODIC REACTIONS

### 7.10.1. Why Bother about Determining a Mechanism?

Some books on electrochemistry do not bother with descriptions of how one may determine the mechanism of an electrode reaction. In particular, if one is concerned only with the "redox reactions" (e.g.,  $\text{Fe}^{3+} + e \rightarrow \text{Fe}^{2+}$ ), the only discussion—though a very important one it is—concerns the physical chemistry of the "fundamental act," the electron transfer from the electrode to  $\text{Fe}^{3+}$  and from  $\text{Fe}^{2+}$  to the electrode.

Such a limited approach is not warranted if one looks at electrochemistry as a whole. Electrochemistry is the underpinning of many practical processes—clean technologies—and it is difficult to see a way out of the pollution caused by our use of fossil fuels for energy, except by conversion to an energy system based on renewable energies and/or (maybe) nuclear power. However, both these energy sources demand distribution systems in electricity and/or hydrogen (Chapter 15). Hence, electrochemistry is bound to play a broad role in the evolution of a stable society. Clearly, the electrochemical processes involved in this evolution bring into play more than simply



one electron-transfer reaction without reaction intermediates. As an example, they involve such processes as the electrochemical oxidation of methanol. If one wants to learn about real electrochemistry, one must be concerned with multistep electrode reactions, with their chemical reactions on the electrode surface, together with coupled transport steps in solution. Catalysis will be a valid concern and will greatly influence the economics of new electrochemical processes in industry. To deal with these reactions at a practical level (in plants and factories), the first necessity is to *understand* them—and that means knowing the steps, often not one or two but several coupled together, that make up the overall reaction.

However, if one is to understand the catalysis of electrode reactions, and the minimization of the energy and economic losses caused by the overpotential, the most important piece of knowledge needed is the rate-determining step in the reaction sequence. After this is known, one can begin to think about how catalysis works and what might be good catalytic surfaces. Before it is known, catalyst development sinks back into exploring hunches.<sup>83</sup>

### 7.10.2. What Does It Mean: “To Determine the Mechanism of an Electrode Reaction”?

There is nothing unique about the determination of the mechanism of electrochemical reactions. Electrochemical kinetics is a parallel field to that of heterogeneous chemical kinetics and basically the mechanism tasks in the two related fields are the same. There are three goals that must be reached consecutively.

**7.10.2.1. *The Overall Reaction.*** This is the apparent reaction, the reaction as seen from afar, the reaction if one asks only what are the reactants and the products. Thus, ethylene can be oxidized electrochemically to  $\text{CO}_2$ . The *overall* reaction is



Basically, the determination of the overall reaction is a matter of analyzing what goes in (ethylene) and what comes out ( $\text{CO}_2$ ), but in the latter case, one must know how much comes out, in a unit time, compared with a unit starting amount of ethylene, and the relation of the rate to pH and gas pressure. This enables one to establish the stoichiometry of the reaction. Of course, one has to measure the coulombs used to obtain a certain amount of  $\text{CO}_2$  and define the potential region of operation. To do this, it is usual to start off by looking at a voltammogram of the reaction under working conditions (Chapter 8). Every mechanism-oriented research paper will contain some voltammograms.

---

<sup>83</sup> One grievous error sometimes made in industrial laboratories that stress the quick fix is the concept that electrochemical processes can be studied by doing experiments on whole cells without examining the processes at the working electrode. One of the several aims of this book is to diminish the occurrence of such attitudes.

One determines the overall reaction by using some of the many tools of chemical analysis. Coulometry, gas chromatography, mass spectroscopy, and, in complex cases, computerized pattern-recognition programs applied to GC-MS data (see Section 7.5.19) are the typical tools used in determining the overall reaction. The current efficiency for the reaction concerned is important here and may vary with potential.

**7.10.2.2. The Pathway.** The pathway of a reaction—an electrochemical reaction as well as other kinds—indicates the successive molecular steps by which the final product is formed.

Determination of the pathways may be a demanding affair where more complex reactions are concerned, particularly when there may be more than one pathway occurring at one time. To make this meaning of “pathway” clear, let the simplest electrode reaction involving a reaction intermediate be chosen: the hydrogen evolution reaction. The overall reaction hardly needs determination. It is (in acid solution)



However, even in such a simple reaction, there are two different paths that the constituent ions and molecules may choose to take. These have already been spelled out in Section 7.2.1 and hence it is only necessary to remind the reader that they are:

Pathway 1: A proton discharge from  $\text{H}_3\text{O}^+$  first forms adsorbed H and this adsorbed H is then assumed (as may be true on some electrodes) to be mobile and to diffuse over the electrode surface, colliding with other adsorbed H's, combining with a few of them to form hydrogen, the final product. In this pathway then, there are two *consecutive* reactions.

Pathway 2: The proton discharges and forms adsorbed H's (as in pathway 1). However, these adsorbed H's are assumed to not readily combine to form  $\text{H}_2$ , as assumed in pathway 1. Hence, the fraction of the surface covered with H builds up until a parallel discharge reaction of  $\text{H}_3\text{O}^+$  onto an adsorbed H occurs, directly forming  $\text{H}_2$ . In this path there are *two parallel* reactions. Thus, the discharge of  $\text{H}_3\text{O}^+$  onto metal sites vacated by adsorbed H that has been taken away to form  $\text{H}_2$  takes place at the same rate as that of the discharge onto adsorbed H. (Every discharge thereon frees up a site onto which  $\text{H}_3\text{O}^+$  may discharge.)

Determining the pathway of reactions involves some of the tools used later on when one determines the rate-determining step. Hydrogen evolution is the most examined reaction in electrochemistry. The pathway on a given electrode can be determined from the results of just two kinds of measurements: (1) FTIR spectroscopy tells of the degree of coverage of the surface, which is negligible for the first path and near to complete for the second. (2) Isotopic analysis (the determination of the H/T reaction rate ratios) gives a clear indication of which path is being taken. Thus, for the first of the two paths, the values of the ratio are small (3–6) and for the second reaction, much larger (10–20).

The example here stresses simplicity. To determine the pathway of more complex reactions (glucose oxidation, for example), one needs to do more, just because there are several alternative pathways. However, if the reaction is complex, it may be enough to find the pathway up to the rds. That, after all, is what determines the overpotential in the steady state and therefore the cell potential and how much electricity will be needed to produce a given amount of product. If it occurs in the first three steps of, e.g., a six-step sequence, the work needed to define the path up to the third step is *much* less (not just 1/2) than one that involves an investigation of the steps after the rds.

**7.10.2.3. The Rate-Determining Step.** Determination of the step that decides the overall rate in a series of consecutive or parallel reactions in heterogeneous catalysis is the most significant part of mechanism determination. It is best to deal with the ideas here in a general way; they will be exemplified in three reactions later on in the section.

One may represent consecutive reactions as



where X is the final product. The rate constant of one of these steps (e.g.,  $B \rightarrow C$ ) is assumed to be *much* less than those of the other steps. One or more steps may involve charge transfer. Then the reactants in the steps before the slow one tend to pile up (a bit like a group of cars stopped before a bridge that is partly closed for repair). If (say) the rate constant of the rds is 1000 times slower than that of any previous step, it is reasonable to regard the earlier reactions as (almost) in equilibrium (i.e., pseudo-equilibrium), waiting for the trickle of molecules to pass through the rds.<sup>84</sup>

Then, *after* the rds, the latter steps can be seen as fast—so fast indeed that every molecule that manages to pass through the rds goes quickly on to the final product, which is rapidly removed in an “open” system (e.g.,  $H_2$  gas escaping into the atmosphere). Alternatively, the final product may be in a closed system. It may build up and send molecules back to the blocked step, the rds. Of course, there is always a net forward reaction rate, but in a closed system the steps after the rds may be considered as being in pseudo-equilibrium, or in an open system (in which there is no back reaction after the rds) as being coupled to the rds.

There are several places in electrochemical reactions where rate-determining steps can occur. First, if a cathode potential is sufficiently negative, transport of reactants to the electrode will not be able to keep pace with the events that transfer charge as the electrode demands. Then, transport in solution and the electrode events have to be satisfied with what the transport rate can bring to the interface. *Transport* is the rds.

<sup>84</sup>To continue the analogy of the bridge under repair, one could see cars held up at the bridge, expecting a wait of some hours, going back and returning every so often to check on the situation. They keep on doing this, i.e., home and the bridge are almost in equilibrium. If the bridge were *closed*, they would set up a true equilibrium, going to and fro until it opened to single-lane traffic and some got through. Then the ones waiting to cross would be in pseudo-equilibrium. The rds, of course, is crossing the bridge.

The most discussed rds is electron transfer at the metal/solution interface, but there may be more than one electron transfer in the overall sequence of several steps, and it is the task of mechanism determination to find out which one is rate determining.

*Surface chemical* reactions among the products of charge transfer (e.g.,  $H_{ads} + H_{ads} \rightarrow H_2$ ) form the rds more frequently than appears to be the case with so much concentration on the first charge-transfer step. The rate at which the reacting radicals arrive on the surface via charge transfer is potential dependent. Hence, although the rds is purely chemical, the concentration of the radicals (e.g.,  $H_{ads}$ ),  $\theta$ , that take part in it is potential dependent and since the rate of the chemical surface reactions are dependent on  $\theta$ , the degree of surface occupancy, the rate of the rate-determining surface reaction itself will be potential dependent.

Finally, but rather rarely, the rate of reactions that occur extremely quickly on the electrode may be determined by the velocity with which the products diffuse away from the electrode back into the solution.

How one finds out what the rds is is the subject of the rest of this section. Suffice it to say here that one devises various hoops through which one makes the reactants jump. One hypothesizes possibilities as to the rds (in complex reactions there may be several) and calculates how the reaction would respond to various stimuli implied by the phrase “jumping through the hoops.” It is hoped that one has devised hoops that are differentiating. By examining the responses, the rds may be identified.

Of course, the reader will understand that what is said here is idealized; that is necessary to convey the essential meaning in a reasonably short space. However, one reservation must be made: It is that once the number of steps exceeds, say, three, one has to use “chemical sense” as well as formal logic. Computer analysis helps in determining mechanism, with pattern recognition available. However, there are a great many possibilities that become visible in analyzing more complex electrode reactions and, in the case of some of them, a chemist *knows* they will not happen and can eliminate them, thus simplifying the analysis. As yet computers don’t know enough general chemistry to exclude highly unlikely steps (e.g.,  $N + N \rightarrow N_2$ ), and this can lead a totally computer-dominated mechanism determination to become futile because without input from chemical knowledge, there are never enough data to decide among the large number of possibilities that a computer recognizes.

Determination of the rds is the central and most important part of a mechanism study. Indeed, if the reaction is a two- or three-step reaction—no more—it may be unnecessary to carry out any experiments to determine the overall reaction, it being obvious that it happens as written (e.g.,  $O_2 + 4H^+ + 4e \rightarrow 2H_2O$ ). Occasionally the pathway is clear without special experimentation for a relatively simpler reaction (e.g.,  $O_2 + 2H^+ + 2e \rightarrow H_2O_2$ ). However, the rds always needs some well-chosen experiments to illustrate the differences in behavior expected from the assumption of alternative choices.

In Table 7.15 some of the methods that are available for mechanism investigations are listed. Sometimes all of these approaches have to be used in investigating a reaction. How many have to be used to achieve a 90% or even 99% certain determination of the

**TABLE 7.15**  
**Some Methods for the Determination of the Mechanism (Including RDS) of**  
**Electrode Reactions**

Method	Type of Information
Rate at constant pressure and temperature as a function of overpotential (Section ?).	Tafel constants $\partial \ln i / \partial \eta$ may give rds, particularly for hydrogen evolution
Rate at constant potential and pressure as a function of temperature (Section 7.5.11)	Gives $\Delta H_{ox}$ . Eliminates rds's with significantly higher $\Delta H_{ox}$ 's
Rotating disk with ring (Section 7.5.14)	Identifies and determines characteristics of films
Ellipsometry and ellipsometric spectroscopy (Section 7.5.16)	Used spectroscopically, determines valence state, etc., of surface atoms. Faster in data processing time than FTIR. An underdeveloped technique
Impedances (real and imaginary) as a function of $\omega$ (The applied ac frequency)	Can isolate $\omega$ ranges in which impedance of one branch of a circuit dominates. Computer simulation allows determination of various $R$ 's in circuit from the impedances. A step with an $R$ at least 10 times greater than another is the likely rds
Fourier transform infrared spectroscopy (FTIR) (Section 7.5.15.2)	Can lead to identification of radicals present on the electrode surface. Such information distinguishes path and rds
Comparison of rate of reaction containing H and one or more of its isotopes	Highly diagnostic for reactions involving protons
STM and AFM (Section 7.5.18)	Can observe surface terrain at 1–2-nm definition; occasionally atomic resolution, in solution. AFM particularly useful in observation of biosurfaces
Computer applications (see Section 7.5.19)	Can be programmed to recognize patterns of behavior characteristic of certain mechanism sequences. Computer simulation is vital in, e.g., impedance spectroscopy

rds? The answer depends on the complexity of the reaction. The much-investigated hydrogen evolution reaction can now be analyzed using only two methods (FTIR determination of the degree of coverage and determination of the separation factor). Much depends on whether it is important to get a 99% probable answer or only a 90% probable one.

Direct methanol oxidation is a candidate for the anodic fuel to run electric surface transportation (Chapter 13). Thus, MeOH would provide a liquid fuel and use of much of the present infrastructure. Here, with a large financial investment at stake in the

choice of the future fuel, it would be worthwhile to reduce any uncertainty in the mechanism of methanol's electrochemical oxidation to  $\text{CO}_2$  because knowledge of this mechanism enhances the possibility of rationally designing an electrocatalyst for the electrochemical oxidation of  $\text{MeOH}$ .<sup>85</sup>

Another consideration is that the rds in a given reaction may change with pH, with temperature, and with catalyst. It would hardly make good sense to go through a detailed and costly investigation on just one electrode material at one set of conditions (see Table 7.15).

### 7.10.3. The Mechanism of Reduction of $\text{O}_2$ on Iron at Intermediate pH's

There is a special importance in the mechanism of  $\text{O}_2$  reduction on iron because of its relevance as the counter-cathodic reaction in corrosion mechanisms that involve Fe more often than other metals. Many of the practical costs of Fe corrosion occur in neutral solution, so that the pH range in the study described here (Jovancicevic, 1986) is between 6 and 9. The experimental methods involved the use of ring-disk analysis (see Section 7.5.14) to detect  $\text{H}_2\text{O}_2$ , an obvious possible intermediate in the measurement of the  $\log i$ -potential relation (Fig. 7.101) to give Tafel constants; and the reaction order with respect to  $\text{O}_2$  and pH.

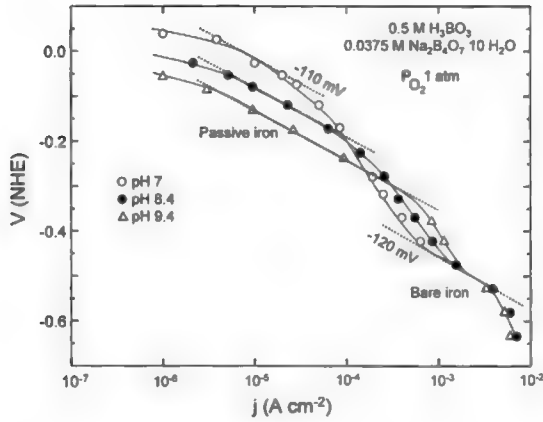
Entirely different behavior with the ring-disk method and other diagnostic criteria is shown for passive and bare iron. However, the Tafel slopes hardly differ—110 mV/decade for passive and -120 mV/decade for bare Fe.

Measurement of  $I_{\text{disk}}/I_{\text{ring}}$  as a function of  $\omega^{-1/2}$  (where  $\omega$  is the angular velocity of the disk) gives a slope that is dependent on  $n$ , the number of electrons in the overall reaction. It shows a decisive outcome; for passive Fe,  $n = 2$  and for bare Fe,  $n = 4$ . Thus, on passive Fe the reduction reaction in the pH range mentioned stops at  $\text{H}_2\text{O}_2$  and on bare iron it continues to  $\text{H}_2\text{O}$ .

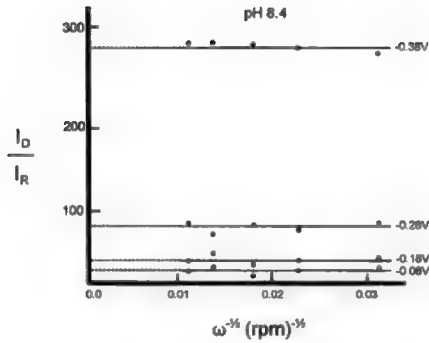
The reaction order results show marked differences between the two kinds of surfaces. Thus, on passive Fe,  $\partial \log i / \partial \text{pH} = -0.4$ , but the same coefficient is 0 for bare Fe. However,  $\partial \ln i / \partial \log p_{\text{O}_2} = 1$  for both passive and bare Fe.

Figure 7.101 shows the detection of  $\text{H}_2\text{O}_2$  on both passive and bare iron. For more negative potentials on bare iron, the  $\text{H}_2\text{O}_2$  amount of  $\text{H}_2\text{O}_2$  in the mechanism sequence is decreased. The most interesting figures are the  $I_{\text{disk}}/I_{\text{ring}}$  plots as a function of  $\omega^{-1/2}$ . The passive Fe shows no dependence of  $I_{\text{disk}}/I_{\text{ring}}$  on  $\omega$ . However, on the bare Fe, there is a potential-dependent slope with a potential-independent intercept. It is clear that at potentials positive to -0.08, Fe is increasingly covered with a passive layer, the intercept is  $1/N$ , and the calculated  $n$  becomes 2 and no longer 4 because it is at more negative potentials (see Figs. 7.102 and 7.103).

<sup>85</sup>In Chapter 15 there is a discussion of a point halfway to powering electric cars by using methanol as a fuel for fuel cells. There the on-board conversion (by re-formation) of methanol (or gasoline) to hydrogen has been proposed (by the Daimler-Benz Company in 1997 in Germany). Hydrogen is usually the fuel of choice for fuel cells. However, it would, of course, be better if one could cut out the re-forming step, and just use methanol directly as the fuel for the fuel cell.



**Fig. 7.101.** Tafel plots for  $\text{O}_2$  reduction on iron in borate buffer solution. (Reprinted from V. Jovancicevic and J. O'M. Bockris, *J. Electrochem. Soc.* **133**(9): 1798. Reproduced by permission of The Electrochemical Society.)



**Fig. 7.102.**  $I_{\text{disk}}/I_{\text{ring}}$  vs.  $\omega^{-1/2}$  on passive layer at different potentials. (Reprinted from V. Jovancicevic and J. O'M. Bockris, *J. Electrochem. Soc.* **133**(9): 1801. Reproduced by permission of The Electrochemical Society.)





**TABLE 7.16**  
**Kinetic Parameters for O<sub>2</sub> Reduction on Passive Film and Bare Iron**

Electrode Surface	Disk Data					Ring Disk Data			
	$\frac{\partial V}{\partial \log i}$	$\frac{\partial \log i}{\partial \log p_{O_3}}$	$\frac{\partial \log i}{\partial \text{pH}}$	$i_{0,O_2}$ (A/cm <sup>2</sup> )	$i(\text{corr})$ A/cm <sup>2</sup>	$J = \left( \frac{I_{\text{disk}}}{I_{\text{ring}}} \right)_{\omega \rightarrow \infty}$	$\frac{\partial I_{\text{disk}}/I_{\text{ring}}}{\partial \omega(\text{rpm})^{1/2}}$	$J_{1/S}$	$S_{J/S}$ (rpm) <sup>-1/2</sup>
Passive iron									
pH 7	-110 mV	1	-0.4	$1.2 \times 10^{-7}$	$1.8 \times 10^{-6}$	1/N	0	1	—
pH 9	-110 mV	1	-0.4	$1.5 \times 10^{-7}$	$2.2 \times 10^{-6}$	1/N	0	1	—
Bare iron									
pH 7	-120 mV	$1 \text{ } p_{O_2} < 0.2$ $1 \text{ } p_{O_2} > 0.3$	0	$8 \times 10^{-15}$	$1.2 \times 10^{-3}$	~300	$1.5-3.0 \times 10^4$	~250	$7 \times 10^{-4}$
pH 9	-120 mV	$1 \text{ } p_{O_2} < 0.2$ $1 \text{ } p_{O_2} < 0.3$	0	$1.5 \times 10^{-13}$	$1.3 \times 10^{-3}$	~300	$1.5-3.0 \times 10^4$	~250	$7 \times 10^4$

Source: Reprinted from V. Jovancicevic and J. O'M. Bockris, *J. Electrochem. Soc.* **133**(9): 1802, 1986, Table 1. Reproduced by permission of The Electrochemical Society, Inc.

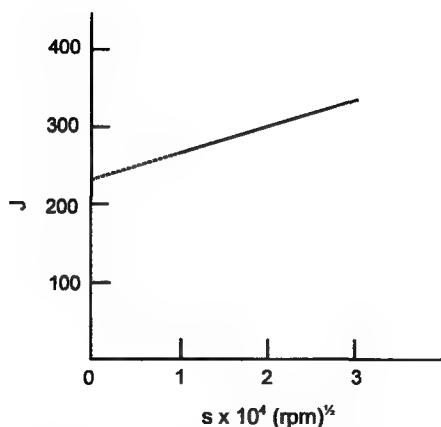


**Fig. 7.104.**  $J$  vs.  $S$  plot on bare iron.

where  $J$  and  $S$  are intercepts and slopes at various potentials, respectively, and  $Z = 0.62 D^{2/3} \nu^{-1/6}$ . However, in an alternative assumption involving the absence of the direct  $4e^-$  formation of  $OH^-$ , Scheme I shows that

$$J = \left( 1 + \frac{SZ}{k_6} \right) \frac{1}{N} \quad (7.239)$$

Equation (7.238) predicts a linear relationship between  $J$  on  $S$  with the intercept greater than 1. Equation (7.239) should yield a linear relationship with an intercept of 1.

Figure 7.104 shows the plot of the value of  $J$  vs.  $S$  obtained for different potentials on the bare iron region from the data plotted in Fig. 7.103. A straight line obtained with an intercept much greater than 1 indicates that  $O_2$  reduction on reduced iron proceeds by the direct four-electron reaction pathway. Formation of  $H_2O_2$  as an intermediate in the consecutive reaction pathway is less than 1 % of the total reduction current. Conversely, in the potential region corresponding to passive iron, the slope,  $S$ , of the  $I_{\text{disk}}/I_{\text{ring}}$  plot is zero, and the intercept  $J = (1/N)$  indicates that  $O_2$  reduction on passive Fe is a two-electron process in which  $H_2O_2$  is the product, and not an intermediate, of the reaction.

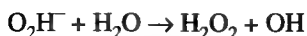
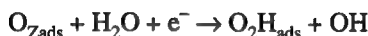
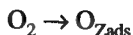
The mechanism argument for the passive layer surface begins with the clear result that the reaction pathway is a  $2e$  pathway (i.e.,  $H_2O_2$ ), while on bare Fe it is a  $4e$  transfer. The possible mechanisms for  $H_2O_2$  formation are shown in Table 7.17. Comparing the predictions of Table 7.17 with the experimental results, only A and C fit. But C involves  $O_2H^+$  formation on a passive layer and seems unlikely for the potential region in which the results obtained are some 0.2 positive to the pzc, i.e., repulsion of a positive radical would occur.<sup>86</sup> Hence, the probable mechanism is A, namely,

<sup>86</sup>This is an example of using human reasoning. As yet, computers are not programmed to take into account radical repulsion in the double layer as a function of the pzc.

**TABLE 7.17**  
**Proposed Mechanisms for Oxygen Reduction on Passive Layer**

rds		Langmuir						Temkin		
		$\partial E/\partial \ln i$		$\partial \log i/\partial \log p_{O_2}$		$\partial \log i/\partial pH$		$\partial E/\partial \ln i$	$\partial \log i/\partial \log p_{O_2}$	$\partial \log i/\partial pH$
		$\theta \rightarrow 0$	$\theta \rightarrow 1$	$\theta \rightarrow 0$	$\theta \rightarrow 1$	$\theta \rightarrow 0$	$\theta \rightarrow 1$			
A <sup>a</sup>	$O_2 \rightarrow O_{2ads}$	$\infty$	—	1	—	0	—	$2RT/F$	1	-0.5
	$O_{2ads} + HO + e^- \rightarrow OH_{ads} + OH^-$	$2RT/F$	$2RT/F$	1	0	0	0	$RT/F$	1	-0.5
	$O_{2H_{ads}} + e^- \rightarrow O_2H^-$	$2RT/3F$	$2RT/3F$	1	0	-1	0	$2RT/F$	0	0
	$O_2H^- + H_2O \rightarrow H_2O_2 + OH^-$	$RT/F$	—	1	0	-1	0	$\infty$	-0.25	0
B <sup>b</sup>	$O_2 + e^- \rightarrow O_{2ad}^-$	$2RT/F$	—	1	—	0	—	$\infty$	1	0
	$O_{2ads} + H_2O \rightarrow O_2H_{ads} + OH^-$	$RT/F$	—	1	0	0	0	$2RT/F$	0	0
	$O_2H_{ads} + e^- \rightarrow O_2H_{ads}^-$	$2RT/3F$	—	1	0	-1	0	$2RT/F$	0	0
	$O_2H_{ads}^- + H_2O \rightarrow H_2O_2 + OH^-$	$RT/2F$	—	1	0	-1	0	$\infty$	-0.25	0
C <sup>c</sup>	$O_2 + H_2O \rightarrow O_2H^+ + OH^-$	$\infty$	—	1	—	0	—	$\infty$	1	0
	$O_2H^+ + e^- \rightarrow O_2H_{ads}$	$2RT/F$	$2RT/F$	1	0	-0.5	0	$2RT/F$	0	0
	$O_2H_{ads} + e^- \rightarrow O_2H_{ads}^-$	$2RT/3F$	$2RT/F$	1	0	-1	0	$2RT/F$	0	0
	$O_2H_{ads}^- + H_2O \rightarrow H_2O_2 + OH^-$	$RT/F$	—	1	0	-1	0	$\infty$	-0.25	0
D <sup>d</sup>	$O_2 + H_2O + e^- \rightarrow O_2H_{ads} + OH^-$	$2RT/F$	0	1	0	0	0	$2RT/F$	1	0
	$O_2H_{ads} + e^- \rightarrow O_{ads} + OH^-$	$2RT/3F$	$2RT/F$	1	0	-1	0	$2RT/F$	0	0
	$O_{ads} + H_2O \rightarrow H_2O_2$	$RT/2F$	—	1	0	-1	0	$\infty$	-0.25	0
	$O_2 + e^- \rightarrow O_{2ads}^-$	$2RT/3F$	—	1	0	0	—	$2RT/F$	1	0
E <sup>e</sup>	$O_{2ads}^- + H_2O + e^- \rightarrow O_2H_{ads} + OH^-$	$2RT/3F$	—	1	-1	-1	—	$2RT/3F$	1	-1
	$O_2H_{ads}^- + H_2O \rightarrow H_2O_2 + OH^-$	$RT/2F$	—	1	0	-1	0	$\infty$	-0.25	0

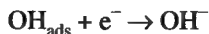
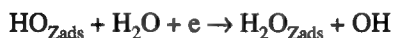
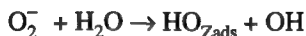
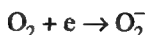
Source: Reprinted from V. Jovancicevic and J. O'M. Bockris, *J. Electrochem. Soc.* **133**(9): 1803 (1986), Table 2. Reproduced by permission of the Electrochemical Society Inc.



As for the reaction on bare iron, the detailed argument would take up too much of the allotted space, and we are illustrating mechanism determination by normal approach. So let it be said only that a discussion of the same type as the one described here gives the most probable rds:



The reactions following  $\text{O}_2 + \text{e}_0^- \rightarrow \text{O}_2^-$  have not yet been determined with any certainty, but may follow the pathway shown:



#### 7.10.4. Mechanism of the Oxidation of Methanol

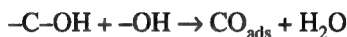
As with many investigations, the primary measurement is one establishing the  $i$ - $V$  relation. For this, steady-state measurements are important, for if the measurement is carried out before the steady-state condition has set in, the value for  $\theta_{\text{radical}}$  will differ from that at steady state—the rds in control may not be the one that controls the long-term operation, for example, of a fuel cell.

The steady-state Tafel lines for methanol oxidation in acid solution are 55–60 mV/decade over the potential range 0.4–0.5 (SHE). When the potential of the working electrode on this scale is made more positive, the Tafel slope changes and becomes 110 mV/decade. These two numerically stated Tafel slopes can readily be reexpressed in electrode kinetic terms to correspond, respectively, to:

For the less anodic section ( $b = 0.05$ – $0.060$ ):  $RT/F$  (thus  $2.303 RT/F = 0.058$  at  $25^\circ\text{C}$ ) for the more anodic section ( $b = 0.110$ ):  $2RT/F$  ( $2.303 2RT/F = 0.112$  at  $25^\circ\text{C}$ ).

In an investigation using potentiodynamic transients to reach the steady state (Section 7.10.5), the number of electrons per site used up in the reaction was calculated and found to vary from 1.2 to 1.5 as the potential in which the measurement was made grew more positive.

An early suggestion (Bagotskii and Vesiliev, 1967) for a mechanism proposed an rds not as an electron transfer reaction but as a reaction on which some radical resulting from the dissociative adsorption of methanol reacted with  $\text{OH}_{\text{ads}}$ , the latter produced from the discharge of water. Then the rds was proposed as

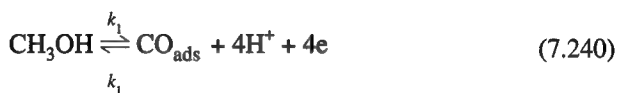


The adsorbed CO, here a *product* of the rds, was seen as reacting further with other adsorbed OH radicals from the discharge of water, finally to form  $\text{CO}_2$ .

When this suggestion was made, *in situ* spectroscopic means for determining the nature of the intermediate radicals in electrode reactions were not available. Later, FTIR spectroscopy was used to establish the nature of the dominating radical on the surface (Chandresakaran and Wass, 1990). Some results are shown in Figs. 7.105 and 7.106.

By noting the frequencies of the peaks in the figures it is possible to identify their origin. Thus, peak B corresponds to adsorbed OH. Peak A, the broad peak at 2170, corresponds most nearly to linearly bonded CO, i.e.,  $\text{M Pt}-\text{C}\equiv\text{O}$ . A peak shows at 1790 when the electrode becomes more positive than 0.65 V, corresponding to bridge-bonded CO, i.e.,  $\text{C}=\text{O}$ , which in independent work has been shown to have a distinguishing peak at  $1800\text{ cm}^{-1}$ .

Thus, the conclusion from the spectroscopic investigations into the steady-state oxidation of methanol is that the surface contains a potential-dependent intermediate, single-bonded CO at less positive potentials, and bridge-bonded CO at the more positive potentials. A possible mechanism fitting the conclusion of the spectroscopy is



The surface concentration of CO can be calculated for reaction (7.240). Thus:



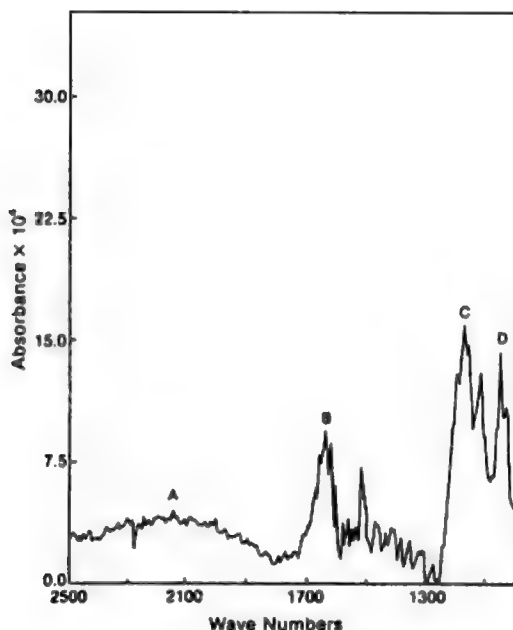


**Fig. 7.105.** Differential IR spectrum of platinum-aqueous sulfuric acid interface containing 0.1 M methanol at 0.1 V (vs. SHE) in the sequence from 0.0 to 0.8 V (vs. SHE). Absorbance maxima were found at 2150 (peak A), 1620 (peak B), 1185 (peak C), and 1050  $\text{cm}^{-1}$  (peak D). (Reprinted from K. C. Chandrasekaran, J. C. Wass, and J. O'M. Bockris, *J. Electrochem. Soc.* **137**(2): 519, 1990. Reproduced by permission of The Electrochemical Society, Inc.)

$$\theta_{\text{CO}} = \frac{K_1 c_{\text{CH}_3\text{OH}} e^{4VF/RT}}{1 + K_2 c_{\text{CH}_3\text{OH}} e^{4VF/RT}} \quad (7.244)$$

would occur if  $K_1 c_{\text{CH}_3\text{OH}} e^{4VF/RT} \ll 1$ , followed by an independence of  $\theta_{\text{CO}}$  with potential (if the above condition reverses at higher V). This analysis allows, then, for the two regions of the Tafel relation observed in several independent studies of the oxidation of methanol.

This account of the mechanism of the oxidation of methanol does not include a “blocking” CO, which many workers have included in their discussions. However,

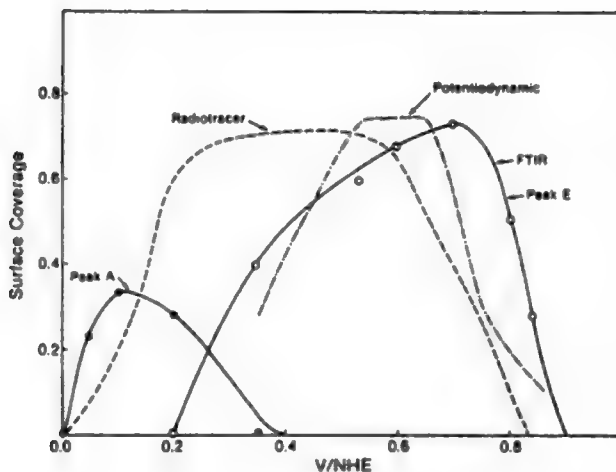


**Fig. 7.106.** Relative areas of peaks A and E as a function of electrode potential. Peak E ( $1790\text{ cm}^{-1}$ ) replaced peak A ( $2150\text{ cm}^{-1}$ ) (Fig. 7.105) at potentials more positive than  $0.4\text{ V}$  (vs. NHE). (Reprinted from K. C. Chandrasekaran, J. C. Wass, and J. O'M. Bockris, *J. Electrochem. Soc.* **137**(2): 520, 1990. Reproduced by permission of The Electrochemical Society, Inc.)

one must reiterate the substantial evidence for heterogeneity of an electrode surface. The CO included in the reaction scheme here is reactive, i.e., less tightly bound. There may indeed be tightly bound  $\text{-CO}$  ("blocking") on some parts of the heterogeneous surface, and it is reasonable to see this blocking as consistent with work done on well-defined electrode surfaces, where some single-crystal orientations are found to be active for methanol oxidation but others are blocked. The situation emphasizes the need to make all fundamental investigations on well-defined (single-crystal) electrode surfaces (as first emphasized by Hubbard) and observe these faces and their constancy after immersion in the solution by measurements and other means.

This mechanism determination is exceptional in its brevity and it depends, basically, upon only two types of measurements, the  $i$ - $V$  relation and FTIR spectroscopy carried out at steady state over a large potential range. Spectroscopic observation of the electrode surface during potential changes will be increasingly valuable to mechanism determination.

What of the future of mechanism determination? Is it not likely that as the decades proceed, the indirect reasoning we now use (interpreting this trend or that to favor one mechanism and to be more likely than the interpretation offered by mechanisms Y, Z, etc.), will fade away, their introductory work done? Thus, in 1989 (Szklaarczyk, Velev,

and Bockris) it became possible (using an STM technique) to distinguish individual atoms on some electrode surfaces. The movement of atoms on electrode surfaces has been registered by Uosaki (1998). May it not be possible within a generation to observe surface reaction mechanisms directly?

## Further Reading

### Seminal

1. R. Parsons, *Trans. Faraday Soc.* **47**: 1332 (1951). General scheme for mechanism determination.
2. M. C. Davies, M. Clark, E. Yeager, and F. Hovorka, *J. Electrochem. Soc.* **106**: 56 (1959). Mechanism of  $\text{H}_2\text{O}_2$  formation.
3. V. S. Bagotskii and Y. B. Vasiliev, *Electrochim. Acta* **12**: 1323 (1967). Mechanism of methanol oxidation.
4. S. Gilmore, *J. Phys. Chem.* **67**: 78 (1963). Mechanism of CO oxidation.
5. A. T. Kühn, H. Wroblowa, and J. O'M. Bockris, *Trans. Faraday Soc.* **63**: 1458 (1967). Mechanics of the oxidation of ethylene.
6. E. Gileadi and L. Duic, *Electrochim. Acta* **13**: 1915 (1968). Mechanism of the oxidation of benzene.

### Modern

1. S. Kunitatsu and H. Kita, *J. Electroanal. Chem.* **149**: 2113 (1986).
2. E. P. Soponeva, S. Hotchandani, B. A. Kisselev, and C. Arbour, *J. Electroanal. Chem.* **387**: 123 (1995).
3. S. I. Mho, B. Ortiz, N. Doddepeneni, and S. M. Paik, *J. Electrochem. Soc.* **142**: 1047 (1995).
4. M. P. Doherty, P. A. Christensen, A. Hamnett, and K. Scott, *J. Electroanal. Chem.* **385**: 39 (1995).
5. K. M. Robertson and W. O'Grady, *J. Electroanal. Chem.* **384**: 139 (1995).
6. H. G. Hambold and X. H. Wang, *Nucl. Instrumen. Meth. Phys. Rev., Sec. B* **97**: 50 (1995).
7. A. K. Jonscher, *J. Mater. Sci.* **30**: 2491 (1995).
8. J. M. Tatiobouet, *Appl. Catalysis A. General*, **148**: 213 (1997).
9. K. Wang, H. A. Gasteiger, N. M. Markovic, and P. N. Ross, *Electrochim. Acta* **41**: 2587 (1996).
10. A. V. Tripkovic and K. D. Popovic, *Electrochim. Acta* **41**: 2385 (1996).
11. W. T. Nappory, H. Laborde, J. M. Leger, and C. Lamy, *J. Electroanal. Chem.* **404**: 153 (1996).
12. A. S. Areco, M. K. Ravikumar, A. K. Schukla, C. Candieno, V. Antenucci, N. Giordano, and A. Hamnett, *J. Appl. Electrochem.* **25**: 528 (1995).
13. T. Feelink, W. Vischer, A. P. Cox, and T. A. R. Van Veen, *Ber. Buns. Phys. Chem.* **100**: 599 (1996).
14. J. W. Schulze and D. Rolle, *Canad. J. Chem.* **75**: 1750 (1997).
15. M. Osawa, K. Yoshi, K. Ataka, and T. Yotsuyanaga, *Langmuir* **10**: 640 (1994). Submillisecond FTIR.



### 7.10.5. The Importance of the Steady State in Electrode Kinetics

In what has been presented so far, it has been made clear that in the example of the hydrogen evolution reaction (h.e.r.), the degree of occupancy of the surface with adsorbed H (i.e., the radical intermediate) builds up with time after the electric current is switched on. The steady state of a reaction is defined as that state at which this buildup of intermediate radicals in the reaction has come to an end. As long as electronic instrumentation is present to keep control of the electrode potential (and the ambient conditions remain the same), the current density—the rate of electrical reaction per unit area—should then be constant. (This assumes a plentiful supply of reactants, i.e., no diffusion control.) It is advisable to add “should be,” because—particularly for electrode reactions on solids that involve the presence of radicals and are therefore subject to the properties of the surface—the latter may change relatively slowly (seconds) and a corresponding (and unplanned) change in reaction rate (observable in seconds and even minutes) may occur (Section 7.5.10).

Now let the reasons for this insistence on the study of the steady state of an electrode reaction be expounded. The main reason is simply that electrochemical reactions are useful at the steady state. It is most desirable for the current density in a reactor carrying out some organic synthesis to remain constant over hours or days while the synthesis is going on. It would not be desirable in a fuel cell producing power to run a car if the rate of the electrochemical reaction in it—hence the power output and thus the speed of the car—varied out of control of the driver.

So, the steady state and the mechanism of the reaction there must be the final objective in electrochemical mechanism determinations. Of course, dynamic intermediate states are met on the way to the steady state (i.e., before it is reached), but one must evaluate the information obtained from them to serve the proper aim: knowledge of the mechanism in the steady state.

In Chapter 8, a study of dynamic methods of investigating electrode reactions is given. It will be shown how to vary the electrode potential systematically and interpret the resulting variations in current so that they provide information on what is going on on the surface. Potentiodynamic measurements are often used, and are indeed essential, in electrochemistry. However, the attractive simplicity of making them and the beguiling variety in the patterns observed on the oscilloscope should not seduce the researcher from his or her aim: determination of a mechanism in the steady state.

Novel and impressive methods for looking at electrode surfaces are available to electrochemists. Such methods (including rapid-response spectroscopy and developments based on scanning tunneling microscopy and its sister techniques) may make it less necessary in the future to derive mechanism information indirectly from analysis of the rate of the reaction as a function of variables. Dynamic spectroscopic methods may make it possible eventually to watch the surface radicals as they vary with potential and time and finally to identify them in the steady state. The cutting edge of the *in situ* techniques moves so quickly that attainment of its eventual aim (following

the movements of individual atoms on the electrode surface in real time!) may well be reached while this book is still in use.

## 7.11. ELECTROCATALYSIS

### 7.11.1. Introduction

Heterogeneous catalysts involve the surfaces of metals, sometimes their oxides, and they are prepared in various ways (e.g., the surface may be roughened) or they may be in powder form to gain greater area. The related subject of electrocatalysis is similar to that of heterogeneous catalysis. Basically, all electrodes that are the site of reactions involving adsorbed intermediates can be regarded as catalysts, although in practice only those on which electrochemical rates are relatively rapid (compared with rates for the same reaction at other electrodes) are thought of as such.

Of course, electrocatalytic reactions are potential dependent in rate, as are all other electrode reactions,<sup>87</sup> and one of the subjects to which attention will be given in the following discussion is the reference potential at which a comparison of electrocatalysts should be made. Table 7.17 contains a comparison of chemical (thermal) and electrochemical (electrical) catalysis.

To consider a hypothetical case, suppose one takes an ion which is to discharge with electron transfer onto an electrode surface and deposit there as an adsorbed radical, X. Then the larger the bond strength of the adsorbed radical with the surface, the easier (faster) the reaction will be. To seek a good catalyst, then, requires a substrate, an electrode, which bonds strongly to X. However, one has to take into account the fact that the bond strength of the adsorbing atoms decreases as the degree of occupancy of the surface with the radical ( $\theta_x$ ) increases (cf. Temkin's isotherm, Section 7.7.4). So some knowledge of  $\theta_x$  in the steady state of the reaction has to be available (or be determined). Only then will it be possible to estimate the relevant bond strength M–X (proportional to the heat of adsorption at that  $\theta_x$ ) and hence predict the degree of catalysis for the discharge of  $X^+$  onto a given metal.

However, there is a second case in respect to bonding. It is possible that the rds is not a discharge of  $X^+$  onto M, an atom in the electrode substrate, but instead is the *desorption* of an adsorbed X from the surface. Obviously, then, a strong bond between the electrode substrate, M, and X, instead of causing a greater velocity of the reaction,

<sup>87</sup>If not all electrode reactions, then electrocatalytic? If one has a redox reaction, an electrode reaction in which nothing happens except that the ion concerned gives up ( $Fe^{2+} \rightarrow Fe^{3+} + e$ ) or receives ( $Fe^{3+} + e \rightarrow Fe^{2+}$ ) an electron, there is no catalysis. Such redox reactions do not involve adsorbed reaction intermediates. Hence, there is no chemical bonding with the electrode surface and no dependence on its nature. However, simple redox reactions are not used much outside the research laboratory and the truth is that most electrode reactions *do* involve intermediates adsorbed onto the electrode and therefore exhibit a rate that is substrate dependent.

will delay it; i.e., each step of the reaction will be more difficult as the M–X bond strength increases.

So much, then, for two essential cases in which the adsorptive bond between an atom of the substrate acts differently, depending on the nature of the rds. This bonding, and how it affects electrocatalysis, is called the *electronic factor*, in electrocatalysis.

Now, there is a second group of factors called *geometric* that influence an electrode reaction rate, i.e., electrocatalysis. These factors will remind the reader of some of the structural matters covered in discussions of chemical catalysis. They refer to the structure and often to the heterogeneity of the catalyst's surface. Active sites on the surface can be identified. Examples of such factors are:

1. *The Lattice Spacing.* This affects particularly the rate of reaction between two radicals on the surface (see Fig. 7.107).

2. *Edges and Kinks.* Although one may at first picture an electrode surface as a flat plane, at high magnification levels, electron microscopy, and particularly scanning tunneling microscopy (see Section 7.5.18), reveals that real surfaces contain a great deal of structure on an atomic level. They contain plenty of vacancies, areas where atoms are missing from the plane. Then there are ledges, places where a crystal plane has emerged above the surrounding surface and forms a ledge, sometimes monatomic but some 10–50 atoms in height. An example of such ledges is shown in Fig. 7.108. Correspondingly, an important configuration on surfaces is the so-called kink site, where two crystal ledges meet and form a corner.

Why should these structures affect catalysis? It is because they affect bonding. In Fig. 7.108, it can be seen that an atom on a planar site coordinates with between one and four surface atoms, depending on how it sits in the site. When it also has the opportunity to bond with further atoms “at the side” (i.e., against a ledge), its coordination number (and hence its bonding) increases and it gets even larger at a kink site.

So, in describing factors in electrocatalysis that can be understood without resorting to quantal concepts, it can be said in summary that an electrode catalyst can be rationally chosen only if one knows what the rds is in the electrode reaction. Then

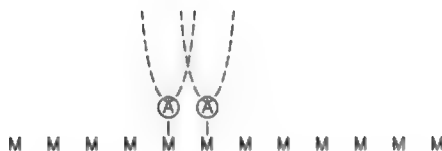


**Fig. 7.107.** If the interatomic distance on the catalyst is too great, the heat of activation (given by the interaction of the potential-energy curves) will be too large. If the interatomic distance is too small, the adsorbed atoms will be in contact and repel.

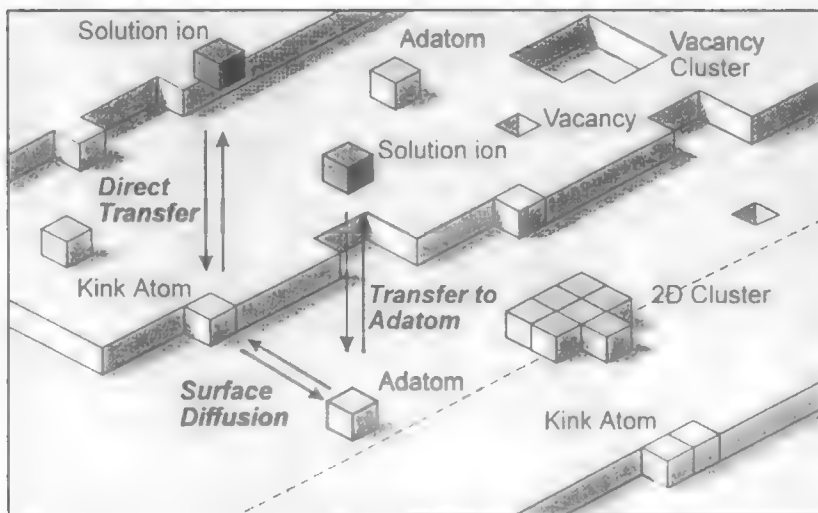


**Fig. 7.108.** The structure of a single face of a crystal with a simple cubic lattice at lower temperatures. (Reprinted from E. Budevski, G. Staikov, and W. J. Lorenz, *Electrochemical Phase Formation and Growth*, p. 17, copyright 1996 John Wiley & Sons. Reproduced by permission of John Wiley & Sons, Ltd.)

the key factor is to choose a material that “bonds right,” i.e., in a way that increases the rate of the rds. Apart from this, the heterogeneity of the surface is vital, and one can at once understand that a surface containing a greater number of defects, kinks, ledges, and holes is likely to be a good catalyst if the rds is such that strong bonding to the radical is helpful (just as a minimization of the heterogeneity will help if the rds indicates that a weak bond would have a positive effect). The way in which these various factors might be collectively taken into account has been discussed (Minevski, 1996), but the complex alloy catalysts that come out of the theory have not yet been examined.

What of the factors that involve quantum mechanics? They concern the electron overlap of bond orbitals and the effect of tunneling *through* a barrier (Chapter 9).

### 7.11.2. At What Potential Should the Relative Power of Electrocatalysts Be Compared?

As has been made abundantly clear in Section 7.2.3, when an electrode reaction is controlled by interfacial reactions—not by transport to the electrode in the solution or (as in semiconductors) within the electrodes—the electrochemical reaction rate depends exponentially on the overpotential. Thus, regarding the approximate equations:

$$i_{\text{cath}} = (i_0) e^{-\alpha n F / RT} \quad (7.27)$$

$$i_{\text{an}} = (i_0) e^{+(1-\alpha)nF/RT} \quad (7.31)$$

respectively for the cathodic and anodic versions of the same reaction, one might at first choose  $i_0$  as the arbiter of electrocatalysis. Then one would take a given reaction (e.g., the oxidation of methanol) and measure its rate on a dozen different electrode materials. Care would have to be taken that the current measured is being given 100% to the oxidation of methanol and not to some competing reaction, e.g., oxide film formation or even (if the potential is sufficiently anodic) oxygen evolution. Then one would list the various  $i_0$ 's against the electrode materials and rate them, taking their catalytic power as being proportional to the  $i_0$ 's for the oxidation of methanol on the various electrode materials. This sounds good and indeed it is the way most academic researchers rate electrocatalysts.

One might go a step further and recall that

$$i_0 = \frac{n}{\nu} F k_0 c_i$$

where these symbols have the meaning previously given to them. Thus,  $n/\nu$  and  $F$  are constants for the reaction concerned and only the reactant concentration,  $c_i$ , is a variable. We can go further and strip the  $i_0$ 's down to the underlying rate constants and compare them; so using  $i_0$  as an arbiter of electrocatalysis seems most reasonable.

However, looking at the problem of the reference potential at which to compare electrocatalysts from a commercial or technological point of view, the  $i_0$  method may not be at all the best way. In practical use—in fuel cells or reactors making compounds electrochemically—the most important economic factor is the overpotential. Insofar as it is large, the cell potential in a reactor will be large and the kilowatt hours needed to produce a unit weight of a product also will be large and expensive. Alternatively, if one wants to let the cell run spontaneously (a fuel cell), a larger  $\eta$  will mean a smaller net potential from the cell and therefore less kilowatts of electricity for a given amount of fuel used.

Now, regard Fig. 7.109. Of the two catalysts, pure platinum and 80-20 Pt-Ru, it is at once clear that the alloy exhibits a higher  $i_0$  than the pure platinum. Further, until a current density of about  $3 \times 10^{-2} \text{ A cm}^{-2}$  for a given potential, a higher current is produced on the alloy than in the pure platinum, confirming the idea (as indicated by a comparison of the  $i_0$ 's) that the alloy is the better catalyst.

What happens if one is a practical engineer and wants to have the largest rate of the reaction unit to make the best use of factory floor space? At potentials above about 0.45 V (Fig. 7.109) it is the reaction on the pure platinum that gives a greater current than that in the alloy. Now which is the better catalyst?

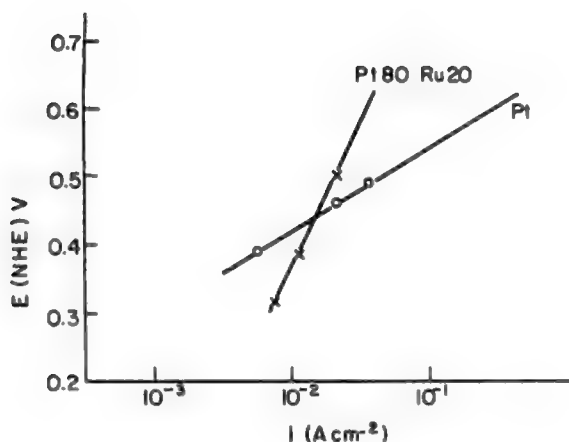


**Fig. 7.109.** Experimental current density–potential relationship for the oxidation of ethylene on platinum and an 80% Pt–20% Ru alloy.

Thus, in comparing  $i_0$ 's and letting the rank of the catalysts be decided by their order, it has been implicitly assumed that the  $\alpha$ 's in Eq. (7.21) are the same for all the electrodes concerned. If that is not the case, the rank of the catalyst will depend on the potential in that section of the Tafel line which is being considered. Practical engineers tend to work at the highest current densities. They would want to rank the catalysts less in terms of exchange current densities and more in terms of the overpotential (near the potential at which they wish to work). If one says, quite arbitrarily, that one will rank the electrocatalysts (electrode materials) by their overpotentials at  $100 \text{ mA cm}^{-2}$ , this would be more helpful to the electrochemical engineer than ranking by exchange current densities or rate constants.<sup>88</sup> So, it all depends on what kind of an electrochem-

<sup>88</sup> The truth is that electrochemical engineers may in fact spurn quantities such as the exchange current density,  $\alpha$ , the transfer coefficient, or  $k_0$ , the rate constant at the reversible potential. A practical engineer must keep his eye on economics. He calls what the fundamental scientist terms overpotential by an older term, the overvoltage. Finally, having to take everything into account, the engineer sometimes talks about "polarization." This term has more than one meaning in electrochemistry, but in respect to cells it means the sum of all the overpotentials (those due to the interfacial processes, the concentration overpotential, and the IR drop).

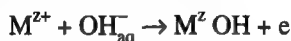
Sometimes in industrial cells, the polarization is surprisingly high. In the famous Hall–Herriault cell from which the world produces its aluminum, it is several volts, partly owing to the potential lost in the IR drop within the electrodes themselves, the anode being made of graphite, which has a resistance far greater than that of metals. Although alternative materials that have a higher conductivity are known, an innate conservatism in the aluminum industry continues to support the use of a cell that wastes large amounts of electricity in its IR drop.

ist you are. And since this book is written for a wide audience, the methods for rating electrocatalysts have been given in Table 7.18.

### 7.11.3. How Electrocatalysis Works

So far, the bonding and surface structure aspects of electrocatalysis have been presented in a somewhat abstract sort of way. In order to make electrocatalysis a little more real, it is helpful to go through an example—that of the catalysis of the evolution of oxygen from alkaline solutions onto substances called perovskites. Such materials are given by the general formula  $\text{RTO}_3$ , where R is a rare earth element such as lanthanum, and T is a transition metal such as nickel. In the electron catalysis studied, the lattice of the perovskite crystal was replicated with various transition metals, i.e., Ni, Co, Fe, Mn, and Cr, the R remaining always La.

Figure 7.110 shows a view of the perovskite lattice. Of course, the diagram shows the surface of a perovskite, and before going any further, the student should spend sufficient time comprehending the surface on which the electrode reaction is to take place, with an understanding of the symbols showing where the La, transition metal, and O's are. One puzzle is cleared up by this diagram. If one contemplates the general empirical formula for perovskites,  $\text{RTO}_3$ , it is not obvious how the  $\text{OH}^-$  ions in an alkaline solution would be able to discharge upon an oxide surface. It would seem that O might be on the surface the  $\text{OH}^-$  would face as it diffused in from the solution and clearly no bonding would occur. However, the slice through the crystal, exposing the surface (Fig. 7.110), shows that in fact the transition metal ion, with its multiple valencies and strong bonding power, is indeed on the surface. So  $\text{OH}^-$  discharges onto the transition metal of the perovskite, M, not onto O's:



Now, the next point to understand is the relation between the rate of the reaction (here measured uniformly for all the perovskites studied at an overpotential of 0.3 V) and the strength of the OH bond to the transition metal. It is made clear from Fig. 7.111 that the stronger the bond strength, the slower the reaction. This is a determinative

**TABLE 7.18**  
**At What Potential Should One Compare Electrode Materials As**  
**Electrocatalysts?**

View of Fundamental Researcher	View of Electrochemical Engineer
Compare the $i_0$ 's. Alternatively, one may compare the corresponding rate constants and the one showing the greatest $i_0$ or $k_0$ is the best.	Compare the overpotentials developed at some practically useful current densities, e.g., $100 \text{ mA cm}^{-2}$ . The catalyst showing the <i>least</i> overpotential at this current density is the best catalyst.

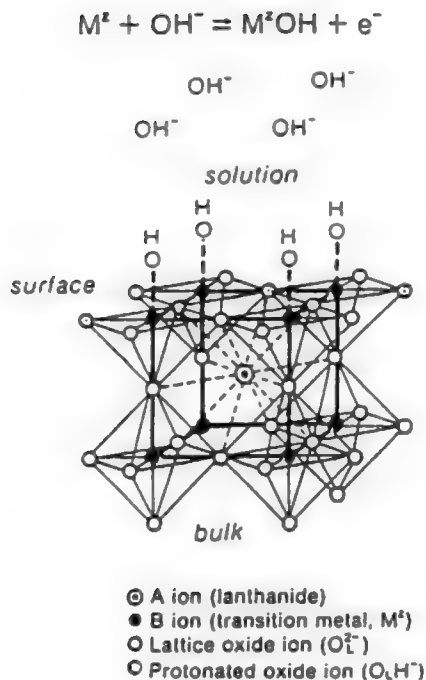
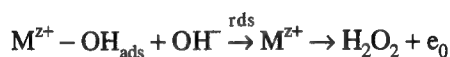


**Fig. 7.110.** Schematic model for the active surface of the perovskite, in which transition metal B is electrochemically active. (Reprinted with permission from J. O'M. Bockris and T. Ottagawa, *J. Phys. Chem.* **87**: 2964, copyright 1983 American Chemical Society.)

piece of information which suggests that the reaction mechanism must involve a *desorption* of OH in the rds. The more difficult this becomes (stronger bonding), the more difficult is it for the reaction to occur.

Any mechanism suggested must involve desorption of OH formed in the first step. The second and rate-determining step in the series going to  $O_2$  is therefore likely to be



The first and second step can be represented in some detail, as shown in Fig. 7.112.

Further steps to finally get  $O_2$  will be beyond the rds and hence not of primary influence on the electrocatalysis process. They could be



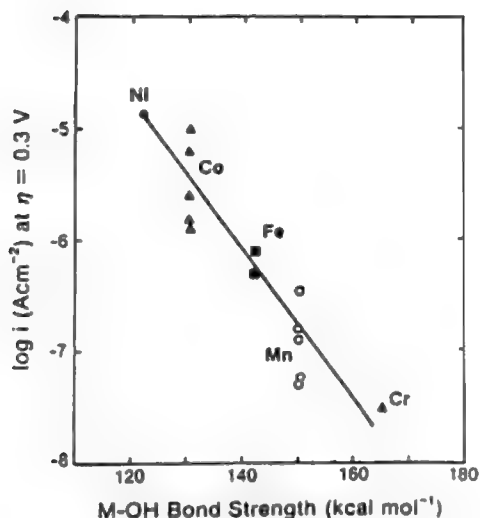
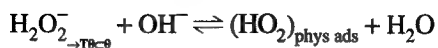


**Fig. 7.111.** Current density (based on real surface area) for oxygen evolution on perovskites at an overpotential of 0.3 V vs. M—OH bond strength. The transition-metal ions (M) in perovskites are indicated with different symbols. (Reprinted from J. O'M. Bockris and T. Ottagawa, *J. Electrochem. Soc.* **131**: 2965, 1984. Reproduced by permission of The Electrochemical Society, Inc.)



Such matters can be represented in a different way in terms of the d-electron configuration of transition metal ions in a molecular orbital scheme (Fig. 7.113).

The considerations of this reaction of  $\text{O}_2$  evolution on an oxide catalyst again show the importance of electronic factors and bonding. However, the discussion covers only the essentials; the reality of the catalysis of perovskites in oxygen evolution involves several other factors that can be referred to here only briefly.

One important matter is the availability of electrons in the oxide, which for a metal would not be a factor because there are always plenty. *Pure* perovskites are nonconductors and before they can be used as electrodes, it is necessary to add to them other substances that increase their conductance. BaO is one substance used. The process is

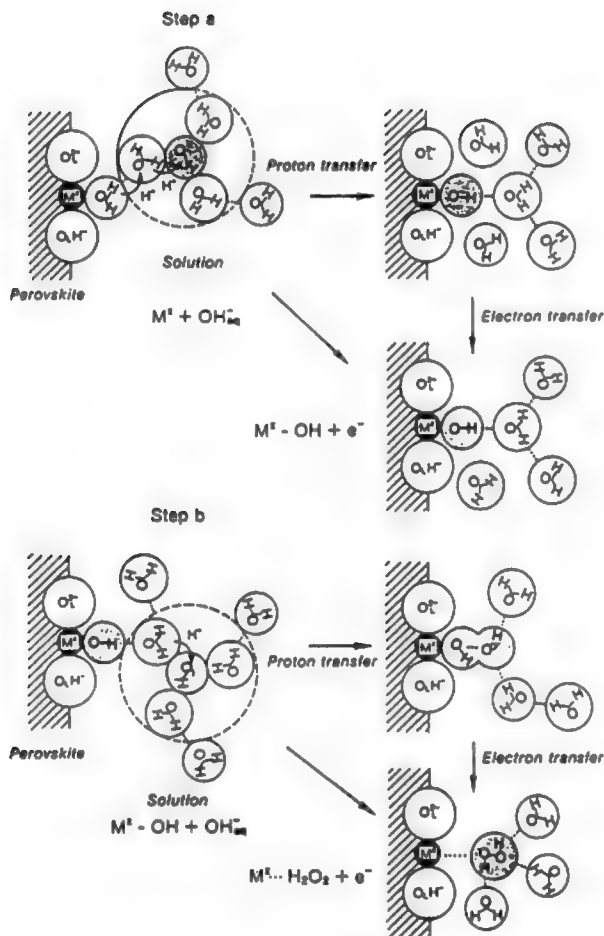


**Fig. 7.112.** Schematic representation of the first and second (rate-determining) steps of the mechanism of the evolution of  $O_2$  on perovskites, involving a series of proton transfers. (Reprinted from J. O'M. Bockris and T. Ottagawa, *J. Phys. Chem.* **87**: 2964, 1983.)

similar to the addition of doping agents to semiconductors (Section 7.4.1). Then it is necessary to know the effect of the adsorbing  $OH$  upon the resulting electron density created by the addition of  $BaO$ . Could it be locally decreased by  $OH^-$  adsorption?

Finally, nothing has been said as yet about the effect of entropy and ordering factors on the geometry of the surface. The discussion looks at  $OH^-$  adsorption and desorption as though it were happening in isolation. What of the buildup of  $OH^-$  on

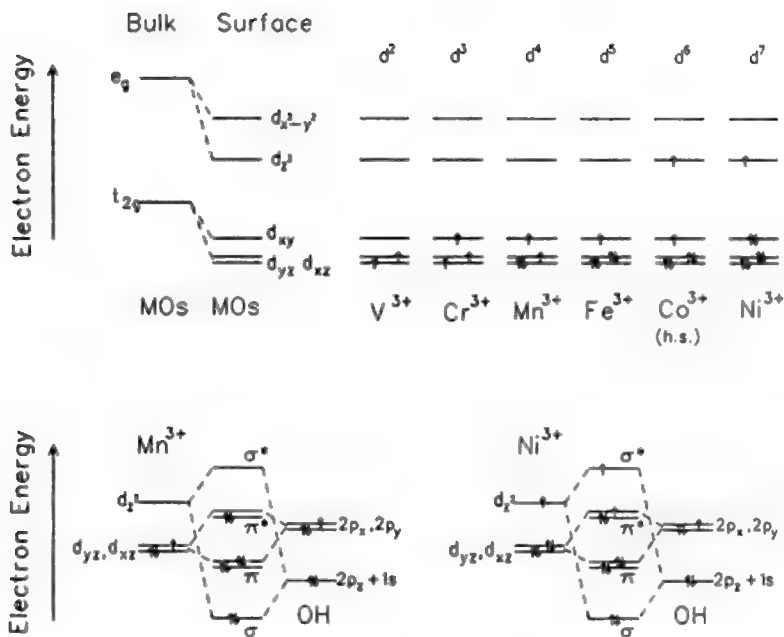


**Fig. 7.113.** d-Electron configuration of transition-metal ions at the surface of perovskites, for the case of magnanites and of nickelates (below). (Reprinted from J. O'M. Bockris and T. Ottagawa, *J. Phys. Chem.*, **87**: 2966, 1983.)

the surface and the lateral repulsive interaction among adsorbed  $OH^-$  ions, which will increase greatly with  $\theta$ ? What of the entropy of activation and how it will affect the reaction rate on the various oxide catalysts?

Such elaborations are beyond the message it was desired to give here; conducting oxides can be electrocatalysts. The catalysis is still due to M–OH bonding, but in an inverse sense to that occurring, say, in  $OH^-$  discharge, when this is rate determining in the evolution of oxygen.

#### 7.11.4. Volcanoes

A widespread phenomenon in chemical catalysis is the volcano. One finds that for a given reaction carried out on a variety of catalysts, one is able to plot the rates on each catalyst so that they pass through a maximum. As to what is plotted on the abscissae, this varies, but it is always a function involving some property of the catalyst, e.g., its heat of sublimation (which would be proportional to its metal–metal bond strength), or the actual bond strength of the catalyst material and an adsorbed radical taking part in the rds, or the interatomic distance among the surface atoms. The

electrocatalytic literature also contains several examples of this phenomenon (Fig. 7.114), and it clearly demands some kind of mechanistic explanation.

A word picture can be given as to why volcanoes occur in electrocatalysis. Consider a series of differing electrode surfaces, on each of which the same reaction occurs. Think of these various electrocatalysts as having a bonding power to some atom in the reactants. If one is thinking, say, of the oxidation of methanol, the important bond may be the M–C bond where M represents the series of catalysts arranged in sequence so that they bind to C to an increasing degree. Now, when the bonding power is minimal, at the beginning of this imaginary series of catalysts,  $\theta$ , the degree of coverage of a unit area of the electrode with an adsorbed reactant will also be small; indeed, perhaps  $< 1\%$ , and so the rate at which the final product ( $\text{CO}_2$  if one begins with  $\text{MeOH}$ ) is produced will be very slow.

As the bonding power of catalyst to the vital reactant in the rds increases in the series of catalysts,  $\theta$  will also increase and hence the rate of production per unit area.

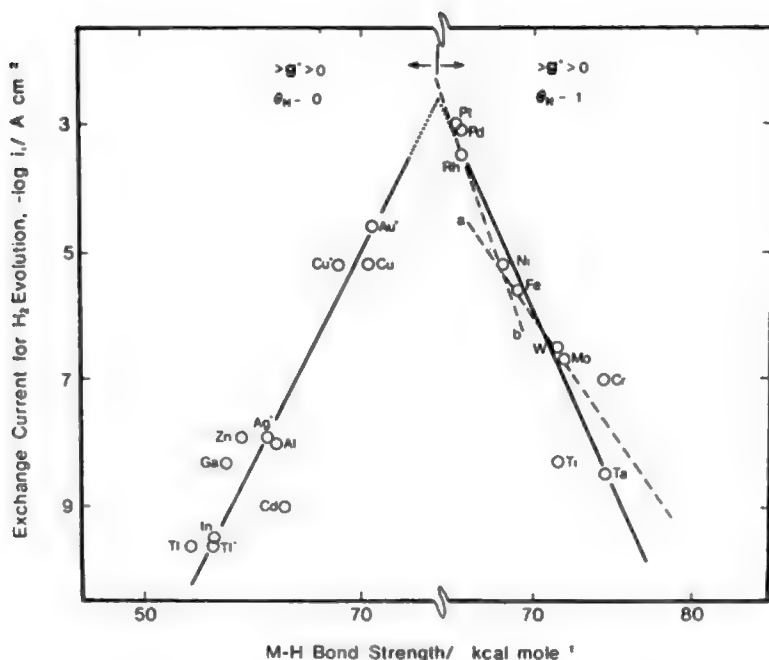


**Fig. 7.114.** A plot of exchange current density for hydrogen evolution reaction vs. M–H bonding strength. (Reprinted from S. U. M. Khan, "Some Fundamental Aspects of Electrode Processes," in *Modern Aspects of Electrochemistry*, Vol. 15, R. E. White, J. O'M. Bockris, and B. E. Conway, eds., Plenum 1983, p. 339.)

This increase will continue as one moves through the series of catalysts, always with increasing bonding power (hence increasing  $\theta$  in the steady state). However, as  $\theta$  increases, the free surface available for adsorption decreases. One has to account for this in the expression for the rate with a  $(1 - \theta)$  term, so that an expression for the reaction rate would be proportional both to  $\theta$  and to  $(1 - \theta)$ . Now, were this clash of increasing  $\theta$  (good) and decreasing availability for adsorption from the solution (bad) the only factor, then

$$\text{Rate} \propto \theta (1 - \theta) \quad (7.245)$$

the maximum rate would be  $d \text{ rate} / d\theta = 0$ , i.e., at  $\theta = 1/2$

The argument given here is simplistic, but it can readily be seen that as the adsorption bond of catalyst to radical increases and  $\theta$  with it, there will occur a value of the bonding strength of the substrate to a radical formed during the oxidation of methanol, for which the value of  $\theta$  will be so large that more than half of the electrode surface will be covered; then the reaction rate will begin to decrease with a further increase in  $\theta$ . Finally, when  $\theta \rightarrow 1$ , nearly all of the surface will be covered with entities taking part in the reaction. Desorption of the products will also be difficult (because of the strong M–C bond), so that the reaction rate will have become very slow, just as it was when the value of the M–C bond strength was very small. In a qualitative sense, then, as the bonding power of the catalyst increases, the reaction rate will increase, pass through a maximum, and then decrease. That is a volcano.

### 7.11.5. Is Platinum the Best Catalyst?

Platinum is so frequently used as an electrode material in electrochemical cells that one tends to think it must be the best catalyst. Platinum is used frequently largely because of its stability and availability, rather than its good catalytic power. It does not dissolve until a highly anodic potential,<sup>89</sup> and it is indeed a good catalyst for some reactions [not to be forgotten is the fact that one can order it from a catalog whereas the other noble metals (except for gold) are more difficult to buy in suitable wire or plate form]. Electrochemical stability is clearly an important element in electrocatalysis—one of several. However, it is interesting to note that the prediction based on the simple model described earlier (that the best catalyst is the one with bonds

<sup>89</sup>The dissolution reaction is:  $\text{Pt} \rightarrow \text{Pt}^{2+} + 2\text{e}$  and the value of its reversible thermodynamic potential is 1.2 V on the normal hydrogen scale. The evolution of  $\text{O}_2$  in acid solution at a current density of, say,  $100 \text{ mA cm}^{-2}$ , needs an overpotential on platinum of nearly 1.0 V, i.e., the electrode potential would be  $\sim >2.0$  V. It follows that at these very anodic potentials platinum *would* tend to dissolve, although its dissolution would be slowed down by the fact that it forms an oxide film at the potentials concerned. Nevertheless, the facts stated show that the alleged stability of Pt may be more limited than is often thought. This is an important practical conclusion because dissolved Pt from an anode may deposit on the cathode of the cell, and instead of having the surface one started with as the cathode, it becomes in fact what is on its surface, platinum.

of intermediate strength; see Fig. 7.114) is borne out with Pt. Thus, if one places Pt among the refractory elements in respect to its melting point, which clearly tends to increase with increasing bond strength, one obtains the results shown in Table 7.19.

Nevertheless, as stated, factors other than bond strength influence the choice of catalyst. Economics is one such factor. Thus  $\text{PbO}_2$  is sometimes called "the poor man's platinum," because it is stable under conditions that are strongly anodic, as in the charging of a lead-acid battery (Chapter 13). Glassy carbon can be a useful anode and is certainly much cheaper than Pt. Refractory compounds such as FeSi and SiC are sometimes used in organic syntheses. TiC is an excellent refractory, conducting at high temperatures, which may eventually become a highly conducting and nonconsumable anode in new methods for the electrolytic production of aluminum, thus reducing the volts wasted in the IR drop through the consumable carbon anodes now used.

### 7.11.6. Bioelectrocatalysis

**7.11.6.1. Enzymes.** As the name implies, bioelectrocatalysis refers to the possible use of enzymes as part of an electrode in electrochemical devices. Enzymes are catalysts that act on the chemical reactions by which the body works. They have remarkable characteristics. The first of these is their astoundingly large catalytic power. The way to measure this is in terms of the *turnover number*: the number of individual catalyzed events that occur per second at a catalytically active site. Whereas in chemical catalysis this number may range between one and one hundred, in enzyme catalysis it ranges between one thousand and ten million. The second characteristic is a stunning specificity. Thus, the enzyme  $\alpha$  glucose oxidase catalyzes  $\alpha$  glucoside bonds; it is inactive toward  $\beta$  glucoside bonds, although the difference between the two is a matter of bond angle only.

What *are* enzymes? One can only give a general answer because the structures are too complex to write down here. Enzymes are proteins, but of a type called *globular* because the polypeptide chain that is a part of all proteins is folded around on itself. Most enzymes need a partner (or coenzyme) to become active. The partner may be as simple as  $\text{Mg}^{2+}$  but as complex as nicotinamide adenine dinucleotide (NAD).

**TABLE 7.19**  
**Melting Points of Some Refractory Elements (°C)**

Lower m.p. than Pt		Higher m.p. than Pt	
Lanthanum	920	Rhodium	1996
Gold	1003	Ruthenium	2427
Palladium	1550	Iridium	2454
Tantalum	1695 = 1770	Osmium	2700
Lutetium	1760	Tungsten	3380

It would be distinctly arrogant to say that we understand how enzymes work. At best we catch glimpses of their action. One model involves the key-and-lock concept—an attempt to rationalize their specificity. A much simplified presentation is shown in Fig. 7.115. The idea is that certain shapes in the enzyme structure are precise fits for a part of the reactant molecule. A famous formulation of this is the Michaelis–Menten kinetics. If E is the enzyme and R is some part of a reactant (a complex biomolecule),



where ER represents the key in the lock, the enzyme with the reactant fitting into it:

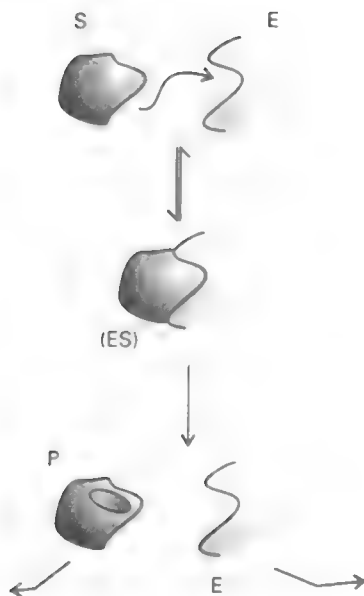
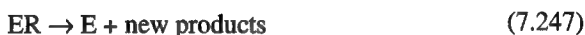


**Fig. 7.115.** The basis of the Michaelis–Menten mechanism of enzyme action. Only a fragment of the large enzyme molecule E is shown. (Reprinted with permission from P. W. Atkins, *Physical Chemistry*, 5th ed., W. H. Freeman, 1994, p. 890, Fig. 25.12.)

Such a mechanism assumes that the reactant adsorbs on the enzyme (both reactant and enzyme are seen as being in solution) and that the adsorption reaction is an equilibrium one. The rds is the release of the new product from the enzyme which—like all catalysts—is regenerated after use.

From (7.246) and (7.247):

$$\frac{[ER]}{[E][R]} = K; ER = K[E][R] \quad (7.248)$$

To form a new product and regenerate the enzyme, then:

$$\text{Rate of reaction} = k_2[ER] = k_2K[E][R]$$

**7.11.6.2. Immobilization.** If enzymes are to be used electrochemically—made part of an electrode—they will have to be taken away from floating around in the dissolved state and adsorbed onto a conducting surface connected to an outside circuit. This process is called *immobilization*. However, a major problem was discovered when ellipsometry was used to follow the adsorption of glucose oxidase on gold (Hitchens and Szucs, 1989). The enzyme adsorbed on the metal from its dissolved state dissociates—in fact falls apart—upon adsorption, emitting in its dissociation some vital parts of its structure. The ellipsometry shows that within minutes of contacting the surface, the enzyme has self-destructed.

Such difficulties can be solved by means of work that goes back to experiments carried out by Eddowes and Hill (1977). Their idea was to allow the giant protein a “soft landing” when it adsorbed on a metal. The concept is shown in Fig. 7.116. To do this, they placed a “modifier” (4,4′-bipyridyl) between the metal surface and the incoming protein from the solution. In the case of the enzyme cytochrome *c*, there are lysine groups, and it is presumed that they are the key to a landing soft enough so that it does not smash up the vital (but extremely fragile) protein structure, which contains the secret of enzyme activity.

Some proteins contain a so-called “heme” group, complex organic structures within the enzyme at the center of which is an iron atom. In respect to electrochemical action, it is necessary for the electron from the underlying metal to reach the iron in the heme group of the adsorbed enzyme and there to cause its reduction to  $\text{Fe}^{2+}$ .

In some proteins, particularly cytochrome *c* (a relatively small enzyme, if still vast compared with a normal ion; its molecular weight is 12,400) electron transfer occurs through the modifier to the heme group. What is surprising is the *rate* at which this electron transfer takes place; it is about the same as that of a fast redox reaction to a simple ion in solution. With such a monster reactant, one might have expected a ponderously slow reaction.

**7.11.6.3. Is the Heme Group in Most Enzymes Too Far Away from the Metal for Enzymes to Be Active in Electrodes?** It has been mentioned that cytochrome *c*, for all its enormous molecular weight, is smallish as biomolecules go.



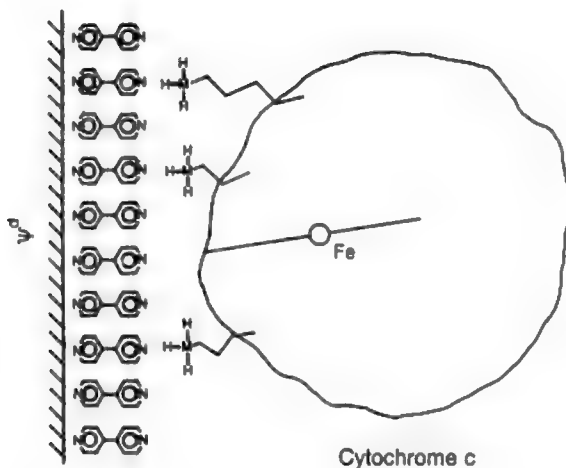


**Fig. 7.116.** Oxidation of glucose mediated by the enzyme glucose oxidase. The catalytic activity produces electrons and oxygen is reduced on the enzyme to produce  $\text{H}_2\text{O}_2$ , which is then electrochemically analyzable. In this way, glucose can be indirectly monitored. (Reprinted from F. A. Armstrong, H. A. O. Hill, and N. J. Walton, *Acc. Chem. Res.* **21**: 407, Fig. 1, copyright 1989, American Chemical Society.)

Most enzymes are in fact much larger. If they are to act electrochemically, and assuming the heme group is roughly at the center, the question arises as to whether this group is too far away from the metal for electron transfer to be possible in one step. By means of the process called *electron tunneling* (see Chapter 9, Section 9.4), electrons can travel in biological situations in “leaps” of 2 nm. If the heme group is, say, 5 nm from the metal inside an adsorbed enzyme, even if the latter has had a successful soft landing and is still intact and catalytically active, it does not seem possible for it to act electrochemically because its heme group is beyond the tunneling power of electrons from or to the metal on which the enzyme has landed.

Acceptance of the idea that there might be a fundamental inability to use the vast catalytic power of enzymes in electrochemical situations would deal a major blow to bioelectrochemistry and provide a challenge so powerful that it would bring funding from the U.S. research funding agencies. One result of this funding has been the work of Delgani and Heller (1990), (see Vol. 1, Section 1.9) who used what might well be called the relay station principle. These workers found it possible to introduce artificial redox centers into giant enzymes and thus to reduce the jump distance for electrons between the redox centers to less than the 2 nm that is their tunneling limit.

**7.11.6.4. Practical Applications of Enzymes on Electrodes.** There is a growing field of biosensors, in which electrochemistry is used in biological situations. For example, ultramicroelectrodes (Section 7.5.4.4) can be used to monitor electroencephalographic activity in the brain.

In respect to the use of enzymes, there are two levels of approaches. In the first, the enzyme is used to carry out a chemical reaction, the result of which is a product that can be monitored electrochemically. The idea is shown in Fig. 7.117. The  $\text{H}_2\text{O}_2$  generated is subject to normal electroanalysis and in this secondary way the glucose, the oxidation of which provided the electrons to reduce the  $\text{H}_2\text{O}_2$ , can be monitored. A successful "wristwatch glucose meter" is important for diabetics, who suffer if the glucose level in their blood (normally monitored by clumsy urine tests only once or twice per day) undergoes irregular variations. The variations could be controlled by an automated insulin intake if a continuous readout of the glucose level in the diabetic's blood were available.

An approach to such a desirable device illustrates the second type of potential use of enzymes in electrochemistry, a direct enzyme electrode. Thus (Fig. 7.117) when glucose undergoes oxidation under the catalytic power of the glucose oxidase, instead of giving electrons to  $\text{O}_2$  and causing the formation of  $\text{H}_2\text{O}_2$ , the enzyme would inject the electrons received during the oxidation of the glucose into an external electronic circuit. A wristwatch meter would then be feasible.

However, there are two difficulties to be overcome. First, and most important, the glucose oxidase has to be immobilized on a modifier (or mediator) attached to a conducting substrate; this can be done using gold on which a monolayer of e.g., bipyridyl is adsorbed. It has to be shown that thus immobilized, the glucose oxidase is sufficiently conducting (relay concept?) to transfer the electron injected into the electrochemically conducting base—through the bipyridyl layer—rather than to the  $\text{O}_2$  dissolved in the blood containing the glucose (as it is doing in Fig. 7.117).

The second problem is to arrange for continuous contact with the diabetic's blood and the electrode material in which the enzyme is adsorbed. Here, ultramicroelectrodes may be possible candidates, for if the diameter of the electrode is sufficiently small

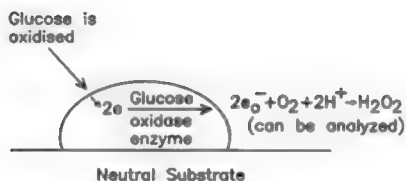


**Fig. 7.117.** Indirect action of an enzyme "electrode." It gives  $\text{H}_2\text{O}_2$  proportionally to the glucose present. The  $\text{H}_2\text{O}_2$  is easily analyzed.

(0.1  $\mu$ ), penetration of the skin is painless. The ultramicroenzyme adsorbed on the modifier would need to be engineered.<sup>90</sup>

Several successful experiments using enzymes on electrodes have been conducted, although the problem of inactivation due to “crash landings” of the enzyme on the electrode during adsorption from solution is a hazard.  $O_2$  reduction and  $H_2$  oxidation have been successfully accelerated by enzyme-covered electrodes.

Some visionary possibilities arise because of the great specificity of enzyme molecules (Vol. 1, Section 1.9). Each disease produces characteristic molecules that are not otherwise present in the blood. If one could find the enzyme that reacts only with the molecule characterizing a specific disease, micropatches of this enzyme could be engineered on a nonconducting surface wired with micropatches of enzyme-covered metal. These would give an electronic signal to an outer circuit if the molecule is present in the blood. Thus would arise the possibility for the diagnosis of many diseases in a single test.

## Further Reading

### Seminal

1. F. P. Bowden and E. K. Rideal, *Proc. Roy. Soc. London* **120A**: 59 (1928). First paper to compare electrode kinetics of  $H_2$  evolution on various substrates.
2. J. Horiuti and M. Polanyi, *Acta Physicochem. URSS* **2**: 505 (1935). First theory of electrocatalysis.
3. B. E. Conway and J. O'M. Bockris, *J. Chem. Phys.* **26**: 532 (1957). Hydrogen evolution catalysts in two groups rationalized.
4. W. T. Grubb, U.S. Patent 2, 913, 511, 1959.
5. A. Damjanovic, A. Dey, and J. O'M. Bockris, *J. Catalysis* **4**: 721 (1965). Catalytic surface of Pt-Rh alloy in solution.
6. A. Damjanovic, V. Brusic, and J. O'M. Bockris, *J. Phys. Chem.* **71**: 2741 (1967). Catalysis of electrochemical  $O_2$  reduction, related to electronic structure of Au/Pd alloys.
7. J. O'M. Bockris and S. U. M. Kahn, *Surface Electrochemistry*, pp. 292–294, Plenum, New York, 1993. Theory of volcano relations in electrochemical reactions.
8. J. O'M. Bockris, R. Mannan, and A. Damjanovic, *J. Chem. Phys.* **48**: 1989 (1968). Electrocatalysis and the electronic work function.

### Modern

1. F. C. Anson, C. L. Ni and J. M. Saveant, *J. Am. Chem. Soc.* **107**: 3442 (1982).
2. A. J. Appleby, in *Comprehensive Treatise of Electrochemistry*, B. E. Conway, J. O'M. Bockris, E. Yeager, S. U. M. Khan, and R. E. White, eds., Vol. 7, p. ? Plenum, New York (1983).
3. J. O'M. Bockris and T. Ottagaewa, *J. Phys. Chem.* **87**: 2960 (1983).

<sup>90</sup>Tarasevich (1986) has claimed a 100-day life for glucose oxidase directly adsorbed on his electronically conducting polypyrrole.

4. Y. B. Vasiliev, V. S. Bagotski, and V. A. Gromyko, *J. Electroanal. Chem.* **176**: 247 (1984).
5. M. S. Taresevitch, *J. Electroanal. Chem.* **206**: 217 (1986).
6. A. Hamlin, *Trends in Electrochemistry*, NATO ASI Series, Vol. 179, p. 19, Reidel, Dordrecht, The Netherlands (1986).
7. M. E. G. Lyons, *Ann. Rep. Chem. Soc.* **87**: 119 (1990).
8. R. Adzic, in *Modern Aspects of Electrochemistry*, B. E. Conway, J. O'M. Bockris, and R. E. White, eds., Vol. 21, p. 1, Plenum, New York (1990).
9. V. S. Bagotski, Y. B. Vasiliev, and V. A. Grinbergi, *J. Electroanal. Chem.* **283**: 359 (1990).
10. C. Quijada, J. L. Vasquez, and A. Aldez, *J. Electroanal. Chem.* **414**: 229 (1990).
11. H. Kita, S. Ye, and K. Sagimuri, *J. Electroanal. Chem.* **297**: 283 (1991).
12. B. E. Conway and T. Tilak, *Advances in Catalysis* **38**: 1 (1992). Major review.
13. S. J. Dong, *Electrochim. Acta* **40**: 2785 (1995).
14. O. A. Petrii, C. Y. Vasina, and Y. D. Seropagin, *Russ. J. Electrochem.* **31**: 1274 (1995).
15. G. Jerkiewicz and A. Zolfaghari, *J. Phys. Chem.* **100**: 8454 (1996).
16. H. Y. Chen, D. M. Zhou, J. J. Xu, and H. Q. Fang, *J. Electroanal. Chem.* **422**: 21 (1997).
17. J. Stepp and J. B. Schlenoff, *J. Electrochem. Soc.* **144**: 155 (1997).
18. J. O'M. Bockris and R. Abdu, *J. Electroanal. Chem.* **448**: 189 (1998).

## 7.12. THE ELECTROGROWTH OF METALS ON ELECTRODES

### 7.12.1. The Two Aspects of Electrogrowth

Electrocatalysis has just been described. One important feature of an electrocatalyst is that it goes through the electrodic reaction unchanged. Its sole function is to act as an electron source or sink and as a surface for the adsorption of any intermediates involved in the reaction. Or, if one prefers to think in terms of the crystalline lattice that constitutes the solid electrocatalyst, it is clear that the lattice neither disintegrates by its constituent particles walking off into solution nor grows by particles from the solution adding onto the lattice permanently. The surface of the electrocatalyst is a stable frontier; it neither advances nor recedes.

But think what happens when a piece of copper is immersed in a silver nitrate solution (Fig. 7.118) and then made an electron-source electrode. The electronation of  $\text{Ag}^+$  ions to silver metal takes place on the copper, and the reddish copper surface becomes coated with a silvery color. A cross section of the electrode shows that the electrode surface has advanced toward the solution (Fig. 7.119). Silver has electrocrystallized on the copper. Thus, the copper electrode has not behaved as an electrocatalyst; it has been altered by electrocrystallization. It is not simply an electron source.

What happens in the electrocrystallization process? How do metals "electro grow" on other metals? There are, strictly speaking, two aspects to this question. The first (Fig. 7.120) involves the process of *deposition*, i.e., the path taken by an ion in solution to move up to and be incorporated in the lattices of the crystals that make up the electrode. The second aspect (Fig. 7.121) concerns the process of *crystallization*, or

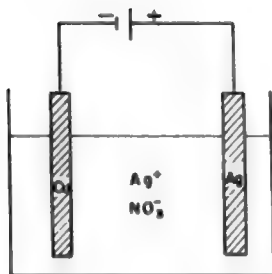


**Fig. 7.118.** An electrochemical cell involving the electronation of  $\text{Ag}^+$  at an electron source (copper cathode).

crystal growth, the name given to the cooperative process by which the individual acts of ionic deposition link up to build up old crystals or grow new ones.

### 7.12.2. The Reaction Pathway for Electrodeposition

The first step in the deposition process is that in which an ion crosses the electrified interface, i.e., the charge-transfer reaction. Picture the situation (Fig. 7.122). A hydrated ion (e.g., a silver ion) is waiting at the OHP. In the direction of the silver metal electrode, there is the three-dimensional network, or lattice, consisting of silver ions cemented together by an electron gas. The silver ions in the lattice each lay claim to an electron of the electron gas; in this sense, they can be said to be neutral and

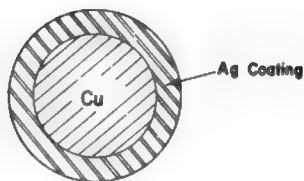


**Fig. 7.119.** An illustration of how the copper cathode in Fig. 7.118 has changed during the electronation of  $\text{Ag}^+$ . Unlike the situation in Fig. 7.118, the copper surface has not been maintained in its original form.

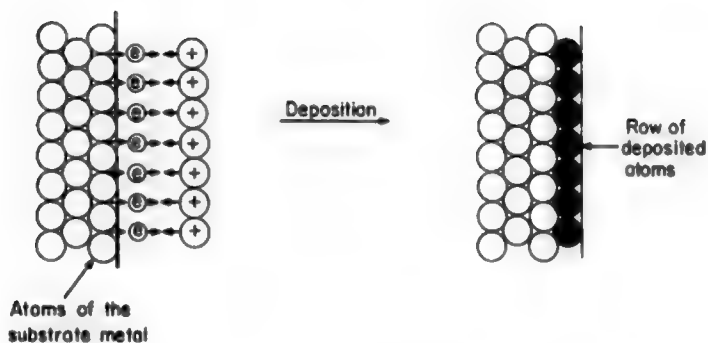


**Fig. 7.120.** The path taken by ions undergoing deposition and lattice incorporation to form a new row of atoms.

referred to as metal atoms, which are, of course, unhydrated. On the other hand, the silver ions in solution are not only charged but undeniably hydrated.

A simple conclusion follows. Before a silver ion from solution becomes part of the metallic lattice (Fig. 7.123), it has to receive an electron and divest itself of its sheath of hydration water. In short, the deposition of an ion consists of *electronation* and *dehydration*. How the ion goes through electronation and dehydration is an interesting story, only the broad outlines of which will be sketched here.

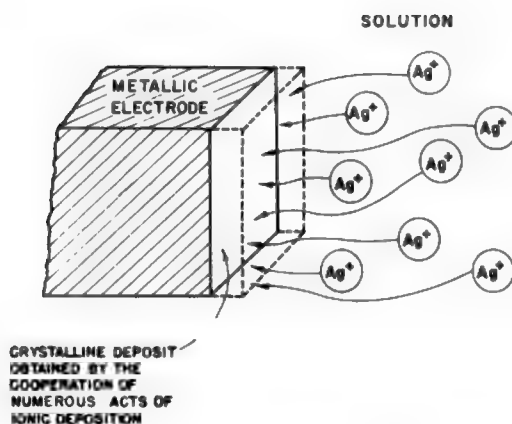


**Fig. 7.121.** The formation of a crystalline deposit involving the deposition of several rows of atoms in a manner identical to that shown in Fig. 7.120.

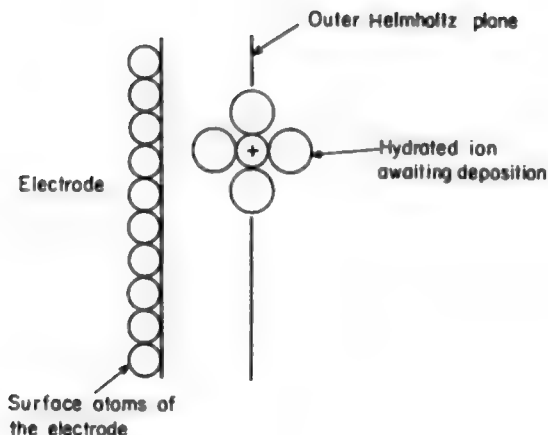


**Fig. 7.122.** Representation of a hydrated ion at the OHP awaiting deposition and lattice incorporation.

### 7.12.3. Stepwise Dehydration of an Ion; the Surface Diffusion of Adions

To answer this question one had to take a more detailed look at the electrode surface. If one does not do this, one might assume that all sites on the electrode look alike. The fundamental point is that an electrode presents a richly differentiated array of sites to an ion crossing the interface.

At first, one can consider that the electrode is a single crystal. Thus, instead of consisting of small crystals separated by grain boundaries, there is one crystal with an uninterrupted network of atoms extending right through its bulk. The surface of such

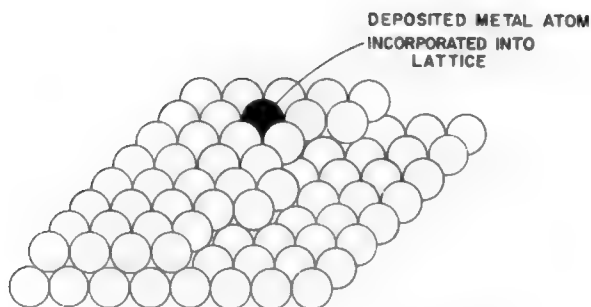


**Fig. 7.123.** The final stage in a metal deposition process, in which the deposited atom becomes incorporated into the lattice.

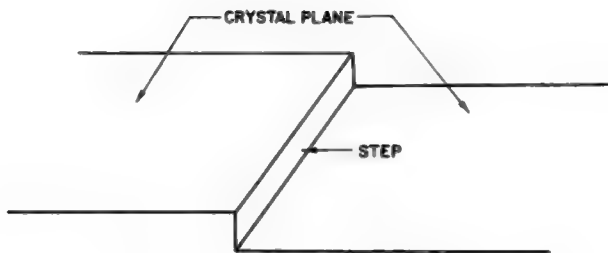


**Fig. 7.124.** Step site upon a crystal lattice.

an ideal crystal is not necessarily a perfect plane. The planes on its surface exhibit steps (Fig. 7.124), kinks (Fig. 7.125), edge vacancies (Fig. 7.126), and holes (Fig. 7.127).

One can do a thought experiment at this stage. Place an ion at each one of these different kinds of sites. It will be partly in contact with metal ions of the substrate, but the remaining space around it can accommodate water molecules. But how many water molecules can be associated with the metal ion on the surface? *That depends on the site.* The maximum number of hydration water molecules with which an adion can associate is available when the adion is sited *on* the plane, and the number progressively decreases as one considers the ion at a step, kink, edge vacancy, and hole (Fig. 7.128). So, if an ion moves from plane to step to kink and then is enveloped in a hole, its surroundings change; it tends to lose a water molecule and acquire a metal atom neighbor with each move.

Now, this description of the stepwise replacement of water molecules by metal ions as nearest neighbors to an ion can be linked up with the charge-transfer reaction. To what site is the ion likely to cross the interface?

One possibility is for the ion to wander about on the solution side of the interface, say, in the OHP, till it comes face to face with a hole site. Then, in one shot, the ion could get electronated, divest itself of its solvent sheath, and dive into the lattice. This would be a direct one-step deposition reaction (Fig. 7.129).

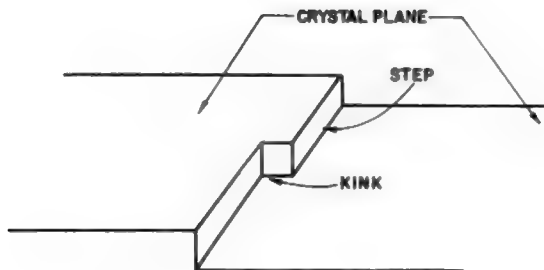


**Fig. 7.125.** Kink site upon a crystal lattice plane.



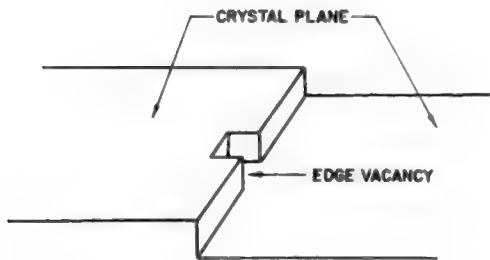


**Fig. 7.126.** Edge vacancy upon a crystal lattice plane.

Alternatively, the ion could jump onto a plane (Fig. 7.130). Two factors favor such a jump to a plane site compared with a direct jump to a hole. First, sites on a smooth plane are far more numerous than the other sites such as holes, kinks, and steps. Second, crossing over to a plane site requires the minimum amount of distortion in the ion–water complex, and hence the minimum energy change from this source. This is an important point because it is connected with basic charge-transfer theory. Before electron tunneling to the ion can occur, the ion–water-sheath bonds have to present themselves in activated form, and it is the stretching and distorting associated with this activation that determines the amount of energy needed for activation (see Section 7.5.11). Since ion transfer to a planar site involves minimum changes in hydration, such transfers have the least activation energy and go fastest compared with the rates of electron transfer at other sites, for example, those to kink sites (Fig. 7.128), where the distortion is relatively greater.

After having landed on a plane, the ion has become a surface adion that still has some charge<sup>91</sup> and therefore some molecules of hydration water associated with it. It has less than the full ionic charge  $ze_0$  of an ion in solution; hence, it must have less than the number of water molecules that hydrate an ion in solution. But the adion has quite a few things to accomplish before it can get incorporated into the metal lattice. It must move on the surface to a step, where it loses one more water molecule, and then move along the step to a kink site (another water molecule lost, Fig. 7.130). A similar process continues. Further, hydration water molecules are replaced by coordinating metal atoms until finally the series of actions ends when this ion, now with “zero” charge, gets embedded in the lattice. The ion is now like any other metal “atom” in the lattice. The deposition process has ended.

How does the ion move on the surface? It cannot drift under an electric field because the field at an interface is normal to the electrode surface (Fig. 7.131) and what is under discussion here is motion parallel to the surface plane. The movements are by a random-walk diffusion process in two dimensions, surface diffusion.

<sup>91</sup>This suggestion of partial charge transfer originated from calculations that gave rise to this statement.



**Fig. 7.127.** Hole vacancy upon a crystal lattice plane.

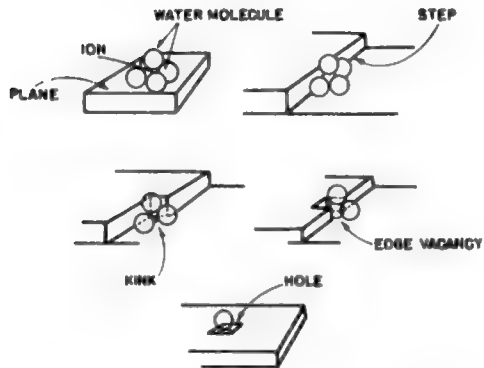


**Fig. 7.128.** Representation of the progressive dehydration of a hydrated ion as its site changes from surface to step to kink to edge vacancy to hole.

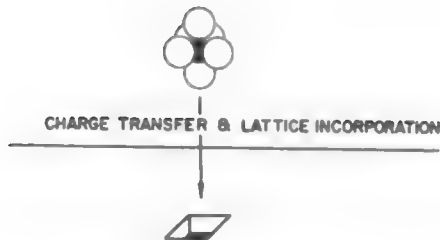


**Fig. 7.129.** Representation of the direct transfer of a hydrated ion to a hole site upon a crystal lattice plane.

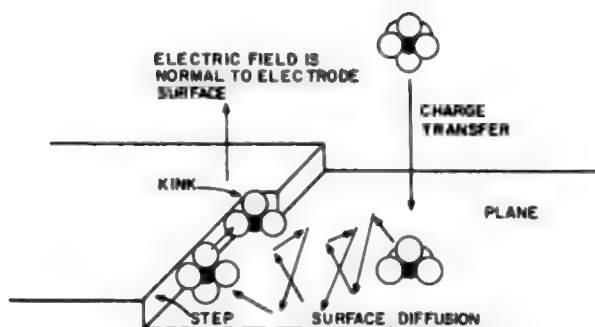


**Fig. 7.130.** Consecutive stages involved in the incorporation of an ion at a kink site.

So, what one is talking about here are the events that take place in getting a hydrated ion out of the solution and into the metal lattice. Initially, charge transfer occurs and an adion is formed; then several phenomena follow—the zig-zag walk across a planar surface (surface diffusion), the “collision” with a step, and a gradual surrendering by the ion of its remaining water molecules as it surrounds itself with other metal atoms. In short, electrodeposition is a multistep reaction of charge transfer followed by surface diffusion to steps (Fig. 7.130), transfer from plane sites to step sites, then diffusion along the step to a kink site (Fig. 7.132), and finally lattice incorporation. Figure 7.133 shows the arrival of several ions at surface sites and the consecutive steps involved in the advance of a step by lattice building.

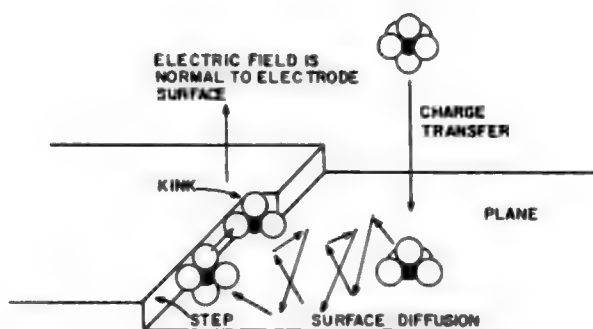


**Fig. 7.131.** Since the surface adion is unaffected by the electric field normal to the electrode surface, in order to reach the step site, the adion diffuses in a random-walk manner.

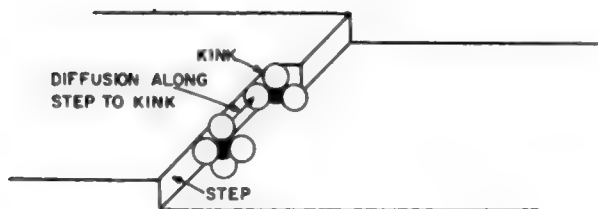


**Fig. 7.132.** Following surface diffusion to a step site, the adion diffuses along the step to a kink site and to final lattice incorporation.

#### 7.12.4. The Half-Crystal Position

The half-crystal position is the same as the position called a “kink” site, and is shown in Fig. 7.134. This term is due to Kossel (1927) and Stranski (1928). The half-crystal position occurs in the way shown in Fig. 7.134. The energy of binding of an atom in the kink position is just half of the total energy of an atom in the bulk of the crystal.

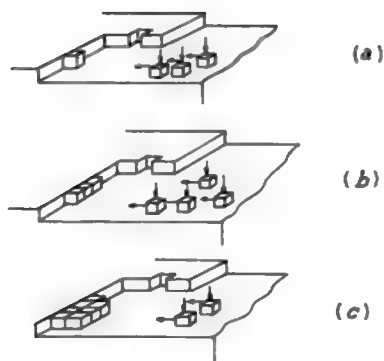


**Fig. 7.133.** Consecutive steps (charge transfer, surface diffusion, and lattice incorporation) involving several ions and showing the advancement of a step by lattice building.

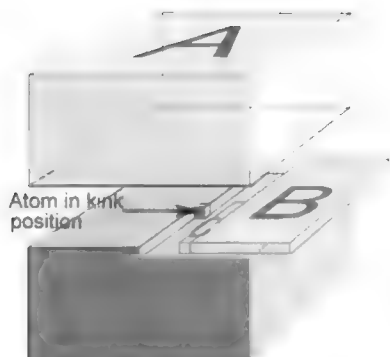


**Fig. 7.134.** The half-crystal (or kink) position. The figure shows the binding energy of an atom in a kink position and how the name “half-crystal position” has been derived. *A* represents the missing part of the bulk crystal above the surface plane, *B* the missing half of the surface plane, and *C* the missing half of the atomic row along the step in front of the kink atom. Together they add the half-crystal to a bulk crystal. (Reprinted from E. Budevski, G. Staikov, and W. J. Lorenz, *Electrochemical Phase Formation and Growth*, 18, copyright © 1996, John Wiley & Sons. Reproduced by permission of John Wiley & Sons, Ltd.)

Kink atoms in electrodeposition have certain characteristics not possessed by other kinds of atoms in building up, or dissolving away, the crystal. Thus, if an atom is removed (dissolved out) from a kink position, the next atom in the row becomes the kink atom. This kink site is regarded as a fundamental stage of the transfer of an atom from a solution to a crystal. It is sometimes called *the growth site* (for cathodic reactions) or the *dissolution site* of the crystal for anodic ones. Thus, dissolving atoms start off at the kink site, either dissolving directly into the solution or diffusing out onto the terrace that surrounds it.

### 7.12.5. Deposition on an Ideal Surface: The Resulting Nucleation

What is assumed in the electrodeposition pathway discussed in the foregoing sections is that one is illustrating the deposition of a metal on the real surface of a metal

of the same atoms as the ion undergoing charge transfer and moving onto the surface. Thus, it concerns the deposition of, say, hydrated  $\text{Ag}^+$  onto a single-crystal plane of silver. However, the single-crystal plane is assumed to have imperfections, as indeed real crystals do. Such irregularities would include edges, often caused by the protrusion into the surface of an emergent screw dislocation.

The discovery of the heterogeneity of surfaces, and in particular of dislocations (see Section 7.12.12), was made in the 1930s (Taylor, 1936), but there had been theoretical work on metal deposition at an earlier time. The model of the surface employed by these earlier workers (Kossel, 1927; Stranski, 1928; Erdey-Gruz, and Volmer, 1931) was a flat plane *without steps and edges* to which the adions produced by ion transfer from the double layer could surface diffuse. The only way a metal could grow on a perfect planar surface without growth sites was by nucleation of the deposited atoms, rather than diffusion to the growth sites shown in Fig. 7.134.

The physical model by means of which one is able to understand the development of the free energy of the growing nucleus involves two energy contributions, the sum of which decide whether it will be stable and grow. The first of these is electrical. If each ion carries a charge of  $z_i e_0$  electrons and the overpotential is  $\eta$ , the *electrical* free energy of cluster formation is  $-z_i e_0 \eta$  per ion. This helps the cluster to form; working against it is the *edge energy* (one is thinking of a 2D atom spread across the surface, and the spreading nucleus is therefore one atom high). One could write:

$$\Delta G = -N z_i e_0 \eta + \Phi(N) \quad (7.249)$$

where  $N$  is the number of atoms in the cluster and  $\Phi(N)$  is the edge energy of the  $N$  adion cluster. Let  $\epsilon$  be the edge energy per unit length and  $P$  the length of the perimeter. Hence, the edge energy is  $\epsilon P$ .

Let the area of one atom be " $s$ ". Hence, the edge area of the cluster is  $Ns$ . If the cluster is circular, its area is  $\pi r_{\text{cluster}}^2$ . Hence,

$$r_{\text{cluster}} = \left( \frac{Ns}{\pi} \right)^{1/2} \quad | \quad P = 2\pi r_{\text{cluster}} = 2\pi \left( \frac{Ns}{\pi} \right)^{1/2} \quad (7.250)$$

Therefore the edge energy =  $\Phi(N) = 2\pi (Ns/\pi)^{1/2} \epsilon = 2\pi^{1/2} \epsilon s^{1/2} N^{1/2}$ .

One puts this expression back in Eq. (7.249) and calculates  $\partial \Delta G / \partial N = 0$ , obtaining (Volmer and Weber (1926):

$$N_{\text{crit}} = \frac{\pi \epsilon^2 s}{(z_i e_0 \eta)^2} \quad (7.251)$$

Then one puts this expression into that for  $\Delta G$  and obtains, for  $\Delta G_{\text{crit}}$

$$\Delta G_{\text{crit}} = \frac{\pi \epsilon^2 s}{z_i e_0 \eta} \quad (7.252)$$

This process of nucleation needs a little more explanation than is given by the above discussion. One can see this if one looks at Fig. 7.135.

The electrical part of the cluster formation energy is negative and always helpful in forming a stable nucleus. The edge energy is a positive contribution to the free energy and tends to make the formation of a cluster more difficult. Thus, the more atoms per cluster, the more positive the energy needed for cluster formation. The diagram shows that (for  $\eta = -10$  mV), the maximum  $\Delta G$  is reached at about 25 atoms. After that, for a higher number in the cluster, the  $\Delta G$  becomes increasingly less positive, and at around 100 atoms finally is numerically negative and hence moves into a region of spontaneous growth as the 2D crystal spreads.

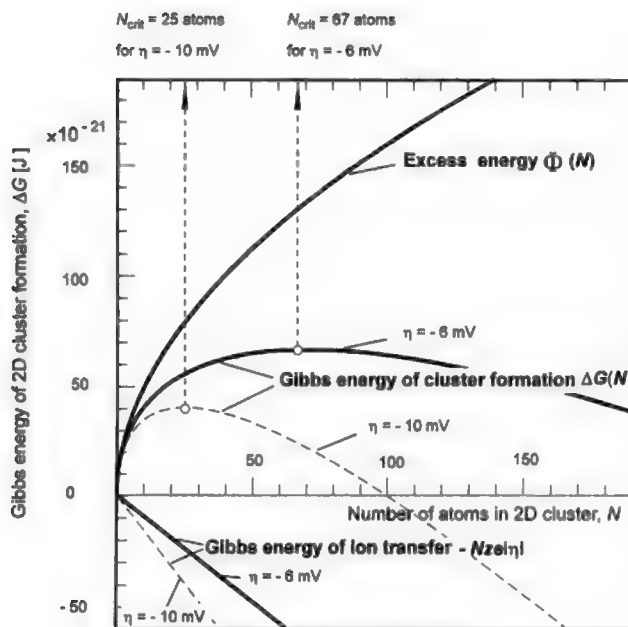


**Fig. 7.135.** Gibbs energy of 2D cluster formation as a function of size  $N$ , with  $\Phi(N) = 2\epsilon(b\Omega N)^{1/2}$ ,  $\epsilon = 2 \times 10^{-13}$  J cm $^{-1}$ ,  $b = 4$  for a square 2D cluster form, and  $\Omega = 4 \times 10^{-16}$  cm $^{-2}$ . The data are taken as most probable values from nucleation rate experiments on an Ag (100) quasi-perfect face. (Reprinted from E. Budevski, G. Staikov, and W. J. Lorenz, *Electrochemical Phase Formation and Growth*, p. 202, copyright © 1996, John Wiley & Sons. Reproduced by permission of John Wiley & Sons, Ltd.)

The question is how do nuclei “make it” to get to the 25 atoms; why do they cling together against a thermodynamic driving force? The quick answer to this is to say: “By means of a fluctuation” (a chance deviation from the expected distribution of energy), but this is not too far off a claim of magic. Fluctuations in molecular events happen, but they happen so rarely that one suspects that in practice, nucleation on a metal surface needs a “nucleating center”—perhaps simply a foreign particle, e.g., an adsorbed anion. A similar problem confronts the explanation of an everyday phenomenon, the condensation of water vapor to liquid rain. One notices that rain falls from dark clouds—those containing the most particles—not from clean white clouds, a hint that nucleation here, too, does not occur by means of a spontaneous fluctuation, but needs a bit of the dust that darkens white clouds.

If real surfaces contain many heterogeneities that act as growth sites, why should one be concerned with formulas for the minimum size of a nucleus that will allow continued growth on a “perfect” site, i.e., one with no growth sites? There are several reasons. On the one hand, it is possible to contrive a surface that is not intersected by screw dislocations, and in practice although such a surface still contains some imperfections, these can be reduced so much that deposition is forced to occur via nucleation and not surface diffusion to growth sites. Further, nucleation will eventually occur on any surface if the overpotential is high enough that surface diffusion to edge sites (as pictured in Fig. 7.133) is insufficient to deal with the avalanche of particles from the solution. Then nucleation will become an additional pathway to crystal growth.

### 7.12.6. Values of the Minimum Nucleus Size Necessary for Continued Growth

As seen from Eq. (7.251), the value of  $N_{\text{crit}}$  depends upon several parameters of the system, e.g., the edge surface energy,  $\epsilon$ . It also depends on the overpotential  $\eta$ , and one can see that the size of the critical cluster decreases with an increase in  $|\eta|$ . For 2D nucleation on quasi-perfect silver single crystals, the number of atoms in the minimum nucleus size at which  $\Delta G$  begins to decrease with an increase in  $N$  varies from 25 to 67 atoms as  $\eta$  varies from  $-10$  to  $-6$  mV.

It is quite difficult to test theories of nucleation—even on specially prepared surfaces—because individual nuclei tend to spread and collide. A novel technique (Fletcher, 1997) involves the use of assemblies of microelectrodes. The nuclei form around them at fixed distances and hence minimize diffusional interactions.

Much smaller values for the minimum number of atoms to form a stable growing crystal are observed for 3D nucleation of various atoms (e.g., Hg, Cu, Pb) on Pt. Here the number of atoms needed for the critical nucleus to ensure that growth continues varies from  $\sim 5$  to 15. If the planar surface of a metal is the catalyst, it is obvious that the fraction of atoms active—the surface ones—is an exceedingly tiny portion of the total number of atoms in the metal used. If, however, one uses small spheres, the fraction of the atoms actually on the surface and hence active in catalysis greatly



increases. One of the best ways to make clusters of about 10 atoms is nucleation in electrodeposition, as discussed in the next section and in Section 7.12.28.

### 7.12.7. Rate of an Electrochemical Reaction Dependent on 2D Nucleation

In interfacial electrochemical reaction rates given by the Butler–Volmer equation (7.24), the current density, or rate of reaction per unit area, is zero at zero overpotential (equilibrium), but significant net currents are observed if the potential of the working electrode is displaced from the reversible potential by only 1 mV. In the case of rate-controlling nucleation, however, there is no detectable current until the overpotential exceeds a few millivolts, after which (at, say, 7 mV), the reaction rate suddenly undergoes an explosive increase.

The physical reason for this is not hard to find and indeed is implied by the formula for the size of the minimum nucleus needed to achieve continued growth. The size of the nucleus gets larger as the overpotential falls. At ~1 mV, the critical nucleus size for silver would be about 400 atoms. As already stated, achieving the critical nucleus needs an antithermodynamic fluctuation, and the frequency of this occurring becomes less likely the larger the number of particles that have to act together in the fluctuation. A similar trend will occur for heterogeneous nucleation triggered by an adion or impurity. Hence, in order to have a *practical* chance of achieving continuous crystal growth by means of 2D nucleation, the overpotential must be several millivolts from equilibrium and the critical nucleus size must be reduced to values less than 100 and perhaps as low as 25. Once the nucleation has started, however, and if nucleation and 2D growth remains the rate-determining step (e.g., is not superseded by surface diffusion to the increasing number of growth sites formed by the nuclei), the current will increase very quickly, as will the size of the growing crystal. This is easily shown mathematically for 2D nuclei. Thus,

$$\text{Rate} = k_1 e^{\frac{-\Delta G_{\text{activation}}}{kT}} \quad (7.253)$$

From Eq. (7.253),

$$\text{Rate} = k_1 e^{-\frac{\pi z e^1}{(z s_e \eta) k T}} \quad (7.254)$$

where  $\eta$  is the numerical value of  $\eta$  (Erdey–Gruz and Volmer, 1931). One can see that, as  $\eta$  becomes numerically greater, the negative exponent falls and the current density increases. The results for an Ag (100) are shown in Fig. 7.136.

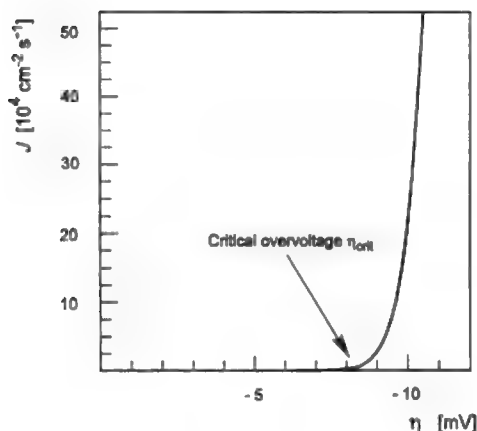


**Fig. 7.136.** Overvoltage dependence of the 2D nucleation rate  $J$  [ $\text{cm}^{-2} \text{s}^{-1}$ ]. Specific edge energy,  $\epsilon = 2 \times 10^{-13} \text{ J cm}^{-1}$ ;  $b = 4$  for a square form;  $T = 318 \text{ K}$ ;  $q_{\text{mon}} = 2 \times 10^{-4} \text{ A s cm}^{-2}$  for a quasi-perfect Ag(100) face and  $A_{2D} = 2 \times 10^{13} \text{ cm}^2 \text{s}^{-1}$ . The data are taken as most probable values from nucleation rate experiments. (Reprinted from E. Budevski, G. Stalkov, and W. J. Lorenz, *Electrochemical Phase Formation and Growth*, p. 203, copyright 1996 John Wiley & Sons. Reproduced by permission of John Wiley & Sons, Ltd.)

### 7.12.8. Surface Diffusion to Growth Sites

The overall process of metal deposition and crystal growth involves several steps. One is the diffusion of ions in the solution to the metal surface. Another is the cathodic deposition step, i.e., the removal of the ion across the interfacial region to land somewhere on a terrace on the metal surface.

Now, just where the ion is most likely to land is a question.<sup>92</sup> There is much structure on the metal surface, but the largest open area for a “landing field” consists of the terraces between steps, as shown in Fig. 7.137. When an ion lands upon a terrace, it at first appears to diffuse aimlessly, but there gradually develops a net movement

<sup>92</sup>Would a deposition directly on a growth site from the solution be preferable? Yes! But there are  $>10^6$  more sites on terraces than growth sites. Although the individual rate constant for a growth site is larger than that for a terrace, most of the ions deposited come to terraces via surface diffusion from planes (Fig. 7.133).

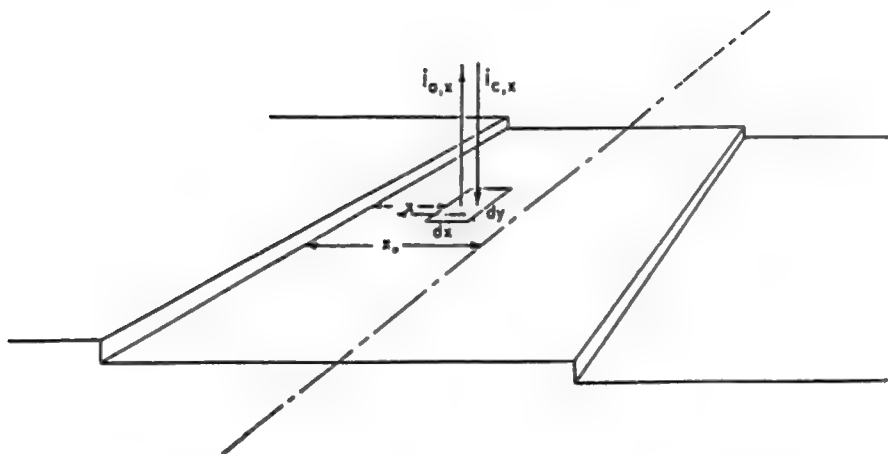


**Fig. 7.137.** The model of the electrode surface. (Reprinted from A. R. Despic and J. O'M. Bockris, *J. Chem. Phys.* **32**: 389, 1960 with the permission of the American Institute of Physics.)

that will follow the direction of the concentration gradient. Sooner or later the diffusing ion will collide with a growth site (likely to be an edge site), and crystal growth will continue from there in a way to be discussed later.

The treatment of this surface diffusion is of interest, among other reasons, because it allows a calculation of the profile of the surface-diffusing adions—where their concentration is greatest and how its rate depends on the dislocation density and other elements of the heterogeneous metal structure.

Despic and Bockris considered an infinitesimal area of the electrode surface (Fig. 7.137). Then:

$$(i_{a,x}/zF) dx dy = (i_{cath,x}/zF) dx dy + D(\partial^2 c_{adion,x}/\partial x^2) dx dy \quad (7.255)$$

where  $i_{a,x}$  is the anodic current density at the surface at a distance  $x$  from the growth line,  $i_{cath,x}$  is the corresponding cathodic current density, and  $c_{adion,x}$  is the adion concentration at  $x$ . Since

$$i_{a,x}/zF = (i_0/zFc_{adion}^0) c_{adion,x} \exp\{[(1-\beta)zF/RT]\eta_a\} = K_{a,\eta} c_{adion,x} \quad (7.256)$$

and

$$i_{cath,x}/zF = (i_0/zF) \exp[-(\beta zF/RT)\eta_a] \quad (7.257)$$

Eq. (7.255) becomes

$$c_{\text{adion},x} - (D/K_{\text{an},\eta})(\partial^2 c_{\text{adion},x}/\partial x^2) = c_{\text{adion}}^{\infty} \quad (7.258)$$

where

$$c_{\text{adion}}^{\infty} = (i_{\text{cath},h}/zFK_{\text{anode},\eta}) = c_{\text{adion}}^0 \exp[-(zF/RT)\eta_a] \quad (7.259)$$

and  $c_{\text{adion}}^{\infty}$  is the adion concentration at a point so distant from the growth line that  $D(\partial^2 c_{\text{adion},x}/\partial x^2) \rightarrow 0$ .

To solve Eq. (7.258), one uses the condition

$$c_{\text{adion},x=0} = c_{\text{adion}}^0 \quad (7.260)$$

corresponding to the assumption that equilibrium remains undisturbed at the growth line, and

$$(dc_{\text{adion},x}/dx)_{x=x_0} = 0 \quad (7.261)$$

Solving Eq. (7.258) with Eqs. (7.260) and (7.261):

$$\begin{aligned} c_{\text{adion},x}/c_{\text{adion}}^0 &= \exp[-(zF/RT)\eta_a] + \frac{1 + \exp[-(zF/RT)\eta_a]}{1 + \exp[-2(i_0/zFv_0)^{1/2}p]} \\ &\times \{ \exp[-2(i_0/zFv_0)^{1/2}p] \exp[(i_0/zFv_0)^{1/2}p(x/x_0)] \\ &+ \exp[-(i_0/zFv_0)^{1/2}p(x/x_0)] \} \end{aligned} \quad (7.262)$$

where

$$p = \exp\{[(1 - \beta)zF/RT]\eta_a\} \quad (7.263)$$

and

$$v_0 = (Dc_{\text{adion}}^0/x_0^2) \quad (7.264)$$

Now,

$$i_x = i_0((c_{\text{adion},x}/c_{\text{adion}}^0) \exp\{[(1 - \beta)zF/RT]\eta_a\} - \exp[-(\beta zF/RT)\eta_a]) \quad (7.265)$$

By introducing Eq. (7.262) into Eq. (7.265), the distributions of adion concentration and current density can be calculated as a function of position,  $x/x_0$ .

The average  $i$  for the electrode surface is obtained by integrating  $i_x$  from  $x = 0$  to  $x = x_0$  and dividing by  $x_0$ . It is

$$i = (i_0 z F v_0)^{1/2} \exp\{[-(1 + \beta)zF/2RT]\eta_a\} \{\exp[(zF/RT)\eta_a] - 1\} \\ \times \frac{1 - \exp[-2(i_0/zFv_0)^{1/2}p]}{1 + \exp[-2(i_0/zFv_0)^{1/2}p]} \quad (7.266)$$

Equation (7.266) can be rewritten as

$$\log y = [(1 + \beta)zF/4.6RT]\eta_a + \log \frac{1 + \exp[-2(i_0/zFv_0)^{1/2}p]}{1 - \exp[-2(i_0/zFv_0)^{1/2}p]} - \log(i_0 z F v_0) \quad (7.267)$$

where

$$y = \{\exp[(zF/RT)\eta_a] - 1\}/i \quad (7.268)$$

When  $(zFv_0/i_0) \rightarrow \infty$ , that is, when the specific rate of the surface diffusion is much faster than that of the transfer reaction, Eq. (7.267) tends to become identical with the Butler–Volmer equation; that is, the current density becomes uniform on the surface. With increasing  $y$  values, the second term of Eq. (7.268) tends toward zero, and the  $y$ – $\eta_a$  relation becomes linear with a slope of  $(1 + \beta)zF/4.6RT$ . It is possible to employ Eq. (7.262) to calculate the concentration profile between the growth sites. Some results are shown in Fig. 7.138.

One can see the cathodic situation as leading at higher overpotential to a surface adion concentration in the middle of terraces so high that 2D nucleation may begin. The current density is by no means uniform. Thus, at high anodic potentials, the midplanes are deserted and adions exist in finite concentrations only near the steps, where the current density is therefore the highest. The actual dissolution current at each point is proportional to the adion concentration there. The treatment outlined above was the first to mathematically describe nonuniform current on a surface in terms of the surface structure. The *mean* adion concentration between growth sites for  $\text{Ag}^+$  deposition onto silver from  $0.1 M \text{AgClO}_4$  is  $\sim 10^{-11} \text{ mol cm}^{-2}$ .

In the results obtained from an analysis of surface diffusion between steps (Fleischmann and Thirsk, 1960; Damjanovic and Bockris, 1963), the model is a simple one. The properties of steps (e.g., their movement and eventual formation of spirals) will be discussed in Section 7.15. Of course, they are not really simple straight edges. Scanning tunneling microscopy has made it possible to obtain images of the steps. A real monatomic step is shown in Fig. 7.139 and is seen to be quite frazzled.

### 7.12.9. Residence Time

At equilibrium, the time of existence of an adion,  $\tau$ , can be calculated by using an equation easily derived from (7.12), i.e.,

$$i_0 = k_{\text{equil}} z F c_{0,\text{adion}} \quad (7.269)$$

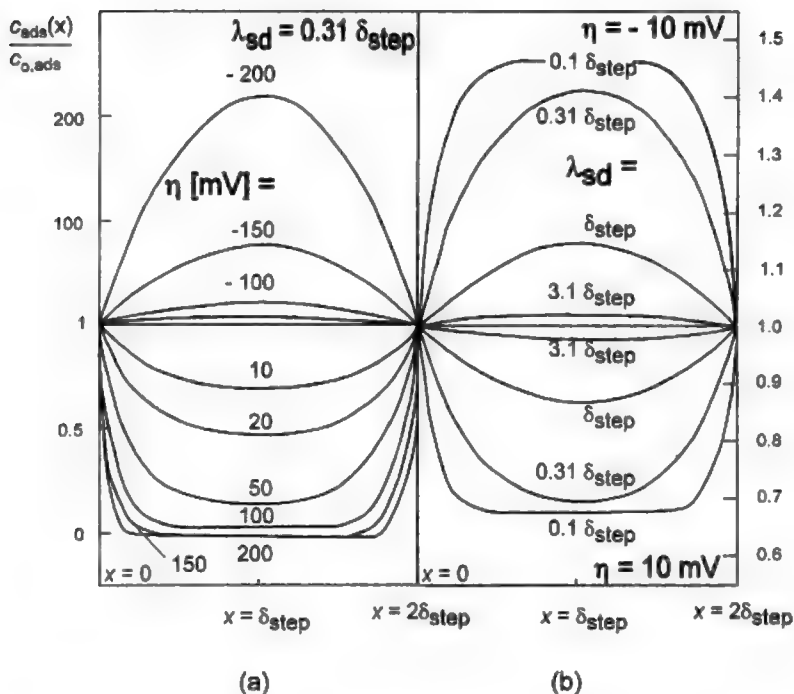


**Fig. 7.138.** Adatom concentration profiles,  $c_{ads}(x)/c_{0,ads}$ , between two steps of growth. (a): for different cathodic (upper part of the plot) and anodic (lower part of the plot) overpotentials at  $\lambda_{sd} = 0.31 \delta_{step}$ . (b): For different surface diffusion (sd) rates  $0.1 \delta_{step} < \lambda_{sd} < 3.1 \delta_{step}$  at 10 mV cathodic and anodic overpotentials;  $\lambda$  is the average distance to the growth site at a fraction of the distance between growth sites. (Reprinted from E. Budevski, G. Staikov, and W. J. Lorenz, *Electrochemical Phase Formation and Growth*, p. 33, copyright © 1996, John Wiley & Sons. Reproduced by permission of John Wiley & Sons, Ltd.)

As  $\tau = 1/k$ , where  $k$  is a rate constant:

$$\tau_{equil} = zF/i_0 c_{0,adion} \quad (7.270)$$

When the overpotential becomes increasingly negative, the residence time of the intermediate adion concentration decreases according to:

$$\tau = zF \frac{c_{0,adions}}{i_0} e^{+\alpha F \eta / RT} \quad (7.271)$$

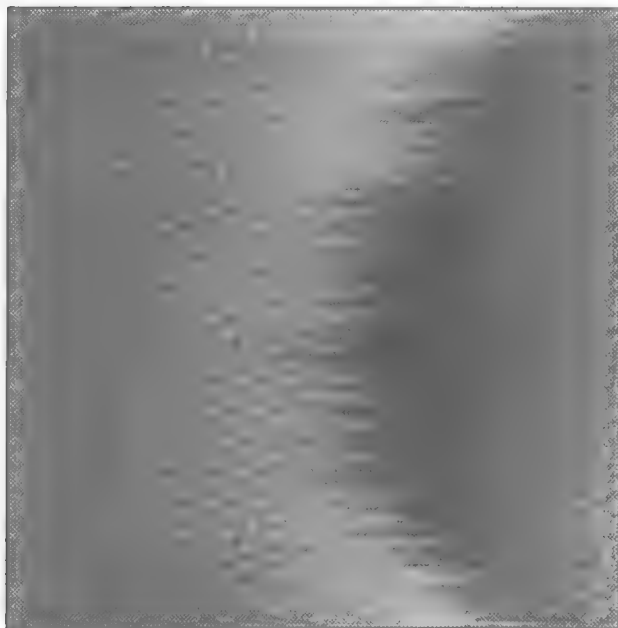


**Fig. 7.139.** *In situ* STM image showing the frazzled appearance of a monatomic step on Ag(111) substrate. System Ag(111)/ $10^{-4}$  M CuSO<sub>4</sub> +  $5 \times 10^{-2}$  M H<sub>2</sub>SO<sub>4</sub> at  $E = 60$  mV vs. SCE and  $T = 298$  K. (Reprinted from E. Budevski, G. Staikov, and W. J. Lorenz, *Electrochemical Phase Formation and Growth*, p. 22, copyright © 1996 John Wiley & Sons. Reproduced by permission of John Wiley & Sons, Ltd.

These expressions are mean values for the whole surface. It was stressed in the last section that in actuality, the adion concentration varies with position; so, therefore, does  $\tau$ .

#### 7.12.10. The Random Thermal Displacement

The Einstein–Smoluchowski equation, derived in Appendix 4.1, relates the mean thermal displacement,  $\lambda$ , to the diffusion coefficient and mean lifetime. For a surface:

$$\lambda^2 = D\tau \quad (7.272)$$

Thus from (7.272),

$$\lambda^2 = D_{\text{surf}} \frac{zF}{i_0} c_{0,\text{adion}} e^{+\alpha F \eta / RT} \quad (7.273)$$

### 7.12.11. Underpotential Deposition

**7.12.11.1. Introduction.** Deposition from a solution of  $M^{z+}$  upon a substrate of the corresponding metal,  $M$  (e.g.,  $Ag^+$  on  $Ag$ ), begins at the thermodynamically reversible potential, at least on surfaces possessing growth sites. However, if one attempts to deposit  $M^{z+}$  on  $S$ , a substrate differing from  $M$  (e.g.,  $Ag^+$  on  $Au$ ), some kind of layer formation on the  $S$  surface begins to occur when it is held at a potential many hundreds of millivolts positive to the reversible potential for  $M^{z+}$  onto  $M$ .<sup>93</sup> The meaning of these statements can be immediately understood by contemplation of Fig. 7.140.

The zero on the potential axis of this figure is the reversible potential for  $Pb^{2+}$  in solution in equilibrium with solid lead. For the experiment portrayed in the figure,  $Pb^{2+}$  is being deposited not on lead but on the 111 plane of silver. One can see (Fig. 7.140) that as the electrode potential is moved in the negative direction, a large electric current suddenly appears at exactly 137 mV positive to the reversible potential of  $Pb^{2+}$  on  $Pb$  (marked as zero). The peak of the current is very narrow and at about 100 mV positive to zero on the figure, the events that caused this peak (a predeposition of  $Pb^{2+}$  onto  $Ag$ ) have died down. Going the other way—anodically dissolving  $Pb$  from an  $Ag$  surface—one sees a parallel peak near 150 mV. A peak also appears at a potential that might be expected if the system were indeed the deposition of  $Pb^{2+}$  onto  $Pb$ , but it seems to be less marked than the “anomalous” peaks described. Normally, for  $M^{z+}$  on  $M$ , deposition will occur at any potential, as long as it is *negative* to the thermodynamically reversible potential. When deposition occurs at a potential *positive* to the thermodynamically reversible potential for  $M^{z+}$  on  $M$ , it is logically called *underpotential deposition* (UPD) (Mills and Willis, 1953). Advances in the study of UPD have been made particularly since the introduction of STM and AFM techniques, which allow direct study of the layers formed.

**7.12.11.2. Some Examples.** Table 7.20 shows values of  $\Delta E$ , the value at which deposition of  $M^+$  on  $S$  begins, relative to the  $M^+$  on  $M$  reversible potential values are given for a number of UPD cases. It can even exceed 1 V in some cases.

One of the reasons that the full study of UPD was delayed until the mid-1970s (Lorenz, 1973) is that it is much more sharply seen on well-defined single-crystal planes than on polycrystals. There was widespread use of single crystals in metal deposition work in the 1970s. This is exemplified in Fig. 7.141, which shows the less sharp peaks for  $Pb^{2+}$  depositing on polycrystalline silver. In contrast are the corresponding phenomena for  $Pb^{2+}$  depositing on  $Ag$  (111) in Fig. 7.142.

<sup>93</sup>This is equivalent to the statement that the deposition started to take place “too soon,” i.e., from a thermodynamic viewpoint, before it was expected to occur.



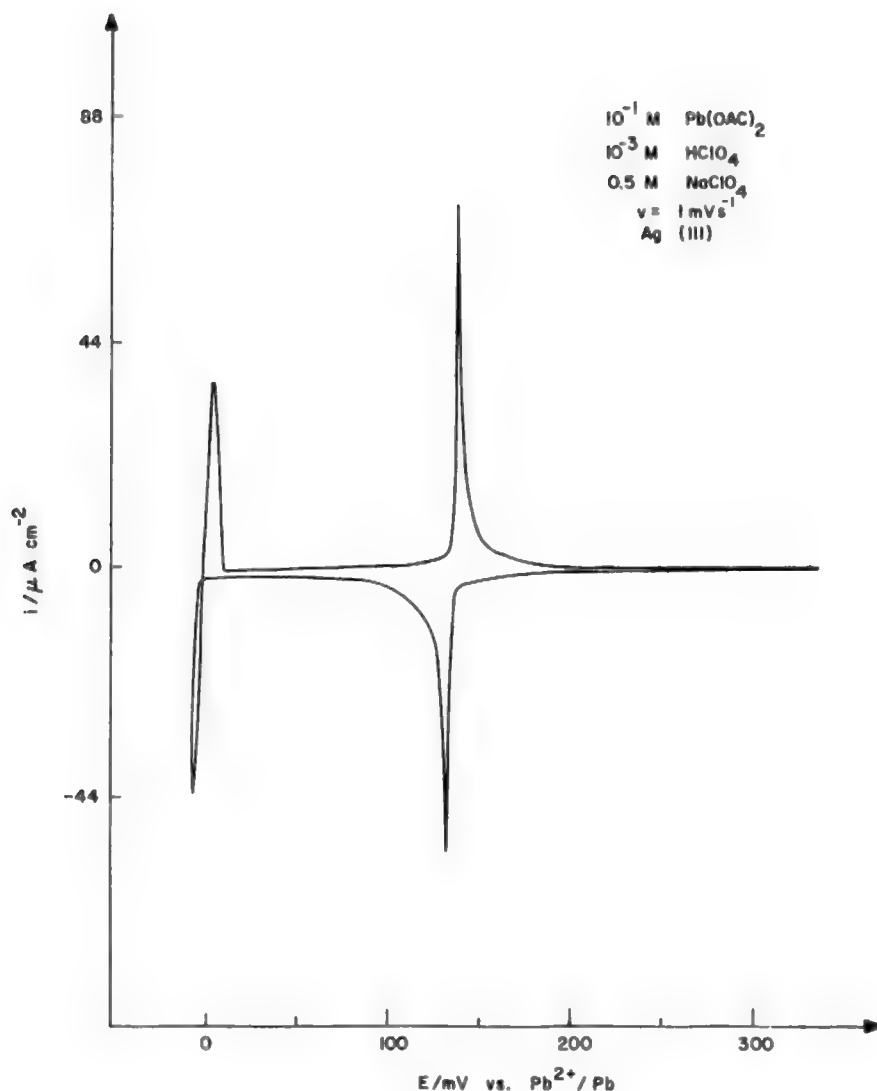


**Fig. 7.140.** Experimentally recorded potential sweep voltammogram for the (111) plane of a silver single crystal in the solution noted in the figure. (Reprinted from A. R. Despic, "Deposition and Dissolution of Metals and Alloys. Part B: Mechanisms, Kinetics, Texture, and Morphology," in *Comprehensive Treatise of Electrochemistry*, Vol. 7, B. E. Conway, J. O'M. Bockris, E. Yeager, S. U. M. Khan, and R. E. White, eds., Plenum, 1983, p. 459.)

**TABLE 7.20**  
**Exchange-Current Densities and the Total Deposition Overpotentials When**  
 **$i = 10^{-2}$  amp cm $^{-2}$  for Copper on Copper Single Crystals**

Crystal face	$i_0$ , amp cm $^{-2}$	Deposition overpotential [mV] when $i = 10^{-2}$ amp cm $^{-2}$
(110)	$2 \times 10^{-3}$	-85
(100)	$10^{-3}$	-125
(111)	$4 \times 10^{-4}$	-185

Some of the basic experiments with UPD have been carried out with Ag onto Au (hkl).<sup>94</sup> This is because the radii of Ag and Au atoms are almost the same, so that the interpretation does not have to involve a steric displacement effect. Figure 7.143 shows the underpotential deposition of Ag on Au (100). The A and D marks on the figure denote a number of underpotential processes. Using STM to study this system indicates that at  $\Delta E > 650$  mV, a stable Ag surface is formed with normal interatomic distance. Between  $200 < \Delta E < 550$  mV, stable domains exist, but now (see Fig. 7.144) they are expanded in respect to their interatomic distance and in comparison with those formed at  $\Delta E > 650$ .

**7.12.11.3. What Are the Causes of Underpotential Deposition?** A physical picture of UPD is fairly easy to grasp. When one thinks of the deposition of a metal on its self, one can comprehend the idea that the energy controlling the potential for deposition is related to its energy of sublimation of the substrate, for this must depend on the sum of the M–M energies, energy of formation of the lattice. However, when  $M^+$  deposits on S, then at least for the first layer (and maybe to a lesser extent for the second and the third), it is the interaction of M with S that counts.<sup>95</sup> If that is greater than the M–M interaction energy, some degree of discharge (hence an electric current)

<sup>94</sup>Au (hkl) indicates a gold single crystal with the face (h,k,l) exposed to the solution. The letters refer to the Miller indices, e.g., 100 or 111, etc.

<sup>95</sup>The calculations referred to here in terms of bond energies are quite approximate and for a clearly explicable reason. The relation of an electrochemical cell potential,  $E$ , to “energy” is via the free energy,  $\Delta G$ . Thus,  $\Delta G = -nFE$  is a well-known equation derived in physicochemical texts. Further,  $\Delta G = \Delta H - T\Delta S$  where  $\Delta S$  is the change in entropy for the electrode process concerned. Hence, in discussing underpotential deposition in terms of bonding only, we are using the incorrect equation  $-nFE = \Delta H$ . The error involved is often not more than 10% at 25°C. In deposition from 1000°C molten salts, it could be a very significant, 30%. A solution to the problem is the calculation of the  $\Delta S$  via a (soon to be available) computer program.

will pass before the regular deposition potential for M on M. This of course is only a qualitative idea, but it does explain why UPD occurs for some systems and not for others. Thus, it may be that the strength of the M–M interaction is greater than that of the M–S—then no UPD will occur.

One quantitative relation has been suggested. It relates  $\Delta E$  (the displacement potential from the  $M^+-M$  potential at which one sees a UPD peak), to  $\Delta\Phi$ , the difference of the work functions of the depositing ion  $M^{z+}$  and S. In fact (Kolb, 1978), empirically:

$$\Delta E = 0.5 \Delta\Phi$$

The relation is illustrated in Fig. 7.145. It is not well rationalized, but at least one can appreciate that deposition involves electron transfer and that electron escape from M and/or S depends upon the work function thereof.

The kinetics by which UPD layers form are qualitatively the processes already discussed. There are the electron transfer kinetics from the metal substrate to the depositing ion and the surface diffusion of the adions formed to edge sites on terraces. Complications occur, however, for there is the adsorption of ions to take care of and that brings up questions of which isotherm to use (Section 6.8). Three kinds of UPD formations are shown in Fig. 7.146. Thus Fig. 7.146 (c) shows 1D phase formation along a monatomic step in the terraces on the single crystal; Fig. 7.146 (b) shows 2D nucleation at a step, and Fig. 7.146 (a) shows 2D nucleation on an atomically flat plane.

Finally, one has to distinguish between underpotential deposition of M on S and alloy formation. Alloys can be formed electrochemically (Brenner, 1942). Underpotential deposition is usually a monatomic step affair. With the alloy, the foreign atoms go on building up until they form part of the new substrate, the alloy.

### 7.12.12. Some Devices for Building Lattices from Adions: Screw Dislocations and Spiral Growths

The steps by which ions from solution are incorporated into the lattice have been described. The next question is obvious. What happens when many ions travel the deposition path, i.e., the path of charge transfer to a plane, surface diffusion to steps, then movement to kinks, and finally lattice incorporation?

As more and more adions join a step, it advances. Electrogrowth is occurring. The more adions incorporated into a step, the farther it advances, but also the closer it comes to the edge of the electrode and, eventually, a stage must come when there is no step on the surface. The step has disappeared (Fig. 7.147). But, according to the deposition mechanism sketched in Section 7.12.3, the existence of steps is a necessary condition. Without steps, the adion concentration on the plane builds up,  $\theta$  increases and makes

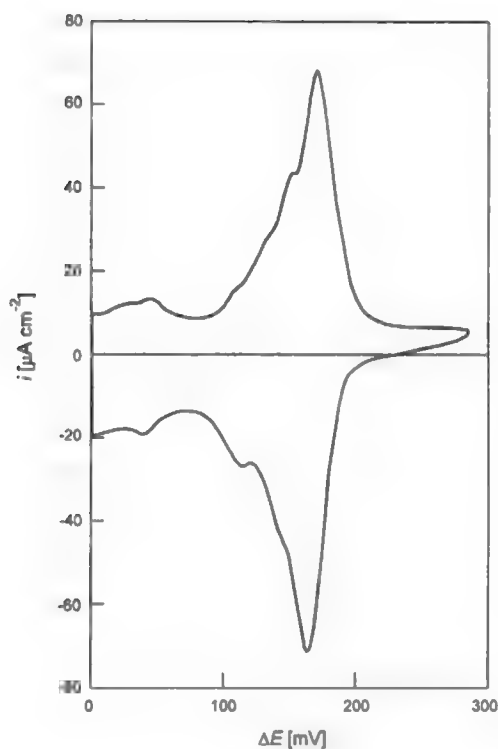


**Fig. 7.141.** Cyclic voltammogram (semi-infinite-linear diffusion conditions) in the system  $\text{Ag}(\text{poly})/5 \times 10^{-2} \text{ M Pb}(\text{ClO}_4)_2 + 5 \times 10^{-1} \text{ M NaClO}_4 + 5 \times 10^{-3} \text{ M HClO}_4$  with  $|dE/dt| = 10 \text{ mV s}^{-1}$  at  $T = 298 \text{ K}$ . (Reprinted from E. Budevski, G. Staikov, and W. J. Lorenz, *Electrochemical Phase Formation and Growth*, p. 49, copyright © 1996 John Wiley & Sons. Reproduced by permission of John Wiley & Sons, Ltd.)

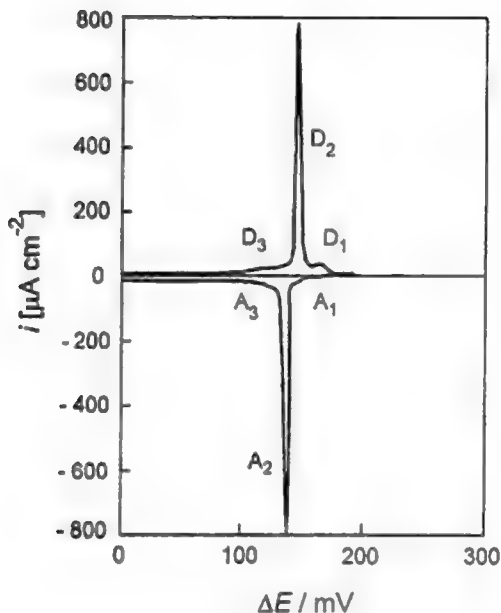


**Fig. 7.142.** Cyclic voltammograms (semi-infinite-linear diffusion conditions) in the system  $\text{Ag}(111)/5 \times 10^{-2} \text{ M Pb}(\text{ClO}_4)_2 + 5 \times 10^{-1} \text{ M NaClO}_4 + 5 \times 10^{-3} \text{ M HClO}_4$  with  $ldE/dt = 10 \text{ mV s}^{-1}$  at  $T = 298 \text{ K}$ .  $A_n$  and  $D_n$  with  $n = 1, 2, 3$  denote cathodic adsorption and anodic desorption peaks, respectively. (Reprinted from E. Budevski, G. Staikov, and W. J. Lorenz, *Electrochemical Phase Formation and Growth*, p. 48, copyright © 1996 John Wiley & Sons. Reproduced by permission of John Wiley & Sons, Ltd.)

it more and more difficult for charge transfer to occur (remember that electronation requires a bare surface), and thus further deposition should stop.

In practice, however, the deposition current just keeps flowing on and electro-growth does not cease. Nature seems to have some trick up her sleeve by which the surface of a crystal is perpetually provided with steps. What is this device?

It turns out to be simple. Nature rarely works with crystals as ideal as the ones considered in Section 7.12.3. Crystals are grown, e.g., from a melt, and in the general rush of crystallization, the majority of crystals grow with built-in defects and imperfections in the way in which their atoms are arranged. It is one type of these imperfections that contains the secret of nonvanishing, self-perpetuating steps. The

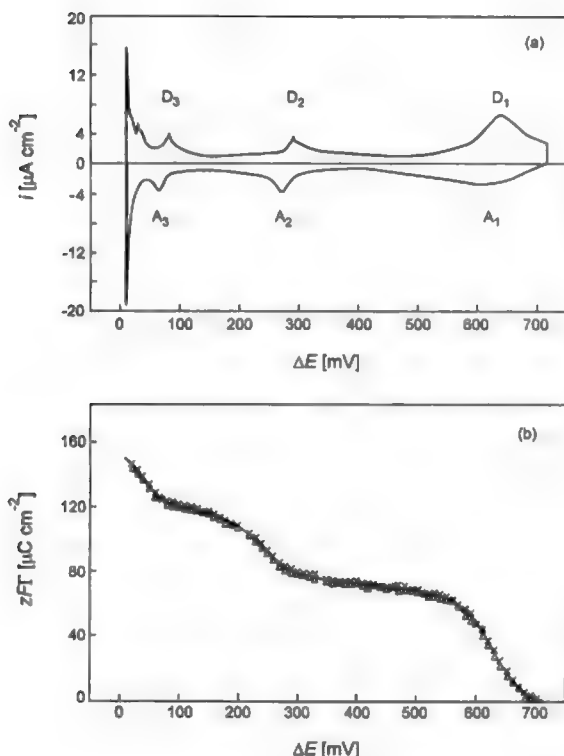


**Fig. 7.143.** Cyclic voltammogram (a) measured under semi-infinite-linear diffusion conditions with  $|\text{d}E/\text{d}t| = 7 \text{ mV s}^{-1}$  in the system  $\text{Au}(100)/5 \times 10^{-3} \text{ M AgSO}_4 + 5 \times 10^{-1} \text{ M H}_2\text{SO}_4$ , and  $\Gamma(E)$  isotherm (b), in the system  $\text{Au}(100)/4.2 \times 10^{-4} \text{ M Ag}_2\text{SO}_4 + 5 \times 10^{-1} \text{ M H}_2\text{SO}_4$  at  $T = 298 \text{ K}$ .  $A_n$  and  $D_n$  with  $n = 1, 2, 3$  denote cathodic adsorption and anodic desorption peaks, respectively. (Reprinted from E. Budevski, G. Staikov, and W. J. Lorenz, *Electrochemical Phase Formation and Growth*, p. 78, copyright © 1996 John Wiley & Sons. Reproduced by permission of John Wiley & Sons, Ltd.)

mechanism by which this type of defect arises has yet to be understood in its details and complications, so what will be done here is to describe a model of a crystal with a defect that is both nonvanishing and self-perpetuating.

Imagine that a perfect crystal is cut, not right through, but only up to a point, and then the part of the crystal on one side of the cut is pushed up or down through one

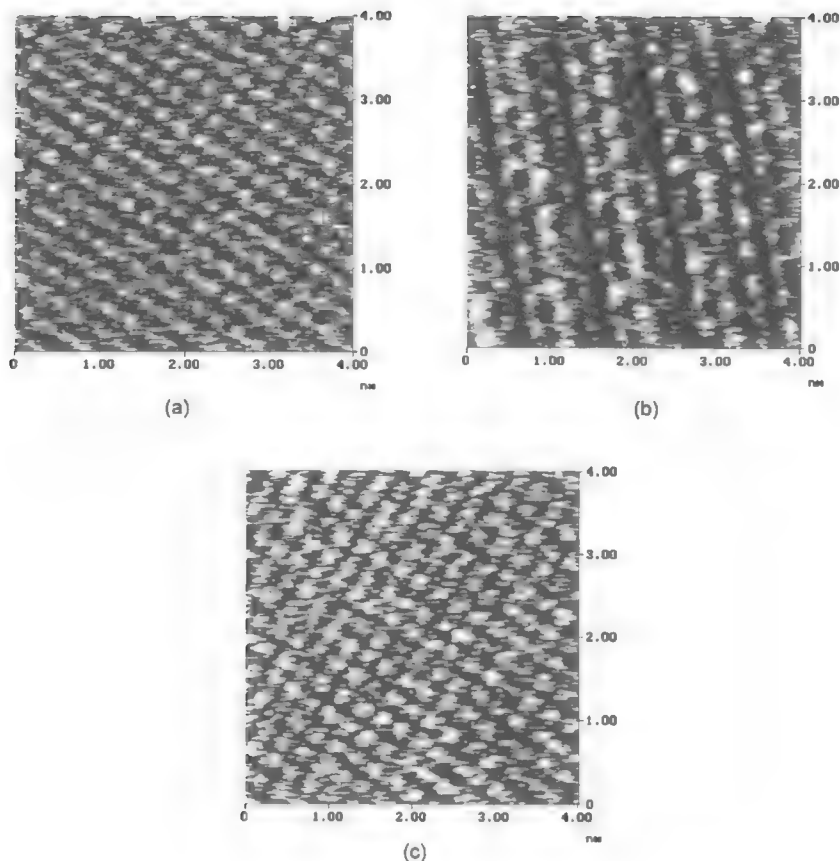


**Fig. 7.144.** *In situ* STM images in the system:  $\text{Au}(100)/5 \times 10^{-3} \text{ M Ag}_2\text{SO}_4 + 10^{-1} \text{ M H}_2\text{SO}_4$  at  $T = 298 \text{ K}$ ,  $\Delta E = 400 \text{ mV}$ ,  $I_T = 3 \text{ nA}$ . (Reprinted from E. Budevski, G. Staikov, and W. J. Lorenz, *Electrochemical Phase Formation and Growth*, p. 79, copyright © 1996 John Wiley & Sons. Reproduced by permission of John Wiley & Sons, Ltd.)

interatomic distance relative to the part of the crystal on the other side of the cut. This is shown in Fig. 7.148. A *dislocation* has been produced in the once-perfect crystal.

The mismatch of atomic layers (arising from the process that formed the single crystal) has made a ledge emerge on the surface. The defect has been advertised on the surface. But think of the atomic layers beneath the surface. The mismatch penetrates (Fig. 7.149) right through the crystal; remember that one whole side of the crystal has been pushed up relative to the other side. A view from above the surface looking down the axis, shown in Fig. 7.149, resembles what one would see if one

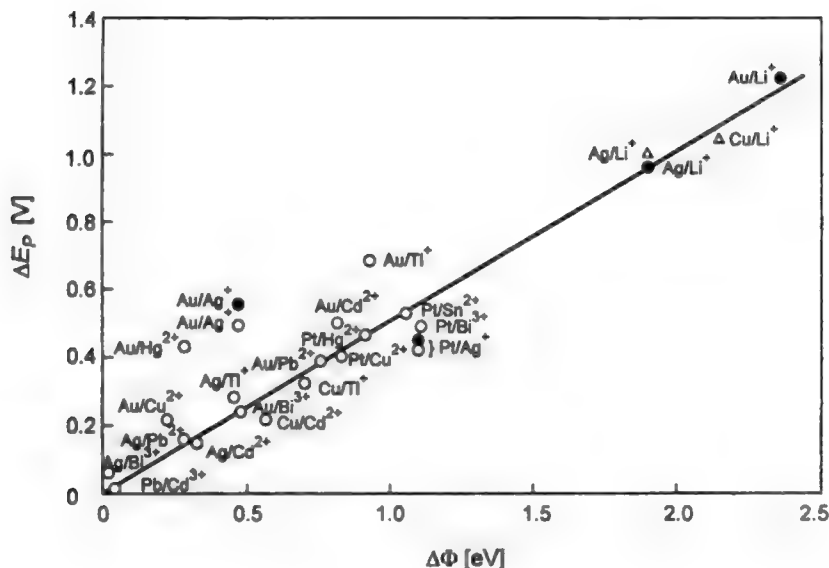


**Fig. 7.145.** Underpotential shift  $\Delta E_p$ , in different  $S(\text{poly})/\text{Me}^{z+}$  systems as a function of the difference of electron work functions of polycrystalline  $S$  and  $\text{Me}$ ,  $\Delta\Phi = \Phi_S - \Phi_{\text{Me}}$ . (Reprinted from E. Budevski, G. Staikov, and W. J. Lorenz, *Electrochemical Phase Formation and Growth*, p. 50, copyright © 1996 John Wiley & Sons. Reproduced by permission of John Wiley & Sons, Ltd.)

looked down upon a spiral staircase from above, but the staircase is spiraling all the way down.

The most important point about the type of defect described above is that it gives rise to a step on the crystal surface. Now consider what happens if adions keep adding on to the step. In the first instance, think about the addition of a whole row of adions starting from the point  $X$  where the step originates at the surface and ending at the edge  $M$  (Fig. 7.150). What is the result of the addition of this row? Has the step disappeared? No. The point  $X$  is still anchored to the same axis normal to the surface, but the step,  $XM'$ , is at an angle to its former position  $XM$  (Fig. 7.150),

Further, however many uniform rows of adions are added to the surface, the step still remains on the crystal surface; all that happens is that its orientation to the surface changes. When the orientation of the step changes by one complete revolution (i.e., an angle of  $2\pi$  radians), the crystal has added on a new layer of atoms in its growth upward. Thus, as the crystal grows, the step rotates about the axis at  $X$  going through the crystal; it winds like a screw (Fig. 7.151), which is why the type of defect has been described by Frank as a *screw dislocation*.



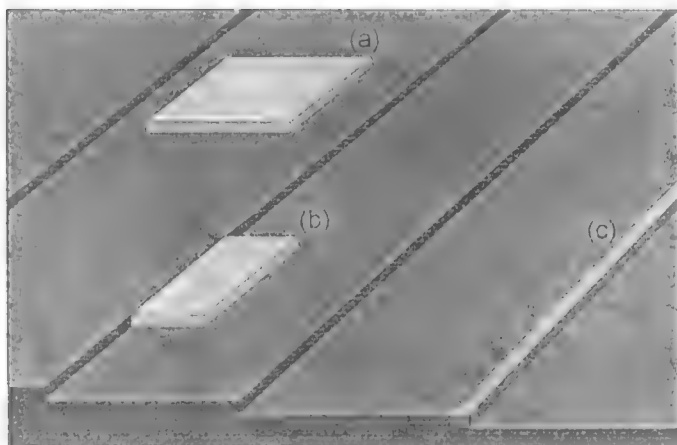


**Fig. 7.146.** Formation of 2D and 1D  $\text{Me}_{\text{ads}}$  phases on stepped foreign substrates. (a) 2D nucleation on atomically flat terraces. (b) 2D nucleation at monatomic steps. (c) 1D  $\text{Me}_{\text{ads}}$  phase formation along monatomic steps at  $\Delta E > \Delta E^*$  for  $\Psi\text{Me}_{\text{ads-ads}}$ . (Reprinted from E. Budevski, G. Staikov, and W. J. Lorenz, *Electrochemical Phase Formation and Growth*, p. 116, copyright © 1996 John Wiley & Sons. Reproduced by permission of John Wiley & Sons, Ltd.)

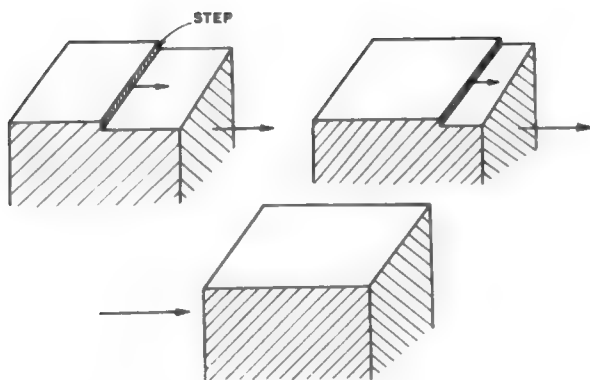


**Fig. 7.147.** Growth step advancement by lattice building until the electrode edge is reached, where the step disappears.

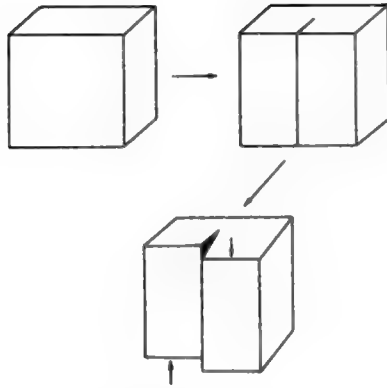


**Fig. 7.148.** Representation of a crystal lattice dislocation. The left half of the crystal has been pushed up, while the right half has been pushed down.

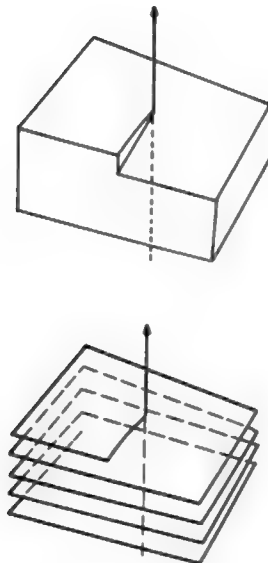


**Fig. 7.149.** A block and atomic-layer representation of a lattice dislocation illustrating the spiral of atomic layers.

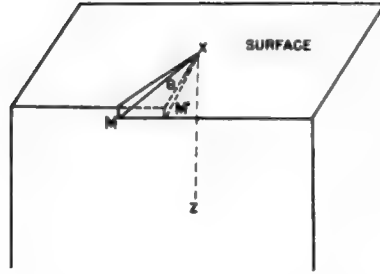


**Fig. 7.150.** The initial stage in the formation of a screw dislocation; the addition of adions to edge  $XM$  moves the step to position  $XM'$ .

What happens, however, if adions do not add on in complete rows all along the step from the screw dislocation axis to the edge of the crystal? Suppose that they add on only up to a fraction  $XY$  of the step length  $XM$  (Fig. 7.152). Then, if this happens several times, another small step  $PQ$  has formed on the surface. This new step, too, can be the recipient of adions, and it can advance. If this process goes on, one obtains an interesting sort of growth. In plan, the growth looks like a spiral; and, in elevation, like a mountain that has been terraced (Fig. 7.153). This is known as a *microspiral* growth.

### 7.12.13. Microsteps and Macrosteps

The steps that have been described so far are microsteps. They are one atomic layer in height and therefore too small to be seen in an optical microscope. But sometimes steps *are* clearly visible in an ordinary optical microscope (Fig. 7.154). Such steps must therefore have a height on the order of a wavelength of light, several thousand angstroms. These are known as *macrosteps*. How do they form?

Numerous reasons for the formation of macrosteps have been suggested, including those by Frank and by Cabrera and Vermilyea. It was considered that the velocity of a microstep was dependent upon two factors, the proximity of the microsteps to



**Fig. 7.151.** Screw-thread spiral analogy to a screw dislocation.

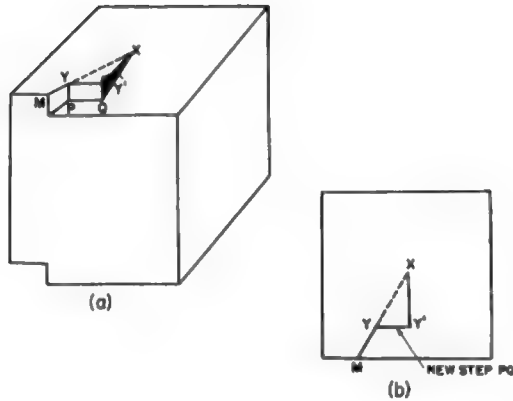


**Fig. 7.152.** An incomplete step  $XM$  movement; lattice building occurring only at  $XY$ , the first stage in the formation of a terraced microspiral growth.

each other—the closer the steps, the more slowly they move since the flux corresponding to a given current density is distributed among *all* steps—and the presence of adsorbed impurities. Ideally, one can consider what will happen when one microstep stops advancing, although the result of this (i.e., microstep bunching) does not depend upon the microstep's coming to a complete halt, but only on the fact that its rate of advance has become slightly less than the steps following it.

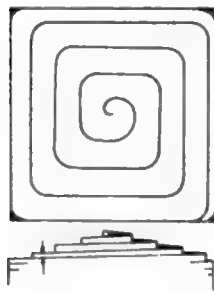


**Fig. 7.153.** Plan and elevation of a microspiral growth. The arrows indicate the thickness of one atomic layer.

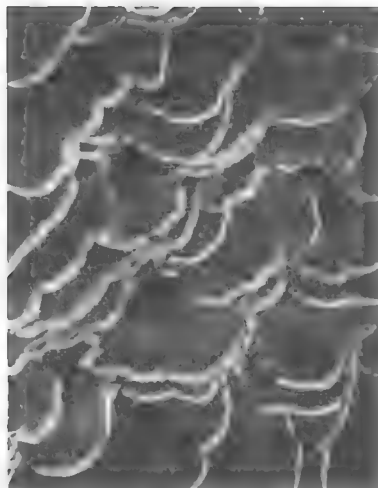


**Fig. 7.154.** Layer type of growth for copper deposition showing macrosteps with irregular edges.

Let it be supposed then that an advancing microstep suddenly stops advancing. The movement may cease, e.g., owing to the adsorption of impurities from solution at the step. On a solid surface with its hierarchy of sites, there will be a hierarchy of free energies of adsorption (see Section 7.7), and it may happen that impurities seek adsorption at steps in preference to adsorption on flat planes.

So think of a microstep which, for a reason such as that given above, has stopped advancing somewhere within the boundary of the crystal (Fig. 7.155). Now imagine that a layer B of atoms is growing on top of layer A. Step B will keep advancing until it comes to the point where the advance of step A is blocked. Layer B will then act as though it has reached the edge of the crystal. If the same process is repeated with another layer C on top of B, and another layer on C, and so on, then there is a pileup of layer upon layer. Microsteps bunch into macrosteps. Sometimes the pileup reaches such proportions that it can be seen in a microscope as a macrostep.

The development of the macrostep through the bunching of microsteps has been described. Now suppose that this bunching mechanism occurs at all the steps of a microspiral. Then, instead of the difference in height between the steps of a microspiral's being one atomic layer (see 7.153), it will be of the same order as in a macrostep, i.e., several thousand angstroms. In short, the result is a macrospiral growth that is clearly visible in a microscope. The observation of macrospiral growths is a clear verification of the role of screw dislocations in sustaining crystal growth.

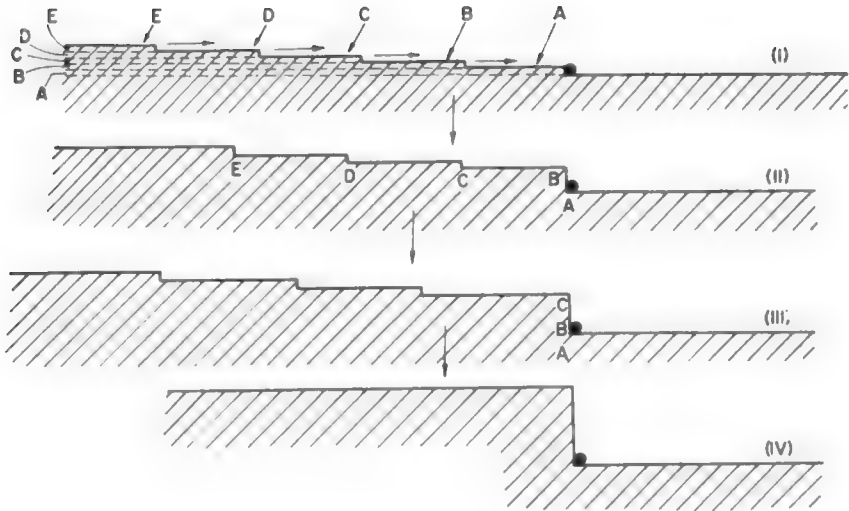


**Fig. 7.155.** Representation of the four successive stages in the formation of a macrostep by microstep bunching.

#### 7.12.14. How Steps from a Pair of Screw Dislocations Interact

It must not be imagined that a single-crystal surface is allotted only one isolated screw dislocation and therefore there will be only one growth spiral. Except in the case of special kinds of very thin rodlike crystals called *whiskers*, even so-called “perfect” single crystals are richly endowed with screw dislocations. Now each screw dislocation generates a rotating step that can in principle span the whole surface. If, therefore, there is more than one screw dislocation, there will be an interaction of the steps generated from each dislocation. In other words, the step rotating from one screw dislocation can collide with the step rotating from another screw dislocation. What happens when these steps collide?

This problem will be side-stepped for a moment, and a simpler one tackled. Consider two steps that are parallel to each other, the type of steps considered in the analysis of the constant-current transient. As ions transfer across the electrified interface and the adions thus formed surface diffuse and become incorporated in the steps, there is an advance of the steps toward each other (Fig. 7.156). Eventually the two steps approach each other, some closely, so that all one is left with is a one-atom-wide and one-atom-deep chasm. The moment this is filled in, the two steps disappear. The collision of the two steps moving toward each other has resulted in their mutual annihilation.

Now back to the original problem. How can the steps emanating from two screw dislocations move toward each other? One way is for the steps to rotate in opposite

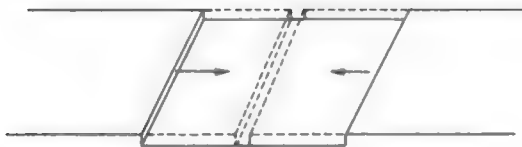


**Fig. 7.156.** The movement of two parallel growth steps toward each other, resulting in their mutual annihilation.

directions. This will happen if one screw dislocation is right-handed and the other is left-handed (Fig. 7.157); they bear the same relation to each other as a right screw thread to a left screw thread.

Consider, therefore, two screw dislocations emerging on the surface (Fig. 7.158) and forming two steps. Suppose that in an ideal case, adions are adding on to the steps uniformly. There comes a stage when the two steps collide. This collision will generally occur at a crystal edge because steps originate at a dislocation axis and extend to the edge of the crystal. A V-shaped step is formed (Fig. 7.159), the region inside the V being one atom layer lower than the outside. Now adions will be incorporated into the inside of the V, but this means that the angle inside the V keeps increasing and eventually it becomes a straight line joining the axes of the two screw dislocations. The step now runs from one axis to another, and further growth must be based on such a step. One half of this step continues to spiral left and the other half spirals right, the final result being the formation of spiral growths with closed loops (Fig. 7.160).

This is only a highly simplified version of the interaction of screw dislocations. The situation is more complicated where there is nonuniform growth along the steps of the two screw dislocations, where both steps are rotating in the same direction, etc.

#### 7.12.15. Crystal Facets Form

One has, therefore, a picture of ions from a solution being transferred onto the electrode surface as adions; of adions joining steps, kinks, etc.; of steps advancing on the surface; of screw dislocations yielding growth spirals; of the surface advancing

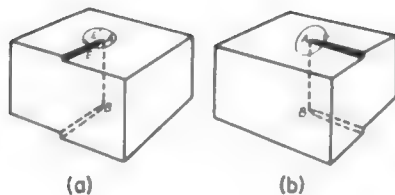


**Fig. 7.157.** (a) Right- and (b) left-handed screw dislocations.

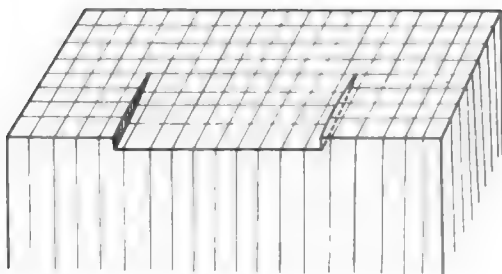


**Fig. 7.158.** Parallel growth steps, each at a screw dislocation, one a left-handed spiral and the other a right-handed spiral.

and occupying more of the solution. But, apart from the macrospiral growths, which require special blockage and bunching mechanisms, the other types of growths (step advance, microspirals, etc.) lead to surface irregularities that are of *atomic* dimensions. The description is too *flat*. In practice, electrodeposits do not consist of smooth-faced, single crystals decorated with an occasional macrospiral. They display the forms and shapes characteristic of crystals; they exhibit facets and also nonuniformities of various kinds, e.g., the formation of complicated and beautiful growths such as dendrites. How do these forms and shapes develop? One has to see things on a grosser scale than steps, kinks, etc.; otherwise one will miss the forest for the trees.

Consider the three-dimensional arrangement of ions in a metal crystal. The ions are close packed. If one imagines a plane cutting the assembly, then depending on the direction of cut, characteristic arrangements of ions are exposed at the surface (Fig. 7.161). Each arrangement is generated by the repetition of a unit pattern. In silver, e.g., the unit patterns might consist (Fig. 7.162) of silver ions in the center of other silver

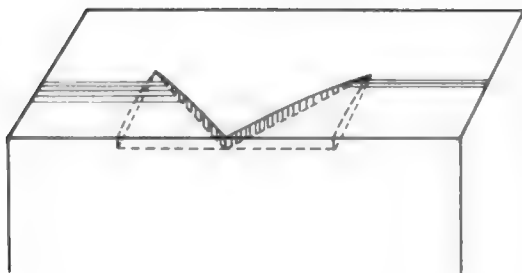


**Fig. 7.159.** The resultant merging of the two growth steps shown in Fig. 7.158, assuming uniform growth on both steps.



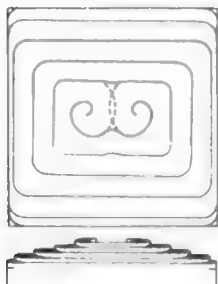


**Fig. 7.160.** Plan and elevation of the final result of two merging screw dislocations; growth spirals similar to those in Fig. 7.153, but with closed loops.

ions arranged in hexagons or squares. The silver ions could also be arranged in rectangles, the long side being  $\sqrt{2}$  times the short side. The regular internal arrangement of ions in a silver crystal is advertising itself at the surface through the characteristic unit pattern that represents different faces of the crystal. This is why they are known as crystal faces. (A small, e.g., 1000-Å square face is known as a *facet*).

The relevance of crystal faces to the subject of electrocrystallization comes up as follows: Each of the crystal faces just described contains all the microfeatures that have been described in previous sections, steps, kinks, etc. Further, the same phenomena of deposition—the ions crossing the electrified interface to form adions, the surface diffusion, lattice incorporation of adions, screw dislocation, growth spirals, etc.—occur on *all* the facets.

What, then, is the difference between electrogrowth on one face compared with that on another? The *rates* of electrogrowth are different on different faces. This phenomenon should not be surprising, for it is generally found that the surface properties of crystals depend on the atomic arrangements that are exposed at the surface.

The explanation of the difference in the rates of electrogrowth on different crystal faces is quite complicated. The differing energetics of two-dimensional nucleation upon different crystal faces have been suggested to account for the different growth rates, but as mentioned earlier in Section 7.12.12, since nucleation is not likely to be involved in crystal growth at low current densities and yet preferential growth is experienced at such conditions, this proposal is not often applicable. The explanation probably lies more in connection with the energies with which adions bond onto the

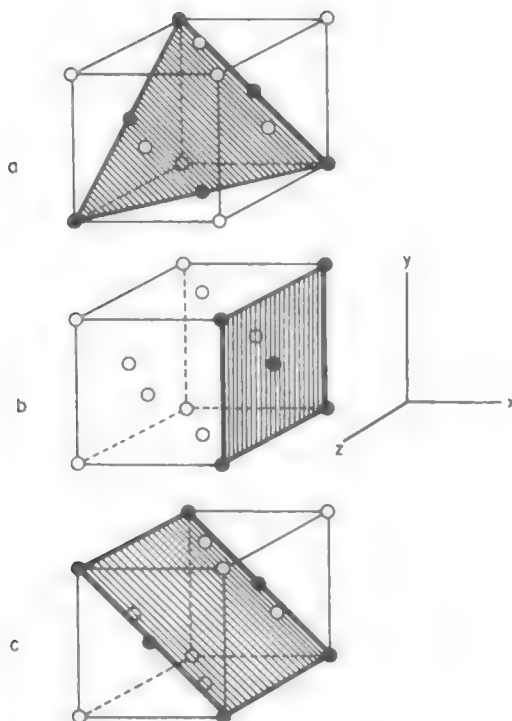


**Fig. 7.161.** Three faces of a cubic lattice showing how the atomic arrangement varies with the direction of the plane chosen.

various types of crystal planes. The number of underlying metal atoms that are in contact with an adion depends on the pattern of atomic arrangement on the surface, i.e., on the particular crystal plane. An adion sitting on the (111), (100), and (110) planes will have 3, 4, and 5 close lattice-atom neighbors, respectively, to which it will be bonded. A situation analogous to this exists when a surface adion diffuses from one lattice site to another and so gains additional lattice-atom neighbors at each step, which finally culminates in lattice incorporation (see Section 7.12.3). Figure 7.130 shows that an adion has 3, 4, and 5 close atom lattice neighbors when it resides at a kink, edge vacancy, and hole, respectively.

Thus, the larger the number of atoms of any crystal plane that are contiguous with the adion, the stronger the bonding and therefore the faster the charge-transfer step. Another possible factor affecting the electrogrowth rate on a particular face is the work function, which is known to be different on different crystal planes. Since the work function helps to determine the ease with which an electron tunnels to the depositing

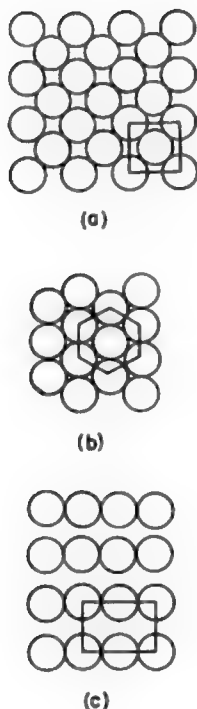


**Fig. 7.162.** Three crystallographic arrangements as seen for the close-packed cubic lattice of silver.

ion, it has an influence on the rate of the charge-transfer reaction (and if this is a local effect, it may not completely cancel out at the metal-metal junction in a cell, as it would otherwise).

This differential deposition rate onto different faces has an important consequence; fast-growing faces tend to grow out of existence and disappear and slow-growing faces tend to survive. This perhaps at first seemingly contradictory assertion follows from simple geometric arguments best grasped from a diagram (Fig. 7.163). The function of crystal faces or diminutive faces, or facets, is a result of the different rates of deposition on different crystal faces of the substrate. This means that even if one carries out deposition on a single-crystal sphere, it soon breaks out (Fig. 7.164) into a rash of those facets that grow slowest.

At this point an objection may be raised. The above argument about faceting may be valid on a sphere, where all possible faces are present (the tangent to the surface at

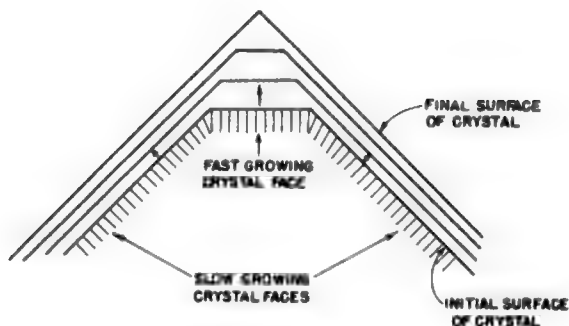


**Fig. 7.163.** The growth of a crystal, illustrating how a fast-growing face grows out of existence, while the slow-growing crystal faces remain.

any point may be considered a hypothetical face), but if deposition is carried out on a flat single-crystal face, where are the different faces to grow at different velocities? There is only one face, it may be said.

The single flat face may be valid as a starting condition, but with continued deposition, all sorts of things happen. The microsteps bunch into macrosteps, and nonuniformities appear on the surface. At the projections, the electric field becomes concentrated and causes faster growth (Fig. 7.165). In this way, the surface of the electrode starts showing sufficient nonflatness for the operation of the law of differential growth velocities of different crystal faces. Then facets start developing on the electrodeposit. This is the crystallographic stage of growth.

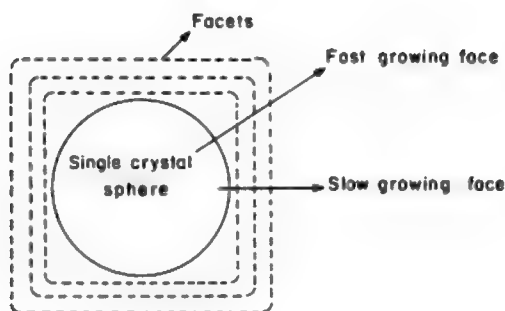


**Fig. 7.164.** Fast- and slow-growing faces as applied to a single crystal sphere. The facets that develop and are observed are those crystal faces with the slowest growth rates.



**Fig. 7.165.** A representation of the concentrated electric field, at a projection, producing a faster growth than at the flat surface.

### 7.12.16. Pyramids

Macrospiral growth, arising from screw dislocations and their rotation, often forms loops of steps and these appear as low cones or pyramids. The slope of the growing pyramid changes if the overpotential is changed during the growth process. Macrospirals can be observed (see Fig. 7.166). The spiral steps have a height of about 10 nm, but the steps are separated by  $10^3$  nm.

### 7.12.17. Deposition on Single-Crystal and Polycrystalline Substrates

In the elementary treatment of the phenomena of electrogrowth being presented here, it is inevitable that several simplifications and idealizations are adopted. Thus it has been assumed so far that the electrodes used were single crystals. Such electrodes, however, have to be specially prepared. The usual piece of metal encountered in everyday life is not a single crystal; X-ray analysis would show that it is a polycrystal, i.e., an agglomerate resulting from many single crystals (sometimes called *grains*) meeting at grain boundaries.

So the question arises: How valid is the picture of deposition developed above when the electrodes are polycrystalline metals? The answer is simple. One can consider the surface exposed to the solution by each grain as a single-crystal microsubstrate and describe the deposition on this microsubstrate in the same terms as those used for single-crystal macrosubstrates. That is, one would have charge transfer followed by surface diffusion, transfer to steps, then to kinks, etc., and one would also have rotating steps resulting from screw dislocations, growth spirals, faceting, etc. In addition, however, at the grain boundaries where the single-crystal microsubstrates meet and the periodic atomic arrangement of each grain is interrupted, the deposition and growth processes will be abnormal. But the actual area of an electrode surface occupied by the grain boundaries is so negligible that the abnormal processes occurring there can be largely ignored. In conclusion, therefore, the basic picture of deposition and growth developed for single crystals is valid as a basis for understanding the electrogrowth of polycrystals.



**Fig. 7.166.** Macrospiral growth observed during electrodeposition of copper in the system:  $\text{Cu (100)}/1\text{ M CuSO}_4 + 1\text{ M H}_2\text{SO}_4$ ,  $T = 298\text{ K}$ . (Reprinted with permission from H. Seiter, H. Fischer, and L. Albert, *Z. Elektrochemie* **63**: 249, 1959.)

### 7.12.18. How the Diffusion of Ions in Solution May Affect Electrogrowth

What next? The situation is replete with possibilities. If the growing electrodeposit is inadequately supplied with metal ions, the nature of the further growth depends on how easily different parts of the electrode secure the supply of ions used to build up the crystal surface. One is talking of the logistic differences between different parts of the advancing crystal front.

One case is where the ions are traveling to the electrode by a process of diffusion. Then the steady-state diffusion problem can be looked at from the diffusion-layer point of view (Section 7.9). The variation of concentration with distance can be approximated to a linear variation, and the linear concentration gradient can be considered to occur over an effective distance of  $\delta$ , the diffusion-layer thickness. Then the diffusion current is given by (Section 7.9.10).

$$i = -DnF \frac{c^0 - c_{x=0}}{\delta} \quad (7.201)$$

If the heights between peaks and recesses on the electrode are small compared with the diffusion-layer thickness  $\delta$  (Fig. 7.167), then  $\delta_{\text{peak}}$  will be less than  $\delta_{\text{recess}}$  and, therefore,  $i_{\text{peak}}$  will be greater than  $i_{\text{recess}}$ . Hence, there will be greater amounts of deposition on the parts of the substrate that stick out. The nonuniformity increases, and the formation of “macrorough” deposits can be understood.

### 7.12.19. About the Variety of Shapes Formed in Electrodeposition

In the last section, a description was given of the amplification of a micropeak on a surface due to faster diffusion to the promontory. However, such concepts only offer a peep at the great proliferation of shapes and sizes possible in electrodeposition (Fig. 7.168).

Among the distinguishable shapes are the simple spreading layers on terraces. These may be monatomic and thus only observable by means of electron microscopy or STM. However, they may also (due to bunching) be more than 100 layers high. Pyramids have already been shown and rationalized. They arise from the rotation of spirals—not microspirals, but macro ones with thicknesses of 100 layers. Boulders, spikes, whiskers, and dendrites (see later discussion on dendrites) may all be formed; and in addition there may be spongy deposits with a surface appearance resembling a leafy plant [see Fig. 7.168(c)].

A theory concerning the electrode kinetics of all these shapes has been given (Popov, 1996). It is quite complicated and involves interactions of differing growth rates, the co-deposition of H, and of course the effects of diffusion, which is sometimes planar but is also spherical if the radius of curvature to which the ions diffuse is less than  $\sim 0.01$  cm. Much more may be done to increase the variety of these shapes and to control them if electrical variables are introduced (e.g., pulsing, superimposed ac, etc.). The area is open for much fascinating research.



**Fig. 7.167.** A representation of a microrough surface where  $\delta_{\text{peak}}$  is less than  $\delta_{\text{recess}}$ , hence, when the growth rate is diffusion-controlled, it will be at the peak than in the recess.

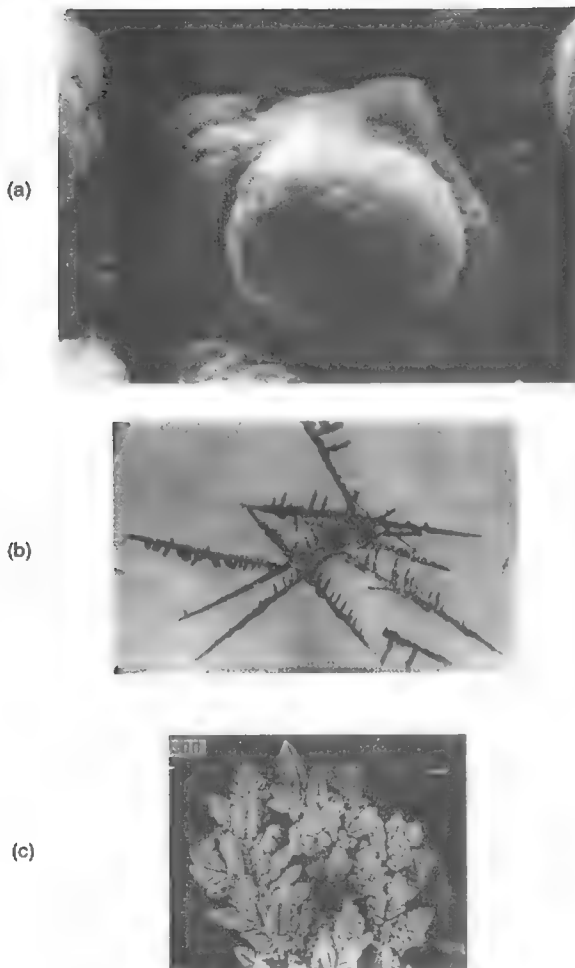


**Fig. 7.168.** (A) SEM photomicrograph of copper powder particles (constant current deposition,  $J_c = 160 \text{ mA cm}^{-2}$ ; magnification  $\times 10,000$ ). (B) Tin powder particles obtained by constant overpotential electrolysis at the overpotential of deposition of 50 mV. (C) SEM micrograph of copper deposits obtained by deposition from  $0.3 \text{ mol dm}^{-3} \text{ CSO}_4$  in  $0.5 \text{ mol dm}^{-3} \text{ H}_2\text{SO}_4$  onto a copper wire electrode (deposition overpotential, 550 mV; magnification, X1500. (A and B, reprinted from M. G. Pavlovic et al., *Hydrometallurgy* **32**: copyright 1993 and K. I. Popov et al., *Hydrometallurgy* **23**: 127 copyright 1989 with permission from Elsevier Science.) (C reprinted with permission from K. I. Popov, N. V. Kestajic, M. I. Cekeraevac, and H. Serb. *Chem. Soc.* **59**: 122, 1994.)



### 7.12.20. Dendrites

There are other ways in which ion transport leads to nonuniform growths. Consider, e.g., the following elementary theory of dendrite formation. Suppose that a macrospiral growth develops on a flat substrate surface. The tip of the spiral has quite a small radius of curvature ( $r \sim 10^{-6}$  cm) and should not be considered a plane sink that stimulates linear diffusion. It is virtually a *point* sink, with the radius of curvature being much less than the diffusion-layer thickness ( $r \ll \delta$ ). Under these conditions, there is spherical diffusion to the point sink (Fig. 7.169), and the limiting current density (see Section 7.9.11) is given by  $DnFc^0/r$  and not  $DnFc^0/\delta$ , as is the case for linear (or planar) diffusion. Since  $r \ll \delta$ , it is obvious that the limiting current density to the spiral tip is much higher than that to a projection with a radius of curvature on the order of the diffusion-layer thickness.

Another feature of the spiral tip is that it has an abnormally high step and kink density and perhaps the tip has a higher exchange-current density for deposition than the corresponding planar surface. If this were so, the activation overpotential would be much less at the tip of the spiral than around its base.

Arguments have been presented by Barton (and also by Hamilton) for both the concentration and activation overpotentials being much less at the tips of macrospiral than on the planar surface. It follows, therefore, that electrogrowth tends to become concentrated at the spiral tip. The tip tends to grow faster than the rest of the substrate. This is part of the basis of the theory of the growth of the long, thin, fast-growing faceted rods that sometimes shoot out from the electrode surface. These *dendrites* usually grow side arms, ending up like mini-Christmas trees (Fig. 7.170).

It must be emphasized here that the study of dendrite formation has important practical implications. In energy-storage devices (batteries), dendrites often rupture the membranous separators and go over to touch the other, electron-sink electrode (anode), which leads to a disastrous short circuit of the cell. In substance producers

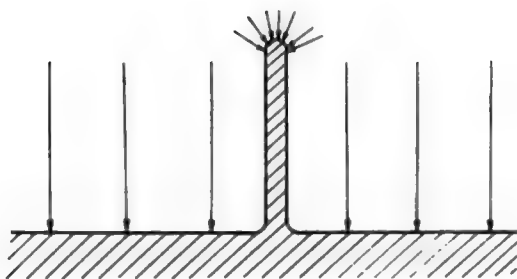


**Fig. 7.169.** The elementary dendrite theory in which the tip of a macrospiral has a radius of curvature  $r \rightarrow \delta$  and hence the growth rate is much greater at the tip than at a flat surface.

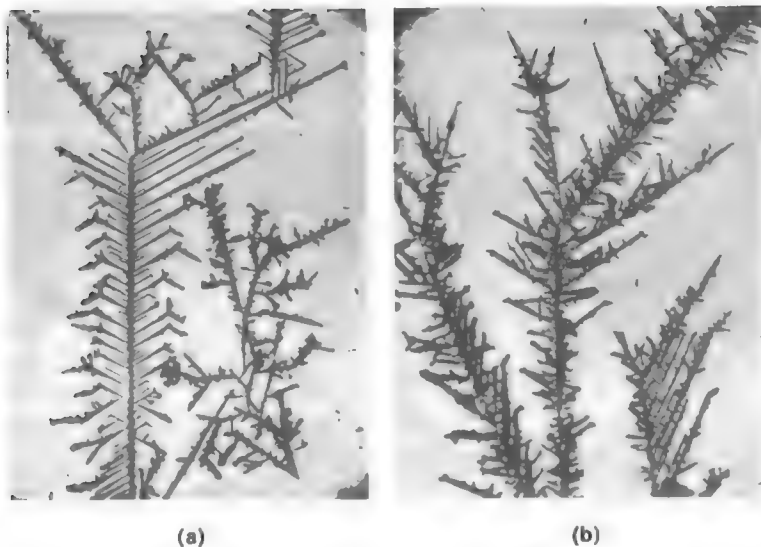


**Fig. 7.170.** (a) Two-dimensional (left) and three-dimensional (right) silver dendrites (after Wranglen). (b) Three-dimensional cadmium dendrites (after Wranglen).

designed for the preparation of metal powders by electrodeposition, dendrite formation is to be avoided because it does not give the desired type of deposit.

#### 7.12.21. Organic Additives and Electrodeposits

The effect of organic substances in solution on the nature of electrocrystallization is an area in which there has been a vast number of facts with little theory explaining them. Here one cannot do more than hint at some of the factors.

In the first place, the adsorption of organic substances is generally dependent on the charge of the electrode. It will be recalled that the relation of the coverage to the electric charge is bell shaped (see Section 6.9.4, Fig. 6.109). A model in which the organic molecule competes for the electrode against water permits a simple view of the process. As a very crude first approximation (see, however, Section 6.9.5), the potential at which there is a maximum adsorption of uncharged organics may be taken as the pzc.

All this only helps one to understand whether the organic adsorbs at the potential difference prevailing at the interface during electrodeposition. But where does it adsorb? Uniformly all over the electrode? This would only lead to an all-round slowing down of growth. Preferentially on some crystal faces but not so much on others? In this case, the ratio of growth velocities of the different faces will be altered from that obtained in the absence of the organic additive, and perhaps the growth rates will get evened out, which will result in smooth, even deposits. Selectively, on the planes? This

will cause a stopping of step movement, perhaps the nucleation of new crystals (fine-grained deposits). Preferentially on micropeaks owing to the greater diffusion of organic molecules to these peaks (Fig. 7.168)? This would lead to smoothing and brightening because the deposit would tend to grow where there is no adsorbed, blocking organic additive, i.e., to fill in the valley. All these effects are in fact observed with the addition of organic solutes to solutions from which electrocrystallization is to occur. But a detailed understanding of how they are related to the structure of the additive is as yet at a very low level. The effects of very small concentrations of additives on crystal-growth forms can be seen in Table 7.21 where the additive is *n*-decylamine.

### 7.12.22. Material Failures Due to H Co-deposition

Certain ions and organics in the solution affect H entry into the metal (Flitt and Bockris, 1991). More is known about this for deposits onto iron and steel than for other metals. Here, for example, cyanide and many organics adsorb and slow down the desorption reaction of H recombination. Consequently, the steady state,  $\theta_H$ , is increased and this tends to accelerate the rate of H diffusion into the metal, resulting eventually in embrittlement. Conversely, anything in the solution that tends to reduce  $\theta_H$  (e.g.,  $\text{NO}_3^-$  and oxidizers) will reduce the tendency of the H to enter into the metal and cause damage.

With steel it is possible to reduce H absorption *mechanically* by plating thin layers of copper and/or nickel onto the steel. These metals absorb H poorly and hence protect the steel.

Something of the complexity of factors affecting the efficiency of metal deposition—the competing reaction always being H co-deposition—can be seen in Fig. 7.171 where there is a maximum in chromium deposition efficiency at about 200 g

**TABLE 7.21**  
**Crystal Growth Morphology for the Electrodeposition of Copper in the Presence and Absence of  $10^{-6}$  mol liter $^{-1}$  *n*-Decylamine**

Deposition-current density (mA cm $^{-2}$ )	Crystal-growth morphology	
	In the presence of <i>n</i> -decylamine	In the absence of <i>n</i> -decylamine
5	Layers	Layers but with larger distances between steps
10	Layers + truncated pyramids	Layers + pyramids, again with larger distances between steps
15	Layers + truncated pyramids + blocks	Layers + pyramids (little tendency for truncated pyramids to form)
20	Polycrystalline	Layers + truncated pyramids + blocks

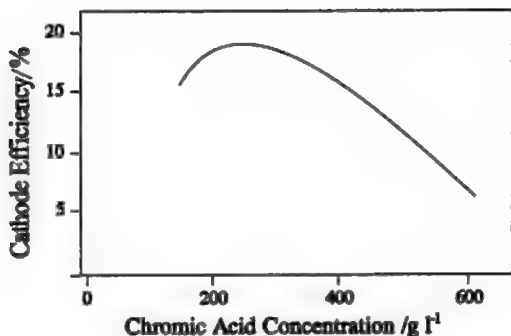


**Fig. 7.171.** Relation between cathode current efficiency and chromic acid concentration. (Reprinted with permission of Chapman and Hall from D. R Gabe, *J. Appl. Electrochem.* 27: 908, Fig. 2, 1997.)

liter<sup>-1</sup> of chromic acid. An increase with concentration of chromium salt would be expected because the limiting diffusion rate for chromate toward the electrode surface increases linearly with its concentration, while that of  $\text{H}_3\text{O}^+$  remains at constant pH. The decrease of the Cr efficiency at higher concentrations occurs probably because of the catalysis given to the  $i_{\text{H}}$  by the increasing coverage of the steel with deposited Cr. The H content of a deposit (e.g., Cr) affects its ductility. About 0.06% H in Cr causes the latter to be “hard,” i.e., to have its ductility diminished.

#### 7.12.23. Would Deposition from Nonaqueous Solutions Solve the Problems Associated with H Co-deposition?

At first sight, electrodeposition of metals from nonaqueous solutions seems to offer a complete solution, there being no source of H present (in a system consisting of e.g., palladium chloride in a phenanthrene-anisole mixture). The potential limits inside which electrodeposition can take place can be far wider than those in aqueous solutions (some 2.0 V). A number of redox potentials in nonaqueous systems are given in Table 7.22.

#### 7.12.24. Breakdown Potentials for Certain Organic Solvents

In many cases, the difference between these potentials—the window of operation without electrochemical decomposition of the solvent—is 3–4 V. In the aqueous case, it may in practice be as little as 1.5 V. On the other hand, even sodium can be electrodeposited from a solution of sodium acetate in ethanolamine. These advantages are countered by three factors that must be considered before a nonaqueous electrodeposition process is chosen as the best solution to co-deposition of H (Section 4.8.3).

**TABLE 7.22**  
**Some Potential Limits in the Use of Battery Systems in Nonaqueous Solution**

Solvent	Salt	$E_{\text{Ox}}$	$E_{\text{Red}}$	Measurement Condition <sup>a</sup>
PC <sup>b</sup>	$\text{Et}_4\text{N}^+ \text{ClO}_4^-$	2.0	-3.5	Glassy carbon; $\text{Ag}^+/\text{Ag}$ ; 50 mV/s; 1.0 mA/cm <sup>2</sup>
PC	$\text{Et}_4\text{N}^+ \text{SbF}_6^-$	2.5	-3.5	
PC	$\text{Et}_4\text{N}^+ (\text{CF}_3\text{SO}_2)_2\text{N}^-$	2.2	-3.8	
PC	$\text{Et}_4\text{N}^+ \text{BEt}_4^-$	1.2	-2.0	
PC	$\text{Et}_4\text{N}^+ \text{BPh}_4^-$	0.1	-3.5	
EM <sup>c</sup>	$\text{Li}^+(\text{CF}_3\text{SO}_2)_2\text{N}^-$	5.8	<-1.0 <sup>d</sup>	Cathode composite; $\text{Li}^+/\text{Li}$ ; 0.1 mV/s; <10 $\mu\text{A}/\text{cm}^2$
EM	$\text{Li}^+\text{ClO}_4^-$	6.0	<-1.0	
EM	$\text{Li}^+\text{CF}_3\text{SO}_3^-$	6.0	<-1.0	
Eip <sup>e</sup>	$\text{Li}^+\text{ClO}_4^-$	6.0	<-1.0	
EsB <sup>f</sup>	$\text{Li}^+\text{ClO}_4^-$	6.0	<-1.0	
PC	$\text{Li}^+\text{ClO}_4^-$	5.0	<-1.0	Platinum; $\text{Li}^+/\text{Li}$ ; 50 mV/s; 1.0 mA/cm <sup>2</sup>
EC	$\text{Li}^+\text{ClO}_4^-$	4.5	<-1.0	
TG	$\text{Li}^+\text{ClO}_4^-$	4.7	<-1.0	
GLN <sup>g</sup>	$\text{Et}_4\text{N}^+ \text{ClO}_4^-$	7.0		
AN <sup>h</sup>	$\text{Et}_4\text{N}^+ \text{CF}_3\text{SO}_3^-$	5.7		
DOL <sup>i</sup>	$\text{Et}_4\text{N}^+ \text{ClO}_4^-$	3.4		

Source: Reprinted from P. Croce et al., *J. Electrochem Soc.* **143**(1), p. 155, Table 1, 1996. Reproduced by permission of the Electrochemical Society.

<sup>a</sup>Working electrode; reference potential; scan rate.

<sup>b</sup>Propylene carbonate.

<sup>c</sup>Ethylmethyl sulfone.

<sup>d</sup>Measurement did not go any more negative.

<sup>e</sup>Ethyl-*iso*-propyl sulfone.

<sup>f</sup>Ethyl-*sec*-butyl sulfone.

<sup>g</sup>Glutaronitrile.

<sup>h</sup>Acetonitrile.

<sup>i</sup>Dioxlane.

1. *Low Limiting Current.* The limiting current in a stationary electrolyte is proportional to the concentration of the depositing ion, i.e., the maximum value is determined by the solubility of the salt. However, this quantity in nonaqueous solutions tends to be at least one and often two orders of magnitude less than the corresponding solubility in aqueous solution. To some extent, this problem can be reduced by using organic salts of the metals, which are much more soluble in nonaqueous solvents, and by using, for example, rotating cylinders or disks to increase the limiting current for a certain concentration of reactant. However, these artifices seldom succeed in approaching the limiting current density offered by a comparable aqueous process. A low limiting current implies a low production rate per unit area of plant space and hence increases cost by requiring more floor space.

2. *Lower Conductivity.* The equivalent conductance of nonaqueous solutions at infinite dilution is often comparable to that of aqueous systems, but it decreases with an increase in concentration more rapidly than the corresponding aqueous systems (the effect of the lower dielectric constant). Since the specific conductivity,  $\kappa$  (that which determines the resistance between cathode and anode) is proportional to  $\Lambda_c$ , the equivalent conductance, the IR drop between the electrodes of a cell in which deposition from nonaqueous solutions is to take place will be greater than that in aqueous solution (see Section 4.8.7). The electricity needed to deposit a given mass of metal is proportional to the total  $E$  between the electrodes, and this includes the IR between the electrodes, which is much greater in the nonaqueous than in the aqueous cases. Hence, nonaqueous deposition will be more costly in electricity (more kilowatt hours per unit of weight deposited) than a corresponding deposition in aqueous solution. The difference may be prohibitive.

3. *Water as a Contaminant.* A typical partial vapor pressure of water in the atmosphere is 15 mm of Hg, i.e., 15/760—about 2%. Thus, any nonaqueous electrochemical cell operating in the air of a laboratory or plant is constantly being struck by molecules, around 1 in 50 being water. Short of making a vacuum-tight apparatus, it is difficult to keep a nonaqueous solution free from water. Countermeasures can include getters (e.g., the use of sodium or aluminum metal spirals or powder), which react with the water to remove it; or a scavenger electrolysis unit to decompose water electrochemically as it enters the cell from the surrounding atmospheres. The problem is that small traces of water ( $\ll 1$  ppm) do not remain dispersed uniformly throughout the solution, but tend to concentrate at surfaces, including those of the electrodes, where they may make the local environment more like that in an aqueous solution.

In summary, electrodeposition of metals from organic solvents may be helpful in relatively short-term fundamental investigations, but it seldom provides an opportunity for an economic large-scale extraction process.<sup>96</sup>

Nevertheless, practical use can be made of the fact that lithium remains unreactive in many solvents (e.g., propylene carbonate, polypropylene, ethanolamine, etc.). Systems using lithium as an anode in the discharge cycle have led to experimental batteries with good prospects (Chapter 13).

---

<sup>96</sup>For many years, attempts have been made to deposit aluminum from nonaqueous solvents, usually a mixture of aromatics in which  $\text{AlBr}_3$  is dissolved. Such a process has been the subject of intense modern work (Gileadi, 1990). Although Al can be successfully plated in thin layers in this way, the limiting currents are so much lower than the relatively high ones ( $0.2 \text{ A cm}^{-2}$ ) of the well-known molten salt process used in industry that there is no question of a large-scale metallurgical process being nonaqueous. It may be advantageous to use such a process in *plating objects with Al* where the high-temperature molten salt process is impractical.

## 7.12.25. Molten Salt Systems Avoid Hydrogen Codeposition

**7.12.25.1. “Nonaqueous.”** It is first necessary to point out a convention. The term “nonaqueous” in electrochemical systems is understood to refer to solution in *organic* solvents. When molten salt systems are intended, they are so named (though, of course, they are also nonaqueous). It was normal until the 1980s to regard “molten” when applied to salts as meaning high temperature, the melting point of NaCl being (850 °C). However, it is now known that some tetraalkylammonium salts can be stable liquids (i.e., “molten” salts) at room temperature (Chapter 5). Further, a series of systems in which  $\text{AlCl}_3$  is dissolved in a series of phosphonium and sulfonium organic compounds are known to have the properties of molten salts, but can be liquids at room temperature.

**7.12.25.2. Advantages of Molten Salts as Solvents for Electrodeposition.** The difficulties associated with H codeposition are mostly avoided by the use of molten salt media. Further, two of the counter difficulties offered by the use of organic solvent systems (low conductivity and low limit of current) are greatly diminished, at least in high-temperature systems ( $250 < T < 1000$  °C). As to the downside of molten salt systems, it is the increased expense of sustaining them in a stable state, mainly ensuring a limited corrosion rate of the containing vessel, and the reduction of contamination of the system with any breakdown products from such corrosion. Residual water—which might well have been thought to have been boiled off at  $>100$  °C—sometimes is retained for many hours in the salt, but is a lesser threat than it is in anhydrous organic systems. The window of operation can be as high as in the nonaqueous systems and is seldom less than 4 V (1.5–1.6 V in aqueous systems).

The most well-known electrodeposition process from the molten state is that of aluminum, which is deposited from a mixture of  $\text{Al}_2\text{O}_3$  in  $\text{AlF}_3\text{-NaF}$  at 965 °C. Other commercial processes involving molten salts exist and are exemplified by the deposition of tantalum and zirconium. Processes for Ti deposition from  $\text{TiCl}_3$  in KCl-LiCl entectics exist. All these escape almost completely<sup>97</sup> from the H co-deposition problem of aqueous electrodeposition.

During the past few decades, semiconductors have revolutionized the electronics industry. The substances are generally required in film form and this favors electrodeposition. The best known among semiconductors that have been successfully electroplated are CdTe, CdSe, CdS, ZnS, and ZnTe (mostly from nonaqueous solutions). The advantage of electrodeposition of semiconductors from molten salts (400–500 °C) is that the higher temperature encourages good crystallization. The downside is that the high-temperature process requires a more complex apparatus, although at temperatures of less than 500 °C, the corrosion difficulty is relatively small and glass apparatus may be usable.

<sup>97</sup>Water may still be a problem (leading, e.g., to the production of oxides) unless it is rigorously eliminated by prolonged heating under vacuum or by means of scavenger electrolysis.

### 7.12.26. Photostimulated Electrodeposition of Metals on Semiconductors

A photoresponse from p-type Si leads to electron ejection to metal ions waiting in the interfacial region and hence to electrodeposition (Kautek, 1991). The practical possibilities are many; for example, the light may be in the form of a laser ray and by moving this, metal can be deposited on the Si base in a form of “writing.” Large displays can be engineered using conducting  $\text{SnO}_2$ -coated glass as a counter-electrode.

### 7.12.27. Surface Preparation: The Established Superiority of Electrochemical Techniques

The traditional method for preparing unusual novel surfaces is to apply a beam of vapor directed against a substrate (chemical vapor deposition, CVD). Use of such techniques is accompanied by three negative characteristics: (1) The lateral resolution of deposits is not better than  $1\text{ }\mu\text{m}$ . Correspondingly, the repeatability of the size of nuclei is poor (owing to the variation in the degree of supersaturation in the vapor). (2) A given operation may involve several environments and hence invite contamination. (3) The substrate heats up as a consequence of the impingement of the vapor and may thus sustain damage.

These features are absent when a surface is prepared by means of electrodeposition or electrodisolution. There is one environment and no local heating. The potentiostat makes it easy to control the size of deposits. Dissolution can be affected as easily as deposition.

Electrochemical cutting (or “machining”) is a technique long used by some automobile manufacturers. The “knife” is a cathode, and when it is brought very near the metal part to be machined (sprayed with solution and wired so that it responds anodically to the approaching “knife”), the anodic section dissolves. With appropriate geometry in the arrangements, any kind of groove can be made and large sections of, for example, steel can be cut or machined with a minimal use of mechanical energy, and at room temperature. Electrochemical micromachining is, correspondingly, a technique of growing importance, as is the use of electrochemically deposited thin films in the magnetic recording devices used by computer systems.

### 7.12.28. Electrochemical Nanotechnology

It is possible to use the tip of an STM device as an electrode and controlled pulses to form reproducibly minute clusters of a few atoms (Kolb, 1993) (Fig. 7.172). Such an achievement illustrates the superiority of electrochemical techniques in achieving resolution to  $1\text{ nm}$ .



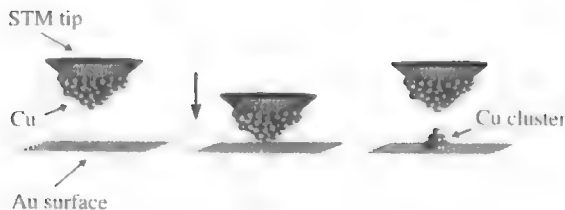


**Fig. 7.172.** Model for tip-induced Cu deposition. (Reprinted from E. Budevski, G. Staikov, and W. J. Lorenz, *Electrochemical Phase Formation and Growth*, p. 301, copyright © 1996 John Wiley & Sons, Reproduced by permission of John Wiley & Sons, Ltd.)

## Further Reading

Electrodeposition is an ancient art. Discoveries in the Middle East have provided evidence of gold plating in 2500 B.C.! Faraday discovered his laws of electrolysis by plating out and weighing materials in 1834. Here, we give references to some outstanding twentieth-century papers.

### Seminal

1. F. Kuhlschutter and J. Torricelli, *Z. Elektrochem.* **38**: 213 (1932). Photography of moving layers in electrogrowth.
2. C. Burton, F. Cabrera, and C. Frank, *Nature* **163**: 398 (1949). Nucleation unnecessary; crystal growth can occur by rotation of spirals originating in screw dislocations.
3. R. Kaischew, *Bull. Acad. Bulg. Sci. Phys.* **1**: 100 (1950). Theory of 2D nucleation.
4. R. Kaischew, E. Budevski, and J. Malinowski, *Z. Physikal. Chem.* **204**: 348 (1955). Nucleation rate.
5. C. Vermilyeo, *J. Chem. Phys.* **28**: 1254 (1956). Screw dislocation theory: kinetics of rotation.
6. O. Kardos and O. Foulke, *American Electroplaters* **43**: 172 (1956). Mechanistic theory of leveling agents.
7. B. E. Conway and J. O'M. Bockris, *Proc. Roy. Soc. London* **248A**: 394 (1958). Calculations on competing steps in electrochemical metal deposition.
8. M. Fleischmann and R. Thirsk, *Electrochim. Acta* **2**: 22 (1960). Potentiostatic transient and crystal growth.
9. J. O'M. Bockris and J. Barton, *Proc. Roy. Soc. London* **268A**: 485 (1962). Quantitative theory of dendritic growth.
10. M. Mullins and P. Hirth, *J. Phys. Chem. Solids* **24**: 1391 (1963). Bunching theory.

### Monograph

1. E. Budevski, G. Staikov, and W. J. Lorenz, *Electrochemical Phase Formation and Crystal Growth*, VCH Publishers, Weinheim (1996).

## Modern

1. E. Budevski, in *Progress in Surface Science*, Vol. II, p. 71, Academic Press, New York (1976).
2. E. Budevski, V. Bortanov, and G. Starkov, *Ann. Rev. Mat. Sci.* **10**: 15 (1980).
3. S. Sweshirajen and S. Bruckenstein, *J. Electrochem. Soc.* **129**: 1202 (1982).
4. B. Scharifker and G. J. Wills, *Electrochim. Acta* **28**: 879 (1983).
5. E. Budevski, in *Comprehensive Treatise in Electrochemistry*, B. E. Conway, J. O'M. Bockris, E. Yeager, S. U. M. Khan, and R. E. White, eds., p. 399, Plenum, New York (1983).
6. Blum, H. D. Abruna, J. G. Gordon, G. I. Borges, M. G. Samant, and O. R. Melroy, *J. Chem. Phys.* **85**: 6732 (1986).
7. M. Szklarczyk, O. Velez, and J. O'M. Bockris, *J. Electrochem. Soc.* **136**: 2433 (1989).
8. R. Sonnenfeld, J. Schneir, and D. K. Hansma, in *Modern Aspects of Electrochemistry*, R. E. White, J. O'M. Bockris, and B. E. Conway, eds., Vol. 21, p. 1, Plenum, New York (1990).
9. C. Kolla, N. Spyrellis, J. Amplard, M. Fromment, and G. Maurin, *J. Appl. Electrochem.* **20**: 1241 (1990).
10. N. Battina, T. Will, and D. M. Kolb, *Faraday Discuss.* **94**: 93 (1992).
11. G. Staynor, *Electrochim. Acta* **37**: 2357 (1992).
12. W. Obretenov, U. Schmidt, W. J. Lorenz, G. Staikov, E. Budevski, D. Carnal, U. Muller, H. Siegenthaler, and E. Schmidt, *J. Electrochem. Soc.* **140**: 692 (1993).
13. S. G. Corcoran, G. S. Chakovova, and K. Siradski, *Phys. Rev. Lett.* **71**: 1588 (1993).
14. V. Battina, A. S. Dakkouri and D. M. Kolb, *J. Electroanal. Chem.* **370**: 370 (1994).
15. M. Ditterlie, T. Will, and D. M. Kolb, *Surface Sci.* **327**: L495 (1995).
16. M. H. Holzle, V. Zwing, and D. M. Kolb, *Electrochim. Acta* **40**: 1237 (1995).
17. P. Mrazek, Y. E. Sung, M. Han, M. Gamboa-Aldeco, A. Wieckowski, C. Chen, and A. Gewirth, *Electrochim. Acta* **40**: 17 (1995).
18. K. Ogaki and K. Itaya, *Electrochim. Acta* **40**: 1249 (1995).
19. U. Schmidt, S. Vinzelberg, and G. Staikov, *Surf. Sci.* **335**: 32 (1995).
20. W. J. Lorenz and G. Staikov, *Surf. Sci.* **335**: 32 (1995).
21. R. T. Porzschke, G. A. Gervasi, S. Vinzelberg, G. Staikov, and W. J. Lorenz, *Electrochim. Acta* **40**: 1469 (1995).
22. T. Leava and W. Schmickler, *Electrochim. Acta* **40**: 37 (1995).
23. Z. Shi, S. Wu, and J. Lipkowski, *Electrochim. Acta* **40**: 9 (1995).
24. W. J. Lorenz and G. Staikov, *Surf. Sci.* **335**: 32 (1995).
25. R. T. Potschke, G. A. Gervasi, S. Vinzelberg, G. Staikov, and D. W. Lorenz, *Electrochim. Acta* **40**: 1469 (1995).
26. A. R. Despic and D. D. Jovic, in *Modern Aspects of Electrochemistry*, B. E. Conway, J. O'M. Bockris, and R. E. White, eds., Vol. 27, p. 143, Plenum, New York (1995).
27. G. Jerkiewicz and A. Zolfaghari, *J. Phys. Chem.* **100**: 8454 (1996).
28. N. M. Markovic, H. A. Gesteiger, Chris A. Lucas, I. M. Tidswell, and P. Ross, *Surf. Sci.* **335**: 91 (1995).
29. K. Shashikata, Y. Matsui, K. Itaya, and M. P. Soriaga, *J. Phys. Chem.* **100**: 20027 (1996).

## 7.13. CURRENT-POTENTIAL LAWS FOR ELECTROCHEMICAL SYSTEMS

### 7.13.1. The Potential Difference across an Electrochemical System

In the introduction to the fundamentals of electrodictics, it was pointed out that the only electrochemical systems of practical interest are those that consist of at least a *pair* of electrode/electrolyte interfaces. In such electrochemical systems, or cells, one electrode can function as an electron sink (or anode) and the other as an electron source (or cathode).

But before trying to understand the behavior of electrochemical systems, or cells, it was considered useful to disassemble, or analyze, them conceptually into two isolated electrode/electrolyte interfaces and then to study single interfaces. This has been done. The whole treatment so far has concerned itself with a single electrode/solution interface<sup>98</sup> and with the current–potential laws that govern its behavior. The Butler–Volmer equation is the key equation for a single interface. The behavior of an electrochemical system, or cell, must be conceptually synthesized from the behavior of the individual interfaces that combine to form a cell.

Consider two electrode/electrolyte interfaces (Fig. 7.173),  $M/S$  and  $M'/S'$ , which are assembled to form an electrochemical system or cell. Recalling that potential differences are always measured between two metals of the same composition, a metal  $M''$  that is identical in composition to  $M$  is attached to  $M'$ . Under these circumstances, the potential difference  $V$  across the whole system, or cell, has been shown [Eq. 6.53] to be given by the inner potential of the electrode on the right minus the inner potential of a wire of the same composition connected to the electrode on the left:

$$\begin{aligned}
 V &= {}^M\Delta^{M''}\phi \\
 &= (\phi_M - \phi_S) + (\phi_S - \phi_{S'}) + (\phi_{S'} - \phi_{M'}) + (\phi_{M'} - \phi_{M''}) \\
 &= {}^M\Delta^S\phi + {}^S\Delta^{S'}\phi + {}^{S'}\Delta^{M'}\phi + (\phi_{M'} - \phi_{M''}) \quad (7.274)
 \end{aligned}$$

where  ${}^S\Delta^{S'}\phi$  is the potential difference between the bulk of the solution  $S$  near the  $M/S$  interface and the bulk of the solution  $S'$  near the  $M'/S'$  interface.

The  ${}^S\Delta^{S'}\phi$  will include (Fig. 7.174) the liquid-junction potential that always arises whenever two solutions of different composition are in contact. But it will be assumed throughout this treatment that the liquid-junction potential has been minimized by the use of salt bridges so that it can be taken as zero. In addition,  ${}^S\Delta^{S'}\phi$  will also include the potential drop in solution. This, in the absence of a liquid-junction potential, is given by

<sup>98</sup>Or, if the treatment considered a cell, the second interface was considered nonpolarizable. i.e., its potential difference was taken to be a constant.

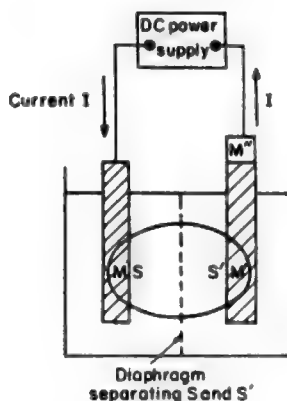


**Fig. 7.173.** An electrochemical system consists of a series of potential drops that constitute the voltage measured between the two wires of equal composition,  $M$  and  $M'$ .

$${}^S\Delta^{S'}\phi = IR \quad (7.275)$$

where  $I$  is the current through the solution, and  $R$  is its resistance. If the resistance is negligible, then the quantity  ${}^S\Delta^{S'}\phi$  tends to zero.

Initially it will be assumed that this special case is applicable. On this basis, Eq. (7.274) reduces to

$$V = {}^M\Delta^S\phi + {}^{S'}\Delta^{M'}\phi + \phi_{M'} - \phi_{M''} \quad (7.276)$$

Since, however, the convention is to express the potential difference across an interface as the inner potential of the *electrode* minus the inner potential of the *electrolyte*, one can use the relation that

$${}^S\Delta^{M'}\phi = -{}^{M'}\Delta^S\phi \quad (7.277)$$

to write

$$V = {}^M\Delta^S\phi - {}^{M'}\Delta^{S'}\phi + (\phi_{M'} - \phi_{M''}) \quad (7.278)$$

This, then, is the potential difference across the whole cell, or electrochemical system, on assuming that there is zero potential difference in the solution, i.e.,  ${}^S\Delta^{S'}\phi = 0$ . The

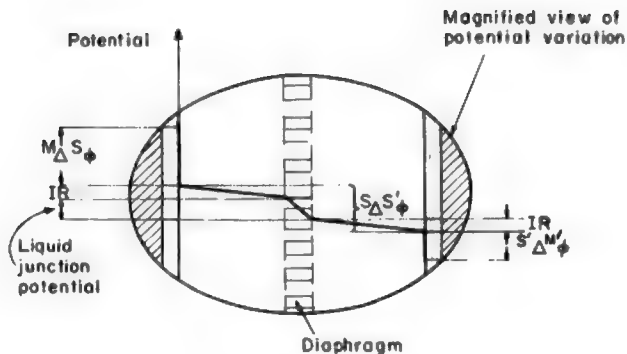


**Fig. 7.174.** A magnified view of the situation in Fig. 7.173 shows that besides the two potential changes at the two metal/solution interfaces, there is also a liquid-junction potential as well as an ohmic drop in both solutions.

potential difference  $V$  is not independent of the current passing through the system because the potential differences across the two individual interfaces  $M/S$  and  $M'/S'$  are functions of the current densities; in fact, that is what the Butler–Volmer equation is all about. (Note that it has been assumed that  $S\Delta S'\phi \approx 0$ . Otherwise, as the current  $I$  changes,  $S\Delta S'\phi = IR$  will also change—another contribution to the variation of  $V$  with  $I$ ). Hence, the cell potential  $V$  depends in general on the current flowing through the electrochemical system. The problem therefore is to understand the laws relating the potential difference across an electrochemical cell to the current  $I$  flowing through it.

### 7.13.2. The Equilibrium Potential Difference across an Electrochemical Cell

Before treating cells with currents flowing across them, an expression will be developed for the zero current or equilibrium potential difference across a cell.<sup>99</sup> Since there is zero cell current, the cell is not connected to either an external current source or an external current sink (or load); one says the cell is on *open circuit*. It is neither a driven cell nor a self-driving system. Each interface therefore must be at equilibrium because the net current is zero across both interfaces.

Hence, both  $M\Delta S\phi$  and  $M'\Delta S'\phi$  in Eq. (7.278) are equilibrium potential differences and may be represented as  $M\Delta S\phi_e$  and  $M'\Delta S'\phi_e$ , respectively, in which case one has for the equilibrium potential difference  $V_e$  across the cell:

$$V_e = M\Delta S\phi_e - M'\Delta S'\phi_e + (\phi_{M'} - \phi_{M''}) \quad (7.279)$$

<sup>99</sup>Corrosion cells (see Chapter 12) are excluded from this analysis because even when a corroding metal is not connected into a circuit, i.e., even when it is on open circuit, the metal is not at equilibrium.

Even though one is considering the simplified situation of equilibrium, one is still faced with the fact that the absolute potential differences across single interfaces are experimentally inaccessible (Section 6.3.1). However, one can always resort to the convention (see Section 6.3.4) of referring all potentials to an SHE which would consist, e.g., of a platinized platinum electrode in contact with hydrogen gas at 1 atm pressure and a solution of hydrogen ions at unit activity.

So one can adopt the following procedure:<sup>100</sup> The quantities  $\Delta\phi_{\text{SHE}}$  and  $\phi_{\text{Pt}}$  are added to and subtracted from the right-hand side of expression (7.279) for the equilibrium cell potential  $V_e$ . Thus,

$$V_e = [{}^M\Delta^S\phi_e - \Delta\phi_{\text{SHE}}^0 + (\phi_{\text{Pt}} - \phi_{\text{M}''})] - [{}^{M'}\Delta^{S'}\phi_e - \Delta\phi_{\text{SHE}}^0 + (\phi_{\text{Pt}} - \phi_{\text{M}'})] \quad (7.280)$$

Examine the terms in the square brackets. What do they represent? They are the potential differences across cells consisting of an SHE coupled with the M/S and M'/S' interfaces. In other words, they are the potential differences of the M/S and M'/S' interfaces relative to the SHE. It is customary to call them *relative potentials* or simply *potentials* of the electrodes M and M'. Thus, Eq. (7.280) becomes

$$V_e = E_{e,\text{M/S}} - E_{e,\text{M'/S'}} \quad (7.281)$$

Since, however, it has been stipulated that the equilibrium situation is being considered, one can use the Nernst expression (7.51) for the equilibrium potentials and write<sup>101</sup>

$$V_e = \left( E_{\text{M/S}}^\circ + \frac{RT}{nF} \ln \frac{a_{\text{A}}}{a_{\text{D}}} \right) - \left( E_{\text{M'/S'}}^\circ + \frac{RT}{nF} \ln \frac{a_{\text{A}'}}{a_{\text{D}'}} \right) \quad (7.282)$$

where A and D are the electron acceptors and donors involved in the electron-transfer reaction at the M/S interface; and A' and D', the corresponding quantities at the M'/S' interface. Thus, the equilibrium-potential differences across cells can be predicted for known  $a_{\text{A}}/a_{\text{D}}$  and  $a_{\text{A}'}/a_{\text{D}'}$  ratios by making use of tabulated values of the standard electrode potentials  $E_{\text{M/S}}^\circ$  and  $E_{\text{M'/S'}}^\circ$ .

### 7.13.3. The Problem with Tables of Standard Electrode Potentials

In consulting tables of standard electrode potentials (see Table 7.23), it is necessary to be aware of an (unfortunate) *difference in conventions* for the *sign* of the  $E^\circ$  values. Consider, e.g., the  $E^\circ$  values for zinc electrodes dipped in  $\text{Zn}^{2+}$  solutions of unit activity and for copper electrodes dipped in  $\text{Cu}^{2+}$  solutions of unit activity. Tables

<sup>100</sup> Compare Eq. (7.280) with (6.18). The potentials that are being added to and subtracted from each side here are the potentials described as constant and arising from the arbitrary designation of the potential of the reference electrode as zero (Section 6.3.4).

<sup>101</sup> To avoid cumbersome notation, it is taken for granted that the standard electrode potential is an *equilibrium* potential and that therefore one can write  $E^\circ$  instead of  $E_e^\circ$ .

**TABLE 7.23**  
**Standard Potentials of Certain Electrode Reactions at 25 °C<sup>a</sup>**

Electrode Reaction	$E^\circ(\text{V})$	Electrode Reaction	$E^\circ(\text{V})$
$\text{Li}^+ + \text{e} \rightleftharpoons \text{Li}$	-3.01	$\text{Cd}^{2+} + 2\text{e} \rightleftharpoons \text{Cd}$	-0.40
$\text{Rb}^+ + \text{e} \rightleftharpoons \text{Rb}$	-2.98	$\text{In}^3 + 3\text{e} \rightleftharpoons \text{In}$	-0.34
$\text{Cs}^+ + \text{e} \rightleftharpoons \text{Cs}$	-2.92	$\text{Tl}^+ + \text{e} \rightleftharpoons \text{Tl}$	-0.34
$\text{K}^+ + \text{e} \rightleftharpoons \text{K}$	-2.92	$\text{Co}^{2+} + 2\text{e} \rightleftharpoons \text{Co}$	-0.27
$\text{Ba}^{2+} + 2\text{e} \rightleftharpoons \text{Ba}$	-2.92	$\text{Ni}^{2+} + 2\text{e} \rightleftharpoons \text{Ni}$	-0.23
$\text{Sr}^{2+} + 2\text{e} \rightleftharpoons \text{Sr}$	-2.89	$\text{Sn}^{2+} + 2\text{e} \rightleftharpoons \text{Sn}$	-0.14
$\text{Ca}^{2+} + 2\text{e} \rightleftharpoons \text{Ca}$	-2.84	$\text{Pb}^{2+} + 2\text{e} \rightleftharpoons \text{Pb}$	-0.13
$\text{Na}^+ + \text{e} \rightleftharpoons \text{Na}$	-2.71	$\text{D}^+ + \text{e} \rightleftharpoons \frac{1}{2}\text{D}_2$	-0.003
$\text{Mg}^{2+} + 2\text{e} \rightleftharpoons \text{Mg}$	-2.38	$\text{H}^+ + \text{e} \rightleftharpoons \frac{1}{2}\text{H}_2$	0.000
$\text{Ti}^{2+} + 2\text{e} \rightleftharpoons \text{Ti}$	-1.75	$\text{Cu}^{2+} + 2\text{e} \rightleftharpoons \text{Cu}$	0.34
$\text{Be}^{2+} + 2\text{e} \rightleftharpoons \text{Be}$	-1.70	$\frac{1}{2}\text{O}_2 + \text{H}_2\text{O} + 2\text{e} \rightleftharpoons 2\text{OH}^-$	0.40
$\text{Al}^{3+} + 3\text{e} \rightleftharpoons \text{Al}$	-1.66	$\text{Cu}^+ + \text{e} \rightleftharpoons \text{Cu}$	0.52
$\text{V}^{2+} + 2\text{e} \rightleftharpoons \text{V}$	-1.5	$\text{Hg}^{2+} + 2\text{e} \rightleftharpoons 2\text{Hg}$	0.80
$\text{Mn}^{2+} + 2\text{e} \rightleftharpoons \text{Mn}$	-1.05	$\text{Ag}^+ + \text{e} \rightleftharpoons \text{Ag}$	0.80
$\text{Zn}^{2+} + 2\text{e} \rightleftharpoons \text{Zn}$	-0.76	$\text{Pd}^{2+} + 2\text{e} \rightleftharpoons \text{Pd}$	0.83
$\text{Ga}^{2+} + 3\text{e} \rightleftharpoons \text{Ga}$	-0.52	$\text{Ir}^{3+} + 3\text{e} \rightleftharpoons \text{Ir}$	1.00
$\text{Fe}^{2+} + 2\text{e} \rightleftharpoons \text{Fe}$	-0.44	$\text{O}_2 + 4\text{H}^+ + 4\text{e}^- \rightleftharpoons 2\text{H}_2\text{O}$	1.23

<sup>a</sup> Although reactions are written as electronation (as recommended by the International Union of Pure and Applied Chemistry), the sign of the standard potential is the same whether electronation or deelectronation is considered (sign invariant).

that follow the *zinc-minus* and *copper-plus* convention report (Table 7.23) that the  $E^\circ$  values for the  $\text{Zn}/\text{Zn}^{2+}$  and  $\text{Cu}/\text{Cu}^{2+}$  electrodes are -0.76 and +0.34 V, respectively. Other tables, particularly those in American textbooks on physical chemistry, follow the *zinc-plus* and *copper-minus* convention and state that the  $E^\circ$  values of  $\text{Zn}/\text{Zn}^{2+}$  and  $\text{Cu}/\text{Cu}^{2+}$  are +0.76 V and -0.34 V respectively. The situation at first appears unlikely because one would think that a standard electrode potential must be an objective fact, not a matter of convention. The situation therefore needs some analysis.

Consider that a cell is set up consisting of an SHE and another electrode, whose standard potential is to be measured. To measure the open-circuit potential of the cell, one can use the Pogendorff compensation method, which consists in applying a potential difference exactly equal and opposed in sign to that produced by the cell itself (see Fig. 7.175). This is effected by adjusting the potentiometer until the galvanometer G shows zero current. The potentiometer reading in such a balanced cell shows then the magnitude of the potential difference across the cell as well as the sign of the charge on the electrode.

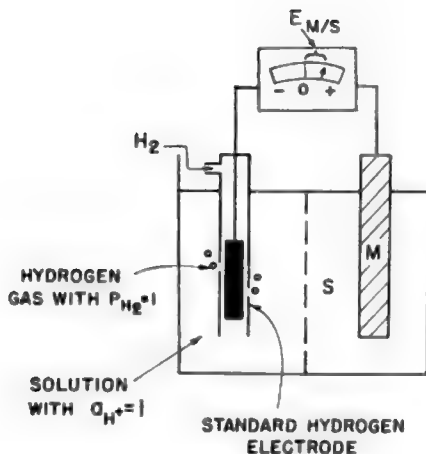
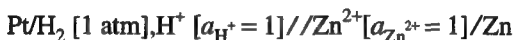
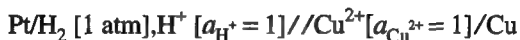


**Fig. 7.175.** The IUPAC convention ascribes to the standard electrode potential the same sign as that experimentally observed when the electrode in question is connected to a cell with the SHE.

These items of information can also be obtained by using a high-input-impedance voltmeter, which, when connected (e.g., across the cell),



shows (1) that the *magnitude* of the potential difference across the cell (i.e., the magnitude of  $E_{\text{Zn}/\text{Zn}^{2+}}^\circ$ ) is 0.76 V and (2) that the zinc electrode is *negative*.<sup>102</sup> A similar measurement across the following cell



indicates that the magnitude of  $E^\circ$  is 0.34 V and that the copper electrode is *positive*.

Now suppose that one decides to affix to the measured magnitude of the  $E_{\text{Zn}/\text{Zn}^{2+}}^\circ$  of a  $\text{Zn}/\text{Zn}^{2+}$  electrode the same sign as the observed polarity of the zinc electrode. Then  $E_{\text{Zn}/\text{Zn}^{2+}}^\circ = -0.76 \text{ V}$ ; and, similarly,  $E_{\text{Cu}/\text{Cu}^{2+}}^\circ = +0.34 \text{ V}$ . It is by this approach that one gets the zinc-minus and copper-plus table. Thus, the rationale behind the zinc-minus-copper-plus convention is based on observed polarities and consequently follows the firmly established electrical convention of assigning the minus

<sup>102</sup>A voltmeter indicates as negative the electrode *from* which electrons flow into the external circuit toward the voltmeter and as positive the electrode *into* which electrons flow from the external circuit.



sign (–) to the electron charge and showing the flow of electrons in an electronic conductor from minus (–) to plus (+).

Note also that if infinitesimally small currents are allowed to flow (see Fig. 7.175) through the galvanometer *G* in one or another direction, (i.e., when the electrode reactions occurring at both electrodes are reversed from their spontaneous direction), the polarity of the electrodes remains unchanged. Thus the sign of the electrode potential remains in this convention invariant, irrespective of whether the electrode processes proceed in the spontaneous or reverse direction, and thus are written as



or



The other convention, called the *American convention*, is based upon the following argument: If a measuring instrument shows the zinc electrode to be negative, it means that the zinc is an electron sink and therefore the site of a spontaneous reaction in which the zinc atoms of the metal transfer electrons to the electrode and become converted into zinc ions. That is, the fact that the zinc electrode is negatively charged implies that the deelectronation reaction  $\text{Zn} \rightarrow \text{Zn}^{2+} + 2\text{e}$  proceeds spontaneously. But if a reaction takes place spontaneously, the corresponding free-energy change  $\Delta G$  must be negative. It is known, however, that  $\Delta G = -nFE$  or  $\Delta G^\circ = -nFE^\circ$  under standard conditions; hence,  $-nFE^\circ$  must be negative, and  $E^\circ$ , positive. Thus, the observed negative polarity of the zinc electrodes suggests that the standard potential for the deelectronation reaction  $\text{Zn} \rightarrow \text{Zn}^{2+} + 2\text{e}$  must be positive, i.e.,  $E^\circ_{\text{Zn}/\text{Zn}^{2+}} = +0.76 \text{ V}$ . The corresponding argument for the  $\text{Cu}/\text{Cu}^{2+}$  electrode suggests that the standard potential for the  $\text{Cu} \rightarrow \text{Cu}^{2+} + 2\text{e}$  reaction must be negative, i.e.,  $E^\circ_{\text{Cu}/\text{Cu}^{2+}} = -0.34 \text{ V}$ . These  $E^\circ$  values corresponding to deelectronations (oxidations), i.e., standard oxidation potentials, are in accordance with the zinc-plus-copper-minus convention, which now appears reasonable from the free-energy point of view.

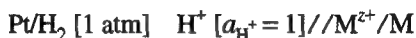
Notice, however, that if the reaction at the  $\text{Zn}/\text{Zn}^{2+}$  interface is reversed and written as an electronation (reduction) rather than a deelectronation, then this electronation does not proceed spontaneously and its free-energy change is positive. This positive value of  $\Delta G^\circ = -nFE^\circ$  implies that  $E^\circ$  must be negative. The standard reduction potentials for the zinc and copper systems are, therefore,  $-0.76$  and  $+0.34 \text{ V}$ , in contrast to the standard oxidation potentials, which are  $+0.76$  and  $-0.34 \text{ V}$ , respectively.

Thus, an unsatisfactory feature of the zinc-plus-copper minus convention has emerged; the sign of the potential varies depending upon whether the electrode reaction is written as an electronation or a deelectronation. *It is a sign-bivariant convention* with respect to the standard potential. In contrast, experiment indicates a unique polarity for an electrode, irrespective of the direction in which the infinitesimally small current is flowing and of the way the interfacial charge-transfer reaction

is written. *The zinc-minus-copper-plus convention is sign invariant* with respect to the potential; this is its distinct advantage.

An important point will now be stressed. If charge-transfer reactions are written as electronations (reductions), e.g.,  $\text{Zn}^{2+} + 2e \rightarrow \text{Zn}$ , the sign of the electrode potential as derived from the free-energy change comes out in agreement with that indicated by the observed polarity of the electrode. This agreement is what prompted the International Union of Pure and Applied Chemistry (IUPAC) to make the following decisions (see Fig. 7.175):

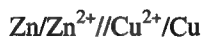
1. The cell implicit in the measurement of a standard electrode potential should be arranged so that the standard hydrogen electrode is on the *left*



2. The measured potential difference across such a cell furnishes the magnitude of the standard electrode potential.
3. The polarity of the electrode on the right, i.e., the sign of the charge on the M electrode, serves to define the sign that is affixed to the  $E^\circ$  value.
4. The charge-transfer reaction implicit in the statement of a standard potential of an  $\text{M}/\text{M}^{z+}$  electrode is an electronation reaction  $\text{M}^{z+} + ze \rightarrow \text{M}$ .

Thus, the IUPAC decision supports the zinc-minus-copper-plus table of standard electrode potentials. The first thing to do, therefore, when consulting a table of standard electrode potentials is to examine the  $E^\circ$  values of the zinc and copper electrodes. If the values are  $-0.76$  and  $+0.34$  V, respectively, the table can be used. If, however, the values are  $+0.76$  and  $-0.34$  V, the convention contravenes the IUPAC decision. To use such a table, one can retain all the magnitudes of the  $E^\circ$  values, but change all the signs of the  $E^\circ$  values; the table will then be in accord with the international convention (Table 7.23).

With this background, consider the calculation of the equilibrium-potential difference  $V_e$  across the cell



According to the international convention, the standard potential of the electrode on the left is always subtracted from that of the right-hand electrode. From Eq. (7.282), one has

$$V_e = \left( E_{\text{Cu}/\text{Cu}^{2+}}^\circ + \frac{RT}{2F} \ln a_{\text{Cu}^{2+}} \right) - \left( E_{\text{Zn}/\text{Zn}^{2+}}^\circ + \frac{RT}{2F} \ln a_{\text{Zn}^{2+}} \right) \quad (7.283)$$

Suppose that a particular table of standard potentials shows that  $E_{\text{Zn}/\text{Zn}^{2+}}^\circ = +0.76$  V and  $E_{\text{Cu}/\text{Cu}^{2+}}^\circ = -0.34$  V. These values are not consistent with the internationally

accepted zinc-minus-copper-plus convention, and therefore the signs are changed to read  $E_{\text{Zn}/\text{Zn}^{2+}}^{\circ} = -0.76$  and  $E_{\text{Cu}/\text{Cu}^{2+}}^{\circ} = +0.34$  V. With these values, the equation becomes

$$V_e = 1.10 + \frac{RT}{2F} \ln \frac{a_{\text{Cu}^{2+}}}{a_{\text{Zn}^{2+}}} \quad (7.284)$$

Now assume that  $a_{\text{Cu}^{2+}}/a_{\text{Zn}^{2+}} = 1$ . Then,  $V_e^{\circ} = 1.10$  V, which means that the copper electrode is positive with respect to the zinc electrode; the sign of the potential difference across a cell corresponds to the polarity of the electrode on the right. For ratios of  $a_{\text{Zn}^{2+}}/a_{\text{Cu}^{2+}}$  other than unity, one can calculate  $V_e$  from Eq. (7.284).

A simple way of visualizing the procedure is to represent all equilibrium potentials on a single vertical axis (Fig. 7.176). Corresponding to any activity ratio  $a_A/a_D$ , there is an equilibrium electrode potential for the interface relative to the SHE. The same is true for the other activity ratio  $a'_A/a'_D$ . Thus, the separation between any two points yields the potential difference across a cell, with the activity ratios corresponding to the points.

### 7.13.4. Are Equilibrium Cell Potential Differences Useful?

There is an important piece of information that emerges from the calculation of the equilibrium cell potential. For example, if unit activities of  $\text{Zn}^{2+}$  and  $\text{Cu}^{2+}$  are taken, it has been found (Section 7.13.3) that the potential difference across the Daniel cell (Fig. 7.2) is

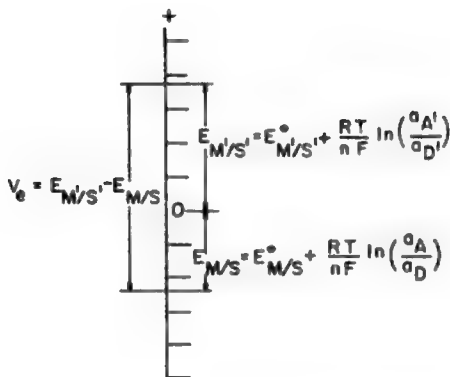


**Fig. 7.176.** Since each electrode potential is referred to the hydrogen scale, the cell voltage, which is equal to the difference in the two electrode potentials, is given by the separation  $V_e$ .

$$V_e^\circ = E_{\text{Cu}/\text{Cu}^{2+}}^\circ - E_{\text{Zn}/\text{Zn}^{2+}}^\circ = 1.1 \text{ V}$$

i.e., the right-hand electrode, copper, is positive with respect to the zinc electrode (Fig. 7.177).

What is the implication of the zinc electrode's being negative and the copper electrode's being positive? It means that relative to the copper electrode, the zinc electrode is negatively charged or bursting with excess electrons, and relative to the zinc electrode, the copper electrode is positively charged or starved of electrons. Hence, when an external electron path (or circuit) is provided, electrons tend to flow out from the zinc electrode, through the external circuit, and into the copper (Fig. 7.178). Thus there tends to be a net deelectronation current  $\text{Zn} \rightarrow \text{Zn}^{2+} + 2e$  at the  $\text{Zn}/\text{Zn}^{2+}$  interface and a net electronation current  $\text{Cu}^{2+} + 2e \rightarrow \text{Cu}$  at the  $\text{Cu}/\text{Cu}^{2+}$

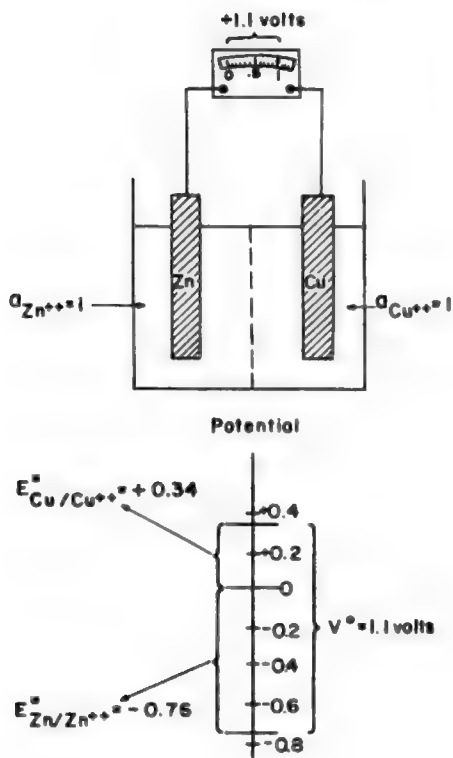


**Fig. 7.177.** In the Daniel cell, the zinc electrode is 1.1 V negative with respect to the copper electrode.

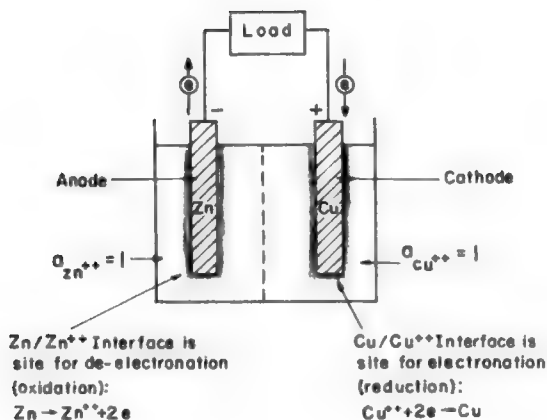
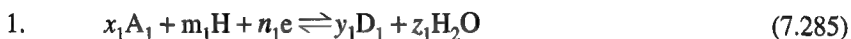


**Fig. 7.178.** The sign of the voltage on the Daniel cell indicates that upon placing a load on the cell, a spontaneous deelectronization will occur on the zinc electrode, and electronation will occur on the copper electrode.

interface. Hence, the zinc electrode tends to function spontaneously as an electron sink and the copper as an electron source electrode.

An interesting result has emerged. When a  $Zn/Zn^{2+}$  interface and a  $Cu/Cu^{2+}$  interface are built into an electrochemical cell or system, one can proceed from the equilibrium electrode potentials and the zero-current cell potential to predict at which interface there will be a tendency for deelectronation (oxidation) and at which a tendency for electronation (reduction), i.e., which electrode will function as the electron source and which as the electron sink.

The result can in fact be generalized. Suppose any two electron-transfer reactions taking place at separated interfaces in a cell are considered (Fig. 7.179)



and



Further, let the equilibrium electrode potentials  $E_{e,1}$  and  $E_{e,2}$  for the two reactions be such that  $E_{e,1}$  is positive with respect to  $E_{e,2}$ . Then there will be a tendency for deelectronation at the electrode that is the site of reaction 2, i.e., electrode 2 will tend to be the electron sink for  $D_2$  and  $H_2 O$ . Correspondingly, there will be a tendency for

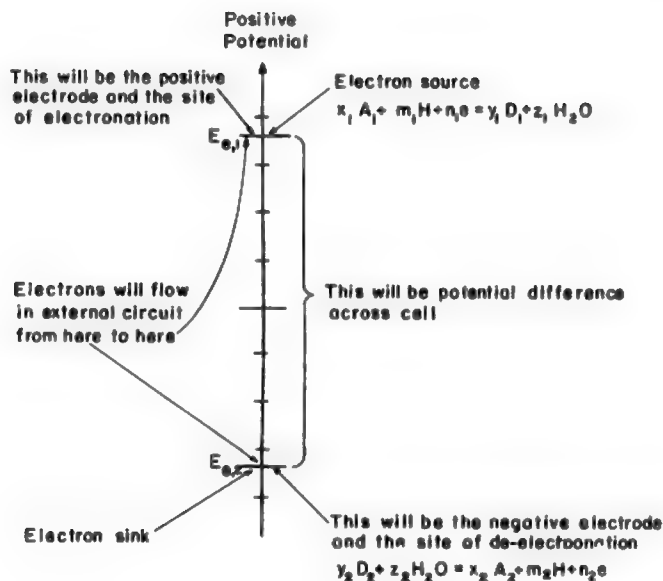


**Fig. 7.179.** A general situation of the potentials of two electrodes connected to a cell and the sites for spontaneous reactions.

electronation at the positive electrode 1, which will tend to be the electron source for  $A_1$  particles.

Thus, the tables of standard electrode potentials predict those processes that tend to occur spontaneously if any pair of listed interfacial systems are built into an electrochemical cell; that with the lower (algebraically, i.e., more negative) standard potential will spontaneously undergo deelectronation (oxidation), while that with the higher potential (i.e., more positive) will spontaneously undergo electronation (reduction).

In this book, the electrode from which electron acceptors in the solution accept electrons has been termed the *electron-source electrode*, and the electrode that receives electrons from electron donors has been termed the *electron-sink electrode*. The conventional terms, introduced by Faraday upon a suggestion by the Reverend Whewell, for an electron-source electrode and an electron-sink electrode are *cathode* and *anode*, respectively.

Consider a driven cell, or substance producer (Fig. 7.180). To make an electronation reaction proceed at a particular electrode, it must function as an electron source for electron acceptors in solution, and must therefore receive an electron flow through the conductor from the power supply. But the terminal of the power supply that pushes out an electron stream is the negative terminal. Thus, to ensure that an electrode

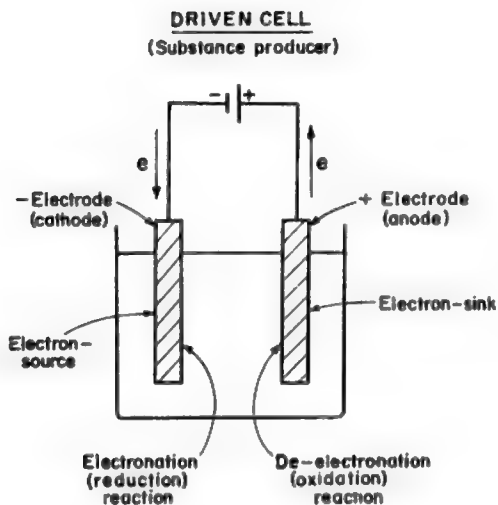


**Fig. 7.180.** In a substance producer, the cathode must be connected to the negative terminal and the anode to the positive terminal of a power supply.

functions as an electron source, or cathode, in an electronation reaction, the electrode must be connected to the negative terminal of the power supply. Similarly, to make an electrode function as an electron sink, or anode, in a deelectronation reaction, the electrode must be connected to the positive terminal of the power supply.

It is important to remember that these terms are connected with the *direction* in which the electrode reaction proceeds and *not* with the electrode interface. Thus, e.g., the  $\text{Zn}/\text{Zn}^{2+}$  interface in a *self-driven electrochemical cell* is an electron sink (anode) since the reaction that is proceeding there is deelectronation  $\text{Zn} \rightarrow \text{Zn}^{2+} + 2e^-$ . By forcing the reaction to proceed in the reverse direction, i.e.,  $\text{Zn}^{2+} + 2e^- \rightarrow \text{Zn}$ , one would make it an electron source (cathode). This can be done by introducing a power supply in the external circuit and thus building a *driven cell*, or substance producer (Fig. 7.180).

On this basis, the terms “anode” and “cathode” have often been taken to signify the positive and negative electrodes, respectively. This conclusion is erroneous since it is only in a driven cell that the cathode is the negative electrode and the anode the positive electrode, as may be shown by considering a self-driving cell or energy producer (Fig. 7.181). In such a cell, the negative electrode is that electrode which serves as an electron sink (anode) with respect to electron donors in the solution; and the positive electrode is that electrode which works as an electron source (cathode) for an electronation reaction. Thus, in a self-driven cell, the anode is the negative terminal

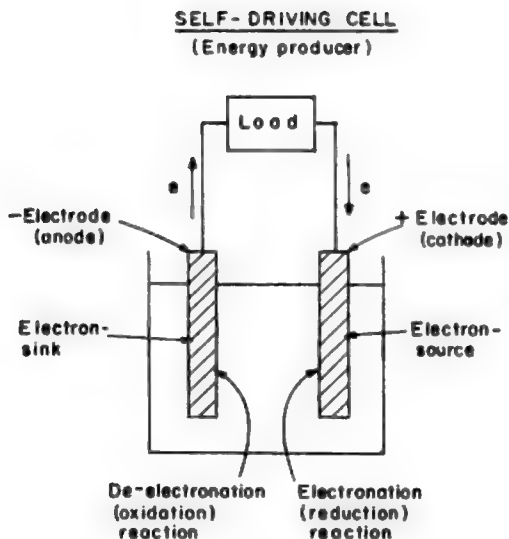


**Fig. 7.181.** In a self-driving cell, the negative electrode is the anode, or an electron sink for deelectronation, and the positive electrode is the cathode, or an electron source for the electronation reaction.

of the cell and the cathode the positive terminal, a situation that is precisely the opposite of that which obtains in an externally driven cell. It is important, therefore, to remember that the terms anode and cathode are connected with the *nature of the reaction* (deelectronation or electronation) at the electrode, and not with its polarity.

### 7.13.5. Electrochemical Cells: A Qualitative Discussion of the Variation of Cell Potential with Current

As long as one is making predictions on the basis of equilibrium cell potentials, one can talk only of tendencies for deelectronation and electronation at the interfaces. Once the system spontaneously drives a current through the external load, the current density at each interface will set up a current-produced potential (i.e., an overpotential)  $\eta$ . What effect will the overpotentials at the two electrodes have on the cell potential  $V$ , an increase or decrease in it? To answer that question, one has to abandon the Nernst framework of equilibrium potentials and think in the Butler-Volmer framework of electrodics.

It is easy to see in a qualitative fashion what happens when an energy-producing, spontaneously acting cell drives a current through an external load. Consider the electron-sink electrode or anode. At its interface with the electrolyte, a net deelec-



tronation current density will flow. The Butler–Volmer equation for the overall reaction at the electron-sink electrode is<sup>103</sup> [see Sections 7.6 and 7.10 and Eq. (7.142)]

$$i_{\text{si}} = \overleftarrow{i}_{\text{si}} - \overrightarrow{i}_{\text{si}} \quad (7.287)$$

$$i_{\text{si}} = i_{0,\text{si}} (e^{\overleftarrow{\alpha}_{\text{si}} F \eta_{\text{si}} / RT} - e^{-\overrightarrow{\alpha}_{\text{si}} F \eta_{\text{si}} / RT}) \quad (7.288)$$

where the subscript si indicates that the electron-sink electrode is being considered. For there to be a *net* deelectronation current density, the first term  $\overleftarrow{i}_{\text{si}}$ , arising from the deelectronation current density (not the *net* current density) at the sink electrode has to be larger than the second term  $\overrightarrow{i}_{\text{si}}$  due to the electronation current density at the same electrode. This requires that  $\eta$  be positive. But

$$\eta_{\text{si}} = \Delta\phi_{\text{si}} - \Delta\phi_{e,\text{si}} = E_{\text{si}} - E_{e,\text{si}} \quad (7.289)$$

where  $\Delta\phi_{\text{si}}$  and  $\Delta\phi_{e,\text{si}}$  are the absolute Galvani potential differences across the interface when a current density  $i$  is passing and when there is equilibrium, and  $E_{\text{si}}$  and  $E_{e,\text{si}}$  are the corresponding relative electrode potentials. Hence,

$$E_{\text{si}} > E_{e,\text{si}} \quad \text{for} \quad i_{\text{si}} > \overrightarrow{i}_{\text{si}} \quad (7.290)$$

This means that the flow of a current through an external load makes the potential of the electron-sink electrode climb in the positive direction (Fig. 7.182).

Similarly, at the electron-source (so) electrode or cathode, the condition for net electronation is

$$\overleftarrow{i}_{\text{so}} < \overrightarrow{i}_{\text{so}} \quad (7.291)$$

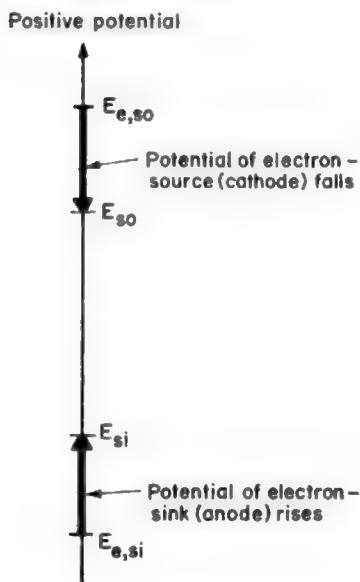
i.e.,

$$\eta_{\text{so}} = -ve \quad (7.292)$$

or

$$E_{\text{so}} < E_{e,\text{so}} \quad (7.293)$$

<sup>103</sup>When one is considering a single interface, there is no ambiguity regarding the interface at which there is a net current density  $i = \overleftarrow{i} - \overrightarrow{i}$ . Here, cells consisting of two interfaces are being discussed. Hence, there are net current densities at two electrodes that must be distinguished by subscripts to indicate which is the electron sink and which is the source.

**ENERGY PRODUCER**

**Fig. 7.182.** When a self-driving cell delivers current to an external load, the potential of the electron sink shifts in the positive direction, while that of the electron source shifts negatively. The net result is a decrease in the cell potential compared with that at an open circuit.

Thus, to drive a current through the external circuit, the potential of the electron sink has to become more positive and that of the electron source more negative (Fig. 7.182). But under zero-current, or equilibrium, conditions, the electrode that tends to be a sink is negative with respect to the electrode that tends to be a source. This means that in the course of driving a current, the potentials of the two electrodes climb toward each other; *the cell potential decreases with cell current in a self-driving cell.*

If it is recalled that on a purely thermodynamic basis, any cell that has a tendency to drive a current through an external load seems capable of being harnessed as an *energy-producing device*, then the conclusion just reached is serious, for it bears the following implication: In the development of an energy-producing device, the variation of cell potential with cell current is as important as, if not more important than,

its open-circuit or equilibrium potential. What is the use of a device, the equilibrium potential of which offers big hope but which decays drastically the moment one tries to draw some current from it?<sup>104</sup> *The crucial problem, therefore, is the quantitative relation between cell potential  $V$  and the actual cell current passed through a load  $I$ .* If it turns out that the fall in potential with current is small, then the actual potential of the cell *in action* at a significant current density is not much different from the theoretical open-circuit potential and the system offers hope of being a good energy producer.

A qualitative understanding of the change of cell potential with current in the case of driven electrochemical systems (*substance producers*) can be developed on similar lines. Here, an external current source has to *oppose* the spontaneous current flow from the cell. That means that it has to promote a net electronation reaction at the electrode that would tend to run spontaneously as a sink and a net deelectronation at the electrode that would tend to be a source.

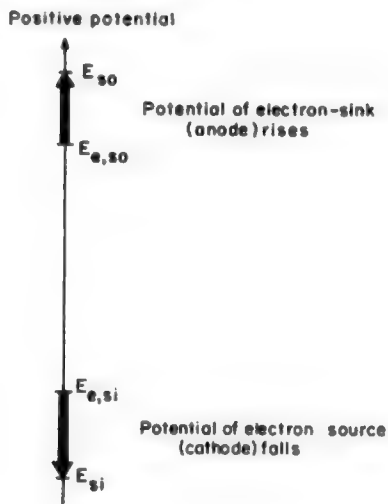
This thinking is based on from the fact that the equilibrium condition ( $i = 0 = \overleftarrow{i} - \overrightarrow{i}$  or  $\overleftarrow{i} = \overrightarrow{i}$  when  $\eta = 0 = E - E_e$  or  $E = E_e$ ) demarcates the regions of the  $i$  vs.  $\eta$  curve where net deelectronation occurs ( $i > 0$  or  $\overleftarrow{i} > \overrightarrow{i}$  when  $\eta > 0$  or  $E > E_e$ ) from the region where net electronation occurs ( $i < 0$  or  $\overleftarrow{i} < \overrightarrow{i}$  when  $\eta < 0$  or  $E < E_e$ ). This means (Fig. 7.183) that the electrode that will function as a source must be driven to more negative potentials ( $E < E_e$ ), and the other electrode, which at equilibrium sits at more positive potentials, must be driven more positive ( $E > E_e$ ). The result is that *the cell potential increases with current in a driven cell*, i.e., it opposes the external cell increasingly as the cell current increases (Fig. 7.184). But how much? One cannot answer this question until one has worked out the quantitative relation between cell potential and current.

### 7.13.6. Electrochemical Cells in Action: Some Quantitative Relations between Cell Current and Cell Potential

At the outset, consider a self-driving, or energy-producing, cell with two interfaces 1 and 2, and let the equilibrium electrode potentials on the hydrogen scale be  $E_{e,1}$  and  $E_{e,2}$ . Suppose  $E_{e,1}$  is more positive than  $E_{e,2}$ . Then, if an external load is provided, electrode 2 will tend to be an electron sink for a net deelectronation reaction and electrode 1 will tend to be an electron source for a net electronation reaction.

If interface 2 is far from equilibrium, one can use the simple one-term exponential form of the current density-potential law (see Eq. (7.31))

<sup>104</sup>In the preelectrode days, essentially before 1950, the attitude of most workers toward electrochemical cells was such that mainly the thermodynamic and diffusion aspects were important. When the cell potentials decreased as the power drawn from them increased, the causes were sought in special phenomena such as *gas layers* on the electrode. The general character of such a decrease, above all its relation to bonding between substrate and reactant and to electrocatalysis (Section 7.11.1), was not realized.

SUBSTANCE PRODUCER

**Fig. 7.183.** When a substance producer is driven at an appreciable rate, the electron sink potential becomes more positive and the electron-source potential becomes more negative. The net result is an increase in the cell potential compared with that at an open circuit.

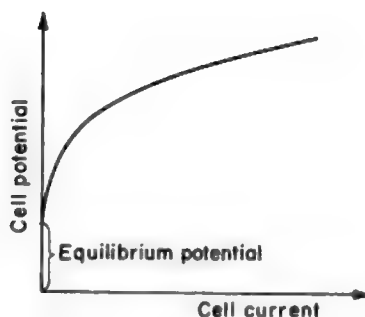


**Fig. 7.184.** The higher the current driven through a substance producer, the larger will be the cell potential opposing the driving cell potential.

$$i_2 = i_{0,2} e^{\tilde{a}_2 F \eta_2 / RT} \quad (7.294)$$

or

$$i_2 = i_{0,2} e^{\eta_2 / \tilde{\lambda}_2} \quad (7.295)$$

where  $\tilde{\lambda}_2$  is the slope of the  $\eta_2$  vs.  $\ln i$  curve and is given by

$$\tilde{\lambda}_2 = \frac{RT}{\tilde{a}_2 F} \quad (7.296)$$

By taking logarithms in Eq. (7.295), the result is

$$\eta_2 = \ln(i_2)^{\tilde{\lambda}_2} - \ln(i_{0,2})^{\tilde{\lambda}_2} \quad (7.297)$$

Similarly, if one assumes that the electronation reaction at interface 1 is far from equilibrium, then since by convention a net electronation current is negative, one has<sup>105</sup>

$$-i_1 = -i_{0,1} e^{-\vec{\alpha}_1 F \eta_1 / RT} \quad (7.298)$$

or

$$i_1 = -i_{0,1} e^{-\eta_1 / \vec{\lambda}_1} \quad (7.299)$$

where

$$\vec{\lambda}_1 = \frac{RT}{\vec{\alpha}_1 F} \quad (7.300)$$

Taking logarithms in Eq. (7.299)

$$\eta_1 = -\ln(i_1)^{\vec{\lambda}_1} + \ln(i_{0,1})^{\vec{\lambda}_1} \quad (7.301)$$

From these relations (7.301) and (7.297) between the current densities  $i_1$  and  $i_2$  and the overpotentials  $\eta_1$  and  $\eta_2$ , at the two electrodes, one has to develop a relation between the current  $I$  flowing through the cell and the potential difference  $V$  across it. This is done in the following way: Since

---

<sup>105</sup>Note that in the electronation reaction,  $\eta$  is a negative quantity.

$$\eta_1 = E_1 - E_{e,1} \quad (7.302)$$

and

$$\eta_2 = E_2 - E_{e,2} \quad (7.303)$$

it is clear that

$$\eta_1 - \eta_2 = (E_1 - E_2) - (E_{e,1} - E_{e,2}) \quad (7.304)$$

But

$$E_1 - E_2 = V \quad (7.305)$$

and

$$E_{e,1} - E_{e,2} = V_e \quad (7.306)$$

Hence,

$$\eta_1 - \eta_2 = V - V_e \quad (7.307)$$

Or

$$V = V_e + \eta_1 - \eta_2 \quad (7.308)$$

Now one must use Eqs. (7.301) and (7.297) to substitute for  $\eta_1$  and  $\eta_2$ . The result is

$$\begin{aligned} V &= V_e - \ln (i_1)^{\vec{\lambda}_1} + \ln (i_{0,1})^{\vec{\lambda}_1} - \ln (i_2)^{\vec{\lambda}_2} + \ln (i_{0,2})^{\vec{\lambda}_2} \\ &= V_e - \ln [(i_1)^{\vec{\lambda}_1} (i_2)^{\vec{\lambda}_2}] + \ln [(i_{0,1})^{\vec{\lambda}_1} (i_{0,2})^{\vec{\lambda}_2}] \end{aligned} \quad (7.309)$$

One still has to transform the current densities into the currents. This is done by recalling that the total *current*  $I_1$  (not current density!) flowing through electrode 1 is equal to the current  $I_2$  through electrode 2, i.e.,

$$I = I_1 = I_2 \quad (7.310)$$

Further, the current density at each electrode is obtained by dividing the total current by the area  $A$  of the interface, i.e.,

$$i_1 = \frac{I}{A_1} \quad \text{and} \quad i_2 = \frac{I}{A_2} \quad (7.311)$$

Combining Eqs. (7.311) and (7.309), one obtains

$$V = V_e - \ln \left[ \frac{I^{\vec{\lambda}_1 + \vec{\lambda}_2}}{A_1^{\vec{\lambda}_1} A_2^{\vec{\lambda}_2}} \right] + \ln [(i_{0,1})^{\vec{\lambda}_1} (i_{0,2})^{\vec{\lambda}_2}] \quad (7.312)$$

This is the general  $I$  vs.  $V$  relation for a cell when there is activation overpotential at the two interfaces, and the  $i$  vs.  $\eta$  relation is taken to be exponential in form. A special case of (7.312) results from assuming electrodes of unit area, i.e.,

$$A_1 = A_2 = 1 \quad (7.313)$$

Then if one uses the following notation,

$$\vec{\lambda}_1 + \vec{\lambda}_2 = q \quad (7.314)$$

and

$$i_{0,\text{cell}}^q = (i_{0,1})^{\vec{\lambda}_1} (i_{0,2})^{\vec{\lambda}_2} \quad (7.315)$$

Eq. (7.312) reduces to

$$V = V_e - \ln I^q + \ln (i_{0,\text{cell}})^q \quad (7.316)$$

or

$$I = i_{0,\text{cell}} e^{-(V-V_e)/q} \quad (7.317)$$

This is an interesting result. First, when the  $i$  vs.  $\eta$  relations at the two electrodes are of the exponential form, then the  $I$  vs.  $V$  relation for the whole cell is also of the exponential form. Second, under these conditions, a plot of what might be called the cell overpotential  $V - V_e$  vs.  $\log I$  should be a straight line (Fig. 7.185). That is, when both the individual interfaces show Tafel behavior, the whole cell shows Tafel behavior. Finally, there is, in the expression for the current-potential relation (7.317) for the whole cell, a quantity  $i_{0,\text{cell}}$  analogous to the equilibrium exchange current density  $i_0$  for a single interface. The quantity  $i_{0,\text{cell}}$  is obtained by extrapolating the  $V - V_e$  vs.  $\log I$  curve back to the equilibrium cell potential  $V_e$ , i.e.,  $V - V_e = 0$ .

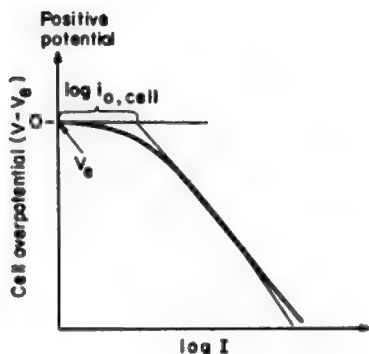


**Fig. 7.185.** In a self-driving cell, the plot of cell overpotential vs. log cell current density should be a straight line if the charge transfers at both electrodes are both rate controlling and valid under the high-field approximation. An apparent  $i_0$  for the cell as a whole can be deduced.

The form of the  $I$  vs.  $V$  relation (7.317) for a cell, which has just been derived, depends upon the assumption that the activation overpotentials  $\eta_1$  and  $\eta_2$  at the two interfaces have pushed the  $i$  vs.  $\eta$  curves into the exponential region. If, instead, the two interfaces are showing ohmic behavior, then one has from Eq. (7.308) and linear  $i$  vs.  $\eta$  relations (7.25):

$$\begin{aligned}
 V &= V_e + \eta_1 - \eta_2 \\
 &= V_e - \frac{RT}{\alpha_1 F} \frac{i_1}{i_{0,1}} - \frac{RT}{\alpha_2 F} \frac{i_2}{i_{0,2}} \\
 &= V_e - I \left( \frac{\vec{\lambda}_1}{A_1 i_{0,1}} + \frac{\vec{\lambda}_2}{A_2 i_{0,2}} \right)
 \end{aligned} \tag{7.318}$$

Thus, when the  $i$  vs.  $\eta$  relations at the two interfaces are linear, the cell potential  $V$  is a linear function of the cell current  $I$ .

There are many ways in which one can go on to make the above  $I$  vs.  $V$  laws for cells more realistic. At the outset, it is necessary to free the treatment from the



assumption that there is no potential drop in the solution due to the passage of current. The potential difference  $S_1 \Delta S_2 \phi$  in the solution is introduced in a straightforward way:

$$V = V_e + \eta_1 - \eta_2 - S_1 \Delta S_2 \phi \quad (7.319)$$

and, since

$$S_1 \Delta S_2 \phi = IR \quad (7.320)$$

where  $R$  is the resistance of the electrolyte,

$$V = V_e + \eta_1 - \eta_2 - IR \quad (7.321)$$

Now the overpotentials  $\eta_1$  and  $\eta_2$  are the total overpotentials at the two interfaces. They must include the activation overpotentials  $\eta_a$  and concentration overpotentials  $\eta_c$ . Thus, Eq. (7.321) can be written

$$V = V_e + \eta_{a,1} + \eta_{c,1} - \eta_{a,2} - \eta_{c,2} - IR \quad (7.322)$$

So, if there are mass-transport limitations on the concentrations of the species involved in the reactions at the two electrodes, expressions for  $\eta_{c,1}$  and  $\eta_{c,2}$  must be introduced. Thus, one can write

$$V = V_e + \eta_{a,1} - \frac{RT}{zF} \ln \left[ 1 - \frac{i_1}{i_{L,1}} \right] - \eta_{a,2} - \frac{RT}{zF} \ln \left[ 1 - \frac{i_2}{i_{L,2}} \right] - IR \quad (7.323)$$

These are matters of detail that will also be discussed more thoroughly in the sections on energy conversion (Chapter 13).

The fundamental point is that in a self-driving cell (Fig. 7.185)—the case treated above—all the terms on the right-hand side of Eq. (7.323) make the cell potential  $V$  at a current  $I$  less than the equilibrium potential  $V_e$ . In a driven cell with (Fig. 7.184)

$$V = V_e + \eta_{a,1} + \eta_{c,1} - \eta_{a,2} - \eta_{c,2} + IR \quad (7.324)$$

all the terms on the right-hand side make  $V$  greater than  $V_e$ . Thus, in a self-driving cell,<sup>106</sup> or energy producer, the equilibrium potential is the *maximum* cell potential, and, in a driven cell, or substance producer, the equilibrium potential is the *minimum* cell potential—compare Fig. 7.184 (a driven cell) with Fig. 7.185 (a self-driving cell).

<sup>106</sup>The existence of self-driving electrochemical mechanisms (i.e., chemical systems that spontaneously produce electrical power) is a concept that has so far been completely neglected in general chemistry (although it has been applied in fuel cells). It may find significant application in biochemistry (Chapter 14).

## 7.14. THE ELECTROCHEMICAL ACTIVATION OF CHEMICAL REACTIONS

A net flow of electrons occurs across the metal/solution interface in a normal electrode reaction. The term “electrocatalysis” is applied to working electrodes that deliver large current densities for a given reaction at a fixed overpotential. A different, though indirectly related, effect is that in which catalytic events occur in a *chemical* reaction at the *gas/solid* interface, as they do in heterogeneous catalysis, though the arrangement is such that the interface is subject to a variation in potential and the rate depends upon it.

To observe such a phenomenon, one needs a solid electrolyte, i.e., a solid in which there is anionic or cationic mobility at some temperature between that of the ambient and, say, 1300 °C. On each side of the solid electrolyte (e.g.,  $\text{Y}_2\text{O}_3^-$  doped  $\text{ZrO}_2$ ), there is an electrode connected to a power source. One electrode acts as a counter-electrode. The other electrode (the catalyst, e.g., Pt, Rh, Ag) is a working electrode (in respect to the normal electrochemical working of the cell involving the “solution”  $\text{ZrO}_2$  and the counter-electrode) but it also has a second function, one of catalysis of a surface chemical reaction occurring on the side of it that is not in contact with  $\text{ZrO}_2$ . Thus it is found that if two gaseous reactants are brought into contact with the outer surface of this working electrode, the rate of the reaction between the gaseous reactants depends on the potential of the electrode. However, the catalytic effect on the gas reaction is not directly connected with the electrochemical reaction occurring in the cell (the chemical reaction catalyzed occurs much faster than any reaction there). For this reason, the effect has attracted to itself a descriptive name: non-Faradaic electrochemical modification of catalytic activity, or NEMCA (Vayenas, 1988). The basic setup is shown in Table 7.24.

When an external potential is applied to the cell described above, the expected charge-transfer reactions occur at the interfaces and current flows throughout the cell. The point is, however, that in addition to these normal events, the rate of the *gas phase chemical reaction*, e.g.,  $\text{C}_2\text{H}_4 + 3\text{O}_2 \rightarrow 2\text{CO}_2 + 2\text{H}_2\text{O}$ , is unexpectedly changed (i.e., accelerated or diminished in rate) by changing the potential of the working electrode.

Thus, the rate of this chemical reaction at the gas/metal interface may be increased as much as 100 times. To be certain that the effect is *not* a part of the electrochemical

**TABLE 7.24**  
**Setup for a NEMCA Experiment**

Gaseous reactants (e.g., $\text{C}_2\text{H}_4 + \text{O}_2$ )	Catalyst working electrode (e.g., Pt, Rh, Ag)	Solid electrolyte (e.g., $\text{ZrO}_2$ - $\text{Y}_2\text{O}_3$ )	Counter-electrode (e.g., Pt)	Auxiliary gas (e.g., $\text{O}_2$ )
---	---	--	------------------------------	-------------------------------------

**TABLE 7.25**  
**Electrochemical Promotional NEMCA Studies**

Reactants	Products	Catalyst	Electrolyte	T(°C)
<b>I. Electrophobic reactions</b>				
C <sub>2</sub> H <sub>4</sub> , O <sub>2</sub>	CO <sub>2</sub>	Pt	YSZ (O <sup>2-</sup> )	260–450
CO, O <sub>2</sub>	CO <sub>2</sub>	Pt	YSZ (O <sup>2-</sup> )	300–550
H <sub>2</sub> S	S <sub>x</sub> , H <sub>2</sub>	Pd	YSZ (O <sup>2-</sup> )	600–750
H <sub>2</sub> , O <sub>2</sub>	H <sub>2</sub> O	Pt	Nafion (H <sup>+</sup> )	25
C <sub>2</sub> H <sub>4</sub> , O <sub>2</sub>	CO <sub>2</sub>	Pt	TiO <sub>2</sub> (TiO <sub>x</sub> <sup>+</sup> , O <sup>2-</sup> )	450–600
<b>II. Electrophilic reactions</b>				
C <sub>2</sub> H <sub>6</sub> , O <sub>2</sub>	CO <sub>2</sub>	Pt	YSZ (O <sup>2-</sup> )	270–500
CH <sub>3</sub> OH, O <sub>2</sub>	H <sub>2</sub> CO, CO <sub>2</sub>	Pt	YSZ (O <sup>2-</sup> )	300–550
CH <sub>4</sub> , O <sub>2</sub>	CO <sub>2</sub>	Au	YSZ (O <sup>2-</sup> )	700–750
C <sub>2</sub> H <sub>4</sub> , NO	CO <sub>2</sub> , N <sub>2</sub>	Pt	β''-Al <sub>2</sub> O <sub>3</sub> (Na <sup>+</sup> )	400

reaction occurring in the cell involving the metal/solid electrolyte interface, it is enough to note that the chemical reaction rate may be as much as  $3 \times 10^5$  greater than the rate at which O<sup>2-</sup> is transported through the solid electrolyte. Table 7.25 contains examples of chemical reactions that have been catalyzed in this electrochemical (non-Faradaic) way. Note the abbreviation YSZ = yttria-stabilized zirconia.

Figure 7.186 shows a schematic representation of the active part of a NEMCA setup. The detailed mechanism by which these effects occur needs further mechanistic

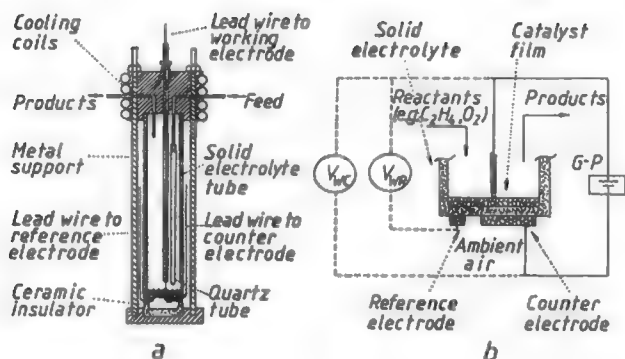


**Fig. 7.186.** Reactor cell (a) and electrode configuration (b) for NEMCA studies using the fuel-cell type design, G-P, galvanostat-potentiostat. (Reprinted with permission from C. G. Vayenas, S. Bebelis, I. V. Yentekakis and H. Glintz, *Catalysis Today* 11: 303, 1992.)

research. However, the principles of an explanation can be understood with the help of Fig. 7.187.

When ions migrate through a solid electrolyte, they diffuse from this onto the gas-exposed surface of the metal electrode. These ions form a double layer (and hence a potential difference) at the metal/gas interface. However, this potential difference (which varies with the electrode potential) in turn changes the work function at the gas/metal interface. The ease of availability of electrons in the bonding of radicals adsorbed from the gas phase onto the electrode increases as the electronic work function of the solid decreases. The chemical reaction rate of the catalyzed reaction depends on the bonding strength of these radicals to the electrode catalyst, which involves electrons from the metal and is therefore dependent on the work function of the metal; this itself is a function of the electrode potential. In this way, a dependence of the rate of the chemical reaction upon the potential of the working electrode can be rationalized.

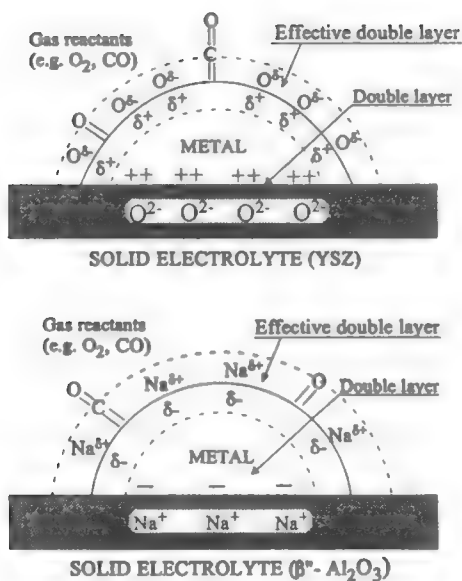


**Fig. 7.187.** Schematic representations of a metal electrode deposited on an  $O^{2-}$ -conducting and on an  $Na^+$ -conducting solid electrolyte, showing the location of the metal-electrolyte double layer and of the effective double layer created at the metal/gas interface due to potential-controlled ion migration (back-spillover). (Reprinted with permission from S. Bebelis, I. V. Yantekakis, and H. G. Lintz, *Catalysts Today* 11: 303, 1992.)

## Further Reading

### Seminal

1. C. Wagner, "Electrolytic Transport of Ions Through Solids," *Adv. Catalysis* **21**: 323 (1970).
2. C. G. Vayenas and H. M. Saltzburg, "Electrochemical Promotion of Chemical Catalysis," *J. Catal.* **57**: 296 (1979).
3. J. Pritchard, "Chemical Catalysts, Electrochemically Caused," *Nature* **343**: 592 (1990).

### Review

1. C. G. Vayenas, M. M. Jaksic, S. I. Bebelis, and S. G. Neophytides, "The Electrochemical Activation of Catalytic Reactions," in *Modern Aspects of Electrochemistry*, J. O'M. Bockris, B. E. Conway, and R. E. White, eds., Vol. 29, p. 57, Plenum, New York (1996).

## 7.15. ELECTROCHEMICAL REACTIONS THAT OCCUR WITHOUT INPUT OF ELECTRICAL ENERGY

### 7.15.1. Introduction

In this book—Chapters 7 and 13—it is demonstrated that there are three types of electrochemical systems. In that most featured, one puts *in* electricity from an outside source and gets *out* substances by forcing a chemical reaction to occur against its free energy gradient (e.g., the electrochemical splitting of water against the tendency of  $\text{H}_2$  and  $\text{O}_2$  to combine). In a type of device less often featured, one puts *in* substances (a fuel for one electrode and oxygen at the other) and gets *out* electricity (first fuel cell principle). The reaction in the cell occurs spontaneously and there is a by-product, the substance produced, as well as the intended product, electricity (second fuel cell principle). The obvious example is the reverse of the last one, and if hydrogen and oxygen are fed to the cell, water and electricity are the result. Now, a third kind of electrochemical device does exist and here one puts in no fuel—nor drives anything with electricity, yet useful<sup>107</sup> electrochemical things happen.

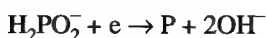
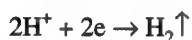
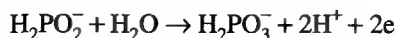
### 7.15.2. Electroless Metal Deposition

It has been known for more than half a century (Brenner and Riddell, 1944) that nickel plating can be made to occur without an external electrical power source. All one needs is a conducting substrate (the object to be plated) and a solution that must contain a nickel salt and some solute which, under the circumstances offered, undergoes electrochemical oxidation on the substrate. It is better to have an "activator," too, e.g., a small patch of a metal catalyst, such as palladium.

---

<sup>107</sup>Not useful things also happen, as in corrosion (Chapter 12).

In essence, what happens is that a substance present in solution (hypophosphate, say) gets electrochemically oxidized and in this process puts some electrons into the metallic catalyst patch, and these electrons then serve to neutralize the  $\text{Ni}^{2+}$  ions in solution and deposit nickel on the substrate. However, some phosphorus is built into the deposit also, and hydrogen is co-evolved along with the deposition of nickel cobalt. Hence, it seems reasonable to write the reactions thus:



A better way to understand all this is to look at Fig. 7.188.

The plating out of cobalt and nickel without the use of an outside power source is an example of a class of processes called *electroless*. In principle, any metal can be electrolessly plated out. A good example is the "gold dip." This is a solution containing auric chloride and an easily oxidizable organic. To give some metallic object a golden sheen (about  $1\ \mu$  inch thick), one dips it in the solution for a few seconds. The organic material delivers electrons to the object and at the same time is oxidized. The electrons are given to the gold ions and they deposit.

There are two big advantages of electroless plating. The first is that one needs no power source or external electric circuit. What one has to pay for, the oxidizable organic material, may well be cheaper than the electricity one would have to use

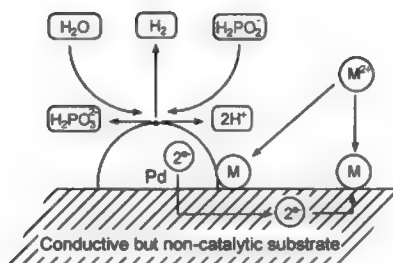


**Fig. 7.188** Electroless deposition on a conducting but noncatalytic substrate if the deposition is based on an electrochemical mechanism. (Reprinted from B. J. Hwang and S. H. Lin, *J. Electrochem. Soc.* **142**: 3749, 1995, Fig. 2. Reproduced by permission of The Electrochemical Society, Inc.)

(including amortization of the electrical equipment) in the alternative use of more normal electrodeposition. The second advantage is in throwing power (Section 7.5.8). In direct deposition there is a tendency to plate irregularly because the resistance offered by the solution opposing the current lines is different from one part of the object to be plated to another. In electroless deposition, one may think that there is a multitude of tiny cathodes and tiny anodes all near each other. There is only a short path between each, and so the plating is uniform and may occur in crevices as well as on open surfaces and plate uniformly in bends. In classical plating with an external power source, the anode is often far from certain parts of the cathode, so that the resulting IR drop may decrease the effective overpotential at distant parts of the object, resulting in nonuniform coating.

### 7.15.3. Heterogeneous “Chemical” Reactions in Solutions

There are several dozen reactions in solution—those that occur in the presence of a metal catalyst, which appear (in terms of the overall reaction) to be chemical, i.e., not to involve electron transfer. For example, nitrobenzene is reduced in solution to aniline by dissolved  $\text{H}_2$  in the presence of colloidal Pt. However, the reaction is catalyzed by colloidal Pt and hence it is a reasonable proposition that it may occur as the net of two partial electrochemical reactions (see Fig. 7.189).

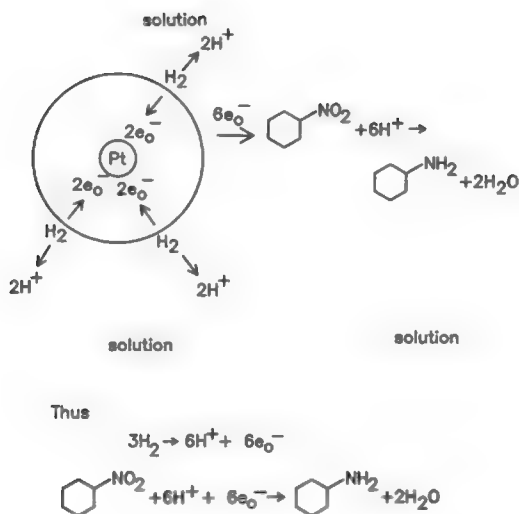


**Fig. 7.189.** Colloidal platinum is sometimes regarded as a catalyst for the reduction of nitrobenzene in solution. A mixed potential alternative is shown.

If apparently chemical reactions can be split up and occur as the sum of two electrochemical partial surface reactions in solution, one may begin to wonder whether electrochemical reactions have a wider realm of application than one had hitherto thought. There is one odd fact to which one might seek an explanation by applying the ideas outlined here. It is that *intensive* drying (say, 100 hr under a high vacuum at a high temperature) causes some semiconductor catalyst surfaces to become catalytically inactive. Does water from moisture dissociate on the surfaces of such catalysts, injecting protons into their surface layers and providing them with surface conductance between the electronating and deelectronating micropatches that the above mechanism demands? With all water gone, protonic surface conductance also would be near zero, and the possibility of cathodic and anodic reactions “communicating” via an electron or proton migration between them on the surface of the semiconductor would cease, as would the catalytic activity normally present.

#### 7.15.4. Electrogenative Synthesis

It is well known that U.S. space vehicles obtain their auxiliary power in space by the use of fuel cells (Chapter 13), electrochemical devices in which the spontaneous tendency of hydrogen to combine with oxygen drives the cell and produces electricity, with water as a by-product (pure enough to drink). It stands to reason then, that one might think of producing substances more economically valuable than water in this “electrogenative” way. Such work is into its first decade and Fig. 7.190 shows an example: benzene is oxidized to phenol with electricity as a by-product. Clearly, the economics of such a process depend on the cost of the  $H_2$  and whether one can sell the electricity. This gives rise to a speculation.

In chemical reactions, those devoted to syntheses, say, there must of course be a negative free-energy change for the reaction to function spontaneously and for the desired product to be produced. Although spontaneous endothermic (cold producing) reactions do exist, nearly all spontaneous reactions evolve heat. However, heat is difficult to collect and send long distances. Thus, insofar as our present chemical syntheses go, heat is a useless by-product of the production of chemicals. Correspondingly, when the expanding gases from a reaction of fuel and oxygen are used to make mechanical energy, most of the heat goes to the surrounding atmosphere in exhaust gases; in a few cases it is used to make steam for household heat.

Just as heat is the by-product of most spontaneous chemical reactions, so electricity is the by-product of the same reactions carried out in an electrogenerative way, such as that illustrated in Fig. 7.190. However, there is one big difference. Electricity can be used as a vector—and sent for hundreds of miles with little loss—and used at the other end. Could such processes become the basis of industrial processes that, as the rule and not the special case, make things electrogeneratively instead of thermally?

Such features could contribute their “waste” electricity to a power internet that would productively utilize among towns and countries the energy now wasted in a



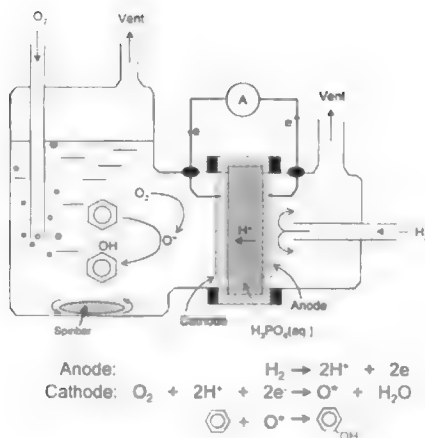


**Fig. 7.190.** Diagram of the reactor for partial oxidation of benzene to phenol during  $\text{O}_2\text{-H}_2$  fuel cell reactions. (Reprinted from K. Otsuka, M. Kunieda, and H. Yamagata, *J. Electrochem. Soc.* **139**: 2382, 1992, Fig. 1. Reproduced by permission of the Electrochemical Society, Inc.)

chemically based<sup>108</sup> industrial economy? Such thoughts are developed further in Section 13.11 in Chapter 13.

### 7.15.5. Magnetic Induction

In the examples given so far in this section, electrochemical cells run spontaneously. Viewed thermodynamically, the cells are running down a free energy gradient, using up the overall chemical free energy of the reaction obtained by adding the electrode reactions that occur in the electrochemical cells. However, there is another entirely different way of bringing about the action of an electrochemical cell without the use of an outside electricity source, or expending fuel. What must be available in the following device is a source of *mechanical* energy (as in hydro or wind resources).

For a radial segment of a rotating metallic disk, driven to spin vertically by a mechanical power source, the linear velocity at a distance  $r$  from the center is  $\omega r$ , where  $\omega$  is the angular velocity of the spinning disk. The induced potential,  $dE$ , due to the

<sup>108</sup>Our present industry is chemically based, not only because manufacturers use chemical reactions for synthesizing materials, but because our energy is obtained from the heat of exothermic chemical reactions (combustion of oil, etc.); however, only about one-third of this heat gets converted to useful energy while the rest goes into the surrounding atmosphere and is wasted.

segment,  $dr$ , is  $v B dr$ , where  $B$  is the magnetic field strength. Because the velocity,  $v$ , is  $\omega r$ , this expression may be rewritten  $\omega r B dr$  (Fig. 7.191). Therefore,  $E = \int \omega B r dr = \omega B (R^2/2)$ . The  $E$  is the potential from the center spindle to the rim of the disk. The device described here is a Faraday disk dynamo or homopolar generator. It produces potentials of a few volts at rpm's in the low thousands, and such potentials are precisely those needed by electrochemical devices.

At present, electrochemical reactors have to take electricity from the grid at, say, 100,000 volts ac. Such electricity has to undergo transformation to a lower voltage and rectification to dc. Not only is power lost in this conversion, but a significant contribution to the cost of the product is the investment in the necessary power management equipment. It follows that when one considers a raw source of energy, instead of using it to drive a generator producing ac at high voltages, it would be better to have it drive a homopolar generator producing low-voltage dc at high currents. Were this change to be introduced throughout the electrochemical industry, the cost of its products (e.g., nylon) would drop.

### Further Reading

1. Dong-Hyun Kim, Koji Aoki, and O. Takano, *J. Electrochem. Soc.* **142**: 3763 (1995).
2. Melvin De Silva and Y. Schachem-Diamond, *J. Electrochem. Soc.* **143**: 3513 (1996).
3. S. Aramyanov, R. Winand, and J. Vereken, *J. Electrochem. Soc.* **143**: 3092 (1996).
4. J. Ghoroghchian and J. O'M. Bockris, *Int. J. Hydrogen Energy* **10**: 101 (1984).

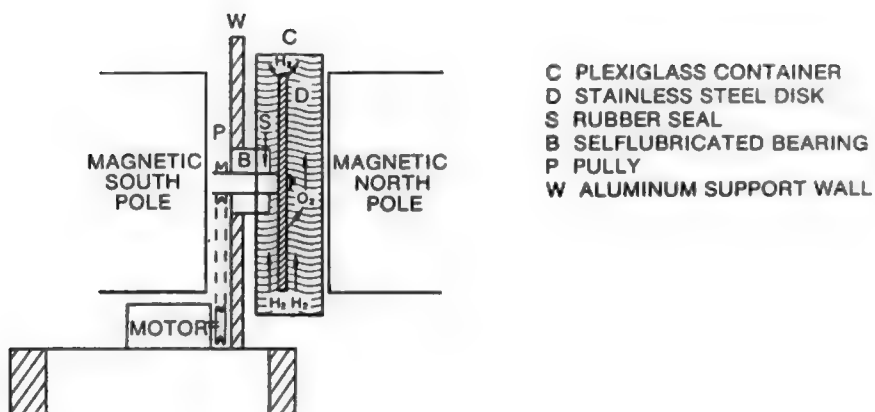


**Fig. 7.191.** Schematic diagram of an *in situ* homopolar generator and electrolyzer (one-unit system). (Reprinted with permission from J. Ghoroghchian and J. O'M. Bockris, *Int. J. Hydrogen Energy* **10**: 101, Fig. 1, 1985.)

## 7.16. THE ELECTROCHEMICAL HEART

It is possible to set up an experiment that involves a pool of Hg and other circuitry. The mercury pool pulsates in a regular way. Two conditions must be simultaneously present to achieve this unexpected phenomenon. One is that the solution contains oxygen or an oxidizing agent. The other is that an iron wire is placed in such a way that the Hg pool contacts the wire when it flattens out in the course of the pulsation, but breaks the contact when it becomes less flat, i.e., turns convex. Figure 7.192 shows a laboratory setup used to demonstrate the phenomenon. It is shown in the “flat” position of the Hg when it is sufficiently extended so as to contact the iron wire.

What happens electrochemically when this contact occurs? It is clear that an electrochemical cell is formed. One can see that it will be a kind of fuel cell. The Fe wire will tend to dissolve anodically ( $\text{Fe} \rightarrow \text{Fe}^{2+} + 2\text{e}^-$ ) and the  $\text{O}_2$  will tend to be reduced cathodically on the Hg ( $\text{O}_2 + 4\text{H}^+ + 4\text{e}^- \rightarrow 2\text{H}_2\text{O}$ ).

To understand the beating of this electrochemical heart (Paik, 1996), it is necessary to think about the changes in potential that occur when the cell switches on and the Hg becomes a cathode to reduce  $\text{O}_2$ . What surface tension changes will these potential changes bring about? When the Hg is in contact with the Fe wire, and reducing  $\text{O}_2$ , its potential moves to a more negative potential than it had before, when

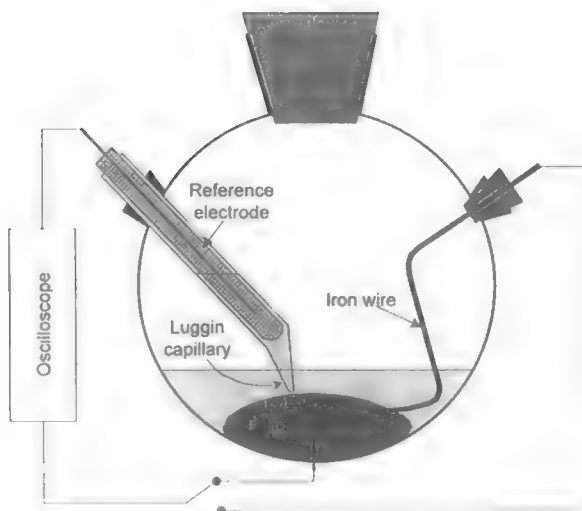


**Fig. 7.192.** A setup for recording the potential of mercury during iron-triggered oscillation in an acidic solution. (Reprinted from C. W. Kim, I-H. Yeo, and W.-K. Paik, *Electrochim. Acta* **41**: 2830, copyright 1996, with permission from Elsevier Science.)

it was “resting.” If one looks at the electrocapillary curve for Hg (see Fig. 7.193), it will be seen that as the Hg potential becomes more negative, the surface tension of the Hg/solution interface increases. This means that the area of the drop will decrease and the drop will become more spherical. It can be seen from Fig. 7.192 that this would mean that the central part of the drop will move higher and the contact with the Fe will be broken. This explains one half of the pulsation (from flat to more convex).

Of course, once the wire and contact is broken, the  $\text{Fe-O}_2$  fuel cell stops functioning, and the potential of the Hg will become more positive again. In Fig. 7.193, one sees at once that the surface tension in turn decreases and the drop therefore flattens. When it does so, it will again make contact with the Fe wire, so the electrochemical cell  $\text{Fe-O}_{2(\text{Hg})}$  will move to the negative side and start reducing  $\text{O}_2$ ; the surface tension will increase and the drop will tend to become spherical again; and the contact will be broken. One can see one has completed *one beat*. It is possible to reproduce a similar phenomenon using an Al wire in an alkaline solution.

Other electrochemical oscillators are known (Wojtowicz, 1972), but none have as yet received practical development. It is not necessary to have specifically iron or aluminum in the system. Any system that undergoes electrochemical oxidation in a potential range so that it can drive the reduction of a substance onto Hg will produce

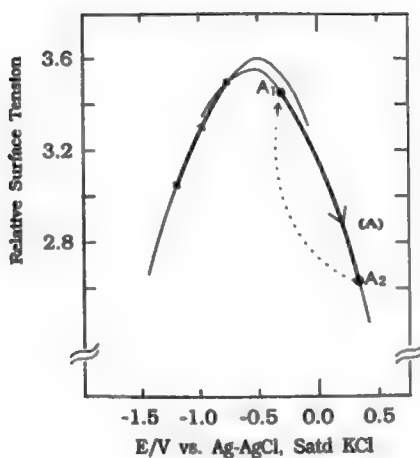


**Fig. 7.193.** The potential range marked on the electrocapillary curve. The potential of the mercury electrode oscillates between the points  $A_1$  and  $A_2$  in the Fe-triggered oscillation. (Reprinted from C. W. Kim, I-H. Yeo, and W.-K. Paik, *Electrochim. Acta* 41: 2833, copyright 1996, with permission from Elsevier Science.)

an oscillating system. Thus, a system in which glucose is oxidized to gluconolactone in the presence of glucose oxidase might be considered. The reaction occurs at about  $-0.4$  V (NHS). Could an oscillating electrochemical system involving glucose in arterial blood as the fuel and  $O_2$  in venous blood as the substance to undergo reduction be engineered to form a fuel cell-powered pump implanted in the body, i.e., an artificial heart?

## Further Reading

### Review

See earlier papers reviewed by J. Wojtowicz, in *Modern Aspects of Electrochemistry*, J. O'M. Bockris and B. E. Conway, eds., Vol. 8, p.47, Plenum, New York (1972).

### Papers

1. B. J. Hwang and S. H. Lin, *J. Electrochem. Soc.* **142**: 3749 (1995).
2. B. Bush and J. Newman, *J. Electrochem. Soc.* **142**: 3771 (1995).
3. S. Nakabayashi, K. Zama, and K. Uosaki, *J. Electrochem. Soc.* **143**: 2258 (1996).
4. C. W. Kim, I. H. Yeo, and W. K. Paik, *Electrochim. Acta* **18**: 2829 (1996).

## EXERCISES

1. The hydrogen evolution reaction is studied on two metals, A and B, in sulfuric acid solutions of  $a = 1$ . The graphic representation of the corresponding Tafel curves is:

If the efficiency of evolution on each metal is 100%, determine the exchange current density and the symmetry factor for the most efficient system. Consider that the experiment is performed at  $25^\circ\text{C}$  and the pressure of the evolving gases is 1 atm. (Zinola)

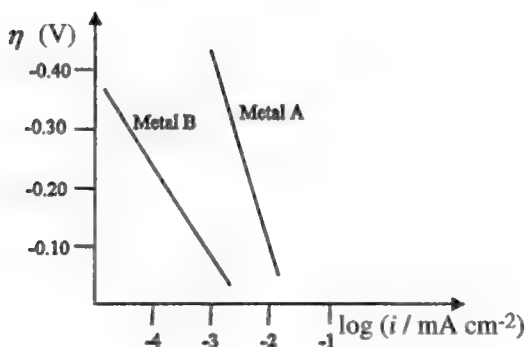


Fig. E7.1

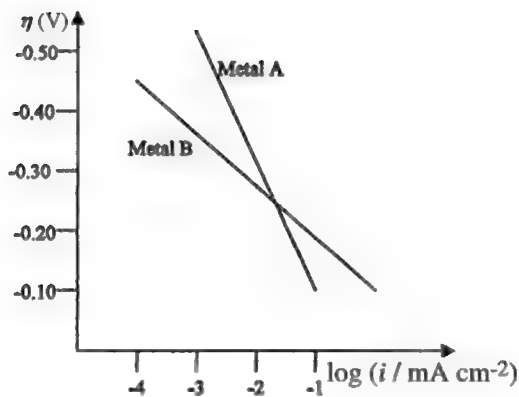


Fig. E7.2

2. (a) Determine  $i_0$  for the hydrogen evolution reaction on silver in acidic media if the corresponding Tafel slope is  $-130 \text{ mV dec}^{-1}$  and  $a = -0.45 \text{ V}$ . (b) If the pH of the previous solution is changed to  $\text{pH} = 1$  at  $25^\circ\text{C}$ , and an electrolyte  $\text{M}^{+2}\text{A}^{-2}$  is added to the solution in a concentration of  $1 \text{ mM}$ , determine the electrode potential for the  $\text{M}^{+2}/\text{M}$  system:

$E_{\text{M}^{+2}/\text{M}}^\circ = -0.25 \text{ V}$ ,  $i_0 = 50 \text{ }\mu\text{A cm}^{-2}$ , and  $(\partial E/\partial \log i)_T = -0.06 \text{ V dec}^{-1}$ .

Consider that the mass transfer phenomena are negligible and that  $\gamma = 0.997$  for a current density of  $100 \text{ }\mu\text{A cm}^{-2}$ . (Zinola)

3. The variation of the overpotential with the current density for the reaction of hydrogen evolution on a mercury cathode in diluted sulfuric acid at  $25^\circ\text{C}$  is:

TABLE E.1

Overpotential (V)	Current Density $\times 10^7 \text{ (A cm}^{-2}\text{)}$
0.60	2.9
0.65	6.3
0.73	28
0.79	100
0.84	250
0.89	630
0.93	1650
0.96	3300

Plot the overpotential against the  $\log |i|$  and determine the parameters of the Tafel equation for the mercury cathode, i.e.,  $\alpha$  and  $i_0$ . (Zinola)

4. For the galvanic couple:  $\text{Pt}/\text{H}_2(1 \text{ atm})/\text{HCl}(\text{aq})//\text{AgCl}(\text{S})/\text{Ag}(\text{S})/\text{Pt}$ , the potential of each electrode was measured with respect to a saturated calomel electrode:

$$E_{\text{Ag}/\text{AgCl}} = 0.0959 \text{ V and } E_{\text{H}^+/\text{H}_2} = 0.3624$$

- (a) Write the reaction that occurs spontaneously, (b) Calculate the open-circuit potential. (c) If the saturated calomel electrode has a value of 0.2444 V in the normal hydrogen scale, determine the potential of each electrode in this scale, (d) Calculate the activity of HCl in the solution. (Zinola)
5. For an electrochemical reaction controlled by the charge-transfer step, (a) define the symmetry factor,  $\beta$ , and the exchange current density,  $i_0$ . (b) Demonstrate in a plot of  $i$  vs.  $F(\eta)$  the influence of  $\beta$ , considering the following cases:  $\beta = 0.20$ ,  $\beta = 0.50$ , and  $\beta = 0.75$ . Consider in the above three cases a constant exchange current density and temperature. Explain the results, (c) Demonstrate the influence of  $i_0$  in the same  $i$  vs.  $F(\eta)$  graph, considering the following cases:  $i_0 = 0.20 \times 10^{-1} \text{ A m}^{-2}$ ,  $i_0 = 0.50 \times 10^{-5} \text{ A m}^{-2}$ , and  $i_0 = 0.75 \times 10^{-9} \text{ A m}^{-2}$ . Consider a constant symmetry factor and temperature. Explain the results. (Zinola)

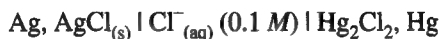
The overpotential for the oxygen evolution reaction on a silver anode in 0.1 N KOH was measured with respect to a reference electrode, at 25 °C.

**TABLE E.2**

$i(\text{mA cm}^{-2})$	1	10	50	100	500	1000	1500
$\eta(\text{V})$	0.58	0.73	0.91	0.98	1.08	1.13	1.14

Make a graph of  $\eta$  vs.  $\log i$  and determine  $i_0$  and  $\beta$ . Calculate the current density at 0.80 V. (Zinola)

6. The zero-current potential (electromotive force) of the cell:



was measured as a function of temperature. The results obtained are listed in Table E.3.

**TABLE E.3**

Temperature (K)	293.3	297.9	303.7	309.1	312.8
$E(\text{V})$	0.0443	0.0458	0.0478	0.0495	0.0508

- (a) Write the cell reaction and equation for the zero-current potential of the cell. (b) Plot the graph of  $E$  vs.  $T$ . (c) Determine the change of free energy and enthalpy for the temperatures given and the change of entropy of the cell reaction. (d) Compare the results obtained at temperature 298 K with the literature data. (Skompska et al.)
7. Calculate the heat of reaction using the experimental data listed in Table E.4. The heat of activation is 30 kJ/mol. (Kim)

TABLE E.4

Overpotential at 25 °C (V)	Current Density at 25 °C (A/cm <sup>2</sup> )	Temperature (°C)	Exchange Current Density (A/cm <sup>2</sup> )
-0.1	0.00025	5	0.00002
-0.15	0.0006	25	0.000043
-0.2	0.0014	45	0.00008
-0.25	0.0034	65	0.00014
-0.3	0.0083	85	0.00023

8. The ratio of the current at a disk electrode to that at a ring electrode as a function of rotation speed was measured as listed Table E.5. Calculate the rate constant of the intermediate's further reaction assuming a diffusion coefficient of  $10^{-5}$  cm<sup>2</sup>/s, a viscosity of  $0.89 \times 10^{-2}$  poise (=g/cm/s), and a density of 1 g/cm<sup>3</sup>.

TABLE E.5

Rotating speed (rpm)	100	200	500	1000	2000
$I_{\text{disk}}/I_{\text{ring}}$	2.59	2.22	1.88	1.72	1.60

9. Calculate the exchange current density and the symmetry factor ( $\beta$ ) of a cathodic reaction:  $A^+ + e^- \rightarrow A$  from Table E.6.

TABLE E.6

Current density (mA/cm <sup>2</sup> )	0.12	0.24	0.48	2.0	6.3	20	63
Overpotential (mV)	-15	-30	-60	-100	-150	-200	-300

10. The electrochemical oxidation of  $H_2O_2$  on passive iron:  $H_2O_2 = O_2 + 2H^+ + 2e^-$  was investigated on a rotating disk electrode in a solution containing 0.10 M NaOH and  $1 \times 10^{-3}$  M  $H_2O_2$ . Limiting diffusion current density and current density at the electrode potential of 700 mV, which is more negative than the limiting current density plateau, were measured as a function of the rotating rate of the disk:

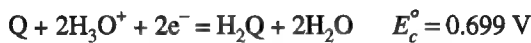


**TABLE E.7**

$\omega(\text{rpm})$	225	400	625	900	1600	2500	3600
$i_L(\text{A m}^{-2})$	5.70	7.60	9.51	11.4	15.2	19.0	22.8
$i_E = -700$ $\text{mV/A m}^{-2}$	4.53	5.39	6.04	6.53	7.24	7.71	8.04

Determine the reaction order with respect to  $\text{H}_2\text{O}_2$  and the kinetic current density at the electrode potential. (Gokjovic)

- How many times higher than the exchange current density does the limiting current density for the electrochemical reaction  $\text{ox}(\text{soln}) + e^- = \text{red}(\text{soln})$  have to be to assume that the reaction is activation controlled at an overpotential of  $-300 \text{ mV}$ ? (Take  $\beta = 0.5$  and  $T = 298 \text{ K}$ .) (Gokjovic)
- The diffusion coefficient of an  $\text{Fe}^{2+}$  ion in  $0.1 \text{ M HClO}_4$  is  $5.7 \times 10^{-10} \text{ m}^2 \text{ s}^{-1}$  and the diffusion coefficient of an  $\text{Fe}^{3+}$  ion in the same solution is  $6.5 \times 10^{-10} \text{ m}^2 \text{ s}^{-1}$  at  $25^\circ\text{C}$ . A Pt electrode (surface area  $0.200 \text{ cm}^2$ ) is immersed in solution containing  $1 \times 10^{-3} \text{ M FeSO}_4$  in  $0.1 \text{ M HClO}_4$ . Calculate the electrode potential of the Pt electrode 100 ms after the switching on of a constant deelectronation current of  $0.100 \text{ mA}$  in the unstirred solution. (Gokjovic)
- A silver wire is immersed in a solution of  $\text{AgNO}_3$  at  $298 \text{ K}$ . What is the minimum concentration of  $\text{AgNO}_3$  in which Ag does not dissolve at an electrode potential of  $0.680 \text{ V}$  vs. SHE? (Gokjovic)
- The stoichiometric equation for the reduction of quinone (Q) to hydroquinone ( $\text{H}_2\text{Q}$ ) is



A Pt electrode is immersed in a solution of pH 7.00 with  $1 \times 10^{-2} \text{ M Q}$  and  $1 \times 10^{-3} \text{ M H}_2\text{Q}$  at  $298 \text{ K}$ . If the electrode potential is externally driven at  $0.600 \text{ V}$  vs. SHE, is that electrode an anode (electron sink) or a cathode (electron source)? (Gokjovic)

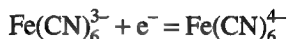
- The redox reaction:  $\text{ox}(\text{soln}) + e^- = \text{red}(\text{soln})$  was investigated in the overpotential range between 10 and 60 mV and following results were obtained:

**TABLE E.8**

$\eta(\text{mV})$	10	20	30	40	50	60
$i(\text{mA cm}^{-2})$	0.0384	0.0768	0.117	0.159	0.206	0.259

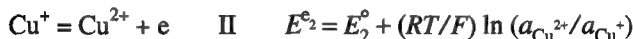
Determine the exchange current density and symmetry factor. (Gokjovic)

## 16. The electrochemical reaction



at Ni exhibits a reaction resistance of  $11 \, \Omega \, \text{cm}^2$  in a solution of  $0.100 \, M \, \text{K}_3\text{Fe(CN)}_6$  and  $\text{K}_4\text{Fe(CN)}_6$  in  $0.100 \, M \, \text{NaOH}$  at  $25^\circ \text{C}$ . Calculate the exchange current density for that reaction in a solution of  $1.0 \, M \, \text{K}_3\text{Fe(CN)}_6$  and  $\text{K}_4\text{Fe(CN)}_6$  in  $0.1 \, M \, \text{NaOH}$ . (Ignore the dependence of the activity coefficients of the complex ions on the concentration.) (Gokjovic)

17. An investigation of the electrochemical reaction  $\text{A} + 3e^- = \text{B}$  revealed that its exchange current density was  $1 \times 10^{-2} \, \text{A m}^{-2}$  and the cathodic Tafel slope  $-39 \, \text{mV dec}^{-1}$ . The slope of the straight line  $i$  vs.  $\eta$ , determined at  $\eta < 20 \, \text{mV}$ , was  $1.17 \, \text{A m}^{-2} \, \text{V}^{-1}$  at  $298 \, \text{K}$ . Calculate the anodic Tafel slope that would be expected. (Gokjovic)
18. The electrochemical reaction  $\text{ox}(\text{sin}) + 2e^- = \text{red}(\text{sin})$  is first order with respect to the reactant ox. The cathodic transfer coefficient is 0.5. How many times is the exchange current density increased when the concentration of ox is increased ten times? (Gokjovic)
19. An investigation of  $\text{O}_2$  reduction on Pt in alkaline solutions showed that the Tafel slope at low current densities was  $-60 \, \text{mV dec}^{-1}$  and that the reaction rate decreased with increasing pH. The slope of the  $E$  vs. pH plot at constant current density was  $-30 \, \text{mV dec}^{-1}$ . What is the reaction order with respect to  $\text{OH}^-$  ions? (Gokjovic)
20. An electrochemical reaction  $\text{I}_2 + 2e^- \rightarrow 2\text{I}^-$  was investigated at a rotating disk electrode in solution that contained  $6.6 \times 10^{-4} \, M \, \text{KI}_3$  and a supporting electrolyte. Calculate the interfacial concentration of an  $\text{I}_3^-$  ion when the current density is  $10 \, \text{A m}^{-2}$  and the rotation rate of the disk is  $3000 \, \text{rpm}$ . [Take  $D(\text{I}_3^-) = 1.14 \times 10^{-9} \, \text{m}^2 \, \text{s}^{-1}$  and  $\nu = 1 \times 10^{-6} \, \text{kg m}^{-1} \, \text{s}^{-1}$ ]. (Gokjovic)
21. Given the two stages



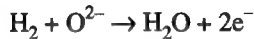
of the total electrode reaction



where  $E^{\circ}_1 = 0.520$ ,  $E^{\circ}_2 = 0.153$ , and  $E^{\circ}_3 = 0.337 \, (\text{V/NHE})$  are the standard equilibrium potentials of reactions I, II, and III, respectively, (a) establish the

relationships between the standard equilibrium potential and the chemical rate constants of the partial reactions. (b) Demonstrate using the kinetic method that  $E_3^\circ = (E_1^\circ + E_2^\circ)/2$ . (Use a symmetry factor=0.5.) (c) Draw the equivalent electric circuit leading to  $E_3^\circ = (E_1^\circ + E_2^\circ)/2$ . (Plonski)

22. In a solid electrolyte fuel cell utilizing  $\text{Y}_2\text{O}_3$ -stabilized  $\text{ZrO}_2$  (YSZ), an  $\text{O}^{2-}$  conductor, as the solid electrolyte,  $\text{H}_2$  and  $\text{O}_2$  are consumed at the anode and cathode, respectively, according to the reactions:



Evaluate the open-circuit emf of the cell at 800, 900, and 1000 °C when at the anode  $p_{\text{H}_2} = 80 \text{ kPa}$ ,  $p_{\text{H}_2\text{O}} = 20 \text{ kPa}$  and at the cathode  $p_{\text{O}_2} = 100 \text{ kPa}$ . (Makri, Pitselis and Vayenas)

23. Figure E7.3 shows the catalytic rate,  $r$ , and catalyst potential,  $V_{\text{WR}}$  (where WR is the catalyst's potential with respect to a reference electrode), response to step changes in current applied during  $\text{C}_2\text{H}_4$  oxidation on a Pt catalyst electrode deposited on YSZ at  $T = 370^\circ\text{C}$ ,  $p_{\text{O}_2} = 4.6 \text{ kPa}$ , and  $p_{\text{C}_2\text{H}_4} = 0.36 \text{ kPa}$ . As shown in Fig. E.7, application of a positive current,  $I$ , causes a 26-fold enhancement in the catalytic rate from its open-circuit value  $r_0 = 1.5 \times 10^{-8} \text{ mol O/s}$  to a new value of  $40 \times 10^{-8} \text{ mol O/s}$ . The catalytic reaction is

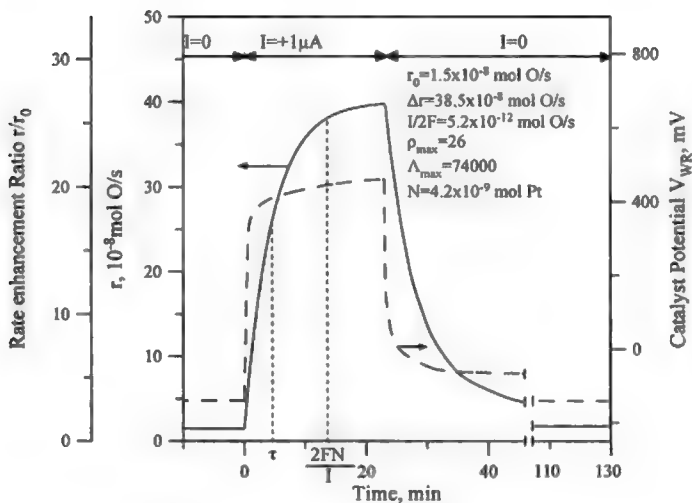
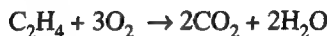


**Fig. E7.3.** Catalytic rate response to step changes in applied currents.

The observed increase,  $\Delta r$ , in catalytic rate, expressed in mol O/s, exceeds by far the rate,  $I/2F$ , of  $\text{O}^{2-}$  supply to the catalyst electrode. Consequently this is an example of electrochemical promotion, or non-Faradaic electrochemical modification of catalytic activity (the NEMCA effect), which results from the migration of promoting  $\text{O}^{2-}$  species on the catalyst surface upon positive current application.

(a) Compute the steady-state Faradaic efficiency,  $\Lambda$ , defined from  $\Lambda = \Delta r/(I/2F)$ . (b) How many extra adsorbed oxygen atoms, O(a), originating from the gas phase react with  $\text{C}_2\text{H}_4$  per each  $\text{O}^{2-}$  supplied to the catalyst? (c) At steady state, i.e., before setting  $I = 0$ , what is the ratio of the rate of reaction of  $\text{O}^{2-}$  with  $\text{C}_2\text{H}_4$  with respect to the rate of reaction of O(a) with  $\text{C}_2\text{H}_4$ ? (Answer  $1/\Lambda$ ). (d) Upon current interruption ( $I = 0$ ), in the second part of the experiment,  $\text{O}^{2-}$  is no longer supplied to the catalyst electrode, but it continues to be consumed by  $\text{C}_2\text{H}_4$ ; consequently, the surface coverage of the promoting  $\text{O}^{2-}$  species decreases and the catalytic rate,  $r$ , also decreases. Assuming that the rate is proportional to the coverage,  $\theta$ , of  $\text{O}^{2-}$  and assuming  $\theta = 0.5$  at current interruption, use the initial  $r$  vs.  $t$  slope upon current interruption to estimate the rate of reaction of  $\text{O}^{2-}$  with  $\text{C}_2\text{H}_4$ . Compare this value with the maximum rate of  $\text{C}_2\text{H}_4$  oxidation (i.e.  $40 \times 10^{-8}$  mol O/s) and explain why their ratio is approximately equal to  $1/\Lambda$ . The Pt catalyst surface area corresponds to  $N = 4.2 \times 10^{-9}$  mol Pt. (e) Explain why the rate relaxation time constant  $\tau$ , defined as the time needed for the rate increase to reach 63% of its steady-state value, is on the order of  $2FN/I$ . (Makri, Pitselis, and Vayenas)

## PROBLEMS

1. The current density for an overall electrochemical reaction ( $\text{A} + 2\text{e}^- \leftrightarrow \text{C}$ ) was measured as a function of the overpotential listed in Table P.1. Develop the mechanism of the reaction and find the rate-determining step, assuming a symmetry factor of 0.5.

TABLE P.1

Overpotential (mV)	Current Density (mA/cm <sup>2</sup> )	Overpotential (mV)	Current Density (mA/cm <sup>2</sup> )
-200	119	20	0.00117
-150	6.4	50	0.00259
-100	0.344	100	0.00701
-50	0.0182	150	0.0186
-20	0.00254	200	0.0492
-10	0.000971	250	0.13
10	0.000657	300	0.345

2. Consider the cell:  $\text{Zn} | \text{ZnSO}_4(c) || \text{CuSO}_4(c) | \text{Cu}$ . The concentration of the salts,  $c$ , is (a)  $0.5 \text{ mol dm}^{-3}$  and (b)  $0.05 \text{ mol dm}^{-3}$ , and the standard electrode potentials are  $E^\circ(\text{Cu}/\text{Cu}^{2+}) = 0.34 \text{ V}$ ,  $E^\circ(\text{Zn}/\text{Zn}^{2+}) = -0.76 \text{ V}$ . The electrodes are connected by a resistor of adjustable resistance. Imagine that the resistance was changed successively from  $100 \text{ M}\Omega$  to  $0.1 \Omega$  and a few measurements of the cell potential were done in each decade.

(a) Write the cell reaction and the equation for the equilibrium potential of the cell and for potential at the current flowing through the cell. Explain the meaning of each term of the equations. Which of the terms depend on the ionic concentration in the cell? (b) Calculate the equilibrium potential of each half-cell for the two concentrations of  $c$ . (c) Sketch a graph of the dependence of each component in your equation on the current flowing in the cell. (d) Sketch a graph of the power output of the cell for the two concentrations of  $c$ . (e) How could you determine the inner resistance of the cell? (f) Calculate the equilibrium constant of the cell reaction at  $298 \text{ K}$ . (Skompska)

3. Butler–Volmer equation: An anodic current  $i_{\text{an}}$  at an electrode/electrolyte interface was recorded as function of overpotential  $\eta$  and the results tabulated as follows:

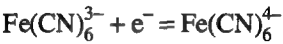
TABLE P.2

$\eta(\text{mV})$	5	10	15	20	25	30	40	50
$i(\text{mA}/\text{cm}^2)$	0.158	0.326	0.505	0.697	0.905	1.131	1.649	2.281

- (a) Calculate the interfacial resistance and find whether this interface is polarizable or nonpolarizable. (b) Will the cathodic current response be larger or smaller than the anodic current? (c) Draw the current dependence on overpotential for both anodic and cathodic regions. (Kang)
4. Here is more impedance study: the simplest cell. In a real-life experiment, one can only work with a complete circuit, which consists of at least two electrodes. Now, to test our newly acquired impedance knowledge on a real-life problem, let's consider a circuit consisting of two identical electrodes. Draw its equivalent circuit and make a try at its impedance expression. Try harder to imagine its Cole–Cole plot. You may also use a computer to simulate the situation by using reasonable parameters. To make the situation less complicated, we assume the interface is ideally polarizable. (Kang)
5. Impedance spectroscopy: a single interface. Draw the equivalent circuits for the following electrode/electrolyte interfaces, then derive their impedance expression and explain what their Cole–Cole plot will look like: (a) An ideally polarizable interface between electrode and electrolyte. (b) An ideally nonpolarizable interface between electrode and electrolyte. (c) A real-life electrode/

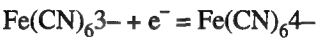
electrolyte interface, which is a mixture of the above two extreme interfaces. (Kang)

6. The kinetic parameters for an Fe dissolution reaction, according to the BDD mechanism, are transfer coefficient  $\tilde{\alpha} = 1.5$  and a reaction order with respect to  $\text{OH}^-$  ions of  $p_{\text{OH}^-, \text{an}} = 1$ , while the kinetic parameters for an  $\text{H}_2$  evolution reaction on Fe in acid solutions are  $\alpha = 0.5$  and  $p_{\text{H}^+, \text{cath}} = 1$ . Using these data, work with the pH dependence of the corrosion potential and the corrosion current density of Fe in acid solutions. (Gokjovic)
7. It is known that double-layer effects are the most pronounced in the reaction of multivalent ions in a dilute solution. According to the calculation of Grahame,  $d^{\text{OHP}} \Delta^3 \phi / d\eta$  in 0.100 M NaF is about 0.05 in the potential region far from the pzc. Evaluate the cathodic and anodic Tafel slope values for the reaction



at 25 °C in a solution of ionic strength  $I = 0.1$  assuming that  $\beta = 0.5$ . (Gokjovic)

8. The electrochemical reaction:



was investigated on passive Fe in a solution of  $5 \times 10^{-3}$  M  $\text{K}_3\text{Fe(CN)}_6$  and  $\text{K}_4\text{Fe(CN)}_6$  in 1.0 M NaOH. A polarization curve was recorded on a rotating disk electrode at 900 rpm and the following results were obtained:

TABLE P.3

<i>E</i> (mV) vs. SHE	430	350	270	190	112	33	−45	−105	−164	−215	−250	−300
<i>i</i> (A m <sup>−2</sup> )	0.102	0.385	1.29	5.05	15.9	34.7	49.6	55.1	57.1	58.0	58.6	58.6

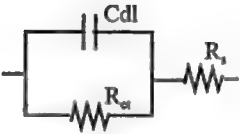
- (a) Calculate kinetic (activation-controlled) current densities for electrode potentials between 430 and −215 mV. Construct Tafel plots using measured and calculated current densities. Evaluate the electrode potential value at which the reaction passes from activation to mixed activation-diffusion control. What is the Tafel slope value? (b) If the polarization curve was recorded at 5000 rpm,

what would be the shift of the transition potential between activation and mixed activation-diffusion control? (Assume that the reaction gets into mixed control when the difference between measured and kinetic current densities is greater than 5%.) (Gokjovic)

- Find the charge-transfer resistance ( $R_{CT}$ ), the double-layer capacitance ( $C_{DL}$ ), and the solution resistance ( $R_{soln}$ ) from the data listed in Table P.4 by using the simplest equivalent circuit for an electrochemical reaction shown in the figure. If the measurement was carried out at equilibrium potential, what is the exchange current? (Kim)

**TABLE P.4**

Frequency ( $H_2$ )	Amplitude $ Z $	Phase angle, $\alpha$
1	3116 $\Omega$	-77.8
10	319	-87
100	33.4	-72.4



- Calculate the critical number of atoms ( $N_{crit}$ ) and the critical free energy change ( $\Delta G_{crit}$ ) for two-dimensional cluster formation ( $A^+ + e^- \leftrightarrow A$ ) assuming that the area of one atom is  $4 \times 10^{-16} \text{ cm}^2$  and the edge energy per unit length is  $2 \times 10^{-13} \text{ J/cm}$  when the overpotential is -5, -10, or -40 mV. (Kim)
- The electrolyte for electrowinning of Zn is an acid solution of  $\text{ZnSO}_4$  of pH 0.5 that contains  $1.20 \text{ mol dm}^{-3} \text{ Zn}^{2+}$ . The exchange current density for Zn deposition in this solution is  $8.0 \text{ A m}^{-2}$ , and for  $\text{H}_2$  evolution is  $5.0 \times 10^{-7} \text{ A m}^{-2}$ . Tafel slope values for both reactions are  $-120 \text{ mV dec}^{-1}$ . If electrolysis is performed under galvanostatic conditions with a current density of  $300 \text{ A m}^{-2}$  and under standard pressure, calculate the current efficiency for the Zn deposition. What is the electrode potential of the cathode? (Ignore the diffusion overpotential of Zn deposition.) (Gokjovic)
- Cadmium is deposited on a rotating disk electrode from a solution that is 0.0100 M in  $\text{CdSO}_4$  and 1.00 M  $\text{H}_2\text{SO}_4$ . The following data are known from the literature:

**TABLE P.5**

Reaction	Solution	$i_0 (\text{A m}^{-2})$	$\alpha$
$\text{Cd}^{2+} + 2e^- = \text{Cd}$	0.0100 M $\text{CdSO}_4$	15	0.45
$2\text{H}^+ + 2e^- = \text{H}_2$	1.00 M $\text{H}_2\text{SO}_4$	$2.5 \times 10^{-3}$	0.50

- (a) Calculate the limiting diffusion current density for the deposition of Cd at 2500 rpm [Take  $D(\text{Cd}^{2+}) = 7.0 \times 10^{-10} \text{ m}^2 \text{ s}^{-1}$  and  $\nu = 1.0 \times 10^{-6} \text{ kg m}^{-1} \text{ s}^{-1}$ .]  
 (b) Estimate the electrode potential at which the limiting diffusion current density for the deposition of Cd is established. (Suppose that  $i \approx 0.999 i_0$ ). (c) Would an  $\text{H}_2$  evolution reaction be expected to occur at the electrode potential calculated in (b)? If it would be, calculate the current efficiency for Cd deposition. (Gokjovic)
13. Copper is deposited at a rotating disk electrode from a solution containing  $0.100 \text{ M CuSO}_4$ . The rotation rate is 1000 rpm. Calculate the thickness of the Cu deposit formed during 30 min if the deposition current density is one-third of the limiting current density. [Take  $D(\text{Cu}^{2+}) = 5.2 \times 10^{-10} \text{ m}^2 \text{ s}^{-1}$ ,  $\nu = 1.0 \times 10^{-6} \text{ kg m}^{-1} \text{ s}^{-1}$ ,  $\rho(\text{a}) = 8.9 \text{ g cm}^{-3}$ .] (Gokjovic)
14. Copper powder is electrodeposited from a solution containing  $0.1 \text{ M CuSO}_4$  and  $0.5 \text{ M H}_2\text{SO}_4$ . The limiting current density for Cu deposition in an unstirred solution of a given composition is  $60 \text{ A m}^{-2}$ . Electrolysis is driven galvanostatically, with a current density 25% higher than the limiting current density. The temperature of the electrolyte is  $25^\circ \text{C}$ . Using kinetic parameters:

TABLE P.6

Electrochemical Reaction	$i_0 (\text{A m}^{-2})$	$\bar{\alpha}$
$\text{Cu}^{2+} + 2\text{e}^- = \text{Cu}$	12	0.5
$2\text{H}^+ + 2\text{e}^- = \text{H}_2$	$1.6 \times 10^{-7}$	0.5

- (a) Calculate the potential value of the cathode at which the limiting current density of Cu deposition is established (assume that the limiting current density is established if  $i = 0.999 i_L$ ). (b) Calculate the potential of the cathode during electrolysis (neglect the change of cathode surface area due to powder deposition). (c) If the diffusion-layer thickness is decreased by stirring to 50% of its value in an unstirred solution and the current density is the same, what is the cathode potential value? (Gokjovic)
15. A copper-cadmium alloy is deposited onto a rotating disk electrode at 2000 rpm in a solution containing  $1 \times 10^{-2} \text{ M CuSO}_4$ ,  $0.100 \text{ M CdSO}_4$ ,  $1 \times 10^{-3} \text{ M H}_2\text{SO}_4$  and  $1.00 \text{ M Na}_2\text{SO}_4$ . It is known from the literature that the exchange current density for Cu deposition in  $1 \times 10^{-2} \text{ M CuSO}_4$  is  $5.5 \text{ A m}^{-2}$  and the exchange current density for Cd deposition in  $0.100 \text{ M CdSO}_4$  is  $84 \text{ A m}^{-2}$ . The cathodic transfer coefficients for the deposition of both metals are 0.50.
- Calculate the current density at which an alloy with 25 mol.% Cu and 75 mol.% Cd should be deposited, assuming that the deposition current density of the alloy is the sum of the deposition current density of individual metals. What is the electrode potential value at that current density? [Take  $D(\text{Cu}^{2+}) = D(\text{Cd}^{2+}) = 5.00 \times 10^{-10} \text{ m}^2 \text{ s}^{-1}$ ,  $\nu = 1 \times 10^{-6} \text{ kg m}^{-1} \text{ s}^{-1}$ ,  $T = 298 \text{ K}$ . The current



density for a hydrogen evolution reaction can be neglected because of the low exchange current density at Cu and Cd.] (Gokjovic)

16. Electrochemical oxidation of hydroquinone was investigated on a rotating disk electrode in a solution containing 0.01 *M* quinone and hydroquinone in 0.5 *M* H<sub>2</sub>SO<sub>4</sub> at 298 K. The following values of current density at different electrode potential values and RDE rotation rates were obtained:

**TABLE P.7**

	<i>i</i> (mA cm <sup>-2</sup> )						
$\omega$ (rpm)	<i>E</i> =0.750 V	<i>E</i> =0.770 V	<i>E</i> =0.790 V	<i>E</i> =0.810 V	<i>E</i> =0.830 V	<i>E</i> =0.870 V	<i>E</i> =1.050 V
500	0.9363	1.846	3.211	4.717	5.887	6.969	7.491
100	0.9717	1.990	3.672	5.784	7.648	9.579	10.59
1500	0.9885	2.061	3.921	6.428	8.815	11.48	12.97
2000	0.9987	2.106	4.087	6.885	9.698	13.03	14.98
2500	1.006	2.137	4.208	7.236	10.41	14.34	16.75
3000	1.011	2.161	4.302	7.519	11.00	15.50	18.35
4000	1.019	2.196	4.442	7.956	11.97	17.48	21.19

The equilibrium potential value was 0.683 V vs. SHE. Assuming that the reaction is first order with respect to hydroquinone, determine the anodic transfer coefficient and exchange current density. (Gokjovic)

17. Water is electrolyzed in a laboratory cell to produce 20 cm<sup>3</sup> min<sup>-1</sup> of H<sub>2</sub> gas at 298 K and 101.3 kPa. An anode and cathode made of stainless steel with dimensions of 5.0 cm × 5.0 cm are placed into the cell parallel to each other at a distance of 4.0 cm. The electrolyte is 6.0 *M* NaOH (mean ionic activity coefficient  $\gamma_{\pm} = 1.28$ ) with a conductivity of 30 S m<sup>-1</sup>. The following data for the reactions at stainless steel in 6.0 *M* NaOH are known from the literature:

**TABLE P.8**

Electrochemical Reaction	$\log(i_0/A \text{ m}^{-2})$	$\alpha$
2H <sub>2</sub> O + 2e <sup>-</sup> = H <sub>2</sub> + 2OH <sup>-</sup>	0.10	0.39
4OH <sup>-</sup> = O <sub>2</sub> + 2H <sub>2</sub> O + 4e <sup>-</sup>	-5.68	0.89

Calculate the cell potential. (Gokjovic)

18. In the case of very fast electrochemical reactions, it can be assumed that an overpotential is caused only by slow transport of reacting particles from the bulk of the solution toward the electrode surface and that the activation overpotential is negligible. What is the error of that approximation for the electrochemical

reaction  $\text{ox}(\text{soln}) + e^- = \text{red}(\text{soln})$  if  $i_L = 10 \text{ mA cm}^{-2}$ ,  $\beta = 0.5$  and (a)  $i_0 = 1 \text{ mA cm}^{-2}$ ; (b)  $i_0 = 10 \text{ mA cm}^{-2}$ ; and (c)  $i_0 = 100 \text{ mA cm}^{-2}$ ?

Instruction: Calculate the current density values as a function of overpotential (in a range of  $-0.200$  to  $0.200 \text{ V}$ ) assuming that the reaction is under mass transport control and under mixed mass transport and charge-transfer control; determine the error of the approximation and plot  $i$ - $\eta$  dependencies. (Gokjovic)

19. An  $I/E$  polarization experiment run at  $298.15 \text{ K}$  on a  $0.6\text{-cm}^2$  active-area platinum electrode at small overpotentials in four aqueous solutions containing a fixed small amount of  $\text{Fe}^{2+}$  and increasing amounts of  $\text{Fe}^{3+}$  gave the following results:

TABLE P.9

$C_{\text{Fe}^{3+}}$ ( $\text{mol dm}^{-3}$ )	0.000066	$C_{\text{Fe}^{3+}}$ ( $\text{mol dm}^{-3}$ )	0.00013	$C_{\text{Fe}^{3+}}$ ( $\text{mol dm}^{-3}$ )	0.00033	$C_{\text{Fe}^{3+}}$ ( $\text{mol dm}^{-3}$ )	0.00066
$E(\text{SCE})/\text{V}$	$I/\mu\text{A}$	$E(\text{SCE})/\text{V}$	$I/\mu\text{A}$	$E(\text{SCE})/\text{V}$	$I/\mu\text{A}$	$E(\text{SCE})/\text{V}$	$I/\mu\text{A}$
0.374	-0.79	0.391	-1.15	0.415	-1.54	0.433	-2.49
0.376	-0.50	0.393	-0.77	0.417	-1.02	0.435	-1.6
0.378	-0.30	0.395	-0.35	0.419	-0.50	0.437	-0.76
0.380	0	0.397	0	0.421	0	0.439	0
0.382	0.28	0.399	0.37	0.423	0.55	0.441	0.75
0.384	0.52	0.401	0.79	0.425	1.05	0.443	1.63
0.386	0.80	0.403	1.18	0.427	1.52	0.445	2.45

(a) Determine the equilibrium potential  $E_{\text{rev}}$  for each solution and plot it against  $\log C_{\text{Fe}^{3+}}$ . What do you get? (b) A student group, correctly mounting the operating cell and correctly adding  $\text{Fe}^{2+}$  and  $\text{Fe}^{3+}$ , had equilibrium potentials fairly constant and  $\approx 0.420 \text{ V}(\text{SCE})$ . What did they forget to do before running the experiment? (c) Plot the four  $\eta$  vs.  $I$  characteristics in one graph. What do you get? (d) Determine the exchange current density  $i_0$  for each solution and plot  $\ln i_0$  vs.  $E_{\text{Rev}}$  and  $\ln i_0$  vs.  $\ln (C_{\text{Fe}^{3+}})$ . What do you get? What is the meaning of the two slopes? Calculate  $\alpha$ . (Mussini)

20. A rotating disk electrode operating at constant angular velocity  $\omega$  provides highly controlled mass transfer. Mass transport to the RDE is uniform on the whole surface, so that it can be discussed along one direction only (i.e., along a  $z$ -axis perpendicular to the surface) with concentration profiles  $c^*$ , electrode surface;  $c^b$ , bulk; a, no faradaic reaction; b, faradaic reaction; c, faradaic reaction in limiting-current conditions.

Using Levich's equation we can determine the diffusion coefficients for the reactant species by measuring the limiting current densities at known angular velocities.

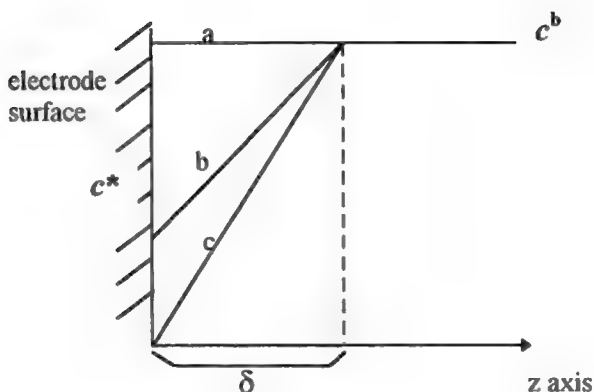


Fig. P7.1

(a)  $I$ - $E$  curves for a Pt rotating disk electrode (radius = 0.1 cm) operating in an aqueous solution of equimolar (0.002 M)  $\text{Fe}(\text{CN})_6^{4-}$  (red)/ $\text{Fe}(\text{CN})_6^{3-}$  (ox) (cinematic viscosity  $\nu = 0.01 \text{ cm}^2/\text{s}$ ) were registered at a slow potential sweep rate ( $\Delta E/\Delta t = 5 \text{ mV/s}$ ) from  $-0.1 \text{ V}$  (SCE) to  $+0.5 \text{ V}$  (SCE), at different rotation speeds. The following anodic and cathodic (LA and LC) limiting diffusion currents were measured for the reaction  $\text{ox} + e = \text{red}$ :

TABLE P.10

Rotations per minute	250	500	1000	1500	2000	3500	4500
$I_{LC}/\mu\text{A}$	-14.5	-21	-30.3	-36.8	-42.2	-55.3	-63.5
$I_{LA}/\mu\text{A}$	13	18.3	25.5	31.3	35.8	47	54

Verify Levich's equation for both the cathodic and anodic reactions and calculate the diffusion coefficients of species ox and red.

(b) Considering the relation between the diffusion-layer thickness  $\delta$  and the angular velocity  $\omega$  implicit in Levich's equation, deduce the limiting diffusion-layer thickness  $\delta$  for  $\omega \rightarrow \infty$ , and the advantage of using an RDE at different rotation speeds in the determination of kinetics parameters of mixed [charge transfer + mass transfer] controlled processes.

21. A practical use of a microelectrode: The advantages of microelectrode techniques are especially pronounced for systems with limited conductivity (e.g., polymer electrolytes), which are popular candidates for state-of-the-art lithium ion batteries, normally with room-temperature conductivities  $\kappa \sim 10^{-4} \text{ S/cm}$ . (a) A researcher is evaluating a newly synthesized lithium polymer electrolyte. He uses a two-electrode cell in which an electrolyte disk of  $0.1 \text{ cm} \times 1.0 \text{ cm}^2$  is

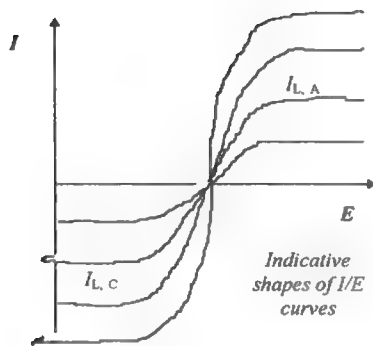


Fig. P7.2

sandwiched between a nickel foil and a lithium foil, the former being the working electrode and the latter being the counter- and reference electrodes. To simulate the real working condition of Li-ion batteries, the researcher sets the current density at  $0.5 \text{ mA/cm}^2$ . Comment on the possible error source if this cell is used to make electrochemical measurements. (b) To eliminate the error source, a fine nickel wire of  $\phi = 10 \mu$  is used as the working electrode. Show quantitatively how much the error has been reduced. (Kang)

22. Assume that the reaction  $\text{ox} + e \rightleftharpoons \text{red}$  at the planar electrode is diffusion controlled. Sketch and correlate the concentration profiles  $C_{\text{ox}} = f(x)$ , where  $x$  is the distance from the electrode surface to the bulk of the solution, with the shape of the current–potential curve for electrolysis carried out at (a) a stationary disk electrode and (b) a rotating disk electrode. Support your explanation by the equations. (Skompska)
23. An aqueous solution of  $0.1 \text{ M}$  sulfuric acid is electrolyzed between two electrodes, which can be made of platinum, gold, or graphite. The electrodes are  $1 \text{ cm}$  apart and have the same area. At that concentration of sulfuric acid, the equivalent conductance is  $234.3 \text{ S cm}^{-2} \text{ eq}^{-1}$ . At a current density of  $0.5 \text{ A m}^{-2}$ , the corresponding values of overpotential of charge transfer are:

$$\eta_{\text{H}_2}/\text{Pt} = -0.56 \text{ V} \quad \eta_{\text{O}_2}/\text{Pt} = 1.43 \text{ V}$$

$$\eta_{\text{H}_2}/\text{Au} = -0.78 \text{ V} \quad \eta_{\text{O}_2}/\text{Au} = 1.53 \text{ V}$$

$$\eta_{\text{H}_2}/\text{C} = -1.16 \text{ V} \quad \eta_{\text{O}_2}/\text{Pt} = 1.19 \text{ V}$$

- (a) Write the reactions for electro-oxidation and reduction that take place in the system. (b) Determine the potential difference that should be applied to the

- electrodes in each case if both electrodes are of the same material. (c) Indicate which combination of electrodes needs the least applied potential difference. For all the combinations, the potential difference at zero current can be taken as 1.23 V. Neglect any concentration overpotential. (Zinola)
24. An electrochemical reaction controlled by charge transfer is studied under an applied potential close to the one that gives a zero-current density. (a) Calculate the differential resistance of the interface if the exchange current density of the reaction is  $5 \times 10^{-4} \text{ mA cm}^{-2}$ , the working temperature is  $20^\circ\text{C}$ , and the number of exchanged electrons is two. (b) Which of these parameters could help determine the polarizability of the system? Explain. (c) Indicate the polarizability of the system by comparing the data obtained with values of exchange current density for the hydrogen evolution in an acidic solution on a platinized-platinum electrode ( $i_{0,\text{H}_2} = 10^{-4.1} \text{ A cm}^{-2}$ ) and on a lead electrode ( $i_{0,\text{H}_2} = 10^{-9.3} \text{ A cm}^{-2}$ ). (d) What modifications would you perform on the system to increase its rate of reaction? (Zinola)
25. According to the scheme in Fig. P7.3, where A is a copper electrode in  $0.1 \text{ M CuSO}_4/\text{H}_2\text{SO}_4$  with a Luggin capillary, B and C are Cu electrodes, S is the switch, and E is a  $0.1 \text{ M CuSO}_4/\text{H}_2\text{SO}_4$  solution, (a) what are instruments 1, 2, and 3 measuring? (b) With switch S opened, what value would instrument 3 measure? (c) If the circuit is closed and electrode B is cathodically polarized, draw the curve  $i = f(\eta)$ , indicating what happens in each segment of the curve. (d) Draw in the same graph the curve for current density vs. overpotential for the case where the solution E is uniformly mixed. (Zinola)
26. An aqueous solution is electrolyzed between two flat electrodes of platinum. The solution contains nickel ions in a concentration of  $1 \text{ mM}$  and sulfuric acid pH 1 at  $25^\circ\text{C}$ . The Tafel parameters for the hydrogen and oxygen evolution reactions on platinum are:  $a_{\text{H}} = -0.09 \text{ V}$  and  $b_{\text{H}} = -0.06 \text{ V dec}^{-1}$ ;  $a_0 = 0.12 \text{ V}$  and  $b_0 = 0.18 \text{ V dec}^{-1}$ . If all the activity coefficients are equal to 1 and the

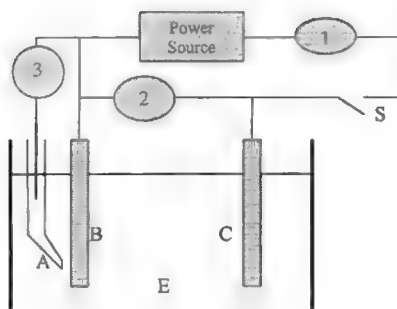


Fig. P7.3

pressure of the hydrogen and oxygen evolution is 1 atm, (a) determine the reactions that take place under these conditions, assuming that the coefficient of mass transfer for the nickel ion is negligible and that the overpotential of ohmic drop is insignificant compared with the activation overpotential. Consider that the activation overpotential for the electrodeposit of nickel is small compared with the hydrogen evolution overpotential when the current density is on the order of  $0.1 \text{ mA cm}^{-2}$ . (b) How much sodium hydroxide must be added to 1 liter of a solution of nickel ions to be able to quantitatively separate nickel without a hydrogen evolution reaction? Assume that nickel ions do not form hydroxide with the added base and that they separate quantitatively when its concentration is less than or equal to  $10^{-6} \text{ M}$ . Consider  $E_{\text{N}^{2+}/\text{N}}^{\circ} = -0.236 \text{ V}$ ,  $E_{\text{H}_2\text{O}/\text{O}_2}^{\circ} = 1.229 \text{ V}$ , and the molecular weight of  $\text{NaOH} = 40 \text{ g mol}^{-1}$ . (Zinola)

27. For the reaction  $\text{A} + \text{BCl}_2 \rightleftharpoons \text{ACl}_2 + \text{B}$  at  $25^\circ\text{C}$ , the value of the equilibrium constant is  $k_{\text{eq}} = 2.93 \times 10^8$ , and the ratio of activities is  $J_a = 49.0$ . (a) Determine  $E$  and  $E^\circ$  of the galvanic pair associated with such a reaction as well as the change in free energy at the same temperature. (b) If the expression for the change of entropy for the system is  $\Delta S = 257 + 8000/T \text{ J K}^{-1} \text{ mol}^{-1}$ , calculate  $E$ ,  $E^\circ$ , and  $\Delta H$  at  $35^\circ\text{C}$  for the same  $J_a$ . Consider  $R = 8.314 \text{ J mol}^{-1} \text{ K}^{-1}$  and  $K^{-1} = 1.987 \text{ cal mol}^{-1} \text{ K}^{-1}$ . (Zinola)
28. The electrolysis of pure water is performed in acidic media between an inert cathode and an inert anode. (a) Write the reactions occurring on both electrodes. Demonstrate that the open-circuit potential is independent of pH of solution when the partial pressure of the evolving gases is equal to the atmospheric pressure.  $E_{\text{CO}_2/\text{H}_2\text{O}}^{\circ} = 1.229 \text{ V}$ . (b) A solution of  $\text{H}_2\text{SO}_4$  needs to be electrolyzed at room temperature using two similar electrodes of platinum and iron. The Tafel constants for the evolution of hydrogen and oxygen are:

TABLE P.11

	$a(\text{V})$	$b(\text{V/decade})$	Metal
$\text{H}_2$	0.09	-0.09	Pt
$\text{H}_2$	0.90	-0.12	Fe
$\text{O}_2$	0.30	0.18	Pt
$\text{O}_2$	0.80	0.24	Fe

What electrodes should be used to obtain a current density of  $0.1 \text{ mA cm}^{-2}$  if mass transfer and ohmic drop effects are neglected? (Zinola)

## MICRO RESEARCH PROBLEM

1. Microresearch: Diffusion control in constant potential mode. The ion concentration gradient in proximity to an electrode surface depends on how the electrode potential state is manipulated by an external electronic device, either

a pulse generator, galvanostat, or potentiostat. So far you have been “an observer” as we solved Fick’s second law for pulse and constant-current polarization and a dropping mercury electrode, but have stopped short of using your own mathematical muscle to tackle those problems. Now that the text leaves the “constant potential polarization” mode unsolved, you should have the fun.

(a) Consider an anion that is free of the influence of migration. State the initial and boundary conditions when the potential of the anode (where oxidation occurs) is held at  $t = 0$  to a constant value that can readily oxidize the anion. (b) Using these conditions, try to solve Fick’s second law and derive an expression of surface concentration,  $c$ , in terms of time as well as distance from the electrode. (Kang)

# CHAPTER 8

## TRANSIENTS<sup>1</sup>

### 8.1. INTRODUCTION

#### 8.1.1. The Evolution of Short Time Measurements<sup>2</sup>

Although a couple of outstanding original publications on electrode kinetics appeared as early as 1928, the bulk of the experimental work in this field was carried out in the second half of the twentieth century. Experimental work with mercury as the electrode was found to be relatively easy. For one thing, because mercury is a liquid at room temperature, there were no crystal planes of differing reactivity to worry about, and mercury drops can easily be renewed, so impurity adsorption with its anticatalytic effects is not a problem.

However, when it came to electrochemical kinetics at *solid* metals, considerable difficulties faced physical electrochemists in the early years. Results under what seemed to be the same conditions of electrode and solution gave wildly differing values for the velocities of reactions at the same overpotential when done in different laboratories.

The reasons for this unsatisfactory state of affairs were eventually discovered. The measurements were lasting for excessive times. In early measurements, it was customary to hold the current density constant at a series of values while the corresponding

---

<sup>1</sup>The full title of this chapter ought to be: "Why one should make measurements in electrode kinetics at short times (i.e., transients) and how to do it." This is really a bit long for a title, so we just used the one word.

<sup>2</sup>The account of transient (i.e., rapid, or short-time) measurements marks one of the areas in which electrochemists had priority. Thus, physical electrochemists (Bowden and Rideal, 1928; Butler and Armstrong, 1936) were making measurements in the submillisecond range long before measurements in such time domains were made in chemistry (by Norrish and Porter, and Eigen, all of whom independently received Nobel prizes).



overpotential was measured over minutes and even hours for each current density. During these times, two phenomena occurred that ruined reproducibility. The first was the effect of impurity adsorption onto the electrode from the solution (mastered for solids by Bockris and Conway, 1949; Figs. 7.32 and 8.1). The second difficulty arose with the use of ill-defined surfaces of polycrystals, in which the distribution of the various crystal faces (with their differing properties) remained unrealized and uncontrolled. This difficulty was not properly solved until much later (by Hubbard in the 1970s).

Both these difficulties depend on changes in the catalytic surface of the electrode, and such changes take time. The idea of making electrode kinetic measurements at *short* times (“transients”) had been introduced by Bowden and Rideal in 1928, but their aim was less to overcome undesired surface changes and more to make use of

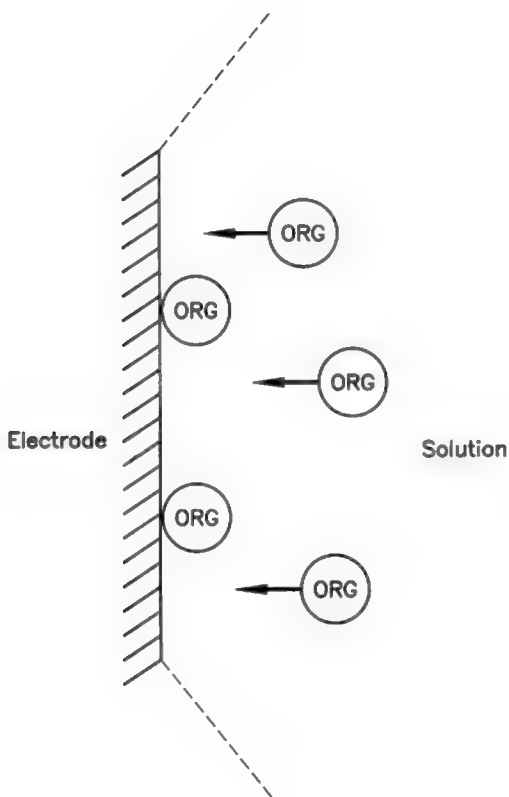


**Fig. 8.1.** Minuscule quantities of impurities in solution adsorbed at active sites on solid electrodes and reduced the activity of the electrode catalyst.

certain properties of potential–time transients to measure the real surface area of the electrode (Fig. 8.2). The ultimate in an unstable electrode surface is one on which new metal is being deposited as a part of the reaction being measured. This led to the first publication in which transients were used to record the overpotential on a millisecond time scale during electrodeposition on a solid, an analogue of high-speed photography (Roitar, Juza, and Polujan, 1939). By varying the time at which the overpotential was measured, it became possible to make conclusions about the situation at various fractions of a monolayer, or, if desired, at longer times for various multilayers of newly deposited metal.

### 8.1.2. Another Reason for Making Transient Measurements

These early transient measurements were then developed with a rather different motive than that described above. Now (cf. Eq. 7.)

$$\frac{1}{i} = \frac{1}{i_F} + \frac{1}{i_L} \quad (8.1)$$

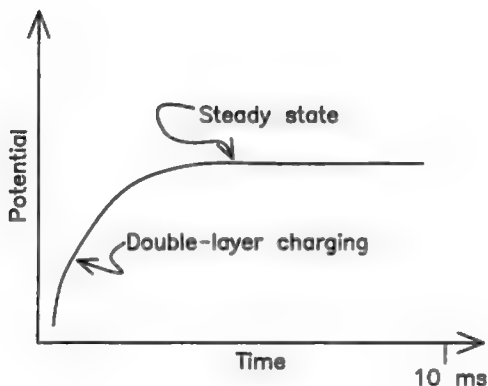


**Fig. 8.2.** An early transient. Current density is constant. Potential builds up first through charging of the double layer, but at a higher potential, electrons pass across the interface, i.e., current flows and the double layer behaves as a leaky capacitor. The very early sections of the transient (double-layer condenser not leaking) can be used to obtain the capacity of the double layer because, there, there is a negligible Faradaic current through the interfacial region and the current goes overwhelmingly to charging the double layer.  $C = (dq/dV) = (idt/dV)$ .

where  $i$  is the measured current density,  $i_F$  the current density due to Faradaic (electron-transfer) processes and  $i_L$  is the limiting diffusion current density.

Obviously, then, if one wants to obtain data dominated by the reaction at the interface, one has to be sure that

$$i_F < 10 i_L$$

Such a condition will give a current density (at least) 90% free from the influence of diffusion control; or, if it is to be 99% (or virtually completely) free of such influences, then the condition would have to be:

$$i_F < 100 i_L$$

Thus, the value of the limiting currents determines the range of current densities over which a Tafel line can be measured, independent of the interference of diffusion (see Fig. 8.3). One needs to take steps to make  $i_L$  as large as possible.

This can certainly be done, e.g., by using a rotating disk electrode, or by using ultramicroelectrodes (Section 7); one can increase  $i_L$  several hundred times compared with its value at a flat plate in a still solution. However, every technique comes with a price tag, which may not only be a dollar one. Thus, if one uses ultramicroelectrodes to give a high  $i_L$ , one has to recall that the currents there are tiny (picoamperes) and

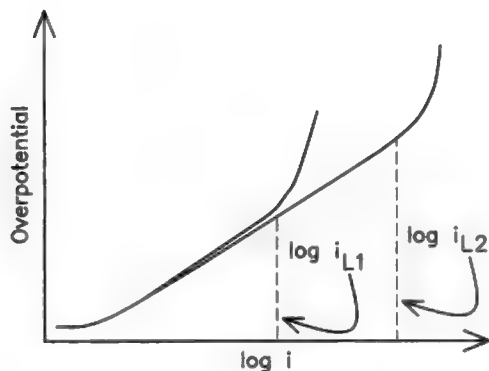


**Fig. 8.3.** A Tafel line. No special effort is made to reduce the limiting current density in case 1 and the Tafel line has a relatively small range, e.g., only  $10^2$  times in current density. In case 2, a rotating disk electrode is used to cause an increased limiting current density, and hence a larger range (say,  $10^4$  times) of current density.

the measurement of such low currents requires special instruments that are available only in a limited number of research laboratories.

Such a consideration, then, turns attention to the *time* dependence of  $i_L$ . Would there be a time domain in which  $i_L$  is very large? The basis of an answer to this question has been given in Section 7.9.10, where discussion shows two time regions in which  $i_L$  is to be considered. To understand the first of these, one must recall Eq. (7.206), the relation between the limiting current density,  $i_L$ , and the diffusion layer thickness,  $\delta$ . It is

$$i_L = \frac{Dz_i F c_i}{\delta} \quad (7.206)$$

However,  $D$ ,  $z_i$ ,  $F$ , and  $c_i$  are time independent ( $c_i$  is the concentration of the reactant in the bulk). It must be the term  $\delta$ , therefore, from which one is to expect a time dependence.

*Region 1:* In this (lower time) region, the diffusion layer grows with time according to (Section 7.9.9):

$$\delta_t = \sqrt{\pi D t} \quad (7.204)$$

Thus:

$$i_L = \frac{Dz_i F c_i}{\sqrt{\pi D t}} \quad (8.2)$$

From (8.2), then,  $i_L$  increases as  $t$  decreases. Thus, at times of 0.1 ms and 1 s,  $i_L$  will be about 100 times more at the lower times than at the higher one.

Use of the lower time would give a big advantage in respect to the upper limits of current density at which an electrode kinetic measurement can be made free of diffusion control. At 0.1 ms, the current density will be free of diffusion effects because it is 100 times higher than that at 1 s, when diffusion will in any case affect the measurement (Fig. 8.4).

Earlier it was pointed out that the use of ultramicroelectrodes could also give a "several hundred" times increase in  $i_L$  compared with the diffusion-free currents at planar electrodes. The advantage of increasing the ability to measure at higher current densities by using short times in a transient technique with a planar electrode is that the magnitude of the currents is normal and is not forced down to the difficult-to-measure picoampere region that microelectrodes require.

*Region 2:* What is the upper limit of the applicability of Eq. (8.2)? There must be one, because as the equation indicates, in a few hours the value of  $\delta$  will be in the centimeter range and will challenge the width of the experimental vessel. Long before this and frequently in the 10-s range, the change of concentration at the interface caused by removal of the reactant (cathodic current) onto the electrode or its oversupply in the neighborhood of the electrode surface by means of dissolution of the electrode

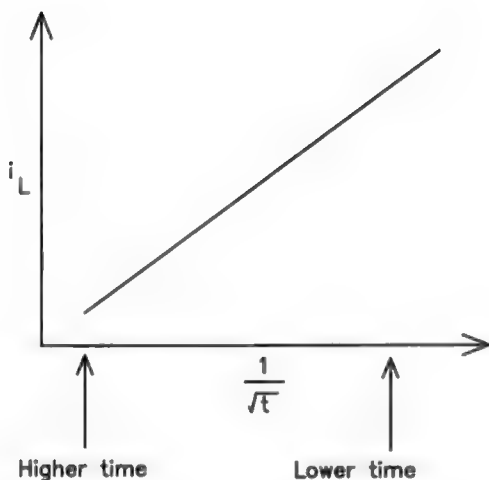


**Fig. 8.4.** As the time increases, the limiting diffusion current density decreases in accordance with  $t^{-1/2}$ . If the only objective is a high limiting current (with no need to reach steady state) it is best to work at the lowest practical times.

(anodic current), the *density* of the solution near the surface changes from that of the bulk of the solution and thereby introduces convection, which stirs the solution near the interface and invalidates Eq. (7.24). Empirically, it is found that this natural convection eventually makes  $\delta$  a constant that is independent of time and has a value around 0.05 cm for solutions at room temperature in the absence of artificial stirring.

So, here is the summary of what we can do to help the experimenter be sure that his or her measurement reflects interfacial and not transport control.<sup>3</sup> (1) Working at short times (microseconds up to a millisecond, say), increases  $i_L$  and therefore lengthens the current density range in which diffusion-free measurements can be made. (2) Working at times  $>$  about 10 s means that natural convection tends to make  $\delta$  constant, i. e., independent of time. However, this time-independent value can still be reduced (and hence  $i_L$  helpfully increased by methods already reviewed (Chapter 7),

<sup>3</sup>Here is the place to point out a certain “attitude” of the authors of this book. It is assumed that the objective of the measurement is to find out all one can about events *on the electrode*. This is the attitude of a physical electrochemist. An electrochemist whose business is otherwise—who wants to measure the concentration of a species in solution (e.g., for analytical purposes)—might take a different view. He or she would want to emphasize transport control and the region *near* the electrode because that would lead to information on the concentration of the entity diffusing.

e.g., the use of a rotating disk electrode at high rpm, or the use of microelectrodes (low radii of curvature).

### 8.1.3. Is there a Downside for Transients?

Are there some counterpoints that may spoil these ideas of using transients to maintain a contamination-free electrode surface during measurement and avoid diffusion control? Yes, there is one. It does not affect the simple type of electrode process (e.g., a “redox” reaction (such as  $\text{Fe}^{3+} + e \rightarrow \text{Fe}^{2+}$ ) because here there are no surface-adsorbed radicals, the variation of which with time may have to be considered. But for a more typical electrochemical reaction (e.g., MeOH oxidation to  $\text{CO}_2$ ) the properties of the adsorbed intermediate radicals that undergo chemical surface reactions, particularly their changes in surface concentration with time at constant potential, are very important. The challenge is created by the fact that when one varies the potential of the electrode, the concentration of the reaction intermediate on the surface changes, but sometimes slowly, i.e., in seconds or even minutes, instead of in milliseconds, a typical time range for a transient. Hence, a danger of using transients is that if the time has been made *too* small, to get a large  $i_L$  and eliminate diffusion (thus making possible a diffusion-free measurement at a very high rate), one may not give intermediate radicals enough time to reach their steady-state surface concentration (Fig. 8.5). In this case, one has to use *extreme* purification, well-defined single-crystal surfaces, and potentiostatic transients, with the current at a given potential continued to steady-state value, even if this takes more than 10 s. However, if the necessary time is such that one enters the time-independent region for  $i_L$  (convection at work), one must keep the working current density at least 10 times below the value  $i_L$  (although this can be increased by methods summarized in Table 7.).

In the rest of this section, the various ways transients can be used to reduce diffusion effects and the effects of contamination of the electrode surface by adsorption from solution will be discussed, as well as any counter-limitations that some types of transient measurements may involve.

### 8.1.4. General Comment on Factors in Achieving Successful Transient Measurements

The majority of fundamental measurements in electrode kinetics are made in one of the types of transients described below. It is meaningless to speak of a “best” transient method, because each electrochemical reaction has its own characteristics, and the large variation in the properties of the reactions concerned means there will be variety in the most appropriate transient method. Some general points follow here. *All* of them must be considered before picking the best technique to use. Further, it must be recalled that the biggest distinction between electrode reactions is in respect to those (few) that occur without adsorbed intermediates and

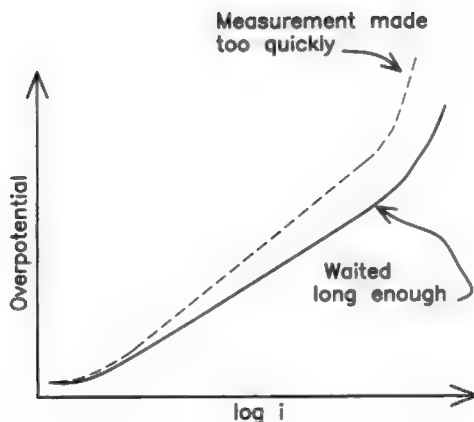


**Fig. 8.5.** In electrochemical reactions involving one or more adsorbed reaction intermediates (sometimes involved in the rate-determining step), the steady-state concentration of the intermediate changes with the potential. However, each intermediate has a time constant to reach the surface coverage corresponding to a given overpotential. The downside of too low a pulse time, or too fast a sweep rate, is that the intermediate concentration does not relax to its appropriate concentration "in time." The Tafel slope (sometimes a significant mechanism indicator) may then differ from that calculated for the assumed path and rate-determining step.

those (many) that involve intermediates which have, however, their own time constants for coming to their steady state after a change in the overpotential applied.

1. It is advantageous from two important points of view (constant surface; high limiting current) to make electrode kinetic measurements as soon as possible after the electrode has been brought into contact with the solution. This can be done, e.g., by preparing an electrode by heating it in an  $\text{H}_2$  atmosphere and then sealing it into an  $\text{H}_2$ -filled glass bulb—the latter to be broken with a probe after introduction of the solution under  $\text{H}_2$  pressure.

2. The *lower* time limit is usually the time needed to charge the double layer to the chosen potential for the measurement.

3. In a typical electrochemical reaction, one has adsorbed intermediates, the buildup of each of which has a characteristic relaxation time that is potential dependent. This may *increase* the minimum acceptable time for a measurement at a chosen potential.

4. Impurities take significant time (up to hundreds of seconds) to become adsorbed to equilibrium on an electrode. Correspondingly, one has to be cautious that variations in the time of the current in a constant potential transient are not caused by the fact that in waiting for an intermediate radical to build up to a constant value, one has run into times long enough for impurities from the solution to become adsorbed. The longer the time needed to attain the steady state in an electrode kinetic measurement, the more it is necessary to maintain a scavenger device (Section 7.5.1) in the solution to keep the impurity concentration low. This is particularly necessary in nonaqueous solutions when there is a constant tendency for water vapor to leak into the dry solution.

The difficulties concerning the relaxation time for intermediate radicals are greatly lessened for redox reactions, where no adsorbed intermediates are involved. However, using such reactions as a way of reducing difficulties with transients will lead one to miss 90% of the reaction's electrochemistry.

## 8.2. GALVANOSTATIC TRANSIENTS

### 8.2.1. How They Work

This is the transient method for which most experience is available. It was introduced by Bowden and Rideal (1928). The name comes from that of Galvani<sup>4</sup> and means, in fact, "current." Thus, "Galvanostatic transient" means "short-term constant current." The circuitry is simple. It consists of nothing more than a measurement cell in series with an adjustable resistance much larger in value than the resistance of the cell, a power source, a rapid action switch, and a cathode ray oscilloscope to record the variation in the potential of the working electrode with time. A typical potential-time relation is shown in Fig. 8.6.

The zero constant starting potential is at A. From A-B, the cathode ray oscilloscope screen may remain blank or show a vertical (i.e., extremely short time) rise in potential. The potential change here represents the IR drop between the end of the Luggin capillary (Section 7.5.7.2) and the electrode. It can be removed electronically from the measurement. During the time corresponding to B-C of the transient, two processes are occurring. The first (which is dominant at the lower time) is the charging of the double layer to correspond to the change in potential. The second (which becomes dominant at the longer time, C) is the passage of electrons across the double layer to ions on the solution side (if the potential is growing more negative). In the period C to D, the double-layer charging is almost finished and nearly all the current is going into the passage of electrons across the double layer. Insofar as C-D takes a significant time to become constant, this may be due to the settling down of the

<sup>4</sup>It was Galvani (1791) who first observed that the leg of a frog he was dissecting twitched when his technician touched it with a scalpel at the moment a nearby electric machine emitted a spark (Vol. 1, Section 1.1).



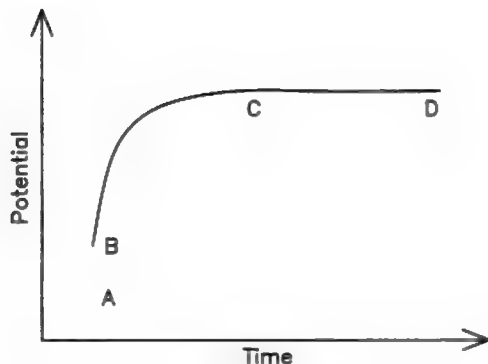


**Fig. 8.6.** The basic Galvanostatic transient, explained in the text.

intermediate radicals taking part in the multistep electrode reaction (Fig. 8.6)<sup>5</sup> It is assumed in the diagram that the time for which the transient lasts is less than the transition time at which diffusion control will set in ( $\delta_t$  having become sufficiently large).

Now, it has already been seen in Chapter 7 that one may write an equivalent circuit for a simple electrode/solution interface as given in Fig. 7.52, where  $R_{\text{soln}}$  is the resistance of the solution;  $R_F$  is the Faradaic resistance; and  $C_{\text{DL}}$  the double-layer capacitance; then the relaxation time<sup>6</sup> is given by:

$$\tau = R_F C_{\text{DL}}$$

The value of  $\tau$  is important for a reason connected with the equation  $\delta_t = (\pi Dt)$ . As long as the time  $t$  in this equation is small, the limiting diffusion current,  $i_L$ , will be large (for  $i_L = DzFc_i/(\pi Dt)^{1/2}$  and hence diffusion control will be negligible  $[(1/i) = 1/i_F + (1/i_L)]$  and the region C-D of the transient will represent the interfacial electrode reaction. (However,  $t$  must be greater than  $\tau$  to reach the steady state.)

Knowing the constant current imposed on the circuit and the “final” potential in the C-D region, the value of the overpotential corresponding to the current can be obtained. Repeating the measurement at a series of constant current densities allows determination of the  $i_0$  and the  $\alpha$  value of Tafel’s equation. If  $i_0$  is available, the corresponding rate constant  $k_0$  can be calculated from the equation  $i_0 = Fk_0\chi c_0$ , where  $\chi$  is the thickness of the reacting layer.

What may go wrong? If the  $i_0$  is sufficiently low and hence (as  $R_F = RT/i_0F$ )  $\tau$  sufficiently high, the  $\delta_t$  may have risen enough so that the limiting diffusion current

<sup>5</sup>This is an “ideal” statement. Other processes that can delay constancy of the potential are crystallographic changes on the electrode surface, particularly if it is a polycrystal (and of course impurity adsorption).

<sup>6</sup> $\tau = R_F C_{\text{DL}}$  is the time for the potential to attain 63% of its final value.

density becomes sufficiently low to affect the measurement  $[(1/i) = (1/i_F) + (1/i_L)]$ . However, there is a way around such a difficulty. Instead of simply switching on a specific constant current density, one uses two pulses, as proposed by Gerischer. The first pulse is the bigger in terms of the current density used and simply has the task of charging up the double layer much more quickly than would be the case if one used the lower working current density alone. Typically, one would use for the first pulse a current density about ten times that for which one wishes to record the “final” potential. Thus, one is making a meaningful kinetic measurement for a given current density much earlier than one would with a simple pulse. However, that means that the  $i_L$  is much higher because of  $\delta_i = (\pi D\tau)$  and hence the kinetic measurement is free of diffusion control. Thereafter, one uses a lower (final) current density, that at which one wishes to measure the overpotential.

## 8.2.2. Chronopotentiometry

*Chronopotentiometry* means, as the name suggests, a measurement in which the change of potential with *time* is important. In fact, Chronopotentiometry is a galvanostatic technique in which (in contrast to the practice in most transient techniques) the times chosen are sufficiently great that the  $i_L$  is low and diffusion becomes potential determining. The relevant equation has already been dealt with (7.192) and is<sup>7</sup>:

$$E = E^\circ + \frac{RT}{nf} \ln \frac{\tau^{1/2} - t^{1/2}}{t^{1/2}} \quad (7.192)$$

The quantity  $\tau$  is the transition time and is in fact the time at which the concentration of the active reactant at the interface is used up and the potential shifts to find another reactant able to diffuse to the surface to maintain the current.

A determination of  $\tau$ , the transition time, involves an  $E-t$  relation such as that in Fig. 8.7. The value of  $\tau$  is given by Sand's equation (7.190), which contains  $c_0$ , the reactant concentrations in solution, so that, if  $\tau$  and  $n$  are known,  $c_0$  can be obtained. This chronopotentiometry is (or was) an analytical technique, but it is no longer much used for the original purpose of determining the concentration of an electroactive reactant in solution because there are more accurate methods. Thus, if the time is short, there may be confusion with double-layer charging time; if the time is too long, irrelevant side reactions may interfere. The method can, however, be used to determine

<sup>7</sup>This equation represents the change of the Nernst *reversible* electrode potential (Section 7.2.7) with time. Is there also an activation overpotential? Yes. However, because the current density during the experiment is constant, any overpotential should be constant (and hence not contribute to a change of potential with time), up until the end of the transient, when the diminution of the reactant concentration and change to another reaction will change the overpotential to that characteristic of the second reaction. However, the important change of potential will be given near the end of the transient when  $t \rightarrow \tau$ , and that is given by Eq.(7.192).

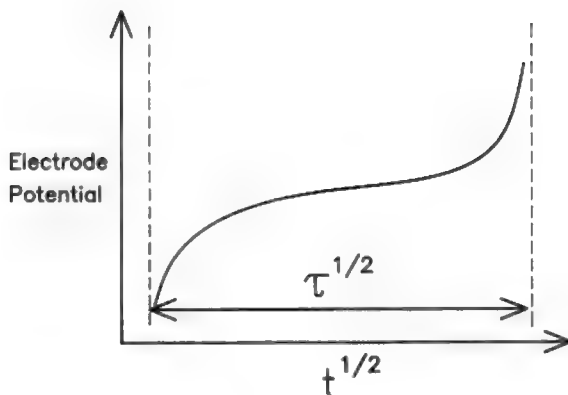


**Fig. 8.7.** A chronopotentiometry diagram. The electrode potential turns up sharply when the diffusion layer is exhausted of material for the electrode reaction. The electrode attempts to seek another source of electrons.

$n$ , the number of electrons in the overall reaction. This quantity must be an integer so that an error of  $\pm 10\%$  will not affect the decision.

### 8.3. OPEN-CIRCUIT DECAY METHOD

#### 8.3.1. The Mathematics

Here one fixes the potential of the working electrode to a certain value and at  $t = t_0$  cuts off the current and observes the decay of the potential. Thus, in general, the current density at an electrode can be written as the sum of the condenser charging current ( $i_C$ ) and the Faradaic current of electrons crossing the double layer ( $i_F$ ). Thus,

$$i_C dt = dq \quad (8.3)$$

By definition:

$$C = \frac{dq}{dV}; \text{ or here } C = \frac{dq}{d\eta_t} \quad (8.4)$$

After the current is switched off:

$$i_C + i_F = 0; \text{ hence } i_C = -i_F \quad (8.5)$$

Or

$$-i_F dt = dq = C d\eta_t \quad (8.6)$$

For an anodic situation and with  $\eta_t > RT/F$ ,

$$-i_0 e^{\alpha\eta_t F/RT} dt = C d\eta_t \quad (8.7)$$

$$\int_{t_0}^t -i_0 dt = \int_{\eta_0}^{\eta_t} C e^{-\alpha\eta_t F/RT} d\eta_t \quad (8.8)$$

With  $t \gg t_0$  and  $\eta_0 \gg \eta_t$

$$-i_0 t = -\frac{RT}{\alpha F} e^{-\alpha\eta_t F/RT}$$

$$\eta_t = \frac{RT}{\alpha F} \ln \frac{RT}{\alpha F i_0} - \frac{RT}{\alpha F} \ln t \quad (8.9)$$

Hence, under the stated conditions, a plot of the varying overpotential  $\eta_t$  during decay against  $\ln t$  gives the Tafel coefficient  $\alpha$ . The intercept will yield  $i_0$  if  $C_{DL}$  is known from an independent source, e.g., a galvanostatic charging curve.

There is an assumption here that during the decay interval of  $t$  s, the double-layer capacity,  $C_{DL}$  remains constant. If it does,  $\eta_t$  will be linear with  $\ln t$  and have the slope of

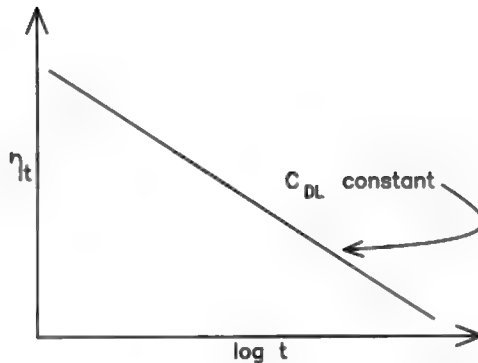


**Fig. 8.8.** The decay of overpotential with time in an open-circuit situation with a constant double-layer capacitance over the decay region. The initial overpotential is anodic and the electrode becomes less positive as the time increases.

$RT/\alpha F$ . One would expect such a result if the double layer is behaving as an ideally polarizable double layer (Section 6.4.3) and there is, e.g., no adsorbed intermediate to slow down the decay. Figure 8.8 shows this case. When there is an adsorbed intermediate radical of significant concentration, the decay method can be used to determine the potential dependence of the fraction of the surface covered by the radical (Conway and Tilak, 1982).

An advantage of open-circuit decay is the absence of IR drop because no current passes through the solution. This is particularly important for work in nonaqueous solutions where the high specific resistance makes the danger of IR errors much more severe than in aqueous solutions.

## 8.4. POTENTIOSTATIC TRANSIENTS

### 8.4.1. The Method

In a potentiostatic transient, the observable quantity is the current density, while what one fixes for a given transient is the electrode potential. An idealized<sup>8</sup> potentiostatic transient (one not showing the effect of diffusion control, which may develop at longer times) is shown in Fig. 8.9.

At times long enough to show some effect of diffusion (not shown in the figure), one has to extract the interfacially controlled Faradaic current from the total current. By carrying out an experiment at a series of potentials, one can obtain the Tafel constants  $\alpha$  and  $i_0$  from a  $\log i_F$  against the overpotential plot. There are several ways to evaluate the Faradaic current,<sup>9</sup> free of diffusion control, which would begin to affect the current at times greater than those corresponding to  $D$  in Fig. 8.9. The simplest (not the most sophisticated)<sup>10</sup> way to obtain  $i_F$  is to recall, once more, the equation:

<sup>8</sup>The shape of actual potentiodynamic transients is sometimes affected by a change in the dominant crystal orientation of facets in polycrystals and by impurity adsorption. There is a conflict between the desire to make short transients ( $< 1$  s) and thus be less affected by diffusion, etc. and the need for radical intermediates to attain steady state at each of the constant potentials used.

<sup>9</sup>The interfacially controlled current is often called *Faradaic* for a historical reason. Among the earliest established electrochemical experiments were those leading to Faraday's laws of electrolysis. Here, the current for a given time was clearly related to the amount of metal deposited. Thus, the term originated in the evidence that this current ("Faradaic") was causing a proportionate change on the surface.

<sup>10</sup>A more sophisticated method involves equations related to those presented in Chapter 4. Thus, it may be shown that

$$\frac{i}{i_{\text{diff}}} = \pi^{1/2}(\lambda) \exp(\lambda^2) \operatorname{erfc}(\lambda)$$

where  $\lambda = k_n(t/D)^{1/2}$  and  $\operatorname{erfc}(\lambda)$  is the error function complement of  $\lambda$ . One can measure  $i$  and calculate  $i_{\text{diff}}$  from  $i_{\text{diff}} = nFDc/(\pi Dt)^{1/2}$ . The rate constant is the desired objective and one can use independent knowledge of  $D$  and a suitable computer program to find what value of  $k$  fits Eq. (8.10).

However, Eq. (8.10) involves two limiting assumptions: that the reaction is first order and that  $\theta_{\text{radicals}}$  tends to zero. Neither of these assumptions is sufficiently general to fit the majority of electrochemical reactions.

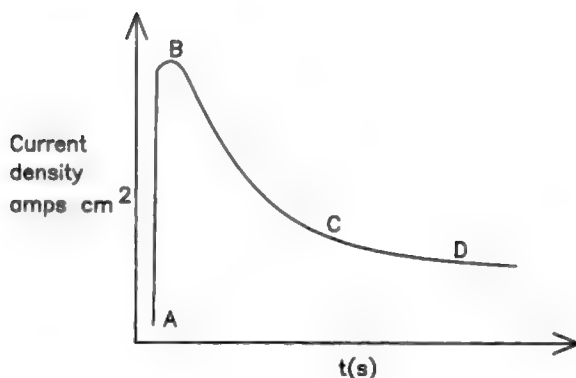


**Fig. 8.9.** A potentiostatic transient. The potential is first set on the potentiostat at the desired value and thus applied to the electrode. From A to B, the current is used in charging the double layer up to the potential chosen. From B to C, the current falls because it is no longer only being used to charge the double layer but increasingly, to drive electrons across the interface—a much more difficult task (i.e., higher resistance than charging the double layer). In C-D, the double layer is almost charged and the current is beginning to become constant (i.e., when all the electrons are used to cross the double layer and none for condenser charging.) The effect of diffusion will be visible if the time is long enough, and will cause the current to decrease beyond D according to Cottrell's equation, with  $t^{1/2}$  (Section 7.9.6).

$$\frac{1}{i} = \frac{1}{i_F} + \frac{i}{i_L}$$

However:

$$i_L = \frac{DzFc_i}{\delta}$$

and as (up to the time at which natural convection intervenes)

$$\delta_t = \sqrt{\pi Dt}$$

one sees that

$$\frac{1}{i} = \frac{1}{i_F} + \kappa t^{1/2}$$

A plot of  $1/i$  against  $t^{1/2}$ , extrapolated to  $t = 0$ , should give  $i_F$ . These matters seem simple enough. However, there are several problems, each solvable; although to varying degrees.

1. It has been assumed that the decline of the current with an increase in time (not shown in the figure) is due only to the onset of a degree of diffusion control, and that the method for obtaining the desired  $i_F$  depends on this assumption. However, there are two other reasons for a decline in current. First, as already stated, the effect of double-layer charging may not be finished in the early part of the  $i_t - t$  plot (between B and C in Fig. 8.9) so that it may be that a straight line between  $1/i$  and  $t^{1/2}$  is observed only if the earlier points are neglected.

Then, another reason for the decline of the current may be buildup of intermediate-surface radicals that diminish the available surface area of the electrode by a time-dependent factor. It is erroneous (in respect to the majority of electrochemical reactions) to assume that the electrode surface remains unchanged during the reaction. What starts out with  $\theta_t \rightarrow 0$  may end with  $\theta_t \approx 1$ . The factor  $(1 - \theta_t)$  may enter into the control of the current. In order to examine this factor, an independent (preferably spectroscopic)<sup>11</sup> method of looking for time-dependent intermediates (which build up  $\theta_t$ ) is desirable.

2. A different difficulty is the IR drop between the end of the Luggin capillary and the electrode. It is the total of the electrode potential *together with* this “IR error” which the potentiostat keeps constant. Thus, since the sum of both these contributions is kept constant, and if a significant IR component varies, then the electrode potential itself varies during the transient, although the very point of the method is that the electrode potential is assumed to remain constant throughout the  $i_t - t$  transient.<sup>12</sup>

There are electronic compensation circuits available to reduce this error, and if the current density is low enough (or the solution highly conducting), it may be negligible. The high resistance of nonaqueous solutions could provide a difficulty (which, however, is not present in the decay transient approach).

## 8.5. OTHER MATTERS CONCERNING TRANSIENTS

### 8.5.1. Reversal Techniques

It is important not to give the impression that all transient techniques neglect intermediate radicals. Some techniques are expressly designed to “catch” them (in contrast to other techniques that neglect them completely). One of the radical-sensitive techniques may be called *reversal*, and refers to information that can be obtained if

<sup>11</sup>There are purely electrochemical methods for finding the amount of simple radicals such as H or O on noble metal electrodes. Basically, they rely upon the assumption that when some electrical variation in the state of the electrode is brought about, the only effect it has is to reduce or augment the H or the O on the electrode surface. Now of course this is not so if the substrate is, say, iron, or indeed all but the noble metals, for there may be a co-dissolution of the substrate, or competing oxide film formation, etc. Spectroscopic methods (e.g., FTIR in a millisecond response version) or ellipsometry are not affected by such difficulties.

<sup>12</sup>This was an easily eliminated error in the galvanostatic transients, where it is a constant quantity, owing to the constancy of the current in a given transient.

one observes the effects of reversing the direction of the current in a galvanostatic experiment, or in the potentiostatic analogue, changing the potential from one in which the reaction gives a limiting current in the cathodic direction to one in which the limiting current is being measured in the anodic direction.

To see what can be done with such techniques, just to open the door on them, one can think of a reaction



Here the intermediate product, I, is an adsorbed radical. It may have great difficulty in going on to B (i.e.,  $k_{+1}$  is small) or it may rapidly go to B ( $k_{+1}$  is large). In the first case, current reversal reproduces A; in the second case, there is no I to send back to A. One can see that at least some knowledge about I can be obtained from a current reversal experiment.

This very short treatment of reversal techniques has the following basis. There are certainly treatments in the literature of chronopotentiometry dealing with current reversal, or reversed-step voltammetry. However, their validity has to be diligently examined in each application. For example, is an assumption of a first-order reaction tacitly involved, when the actual solution may correspond to a fractional reaction order? Another reason for the limited treatment has an eye on the future. There are those who see in the rapid development of *in situ* spectroscopic techniques (see, e.g., Section 6.3), together with advances in STM and AFM, the future of surface analysis in electrochemistry. If these surface spectroscopic techniques continue to grow in power, and give information on surface radicals in time ranges as short as milliseconds, transient techniques to catch intermediate radicals adsorbed on surfaces may become less needed.

## 8.5.2. Summary of Transient Methods

**TABLE 8.1.**  
**Some Transient Methods**

Name of Transient	How Is It Carried Out?	Positive Points	Negative Points
Galvanostatic	Observe potential during constant current pulse	IR drop easily allowed for; observable on oscilloscope	Relaxation time may be too slow; transient runs into diffusion control
Double pulse galvanostatic	Use two pulses; first a large one charges the double layer; second a smaller one runs the reaction	Fast chargeup; avoids slow relaxation time	Difficulties are secondary, e.g., possible surface change during pulse. If pulse too short, may not get to steady state; too long, diffusion control



TABLE 8.1.  
Continued

Name of Transient	How Is It Carried Out?	Positive Points	Negative Points
Chronopotentiometry	Galvanostatic transient but under conditions that encourage diffusion control. Observe transition time	Determine $n$ , number of electrons in overall reaction; a valuable parameter, not easy otherwise to determine	As analytical technique to determine concentration is sloppy and may be affected by double-layer charging; need to know $D$ and $n$ independently
Decay	Bring electrode to potential in Tafel region, then open the circuit so that $i = 0$ . Observe decay of potential	Because no $i$ through solution, IR drop is zero. Excellent for nonaqueous solution work	Simple analyses show $\eta$ , linear with $\log t$ . If not, presence of radical indicated
Potentiostatic	Fix potential with potentiostat and observe current as $f(t)$ to steady state. Repeat at many fixed potentials	Intellectually attractive because it mirrors a chemical reaction with fixed energy of activation for each potential	Potentiostat makes ( $IR + \eta$ ) a constant, may mean $\eta$ varies unintentionally with time unless IR error electronically compensated.
Reverse pulse	Reverse $i$ in galvanostat or change $\eta$ from + to - in potentiostat cases, respectively	Can give information by intermediate radicals	However, math analysis involving diffusion and intermediate radicals difficult and may involve inapplicable assumptions. Spectroscopic methods better radical catchers?

### 8.5.3. "Totally Irreversible," etc.: Some Aspects of Terminology

Fundamental electrode process chemistry, "electrodics," gave rise to so many useful analytical applications that the resulting subfield of electroanalytical chemistry has become a tail that wags the dog. The contributions of electrochemists primarily interested in analysis are not only of large extent but are also broad in interest. Further, the work done by those in the analytical field often contributes novel advances to fundamental electrochemistry.

Nevertheless, it must be recalled that there is a different tilt among those who were introduced to electrode process chemistry because they wished to use it in increasingly sophisticated analytical techniques and those whose main aim is to increase knowledge

of what goes on on surfaces during an electrochemical situation.<sup>13</sup> This difference in emphasis can be readily seen in the development of transient methods in respect to the time domain of interest in transient techniques. Thus, the electroanalytical chemist is more interested in diffusion-controlled processes and in conditions (such as longer times) that will emphasize transport effects. With such interests in mind, events at the interface will be seen as a complication to the study of transport and reactions in solution. Conversely, the physical chemist will see transport as a complication to his or her interest in the surface itself and what goes on there with the aim of factoring out the involvement of diffusion. Hence, the physical chemist tends to go for shorter experiments, although the shortness of the time is limited by the relaxation time of intermediate radicals.

These matters show up in terminology. For the physical electrochemist, there is the state of thermodynamic reversibility, the domain of the Nernst equation, and this state is the bedrock and the base from which he or she starts out. When a reaction departs from equilibrium in the cathodic and anodic direction, it has a degree of irreversibility in the thermodynamic sense. Thus, for overpotentials less than  $RT/F$ , one refers to the linear region ( $i \propto | \eta |$ ), where departure from reversibility is small enough to be measured in millivolts. If  $| \eta | > RT/F$  (about 26 mV at room temperature), the reaction is simply and straightforwardly irreversible; the forward reaction has been made to become much faster than the back-reaction.

However, if one calls a reaction irreversible in the thermodynamic sense, this does not mean that it cannot be reversed! Reduction of oxygen to water is one of the more irreversible electrode reactions known (in this thermodynamic sense), and therefore it always runs (for a significant rate) at a large negative overpotential. However, it is simple to reverse the direction of the current and oxidize water to produce oxygen, with a large positive overpotential. Thus, the physical electrochemist regards the term "irreversible" as the converse of the thermodynamic term "reversible," but not in respect to the direction in which the reaction may be caused to go. If thermodynamic equilibrium has been left behind, an "irreversible" event is occurring. The term used in this way is not meant to indicate that there is no possibility of turning the reaction around in direction; indeed, there is a measure of the degree of thermodynamic

<sup>13</sup>Corresponding to a division among electrochemists as to their main objective (analytical or physical), one finds that within U.S. universities the electroanalytically active electrochemists belong naturally to the analytical division. However, the electrochemists whose interests are not in analysis vary in the home they find. The most fundamental chemists (and particularly the quantum theorists) are housed in physical chemistry divisions, while the organoelectrochemists clearly choose organic divisions. Others are in chemical engineering, materials science, electrical engineering, and biochemistry departments. Insofar as the university is sufficiently future conscious, it may have an environmental division in which electrochemists play a strong role in researching, e.g., pollution-free power sources for cars, photovoltaics, water splitting with solar light, and electrochemical procedures for wastewater purification and the remediation of wastes.

irreversibility, and this is the overpotential needed to drive the reaction in one direction at a given rate.

The electroanalytical chemist tends to use terms such as “reversible” and “irreversible” in a subtly different way, although the difference is more one of semantics rather than final understanding. Thus, the phrase “totally irreversible” is used by electroanalytical practitioners for reactions in the Tafel region [ $|\eta| \gg (RT/F)$ ]. The physical electrochemist most certainly views such reactions as being thermodynamically irreversible, and distinctly so. However, it seems that the use of the term “totally” irreversible may lead to misunderstanding, for it does not seem consistent with the ease of reversal in *direction*, which in practice can be made to occur even with the most (thermodynamically) “irreversible” reactions.

Correspondingly, the electroanalytical chemist frequently refers to electrode processes having a finite rate as “reversible” when they have moved only a small degree away from equilibrium. This happens as a result of the competition between  $i_L$  and  $i_F$ , the diffusion-controlled limiting current and the interfacially controlled Faradaic current.

If  $i_L \ll i_F$ , the reaction is largely diffusion controlled and the overpotential that arises from the electron transfer and other interfacial processes may be negligible. Then, as an approximation, the Nernst equation is applied, as has been seen in the section on chronopotentiometry. “Quasi-reversible” might give rise to less misunderstanding for the  $\eta$  vs.  $i$  region the physical electrochemist thinks of as “linear,” but electroanalytical chemists tend to use the term “quasi-reversible” for the region in which there is mixed control, i.e., the realm in which both  $i_L$  and  $i_F$  are of the same order of magnitude.<sup>14</sup> These matters are summarized in Table 8.2.

### 8.5.4. The Importance of Transient Techniques

The variety of possibilities with transients, and the fact that each has its own characteristic limitations, may drive the reader to ask whether one cannot just switch on a potential and wait for the current to become constant, etc. Indeed, this was just what electrochemists used to do in the first half of the century. It is one of the reasons why progress in electrochemical kinetics is measured almost entirely by work done in the second half. He or she who switches on and waits for constancy of potential should plan to come back after a late lunch, or perhaps after supper. The potential will still be varying unless very great care has been taken to constantly remove contaminants and provide a certain crystal orientation in contact with the solution. Even then, H atoms may diffuse into the substrate and change its character; and O may build up oxide films, etc.

<sup>14</sup>One is reminded of the gasoline tank that some would call “half full” and others “half empty.” The electroanalytical chemists like the term “reversibility” and when reality forces a departure from it, they still remain near it. Conversely, physical electrochemists like irreversibility—it shows properties they want to measure.

**TABLE 8.2.**  
**Terminological Alternatives in Electrodeics**

	Physical Chemistry Tilt	Electroanalytical Tilt
Reversible	Meaning comes directly from thermodynamics. Means: "at equilibrium" and applicable equation is that of Nernst	Agrees with physical chemistry definition but extends to situation in which diffusion is rate determining; interfacial processes provide negligible influence from <i>their</i> overpotential. Although $i > 0$ , such situations called reversible and Nernst applied
Linear region	Used when $\eta < RT/F$ and $i \propto \eta$	Not used
Quasi-reversible	Less used	The interfacial overpotential is $< RT/F$ and the reaction is controlled both by diffusion and interfacial processes
Irreversible	If $i > 0$ , i.e., departure from equilibrium, situation is irreversible in the thermodynamic sense. If $ n\eta  < RT/F$ , reaction is in "reversible region" and there is a linear relation of $i$ to $\eta$	Uses phrase "totally irreversible" for $ n\eta  > RT/F$ Tafel region
Emphasis	Aims principally to eliminate influence diffusion, observe interfacial happenings. Prefers Tafel region	Aims principally to reduce influence interfacial happenings, observe diffusion; monitor entities in solution. Prefers "reversible" region
Archetypal reaction	$2H^+ + 2e \rightarrow H_2$	$Fe^{3+} + e \rightarrow Fe^{2+}$

The point is that measurements of the dependence of the *rate* of the electrode reaction on important variables—potential, concentration, temperature, pressure, etc.—must be made under conditions in which the influences of contamination and diffusion control are eliminated. If, for example, when one varies the pressure, some other influence is at work (say, H diffusing into the electrode material and changing the properties of the surface), then of course an innocent analysis of the result of pressure variation (which may take many minutes to accomplish) as though the changes observed were due only to that variation and not contamination of the electrode surface, may yield puzzling conclusions.

Keeping the time short *is* very helpful in decreasing the uncertainties that develop as the time of exposure to solution increases, and in decreasing the effect of diffusion control. Each transient method has to be treated individually and each one, when used incorrectly, can obscure the physicochemical events at the interface (Table 8.1). Thus, to go to times that are *too* short ( $< 1 \mu s$ ) will tend to mix the effects of the time constants

of the instrument upon the results. Times that are “too long” may lead to the onset of diffusion control.

For electrochemists whose principal objective is analysis of constituents in solution, the path is straighter and the hill less steep. The reaction model often used is a redox reaction in which the interfacial reaction is simply electron transfer, and surface chemical reactions among radicals can be neglected. The electrode is regarded as stable during the reaction and is not intended to take any chemical part in it. The function of the surface is not electrocatalytic, it is simply to be a source and sink of electrons, the energy of which may be controlled by variation of the electrode potential.

By contrast, pity the physical electrochemist! Compared with his electroanalytical colleague, his burden is heavier, his road twistier. On *his* stage may play a panoply of most of chemistry's atoms. His electrodes may be platinum, but they are more likely to be iron or semiconductors such as doped gallium phosphide or even semi-insulators such as proteins. His expenses will be greater, also, for he will want to work, at least in research laboratories, with single crystals having a face of specific crystallographic orientation in contact with the solutions. This requires hefty expenses for instrumentation, which is increasingly spectroscopic in nature.

For these researchers, transients are not merely helpful but essential. Because each method has limitations, it is desirable to use two and even three transient methods for one reaction. Rotating disk and microelectrode techniques and the steady-state methods, summarized in Table 7. , may be added to the armory. In the background are the developing *in situ* spectroscopic methods, which, if their time of operation can be made short enough,<sup>15</sup> may eventually do some of the things the transient methods purport to achieve. For reactions with intermediates, spectroscopic methods may eventually offer more information than do transients, even though some of these are oriented to give information on intermediates.

## 8.6. CYCLIC VOLTAMMETRY

### 8.6.1. Introduction

Two transient techniques (galvanostatic and potentiostatic) have been presented; in each of these either current or potential, respectively, is kept constant during the observed variation of the other. It is hardly surprising, therefore, to discover that, since the 1950s, it has been the practice of many electrochemists to vary current and potential at the same time. The basic technique is called *linear*

---

<sup>15</sup>By the end of the twentieth century, FTIR techniques, which in the 1980s required several minutes for a measurement, were being described in research papers as reaching below the millisecond range. Ellipsometric spectroscopy can also be developed as a transient technique, although it has the limitation that the electrode surface must be specularly reflecting;

*sweep voltammetry*, but also by the more intimate term, “the potential sweep” technique.

In terms of the earlier material, this technique is nearest to the potentiostatic technique, but because here the potential is made to vary linearly with time (i.e., it is not static), the more appropriate name is *potentiodynamic*. As far as the electrode, cell, etc., are concerned, one has the same setup as with potentiostatic transients; the difference is that instead of being fixed at a given value while the  $i_p$  is observed, the potential is made to change at a constant rate over a chosen potential range. The range of acceptable values for the “sweep rate” is something to be discussed in detail later, but it may be stated now that a typical value is  $10 \text{ mV s}^{-1}$ .

In the linear sweep technique, a recording of the current during the potential sweep (say, from 0.0 V on the normal hydrogen scale to 1.2 V positive to it in a  $1 \text{ M H}_2\text{SO}_4$  solution) completes one act of the basic experiment. However, and hence the title of this part of the chapter, the electronics can be programmed so that when the electrode potential reaches 1.20 V, it begins a return sweep, going from 1.2 to 0.00 V, NHS. Completion of the two sweeps and back to the starting point is one act in what is called *cyclic voltammetry*.<sup>16</sup> The current is displayed on a cathode ray oscilloscope screen on an XY recorder, and it is normal to carry out not one but several and often many cycles. Much information is sometimes contained in the difference between the second and other sweeps in comparison with the first (Fig. 8.10).

The name “electrochemical spectra” is sometimes given to the results of this kind of experiment because the maxima that develop are reminiscent of absorption spectra in chemistry. Thus, in the latter, one varies the energy of incident photons, and these are absorbed when their energy overlaps the energy of some molecular activity (e.g., a vibration in a molecule on which the light is incident). In electrochemical spectra, one varies the energy of the electronic states in the electrode, and the electrons exit, or are received, when their energy (or the energy of empty electronic states in the electrode) overlaps the energy of an electronic state (empty or filled, respectively) in an ion or molecule in the layer of solution next to the electrode. Thus the events in the electrochemical case are analogous, if not similar, to those in absorption spectroscopy (Khan, 1977).

There is no doubt that if one looks at the whole of the electrochemical field around the century's end, cyclic voltammetry has been the most frequently used technique. Indeed, it is the experiment with which all electrochemists begin their studies. It is a kind of “road map” or “fingerprint” for the experiment, indicating the potential region in which there is electrodic activity. Because of the very large scope of the technique, it is worth briefly describing its origin.

<sup>16</sup> The term “voltammetry” may be contrasted with a term such as “potentiometry.” Of course, the use of “volt” comes from Volta, who in 1800 reported the first electric battery. In a similar way, one refers to “amps” as a measurement of current because of the very early work of Ampere on electrical circuits. The trend now is to use the generic term (potential, current) instead of the historical one (volt, ampere).

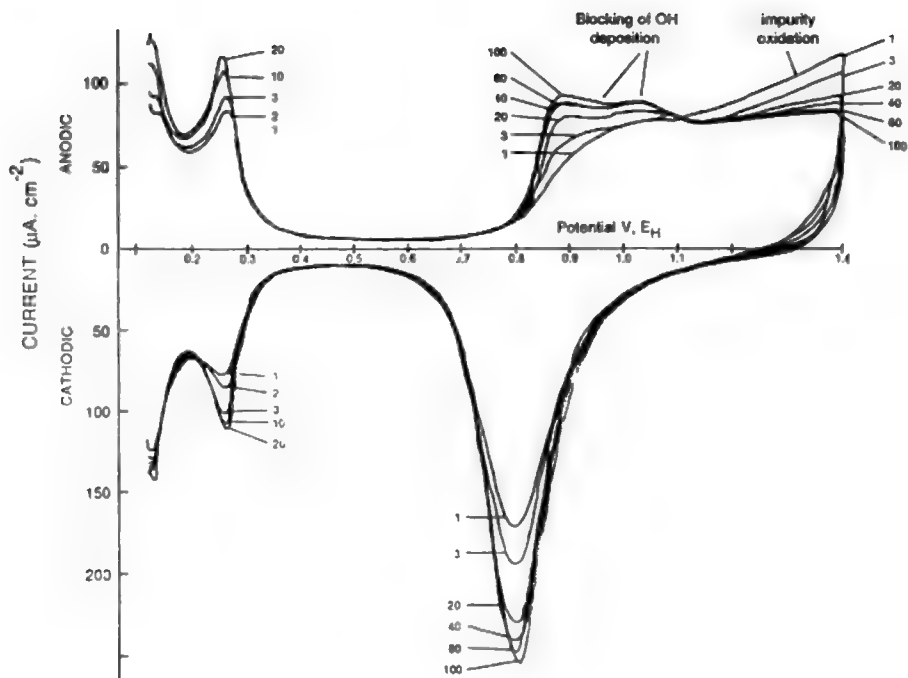


**Fig. 8.10.** Potentiodynamic  $i$ - $v$  profile for a platinum electrode surface in 0.5 M  $\text{H}_2\text{SO}_4$  solution, showing the effect of potential cycling on cleanup of the surface. The two lines shown are for the first "lower" and the twentieth "higher" sweep. (Reprinted from H. Angerstein-Kozłowska, in *Comprehensive Treatise of Electrochemistry*, E. Yeager, J. O'M. Bockris, B. E. Conway, and S. Sarangapani, eds., Vol. 9, p. 28, Plenum, 1984.)

### 8.6.2. Beginning of Cyclic Voltammetry

There is no doubt that linear sweep voltammetry originated in a technique invented by Jaroslav Heyrovsky<sup>17</sup> (1922). This method, called *polarography*, involved the observation of the current at a developing mercury drop as the potential was slowly varied in the direction positive to negative. The polarographic method became a powerful tool for chemical analysis, although it was limited to systems that underwent electrode reactions in the range of potential in which the liquid mercury drops were not themselves oxidized. Because of this latter limitation, there grew out

<sup>17</sup>Jaroslav Heyrovsky worked at Charles University in Prague, Czechoslovakia, before WWII and later at the Polarographic Institute in the same city. He received the Nobel prize for his invention of polarography in 1959. Heyrovsky's contribution was largely experimental and the principal equation, which represented the diffusion-controlled current at a time  $t$  during the growth of a drop, was first derived by a Czech schoolteacher, D. Ilkovic (1938).

of polarography the use of solid stationary electrodes of platinum, which allowed experiments in a more anodic part of the potential spectrum and thus a greater range in analysis. The names clearly associated with the foundation of the theory of such systems are Randies<sup>18</sup> (1947) and Sevcik (1948). At the same time, ac polarography was also introduced by Breyer and Gutmann<sup>19</sup> (1947).

### 8.6.3. The Range of the Cyclic Voltammetric Technique

The reach of cyclic voltammetry is vast. It has been applied to the investigation of simple electron-transfer reactions; those with two successive electron transfers (so-called EE reactions); and with multiple electron transfers (EEE) involving electron transfer to and from compounds, say, with several benzene rings. The technique has been applied to complex sequences in which an electron transfer is followed by a chemical reaction step, and then by another electron transfer (ECE reactions), etc. The complexity of some of the reaction sequences investigated by cyclic voltammetry lends itself well to calculations that need computers; the classic work of Feldburg in this direction (digital simulation) has been already mentioned (Section 7.5.19.2).

Several techniques arising from cyclic voltammetry help the interested reader to peer into the future. Derivative polarograph ( $di/dV$  against  $V_p$ ) increases the sharpness of detection of dissolved radicals and molecular fragments. Microelectrodes can be used with potential sweep circuitry. The use of varying electrical wave forms (instead of the linear potential variation) offers much to be learned in the future. Automation and the use of pattern recognition in mechanism evaluations are techniques that will be increasingly developed. The first step will always be to obtain the voltammogram.<sup>20</sup>

<sup>18</sup>J. E. B. Randles, a lecturer at the University of Birmingham, England, made a second seminal contribution to electrochemistry in publishing (at the Faraday meeting of 1947) an analysis of the impedance of a circuit containing not only diffusion but also interfacial electron transfer. His equation showed how to obtain  $i_0$  from an impedance  $-1/\omega^{1/2}$  plot. Randles' publication was very influential, although a similar analysis had been published by Dolin and Erschler in Russia in 1940, but was not easily available in the West because of difficulties of communication during WWII. Randies' contributions to electrochemistry include a molecular model for redox reactions and a rare measurement of a volta potential (Appendix 6.1).

<sup>19</sup>Felix Gutmann's contributions to electrochemistry, though less well recognized than Randles' early impedance analysis, include, in addition to the introduction of ac polarography, the first paper on the analysis of electronic noise at electrodes; the charge-transfer-oriented mechanism of action of the antidepressant chlorpromazine; and a description of biological metabolism in terms of a fuel cell-like system within the mitochondria contained in biological cells.

<sup>20</sup>One of the authors' aims is to equip the reader so that he or she can understand the terms used in the electrochemical literature. However, particularly in this chapter, this may lead to a certain lack of consistency. Thus, the most rational name for the techniques being described seems to center on the term "potentiodynamic." Terms such as "voltammetry" and "voltammogram" (used freely in modern literature) spring from an earlier era in which "voltage" and "overvoltage" were used, although now voltage is replaced by the more logical "potential."



### 8.6.4. Cyclic Voltammetry: Its Limitations

With a technique having such a vast expanse of application, it may be readily asked if there are no limitations, no areas where the method fails, no pitfalls in interpretation. Of course, the answer must be in the affirmative to all these questions. In a *global* kind of way, the downside of the giant octopus that developed from the falling drops of mercury used in the polarography that preceded cyclic voltammetry occurred as follows:

1. Historically, the potential sweep technique and cyclic voltammetry were developed for *analysis* (as successors to polarography) and much of the theoretical development is concerned with the situation under conditions of *diffusion control*, for that is where the analytical applications are most readily made. In many of these approaches, the underlying assumption is that the electron transfer that must necessarily occur at the interface is a fast process and plays little part in determining the dependence of the observed current upon potential or upon the concentration of the reactant. However, these assumptions may not always apply.

2. When the reaction has adsorbed chemical intermediates, the surface concentration of which is potential dependent, the situation is difficult and was first put into a quantitative theory by Conway and Gileadi in 1962 and in more detail by Srinivasan and Gileadi in 1967. However, these pioneer authors dealt with submonolayers of simple entities such as H. How to deal with the potential-dependent intermediates in such a (still fairly simple) reaction such as methanol oxidation is not yet in sight. (It can be done in principle, but there is still no knowledge of the kinetics of the reactions of the radical intermediates and how they are connected to the sweep rate.)

3. Reactions in which the nature of the substrate is vital (e.g., as in electrocatalysis, corrosion, electrodeposition) do not offer opportunities for application of a technique in which the substrate is regarded essentially as an electron source or sink, rather than as an electrocatalyst. The very large field of bioelectrochemistry (which involves concepts such as enzymes as electrodes and even offers electrochemical mechanisms for metabolism) would offer difficulties for potential sweep applications because of the very high resistance of the substrate.<sup>21</sup>

As will be seen, the rate at which the potential is changed (i.e., the sweep rate) becomes very important. For complex reactions, it may have to be so slow ( $0.01 \text{ mV s}^{-1}$ ) that cyclic voltammetry approaches a potentiostatic (rather than a potentiodynamic) technique. On the other hand, too large a sweep rate may yield parameters that are not those of the steady state and hence are difficult to fit into a mechanism of consecutive reactions in which the attainment of a steady state ( $\partial\theta/\partial t = 0$ ) at each potential is a basic assumption. Thus, determining the mechanisms of reactions that are to function in steady-state devices such as fuel cells or reactors is more likely to

<sup>21</sup>Conversely—and just in bioelectrochemistry—derivatives of potentiodynamic techniques have found application—e.g., in determining on a micron scale the products produced by biological cells (Chapter 14).

be relevant if it is carried out by means of potentiostatic transients, together with a sample of spectroscopic techniques.

### 8.6.5. The Acceptable Sweep Rate Range

There are a number of criteria that will influence the acceptable range of sweep rates. Some of these (the relaxation time of intermediates in organic oxidation reactions, etc.) may be very specific to the system and have to be discovered by trial and error. Here, we will use just two rather general criteria that can give us some very rough ideas as to the window in which one can work.

**8.6.5.1. What Would Make a Sweep Rate Too Fast?** It is clear that an influence of the condenser charging current  $C(dV/dt)$  must be avoided. If, therefore, the lowest current density to be measured meaningfully is, say,  $10 \mu\text{A cm}^{-2}$ , a necessary condition is one in which the (irrelevant) charging current is  $\ll 10 \mu\text{A cm}^{-2}$ .

$$C \frac{dV}{dt} < 1 \times 10^{-6} \text{ A cm}^{-2}$$

Then, with a typical  $C_{\text{DL}} \approx 50 \mu\text{F cm}^{-2}$ ,

$$\frac{dV}{dt} < 20 \text{ mVs}^{-1}$$

Of course, this figure will be increased proportionately if one is measuring not less than, say,  $1 \text{ mA cm}^{-2}$ . Then  $dV/dt$  (on this criterion alone) could be as high as  $2000 \text{ mVs}^{-1}$ .

**8.6.5.2. What Would Make a Sweep Rate Too Slow?** One general criterion that can be taken here is that the time in which  $(\pi Dt)^{1/2} = \delta$ , an assumption used in the theory of potentiodynamic transients, remains valid. It is an experimental fact that  $\delta$  at an electrode in a still solution for a long time ( $> 10 \text{ s}$ , say) is about  $0.05 \text{ cm}$  and constant because natural convection stirs the solution and wipes out the concentration gradient set up by diffusion alone. Hence, one can assume that the limit of validity of  $\delta_t = (\pi Dt)^{1/2}$  is a time at which becomes  $\delta$  equal to  $0.05 \text{ cm}$ . Using a typical value of  $D (= 3 \times 10^{-5} \text{ cm}^2 \text{ s}^{-1})$ , one obtains

$$\tau_{\text{limit}} = \frac{0.05^2}{3.1 \times 10^{-5}} = 27 \text{ s}$$

For the pseudo-capacity of adsorbed intermediates and for double-layer charging, cyclic voltammetric currents increase linearly with the sweep rate. For diffusion-controlled currents, the variation of the current increases with the square root of the sweep rate.

The range of potentials over which potential sweep experiments are carried out in aqueous solutions is from around 0.00 to 1.5 V on the NHS. This is to avoid hydrogen evolution on the negative side and  $O_2$  evolution on the positive side (pH 0). *If, then, one had a steady current*, the limitingly slow sweep rate would be one that covers 1500 mV in 27 s. On this basis, the lowest sweep rate should be about  $50 \text{ mV s}^{-1}$ .

This is higher by some 10 times than the  $5\text{--}10 \text{ mV s}^{-1}$  that is often used in successful potential sweep experiments. However, the above result was obtained on the assumption of a constant limiting current passed during the entire 1500 mV of sweep. In fact, during much of a sweep, the current density will be a very low “charging current” and the movement of ions under limiting current conditions will not take place (but does occur during peaks in which the limiting current is reached).

Thus, a sweep rate so slow that it will outrun the validity of  $\delta_r = (\pi Dt)^{1/2}$  will be much less than the  $55 \text{ mV s}^{-1}$  calculated on the basis of a constant current density during the sweep. If one makes a guestimate that a typical sweep has a full limiting current for 5% (1/20th) of the sweep time, then the acceptable minimum sweep rate would be around  $55/20 = 2.5 \text{ mV s}^{-1}$ .

As must be the case, the maximum and minimum sweep rates ( $2\text{--}20 \text{ mV s}^{-1}$ ?) depend on assumptions (e.g., the minimum current density to be measured or the fraction of the time during a sweep in which the limiting current is reached). Depending on these variables, then, one can only conclude that the rate may vary according to the reaction characteristics and for likely current densities between about 1 and  $100 \text{ mV s}^{-1}$ .

Sweep rates as low as  $0.05 \text{ mV s}^{-1}$  or as high as  $100 \text{ V s}^{-1}$  are occasionally found in the electrode kinetic literature; one would have to examine the detailed conditions to understand whether experiments at either end of this great range can avoid being affected by natural convection (for the slowest sweeps) and by double-layer charging for the highest ones.

### 8.6.6. The Shape of the Peaks in Potential–Sweep Curves

An archetypal potential–sweep curve (say, with a redox couple in solution) is portrayed in Fig 8.11. The essence is that as the potential of the working electrode is made to move in the anodic direction, there arises a potential at which the current starts to increase (the reversible potential of the redox couple has been reached), passes through a maximum (the peak), and decreases. Then in a cyclic voltammogram, as the potential is ramped back again, from the anodic side toward the cathodic, the sign of the current tends to become reversed (i.e., to become negative or cathodic) and the cathodic-to-anodic sweep is only qualitatively replicated. In very simple reactions (e.g., a redox couple), and particularly when the range of the sweep is insufficiently anodic to form an oxide, the peak on the cathodic side will be nearly the same as that on the anodic side. However, it is more usual for the substrate (Pt) to become oxidized during the cathodic-to-anodic sweep and then when the potential moves into a range at which the oxide is reduced, a corresponding

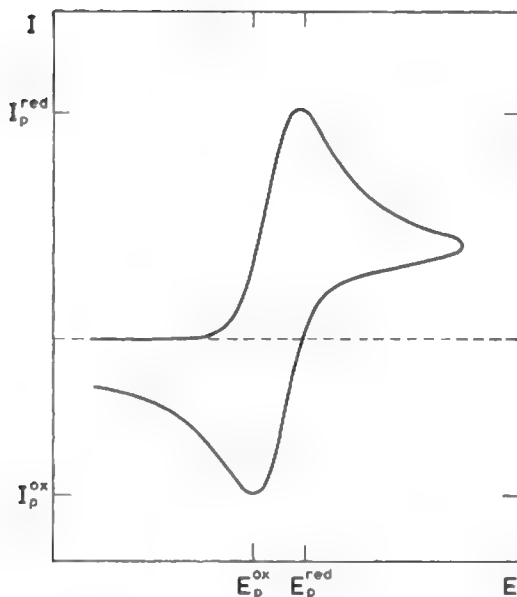


**Fig. 8.11.** A cyclic voltammogram for a reversible charge-transfer reaction. (Reprinted from V. D. Parker, "Linear Sweep and Cyclic Voltammetry," in *Comprehensive Chemical Kinetics, Electrode Kinetics, Principles and Methodology*, C. H. Bamford and R. C. Compton, eds., copyright 1986, p. 148, with permission from Elsevier Science.)

cathodic current (and cathodic maximum) will be seen. There may be specific features ("blips") in the anodic curve not in the cathodic one, or vice versa.

The main thing to be interpreted is the peak itself, the principal characteristic of the potential sweep. The processes corresponding to each peak differ only in finer detail, specific to the reaction encountered. Basically, they can be explained in terms of the effect of potential on the Faradaic (electron transfer) current,  $i_F$ , and of time on the value of the limiting current,  $i_L$ .

Now, from Eq. (7.236)

$$i = \frac{i_F i_L}{i_F + i_L} \quad (7.236)$$

It is known that  $i_F$  increases exponentially with increasingly positive potential (in an anodic process), as long as the potential is more positive than that of the reversible potential. Correspondingly:

$$i_L \propto \frac{1}{\delta_i} \quad (8.12)$$

and hence ( $\delta_i = \sqrt{\pi D t}$ )

$$i_L \propto \frac{1}{\sqrt{t}} \quad (8.13)$$

Consider now the advance of the potential of the working electrode toward the positive side in Fig. 8.12 and let the time be small near the beginning of the sweep. It follows from Eq. 8.13 that  $i_L$  will be large and one can see from Eq. (7.236) that

$$i \approx i_F$$

In the initial steep ascent part of the current density then, one is just viewing a part of a normal  $i - \eta$  curve under interfacial control, the beginning of the normal exponential (Tafelian) relation of current to overpotential. At such low times,  $\delta_i$  is small and hence  $i_L$  is too large to have an observable effect.

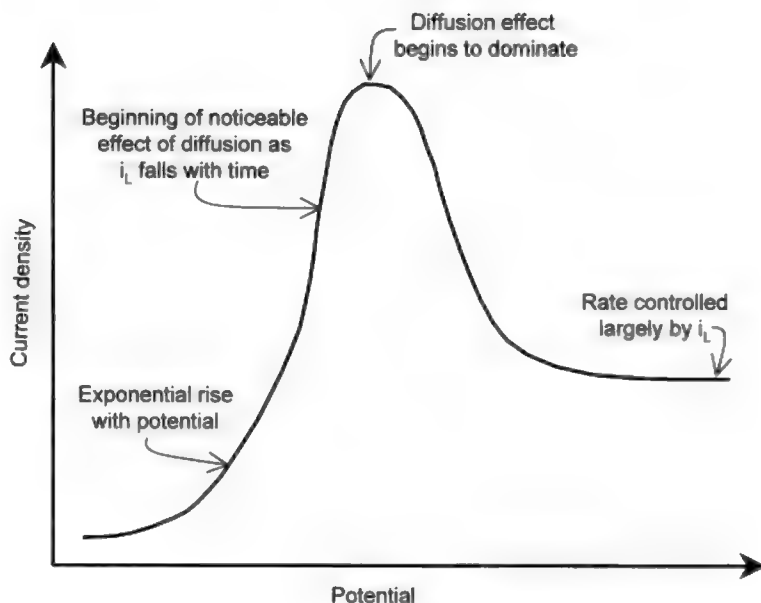


**Fig. 8.12.** The structure of a potentiodynamic sweep. At the beginning, the current is dominated by the Faradaic electron transfer. As time increases,  $i_L$  decreases and hence begins to affect the current. At the maximum, both types of influence are equal. At higher times, diffusion control dominates the situation.

As the time increases and the potential grows more positive,  $i_F$  continues to increase exponentially. However, from Eq. 8.13,  $i_L$  becomes smaller, following  $1/\sqrt{t}$ . Looking back at Eq. (7.236), it is seen that when eventually,

$$i_L \ll i_F$$

$$i \approx i_L$$

Thus, as  $i_L$  continues to fall with increasing time, the  $i - \eta_t$  relation will fall after a maximum to a decreasing, diffusion-controlled value. The essentials of all this are shown in outline in Fig. 8.12.

The peak has thus been explained, albeit quasi-quantitatively. It is known empirically that, as  $s$ , the sweep rate, increases, the peak occurs at a higher value of the current density. The reason for this is not difficult to grasp if one realizes that with a larger sweep rate, the potential will reach a higher (more positive) value in a fixed time, say, in 10 s. Now, after 10 s,  $\delta_t$  and hence the  $i_L$  value will be the same, independent of the sweep rate. However,  $i_F$  will be greater after 10 s at a higher than at a lower sweep rate. Since the maximum current occurs when

$$i_L = i_F$$

the peak current will occur at a higher value of  $i_L$ .

### 8.6.7. Quantitative Calculation of Kinetic Parameters from Potential-Sweep Curves

In Section (8.6.5) it was argued that the value of the sweep rate must be less than that which would cause the capacitative charging current to be significant compared with the total current and greater than a value that in the potential range of the sweep would cause  $\delta_t$  to reach a value at which natural convection would cause the breakdown of the relation  $\delta_t = \sqrt{\pi D t}$ .

Correspondingly, a quasi-quantitative picture has been given of the formation of a peak. The current peak occurs in a potential-sweep relation when the potential moves past the region of the reversible potential for a process so that the current climbs exponentially with an increase in potential until it runs into the limiting current, declining (and hence becoming more assertive) with an increase in time. After the current peak, the current density declines to correspond eventually to the diffusion-controlled limiting current, according to  $i_L$ , and  $1/\sqrt{t}$ .

However, when one gets down to detailed quantitative equations to represent real, actual reactions with several steps in consecutive sequence, the mathematics become very complex. Thus, the change in the limiting current with time introduces complications that one tries to avoid in other transient methods by working at low times (constant current or constant potential approaches) or at times sufficiently high that the current becomes entirely diffusion controlled. However, taking into account the

effect of varying the potential while measuring the current increases risk, especially if adsorbed intermediates are involved. For, what is the meaning of “steady state” when the potential is continually changing?

The quantitative treatment for  $i$  as a function of a varying  $\eta$ , was first solved analytically by Sevcik in 1948. The solution involves Laplace transformation and the error function complement expressions applied in Vol. 1, Section (4.2.11). It is better to quote here the rather simpler equations that can be found if one takes the entire surface as available for the exchange of electrons, i.e., the easy case of  $\theta = 0$ . Then (Gileadi, 1993),<sup>22</sup> with this assumption, the peak potential is related to the rate constant ( $k_f$ ) for the interfacial reaction, to the Tafel constant  $b$ , and to the sweep rate  $s$ , by the equation:

$$E_{\text{Tafel region}} = E_0 + b/2 [1.04 - \log b/D - 2 \log k_f + \log s]$$

In  $\theta = 0$  situations in which the equation is applicable, a plot of  $E_{\text{Tafel region}}$  against  $\log s$  gives the Tafel constant from the slope  $b$  and  $k_f$  arises from the intercept at the reversible potential  $E$ , in analogy to  $i_0$  ( $i_0 = F\chi k_0 c_0$ ).

Correspondingly, with the same assumption of  $\theta = 0$ , Gileadi's version of the peak current is

$$i_{p(\text{Tafel})} = (3.01 \times 10^5 n \alpha^{1/2} D^{1/2} c_0) s^{1/2}$$

Here  $n$  is the number of electrons in the overall reaction, and can be independently determined by chronopotentiometry.

The difficulty of dealing with a quantitative theory that involves peaks due to the adsorption or desorption of materials (i.e.,  $\theta > 0$ ) is that one has to know the kinetic rate constants for the surface reactions that are often part of an overall sequence. Equilibrium equations involving the adsorption energies of the intermediates (Gosser 1993) are not enough, i.e., the intermediate may be part of a rate-determining reaction and not at equilibrium.

### 8.6.8. Some Examples

Figures 8.13 to 8.15 show several examples of cyclic voltammetric curves. The figures given are intentionally varied in complexity. Computer simulation of these cyclic voltammograms can, however, be carried out (Gosser, 1993).<sup>23</sup>

<sup>22</sup>The summary given by this author rests on the work of several theorists who followed the work of Sevcik. Among the most outstanding of these is Paul Delahay who, with Strassner and others in 1951–1953 contributed much to the basic theory of linear sweep voltammetry with partial interfacial control.

<sup>23</sup>Students interested in programs for such simulations should contact Prof. David K. Gosser, Chemistry Department, City College of New York, NY, 10031.

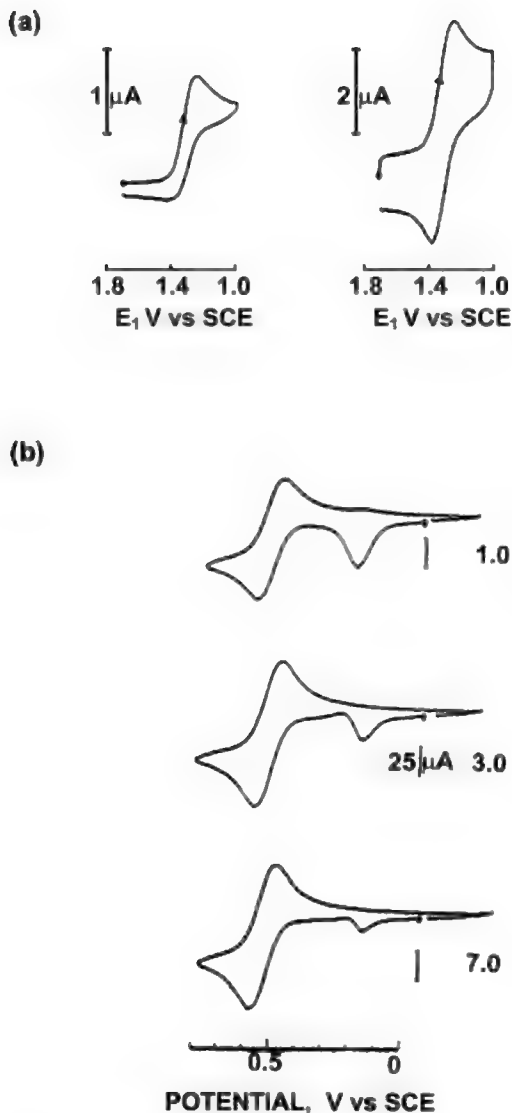


**Fig. 8.13.** (a) Cyclic voltammograms for  $\text{NO}_2^+$  in acetonitrile at scan rates of  $0.1$  and  $7 \text{ V/s}$ . (b) Experimental CVs for the oxidation of  $1.7 \times 10^{-3} \text{ M MnMe}$  in the presence of various molar ratios of phosphine ligand and manganese complex. (Reprinted from D. Gosser, *Cyclic Voltammetry*, pp. 74, 77, 84, copyright © 1993, VCH-Wiley. Reprinted by permission of John Wiley & Sons, Inc.)



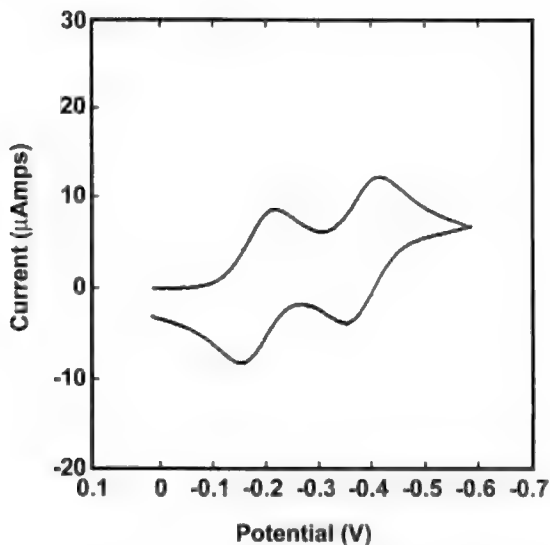


**Fig. 8.14.** Current–potential relation for two-electron transfer for  $E_1 > E_2$ . The scan rate is  $0.1 \text{ mV s}^{-1}$ . (Reprinted from D. Gosser, *Cyclic Voltammetry*, pp. 74, 77, 84, copyright © 1993, VCH-Wiley. Reprinted by permission of John Wiley & Sons, Inc.)

### 8.6.9. The Role of Nonaqueous Solutions in Cyclic Voltammetry

Nonaqueous solutions are often the subject of voltammetric examinations, particularly when larger organic molecules (polycyclic hydrocarbons and biomolecules) are to be examined, for it is only in such solvents that the big organics are sufficiently soluble to give significant currents. Here it is vital to keep the solution dry, e.g., by the use of powdered aluminum as a getter. A typical cell for this purpose is shown in Fig. 8.16.

### 8.6.10. Two Difficulties in Cyclic Voltammetric Measurements

It was stressed at the beginning of this section that cyclic voltammetry is the most widely used electrochemical technique, not only for the original purpose of analyzing the content of a solution, growing out of Heyrovsky's original polarography on Hg drops, but also for the rapid examination of many kinds of electrochemical relations. However, weighing against a technique ubiquitous in all electrochemistry are two difficulties in understanding the results obtained, and it is only if these difficulties are properly understood and accounted for that one may be able (using

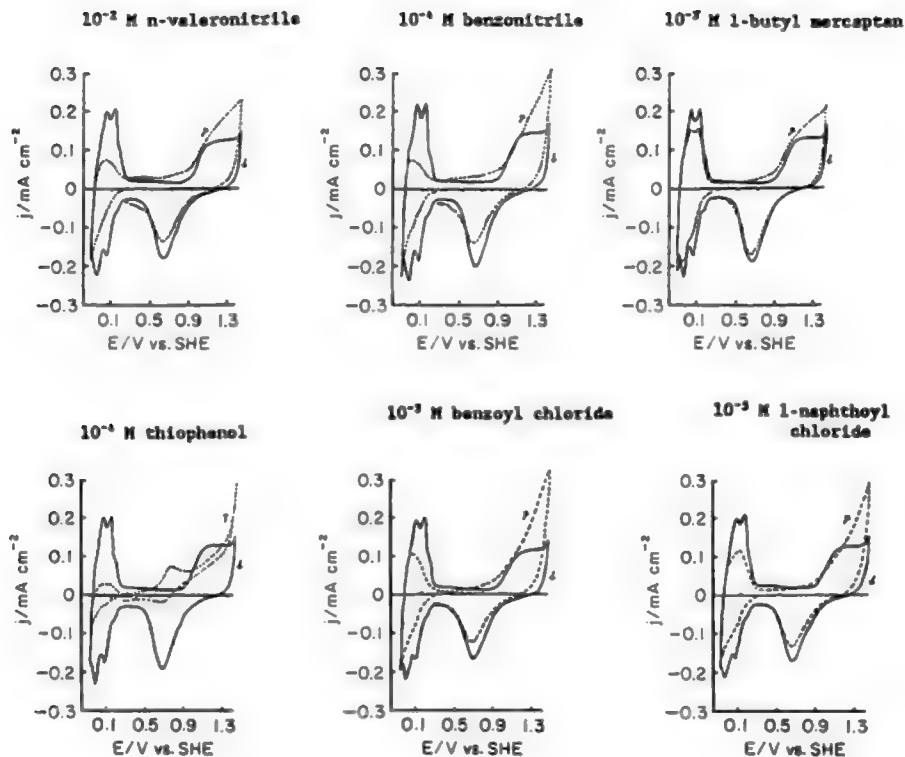


**Fig. 8.15.** Cyclic voltammograms for the adsorption and oxidation-reduction for a number of organics at platinum. The sweep rate is  $50 \text{ mV s}^{-1}$ . (Reprinted from J. O'M. Bockris and K. T. Jeng, *J. Electroanal. Chem.* **330**: 561, copyright 1992, Fig. 5 with permission from Elsevier Science, The Boulevard, Langford Lane, Kidlington, OX516B, UK.)

cyclic voltammetry) to obtain data of a value comparable to those of the several other (often, simpler) transient methods presented earlier.

1. The first difficulty involves steady state. In this book, it has been stressed that fundamental electrochemistry is not limited to simple redox reactions with no adsorbed radical intermediates, and that we must accept the indisputable fact that most electrode reactions involve intermediates, and their concentration depends not only on the electrode potential but also on time during the potential sweep. Thus, unless the surface concentration of the intermediates is negligible or their relaxation times much faster than those of the sweep rate, the steady-state value of  $\theta_1$ ,  $\theta_2$ , etc. (of the various adsorbed radicals) may not be "felt" by the current registered in the sweep. However, when one writes a reaction sequence:

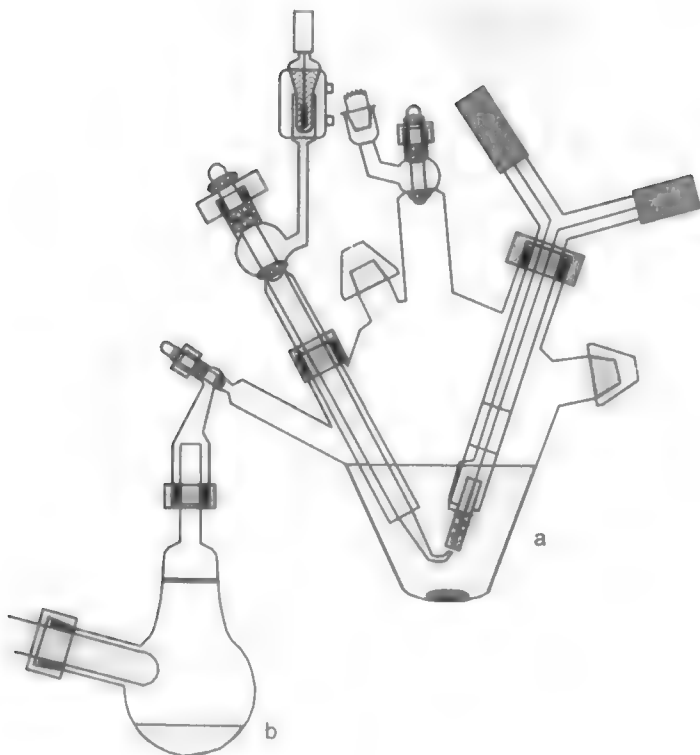


**Fig. 8.16.** Electrochemical cell for voltammetric experiments under “superdry” conditions: (a) Measuring cell with three-electrode arrangement, (b) Drying vessel with superactive aluminum. (Reprinted with permission from J. Heinze, *Angewandte Chemie* 23: 831, copyright 1986, Wiley-VCH Verlag.)



and then:



it is assumed in the analyses that all the radicals (B and C) have had time to adjust to their appropriate surface concentrations (i.e., to the values of the  $\theta$ 's corresponding in the steady state to a specific constant potential). It is much more difficult to analyze a situation in which the values of  $\theta$  are never content and it has only been done so far in very simple cases (Section 8.7).

This challenge of being able to give information on the steady state of the typical (surface intermediate involving) electrochemical reaction is intrinsic to the potential

sweep method. The difficulty of estimating the effect of assuming that the radicals “immediately” follow the potential is that adsorption experiments (e.g., of organics on Pt) suggest that the order of magnitude for the relaxation time for adsorption of organics from solution on polycrystals is 10–100 s. Adjustment of the  $\theta_n$  “immediately” as the potential changes is not a realistic assumption (Fig. 8.17). But if the  $\theta$ 's are not synchronized with the potential, the results (and the rate constants and  $\alpha$ 's) do not correspond to the reaction sequences that we write down and try to analyze to find a mechanism for the reaction (Gileadi and Stoner, 1969).

Such objections do not apply to a redox-type situation ( $\text{Fe}^{3+} + e = \text{Fe}^{2+}$ ) and for which there are no radical intermediates. They apply only in a muted form when the cyclic voltammetric method is used in some kind of analysis of the content of the solution. However, they do apply to mechanism studies of electrochemical reactions involving intermediates as adsorbed radicals, and that means that they apply to most electrochemical reactions.

2. A more subtle objection applies to the usually uncompensated nature of the “IR error” discussed in Section 7.5.4. It will be recalled that in a potentiostatic

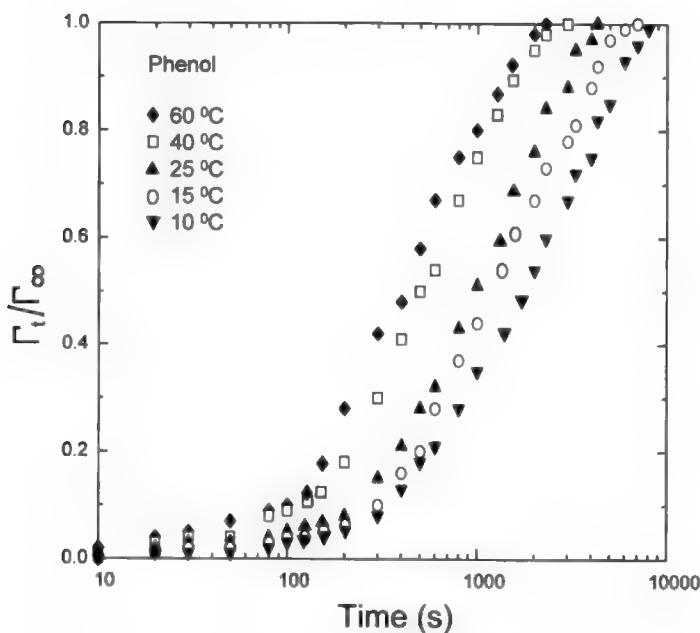


**Fig. 8.17.** Adsorption kinetics for phenol on polycrystalline platinum from 0.01 M HCl solution. (Reprinted from J. O'M. Bockris and K. T. Jeng, *J. Electroanal Chem.* **330**: 550, copyright 1992, Fig. 5 with permission from Elsevier Science, The Boulevard, Langford Lane, Kidlington OX5 16B, UK.)

technique, the potentiostat keeps the total of the IR drop potential and the electrode potential constant. In a potential sweep, between the peaks, the current is very low (it's simply the charging current) and the IR error negligible. However, near the current peak, the current (and hence the IR error) maximizes and this means that the actual *electrode* potential deviates to a maximum amount from that indicated. In fact, this is equivalent effectively to a reduction in sweep rate since the potential actually applied to the electrode in the peak region is less than it would be in the absence of the uncompensated IR. However, the information on current–potential relations is drawn from the peaks, just where the IR error is at maximum (Gileadi, 1993).

This source of error in potential sweep measurements will apply to sweep measurements made for all kinds of electrode reactions, not only those involving intermediates. It will be a strong source of error, particularly when nonaqueous solutions are used because there, the resistance of the solution (and hence the IR error) can be particularly large.

### 8.6.11. How Should Cyclic Voltammetry be Regarded?

As stated earlier, cyclic voltammetry is a good road map when one first comes to examine an electrode reaction. It gives the researcher some idea of the potential near which there is reactivity. Cyclic voltammetry should always be used to get some idea of things at the beginning of an electrode kinetic investigation.<sup>24</sup>

However, if quantitative results are needed, and particularly if intermediates occupy a significant fraction of the electrode surface, one needs to turn from cyclic voltammetry as a technique and approach the reaction with two or more transient techniques in which the errors are more quantitatively understood and brought under control (Table 8.1), than for the case in which current and potential are changing simultaneously. One also needs, as the new century begins, to use spectroscopic approaches in a routine way to monitor the surface, and to couple one or two of these methods with the electrical measurements in all investigations of reactions on electrode surfaces.

## 8.7. LINEAR SWEEP VOLTAMMETRY FOR REACTIONS THAT INCLUDE SIMPLE ADSORBED INTERMEDIATES

### 8.7.1. Potentiodynamic Relations that Account for the Role of Adsorbed Intermediates

Throughout the foregoing discussion, it has been stressed that theoretical treatments of linear sweep voltammetry are usually applicable to situations in which the

<sup>24</sup>The phrase “some idea” implies an imperfection and is intended. Thus, one does not know the electrode potential as a function of current density at the peak because the potential is mixed up with a changing IR error and diffusion control. This could be negligible, but it may also be significant.

coverage  $\theta$ , with radicals, is taken as limitingly small and neglected in the kinetic calculations. In fact, the question of concentration of the adsorbed intermediate radical has been made a bone of contention in respect to potential sweep measurements, it being hinted that they are accounted for, the analysis may become too difficult.

However, a number of treatments specifically oriented in this direction have been developed (Conway and Gileadi, 1962; Srinivasan and Gileadi, 1967; Conway and Stonehart, 1977). In these, a Frumkin-type isotherm (6.8.9) is used, i.e.,

$$\frac{\theta}{1-\theta} = K e^{-g\theta} e^{VF/RT} \quad (8.14)$$

Thus, if one considers an anodic discharge reaction onto a surface on which the coverage is  $\theta$  (and assuming one is outside the reversible region), then (with  $\beta = 1/2$ ):

$$i = k_1(1-\theta) e^{VF/2RT} e^{-g\theta/2} \quad (8.15)$$

in differential form, as  $V = V_i + \nu t$ , with  $\theta \rightarrow 0$ :

$$di/dt = k_1^{FV/2RT} [(1-\theta)\nu F/2RT - d\theta/dt] \quad (8.16)$$

where  $\nu$  is the sweep rate in volts per second.

The current will thus reach a maximum when  $di/dt = 0$ ; that is,

$$d\theta/dt = (1-\theta) \nu F/2RT \quad (8.17)$$

If  $Q$  is the charge required to form a monolayer of adsorbed intermediates, the current is

$$i = Q d\theta/dt \quad (8.18)$$

Hence the maximum current is

$$i_p = Q(1-\theta) \nu F/2RT \quad (8.19)$$

The potential corresponding to the peak current can be obtained from Eqs. (8.19) and (8.15) as

$$V_p = \frac{2RT}{F} \ln \frac{QF}{2k_1RT} + \frac{2RT}{F} \ln \nu \quad (8.20)$$

Thus the peak position changes with sweep rate, and the slope of the  $V_p - \ln \nu$  relation is  $2RT/F$ . As shown later,  $V_p$  is independent of sweep rate for the highly reversible case. This criterion offers an easy indication of whether the reaction falls into the class of highly irreversible reactions assumed in the deduction.

From Eqs. (8.15) and (8.18)

$$Q \, d\theta/dt = k_1(1 - \theta) e^{V_F/2RT} \quad (8.21)$$

$$V = V_i = vt \quad (8.22)$$

$$-d \ln(1 - \theta) = (k_1/Q) e^{FV_i/2RT} e^{V_i F/2RT} dt \quad (8.23)$$

whence

$$-d \ln(1 - \theta) = (k_1/Q)(2RT/\nu F) e^{FV_i/2RT} e^{V_i F/2RT} + B \quad (8.24)$$

At  $t=0$ ,  $\theta = 0$ . It follows that

$$-\ln(1 - \theta) = [(k_1/Q)(2RT/\nu F) e^{FV_i/2RT} e^{V_i F/2RT} - 1] \quad (8.25)$$

From Eqs. (8.15) and (8.25)

$$\ln i = \ln k_1 - (k_1/Q)(2RT/\nu F) e^{FV_i/2RT} (e^{(V-V_i)F/2RT} - 1) + VF/2RT \quad (8.26)$$

This equation gives the  $i$ — $V$  characteristics independent of  $\theta$ . A linear Tafel plot with a slope of  $b = 2RT/F$  is obtained only if the second term on the right-hand side is negligible in comparison with the third. The deviations from this slope depend on the sweep rate and are minimal at small sweep rates.

To find  $i_p$ , substitution of  $V = V_p$  from Eq. (8.20) gives

$$\ln i_p = \ln \left( \frac{QF}{2RT} \nu \right) + \left( \frac{2k_1RT}{QF\nu} e^{V_p F/2RT} - 1 \right) \quad (8.27)$$

If

$$\frac{2k_1RT}{QF\nu} e^{V_p F/2RT} \ll 1 \quad (8.28)$$

then

$$\ln i_p = \ln \left( \frac{QF}{2RT} \nu \right) - 1 \quad (8.29)$$

or

$$i_p = \frac{QF}{e2RT} \nu \quad (8.30)$$

The peak current is hence proportional to the sweep rate with an adsorption pseudo-capacitance of

$$C_p = \frac{dq}{dV} = \frac{d(i dt)}{dV} = \frac{di}{d\nu} = i_p/\nu = QF/e2RT \quad (8.31)$$

independent of the sweep rate. The pseudo-capacitance plot varies with the sweep rate as shown in Fig. 8.18.

This analysis gives the basis and principles of a more advanced treatment of potential sweep kinetics than treatments that neglect adsorbed intermediates. However, although such an approach can be applied, e.g., to the deposition of  $\text{Cl}^-$  on an inert surface, or to simple situations involving, e.g., H or O, the situation of a radical involving successive chemical reactions, along with charge transfers, needs too much information about the individual kinetic behavior of the intermediates to make it quantitatively feasible to analyze the resulting cyclic voltammogram (Conway and Koslowska, 1991).

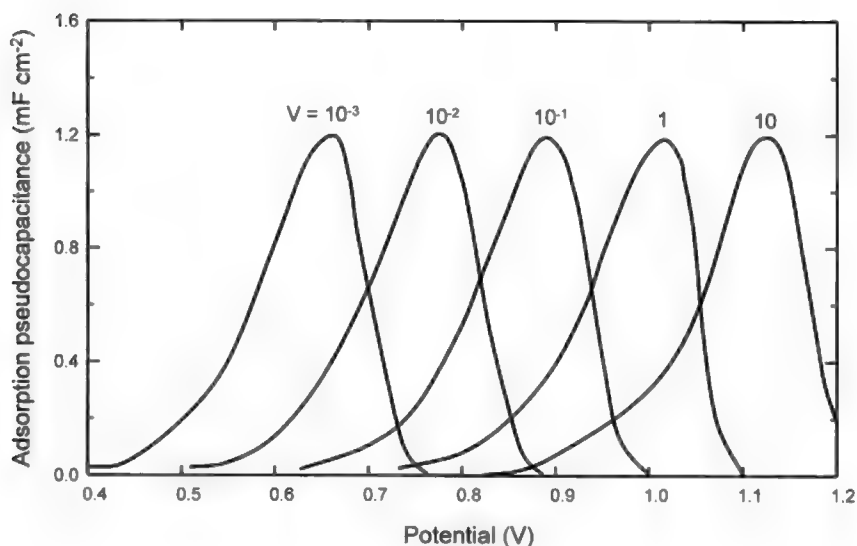


**Fig. 8.18.** Calculated pseudo-capacitance potential plots of the “Tafel approximation” case ( $k_i = 10^{11}$ ) for an increasing series of sweep rates  $\nu$ . (Reprinted from S. Srinivasan and E. Gileadi, *Electrochim. Acta* 11: 321, copyright 1966, Fig. 1, with permission from Elsevier Science, The Boulevard, Langford Lane, Kidlington OX5 16B, UK.)



Thus, potential sweep techniques and cyclic voltammetry are excellent tools for the early stages of an investigation. However, they must never be the only tools used.

## FURTHER READING

### Seminal

1. J. Heyrovsky, *Chem. Listy* 16:256 (1922). Foundation of polarography.
2. F. P. Bowden and E. K. Rideal, *Proc. Roy. Soc. London* **120A**: (1928). First transients in electrochemistry.
3. J. A. V. Butler and L. Armstrong, *Trans. Faraday Soc.* 29:1261 (1933). Galvanostatic transients.
4. D. Ilkovič, *J. Chim. Physique* 35:129 (1939). First theory of polarography.
5. P. Dolin and B. Erschler, *Acta Physicochem. URSS* 13:747 (1940). First impedance analysis to give  $i_0$ .
6. A. Hickling, *Trans. Faraday Soc.* 38:27 (1942). First electronic potentiostat.
7. J. E. B. Randies, *Discuss. Faraday Soc.* 1:11 (1947). Analysis of the impedance of the interface.
8. A. Sevcík, *Coll. Czech. Chem. Comm.* 13:349 (1948). First analytical theory of linear sweep voltammetry.
9. J. E. B. Randies, *Trans. Faraday Soc.* 44:327 (1948). Graphical solution in linear sweep voltammetry.
10. N. Tanaka and R. Tamamushi, *Bull. Chem. Soc. Jpn.* 22:187 (1949). Theory of polarography in the presence of interfacial control.
11. B. Breyer, F. Gutmann, and S. Hacobian, *Aust. J. Sci. Res., Ser. A.* 3:58, 517 (1950). Foundation of ac polarography.
12. J. O'M. Bockris and E. C. Potter, *J. Electrochem. Soc.* 99:169 (1952). First theory of the decay transients.
13. H. Gerischer and W. Vielstich, *Z. Electrochem.* 56:380 (1952). First potentiostatic transients.
14. J. E. Strassner and P. Delahay, *J. Am. Chem. Soc.* 74:6232 (1952). First rate constant calculated from a polarographic wave.
15. F. G. Will and C. A. Knorr, *Z. Elektrochem.* 64:258 (1960). First analysis of O and H with potential sweep approach.
16. E. Gileadi, G. Stoner, and J. O'M. Bockris, *J. Electrochem. Soc.* 113:585 (1966). Calculation of errors in the determination of kinetic parameters arising from potential sweep rates that are too high.
17. E. Gileadi and S. Srinivasan, *Electrochim. Acta* 11:321 (1966). First quantitative analysis of potential sweeps involving adsorbed intermediates.

### Modern

1. H. Angerstein-Kozłowska, J. Klinger, and B. E. Conway, *J. Electroanal. Chem.* **75**:61 (1977).
2. D. D. MacDonald, *Transient Techniques in Electrochemistry*, Plenum, New York (1977).
3. H. Angerstein-Kozłowska and B. E. Conway, *J. Electroanal. Chem.* **95**:1 (1979).

4. B. E. Conway and H. Angerstein-Kozłowska, *Acc. Chem. Res.* **14**:49 (1981).
5. Southampton Group, *Instrumental Methods in Electrochemistry*, Ch. 6, Ellis Harwood, Chichester, U. K. (1985).
6. V. D. Parker, "Linear Sweep and Cyclic Voltammetry," in *Electrode Kinetics, Principles and Methodology*, C. H. Bamford and R. G. Compton, eds., Ch. 4, p. 197, Elsevier, Amsterdam (1986).
7. M. Sluyters-Rehbach and J. H. Sluyters, "Alternating Current and Pulse Methods," in *Electrode Kinetics, Principles and Methodology*, C. H. Bamford and R. C. Compton, eds., Elsevier, Amsterdam (1986).
8. J. Clavilier, "Characterization of Platinum at Stepped Surface," in *Electrochemical Surface Sciences*, M. Soriaga, ed., Ch. 14, American Chemical Society, Washington, DC (1988).
9. A. Wieckowski, "Electrochemistry at Well-Defined Surfaces," in *Electrochemical Surface Sciences*, M. Soriaga, ed., Ch. 17, American Chemical Society, Washington, DC (1988).
10. K. M. Radish, Q. Y. Ku, and J. E. Anderson, in *Electrochemical Surface Sciences*, M. Soriaga, ed., Ch. 31, American Chemical Society, Washington, DC (1988).
11. A. Szucs, G. D. Hitchens, and J. O'M. Bockris, *Bioelectrochem. Bioenergetics*, 21:133 1989.
12. David K. Gosser, *Cyclic Voltammetry and Reaction Mechanism (Computer Simulations)*, VCH Publishers, Weinheim (1993).
13. E. Gileadi, *Electrode Kinetics for Chemists, Engineers and Material Scientists*, Ch. 25, VCH Publishers, Weinheim (1993).
14. L. M. A. Brett and A. M. O. Brett, *Electrochemistry*, Ch. 9, p. 174, Oxford Science Publications (1993).
15. K. B. Oldham and J. C. Myland, *Fundamentals of Electrochemical Science*, Ch. 11, Academic Press, San Diego (1994).
16. M. Rudolph, "Digital Simulation in Electrochemistry," in *Physical Electrochemistry*, I. Rubenstein, ed., Ch. 3, Marcel Dekker, New York (1995).
17. T. Fukuda and Akiko Aramata, *Proc. Electrochem. Society* **96-97**:96 (1996).
18. M. Osawa, K. Ataka, and K. Yoski, *Proc. Electrochem. Soc.* **96-98**:108 (1996).
19. A. Zoltaghari, G. Jerkiewicz, V. E. Sung, and A. Wieckowski, *Proc. Electrochem. Soc.* **96-98**:150 (1996).
20. J. Skin and C. Korzeniewski, *Electrochem. Soc. Proc.* **96-98**:291 (1996).

## EXERCISES

1. (a) State clearly two reasons why one uses transient measurements in electrode kinetics, (b) Give one specific practical example for each of these two reasons. (Bockris)
2. (a) What is the equation for "the capacitive current density?" (b) When one talks of "transients" what is a lower limit in a useful time interval using normal electrochemical instrumentation? (c) What sort of time would be "too long" to be called "a transient?" (d) What are typical potential sweep rates (volts s<sup>-1</sup>) commonly found in the literature? (Bockris)

3. The use of cyclic voltammetric measurements has been said by some to be open to misunderstanding when applied to electrode reactions involving adsorbed intermediates, oxide and sulfide layers, or in metal deposition. (a) What sort of misunderstandings? (b) Why is it said (Gileadi, 1993) that it is always good to start an investigation using cyclic voltammetry, but this method can never be the only method in a mechanism investigation? (Bockris)
4. For a constant current (i.e., galvanostatic) transient, the basic relation for a constant is

$$\left(i_{\text{total}}\right)_{\text{const}} = C \frac{dV}{dt} + i_F$$

where  $C$  is the double-layer capacitance ( $50 \mu\text{cm}^{-2}$ ) and  $i_F$  is the Faradaic current. The latter can be expressed by the Butler–Volmer equation, but with  $\eta = \eta_p$ , i.e., the overpotential is parallel to the electrode potential.

Take  $i_0 = 10^{-6} \text{ A cm}^{-2}$  at  $25^\circ\text{C}$ . Explore the appropriate time and potential range to form a galvanostatic transient relation with the parameters stated. (Note: The so-called “rise time” of the potential is about  $4 C R'$ , where  $R' = \partial V / \partial \ln i$ . Calculate the full  $V$ - $t$  curve to 99% of the steady state. (Bockris)

5. In chronopotentiometry, conditions are chosen so that transport in the solution is rate controlling. A solution contains  $0.001 \text{ M Cd(NO}_3)_2$  (with  $1 \text{ M KNO}_3$ ) and the constant current applied is  $0.10 \text{ A cm}^{-2}$ . The quarter-time potential is  $0.57 \text{ V}$  vs. standard calomel. Use Sand’s equation to calculate the transition time,  $\tau$ , and plot the electrode potential as a function of time. (Bockris)
6. (a) Compare and contrast the regions of applicability of equations due to Sand and Cottrell. In a certain experiment carried out at constant potential in a diffusion-controlled region, the slope of the  $i$ - $t^{-1/2}$  line is  $10^{-3} (D \text{ in cm}^2 \text{ s}^{-1}, C \text{ in mol cm}^{-3})$  and  $t$  in seconds. (b) What is the concentration of the reactant? (Bockris)
7. Define and explain the following terms for electrode kinetics: irreversible, quasi-reversible, linear region, and reversible. (Bockris)
8. The transition time in the galvanostatic mode is listed in Table E1. The concentration of electroactive species is  $0.1 \text{ M}$  and the diffusion coefficient is  $10^{-5} \text{ cm}^2/\text{s}$ . Find the number of electrons transferred and draw a current-time response in a potentiostatic mode.

TABLE E.1

Current density (mA/cm <sup>2</sup> )	10	12	14	16	18
Transition time (s)	29.16	20.25	14.88	11.39	9

9. (a) Develop the formulas describing the open-circuit potential decay  $\eta$  vs.  $T$  (after the current is cut off) for the reaction  $\text{Me}^{2+} + 2e = \text{Me}$ , under the hypotheses that the symmetry factor  $\beta = 1/2$ , and the diffusion does not interfere, (b) Establish the conditions the decay overpotential must fulfill so that the anodic decay transient can be approximated by the formula

$$\eta = (1/2\alpha) \ln (C_{\text{DL}}/(2\alpha i_0 t)) \quad (1)$$

where  $\alpha = \beta z F / RT$ , and  $C_{\text{DL}}$  is the double-layer capacity. Accept an error of 10% for every approximation, (c) Let us consider that in order to use formula (1) to determine the electrode characteristics  $C_{\text{DL}}/(2\alpha i_0)$ , the linear relationship  $\eta$  vs.  $T$  must be obeyed over an overvoltage range as large as 21 mV. Establish the interval of  $\eta$  values and the minimum value of  $\eta_0$ . (Plonski)

10. (a) Develop the formulas describing the open-circuit potential decay  $\eta$  vs.  $T$  (after the current is cut off) for the reaction  $\text{Me}^{2+} + 2e = \text{Me}$ , after a galvanostatic, step current leading to a very low overpotential value ( $< 20$  mV) passes the circuit. Take the symmetry factor  $\beta = 1/2$ , and ignore the mass transfer effects. Figure E8.1 shows the rising and the decay part of a cathodic galvanostatic transient recorded under the following conditions:

working electrode: disk Cu,  $A_{\text{Cu}} = 1 \text{ (cm}^2\text{)}$ , roughness factor: 1.5

rotating disk speed:  $N = 2000 \text{ rpm}$

counter-electrode: Cu;  $I = -1 \text{ mA}$

electrolyte:  $2.5 \times 10^{-3} \text{ M CuSO}_4$ , pH 5

solution viscosity  $\rho = 0.01 \text{ (g cm}^{-1}\text{s}^{-1}\text{)}$ ;  $D_{\text{Cu}^{2+}} = 7.2 \times 10^{-5} \text{ (cm}^2 \text{s}^{-1}\text{)}$

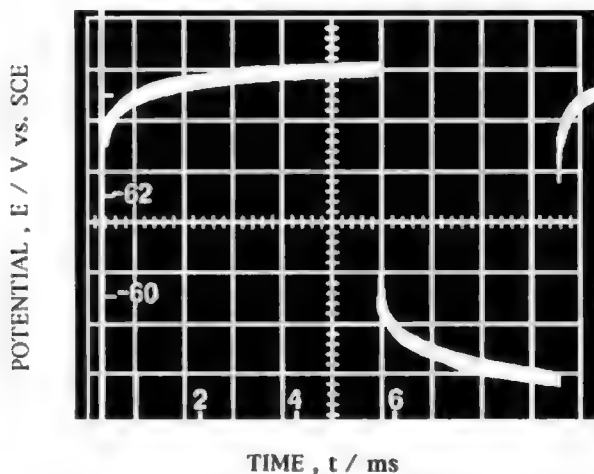


Fig. E8.1

(b) Verify whether this transient satisfies the hypothesis under which the approximate formulas for the  $\eta$  vs.  $t$  curve have been derived in terms of the lack of diffusion and the particular case:  $\eta < 20 \text{ mV}$ ; take into consideration both the stagnant and the rotating electrode.

(c) Using the data measured on the decay part of the transient and knowing that  $\beta = 0.5$ , verify whether these data satisfy the approximated formulas. If not, mention some possible causes. (Plonski)

11. The initial sweep peak current (amperes) for a reversible one-electron reduction at the electrode in the cyclic voltammetric experiment is given by

$$i_p = 0.4463nFA \left[ \frac{nF}{RT} \right]^{1/2} C_{\text{ox}} D^{1/2} \nu^{1/2}$$

where

$C_{\text{ox}}$  = concentration of the electroactive species ( $\text{mol/cm}^3$ )

$A$  = area of the electrode ( $\text{cm}^2$ )

$D$  = diffusion coefficient

$\nu$  = scan rate, in volts per second

(a) For an electrode of  $0.01 \text{ cm}^2$ , a solution concentration of  $1.00 \text{ mM}$ , a diffusion coefficient of  $5.0 \times 10^{-6} \text{ cm}^2/\text{s}$ , and a scan rate of  $1.0 \text{ V/s}$ , what will the peak current be? (b) How will the peak current vary with a doubling in concentration? scan rate? electrode area? diffusion coefficient? (c) How can the cyclic voltammetric experiment be used to estimate a diffusion coefficient? (Gosser)

12. The peak potential for a reversible one-electron reduction is not equal to the reduction potential, but is shifted in a negative direction. The exact amount is given by

$$E_p = E^{\circ'} - 1.109 [RT/nF]$$

The reduction potential is also the average of the cathodic and anodic peak currents.

$$E^{\circ'} = \frac{E_{p,\text{cathodic}} + E_{p,\text{anodic}}}{2}$$

If the forward reduction peak is observed at  $-289 \text{ mV}$ , what is the reduction potential and the expected location of the reverse oxidation peak? (Gosser)

13. The electrochemical circuit in the CV experiment, like other electrochemical experiments, contains an IR drop due to the solution resistance and the current. For the one-electron process as described in the above problem, what scan rate could be used so that the IR drop is less than  $10 \text{ mV}$ , if the solution resistance is  $5000 \text{ ohms}$ ? (Gosser)

## PROBLEMS

- Figure 8.9 shows a somewhat idealized potentiostatic relation. Here, a potentiostat controls the electrode potential and one observes the current as a function of time. At higher times, the current becomes transport controlled. How may one eliminate this influence and get back to a part of the  $(i)_v-t$  relation influenced by neither double-layer charging nor diffusion control so that the exchange current and rate constant of the electrode reaction can be obtained? (Bockris)
- (a) Compare constant current and constant potential methods of obtaining the basic parameters ( $\alpha$  and  $i_0$ ) of an electrode reaction in the Tafel region, (b) How does one find the steady state for reactions involving an intermediate on a solid electrode in the results obtained by either method? (c) What of the IR drop—can it be eliminated more easily on the galvanostatic approach than on the potentiostatic? (d) Does the potentiostatic approach give results in a form easier to interpret, i.e., at constant “electrochemical energy of activation?” (Bockris)
- In Fig. 8.17 experimental results are shown for the values of the adsorption of an organic substance as a function of time at constant potential and several temperatures for the adsorption of phenol on Pt. At 60°C, the occupancy of surface after 100 s is around 0.1, and at 1000 s it is 0.6. To reach steady state or equilibrium, it takes  $\sim 10^3$  s.

Consider now a potential sweep relation. As the potential changes, surface occupancy changes. What will the sweep rate have to be so the results reflect the happenings within 10% of the equilibrium coverage for each potential? (Assume the surface reaction is with the adsorbed organic and the latter is in equilibrium with the dissolved species in solution.) (Bockris)

- Potential sweep relations consist of current–potential curves in which the potential is varied in a regular manner and the corresponding current is recorded. Cyclic “voltammetry” is this experiment but with the potential sweep—and the resulting current—plotted for the cathodic  $\rightarrow$  anodic direction, followed by a sweep in the anodic  $\rightarrow$  cathodic direction. Several such diagrams are shown in the text.
  - Why mechanistically do these curves have peaks? (b) What does the potential of a current peak represent? (c) How may a rate constant be obtained by the study of such peaks? (Bockris)
- An electrode reaction for which the exchange current density is  $10^{-6} \text{ A/cm}^2$  is proceeding in a galvanostatic mode with a current density of  $10^{-4} \text{ A/cm}^2$ . Calculate the overpotentials measured at times of  $10\tau$ ,  $100\tau$ , and  $1000\tau$ , where  $\tau$  is the relaxation time of the interface (capacitance =  $50 \text{ } \mu\text{F/cm}^2$ ), when the concentration and diffusion coefficient of the electroactive species ( $A^+$ ) are  $10 \text{ mM}$  and  $10^{-5} \text{ cm}^2/\text{s}$ . The symmetry factor is 0.5. (Kim)

6. The overpotential measured at a current density of  $10^{-5} \text{ A/cm}^2$  was +0.236 V. The decay of the overpotential with the cut off of the current was observed as listed Table P.1. Calculate the double-layer capacitance, the exchange current density, and the transfer coefficient for the electrochemical reaction. (Kim)

**TABLE P.1**

Time after cutoff (s)	2	4	6	8
Overpotential (mV)	166	148	138	130

7. Calculate the lower limit and the upper limit for the sweep rate in a cyclic voltammetry. The double-layer capacitance is  $50 \mu\text{F/cm}^2$  and the diffusion coefficient is  $10^{-5} \text{ cm}^2/\text{s}$ . The measurable current density is  $100 \mu\text{A/cm}^2$  and the sweep range is 1.0 V. (Kim)
8. One obtains the data listed in Table P.2 for an electrochemical reaction involving a chemisorbed species on the electrode surface. Calculate the amount of charge required to form a monolayer of adsorbed intermediates and the rate constant for the formation of the intermediate on the surface under highly irreversible conditions. (Kim)

**TABLE P.2**

Sweep rate (mV/s)	0.1	1	10	100
Peak current density ( $\text{A/cm}^2$ )	$6.9 \times 10^{-8}$	$7.0 \times 10^{-7}$	$6.8 \times 10^{-6}$	$6.9 \times 10^{-5}$
Peak potential (V)	0.387	0.505	0.623	0.742

9. The  $I$  vs.  $E$  (current vs. potential) characteristics of a platinum electrode (geometric surface  $0.185 \text{ cm}^2$ ) in  $0.5 \text{ M H}_2\text{SO}_4$  obtained by cycling the electrode potential [Fig. P8.1(a)] in the range  $-0.150 \text{ V} < E < -0.250 \text{ V (SCE)}$  (in which no Faradaic reaction takes place) at different potential sweep rates  $\Delta E/\Delta t$  are shaped as in Fig. P8.1(b).

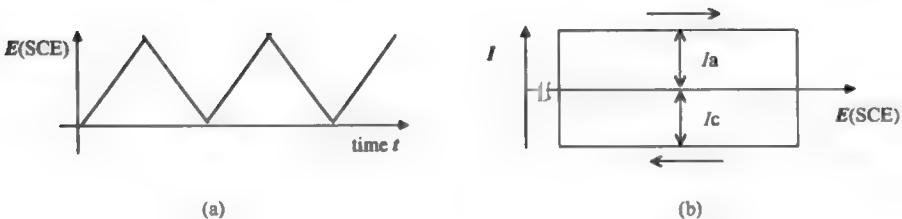


**Fig. P8.1.**

with

**TABLE P.2**

$\Delta E/\Delta t/(\text{mV/s})$	20	30	50	80	120
$ I_{\text{an}}  +  I_{\text{cath}} /(\mu\text{A})$	2.2	2.95	4.6	6.6	9.1

Calculate the capacity of the electrode/solution interface system and the active surface of the electrode, given the specific capacity factor  $20 \mu\text{F}/\text{cm}^2$ . (Mussini)

10. Metal deposition or stripping and capacitance under constant current, (a) What is the potential transient in the case of metal deposition under constant current ( $I = 10 \text{ mA}/\text{cm}^2$ )? Derive its transition time  $\tau$ . Consider silver deposition on a silver substrate as an example ( $E_{\text{Ag}} = 0.799 \text{ V}$ ,  $D_{\text{Ag}} = 1.65 \times 10^{-5} \text{ cm}^2/\text{s}$  at room temperature), (b) If this process is reversed (i.e., silver is stripped from the silver substrate electrode), what should the expression be? Suppose the initial solution does not contain silver salt, (c) What will the potential be at  $t = 0$ ?

Let's assume that the silver electrode is composed of a thin layer of silver plated on a polished noble metal. Then at the time when all of the silver is stripped, the potential of the electrode will "shoot" to higher (more positive) territory until the next species in the electrolyte gets oxidized. Suppose this next anodic process is decomposition of water, (d) Calculate the time it takes to raise the electrode potential to oxygen evolution. (Kang)

11. Diffusion control: constant flux mode. Table P.3 contains the potential transient data obtained on a platinum working electrode (against SHE) immersed in an aqueous solution of  $0.1 \text{ M}$  ferric perchlorate and  $1.0 \text{ M}$  ammonium perchlorate. The experiment was carried out at a constant current of  $10 \text{ mA}/\text{cm}^2$ , and the diffusion coefficient of both reactant and product is assumed to be  $10^{-5} \text{ cm}^2/\text{s}$ .

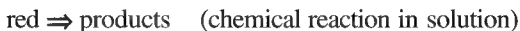
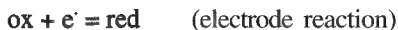
**TABLE P.3**

$t(\text{s})$	1.0	2.0	3.0	4.0	5.0	6.0	7.0	7.2	7.25
$E(\text{V})$	0.7828	0.7667	0.7543	0.7424	0.7292	0.7115	0.6735	0.6506	0.6200

(a) Calculate the transition time for this system. (b) Derive the standard reduction potential for this redox system. (c) At what time does the measured electrode potential equal the standard reduction potential for this redox system? (d) Derive a general expression and discuss its possible use in standard potential measurement. (Kang)



12. The EC mechanism is a standard departure for discussing electrochemical mechanisms. It represents a one-electron electrode reaction coupled to a chemical reaction in solution:



In light of the Nernst equation, how do you think that the potential for a reduction peak will shift if the reductant is quickly removed by a coupled chemical reaction? (Gosser)

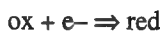
13. It is said that the CV response has a peak because the electroactive substance is depleted faster than diffusion can replace it near the electrode. The relationship between the current at the electrode and the diffusion gradient at the surface is

$$I/nFA = -J_{\text{ox}} = -D_{\text{ox}} \frac{\Delta C}{\Delta X}$$

for a small change in  $x$ .

Draw a rough sketch of the concentration of  $C_{\text{ox}}$  as a function of distance from the electrode for the following potentials in the CV experiment. Show the relative gradients: 1/2 V before the reduction potential, at the reduction potential, at the peak potential, and 1/2 V after the peak potential. (Gosser)

14. As the technology of electrode fabrication has advanced, the use of microelectrodes in electrochemistry has allowed new kinds of experiments to be done. Explain why the use of microelectrodes in CV allows fast scan experiments (up to 1,000,000 V per second) to be done. (Gosser)
15. The effects of complex coupled chemical reactions are sometimes more pronounced for a transient experiment than for a steady-state experiment, (a) Compare the experimental result obtained with a steady-state experiment and a CV (transient) experiment in the case of an EC mechanism, (b) In each case, how will the current response curve reflect the rate of the coupled chemical reaction? (Gosser)
16. Consider a catalytic reduction where the electroactive species is regenerated:



- (a) What is the maximum peak current that can be observed, if  $[\text{S}] = 3 * [\text{ox}]$ ?  
 (b) How will the peak current change if the scan rate is increased? (Gosser)

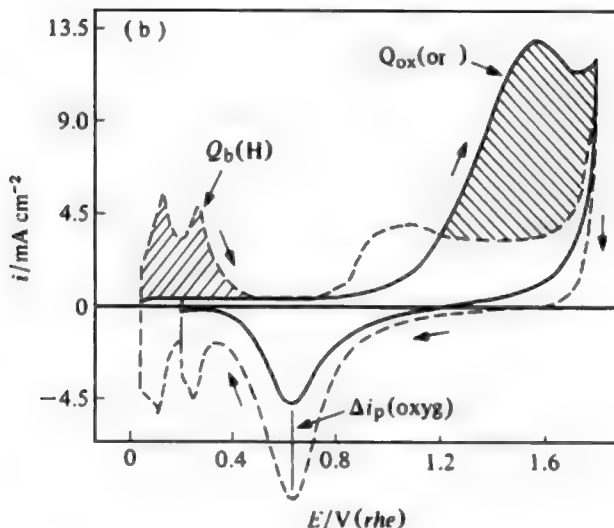


**Fig. P8.2.** Voltammograms of platinum in 0.5 M H<sub>2</sub>SO<sub>4</sub> + 0.1 M propargyl alcohol ( $E_{\text{ads}} = 0.2$  V;  $t_{\text{ads}} = 100$  s; 25° C. (a)  $\nu = 0.1$  V s<sup>-1</sup> and (b)  $\nu = 5$  V s<sup>-1</sup>. (Reprinted from R. S. Goncalves, J-M. Leger, and C. Lamy, "Electrochemical Studies of the Adsorption of Propargyl Alcohol on a Smooth Platinum Electrode in Acid Medium," *Electrochim. Acta* **34**(3), Fig. 2, p. 425. Copyright 1989 Pergamon Press.)

17. This problem concerns the study, by means of cyclic voltammetry, of organic molecules adsorbed on Pt at 25°C. The coverage for each concentration,  $C_i$ , was determined from the accompanying voltammograms (see Fig. P8.2) by determining the coverage with H on the Pt in the presence and absence of the organic. The following relation was used and Table P.4 gives the results of  $\theta_i$  as a function of  $C_i$ .

$$\theta_i = \frac{Q_H^\circ - Q_H}{Q_H^\circ}$$

**TABLE P.4**

$10^6 C_i(\text{M})$	0.368	0.736	1.108	1.488	1.881	2.293	2.731	3.205	3.728	4.319
$\theta_i$	0.049	0.101	0.153	0.202	0.254	0.294	0.350	0.399	0.441	0.511
$10^6 C_i(\text{M})$	5.004	5.821	6.832	8.136	9.916	12.53	16.83	25.34	50.70	
$\theta_i$	0.556	0.601	0.665	0.694	0.767	0.817	0.851	0.903	0.958	

(a) Draw the isotherms for adsorption, representing  $\theta$  as a function of  $\log E_i$ . (b) Show that the results are consistent with Frumkin's isotherm:

$$\frac{\theta_i}{1 - \theta_i} e^{g\theta_i} = KC_i$$

(c) By deducing the value of the parameter,  $g$ , for interaction between the molecules, calculate the equilibrium constant,  $K$ . (d) Also calculate the free enthalpy of adsorption,  $\Delta G_{\text{ads}}$  in kilojoules  $\text{mol}^{-1}$ . (e) Show that one may also determine the factor  $g$  from an inflection on the  $\theta$ - $\log C_i$  relation. Again, evaluate  $g$  and  $K$ .

The equilibrium constant depends on the potential by the relation

$$K = K_0 \exp \left[ \frac{nF}{RT} (E - E_0) \right]$$

where  $K_0$  is the equilibrium constant at the standard potential,  $E_0$ , for the system, (f) Show that the voltammetric curve  $i = f(E)$  passes through a maximum. ( $dE/dt = V$  is called the *sweep rate* and  $Q_0$  is the quantity of electricity needed to oxidize a fully covered surface. ( $E_0 = 0.5 \text{ V}$  vs. NHS;  $V = 50 \text{ mV s}^{-1}$ ,  $Q_0 = 200 \mu\text{C cm}^{-2}$ ;  $n = 2$ ; the value of  $g$  can be calculated from the experiment). (Lamy)

## MICRO RESEARCH PROBLEMS

1. The study here is of a fuel cell intended to run a 10-kW car using ethylene glycol as a fuel.

### *Equilibrium Study*

(a) Write the electrochemical reactions occurring in an acid ( $\text{H}_2\text{SO}_4$  0.5 M) and an alkaline (KOH 1 M) medium for the complete oxidation of ethylene glycol. Write the equation for the reduction of oxygen in acid and alkaline media. (b) Calculate the standard potential with respect to the normal hydrogen electrode for the reactions in the cell considering as an approximation 1 M concentrations and assuming the activities of all the reactants are unity. (c) Calculate the maximum possible energy density of this cell in kilowatt hours/kilogram. The following data are given for the combustion in oxygen of the following compounds.

Compound	$\Delta G^\circ$	$\Delta H^\circ$
	$\leftarrow \text{kcal/mol} \rightarrow$	
$\text{H}_2$	-56.7	-68.3
Ethylene glycol (EG)	-272.6	-281.9

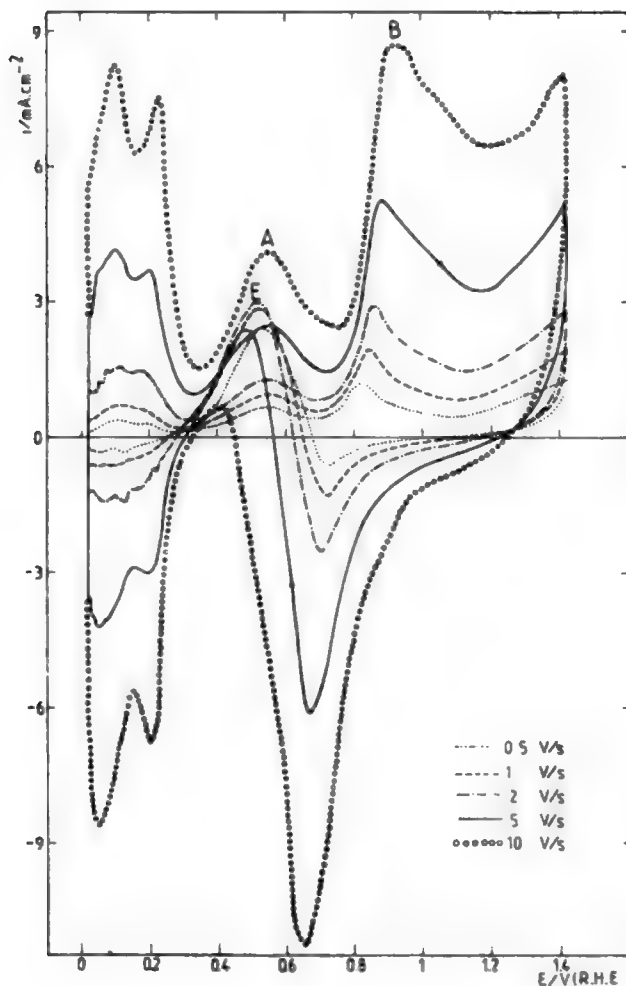


**Fig. M8.1.** Voltammograms of Pt in  $\text{H}_2\text{SO}_4$  0.5 M + EG 0.1 M at  $25^\circ\text{C}$ . Effect of the variation in the sweep rates. (Reprinted from F. Kadirgan, B. Beden, and C. Larry, "Electrocatalytic Oxidation of Ethylene-Glycol," *J. Electroanal. Chem.* **136**, Fig. 3, copyright 1982, p. 124, with permission from Elsevier Science.)

#### *Voltammetric Data*

A voltammetric study, as a function of the variation of the sweep rate in the electrochemical oxidation of EG in acid (as above) led to the following collection of curves (Fig. M8.1). From the data it is possible to obtain the potentials

and current densities of the peaks as a function of the sweep rate; these results are given in Table M.1.

**TABLE M.1**

$v(\mu\text{V s}^{-1})$	0.01	0.03	0.1	0.32	1	3	10	32	100	998
$E_p(\text{mV})$	47	49	48	46	65	96	157	218	276	400
$i_p(\text{mA cm}^{-2})$	1.9e-4	6.1e-4	1.9e-3	6.3e-3	0.019	0.044	0.15	0.45	1.45	14.2

(a) Plot on a semilogarithmic scale the characteristics  $E_p$  and  $i_p$  as a function of  $v$ . What is the rate-determining step? (b) Calculate  $\alpha$ ,  $n$ , where  $\alpha$  is the transfer coefficient and  $n$  is the number of electrons in the rate-determining step. Calculate the standard rate constant and the exchange current density for the anodic reaction.

### *The Stationary Cell*

Table M.2 contains data for the cell potential as a function of  $\log i$ .

**TABLE M.2**

$i(\text{mA cm}^{-2})$	1	5	10	25	50	100	200	500	1000	1600
$E(\text{V})$	1.54	1.35	1.30	1.20	1.11	1.02	0.91	0.69	0.42	0.15

(a) Show that this curve can be described by the equation

$$E = E_0 - a i - b \ln i$$

To do this, it may be helpful to plot the derivative  $dE/di$  as a function of  $1/i$ , deducing from it the coefficients  $a$  and  $b$ . One can then calculate the value of  $E_0$  from the initial curves, (b) Establish theoretically the law  $E = f(\ln i)$ . Find from the experimental data the resistance of the electrolyte  $R_e$ , the product  $\alpha_2 n_2$ , and the exchange current density for the reduction of oxygen, (c) Calculate the maximum current and maximum power of the cell. (d) What electrode surface would be necessary to obtain twice the normal power of the cell? You are given:

$$R = 8.314 \text{ J/mol, } 1 \text{ cal} = 4.185 \text{ J, and } F = 96,490 \text{ C.}$$

## CHAPTER 9

# SOME QUANTUM-ORIENTED ELECTROCHEMISTRY

### 9.1. SETTING THE SCENE

When Galvani and, separately, Volta, made their first hesitant electrochemical experiments, in the eighteenth century, the electricity with which they dealt was not understood. Faraday's laws of 1834 (relating the amount of metal deposited in electrolysis to the amount of electricity passed) hinted at a particulate nature for electricity, and by 1897 J. J. Thompson had measured electric charge to mass ratio ( $e/m$ ) for the charged "cathode corpuscles" he found in gas discharge tubes. By 1912, Millikan had measured the charge,  $e_0$ , on such particles, so that their mass was also known. The realization that the passage of electricity consists of the flow of these "electrons" is less than 100 years old.

The electron is the quintessential particle in electrochemistry. But it has turned out that its properties bear within them a mystery, the nature of which is still debated. For Davidson and Germer (1927), and then G. P. Thompson (1928) found that the corpuscles that J. J. Thompson (1897) had measured possessed a Jekyll and Hyde character. Material corpuscles they could be (with definite mass and charge) but lo!—they could also behave as if they were *waves*.

Earlier on, in 1901, experimental results on the variation of the intensity of radiation from hot black bodies as a function of the wavelengths emitted by the radiation led Planck to suggest that energy itself went about as "quanta," bits of energy, the amount of energy in each bit being related to the frequency of the radiation concerned. Bohr's 1913 interpretation of the H atom spectra then involved an assumption to which he needed to fit the facts: only certain frequencies of radiation were "allowed." The radiations emitted from hot atoms consisted of a number of spectral lines having frequencies of  $\nu_1$ ,  $\nu_2$ , and  $\nu_3$ , etc. The positions in the atoms issuing

radiation at these specific frequencies are called *quantum states*. Electrons could be in these states, but not in others.

By 1926, just in time for Davidson and Germer's 1927 experiment, Schrödinger put into mathematical form an idea due to de Broglie (1924). It was that the sometimes wavelike character of electrons could be the basis of the quantum states. The waves had to "fit into" the space available (e.g., the distance between two nuclei in a solid), and it was this need to fit and make a "standing wave" that made only certain states—certain wavelengths (or energies)—possible.

All this material is described in introductory textbooks of physics and chemistry. However, it is interesting to recall the headlines here because the very first application to a chemical theme of the ideas of waves in quantum mechanics was to explain how electrons were emitted from, or accepted by, electrodes. This was the achievement of Ronald Gurney,<sup>1</sup> the first physical electrochemist, and much of this chapter is based on developments that sprang from his seminal paper of 1931. In this paper, he related electric currents across the electrode solution interface to the tunneling of electrons through energy barriers formed between the electrode and the ions or molecules in the first layer next to the electrode (possessing "electronic states").

Our chapter has two broad themes. In the first, we will consider some aspects of quantum states relevant to electrochemical systems. In the second, the theme will be the penetration of the barrier and the relation of the current density (the electrochemical reaction rate) to the electric potential across the interface. This concerns a quantum mechanical interpretation of Tafel's experimental work of 1905, which led (1924–1930) to the Butler–Volmer equation.

---

<sup>1</sup>Gurney's seminal contribution to the way electrons exchange with metals in contact with solution sprang out of his work with Condon on an even more fundamental problem, the physics of the stability of nuclei. In a classical world, particles in nuclei—the protons and neutrons—ought to stay inside because energetically, they do not have the energy to jump out of the deep energy well that contains them. By applying the recently published Schrödinger equation of 1926, Condon and Gurney showed in 1929 that some particles in heavy nuclei could "leak out" of the nuclei by the new quantum mechanical idea of "tunneling." Gurney saw the analogy between this energy well in the nucleus and the energy well of electrons in metals; if the walls of the former could be tunneled through, electrons could also tunnel out of metals to waiting acceptor states in ions in solution.

Gurney then collaborated with the eminent Cambridge (U.K.) physicist, Nevil Mott, to co-author a book, *Electronic Processes in Crystals* (1936), which provided the foundation of solid state physics. Some years later there followed *Ions in Solution*, the first book to treat solution J electrochemistry at a quantum level.

This brilliant career ran into WWII. Gurney was in Norway when war broke out, and return to England was not practical. Much of the war was spent in Russia and when Gurney finally reached the United States (traveling eastward), he fell under the suspicion of American authorities; had he perhaps been infected with Communism? His tragic end took place on a New York street in 1953, in collapse from a heart attack, brought on, it has been said, by the overzealous treatment he had received from U.S. immigration officials.

### 9.1.1. A Preliminary Discussion: Absolute or Vacuum-Scale Potentials

In conventional electrochemistry, the scale of electrode potentials (see Section 6.4.15) is an arbitrary one. Although it is obvious that the potential of the standard hydrogen electrode cannot be zero, it is arbitrarily taken as such and all the “electrode potentials” are in fact cell potentials, the cell consisting of the given electrode (e.g., a copper electrode in a cupric nitrate solution) and the other electrode making up the cell being always the same, the standard hydrogen electrode (Section 7.5.7.3). This arrangement is exactly analogous to one way of expressing temperature—the use of the Celsius scale—in which the melting point of ice and the boiling point of water at 1 atm are arbitrary choices of temperatures to form a scale of one hundred divisions.

Until 1967, no value of the hydrogen electrode potential itself was known. Then a value for the quantity

$${}^{\text{ref}}\Delta^{\text{S}}\phi - \mu_e^{\text{ref}}/F \quad (9.1)$$

was calculated (Lohman, 1967; Bockris and Argade, 1968) where “ref” refers to the electrode in a solution of unit activity of  $\text{H}^+$  in equilibrium with  $\text{H}_2$  at 1 atm and  $\mu_e$  is the chemical potential of the electron in the metal of the reference electrode when its electrons are in equilibrium with protons in the solution, as described. Various numerical values have been theoretically calculated for the quantity (9.1), and  $4.6 \pm 0.2$  V seems to cover them. The quantity is regarded by most people as the absolute potential of the standard hydrogen electrode.

Knowledge of the numerical value of the entity represented by Eq. (9.1) allows one to make up cells that give the potential of an electrode “on the absolute scale,” just as the Celsius scale was later shown to be expressed on the absolute or Kelvin scale of temperatures, in which there is a rationally based zero at  $-273^\circ\text{C}$ . Thus, to find the “absolute” value,  $V_{\text{M,abs}}$  of an electrode potential expressed on the standard hydrogen scale, one writes

$$V_{\text{M,abs}} = V_{\text{M,H}_2 \text{ scale}} + 4.6 \quad (9.2)$$

In what sense is this potential absolute? It refers back, eventually, to the free energy of a hypothetical stationary electron and a hypothetical stationary proton in the gas phase. In *this* sense, it is reasonable to call the quantity given by Eq. (9.2) “absolute,” for a stationary electron or proton has no entropy and the potential energy of a stationary isolated particle must be zero.

However, some electrochemists prefer to call potentials calculated from Eq. (9.2) potentials on the “vacuum scale,” rather than an “absolute,” potential. Thus, “absolute” is a loaded word and requires detailed explanation. Some chemists are surprised when one identifies the word “electrode potential” with (9.1), for they tend, intuitively, to identify a quantity so named with  ${}^{\text{M}}\Delta^{\text{S}}\phi$ , the potential difference across the interphase. To avoid controversy that might arise concerning the justice of calling  ${}^{\text{ref}}\Delta^{\text{S}}\phi - \mu_e^{\text{ref}}/F$



an absolute *electrode* potential, it may be better, say some, to call such potentials *vacuum scale* potentials, for this phrase is not loaded with meaning as is the word “absolute.” If asked what a vacuum scale electrode potential is, one can explain the meaning of (9.1) and show how it is used in (9.2), which gives, by definition, a vacuum scale of potential (Gerischer, 1960).

What has this to do with quantum-oriented electrochemistry? Very much! For in the work we are to cover, the energy of a particle in a system is usually expressed with respect to a state in which its energy is zero (and often stationary in a vacuum, i.e., at an infinite distance from particles with which it might interact). However, one cannot discuss particles at the electrochemical interface, or those moving across it, without taking into account the electrical potential that is the origin of part of their energy. What is the value of that potential? It clearly won’t do to express it on an arbitrary scale, where the numerical value carries a hidden quantity masquerading as zero. It must be on the same energy scale as the energy of the other particles and relate back to the work done to take them to the final state in which they make up an electrode potential from a state in which their energy may confidently be placed equal to zero.

## 9.2. CHEMICAL POTENTIALS AND ENERGY STATES OF “ELECTRONS IN SOLUTION”

### 9.2.1. The “Fermi Energy” of Electrons in Solution

In the last section it was shown that instead of representing an “electrode potential” on a *relative* scale (arbitrarily setting the standard hydrogen electrode potential equal to zero), it is possible to numerically calculate the actual value of the latter, with a reference state of zero energy for the stationary electron at infinity in a vacuum.

In calculating this “absolute” or “vacuum scale” potential of the standard hydrogen electrode, the expression quoted as an “electrode potential” was

$${}^M\Delta^S\phi - \mu_e^M/F \quad (9.3)$$

where  ${}^M\Delta^S\phi$  is the Galvani (inner) potential difference at the interface and  $\mu_e^M$  is the chemical potential of the electron in the metal. In a conceptual sense, the expression implies that an electrode potential is the algebraic sum of the energy needed to transfer an electron from infinity to the interior of the electrode, together with the electrical work ( $F{}^M\Delta^S\phi$ ) of passing an electron from the interior of the metal to the interior of the solution. This of course immediately brings up the question of an “electron in the solution.” Hydrated electrons can certainly be created in solution, but in this case the

---

<sup>2</sup>Of course, this is a hypothetical state, but easy to imagine. It is necessary to have it stationary; otherwise it would have translational entropy. The condition “at infinity” means that the electron in its reference state is too far away from anything to experience an energy of interaction.

concept is an electron in a state within an ion, for it is generally in the electronic states of ions in solution that electrons exchange with metals; i.e., interfacial electrochemistry takes place.

Some interesting thoughts arise if one follows this concept of an electrode potential [Eq. (9.1)] somewhat further. Thus, from Eq. (9.3),

$$FV_{\text{abs}} = F^M \Delta \phi - \mu_e^M$$

Hence:

$$FV_{\text{abs}} = F\phi^M - F\phi^S - \mu_e^M$$

Or,

$$\bar{\mu}_e^M = -FV_{\text{abs}} - F\phi^S \quad (9.4)$$

In (9.4),  $\bar{\mu}_e^M = F\phi^M + \mu_e^M$  is the electrochemical potential of the electron in the metal with which an electron in an ion in solution is in equilibrium (Section 6.4.13), and  $\phi^S$  is the inner potential of the solution.

Now in the study of chemical equilibria, at an interface between a phase  $\alpha$  and a phase  $\beta$ , any entity,  $i$ , adjusts its different concentrations in the two phases so that the chemical potentials in them are equal. Thus:

$$\mu_i^\alpha = \mu_i^\beta$$

Correspondingly, at *charged* interfaces, and in particular between a metal, M, and a solution, S, for an electron and in equilibrium:

$$\bar{\mu}_e^M = \bar{\mu}_e^S \quad (9.5)$$

where the subscript  $e$  indicates the electron, and  $\bar{\mu}$  is called, logically, the *electrochemical potential*; it is related to the chemical potential by  $\phi$ , the inner potential of the phase concerned (see Section 6.4.13).

$$\bar{\mu}_e = \mu_e^- - \phi F \quad (9.6)$$

Then (Bockris and Khan, 1983), from Eq. (9.5) (only at equilibrium),

$$\bar{\mu}_e^S = -FV_{\text{abs}} - F\phi^S \quad (9.7)$$

This electrochemical potential has a name. It is called the *Fermi energy of the electron in solution*, and the name arises because if one expels an electron into a vacuum, the electrons come (overwhelmingly, if not entirely) from the Fermi level of electrons in

the metal. Correspondingly, the concept is that the electrons “in solution” (albeit carried about in the outermost electron levels of ions) exchange with electronic states in the most available states in the metal, the topmost occupied states or the Fermi level.

Electrons in metals obey a different “distribution law” (the law that indicates how the number of electrons varies with the energy state they are in) from the corresponding quantity for, say, molecules in gases. Because the electrons in solution are in equilibrium with the electrons in the Fermi level of the metal, electrochemists have referred to the  $\bar{\mu}_e^S$  as the Fermi energy of electrons in solution (see later discussion).

It can be seen from Eq. (9.6) that the quantity concerned is not so easy to determine because although we can determine  $V_{\text{abs}}$ , as described in Section 6.4.15,  $\phi^S$  is not directly measurable. However, one can at least minimize the difficulty by adopting a convention with a good history and referring to numerical values for the special condition of a charge-free interface. (This is also the tacit condition assumed in the measurement of the work function.)

Now (Section 6.4.10),

$$\phi = \psi + \chi \quad (9.8)$$

Then, adopting the condition of the pzc (Section 6.6.6), i.e.,  $q = 0$ , it follows that the outer potential of the phase concerned,  $\psi$ , is zero. Hence,

$$(\phi)_{q=0} = \chi \quad (9.9)$$

so that  $(\phi_S)_{q=0} = \chi^S$ , the surface potential of the solution. Although this quantity is by no means well known, values estimated for it (Trasatti, 1998) show it to be about +0.1 V.

Hence, from Eq. (9.3),<sup>3</sup>

$$(\bar{\mu}_e^S)_{q=0} = -FV_{\text{abs}} - F\chi^S \quad (9.10)$$

However, it has been noted that at present  $V_{\text{abs}}$  (hydrogen electrode) is known to be only  $\pm 0.2$  V, so that within this degree of uncertainty and in the presence of a certain reversible electrochemical reaction, the electrochemical potential of an electron in solution with a metal at the pzc is  $-FV_{\text{abs}}$  of that process (i.e., the  $\chi_S$  is neglected as an approximation because the uncertainty in  $V_{\text{abs}}$  is greater than the uncertainty in  $\chi_S$ ). Hence, the Fermi energy of electrons in solution is approximately  $-FV_{\text{abs}}$  (at the pzc of an electrode and at the process in which the electrons are taking part).

Before leaving this subject, it is a good idea to remark that the term “Fermi energy of electrons in solution” is not the most helpful one and has led to a degree of misunderstanding. Thus, as mentioned, the Fermi level *in a metal* deals with electrons that obey a certain distribution law. This law arises from Pauli’s principle: Only two

<sup>3</sup>For Eq. (9.10) to be valid, the interface should be at equilibrium at  $V_{\text{pzc}}$  during the charge-transfer process.

electrons can be in the same state and they must have opposite spins. In a metal, the principle can be shown to imply that at the Fermi energy level, the probability of occupancy by an electron of a state is exactly 1/2.

The electrons in the Fermi level in a metal—those that undergo the Fermi distribution law—are *mobile* and that is where the difference comes from electrons in solution which are, in fact, in the bound levels of ions. Such electrons are not mobile and the statement that they have a *Fermi* energy may therefore be misleading, for they do not obey the same distribution law as the electrons with which they are in equilibrium.<sup>4</sup>

## 9.2.2. The Electrochemical Potential of Electrons in Solution and Their Quantal Energy States

A thermodynamic quantity, such as the electrochemical potential of an electron in solution, represents the partial molar free energy of the electron (whatever may be its neighborhood) in the mixture of ions and solvent. On the other hand, in quantum treatments, the energy associated with the properties of a mole of a substance is the sum of the energies of its quantum states, taking into account their degree of occupancy, which depends on temperature and, in electrochemical systems, the potential of the phase in which they exist. At room temperature, the most important energy quantity in solution is usually the ground vibrational state of the first electronic state of the ion-exchanging electrons with the metal. Let us, therefore, consider such electronic states of ions in solution.

The relation between thermodynamic and molecular quantities is given in terms of partition functions. In the case of the free energy, one finds:

$$G_e = -n_e kT \ln f_e$$

where  $f_e$  is the electronic partition function of the electron in ions in solution, and  $n_e$  is the number of electron states per unit volume. Hence,

$$\mu_e = -kT \left[ \ln f_e + \left( \frac{\partial \ln f_e}{\partial \ln n_i} \right)_{T,p,n_j \neq i} \right]$$

In sufficiently dilute solutions, the partition function for the electron in solution will be negligibly dependent on concentration. Under these conditions:

$$\mu_e \simeq -kT \ln f_e$$

<sup>4</sup>Of course, this *energy* of electrons in solution is numerically equal to the Fermi energy of electrons in the metal. However, in respect to the applicable distribution law, that which applies to the "electrons in solution" is not that which applies to electrons in the metal.

However, in general

$$f = \sum_{i=0}^{i=\infty} e^{-\epsilon_i/kT} = e^{-\epsilon_0/kT} + e^{-\epsilon_1/kT} + e^{-\epsilon_2/kT} + \dots$$

where  $\epsilon_0$  is the energy of the electron in solution in its ground state,  $\epsilon_1$  in the first excited state, etc., and  $kT=0.025$  eV. However,  $\epsilon_0 < \epsilon_1 < \epsilon_2$ , etc. Hence

$$\bar{\mu}_e \approx kT \ln e^{-\epsilon_0/kT} = \epsilon_0$$

Thus, in dilute solution, the electrochemical potential of the electron corresponds to the energy of the ground state of the electronic ions in the solution concerned. If the electron is taking part in a redox equilibrium and a value of the concentration in solution can be found for which there is equilibrium at the pzc, then the approximate value of this quantity (in energy units) is  $F(V_{\text{pzc}})_{\text{abs}}^5$

### 9.2.3. The Importance of Distribution Laws

Distribution functions are usually first met in physical chemistry when the crude treatment of molecular velocities in the kinetic theory of gases (all the molecules taken as having the same mean speed) is replaced by Maxwell's seminal equation showing that the number of molecules having velocities between narrow limits depends very much on what velocities are chosen. This is shown in Fig. 9.1. Thus, this first and basic distribution law of Maxwell, the distribution of velocities, gives an unexpected result (the nonsymmetrical nature of the distribution), which still causes us to think, more than a century after its publication.

What of the distribution of energy states in solution? This is important in electrochemistry because it is so simple to vary the energy of electrons in an electrode over wide energy ranges by means of outside electronic circuitry. However, electron transfer occurs, as will be established below, when the energies of the state of electrons in the metal overlap with those of the energy of the electronic state in solution (Section 9.4.2). Now, the operation of a potentiostat can vary the energies of electrons in electrodes over a large range of potential as much as  $\pm 3$  eV. It follows that electronic states in solution must be available over this range if there is to be electron transfer, from electrode to solution or solution to electrode.<sup>6</sup> The *number* of states available in the solution at each energy level will play a major role in determining the rate of an electrode reaction and how it varies with the electrode potential. The importance of

<sup>5</sup>This conclusion depends on the experimental attainment of equilibrium between electrons in the metal and those in ions in solution. This may not always be an attainable state.

<sup>6</sup>It is not implied that this huge range of energies will be available in one system. However, the linearity of Tafel plots over more than 1 eV suggests that in systems in which such linearity is observed, vibrational-rotational states covering this range are available in solution.

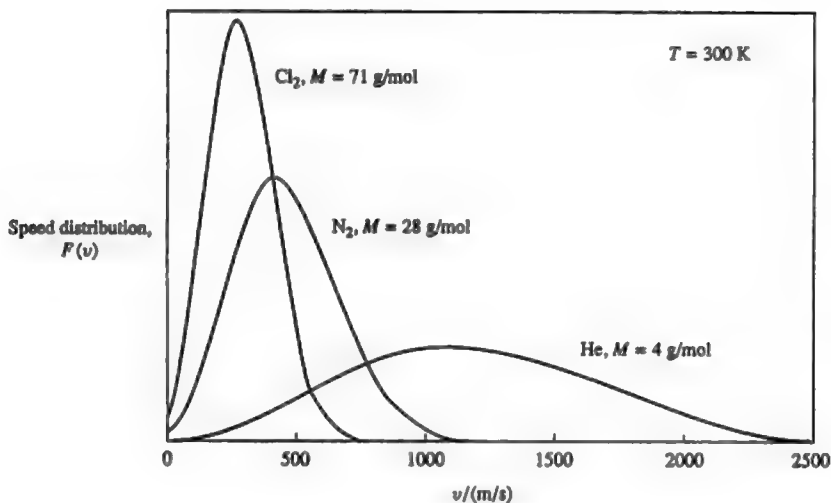


**Fig. 9.1.** The Maxwell distribution of molecular speeds for oxygen at 300. (Reprinted from J. Noggle, *Physical Chemistry*, 3rd ed., Benjamin Cummings, 1996, p. 42.)

the shape of the distribution function, which gives the number of electron states available in ions or molecules in solution over a narrow band of energies and how this number varies with the energy chosen, can then be appreciated.

#### 9.2.4. Distribution of Energy States in Solution: Introduction

One is familiar with the idea of discrete and definite electronic states in molecules, as revealed by molecular spectroscopy. Each electronic state possesses a number of vibrational states that are occupied to a great extent near the ground state at normal temperatures. Each vibrational state has, if the steric conditions are enabling, a number of rotational states associated with it, and for gas molecules both the vibrational and the rotational states can easily be observed and measured spectroscopically. Correspondingly, the distribution of the vibrational states in solids (phonon spectra) is easily measurable.

However, in solutions, there is what is called “line” broadening, i.e., the characteristic shapes seen in molecular spectra in the gas phase are substantially wider in the range of energies they cover. Thus, the separability by means of spectroscopic measurements of the vibrational and rotational states in solution is greatly reduced.

This line broadening is caused by repeated collisions between the entities in solution, which occur with a far greater intensity than for molecules in gases. The collisions are largely with the solvent members of a “cage” in which each solute particle remains for hundreds of thousands of vibratory movements before it escapes

to make a diffusive step. Each of these collisions imparts to what would have been a regular and repeated vibration of a bond, an unscheduled shove, and this sporadic addition or subtraction to the vibrational and rotational energy smooths out the tiny differences between them. There are two models that form the basis for the deduction of distribution laws for energy states in solution.

**9.2.4.1. The Gaussian Distribution Law.** Here, one concentrates one's attention upon the ground vibrational state of the solvated ion, noting the much smaller degree of occupancy of the higher vibrational states in an electronic state. To have a distribution of energies in the ground state sounds like an oxymoron. That it can nevertheless be so was suggested by Gerischer<sup>7</sup> in 1960 and this remained the most popular theory of the distribution of energy states from the early 1960s through the mid-1980s, so that a great number of diagrams representing it (Fig. 9.2) exist in the literature.

The argument may be put as follows. It must be mainly the ground states of solvated ions and molecules that exchange electrons with an electrode (because of the high degree of occupancy compared with other states). Now the ground state of electrons in solution (i.e., of electrons in ions in solution) shows a *range* of energy states resulting from the fluctuations in energy that occur with any energy state in solution and give rise to line broadening. The basic phenomenon is the chance-dependent variation of the energy of any state dependent upon the perpetual buffeting of the entity concerned by its neighboring molecules and ions.

This model suggests at once the *type* of distribution of energy that will result. It must involve the law governing chance events, the Gaussian distribution law. Thus, if one repeatedly shoots a bullet at a target, and the causes giving rise to the near-misses of the bullseye are all due to chance (e.g., ticks in the nervous system of the aimer), the number of near-misses is related to distance from the target ( $x$ ) by a so-called error function:

$$P(x)dx = \frac{1}{\sqrt{2\pi\sigma^2}} e^{-x^2/2\sigma^2} dx$$

---

<sup>7</sup>Heinz Gerischer was unchallenged as the leading physical electrochemist in Germany from 1960 to 1980. He was one of the first to use potentiostatic transients to establish mechanisms, particularly those involving adsorbed H. His work stressed the physics on which electrode processes rested. He suggested the vacuum scale of potentials and contributed seminally over his whole career to semiconductor electrochemistry and photoelectrochemistry (see Chapter 10). After a period as professor at the University of Munich, he became director of the prestigious Max Planck Institute in Berlin, where he remained for 24 years. Partly because of his association with leading American electroanalytical chemists, his influence on electrochemistry was widely felt, particularly his emphasis upon a Gaussian distribution of energy states in solution, and because of opinion that semiconductor electrode kinetics occurred as a function of happenings inside the semiconductor and was not affected by surface states.

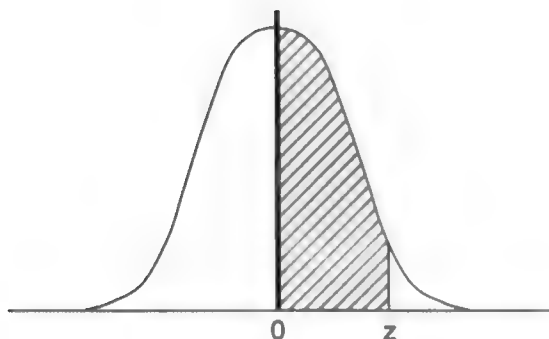


**Fig. 9.2.** Probability of random events: the Gaussian distribution. (Reprinted from R. A. Serway, C. J. Moses, and C. A. Moyer, *Modern Physics*, 2nd ed., Saunders College Publishing, 1997, p. 208. Reproduced with permission of Harcourt Brace.

where  $\sigma = \sqrt{n\lambda^2}$ , where [in terms of a random walk (Section 4.2.5)]  $\sigma$  is the root mean square from the origin to the end of the random walk. Thus, the probability of the event is independent of the sign of  $x$ . Correspondingly, any function that has the form  $e^{-ax^2}$  is called a *Gaussian Function* (Fig. 9.2).

Correspondingly, in terms of the energy of the ground state, it is possible to show (Morrison, 1980) that the distribution law (fraction of particles having an energy,  $E$ ) follows according to a Gaussian model as

$$D(E) = \frac{1}{4\pi E_s kT} \exp \left[ -\frac{(E_0 - E)^2}{4\pi E_s kT} \right]$$

where  $E_0$  is the undisturbed ground state energy and  $E_s$  is a so-called reorganization energy (see Section 9.6.3). Thus, in this view, the probability of finding a state of energy  $E$  in a solvated ion varies in a Gaussian manner around the ground state of such ions.

A diagram illustrating this is given in Fig. 9.3. Here, the *numbers* of states with specific energies are plotted as abscissae and the energy is plotted as ordinates. Such distribution laws are sometimes given the affectionate name of “shoelace” curves. Turning them through 90° counterclockwise shows two Gaussian distribution curves for the energy available in the ions in solution in their exchange with electrons in the metal. The question of course is to what extent the Gaussian distribution law for electron states in solution gives results consistent with electrochemical observations. There are two points that bear on this.



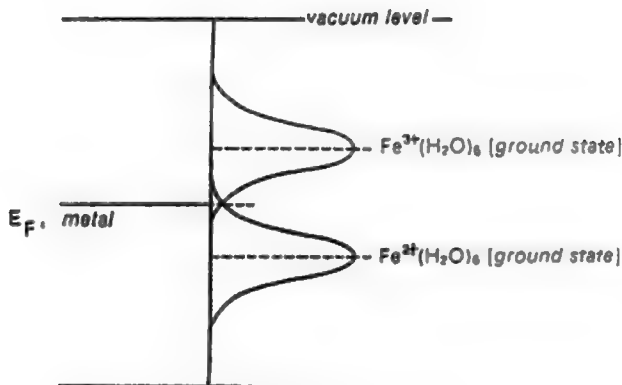


**Fig. 9.3.** A schematic bell-shaped diagram of the distribution of electronic states of redox ions at an electrode/solution interface (fluctuation theory). (Reprinted with permission of the American Institute of Physics from J. O'M. Bockris and S. U. M. Khan, *Appl. Phys. Lett.* **42**: 124 (1983).

A plot of the probability of finding a state against the energy of that state falls off more quickly in a Gaussian distribution than in the Boltzmannian one. Calculation shows that the large electrical potential range over which it is possible to satisfy the Butler–Volmer equation (say,  $\pm 1.0$  eV), would be difficult to reach by energy changes caused by fluctuations in the ground state due to collisions that are unlikely to exceed, say,  $10 kT$  (0.25 eV).

If one introduces an overpotential into a distribution law such as that given by Morrison, one obtains for the current density of a cathodic reaction at an overpotential,  $\eta$ , in a reaction the standard free energy of which  $\Delta G^\circ$ ,

$$i = A \exp \left( - \frac{(E_s + \Delta G^\circ + \eta F)^2}{4E_s kT} \right)$$

and such a model gives *curved* Tafel lines and a maximum in the relation of  $i$  to  $\eta$  (Khan and Bockris, 1983), which is not observed for electron-transfer processes at electrodes (Section 9.4.14).

The great importance of the Tafel relation—because it is too widely observed to be applicable in electrode kinetics—does not seem to have been appreciated during the time (about 1960–1980) in which Gaussian concepts were frequently used to present a quantal approach to electrode kinetics. Supporting a theoretical view that does not yield what is in effect the first law of electrode kinetics is similar to supporting a theory of gas reactions that does not lead to the exponential dependence of rate on temperature. It represents a remarkable historical aberration in the field. Thus the

Gaussian theory of the distribution of energy among states in solution is not the whole story (although, of course, the ground state is bound to have some distribution in its energy according to the Gaussian law).

**9.2.4.2. The Boltzmannian Distribution.** The general theory of chemical reaction rates is associated with the reactivity of rarely occurring, highly energetic states. It seems improbable that electrochemical reactions in solution will differ radically from chemical reactions in solution so as not to involve states above the ground state.

Thus, if one thinks of a cathodic reaction, an electron of a given energy that is still in the electrode and seeking an equal energy state in an ion-solvent complex to which it can make a radiationless quantum mechanical transition, is confronted with energy states in the ion-solvent complex distributed according to Boltzmann's law. The probability of the availability of a state,  $E$ , above the ground state of the ion-solvent system is  $e^{-E/RT}$ . Thus the distribution law for electrons in solution seems to be solved by realizing that one means the electronic energy in the vibration rotation levels of ion-solvent bonds and, by applying Boltzmann's law, admitting that states above the ground state take part in electrode reactions. At first it seems that this would mean a distribution for (e.g.) the energy in an  $\text{H}_3\text{O}^+$  ion as shown in Fig. 9.4. This implies a maximum (and limiting) current density when the electrode potential brings the energy of electrons in the Fermi level (Section 9.2.1) up to that of the ground state of the entity that is to have acceptor states for electrons from the cathode. Such a diagram was first introduced by Gurney in 1931 (Fig. 9.4).

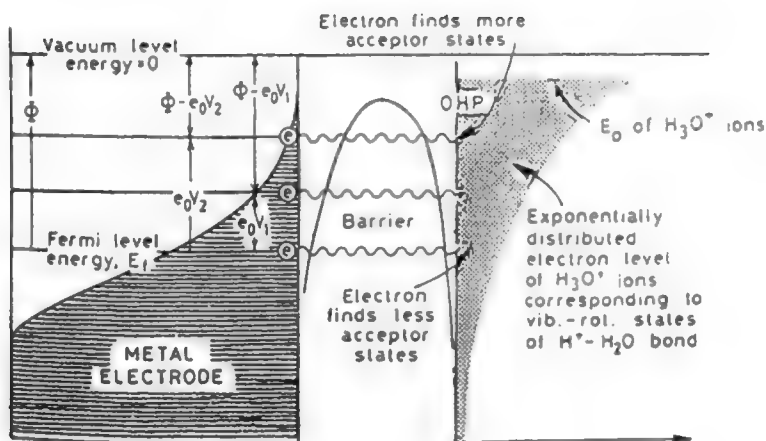


**Fig. 9.4.** Schematic diagram of the potential energy barrier at the interface. The electron energy levels and their distribution in the electrode and in the solution are shown. (Reprinted from J. O'M. Bockris and S. U. M. Khan, *Quantum Electrochemistry*, Plenum, 1979, p. 264.)

However, one must not blithely overthrow in its entirety one model for another. The argument introduced by Gerischer concerning the disturbance of the ground state due to collisions in solution still has some force. Thus the original portrayal of energy levels in solution by Gurney should be modified and the ground state judder caused by the energy of ion-solvent collisions taken into account. It follows that the number of molecules having the energy of the ground state will suffer some degree of "fuzziness," reflecting the decrease in definition of the exact energy associated with the state, owing to the collisional effects which in the Gaussian view were supposed to be the whole cause of the distribution of states in solution. Figure 9.5 shows the resulting distribution of electronic states in redox ions in solution as the shoelace curves of the Gaussian distribution.

An objection to consideration of vibrational states above the ground state (Levich, 1970) was that if such states were indeed involved in electron transfer, then there would be no smooth Tafel lines because as a change in overpotential altered the energy of the Fermi level (from which, e.g., cathodic electrons come), matching levels in the solution species would not be available until the next vibrational state, perhaps 1/2 eV away, was reached by the change in the electrode potential. Hence, in this picture, the

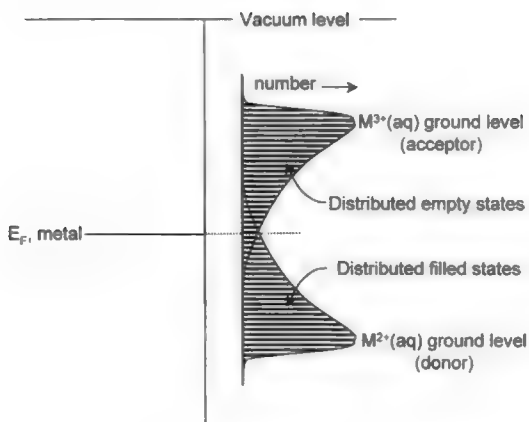


**Fig. 9.5.** Schematic representation of acceptor (empty) and donor (filled) electronic states of ions in solution. The states are distributed in solution according to the Maxwell-Boltzmann law. Fluctuations of all states (i.e., ground and other higher energy states) are considered to give rise to a continuum distribution (vibrational model). (Reprinted with permission from J. O'M. Bockris and S. U. M. Khan, *J. Phys. Chem.* **87**: 2599 copyright 1983 American Chemical Society.)

$\log i - \eta$  relation, instead of being linear would be stepped. However, such an argument is not applicable because the jiggling of the ion-solvent entities in solution smooths out the difference between the energy levels and makes energy states available according to the Boltzmann law, which deals here in practice with a continuum of energy states in the solution species.

## 9.2.5. The Distribution Function for Electrons in Metals

The probability of the occupancy of an energy state involving electrons in metals is found by considering the number of distinguishable arrangements of the total number of cells, reduced by the product of the number of arrangements of electrons with the same energy (which are therefore indistinguishable) and of empty cells (which are also indistinguishable). The number of cells will be greater than the number of electrons, and because each electron has the possibility of having either of two directions of spin in the ground state, there will be two cells for each electron. The final expression for the probability of occupancy of cells at any energy (of the electrons) turns out to be:

$$P_E = \frac{1}{(E - E_f)/e^{kT} + 1}$$

where  $E_f$  is an energy characteristic of the metal, varying from about 1 to about 5 eV. It is easy to see that (Fig. 9.6) at electron energies significantly less than  $E_f$ , the exponential in the denominator becomes negligible compared with unity, so that the

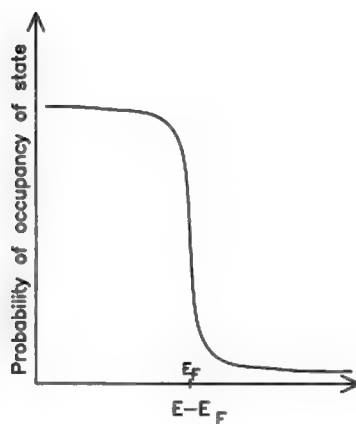


**Fig. 9.6.** The probability of the filling of states in a metal as a function of energy below or above the Fermi level.

probability of occupancy of the cells reaches a maximum ( $\approx 1$ ); that when  $E = E_f$ , the probability is that the occupancy of the states will be  $1/2$ , and that when  $E \gg E_f$ , the exponential term is much more than unity and

$$P_E \approx e^{(E-E_f)/kT}$$

Thus, one is back with Boltzmann's law.

How much more positive than  $E_f$  does the electron energy have to be for us to relax the Fermi–Dirac law and use the simpler Boltzmann expression? From

$$e^{(E-E_f)/kT} > 10$$

one finds  $E - E_f > 2.303$  (0.025) eV at 25 °C, i.e.,  $E$  has to be only  $2 kT$  eV above the Fermi level<sup>8</sup> for the Boltzmann approximation to be an acceptable approximation of Fermi's law for the probability of the occupancy of cells. How far from the Fermi level (probability of occupancy  $1/2$ ) does  $E$  have to fall for the probability of occupancy to rise to 90%? The answer is about  $2 kT$ .

These are important results for practical (and approximate!) electrochemical calculations. As far as the occupancy of electronic states *above* the Fermi level is concerned, it becomes negligible so quickly (recall that the practical electrochemical scale is a few electron volts), and the occupancy is so high *at* the Fermi level that electrochemists usually use the rule that the only metal electrons they should count are those at the Fermi level; they neglect electrons having energies below or above that of the Fermi level.

Neglecting the electrons below the Fermi level might at first cause some dismay. Do not states having energies less than  $E_f$  have a very high probability of being filled? The argument runs this way: that as one departs from the Fermi level toward lower energies, the electronic states are indeed tending to be full (i.e.,  $P_E \rightarrow 1$ ). But filled electronic states will not yield available electrons, for electrons there become immobilized as the levels fill and hence will not take part in a cathodic or anodic current.

Clearly, these statements are based on approximations and are roughly applicable at 25 °C. There is so much else to explore in fundamental electrode kinetics at this time that no one has given priority to finding out whether a closer approximation concerning the availability of electrons of energies near to, and particularly below, the Fermi level would be worth examining. It would certainly be necessary to seek a better approximation at temperatures well above 25 °C (e.g., at 1000 K). At energies significantly below 25 °C, the statements on the dominance of Fermi level electrons become increasingly applicable.

All this material about the Fermi–Dirac equation for the probability of filling of the electron states comes down in practice to one approximation: Electrons taking part in electrode processes are from the Fermi level and hence have the Fermi level energy.

<sup>8</sup>Thus,  $kT$  at 300 K is about 0.025 eV.

It is that which moves when the electrode potential changes. The practical usefulness of the approximation can be seen when one learns (Section 9.2.4) that electron transfer in quantum mechanical tunneling is radiationless. It also makes it clear why we should be interested in the distribution law for electronic states in solution. For, as the electrode potential changes, the Fermi level also changes<sup>9</sup> and hence the energy of the available electrons. The overlap of the energy of these Fermi-level electrons with those states having the same energies in solution depends then upon the shape of the distribution function for electronic energy states in solution.

### 9.2.6. The Density of States in Metals

The Fermi–Dirac distribution law gives the *probability of the occupancy* of states within a small energy range of  $E$  to  $E + dE$ . However, for kinetic calculations, it is necessary to know the number of electrons per unit volume which have energies between  $E$  and  $E + dE$ . This is certainly proportional to the Fermi–Dirac probability of occupancy of these states, but to convert to the number of electrons in the small energy interval,  $E$  and  $E + dE$ , one must multiply by the density of states ( $\rho_E$ ) having the energy  $E$  to  $E + dE$  whether they are occupied or not. This is given by

$$\rho_E = \frac{1}{2\pi^2} \left( \frac{2m_e}{\hbar^2} \right)^{3/2} E^{1/2}$$

where  $\hbar^2 = h/2\pi$  and  $m_e$  is the real mass of the electron.

The full Fermi–Dirac distribution law (as distinct from the Fermi–Dirac probability of occupancy expression) is therefore

$$\eta_{e,E \rightarrow E+dE} = \frac{1}{2\pi^2} \left( \frac{2m_e}{\hbar^2} \right)^{3/2} \frac{E^{1/2} dE}{\exp \left[ \frac{E - E_f}{kT} \right] + 1}$$

Both the density of states and the quantity  $\rho_E$  for  $E$  to  $E - dE$  (the full distribution law) are plotted in Fig. 9.7.

<sup>9</sup>Why does the energy of electrons *inside* a metal depend upon the electrical potential difference across its interface with the solution? The reason is that the energy of electrons at the Fermi level is equated to  $\bar{\mu}_e^M$  and this quantity is then equal to  $\mu_e^M$ , the chemical potential of electrons within the metal, which is independent of the electrode potential—together with  $\phi_M$ , the inner potential of the metal, which is a function of the electrode potential. Thus, looked at *from outside the electrode*, the Fermi level of the metal moves with potential because it is a function of the metal's inner potential.

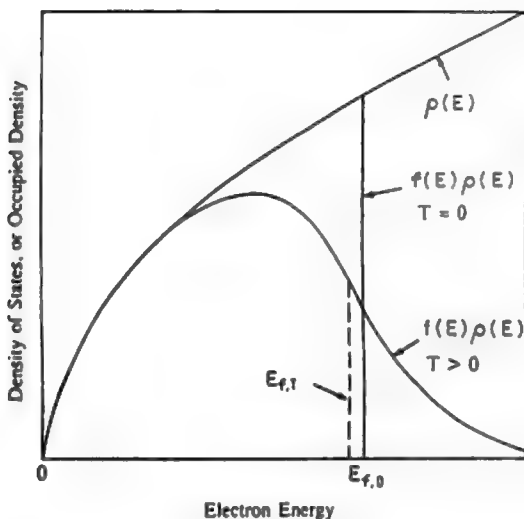


**Fig. 9.7.** The density of electronic states as a function of energy on the basis of the free electron model and the density of occupied states dictated by the Fermi–Dirac occupancy law. At a finite temperature, the Fermi energy moves very slightly below its position for  $T = 0$  K. The effect shown here is an exaggerated one; the curve in the figure for  $T > 0$  would with most metals require a temperature of thousands of degrees Kelvin. (Reprinted from J. O’M. Bockris and S. U. M. Khan, *Quantum Electrochemistry*, Plenum, 1979, p. 89.)

## Further Reading

1. H. Gerischer, *Z. Physikal. Chem.* **26**: 223 (1960). Absolute potential; Fermi level in solution.
2. P. Lohman, *Z. Naturforsch.* **A22**: 843 (1967). Calculation of the value of the absolute potential of the hydrogen electrode.
3. M. Ali Omar, *Elementary Solid State Physics*, Addison-Wesley, Reading, MA (1975). Fermi’s law, etc.
4. J. O’M. Bockris and S. U. M. Khan, *Appl. Phys. Lett.* **42**: 124 (1983). Fermi levels in solution.
5. S. U. M. Khan and J. O’M. Bockris, *J. Phys. Chem.* **87**: 2599 (1983). Electron transfer theory.

6. H. Reiss, *J. Phys. Chem.* **89**: 3783 (1985). Absolute potentials.
7. S. Trasatti, in *Trends in Interfacial Electrochemistry*, A. Fernando Silva, ed., Vol. 179, NATO ASI Series 179, Reidel, Dordrecht (1986). The potential of oriented water at a metal/solution interface.
8. J. O'M. Bockris and S. Argade, *J. Chem. Phys.* **49**: 5133 (1986). Calculation of the value for the absolute potential of the hydrogen electrode and of a Galvani potential.
9. S. U. M. Khan, R. Kainthla, and J.O'M. Bockris, *J. Phys. Chem.* **91**: 594 (1987). Absolute potentials.
10. J. Goodisman, *Electrochemistry: Theoretical Foundations*, Wiley, New York (1987).
11. A. M. Kuznetsov, *Charge Transfer in Physics, Chemistry and Biology*, Gordon and Breach, Luxembourg (1995). Broad treatment of many aspects of charge transfer; only two out of twenty chapters are directly electrochemical.
12. R. J. Dewayne Miller, G. McLendon, A. J. Nozik, W. Schmickler, and Frank Willig, *Surface Electron Transfer*, VCH Publishers, New York (1995). Advanced discussions.
13. W. Schmickler, *Interfacial Electrochemistry*, Oxford University Press, Oxford (1996). A brief summary.

## 9.3 POTENTIAL ENERGY SURFACES AND ELECTRODE KINETICS

### 9.3.1. Introduction

Most students have been exposed to an equation first suggested by Svante Arrhenius in Sweden, which indicates that the velocity of a chemical reaction climbs with an increase in temperature in an exponential way:

$$V_{\text{reac}} \propto e^{-E/RT}$$

where  $E$  is the energy of activation. The law led to an idea that has dominated the study of the mechanism of chemical reactions for more than a century: *Only sufficiently energized molecules react*. In the gas phase, it turns out that the fraction of collisions that lead to a chemical change is extraordinarily small, according to the reaction and temperature—between about  $10^{-5}$  and  $10^{-20}$  of the total number.

This theory, that only “hot” molecules react, is responsible for a diagram found in all physicochemical texts—the plot of the energy of some representative point in a reaction against a distance coordinate. Such curves (Fig. 9.8) are qualitatively uniform; going from left to right, one starts off with the reactant system having a certain energy. Then the energy climbs to a maximum value. That value diminished by the initial value of the energy of the system is the energy of activation, the energy necessary to make the vital step in the reaction occur; the distance coordinate corresponding to it indicates the location of the heart of the reaction, the representative point. Then the energy goes down (gets more negative) to a final value of the potential energy, that of the product system.



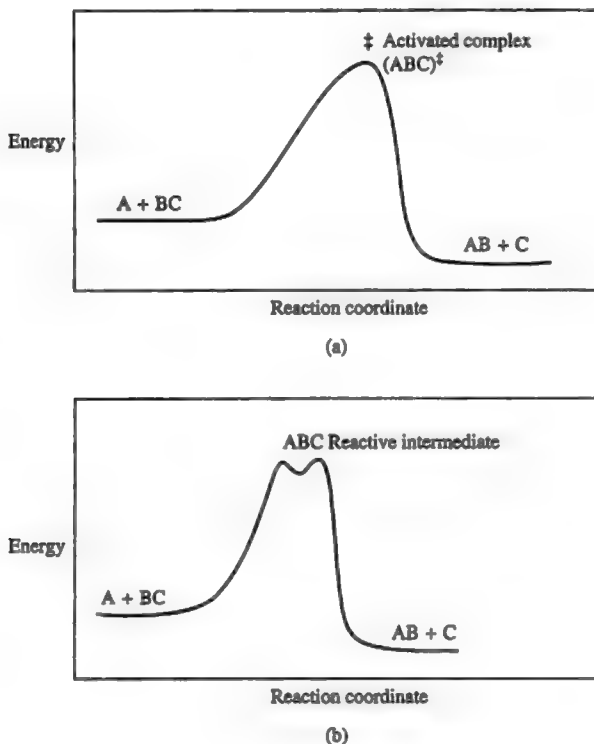
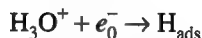


**Fig. 9.8.** Activated complex compared with a reactive intermediate. If there is a well at the intermediate state (with a depth greater than  $k_b T$ ), the intermediate is called a *reactive intermediate* rather than an *activated complex*. (Reprinted from J. Noggle, *Physical Chemistry*, 3rd ed., Benjamin Cummings, 1996, p. 536.)

The situation in electrochemistry is similar to that outlined above for chemistry. However, in the electrochemical case, there is also a component of electrical energy, the energy of an electrical charge,  $e_0^-$ , passing through a potential difference in the interphasial region, which contributes to the potential energy that makes up the energy–distance curves in chemical reactions. It turns out that the electrical energy contributes to a decrease or increase in the activation energy by about one half of the total electrical energy,  $e_0 \Delta\phi$ , of the interphasial region. This much has been understood since 1930 (Volmer and Erdey–Gruz). One sees that enlightenment came to the electrochemists who used such diagrams about a generation after Arrhenius' 1889 work, which provided the basis of the chemical diagrams in Fig. 9.8. By 1935, physical electrochemists could see potential–energy distance relations that looked quite similar to the good old energy of activation curves used by the physical chemists.

### 9.3.2. The Basic Potential Energy Diagram

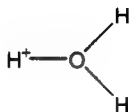
To illustrate a potential energy diagram in an electrochemical reaction, it is helpful to use as an example the proton-transfer reaction:



This reaction is about the simplest that involves intermediate radicals (adsorbed H atoms waiting to combine to form  $\text{H}_2$ ). A study of potential energy diagrams such as that described below can be used to comprehend why a change in the electrode potential changes the reaction rate, and thus to understand the basis of electrocatalysis.

The diagram can be made clear if one restricts it at first to a presentation of the reaction on *one* metal (e.g., mercury) and one electrode potential. Then the figure would look like Fig. 9.9.

The plot is of the potential energy of a representative point in the reaction and its variation with distance as the proton converts to an adsorbed H atom. There are two components in it. Component X is the potential energy–distance relation of the proton in the hydroxonium ion:



The  $\text{H}^+ - \text{O}$  bond here vibrates at around  $10^{14} \text{ s}^{-1}$  while the  $\text{H}_3\text{O}^+$  ion itself is for about  $10^{-8}$  to  $10^{-2} \text{ s}$  in contact with the electrode.<sup>10</sup> The potential energy curve, X, has a zero-point energy. If it were in the gas phase, it would manifest a number of distinguishable vibrational and rotational levels. Here they are smoothed out by the buffeting that the ion (being still a part of the solution) obtains from its nearest-neighbor particles. Thus, the proton can have any energy up to the crossing point at Z. The distribution law we have discussed (Section 9.2.4) will be effective, i.e., the chance of finding a proton  $\Delta E$  above the ground state is  $e^{-\Delta E/RT}$ .

The other (or Y) curve represents the variation with distance of the energy of the adsorbed H atom as it vibrates on the metal surface. This M–H bond waggles as well as stretches, but in Fig. 9.10 only the stretching away from and toward the electrode

<sup>10</sup>Such values are guestimates based on the rate constant for desorption,  $\nu e^{-E/RT}$ , so that the residence time is

$$1/\nu e^{E/RT} \sim 10^{-14} e^{E/RT} \text{ s.}$$

Now,  $E$ , the activation energy for the desorption of  $\text{H}_3\text{O}^+$  from various metals, will correspond to the weak bond formed in ion adsorption (Bockris and Gamboa, 1992). It is possible to find a range of  $E_a$  from 20–80  $\text{kJ mol}^{-1}$ . Such figures give a range for  $\tau_{\text{residence}}$  of  $10^{-8}$  to  $10^{-2} \text{ s}$ .

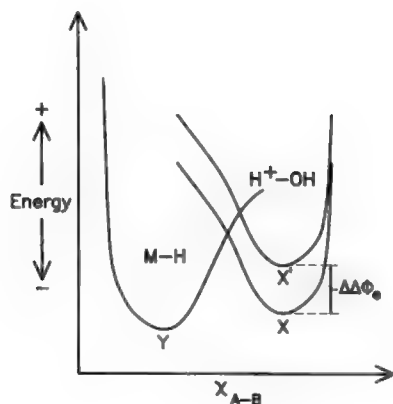
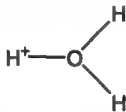


**Fig. 9.9.** The potential energy curves that make up a one-dimensional representation of the variation of energy of the molecules indicated. It represents the energy variation during a reaction. The Y curve shows the changes in energy of the atomic  $H^+$  metal bond on the electrode surface. The X curve is more complicated. As shown, it represents the variation in the energy as  $H^+-O$  as the  $H^+-O$  distance varies. However, what is not shown in the figure is that the X curve includes the energy of the electron in the metal. Hence, what is shown is at a fixed potential. If the potential varies, so would the vertical position of the X curve. Clearly, the presentation greatly simplifies reality. Thus, the M-H moiety is surrounded by water molecules that will change their position with potential and hence affect the energy of M-H by dipole-dipole interactions. The



moiety is really part of a solvated  $H_3O^+$  ion and will be affected in energy by the surrounding water molecules. These influences are neglected in the "bare bones" figure shown. The distance  $X_{A-B}$  applies either to M-H or  $H^+-O$ . Note that the effect of the electrical potential difference across the interface will be much more on the  $H^+$  ion than on the electric dipole, which is made up of the adsorbed M-H entity on the electrode surface.

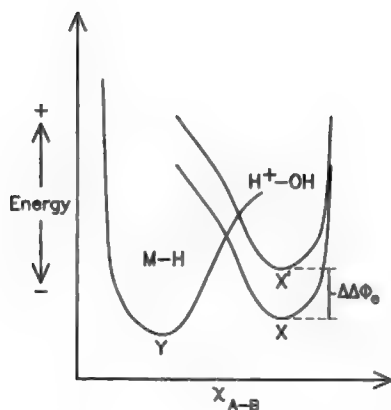
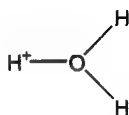


**Fig. 9.10.** This schematic shows three potential energy curves. One belongs to M-H, the potential energy variations during the vibrations of the adsorbed H. The two on the right of the schematic both represent the same thing, anharmonicity; i.e., the potential energy curves are no longer represented by  $U_k = kx^2$  because the oscillations of the O-H<sup>+</sup> bonds are only harmonic near the bottoms of the curves. The difference in the two curve bottoms and the two intersection points is that they are, respectively, the energies of activation for the reaction: (i) then no change of potential  $\Delta\Delta\phi$  is applied in (ii) (for the higher one) then the potential is changed by  $\Delta\Delta\phi$ . For simplicity of comprehension, portrayal of the zero-point energy in these potential energy curves has been left out. Also, the potential energy curves do not intersect sharply as shown, but are smoothed out so that the diagram represents two energy barriers at potentials differing by  $\Delta\Delta\phi_0$ .

is shown. There is here, also, a continuum of energy states, and there is a chance (greatly diminishing in probability with increasing energy) that the vibrating H in M–H on the electrode surface will be in any energy state up to those at the intersection of the curves. Note that the effect of the electrical potential difference across the interface will be much more on the  $\text{H}^+$  ion than on the electric dipole, which is made up of the adsorbed M–H entity on the electrode surface. The probability of the occupancy of states above the zero-point energy level in  $Y$  is given by a Boltzmann factor.

One has to choose a direction for the reaction and it will be the forward direction,  $\text{H}_3\text{O}^+ + e_0^- \rightarrow \text{MH}$ , from right to left in the diagram. Then, seen in slow motion, one observes that very very occasionally, the proton in one of the



vibrations (occurring at about  $10^{14} \text{ s}^{-1}$ ) will have an energy corresponding to that of  $Z$ .

The energy corresponding to  $Z$  must be such that the empty electron energy state, there would have the same energy as that of an electron in the Fermi level in the metal. A quantum mechanical transfer of an electron from the metal to  $\text{H}^+$  occurs if the transfer involves no change in energy, and so the conditions for that are reached at  $Z$  and there is a finite probability that the critical happening will occur and the proton will transfer to the curve  $Y$ , becoming thereby an adsorbed H atom. It is true that at  $Z$ , the H atom just produced will be “hot,” but after a short time (some  $10^{-8} \text{ s}$ ) it will adjust and take up the energy distribution of any other adsorbed H on the mercury surface.

This estimate of the lifetime of the excited state resulting from the charge transfer described here results from seeing a principal process in the deexcitation as the rotation of a water molecule (originally attached to the proton) away from the position in the first layer next to the electrode from which the proton transfer from  $\text{H}_3\text{O}^+$  occurred. The rotating rate of a free molecule is  $\sim 10^9 \text{ s}^{-1}$ , but in solution there will be a hindrance to such a motion by the tendency to re-form H bonds and become part of the water structure. There is some evidence that the potential energy barrier for hindered rotation in this situation is quite low, about  $6 \text{ kJ mol}^{-1}$ . Accepting this reduces the rotation rate to  $10^9 e^{-E/RT} = 10^9 e^{-6000/8.315.298}$  at room temperature  $\approx 10^8 \text{ s}^{-1}$ , i.e.,  $10^{-8} \text{ s}$ .

How are these potential energy curves constructed? That is not a question to be answered in detail in this book. However, let it be said that one needs knowledge of the quantum mechanics of chemical bond formation to do it. Owing partly to the work by Anderson (1990), there is software that enables one (in hours, not days) to calculate the potential energy quantities needed in particular for the M–H bond strengths at

various degrees of stretching. Quasi-quantitative calculations of curves such as those shown in Fig. 9.10 have been made since 1948 (Parsons). Similar diagrams can now be constructed for more complex electrode reactions, although as the type of molecule involved increases in complexity, the practicality of the computer calculation becomes limited by time and expense.

### 9.3.3. Electrode Potential and the Potential Energy Curves

How is the effect of electrode potential to be introduced into the potential energy diagrams? This can be done by realizing that in the reaction



one can regard the  $\text{H}_3\text{O}^+$  present in the solution in contact with the electrode, and the electron in the metal, as one state. Then, instead of the state " $\text{H}_3\text{O}$ " being calculated, along with its continuum of excited levels, it is possible to take into account also the energy of the electron ( $\text{H}_3\text{O}^+ + e_{\text{M}}$  is called *the initial state*) by adjusting the entire potential energy curve  $X$  up and down vertically, according to the change of energy contributed by the energy of the electron at the Fermi level of the metal. Thus, if the curve  $X$  is adjusted vertically upward (reflecting an increase in the electrochemical potential ( $\bar{\mu}_e^{\text{M}}$ ) of the electron in the metal, the potential energy of the initial state ( $\text{H}_3\text{O}^+ + e_{0(\text{M})}^-$ ) becomes less negative, by  $\Delta\phi e$ , and the state becomes less stable until the equal energy condition for transfer is met at point  $X$ .

At first sight one might think (Fig. 9.10) that the movement of the ground state,  $X$ , upwards is equaled by the movement of  $Z$  upward by the same amount, so that there would be no change in the energy of activation, which is the  $X$ - $Z$  vertical distance. However, while the ground state moves up by the energy  $\Delta\phi e_0$  when the potential is changed by  $\Delta\phi$ , the intersection point  $Z$  moves up a lesser amount by a factor called  $\beta$  because it meets curve  $Y$  at an angle.

Thus, if the ground state of the initial state (made up by  $\text{H}_3\text{O}^+ + e_0^-$ ) moves up more than  $Z$  does, the energy of activation for proton transfer gets less. Since the reaction velocity is proportional to  $e^{-\Delta E/RT}$ , making the potential of the electrode more negative (the energy less negative) makes the reaction go faster.

**9.3.3.1. A Simple Picture of the Symmetry Factor.** In order to employ simple geometry, one now ignores the curvature of the Morse curves and considers that the potential energy barrier near the intersection point is made up of straight lines (Fig. 9.11). This simplifying analogue of the barrier is useful for a first-base discussion of the symmetry factor  $\beta$ .

At the outset, recall how the symmetry factor was introduced (Section 8.2.4). The charge-transfer reaction was roughly pictured as the jump of an electron acceptor toward the electrode during which, somewhere en route, an electron jumped to the particle and completed its job of electro-nation. Representing the energy of the system

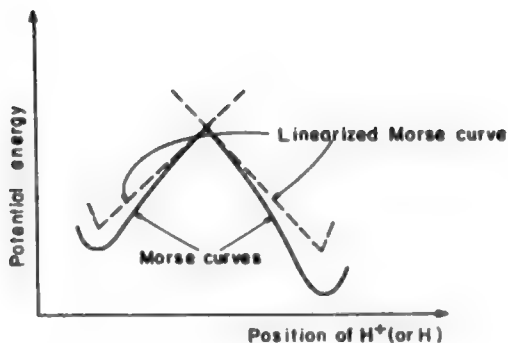


**Fig. 9.11.** For the sake of simplicity, the Morse curves can be linearized, and the model thus obtained can be considered sufficiently real for general (if approximate) considerations.

by a point on an energy–distance curve, the progress of the jump could be charted by the movement of the representative point across a potential energy barrier. Once the point climbed to the top of the barrier (the activated state), the rest of the jump was assured (automatic). But this climb to the peak (or activation) requires some work to be done. The chemical work is done by or on the ion in climbing the barrier in the presence of the electric field at the interface than without it. The question is: How is the extra electrical work of activation to be computed?

The first approach (Section 8.2.4) at this computation ran along the following lines: The electrical work of activation arises because in the activation process charges have to be moved through the difference of potential between the initial and activated states, i.e., from  $x_1 + x_2$  to  $x_1$  in Fig. 8.17. It was necessary, therefore, to know what fraction of the total jump distance is the distance between the initial state and the barrier peak. This distance ratio was defined as the symmetry factor  $\beta$ , i.e.,

$$\beta = \frac{\text{Distance along reaction coordinate between initial and activated states}}{\text{Distance along reaction coordinate between initial and final states}}$$

The essential point that emerges from this first discussion of  $\beta$  is that only a fraction of the potential difference across the double layer, not the whole potential difference, is operative on the reaction. That there is a fraction  $\beta$  becomes clear; what the fraction is remains a problem as long as the barrier shape is not known. This point of view must only be considered as the first murmuring of a theory of  $\beta$ , the symmetry factor.

A different (second) approach may be adopted. The main point in this new approach is that the value of  $\beta$  will be shown to depend on the *relative slopes of the potential energy–distance curves* representing the energies of the particles (rather than

the position of the summit of the potential energy barrier within the path of the ion in its jump from double layer to electrode [Section 8.2.4]).

Suppose that a potential difference  $\Delta\phi$  is applied across the interface. How does this affect the barrier obtained if one linearizes the Morse curves for the electrodic reaction



The curve (or rather its linearized version) for the stretching of the M-H bond in the system  $\text{M-H} + \text{H}_2\text{O}$  will not be influenced by the field because the particles M-H and  $\text{H}_2\text{O}$  are not charged.

The effect of the electric field on the linear curve for the stretching of the H-OH bond in the system  $\text{M(e)} + \text{H}^+ - \text{OH}_2$  has to be thought about now. When the potential difference across the interface is changed (from 0 to  $\phi$ ), the energy of the  $\text{H}^+ - \text{OH}_2$  part of the system suffers little change, but the energy of the electron in the metal [and thus the energy of the left-hand side of (9.11)] is altered by an amount that is easily calculable. The change in electron energy is equal to the change in potential times the electronic charge. Hence the total change in energy of the initial state (the electron in the metal and  $\text{H}^+ - \text{OH}_2$  at the OHP) is  $e_0\Delta\phi$  per system, or  $F\Delta\phi$  per mole of systems  $\text{M(e)} + \text{H}^+ - \text{H}_2\text{O}$ . What this implies is that the linear version of the Morse curve for  $\text{H}^+ - \text{OH}_2$  stretching in the system  $\text{M(e)} + \text{H}^+ - \text{H}_2\text{O}$  is *shifted vertically* through an energy  $F\Delta\phi$  (Fig. 9.12).

The vertical shift has arisen from the application of an absolute potential difference of  $\Delta\phi$  to a hypothetical interface, initially with zero potential difference across it, i.e.,  $\Delta\phi = 0$ . But the argument is valid for any change of potential across the interface. Thus, if the double-layer potential is initially  $\Delta\phi_e$  (i.e., the interface is at equilibrium) and then the potential is change to  $\Delta\phi$ , the Morse curve for the initial state is shifted vertically through an energy  $F(\Delta\phi - \Delta\phi_e)$ , or  $F\eta$ .

As a consequence of the vertical shift of one linear curve, the critical activation energy for the reaction (the main factor upon which its rate depends) is altered from  $E_e^*$  at equilibrium (i.e.,  $AF$  in Fig. 9.13) to  $E_\eta^*$  the overpotential  $\eta$  (i.e.,  $HD$  of Fig. 9.13). *The difference  $\Delta E^*$  between the two activation energies has resulted from the electrical energy  $F\eta$  that has been introduced into the reaction.* What is the relationship between  $\Delta E^*$  and  $F\eta$ ? The change  $\Delta E^*$  in activation energy decides the net current output; the  $F\eta$  is the input electrical energy channeled into the interface. One seeks to know how much the activation energy decreased for the given energy input  $F\eta$ .

In terms of the linear analogue, the question is answered by a trivial exercise in geometry (see Fig. 9.13). One has

$$AB = FE = \frac{E_e^*}{\tan \gamma} [\text{from } \triangle AEF] \quad \text{and} \quad AB = \frac{GE - E_e^*}{\tan \theta} [\text{from } \triangle ABG]$$

and therefore,



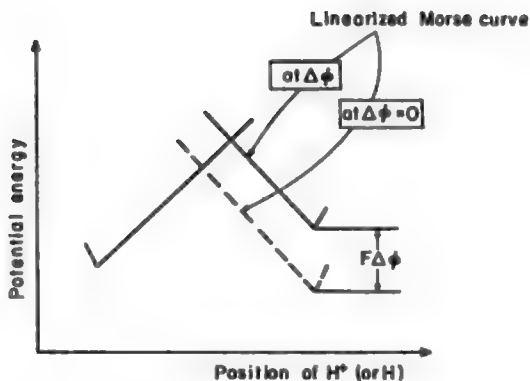


**Fig. 9.12.** When the potential difference across the interface is changed from zero to a value  $\Delta\phi$ , the Morse curve of the initial state is shifted vertically by the amount of electrical energy  $F\Delta\phi$ .

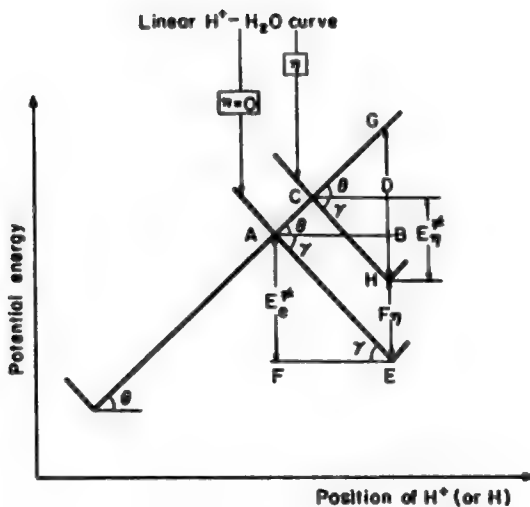


**Fig. 9.13.** As a consequence of the vertical shift of one linear curve, the critical activation energy is altered.

$$E_e^\ddagger = \frac{\tan \gamma}{\tan \theta} (GE - E_e^\ddagger) \quad (9.12)$$

Further,

$$CD = \frac{E_\eta^\ddagger}{\tan \gamma} [\text{from } \triangle CDH] \quad \text{and} \quad CD = \frac{GH - E_\eta^\ddagger}{\tan \theta} [\text{from } \triangle CDG]$$

Hence,

$$E_\eta^\ddagger = \frac{\tan \gamma}{\tan \theta} (GH - E_\eta^\ddagger) \quad (9.13)$$

By making use of Eqs. (9.12) and (9.13), it follows that a change in activation energy

$$\begin{aligned} \Delta E^\ddagger &= E_e^\ddagger - E_\eta^\ddagger \\ &= \frac{\tan \gamma}{\tan \theta} (GE - GH) - (E_e^\ddagger - E_\eta^\ddagger) \\ &= \frac{\tan \gamma}{\tan \theta} (F\eta - \Delta E^\ddagger) \end{aligned}$$

or

$$\Delta E^\ddagger = \left( \frac{\tan \gamma}{\tan \gamma + \tan \theta} \right) F\eta \quad (9.14)$$

This is a basic result. The change in activation energy due to a change the electric field in the double layer has been computed. It depends on the input electric energy  $F\eta$  and a trigonometric function which cannot exceed unity. This fraction determines how much of the input electric energy fed into the interface goes toward affecting the activation energy and therefore the net rate of the reaction. The fraction has the basic characteristics of the symmetry factor, with which it will be identified.

Thus, it has been shown, by linearizing Morse curves, that (Fig. 9.13):

$$\beta = \frac{\text{Change of activation energy, } \Delta E^\ddagger}{\text{Change of electrical energy, } F\eta} = \frac{\tan \gamma}{\tan \theta + \tan \gamma} \quad (9.15)$$

One had proceeded previously (in the derivation of the Butler–Volmer equation, Section 7.2.3) on the basis that  $\Delta E^\ddagger = \beta F\eta$ , and it is fair to ask: What new knowledge has emerged? The symmetry factor has now been given in terms of the slopes ( $\tan \gamma$  and  $\tan \theta$ ) of the linearized Morse curves, and these slopes are related to those

*molecular* quantities (e.g., force constants of the molecular bonds involved) which determine the shape and surfaces of potential energy–distance relations (linearized for simplicity).

The symmetry factor  $\beta$  is obviously a central entity in electrodics and a fundamental quantity in the theoretical treatment of charge transfer at surfaces, particularly in relating electrode kinetics to solid-state physics.

**9.3.3.2. Is the  $\beta$  in the Butler–Volmer Equation Independent of Overpotential?** In order to consider the influence of the current-producing current-produced) overpotential  $\eta$  on the activation energy, the Morse curves used to synthesize the potential-energy barrier were linearized, and one linear curve was shifted vertically through an energy  $F\eta$ . During the shift brought about by a change in interfacial potential difference, the slopes  $\tan \gamma$  and  $\tan \theta$  of the linear curves were maintained constant (Fig. 9.130). On this approximate basis, the symmetry factor, which is a function only of the slopes  $\gamma$  and  $\theta$  of the linear curves, appears to remain constant during a change in potential.

Is this result a feature of barriers at interfaces or merely a consequence of shifting a *linear* curve? It is clear that once a linear curve is displaced vertically, it cannot but yield a *parallel* shift of the curve and therefore a constant  $\beta$ . The apparent constancy of  $\beta$  with potential is a result of the linearization of the potential energy–distance curves.

A glance at Fig. 9.14 shows, however, that, when the activation energy at equilibrium,  $E_e^\ddagger$ , is large, i.e., for electrode reactions of low exchange-current density  $i_0$  [cf. Eq. (7.21)], the slopes of the linear curves and, hence,  $\beta$  do not change significantly with overpotential. Such changes in  $\beta$  become likely only for reactions which have very low equilibrium activation energies (i.e., very high  $i_0$ 's). One can take it, therefore, that, for all but very fast electrode reactions, the symmetry factor  $\beta$  will be independent of overpotential  $\eta$  over a reasonably large (e.g., hundreds of millivolts) range of potentials. At sufficiently high overpotentials, the curves will be changed in relative position sufficiently that they will begin to intersect at positions of differing curvature (real, rather than idealized, potential energy curves tend to decrease in slope near their minima). As soon as the curvature of one of the potential energy–distance curves at the point of intersection begins to change compared with that of the other curve,  $\beta$  begins to change (see Eq. A1 in the appendix).

### 9.3.4. How Bonding of Surface Radicals to the Electrode Produces Electrocatalysis

Curve Y (Fig. 9.10) has been shown to have within it the explanation of why a change in potential affects reaction rates in electrochemistry. Curve X will now be shown to manifest, in a very elementary and simple way, one aspect of electrocatalysis.

Thus, in a thought experiment, let it be supposed (Fig. 9.15) that one could change at will the substrate metal onto which protons are discharged. One might think that the

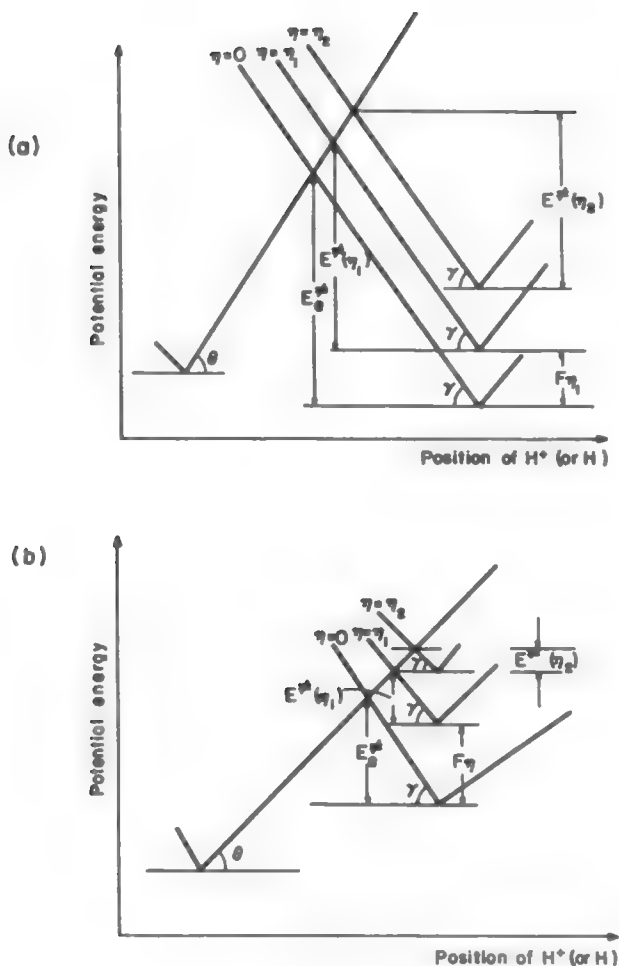


**Fig. 9.14.** The influence of overpotential on the symmetry factor  $\beta$ : (a) reaction of low  $i_0$ ;  $\beta$  independent of  $\eta$ ; (b) reaction of high  $i_0$ ;  $\beta$  dependent on  $\eta$ , tending to zero in the limit of high  $\eta$ .

electrode material could be changed from, say, mercury to, say, nickel. Then, in Fig. 9.15 the fact that the bond strength of H to Ni has a larger value (the H atom is bound more deeply) than that of H on Hg produces the change seen in the figure. One can see that now the energy of activation for proton discharge on Ni (and assuming the overpotential and all other factors influencing the reaction remain the same) is less than that on Hg. But if that is so, the velocity of the proton discharge reaction on Ni will be greater than that on Hg, i.e., electrocatalysis has occurred as one changes the

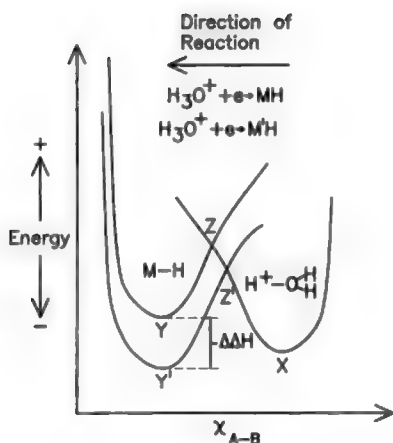
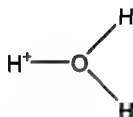
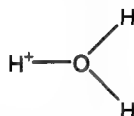


**Fig. 9.15.** This schematic is subject to the same reservations as that in Figs. 9.9 and 9.10. It shows the potential energy variation during the vibration of M-H and



It is as though M-H and



were isolated entities. In fact, they are influenced by their surroundings. Nevertheless, they have a heuristic purpose. They clearly show the essence of what is happening; the  $\text{H}^+$  is activated and reacts to form H adsorbed on M.

This particular schematic illustrates the rudiments of electrocatalysis. If the proton discharge reaction is rate determining, the energy of activation for one potential is influenced by the intersection point, 2. In fact, the energy of activation of the reaction is the vertical distance X to Z. This is valid for the electrode material M. But when M changes to  $\text{M}_-$ , the energy of adsorption of H on M changes by  $\Delta\Delta H$  for adsorption on  $\text{M}_-$ . At first sight, one might think that the activation energy is changed to  $\Delta\Delta H$ . However, the intersection point moves also, but only by  $\beta\Delta\Delta H$  ( $0 < \beta < 1$ ). Hence the change in activation energy is  $(1 - \beta)\Delta\Delta H$ . As the activation energy is lowered, the rate of reaction increases: electrocatalysis.

electrode surfaces from the weakly bonded Hg to the more strongly bonded Ni (Horiuti and Polanyi, 1935).

### 9.3.5. Harmonic and Anharmonic Curves

In the preceding sections, several potential energy curves associated with electrode reactions have been presented. Their purpose is heuristic and they are therefore schematic in nature. Nevertheless, they resemble carefully calculated curves in which molecular dynamics and computer software have been used to obtain the potential energy curves at the various displacements from equilibrium (Rose and Benjamin, 1996; Xia and Berkowitz, 1997) (Fig. 9.16).

It can be seen at once that no simple relation (in particular not  $U_x = kx^2$ , a simple harmonic relation) can represent these potential energy–distance relations. As known since the 1930s, from gas phase spectroscopy, curves with the appearances of those shown in Figs. 9.15 and 9.16 can be represented in form by an empirical relation, the Morse equation:

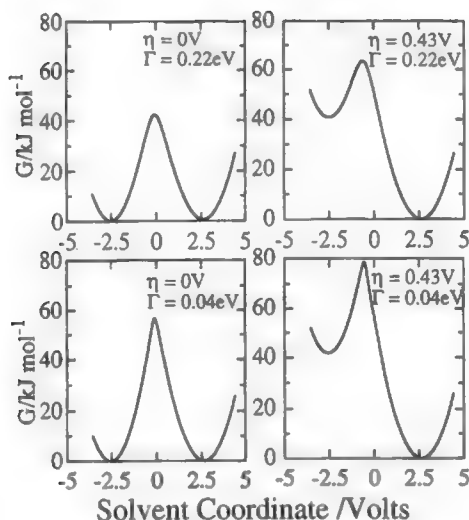


**Fig. 9.16.** Adiabatic free energy curves for the electron-transfer reaction for  $\text{Fe}^{3+} + \text{e}^- \leftrightarrow \text{Fe}^{2+}$  for an overpotential  $\eta$  and electronic coupling coefficient,  $\Gamma$ . (Reprinted from I. Benjamin and D. A. Rose, *J. Chem. Phys.* **100**: 3545, 1994 with permission of the American Institute of Physics.)

$$U_V = -D_e(1 - e^{-a(r-r_e)})^2 \quad (9.16)$$

where  $D_e$  is the dissociation energy in a hypothetical A–B bond,  $r_e$  is the equilibrium distance of A–B,  $r$  is any distance reached in the oscillation of the bond, and  $a$  is a constant of the system. Insofar as a relation established in gas phase spectroscopy can be used to represent energy changes in solution, and recalling the limitations of a one-dimensional presentation, the Morse equation represents features of the type of  $U_x - x$  relation that eventually controls the velocity of electrode reactions.

However, it is of interest to use the Taylor–MacClaurin expansion procedure on the Morse equation and see what happens if one takes  $a(r - r_e)$  as  $\ll 1$ . One obtains at once:

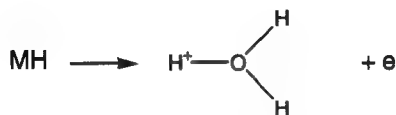
$$U_x = -D_e a(r - r_e)^2$$

a relation, then, which is harmonic, i.e., has the form  $U_x = -kx^2$ , where  $x$  is the distance the oscillator has been displaced from its position at equilibrium.

Hence, and this will soon turn out to be rivetingly important in obtaining consistency with well-known electrode kinetic laws, only for a low overpotential (in practice until about 0.2 V) is the potential energy–distance relation to be taken as harmonic. At greater potentials, *it does not have a harmonic shape* and theories that retain the idea of a harmonic energy–distance relation will give results (e.g., curved Tafel lines) inconsistent with the behavior of electrochemical reactions. Electrode kinetics wrongly based on harmonic potential energy curves even predict that the current density maximizes at a certain overpotential, a result not observed in more than 50 years of experimentation on the rate–overpotential relation called Tafel's law (Section 9.6.4).

### 9.3.6. How Many Dimensions?

The potential energy curves shown in Figs. 9.15–9.17 are one-dimensional relations. They show the variation of the energy of the systems as the representative point goes orthogonally to and from the electrode. In a reaction such as



or its converse, this seems to be quite a fair approximation, simple to understand, and not very far from reality. However, one does not have to seek much further in electrode reactions to understand that the movement of the molecules in the formation of the activated state at electrodes involves several directions. This need to calculate in more

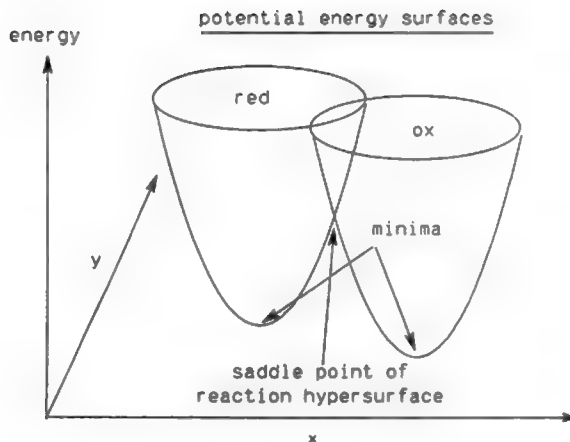


**Fig. 9.17.** Schematic diagram of the potential energy surfaces for an electron transfer reaction; the generalized coordinates  $x$  and  $y$  correspond to inner and outer sphere modes, respectively. (Reprinted from R. J. D. Miller, G. L. McLendon, A. J. Nozik, W. Schnickie, and F. Willig, *Surface Electron Transfer Processes*, p. 58, copyright © 1995 VCH-Wiley. Reprinted by permission of John Wiley & Sons, Inc.)

than the one direction does not strain our resources very much today, but showing the results in a diagram is not so easy. Thus, in Fig. 9.17 a *two-dimensional* diagram is shown.

As the reaction becomes more complex, the potential energy relations representing it will be expressed in *several* dimensions. Even a reaction such as  $\text{O}_2 + \text{H}^+ + \text{e} \rightarrow \text{OH}_{\text{ads}} + \text{O}_{\text{ads}}$  needs six dimensions. However, the technique for calculating such relations will be left to the reading list (e.g., Bockris and Sidik, 1998).

## 9.4. TUNNELING

### 9.4.1. The Idea

In classical mechanics, a particle, the energy of which is  $U_{\text{M}}$  below the top of an energy well, cannot escape from its well unless it possesses a kinetic energy greater than  $U_{\text{M}}$ . Thus, in particular, the particles that make up atomic nuclei should be particularly stable because they are buried in energy wells that are much deeper than any known in normal chemistry. However, in contradiction to this conclusion from classical mechanics, a number of discoveries were made (1903–1908) which showed



that particles (later found to be electrons and helium nuclei) do escape spontaneously from the nuclei of some heavy atoms.

As mentioned earlier, it was Condon and Gurney (1929) who solved the problem of how they do it, by a remarkable application of quantum mechanical concepts which were at the time quite new. Thus, according to the very original (and seminal) suggestion of de Broglie (1924), all particles are “accompanied” by a wave. Condon and Gurney saw the possibility that the *wave* might penetrate the energy barrier, just as in an analogy a ray of light penetrates a semitransparent layer. But in de Broglie’s model, the wave is accompanied by its particle. Thus, the particle also must “penetrate” the barrier; hence the name “tunneling.”

Quantum mechanical tunneling is a fertile idea with many applications in chemistry. It will be seen that in practice calculations using its concepts make a significant difference with very light particles, e.g., electrons and (to a much lesser degree) protons. But these are exactly the particles that hold center stage in interfacial electrochemistry. Indeed, without quantum mechanical tunneling, no electric currents across interfaces could occur.<sup>11</sup>

## 9.4.2. Equations of Tunneling

Consider the one-dimensional rectangular potential energy barrier shown in Fig. 9.18. Then, considering the potential energy of the particle  $U(x) = 0$ .

$$\begin{aligned} U(x) &= 0, & x < 0 & & \text{in region I} \\ U(x) &= U_0, & 0 < x < a & & \text{in region II} \\ U(x) &= 0, & x > a & & \text{in region III} \end{aligned} \tag{9.17}$$

If the total energy of a particle is less than  $U_0$ , then classical mechanics denies passage of the particle from region I to the other side of the barrier at region III. Indeed, in the classical view, the particle is like a ball that someone is trying to throw over a wall, but the person does not have the strength to throw it high enough for passage.

The Schrödinger wave equation for a particle in the potential energy regions I and III can be written as

$$-\frac{\hbar^2}{2m} \frac{d^2\psi(x)}{dx^2} = E\psi(x)$$

for in I and III the particle has zero potential energy.

In region II, however, the particle is taken as having some potential energy  $U_0$ . Then, for this region,

<sup>11</sup>The fact is that the calculated rate of electrochemical reactions over (and not through) energy barriers is far too low to be compared with the orders of magnitude observed in experiments.

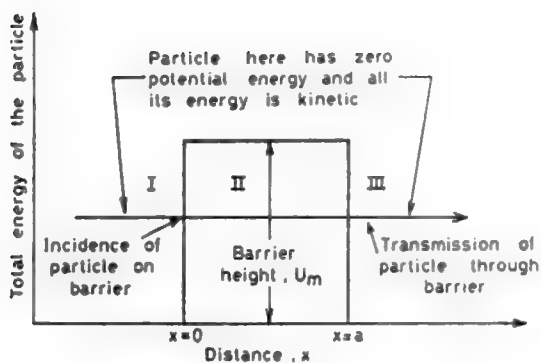


**Fig. 9.18.** A schematic diagram of a rectangular potential energy barrier for a tunneling particle. In regions I and III, the particle has a total energy equal to kinetic energy. In region II, the particle experiences a potential energy barrier of height  $U_m$  and width  $a$ . Within the barrier, the potential energy is constant. (Reprinted from J. O'M. Bockris and S. U. M. Khan, *Quantum Electrochemistry*, Plenum, 1979, p. 236.)

$$\frac{\hbar^2}{2m} \frac{d^2\psi(x)}{dx^2} = (U_0 - E)\psi(x) \text{ for } E < U_0$$

Now, in regions I and II, the particle is “free” in the sense that it has only kinetic energy (though not enough to top the barrier). For these two regions, the solution of Schrödinger’s equation is

$$\psi_I(x) = A \exp(ik_1x) + B \exp(-ik_1x) \quad \text{in region I} \quad (9.18)$$

$$\psi_{III}(x) = C \exp(ik_1x) + D \exp(-ik_1x) \quad \text{in region III} \quad (9.19)$$

where

$$k_1 = (2mE/\hbar^2)^{1/2} \quad (9.20)$$

is the wave number of the particle in terms of its energy  $E$  and mass  $m$ . The two terms,  $\exp(ik_1x)$  and  $\exp(-ik_1x)$  of Eqs. (9.18) and (9.19) describe an incident particle that moves from left to right and right to left, respectively.

In region II, the Schrödinger equation for  $E < U_0$  has the solution:

$$\Psi_{\text{III}}(x) = F \exp(+k_2 x) + G \exp(-k_2 x) \quad (9.21)$$

where

$$k_2 = \left[ \frac{2m(U_0 - E)}{\hbar^2} \right]^{1/2} \quad (9.22)$$

Inspection of the equation for  $\Psi_{\text{II}}$  and  $\Psi_{\text{III}}$  show that there is a finite probability amplitude that the particle will be found in regions II and III, although classically this is not possible. The passage through to region III is called *tunneling*. Furthermore, because the de Broglie wave passes through the barrier without a change in frequency, the accompanying particle has the same energy after passage through the barrier as it had before.

### 9.4.3. The WKB Approximation

In Fig. 9.19, a sample rectangular barrier is shown and the solution to the Schrödinger equation given above depends on the independence of the potential energy with distance in the barrier. This is an unrealistic approximation if the aim is to represent the real energy barrier in a chemical situation where the sides of the barrier slope and the top is curved. For a more realistic model, the mathematical solutions become heavy going. Wentzel, Kramer, and Brillouin (WKB) suggested some approximations to treat such cases. On the basis of this work, Gamow (1928) obtained an equation for the probability of tunneling through a barrier that is reasonably simple and which, for a parabolic barrier (nearer to the real barrier in chemistry), comes to

$$P_T = \exp \left( -2 \int_a^b \left\{ \frac{8\pi^2 m}{h^2} [U(x) - E] \right\}^{1/2} dx \right)$$



**Fig. 9.19.** A rectangular potential barrier. (Reprinted from J. O'M. Bockris and S. U. M. Khan, *Quantum Electrochemistry*, Plenum, 1979, p. 251.)

$$\begin{aligned}
&= \exp \left\{ -2 \left( \frac{8\pi^2 m}{h^2} \right)^{1/2} \int_{-a}^a [U(x) - E]^{1/2} dx \right\} \\
&= \exp \left[ -\frac{4\pi}{h} (2m)^{1/2} \frac{\pi}{2} a (U_0 - E)^{1/2} \right] \\
&= \exp \left\{ -\frac{4\pi^2}{h} \frac{2a}{4} [2m(U_0 - E)]^{1/2} \right\} \\
&= \exp \left\{ -\frac{\pi^2 l}{h} [2m(U_0 - E)]^{1/2} \right\} \tag{9.23}
\end{aligned}$$

where  $l = 2a$  is the width of the barrier and  $U_0$  is the barrier maximum (Fig. 9.20).

The corresponding equation for a rectangular barrier is

$$P_T = \exp \left( \frac{-4\pi l}{h} [2m(U_0 - E)]^{1/2} \right) \tag{9.24}$$

and seems to be somewhat surprisingly more used than Eq. (9.23).

Inspection of Gamow's equation shows that the probability of tunneling through a barrier decreases exponentially as the potential energy, mass of the particle tunneling, and distance to be tunneled increase. Using typical values for chemical reactions ( $U_0$  1–5 eV), one finds that chemical barriers can be significantly penetrated by electrons, even if the path length (as in some biochemical situations) is up to 20 Å.

The only other particles that appear to tunnel atomic distances with chemical energies are hydrogen and its isotopes, deuterium and tritium. Because these particles

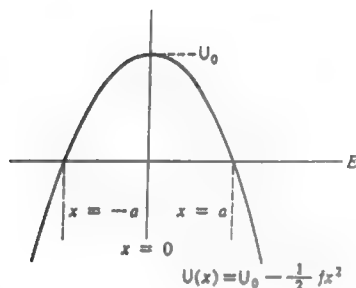


**Fig. 9.20.** The parabolic potential barrier. (Reprinted from J. O'M. Bockris and S. U. M. Khan, *Quantum Electrochemistry*, Plenum, 1979, p. 250.)

are more than 1000 times heavier than the electron, the probability of their tunneling will be very much less than that of the electron. Nevertheless, for distances of 1–2 Å, some degree of barrier penetration by these particles can occur. It is important because one knows the relative masses of the three isotopes, while Gamow's equation gives a prediction of the relative states of barrier penetration (e.g., at an electrode). The interpretation of the relative rates in the evolution of H and its two isotopes can sometimes provide information that leads to a differentiation among mechanisms of the interfacial reaction that is occurring (Srinivasan and Matthews, 1965).

#### 9.4.4. The Need for Receiver States

There is an important condition that greatly influences the numerical answer obtained in a tunneling calculation. Thus, the Gamow equation cited earlier [Eq. (9.24)] for the tunneling probability has within it the assumption that the reaction is radiationless, i.e., that the *final* state for the electron after tunneling has the same energy as that of the electron before the tunneling started. This condition is tacitly assumed in Gamow's equation, but it has to be actualized in a calculation of a real situation by multiplying it by the probability of finding a receiver state of the same energy in the solution. This is the consequence of the rule that the tunneling is radiationless. Thus, if one is considering electron transfer to  $\text{H}_3\text{O}^+$ , and the Fermi energy in the metal is  $E_F$ , then what is of interest for the calculation is not only the probability of penetrating through the barrier (assuming that the probability of finding a receiver state is unity), but also the probability of finding energy states of  $E_F \pm dE_F$  in an excited  $\text{H}^+ - \text{O}$  particle bound in an  $\text{H}_3\text{O}^+$  adsorbed at an electrode.

#### 9.4.5. Other Approaches to Quantum Transitions and Some Problems

In general, transitions in chemistry are treated in terms of quantal concepts. However, according to the correspondence principle, quantal calculations of vibration approximate classical ones when  $\hbar\omega/kT \ll 1$ , where  $\omega/2\pi$  is the frequency (e.g., of a vibration) involved. Now, most of the vibrations between ions in complexes in solution or ions and water molecules in hydration sheaths do not obey this criterion and so should be treated quantally. It must be admitted that at the century's end, realistic *ab initio* calculations in chemistry were still difficult to make and some examples exist in the literature in which unwarranted use of classical approximations has been made (Kuznetsov, 1990).

Another example in which the attraction of ease of mathematical handling has involved authors in unrealistic steps<sup>12</sup> concerns the assumption that oscillators met

<sup>12</sup>A pessimistic Taoist saying runs: "Those who speak don't know and those who know, don't speak." This reminds one that most physical electrochemists don't know much quantum mechanics and most quantum mechanics don't know much (of the facts of) electrochemical kinetics. So, neither kind of specialist should speak until much more of the other's discipline has been learned. Then, presumably, they would know, but—following the Taoists' wisdom—not speak!

with in electrochemical systems are all executing simple harmonic motion, i.e., that their energy can be represented by  $U_x = kx^2$ , where  $x$  is the displacement above the ground state. As mentioned in Section 9.3.5, such assumptions are valid only for energies up to about 0.2 eV from equilibrium. Treating an electrochemical reaction over the range of overpotential that exists in the literature ( $\sim 1$  eV) involves accounting for anharmonicity. This involves a heavier mathematical burden than most authors have wished to undertake. However, the harmonic approximation does not lead to equations consistent with Tafel's law.

A third matter to mention here is that the WKB approximation outlined above is limited in the realm in which it is valid. It is more applicable to protons than to electrons (Bockris and Sen, 1973). Other quantum mechanical methods of a quite different nature can be used<sup>13</sup> (D. Miller, 1995) and have been applied to make numerical quantal calculations of the rate of redox reactions (Khan, Wright, and Bockris, 1977; Newton, 1986), but they depend on a knowledge of wave functions which, for electron levels in hydrated ions in solution, may still be too primitive for calculations of rate.

#### 9.4.6. Tunneling Through Adsorbed Layers at Electrodes and in Biological Systems

A lively subsection in applications of quantum theory to transitions at electrodes concerns the tunneling of electrons through oxide films. This work has been led by Schmickler (1980, 1996), who has used a quantum mechanical approach known as resonance tunneling to explain the unexpected curvature of Tafel lines for electron transfer through oxide-covered electrodes (Fig. 9.21).

The basic idea of resonance tunneling relies on the reasonable assumption that there are impurity states in the oxide film (regarded as a semiconductor), the energy of which is in resonance with that of electrons in the metal on which the film has been formed. One considers the situation in terms of two coordinated tunnel transfers, one from the metal to the impurity state and then from the impurity state to an ion adsorbed at the oxide/solution interface.

Much use has also been made of tunneling concepts in work on electron transfer from electrode to enzymes in solution, some of which adsorb on the electrode (Tarasevich, 1983). Most enzymes are huge in size ( $r > 50$  Å) compared with the hydrated ions usually considered. They contain a heme group that is a metal ion that must be reached by an electron if reduction is to occur. This would seem to introduce a hindrance to the development of the theory of enzyme electrochemistry. An electron

<sup>13</sup>Those who wish to extend their skills in this direction here should investigate "Fermi's golden rule," a general quantum mechanical expression for transition probability. It runs

$$P_T = 2\pi/\hbar |T|^2 \rho(E_F),$$

where  $|T|^2$  is the square of the transition matrix, and  $\rho$  the density of states at the Fermi level in the metal. The expression for  $T$  involves the wave function of the electron in the metal (well treated), but also that for the electron in the hydrated ion, where the approximations may be severe.

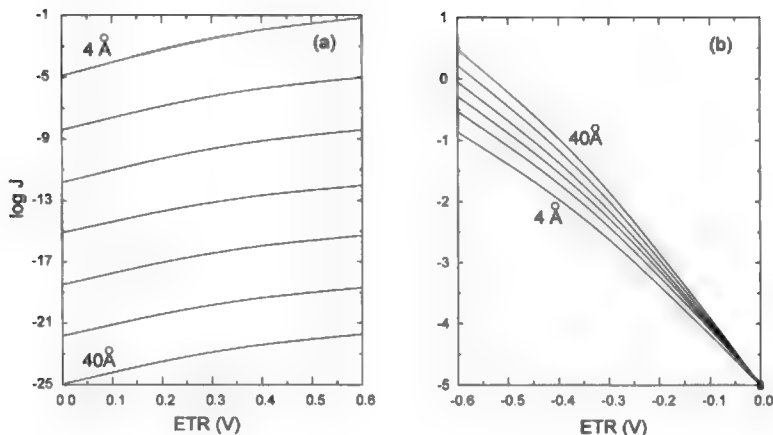


**Fig. 9.21.** Tafel plots of the (a) anodic and (b) cathodic current densities for film thickness varying from 4 to 40 Å in steps of 6 Å. The cathodic curves have been normalized for  $\eta = 0$ . Barrier height = 1.5 eV.  $VL = VR = 1.5$ ; harmonic. (Reprinted with permission from W. Schmickler and J. Ulstrup, *J. Chem. Phys.* **19**: 217, Fig. 3, copyright 1989, American Chemical Society.)

attempting to reach the heme group would not pass easily into the conduction band of the enzyme through  $> 25$  Å of complex organic structure. Tunneling from electrode to heme might be feasible, but the distances strain the electrons' tunneling ability, which has been found to decline markedly at  $x > 20$  Å. To address this, the introduction of "relay stations" (artificially inserted redox ions) has been successfully used to reduce the gap over which the electrons have to tunnel (Heller, 1990) (Fig. 1.12).

## 9.5. SOME ALTERNATIVE CONCEPTS AND THEIR TERMINOLOGY

### 9.5.1. Introduction

Our book is intended to be a *basic* text in physical electrochemistry; it is not a comprehensive monograph for research workers (see Bockris and Khan, 1993). Nevertheless, it is desirable to equip the student with knowledge of some of the relevant terminology of topics at the frontier around the year 2000. Three of these are presented here.

### 9.5.2. Outer Shell and Inner Shell Reactions

The concept of inner and outer shells arises from an earlier stage in the development of the theory of electrochemical reactions when it was thought that some

electrode reactions received the activation necessary for reaction “from the outer shell.” The only molecular description of what this might mean is due to Levich (1970) and is described later in the section on mechanisms of activation (Section 9.5.2). It is now realized that few outer shell reactions exist, and the typical electrochemical reaction is associated largely with interactions between the ion concerned and the nearby (first layer of) water in the hydration sheath surrounding it. “Inner shell” referred historically to the vibrating interactions of the central metal in a complex ion [e.g., Fe in  $\text{K}_3\text{Fe}(\text{CN})_6$ ] with the surrounding ligands, in the example, Fe-CN vibrations. However, most electrochemical reactions do not involve complex ions. The “inner shell” in the charge-transfer reactions of  $\text{Ag}^+$  depositing on Ag metal is the  $\text{Ag}^+$  surrounded by its sheath of hydration waters.

### 9.5.3. Electron-Transfer and Ion-Transfer Reactions

Interfacial electrochemistry is about electric charges at interfaces between phases, one of which is an electron conductor and the other an ion conductor. The kinetic part of the subject is about the rate at which these charges transfer across the interphase. However, this definition clearly embraces two limiting cases.

One of these, electron transfer, actually occurs in the ideal definitional sense. It applies to the few overworked redox reactions where there is no adsorbed intermediate. The ion in a cathodic transfer is located in the interfacial region and receives an electron (ferric becomes ferrous) without the nucleus of the ion moving. Later (perhaps as much as  $10^{-9}$  s later), a rearrangement of the hydration sheath completes itself because that for the newly produced ferrous ion in equilibrium differs (in equilibrium) substantially from that for the ferric. Now (even in the electron transfer case) the ion moves, but the definition remains intact because it moves *after* electron transfer. The amounts of such small movements (changes in the ion-solvent distance for  $\text{Fe}^{2+}$  and  $\text{Fe}^{3+}$  ions in equilibrium) are now known from EXAFS measurements.

*Ion-transfer* reactions are clearly exemplified by proton transfer in the case (e.g.,  $\text{H}_2$  evolution on Hg) in which the transfer of a proton from its hydration sheath to the electrode is rate determining. However, ion-transfer reactions can only be clearly defined as a hypothetical ideal (the proton transfers to the electrode and becomes an adsorbed *atom*). The reality is that the electron also emits from the metal. Further, the status of the adsorbed entity that exists after transfer may not have zero charge, i.e., be an atom in the normal sense (partial charge transfer; Conway and Bockris, 1958; Lorenz, 1961; Vetter and Schultze, 1972).

### 9.5.4. Adiabatic and Nonadiabatic Electrode Reactions

The terms “adiabatic” and “nonadiabatic” are confusing. Thus, students who approach kinetics at an electrochemical interface via studies of chemistry will be used to the term “adiabatic.” In thermodynamics, adiabatic indicates a process in which no heat enters or escapes from the system, e.g., from the vessel in which the reaction



occurs. A Dewar flask has adiabatic walls. Nonadiabatic means, correspondingly, a situation in which heat *does* escape from or enter into the vessel during the reaction. These two terms are used in quantum discussions of electrode reactions, but the meaning there is remote from that used in thermodynamics.

The one-dimensional potential energy–distance cut orthogonal to the electrode marked P-R in Fig. 9.22 represents, at a simplified level, what we have seen before in discussing the happenings in potential energy curves. It consists, in fact, of two half-curves, the initial state partly to the right of  $B_0$  and the final state partly to the left thereof. Considerable rounding occurs near the maximum of the two half curves (not shown in earlier, simpler curves) owing to mutual interaction and resonance.

In spite of its simplicity, the basic features of a simple reaction (e.g., proton transfer from  $\text{OH}_3^+$  to adsorbed H) can be made out in this diagram. A reaction here is called *adiabatic* if the representative points *stay on this (lower) curve* during the course of a transition from the initial state (the minimum on the right) to the final state (the minimum on the left) as in Fig. 9.18.

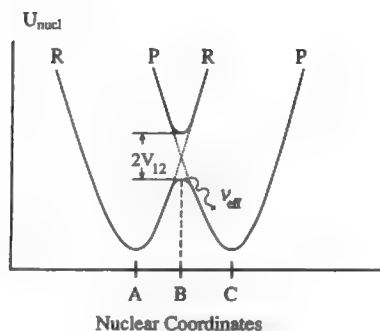


**Fig. 9.22.** Electron-transfer reaction curves. The potential energy of the system is drawn as a function of the nuclear coordinate surface. The parabolic surface that signifies that the nuclear displacements are within harmonic limits of their respective internuclear potentials is the key feature. (Reprinted from R. J. D. Miller, G. McLendon, A. J. Nozik, W. Schmickler, and F. Willig, *Surface Electron Transfer Processes*, p. 9, copyright © 1995 VCH-Wiley. Reprinted by permission of John Wiley & Sons, Inc.)

An adiabatic reaction is the simplest way a reaction can occur. This meaning here bears perhaps a faint resemblance to that of thermodynamics. For in an adiabatic reaction, there is relative simplicity of concept; nothing disturbs, no other state interferes.

Now, there is another and rather disturbing possibility for reactions. Thus, in Fig. 9.22, at the transition point there is a finite probability that the activated complex will pass to a higher electronic state, represented by RP. The curve RP is a single potential energy curve, that of the activated complex. The lifetime in the upper state is likely to be short, however, and the complex there is likely to dissociate and fall back to the initial state. It is easy to accept the term “nonadiabatic” for such a situation. Again, some remote resemblance to the thermodynamic meaning (interfered with by heat coming in or leaving) exists; the reaction is disturbed by transfer to another state.

What is the probability of a reaction transferring to the upper curve and not staying on the lower one? It depends on the magnitude of the energy distance  $2V_{12}$  (Fig. 9.22). Very small values of  $V_{12}$ , i.e., a small energy gap between the maximum of the lower curve and the minimum of the upper curve, will make it easy for the reaction to become nonadiabatic. Any introduction of nonadiabaticity will slow the reaction down. If the reaction makes 1000 attempts to pass through the summit of the lower curve to the final state, staying on the lower curve, and only 1% of these attempts succeeds, the reaction is reduced in velocity (compared with what it would have been if it had stayed adiabatic) by 100 times.

Thus, adiabatic reactions are relatively fast, faster than the corresponding nonadiabatic ones. There is a famous theory, deduced independently in the early days of quantum mechanics (1932) by Landau in Moscow and Zener in Cambridge, Massachusetts; their formula shows that the probability of a nonadiabatic change depends exponentially on  $e^{-aV_{12}}$  where the parameter,  $a$ , has quantities describing the curves of Fig. 9.22, but is little temperature dependent. Thus, the smaller  $V_{12}$  (the closer together the curves at the point of nearest approach), the more likely it is that a successful adiabatic crossing on the lower curve will be lost and a successful reaction will be deterred by its becoming nonadiabatic, i.e., the majority of the transfers end up back at the starting point.

As a generalization, nonadiabaticity tends to be greater in redox reactions than for the ion-transfer reactions (e.g.,  $\text{O}_2 + 4\text{H}^+ + 4\text{e} \rightarrow 2\text{H}_2\text{O}$ ) where the value of  $V_{12}$  can be as much as 0.5 eV (Newton, 1986; Bockris and Sidik, 1998). Such reactions will be largely adiabatic.

## 9.6. A QUANTUM MECHANICAL DESCRIPTION OF ELECTRON TRANSFER

### 9.6.1. Electron Transfer

The heart of interfacial electrochemical kinetics is electron transfer—metal to solution and solution to metal. The electron is a particle, the movement and properties

of which (particularly in its passage through energy barriers) can only be dealt with if one views it as behaving quantum mechanically. It is therefore worthwhile to give right now a description of what happens at the electronic and molecular level during electron transfer.

In doing this, two different kinds of particles will be held in mind. The one will be the strongly hydrated ferric ion, the other the  $\text{H}_3\text{O}^+$  ion. The transfer described will be the cathodic one. The loss of generality by these limitations is compensated by focusing on familiar objects.

One can begin here by thinking of  $\text{Fe}^{3+}$  and/or  $\text{H}_3\text{O}^+$  bobbing about in the solution; no space will be used in describing how each particle gets to the interfacial region (Section 4.3) and adsorbs there. Nor will we bother just now to enter into the interesting questions of the nature of the adsorption and the precise location of the ions (Section 6.8.2), whether as a part of the first layer of water molecules attached to the metal surface or in the next layer outside it.

Now the hydrated ion sits there near the electrode and there is a simple phenomenological calculation we can easily make, and that is the range of its turnover numbers. This is the number of times a given site on the electrode surface goes into action and successfully deals with an electron per second. In order to come up with specific numbers, it is necessary to make some rough-and-ready assumptions; the first will be that one site in 100 on the electrode surface is covered with ions and can be considered as a potential electron receiver. The next assumption is that the current density is  $10^{-3} \text{ A cm}^{-2}$ , i.e.,  $1 \text{ mA cm}^{-2}$ , and one can see at once that this means that  $(10^{-3}/F) \times N_A$ , where  $F$  equals the Faraday transfer and  $N$  is the number of electrons  $\text{cm}^{-2} \text{ s}^{-1}$  to which  $1 \text{ mA cm}^{-2}$  is equivalent. With  $9.45 \times 10^4 \text{ C mol}^{-1}$  for the faraday,  $F$ , and  $6.023 \times 10^{23}$  for Avogadro's number one arrives at  $6 \times 10^{15}$  electrons  $\text{cm}^{-2} \text{ s}^{-1}$ . The number of atoms  $\text{cm}^{-2}$  on a metal clearly depends on the radius of the metal's atom and will be taken here as a typical  $10^{15} \text{ cm}^{-2}$ . Since only 1% of them are taken as being active, one has  $10^{13}$  atoms  $\text{cm}^{-2}$  passing  $6 \times 10^{15}$  electrons to the solution, or 600 actions per atom site  $\text{s}^{-1}$ .

One  $\mu\text{A cm}^{-2}$  is very much in the useful electrochemical range and then a given site, within present assumptions, would only have to be active every 0.6 s. At the other end of the usual current density scale,  $1 \text{ A cm}^{-2}$ , the number would be up to  $6 \times 10^5 \text{ s}^{-1}$ . These are simple concepts.

Next, let the focus be on one of the chosen ions, say,  $\text{Fe}^{3+}$ , and its hydration sheath (somewhat distorted by adsorption in the double layer). The energy levels in this ion at 300 K are predominantly in the ground state. Because the tunneling of the electron to the ion is taken to occur from the Fermi level of the metal and to be radiationless, the energy states in the ion are the ones of interest for electron transfer. This means that the electrons will be likely to find a home only in electronic states of the hydrated  $\text{Fe}^{3+}$  ion, well above the ground state.

How do these distributed energy states exist, i.e., from where do they obtain their energy and deliver it back again (for equilibrium with the surrounding solution is

assumed)? The answer lies in the “heat bath” of the surrounding water, where there is a series of distributed energies, largely in the form of librators of the water, which, near one of the adsorbed ions on which attention is concentrated, will have reassumed its 3D structure of liquid water (this structure is interrupted near the electrode). It is possible to give a quantum mechanical theory of the transfer of librational energy to the adsorbed ions (Khan, 1984), but a detailed mathematical description of this will be postponed so that more attention can be given to the principal act, the actual electron transfer.

It can be imagined that electrons in the electrode's surface are constantly reaching for ways to transfer. They are, so to speak, tuned to the signal that (for a give site) there is available an empty energy state having the same Fermi energy as the activated energy site in the receiver ion, 3–5 Å away in the double layer. *How* to jump is the electron's problem.

Briefly, the electron has choices. This is because there are two states to which it can transfer, and these are represented in Fig. 9.23. There is a probability that the electron may go to the higher state, but there becomes unstable and relaxes back to its starting point again. Or, the electron may go to the lower state, making an excited  $\text{Fe}^{2+}$  (or, for transfer to  $\text{H}_3\text{O}^+$ , a highly unstable H).

On the whole, it is more likely in the case of  $\text{Fe}^{3+}$  that the electron will opt for the “upper state,” the one in the discussion given in Section 9.5.4 about nonadiabatic transfers. Perhaps 10 electrons may go to this upper state (one is referring here more to  $\text{Fe}^{3+}$ ) and uselessly fall back again into the metal, the “never made it,” transfer. One electron out of ten, say, spends more and more of its time in the lower state and finally becomes localized there in the valence shell of the  $\text{Fe}^{2+}$  ion, although this  $\text{Fe}^{2+}$  has suddenly become an unstable entity, for it still has an activated  $\text{Fe}^{3+}$  hydration shell. There is then the relaxing or cooling down of the newly formed  $\text{Fe}^{2+}$  ion with the wrong hydration shell, the one which, as a result of the thermal energy picked up from the heat bath, led to the special formation around  $\text{Fe}^{3+}$  so that there were electron levels in it having an energy equal to that of the electron at the Fermi level. The  $\text{Fe}^{2+}$  ion finally reaches the equilibrium state for the  $\text{Fe}^{2+}$  hydrated. This means a movement away from the ion of several water molecules and an increase in the average distance of  $\text{Fe}^{2+}\text{--OH}_2$  compared with that for  $\text{Fe}^{3+}\text{--OH}_2$ .

Let the  $\text{Fe}^{2+}$  ion be abandoned for the moment to describe the somewhat different events with  $\text{H}_3\text{O}^+$  a femtosecond after electric transfer. For transfer to  $\text{Fe}^{3+}$  when the electron leaves the metal and in an interval of  $10^{-15}$  s transfers to the hydrated ion awaiting it, the decisive quantity is  $V_{12}$  in Fig. 9.22. It is liable to be very small, for  $\text{Fe}^{3+}$  and similar redox species, less than 0.1 eV; and so the probability of the useless nonadiabatic electron transfer will be large and the successful rate of formation of  $\text{Fe}^{2+}$  relatively small.

With  $\text{H}_3\text{O}^+$ , the situation is different from that of the redox reaction. There is stronger coupling between the electron and the nuclear motion in

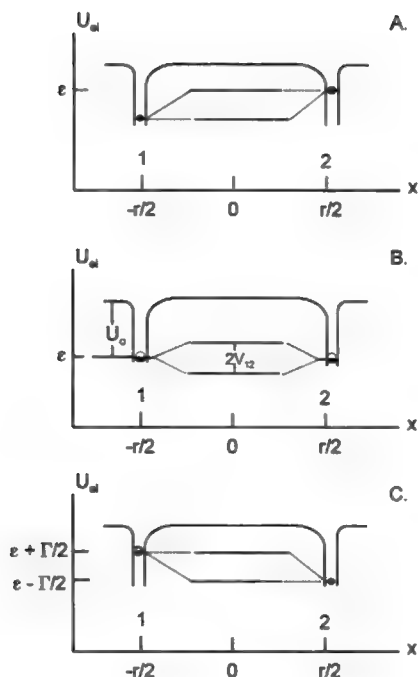
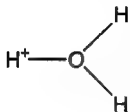


**Fig. 9.23.** Square-well model for electronic mixing between two discrete states. The displacement toward resonance is derived from modulation of the energy levels by the coupling of the electronic levels to the nuclear motion of the surrounding medium. In configuration A, the electron is localized at the donor site; B corresponds to the condition of quantum resonance between the two states; C corresponds to the nuclear configuration in which the electron becomes localized on the acceptor site (Reprinted from R. J. D. Miller, G. McLendon, A. J. Nozik, W. Schmickler, and F. Willig, *Surface Electron Transfer Processes*, p. 4, copyright © 1995 VCH-Wiley. Reprinted by permission of John Wiley & Sons, Inc.)



The surrounding medium and its relaxation time determine the time for the nuclear fluctuations that are to couple with the electron and to capture it, annulling the charged state of  $\text{H}_3\text{O}^+$ .

When these details were first discussed by Gurney (a physicist), in 1931, it was not realized that the adiabatic reception of the electron in  $\text{H}_3\text{O}^+$  depended on a coupling of the motion of the H that was previously the proton in  $\text{H}_3\text{O}^+$  with the metal surface orbitals to which it must bond to become an adsorbed H—the intermediate radical of which has already been discussed. Hence, in Gurney's famous first publication, H had not, to use a phrase, come in from the cold; it was left out of contact with the electrode, and lack of bonding to the metal led to improbably high values for the calculated heat of activation for the proton discharge reaction.

This error in Gurney's first paper was corrected by the physical chemist Butler (1936)—of the Butler–Volmer equation—who accounted for the coupling between surface orbitals of the metal and the newly born H from  $\text{H}_3\text{O}^+$ . The *chemical* importance of this formation of the adsorbed radical is great. It rationalizes in quantum mechanical terms the explanation of electrocatalysis, a heuristic view of which had been given by Horiuti and Polanyi a year before, in 1935. But the quantum mechanical significance is in the value of  $V_{12}$ . The energy of the lower curve (PB in Fig. 9.22) is pulled *down*, made more negative in potential energy by the coupling of the H–O vibrational modes to those of M–H in the electrode. In this way,  $V_{12}$  is increased, e.g., to 0.5 eV. The result is a greater separation of the lower (adiabatic) energy pathway (see Fig. 9.23) from the higher one, and the probability of the nonadiabatic (wasteful, slow) pathway is diminished toward a negligible value (McClendon, 1995). A corresponding result is a major lowering in the calculated energy of activation of the reaction.

It is now necessary to return to the diagram (9.22), the first version of which was due to Landau (and in the same year, 1932, to Zener), which was used in Section 9.5.4 to explain the idea of adiabatic and nonadiabatic transfer. The figure represents a one-dimensional slice through the three-dimensional energy variations surrounding the electron transfer to one ion (Fig. 9.23). At point B, there is resonance between the donor and acceptor levels, brought about with the aid of the heat bath and the fluctuations of energy to which it gives rise. The lower curve, therefore, contains the adiabatic crossing point, which was earlier referred to as the transition state.

All these details of energy and interactions are dependent on Boltzmann and the distribution law. The probability of maintaining the molecular configurations implied in the diagrams (particularly the summit) can be calculated by determining the probability of their existence by means of Boltzmann's law.

### 9.6.2. The Frank–Condon Principle in Electron Transfer

According to the Frank–Condon principle, because nuclei are so much more massive than electrons, an electronic transition to an ion occurs in a time too small for a significant change in the position of the nucleus to occur during it. In order to appreciate the applicability of this principle to the situation with an electron transfer in a redox reaction, consider the situation of ferric ion in the double layer prior to an electron transfer. The water molecules around it are oscillating (vibrating and librating) in their various states and have numerous configurations. At a certain moment, a configuration is set up such that the ion solvent complex has electron states (for a cathodic reaction) corresponding to that of the Fermi energy, i.e., the energy of the electron waiting to transfer. According to the Frank–Condon principle, then, at this moment, the  $\text{Fe}^{3+}\text{--OH}_2$  bonds will be (as far as the fast-moving electron is concerned) frozen in length and position, i.e., the solvent geometry will be (in effect) frozen (see the Frank–Condon principle) and the electron has a certain (very short) time in which this frozen state allows transfer at an apparently constant energy.

Corresponding to the Frank–Condon principle is an associated concept called the *Frank–Condon factors*. Thus, when an electronic transition occurs from the vibrational levels of a lower vibrational state to the corresponding vibrational levels of a higher electronic state, there are various intensities of transition, depending on the vibrational states to which a transition is made.

Development of the Frank–Condon principle in quantum mechanical terms (involving a transition dipole moment<sup>14</sup>) allows a calculation of the intensities referred to in terms of a series of Frank–Condon factors by which expressions for the transition probabilities are multiplied to obtain a net transition probability from one level to another for an electron-transfer process.

### 9.6.3. What Happens if the Movements of the Solvent–Ion Bonds Are Taken as a Simple Harmonic? An Aberrant Expression for Free Energy Activation in Electron Transfer

A well-known expression (Marcus, 1956) arises when the energy changes in the solvent–ion distances in the rearrangements concerned with electron transfer are taken to be harmonic, i.e., that  $U_x = kx^2$ . This expression has been discussed (Levich and Dogonadze, 1983) in a quantum mechanical context with the implication that its derivation depends on quantum mechanical considerations. However, the association

<sup>14</sup>Transition dipole moments are concerned with the dipole that exists in a molecular vibration when it adjusts itself to the frequency of the electromagnetic radiation with which it is in resonance (and about to undergo a transition). The values of such transition dipole moments can be calculated quantum mechanically (which is lengthy and approximate). If a bond is considered within a series of similar bonds for which reliably calculated transition dipole moments are available, an interpolation of the relevant value may be sufficient (Bockris and Carbajal, 1987).

with quantum (really spectroscopic) concepts is only in the application of the Frank-Condon principle (Fig. 9.24). Then the following derivation applies:

$$G_R = kq^2 \quad (9.25)$$

for the reactant system and

$$G_P = k(q - d)^2 + \Delta G^\circ \quad (9.26)$$

for the product system, where  $d$  is the displacement between the reactant and product system corresponding to the respective equilibrium positions. At the activated state, the two reactant and product system parabolas intersect where

$$G_R = G_P \quad (9.27)$$

Now using Eqs. (9.25) and (9.26) in Eq. (9.27), one can find the solvent coordinate corresponding to the activated state  $q^*$  as

$$kq^{*2} = k(q^* - d)^2 + \Delta G^\circ$$

or

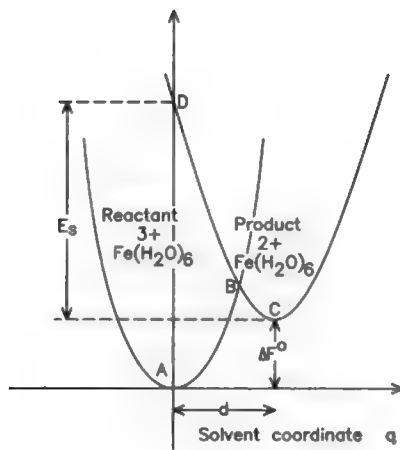


**Fig. 9.24.** The free energy versus solvent coordinate curve showing the relation between reorganization energy  $E_s$ , free energy of reaction  $\Delta F^\circ$ , and free energy of activation  $\Delta F^\ddagger$ .



$$kd^2 - 2kdq^* + \Delta G^\circ = 0 \quad (9.28)$$

From the definition, the reorganization energy is the energy of the product system when its solvent coordinate is still the same as that of the reactant state, i.e., where  $q = 0$ . Thus, putting  $q = 0$  in Eq. (9.28), one gets

$$G = kd^2 = E_s \quad (9.29)$$

where  $E_s$  is the construct shown in the diagram.<sup>15</sup>

Putting Eq. (9.27) in Eq. (9.29), one obtains after rearrangement

$$q^* = \frac{kd^2 + \Delta G^\circ}{2kd} = \frac{(E_s + \Delta G^\circ)}{2kd} \quad (9.30)$$

The free energy of activation  $\Delta G^\ddagger$  is given as

$$\Delta G^\ddagger = kq^{*2} = k \frac{(E_s + \Delta G^\circ)^2}{4k^2 d^2} = \frac{(E_s + \Delta G^\circ)^2}{4E_s} \quad (9.31)$$

In Eq. (9.31),  $\Delta G^\circ$  is the standard thermodynamic free energy change in the reaction.

Now, the simplified model shown represents equilibrium, and the  $\Delta G^{\circ\ddagger}$  is the free energy of activation for the forward direction of the reaction at the reversible potential. To represent the forward direction at any other potential,  $V$ , one finds beyond the reversible potential.

$$\Delta G^{\circ\ddagger} = \frac{(E_s + \Delta G^\circ + \eta E)^2}{4E_s} \quad (9.32)$$

<sup>15</sup>This term, "the reorganization energy," is in fact a mathematical construct [Eq. (9.29)]. It does not apply to an actual state in thermal electron transfer. Thus, consider an electron transfer to a ferric ion that has just been stimulated by a photon arriving in the metal. The product would be an activated ferrous ion with the energy corresponding to  $D$  in Fig. 9.22 (i.e., this would be the energy of the excited ferrous ion far from equilibrium). The hypothetically formed ion would then relax to the equilibrium state at  $C$  and this relaxation energy is the  $E_s$ , called in the present deduction, the "reorganization energy." The mathematical construct nature of  $E_s$  must be stressed. Although often mentioned in the literature by electrochemists (and some quantum physicists, too!) who wanted to go on with the traditional quadratic energy variation model of Weiss and Marcus (Section 9.7.2), there are no ions that undergo the reorganization indicated by the phrase "reorganizational energy" [Eq. (9.29)]. The ions reorganize to the intersection point of the potential energy curves ( $B$  in Fig. 9.24), whereupon the electron transfer occurs.

On the other hand, although the reorganization energy is a construct (like the Fermi energy of electrons in an intrinsic semiconductor in the middle of a region with no electrons), it is easy to imagine. Thus, in Fig. 9.24 at  $D$ , the *ferrous* ion would just have been formed by a vertical electronic transition and be with all the solvent structure of the *ferric* ion. But not  $C$ ; the ferrous ion has its solvation shell, reorganized from that of the ferric ion.

This expression can be rewritten<sup>16</sup>:

$$\Delta G^{\circ\ddagger} = \left[ \frac{1}{4} E_s + \frac{1}{2} \Delta G^\circ + \frac{\Delta G^{\circ\ddagger}}{4E_s} \right] + \frac{1}{2} \eta F \left[ 1 + \frac{\Delta G^\circ}{E_s} \right] + \frac{\eta^2 F^2}{4E_s} \quad (9.33)$$

However,

$$i = nF \frac{kT}{h} c_i e^{-\Delta G^{\circ\ddagger}/RT} \quad (9.34)$$

Hence, from Eq. (9.28),

$$\beta = -\frac{RT}{F} \frac{\partial \ln i}{\partial \eta} = \frac{1}{2} \left[ 1 + \frac{\Delta G^\circ}{E_s} \right] + \frac{\eta F}{2E_s} \quad (9.35)$$

Also

$$i = nFk e^{-\alpha \eta F/RT} \quad (9.36)$$

$$\frac{\partial \ln i}{\partial \eta} = -\alpha F/RT$$

$$-\frac{RT}{F} \frac{\partial \ln i}{\partial \eta} = \alpha = \frac{1}{2} \left( 1 + \frac{\Delta G^\circ}{E_s} \right) + \frac{\eta F}{2E_s} \quad (9.37)$$

#### 9.6.4. The Primacy of Tafel's Law in Experimental Electrode Kinetics

Arrhenius' law<sup>17</sup> for the variation of the velocity of reactions with temperature was followed in 1905 by Tafel's equation for the variation of the electrochemical reaction rate with potential. The two laws may be compared:

$$V_{\text{Arrhenius}} = Ae^{-E/RT}; V_{\text{Tafel}} = A'e^{-\alpha \eta F/RT}$$

<sup>16</sup>In some presentations this equation has been applied to isotopic reactions in solution. There is in effect a negligible  $\Delta G^\circ$  if the redox ions in equilibrium are isotopes. Thus, one could find in solution:  $n_1 A^{2+} + n_2 A^{3+} \rightarrow n_1 A^{3+} + n_2 A^{2+}$  With  $\Delta G = 0$ ,

$$\Delta G^{\circ\ddagger} = \frac{1}{4} E_s + \frac{1}{2} \eta F + \frac{\eta^2 F^2}{4E_s}$$

However, this simplification obviously does not apply to real electrochemical reactions. This harmonic oscillator model is described here because it is so well known. It will be compared with experiment in Section 9.6.3.

<sup>17</sup>As is often the case in deciding the names attached to equations in science, Arrhenius' equation was actually deduced by Van Hoff (1884). However, Arrhenius developed it and used it a lot, so it is known under his name!

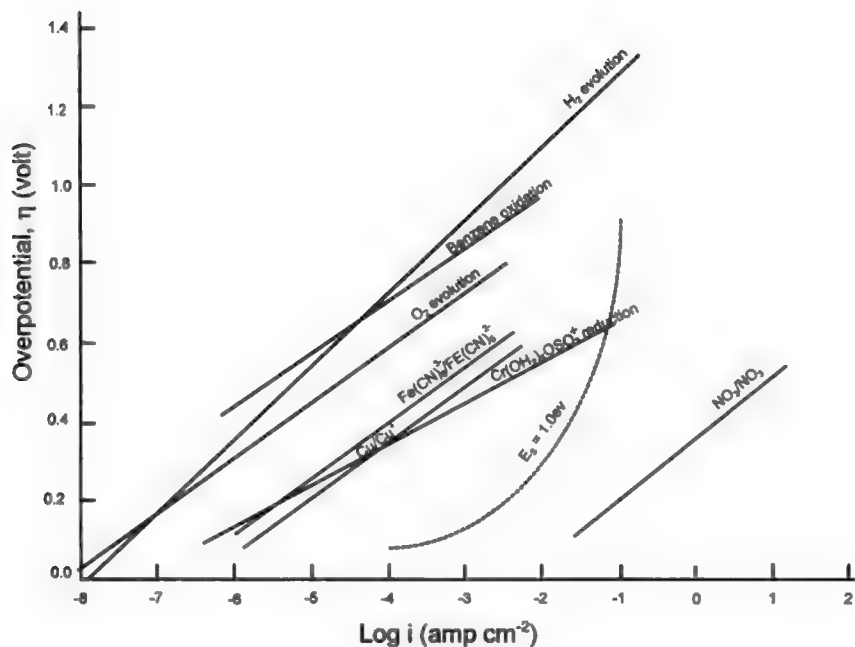


**Fig. 9.25.** (a) Tafel plots of numerous reactions: reduction of benzene, oxidation of Cu in solid electrolyte, reduction of  $\text{NO}_3^-$  in molten salt, reduction of  $\text{Fe}^{3-}(\text{CN})_6$ ,  $\text{H}_2$  evolution reaction,  $\text{O}_2$  evolution reaction,  $\text{Cr}(\text{OH})_5\text{OSO}_3^+$  reduction, and the theoretical plots from the continuum theory expression (—) for an  $E_s$  value of 1.0 eV. (Reprinted with permission from S. U. M. Khan and J. O'M. Bockris, *J. Phys. Chem.* **87**: 2601, copyright 1983 American Chemical Society.)

where  $A$  and  $A'$  are constants that include the concentration of the reactants. When one realizes that the expression  $\alpha\eta F$  has the dimension of energy, it is seen that the two laws are the same form.<sup>18</sup>

*Tafel's law is the primary law of electrode kinetics*, in the sense that Arrhenius' law is the basic law of thermal reaction. It applies universally to all processes that are controlled in rate by the interfacial transfer of electrons or by a rate-determining surface reaction that may be coupled to the interfacial electron [Fig. 9.25(a)]. Redox reactions without surface intermediates demonstrate Tafel's law well [Fig. 9.25(b)].

<sup>18</sup> It seems likely that Tafel's law applies to a greater swath of reactions occurring spontaneously in nature than does the law of Arrhenius. Very widespread natural happenings (corrosion, photosynthesis, metabolism) all depend for their rate on interfacial charge transfer and are subject then, in respect to the rate of the constituent processes at the molecular level, to Tafel's law. Remarkably, although Arrhenius equation is perhaps the best known in chemistry, and its form is widely recognized by most scientists, those who are familiar with Tafel's law are limited to maybe a thousand physical electrochemists.

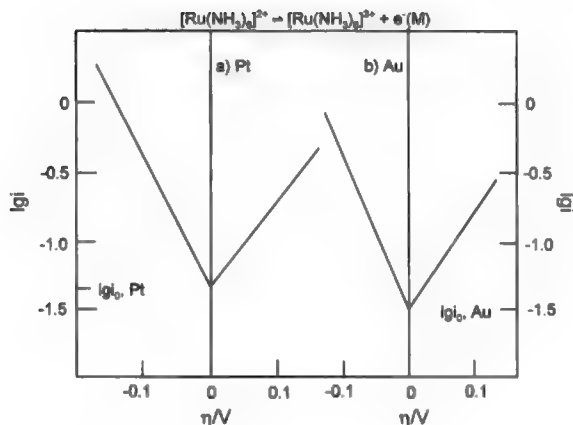


**Fig. 9.25. (b)** Tafel plots for the system  $[\text{Ru}(\text{NH}_3)_6]^{2+/3+}$  at 20 °C. (Reprinted with permission from T. Iwasita, W. Schmickler, and J. W. Schultze, *Phys. Chem.* **89**: p. 142, copyright 1985 American Chemical Society.)

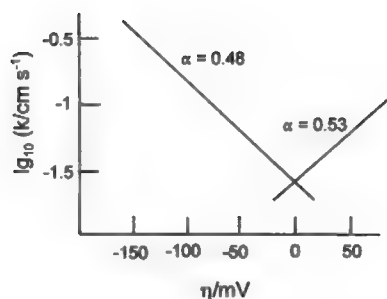


**Fig. 9.25. (c)** Tafel plots for the exchange of the acetylcholine ion between an aqueous solution and one containing organic molecules; the branch on the right-hand side corresponds to transfer from the aqueous to the organic solution. (Reprinted from Wolfgang Schmickler, *Interfacial Electrochemistry*. Copyright © 1996 by Oxford University Press, Inc. Used by permission of Oxford University Press.)

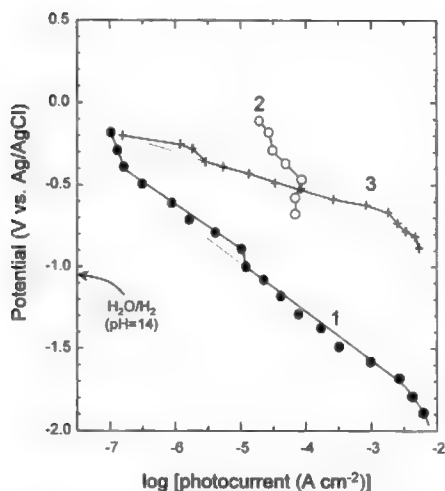


**Fig. 9.25.** (d) Tafel plots of log-photocurrent vs. potential for *p*-InP and *p*-GaP. Curve 1, *p*-InP in 1 M NaOH; curve 2, *p*-InP in 1 M NaOH + 3 mM methyl viologen; curve 3, *p*-GaP in 1 M NaOH. (Reprinted from K. Uosaki and H. Kita, *Solar Energy Materials*, Vol. 7, p. 424, Fig. 2, 1983, with kind permission from Elsevier Science-NL, Sara Burgerhartstraat 25, 1055 KV Amsterdam, The Netherlands.)

Tafel's law applies also in current density ranges well below that of the limiting current at semiconductor/solution interfaces and to photoelectrochemical reactions. Its application to liquid-liquid interfacial electron transfer is also good [see Fig. 9.25(d)] (Schmickler 1995). In hydrogen evolution, it has been followed down to the picoampere region and up to 100 A cm<sup>-2</sup>.

A thoroughgoing restudy of Tafel's law, involving the use of fast-flow techniques to avoid the introduction of diffusion control at high rates (Iwasita, Schmickler, and Schultze, 1985) shows excellent verification.<sup>19</sup> Tafel's law is one of the most tested and verified laws in nature. It is also one with the broadest applicability (e.g., in interfacial charge-transfer control, e.g., corrosion metabolism and photosynthesis). In

<sup>19</sup>Of course, Tafel's law applies to reactions under *interfacial* charge-transfer control. Tests of it need conditions that maintain that control over the current density range investigated, so that the same surface is maintained (e.g., the experimental conditions do not stray into a potential region in which an oxide film is formed). Tafel's law can be made to fail by implanting on a surface a scaffolding of organic structures with an unknown variation of the barrier height with potential (Miller and Graetzel, 1991), or passing the electrons concerned through semiconducting oxide films (Schmickler, 1981) where the rate-determining step changes from charge transfer at the interface to electron transport in the structure concerned.

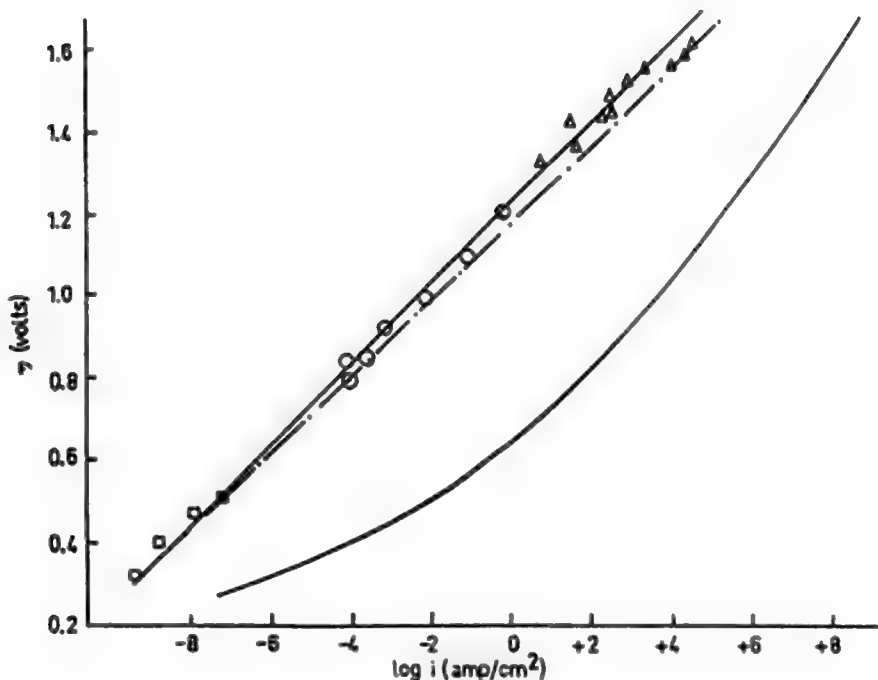


**Fig. 9.25.** (e) The hydrogen evolution reaction over the Tafel relation which is linear over eleven orders of magnitude (experimental points). Curved line: Marcus expression with assumption of harmonic oscillators. (Reprinted from J. O'M. Bockris and S. U. M. Khan, *Quantum Electrochemistry*, Plenum 1979, p. 228.)

spite of almost a century of confirming data, however, there is still a research frontier in the study of Tafel's law. Is there an overpotential at which it will break down? Does it apply at very low temperatures (Wass, 1990)?

Why did we introduce this purely experimental material into a chapter that emphasizes theoretical considerations? It is because the ability to replicate Tafel's law is the first requirement of any theory in electrode kinetics. It represents a filter that may be used to discard models of electron transfer which predict current-potential relations that are not observed, i.e., do not predict Tafel's law as the behavior of the current overpotential reaction free of control by transport in solution.

## 9.7. FOUR MODELS OF ACTIVATION

### 9.7.1. Origin of the Energy of Activation

The quantal aspect of electrochemical reactions so far presented has described what happens in an electron transfer in terms of molecular movements. In these

descriptions it is assumed that the ion–solvent complexes concerned have been “activated” so that suitable empty states are available for the electron. There are no fewer than four models by which the energetics aspects of electron-transfer reactions are described.

### 9.7.2. Weiss–Marcus: Electrostatic

The first is due to Weiss (1954) and is, like the later theory of Marcus (1956), entirely electrostatic. Weiss was the first to introduce the Frank–Condon principle to the model for the energy changes concerned. He took account of the changes in ionization energy and of electron affinity occurring in the reaction. Weiss was also the first to point out the existence of the adiabatic and nonadiabatic modes of transfer for ions in solution, and followed Gurney in assuming a *Boltzmann* distribution of the energy states. Weiss involved electron tunneling at electrodes (cf. Gurney 1931) and applied Landau’s modification of the Born equation to calculate what he called the “energy of the orientation of dipoles” as a consequence of electron transfer (Marcus later called this idea *reorganization energy*). Weiss’s paper for the first time contained the equation

$$\Delta G^\circ = \frac{z_i^2 e_0^2}{2R_i} \left( \frac{1}{\epsilon_{\text{opt}}} - \frac{1}{\epsilon_{\text{stat}}} \right)$$

where  $R$  is the radius of the ion and the first layer of waters and  $\epsilon_{\text{opt}}$  and  $\epsilon_{\text{stat}}$ , are, respectively, the optical and static dielectric constants later used by Marcus. Weiss regarded the total hydration energy in terms of Born’s equation as  $-(z_i^2 e_0^2 / 2R_i)(1/\epsilon_{\text{stat}})$  and the part due to the distortion of electronic shells as  $-(z_i^2 e_0^2 / 2R_i)(1/\epsilon_{\text{opt}})$ . The difference, then, would be what was left over from the total after taking away the electronic distortion part—the dipole orientation energy occurring outside the first layer of water dipoles. Energy changes in this first layer were allowed for by calculating, electrostatically, the energy needed for electrons to pass through it.<sup>20</sup>

Marcus (1956) simplified Weiss’s 1954 theory by neglecting the changes in ionization energy and electron affinity in redox reactions, and all changes in the inner sphere, although the total of these would amount to several electron volts. He considered only the adiabatic case, although he concentrated on redox reactions where a degree of nonadiabaticity is expected. Electron tunneling was implied with a probability of unity and the energetics of the redox process were supposed to occur entirely in terms of changes in hydration energy. Following Weiss, Marcus also used

<sup>20</sup>Weiss’s considerations in the original and seminal paper of 1954 included founding discussions of the energetics of electron transfer to complex ions and particularly discussion of biochemical redox processes in solutions with electron transfer to heme groups.

the Born–Landau expression to calculate the energy changes on electron acceptance. The dipoles adjusted to the new charge caused by neutralization.

Now, typical values of  $E_s$  and  $\Delta G^\circ$  for redox reactions are 20 and 15 kcal/mol, respectively. Hence,  $\Delta G^\circ/E_s \sim 0.75$ . Using Eq. (9.35) and  $\eta = 0.5$ , the value of  $\beta$  is 0.96 (compare experimental values of  $0.5 \pm 0.1$ ). Equation (9.35) clearly fails the test of a constant  $\beta$  independent of potential over a potential range of about 1 eV.

Marcus stressed that only harmonic modes  $U = k_x^2$  were involved in the ion–solvent interactions and went further than Weiss in formulating a simple equation for the rate of adiabatic electron transfer, taking the case of an isotopic reaction so that the  $\Delta G^\circ$  term was eliminated. Under this condition and using Eq. (9.32), the current density (or electrochemical reaction rate) at a given overpotential  $\eta$ , in the cathodic direction ( $\eta$  is negative) is

$$i \propto e^{-\Delta G^{\text{ox}}/RT}$$

$$\propto e^{\frac{-E_s + \Delta G^\circ + \eta F}{4E_s RT}}$$

Using a proportionally constant  $A'$  and Eq. (9.33):

$$i = A' e^{\frac{-E_s + \Delta G^\circ + \eta F}{4E_s RT}}$$

The first term in Eq. (9.33) is independent of potential, so that (combining it with  $A'$ ):

$$i = A e^{-\frac{1}{2} \frac{\eta F}{RT} \left( \frac{1 + \Delta G^\circ}{E_s} \right)} e^{-\eta^2 F^2 / 4E_s RT} \quad (9.38)$$

However, the form of (9.38) is not that of the first (cathodic) term in the familiar Butler–Volmer equation (7.24), which itself does indeed give the experimentally required Tafel law at  $\eta > RT/F$ .

What conditions would be necessary for (9.38) to give Tafel's law (9.36) and replicate the Butler–Volmer equation (Section 7.2.3)? Suppose (as with isotopic reactions)  $\Delta G^\circ = 0$ , then,

$$i = A e^{-\frac{1}{2} \eta F / RT} e^{\frac{-\eta^2 F^2}{4E_s RT}}$$

The required form is simply

$$i = A e^{-\frac{1}{2} \eta F / RT}$$



So, one has to ask what value of  $e - (\eta^2 F^2 / 4E_S RT)$  would be “negligible,” i.e.,  $\eta^2 F^2 / 4E_S RT$  is about unity.

To find this, one needs to know typical value of  $E_S$ . The data on this quantity are more or less limited to those redox reactions again and there one learns that (in kilojoules  $\text{mol}^{-1}$ ):

$$40 < E_S < 120$$

Take a mean value of 80 (i.e., 0.83 eV). Numerical calculations show that  $\eta < 0.2$  V is the condition up to which 9.38 yields the experimental version of Tafel’s law (of course, the value depends on the  $E_S$  chosen and the allowed  $\eta$ , for the applicability of 9.38 will be roughly halved at the lower limit and doubled at the higher one. In any case, this harmonic approximation, which is involved in the Weiss–Marcus theory, cannot be applied to the experimental current-potential data, which in reality extend over 0.2 V and even 1.0 V (for hydrogen and oxygen evolution).

Correspondingly, a typical value for  $\Delta G^\circ / E_S$  [cf Eq. (9.3)] is 0.5 so that  $(\partial \eta / \partial \ln i) = (2RT / 1.5F) = 1.3(RT / F)$ . Although observed values of this coefficient vary from  $RT / 4F$  to  $2RT / F$ , and sometimes above this, the figure for the majority of electrochemical reactions is very near  $2RT / F$  and thus the formation of the rate–overpotential relation to which this Weiss–Marcus harmonic energy variation theory gives rise is not consistent with experiment (Fig. 9.26).

### 9.7.3. George and Griffith’s Thermal Model

George and Griffith (1959) were the first to derive a theoretical expression (thermal) for the free energy of activation in redox reactions. They regarded the free energy of activation as arising from the vibrations of the nearest-neighbor bonds, be they the groups within a complex e.g.,  $\text{Co}-(\text{CN})_n$  or the ion–solvent bonds,  $\text{M}^+-(\text{OH}_2)_M$  (see Fig. 9.27).

The final expression for the free energy of activation from the George and Griffith theory is

$$\Delta G_0^\ddagger(\text{electrochemical}) = \frac{1}{4} n \left( \frac{f_1 f_2}{f_1 + f_2} \right) (\Delta r)^2$$

where  $n$  is the number of ligands or solvent molecules in the first layer around an ion;  $f_1$  and  $f_2$  are the force constants in the lower and higher valence states of ions, respectively; and  $\Delta r$  is the difference in the distance between nucleus and ligand for the higher and lower valence states of ions at equilibrium. Both  $n$  and  $\Delta r$  have been known quite extensively since 1998 as a result of EXAFS studies. In contrast to the discrepant calculation of  $\Delta G_{\text{theoret}}^{\text{ox}}$  which arises from Marcus’s development of Weiss’s electrostatic view, the George and Griffith equation does quite well (Fig.

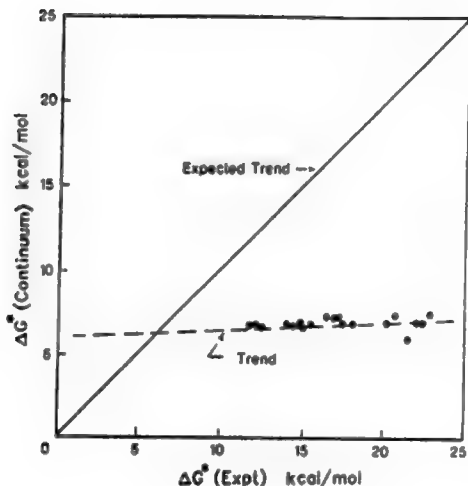


**Fig. 9.26.** Plot of  $\Delta G^*$  from the electrostatic theory of activation vs.  $\Delta G^*$  (expt) for electrochemical redox reactions. (Reprinted from S. U. M. Khan and J. O'M. Bockris, in *Proceedings of The Symposium on the Chemistry and Physics of Electrocatalysis*, J. D. E. McIntyre, M. J. Weaver, and E. Yeager, eds., Vol. 84, p. 34, Electrochemical Society, 1984. Reproduced by permission of The Electrochemical Society, Inc.)

9.28). Marcus later (1963) added the George and Griffith expression to the electrostatically calculated results of his first theory.<sup>21</sup>

#### 9.7.4. Fluctuations of the Ground State Model

The theory of the ground-state model advocated largely by Gerischer was described in Section 9.2.4. It results in a standard free energy of activation that is proportional to the *square* of the sum of the reorganization energy, a standard free energy of overpotential in which the resulting dependence of the log *i* on potential is not Tafelian and is thus discrepant with the main law of electrode kinetics.

<sup>21</sup>The absence of quotation in the chemical literature of the prior publications by Weiss, and of George and Griffith, to those of Marcus, is difficult to rationalize in the case of Weiss's work, which was published in a series of papers in the prominent *Proceedings of the Royal Society* (U.K.), which is easily available. Further, Joseph Weiss was a leading name in redox chemistry of the 1950s. The main elements of the ideas about redox reactions published 2 years later by Marcus had indeed been published by Weiss in the earlier papers! However, the absence of reference also to the prior George and Griffith 1959 paper in Marcus's 1963 application of the same idea is easier to understand, for it was published in an edited volume on enzymatic reactions, which is not normally on the reading list of a physical electrochemist.

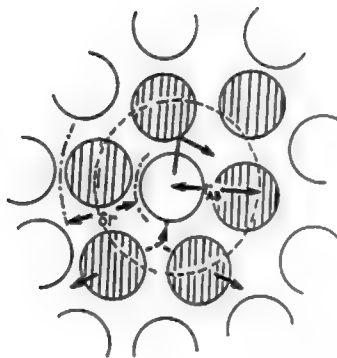


**Fig. 9.27.** Movement of a reference molecule in a liquid and the collision process. (Reprinted from J. O'M. Bockris and S. U. M. Khan, *Quantum Electrochemistry*, Plenum, 1979, p. 160.)

### 9.7.5. The Librator Fluctuation Model

Levich (1970) suggested a molecular model to rationalize the phrase “outer sphere activation.” Thus, the lack in Marcus’s original (1956) model of any explicit accounting for the influence of the first hydration layer led to the idea that the activation must arise “outside the first sphere.”

Levich’s theory involved the “polaron,” the quantum of electrostatic interaction energy (cf. phonon as the quanta of vibrational energy). Considering a dipole librator, more than one molecular diameter from a given ion, Levich pointed out that the librative energy of the water dipole would be about 0.001 eV. He conceived of polarons as transmitting this energy to a central ion.

However, and this was the essence of Levich’s view, any given ion would suffer fluctuations in its electrostatic interactions—brief moments in which the ion’s energy would be made more positive, less stable—and thus bring the energy levels of an ion adsorbed at an electrode into the range of the Fermi energy of electrons in the metal so that radiationless electron tunneling for electrons could occur.

How would these electrostatic fluctuations occur? Levich took 1 eV as the necessary activation energy and this implied a *coordinated* libration of about 1000 librators (cf. the energy of 0.001 eV per librator). Levich took the attitude that in any practical setup, “one could be sure” (no calculation was given) that at any given moment, there would be  $10^3$  molecules (among, say,  $10^{25}$ ) fluctuating in a coordinated way. These fluctuations could de-stabilize an ion at the electrode and it could undergo electron transfer. This model is described here because of its ingenious nature. It has

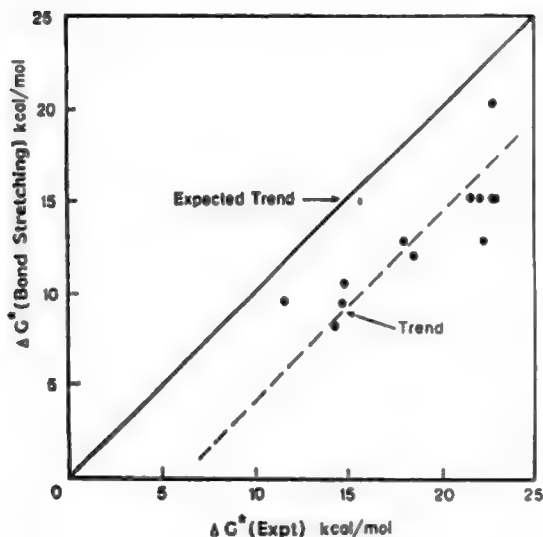


**Fig. 9.28.** Plot of  $\Delta G^*$  (bond stretching) vs.  $\Delta G^*$  (expt) for electrochemical redox reactions. (Reprinted from S. U. M. Khan and J. O'M. Bockris, in *Proceedings of The Symposium on the Chemistry and Physics of Electrocatalysis*, J. D. E. McIntyre, M. J. Weaver, and E. Yeager, eds., Vol. 84, p. 35, Electrochemical Society, 1984. Reproduced by permission of The Electrochemical Society, Inc.)

been shown (Sen, 1973), however, that it does not allow a sufficient number of activations per unit time to account for normal current densities.

### 9.7.6. The Vibron Model

In the Gurney model of charge transfer, species in solution were considered to be activated by thermal (not electrostatic) energy transfer from the surrounding solvent molecules. The solvent acts as a heat (phonon) bath to supply energy to reacting species, so that radiationless electron transfer becomes possible to or from some of them. However, Gurney did not make any quantum mechanical formulation of the thermal energy transferred to the central ion in a condensed medium.

According to the phonon-vibron coupling (PVC) model (Khan, 1993), an ion in a condensed medium becomes activated as a result of the transfer of energy to it from phonons produced by the surrounding solvent oscillators (Fig. 9.29). The phonon-vibron model can be visualized in the following way: Energy transfer occurs from the surrounding phonon waves by a coupling of the interaction between them and the energy of the inner sphere ion-solvent bond oscillators. Thus, energy is transferred to

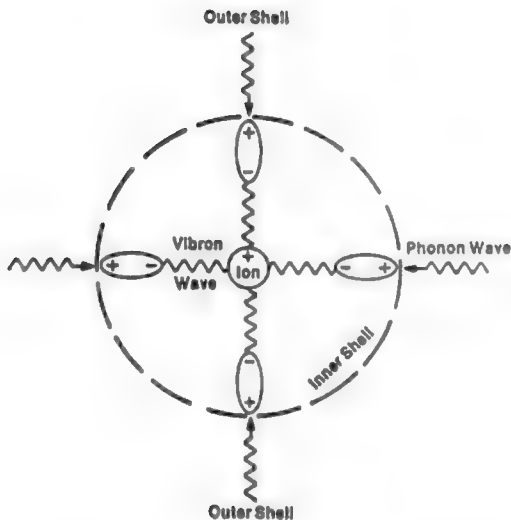


**Fig. 9.29.** Schematic diagram of a phonon-vibron coupling model. (Reproduced from J. O'M. Bockris and S. u. M. Khan, *Surface Electrochemistry*, Plenum, 1993, p. 448.)

solvent oscillators in contact with the ion, and the associated bond undergoes a transition from the ground state to a higher quantum state. When a sufficiently high quantum state is reached, radiationless electron transfer from or to an electrode can occur. The model has received a mathematical formulation. This model is a quantum mechanical rationalization of the George and Griffith thermal model described above. (See a formulation of the current potential relation in Section 9.9.)

## 9.8. BOND-BREAKING REACTIONS

### 9.8.1. Introduction

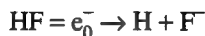
It has been a characteristic of the discussion that sprang from the Weiss-Marcus views that the comparison of theory with experiments was made largely with redox reactions. It is understandable that theorists have concentrated on these reactions, for they are simpler than the bond-forming reactions which are, however, much more numerous in reality than nonbonding redox reactions.

The future of calculations in electrochemical kinetics must involve bond-breaking reactions because most electrochemical reactions involve them. The work of Savéant (1992)



reactivates the earlier work of Gurney and of Butler (published in the 1930s) on proton transfer. Savéant used Morse's equation to represent the potential energy curves in place of the harmonic relations ( $U = kx^2$ ) used by others (see Fig. 9.30). It is of interest that Savéant concluded that about 80% of the activation energy was due to bond activation (George–Griffith model) and only 20% was connected with the electrostatics of solvent polarization (Weiss and Marcus).

Perez (1992) has made an analysis of



in solution using a Monte Carlo simulation (Fig. 9.31). Perez and co-workers concentrated on ascertaining whether the bond activation of George and Griffith and the electrostatic changes of Weiss and Marcus could be separated (as is usually assumed).

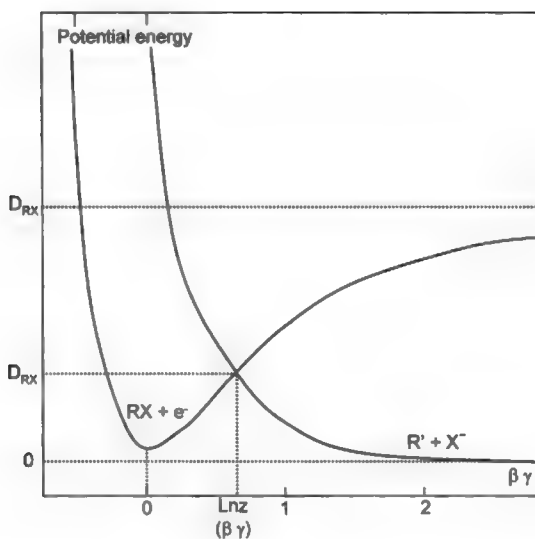


**Fig. 9.30.** Morse curves for the reactants and products at zero driving force ( $\nu$ , elongation of the  $R$ - $X$  distance from the equilibrium;  $B = \nu_0(2\pi^2\mu/D_{RX})^{1/2}$ ;  $\nu_0$ , vibration frequency;  $\mu$ , reduced mass;  $D_{RX}$ , bond dissociation energy). (Reprinted with permission of J. M. Savéant, *J. Am. Chem. Soc.* **109**: 6788 copyright 1992 American Chemical Society.)

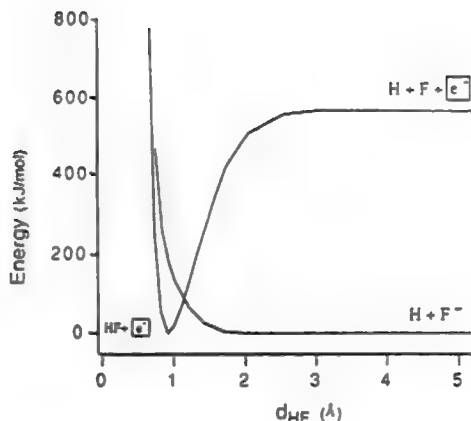
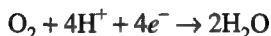


**Fig. 9.31.** Fitted cubic curves representing solute internal energy with respect to the  $d_{\text{HF}}$  distance, corresponding to the precursor and the successor complexes.  $e^-$  represents an electron inside an electrode. (Reprinted from V. Perez, J. M. Leuch, and J. Bertran, *J. Computational Chem.*, **13**: 1057. Copyright © 1992 John Wiley & Sons. Reprinted by permission of John Wiley & Sons, Inc.)

Their conclusion tended to the negative on this. They also concluded that quadratic approximations for energy variations were not applicable.

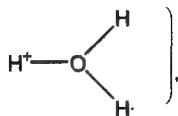
Bockris and Sidik (1998) tackled the calculation of the important bond-breaking oxygen reduction reaction



They followed the conclusion of Damjanovic and Brusic that the rate-determining step in acid solution was



and generated a potential energy surface that involved a combination of experimental values entered into Morse-type relations (for the O-D stretching and that of



but, in the interaction of O and OH with the metal, they used a semiempirical quantum mechanical technique due to A. B. Anderson called the atom superposition electron delocalization molecular orbital method (ASED-MO).

Three further calculations were made on the basis of the 6D potential energy surface generated:

1. The degree of nonadiabaticity was calculated using Landau–Zener formalism and involved a calculation of the transition matrix according to
2. A proton tunneling calculation involving a realistic energy barrier was made (and had a significant effect in increasing the reaction rate).
3. An entropy of activation was calculated so that the  $\Delta G^{\circ\ddagger}$  could be determined from the  $\Delta E^{\circ\ddagger}$  of the potential energy surface.

There is, of course, uncertainty in all such calculations made. When these are added together, the uncertainties are sufficiently great to make direct comparison with the experimental rate too exacting a comparison. However, calculations of the type made have the following contributions. First, they clarify what happens in the reaction concerned, particularly since it is a more complex bond-breaking case. Second, they indicate the direction for research on electrocatalysis and allow trends to be set as to what is demanded from the substrate to optimize the rate. Correspondingly, they allow calculation of the effect that changing the solvent has on the energy of activation.

## 9.9. A QUANTUM MECHANICAL FORMULATION OF THE ELECTROCHEMICAL CURRENT DENSITY

### 9.9.1. Equations

Consider an electron-transfer reaction:



One can write the rate of the electron-transfer process as proportional to the probability factors formulated originally by Gurney. Thus one obtains

$$i_c = eQ^{-1}\delta_{ci}\int \rho(E)f(E)P_T(E)P_{act}(E)dE \quad (9.40)$$

where  $P$  is the density of state;  $P_{act}$  is the probability of having the solution species in the activated state;  $P_T$  is the probability of tunneling through the barrier;  $\delta$  is the distance between the center of the ion in the OHP and the electrode surface and the normalization factor  $Q$  for the electrons in the various energy states can be expressed as



$$Q = \int_0^x \rho(E)f(E)dE = A \int_0^{\infty} E^{1/2}f(e)dE \quad (9.41)$$

After integration

$$Q = A(\pi/4)^{1/2}(kT)^{3/2} \quad (9.42)$$

where  $A$  is a constant, and the Fermi function has been approximated to an exponential function for  $E > kT$  to solve the integral in Eq. (9.41). However, this approximation to the Fermi function has been made to obtain an analytical value of  $Q$ , and numerical integration will be needed for accurate results.

Now, using Eq. (9.42) in Eq. (9.40), one obtains:

$$i_c = 2e\delta c_i(1/\pi)^{1/2}(kT)^{-3/2} \int E^{1/2}f(E)P_T(E)P_{act}(E)dE \quad (9.43)$$

when  $A$  cancels with the term  $A$  in  $\rho(E) = AE^{1/2}$ . In Eq. (9.43), the Fermi distribution function is expressed in the normal way, and  $P_T(E)$  can be given by the WKB tunneling expression. An extension of these equations using a Morse-type treatment for the potential energy of the ion–solvent interaction leads to current–potential curves that are linear, over about 1 eV, in potential range and thus comply with the need to replicate Tafel's law.

## 9.10. A RETROSPECT AND PROSPECT FOR QUANTUM ELECTROCHEMISTRY

### 9.10.1. Discussion

There is no doubt that this field, like few others, owes very much to its founder, Ronald Gurney, because of the fast start he gave it by applying quantum mechanics to interfacial electron transfers shortly after the publication of Schrödinger's wave equation (1926). The early seminal contributions (to which must be added that of J. A. V. Butler in the same period)<sup>22</sup> founded quantum electrochemistry and led to its broader development by Gerischer (1960), in particular the idea of the absolute scale of potentials and the equation

$$V_{abs} = V_{SHE} + 4.6$$

The essentials of quantum kinetics were in place by 1954, Weiss having added to the Gurney theory a comprehensive theory of redox reactions. By this date, tunneling, adiabatic and non-adiabatic electron transfer, the simplicity introduced by considering redox reactions between isotopes, the separate contribution from outer sphere and inner sphere, and in particular the equation for the reorganization energy involving  $\epsilon_{opt}$  and  $\epsilon_{stat}$  had all been published.

<sup>22</sup>Quantitative developments of these early formulations of a quantum theory of electrode processes were developed by Parsons (1951) and Conway (1957).

Marcus (1956) used some of these ideas (outer sphere and adiabatic only) to formulate an equation for the rate of electron transfer to redox particles, although in doing so he left out the influence of the first ion–solvent layer. He applied his equations at first to isotopic reactions, whereupon the expressions became very simple and attractive and hence were applied by many researchers, though to normal reactions. But when the original equations were used to calculate  $\Delta G^{\circ\ddagger}$  electrodic (for redox reactions in solution), the equations proved inadequate and even predicted maxima in Tafel plots. The stark lack of agreement [in Eq. (9.28)] between the experimental and theoretical electrostatics associated with the Weiss–Marcus theory shows that the Born equation is inadequate in determining the activation energy in a redox reaction, the disagreement with the Butler volume equation and Tafel’s law being a consequence of the harmonic approximation for the potential energy–distance relations.

A rescue in terms of agreement with experiment was offered in 1959 by George and Griffith, who formulated the first equation for  $\Delta G^{\circ\ddagger}$  dependent on the vibrational energy of the inner sphere (the first ion–solvent layer), which had been counted by Weiss but left out by Marcus. The importance of the somewhat vaguely defined outer sphere began to fade and the George and Griffith equation of 1959 was adopted into a revised equation for the rate given by Marcus in 1968.

These contributions were taken explicitly to a quantum mechanical level by Levich during the 1960s and then by Schmickler, who finally published an elegant summary of quantum electrode kinetics in 1996. Schmickler stressed the quantum mechanical formulation made by Levich, Dogonadze, and Kuznetsov. However, his summary of the quantum mechanical formulation of electrode reactions still possesses the Achilles heel of earlier formulations; it is restricted to nonbond-breaking, seldom-occurring outer-sphere reactions and involves the harmonic approximation for the energy variation, which is the main reason of such theories cannot replicate Tafel’s law (Khan and Sidik, 1997).

In parallel with the formulation of electrode kinetics found in Schmickler’s book, there began a new wave, led by those who broke through the barrier of the harmonic approximation and the outer-sphere reaction. The first of these new papers was authored by Savéant (1992). Savéant’s formulation implicitly uses the vibrational mode of activation (George and Griffith, 1959) to about 80%. Thus, Savéant opened a gate to a development that will clearly dominate the field in the future, namely, computer simulation studies, such as those published by Benjamin, Berkowitz, Khan and Sidik, Perez, Voth, and others (1998)—and, above all, to a theory of bond-breaking reactions to supplement and replace the primitive models in the 1930s–1950s.

## Further Readings

### Seminal

1. R. W. Gurney, *Proc. Roy. Soc. London*, **A134**: 127 (1931). The founding paper of quantum electrochemistry. Treatment of quantum mechanical transfer applied to protons at an electrode. However, the bond to the metal was not made.

2. J. Horiuti and J. C. Polanyi, *Acta Physicochim. URSS* **2**: 505 (1935). Potential energy curves given for the discharge of protons onto metals. Effect of change of metal bond shown; foundation of electrocatalysis.
3. J. A. V. Butler, *Proc. Roy. Soc. London* **A157**: 423 (1936). Quantum mechanical Gurneyian approach corrected for bonding to metal.
4. R. Parsons and J. O'M. Bockris, *Trans. Faraday Soc.* **47**: 914 (1951). Gurney–Butler approach applied quantitatively to proton discharge (numerical).
5. J. Weiss, *Proc. Roy. Soc. London* **A222**: 128 (1954). First electron transfer theory in terms of electrostatic changes, including energy of reorganization,  $\epsilon_{\text{opt}}$  and  $\epsilon_{\text{stat}}$ , adiabatic and nonadiabatic theory, and much else.
6. R. Kubo and Y. Toyozawa, *Prog. Theoret. Phys.* **130**: 411 (1955). Early formation of reorganization energy in electron transfer.
7. R. A. Marcus, *J. Chem. Phys.* **24**: 966 (1956). Follows Weiss-like model, but explicitly applied to rate calculation. Harmonic oscillators.
8. B. E. Conway and J. O'M. Bockris, *Canad. J. Chem.* **35**: 1124 (1957). Gurney–Butler approach to electrochemical desorption of adsorbed H. 3D models of potential surface for the reaction (numerical).
9. P. George and J. Griffith, in *Enzymes*, P. D. Boyer, H. Lardy and K. Myrback, eds., Vol. 1, p. 347, Academic Press, New York (1959). The first quantitative formulation of vibrational activation for redox reactions from first-layer ligands.
10. V. Levich and R. R. Dogonadze, *Dokl. Akad. Nauk. SSSR* **124**: 123 (1959). Hamiltonian formulation for electron transfer; dielectric polarization approach. Quantum aspects of Weiss–Marcus model developed.

The basic division between the roots and the “more modern” papers is arbitrary (1931–1964 is about one generation). The basic theory of proton and electron transfer at electrodes was formulated by Gurney in 1931 and by Weiss in 1954.

### Modern

1. R. A. Marcus, *J. Chem. Phys.* **93**: 679 (1965). The addition of the George and Griffith theory (vibrational activation) to electrostatics of electron transfer.
2. J. O'M. Bockris and D. B. Matthews, *J. Chem. Phys.* **44**: 298 (1966). Quantal properties of the proton experimentally established.
3. V. G. Levich, in *Physical Chemistry: An Advanced Treatise*, H. Eyring, D. Henderson, and W. Jost, eds., Vol. 9B, Ch. 12, Academic Press, New York (1970). A review stressing polaron theory in a rationalization in quantal terms of outer-sphere activation.
4. J. O'M. Bockris, D. B. Matthews, and S. U. M. Khan, *J. Res. Inst. Catal.* **22**: 1 (1974). The  $\Delta G^{\text{ox}}$  calculated from the electrostatic model of Weiss–Marcus is discrepant with experimental trends, but a vibrational energy based theory fits well.
5. S. U. M. Khan, P. Wright, and J. O'M. Bockris, *Elektrokhimya* **13**: 914 (1977). The first application of time-dependent perturbation theory to quantum electrode kinetics; redox reactions.
6. J. O'M. Bockris and S. U. M. Khan, *Quantum Electrochemistry*, Plenum, New York (1979). A monograph.

7. W. Schmickler, *J. Electroanal. Theory* **100**: 533 (1979). Theory of electrodic currents through coatings (and oxide films) in terms of resonance tunneling. Tafel lines curve.
8. W. Schmickler, *J. Electroanal. Chem.* **204**: 31 (1986). A discussion of the influence of the choice of Hamiltonian on electron-transfer theory.
9. L. A. Curtis, J. W. Halley, J. Hautmann, and A. Bakman, *J. Chem. Phys.* **86**: 2319 (1987). Molecular dynamics gives "activation energies" in agreement with experiment 3 times larger than those of Weiss–Marcus.
10. J. W. Halley and J. Hautmann, *Phys. Rev. B* **38**: 11704 (1988). First molecular dynamic simulation of interfacial electron transfer.
11. J. O'M. Bockris and J. Wass, *J. Electroanal. Chem.* **267**: 325 (1989). Electrode kinetics at the superconductor/solution interface.
12. A. M. Kuznetsov, in *Modern Aspects of Electrochemistry*, J. O'M. Bockris, B. E. Conway and R. White, eds., Vol. 20, Ch. 2, Plenum, New York (1990). A review stressing the dielectric continuum viewpoint.
13. W. Schmickler, *J. Electroanal. Chem.* **284**: 269 (1990). A theory of the variation of the transfer coefficient with temperature.
14. A. B. Anderson, *J. Electroanal. Chem.* **280**: 37 (1990). Molecular orbital theory and the influence of electrode potential.
15. C. E. D. Chidsey, *Science* **251**: 919 (1991). Theory of electron transfer at gold covered by a thick layer of organic material.
16. J. M. Savéant, *J. Am. Chem. Soc.* **109**: 6288 (1992). Anharmonic analysis of  $R-X + e_0^- \rightarrow R + x^-$ . Activation energy is made up of 80% bond breaking.
17. V. Perez, J. M. Leach, and J. Bertran, *J. Computational Chem.* **13**: 1057 (1992). A Monte Carlo approach to bond-breaking reactions at electrodes.
18. M. J. Weaver, *Chem. Rev.* **92**: 463 (1992). A review, oriented to mechanism determination for redox reaction.
19. A. B. Anderson, *Int. J. Quantum Chem.* **49**: 581 (1994). How electron density affects the electron-transfer rate.
20. P. J. Russky and J. D. Simon, *Nature* **370**: 263 (1994). The solvent medium affects the rate of electron transfer.
21. D. A. Rose and E. Benjamin, *J. Chem. Phys.* **100**: 3545 (1994). Molecular Dynamic Simulation of the free energy function in  $Fe^{3+} + e \rightarrow Fe^{2+}$ .
22. W. Schmickler, *Chem. Phys. Lett.* **237**: 152 (1995). Electron-transfer and ion-transfer reactions at electrodes distinguished.
23. J. B. Strauss, A. Calhoun, and G. Voth, *J. Chem. Phys.* **65**: 529 (1995). Molecular dynamic (MD) simulation of charge transfer at the interface.
24. Z. Nagy, J. P. Bleau, N. C. Hung, L. A. Curtiss, and D. J. Zurewski, *J. Electrochem. Soc.* **142**: 1887 (1995).
25. W. Schmickler, *Interfacial Electrochemistry*, Oxford University Press, Oxford (1996). A 284-page encapsulation of selected elements of the theory assuming harmonic oscillators.
26. A. Calhoun and G. Voth, *J. Phys. Chem.* **100**: 10746 (1996). Molecular dynamic simulation in redox reactions.

27. E. Benjamin, in *Modern Aspects of Electrochemistry*, R. H. White, B. E. Conway, and J. O'M. Bockris, eds., Vol. 31, Ch. 3, Plenum, New York (1997). Molecular dynamic simulation in interfacial electrochemistry.
28. S. U. M. Khan, in *Modern Aspects of Electrochemistry*, R. H. White, B. E. Conway, and J. O'M. Bockris, eds., Vol. 31, Ch. 2, Plenum, New York (1997). Quantum mechanical contributions to electrode kinetics.
29. J. O'M. Bockris and R. Sidik, *J. Electroanal. Chem.* **448**(2): 189 (1998). A semiquantitative quantum theory of the oxygen reduction reaction.

## APPENDIX. THE SYMMETRY FACTOR; DO WE UNDERSTAND IT?

### A.1. Introduction: Gurney–Butler

When the symmetry factor was introduced by Volmer and Erdey–Gruz in 1930, it was thought to be a simple matter of the fraction of the potential that helps or hinders the transfer of an ion to or from the electrode (Section 7.2). A more molecularly oriented version of the effect of  $\beta$  upon reaction rate was introduced by Butler, who was the first to apply Morse-curve-type thinking to the dependence of the energy–distance relation in respect to nonsolvent and metal–hydrogen bonds.

Consider a linear analogue of Fig. 9.9. This figure is a simplification<sup>23</sup> of the potential energy–distance relations when there is a vibrational stretching of the  $\text{H}^+ - \text{O}$  bond in the system  $\text{M}(\text{e}) + \text{H}^+ - \text{OH}_2$  or the  $\text{M} - \text{H}$  bond in the system  $\text{M} - \text{H} + \text{H}_2\text{O}$ . It is concerned with proton stretching as a precondition for electron tunneling. It is obvious (Fig. 9.28) that

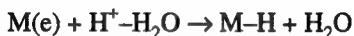
$$\frac{\overrightarrow{\Delta\epsilon}}{\overrightarrow{\Delta E_0}} = \frac{AB \tan \gamma}{AB(\tan \gamma + \tan \theta)} = \frac{\tan \gamma}{\tan \gamma + \tan \theta} \quad (\text{A.1})$$

But  $\tan \gamma / (\tan \gamma + \tan \theta)$  is none other than the symmetry factor  $\beta$  of Eq. (7.24). This is perhaps a surprising realization. The ratio  $\overrightarrow{\Delta\epsilon} / \overrightarrow{\Delta E_0}$ , which is so crucial to the fundamental picture of charge transfer according to the Gurney model involving a critical bond stretching as a precondition for tunneling, is in fact the symmetry factor  $\beta$ . Since, however,  $\beta$  has already been shown to be equal to the change in the activation energy of the reaction produced by a change  $\Delta\phi$  in the potential difference from the metal to the OHP, one can write

$$\frac{\overrightarrow{\Delta\epsilon}}{\overrightarrow{\Delta E_0}} = \beta = \frac{\text{Change in activation energy}}{\text{Change in interfacial potential}} \quad (\text{A.2})$$

<sup>23</sup>It will be noted that if the initial state involves a particular electronic state (e.g., the ground state), then that state is considered to be maintained throughout the passage of the electron. In other words, it is assumed that there are no transitions to a higher electronic state during the reaction. Such reactions are termed “adiabatic.”

The picture begins to come somewhat into focus. Starting off with some basic mechanics of electrons, one was able to define the quantum mechanical condition for the tunneling of electrons from a metallic donor to electron acceptors through an electron–energy barrier. The tunneling condition could be expressed in terms of an energy barrier for ion movement, e.g., the movement of protons toward the metal in the reaction:



Tunneling becomes possible only when the proton has reached a position between the metal surface and the  $\text{H}_2\text{O}$  corresponding to the barrier peak in, e.g., Fig. 9.32. The former assumption that a reaction step occurs when the energy of the system climbs to the peak is correct, but now a rational quantum mechanical basis has been given, and the electrons rather rightfully have been placed in the central role in charge transfer, instead of the ions and bond stretching as in the earlier model. The ion stretching is very important, but this is so *only because of the need for the tunneling electrons to find a state in the acceptor particle equal in energy to the one (in the metal) from which they came, which is the condition for radiationless tunneling.*

The energy  $\Delta\epsilon$  required to stretch the  $\text{H}^+ - \text{H}_2\text{O}$  bond to the critical condition for electron tunneling is a *fraction* of the energy gap  $\Delta E_0$ , which must be closed to make

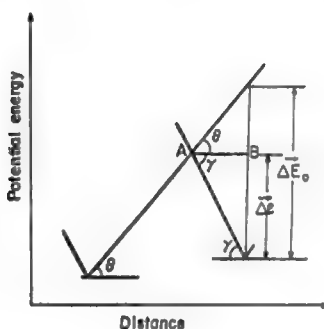


**Fig. 9.32.** A linear analogue to the potential energy barrier for electron tunneling shows that the ratio of  $\tan \gamma$  to  $\tan \gamma + \tan \theta$  is equal to the ratio of energies  $\Delta H_-$  to  $\Delta H_0$ , the ratio of the tangents being equal to the symmetry factor  $\beta$ . This gives the symmetry factor new physical meaning.

tunneling possible. The fraction  $\vec{\Delta\epsilon}/\vec{\Delta E}_0$  of the earlier discussion turns out to be none other than the symmetry factor  $\beta$  of the former treatment. This is the fundamental theory of the symmetry factor in terms of electron and proton mechanics. It bears out the following intuition, which arose from a comparison of current–potential laws for electrode–electrolyte and semiconductor  $n$ – $p$  junctions: A symmetry factor arises in the relation of current to potential when atom movements are a prerequisite for charge transfer across an electrified interface, but is absent when this is not so. Obtaining  $\beta$  in this way gives a more or less constant value over more than 1 eV. Hence, *Tafel's law is deducible*. It also rationalizes the extreme values discussed in the next section.

## A.2. Activation less and Barrierless

The approach to  $\beta$  given above is a simplification, although it does show why the effect of the change in the electrode potential on the charge-transfer rate is less than that expected if the full potential were applied, an important realization. Another virtue of the early theory is the basis it gives to a theory of electrocatalysis.

Interesting possibilities arise in these potential energy–distance curves if they are not drawn in the extreme simplification of straight lines (see Fig. 9.33), but with the natural curvature that potential energy–distance relations have. Thus, Fig. 9.33 shows the simplified situation where, from the formula given above for  $\beta$  it can be seen that with approximately equal slopes of the potential energy curves near the intersection point, equal slopes of the value of  $\beta$  will be about one-half, as is often observed.

On the other hand, what happens when the overpotential is increased sufficiently? Then one gets a curve where one can pass to the initial state from the final state without any activation at all (Kabanov, 1936) [Fig. 9.33(b)]. Such a state would give rise to the “end of electrode kinetics”; there would no longer be any further dependence of the reaction rate upon potential.

Now, another possibility is to consider what would happen if one lowered the overpotential sufficiently. Then one gets what is shown in Fig. 9.33(c), which some workers (Krishtalik) have called *barrierless processes* because the transfer between the initial and final state becomes simply the heat of the reaction.

The interpretation of  $\beta$ , then, in terms of the gradients of the potential energy surfaces in electrode kinetics seems a reasonable one, and it does lead to values of  $\beta$  that are in fairly good accord with those observed. They are always near one-half but seldom exactly one-half, and that is just what potential energy surfaces indicate when calculations are made.

## A.3. The Dark Side of $\beta$

However, this “everything is alright” attitude toward  $\beta$  is less than justified, and that is why we have put the discussion of it in an appendix. It is really work in progress and the understanding of  $\beta$  is still in a state in which one might say “it may be like this . . . .”

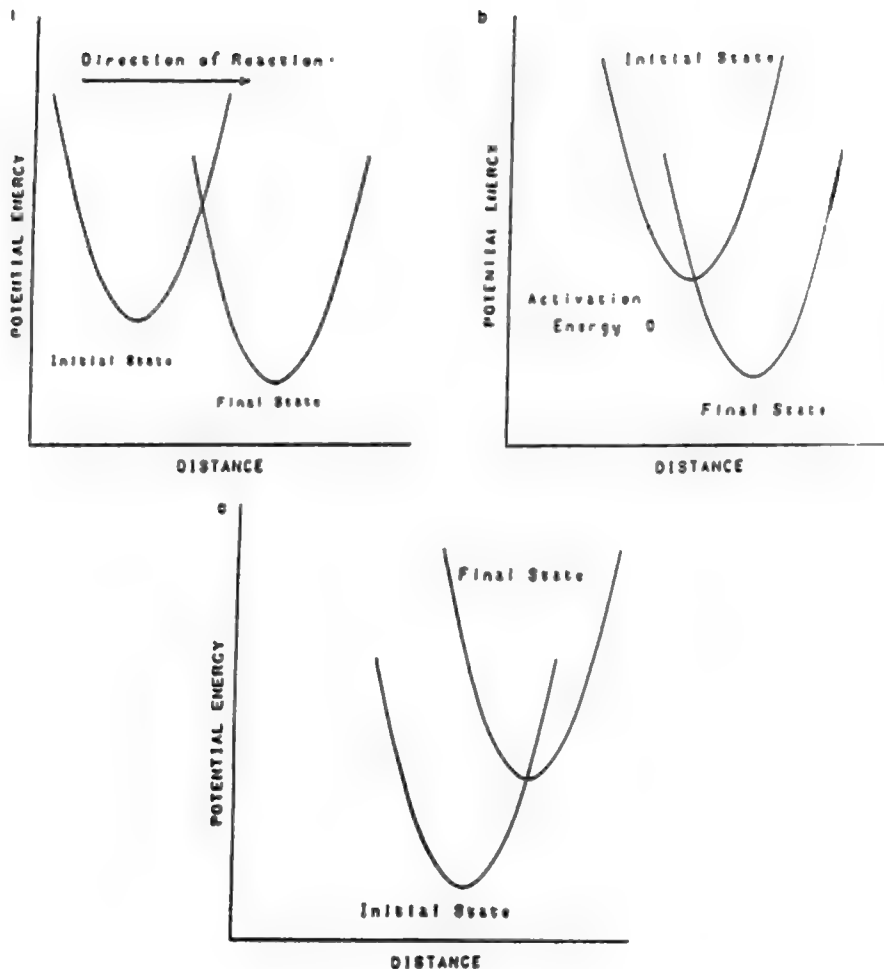


**Fig. 9.33.** Potential-energy–distance curves for (a) a typical electrode reaction, (b) an activationless electrode reaction, and (c) a barrierless electrode reaction. (Reprinted from J. O'M. Bockris and S. U. M. Khan, *Surface Electrochemistry*, Plenum, 1993, p. 278.)

There are three things that make us want to do more work to obtain a more precise picture of  $\beta$ :

1. As shown in Section (7.2), the  $\beta$  ("the symmetry factor") is often observed as part of the "transfer coefficient," which is a more all-embracing coefficient that multiplies the potential at the interface and involves considerations of where



the charge-transfer step comes in a sequence of consecutive reactions. In these cases one can get values of  $\alpha$  (the multistep version of  $\beta$ ) that are far from one-half in an entirely rational way which can be understood. So, if one finds an anomalous value of  $\beta$  such as 0.25, one should not necessarily assume that one has a vastly nonsymmetrical barrier, but go back to the general equation that relates the multistep  $\alpha$  to the single-step  $\beta$  and see if a rationalization can be made with  $\beta$  near one-half.

2. In *some reactions* (Conway, 1985) it seems that  $\alpha$  (perhaps  $\beta$ ) varies with temperature in a way that would be difficult to explain in terms of the potential energy curve explanation for  $\beta$  that is given here.
3. There is no doubt [see Fig. 9.25(e)] that the constancy of the slope of the Tafel equations (and therefore of  $\alpha$  and probably  $\beta$ ) stretches over a large potential range and for some ion-transfer reactions may be more than 1.5 V. It seems difficult to fit this remarkable constancy of  $\beta$  over such potential intervals. What is needed are experimental details on much longer potential ranges in the measurement of Tafel lines, particularly for redox processes where the potential range of the Tafel lines examined so far is more in the region of 0.6 V and not 1.5 V as for the ion-transfer reactions. In addition, an extended examination of the temperature dependence of  $\beta$  is needed. The coefficient  $\beta$  in electrode kinetics has exhibited anomalous aspects since its introduction into electrode kinetic theory by Erdey-Gruz and Volmer in 1930. In summary,  $\beta$  should be constant with temperature, but it sometimes varies; it should vary with potential, but over a surprisingly long range of potentials.

## EXERCISES

1. (a) Describe in terms of a diagram the “vacuum scale of potentials.” An electrode has a potential on the standard H scale of +0.4 V. Find its potential in the vacuum scale of potentials. (b) What would be its *energy* in electron volts? (Bockris)
2. (a) Draw the fundamental electrochemical cell: two electrodes of different metals in solution, involving a metal–metal boundary and a voltmeter in the circuit. (b) Using this diagram, point out the various sites of potential differences in the electrochemical cell, at open circuit. (c) Which potential differences are involved in the vacuum scale of potentials? (d) In what way does the potential energy of a stationary electron at infinity come into the considerations? (Bockris)
3. All scientists know Maxwell’s law concerning the fractions of molecules present at a certain speed and how this fraction varies with their speed. This is the best-known distribution law. State other distribution laws and represent each graphically in an electrochemical context. (Bockris)
4. (a) What does the well-known Fermi distribution law represent? Give a *precise* answer. Quantum mechanical “tunneling” of electrons was introduced into

electrochemistry by Gurney in 1931 (cf. Schrödinger's equation, 1926). Gurney calculated (Section 9.4.1) that the probability of the rate of escape of electrons from a metal *over* a barrier (i.e., the work function) would be too small to be consistent with the observed current densities of electrochemical kinetics.

In electrochemistry, electron tunneling in cathodic reactions takes place from the Fermi level to some specific energy state in ions in solution (radiationless tunneling). In Gamow's equation, is implicitly assumed that there is an energy state available to receive the tunneling electron. (b) Does this mean that simple calculations of probability of transition made with the Gamow approximation are too high or too low compared with those that take into account the probability of the presence of an appropriate empty state? Reason out your answer. (Bockris)

5. One equation that does express the shape of the potential-energy–distance curve for the interaction of two particles is the Morse equation<sup>24</sup>:

$$U_r = D_e(1 - e^{-a(r-r_e)})^2$$

where  $D_e$  is the dissociation from energy, the distance apart,  $r$  of ion and solvent molecule or the metal and an adsorbed radical, that distance at equilibrium, and  $a$  is a constant. (a) Find the force constant-near equilibrium for the interaction expressed by this equation. Show that for  $a(r - r_e) < 1$ , the oscillations of the interacting pair are harmonic. (b) Is this harmonic oscillator condition likely to remain for solvent movements in electron transfer? Discuss! (Bockris)

6. Define the following terms: librator, polaron, fluctuation of the ground state, phonon, vibron, activationless, and barrierless. (Sidik)
7. What is the physical meaning of  $E$  in the Fermi–Dirac law? (b) How is it related to  $\mu_e^M$  in Fig. 9.4? (Sidik)
8. (a) Determine the WKB tunneling probability of an electron from the Fermi level of a Pt electrode to an equally distributed energy state of an  $\text{H}_3\text{O}^+$  ion in solution near the electrode at a distance of  $d = 3 \text{ \AA}$  when the barrier height,  $U_m = 3.5 \text{ eV}$  measured from the Fermi level, (b) What is the tunneling probability when the barrier is assumed to be parabolic? (c) What is the tunneling probability when the barrier is of a square type? (Khan)

<sup>24</sup>Applying the Morse equation to the approach of atoms to each other in solution is an easy (partial) way out of something quite difficult. However, Morse's equation pertains to the interaction of two isolated particles in the gas phase. In solution, no particle can be isolated, and many interact. There are now computer programs that allow a more accurate version of  $U_r$ 's to be obtained, although basically they are still particle–particle two-body interactions (Section 5.3.4). At least for heuristic purposes, it is good to have (as in the Morse equation) an analytical equation that can be studied and that gives the student “a feel” for what is going on.

9. What is the Born solvation energy of  $\text{Fe}^{3+}$  in water having a dielectric constant of 78, and what is its value when it is in ethanol, which has dielectric constant of 36? (b) What is the self-energy of  $\text{Fe}^{3+}$  in a vacuum? (c) Is there any meaningful difference between the Born solvation energy and the self-energy of an  $\text{Fe}^{3+}$  ion? The radius of this ion is  $0.64 \text{ \AA}$  and the diameter of water is  $2.76 \text{ \AA}$ . (c) Where do you think there is a possible flaw in Born's solvation equation? (Khan)
10. (a) Define nonadiabaticity for an electron-transfer reaction, e.g.,  $\text{Fe}^{3+} + \text{e}_0^- \rightarrow \text{Fe}^{2+}$ . (b) Does temperature affect the degree of nonadiabaticity of a reaction? (c) Discuss your answer. (Sidik)
11. Calculate the tunneling probability of an electron and proton through a parabolic barrier of height  $1 \text{ eV}$  and width of  $20 \text{ \AA}$ . Assume  $E_{\text{particle}} = 1/2$  barrier height and that a receptor state is available for the tunneling particle. (Sidik)

## PROBLEMS

1. What does the phrase "electrons in solution" mean? If one injects electrons into an aqueous solution, they have a short lifetime and rapidly enter into a reaction with the species present. Which of the following answers is correct? (a) The "energy of an electron in solution" is valued only in a thought experiment. There is no electron present in the energy gap region of an ideal pure semiconductor (undoped), yet it has a Fermi level energy halfway between the conductivity and valence bonds. This Fermi energy of the nonexistent electrons in the semiconductor is analogous to the Fermi energy of the nonexistent electron in solution. (b) The electrons in solution are real enough. They are the electrons in the electronic shells of ions in solution—those that take part in reactions with electrodes. (Bockris)
2. Electrochemists take the electrons they deal with in metal electrodes as those having an energy equal to that of the "Fermi level." (a) What, precisely, is this Fermi level? Draw a diagram to illustrate your answer. (b) What kind of energy is referred to at which level of electrons? (c) Is it a kinetic or a potential energy, or a sum of both?

Electrochemists implicitly assume that the number of available electrons above or below the Fermi level is so small that it may be neglected. (d) Examine this assumption at two temperatures,  $300$  and  $1000 \text{ K}$ .

(e) Find the probability of occupying empty electronic states at the Fermi level; at an energy  $0.1 \text{ eV}$  above and below the Fermi level; at  $0.5 \text{ eV}$  above and below the Fermi level; and in a metal having a Fermi energy of  $5 \text{ eV}$ . (f) After you have made the calculations, state your now informed opinion as to the degree of correctness of the usual electrochemical assumption that electrons that take

part in electrochemical reactions all come from the Fermi level. Distinguish carefully between the situation at 300 and at 1000 K. (Bockris)

3. (a) Write the definition of the “density of states.” (b) What are its dimensions? (c) What does it mean, physically?

The normal expression for the density of states in a metal is an approximation based on the “free electron” theory of metals. It is possible to determine this quantity experimentally. (d) In what part of the density-of-state–energy relation is there likely to be the greatest discrepancy with free electron theory and why?

The Fermi distribution law deals with the probability of occupancy by electrons in metals of states of a given energy. The density of states represents a number of states per unit volume having a given energy. (e) What, then, is an expression for the number of electrons per cubic centimeter having an energy between  $E$  and  $E + dE$ ?

4. According to the Frank–Condon principle, electronic transitions occur so much faster than nuclei so that during an electronic transition, the nuclei involved can be considered to be stationary. Consider a hydrated ferric ion in the first layer of ions going out from the electrode. Most of the electrons waiting their chance to jump to a state of equal energy in a hydrated ion have an energy near ( $\pm 0.05$  eV) the energy of electrons in the Fermi level. The ferric ion, under the influence of its interaction with its hydrating water, represents a fluctuating system having many vibration–rotation electronic states. There will be a certain probability of a suitable electronic state being present. (Bockris) Describe the applicability of the Frank–Condon principle to this electronic transition. It clearly creates a ferrous ion, but what of the hydration sheath for a short time around the moment the electrons jump? What is its solvation energy for a time just after the arrival of the electron? (Bockris)
5. Weiss published a paper in 1954 giving a number of modeling ideas concerning the molecular-level mechanism of redox reactions in solution. In 1956 Marcus published (independently) a paper containing similar ideas, but also applied them to electrode reactions. From these works there followed an equation:

$$\Delta G^{\text{ox}} = \frac{(E_s + \Delta G^\circ)^2}{4E_s}$$

where  $\Delta G^{\text{ox}}$  is the standard free energy of activation,  $E_s$  is the “reorganization energy”, and  $\Delta G^\circ$  is the standard free energy of the chemical reaction. In an electrochemical reaction,  $\Delta G^\circ$  becomes  $\Delta G^{\text{ox}} = \Delta G^\circ \pm \eta F$ , where  $\eta$  is the over-potential corresponding to a given current density. Show that such an equation cannot give rise to Tafel’s law. (Bockris)

6. Data are available for many electrochemical reactions (Fig. ??) which show that a Tafel relation of good linearity exists over a relatively large potential region, e.g., up to 1 V. This implies that the symmetry factor,  $\beta$ , and in some cases the transfer coefficient,  $\alpha$ , are potential invariant over the range stated. Examine this result, first in terms of the Weiss–Marcus theory and then in terms of equations that would represent the anharmonicity of the relation for the potential energy of ion–solvent bonds. Regions of great constancy of  $\beta$  (or  $\alpha$ ) imply a force constant independent of potential. Can you rationalize this? (Bockris)

## MICRO RESEARCH PROBLEM

1. In the Weiss–Marcus theory of “reorganizational energy” that leads to an expression for the rate of redox reactions, there are several concepts that need investigation. You should refresh your knowledge of this theory from what is given in this book and then use the references in the reading list to take you further in thinking about the following questions:

In some presentations of this theory, the Frank–Condon principle is mentioned, (a) Why do you think that is? (b) In what part of the theory do you see this principle applied?

In the theory, two dielectric constants are used. One is the normal dielectric constant for dilute aqueous solutions, which is around 80. However, there is also an  $\epsilon_{\text{opt}}$ , the “optical” dielectric constant, the one that is the dielectric constant for happenings at very low times, before any part of the surrounding system reacts to the applied field, except the electronic shells of the solvent. (c) What is the physical argument in Weiss’s paper, which first introduced an equation containing the element  $(1/\epsilon_{\text{opt}}) - (1/\epsilon_{\text{stat}})$ ? (d) What does this reorganization energy mean for molecular movements? Spell out your answer in clear language, with diagrams.

A simple system used to illustrate the Weiss–Marcus theory is the cathodic reduction of  $\text{Fe}^{3+}$  to  $\text{Fe}^{2+}$ . Go back to Chapter 2 and review your ideas on hydration shells; find this quantity for  $\text{Fe}^{3+}$  and  $\text{Fe}^{2+}$ . (e) Using molecular models, calculate a radius for the  $\text{Fe}^{3+}-(\text{OH}_2)_n$  hydrated ion and calculate a corresponding value for  $\text{Fe}^{2+}-(\text{OH}_2)_m$ . In the Weiss–Marcus theory, in the calculation of the reorganization energy, these radii are taken as the same. (f) Correct? Discuss! If not, calculate the error in  $E_s$  arising from the assumption.

In the Marcus version of the theory,  $\Delta G^\circ$ , the standard free energy change of the reaction considered is taken as zero. (f) When will this apply? (h) What error in the calculation of the energy of activation would neglect of  $\Delta G^\circ$  cause in the calculated energy of activation for  $\text{Fe}^{3+} + e_0^- \rightarrow \text{Fe}^{2+}$ ? Give a list of papers and books you consulted in researching your answer.

# INDEX

- Absolute electrode potential, 1059, 1457
  - definition, 837
  - measurement, 840
  - for reference hydrogen electrode, 870
- Absorbance, 800
- Absorption coefficient, ellipsometry, 1148, 1152
- Absorption spectroscopy, and electrokinetics, 1145
- ac impedance, information on electrode
  - processes, 1131, 1134
  - bridges, 1128
- Acetonitrile, adsorption, 981
- Activation overpotential, 1232
- Activation potential, in polarography, 1244
- Active sites for adsorption, 928
- Activity
  - mean ionic, 865
- Additives, during electrodeposition, 1339
  - selectivity of, 1339
- Admittance, 1130
- Adsorbate, 969
- Adsorbed ions, specifically, 886
- Adsorbent, 969
- Adsorption, 971
  - contact, 959
  - electrical field, 929
  - and equation of state, 931
  - ionic, summary, 964
  - irreversible, 969, 970
  - lattice gas models of, 965
  - nonlocalized, 928, 958
  - organic and inorganic, 972
  - of intermediates, 1192
- Adsorption (*cont.*)
  - and partition functions, 937
  - theoretical methods to study, 965
- Adzic, 1207
- Alloy formation during underpotential deposition, 1316
- Aluminum deposition, 1343
- Ampere, 1423
- Amyl-alcohol, adsorption, 979
- Anderson, 1478
- Angerstein-Kozłowska, 1203
- Anharmonic curves, 1487
- Anode, 1050, 1348, 1359, 1361
- Argade, and absolute electrode potential, 839, 840, 1457
- Armstrong, 1401
- Arrhenius equation, 1115, 1507
- Arrhenius, Svante, 1473
- Asaki, 1159, 1313
- Auger electron spectroscopy (AES), 787
- Automated mechanism analysis in
  - electrochemical measurements, 1163
- $\beta$ -particles**, 804, 806
- Backscattering factor, 806
- Bagotskii, oxidation of methanol, 1270
- Barton, 1098, 1338
- Batteries and fuel cells, 1040
- Baxendale, 1122
- Benjamin, 1487
- Benzene oxidation, 1377
- Berkowitz, potential energy curves, 1487
- Beer-Lambert law, 800

- Binding energy
  - in electrodeposition, 1301
  - of the electron to the metal, 834
  - of hydrogen, 1191
  - of water, 1191
- Binning, 1158
- Bioelectrocatalysis, 1287
  - enzymes, 1287, 1495
  - definition, 1287
- Biosensors, 1290
- Blomgren, and organic adsorption, 982
- Bockris, 1273, 1402, 1459, 1466, 1475, 1489, 1497, 1499
  - and absolute electrode potential, 839, 840
  - and bond breaking reactions, 1520
  - and cryostat, 1121
  - and electrode kinetics, 1091
  - and electrode potential, 1457
  - and electrodeposition, 1308, 1310
  - and isotherms, 936
  - and material failure, 1340
  - and microelectrodes, 1098
  - and quantal calculations, 1495–1497
  - scanning tunneling microscopy, 1158, 1273
  - and surface potential determination, 893
- Bockris–Devanathan–Muller model of water, 898
- Bockris–Habib’s model of water, 899
- Bode plot, impedance, 1129
- Bohr, 1455
- Bond, 1099
- Bond-breaking reaction, 1518
  - potential energy curves, 1519
  - bond activation, 1519
  - George–Griffith model, 1519
  - Wiss–Marcus model, 1519
- Bond strength, in electrocatalysis, 1287
- Boulders, electrodeposition, 1336
- Bowden, 1402
- Bowden, transients, 1401, 1409
- Brenner, alloy formation, 1316
- Breyer, ac polarography, 1425
- Brusic, 1154
- Buck, 1121
- Buffer in electrokinetic measurements, 1122
- Butler, J. A. V., 1048, 1401, 1503, 1526
- Butler–Volmer, equation, 1052, 1053, 1066, 1067, 1075, 1176, 1188, 1231, 1249, 1348, 1361, 1456
  - and electrodeposition, 1205
  - high overpotential region, 1054, 1179
  - low overpotential region, 1054, 1179, 1185
- Butler–Volmer, equation (*cont.*)
  - multistep reaction, 1176, 1179
  - non-equilibrium, 1191
  - theory of diffusion, 1217
- Butyl compounds, adsorption, 979
- Cabrera, electrodeposition, 1324
- Cahan, 1154
- Calomel electrode, 815, 1109
- Capacitance, 1120
  - differential, 861, 910, 911
  - integral, 861, 959
  - of the interface, determination, 859, 911
  - of condenser, 861
- Capacitor–resistor, impedance of, 1125
- Capacity
  - of contact adsorption, 960, 963
  - curve, 960
    - and the capacity hump, 962
    - and the capacity minimum, 962
    - and the constant capacity region, 961
  - curves and metal properties, 887, 888
  - of diffuse charge, 884
  - of Gouy–Chapman, in Stern model, 884
  - of Helmholtz–Perrin, in Stern model, 884
  - interfacial, 959
  - of parallel plate condenser, 875
  - potential curve, 965
- Capillary electrometer, 849
- Carslaw, 1216
- Catalysis, mechanism of electrodic reactions, 1258
  - in redox reactions, 1275
  - and enzymes, 1287
- Cathodic deposition, 1307
- Cathode, 1050, 1348, 1359, 1361
- Chandrasekaran, methanol oxidation, 1269
- Chapman, 877
- Charge carriers at the electrode, concentration of, 1247
- Charge density of electrode, determination, 858
- Charge of double layer, 1217
- Charge transfer, 1213
  - mechanism, 1294
  - overpotential and, 1172
  - rate determining step and, 1179
  - steady state and, 1213
  - transport in electrolyte, 1211
- Charge transfer, equilibrium at interface
  - kinetic treatment, 1058
  - Nernst’s equilibrium treatment, 1058
  - polarography, 1240
  - thermodynamics, 1057

- Charge transfer reaction of organic molecules, 969, 970
- Charge transfer resistance, 1056
- Charge transfer overpotential, 1231
- Charge transfer, partial, 922, 954
- Charges in solution, 882
  - chemical interactions, 830
- Charging current, 1056
- Charging time, 1120
- Chemical catalysis, 1252
- Chemical and electrochemical reactions, differences, 937
- Chemical equilibrium, 1459
- Chemical kinetics, 1122
- Chemical potential, 937, 1058
  - definition, 830
  - determination, 832
  - of ideal gas, 936
  - interactions, 835
  - of organic adsorption, 975
  - and work function, 835
- Chemical reaction states, reactivity of states, 1467
- Chemical reaction, as a basic step, 937, 1473
  - adiabatic, definition, 1497
  - at gas/solid interphase, 1371
  - heterogeneous, in solution, 1376
  - non-adiabatic, definition, 1497
  - reactivity of molecules in, 1473
  - velocity of, 1473
- Chemical step as rate determining step, 1179
- Chemical vapor deposition, disadvantages, 1345
- Chemical work of water adsorption, 907
- Chemisorption, 922, 1070
- Chi potential, 824
- Chronopotentiometry, galvanostatic transients, 1411
  - as analytical technique, 1411
  - activation overpotential, 1411
- Clavilier, and single crystals, 1095
- Cluster formation
  - energy of, 1304
  - and Frumkin isotherm, 1197
- Cobalt–nickel plating, 1375
- Cold combustion, definition, 1041
- Cole–Cole plot, impedance, 1129, 1135
- Colloidal particles, 880, 882
  - and differential capacity, 880
- Complex impedance, 1135
- Computer simulation, 1160
  - of adsorption processes, 965
  - and overall reaction, 1259
  - and rate determining step, 1260
- Computers in electrochemistry, 1159, 1162
  - robotization to control experiments, 1162
  - pattern recognition analysis, 1162
- Condenser, 1117
  - capacitance of, 861
  - model of parallel-plate, 873, 875, 961
    - asymmetry of electrocapillary curves, 876
  - capacity, 875
  - differential capacity, 876
  - and Lippman equation, 875
  - and water–dipole layer, 905
  - potential difference, 875
- Condon, 1456, 1490
- Conductive oxides, in electrocatalysis, 1284
- Conductivity, 1172, 1175, 1185
  - and stoichiometric number, 1183
- Configurational entropy, 914
- Consecutive reactions, pathway, 1259
- Constructive interference of waves, 789
- Contact adsorption, 845, 919, 920, 922, 926, 948, 959
- Contact potential difference, 809
- Convection
  - diffusion layer, 1233
  - diffusion mechanism, 1229
  - effect on potential-time transients, 1229
  - in electrochemical systems, 1226
  - Fick's first law and, 1227
  - flux, 1228
  - interfacial concentration, 1225
  - laminar flow, 1226, 1227
  - natural, 1226, 1229
  - nature of, 1226
  - transition time, 1225
  - turbulent flow, 1226, 1234
  - types of flow, 1226
  - vortices, 1226
- Convenient standard state, 936
- Conventional standard state, 936
- Conway, 936, 1091, 1125, 1203, 1402, 1426, 1441, 1497, 1522, 1530
- Conway and Angerstein-Kozłowska isotherm, 943
- Corrosion, 1041
  - as an electrochemical reaction, 1042
  - inhibition by organic molecules, 1192
- Corrosion cell, 1350
- Cottrell, 1224, 1225
- Cottrell's equation, 1415
- Coulombic forces, 819, 946
- Coulometry and determination of overall reaction, 1259



- Couple reaction, 1169
- Cryostat, cooling by, 1121
- Crystal facets
  - disappearance, 1332
  - formation, 1328
  - rate of electrogrowth, 1330
- Crystal growth, during electrodeposition, 1307, 1328
- Crystal planes, 1202, 1315, 1331
  - cleavage of, 1202
  - electrocrystallization, importance, 1330
  - reactivity, 1201
  - well defined, 1202, 1207
- Crystallization, 1293
- Crystallographic stages of growth, 1333
- Current density, 1046, 1049, 1111
  - anodic, 1051, 1052
  - cathodic, 1051, 1052
  - diffusion controlled, 1256
  - of disk and ring in rotating disk electrode, 1142
  - distribution, 1112
  - during electrodeposition, 1309, 1310
  - faradaic, 1250
  - limiting, 1235, 1237, 1246, 1248, 1255
  - multistep reaction and, 1173
  - net, 1066, 1081
  - quantum mechanical formulation, 1521
  - semiconductors, 1080
  - transport controlled reactions, 1254
- Current-overpotential curves, 1051, 1172, 1255; *see also* potential-current
- Current-potential law, 1348
- Current-potential relation
  - electrical migration, 1253
  - at semiconductors, 1082
- Current-step measurements, 1119
- Currie, 1125
- Cytochrome c, 1289
  
- Daimler-Benz company, 1263
- Damaskin-Frumkin, and water, 899
- Damjanovic, 1141, 1310, 1520
- Daniel cell, 1356
- Dannenberger, organic adsorption, 979
- De Broglie, 1456, 1490
- Debye-Hückel theory, 877
  - and total diffuse charge in solution, 879
- De-electronation, 1047, 1049, 1066, 1178, 1358
  - and transport controlled reaction, 1252
- Deformation of ions upon adsorption, 964
  
- Degrees of freedom of adsorbed ions, 928, 958
- Delgani, 1290
- Delocalization of electrons
- Destructive interference of waves, 789
- Dendrites, electrodeposition, 1336, 1338
  - point sink during formation of, 1338
- Deposition of metals, 1293; *see also* electrodeposition, metal deposition
- Despic, electrodeposition, 1308
- Deuterium, reaction rate, advantages, 1154
- Dielectric constant
  - definition, 898
  - variation at the interface, 897
- Dielectric, saturated, 898
- Differential capacity
  - of parallel plate condenser, 876
  - of Stern model, 884
  - variation with potential, 915
- Diffraction, definition, 789
- Diffraction pattern, 790
- Diffuse charge capacity, 884
- Diffusion-activation equation, 1247
- Diffusion, 1212, 1226
  - Butler-Volmer equation and, 1217
  - controlled reaction rates, 1213, 1218
  - convective mechanism, 1229
  - flux-equality equation, 1213
  - heat flow and, similarities, 1215
  - interfacial response at constant current, 1216, 1218
  - Laplace transformation, 1215
  - Nernst's equation and, 1217
  - non-steady, 1254
  - as rate determining step, 1261
  - Schlieren method, 1235
  - semi-infinite linear, 1216, 1234, 1255
  - in solution and electrodeposition, 1335
  - spherical, 1216, 1239
  - time dependence of current under, 1224
- Diffusion control, 1248
  - current-overpotential, 1248, 1250, 1255
  - currents, 1256
  - and electrochemical processes, 1254
  - limiting current density, 1250, 1255
- Diffusion flux, and electrical migration, 1254
- Diffusion layer, 1228, 1232, 1255
  - an artifice concept, 1233
  - convection and, 1233
  - interferometry and, 1234
  - limiting current density and, 1237
  - Nernst, 1233

- Diffusion layer (*cont.*)
  - polarography, 1246
  - thickness, 1335
  - turbulent flow and, 1234
- Diffusion coefficient, and rotating disk electrode, 1141
- Diffusion into electrodes, and potentiostatic and galvanostatic measurements, 1121
- Diffusion problems, and computer simulation, 1161
- Diffusion, surface, during electrodeposition, 1296, 1298, 1300, 1307, 1310
- Dimensions, of surface irregularities, 1329
- Dimers of water, 975
  - definition, 899, 902
  - surface coverage, 904
- Dipole
  - dipole interactions, organic adsorption, 977
  - preferential orientation, 823
  - water, 871, 899
- Dipole moment, 905
- Dipole potential, 824, 897
  - of water, 909
- Dislocation, 1303, 1320
- Dispersion forces, 819, 896, 921, 944, 946, 964, 977, 1195, 1197
  - and metal-water interaction, 896
- Dissolution site, during electrodeposition, 1302
- Distribution function for electrons in metals, 1469
  - Boltzmann law, 1470
  - density of states in metals, 1471
  - Fermi-Dirac law, 1470, 1471
  - Fermi level, 1470
  - probability of occupancy of cells, 1469
  - quantum mechanical tunneling, 1471
- Distribution law of electronic states, 1460
  - Boltzmann, 1466, 1470
  - Gaussian, 1464, 1465
  - overpotential and, 1466
  - Maxwell-Boltzmann, 1468
  - in redox ions in solution, 1468
  - Tafel curves and, 1466
  - vibrational states, 1468
- Dolin, 1303, 1320
- Doping, 1074
- Double layer, 869, 873, 1043
  - charging process of, 1217
  - electric field of, 1035
  - dimensions of, 1035
  - impedance of, 1134
- Driven cell device, 1036
- Dropping-mercury electrode, 1237, 1401
- Dolin, 1425
- ecm, 853
- Edges
  - in electrocatalysis, 1276
  - energy of, in electrodeposition, 1303
  - vacancies, in electrodeposition, 1297
- Eddowes, enzymes, 1289
- e-i* junction, 1081
- Einstein-Smoluchowski equation, electrodeposition, 1312
- Elastic backscattered electrons, 794
- Electric current density, 1046
- Electric field, 1035
  - and adsorption, 929
  - definition, 818
  - electron transfer under an, 1042, 1044
  - force, 921, 964
  - rate of ions crossing interface under, 1046
- Electric power source, 1048
- Electrical work of water adsorption, 907
- Electricity producer, 1039
- Electrified interfaces, 871
  - potential differences, 806
  - retrospect and prospect, 869
- Electroanalytical chemistry, 1057, 1419, 1422
- Electrocapillary
  - curves, 849, 852
    - asymmetry, 876
    - definition, 849
    - importance, 852
    - maximum, 853
    - and potential of zero charge, 861
    - thermodynamic conditions, 858
  - equation, for liquids, 858
  - equation, for solids, 858
  - maximum, determination in liquid electrodes, 861
  - maximum, and electrocapillary curves, 861
  - measurements, definition, 848
  - thermodynamics, summary, 866
- Electrocatalysis, 1252, 1275, 1293, 1371, 1503
  - adsorbed radicals in, 1275
  - bond strength, 1287
  - comparison of different systems, 1277
  - conductive oxides in, 1284
  - desorption in, 1275
  - edges and kinks, 1276
  - electrochemical engineers and, 1279
  - electronic factors in, 1276

Electrocatalysis (*cont.*)

- entropy, 1283
- exchange current density and, 1278
- geometric factors in, 1276, 1283
- heterogeneous, 1275
- how it works, 1280
- hydrogen evolution, 1284
- lattice spacing in, 1276
- methanol oxidation, 1284
- overpotential as a measure of, 1278
- oxygen evolution, 1280
- rate determining step in, 1276
- surface heterogeneity, 1276
- Temkin isotherm in, 1275
- volcanoes in, 1284

## Electrocatalysts

- enzymes, 1287, 1495
- glassy carbon, 1287
- lead oxide, 1287
- perovskites, 1280, 1282
- platinum, 1286
- silicio carbide, 1287
- titanium carbide, 1287

## Electrochemical cell

- definition, 808
- driven, 1360
- effect on potential difference, 1104
- general arrangement, 1104, 1106
- and overpotential, 1104
- potential difference, 809
- self-driven, 1360
- three electrode, 1105

## Electrochemical “cutting”, 1345

## Electrochemical devices, 1036, 1039

## Electrochemical equilibrium, 1066

## Electrochemical heart, the, 1380

## Electrochemical interface, real, 1133

Electrochemical kinetics, *see also* electrode kinetics

- effect of structure of interphasial region, 1067
- and equilibrium, 1049
- and thermodynamics, bridge between, 1048

## Electrochemical “machinery”, 1345

## Electrochemical nanotechnology, 1345

## Electrochemical oscillators, 1377

## Electrochemical potential, 1058, 1459

- of adsorbed species, 933
- definition, 830
- as a driving force in transport of charges, 832
- and Nernst’s equation, 1064
- of species in solution, 933
- and thermodynamic equilibrium, 833

Electrochemical potential (*cont.*)

- as a total potential, 832

## Electrochemical reaction rate, 1049, 1115

- at equilibrium, 1124

## Electrochemical reactions, 1041

- activationless, 1528
- adiabatic, 1497, 1499, 1503, 1526
- barrierless, 1528
- bond breaking, 1518
- digestive processes, 1037
- galvanostatic control, 1219
- glucose oxidation, photosynthesis, corrosion, 1038
- impedance of, 1128
- nature of, 1357
- non-adiabatic, definition, 1497, 1499, 1501
- potentiostatic control, 1219
- prediction of, in electrochemical cell, 1354
- and production of electricity, 1037
- reactivity of molecules in, 1470
- without input of electrical energy, 1370

## Electrochemical spectra, 1419

## Electrochemical systems

- electricity producer, 1370
- electroless, 1370
- mechanical energy in, 1374
- substance producer, 1370

## Electrochemical unidevices, 1041

## Electrochemistry, definition, 1032

- analytical, objectives, 1406, 1422
- chemical and electrical parts of, 1032
- computers in, 1159
- frontier topics, terminology, 1496
- physical, objectives, 1406, 1419, 1422
- and quantum calculations, 1494, 1521
- quantum, retrospect and prospect, 1522

## Electrode, 1103

- absolute electrode, 837, 840, 871, 1457
- activation of, 1095
- auxiliary, *see* reference electrode, 1105
- calomel, 815, 857, 1109
- charge density, determination, 858
- counter, 1105
- electrolyte interface
  - first and second laws of thermodynamics, 855
  - work at an, 855
- hydrogen, 815, 840, 857
- indicator, 1113
- ion interactions, 964
- ion selective reference electrode, 1110
- mercury as, 1401

Electrode (*cont.*)

- micro-, 1097
- polycrystalline, 1094
- potential
  - absolute, definition, 837, 1457
  - definition, 816
  - measurement, 840, 1112
  - vacuum, 1457
- properties and organic adsorption, 979
- purification, 1095
- real area of, 1095
- reversible, 834, 1113, 1411
- reversible hydrogen, 815
- roughness factor of, 806, 1096
- secondary reference, 815, 1109
- silver–silver chloride, 815, 1110
- single crystal, 1095, 1103, 1201, 1209
- solid, determination of potential of zero charge, 861
- solid metals as, 1401
- standard hydrogen electrode, 840, see also “hydrogen electrode”
- thin evaporated films, 1095
- ultramicro-, 1098
- working, potential, 1061

## Electrode kinetics, 1035, 1441

- absorption spectroscopy, 1145
- buffer use in, 1122
- effect of impurities on, 1087
- electrode surface changes during, 1118
- electronic instrumentation, 1108
- energy of activation, 1118, 1119, 1195
- isotopes reaction rates, 1151
- isotopic effects in, 1150, 1152, 1503
- partial pressure, 1119, 1120
- pressure effect, 1119
- quantum oriented, 1451, 1454, 1517
- radioactive particles and, 1151
- of semiconductors, 1070, 1082
- solution preparation, 1087
- spectroscopic approaches, 1141
- techniques of, 1087
- temperature control in, 1117
- thin layer cell in, 1099
- volume change of the system, 1120

## Electrode shapes, 1144

- cone, cylindrical, and jet electrodes, 1144

## Electrode surface

- changes of, during electrokinetic measurements, 1122
- novel methods to study, 1274

Electrode surface (*cont.*)

- preparation, 1094

## Electrodeposition, 1294

- aluminum, 1343
- binding energy, 1301
- Butler–Volmer equation in, 1306
- cathodic deposition, 1307
- charge transfer reaction, 1294
- cluster formation energy, 1304
- concentration of adions during, 1309, 1311
- crystal facets, 1328, 1330
- crystal growth, 1303
- current density during, 1309, 1310
- dehydration of ions during, 1296
- diffusion of adions, 1307
- diffusion layer thickness, 1335
- diffusion in solution, effect on, 1335
- dislocation in, 1303, 1320
- dissolution site in, 1302
- edge energy, 1303
- electrical free energy, 1303
- electrogrowth, 1317
- electionation of ions during, 1295
- Einstein–Smoluchowski equation, 1312
- Faraday and, 1346
- fluctuations during, 1305
- free energy of growing nucleus, 1303
- getters, 1343
- grains, 1334
- growth site in, 1302, 1307
- half-crystal position, 1301
- heterogeneity of surfaces and, 1303, 1305, 1308
- history of, 1346
- hydration of ions during, 1295, 1298
- importance, 1338
- kink atoms, importance in, 1302
- lithium as anode in, 1343
- macrospiral, 1326
- macrosteps, 1324
- mechanism of, 1294, 1297, 1298, 1300, 1307
- microelectrodes used to study, 1305
- microspiral growth, 1324
- microsteps, 1324
- movement of adions during, 1298
- nonuniform current distribution during, 1310
- nucleating center during, 1305
- nucleation in, 1302
- nucleation in two dimensions, 1306
- nucleus size, 1305, 1306
- one-step deposition reaction, 1297

- Electrodeposition (*cont.*)
- organic additives, 1339
  - overpotential, 1305, 1306, 1338
  - partial charge transfer and, 1298
  - photostimulated, on semiconductors, 1345
  - point sink, dendrites formation, 1338
  - polycrystals, 1334
  - random thermal displacement, 1312
  - rate of electrochemical reaction, 1306
  - rate of faces growth, 1332
  - residence time, 1310
  - scanning tunneling microscopy and, 1310
  - scavenger electrolysis, 1343
  - single crystals and, 1296, 1303, 1334
  - step properties, 1310, 1321
  - stages of growth, crystallographic, 1333
  - surface diffusion, 1296, 1298, 1300, 1307, 1310
  - transfer reactions, 1310
  - underpotential, 1313
- Electrodeposition, shape of, 1336
- boulders, 1336
  - control, 1336
  - dendrites, 1336, 1338
  - pyramids, 1334, 1336
  - screw dislocation, 1303, 1321, 1326, 1327
  - spiral growth, 1316, 1328
  - spikes, 1336
  - terraces, 1307, 1336
  - whiskers, 1327, 1336
- Electrodes, 1035, 1211
- effect of ionics on, 1073
  - transport controlled, 1216, 1231
- Electroencephalogram, and ultramicroelectrodes, 1291
- Electrogenative synthesis, 1377
- Electrogrowth of metals on electrodes, 1293; *see also* Electrodeposition
- Electrokinetic potential, 1069
- and Galvani potential difference, 1069
- Electroless, 1374
- activator in, 1374
  - advantages, 1375
  - cobalt–nickel plating, 1375
  - metal deposition by, 1374
  - process of, 1375
  - throwing power, 1376
- Electrolysis of water, 1162
- Electrolyzer, 1036
- Electron
- delocalization, 923
  - partial molar free energy of, 834
- Electron (*cont.*)
- spillover, 889, 891
  - wave nature, 788, 1455
- Electron acceptor, 1060, 1067
- Electron donor, 1060, 1067
- Electron–hole recombination process, 1076
- Electron in semiconductors
- concentration, as a function of overpotential, 1084
  - current density, 1080
- Electron microscopy, 1157, 1276
- Electron mobility, 1076
- Electron spectroscopy for chemical analysis (ESCA), 794
- Electrons in solution
- electrochemical potential, 1461
  - energy states of, 1458
  - Fermi energy of, 1458, 1459
  - partition function, 1461
  - quantal energy states, 1461
- Electron transfer, 1035, 1042, 1500
- activation, models, 1511
  - adiabatic, 1503, 1526
  - and electrocatalysis, 1503
  - enzymes, 1495
  - Fermi level, 1501
  - Frank–Condon principle, 1504
  - free energy of activation, 1504
  - harmonic, 1504
  - interfacial potential, 1044
  - non-adiabatic, 1501, 1503
  - number of, in multistep reaction, 1177
  - paths of, 1501
  - quadratic energy variation, 1506
  - quantum mechanics, 1499
  - radiationless, 1500
  - rate of, effect of electric field, 1044
  - reaction, definition, 1497
  - reaction, interfacial, 1052, 1055
- Electron transfer, interfacial, 1035
- free energy of activation, 1042
- Electronation, 1047, 1049, 1066, 1295, 1358
- step, 1173
- Electronic forces, 944
- Electronic states, 1456, 1466
- acceptor, of ions in solution, 1468
  - donor, of ions in solution, 1468
  - vibrational, 1463
- Electroneutrality at interfaces, 864
- Electroplating, 1112
- Electrosorption valence, 923

- Ellipsometry, 787, 1139, 1147  
 absorption coefficient, 1148, 1152  
 automatic, 1153  
 Ellipsometry, 787, 1139, 1147  
 disadvantages, 1154  
 in electrochemistry, 1148  
 enzymes and, 1289  
 Fresnel's equations in, 1151  
 fundamentals, 1148  
 phase difference of light, 1148  
 polarized light, 1147  
 refractive index, determination with, 1148, 1151  
 reflection coefficient, 1151  
 sensitivity, 1148, 1149, 1153  
 as a spectroscopic technique, 1148, 1152  
 thickness of thin layers, measurement by, 1148, 1151  
 transients in, 1422
- Energy  
 of adsorption, 940  
 of adsorption of water, 912  
 binding, 834, 1191, 1484  
 distribution of site, 952  
 of interaction, ion, 945  
 of interaction, water, 945  
 partial molar free, of an electron, 834
- Energy of activation, 1122, 1123, 1199  
 barrier, transport process, 1212  
 origin, 1511
- Energy barrier  
 for multistep reactions, 1180  
 symmetry, 1055
- Energy states in solution, 1462, 1463  
 Boltzmann distribution law, 1466  
 distribution, 1462, 1464  
 ground state, 1464, 1468  
 number of, 1462
- Enthalpy  
 of adsorption, 926, 956, 964  
     and variation with ionic coverage, 927  
 of contact adsorption, 926  
 of ion-electrode, 924, 944  
 of water-electrode interaction, 944, 924  
 of water-ion interaction, 924
- Entropy  
 of adsorption, 926, 928, 956, 964  
 charge dependence, 913  
 charge independence, 913  
 configurational, 914  
 of contact adsorption, 926
- Entropy (*cont.*)  
 electrocatalysis and, 1283  
 on ion-electrode, 924, 944  
 librational, 914, 915  
 vibrational, 914, 915  
 of water-electrode interaction, 944, 924  
 of water-ion interaction, 924
- Enzymes, 1287, 1495  
 application, 1291  
 biosensors, 1291  
 characteristics, as catalysts, 1287  
 cytochrome C, 1289  
 in electrochemistry, 1289, 1291  
 electro-tunneling in, 1290  
 ellipsometry and, 1289  
 glucose meter, 1291  
 glucose oxidase, 1291  
 heme group, 1289, 1290  
 how they work, 1288  
 immobilization, 1289  
 Michaelis-Menten mechanism, 1288  
 specificity, 1287  
 turnover number, 1287  
 ultramicroelectrodes, 1291  
 what they are, 1287
- Equation of state  
 for adsorption, 931  
 and surface excess, 931  
 virial, in two dimensions, 931
- Equilibrium, of interfacial reaction, 1047, 1052
- Equivalent circuit, 814, 1134  
 of ideally polarized and nonpolarized interfaces, 814
- Erdey-Gruz, 1048, 1306, 1474
- Erschler, 1133, 1134, 1425
- Ethylene oxidation, anodic, 1052, 1258
- Exchange current density, 1049, 1066  
 correction of, 1069  
 definition, 1053  
 electrocatalysis and, 1278  
 impedance and, 1136  
 interfacial reaction, 1047  
 and partly polarizable interface, 1056
- Excited states, lifetime, 1478
- Exothermic reaction, 1041
- Ex situ* techniques, 785, 788, 1146
- Failure of materials, hydrogen coadsorption, 1340
- Faradaic resistance, 1175
- Faradaic current density, 1250, 1404, 1414
- Faraday, Michael, 1050, 1346

- Faraday, Michael (*cont.*)  
 and electrode names, 1359
- Faraday law, 1455
- Fawcett's model of water, 899
- Feldberg, diffusion problems, 1160, 1425
- Fermi distribution law, 1082
- Fermi–Dirac law, 1470, 1471
- Fermi golden rule, 1495
- Fermi level, 1470, 1501  
 and electrochemical potential, 1471  
 of electrons in solution, 1459, 1460
- Fick's first law, 1214, 1227, 1233, 1243, 1253, 1255
- Fick's second law, 1160, 1218, 1229, 1233, 1239
- Finite differential method, 1160
- Fleischmann, 1099, 1146, 1310
- Fletcher, electrodeposition, 1305
- Flip-up state of water, 899, 902, 906, 915, 975
- Flitt, material failure, 1340
- Flop-down state of water, 899, 906, 906, 915, 975
- Flory, 941
- Flory–Huggins type isotherm, 941, 942, 944, 965
- Flux-equality condition, 1213
- Forces  
 chemical, 897  
 Coulombic, 819, 946  
 dispersion, 819, 896, 921, 925, 944, 946, 964, 977, 1197  
 electric field, 921, 964  
 electronic nature forces, 921, 944  
 image, 819, 921, 924, 946, 964  
 lateral, 897, 927, 954, 964, 983  
 London, 896  
 involved in organic adsorption, 971  
 short range, 819
- Fourier transform infrared spectroscopy (FTIR), 800, 1147  
 and mechanism of reactions, 1147, 1259  
 and methanol oxidation, 1270  
 and radical intermediates, 1147  
 and time measurement, 1147  
 transients in, 1422
- Fourier transformation, 799
- Frank, electrodeposition, 1321, 1324
- Frank–Condon principle, 1504
- Free energy, 1506  
 of adsorption, 926, 956, 964, 1197, 1199  
 of adsorption, organic adsorption, 971  
 of contact adsorption, 926  
 and electrodeposition, 1303
- Free energy (*cont.*)  
 of flip-up and flop down, water molecules, 906, 915  
 of ion–electrode, 924, 944  
 partial molar, of an electron, 834  
 of redox reactions, 1513  
 standard electrochemical, of adsorption, 935  
 of water–electrode interaction, 944, 924  
 of water–ion interaction, 924
- Free energy of activation, 1506, 1511, 1515  
 electron transfer, 1504, 1506  
 librator fluctuation model, 1516  
 phonon–vibron model, 1517  
 in redox reactions, 1514  
 standard, multistep reaction, 1180, 1182  
 vibron model, 1513
- Free sites of adsorption, 937, 938
- Fresnel's equations in ellipsometry, 1151
- Frequency, impedance, 1127, 1128, 1132, 1135
- Frumkin, A. N., 1070, 1141
- Frumkin isotherm, 938, 942, 965, 982, 1195, 1439  
 and cluster formation, 1197
- Frumkin–Damaskin, water model, 899
- Frumkin–Temkin isotherm, 1195  
 in electrode kinetics, 1198, 1200
- Fuel cell, 1039, 1040, 1042, 1156, 1377  
 advantages, electric cars, 1040  
 iron–oxygen fuel cell, 1381
- Galvani, 1409
- Galvanostatic transients, 1409, 1412  
 chronopotentiometry, 1411  
 circuitry, 1409  
 methodology, 1409  
 problems, 1410  
 two pulses, 1411
- Galvani potential, 826, 1057, 1069, 1458
- Galvani potential difference, and electrochemical kinetics, 1069
- Galvanostatic control of electrochemical reactions, 1223
- Galvanostatic techniques, 1115, 1116, 1118  
 advantages, 1118  
 and impurities on electrodes, 1120  
 skin effect in, 1121
- Gamboa-Aldeco, M., 786, 805, 925, 927, 929, 930, 965, 1475
- Gamov, equation of tunneling, 1492
- Gamow, 1155
- Gas chromatography, and determination of overall reaction, 1259

- Gauss' law, 879  
 Germer, Davidson, 1455  
 Germanium, properties as semiconductor, 1076  
 George-Griffith's thermal model, 1514, 1519  
 Gerischer, 1411, 1458, 1464, 1468, 1515  
 Getters, electrodeposition, 1343  
 Gibbs' angle, 842  
 Gibbs, J. Willar, 842  
 Gibbs' surface excess, definition, 845  
 Gibbs–Duhem relation, 856  
 Gileadi, 1426  
 Glass scintillator, 804  
 Glassy carbon, as electrocatalyst, 1287  
 Glucose meter, 1291  
 Glucose oxidase, 1291  
 Glucose oxidation, as an electrochemical reaction, 1041  
 Gonometer, 1202  
 Gouy, 877  
 Gouy–Chapman  
   capacity, in Stern model, 884  
   charge, 882  
   diffuse-charge model of the double layer, 876  
   model, 959  
   model and similarity to ion–ion interactions, 877  
 Graetzel, 1510  
 Graham, David C., 843, 886  
 Grains, electrodeposition, 1334  
 Greenler theorem of IR spectroscopy, 801  
 Ground state  
   fluctuations, 1515  
   potential energy curves, 1479  
 Growth site, during electrodeposition, 1302, 1307  
 Guidelli's model of water, 899  
 Guidelli, 971, 1343  
 Gurney, Ronald, 1456, 1467, 1490, 1503, 1526  
 Gutmann, Felix, ac polarography, 1425  
  
 Habib, and surface potential determination, 893  
 Habib–Bockris' model of water, 899  
 Habib–Bockris isotherm, 943, 949  
 Half-crystal position, electrodeposition,  
 Half-wave potential in polarography, 1244  
 Hamelin, 1209  
 Hamilton, dendrites, 1338  
 Hamnet, 1133  
 Harmonic curves, 1487, 1495  
   solvent–ion bonds, 1504  
 Harmonic electron transfer, 1504  
 Heat of adsorption, 940  
 Heat of adsorption (*cont.*)  
   dependence on coverage, 1194  
   independence on coverage, 1193  
 Heat of activation, 1122  
   apparent, 1123  
 Heat transfer  
   flow, comparison with diffusion, 1215  
   theory of, 1215  
 Heller, 1290, 1496  
 Helmholtz plane  
   inner, 919, 922, 959, 961, 962  
   outer, 872, 882, 959, 961, 962, 1069, 1213, 1232  
 Helmholtz–Perrin  
   capacity, in Stern model, 884  
   charge, 882  
   theory, 873, 959, 961  
 Helmholtz, 873  
 Heme group, 1289, 1290, 1495  
 Heterogeneity of surfaces, 952, 954, 955, 975, 977, 978, 983  
   and electrocatalysis, 1277, 1283  
   and electrodeposition, 1303, 1308  
   and ionic adsorption, 928  
   ionic isotherm for, 944, 953, 954  
   and methanol oxidation, 1272  
   and Temkin isotherm, 938, 1195  
 Heyrovski, Jaroslav, 1237, 1424  
 Hickling, 1118  
 High overpotential case, Butler–Volmer equation, 1054, 1179  
 High resolution electron energy loss spectroscopy (HREELS), 787  
 Hill, enzymes, 1289  
 Hitchens, enzymes, 1289  
 Hole  
   current density, 1080  
   -electron recombination process, 1076  
   mobility, 1076  
   movement, in semiconductors, 1076  
   transfer of, in n–p junctions, 1082  
 Holes in electrodeposition, 1297  
 Huggins, 941  
 Horiuti, 1483, 1499  
 Hubbard, 979, 1099, 1142, 1205, 1206, 1266, 1398  
 Huq, electrode kinetics, 1087  
 Hydration sheath, 871, 964, 1512  
 Hydrocarbon, electrooxidation, mechanism determination, 1152



- Hydrogen evolution reaction, mechanism, 1135, 1151, 1163, 1164, 1189
  - catalytic pathway, 1163, 1194, 1255
  - electrocatalysis, 1280
  - Frumkin-Temkin isotherm, 1194
  - Langmuir isotherm, 1194
- Hydrogen coadsorption
  - breakdown potential, 1337
  - effect of low conductivity, 1338
  - equivalent conductance and, 1339
  - low limiting current, 1338
  - material failure, 1336
  - molten salts in, 1340
  - in nonaqueous solutions, 1337
  - and organic adsorption, 1336, 1337
  - from organic solvents
    - water as contaminant
- Hydrogen electrode, 857, 924
  - absolute electrode potential, 870
  - absolute potential of standard, 1457
  - and ion size, 924
  - reversible, 815, 1207
  - standard, 1060, 1061, 1108, 1207, 1351
- Hydrogen peroxide, 1139
- Ideal gas, standard state, 936
- Ilkovic equation, 1246
- Ilkovic, D., polarography, 1424
- Image dipole, 896
- Image forces, 819, 924, 921, 946, 964
  - and metal–water interactions, 896
- Imaginary impedance, 1128, 1135, 1160
- Imaginary number, 1129
- Impedance spectroscopy, 1127, 1160
  - ac and dc, 1134
  - ac, information on electrode processes, 1131
  - Bode plot, 1129
  - capacitor–resistor, 1129
  - Cole–Cole plot, 1129, 1135
  - complex, 1135
  - computer control, 1163
  - double layer, 1134
  - electrochemistry and, 1132, 1134, 1138
  - electron transfer reactions in, 1136
  - exchange current density obtained from, 1136
  - experimental methodology, 1128
  - frequency, 1127
  - frequency range, 1128, 1132, 1135
  - imaginary, 1128, 1135, 1160
  - limitations, 1138
  - Impedance spectroscopy (*cont.*)
    - measurements of electrochemical systems, 1132
    - mechanism indicating plot, 1135
    - microroughness, effect on, 1139
    - Moiré's theorem, 1128
    - out of phase, 1127
    - of oxide covered electrode, 1136
    - phase angle, 1127, 1129
    - phase difference, 1127
    - potential response, 1129
    - rate constants obtained from, 1136
    - real, 1128, 1135
    - of semiconductors, 1136
    - solution, 1134
    - stabilization of electrode surface in, 1138
    - of surface states, 1138
    - Warburg, 1133, 1134
    - Z-log W plot, 1127
- Impurities, effect on electrode kinetics, 1091, 1120
- Indicator electrodes, 1111
- Indifferent ions, see supporting electrolyte
- Infrared
  - Greenler theorem of, light, 801
  - radiation, 797
  - spectroscopy, 1146
  - surface selection rules, 801
- Intermediate, adsorption of, 1192
- Interferometry, and diffusion layer, 1234
- Infrared spectroscopy (IR), 787, 797
  - conditions for adsorption detectability in, 803
  - relation of incidence angle with adsorbed molecules, 803
- Inhibitor, organic molecules as, 968, 1192
- Inner Helmholtz plane, 919, 922, 959, 961
- Inner shell reaction, definition, 1496
- Inner potential, 826, 830, 857, 1059
  - as an absolute potential, 829
  - difference, 869
  - measurability, 829
  - as a non practical potential, 829
- In situ* measurements, 1146
- In situ* microscopy, atomic scale, 1157
- In situ* techniques, 783, 788
- Interaction with matter, 795
- Interface, 845, 848, 1035
- Interfaces
  - nonpolarizable, 812, 857, 1055, 1111
  - polarizable, 812, 858, 863, 1055, 1056
  - potential differences, 806

- Interfacial concentration
  - convection, 1225
  - dependence on ionic transport, 1072
  - Nernst equation and, 1220, 1230
  - variation with time, 1220
- Interfacial control, 1248
- Interfacial reaction
  - chemical term, 1046
  - equilibrium of, 1047, 1123
  - exchange current density of, 1047
- Interfacial region, model, 873
- Interfacial tension, 847, 848
- Interferogram, 1146
- Interphase, 845, 1035
- Interferometer
  - Michelson, 798
  - wavenumber, 799
- Interference patterns, 790
- Ion dissolution reaction, 1189
- Ion–electrode interaction energy, 924, 944, 945, 964
- Ionic adsorption, 919
  - active sites, 928
  - contact, 919, 920, 922, 948
  - degrees of freedom, 928, 958
  - on heterogeneous surfaces, 928
  - mobility of the ion, 928, 958
  - summary, 964
- Ionic deformation upon adsorption, 964
- Ionic strength, multistep reactions, 1189
- Ion–solvent interactions, 964
- Ionics, 1207
- Ion transfer reaction, 1055, 1497
- Ion mobility during adsorption, 928, 958
- Irreversible adsorption of organic molecules, 969, 970
- Irreversible reaction, 1251, 1419
- Isoconic, definition, 933, 978, 982
- Isotherm, 932, 964, 1197
  - applicability, 941
  - and charge transfer, 954, 955
  - Conway and Angersein–Kozłowska, 943
  - definition, 933
  - in electrode kinetics, 1197
  - Flory–Huggins type, 941, 942, 944, 965
  - Frumkin, 938, 942, 965
  - Frumkin–Temkin, 1197, 1198
  - Habib–Bockris, 943
  - for heterogeneous systems, 944, 953, 954, 955
  - ionic, 944
  - and ion size, 954, 955
  - Isotherm (*cont.*)
    - Langmuir, 936, 937, 938, 942, 965, 1197, 1198
    - and lateral interactions, 954, 955
    - logarithmic, 941, 1196
    - long range interaction, 936
    - Parsons, 943
    - short range interaction, 936
    - and solvent displacement, 954, 955
    - standard states, 936
    - Temkin, 938, 942, 944, 965
    - virial, 936
- Isotopes, radioactive, 801
  - difference in reaction rates, 1155
- Isotopic effects in electrode kinetics, 1154
  - determination of electroorganic reaction mechanism, 1156
  - pathway determination, 1259
- Isotopic reactions in solution, 1507
- Ivanov, 1140
- Iwasita, 1510
- Jaeger, 1216
- Jellium model of the metal, 890
  - and crystal structure, 892
  - and pseudo potentials, 892
  - and surface of potential, 893
- Jeng, organic adsorption, 975, 979
- Jovancevic, 1125, 1263
- Junction
  - e–i*, 1081
  - n–p*, 1074, 1081
  - transistor, 1075
- “just outside” the metal, definition, 834
- Juza, transients, 1403
- Kabanov, 1528
- kang, 1121
- Khan, 1423, 1459, 1466, 1495, 1496, 1501, 1517
- Kautek, 1345
- Kinematic viscosity, in rotating disk electrode, 1141, 1234
- Kinetics of underpotential deposition, 1316
- Kingston, 1082
- Kinks, 1276, 1297
  - importance in electrodeposition, 1302
- Kirchhoff’s first law, 1213
- Kirchhoff’s second law, 811
- Kolb, underpotential deposition, 1315, 1345
- Kosłowska, 1441
- Kossel, electrodeposition, 1301, 1303

- Krishtalik, 1528
- Krznanric, organic adsorption, 979
- Kuznetsov, quantal calculations, 1494
- Laminar flow, 1226, 1227
- Landau, 1499, 1503
- Lange and Miscenko, 823, 1059
- Langmuir isotherm, 936, 937, 938, 942, 965, 1196
  - applicability at high coverages, 1197
  - in electrode kinetics, 1200
- Langmuir equation, electrochemical version of, 1194
- Lateral interaction forces, 897, 927, 963, 964, 972, 977, 978, 983
- Lateral interaction work of water adsorption, 907
- Lateral interactions of ionic adsorption, 924, 944
- Lateral interactions and Frumkin's isotherm, 938
- Lattice gas models of adsorption, 965
- Lattice spacing, 1276
- Laue pattern, 793
- Lead deposition, underpotential deposition, 1313
- Lead oxide, as electrocatalyst, 1287
  - in lead acid battery, 1287
- Levich, V. G., 1140, 1468, 1516
- Levich equation, 1141, 1234
- Librational entropy, 914, 915
- Librational motion of adsorbed ions, 928
- Librator fluctuation model, 1516
- Libratory motion, 915
- Light interaction and molecular dipole moment, 803
- Light
  - polarization of, and adsorption, 803
  - polarized, 800, 801
  - p*-polarized, 802
  - s*-polarized, 802
- Limiting current, 1255
  - definition, 1097
  - diffusion control, 1250
  - diffusion layer, 1237, 1246, 1248
  - importance, 1235
  - in semiconductor electrodes, 1088
- Linear absorption coefficient, 806
- Lipkowski, and surface tension of solid/solution interfaces, 850
- Lippman equation, 858, 875
- Liquid metals
  - advantages, 848
  - determination of electrocapillary maximum, 861
- Lithium as anode during electrodeposition, 1343
- Logarithmic isotherm, 941
- Lohman, electrode potential, 1457
- London forces, 896
- Long range interactions, 936
- Lorenz and Salie, and partial charge transfer, 922
- Lorenz, 1313, 1497
- Louis de Broglie postulate, 788
- Low energy electron diffraction (LEED), 788, 787, 790
- Low overpotential case, Butler-Volmer equation, 1054, 1179, 1185
- Luggin capillary, 1097, 1105, 1107
  - ohmic drop correction in, 1108
- Mc Donald, D. D., 1139
- Mc Donald, J. R., 1139
- McClendon, 1503
- Macrosteps, electrodeposition, 1324
- Magnetic induction, 1378
- Marcus, 1506, 1512, 1516
- Mass action law, and reactions in quasi-equilibrium, 1184
- Mass spectroscopy, and determination of overall reaction, 1259
- Matthews, hydrogen tunneling, 1494
- Maxwell's demon, 842
- Maxwell law, particle velocity, 1462
- Mean ionic activity, 865
- Mechanism of electrodic reactions, see also "pathway"
  - catalysis, 1258
  - ethylene oxidation, 1258
  - goals of, 1258
  - importance, 1257
  - methanol oxidation, 1262, 1269
  - methods used to study, 1261
  - overall reaction, 1258
  - oxygen reduction on iron, 1263, 1265
  - pathway, 1259
  - rate determining step, 1260
  - ring disk electrode, 1263
  - stepwise, 1257
  - voltammograms, 1258
- Menstätter, 1082
- Mercaptohexadecanol, adsorption, 979
- Mercury in electrode kinetics, 1093, 1195
- Mercury solution interface, ideal polarizable interface, 848
- Metal capacity, 888
  - determination, 890
  - water interactions, 896, 897

- Metal deposition, 1144, 1293; *see also* electrodeposition
- Metal oxidation reaction, 1144
- Metal, spillover electrons of, 889, 891
- Metal–solution properties, 887  
and capacity curves, 887
- Metal–solvent interactions, 964
- Metals, liquid, advantages, 848
- Methanol, electrooxidation  
electrocatalysis, 1284  
FTIR spectroscopy and, 1270  
heterogeneity of the electrode, 1272  
mechanism, 1262, 1269  
on platinum single crystals, 1207  
potentiodynamic transients, 1269  
rate determining step, 1270  
rotating disk electrode, 1139  
Tafel plots, 1265
- Michelson interferometer, 798
- Microelectrodes, 1097, 1103, 1291  
advantages and disadvantages, 1097, 1098, 1100, 1404  
applications, 1102  
arrays of, 1100  
electrodeposition and, 1305  
enzymes and, 1291  
limiting diffusion current in, 1098  
reduction of ohmic errors by, 1089
- Microwave radiation, 797
- Microspiral growth, 1324, 1326
- Michaelis–Menten mechanism, enzymes, 1288  
Migration, 1212, 1226  
current–potential relation, 1253  
diffusion flux and, 1254  
electrical, 1253, 1256  
Fick’s law, 1253  
steady state, 1253
- Miller, David, 1495, 1510
- Miller indexes, 1202, 1315
- Millikan, 1455
- Mills, underpotential deposition, 1313
- Minevski, 1277
- Miscenko and Lange, 823
- Moirre’s theorem of impedance, 1128
- Molecular dipole moment and light interaction, 803
- Molecular dynamic simulation, adsorption  
process, 965
- Molten salt  
electrodeposition on semiconductors, 1344  
in hydrogen coadsorption, 1344
- Monomers of water, 899
- Monsanto, 1039
- Monte Carlo simulation of adsorption, 965
- Morse curves, 1480, 1483
- Morrison, electron distribution law, 1465
- Mott, Nevil, 1456
- Multistep reactions, 1166  
Butler–Volmer equation in, 1176, 1179  
concentration terms, 1189  
coverage, 1168  
current density in, 1174  
current density–overpotential curves, 1172  
de-electronation reaction as a, 1178  
electron transfer number in, 1177  
energy barrier in, 1180  
hydrogen reaction as a, 1171  
ionic strength, 1189  
potential, 1189  
rate determining step in, 1180  
resistivity of the reaction in, 1174  
silver discharge as a, 1171  
standard free energy of activation, 1180, 1182  
steady state conditions in, 1173  
supporting electrolyte, 1190, 1253  
terminology, 1167
- Nanotechnology, 1345
- n-semiconductor, in thermal reactions, 1086  
as cathode, 1087
- n-p* junction, 1074, 1081  
transfer of holes or electrons in, 1082
- n-p* semiconductor  
current density, 1081
- Naphtyl compounds, adsorption, 979, 982
- Nekrassow, 1141
- Nernst, W., 1057
- Nernst’s equation, 857, 1057, 1058, 1060, 1062, 1066, 1255, 1351  
diffusion layer, 1233  
electrochemical potential, 1064  
equilibrium potential difference, 1061  
importance, 1064  
interfacial concentration and, 1220, 1230  
polarography and, 1240  
and semiconductors, 1084  
standard electrode potential, 1061  
theory of diffusion, 1217
- Neugebirt, 1146
- Newton, 1495, 1499
- Nicotinic acid, adsorption, 979
- Ni–NiO<sub>2</sub>** electrodes, 1144

- Nikitas, isotherms, 936, 952, 1195
- Nitrobenzene reduction, 1376
- Nonaqueous solutions, coadsorption of hydrogen
  - and organic molecules, 1340; *see also* hydrogen coadsorption
- Non-faradaic electrochemical modification of catalytic activity, 1371
- Nonlocalized adsorption, 928, 958
- Nonpolarizable interfaces, 812, 857, 1055, 1060, 1111
  - equivalent circuit of ideally, 814
  - ideally, 813
  - and thermodynamic equilibrium, 834
- Nucleation, during electrodeposition, 1302, 1305
  - size of, 1305, 1302
  - two dimensional, 1306
  - two dimensional, during underpotential deposition, 1316
- Nylon synthesis, as an electrochemical process, 1039
- O'Brien, 1235
- Ohmic drop, 811, 1089, 1108
- Ohmic resistance, 1175
- Ohm's law, 1127, 1172
- Open circuit cell, 1350
- Open circuit decay method, 1412
- Order of electrodic reaction, definition 1187, 1188
  - cathodic reaction, 1188
  - anodic reaction, 1188
- Organic adsorption, 968, 978, 1339
  - additives, electrodeposition, 1339
  - aliphatic molecules, 978, 979
  - and the almost-null current test, 971
  - aromatic compounds, 979
  - charge transfer reaction, 969, 970
  - chemical potential, 975
  - as corrosion inhibitors, 968, 1192
  - electrode properties and, 979
  - electrolyte properties and, 979
  - forces involved in, 971, 972, 977, 978
  - free energy, 971
  - functional groups in, 979
  - heterogeneity of the electrode, 983, 1195
  - hydrocarbon chains, 978, 979
  - hydrogen coadsorption and, 1340
  - hydrophilicity and, 982
  - importance, 968
  - and industrial processes, 968
  - irreversible, 969, 970
  - isotherms and, 982, 983
- Organic adsorption (*cont.*)
  - lateral interactions, 983
  - and the maximum of the coverage-potential curve test, 971
  - naphtyl compounds, 982
  - and the parabolic coverage-potential curve test, 970
  - potential dependence of, 972
  - pyridine, 983
  - reversible, 969, 970
  - reorientation process in, 979
  - roughness of the electrode and, 979
  - solubility and, 982
  - single crystals and, 979
  - structure, size and orientation of molecules, 978
  - as a substitution process, 973, 978
- Organoelectrochemistry, 970
  - effect of electrochemical reaction rates in, 1070
- Orientation of water at the interface, 912
- Orientation of adsorbed organic molecules, 979
- Outer Helmholtz plane, 872, 919, 922, 959, 961, 1069, 1213, 1232
- Outer potential, 821, 830, 1069
  - a thought experiment, 822
  - difference, 822
  - measurability, 829
- Outer sphere, 1127
  - reaction, definition, 1496
- Overall reaction, 1167, 1258
  - computer simulation and, 1259
  - coulometry, 1259
  - gas chromatography and, 1259
  - mass spectroscopy and, 1259
- Overall order of electrodic reaction, 1187
- Overpotential, 1066, 1078, 1115, 1116, 1171, 1370, 1466
  - activation, 1231, 1232, 1368
  - charge transfer and, 1172
  - charge transfer, 1131
  - concentration, 1230
  - conductivity and, 1175
  - vs. coverage, isotherms, 1197
  - definition, 1050, 1051
  - in electrochemical cell, 1361
  - electrodeposition and, 1305, 1306, 1338
  - as a measure of electrocatalysis, 1278
  - rate of electrochemical reaction and, 1197
  - symmetry factor dependence with, 1484
- Oxygen reduction, cathodic, 1052, 1140

- Oxygen reduction, cathodic (*cont.*)
  - on bare iron, 1263
  - on gold single crystals, mechanism, 1207
  - importance, 1263
  - mechanism, 1263
    - on iron, 1265
  - order of reaction, 1263
  - overall reaction, 1263
  - on passive iron, 1263
  - Tafel lines, 1207
  - on well defined crystal planes, 1207
- Oxygen evolution, 1091
  - on perovskites, 1280
- p*-semiconductor, 1086
  - as anode, 1087
- Paik, and ellipsometry, 1152
  - and the electrochemical heart, 1380
- parallel reactions, 1168, 1259
  - and rotating disk electrode, 1141
- Parsons, 899, 931, 943, 1479, 1522
- Parsons–Zobel plot, 890
- Partial charge transfer, 922, 1298, 1497
- Partition functions of adsorbed species, 937
- Pattern recognition analysis, use of computers in, 1162
- Pathway of reaction, 1167
  - consecutive reactions, 1259
  - definition, 1259
  - and FTIR spectroscopy, 1259
  - hydrogen evolution reaction, 1259
  - isotopic analysis, 1259
  - mechanism, 1259
  - parallel reactions, 1259
- Permittivity of free space, 875
- Perez, 1519
- Perovskites, 1280, 1282
- Perrin, 873
- Perrin-Helmholtz theory, 873
- Phase angle, impedance, 1129
- Phase difference, impedance, 1127
- Phase formation, one dimensional, underpotential deposition, 1316
- Phenyl compounds, 979
- Phonon spectra, 1463
- Phonon, 1517
- Phonon–vibron coupling, 1517
- Photoactivity of semiconductor electrodes, 1089
- Photoelectrochemistry, 1089
- Photoelectrodes, 1088
- Photomultiplier tube, 805
- Photosynthesis, 1090
  - as an electrochemical reaction, 1042
- Photoelectrochemistry, 1074
- Physisorption, 922
- Plating with aluminum, 1343
- Platinum
  - advantages as electrocatalyst, 1286
  - black, 1108
- Pogendorff, 1352
- Polanyi, 1487, 1503
- Polarizable interfaces, 812, 1055, 1134
  - equivalent circuit of ideally, 814
  - fundamental equation, 858
  - ideally, 813, 848
  - mercury–solution interface, 848
  - partly, interface and exchange current density, 1056
  - surface tension, 863
- Polarization of light and adsorption, 803
- Polarized light, 800, 801, 1147
- Polarography, 1237, 1424
  - activation potential in, 1244
  - assumptions in, 1244
  - charge transfer equilibrium, 1240
  - condition, 1238
  - current–potential relationship in, 1244
  - diffusion layer in, 1246
  - drop area in, 1245
  - Fick's first law, 1243
  - half-wave potential, 1244
  - mean current–potential relationship, 1238
  - Nernst equation, 1240
  - spherical diffusion in, 1239
- Polarographic wave, 1244
- Polaron, 1516
- Polujan, transients, 1403
- Polycrystalline electrodes, 190, 1201
  - in electrodeposition, 1334
  - and transients, 1402
- Pons, 1146
- Popov, 1336
- Potential
  - absolute, 1059
  - chemical
    - definition, 830
    - determination, 832
  - chi, 824
  - difference of, 806; *see also* potential difference
  - difference of metal/solution interface, contributions, 818

Potential (*cont.*)

- dipole, 824
- of electrode, 821, 900, 924
- of electrode, definition, 816, 821
- electrochemical, 1058
  - definition, 830
  - as driving force in transport of charged species, 832
  - and thermodynamic equilibrium, 833
  - as a total potential, 832
- electrokinetic, 1069
- equilibrium, 1351
- Galvani, 826, 1057, 1455
- inner, 830, 1059
  - as absolute potential, 829
  - difference, 826, 857, 869
  - measurability, 829
  - as a nonpractical potential, 829
- measurement of, 811, 1112, 1125
- multistep reactions, 1189
- outer, 821, 830
  - difference, 822, 869
  - measurability, 829
  - a thought experiment, 822
- psi, 822
- potential energy curves, 1479
- relative, 1351
- relative electrode, 815, 1059
- reversible, and reaction rate, 1124
- of solution, 821
- standard electrode, conventions 1351; *see also* standard electrode potential
- surface, 830, 887, 888
  - measurability, 829
  - potential difference, 869
  - in solution, 826
  - a thought experiment, 823
  - in vacuum, 823
  - of water dipole layer, 904
- Volta, difference, 822
- working electrode, 1061
- of zero charge, 887, 946, 971
  - definition, 840
  - determination on solid electrodes, 861
  - and electrocapillary curves, 861

Potential-current relationship

- in driven cells, 1364
- in self driven cells, 1363
- variation of, 1361

Potential changes, measurement, 811

Potential difference, 1043, 1067, 1348

Potential difference (*cont.*)

- across electrified interfaces, 806
- across an electrochemical cell, measurability, 1160
- cell, effect on, 1104
- contact, 809
- displacement, in underpotential deposition, 1316
- in an electrochemical cell, 809
- equilibrium, across an electrochemical cell, 1350, 1356
- inner, 826, 869
- measurement of a single, 807
- measurement, 811
- of metal-solution interface, contributions, 818
- outer, 822, 869
- of parallel plate condenser, 875
- surface, 869
- Volta, 822
- Potential energy, definition, 818, 1475, 1481
- Potential energy curves, 1199, 1200, 1473, 1498, 1519
  - activated state, 1480
  - adsorption process, 965
  - anharmonic curves, 1487
  - basic diagram, 1475, 1478
  - dimensions, 1488
  - electrode potential, 1479
  - ground state, 1479
  - harmonic, 1487
  - initial state, 1479
  - Morse curves, 1480
  - potential energy, 1481
  - symmetry factor, 1479
- Potential step measurements, 1119
- Potential variation with distance in solution, 884
- Potentiostat, 1118
- Potentiostatic control of electrochemical reactions, 1223
- Potentiostatic techniques, 787, 1115, 1118
  - and impurities on electrodes, 1120
  - potential interval measurements, 1121
- p-polarized light, 802
- Potentiodynamic techniques, 1423, 1438
  - vs. potentiostatic techniques, 1426
- Potentiostatic transients, 1414
  - difficulties in, 1415
  - double layer charging, 1416
  - radicals in, 1416
  - IR drop in, 1416
- Prandtl layer, 1228

- Pressure, 931
- Pressure changes in region outside the ion's inner shell, 1126
- Proton transfer reaction, intermediate radicals, 1475
- Pseudo capacitance, 1431
- Pseudo equilibrium, 1198
  - definition, 1169
  - rate determining step and, 1260
- Pseudo potential, and jellium model, 892
- Psi potential, 822
- Pyramids, electrodeposition, 1334, 1336
- Pyridine, 983
  
- Quasi-equilibrium
  - and law of mass action in reactions in, 1184
  - and rate determining step, 1176
- Quasi-reversibility, definition, 1420
- Queueing theory
- Quantum electrochemistry, retrospect and prospect, 1522
- Quantum mechanical tunneling, 1471, 1499
- Quantum states, 1456
  - of electrons in solution, 1461
- Quantum transitions, 1494
  
- Radiationless quantum mechanical transition, 1467
- Radicals, 1139, 1147, 1193, 1416
  - adsorbed, in electrocatalysis, 1275
  - determination by rotating disk electrode, 1140
  - intermediate, in methanol oxidation, 1270
- Radiation
  - infrared, 797
  - microwave, 797
  - ultraviolet, 797
  - visible, 797
- Radioactive isotopes, 804
- Radiochemical
  - in electrochemistry, 804
  - techniques, 787, 806
- Raleigh, 1159
- Randles, 1134, 1425
- Random thermal displacement, electrodeposition, 1312
- Rate constant, 1168
- Rate determining step, 1157, 1168, 1212, 1404
  - computer analysis in, 1261
  - conductivity and, 1175
  - determination of, 1261
  - diffusion, 1261
- Rate determining step (*cont.*)
  - electrocatalysis and, 1276
  - methanol oxidation, 1270
  - in multistep reactions, 1180
  - overpotential and, 1175
  - places where it can occur, 1260
  - pseudo-equilibrium, 1260
  - quasi equilibrium and, 1176
  - reaction mechanism and, 1260
  - steady state and, 1176
  - surface chemical reactions and, 1261
- Real impedance, 1128, 1135
- Reciprocal relation, the, 1250
- Recombination reaction, 1168
- Receiver states, 1494
- Reddy, 1163
- Redox reactions, 1092, 1220
  - catalysis and, 1275
  - free energy, 1513
- Reference electrode, 1104, 1108, 1113
  - potential, 819, 874
- Refractive index, determination with ellipsometry, 1148, 1151
- Reflection coefficient, 1151
- Residence time, definition, 1310
- Reversal techniques, determination of intermediate radicals, 1416
- Reversible adsorption of organic molecules, 969, 970
- Reversible, definition, 1419
- Reversible electrode, definition, 834, 1113
- Reversible hydrogen electrode, 815, 1207
- Reversible reaction, 1251
- Reversible region, 1255
- Resistance, 1172
  - faradaic, 1175
  - ohmic, 1175
- Resistivity of the reaction, multistep reaction, 1174
- Rice, 887
- Rideal, transients, 1401, 1402, 1409
- Ring-disk electrode, 1140, 1143
  - mechanism determination, 1263
  - ring current in, 1142
- Robotization to control experiments, use of computers for, 1162
- Rohrer, 1157
- Roitar, transients, 1403
- Roscoe, 1159
- Rose, potential energy curves, 1487
- Rotating disk electrode, 1139



Rotating disk electrode (*cont.*)

- diffusion coefficient, 1141
- diffusion layer in, 1234
- disk current in, 1141
- ECE reactions determination by, 1144
- electrooxidation of methanol, 1139
- kinematic viscosity, 1141, 1234
- intermediate radicals, determination of, 1139, 1193
- mechanism determination, 1144
- metal deposition and, 1144
- metal oxidation and, 1144
- parallel reactions, 1141
- radicals, determination, 1140
- ring and, 1140; *see also* ring-disk electrode
- rotation rates
- stirring, 1140
- Temkin conditions in, 1142

Rotational motion of adsorbed ions, 928

Roughness factor of the electrode, 806, 979, 1096

Salic and Lorenz and partial charge transfer, 922

Sands' equation, 1120, 1220, 1223, 1411

Saturated dielectric, 898

Savéant, 1518

Scanning tunneling microscopy (STM), 787, 1157

- bioelectrochemistry and, 1159
- electrochemistry and, 1158
- electrodeposition and, 1310
- nanotechnology, 1345
- piezoelectric crystal, 1158
- tunneling current, 1157
- underpotential deposition, 1313, 1315

Scavenger electrolysis, electrodeposition, 1343

Schlieren method, diffusion layer, 1235

Schmickler, 1495, 1510

Schrödinger equation, 1456, 1490

Schultze 923, 1497, 1510

Screw dislocation, 1303, 1316, 1321, 1326

Secondary reference electrode, 815, 1109

Self-consumed electrode, 1040

## Semiconductors

- Boltzmann term, 1078
- computer simulation, 1161
- current density, 1078, 1081
- current potential relation, 1082
- doping, 1073
- effect of light on, 785
- $e-i$  junction, 1081
- electrode kinetics of, 170
- electrodeposition on, 1344

Semiconductors (*cont.*)

- equilibrium in, 1076
- exponential law, 1081
- germanium as, properties, 1076
- hole movement, 1076
- impedance of, 1136
- importance of, 785
- limiting current, 1088
- n-, in thermal reactions, 1086
- n-p junction, 1073, 1081
- p- in thermal reactions, 1086
- photoactivity of, 1089
- photoelectrochemistry, 1073
- photostimulated electrodeposition on, 1345
- potential variation with distance in, 1082
- silicon as, properties, 1076
- surface states, 1086
- symmetry factor in, 1082
- thermal reactions, definition, 1088

Sen, 1495

Sevcik, voltammetry, 1425

"Shoelace" curves, 1465, 1468

Sidik, 1489, 1499, 1520

Silicio carbide, as electrocatalyst, 1283

Silicon, properties as semiconductor, 1072

Silver-silver chloride reference electrode

Single crystal electrodes, 1091, 1099, 1197

in electrochemistry, 1205

in electrodeposition, 1292, 1299, 1330

fabrication, 1198

gonometer, 1198

kinetics, 1206

Miller indexes, 1198

orientation, 1198

reactivity of, 1201, 1205

underpotential deposition, 1309

usefulness in technology, 1205

Short range forces, 819, 936

Silver-silver chloride electrode, 815

Single flat face, electrodeposition, 1329

Single step reaction, 1162

Site energy distribution, 952

Size, of ion, and isotherms, 954

Skin effect in current measurements, 1121

Solid electrodes, determination of potential of zero charge, 861

Solution, potential of, 821

Solution resistance, impedance electrochemistry, 1133, 1134

Solution spectroscopy, 1463

Solution, steps of purification of, 1093, 1094

- Solution, steps of purification of (*cont.*)  
 by scavenging, 1093  
 by UV radiation, 1093
- Solvation, 964
- Solvent displacement, and isotherms, 954, 955
- Solvent excess entropy at the interface, 912
- Solvent interactions, 923, 964
- Soriaga, M., 1103, 1146
- Specifically adsorbed ions, 886
- Spectrometer, 797
- Spikes, electrodeposition, 1336
- Spillover electrons, of metal, 889
- Spiral growth, electrodeposition, 1316, 1324,  
 1326, 1324, 1328
- s-polarized light, 802
- Srinivasan, S., 1439, 1494
- Standard electrode potential  
 American convention, 1354  
 convention, 1351  
 IUPAC convention, 1355  
 prediction of reactions, 1359  
 the zinc-minus and copper-plus convention,  
 1352
- Standard states, isotherms, 936  
 convenient, 936  
 conventional, 936
- Stanski, electrodeposition, 1301, 1303
- Standard hydrogen electrode, 1108; *see also*  
 hydrogen electrode  
 potential, definition, 840, 1060, 1061
- Steady state, 1147, 1212  
 current, 1248  
 current-potential relation, transport control,  
 1246  
 definition, 1115, 1274  
 electrical migration, 1253  
 effect of charge transfer, 1212  
 importance, in electrode kinetics, 1274  
 multistep reaction, 1173  
 rate determining step and, 1176
- Step, electrodeposition, 1310, 1321, 1324  
 formation from screw dislocations, 1327
- Stepwise mechanism of electrodic reactions,  
 determination, 1257
- Stern model, 882, 959  
 charge in solution, 882  
 differential capacity, 884  
 potential variation with distance, 884
- Stoichiometric number, 1182
- Stonehart, 1439
- Substance producer device, 1036
- Supporting electrolyte, 1190, 1216, 1235
- Surface area of drop, in polarography, 1244
- Surface concentration, 805
- Surface coverage, 933  
 at equilibrium in multistep reactions, 1191  
 at nonequilibrium, 1191
- Surface coverage factor, 1190
- Surface excess, 843, 845, 856, 866, 870  
 and amount adsorbed, 845  
 definition, 845  
 determination, 846, 847, 862  
 and equation of state, 931  
 importance, 846  
 as a macroscopic concept, 846  
 and reference electrode, 862
- Surface selection rules, 801
- Surface preparation, and electrochemical  
 techniques, 1345
- Surface potential, 830, 887, 888  
 calculation of, 893  
 and jellium model, 893  
 measurability, 829  
 in solution, 826, 1460  
 a thought experiment, 823  
 in vacuum, 823  
 of water dipole layer, 904  
 and work function, 835
- Surface pressure, definition, 931
- Surface states, 1082, 1083  
 definition, 1086  
 effect on semiconductors electrode kinetics,  
 1086  
 impedance of, 1138
- Surface tension, 847, 855, 931  
 of liquids, 848  
 of polarizable interface, 863  
 of solids, 850  
 variation with solution concentration, 863
- Symmetry factor, 1044, 1051, 1068, 1071, 1078,  
 1082, 1526  
 the dark side of, 1528  
 definition, 1483  
 dependence with overpotential, 1484  
 importance, 1484  
 Morse curves, 1483  
 potential energy curves, 1479  
 and transfer coefficient, 1186  
 variation with temperature, 1530
- Szklarczyk, M., 1158, 1272
- Szucs, enzymes, 1289

- Tafel equation, 1054, 1066, 1106, 1115, 1133,  
1249, 1404, 1440, 1456, 1507, 1528  
applications, 1508  
and distribution of electronic states,  
importance, 1466  
importance, 1508  
in quantum calculations, 1495  
in semiconductors, 1085  
tunneling, 1495
- Tafel, Julius, 1106
- Tafel lines, oxygen reduction, 1207
- Tamm states, 1082
- Tarasevich, 1495
- Taylor, electrodeposition, 1303
- Temkin isotherm, 927, 938, 1195  
coverage variation with concentration,  
1196  
coverage variation with potential, 1196  
in electrocatalysis, 1275
- Temkin conditions, 942, 944, 965, 983, 1122,  
1142, 1199
- Temperature control in electrode kinetics, 1121
- Terraces, electrodeposition, 1307, 1336
- Thermal desorption spectroscopy (TDS), 787
- Thermal reactions in semiconductors, definition,  
1088
- Thermodynamic equilibrium  
and electrochemical potential, 833  
and nonpolarizable interfaces, 834
- Thermodynamics, first and second laws, 854
- Thermodynamics of interfacial charge transfer at  
equilibrium, 1057
- Thickness of thin layers, measured by  
ellipsometry, 1148, 1151
- Thin layer cells, 1146  
adsorption in, 1103  
in electrode kinetics, 1103
- Thiophenol, adsorption, 979
- Thirsk, electrodeposition, 1310
- Thompson, G. P., 1455
- Thompson, J. J., 1057, 1455
- Throwing power, 1112
- Throwing power, electrodeless, 1376
- Titanium carbide, as electrocatalyst, 1287
- Transfer coefficient and symmetry factor, 1186,  
1529
- Transfer reaction, electrodeposition, 1310
- Transients, 1119, 1401, 1417, 1422  
definition, 850  
diffusion current, 1404  
electrode surface area using, 1403
- Transients (*cont.*)  
electron transfer current, 1404  
faradaic current, 1404  
galvanostatic, 1409, 1411, 1412  
heterogeneity, effect on, 1414  
how to have successful, 1407  
intermediates, 1408  
importance, 1403, 1407, 1420  
impurities, effect on, 1402, 1409  
interfacial control in, 1406  
irreversibility in, 1419  
lower time region in, 1405  
measurement time, 1408  
as a method to avoid impurities, 1093  
potential-time, 1220, 1221  
potentiostatic, 1414  
rate determining step in, 1404  
Tafel region in, 1404  
upper time region in, 1405
- Transition time, 1120
- Transition time, definition, 1217, 1221, 1222,  
1223, 1255  
and convection, 1225
- Translational motion of adsorbed ions, 928
- Transport process, 1216  
controlled reaction by, 1217, 1246, 1252  
convection, 1225, 1226  
current density, 1254  
diffusion, 1212  
flux, 1203  
net current density, 1203  
migration, 1212, 1225  
summary, 1254
- Trasatti, isotherms, 936, 981
- Trasatti, surface potential of solution, 1460
- Tritium, reaction rate, advantages, 1155
- Tunneling current, in scanning tunneling  
microscopy, 1157
- Tunneling, 1455  
definition, 1490  
deuterium, 1493  
of electrons, 1456, 1489, 1527  
equation of, 1490  
heme, 1495  
hydrogen, 1493  
parabolic potential barrier in, 1493  
probability of, 1492  
rectangular potential barrier in, 1492  
relay stations, electron, 1496  
resonance, 1495  
Schrödinger wave equation, 1490

Tunneling (*cont.*)

through adsorbed layers in biological systems, 1495

tritium, 1493

WKB approximation, 1492

## Turbulent flow, 1226

and diffusion layer, 1234

## Turnover number, enzymes, 1287

## Ultramicroelectrodes, 1098

## Ultraviolet photoelectron spectroscopy (UPS), 787

## Ultraviolet radiation, 797

## Underpotential deposition, 1121, 1313

alloy formation during, 1316

causes of, 1315

definition, 1313

displacement potential, 1316

kinetics of, 1316

lead deposition, 1313

one-dimensional phase formation in, 1316

scanning tunneling microscopy used to study, 1313, 1315

single crystals in the study of, 1313

two dimensional nucleation in, 1316

work function and, 1316

## Unielectrodes, 1036

## Uosaki, 1273

## Urea, adsorption, 979

## Van Hoff, 1507

## Vayenas, 1371

## Velev, 1121, 1122, 1272

## Vermilyea, electrodeposition, 1324

## Vesiliev, oxidation of methanol, 1269

## Vetter, 1497

## Vetter and Schulze, charge transfer, 923

## Vibrational entropy, 914, 915

## Vibrational motion of adsorbed ions, 928

## Vibron model, 1517

## Virial equation of state in two dimensions, 931

## Virial isotherm, 936

## Visible radiation, 797

## Volcanoes, in electrocatalysis, 1284

## Volmer, Max, 1048, 1474

## Volmer, Weber, electrodeposition, 1303, 1306

## Volta, 1423, 1455

## Volta potential difference, 822

## Voltammetry, 1432, 1434

cyclic, 1422, 1423

diffusion control reactions, 1426

electron transfer reaction, 1424

Voltammetry (*cont.*)

in electrokinetics, 1438

history, 1424

IR error, 1437

limitations, 1426

linear sweep, 1423, 1438

in non-aqueous solutions, 1434

pseudo-capacitance, 1441

range, 1425

redox type reactions, 1437

reversed-step, 1417

shape of peaks, 1428

steady state in, 1432, 1435

sweep rate, 1423, 1426, 1427

## Voltammogram, of clean surface, 1203

of hydrogen adsorption on platinum single crystals, 1205

electrocatalysis and, 1206

mechanism determination and, 1258

## Voltmeter, high-input impedance, 1353

## Vortices, convection, 1226

## Waiting lines in electrochemical reactions, 1169

## Waiting time theory, 1170

## Warburg impedance, 1133, 1134, 1223

## Washington, G., 1164

## Wass, 1121, 1270, 1511

## Water

adsorption

chemical work of, 907

electrical work of, 907

lateral interaction work, 907

binding energy of, 1191

Bockris-Devanathan-Muller model of, 898

coverage of electrode by, 895

Damaskin and Frumkin model of, 899

dimers, 975

definition, 899, 902

surface coverage, 904

dipole, 871, 899

dipole differential capacity of, 910, 911

dipole layer

and surface potential, 904

and parallel plate condenser, 905

dipole potential of, 909

-electrode interaction energy, 944, 924, 945

energy of adsorption of, 912

equilibrium cycle of, 903

Fawcett model of, 899

flip-up state of, 899, 902, 906, 975

flop-down state of, 899, 906, 906, 975

Water (*cont.*)

- free energy of flip-up and flop down waters, 906, 915
- Guidelli model of, 899
- Habib and Bockris, 899
- at the interface, importance of, 918
- ion interaction energy, 924
- metal interactions, 896
  - chemical forces, 897, 972
  - lateral forces, 897
- monomers of, definition, 899
- orientation of, 898
- Parsons model of, 899
- and potential of the electrode, 900, 924
- preferential orientation of, 912
- and solvent excess entropy, 912
- the "three-state water model" 898, 899

Wave nature of electrons, 788

Wavenumber, 799

Waves

- constructive interference of, 789
- destructive interference of, 789
- diffraction pattern, 790
- in-phase, 789
- interaction with matter, 788, 790
- interference, 790
- out-of-phase, 789

Weiss, 1506, 1512

Weiss-Marcus harmonic energy variation theory, 1513, 1519

Wenking, 1118

Wentzel-Kramer-Brillouin approximation, tunneling, 1492

Whewell, Reverend, 1050

Whiskers, 1327, 1336

White, and organic adsorption, 979

Wieckowski, A., 1146

Will, 1205

Willis, underpotential deposition, 1313

Wojtowicz, 1381

Work function of the metal, 887

- and chemical potential, 835
- definition, 835
- in electrochemistry, 835
- and surface potential, 835
- underpotential deposition and, 1316

Working electrode, potential, 1061

Wright, 1495

Xia, potential energy curves, 1487

X-ray diffraction, 793

X-ray photoelectron spectroscopy (XPS), 787, 794  
information obtained from, 796

X-rays, definition, 794

Zener, 1499, 1503

Zero charge, potential of, 887, 946, 971

- definition, 840
- determination on solid electrodes, 861
- and electrocapillary curves, 861

Zero point energy, influence of isotopic reaction rate, 1155

Z-log W plot in impedance, 1127